Rolf Rannacher
Adélia Sequeira
Editors

Advances in Mathematical Fluid Mechanics

Springer

Advances in Mathematical Fluid Mechanics

Rolf Rannacher · Adélia Sequeira
Editors

Advances in Mathematical Fluid Mechanics

Dedicated to Giovanni Paolo Galdi on the Occasion of his 60th Birthday

Springer

Editors
Rolf Rannacher
Institut für Angewandte Mathematik
Universität Heidelberg
Im Neuenheimer Feld 293/294
69120 Heidelberg
Germany
rannacher@iwr.uni-heidelberg.de

Adélia Sequeira
Department of Mathematics
Centre for Mathematics and its Applications
Instituto Superior Técnico/UTL
Av. Rovisco Pais, 1
1049-001 Lisboa
Portugal
adelia.sequeira@math.ist.utl.pt

ISBN 978-3-642-04067-2 e-ISBN 978-3-642-04068-9
DOI 10.1007/978-3-642-04068-9
Springer Heidelberg Dordrecht London New York

Library of Congress Control Number: 2010920233

Cover illustration: Simulations performed by Otto Mierka/Stefan Turek based on FeatFlow (www.featflow.de)

Cover design: WMXDesign GmbH, Heidelberg

Printed on acid-free paper

Springer is part of Springer Science+Business Media (www.springer.com)

Dedicated to Giovanni Paolo Galdi, on the occasion of his sixtieth birthday

Giovanni Paolo Galdi

Foreword

The present volume celebrates the 60th birthday of Professor Giovanni Paolo Galdi and honors his remarkable contributions to research in the field of Mathematical Fluid Mechanics. The book contains a collection of 35 peer reviewed papers, with authors from 20 countries, reflecting the worldwide impact and great inspiration by his work over the years. These papers were selected from invited lectures and contributed talks presented at the *International Conference on Mathematical Fluid Mechanics* held in Estoril, Portugal, May 21–25, 2007 and organized on the occasion of Professor Galdi's 60th birthday. We express our gratitude to all the authors and reviewers for their important contributions.

Professor Galdi devotes his career to research on the mathematical analysis of the Navier-Stokes equations and non-Newtonian flow problems, with special emphasis on hydrodynamic stability and fluid-particle interactions, impressing the worldwide mathematical communities with his results. His numerous contributions have laid down significant milestones in these fields, with a great influence on interdisciplinary research communities. He has advanced the careers of numerous young researchers through his generosity and encouragement, some directly through intellectual guidance and others indirectly by pairing them with well chosen senior collaborators. A brief review of Professor Galdi's activities and some impressions by colleagues and friends are included here.

This project could not have been successfully concluded without the generous support of some collaborators and several Portuguese institutions. Special thanks are due to João Janela for the careful preparation of the final version of this book, and also to Thomas Wick for his precious help. The financial and technical support of *Fundação para a Ciência e a Tecnologia (FCT), Fundação Calouste Gulbenkian, Fundação Luso-Americana para o Desenvolvimento (FLAD)* and of *Centro de Matemática e Aplicações (CEMAT), Instituto Superior Técnico*, are gratefully acknowledged. Finally, a special thanks to Springer-Verlag for accepting to publish this work.

On behalf of all collaborators and friends of Professor G.P. Galdi we wish him many more years of continued high energy, great enthusiasm and further impressive mathematical achievements.

Heidelberg, Germany — Rolf Rannacher
Lisboa, Portugal — Adélia Sequeira

Short Biography

Giovanni P. Galdi was born in Naples, Italy, on January 3, 1947, where he received his University degree (Laurea) in Physics from the University of Naples in 1971.

He is, currently, the William Kepler Whiteford Professor of Engineering and Professor of Mathematics at the University of Pittsburgh. He is also Adjunct Faculty at the Tata Institute of Fundamental Research in Mumbai, India. Before joining the faculty at the University of Pittsburgh in the Fall semester 1999, in the years 1980–1985 he was Professor at the Department of Mathematics of the University of Naples (Italy) and, from 1985 until 1998, he was Professor at the Institute of Engineering of the University of Ferrara (Italy).

Professor Galdi founded and organized the School of Engineering of the University of Ferrara in 1989, where he was the Dean from 1989 until 1995. He has been Visiting Professor in several academic institutions, including the University of Glasgow (Scotland), University of Minnesota (USA), University of Paderborn (Germany), University of Pretoria (South Africa), TIFR, Bangalore (India), Fudan University, Shanghai (China), University of Waseda, Tokyo (Japan), Czech Academy of Science (Czech Republic), Steklov Institute of Mathematics, the St Petersburg Branch (Russia), University of Paris-Sud XI, Orsay (France), Instituto Superior Tecnico, Lisbon (Portugal), and University of Pisa (Italy).

In the years 2003 and 2009 he was awarded the Mercator-Gastprofessuren from Deutschen Forschungsgemeinschaft (DFG).

He is a member of the Editorial Board of several scientific Journals, including *European Journal of Mechanics B/Fluids*. He is also co-founder and Editor in Chief of the *Journal of Mathematical Fluid Mechanics*, and of the Series *Advances in Mathematical Fluid Mechanics*, published by Birkhäuser-Verlag, Basel, Boston.

Professor Galdi has (co) authored over 130 original research papers and 6 books, and (co) edited 13 books, dedicated mostly to hydrodynamic and magnetohydrodynamic stability, mathematical theory of the Navier-Stokes equations, non-Newtonian fluid mechanics and fluid-solid interactions. In particular, his two-volume book "An Introduction to the Mathematical Theory of the Navier-Stokes Equation", first published with Springer-Verlag in 1994, is a classical milestone in the steady-state theory of the Navier-Stokes equations.

Paolo Galdi – The Man and the Mathematician

During the 1960s I worked hard on the Navier-Stokes equations, writing a number of papers. Then I sensed that the problems weren't getting easier, on top of which competition was moving in, so I looked for other things to do. My instincts soon found expression in reality when G.P. Galdi appeared on the scene; he would have been a formidable competitor and I'm happy I didn't have to face that challenge. He had a voracious appetite for knowledge, and I recall repeated requests for reprints of my papers. At that time, e-mail was not yet suitable for exchanging manuscripts, and reprints were generally sent as hard copies through postal services. He requested an early paper, which I dutifully sent him. Postal service between USA and Italy was rather slow, and apparently he lost patience, as shortly later he requested the same paper again. I assumed then that he wanted a later paper, and sent him that one. That seems to have arrived prior to the one he wanted, as I then got still another request from him. Again there was confusion, and I sent him still another paper. Ever since, he has been repeatedly accusing me (publicly) of sending him things he didn't want.

Never mind! It is clear that he read all the papers (also those written by others), absorbed their content, and then carried the theory further in new ways that have left a permanent imprint with his signature. A case close to my heart is his 1997 paper with Heywood and Shibata, in which the dissertation problem that I gave to John Heywood about 1965, on which Heywood at the time made deep initial progress, was finally solved. Beyond that is his impressive recasting of my own results on exterior problems into function space settings, and his extensions of the results to rotating and more general periodic motions. Galdi became – and continues to be – a central figure in describing and clarifying some of the most profound problems in modern hydromechanics. He has established himself as one of the few top contributors to a theory that has attracted worldwide interest and activity, and as a person who has stimulated and encouraged the creative achievements of many others. He is in fact in large part responsible for the present worldwide interest, by calling attention to the beauty, depth and underlying unity of the many open problems.

Stanford, California — Robert Finn

As many people have commented, "Paolo Galdi is a very special person". His enthusiasm, generosity, kindness and discernment have made him a most valuable colleague to the whole community of researchers working on topics in fluid dynamics.

Paolo's own contributions to fluid dynamics have been very significant and wide ranging. As an Editor of the *Handbook of Mathematical Fluid Dynamics*, I was very pleased to include an article by Paolo "On the motion of a rigid body in a viscous fluid" which covered an interesting sub-class of important fluid applications, and illustrated Paolo's versatility.

Through hard work and dedication, Paolo, John Heywood and Rolf Rannacher have created a major journal in the field, *The Journal of Mathematical Fluid Dynamics*, which has encouraged the resurgence of a classical topic in mathematics that is again taking center stage in partial differential equations.

I was honored and delighted to be part of the wonderful celebration of Paolo's 60th birthday that Adélia Sequeira and her colleagues organized in Estoril in 2007.

Los Angeles, California Susan Friedlander

I am not sure when I first met Paolo. I think it was in 1976 when I published my book on the stability of fluid motions. The mathematicians in Naples, under Salvatore Rionero, had taken an interest in the energy theory of stability. Paolo was a student of Rionero. I had published papers on that subject which led to my 1976 book on the stability of fluid motions. I was greatly stimulated to go in this direction by papers of James Serrin. I think that Mariolina Padula, Paolo's wife then, was also Rionero's student. She was, in any case, very active in math and she and Paolo would study together. Paolo and Mariolina came to the US I think in 1976. I do not know how their trip was financed. In any case, my wife then (Ellen) and I had a little party in our house which was on a lake in Minnesota. James Serrin was also a guest. I think it was in 1976 because Paolo reminded me that my book had arrived from Springer that very day. I think that Paolo and Mariolina were very impressed to meet with persons they though so great in an environment so different that via Mezzacannone. This is the time that Paolo and I became fast friends. I like to say that people from Minneapolis and Naples are natural friends since Minneapolitans can be thought to be small persons from Naples.

The next stage of our friendship developed in successive trips to Italy. These trips were arranged by Professor Rionero. In the first trip, Paolo and Mariolina invited me to their home. There, I learned about Paolo's special talents in the arts as a painter specializing in portraits of Donald Duck and as a fine pianist specializing in Chopin. I loved Naples. For years in the early 1980s I taught in the summer school in Ravello. These were very pleasant summers. In 1982, I practiced there to run the original marathon in Greece. I would run up to Valico di Chiunzi and back, chased always by angry Italian dogs. The further south you go in Europe, the greater are the number of female math students and there were many nice ragazzi in Ravello. I remember one handsome Italian mathematician from Bologna telling me that his marriage license was not valid in the South. Later, it was not valid in the north.

I had many intimate conversations with Paolo in the cafes in Ravello. At this time he was drifting to a more rigorous approach to mathematics. I urged him to continue his studies on the applied side, warning him that if he followed his desire he would have to compete with fine mathematicians much better prepared than he. At that time, he was working on energy theory on unbounded domains. To complete his results, he needed some powerful Navier Stokes theorems. I think the work of Leray was involved in his theorems. He was intense about mathematics and had gone beyond the energy theory of stability which frankly is a theory which demands that you know how to use the divergence theorem and integrate by parts. Gradually, our trajectories in science grew apart. Paolo was encouraged to prepare his now well known Springer monograph on the Navier Stokes equations by Clifford Truesdell, who at an earlier time was also my mentor but later my tormentor.

In 1991, Paolo and Salvatore visited me again in Minneapolis. I had developed a theory for miscible liquids and showed that mixtures of incompressible mixing liquids are compressible and obtained a new theory of diffusion. The velocity is not solenoidal. Paolo found that a certain combination of the velocity and expansion velocity was divergence free. It turns out that this combination is equivalent to a volume averaged velocity. It is a great result, which we used in all subsequent papers.

Paolo is a very special, outgoing and supportive person. He has that magic personality which radiates interest and concern about others wherever he goes. He engages all persons and elevates their level of well being. Maybe this is why he has so many friends all over the world and at the great birthday meeting celebrated by this volume.

I know three mathematicians from the applied side who developed a burning desire to be the master of rigorous mathematics. This goal is at the top of a mountain. One of these mathematicians in Klaus Kirchgässner, another is Edward Fraenkel and the third is Paolo. It was a difficult journey, but Paolo has reached the summit without forgetting the applied side. It is my pleasure to wish happy 60th birthday to this good friend, great man and fine mathematician.

Minneapolis, Minnesota Daniel D. Joseph

Naples, via Mezzocannone, 8, early Seventies. It is here, in this stern and monumental environment where Tommaso d'Aquino gave his theological lectures, that I, a young student of Mathematics, take my first steps in the field of mathematical research. Professor Salvatore Rionero introduces and guides me into this world where at first I feel awe. Further than him, I owe his young co-worker Giovanni Paolo Galdi my quick and complete adaption, so that I could feel quite at ease among those great staircases and those lecture halls where one could smell the odor of history. There had lived and worked mathematicians of the level of Ernesto Cesaro, Roberto Marcolongo, Mauro Picone and Renato Caccioppoli and there still worked in that period great masters like Alfredo Franchetta, Carlo Miranda and Carlo Tolotti.

Paolo, as I called him at once since at once we became friends, was for me a most precious guide towards that world which seemed to me very far and difficult to reach. Paolo addressed me to the journals he deemed more suitable for my kind of research, gave me his advice, but above all stimulated me with his observations and his sparkling conversation. Our friendship and our work relations consolidated in time. I always remember the wonderful evenings passed together, when Paolo, as a true showman, was the life and soul of the company with his pleasantness and his skill as a piano player; or the football games played on Saturday in a small pitch on one of the finest hills of Naples. I always remember the days Marina and I spent at the seaside together with Paolo, Mariolina, Adriana and Giovanni, swimming in the crystal clear waters of Calabria and playing on the beach. Memories the time will never wipe out, even though life has assigned to each of us a different road to follow.

Caserta, Italy Remigio Russo

Christian Simader met Paolo Galdi for the first time in 1988, exactly 20 years ago. He describes this meeting as follows: "In the spring 1987 I was a visitor at the University of Catania in Sicily, where I gave several lectures. One was devoted to the Helmholtz decomposition of vector fields. Shortly before this visit, Hermann Sohr and I found an elementary proof of this theorem. Professor Giuseppe Mulone suggested I contact Professor Galdi from Ferrara who, at the time, was writing a book on the Navier-Stokes equations. In April 1988, my wife and I intended to participate in an intensive Italian language course at Venice. Shortly before we left for Venice, I realized that Ferrara is close to Venice, so I immediately contacted Professor Galdi who invited me to come to Ferrara. At that time I was already familiar with many of his papers, but I had never met him in person. These papers impressed me deeply because of their clearness, accuracy and profoundness. Therefore, I had the impression that the author had to be a mature mathematician, much older than I was. Our first appointment was in a hotel in Ferrara. Precisely at the time of our appointment, a young couple entered the lounge and was obviously looking for someone. After some seconds, I asked the man if he was Professor Galdi. He said yes and I introduced my wife and myself. He was very surprised – and told me that he thought vice versa that I had to be much older. From his mathematical studies with Professor Carlo Miranda at Naples, he knew my old Springer Lecture Notes from 1972 which in fact was an English translation (at least I regarded it so) of my thesis from 1968. So we laughed a lot and spent a very nice evening together, enjoying a wonderful dinner. My wife and I had the impression of a very sympathetic and cultured couple, interested in many topics – clearly very much in mathematics. This impression was deepened in the following days, especially when we met their three children. Briefly expressed, it was reciprocal sympathy at the first view. At that time, the joint work with Hermann Sohr on the L-Dirichlet problem for the Laplacian in exterior domains was in progress. The problem turned out to be much more difficult than we expected. Though clearly we had Stokes' system in mind, we regarded this problem as a first step and as a type of model to find the appropriate function spaces. At that time, we worked with function spaces which in certain cases ($1 < q < n$) turned out to be too "small" and we had to impose a certain compatibility condition on the data such that we could prove existence and uniqueness of weak L-solutions in exterior domains. I presented a lecture on the results Hermann and I had achieved. Afterwards Paolo (meanwhile, we had begun to use first names) told me, that he was studying the corresponding problem for Stokes' system. Some weeks after returning to Bayreuth, Paolo called me and asked again for our compatibility condition which turned out to be different from the one he found. So I returned to Ferrara and we started to jointly work on the exterior Stokes' system. It turned out that we have a similar mathematical taste and a similar way in regarding problems. These similarities, simplified our collaboration very much. But there were also differences: Paolo knew a magnitude more about Stokes' problem than I did and he was much faster in thinking and calculating. But it was a very happy collaboration and within some days we solved the problem completely and the joint paper appeared 1992 in the Archive. But to tell the truth, 90% of the paper is due to Paolo. In the sequel, I often visited Ferrara which also gave me the opportunity to meet many truly sympathetic, excellent mathematicians from all over the world. In 1991 Deutsche Forschungsgemeinschaft (DFG) installed a research group "Equations of Hydrodynamics" at the University of Bayreuth (members: Professors F. Busse, C. G. Simader, M. Wiegner, W. von Wahl (all Bayreuth) and H. Sohr (Paderborn)) which worked until the spring 1998. This group provided us the financial basis to invite Paolo to Bayreuth and Paderborn, where a fruitful collaboration with Hermann Sohr started too. This was very important since at that time Hermann did (not yet) like to travel.

Now, we can continue to jointly describe our impressions of Paolo. In May 1992, mainly Professors I. Straskraba and R. Salvi organized a meeting on Navier-Stokes equations in the wonderful Villa Monastero in Varenna. This meeting was followed by many other meetings in the castle of Thurnau near Bayreuth (1992), Cento/Italy (1993), Funchal/Madeira (1994), Toulon-Hyeres/France (1995), Pretoria/South Africa (1996) and again in Varenna (1997). It was surely Paolo's influence that both very young mathematicians as well as very experienced mathematicians were included for these scientific gatherings. In addition to an enormous number of very important papers, to Paolo's persistent merit are the two volumes of "An Introduction to the Mathematical Theory of the Navier-Stokes Equations" which was finished in 1992 and appeared in 1994. At that time, these books represented the state of the art in this field. His book is both very precise and readable. Besides, including an excellent preface, there is an introduction to each chapter where the reader is clearly introduced to the aims of the chapter and the underlying ideas. Due to our knowledge, many young people became fascinated by this book for the

Navier-Stokes equations. We are very much indebted to Paolo as a friend and as an outstanding scientist. We wish him (and us too) the chance to celebrate many further birthdays together, such as the 70th, 80th, 90th and. . . .

Bayreuth, Germany Christian G. Simader
Paderborn, Germany Hermann Sohr

Contents

Contributors

Chérif Amrouche Laboratoire de Mathématiques Appliquées, UMR CNRS 5142, Université de Pau et des Pays de l'Adour, IPRA, 64000 Pau, France, cherif.amrouche@univ-pau.fr

Guy Bayada INSA de Lyon, Institut Camille Jordan CNRS UMR 5208 & Lamcos CNRS UMR 5259, Bât. L. de Vinci, F-69621 Villeurbanne, France, guy.bayada@insa-lyon.fr

Josef Bemelmans Institut für Mathematik RWTH-Aachen, Aachen, Germany, bemelmans@instmath.rwth-aachen.de

Luigi C. Berselli Dipartimento di Matematica Applicata "U. Dini," Università di Pisa, I-56127 Pisa, Italy, berselli@dma.unipi.it

Tomáš Bodnár Department of Technical Mathematics, Faculty of Mechanical Engineering, Czech Technical University, 121 35 Prague 2, Czech Republic, bodnar@marian.fsik.cvut.cz

Eric Bonnetier LJK-IMAG, UMR 5523 CNRS, 38041 Grenoble cedex 9, France, Eric.Bonnetier@imag.fr

Didier Bresch LAMA, UMR 5127 CNRS, Université de Savoie, 73217 Le Bourget du Lac cedex, France, Didier.Bresch@univ-savoie.fr

Roberto Camassa Department of Mathematics, University of North Carolina, Chapel Hill, NC 27599, USA, camassa@email.unc.edu

N. Cavallini Research Center "Mathematics for Technology", University of Ferrara, Scientific-Technological Campus, 44100 Ferrara, Italy, nicola.cavallini@unife.it

Alexey Cheskidov Department of Mathematics, University of Chicago, Chicago, IL 60637, USA, acheskid@math.uchicago.edu

Bong Jae Chung Department of Marine Sciences, University of North Carolina, Chapel Hill, NC 27599, USA, bjchung@email.unc.edu

Bong Jae Chung Department of Marine Sciences, University of North Carolina-Chapel Hill, Chapel Hill, NC 27599, USA, bjchung@email.unc.edu

Laurent Chupin INSA de Lyon, Institut Camille Jordan CNRS UMR 5208, F-69621 Villeurbanne, France, laurent.chupin@insa-lyon.fr

Luisa Consiglieri Department of Mathematics and CMAF, Sciences Faculty, University of Lisbon, 1749-016 Lisboa, Portugal, lcconsiglieri@fc.ul.pt

Vincenzo Coscia Department of Mathematics, University of Ferrara, 44100 Ferrara, Italy, cos@unife.it

Hugo Beirão da Veiga Dipartimento di Matematica Applicata "U. Dini" Università di Pisa, 56127-Pisa, Italy, bveiga@dma.unipi.it

Paula de Oliveira CMUC-Department of Mathematics, University of Coimbra, Coimbra, Portugal, poliveir@mat.uc.pt

Hermenegildo B. de Oliveira FCT – Universidade do Algarve, Campus de Gambelas 8005-139 Faro, Portugal, holivei@ualg.pt

Paul Deuring Université Lille Nord de France, F-59000 Lille, France; ULCO, LMPA, F-62228 Calais, France, Paul.Deuring@lmpa.univ-littoral.fr

Michael Durka Department of Mechanical Engineering and Materials Science, University of Pittsburgh, Pittsburgh, PA 15261, USA, mjd4+@pitt.edu

Reinhard Farwig Department of Mathematics, Darmstadt University of Technology, 64283 Darmstadt, Germany, farwig@mathematik.tu-darmstadt.de

José Augusto Ferreira CMUC-Department of Mathematics, University of Coimbra, Coimbra, Portugal, ferreira@mat.uc.pt

Robert Finn Department of Mathematics, Stanford University, Stanford, CA, USA, finn@math.stanford.edu

Franco Flandoli Dipartimento di Matematica Applicata "U. Dini," Università di Pisa, I-56127 Pisa, Italy, flandoli@dma.unipi.it

Susan Friedlander Department of Mathematics, Statistics and Computer Science, University of Illinois, Chicago, IL 60607, USA, susan@math.northwestern.edu

Elfriede Friedmann Department of Applied Mathematics, University Heidelberg, 69120 Heidelberg, Germany, friedmann@iwr.uni-heidelberg.de

Bérénice Grec Ecole Centrale de Lyon, Institut Camille Jordan CNRS UMR 5208, F-69621 Villeurbanne, France, berenice.grec@insa-lyon.fr

Antony A. Hill School of Mathematical Sciences, University of Nottingham, Nottingham, NG7 2RD, UK, antony.hill@nottingham.ac.uk

Philip Howard Department of Statistics, University of North Carolina, Chapel Hill, NC 27599, USA, pdhoward@email.unc.edu

Jaroslav Hron Institute of Mathematics, Charles University, Prague, Czech Republic, hron@karlin.mff.cuni.cz

João Janela Department of Mathematics/ISEG and CEMAT/IST, 1200 Lisboa, Portugal, jjanela@iseg.utl.pt

Daniel D. Joseph University of Minnesota, Minneapolis, MN; University of California, Irvine, CA, USA, joseph@aem.umn.edu

Hideo Kozono Mathematical Institute, Tôhoku University, Sendai, 980-8578 Japan, kozono@math.tohoku.ac.jp

Petr Kučera Department of Mathematics, Faculty of Civil Engineering, Czech Technical University, 16629 Prague 6, Czech Republic, kucera@mat.fsv.cvut.cz

Mads Kyed Institut für Mathematik, RWTH-Aachen, Aachen, Germany, kyed@instmath.rwth-aachen.de

Elena Martín E. T. S. Ingenieros Industriales, Universidad de Vigo, Vigo, Spain, emortega@uvigo.es

Richard McLaughlin Department of Mathematics, University of North Carolina, Chapel Hill, NC 27599, USA, rmm@email.unc.edu

Vuk Milišić LJK-IMAG, UMR 5523 CNRS, 38041 Grenoble cedex 9, France, Vuk.Milisic@imag.fr

Alexandra Moura CEMAT/IST, 1049-001 Lisboa, Portugal, almoura@math.ist.utl.pt

Yuliya V. Namlyeyeva Institute of Applied Mathematics and Mechanics of NAS of Ukraine, 83114 Donetsk, Ukraine, namleeva@iamm.ac.donetsk.ua

Joachim Naumann Mathematical Institute, Humboldt University Berlin, 10099 Berlin, Germany, jnaumann@math.hu-berlin.de

Šarka Nečasová Mathematical Institute of Academy of Sciences, 11567 Prague 1, Czech Republic, matus@math.cas.cz

Jirí Neustupa Mathematical Institute of the Czech Academy of Sciences, 115 67 Praha 1, Czech Republic, neustupa@math.cas.cz

Abderrahim Ouazzi Institute of Applied Mathematics, TU Dortmund, D-44227 Dortmund, Germany, abderrahim.ouazzi@math.uni-dortmund.de

Patrick Penel Département de Mathématique & Laboratoire "Systèmes Navals Complexes", Université du Sud Toulon–Var, 83957 La Garde cedex, France, penel@univ-tln.fr

Julia Portl Interdisciplinary Center for Scientific Computing (IWR), University Heidelberg, 69120 Heidelberg, Germany, julia.portl@iwr.uni-heidelberg.de

Rolf Rannacher Institute of Applied Mathematics, University of Heidelberg, D-69120 Heidelberg, Germany, rannacher@iwr.uni-heidelberg.de

Ulrich Razafison MAPMO, UMR CNRS 6628, Fédération Denis Poisson, bât. Mathématiques, B. P. 6759, Orléans cedex 2, France, ulrich.razafison@math.cnrs.fr

Mudassar Razzaq Institute of Applied Mathematics, TU Dortmund, Germany, mrazzaq@math.uni-dortmund.de

Thomas Richter Institute of Applied Mathematics, University Heidelberg, 69120 Heidelberg, Germany, thomas.richter@iwr.uni-heidelberg.de

Anne M. Robertson Department of Mechanical Engineering and Materials Science, McGowan Institute for Regenerative Medicine, Center for Vascular Remodeling and Regeneration (CVRR); University of Pittsburgh, Pittsburgh, PA 15261, USA, rbertson@pitt.edu

Remigio Russo Dipartimento di Matematica, Seconda Università di Napoli, 81100 Caserta, Italy, remigio.russo@unina2.it

Adélia Sequeira Department of Mathematics and CEMAT, Instituto Superior Técnico, Technical University of Lisbon, 1049-001 Lisbon, Portugal, adelia.sequeira@math.ist.utl.pt

Yoshihiro Shibata Department of Mathematics, Research Institute of Science and Engineering, Waseda University, Tokyo 169-8555, Japan, yshibata@waseda.jp

Roman Shvydkoy Department of Mathematics, Statistics and Computer Science, University of Illinois, Chicago, IL 60607, USA, shvydkoy@math.uic.edu

Christian G. Simader Universität Bayreuth, D-95447 Bayreuth, Germany, Christian.Simader@uni-bayreuth.de

Zdenek Skalák Czech Technical University, 16612 Prague 6, Czech Republic, skalak@mat.fsv.cvut.cz

Igor Igorievich Skrypnik Institute of Applied Mathematics and Mechanics of NAS of Ukraine, 83114 Donetsk, Ukraine, iskrypnik@iamm.donbass.com

Hermann Sohr Faculty of Computer Science, Electrical Engineering and Mathematics, University of Paderborn, 33098 Paderborn, Germany, hsohr@math.uni-paderborn.de

Ivan Straškraba Mathematical Institute, Academy of Sciences of the Czech Republic, 11567 Prague 1, Czech Republic, strask@math.cas.cz

Brian Straughan Department of Mathematical Sciences, Durham University, Durham, DH1 3LE, UK, brian.straughan@durham.ac.uk

Stefan Turek Institute of Applied Mathematics, TU Dortmund, Germany, ture@featflow.de

Ashwin Vaidya Department of Mathematics, University of North Carolina, Chapel Hill, NC 27599, USA, avaidya@email.unc.edu

Werner Varnhorn Fachbereich Mathematik, Universität Kassel, 34109 Kassel, Germany, varnhorn@mathematik.uni-kassel.de

José M. Vega E. T. S. Ingenieros Aeronáuticos, Universidad Politécnica de Madrid, Madrid, Spain, vega@fmetsia.upm.es

Jörg Wolf Mathematical Institute, Humboldt University Berlin, 10099 Berlin, Germany, jwolf@math.hu-berlin.de

Zijing Zeng Department of Mechanical Engineering and Materials Science, University of Pittsburgh, Pittsburgh, PA 15261, USA, ziz3+@pitt.edu

Isotropically and Anisotropically Weighted Sobolev Spaces for the Oseen Equation

Chérif Amrouche and Ulrich Razafison

Abstract This contribution is devoted to the Oseen equations, a linearized form of the Navier-Stokes equations. We give here some results concerning the scalar Oseen operator and we prove Hardy inequalities concerning functions in Sobolev spaces with anisotropic weights that appear in the investigation of the Oseen equations.

Keywords Oseen equations · Anisotropic weights · Hardy inequality · Sobolev weighted spaces

1 Introduction

In an exterior domain Ω of $\mathbb{R}^3$, the Oseen system is obtained by linearizing the Navier-Stokes equations, describing the flow of a viscous fluid past the obstacle $\mathbb{R}^3 \setminus \overline{\Omega}$, around a nonzero constant vector which is the velocity at infinity (see [13]). When $\Omega = \mathbb{R}^3$, the system can be written as follow:

$$\begin{aligned} -\nu\Delta \boldsymbol{u} + k\frac{\partial \boldsymbol{u}}{\partial x_1} + \nabla\pi &= \boldsymbol{f} \ \text{ in } \mathbb{R}^3, \\ \operatorname{div} \boldsymbol{u} &= g \ \text{ in } \mathbb{R}^3, \end{aligned} \tag{1}$$

where we add the condition at infinity

$$\lim_{|\boldsymbol{x}|\to\infty} \boldsymbol{u}(\boldsymbol{x}) = \boldsymbol{u}_\infty. \tag{2}$$

The data are the viscosity of the fluid ν, the external forces acting on the fluid $\boldsymbol{f}$, a function g, a constant vector $\boldsymbol{u}_\infty$ and a real $k > 0$. The unknowns are the velocity of the fluid $\boldsymbol{u}$ and the pressure function π. Let us now notice that the pressure satisfies the Laplace equation

C. Amrouche (✉)
Laboratoire de Mathématiques Appliquées, UMR CNRS 5142, Université de Pau et des Pays de l'Adour, IPRA, 64000 Pau, France
e-mail: cherif.amrouche@univ-pau.fr

R. Rannacher, A. Sequeira (eds.), *Advances in Mathematical Fluid Mechanics*,
DOI 10.1007/978-3-642-04068-9_1,

$$\Delta\pi = \operatorname{div}\boldsymbol{f} + \nu\Delta g - k\frac{\partial g}{\partial x_1}, \tag{3}$$

and each component u_i of the velocity satisfies

$$-\nu\Delta u_i + k\frac{\partial u_i}{\partial x_1} = f_i - \frac{\partial \pi}{\partial x_i}. \tag{4}$$

Hence we see that the Oseen problem (1) is related to the following equation:

$$-\nu\Delta u + k\frac{\partial u}{\partial x_1} = f \text{ in } \mathbb{R}^3. \tag{5}$$

Therefore, the results arising from the analysis of (5) can be used for the investigation of the Oseen problem (1). To prescribe the growth or the decay properties of functions at infinity, we consider here weighted Sobolev spaces where the weight reflects the decay properties of the fundamental solution $\mathcal{O}$ of (5) defined by

$$\mathcal{O}(\boldsymbol{x}) = \frac{1}{4\pi\nu|\boldsymbol{x}|}e^{-k(|\boldsymbol{x}|-x_1)/2\nu}. \tag{6}$$

Note now that, at infinity, $\mathcal{O}$ has the same following decay properties than the fundamental solution of Oseen

$$\mathcal{O}(\boldsymbol{x}) = O(\eta_{-1}^{-1}(\boldsymbol{x})), \quad \nabla\mathcal{O}(\boldsymbol{x}) = O(\eta_{-3/2}^{-3/2}(\boldsymbol{x})), \quad \partial^2\mathcal{O}(\boldsymbol{x}) = O(\eta_{-2}^{-2}(\boldsymbol{x})), \ldots.$$

where $\eta_\beta^\alpha(\boldsymbol{x}) \equiv \eta_\beta^\alpha = (1+|\boldsymbol{x}|)^\alpha(1+|\boldsymbol{x}|-x_1)^\beta$ will be the weight function considered. Equation (5) has been investigated by Farwig (see [6]) in weighted L^2-spaces, with the weight η_β^α.

Furthermore, for $r = |\boldsymbol{x}|$ sufficiently large, we obtain the following anisotropic estimates (see [11]):

$$\begin{aligned} &|\mathcal{O}(\boldsymbol{x})| \le C\,r^{-1}(1+s)^{-2}, \quad \left|\frac{\partial\mathcal{O}}{\partial x_1}(\boldsymbol{x})\right| \le C\,r^{-2}\,(1+s)^{-\frac{3}{2}}, \\ &\left|\frac{\partial\mathcal{O}}{\partial x_j}(\boldsymbol{x})\right| \le C\,r^{-\frac{3}{2}}\,(1+s)^{-\frac{3}{2}}\left(1+\frac{2}{r}\right), \quad j=2,3, \quad \text{if } n=3, \end{aligned} \tag{7}$$

$$\begin{aligned} &|\mathcal{O}(\boldsymbol{x})| \le C\,r^{-\frac{1}{2}}(1+s)^{-1}, \quad \left|\frac{\partial\mathcal{O}}{\partial x_1}(\boldsymbol{x})\right| \le C\,r^{-\frac{3}{2}}\,(1+s)^{-1}, \\ &\left|\frac{\partial\mathcal{O}}{\partial x_2}(\boldsymbol{x})\right| \le C\,r^{-1}\,(1+s)^{-1}, \quad \text{if } n=2. \end{aligned} \tag{8}$$

Note also the following properties:

$$\forall p > 3,\ \ \mathcal{O} \in L^p(\mathbb{R}^3) \quad \text{and} \quad \forall p \in]\frac{3}{2}, 2[,\ \ \nabla\,\mathcal{O} \in \boldsymbol{L}^p(\mathbb{R}^3), \tag{9}$$

$$\forall p \in]2, 3[,\ \ \mathcal{O} \in L^p(\mathbb{R}^3) \quad \text{and} \quad \forall p \in]\frac{4}{3}, \frac{3}{2}[,\ \ \nabla\,\mathcal{O} \in \boldsymbol{L}^p(\mathbb{R}^3), \tag{10}$$

$$\mathcal{O} \in L^1_{\text{loc}}(\mathbb{R}^n) \quad \text{and} \quad \nabla\,\mathcal{O} \in \boldsymbol{L}^1_{\text{loc}}(\mathbb{R}^n), \qquad \text{for } n = 2, 3. \tag{11}$$

Observe that when $\boldsymbol{f} \in \mathcal{D}(\mathbb{R}^3)$, then $u = O * f$ is a solution of (5). We have also $u = \mathcal{F}^{-1}(m_0(\xi)\mathcal{F}f)$, with $m_0(\xi) = (|\xi|^2 + ik\xi_1)^{-1}$ and $\dfrac{\partial u}{\partial x_j} = \mathcal{F}^{-1}(m_1(\xi)\mathcal{F}f)$, with $m_1(\xi) = i\xi_j(|\xi|^2 + ik\xi_1)^{-1}$. Here $\mathcal{F}f$ is the Fourier transform of f.

2 Scalar Oseen Potential in Three Dimensional Space

This section is devoted to the L^p estimates of convolutions with Oseen kernels. Before that, we introduce some basic weighted Sobolev spaces. We first set $\varrho(\boldsymbol{x}) = (1+ \mid \boldsymbol{x} \mid^2)^{\frac{1}{2}}$, $\lg \varrho = \ln(1 + \varrho)$ and we define

$$W_0^{1,p}(\mathbb{R}^3) = \left\{ v \in \mathcal{D}'(\mathbb{R}^3);\ \frac{v}{\omega_1} \in L^p,\ \nabla v \in L^p(\mathbb{R}^3) \right\},$$

with $\omega_1 = \varrho$ if $p \neq 3$, $\omega_1 = \varrho \lg \varrho$ if $p = 3$ and $W_0^{-1,p'}(\mathbb{R}^3) = (W_0^{1,p}(\mathbb{R}^3))'$. We recall that $\mathcal{D}(\mathbb{R}^3)$ is dense in $W_0^{1,p}(\mathbb{R}^3)$ and the constant functions belong to $W_0^{1,p}(\mathbb{R}^3)$ if $p \geq 3$. We now introduce a second family of weighted spaces:

$$\widetilde{W}_0^{1,p}(\mathbb{R}^n) = \left\{ v \in W_0^{1,p}(\mathbb{R}^n),\ \frac{\partial v}{\partial x_1} \in W_0^{-1,p}(\mathbb{R}^n) \right\}$$

and we can prove that

$$\mathcal{D}(\mathbb{R}^n) \text{ is dense in } \widetilde{W}_0^{1,p}(\mathbb{R}^n).$$

Theorem 1 *Let* $f \in L^p(\mathbb{R}^3)$. *Then* $\dfrac{\partial^2 \mathcal{O}}{\partial x_j \partial x_k} * f \in L^p(\mathbb{R}^3)$ *(in the sense of principal value),* $\dfrac{\partial \mathcal{O}}{\partial x_1} * f \in L^p(\mathbb{R}^3)$ *and the following estimate holds*

$$\| \frac{\partial^2 \mathcal{O}}{\partial x_j \partial x_k} * f \|_{L^p(\mathbb{R}^3)} + \| \frac{\partial \mathcal{O}}{\partial x_1} * f \|_{L^p(\mathbb{R}^3)} \leq C \| f \|_{L^p(\mathbb{R}^3)}. \tag{12}$$

Moreover,
(1) if $1 < p < 2$, *then* $O * f \in L^{\frac{2p}{2-p}}(\mathbb{R}^3)$ *and satisfies*

$$\|O * f\|_{L^{\frac{2p}{2-p}}(\mathbb{R}^3)} \leq C\|f\|_{L^p(\mathbb{R}^3)}. \tag{13}$$

(2) If $1 < p < 4$, *then* $\dfrac{\partial \mathcal{O}}{\partial x_j} * f \in L^{\frac{4p}{4-p}}(\mathbb{R}^3)$ *and verifies the estimate*

$$\left\| \frac{\partial \mathcal{O}}{\partial x_j} * f \right\|_{L^{\frac{4p}{4-p}}(\mathbb{R}^3)} \leq C\|f\|_{L^p(\mathbb{R}^3)}. \tag{14}$$

Proof By Fourier's transform, from Eq. (5) we obtain:

$$\mathcal{F}\left(\frac{\partial^2 \mathcal{O}}{\partial x_j \partial x_k} * f\right) = \frac{-\xi_j \xi_k}{\boldsymbol{\xi}^2 + i\xi_1}\mathcal{F}(f).$$

Now, the function $\xi \mapsto m(\xi) = \dfrac{-\xi_j \xi_k}{\boldsymbol{\xi}^2 + i\xi_1}$ is of class $\mathcal{C}^2$ in $\mathbb{R}^3 \setminus \{0\}$ and satisfies for every $\alpha = (\alpha_1, \alpha_2, \alpha_3) \in \mathbb{N}^3$

$$\left| \frac{\partial^{|\alpha|} m}{\partial \boldsymbol{\xi}^\alpha}(\boldsymbol{\xi}) \right| \leq C|\boldsymbol{\xi}|^{-\alpha},$$

where, $|\alpha| = \alpha_1 + \alpha_2 + \alpha_3$ and C is a constant not depending on $\boldsymbol{\xi}$. Then, the linear operator

$$\mathcal{A} : f \mapsto \frac{\partial^2 \mathcal{O}}{\partial x_j \partial x_k} * f(\boldsymbol{x}) = \int_{\mathbb{R}^3} e^{ix\boldsymbol{\xi}} \frac{-\xi_j \xi_k}{\boldsymbol{\xi}^2 + i\xi_1}\mathcal{F}f(\boldsymbol{\xi})\, d\boldsymbol{\xi}$$

is continuous from $L^p(\mathbb{R}^3)$ into $L^p(\mathbb{R}^3)$ (see Stein [15], Theorem 3.2, p. 96). Therefore, $\dfrac{\partial^2 \mathcal{O}}{\partial x_j \partial x_k} * f \in L^p(\mathbb{R}^3)$ and satisfies

$$\|\frac{\partial^2 \mathcal{O}}{\partial x_j \partial x_k} * f\|_{L^p(\mathbb{R}^3)} \leq C\|f\|_{L^p(\mathbb{R}^3)}.$$

We also have

$$\mathcal{F}\left(\frac{\partial \mathcal{O}}{\partial x_1} * f\right) = \frac{i\xi_1}{\boldsymbol{\xi}^2 + i\xi_1}\mathcal{F}(f)$$

and since the function $\boldsymbol{\xi} \mapsto m_1(\boldsymbol{\xi}) = \dfrac{i\xi_1}{\boldsymbol{\xi}^2 + i\xi_1}$ have the same properties than $m(\boldsymbol{\xi})$, it follows that $\dfrac{\partial \mathcal{O}}{\partial x_1} * f \in L^p(\mathbb{R}^3)$ and satisfies the estimate

$$\left\| \frac{\partial \mathcal{O}}{\partial x_1} * f \right\|_{L^p(\mathbb{R}^3)} \leq C \| f \|_{L^p(\mathbb{R}^3)},$$

which proves the first part of the proposition and Estimate (12). Next, to prove inequalities (13) and (14), we adapt the technique used by Stein [15] who studied the convolution of $f \in L^p(\mathbb{R}^n)$ with the kernel $|\boldsymbol{x}|^{\alpha-n}$. Let us decompose the function K as $K_1 + K_\infty$ where,

$$\begin{aligned} &K_1(\boldsymbol{x}) = K(\boldsymbol{x}) \quad \text{if} \ |\boldsymbol{x}| \leq \mu \quad \text{and} \quad K_1(\boldsymbol{x}) = 0 \quad \text{if} \ |\boldsymbol{x}| > \mu, \\ &K_\infty(\boldsymbol{x}) = 0 \qquad\quad \text{if} \ |\boldsymbol{x}| \leq \mu \quad \text{and} \quad K_\infty(\boldsymbol{x}) = K(\boldsymbol{x}) \ \text{if} \ |\boldsymbol{x}| > \mu. \end{aligned} \tag{15}$$

The function K will denote successively $\mathcal{O}$ and $\dfrac{\partial \mathcal{O}}{\partial x_j}$ and μ is a fixed positive constant which need not be specified at this instance. Next, we shall show that the mapping $f \mapsto K * f$ is of *weak-type* (p, q), with $q = \dfrac{2p}{2-p}$ when $K = \mathcal{O}$ and $q = \dfrac{4p}{4-p}$ when $K = \dfrac{\partial \mathcal{O}}{\partial x_j}$, in the sense that:

$$\text{for all } \lambda > 0, \quad \text{mes}\,\{\boldsymbol{x}\,;|(K * f)(\boldsymbol{x})| > \lambda\} \leq \left(C_{p,q} \frac{\| f \|_{L^p(\mathbb{R}^3)}}{\lambda} \right)^q. \tag{16}$$

Since $K * f = K_1 * f + K_\infty * f$, we have now:

$$\text{mes}\,\{\boldsymbol{x}\,;|K * f| > 2\lambda\} \leq \text{mes}\,\{\boldsymbol{x}\,;|K_1 * f| > \lambda\} + \text{mes}\,\{\boldsymbol{x}\,;|K_\infty * f| > \lambda\}. \tag{17}$$

Note that it is enough to prove inequality (16) with $\| f \|_{L^p(\mathbb{R}^3)} = 1$. We have also:

$$\text{mes}\,\{\boldsymbol{x}\,;|(K_1 * f)(\boldsymbol{x})| > \lambda\} \ \leq \ \frac{\| K_1 * f \|^p_{L^p(\mathbb{R}^3)}}{\lambda^p} \ \leq \ \frac{\| K_1 \|^p_{L^1(\mathbb{R}^3)}}{\lambda^p}, \tag{18}$$

and

$$\| K_\infty * f \|_{L^\infty(\mathbb{R}^3)} \leq \ \| K_\infty \|_{L^{p'}(\mathbb{R}^3)}. \tag{19}$$

(1) *Estimate (13)* Observe that $\mathcal{O}_1 \in L^1(\mathbb{R}^3)$ and $\mathcal{O}_\infty \in L^{p'}(\mathbb{R}^3)$ for $1 \leq p < 2$. Then, the integral $\mathcal{O}_1 * f$ converges almost everywhere and $\mathcal{O}_\infty * f$ converges everywhere. Thus, $\mathcal{O} * f$ converges almost everywhere. But

$$\forall \mu > 0, \quad \| \mathcal{O}_1 \|_{L^1(\mathbb{R}^3)} \ \leq \ C\mu. \tag{20}$$

Next, by using (7), we have for any $p' > 2$:

$$\forall \mu > 0, \quad \| \mathcal{O}_\infty \|_{L^{p'}(\mathbb{R}^3)} \leq C\mu^{\frac{2-p'}{p'}}. \tag{21}$$

Choosing now $\lambda = C\mu^{\frac{2-p'}{p'}}$ or equivalently $\mu = C'\lambda^{\frac{p}{p-2}}$. Then from (21) and (19) we have $\|\mathcal{O}_\infty * f\|_{L^\infty(\mathbb{R}^3)} < \lambda$ and so mes$\{\boldsymbol{x}\ ;\ |\mathcal{O}_\infty * f| > \lambda\} = 0$. Finally, for $1 \le p < 2$, we get from inequalities (20), (17) and (18):

$$\text{mes}\,\{\boldsymbol{x} \in \mathbb{R}^3;\ |(O * f)(\boldsymbol{x})| > \lambda\} \ \le\ \left(C_p \frac{1}{\lambda}\right)^{\frac{2p}{2-p}}. \tag{22}$$

Therefore, for $1 \le p < 2$, the operator $R : f \mapsto O * f$ is of *weak-type* $\left(p, \dfrac{2p}{2-p}\right)$.

(2) *Estimate (14)*. Here we take $K = \dfrac{\partial \mathcal{O}}{\partial x_j}$. First, according to (12), $\dfrac{\partial \mathcal{O}}{\partial x_1} * f \in W^{1,p}(\mathbb{R}^3)$ then, by the Sobolev embedding results, we have in particular, $\dfrac{\partial \mathcal{O}}{\partial x_1} * f \in L^{\frac{4p}{4-p}}(\mathbb{R}^3)$. It remains to prove Estimate (14) for $j = 2, 3$. First we have:

$$\left\| \frac{\partial \mathcal{O}}{\partial x_j} \right\|_{L^1(\mathbb{R}^3)} \le c\mu, \ \text{ if } \ \mu \le 1 \ \text{ and } \ \left\| \frac{\partial \mathcal{O}}{\partial x_j} \right\|_{L^1(\mathbb{R}^3)} \le c\mu^{\frac{1}{2}}, \ \text{ if } \ \mu > 1.$$

Furthermore, we have for $p' > \frac{4}{3}$:

$$\int_{|\boldsymbol{x}|>\mu} \left| \frac{\partial \mathcal{O}}{\partial x_j}(\boldsymbol{x}) \right|^{p'} d\boldsymbol{x} \ \le\ C\mu^{4-3p'}, \quad \text{if } \ \mu \le 1,$$

$$\int_{|\boldsymbol{x}|>\mu} \left| \frac{\partial \mathcal{O}}{\partial x_j}(\boldsymbol{x}) \right|^{p'} d\boldsymbol{x} \ \le C\mu^{\frac{4-3p'}{2}}, \quad \text{if } \ \mu > 1.$$

Summarising we obtain:
(a) If $0 < \mu < 1$,

$$\int_{|\boldsymbol{x}|<\mu} \left| \frac{\partial \mathcal{O}}{\partial x_j}(\boldsymbol{x}) \right| d\boldsymbol{x} \ \le c\mu \quad \text{and} \quad \int_{|\boldsymbol{x}|>\mu} \left| \frac{\partial \mathcal{O}}{\partial x_j}(\boldsymbol{x}) \right|^{p'} d\boldsymbol{x} \ \le C\mu^{4-3p'},$$

(b) if $\mu \ge 1$,

$$\int_{|\boldsymbol{x}|<\mu} |\frac{\partial \mathcal{O}}{\partial x_j}(\boldsymbol{x})|\, d\boldsymbol{x} \ \le c\mu^{\frac{1}{2}} \quad \text{and} \quad \int_{|\boldsymbol{x}|>\mu} |\frac{\partial \mathcal{O}}{\partial x_j}(\boldsymbol{x})|^{p'}\, d\boldsymbol{x} \ \le C\mu^{\frac{4-3p'}{2}}.$$

Setting $\lambda = C\mu^{\frac{4-3p'}{p'}}$ in the case (a) or $\lambda = C\mu^{\frac{4-3p'}{2p'}}$ in the case (b), we get in both cases:

$$\text{mes}\,\{\boldsymbol{x} \in \mathbb{R}^3;\ |K * f(\boldsymbol{x})| > \lambda\} \ \le\ \left(C_p \frac{1}{\lambda}\right)^{\frac{4p}{4-p}}. \tag{23}$$

Thus, for $1 \leq p < 4$, the operator $R_j : f \mapsto \dfrac{\partial \mathcal{O}}{\partial x_j} * f$ is of *weak-type* $\left(p, \dfrac{4p}{4-p}\right)$. Applying now the Marcinkiewicz interpolation's theorem, we deduce that, for $1 < p < 2$, the linear operator R is continuous from $L^p(\mathbb{R}^3)$ into $L^{\frac{2p}{2-p}}(\mathbb{R}^3)$ and for $1 < p < 4$, R_j is continuous from $L^p(\mathbb{R}^3)$ into $L^{\frac{4p}{4-p}}(\mathbb{R}^3)$. $\square$

Remark 1 Another proof of Theorem 1 consists in using Fourier's approach. Let $(f_j)_{j\in\mathbb{N}} \subset \mathcal{D}(\mathbb{R}^3)$ be a sequence which converges to $f \in L^p(\mathbb{R}^3)$. Then the sequence $(u_j)_{j\in\mathbb{N}}$ given by:

$$u_j = \mathcal{F}^{-1}(m_0(\boldsymbol{\xi})\mathcal{F} f_j), \quad m_0(\boldsymbol{\xi}) = (|\boldsymbol{\xi}|^2 + i\xi_1)^{-1}, \tag{24}$$

satisfies the equation $-\Delta u_j + \frac{\partial u_j}{\partial x_1} = f_j$. Let us recall now the (see [15]):

Lizorkin Theorem *Let $D = \{\boldsymbol{\xi} \in \mathbb{R}^3;\ |\boldsymbol{\xi}| > 0\}$ and $m : D \longrightarrow \mathbb{C}$, a continuous function such that its derivatives $\dfrac{\partial^k m}{\partial \xi_1^{k_1} \partial \xi_2^{k_2} \partial \xi_3^{k_3}}$ are continuous and verify*

$$|\xi_1|^{k_1+\beta}\, |\xi_2|^{k_2+\beta}\, |\xi_3|^{k_3+\beta} \left| \frac{\partial^k m}{\partial \xi_1^{k_1} \partial \xi_2^{k_2} \partial \xi_3^{k_3}} \right| \leq M, \tag{25}$$

where $k_1, k_2, k_3 \in \{0, 1\}$, $k = k_1 + k_2 + k_3$ and $0 \leq \beta < 1$. Then, the operator

$$\mathcal{A} : g \longmapsto \mathcal{F}^{-1}(m_0\, \mathcal{F} g),$$

is continuous from $L^p(\mathbb{R}^3)$ into $L^r(\mathbb{R}^3)$ with $\frac{1}{r} = \frac{1}{p} - \beta$.

Applying this continuity property with $f_j \in L^p(\mathbb{R}^3)$ and $\beta = \frac{1}{2}$, we show that (u_j) is bounded in $L^{\frac{2p}{2-p}}(\mathbb{R}^3)$ if $1 < p < 2$. Thus, this sequence has a subsequence still denoted by (u_j) which converges weakly to u and which satisfies $Tu = f$. For the derivative of u_j with respect to x_1, the corresponding multiplier is of the form $m(\boldsymbol{\xi}) = i\xi_1(|\boldsymbol{\xi}|^2 + i\xi_1)^{-1}$. It follows that (25) is satisfied for $\beta = 0$ and $\dfrac{\partial u}{\partial x_1} \in L^p(\mathbb{R}^3)$. The same property takes place for the derivatives of second order with $m(\boldsymbol{\xi}) = \xi_k \xi_l (|\boldsymbol{\xi}|^2 + i\xi_1)^{-1}$. Finally, we verify with $\beta = \frac{1}{4}$, that the derivative of (u_j) with respect to x_k is bounded in $L^{\frac{4p}{4-p}}(\mathbb{R}^3)$, which implies $\dfrac{\partial u}{\partial x_k} \in L^{\frac{4p}{4-p}}(\mathbb{R}^3)$. $\square$

Theorem 1 states that $\frac{\partial^2 \mathcal{O}}{\partial x_j \partial x_k} * f \in L^p(\mathbb{R}^3)$ and under some conditions on p, $\frac{\partial \mathcal{O}}{\partial x_j} * f \in L^{\frac{4p}{4-p}}(\mathbb{R}^3)$ and $O * f \in L^{\frac{2p}{2-p}}(\mathbb{R}^3)$. Now, using these results and the classical Sobolev embedding results, we have the following (see also [3]–[5]):

Theorem 2 *Let $f \in L^p(\mathbb{R}^3)$.*

(1) Assume that $1 < p < 4$. Then $\nabla \mathcal{O} * f \in \boldsymbol{L}^{\frac{4p}{4-p}}(\mathbb{R}^3)$ with the estimate (14). Moreover,

(i) if $1 < p < 3$*, then* $\nabla\mathcal{O} * f \in \boldsymbol{L}^{\frac{3p}{3-p}}(\mathbb{R}^3)$ *with the estimate*

$$\|\nabla\mathcal{O} * f\|_{\boldsymbol{L}^{\frac{3p}{3-p}}(\mathbb{R}^3)} \leq C\|f\|_{L^p(\mathbb{R}^3)}. \tag{26}$$

(ii) If $p = 3$*, then* $\nabla\mathcal{O} * f \in \boldsymbol{L}^r(\mathbb{R}^3)$ *for any* $r \geq 12$ *and satisfies*

$$\|\nabla\mathcal{O} * f\|_{\boldsymbol{L}^r(\mathbb{R}^3)} \leq C\|f\|_{L^p(\mathbb{R}^3)}. \tag{27}$$

(iii) If $3 < p < 4$*, then* $\nabla\mathcal{O} * f \in \boldsymbol{L}^\infty(\mathbb{R}^3)$ *and verifies the estimate*

$$\|\nabla\mathcal{O} * f\|_{\boldsymbol{L}^\infty(\mathbb{R}^3)} \leq C\|f\|_{L^p(\mathbb{R}^3)}. \tag{28}$$

(2) Assume that $1 < p < 2$*. Then* $O * f \in L^{\frac{2p}{2-p}}(\mathbb{R}^3)$ *with the estimate (13). Moreover,*
(i) if $1 < p < \frac{3}{2}$*, then* $O * f \in L^{\frac{3p}{3-2p}}(\mathbb{R}^3)$ *and satisfies*

$$\|O * f\|_{L^{\frac{3p}{3-2p}}(\mathbb{R}^3)} \leq C\|f\|_{L^p(\mathbb{R}^3)}. \tag{29}$$

(ii) If $p = \frac{3}{2}$*, then* $O * f \in L^r(\mathbb{R}^3)$ *for any* $r \geq 6$ *and*

$$\|O * f\|_{L^r(\mathbb{R}^3)} \leq C\|f\|_{L^p(\mathbb{R}^3)}. \tag{30}$$

(iii) If $\frac{3}{2} < p < 2$*, then* $O * f \in L^\infty(\mathbb{R}^3)$ *and the following estimate holds*

$$\|O * f\|_{L^\infty(\mathbb{R}^3)} \leq C\|f\|_{L^p(\mathbb{R}^3)}. \tag{31}$$

Proof (1) If $1 < p < 4$, the previous theorem asserts that $\frac{\partial\mathcal{O}}{\partial x_j} * f \in L^{\frac{4p}{4-p}}(\mathbb{R}^3)$ and $\frac{\partial^2\mathcal{O}}{\partial x_j \partial x_k} * f \in L^p(\mathbb{R}^3)$. If $1 < p < 3$, there exists a unique constant $k(f) \in \mathbb{R}$ such that $v = \frac{\partial\mathcal{O}}{\partial x_j} * f + k(f) \in W_0^{1,p}(\mathbb{R}^3)$. Then $k(f) = v - \frac{\partial\mathcal{O}}{\partial x_j} * f \in W_0^{1,p}(\mathbb{R}^3) + L^{\frac{4p}{4-p}}(\mathbb{R}^3)$. As none of both spaces contains constants then $k(f) = 0$, which implies that $\frac{\partial\mathcal{O}}{\partial x_j} * f \in W_0^{1,p}(\mathbb{R}^3)$. Now, the Sobolev embedding results yield $\frac{\partial\mathcal{O}}{\partial x_j} * f \in L^{\frac{3p}{3-p}}(\mathbb{R}^3)$ and Estimate (26). If $p \geq 3$, again by the previous theorem, we have $\frac{\partial\mathcal{O}}{\partial x_j} * f \in W_0^{1,p}(\mathbb{R}^3)$. Then $\frac{\partial\mathcal{O}}{\partial x_j} * f \in BMO(\mathbb{R}^3)$ if $p = 3$. Applying now the interpolation theorem between $BMO(\mathbb{R}^3)$ and $L^p(\mathbb{R}^3)$, we get $\frac{\partial\mathcal{O}}{\partial x_j} * f \in L^r(\mathbb{R}^3)$ for any $r \geq 12$. By Sobolev embedding results, if $3 < p < 4$, we have $\frac{\partial\mathcal{O}}{\partial x_j} * f \in L^\infty(\mathbb{R}^3)$, and the case (1) is proved.
(2) By the previous theorem, if $1 < p < 2$, we have $O * f \in L^{\frac{2p}{2-p}}(\mathbb{R}^3)$ and $\nabla\mathcal{O} * f \in \boldsymbol{L}^{\frac{3p}{3-p}}(\mathbb{R}^3)$. Now by Sobolev embedding results, $O * f \in L^{p^*}(\mathbb{R}^3)$, where $\frac{1}{p^*} = \frac{3-p}{3p} - \frac{1}{3} = \frac{1}{p} - \frac{2}{3}$ if $1 < p < \frac{3}{2}$, which yields (26). For the remainder of the

proof, we use the same arguments that in the previous case with $O * f$ instead of $\frac{\partial \mathcal{O}}{\partial x_j} * f$ and $\frac{\partial \mathcal{O}}{\partial x_j} * f$ instead of $\frac{\partial^2 \mathcal{O}}{\partial x_j \partial x_k} * f$. □

Remark 2 In Farwig and Sohr [7], Theorem 2.3 proves existence of solutions to the Oseen equations with forces in L^p, thanks to the Lizorkin theorem's. These solutions, which are not explicit, belong to homogeneous Sobolev spaces. Here, in Theorem 1, we prove some continuity properties for the Oseen potential, without using Lizorkin theorem's, and in Theorem 2, we complete those properties, thanks to Sobolev embeddings and we find the same results as the ones given in [7].

Remark 3 (i) We can also have the result given by Theorem 2, by showing that $\mathcal{O} \in L^{2,\infty}(\mathbb{R}^3)$, i.e.

$$\sup_{\mu>0} \mu^2 \operatorname{mes}\{\boldsymbol{x} \in \mathbb{R}^3;\ \mathcal{O}(\boldsymbol{x}) > \mu\} < +\infty. \tag{32}$$

So that, for any $1 < q < 2$, according to weak Young inequality (cf. [14], Chap. IX.4), we obtain:

$$\|O * f\|_{L^{\frac{2q}{2-q},\infty}(\mathbb{R}^3)} \leq C\|\mathcal{O}\|_{L^{2,\infty}(\mathbb{R}^3)}\|f\|_{L^q(\mathbb{R}^3)}. \tag{33}$$

Let now $p \in]1, 2[$. There exist p_0 and p_1 such that $1 < p_0 < p < p_1 < 2$ and such that the operator $R : f \longmapsto O * f$ is continuous from $L^{p_0}(\mathbb{R}^3)$ into $L^{\frac{2p_0}{2-p_0},\infty}(\mathbb{R}^3)$ and from $L^{p_1}(\mathbb{R}^3)$ into $L^{\frac{2p_1}{2-p_1},\infty}(\mathbb{R}^3)$. The Marcinkiewicz theorem allows again to conclude that the operator R is continuous from $L^p(\mathbb{R}^3)$ into $L^{\frac{2p}{2-p}}(\mathbb{R}^3)$
(ii) The same remark remains valid for $\nabla \mathcal{O}$ that belongs to $\boldsymbol{L}^{\frac{4}{3},\infty}(\mathbb{R}^3)$. □

Using the Young inequality with the relations (10) and (11), we get the following result:

Proposition 1 *Let $f \in L^1(\mathbb{R}^3)$. Then*
(1) $O * f \in L^p(\mathbb{R}^3)$ for any $p \in]2, 3[$ and satisfies the estimate

$$\|O * f\|_{L^p(\mathbb{R}^3)} \leq C\|f\|_{L^1(\mathbb{R}^3)}, \tag{34}$$

(2) $\nabla\mathcal{O} * f \in \boldsymbol{L}^p(\mathbb{R}^3)$ for any $p \in]\frac{4}{3}, \frac{3}{2}[$ and the following estimate holds

$$\|\nabla\mathcal{O} * f\|_{\boldsymbol{L}^p(\mathbb{R}^3)} \leq C\|f\|_{L^1(\mathbb{R}^3)}. \tag{35}$$

Remark 4 Taking "formally" $p = 1$ in Theorem 2, we find that $O * f \in L^q(\mathbb{R}^3)$ for any $q \in]2, 3[$ and $\nabla\mathcal{O} * f \in L^q(\mathbb{R}^3)$ for any $q \in]\frac{4}{3}, \frac{3}{2}[$. We notice that they are the same results obtained in Theorem 1 by using the Young inequality.

Now, we are going to study the Oseen potential $O * f$ when f belongs to $W_0^{-1,p}(\mathbb{R}^3)$. For that purpose, we give the following definition of the convolution of f with the fundamental solution $\mathcal{O}$:

$$\forall \varphi \in \partial(\mathbb{R}^3), \quad \langle O * f, \varphi \rangle =: \langle f, \check{\mathcal{O}} * \varphi \rangle_{W_0^{-1,p}(\mathbb{R}^3) \times W_0^{1,p'}(\mathbb{R}^3)}, \tag{36}$$

where $\check{\mathcal{O}}(\boldsymbol{x}) = \mathcal{O}(-\boldsymbol{x})$. With the L^∞ weighted estimates obtained in [11] (Theorems 3.1 and 3.2), we get an estimate on the convolution of $\check{\mathcal{O}}$ with a function $\varphi \in \mathcal{D}(\mathbb{R}^3)$ which we shall use afterward as follow

Lemma 1 *For any $\varphi \in \mathcal{D}(\mathbb{R}^3)$ we have the estimates*

$$|\check{\mathcal{O}} * \varphi(\boldsymbol{x})| \le C_\varphi \frac{1}{|\boldsymbol{x}|(1 + |\boldsymbol{x}| + x_1)}, \tag{37}$$

$$|\nabla \check{\mathcal{O}} * \varphi(\boldsymbol{x})| \le C_\varphi \frac{1}{|\boldsymbol{x}|^{\frac{3}{2}}(1 + |\boldsymbol{x}| + x_1)^{\frac{3}{2}}}, \tag{38}$$

where C_φ depends on the support of φ.

Remark 5 (1) The behaviour on $|\boldsymbol{x}|$ of $\check{\mathcal{O}} * \varphi$ and its first derivatives is the same that of $\check{\mathcal{O}}$, but the behaviour on $1 + s'$ is slightly different (see (7)).
(2) From Estimates (37) and (38) we find that

$$\forall q > \frac{4}{3}, \quad \check{\mathcal{O}} * \varphi \in W_0^{1,q}(\mathbb{R}^3). \tag{39}$$

(3) In (37) and (38), when φ tends to zero in $\mathcal{D}(\mathbb{R}^3)$, then C_φ tends to zero in $\mathbb{R}$.

The next theorem studies the continuity of the operators R and R_j when f belongs to $W_0^{-1,p}(\mathbb{R}^3)$ (see also [1] and [3]–[5]).

Theorem 3 *Assume that $1 < p < 4$ and let $f \in W_0^{-1,p}(\mathbb{R}^3)$ satisfying the compatibility condition*

$$\langle f, 1 \rangle_{W_0^{-1,p}(\mathbb{R}^3) \times W_0^{1,p'}(\mathbb{R}^3)} = 0, \quad \text{when } 1 < p \le \frac{3}{2}. \tag{40}$$

Then $O * f \in L^{\frac{4p}{4-p}}(\mathbb{R}^3)$ and $\nabla \mathcal{O} * f \in \boldsymbol{L}^p(\mathbb{R}^3)$ with the following estimate

$$\|O * f\|_{L^{\frac{4p}{4-p}}(\mathbb{R}^3)} + \|\nabla \mathcal{O} * f\|_{\boldsymbol{L}^p(\mathbb{R}^3)} \le C \|f\|_{W_0^{-1,p}(\mathbb{R}^3)}. \tag{41}$$

Moreover,
(i) if $1 < p < 3$, then $O * f \in L^{\frac{3p}{3-p}}(\mathbb{R}^3)$ and the following estimate holds

$$\|O * f\|_{L^{\frac{3p}{3-p}}(\mathbb{R}^3)} \le C \|f\|_{W_0^{-1,p}(\mathbb{R}^3)}. \tag{42}$$

(ii) If $p = 3$, then $O * f \in L^r(\mathbb{R}^3)$ for any $r \ge 12$ and satisfies

$$\|O * f\|_{L^r(\mathbb{R}^3)} \le C \|f\|_{W_0^{-1,p}(\mathbb{R}^3)}. \tag{43}$$

(iii) If $3 < p < 4$*, then* $O * f \in L^{\infty}(\mathbb{R}^3)$ *and we have the estimate*

$$\|O * f\|_{L^{\infty}(\mathbb{R}^3)} \leq C\|f\|_{W_0^{-1,p}(\mathbb{R}^3)}. \tag{44}$$

Proof Let $1 < p < 4$. By Lemma 1 and Remark 5 point (3), if $\varphi \to 0$ in $\mathcal{D}(\mathbb{R}^3)$, then $C_\varphi \to 0$ where C_φ is defined by (37). Thus, $\check{\mathcal{O}} * \varphi \to 0$ in $W_0^{1,p'}(\mathbb{R}^3)$ for all $p \in]1, 4[$, which implies that $O * f \in \mathcal{D}'(\mathbb{R}^3)$. Next, there exists $\Phi \in \boldsymbol{L}^p(\mathbb{R}^3)$ such that

$$f = \operatorname{div} \Phi \quad \text{and} \quad \|\Phi\|_{\boldsymbol{L}^p(\mathbb{R}^3)} \leq C\|f\|_{W_0^{-1,p}(\mathbb{R}^3)}. \tag{45}$$

According to (12), we have for any $\varphi \in \mathcal{D}(\mathbb{R}^3)$,

$$\left| \left\langle \frac{\partial \mathcal{O}}{\partial x_j} * f, \varphi \right\rangle_{\mathcal{D}'(\mathbb{R}^3)\times\mathcal{D}(\mathbb{R}^3)} \right| = \left| \left\langle \Phi, \nabla \frac{\partial}{\partial x_j} \check{\mathcal{O}} * \varphi \right\rangle_{\boldsymbol{L}^p(\mathbb{R}^3)\times\boldsymbol{L}^{p'}(\mathbb{R}^3)} \right|$$
$$\leq C\|f\|_{W_0^{-1,p}(\mathbb{R}^3)}\|\varphi\|_{L^{p'}(\mathbb{R}^3)}.$$

Then we deduce the second part of (41). We also have for all $\varphi \in \mathcal{D}(\mathbb{R}^3)$:

$$\langle O * f, \varphi\rangle_{\mathcal{D}'(\mathbb{R}^3)\times\mathcal{D}(\mathbb{R}^3)} = -\langle \Phi, \nabla \check{\mathcal{O}} * \varphi\rangle_{\boldsymbol{L}^p(\mathbb{R}^3)\times\boldsymbol{L}^{p'}(\mathbb{R}^3)},$$

and by (14):

$$|\langle O * f, \varphi\rangle_{\mathcal{D}'(\mathbb{R}^3)\times\mathcal{D}(\mathbb{R}^3)}| \leq C\|f\|_{W_0^{-1,p}(\mathbb{R}^3)}\|\varphi\|_{L^{\frac{4p}{5p-4}}(\mathbb{R}^3)}.$$

Note that $1 < p < 4 \iff 1 < \frac{4p}{5p-4} < 4$. Consequently, we have the first part of (41). Moreover, by Sobolev embeddings, $O * f \in L^{\frac{3p}{3-p}}(\mathbb{R}^3)$ if $1 < p < 3$, $O * f$ belongs to $L^r(\mathbb{R}^3)$ for all $r \geq 12$ if $p = 3$ and belongs to $L^{\infty}(\mathbb{R}^3)$ if $3 < p < 4$. Thus, we showed that if $1 < p < 4$, the operators R and R_j are continuous. □

Corollary 1 *Assume that* $1 < p < 4$*. If* u *is a distribution such that* $\nabla u \in \boldsymbol{L}^p(\mathbb{R}^3)$ *and* $\frac{\partial u}{\partial x_1} \in W_0^{-1,p}(\mathbb{R}^3)$*, then there exists a unique constant* $k(u)$ *such that* $u + k(u) \in L^{\frac{4p}{4-p}}(\mathbb{R}^3)$ *and*

$$\| u + k(u) \|_{L^{\frac{4p}{4-p}}(\mathbb{R}^3)} \leq C(\| \nabla u \|_{\boldsymbol{L}^p(\mathbb{R}^3)} + \| \frac{\partial u}{\partial x_1} \|_{W_0^{-1,p}(\mathbb{R}^3)}). \tag{46}$$

Moreover, if $1 < p < 3$*, then* $u + k(u) \in L^{\frac{3p}{3-p}}(\mathbb{R}^3)$*, where* $k(u)$ *is defined by:*

$$k(u) = -\lim_{|\boldsymbol{x}|\to\infty} \frac{1}{\omega_3} \int_{S_2} u(\sigma|\boldsymbol{x}|)\, d\sigma, \tag{47}$$

where, ω_3 denotes the area of the sphere S_2 and u tends to the constant $-k(u)$ as $\boldsymbol{x}$ tends to infinity in the following sense:

$$\lim_{|\boldsymbol{x}|\to\infty}\int_{S_2}|u(\sigma|\boldsymbol{x}|)+k(u)|\,d\sigma=0. \tag{48}$$

If $p=3$, then $u+k(u)$ belongs to $L^r(\mathbb{R}^3)$ for any $r\geq 12$. If $3<p<4$, then u belongs to $L^\infty(\mathbb{R}^3)$, is continuous in $\mathbb{R}^3$ and tends to $-k(u)$ pointwise.

Proof We set $g=-\Delta u+\frac{\partial u}{\partial x_1}\in W_0^{-1,p}(\mathbb{R}^3)$. Since $\mathcal{P}_{[1-\frac{3}{p'}]}$ contains at most constants and according to the density of $\partial(\mathbb{R}^3)$ in $\widetilde{W}_0^{1,p}(\mathbb{R}^3)$, then g satisfies the compatibility condition (40). By the previous theorem, there exists a unique $v=\mathcal{O}*g\in L^{\frac{4p}{4-p}}(\mathbb{R}^3)$ such that $\nabla v\in L^p(\mathbb{R}^3)$ and $\frac{\partial v}{\partial x_1}\in L^p(\mathbb{R}^3)$, satisfying $T(u-v)=0$, where T is the Oseen operator, with the estimate:

$$\|\, v\,\|_{L^{\frac{4p}{4-p}}(\mathbb{R}^3)}\leq C(\|\,\nabla u\,\|_{\boldsymbol{L}^p(\mathbb{R}^3)}+\|\,\frac{\partial u}{\partial x_1}\,\|_{W_0^{-1,p}(\mathbb{R}^3)}). \tag{49}$$

Setting $w=u-v$, we have for all $i=1,2,3$, $\frac{\partial w}{\partial x_i}\in L^p(\mathbb{R}^3)$ and satisfies $T(\frac{\partial w}{\partial x_i})=0$. Then by an uniqueness argument, we deduce that $\nabla u=\nabla v$ and consequently there exists a unique constant $k(u)$, defined by (47), such that $u+k(u)=v$. The last properties are consequences of Sobolev embeddings. □

Remark 6 Let $u\in\mathcal{D}'(\mathbb{R}^3)$ such that $\nabla u\in\boldsymbol{L}^p(\mathbb{R}^3)$.
(i) If $1<p<3$, we know that there exists a unique constant $k(u)$ such that $u+k(u)\in L^{\frac{3p}{3-p}}(\mathbb{R}^3)$. Here, the fact that in addition $\frac{\partial u}{\partial x_1}\in W_0^{-1,p}(\mathbb{R}^3)$ we also have $u+k(u)\in L^{\frac{4p}{4-p}}(\mathbb{R}^3)$, with $\frac{4p}{4-p}<\frac{3p}{3-p}$.
(ii) If $3\leq p<4$, for any constant k, $u+k$ belongs only to $W_0^{1,p}(\mathbb{R}^3)$ but not to the space $L^r(\mathbb{R}^3)$. But, if moreover $\frac{\partial u}{\partial x_1}\in W_0^{-1,p}(\mathbb{R}^3)$ then, $u+k(u)\in L^{\frac{4p}{4-p}}(\mathbb{R}^3)$ for some unique constant $k(u)$. Moreover $u+k(u)\in L^r(\mathbb{R}^3)$ for any $r\geq\frac{4p}{4-p}$ and $u\in L^\infty(\mathbb{R}^3)$ if $p>3$.

3 Weighted Hardy Inequalities

In this section, our aim is to give some weighted anisotropic Hardy inequalities in $\mathbb{R}^n$ with $n\geq 2$.
For $\alpha,\beta\in\mathbb{R}$, we consider the anisotropic weight functions

$$\eta_\beta^\alpha=(1+r)^\alpha(1+s)^\beta,$$

with

$$s=s(\boldsymbol{x})=r-x_1.$$

We define the weighted space

$$L^p_{\alpha,\beta}(\mathbb{R}^n) = \{v \in \mathcal{D}'(\mathbb{R}^n), \quad \eta^\alpha_\beta v \in L^p(\mathbb{R}^n)\},$$

which is a Banach space for its natural norm given by

$$\|v\|_{L^p_{\alpha,\beta}(\mathbb{R}^n)} = \|\eta^\alpha_\beta v\|_{L^p(\mathbb{R}^n)}.$$

We introduce the first family of weighted Sobolev spaces,

$$\begin{aligned}
W^{1,p}_{\alpha,\beta}(\mathbb{R}^3) &= \left\{v \in L^p_{\alpha-\frac{1}{2},\beta}(\mathbb{R}^n), \nabla v \in \lambda^p_{\alpha,\beta}(\mathbb{R}^n)\right\},\\
X^{1,p}_{\alpha,\beta}(\mathbb{R}^3) &= \left\{v \in L^p_{\alpha-\frac{1}{2},\beta-\frac{1}{2}}(\mathbb{R}^n), \nabla v \in \lambda^p_{\alpha,\beta}(\mathbb{R}^n)\right\},\\
Y^{1,p}_{\alpha,\beta}(\mathbb{R}^3) &= \left\{v \in L^p_{\alpha-1,\beta}(\mathbb{R}^n), \nabla v \in \lambda^p_{\alpha,\beta}(\mathbb{R}^n)\right\}.
\end{aligned}$$

These are Banach spaces for their natural norms. Observe that

$$W^{1,p}_{\alpha,\beta}(\mathbb{R}^3) \subset X^{1,p}_{\alpha,\beta}(\mathbb{R}^3) \subset Y^{1,p}_{\alpha,\beta}(\mathbb{R}^3).$$

All the local properties of the spaces $W^{1,p}_{\alpha,\beta}(\mathbb{R}^3)$, $X^{1,p}_{\alpha,\beta}(\mathbb{R}^3)$ and $Y^{1,p}_{\alpha,\beta}(\mathbb{R}^3)$ coincide with those of classical Sobolev spaces $W^{1,p}(\mathbb{R}^n)$. Moreover, we have the following properties:

Proposition 2 *The space $\mathcal{D}(\mathbb{R}^n)$ is dense in $W^{1,p}_{\alpha,\beta}(\mathbb{R}^3)$ (resp. in $X^{1,p}_{\alpha,\beta}(\mathbb{R}^3)$ and in $Y^{1,p}_{\alpha,\beta}(\mathbb{R}^3)$).*

Proof It relies on a truncation procedure. Let $u \in W^{1,p}_{\alpha,\beta}(\mathbb{R}^3)$, $\varphi \in \mathcal{D}(\mathbb{R}^n)$, with $0 \le \varphi(\boldsymbol{x}) \le 1$, $\varphi(\boldsymbol{x}) = 1$ if $r \le 1$, $\varphi(\boldsymbol{x}) = 0$ if $r \ge 2$, and set $\varphi_k(\boldsymbol{x}) = \varphi(\boldsymbol{x}/k)$, $u_k = u\varphi_k$. We have

$$\begin{aligned}
\|u_k - u\|^p_{W^{1,p}_{\alpha,\beta}(\mathbb{R}^3)} &= \|u_k - u\|^p_{L^p_{\alpha-\frac{1}{2},\beta}(\mathbb{R}^n)} + \|\nabla(u_k - u)\|^p_{L^p_{\alpha,\beta}(\mathbb{R}^n)}\\
&\le \|(\varphi_k - 1)u\|^p_{L^p_{\alpha-\frac{1}{2},\beta}(\mathbb{R}^n)} + C\|(\varphi_k - 1)\nabla u\|^p_{L^p_{\alpha,\beta}(\mathbb{R}^n)}\\
&+ C\|u\nabla\varphi_k\|^p_{L^p_{\alpha,\beta}(\mathbb{R}^n)},
\end{aligned} \tag{50}$$

where C is a positive real. Since $u \in W^{1,p}_{\alpha,\beta}(\mathbb{R}^3)$, it is clear that the first two terms of the right hand side of (50) tend to zero, when k tends to ∞. Now, the last term of (50) can be written,

$$\|u\nabla\varphi_k\|^p_{L^p_{\alpha,\beta}(\mathbb{R}^n)} = \int_{\{k\le r\le 2k\}} \eta^{\alpha p}_{\beta p}|u\nabla\varphi_k|^p d\boldsymbol{x}$$

and, since $|\nabla\varphi_k(\boldsymbol{x})| \leq \dfrac{1}{k}|\nabla\varphi(\boldsymbol{x}/k)|$, we arrive at

$$\|u\nabla\varphi_k\|^p_{L^p_{\alpha,\beta}(\mathbb{R}^n)} \leq C\int_{\{k\leq r\leq 2k\}} \eta_{\beta p}^{(\alpha-1)p}|u|^p d\boldsymbol{x}.$$

Recalling that $u \in W^{1,p}_{\alpha,\beta}(\mathbb{R}^3)$, this last quantity tends to zero as k tends to ∞. Then, since each u_k has a compact support and the topologies of $W^{1,p}_{\alpha,\beta}(\mathbb{R}^3)$ and $W^{1,p}(\mathbb{R}^n)$ coincide on this support, the statement of the proposition follows from the density of $\mathcal{D}(\mathbb{R}^n)$ in $W^{1,p}(\mathbb{R}^n)$. The proof is the same for the two other spaces. □

The previous proposition implies that the dual spaces respectively denoted $W^{-1,p'}_{-\alpha,-\beta}(\mathbb{R}^n)$, $X^{-1,p'}_{-\alpha,-\beta}(\mathbb{R}^n)$, $Y^{-1,p'}_{-\alpha,-\beta}(\mathbb{R}^n)$ are subspaces of $\mathcal{D}'(\mathbb{R}^n)$. Let ϱ be the weight function $\varrho = 1 + r = \eta_0^1$ and $\lg r = \ln(1+\varrho)$. For $\alpha \in \mathbb{R}$, we recall the following weighted Sobolev spaces

$$W^{0,p}_\alpha(\mathbb{R}^n) = \{u \in \mathcal{S}'(\mathbb{R}^n),\, \varrho^\alpha u \in L^p(\mathbb{R}^n)\} = L^p_{\alpha,0}(\mathbb{R}^n), \tag{51}$$

$$W^{1,p}_\alpha(\mathbb{R}^n) = \{u \in W^{0,p}_{\alpha-1}(\mathbb{R}^n),\, \nabla u \in \mathbf{W}^{0,p}_\alpha(\mathbb{R}^n)\},\ \text{if } \frac{n}{p}+\alpha \neq 1, \tag{52}$$

$$W^{1,p}_\alpha(\mathbb{R}^n) = \{(\lg r)^{-1}u \in W^{0,p}_{\alpha-1}(\mathbb{R}^n),\, \nabla u \in \mathbf{W}^{0,p}_\alpha(\mathbb{R}^n)\},\ \text{if } \frac{n}{p}+\alpha = 1. \tag{53}$$

We have the following identity:

$$W^{1,p}_\alpha(\mathbb{R}^n) = Y^{1,p}_{\alpha,0}(\mathbb{R}^n) \quad \text{if} \quad \frac{n}{p}+\alpha \neq 1.$$

We will now prove some one-dimensional inequalities.

Lemma 2 *Let* $\gamma \in \mathbb{R}$ *satisfy* $\gamma + \dfrac{n-1}{2} > 0$ *and* $\theta^* \in]0,\pi/2[$. *Then for any positive measurable function* f *defined on* $]0,\theta^*[$, *such that*

$$\int_0^{\theta^*}(1-\cos\theta)^{\gamma+\frac{p}{2}}(\sin\theta)^{n-2}[f(\theta)]^p d\theta < +\infty,$$

one has

$$\int_0^{\theta^*}(1-\cos\theta)^{\gamma}(\sin\theta)^{n-2}[F(\theta)]^p d\theta \leq C\int_0^{\theta^*}(1-\cos\theta)^{\gamma+\frac{p}{2}}(\sin\theta)^{n-2}[f(\theta)]^p d\theta, \tag{54}$$

with

$$F(\theta) = \int_\theta^{\theta^*} f(t)dt. \tag{55}$$

Proof Let us first notice that on $]-\frac{\pi}{2}, \frac{\pi}{2}[$, the following inequality holds

$$\frac{1}{2}\sin^2\theta \leq 1-\cos\theta \leq \sin^2\theta. \tag{56}$$

We now set

$$J = \int_0^{\theta^*} (1-\cos\theta)^\gamma (\sin\theta)^{n-2} (F(\theta))^p d\theta.$$

In view of Inequality 56, we find

$$\begin{aligned} J &= \int_0^{\theta^*} (1-\cos\theta)^\gamma (\sin\theta)^{n-3} \sin\theta (F(\theta))^p d\theta \\ &\leq 2^{(n-3)/2} \int_0^{\theta^*} (1-\cos\theta)^{\gamma+\frac{n-3}{2}} \sin\theta (F(\theta))^p d\theta. \end{aligned}$$

From (55) and since $\gamma + \frac{n-1}{2} > 0$, an integration by parts yields

$$J \leq C \int_0^{\theta^*} (1-\cos\theta)^{\gamma+\frac{n-1}{2}} f(\theta) (F(\theta))^{p-1} d\theta.$$

Using the Hölder inequality, we obtain

$$J \leq C \int_0^{\theta^*} (1-\cos\theta)^{\gamma+\frac{n-1}{2}p} (\sin\theta)^{-(n-2)(p-1)} (f(\theta))^p d\theta$$

and from (56), we prove (54). □

Remark 7 By the same way, we can prove that, if $\gamma \in \mathbb{R}$, satisfy $\gamma + \frac{1}{2} > 0$ and $\theta^* \in]0, \pi/2[$, then for any positive measurable function f defined on $]-\theta^*, 0[$, such that

$$\int_{-\theta^*}^0 (1-\cos\theta)^{\gamma+\frac{p}{2}} [f(\theta)]^p d\theta < +\infty,$$

one has

$$\int_{-\theta^*}^0 (1-\cos\theta)^\gamma [F(\theta)]^p d\theta \leq C \int_{-\theta^*}^0 (1-\cos\theta)^{\gamma+\frac{p}{2}} [f(\theta)]^p d\theta, \tag{57}$$

with

$$F(\theta) = \int_{-\theta^*}^{\theta} f(t) dt.$$

Remark 8 (i) As a consequence of inequality (54) for $n = 2$ and inequality (57), for any $w \in \mathcal{D}(]-\theta^*, \theta^*[)$ with $\gamma + \frac{1}{2} > 0$, one has

$$\int_{-\theta^*}^{\theta^*} (1-\cos\theta)^{\gamma} |w(\theta)|^p d\theta \leq C \int_{-\theta^*}^{\theta^*} (1-\cos\theta)^{\gamma+\frac{p}{2}} |w'(\theta)|^p d\theta. \tag{58}$$

(ii) Inequality (54) also implies that for any $w \in \mathcal{D}([0, \theta^*[)$, $\gamma + \frac{n-1}{2} > 0$, one has

$$\int_{0}^{\theta^*} (1-\cos\theta)^{\gamma} (\sin\theta)^{n-2} |w(\theta)|^p d\theta \leq C \int_{0}^{\theta^*} (1-\cos\theta)^{\gamma+\frac{p}{2}} (\sin\theta)^{n-2} |w'(\theta)|^p d\theta. \tag{59}$$

We now consider the sector

$$S = S_{R,\lambda} = \{\boldsymbol{x} \in \mathbb{R}^n,\ r > R,\ 0 < s < \lambda r\}, \quad \text{with } R > 0 \quad \text{and } 0 < \lambda < 1. \tag{60}$$

We start to prove a Hardy-type inequality in the sector S.

Lemma 3 *Let* $\alpha, \beta \in \mathbb{R}$ *such that* $\beta > \max(0, (1-n+p)/2p)$. *Then we have*

$$\forall u \in \mathcal{D}(S), \quad \|u\|_{L^p_{\alpha-\frac{1}{2},\beta-\frac{1}{2}}(S)} \leq C \|\nabla u\|_{L^p_{\alpha,\beta}(S)}. \tag{61}$$

Proof Let u be in $\mathcal{D}(S)$. Since $\beta > 0$, it is enough to prove

$$I = \int_S (1+r)^{(\alpha-\frac{1}{2})p} s^{(\beta-\frac{1}{2})p} |u|^p d\boldsymbol{x} \leq C \int_S (1+r)^{\alpha p} s^{\beta p} |\nabla u|^p d\boldsymbol{x}. \tag{62}$$

Indeed, let us assume that inequality (62) holds. Then, if $0 < \beta < \dfrac{1}{2}$, thanks to (62), we have

$$\begin{aligned}
\int_S (1+r)^{(\alpha-\frac{1}{2})p} (1+s)^{(\beta-\frac{1}{2})p} |u|^p d\boldsymbol{x} &\leq \int_S (1+r)^{(\alpha-\frac{1}{2})p} s^{(\beta-\frac{1}{2})p} |u|^p d\boldsymbol{x} \\
&\leq C \int_S (1+r)^{\alpha p} s^{\beta p} |\nabla u|^p d\boldsymbol{x} \\
&\leq C \int_S (1+r)^{\alpha p} (1+s)^{\beta p} |\nabla u|^p d\boldsymbol{x}.
\end{aligned}$$

Now, if $\beta \geq \dfrac{1}{2}$,

$$\begin{aligned}
\int_S (1+r)^{(\alpha-\frac{1}{2})p} (1+s)^{(\beta-\frac{1}{2})p} |u|^p d\boldsymbol{x} &\leq C \int_S (1+r)^{(\alpha-\frac{1}{2})p} (1+s^{(\beta-\frac{1}{2})p}) |u|^p d\boldsymbol{x} \\
&\leq C \int_S (1+r)^{\alpha p} (s^{p/2} + s^{\beta p}) |\nabla u|^p d\boldsymbol{x}
\end{aligned}$$

and we obtain (61). First, we prove inequality (62) for the case $n \geq 3$. Let $\theta = (\theta_1, \theta_2, \dots, \theta_{n-1}) \in]0, \pi[^{n-2} \times]0, 2\pi[$, $R > 0$, $\theta^* \in]0, \frac{\pi}{2}[$ fixed and consider

$$\Delta = \{(r, \theta) \in \mathbb{R}^+ \times]0, \pi[^{n-2} \times]0, 2\pi[, r > R, \theta_1 \in]0, \theta^*[\}. \tag{63}$$

To establish (62), we introduce the generalized spherical coordinates

$$\begin{aligned} &x_1 = r\cos\theta_1, \;\; x_2 = r\sin\theta_1\cos\theta_2, \dots, \;\; x_{n-1} = r\sin\theta_1 \dots \sin\theta_{n-2}\cos\theta_{n-1}, \\ &x_n = r\sin\theta_1 \dots \sin\theta_{n-2}\sin\theta_{n-1}, \end{aligned} \tag{64}$$

where $(r, \theta) \in \Delta$. Now taking $u(\boldsymbol{x}) = v(r, \theta)$ and observing that

$$\left|\frac{\partial v}{\partial \theta_1}\right| \leq r|\nabla u|,$$

it is sufficient to prove that

$$\begin{aligned} I &= \int_\Delta (1+r)^{(\alpha-\frac{1}{2})p}(r - r\cos\theta_1)^{(\beta-\frac{1}{2})p} r^{n-1}(\sin\theta_1)^{n-2}|v|^p dr d\theta \\ &\leq C\int_\Delta (1+r)^{\alpha p}(r - r\cos\theta_1)^{\beta p} r^{n-1}(\sin\theta_1)^{n-2} r^{-p}\left|\frac{\partial v}{\partial\theta_1}\right|^p dr d\theta. \end{aligned} \tag{65}$$

We immediately have

$$I \leq \int_\Delta (1+r)^{\alpha p} r^{\beta p}(1-\cos\theta_1)^{(\beta-\frac{1}{2})p} r^{n-1}(\sin\theta_1)^{n-2} r^{-p}|v|^p dr d\theta. \tag{66}$$

We now set

$$J = \int_0^{\theta^*} (1-\cos\theta_1)^{(\beta-\frac{1}{2})p}(\sin\theta_1)^{n-2}|v|^p d\theta_1.$$

Since $\beta > (1-n+p)/2p$, we have $(\beta - \frac{1}{2})p + \frac{n-1}{2} > 0$. Moreover $u \in \mathcal{D}(S)$ implies that, for $(r, \theta) \in \Delta$, the function $\theta_1 \to v(r, \theta)$ belongs to $\mathcal{D}([0, \theta^*[)$. Therefore from (59), we get

$$J \leq C\int_0^{\theta^*} (1-\cos\theta_1)^{\beta p}(\sin\theta_1)^{n-2}\left|\frac{\partial v}{\partial\theta_1}\right|^p d\theta_1. \tag{67}$$

In view of inequalities (66) and (67), we obtain (65).

We now continue the proof of (62) for the case $n = 2$. We define

$$\Delta = \{(r, \theta) \in \mathbb{R}^+ \times]-\pi, \pi[, \;\; r > R, \;\; \theta \in]-\theta^*, \theta^*[\} \tag{68}$$

and we introduce the polar coordinates

$$x_1 = r\cos\theta \ , \ \ x_2 = r\sin\theta, \tag{69}$$

where $(r,\theta) \in \Delta$. Taking $u(\boldsymbol{x}) = v(r,\theta)$, it is sufficient to prove

$$\begin{aligned} I &= \int_{-\theta^*}^{\theta^*}\int_R^{\infty}(1+r)^{(\alpha-\frac{1}{2})p}(r-r\cos\theta)^{(\beta-\frac{1}{2})p}r^2|v|^p drd\theta \\ &\leq C\int_{-\theta^*}^{\theta^*}\int_R^{\infty}(1+r)^{\alpha p}(r-r\cos\theta)^{\beta p}r^{2-p}\left|\frac{\partial v}{\partial\theta}\right|^p drd\theta. \end{aligned} \tag{70}$$

Proceeding as for the case $n \geq 3$ and the use of inequality (58) give us Inequality (70). □

Let R be a positive real number fixed large enough. In the sequel, we will need the following Hardy-type inequality (*cf.* Hardy-Littlewood-Polya [9] : we have

$$\forall f \in \mathcal{D}(]R,\infty[), \quad \int_R^{+\infty}|f(r)|^p r^{\gamma}dr \leq C\int_R^{+\infty}|f'(r)|^p r^{\gamma+p}dr, \quad \text{with } \gamma+1 \neq 0. \tag{71}$$

Let now B_R denotes the open ball centered at the origin and with radius R and $B'_R = \mathbb{R}^n \setminus \overline{B}_R$. We are going to prove inequality (61) for a function $u \in \mathcal{D}(B'_R)$.

Lemma 4 *Let* $\alpha, \beta \in \mathbb{R}$ *satisfy* $\beta > \max(0, (1-n+p)/2p)$ *and* $\alpha+\beta+n/p-1 \neq 0$.*Then, for any large enough positive real number R, we have*

$$\forall u \in \mathcal{D}(B'_R), \quad \|u\|_{L^p_{\alpha-\frac{1}{2},\beta-\frac{1}{2}}(B'_R)} \leq C\|\nabla u\|_{L^p_{\alpha,\beta}(B'_R)}. \tag{72}$$

Proof Let u be in $\mathcal{D}(B'_R)$. We introduce the open set

$$D_{R,\lambda} = \{\boldsymbol{x} \in \mathbb{R}^n, r > R, \lambda r < s\}$$

and the following partition of unity

$$\varphi_1, \varphi_2 \in \mathcal{C}^{\infty}(B'_R), \quad 0 \leq \varphi_1, \varphi_2 \leq 1, \quad \varphi_1 + \varphi_2 = 1 \text{ in } B'_R,$$

with

$$\begin{aligned} &\varphi_1 = 1 \text{ in } S_{R,\lambda/2}, \quad \text{supp}\,\varphi_1 \subset S_{R,\lambda} \\ &\text{and } |\nabla\varphi_1(\boldsymbol{x})| \leq \frac{C}{|\boldsymbol{x}|}, \ \boldsymbol{x} \in S_{R,\lambda} \cap D_{R,\lambda/2}. \end{aligned} \tag{73}$$

We have

$$\|u\|_{L^p_{\alpha-\frac{1}{2},\beta-\frac{1}{2}}(B'_R)} \leq \|u\varphi_1\|_{L^p_{\alpha-\frac{1}{2},\beta-\frac{1}{2}}(B'_R)} + \|u\varphi_2\|_{L^p_{\alpha-\frac{1}{2},\beta-\frac{1}{2}}(B'_R)}.$$

Let us prove that

$$\|u\varphi_1\|_{L^p_{\alpha-\frac{1}{2},\beta-\frac{1}{2}}(B'_R)} \leq C\|\nabla u\|_{L^p_{\alpha,\beta}(B'_R)}. \tag{74}$$

Since $u\varphi_1 \in \delta(S_{R,\lambda})$ and $\beta > \max(0, (1-n+p)/2p)$, Lemma 3 yields

$$\|u\varphi_1\|_{L^p_{\alpha-\frac{1}{2},\beta-\frac{1}{2}}(S_{R,\lambda})} \leq C\|\nabla(u\varphi_1)\|_{L^p_{\alpha,\beta}(S_{R,\lambda})}. \tag{75}$$

Furthermore, we have

$$\begin{aligned}\|\nabla(u\varphi_1)\|^p_{L^p_{\alpha,\beta}(S_{R,\lambda})} &\leq C\int_{S_{R,\lambda}} (1+r)^{\alpha p}(1+s)^{\beta p}|\nabla u|^p d\boldsymbol{x}\\ &\quad + C\int_{S_{R,\lambda}\cap D_{R,\lambda/2}} (1+r)^{\alpha p}(1+s)^{\beta p}|u\nabla\varphi_1|^p d\boldsymbol{x}.\end{aligned} \tag{76}$$

Since $s \sim r$ in $S_{R,\lambda} \cap D_{R,\lambda/2}$ and from (73), for the second term of the right hand side of (76), we find

$$\begin{aligned}&\int_{S_{R,\lambda}\cap D_{R,\lambda/2}} (1+r)^{\alpha p}(1+s)^{\beta p}|u\nabla\varphi_1|^p d\boldsymbol{x}\\ &\qquad \leq C\int_{S_{R,\lambda}\cap D_{R,\lambda/2}} (1+r)^{(\alpha+\beta-1)p}|u|^p d\boldsymbol{x}\\ &\qquad \leq C\int_{S_{R,\lambda}\cap D_{R,\lambda/2}} r^{(\alpha+\beta-1)p}|u|^p d\boldsymbol{x}.\end{aligned} \tag{77}$$

Now, we introduce the generalized spherical coordinates defined by (64), where $(r,\theta) \in \mathbb{R}^+\times]0,\pi[^{n-2}\times]0,2\pi[$, for the case $n \geq 3$, or the polar coordinates defined by (69), where $(r,\theta) \in \mathbb{R}^+\times]-\pi,\pi[$, for the case $n = 2$. We take $u(\boldsymbol{x}) = v(r,\theta)$ and, recalling that $\alpha+\beta+n/p-1 \neq 0$, we apply (71) to the function $r \to v(r,\theta)$. Thus, it comes

$$\int_R^{+\infty} |v|^p r^{(\alpha+\beta-1)p+n-1} dr \leq C\int_R^{+\infty} \left|\frac{\partial v}{\partial r}\right|^p r^{(\alpha+\beta)p+n-1} dr,$$

which immediately yields

$$\begin{aligned}\int_{S_{R,\lambda}\cap D_{R,\lambda/2}} r^{(\alpha+\beta-1)p}|u|^p d\boldsymbol{x} &\leq C\int_{S_{R,\lambda}\cap D_{R,\lambda/2}} r^{(\alpha+\beta)p}|\nabla u|^p d\boldsymbol{x}\\ &\leq C\int_{S_{R,\lambda}\cap D_{R,\lambda/2}} (1+r)^{\alpha p}(1+s)^{\beta p}|\nabla u|^p d\boldsymbol{x}.\end{aligned} \tag{78}$$

Summarizing (75), (76), (77) and (78), we deduce (74). Let us now prove that

$$\|u\varphi_2\|_{L^p_{\alpha-\frac{1}{2},\beta-\frac{1}{2}}(B'_R)} \leq C\|\nabla u\|_{L^p_{\alpha,\beta}(B'_R)}. \tag{79}$$

Since the support of φ_2 is included in $D_{R,\lambda/2}$ and $\varphi_2 \leq 1$, we have

$$\begin{aligned}\|u\varphi_2\|^p_{L^p_{\alpha-\frac{1}{2},\beta-\frac{1}{2}}(B'_R)} &= \int_{D_{R,\lambda/2}} (1+r)^{(\alpha-\frac{1}{2})p}(1+s)^{(\beta-\frac{1}{2})p}|u\varphi_2|^p d\boldsymbol{x}\\ &\leq \int_{D_{R,\lambda/2}} (1+r)^{(\alpha-\frac{1}{2})p}(1+s)^{(\beta-\frac{1}{2})p}|u|^p d\boldsymbol{x}.\end{aligned}$$

Moreover, recalling that $s \sim r$ in $D_{R,\lambda/2}$, we get

$$\int_{D_{R,\lambda/2}} (1+r)^{(\alpha-\frac{1}{2})p}(1+s)^{(\beta-\frac{1}{2})p}|u|^p d\boldsymbol{x} \leq C\int_{D_{R,\lambda/2}} r^{(\alpha+\beta-1)p}|u|^p d\boldsymbol{x}.$$

Next, we use generalized spherical coordinates for $n \geq 3$ or polar coordinates for $n = 2$, with $u(\boldsymbol{x}) = v(r,\theta)$. Since $\alpha+\beta+n/p-1 \neq 0$, inequality (71) yields

$$\int_R^{+\infty} r^{(\alpha+\beta-1)p+n-1}|v|^p dr \leq C\int_R^{+\infty} r^{(\alpha+\beta)p+n-1}\left|\frac{\partial v}{\partial r}\right|^p dr,$$

which implies that

$$\begin{aligned}\int_{D_{R,\lambda/2}} r^{(\alpha+\beta-1)p}|u|^p d\boldsymbol{x} &\leq C\int_{D_{R,\lambda/2}} r^{(\alpha+\beta)p}|\nabla u|^p d\boldsymbol{x}\\ &\leq C\int_{D_{R,\lambda/2}} (1+r)^{\alpha p}(1+s)^{\beta p}|\nabla u|^p d\boldsymbol{x}.\end{aligned}$$

The previous inequalities yield (79) and that concludes the proof. □

We are now in a position to give the following Hardy-type inequality.

Theorem 4 *Let* $\alpha, \beta \in \mathbb{R}$ *satisfy* $\beta > \max(0, (1-n+p)/2p)$ *and* $\alpha+\beta+n/p-1 \neq 0$. *Let* $j' = \min(j, 0)$*, where* j *is the highest degree of the polynomials contained in* $X^{1,p}_{\alpha,\beta}(\mathbb{R}^3)$*. Then, we have*

$$\forall u \in X^{1,p}_{\alpha,\beta}(\mathbb{R}^3), \quad \inf_{\lambda\in\mathbb{P}_{j'}} \|u+\lambda\|_{L^p_{\alpha-\frac{1}{2},\beta-\frac{1}{2}}(\mathbb{R}^n)} \leq C\|\nabla u\|_{L^p_{\alpha,\beta}(\mathbb{R}^n)}. \tag{80}$$

In other words, the semi-norm $|\,.\,|_{X^{1,p}_{\alpha,\beta}(\mathbb{R}^3)}$ *defines on* $X^{1,p}_{\alpha,\beta}(\mathbb{R}^3)/\mathbb{P}_{j'}$ *a norm which is equivalent to the quotient norm.*

Proof The proof of this theorem is similar to that given in Amrouche-Girault-Giroire [2] (Theorem 8.3, p. 598). □

Remark 9 Note that the particular case $n = 3$, $p = 2$, $\beta > 0$ and $\alpha + \beta + \frac{1}{2} > 0$ of previous theorem for was proved by Farwig (see [6]). Next, observe that the previous theorem also improves the inequalities proved in [10] (Lemma 2.3) for the case $n = 3$, $p = 2$, $\beta > 0$, $\alpha \geq 0$ and $\alpha + \beta < \frac{3}{2}$.

Lemma 5 *Let α, β be two reals such that $\beta \leq 0$ and $\alpha + n/p - 1 < 0$ or $\alpha + \beta + n/p - 1 > 0$. Then, for any large enough positive real number R, we have*

$$\forall u \in \mathcal{D}(B'_R), \quad \|u\|_{L^p_{\alpha-1,\beta}(B'_R)} \leq C\|\nabla u\|_{L^p_{\alpha,\beta}(B'_R)}. \tag{81}$$

Proof Let $u \in \mathcal{D}(B'_R)$. We first prove (81) for $n \geq 3$. Let $\theta = (\theta_1, \dots, \theta_{n-1})$ and consider the following set

$$D = \{(r, \theta) \in \mathbb{R}^+ \times]0, \pi[^{n-2} \times]0, 2\pi[, r > R\}.$$

We introduce the generalized spherical coordinates (64) with $(r, \theta) \in D$. Taking $u(\boldsymbol{x}) = v(r, \theta)$, inequality (81) is equivalent to

$$\begin{aligned} I &= \int_D r^{(\alpha-1)p+n-1}(1 + r - r\cos\theta_1)^{\beta p}(\sin\theta_1)^{n-2}|v|^p dr d\theta \\ &\leq C \int_D r^{\alpha p+n-1}(1 + r - r\cos\theta_1)^{\beta p}(\sin\theta_1)^{n-2} \left|\frac{\partial v}{\partial r}\right|^p dr d\theta. \end{aligned} \tag{82}$$

We define $\tilde{r}(\theta_1) = \dfrac{1}{1 - \cos\theta_1}$ and $\tilde{\theta} \in]0, \pi[$ such that $R = \dfrac{1}{1 - \cos\tilde{\theta}}$. We divide D into three subdomains:

$$\begin{aligned} D_1 &= \{(r, \theta) \in D, R < r < \tilde{r}(\theta_1), 0 < \theta_1 < \tilde{\theta}\} \ \text{ where } 1 + r - r\cos\theta_1 \sim 1, \\ D_2 &= \{(r, \theta) \in D, r > \tilde{r}(\theta_1), 0 < \theta_1 < \tilde{\theta}\} \ \text{ where } 1 + r - r\cos\theta_1 \sim r - r\cos\theta_1, \\ D_3 &= \{(r, \theta) \in D, r > R, \tilde{\theta} < \theta_1 < \pi\} \ \text{ where } 1 + r - r\cos\theta_1 \sim r - r\cos\theta_1. \end{aligned}$$

Thus, we obtain

$$I \sim I_1 + I_2 + I_3,$$

with

$$\begin{aligned} I_1 &= \int_{D_1} r^{(\alpha-1)p+n-1}(\sin\theta_1)^{n-2}|v|^p dr d\theta, \\ I_2 &= \int_{D_2} r^{(\alpha+\beta-1)p+n-1}(1 - \cos\theta_1)^{\beta p}(\sin\theta_1)^{n-2}|v|^p dr d\theta, \\ I_3 &= \int_{D_3} r^{(\alpha+\beta-1)p+n-1}(1 - \cos\theta_1)^{\beta p}(\sin\theta_1)^{n-2}|v|^p dr d\theta. \end{aligned}$$

Let us now estimate the three integrals. Since $\alpha + \dfrac{n}{p} - 1 \neq 0$, an integration by parts and the Hölder's inequality yield

$$\int_R^{\tilde{r}(\theta_1)} r^{(\alpha-1)p+n-1}|v|^p dr \leq \frac{1}{(\alpha-1)p+n}(\tilde{r}(\theta_1))^{(\alpha-1)p+n}|v(\tilde{r}(\theta_1),\theta))|^p$$
$$+\frac{p}{|\alpha p - p + n|}\left(\int_R^{\tilde{r}(\theta_1)} r^{(\alpha-1)p+n-1}|v|^p dr\right)^{1/p'}\left(\int_R^{\tilde{r}(\theta_1)} r^{\alpha p+n-1}\left|\frac{\partial v}{\partial r}\right|^p dr\right)^{1/p},$$

and consequently

$$I_1 \leq$$
$$\frac{1}{(\alpha-1)p+n}\int_0^{2\pi}\int_0^{\pi}\cdots\int_0^{\pi}\int_0^{\tilde{\theta}}(\tilde{r}(\theta_1))^{(\alpha-1)p+n}(\sin\theta_1)^{n-2}|v(\tilde{r}(\theta_1),\theta)|^p d\theta_1\ldots d\theta_{n-1}$$
$$+C\int_{D_1} r^{\alpha p+n-1}(\sin\theta_1)^{n-2}\left|\frac{\partial v}{\partial r}\right|^p dr d\theta. \quad (83)$$

Similarly, since $\alpha + \beta + \dfrac{n}{p} - 1 \neq 0$, we get for the two other integrals

$$I_2 \leq -\frac{1}{(\alpha+\beta-1)p+n}I_2'$$
$$+C\int_{D_2} r^{(\alpha+\beta)p+n-1}(1-\cos\theta_1)^{\beta p}(\sin\theta_1)^{n-2}\left|\frac{\partial v}{\partial r}\right|^p dr d\theta, \quad (84)$$

with

$$I_2' =$$
$$\int_0^{2\pi}\int_0^{\pi}\cdots\int_0^{\pi}\int_0^{\tilde{\theta}}\tilde{r}(\theta_1)^{(\alpha+\beta-1)p+n}(1-\cos\theta_1)^{\beta p}(\sin\theta_1)^{n-2}|v(\tilde{r}(\theta_1),\theta)|^p d\theta_1\ldots d\theta_{n-1},$$
$$I_3 \leq C\int_{D_3} r^{(\alpha+\beta)p+n-1}(1-\cos\theta_1)^{\beta p}(\sin\theta_1)^{n-2}\left|\frac{\partial v}{\partial r}\right|^p dr d\theta. \quad (85)$$

Summarizing (83), (84), (85), we obtain

$$I \leq C\int_D r^{\alpha p+n-1}(1+r-r\cos\theta_1)^{\beta p}(\sin\theta_1)^{n-2}\left|\frac{\partial v}{\partial r}\right|^p dr d\theta +$$
$$\frac{1}{(\alpha-1)p+n}\int_0^{2\pi}\int_0^{\pi}\cdots\int_0^{\pi}\int_0^{\tilde{\theta}}(\tilde{r}(\theta_1))^{(\alpha-1)p+n}(\sin\theta_1)^{n-2}|v(\tilde{r}(\theta_1),\theta)|^p d\theta_1\ldots d\theta_{n-1}$$
$$-\frac{1}{(\alpha+\beta-1)p+n}I_2'.$$

Recalling that $(\tilde{r}(\theta_1)(1-\cos\theta_1))^{\beta p} = 1$, and since $\beta \le 0$ with $\alpha + \dfrac{n}{p} - 1 < 0$ or $\alpha + \beta + \dfrac{n}{p} - 1 > 0$, we have

$$\frac{1}{(\alpha-1)p+n} - \frac{1}{(\alpha+\beta-1)p+n} \le 0.$$

Thus, we deduce inequality (82).

For the case $n = 2$, we use polar coordinates (69), with $(r,\theta) \in D$, where

$$D = \{(r,\theta) \in \mathbb{R}^+ \times]-\pi,\pi[, r > R\}.$$

We set $\tilde{r}(\theta) = \dfrac{1}{1-\cos\theta}$ and $\tilde{\theta}$ such that $R = \dfrac{1}{1-\cos\tilde{\theta}}$. We devide D as follow

$$D_1 = \{(r,\theta) \in D, R < r < \tilde{r}(\theta), -\tilde{\theta} < \theta < \tilde{\theta}\}$$
$$D_2 = \{(r,\theta) \in D, r > \tilde{r}(\theta), -\tilde{\theta} < \theta_1 < \tilde{\theta}\}$$
$$D_3 = \{(r,\theta) \in D, r > R, \theta \in]-\pi, -\tilde{\theta}[\cup]\tilde{\theta},\pi[\}.$$

We then proceed as for the proof of the case $n \ge 3$. □

Now proceeding as for the case $\beta > 0$, we obtain the Hardy-type inequality.

Theorem 5 *Let α, β be two real satisfying $\beta \le 0$ and $\alpha + \dfrac{n}{p} - 1 < 0$ or $\alpha + \beta + \dfrac{n}{p} - 1 > 0$. Let $j' = min\,(j, 0)$, where j is the highest degree of the polynomials contained in $Y^{1,p}_{\alpha,\beta}(\mathbb{R}^3)$. Then we have*

$$\forall u \in Y^{1,p}_{\alpha,\beta}(\mathbb{R}^3), \quad \inf_{\lambda \in \mathbb{P}_{j'}} \|u+\lambda\|_{L^p_{\alpha-1,\beta}(\mathbb{R}^n)} \le C\|\nabla u\|_{L^p_{\alpha,\beta}(\mathbb{R}^n)}. \tag{86}$$

In other words, the semi-norm $|\,.\,|_{Y^{1,p}_{\alpha,\beta}(\mathbb{R}^3)}$ defines on $Y^{1,p}_{\alpha,\beta}(\mathbb{R}^3)/\mathbb{P}_{j'}$ a norm which is equivalent to the quotient norm.

Remark 10 For the case $\beta = 0$, we get the result proved by Amrouche-Girault-Giroire [2] for the space $W^{1,p}_{\alpha}(\mathbb{R}^n)$ when $\alpha + \dfrac{n}{p} - 1 \ne 0$.

References

1. C. Amrouche and H. Bouzit, L^p – inequalities for scalar Oseen potential. J. Math. Anal. Appl. **337** (2008), 753–770
2. C. Amrouche, V. Girault and J. Giroire, Weighted Sobolev spaces for Laplace's equation in $\mathbb{R}^n$. J. Math. Pures. Appl. **73** (1994), 579–606

3. C. Amrouche and U. Razafison, Weighted Sobolev spaces for a scalar model of the stationary Oseen equations in $\mathbb{R}^3$. J. Math. Fluid Mech. **9** (2007), 181–210
4. C. Amrouche and U. Razafison, The stationary Oseen equations in $\mathbb{R}^3$. An approach in weighted sobolev spaces. J. Math. Fluid Mech. **9** (2007), 211–225
5. C. Amrouche and U. Razafison, Espaces de Sobolev avec poids et équation scalaire d'Oseen dans $\mathbb{R}^n$. C. R. Math. Acad. Sci. Paris. **337**(12) (2003), 761–766
6. R. Farwig, A variational approach in weighted Sobolev spaces to the operator $-\Delta + \partial/\partial x_1$ in exterior domains of $\mathbb{R}^3$. Math. Z. **210**(3) (1992), 449–464
7. R. Farwig and H. Sohr, Weighted estimates for the Oseen equations and the Navier-Stokes equations in exterior domains. Ser. Adv. Math. Appl. Sci. **47** (1998), 11–30
8. G. P. Galdi, *An Introduction to the Mathematical Theory of the Navier-Stokes Equations* – Vol. I. Springer Tracts in Natural Philosophy, 38, Springer-Verlag, Berlin, 1994
9. G. H. Hardy, J. E. Littlewood and G. Pólya, *Inequalities.* Cambridge University Press, New York, 1952
10. S. Kračmar, Š. Nečasová and P. Penel, Anisotropic L^2-estimates of weak solutions to the stationary Oseen type equations in $\mathbb{R}^3$ for rotating body. RIMS Kokyuroku Bessatsu **B1** (2007), 219–235
11. S. Kračmar, A. Novotný and M. Pokorný, Estimates of Oseen kernels in weighted L^p spaces. J. Math. Soc. Japan **53** (2001), 59–111
12. P. I. Lizorkin, (L^p, L^q) – multipliers of Fourier integrals. Dokl. Akad. Nauk SSSR **152**, (1963), 808–811
13. C. W. Oseen, *Neuere Methoden und Ergebnisse in der Hydrodynamik.* Akadem. Verlagsgesellschaft, Leipzig, 1927
14. M. Reed and B. Simon, *Fourier Analysis Self-Adjointness.* t.II Academic Press New York, 1975
15. E. M. Stein, *Singulars Integrals and Differentiability Properties of Functions.* Princeton University Press. Princeton, NJ, 1970

A New Model of Diphasic Fluids in Thin Films

Guy Bayada, Laurent Chupin, and Bérénice Grec

Abstract In this work, we are interested in the modelling of diphasic fluids flows in thin films. The diphasic aspect is described by a diffuse interface model, the Cahn-Hilliard equation. The specific geometry (thin domain) allows to replace heuristically the usual Navier-Stokes equations by an asymptotic approximation, a modified Reynolds equation (in which the pressure and the velocity are uncoupled), where the viscosity depends on the composition of the mixture. An existence result on the limit system is stated. since the boundary conditions are chosen in order to model the injection phenomenon, previous results on the Cahn-Hilliard equation cannot be applied, and new estimates have to be obtained. Moreover, we present numerical simulations for lubrication applications to improve the understanding of the cavitation phenomenon.

Keywords Diphasic flows · Cahn-Hilliard equation · Existence result · Numerical simulations · Lubrication

1 Introduction

In lubrication applications, the flow of a fluid between two close surfaces in relative motion is described by an asymptotic approximation of the Navier-Stokes equations, the Reynolds equation. This equation is much easier to study, since the pressure and the velocity can be uncoupled. Indeed, the pressure is shown to be independent of the normal direction to the surfaces, this simplification leads to an equation on the pressure only, and the velocity can be deduced from the pressure. This approach was introduced by Reynolds, and has been rigorously justified in [2] for the Stokes equation, and generalized afterwards in many works (Navier-Stokes equations [1], unsteady case [3], compressible fluid (for some perfect gases law) [12]). It is of

B. Grec (✉)
Ecole Centrale de Lyon, Institut Camille Jordan CNRS UMR 5208, Jean Capelle,
F-69621 Villeurbanne
e-mail: berenice.grec@insa-lyon.fr

R. Rannacher, A. Sequeira (eds.), *Advances in Mathematical Fluid Mechanics*,
DOI 10.1007/978-3-642-04068-9_2,

interest to investigate how this approach can be used for the case of a two fluid flow. A partial answer to this question has been given in [13].

There are two different approaches to describe multi-phase fluids. The most frequent one in the previous works on the subject for lubrication applications is to consider the interface to be sharp. It consists in introducing a variable viscosity $\eta(x, y)$, which is either equal to the viscosity η_1 of one fluid or the viscosity η_2 of the other fluid (that is to say that the fluids are supposed to be non-miscible). The behavior of η is described by a transport equation. In that case, under an assumption on the interface, the asymptotic equations can be interpreted as a generalized Buckley-Leverett equation coupled with a generalized Reynolds equation [13]. One of the main disadvantages of the method is that the fluid interface is supposed to be the graph of a function, which hinders for example the formation of bubbles. In addition, this kind of models only takes into account hydrodynamical effects between the two phases.

The second class of models describing diphasic flows are the so-called diffuse interface models. These models are not only based on mechanical considerations but also on chemical properties at the interface between the two fluids, which enable an exchange between the two phases. In this chapter, we use the Cahn-Hilliard equation, which involves an interaction potential. To this end, we introduce an order parameter φ, for example the volumic fraction of one phase in the mixture. This kind of model has already been studied for the complete Navier-Stokes equations in [6, 10].

In this chapter, we describe the governing equations (in Sect. 2) for a diphasic fluid in thin flows, and explain how this model is derived from the Navier-Stokes and the Cahn-Hilliard equation. In Sect. 3, we state an existence result and sketch out its proof. Lastly, in Sect. 3, the numerical scheme used for simulations of this model is detailed, and some numerical results are given.

2 Governing Equations

In order to derive the governing equations, we first recall briefly the approach for obtaining the Reynolds equation from the Navier-Stokes equations. Then we introduce the Cahn-Hilliard equation, which models a mixture of fluids. Last, we obtain the full model for two fluids in a thin domain.

2.1 Modelling One Fluid in a Thin Domain

For $\varepsilon > 0$, let Ω^ε be a thin domain

$$\Omega^\varepsilon = \left\{(x, y) \in \mathbb{R}^2,\ 0 < x < L,\ 0 < z < \varepsilon h(x)\right\},$$

with h a regular mapping from $[0, L]$ to $\mathbb{R}_+^*$ which is supposed to satisfy $0 < h_m \leq h(x) \leq h_M$. The usual Navier-Stokes equations describe an incompressible fluid flow, coupling the velocity $\mathbf{u} = (u, v)$ and the pressure p, which depend on the physical parameters of the fluid (the density ϱ, the viscosity η), and the external forces $\mathcal{F}$ (for example the gravity term ϱg):

$$\varrho\,(\partial_t \mathbf{u} + \mathbf{u}\cdot\nabla\mathbf{u}) - \operatorname{div}(\eta D(\mathbf{u})) + \nabla p = \mathcal{F}, \qquad \operatorname{div}\mathbf{u} = 0. \tag{1}$$

In lubrication applications, it is important to take the shear effects into account, and the following boundary conditions are used: Dirichlet boundary conditions are imposed on the velocity on $\{z = 0\}$ and $\{z = \varepsilon h(x)\}$:

$$\forall x \in]0, L[\quad u(x, 0) = s, \qquad u(x, \varepsilon h(x)) = v(x, 0) = v(x, \varepsilon h(x)) = 0. \tag{2}$$

It has been showed in [2] that in a thin domain, the conditions on $\mathbf{u}$ on the lateral part of the boundary only occur in the limit problem (i.e. when $\varepsilon \to 0$) by means of the input flow: indeed, any lateral boundary condition corresponding to a given input flow will lead to the same limit problem. Therefore the lateral boundary conditions are not given explicitly, only the input flow q is given:

$$\int_0^{h(0)} \mathbf{u}|_{x=0}\cdot\nabla = q, \tag{3}$$

where ∇ is the external normal to $\partial\Omega$.

With the aid of asymptotic expansions, one shows that the Navier-Stokes equations (1) tend formally to the Reynolds equation when ε tends to zero. It has been proved in [1] that this limit can be justified rigorously. Introducing the rescaled domain

$$\Omega = \left\{(x, y) \in \mathbb{R}^2,\ 0 < x < L,\ 0 < y < h(x)\right\},$$

the following steady-state equation is obtained to the limit $\varepsilon \to 0$:

$$\partial_y\left(\eta\,\partial_y u\right) = \partial_x p, \qquad \partial_y p = 0, \qquad \partial_x u + \partial_y v = 0. \tag{4}$$

The usual procedure to obtain the Reynolds equation is to integrate twice (4) with respect to y, and make use of the boundary conditions (2), u can be expressed as a function of p. The incompressibility condition enables to obtain an equation on the pressure only, the Reynolds equation:

$$\partial_x\left(\frac{h^3}{12\eta}\partial_x p\right) = s\,\partial_x\left(\frac{h}{2}\right). \tag{5}$$

The velocity $\mathbf{u}$ is given as a function of p:

$$u(x, y) = \frac{y(y-h)}{2\eta}\partial_x p + s\left(1 - \frac{y}{h}\right) \qquad \text{and} \qquad v(x, y) = -\int_0^y \partial_x u(x, z)\,dz. \tag{6}$$

The boundary conditions on p are deduced from the ones on $\mathbf{u}$. Indeed, the choice of q corresponds to a Neumann condition on p at $x = 0$: it follows from (6) that

$$q = \int_0^{h(0)} u(0, y)dy = -\partial_x p(0)\frac{h(0)^3}{12\eta} + \frac{sh(0)}{2}.$$

This expression determines $\partial_x p(0)$ as a function of q. Moreover, since the pressure p is defined up to a constant, we have to impose another condition. Finally, the boundary conditions on p read:

$$\partial_x p(0) = \frac{12\eta}{h(0)^3}\left(\frac{sh(0)}{2} - q\right), \qquad p(L) = 0. \tag{7}$$

2.2 Modelling a Mixture in a Thin Domain

2.2.1 Modelling a Mixture and Taking the Surface Tension into Account

In order to describe the mixture of two miscible fluids, we introduce an order parameter $\varphi \in [-1, 1]$ (corresponding to the volumic fraction of one fluid in the flow). Then all physical parameters are written as functions of φ. The viscosity $\eta(\varphi)$ of the mixture is given as function of the viscosities of the two fluids η_1 and η_2 by:

$$\frac{1}{\eta(\varphi)} = \begin{cases} \dfrac{1+\varphi}{2\eta_1} + \dfrac{1-\varphi}{2\eta_2} & \text{if} \quad \varphi \in [-1, 1], \\ 1/\eta_1 & \text{if} \quad \varphi > 1, \\ 1/\eta_2 & \text{if} \quad \varphi < -1, \end{cases} \tag{8}$$

so that $\varphi = 1$ and $\varphi = -1$ correspond to the fluids of viscosity η_1 and η_2 respectively.

In a similar way, the density ϱ of the mixture can be defined as a function of φ. However, the non homogeneous case $\varrho_1 \neq \varrho_2$ induces further difficulties (see [8]) due to the loss of the local conservation equation for the density. We do not wish to take these effects into account in this paper. Therefore, we restrict ourselves to the case $\varrho_1 = \varrho_2$ (as in [6] for example).

In order to describe the evolution of φ, we introduce the Cahn-Hilliard equation, which is composed of both a transport term, taking the mechanical effects into account, and a diffusive term modelling the chemical effects. The Cahn-Hilliard equation reads in a dimensionless form:

$$\partial_t \varphi + \mathbf{u} \cdot \nabla\varphi - \frac{1}{\text{Pe}} \operatorname{div}(B(\varphi)\nabla\mu) = 0, \tag{9a}$$

$$\mu = -\alpha^2 \Delta\varphi + F'(\varphi). \tag{9b}$$

The variable μ is the chemical potential, $B(\varphi)$ is called mobility, Pe is the Péclet number, α is an non-dimensional parameter measuring the thickness of the diffuse interface, and the function F is called Cahn-Hilliard potential. The physical-relevant assumption on F is that it must have a double-well structure, each of them representing one of the two fluids. A realistic choice for F is given by a logarithmic form $F(x) = 1-x^2+c\,((1+x)\log(1+x)+(1-x)\log(1-x))$, or its polynomial approximation $F(x) = (1-x^2)^2$. The mathematical hypotheses imposed on F match these two choices, and allow some more general profiles. As far as the mobility B is concerned, it is supposed to be regular, positive, and bounded from above and from below: $0 < B_m \le B(\varphi) \le B_M$. Let us mention that other functions B can be considered, in particular the degenerate case $B(x) = (1-x^2)^r$, with $r \ge 0$. This case has been studied in [6], but introduces further mathematical difficulties.

This equation is equipped with boundary conditions on φ and μ. Unlike the previous works [6, 10], we are interested in modelling injection phenomena, therefore we consider a Dirichlet condition on φ on the left-hand side of the boundary. In order to state the boundary conditions mathematically, we define different parts of the boundary $\Gamma = \partial\Omega$ as follows: let $\Gamma_l = \{(x, y) \in \Gamma, x = 0\}$ be the left-hand part of the boundary (see Fig. 1). Let φ_l is a given function satisfying $\varphi_l \in H^{5/2}(\Gamma_l)$, with a compatibility condition reading

$$\exists(\varphi_1, \varphi_2) \in \mathbb{R}^2, \quad \exists r > 0, \qquad \varphi|_{[0,r]} = \varphi_1, \quad \varphi|_{[h(0)-r,h(0)]} = \varphi_2.$$

The boundary conditions read

$$\varphi|_{\Gamma_l} = \varphi_l, \qquad \frac{\partial\varphi}{\partial\nabla}\Big|_{\Gamma\setminus\Gamma_l} = 0, \qquad \mu|_{\Gamma_l} = 0, \qquad \frac{\partial\mu}{\partial\nabla}\Big|_{\Gamma} = 0. \tag{10}$$

In order to take into account the surface tension effects, we add to the external forces $\mathcal{F}$ in (1) an additional term $\kappa\mu\nabla\varphi$, where κ is the capillarity coefficient (related to the surface tension). The Navier-Stokes equation becomes:

$$\varrho\,(\partial_t \mathbf{u} + \mathbf{u}\cdot\nabla\mathbf{u}) - \operatorname{div}(\eta D(\mathbf{u})) + \nabla p = \kappa\mu\nabla\varphi, \qquad \operatorname{div}\mathbf{u} = 0. \tag{11}$$

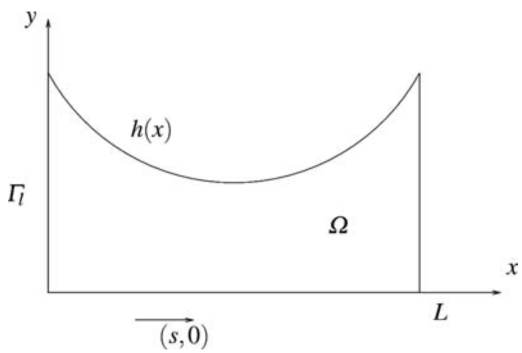

Fig. 1 Domain Ω of boundary Γ and notations for the boundary conditions on φ and on $\mathbf{u}$

The system (11)–(9) has been studied in [6, 10].

2.2.2 Modelling Diphasic Flows in a Thin Domain

Formally, we can pass to the limit in (11) as ε tends to zero similarly to Sect. 2.1. However, it remains to make a choice for the non-dimensionalization of the additional parameters: in this work, κ is chosen to be of order ε (thus the term $\kappa\mu\nabla\varphi$ in (11) vanishes when passing to the limit).

Passing formally to $\varepsilon \to 0$, we get again (4), with η non constant. After integrating twice the first equation of (4) and making use of the boundary conditions, we find

$$u = \left(B - \frac{\widetilde{B}}{\widetilde{A}}A\right)\partial_x p + \left(1 - \frac{A}{\widetilde{A}}\right)s \tag{12}$$

where

$$A(x,y) = \int_0^y \frac{dz}{\eta(\varphi(x,z))}, \quad B(x,y) = \int_0^y \frac{zdz}{\eta(\varphi(x,z))}, C(x,y) = \int_0^y \frac{z^2dz}{\eta(\varphi(x,z))}$$

and $\widetilde{A}(x) = A(x,h(x))$, $\widetilde{B}(x) = B(x,h(x))$, $\widetilde{C}(x) = C(x,h(x))$.

As before we use the fact that $\mathbf{u}$ is divergence-free and the boundary conditions to obtain

$$\int_0^{h(x)} \partial_x u(x,z)\,dz = \partial_x \int_0^{h(x)} u(x,z)\,dz = 0.$$

After integrating (12), we have

$$\partial_x\left(\widetilde{D}\partial_x p\right) = s\partial_x\left(\widetilde{E}\right) \tag{13}$$

where

$$\widetilde{D} = \left(\widetilde{C} - \frac{\widetilde{B}^2}{\widetilde{A}}\right) \quad \text{and} \quad \widetilde{E} = \frac{\widetilde{B}}{\widetilde{A}}.$$

The velocity $\mathbf{u} = (u, v)$ is determined from the pressure by:

$$u = \left(B - \frac{A\widetilde{B}}{\widetilde{A}}\right)\partial_x p + \left(1 - \frac{A}{\widetilde{A}}\right)s \qquad \text{and} \qquad v = -\int_0^y \partial_x u(x,z)\,dz. \tag{14}$$

The whole system (Reynolds and Cahn-Hilliard equations) reads, in the case where the capillarity coefficient κ is of order ε:

$$\begin{cases} \partial_x(\widetilde{D}(\varphi)\,\partial_x p) = s\,\partial_x \widetilde{E}(\varphi) \\ u(x,y) = \left(B - \dfrac{A\widetilde{B}}{\widetilde{A}}\right)\partial_x p + s\left(1 - \dfrac{A}{\widetilde{A}}\right) \\ v(x,y) = -\displaystyle\int_0^y \partial_x u(x,z)dz \\ \partial_t\varphi + u\,\partial_x\varphi + v\,\partial_y\varphi - \dfrac{1}{\mathrm{Pe}}\,\mathrm{div}(B(\varphi)\nabla\mu) = 0 \\ \mu = -\alpha^2\Delta\varphi + F'(\varphi). \end{cases} \tag{15}$$

with the boundary conditions (2), (3), (7), (10), and the initial condition $\varphi|_{t=0} = \varphi_0$, for $\varphi_0 \in H^1(\Omega)$ compatible with the boundary conditions.

Remark 1 It is to be noticed that the non-dimensionalization choices for α and $B(\varphi)$ imply that the thin film effect only changes the Reynolds equation, and not the Cahn-Hilliard equation. Other choices lead to different equations, which deserve further studies.

3 Theoretical Results

Let us state the following existence theorem (the full details of the proof are given in [4]).

Theorem 1 *Let us denote* $X(\Omega) = \{f \in H^1(\Omega) \cap L^\infty(\Omega),\ \partial_y f \in H^1(\Omega)\}$. *Under some smallness assumptions on* $|\Omega|$ *and under a condition on* F *(somehow more general than convexity), there exists a solution* $(p, \mathbf{u}, \varphi, \mu)$ *of* (15)*, equipped with its initial and boundary conditions, such that*

$$\partial_x p \in L^\infty(0,\infty; H^1(0,L) \cap L^\infty(0,L)), \quad u \in L^\infty(0,\infty; X(\Omega)),$$
$$v \in L^\infty(0,\infty; L^2(\Omega)),\ \varphi \in L^\infty(0,\infty; H^2(\Omega)) \cap L^2_{loc}(0,\infty; H^3(\Omega)),$$
$$\mu \in L^2_{\mathrm{loc}}(0,\infty; H^1(\Omega)).$$

Proof We just sketch out the main steps of the proof, pointing out the main difficulties and differences with previous works [6, 10]. The main idea consists in writing a unique equation on φ by expressing $\mathbf{u}$ and p as a function of φ.

1. Since the Reynolds equation (13) is an elliptic equation on p, we have to prove first the regularity of p as a function of φ, and then deduce the regularity of $\mathbf{u}$ by (14). For the regularity of p, the proof divides in two steps; first the proof of the regularity of the coefficients $\widetilde{D}$, $\widetilde{E}$, and then the coercivity of the elliptic operator $\partial_x(\widetilde{D}\partial_x\cdot)$.
2. For the Cahn-Hilliard equation, the usual approach is to use Galerkin approximations, thus reducing the system to finite dimension, and proving the convergence of these approximations.

We then obtain some a priori estimates on φ and μ in appropriate norms, by multiplying (9a) by μ and (9b) by φ and $\Delta\varphi$, and integrating over Ω:

- The loss of the capillarity term in the limit problem induces difficulties, since usually it cancels with the convection term $\mathbf{u} \cdot \nabla\varphi$ in the Cahn-Hilliard equation. Here, this term of the Cahn-Hilliard equation has to been estimated in order to obtain a priori estimates, and deduce the existence theorem.
- Let us point out that the regularity obtained on the second component v of the velocity is weaker than the regularity obtained with the full Navier-Stokes system ($v \notin L^\infty(\Omega)$). Therefore, the two components of the convection term of the Cahn-Hilliard equation have to be treated separately.
- The boundary conditions on φ take into account the fluid injection phenomena, and correspond to a non homogeneous Dirichlet condition on the left-hand side of the domain, instead of the homogeneous Neumann condition considered e.g. in [6]. This induces many boundary terms coming from the integration by parts which have to be estimated. It is to be emphasized that the non-conservation of the flow (because of the injection) generates estimates of a slightly different type, which are to be dealt with. Moreover, since the mean value $m(\varphi)$ of φ is not constant, classical inequalities on $\varphi - m(\varphi)$ as Poincaré inequality cannot be applied. We have to work with the boundary value of φ given on the left-hand side of the domain, and control the terms induced.

3. A Gronwall argument allows to conclude that $\varphi \in L^\infty(0, \infty; H^2(\Omega))$. From the a priori estimates follow weak convergences. For the convergence of the non-linear term $\mathbf{u} \cdot \nabla\varphi$, we estimate the time derivatives, which allows to conclude the Galerkin process. □

4 Numerical Simulations

4.1 The Numerical Scheme

In order to simulate the behavior of a diphasic flow in thin film, we introduce a numerical scheme for the system (15), which consists in two steps. The first step is the computation of the pressure and the velocity by (13) and (14). For the Reynolds equation, the derivatives are discretized by finite differences, and the integrals (in the coefficients) by the trapezoidal method. Then, the Cahn-Hilliard equation is solved using a method similar to the one introduced in [7, 9].

4.1.1 Time Discretization

For the Cahn-Hilliard equation (9a) and (9b), the time discretization is done with a variable time step δt. First, knowing the values φ^n, μ^n at instant t^n, the first step consists in computing the solution $\varphi^{n+1/2}$, $\mu^{n+1/2}$ of the Cahn-Hilliard equation without the convection term, using a θ-method. More precisely, we consider the following scheme

$$\begin{cases} \dfrac{\varphi^{n+1/2} - \varphi^n}{\delta t} - \dfrac{1}{\mathrm{Pe}} \operatorname{div} \left(B(\varphi^n) \nabla (\theta \mu^{n+1/2} + (1-\theta)\mu^n) \right) = 0, \\ \theta \mu^{n+1/2} + (1-\theta)\mu^n + \alpha^2 \Delta (\theta \varphi^{n+1/2} + (1-\theta)\varphi^n) = \\ \qquad\qquad\qquad\qquad\qquad\qquad F'(\theta \varphi^{n+1/2} + (1-\theta)\varphi^n). \end{cases}$$

The parameter θ is chosen greater than 0.5 in order to ensure the stability, but close enough to 0.5 so that the precision remains good (for example $\theta = 0.6$). This non-linear system is solved with a fixed point method. From a practical point of view, a few iterations are needed for the method to converge.

For the convection part, knowing $\varphi^{n+1/2}$, we compute φ^{n+1} (and then we deduce μ^{n+1} from φ^{n+1} by (9b)). To this end, we define the convection operator K by $K(f) = \mathbf{u} \cdot \nabla f$. The third-order Runge-Kutta scheme reads

$$\varphi^{n+1} - \varphi^{n+1/2} = -\delta t K(\varphi^{n+1/2}) + \frac{1}{2}\delta t^2 K^2(\varphi^{n+1/2}) - \frac{1}{6}\delta t^3 K^3(\varphi^{n+1/2}).$$

4.1.2 Space Discretization

The domain considered here is not rectangular, but since there is no particular point where the mesh should be finer, we consider a regular rectangular mesh of uniform cells, and we re-write all the equations in a rescaled rectangular domain.

For a cell (i, j), the values of p, φ and μ are sought at the center of the cells (of coordinates (i, j)), the values of u at the point of coordinates $(i + 1/2, j)$ and the values of v at $(i, j + 1/2)$. The boundary conditions are discretized in an usual way, introducing artificial unknowns around the physical domain.

We define a finite-difference centered discretization of the convection operator K. In order to ensure that this discretization is L^∞-stable, we use some limiters in the discretization, as proposed for example in [11], and then applied to the Cahn-Hilliard equation in [9]. For this scheme, the C.F.L. (Courant-Friedrich-Levy) condition reads

$$\frac{\delta t}{\delta x} \max_{i,j}(|u_{i+1/2,j}| + |u_{i-1/2,j}|) + \frac{\delta t}{\delta y} \max_{i,j}(|u_{i,j+1/2}| + |u_{i,j-1/2}|) \leq 1.$$

4.2 The Numerical Results

In the field of lubrication, it is of interest to compare the results obtained with the Cahn-Hilliard model with previous results using the Buckley-Leverett equation, for example in [5]. Therefore, we choose the two viscosities of the two fluids to be of ratio $\eta_1/\eta_2 = 10^{-3}$ (which corresponds to the modelling of a lubricant of viscosity η_2 and air). We simulate a flow between two surfaces in relative motion (i.e. with shear effects). The lubricant is supposed to be adhering to the moving surface, and the geometry chosen corresponds to a convergent-divergent upper surface: $L = 1$,

$h(x) = \frac{1}{3}\big(2(2x-1)^2+1\big)$. In order to work in a rectangular domain, the equations are rescaled. The mesh grid has 1000 elements, and we choose the following numerical data: for the shear velocity $s = 1$, for the input flow $q = 0.28$. The injection height is chosen equal to 0.45 (i.e. for $y \in [0, 0.45]$, lubricant is injected, and for $y \in [0.45, 1]$, air is injected). As for the time evolution, the first simulations are similar to the ones obtained in [5], until a saturation point appears. Then the behavior of the two fluids is significantly different, and we present the numerical simulations in Fig. 2 (the black region corresponds to $\varphi = -1$, i.e. the fluid of viscosity η_2, the lubricant).

The velocity field obtained in this simulation is similar to the one obtained in previous works. Let us stretch out that the velocity reverses at the left-hand side of the saturation zone. In our model, there is no hypothesis forcing the boundary between the lubricant and air to be the graph of a function. Therefore, on the contrary to [5], the fluid is not limited by a fictive vertical boundary at the left-hand side of the saturation zone, and the saturation profile is consistent with the velocity field.

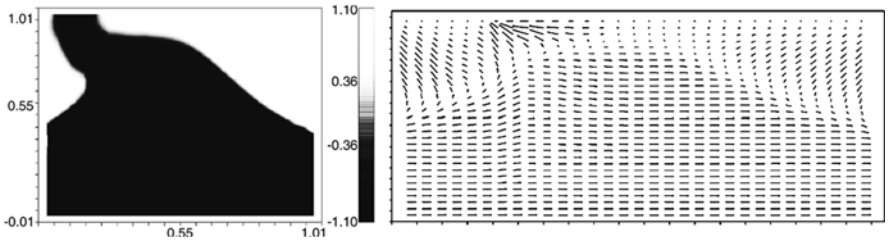

Fig. 2 Saturation profile (repartition of the two fluids) and velocity field in the thin rescaled domain with convergent-divergent upper surface

References

1. Assemien, A., Bayada, G., Chambat, M.: Inertial effects in the asymptotic behavior of a thin film flow. Asymptot. Anal. **9**(3), 177–208 (1994)
2. Bayada, G., Chambat, M.: The transition between the Stokes equations and the Reynolds equation: A mathematical proof. Appl. Math. Optim. **14**(1), 73–93 (1986)
3. Bayada, G., Chambat, M., Ciuperca, I.: Asymptotic Navier-Stokes equations in a thin moving boundary domain. Asymptot. Anal. **21**(2), 117–132 (1999)
4. Bayada, G., Chupin, L., Grec, B.: Some theoretical results concerning diphasic fluids in thin films. Submitted (2009)
5. Bayada, G., Martin, S., Vázquez, C.: About a generalized Buckley-Leverett equation and lubrication multifluid flow. Eur. J. Appl. Math. **17**(5), 491–524 (2006)
6. Boyer, F.: Mathematical study of multi-phase flow under shear through order parameter formulation. Asymptot. Anal. **20**(2), 175–212 (1999)
7. Boyer, F.: Theoretical and numerical study of multi-phase flows through order parameter formulation. In: International Conference on Differential Equations, Vols. 1, 2 (Berlin, 1999), 488–490. World Science Publication, River Edge, NJ (2000)
8. Boyer, F.: Nonhomogeneous Cahn-Hilliard fluids. Ann. Inst. H. Poincaré Anal. Non Linéaire **18**(2), 225–259 (2001)

9. Boyer, F., Chupin, L., Fabrie, P.: Numerical study of viscoelastic mixtures through a Cahn-Hilliard flow model. Eur. J. Mech. B Fluids **23**(5), 759–780 (2004)
10. Chupin, L.: Existence result for a mixture of non Newtonian flows with stress diffusion using the Cahn-Hilliard formulation. Discrete Contin. Dyn. Syst. Ser. B **3**(1), 45–68 (2003)
11. Godlewski, E., Raviart, P.A.: Hyperbolic Systems of Conservation Laws, Mathématiques & Applications (Paris) [Mathematics and Applications], Vol. 3/4. Ellipses, Paris (1991)
12. Marušić-Paloka, E., Stracević, M.: Rigorous justification of the Reynolds equations for gas lubrication. C. R. Mécanique **33**(7), 534–541 (2005)
13. Paoli, L.: Asymptotic behavior of a two fluid flow in a thin domain: From Stokes equations to Buckley-Leverett equation and Reynolds law. Asymptot. Anal. **34**(2), 93–120 (2003)

On the Global Integrability for Any Finite Power of the Full Gradient for a Class of Generalized Power Law Models $p < 2$

Hugo Beirão da Veiga

Abstract In the following we consider a class of non-linear systems that covers some well known generalized Navier-Stokes systems with shear dependent viscosity of power law type, $p < 2$. We show that weak solutions to our class of systems have integrable gradient up to the boundary, with any finite exponent. This result extends, up to the boundary, some of the interior regularity results known in the literature for systems of the above power law type. Boundedness of the gradient, up to the boundary, remains an open problem.

Keywords Navier-Stokes equations · Power law model · Regularity up to the boundary

1 Main Result

In the following we prove $W^{1,q}(\Omega)$-regularity up to the boundary, for any finite power q, for solutions of the system (5) under very weak assumptions on the non-linear term $G(x, \nabla u)$. Our proof, based on a bootstrap argument and Stokes-elliptic regularization (see [3]), is elementary. Nevertheless, the Theorem 1 below extend to a larger class of operators, and up to the boundary, some of the well known results in the literature.

In the sequel Ω is a bounded, connected, open set in $\mathbb{R}^3$, locally situated on one side of its boundary Γ, a manifold of class C^2.

Below we consider solutions to the following class of stationary Navier-Stokes equations for flows with shear (more generally, gradient) dependent viscosity

H. Beirão da Veiga (✉)
Dipartimento di Matematica Applicata "U. Dini" Università di Pisa,
Via F. Buonarroti, 1, 56127-Pisa, Italy
e-mail: bveiga@dma.unipi.it

R. Rannacher, A. Sequeira (eds.), *Advances in Mathematical Fluid Mechanics*,
DOI 10.1007/978-3-642-04068-9_3, © Springer-Verlag Berlin Heidelberg 2010

$$\begin{cases} -\nabla \cdot T(u,\pi) + (u \cdot \nabla)\, u = f, \\ \nabla \cdot u = 0\,, \end{cases} \tag{1}$$

under suitable boundary conditions. T denotes the Cauchy stress tensor

$$T = -\pi\, I + \nu_0\, \mathcal{D}\, u + G(x, \nabla u) \tag{2}$$

and $\mathcal{D}\, u$ is the symmetric gradient, i.e.,

$$\mathcal{D}\, u = \frac{1}{2}\,(\nabla\, u + \nabla\, u^T)\,.$$

Here ν_0 is a strictly positive constant and G is a tensor with components G_{ij}, $i, j = 1, 2, 3$. Note that

$$G = G(x, \mathcal{D}u)$$

is a particular case of $G(x, \nabla u)$. We set

$$|S|^2 = \sum S_{k\,l}^2\,,$$

where $S = S_{kl}$ is a tensor. In the following we assume that $G(x, S)$ satisfies the classical Caratheodory conditions (measurability in x for each S, continuity in S for a.a. x), together with

$$|G(x, S)| \leq c\,(1 + |S|)^{p-1} \tag{3}$$

for some $p \in (1, 2)$. As a particular case of (3), one may have

$$|G(x, S)| \leq c\,(1 + |S|)^{\mu(x)-1} \tag{4}$$

provided that $\mu(x) \leq p < 2$, almost everywhere in Ω. This particular case is related to the theory of electro-rheological fluids. See [8].

It is worth noting that $G(x, \nabla u)$ may depend on each of the first order derivatives $\partial_i\, u_j$ in a totally independent way. In particular, there are not convexity-related assumptions here.

Without loss of generality we assume that $\nu_0 = 1$. From (1) we get

$$\begin{cases} -\,\Delta\, u + \nabla \cdot\, G(x, \nabla\, u) + (u \cdot \nabla)\, u + \nabla\, \pi = f\,, \\ \nabla \cdot u = 0\,. \end{cases} \tag{5}$$

In order to fix ideas we assume here the homogeneous Dirichlet boundary condition

$$u_{|\Gamma} = 0\,. \tag{6}$$

However, many other boundary conditions fall within the above scheme. Actually, it is sufficient that an estimate like (21) holds for the usual Stokes linear system (20) under the desired boundary condition. We may also assume a non-homogeneous Dirichlet boundary condition $u_{|\Gamma} = a(x)$, if $a \in W^{1,+\infty}(\Gamma)$ satisfy the necessary compatibility condition

$$\int_\Gamma a \cdot n \, d\Gamma = 0\,.$$

We take into account any possible weak solution u,

$$u \in W_0^{1,p}(\Omega)\,. \tag{7}$$

Note that (7) may be replaced by $u \in W_0^{1,2}(\Omega)$ (see (11) and (12)). Spaces $W_0^{1,q}(\Omega)$ are endowed here with the norm $\|\nabla u\|_q$.

Remark 1 Our assumptions do not necessarily imply the existence of a solution. However, and this is a crucial point here, many well known existence theorems fall within the assumptions made here.

Our main result is the following.

Theorem 1 *Assume that* (3) *holds and that*

$$f \in L^3(\Omega)\,. \tag{8}$$

Let u *be a solution of problem* (5), (6) *in the class* (7). *Then*

$$u \in W^{1,q}(\Omega) \quad \forall q < +\infty\,. \tag{9}$$

In particular

$$u \in C^{0,\alpha}(\overline{\Omega})\,, \quad \forall \alpha < 1\,. \tag{10}$$

Theorem 1 allows the extension up to the boundary of some of the interior regularity results known in the literature, obtained under much restrictive assumptions on G. In [6], Theorem 3.2.3, it is proved that $\mathcal{D}u \in L^\infty_{loc}(\Omega)$. In Remark 3.2.5 it is pointed out that this last result implies (9) locally in Ω. In Theorem 3.2.1 (10) is proved locally in Ω. See also [5]. Finally, in reference [4], the author proves (9) under more classical assumptions on G.

It remains open, in particular, the conjecture proposed in [6] Remark 3.2.9, namely, to prove that $\mathcal{D}u \in L^\infty(\Omega)$. Actually, by taking into account (9), we may even expect that, in our very general context, $\nabla u \in L^\infty(\Omega)$.

For interior partial regularity results we also refer the reader to [2] (see, in particular, Lemma 3.14) and to [1] and references therein.

Finally we refer to [7] where the authors prove the existence of globally smooth solutions in the two dimensional case under suitable conditions.

2 Proof of Theorem 1

From (5) and (6) we get the "energy estimate"

$$\|\nabla u\|_2^2 \leq \|f\|_{-1,2}\,\|\nabla u\|_2 + c\,\|\nabla u\|_1 + c\,\|\nabla u\|_p^p\,. \tag{11}$$

In particular, it readily follows that

$$\|\nabla u\|_2^2 \leq c(1 + \|f\|_{-1,2})\,. \tag{12}$$

The symbol c denotes, here and in the sequel, positive constants that may depend, at most, on Ω. The same symbol may denote distinct constants.

Note that under any of the typical assumptions that lead to an existence theorem, the term $\|\nabla u\|_p^p$ appears in the left hand side instead of in the right hand side of Eq. (11).

We start by the following result.

Lemma 1 *Let $u \in W_0^{1,p}(\Omega)$ be a weak solution of problem* (5), (6). *Then*

$$\nabla u \in L^3(\Omega)\,. \tag{13}$$

Proof We start by noting that

$$f \in L^3(\Omega) \subset W^{-1,q}(\Omega)\,, \quad \forall q < \infty\,, \tag{14}$$

and that (since $\nabla u \in L^2$)

$$(u \cdot \nabla)\,u \in L^{\frac{3}{2}}(\Omega) \subset W^{-1,3}(\Omega)\,. \tag{15}$$

Set, for each non-negative integer m,

$$r_m = \min\left\{3,\ \frac{2}{(p-1)^m}\right\}. \tag{16}$$

Let us show that

$$\nabla u \in L^{r_m}(\Omega)\,, \quad \forall\, m\,. \tag{17}$$

Clearly (17) holds for $m = 0$. Next we assume that (17) holds for some m and show it for $m + 1$. If $r_m = 3$ then $r_{m+1} = 3$, and the thesis follows. If $r_m < 3$, by appealing to (3) one shows that

$$G(x, \nabla u) \in L^{\frac{2}{(p-1)^{m+1}}}(\Omega) \subset L^{r_{m+1}}(\Omega). \tag{18}$$

In particular, from (14), (15) and (18) it follows that

$$f - \nabla \cdot G(x, \nabla u) - (u \cdot \nabla) u \in W^{-1, r_{m+1}}(\Omega). \tag{19}$$

Well know regularity results, see [3], for the linear Stokes system

$$\begin{cases} -\Delta w + \nabla \widetilde{\pi} = F, \\ \nabla \cdot w = 0, \\ w_{|\Gamma} = 0, \end{cases} \tag{20}$$

state that

$$\|\nabla w\|_q \leq C_q \, \|F\|_{-1,q} , \tag{21}$$

where C_q denotes a suitable positive constant. So, from (19), it follows that (17) holds with m replaced by $m + 1$. Hence it holds for each index m. This shows (13). □

Lemma 2 *Let* $u \in W_0^{1,p}(\Omega)$ *be a weak solution of problem* (5), (6). *Then*

$$\nabla u \in L^6(\Omega). \tag{22}$$

Proof The proof follows that of the previous lemma. Now, since $\nabla u \in L^3(\Omega)$, it follows that $(u \cdot \nabla) u \in L^2(\Omega) \subset W^{-1,6}(\Omega)$. This is used here in place of (15). Furthermore, the exponents r_m, defined by (16), are now replaced by

$$s_m = \min \left\{ 6, \frac{3}{(p-1)^m} \right\}. \tag{23}$$

Details are left to the reader. □

The proof of Theorem 1 follows the same lines. Now we appeal to the fact that $\nabla u \in L^6(\Omega)$ yields

$$f - (u \cdot \nabla) u \in L^3(\Omega) \subset W^{-1,q}(\Omega), \quad \forall q < \infty .$$

Set $t_m = \frac{2}{(p-1)^m}$. Clearly $\nabla u \in L^{t_0}(\Omega)$. If $\nabla u \in L^{t_m}(\Omega)$ then

$$f - \nabla \cdot G(x, \nabla u) - (u \cdot \nabla) u \in W^{-1, t_{m+1}}(\Omega).$$

This leads to $\nabla u \in L^{t_{m+1}}(\Omega)$. So $\nabla u \in L^{t_m}(\Omega)$ for all m. This proofs (9).

Remark 2 It is worth noting that if the constants C_q were uniformly bounded for large values of q then we could easily prove the uniform boundedness of the norms $\|\nabla u\|_q$, hence the Lipschitz continuity of u up to the boundary. However, it may be proved, see [9], that for the scalar equation $-\Delta w = F$ under the homogeneous Dirichlet boundary condition, one has $\|w\|_{2,q} \leq C_q \|F\|_q$, where $C_q \approx q$, as $q \to \infty$. At best, we expect this same behavior for the constants C_q in the case of the Stokes problem (20). By merely assuming this behavior, specific estimates obtained by following our proof do not lead to the above uniform boundedness.

References

1. Apushkinskaya D., Bildhauer, M., Fuchs, M.: Steady states of anisotropic generalized Newtonian fluids. J. Math. Fluid Mech. **7**, 261–297 (2005)
2. Bildhauer, M.: *Convex Variational Problems*. Lecture Notes in Mathematics, 1818. Springer-Verlag, Berlin (2003)
3. Cattabriga, L.: Su un problema al contorno relativo al sistema di equazioni di Stokes. Rend. Sem. Mat. Univ. Padova **31**, 308–340 (1961)
4. Crispo, F.: A note on the global regularity of steady flows of generalized Newtonian fluids. Portugaliae Math. **66**, 211–223 (2009)
5. Fuchs, M.: Regularity for a class of variational integrals motivated by nonlinear elasticity. Asymp. Analysis **9**, 23–38 (1994)
6. Fuchs, M.: Seregin G.: *Variational Methods for Problems from Plasticity Theory and for Generalized Newtonian Fluids*. Lecture Notes in Mathematics, 1749. Springer-Verlag, Berlin (2000)
7. Kaplický, P., Málek, J., Stará, J.: $\mathcal{C}^{1,\alpha}$-solutions to a class of nonlinear fluids in two dimensions-stationary Dirichlet problem. POMI, **259** , 89–121 (1999)
8. Ružičza M.: Modeling, mathematical and numerical analysis of electrorheological fluids. Appl. of Math. **49**, 565–609 (2004)
9. Yudovich, V.I.: Some estimates connected with integral operators and with solutions of elliptic equations. Soviet Math. Dokl. **2** , 746–749 (1961)

Steady Flow Around a Floating Body: The Rotationally Symmetric Case

Josef Bemelmans and Mads Kyed

Abstract We investigate the steady motion of a viscous incompressible fluid around a floating body which is rotating with a constant angular velocity. The fluid flow is described by a free boundary problem for the Navier-Stokes equations, where the free boundary consists of the capillary surface of the fluid and the wetted part of the floating body.

Keywords Free boundary problems · Navier-Stokes equations · Capillarity (surface tension) · Rotating fluids

1 Introduction

In this paper we consider the stationary flow of a viscous incompressible fluid which is generated by a circular cylinder $\mathcal{C}$ or by a more general rotationally symmetric body $\mathcal{B}$ that is partly immersed in it and that rotates with prescribed angular velocity. We formulate the problem for a floating cylinder first and describe in Sect. 4 how to proceed in the general case. The density of $\mathcal{C}$ is assumed to be smaller than that of the fluid, and therefore the cylinder is floating on the liquid; hence the position of $\mathcal{C}$ is a further unknown of the problem. The upper boundary of the fluid consists of a capillary surface, such that we are about to solve the free-boundary problem (Fig. 1)

$$\begin{cases} -\mu\,\Delta\,\underline{v} + Dp + \varrho\,(\underline{v}\cdot D)\,\underline{v} = -\varrho\,g\,\underline{e}_3 & \text{in } \Omega\,, \\ \operatorname{div}\underline{v} = 0 & \text{in } \Omega\,, \end{cases} \tag{1}$$

J. Bemelmans (✉)
Institut für Mathematik, RWTH Aachen, D-52062 Aachen, Germany
e-mail: bemelmans@instmath.rwth-aachen.de

R. Rannacher, A. Sequeira (eds.), *Advances in Mathematical Fluid Mechanics*,
DOI 10.1007/978-3-642-04068-9_4, © Springer-Verlag Berlin Heidelberg 2010

where, putting $r = \sqrt{x_1^2 + x_2^2}$ and $z = x_3$, the domain Ω occupied by the fluid is given by

$$\Omega := \Big\{x \in \mathbb{R}^3 \mid 0 \le r < R\,, \quad \begin{array}{ll} 0 < z < a + \alpha(r) & \text{for } 0 \le r < r_0\,, \\ 0 < z < \zeta(r) & \text{for } r_0 \le r < R \end{array} \Big\}\,. \tag{2}$$

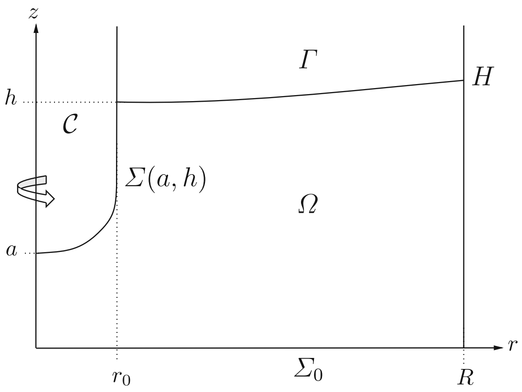

Fig. 1 Floating cylinder in a bounded fluid reservoir

Here μ denotes the coefficient of viscosity, ϱ the density of the fluid, and g the gravitational constant. We shall impose a no-slip boundary condition on the fluid-structure boundaries. Consequently, on the wetted part of $\mathcal{C}$,

$$\Sigma(a,h) := \Big\{x \in \mathbb{R}^3 \mid \begin{array}{ll} z = a + \alpha(r) & \text{for } 0 \le r < r_0\,, \\ a + r_0 \le z < h & \text{for } r = r_0 \end{array} \Big\}\,, \tag{3}$$

we impose the boundary condition

$$\underline{v}(x) = \underline{\omega} \wedge x \quad \text{on } \Sigma(a,h)\,, \tag{4}$$

where $\omega = (0, 0, \omega_3) \in \mathbb{R}^3$ is the angular velocity of $\mathcal{C}$. On the bottom,

$$\Sigma_0 := \big\{x \in \mathbb{R}^3 \mid 0 \le r < R\,,\ z = 0\big\}\,,$$

and the wetted part of the lateral boundary of the container,

$$\Sigma(H) := \big\{x \in \mathbb{R}^3 \mid r = R\,,\ 0 \le z < H\big\}\,,$$

we have

$$\underline{v} = 0 \quad \text{on } \Sigma_0 \cup \Sigma(H)\,. \tag{5}$$

On the capillary surface, Γ, that separates the fluid from the atmosphere above it, we impose the mixed boundary condition

$$\underline{v} \cdot \underline{n} = 0\,,\ \underline{\tau}_k \cdot \underline{\underline{T}}(\underline{v}, p) \cdot \underline{n} = 0 \quad \text{on } \Gamma \quad (k = 1, 2)\,, \tag{6}$$

where $\underline{n}$ is the exterior normal to Ω, and $\underline{\tau}_1, \underline{\tau}_2$ span the tangent plane on Γ. As usual

$$\underline{\underline{T}}(\underline{v}, p) := -p\underline{\underline{I}} + \mu\,(D\underline{v} + D\underline{v}^T)$$

denotes the stress tensor of the fluid. The capillary surface is the graph of a real function $\zeta = \zeta(r)$,

$$\Gamma := \left\{x \in \mathbb{R}^3 \mid z = \zeta(r)\,,\ r_0 < r < R\right\}, \tag{7}$$

which satisfies

$$\frac{1}{r}\,\frac{d}{dr}\left(\frac{r\zeta_r}{\sqrt{1+\zeta_r^2}}\right) = \sigma\,\underline{n} \cdot \underline{\underline{T}}(\underline{v}, p) \cdot \underline{n} \quad \text{for } r_0 < r < R \tag{8}$$

together with the boundary conditions

$$\frac{d\zeta}{dr}(r) = 0 \quad \text{for } r = r_0 \text{ and } r = R\,. \tag{9}$$

Note that (9) implies that the capillary surface meets the rigid walls at a right angle. As the fluid is assumed to be incompressible, we further require

$$\operatorname{vol}\Omega = V_0\,. \tag{10}$$

This condition determines the height of the capillary surface:

$$h_0 := \zeta(r_0) \text{ and } h_R := \zeta(R). \tag{11}$$

Finally, we have the equilibrium condition

$$\int_{\Sigma(a,h)} \underline{\underline{T}}(\underline{v}, p) \cdot \underline{n}\, d\sigma = m\, g\, \underline{e}_3\,, \tag{12}$$

where m denotes the mass of $\mathcal{C}$. From this condition, the depth to which $\mathcal{C}$ is immersed in the fluid can be be determined. We shall use a to denote this depth.

In order to avoid a complicated analysis of (1) in domains with corners, we assume that the lower half of a ball is attached to the cylinder $\mathcal{C}$ such that its boundary is smooth where it is in contact with the fluid. In a similar way, the assumption (9) on the capillary angle allows for regular solutions $\underline{v}$ and p up to the ridge at the fluid-structure contact line.

The free-boundary problem (1)–(12) can also be solved for an unbounded layer of fluid. In this case Σ_0 and Γ extend to infinity, which means that $\zeta = \zeta(r)$ is defined on (r, ∞). We then require

$$\lim_{r\to\infty} \zeta(r) = h_\infty \tag{13}$$

and

$$\lim_{x_1^2+x_2^2\to\infty} \underline{v}(x) = 0, \tag{14}$$

Our main proof of existence is based on the implicit function theorem; in order to apply it one has to find suitable function spaces for $\underline{v}$, p and ζ such that the nonlinear mapping that is defined by the equations in Ω and on the boundary of Ω has a Frechet-derivative which is an isomorphism on these spaces. Following Sattinger [8] we work in Hölder-spaces, namely $u = (\underline{v}, p, \zeta, a) \in \mathcal{X} := C^{2,\alpha} \times C^{1,\alpha} \times C^{3,\alpha} \times \mathbb{R}$, and we first show that a sequence of successive approximations $(\underline{v}_n, p_n, \zeta_n, a_n)$ is well-defined on $\mathcal{X}$ in the sense that for any $(\underline{v}_n, p_n, \zeta_n, a_n) \in \mathcal{X}$ the next approximation lies in the same space. We then show that the difference of two approximations is small in the norm of $\mathcal{X}$ provided the data are small.

As the functions $(\underline{v}_n, p_n)$ and $(\underline{v}_{n+1}, p_{n+1})$ are solutions to the Navier-Stokes equations in different domains this requires several transformations onto a standard domain; when constructing these mappings one has to take several side conditions into account.

The flow generated by a rotating cylinder whose position is fixed, rather than determined by the force of buoyancy, is the topic of the first free-boundary problem for the Navier-Stokes equations that could be solved analytically; D.H. Sattinger proved in [8] existence and uniqueness of a classical solution if the angular velocity is small. We not only apply the approximation scheme from [8] but also construct the transformations of the domains Ω_n in such a way that we can use the careful calculations from [8] that eventually yield regularity of the solution up to the ridge where the capillary surface Γ and the cylinder $\mathcal{C}$ meet.

2 Approximation Scheme

To define the approximation scheme that eventually leads to a solution of the free-boundary problem, we start with the static configuration $\Omega_0 = \Omega(a_0, \zeta_0)$, where $\zeta_0(r) = h_0$ on $[r_0, R]$, $\underline{v}_0(x) \equiv 0$ and $p_0(x) = \text{const}$ on Ω. The cylinder is in equilibrium which means that

$$\varrho\, V(a_0, h_0) = \varrho_0\, \text{vol}(\mathcal{C})\ , \tag{15}$$

where $V(a_0, h_0)$ is the volume of the part of $\mathcal{C}$ lying below the fluid-cylinder contact line, see Fig. 2.

Fig. 2 Static configuration

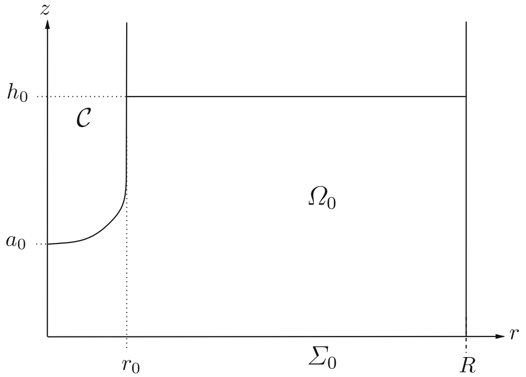

First we solve the Navier-Stokes equations (1) in Ω_0 under the boundary conditions (4), (5), and (6), and we denote the solution by $(\underline{v}_1, p_1)$. From this we calculate

$$\underline{n}_0(x) \cdot \underline{\underline{T}}(\underline{v}_1(x), p_1(x)) \cdot \underline{n}_0(x) \quad \text{for } x \in \Gamma_0 \ ,$$

and we consider this quantity as a function $g_1 = g_1(r)$, $r \in (r_0, R)$. For this g_1 we solve the mean curvature equation (8) with the Neumann boundary condition (9). Its solution ζ_1' is unique up to an additive constant c_1. Next we calculate the stress tensor on the wetted part of $\partial\mathcal{C}$:

$$\underline{t}_1(x) := \underline{\underline{T}}(\underline{v}_1(x), p_1(x)) \cdot \underline{n}_0(x) \quad \text{for } x \in \Sigma\,(a_0, h_0).$$

The cylinder will generally no longer be in equilibrium with this force, but either plunge deeper into the fluid or rise higher out of it. This change in position will be described by the new height a_1 of $\mathcal{C}$ above the bottom of the container. The solution $(\underline{v}_1, p_1)$ is rotationally symmetric; the stress vector $\underline{t}_1(x),\ x \in \Sigma\,(a_0, h_0)$, may have an r-component that is different from zero, but due to the symmetry, the resultant of $\underline{t}_1(x)$ over $\Sigma\,(a_0, h_0)$ is a vector that points in the z-direction. When we determine a_1 we must take the volume constraint (10) into account; a decrease in the height of $\mathcal{C}$ results in an increase of the free boundary by some constant and vice versa. This determines c_1, and we set $\zeta_1(r) := \zeta_1'(r) + c_1,\ h_1 := \zeta_1(r_0),\ H_1 := \zeta_1(R)$. For the corresponding new domain $\Omega_1 := \Omega(a_1, \zeta_1)$ we have

$$\text{vol}(\Omega_1) = V_0 \ . \tag{16}$$

Furthermore

$$\varrho V(a_1, h_1)\, g\, \underline{e}_3 = \int\limits_{\Sigma(a_0,h_0)} \underline{t}_1(x) d\sigma(x) \ . \tag{17}$$

To obtain the next approximation we solve (1) in Ω_1 with boundary conditions (4) on $\Sigma(a_1, h_1)$, (5) on $\Sigma_0 \cup \Sigma(H_1)$ and (6) on Γ_1, the graph of ζ_1. We call the solution (v_2, p_2) and construct from it a_2 and ζ_2 as we did for a_1 and ζ_1.

In the case of an unbounded layer we argue somewhat differently because the solution of the mean curvature equation (8) on (r_0, ∞) with boundary data

$$\frac{d\zeta}{dr}(r) = 0 \quad \text{for } r = r_0 \tag{18}$$

and (13) is now uniquely determined. From $(\underline{v}_1, p_1)$ we calculate $g_1(r)$ as before and solve (8), (18), (13) for this g_1. The solution $\zeta_1 = \zeta_1(r)$ attains some value $h_1 = \zeta_1(r_0)$ at the boundary. When we next compare

$$\int_{\Sigma(a_0,h_0)} \underline{t}_1(x) d\sigma$$

with $\varrho_0 \, V(a_0, h_0) \, g \, \underline{e}_3$, we can change a_0 into a_1 such that

$$\varrho_0 V(a_1, h_1) \, g \, \underline{e}_3 = \int\limits_{\Sigma(a_0,h_0)} \underline{t}_1(x) \, d\sigma(x) \tag{19}$$

because in an unbounded reservoir we need not compensate the height of the free boundary if we change a_0.

The successive approximation is based on the following existence theorem.

Theorem 1 *Let Ω_0 and Γ_0 be defined as above. Then there exists a unique solution $(\underline{v}, p) \in C^{2,\alpha}(\overline{\Omega}_0) \times C^{1,\alpha}(\overline{\Omega}_0)$ with $\int_{\Omega_0} p = 0$ to the stationary Stokes equations*

$$\begin{cases} -\mu \Delta \underline{v} + Dp = -\varrho \, g \, \underline{e}_3 & \text{in } \ \Omega_0 \, , \\ \operatorname{div}(\underline{v}) = 0 & \text{in } \ \Omega_0 \, , \end{cases} \tag{20}$$

with boundary conditions (4) *on $\Sigma(a_0, h_0)$,* (5) *on $\Sigma_0 \cup \Sigma(h_0)$, and* (6) *on Γ_0.*

For the existence of a unique solution that is regular up to the smooth part of the boundary we refer to [11]. Regularity up to the fluid-structure contact line has been shown in [8] by a reflection argument that can be applied because of the following compatibility conditions: In cylindrical coordinates $\underline{v} = (v_r, v_\vartheta, v_z) \equiv (u, v, w)$ the boundary conditions (4) and (6) read

$$\begin{aligned} & u = w = 0 \, , \ v = \text{const} \quad \text{on } \Sigma(a_0, h_0) \, , \\ & \frac{\partial u}{\partial z} = \frac{\partial v}{\partial z} = w = 0 \quad \text{on } \Gamma_0 \, . \end{aligned} \tag{21}$$

On $\Sigma \, (a_0, h_0)$ derivatives of $\underline{v}$ with respect to ϑ and z vanish, and the same holds on Γ_0 for derivatives in r- and in ϑ-direction. If one inserts these values into the equations of motion one gets the following compatibility conditions in the corner:

$$\frac{\partial u}{\partial r} = 0\,,\ \frac{\partial^2 w}{\partial r^2} = 0\,,\ \frac{\partial w}{\partial r} = 0\,,\ \frac{\partial^2 u}{\partial r \partial z} = 0\,,\ \frac{\partial p}{\partial z} = 0\,. \tag{22}$$

Regularity is there shown by first extending the solution across $r = r_0$ and after that by reflecting it across the plane $\{z = h_0\}$.

The results of Theorem 1 hold for more general domain Ω where Γ need not be planar, but still meets the cylinder $\mathcal{C}$ at a right angle.

In this case the domain Ω is transformed onto Ω_0, and in the new coordinates the equations of motion become rather involved, cf. (28) below. It is essential that near the corner the transformation affects only the z-component such that the compatibility conditions (22) remain basically unchanged.

The solutions obtained in Theorem 1 are of class $C^{2,\alpha}(\overline{\Omega}_0) \times C^{1,\alpha}(\overline{\Omega}_0)$ as long as the boundary is of class $C^{3,\alpha}$ – apart from the corner points. Therefore the approximation $(\underline{v}_n, p_n, \zeta_n)$ will be in the same space $\mathcal{X} := C^{2,\alpha} \times C^{1,\alpha} \times C^{3,\alpha}$ as $(\underline{v}_{n-1}, p_{n-1}, \zeta_{n-1})$ if the solution ζ_n of (8) with data $\underline{n} \cdot \underline{\underline{T}}(\underline{v}_{n-1}, p_{n-1}) \cdot \underline{n} \equiv g_{n-1}$ is of class $C^{3,\alpha}$. Now for $\zeta_{n-1} \in C^{3,\alpha}$ the normal $\underline{n}$ to its graph is of class $C^{2,\alpha}$; for $(\underline{v}_{n-1}, p_{n-1}) \in C^{2,\alpha} \times C^{1,\alpha}$ we have $\underline{\underline{T}}(\underline{v}_{n-1}, p_{n-1}) \in C^{1,\alpha}$, hence $g_{n-1} \in C^{1,\alpha}$. Then clearly a solution to (8) is of class $C^{3,\alpha}$. Existence of such solutions can be shown by proving a-priori estimates or by variational methods, see [4].

Remark 1 Free-boundary problems for an infinite layer of fluid that is bounded on top by a capillary surface have been investigated by R.S. Gellrich in [5] and [6]. Her results can be applied to the problem above, where Ω is an infinite layer with boundary conditions (13) and (14), since the presence of a bounded floating body does not affect the properties of the solution at infinity.

3 A Solution to the Free-Boundary Problem for a Cylinder

The sequence of successive approximations $\{\underline{v}_n, p_n, \zeta_n, a_n\}$ converges if we can estimate the differences $\underline{v}_n - \underline{v}_m$ etc. in appropriate norms. While all ζ_n are defined on the same domain $[r_0, R]$, this is not the case for $\underline{v}_n$ and p_n. Therefore we construct diffeomorphisms $\underline{W}_n : \overline{\Omega}_0 \to \overline{\Omega}_n$, such that we can define $\underline{v}_{n+1}$ on $\underline{W}_n^{-1}(\overline{\Omega}_n)$. Once all functions v_m are defined on $\overline{\Omega}_0$ we can estimate their differences.

We now describe the construction of the transformation $\underline{W} : \overline{\Omega}_0 \to \overline{\Omega}$ as well as the transformed equations and the unknowns. We omit from now on the index n for simplicity.

If $\underline{W} : \overline{\Omega}_0 \to \overline{\Omega}$ is a diffeomorphism we set

$$g_{ij} := \frac{\partial \underline{\underline{W}}}{\partial x_i} \cdot \frac{\partial \underline{\underline{W}}}{\partial x_j} \tag{23}$$

for the corresponding metric tensor. Then the original vector field $\underline{v}$ has components v^i defined on Ω_0 by

$$v^i := g^{ij}\,(\underline{v}\cdot\frac{\partial \underline{W}}{\partial x_j})\,, \tag{24}$$

cf. [8, Chap. 3] or for a more general presentation [1, §8]. We denote the covariant derivative of v^i by $v^i_{,j}$ and set

$$v_i := g_{ij}\, v^j \tag{25}$$

$$D_{ij} := \frac{1}{2}(v_{i,j} + v_{j,i}) \tag{26}$$

$$D^i_j := g^{i\,m}\, D_{mj}. \tag{27}$$

D^i_j is the transformed deformation tensor. Then we get the Navier-Stokes equations in the new variables:

$$\begin{cases} -2\mu\, g^{jk}\, D^i_{j,k} + g^{ij}\dfrac{\partial p}{\partial x_j} + v^j v^i_{,j} = 0 \quad \text{in } \Omega_0\,, \\ \hfill v^i_{,i} = 0 \quad \text{in } \Omega_0\,. \end{cases} \tag{28}$$

The boundary conditions on $\Sigma(a,h)$ are

$$g_{ij}\, v^i\, e^j_r = 0\,,\;\; g_{ij}\, v^i\, e^j_\vartheta = \omega\,,\;\; g_{ij}\, v^i\, e^j_z = 0\,, \tag{29}$$

where $\underline{e}_r, \underline{e}_\vartheta, \underline{e}_z$ are the basis vectors. On the free surface we now have

$$v^i n_i = g_{ij} v^i n^j = 0\,,\; (-p g_{ij} + 2D_{ij}) n^j = \sigma \mathcal{H} n_i\,, \tag{30}$$

where $\mathcal{H}$ is the mean curvature.

The construction of $\underline{W}$ takes three properties of Ω into account: The height of $\mathcal{C}$ above $\{z=0\}$ changes from a_0 to a, Ω must have the same volume as Ω_0, and the upper surface is $z=\zeta(r)$ instead of $z=h_0$. First we define $\underline{L} : \overline{\Omega}_0 \to \overline{\Omega}'_0$, where Ω'_0 is defined as Ω_0 but with a_0 replaced by a and h_0 replaced by $h'_0 := h_0 + a - a_0$, i.e. the cylinder and the boundary Γ_0 have been lowered by $a - a_0$ (or rather raised by that amount). We define

$$\underline{L}(r,\vartheta,z) := (r,\vartheta, f_1(z))$$

with

$$f_1(z) := \begin{cases} z + a - a_0 & \text{for } a_1 \le z \le h_0\,, \\ z + a - a_0 + \dfrac{a_0 - a}{a_1^4}(z - a_1)^4 & \text{for } 0 \le z \le a_1\,. \end{cases}$$

Here a_1 is some height less than $\frac{1}{2}\min(a, a_0)$. Note that f_1 is a smooth function, and near the contact point the deformation is a translation in z-direction. Now the volume of Ω_0' differs from V_0 by $2\pi R^2(a_0 - a)$. We compensate this by the transformation $\underline{M} : \overline{\Omega_0'} \to \overline{\Omega_0''}$, where Ω_0'' is of the same form as Ω_0' but the upper surface is now $z = h_0'' := h_0' + \alpha$, where α satisfies

$$R^2(a_0 - a) = (R^2 - r_0^2)\alpha \,.$$

We fix some height $h_2 < h_0'$ and define

$$f_2(z) := \begin{cases} z & \text{for } 0 \le z \le h_2 \,, \\ z + \dfrac{a_0 - a + \alpha}{(h_0' - h_2)^4}(z - h_2)^4 & \text{for } h_2 \le z \le h_0' \,, \end{cases}$$

and

$$\underline{M}(r, \vartheta, z) := (r, \vartheta, f_2(z)) \,.$$

Finally, we transform Ω_0'' onto Ω, where the upper surface is now given by $z = \zeta(r)$. Moreover, as the solution ζ to (8), (9) is unique up to an additive constant, we may assume

$$\int_{r_0}^{R} (\zeta(r) - h_0'')\, r\, dr = 0 \,.$$

As before we define

$$f_3(z) := \begin{cases} z & \text{for } 0 \le z \le h_2 \,, \\ z + \dfrac{\zeta(r) - h_0''}{(h_0'' - h_2)^4}(z - h_2)^4 & \text{for } h_2 \le z \le h_0'' \,, \end{cases}$$

and set $\underline{N}(r, \vartheta, z) = (r, \vartheta, f_3(z))$. Then $\underline{W} = \underline{N} \circ \underline{M} \circ \underline{L}$ maps Ω_0 onto Ω, and if we compare this mapping with the transformation $\underline{W}$ in [8, (3.1)] we see that it is of the same form because the quantities $|a_0 - a|$, $|h_0'' - h_0'|$, and $|\zeta(r) - h_0''|$ are small if the angular velocity ω is small. Therefore Theorem 5.1 from [8] can be applied, and we obtain a solution to the free-boundary problem (1)–(12).

4 A Solution to the Free-Boundary Problem for a Rotationally Symmetric Body

We now extend the reasoning from before to the case of a rotationally symmetric body $\mathcal{B}$ that is not necessarily a cylinder. If we now consider different heights a of the body above $\{z = 0\}$, the corresponding capillary surfaces $\zeta_0(r)$ are no longer constants; and these functions will be defined on different intervals $[r_1, R]$ where r_1 depends on a, see Fig. 3. We can, however, use the same transformations $\underline{W}$ as

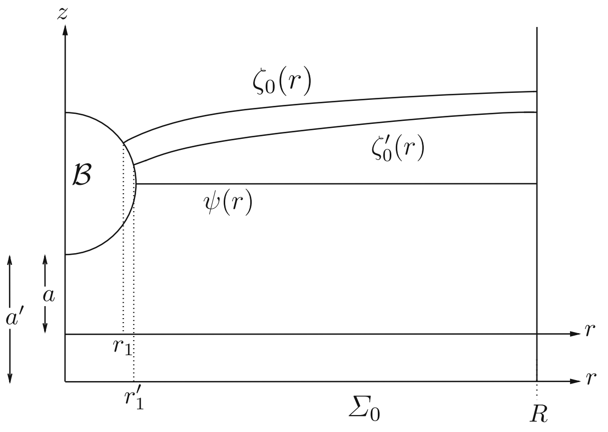

Fig. 3 Floating body in a bounded fluid reservoir

before if we introduce a coordinate system that consists of a family of capillary surfaces $\zeta = \zeta(r, \alpha)$, where α refers to the volume that is included by ζ. These functions correspond to the surfaces $z = \alpha = \text{const}$ in the previous case, which are also capillary surfaces including different volumes for different values of α. Curves that are perpendicular to the family $\zeta = \zeta(r, \alpha)$ replace the z-coordinate.

We assume $\mathcal{B}$ to be convex because we want to exclude situations where the region occupied by the fluid is no longer connected. For a convex body $\mathcal{B}$ there exists a point $P \in \partial\mathcal{B}$ such that the normal vector in P points into the r-direction. The curve that describes $\partial\mathcal{B}$ between 0 and P is the graph of a function $\psi = \psi(r)$, and $P = (r_2, \psi(r_2))$. For $r > r_2$ we set $\psi(r) = \psi(r_2)$. Then the capillary surfaces $\zeta = \zeta(r)$ for which $\int(\zeta(r) - \psi(r))\, r\, dr$ is positive are solutions to the following variational problem:

Theorem 2 *Let $\psi = \psi(r)$, $0 \leq r \leq R$, as defined above. For $\zeta = \zeta(r)$, $0 \leq r \leq R$, set*

$$I^+ := [0, R] \cap \{r \mid \zeta(r) > \psi(r)\}.$$

Then the variational problem

$$\mathcal{F}(\zeta) := \int\limits_{I^+} \sqrt{1 + \zeta_r^2(r)}\, r\, dr + \frac{k}{2} \int_{I^+} \zeta^2(r)\, r\, dr \;\to Min \tag{31}$$

in

$$\mathcal{E} := \left\{\zeta \in BV[0, R] \mid \zeta(0) = \psi(0)\,,\; \zeta(r) \geq \psi(r)\,,\; \int_{I^+} (\zeta(r) - \psi(r))\, r\, dr = V_0\right\}$$

has a unique solution $\zeta \in \mathcal{E}$.

The solvability of this problem and many properties of the solutions are well-known, cf. [3]. The set $\{r \mid \zeta(r) > \psi(r)\}$ is a single interval $(r_1, R]$, and ζ satisfies the Euler-Lagrange equation

$$\frac{d}{dr}\left(\frac{r\,\zeta_r(r)}{\sqrt{1+\zeta_r^2(r)}}\right) = kr\,\zeta(r) + \lambda\, r \quad \text{for } r \in (r_1, R)\,, \tag{32}$$

and in the endpoints r_1 and R we have

$$\zeta_r(R) = 0 \tag{33}$$

and

$$1 + \psi_r(r_1)\,\zeta_r(r_1) = 0\,. \tag{34}$$

Condition (33) is the same as in (9) before, whereas (34) is a transversality condition, cf. [2, p. 44]:

$$r_1\sqrt{1+\zeta_r^2(r_1)} + \Big[\psi_r(r_1) - \zeta_r(r_1)\Big]\frac{r_1\,\zeta_r(r_1)}{\sqrt{1+\zeta_r^2(r_1)}} = 0\,. \tag{35}$$

Equation (34) follows immediately from (35), and it states that the graphs of ψ and ζ meet under a right angle. The Lagrange multiplier λ can be calculated explicitly from (32):

$$\int_{r_1}^{R} \frac{d}{dr}\left(\frac{r\,\zeta_r(r)}{\sqrt{1+\zeta_r^2(r)}}\right) dr = k\int_{r_1}^{R} \zeta(r)\,r\,dr + \lambda\int_{r_1}^{R} r\,dr\,,$$

hence we get

$$\lambda = \frac{2}{R^2 - r_1^2}\left(\frac{r_1}{\sqrt{1+\psi_r^2(r_1)}} - k\int_{r_1}^{R}\zeta(r)\,r\,dr\right),$$

and as the last integral is $V_0 + \int_{r_1}^{R}\psi(r)\,r\,dr$, we see that λ depends on V_0 monotonically. For $\lambda_1 < \lambda_2$ the corresponding solutions ζ_1 and ζ_2 from Theorem 2 satisfy $\zeta_1(r) \geq \zeta_2(r)$, and in particular

$$\zeta_1(r) > \zeta_2(r) \tag{36}$$

for all r with $\zeta_2(r) > \psi(r)$. This monotone behavior was proved in [9, Theorem 4.23], see also [10].

We can now proceed as in the previous chapter. To a given V_0 there exists a unique solution ζ_0 as in Theorem 2, and to $V_\alpha \in (V_0 - \varepsilon, V_0 + \varepsilon)$ we obtain corresponding solutions ζ_α with the properties above.[1] Then we introduce coordinates ϱ and η where ϱ is the parameter of arc length on the graph of ζ_0 and η on the curves perpendicular to the family ζ_α. Locally the boundary of $\mathcal{B}$ is described by $\{\varrho = 0\}$, which means that it is a cylinder in these coordinates. Therefore we can use the same transformation as in Sect. 3 for the successive approximations $\{\underline{v}_n, p_n, \zeta_n, a_n\}$ to the free-boundary problem. Consequently, we obtain the following theorem of existence.

Theorem 3 *Let $\mathcal{B}$ be a convex and rotationally symmetric body with the properties described in the introduction. Then the free-boundary problem* (1)–(12) *has a unique solution* $(\underline{v}, p, \zeta, a)$ *for ω sufficiently small.*

Remark 2 The reasoning from this chapter cannot be extended to the case of an unbounded layer of fluid, because in that case the capillary surface does no longer include a finite volume, and therefore we do not have a Lagrange multiplier as above.

Remark 3 After submitting the manuscript we learned that the free boundary problem that was investigated by Sattinger has been solved in Sobolev spaces by Jin in [7].

References

1. Aris, R.: *Vectors, Tensors, and the Basic Equations of Fluid Mechanics.* Englewood Cliffs, NJ: Prentice-Hall (1962)
2. Bolza, O.: *Vorlesungen über Variationsrechnung.* Leipzig: B.G. Teubner (1909)
3. Buttazzo, G., Giaquinta, M., Hildebrandt, S.: *One-Dimensional Variational Problems. An introduction.* Oxford Lecture Series in Mathematics and its Applications, 15. Oxford: Clarendon Press (1998)
4. Finn, R.: *Equilibrium Capillary Surfaces.* Grundlehren der Mathematischen Wissenschaften, 284. New York etc.: Springer-Verlag (1986)
5. Gellrich, R.: Freie Randwertprobleme der Stationären Navier-StokesGleichungen bei Nichtkompakten Rändern. Ph.D. Thesis, Universität des Saarlandes (1991)
6. Gellrich, R.: Free boundary value problems for the stationary Navier-Stokes equations in domains with noncompact boundaries. Z. Anal. Anwend. **12**(3), 425–455 (1993)
7. Jin, B.J.: Free boundary problem of steady incompressible flow with contact angle $\frac{\pi}{2}$. J. Differ. Eqn. **217**(1), 1–25 (2005)
8. Sattinger, D.: On the free surface of a viscous fluid motion. Proc. R. Soc. Lond. Ser. A **349**, 183–204 (1976)
9. Schindlmayr, G.: Kapillarität im Kegel und in allgemeineren skalierten Gebieten. Ph.D. Thesis, RWTH-Aachen (1998)
10. Schindlmayr, G.: Capillary surfaces in non-cylindrical domains. Z. Anal. Anwend. **19**(3), 747–762 (2000)
11. Solonnikov, V., Scadilov, V.: On a boundary value problem for a stationary system of Navier-Stokes equations. Proc. Steklov Inst. Math. **125**, 186–199 (1973)

[1] In the field theory of the calculus of variations this family is called a field of extremals.

On a Stochastic Approach to Eddy Viscosity Models for Turbulent Flows

Luigi C. Berselli and Franco Flandoli

Abstract The aim of this note is twofold: we review some basic results which are at the basis of the derivation of eddy viscosity methods for large eddy simulation (LES) and we also try to combine them with the Stochastic approach to the Navier-Stokes equations. In particular, we propose a stochastic approach to the introduction of eddy viscosity LES methods and we evaluate by means of probabilistic techniques generalizations of the Lilly's constant. Next, we propose some heuristic for alternate modeling of sub-grid-scale terms and we apply scaling techniques to the derivation of a model for channel flows.

Keywords Navier-Stokes equations · Turbulence · LES · Stochastic modeling

1 Introduction

In this paper we consider the 3D Navier-Stokes equations describing an incompressible viscous Newtonian fluid with constant (equal to one) density

$$\begin{cases} \dfrac{\partial u}{\partial t} + \nabla \cdot (u \otimes u) + \nabla \pi - \nu \Delta u = f, \\ \text{div } u = 0, \\ u|_{t=0} = u_0. \end{cases} \tag{1}$$

It is well-known that mathematical difficulties arise in the study of the well-posedness of the Cauchy problem: If the viscosity is large (compared to the data), then a unique smooth solution exists for all positive times. For arbitrary positive viscosity and L^2-initial data (and external force) then existence of Leray-Hopf weak solutions is known since about 1930, while proving global regularity (or breakdown of smooth solutions) is a challenging problem, see the review in Galdi [18]. On the

L.C. Berselli (✉)
Dipartimento di Matematica Applicata "U. Dini," Università di Pisa, Via F. Buonarroti 1/c, I-56127 Pisa, ITALY
e-mail: berselli@dma.unipi.it

R. Rannacher, A. Sequeira (eds.), *Advances in Mathematical Fluid Mechanics*,
DOI 10.1007/978-3-642-04068-9_5,

other hand, these difficulties are also reflected by the fact that for small values of the viscosity $\nu > 0$ the flow becomes unstable and with a chaotic behavior. At present state-of-the-art performing accurate direct numerical simulations is not possible. In fact, the so called "K-41," Kolmogorov's 1941 theory [22], predicts that the size of the smallest persisting scale is

$$\mathcal{O}\left(\frac{\nu^3}{\varepsilon}\right)^{\frac{1}{4}},$$

where ε is the kinetic-energy injection rate.

It is interesting to observe that *experimentally* $\varepsilon \simeq u'^3/l$ where u' is the RMS turbulence intensity, while l is the scale or the largest eddy, which is comparable to the length scale L, cf. Pope [37, p. 183]. It is then possible to define Re, the Reynolds number and it turns out that N_d the number of degrees of freedom needed to fully resolve turbulence in the 3D case is

$$N_d = \mathcal{O}(\mathrm{Re}^{\frac{9}{4}}),$$

and for real-life flows this is completely out of range also for the most powerful supercomputers. We point out that the K-41 theory is based on a mixing of pure statistical methods with audacious physical guesswork and dimensional analysis. The link with this various theoretical questions and the statement of the precise mathematical hypotheses underlying the K-41 theory is addressed, e.g., in Frisch [17], Kupiainen [23], and in Flandoli et al. [16].

The aim of this paper is to review some well-known facts in physics of fluids and to try to give different explanations of some results, together with possible generalizations in the field of LES of turbulent flows. In particular, we present a different (based on a stochastic approach) derivation of eddy viscosity (EV) methods.

The approach of LES is that of finding suitable equations in which the smallest scales are cut-off, even if their effect on larger scales is still taken into account (even if in a non completely exact way). To this end we give the following definition.

Definition 1 The function $\overline{u}$, is an approximation of the solution u of (1), such that $\overline{u}$ contains only "large scales," and consequently it is a computable quantity.

Deriving a suitable system of partial differential equations satisfied by $\overline{u}$ is one of the main issues in the mathematical theory of LES, see the review in Berselli, Iliescu, and Layton [4].

Here, we want to focus on one of the earlier LES models, the Smagorinsky model (hence $\overline{u}$ will be a solution to system (4) below or of some generalizations) and we shall consider the following natural generalization of the Smagorinsky EV term:

$$\nu_T = 2\left(C_{S,p}\delta\right)^{\frac{2}{3}p}\left|\sqrt{2}\nabla^s\overline{u}\right|^{p-2}, \qquad \text{for } p \geq 2, \tag{2}$$

where $\nabla^s\overline{u} = \frac{1}{2}(\nabla\overline{u} + \nabla\overline{u}^T)$.

A stochastic approach to parameterization of LES seems promising, see also the recent results of Duan and Nadiga [14] and Du and Duan [13]. More precisely, here we want to present a new justification, based on a combination of scaling arguments and techniques from probability, of the fact that $\overline{u}$ should be a large scale approximation of u. In addition, we derive in a manner a little different from usual the value of the Lilly's-Smagorinsky constant in the more general context of p-fluids.

Moreover, we are trying to glue open problems, mathematical techniques, perspectives, and motivations coming form several fields rather far away each other. Hence, we think it would be helpful to have such a review in order to make a wider community aware of several results. As a by product, we propose some new results (or partially restatement of known facts). The interdisciplinary nature of the problem of understanding, describing, and predicting by means of accurate numerical simulations the behavior of turbulent flows seems to be a perfect playground to try to employ (perhaps not in a very rigorous way) tools well-established in other research topics. Consequently, we try to give some hints, not focusing on real technical points, but just on the underlying ideas. The reader should not be an expert of stochastic differential equations, analysis of partial differential equations, numerical simulations of fluids *etc*... to understand the main points. At the same time we apologize for not proving any deep and analytical results, because we are aware that the rigorous justification of every single step -if possible- would take too much effort and will hide the main results we are proposing. We remark that several arguments of this note are heuristic and we make computations at a formal level assuming the necessary regularity. Only a few fragments can be rigorously handled and will be reported elsewhere. The reader can find rigorous contributions to the theory of stochastic Navier-Stokes equations, see for instance the review in Flandoli [15]. See also Kupiainen [23] for a review of the use of Itô calculus and scaling transformations (which will be our two main tools).

Plan of the paper. In Sect. 2 we review the basic tools of LES and of Stochastic calculus, with their applications to the Navier-Stokes equations. In particular, we introduce Kolmogorov's scaling transformations, which are of interest for our approach. In Sect. 3 we employ scaling and asymptotic techniques to derive our family of LES models and to give our justification of the fact that $\overline{u}$ is an approximation of the large scales of u. In Sect. 3.5 we propose a slightly new way to evaluate Lilly's constant, which generalizes to more general exponents. Finally, in Sect. 3.6 we also propose a scaling argument to derive suitable channel flow approximation of turbulent flows.

2 Two Approaches to Turbulent Flows: LES and Stochastic Partial Differential Equations

In this section we review the basic tools we shall need later on and we refer to the extensive bibliography for further details.

2.1 The Paradigm of Large/Small Scales

As we claimed in the introduction, real-life flows develop very small scales. From the computational point of view several approximate methods have been proposed in order to truncate the smallest (and impossible to be accurately described) ones. The inner consistency of these methods is that the effect of the unresolved scales should be taken into account in some way, and not simply disregarded as in the classical Galerkin method. Various techniques based on time averaging, space averaging, scale similarity, variational multiscale methods *etc*... have been proposed, see the review in Berselli, Iliescu, and Layton [4], in Sagaut [40] and in Lesieur, Métais, and Comte [28].

It is peculiar that in several applications, or at least to debug, check performances, and also to stabilize complicate methods it is still well-diffused the "probably oldest" LES Model: the Smagorinsky model introduced in 1963 to perform simulations for weather prediction. In this case $\overline{u}$ represents an approximation of the velocity u, recall Definition 1, where the cut-off length δ is tuned on the size of the computational grid. The effect of the unresolved scales is taken into account by using the hypothesis that

> ... a turbulent flow is dissipative in mean.

This assumption leads to the class of EV-methods introduced for the first time by Boussinesq [5], who proposed that this *ansatz* is taken into account by an additional turbulent stress tensor

$$\tau = \nu_T \, \nabla^s \overline{u},$$

where ν_T is function of the turbulent flow. Later Smagorinsky [42] proposed the following constitutive relation for the turbulent stress viscosity:

$$\nu_T = (C_S \delta)^2 |\sqrt{2} \nabla^s \overline{u}|, \tag{3}$$

where $\delta > 0$ is the sub-grid-scale characteristic length (taken proportional to the size of the grid in the numerical approximation) and

$$|\nabla^s \overline{u}| := \sqrt{\sum_{i,j=1}^{3} 2[\nabla^s \overline{u}]_{ij} [\nabla^s \overline{u}]_{ij}}.$$

The classical Smagorinsky approximation is given by the solution of the equations

$$\begin{cases} \dfrac{\partial \overline{u}}{\partial t} + \nabla \cdot (\overline{u} \otimes \overline{u}) - \nabla \cdot \left(\nu + 2 (C_S \delta)^2 \left| \sqrt{2} \nabla^s \overline{u} \right| \right) \nabla \overline{u} + \nabla \overline{\pi} = \overline{f}, \\ \qquad\qquad\qquad\qquad\qquad\qquad\qquad\qquad\qquad\qquad \operatorname{div} \overline{u} = 0, \\ \qquad\qquad\qquad\qquad\qquad\qquad\qquad\qquad\qquad\qquad \overline{u}|_{t=0} = \overline{u}_0. \end{cases} \tag{4}$$

System (4) have been used in LES with the hope that $\overline{u}$ approximates u at large scales, but small scale structures are almost absent in $\overline{u}$. Motivations and numerical experiments supporting this LES model can be found, e.g., in Moin and Kim [34], Rodi et al. [39], and Breuer and Jovicic [6]. More precisely, the Smagorinsky model is capable of representing both the $k^{-\frac{5}{3}}$ law and the theoretical decay (with respect to time) of kinetic energy for homogeneous isotropic turbulence. Interesting computations also with Finite Element Methods (instead of classical spectral ones) have been performed by Chalot et al. [7].

For completeness, we also point out that the class of EV methods is too narrow to include all phenomena present in turbulent flows. For instance criticism against Smagorinsky model may be that: it does not work correctly near walls (computations of a mixing layer are too dissipative since this model seems incapable of discriminating between the mean shear and the shear associated with fluctuations); The value of C_S (which is calculated for homogeneous and isotropic flows) is too large in presence of walls; The Smagorinsky model cannot take into account of back-scatter of energy as scale similarity methods can do.

On the other hand, EV models have good stability properties and the are a building block for some advanced LES methods. See for instance the *dynamic model* of Germano et al. [20] based on an adaptive evaluation of $C_S = C_S(x,t)$ and also the recent *selective Smagorinsky model* proposed by Cottet, Jiroveanu, and Michaux [10], based on triggering of the dissipative term in presence of regions of *high vortex-activity.*

We recall that the Smagorinsky model (and its generalizations) became also a paradigm for the modeling of several phenomena involving non-Newtonian fluids, see the review in Galdi [19]. The first mathematical studies can be found in Ladyžhenskaya [24], Lions [32] and for the mathematical foundation see also Málek et al. [33]. Fine properties of regularity have been recently obtained, see Beirão da Veiga [1, 2].

2.2 Preliminaries on Stochastic Navier-Stokes Equations

In this section we consider the Navier-Stokes equations (1) in $T_L =]-L, L[^3$ with periodic boundary conditions, and with $f = \dot{W}$

$$\begin{cases} \dfrac{\partial u}{\partial t} + \nabla \cdot (u \otimes u) + \nabla \pi - \nu \Delta u = \dot{W}, \\ \operatorname{div} u = 0, \\ u|_{t=0} = u_0, \end{cases} \tag{5}$$

where f is a wildly oscillating function. We recall some basic assumptions and results which will be needed later on.

2.2.1 On White Noise

We recall the basic hypotheses on the noise exciting the fluid at large scales. We assume that the *white noise* has the form, for some $N \in \mathbb{N}$,

$$\dot{W}(x,t) := \sum_{k=1}^{N} \sigma_k e_k(x) \frac{dW_k(t)}{dt}, \tag{6}$$

and observe that we require the sum to be finite. To be more specific, consider a torus T_L, employ the (scaled) L^2-scalar product

$$\langle f, g \rangle := \frac{1}{L^3} \int_{T_L} f(x) \cdot g(x)\, dx,$$

for vector fields $f, g \in L^2(T_L; \mathbb{R}^3)$, and assume that $\{e_k\}_{k=1,\dots,N}$ are orthonormal vector fields on $L^2(T_L)$. Moreover, assume that $W_k(t)$ are independent Brownian motions, identified with the components of the canonical process $W(t,\omega) := \omega(t)$ on the space Ω of real continuous functions $\omega(\cdot)$ on $[0,+\infty[$, equipped with the Wiener measure P. The assumption that the sum in (6) is finite reflects the idea that the noise acts at large scales, hence that it cannot act as a direct perturbation of all small scales. Finally, we define

$$\sigma^2 := \sum_{k=1}^{N} \sigma_k^2,$$

which will be linked with the kinetic energy input.

2.2.2 On a Stochastic LES Model

To explain why we expect that $\overline{u}$ should be a large scale approximation of u (for every $p \geq 2$), we analyze the stochastic partial differential equation

$$\begin{cases} \dfrac{\partial \overline{u}}{\partial t} + \nabla \cdot (\overline{u} \otimes \overline{u}) - \nabla \cdot \left(\nu + 2 \left(C_{S,p} \delta \right)^{\frac{2}{3}p} \left| \sqrt{2} \nabla^s \overline{u} \right|^{p-2} \right) \nabla \overline{u} + \nabla \overline{\pi} = \dot{W}, \\ \nabla \cdot \overline{u} = 0, \end{cases} \tag{7}$$

and the corresponding stochastic Navier-Stokes equations (1), with f equals to a white noise $\dot{W}$ acting at large scales. Specific scaling properties of the white noise and Itô calculus allow us to develop the analysis which will be presented here.

The generalization with $p \neq 3$, is not only natural from the view point of the method presented in this note. We believe it is useful for two reasons: First, values of p larger than 3 allow one to develop numerical schemes of higher degree, see Layton [25] and Iliescu [21]. Next, there is hope that suitable large values of p may mitigate the over-damping observed in many numerical simulations with the Smagorinsky equations. We explain the reasons for this hope in Sect. 3.4 below.

It is worth to mention that generalizations of the classical Smagorinsky model have already been proposed in the literature, see Sect. 3.2.

2.2.3 Existence and Balance Laws for Stochastic Navier-Stokes Equations

The concept of solution and questions of uniqueness and regularity are reviewed for instance in Flandoli [15]. Without entering too technical details on the precise notion of solution, we recall that it is possible to prove that there exists a weak solution $u(x, t, W)$ such that with probability one:

$$u \in C_w([0, T]; L^2) \cap L^2(0, T; H^1)$$

and

$$\frac{d}{dt}\left(u - \sum_{k=1}^{N} \sigma_k e_k\,(x)\,W_k\,(t)\right) \in L^{\frac{4}{3}}(0, T; H^{-1}),$$

and we refer, for instance, to Bensoussan and Temam [3]. The solution u clearly depends on x, t, and W. Hence, it can be seen as a stochastic process, i.e., a parameterized collection of random variables. The parameter t represents time (for each t we have a random variable), while W represents an individual experiment. Since we consider homogeneous fully developed turbulence, in the sequel we shall assume that:

> The velocity u is a time-stationary, space-homogeneous solution, with sufficient regularity to perform Itô calculus.

In this case time-stationary does not mean that u is time independent, but that the velocity u at time t has the same distribution (as a random variable) as the velocity at time $t + h$, for each $h > 0$.

With this assumption it is easy to prove (formally, see footnote at page 62) that, for each space-time point (x, t)

$$\nu\,\mathbb{E}\left[|\nabla u|^2\right] = \frac{\sigma^2}{2}. \tag{8}$$

Here the symbol $\mathbb{E}[\,\cdot\,]$ denotes expectation with respect to the probability measure underlying the white noise:

$$\mathbb{E}[X] := \int X(W)\,dP(W) = \int_{\mathbb{R}} x\,d\mu_X(x),$$

where μ_X is the distribution of the scalar random variable X. This balance relation motivates the following definition (cf. with the quantity ε defined at page 56):

Definition 2 The quantity

$$\varepsilon := \frac{\sigma^2}{2} \tag{9}$$

is the energy density (energy per unit volume) injected by the noise into the fluid.

We give a sketch of the computations with Itô's calculus (cf. Øksendal [35]) behind the derivation of (8). The Itô's formula is a generalization of the chain rule to stochastic integrals. It states that for a C^2 function $g : [0, \infty) \times \mathbb{R}^n \to \mathbb{R}^m$ and a n-dimensional Itô's process X_t, then $Y_t = g(t, X_t)$ is again an Itô process and

$$dY_k = \frac{\partial g_k}{\partial t}(t, X)dt + \sum_{i=1}^{n} \frac{\partial g_k}{\partial x_i}(t, X)dX_i + \frac{1}{2}\sum_{i,j=1}^{n} \frac{\partial^2 g_k}{\partial x_i \partial x_j}(t, X)dX_i dX_j, \qquad 1 \le k \le m,$$

where we have written $dX_i dX_j$ to help intuition, but the more precise term $d[X_i, X_j]$ should be used, involving the concept of mutual quadratic variation. By applying the above formula to $\frac{|u|^2}{2}$ it follows that, for every sufficiently regular[1] solution of the stochastic Navier-Stokes equations, we have

$$d\left(\frac{1}{2}\int_{T_L} |u|^2\, dx\right) + \left(\nu \int_{T_L} |\nabla u|^2\, dx\right) dt = dM + \frac{1}{2}\sum_{k=1}^{N}\left(\int_{T_L} \sigma_k^2 e_k^2 dx\right) dt,$$

where M is a martingale (we do not recall this concept based on conditional expectation at different times, but only use the property $\mathbb{E}[M_t] = 0$). Hence, for time-stationary solutions

$$\nu \mathbb{E}\left[\int_{T_L} |\nabla u|^2\, dx\right] = L^3 \frac{\sigma^2}{2}, \tag{10}$$

(and the scaling factor $\frac{1}{L^3}$ in the definition of the above scalar product is essential here.) We get (8) in the case of space-homogeneous solutions, but (10) is already sufficient to motivate the concept of energy density injected by the noise into the fluid.

We observe that, contrary to the deterministic Navier-Stokes, there is a more clear expression for the energy dissipation. In the deterministic case the energy balance (formally) gives

$$\frac{1}{2}\frac{d}{dt}\int_{\Omega} |u(x,t)|^2 dx + \nu \int_{\Omega} |\nabla u(x,t)|^2 dx = \int_{\Omega} f(x,t) u(x,t)\, dx$$

and, even if the solution is supposed to be stationary (or similarly if it is integrated over very large time-intervals), it turns out that the power input *depends* on the solution u itself! This difference is one of the main features of a statistical approach to the Navier-Stokes equations.

[1] This calculation cannot be rigorously performed in the 3D case, since we do not know that solutions are smooth enough. In this case the *inequality* corresponding to the *equality* (10) can be proved by means of Galerkin approximation.

Finally, since we shall work with the modified equations we need the analog of relation (10) for equation (7). With the same arguments above sketched one gets

$$\nu\,\mathbb{E}\left[\int_{T_L} |\nabla \overline{u}|^2\,dx\right] + \left(C_{S,p}\delta\right)^{\frac{2}{3}p}\,\mathbb{E}\left[\int_{T_L} \left|\sqrt{2}\nabla^s \overline{u}\right|^p dx\right] = L^3\frac{\sigma^2}{2}, \qquad (11)$$

for time-stationary solutions to system (7).

2.3 Brownian Scaling

Beside Itô's calculus, the second essential ingredient of our arguments are scaling transformations.

Lemma 1 *Denoting equality in law between (generalized) stochastic processes by $\stackrel{\mathcal{L}}{=}$, we have the following classical result for white noises:*

$$\lambda^{\beta/2}\dot{W}\left(x,\lambda^\beta t\right) \stackrel{\mathcal{L}}{=} \dot{W}\left(x,t\right), \qquad (12)$$

for every $\lambda > 0$ *and* β.

Instead of a rigorous proof, let us explain (12), at the intuitive level. It is well known (see [35]) that a one dimensional Brownian motion $W_k(t)$ is invariant under the (Brownian) scaling

$$\lambda^{-\beta/2}W_k\left(\lambda^\beta\cdot\right) \stackrel{\mathcal{L}}{=} W_k\left(\cdot\right).$$

The corresponding white noise $\frac{dW_k}{dt}(t)$ is invariant under the following scaling

$$\lambda^{\beta/2}\frac{dW_k}{dt}\left(\lambda^\beta t\right) \stackrel{\mathcal{L}}{=} \frac{dW_k}{dt}\left(t\right),$$

because

$$\begin{aligned}
\lambda^{\beta/2}\frac{dW_k}{dt}\left(\lambda^\beta t\right) &\sim \lambda^\beta\frac{\lambda^{-\beta/2}W_k\left(\lambda^\beta t+dt\right)-\lambda^{-\beta/2}W_k\left(\lambda^\beta t\right)}{dt}\\
&\overset{dt=\lambda^\beta dt'}{\sim} \lambda^\beta\frac{\lambda^{-\beta/2}W_k(\lambda^\beta t+\lambda^\beta dt')-\lambda^{-\beta/2}W_k(\lambda^\beta t)}{\lambda^\beta dt'}\\
&\sim \lambda^\beta\frac{W_k\left(t+dt'\right)-W_k\left(t\right)}{\lambda^\beta dt'}\\
&\sim \frac{dW_k}{dt}\left(t\right).
\end{aligned}$$

The claim (12) for a finite dimensional noise follows from the previous one.

We use the information in Lemma 1 to perform suitable scaling transformation of the equations. In the next section we shall perform scaling transformations of the form

$$\dot{W}^{\lambda}(x,t) := \lambda^{2\alpha+1}\dot{W}\left(\lambda x, \lambda^{\alpha+1}t\right).$$

This is again a white noise on the torus $T_{L/\lambda}$ and it acts on the fluid through the orthonormal fields $e_k(\lambda x)$ (so it acts at larger scales than $\dot{W}$, if $\lambda < 1$). The essential point of our argument is given by the following statement.

Lemma 2 *The energy density injected by the noise* $\dot{W}^{\lambda}(x,t)$ *into the fluid is* $\frac{\sigma^2}{2}$, *the same as for* $\dot{W}(x,t)$, *if and only if*

$$\alpha = -\frac{1}{3}.$$

Proof From (12), we get

$$\dot{W}^{\lambda}(x,t) = \lambda^{2\alpha+1}\dot{W}\left(\lambda x, \lambda^{\alpha+1}t\right) \stackrel{\mathcal{L}}{=} \lambda^{\frac{3}{2}\alpha+\frac{1}{2}}\dot{W}(\lambda x, t)$$

and thus its injected energy density is

$$\lambda^{\frac{3}{2}\alpha+\frac{1}{2}}\frac{1}{2}\sum_{k=1}^{N}\sigma_k^2,$$

which equals ε in Eq. (9) (for all $\lambda > 0$) if and only if $\alpha = -\frac{1}{3}$. □

This lemma will be used later on to detect the most suitable scaling transformations needed to study statistical properties of the flow.

3 Scaling Transformations and Derivation of Generalized Smagorinsky Models

In this section we give a derivation of the EV model (7). As we shall see from the derivation, our main goal will be that of having a model consistent (in some sense) with K-41. In this respect we see that the consistency of a LES model with the K-41 theory seems a first natural request. Similar calculations (aimed at different K-41-consistency, as reproducing the $k^{-\frac{5}{3}}$ behavior) have been previously performed by several authors, see, e.g., Lesieur et al. [28] and Layton and Neda [26, 27].

3.1 Derivation of a Family of Eddy Viscosity Models

We now derive the expression

$$\nu_T := 2\left(C_{S,p}\delta\right)^{\frac{2}{3}p}\left|\sqrt{2}\nabla^s\overline{u}\right|^{p-2}$$

for the turbulent viscosity in (7) and in particular the precise scaling exponent for the "length" $\delta > 0$.

Theorem 1 *Equation (7) with the additional turbulent viscosity*

$$\nu_T = 2\left(C_{S,p}\delta\right)^{r}\left|\sqrt{2}\nabla^s\overline{u}\right|^{p-2}, \qquad r \in \mathbb{R}$$

is consistent with K-41 if and only if

$$r = \frac{2p}{3}.$$

Proof Let us consider the EV equation (7)

$$\frac{\partial\overline{u}}{\partial t} + \nabla\cdot(\overline{u}\otimes\overline{u}) - \nabla\cdot\left(\nu + 2\left(C_{S,p}\delta\right)^{r}\left|\sqrt{2}\nabla^s\overline{u}\right|^{p-2}\right)\nabla\overline{u} + \nabla\overline{\pi} = \dot{W}, \qquad (13)$$

with an arbitrary $r > 0$.

For more transparency in the calculations, let us employ the family of scaling transformation

$$\overline{u}^{\lambda}(t,x) := \lambda^{\alpha}\overline{u}\left(\lambda^{\alpha+1}t, \lambda x\right) \qquad \overline{\pi}^{\lambda}(t,x) := \lambda^{2\alpha}\overline{\pi}\left(\lambda^{\alpha+1}t, \lambda x\right), \qquad (14)$$

indexed by $\alpha \in \mathbb{R}$ and which we shall specialize later on. We have the following equalities for the Navier-Stokes equations and for the EV model (13), with the arbitrary coefficient $r \in \mathbb{R}$:

$$\left[\frac{\partial\overline{u}^{\lambda}}{\partial t}+\nabla\cdot\left(\overline{u}^{\lambda}\otimes\overline{u}^{\lambda}\right)-\left(\lambda^{\alpha-1}\nu\right)\Delta\overline{u}^{\lambda}\right](t,x)$$
$$=\lambda^{2\alpha+1}\left[\frac{\partial\overline{u}}{\partial t}+\nabla\cdot(\overline{u}\otimes\overline{u})-\nu\Delta\overline{u}\right]\left(\lambda^{\alpha+1}t,\lambda x\right),$$

$$\left[\nabla\cdot\left(2\left(C_{S,p}\delta\right)^{r}\left|\sqrt{2}\nabla^{s}\overline{u}^{\lambda}\right|^{p-2}\right)\nabla^{s}\overline{u}^{\lambda}\right](x,t)$$
$$=\lambda^{(p-1)(\alpha+1)+1}\left[\nabla\cdot\left(2\left(C_{S,p}\delta\right)^{r}\left|\sqrt{2}\nabla^{s}\overline{u}\right|^{p-2}\right)\nabla^{s}\overline{u}\right]\left(\lambda^{\alpha+1}t,\lambda x\right),$$

$$\nabla\overline{\pi}^{\lambda}(t,x)=\lambda^{2\alpha+1}\nabla\overline{\pi}\left(\lambda^{\alpha+1}t,\lambda x\right).$$

Thus, we get the following rescaled form of the equations for the p-fluid

$$\left[\frac{\partial\overline{u}^{\lambda}}{\partial t}+\nabla\cdot\left(\overline{u}^{\lambda}\otimes\overline{u}^{\lambda}\right)+\nabla\overline{\pi}^{\lambda}\right](t,x)$$
$$-\nabla\cdot\left(\lambda^{\alpha-1}\nu+\lambda^{3\alpha+1-p(\alpha+1)}2\left(C_{S,[}\delta\right)^{r}\left|\sqrt{2}\nabla^{s}\overline{u}^{\lambda}\right|^{p-2}\right)\nabla^{s}\overline{u}^{\lambda}(t,x)=$$
$$=\lambda^{2\alpha+1}\left[\frac{\partial\overline{u}}{\partial t}+\nabla\cdot(\overline{u}\otimes\overline{u})+\nabla\overline{\pi}-\right.$$
$$\left.\nabla\cdot\left(\nu+2\left(C_{S,p}\delta\right)^{r}\left|\sqrt{2}\nabla^{s}\overline{u}\right|^{p-2}\right)\nabla^{s}\overline{u}\right]\left(\lambda^{\alpha+1}t,\lambda x\right).$$

This shows that if $\overline{u}$ solves (13) on the torus T_L, with the still generic coefficient $\left(C_{S,p}\delta\right)^{r}$ in place of $\left(C_{S,p}\delta\right)^{\frac{2}{3}p}$, then

$$\frac{\partial\overline{u}^{\lambda}}{\partial t}+\nabla\cdot\left(\overline{u}^{\lambda}\otimes\overline{u}^{\lambda}\right)+\nabla\overline{\pi}^{\lambda}$$
$$-\nabla\cdot\left(\lambda^{\alpha-1}\nu+\lambda^{3\alpha+1-p(\alpha+1)}2\left(C_{S}\delta\right)^{r}\left|\sqrt{2}\nabla^{s}\overline{u}^{\lambda}\right|^{p-2}\right)\nabla^{s}\overline{u}^{\lambda}=\dot{W}^{\lambda},$$

where $\dot{W}^{\lambda}$ is defined by (2.3).

To identify $r\in\mathbb{R}$ we need two properties:

1. We ask that the energy density injected by $\dot{W}^{\lambda}$ is the same as the energy density injected by $\dot{W}$. By Lemma 2, this is true for $\alpha=-\frac{1}{3}$. For a reason that will be clear below, we call *Kolmogorov scaling transformation* the change of variable (14) when $\alpha=-\frac{1}{3}$.
2. We ask that the coefficient $\lambda^{3\alpha+1-p(\alpha+1)}\delta^{r}$ in the EV term is of order one when $\lambda=\delta$. Since $\alpha=-\frac{1}{3}$, this requires

$$r = \frac{2}{3}p.$$

By using the results of the previous section we derived the model (7) and we have identified the exponent that the *smallest resolved scale length* $\delta > 0$ should assume to have a statistical consistency with the Navier-Stokes theory. □

Remark 1 The scaling transformation we are using (well-known since the work of Kolmogorov and Obukhov) is rather different from the scaling used in the analytical theory of partial regularity for Navier-Stokes equations. In fact, the standard parabolic scaling is at the basis of some well-known regularity criteria due to Leray, Prodi, Serrin, Sohr…, see [18]: If the pair (u, π) solves (1) then so does the family $(u_\lambda, \pi_\lambda)_{\lambda>0}$ defined by

$$u_\lambda(x,t) := \lambda\, u(\lambda x, \lambda^2 t) \qquad \pi_\lambda(x,t) := \lambda^2\, \pi(\lambda x, \lambda^2 t).$$

With this transformation the *viscosity* does not change, but the energy input changes. Hence, the use of different scaling transformations can be used to extract different information from the equations. In particular, the scaling we use (and a whole one-parameter family) keeps the material derivative $\frac{D}{Dt} := (\partial_t + u \cdot \nabla)$ unchanged and this explains the relevance in the study of Euler equations or also in presence of very small viscosities.

Remark 2 The use of Kolmogorov's scaling is at the basis of the Onsager's conjecture. In particular, the scaling transformation is compatible with $C^{0,1/3}$-functions. The problem of energy conservation for non-smooth functions has been recently addressed in Cheskidov et al. [9].

3.2 Comparison with Alternate Scaling Previously Proposed

We observe that the exponent $r = \frac{2p}{3}$ in (7) is different from other ones which have been previously obtained (even if with different intents). We review some of these results: Smagorinsky model is most successful when used with second order finite difference methods for which it gives a perturbation of $\mathcal{O}$(discretization error) in the smooth/laminar flow regions. For higher order methods (say, order $p-1$) a natural generalization is thus (see Layton [25])

$$\nu_T = (C_{S,p}\delta)^{p-1}\, |\nabla^s \overline{u}|^{p-2} = \begin{cases} \mathcal{O}(\delta^{p-1}) & \text{in smooth regions,} \\ \mathcal{O}(\delta) & \text{in the smallest resolved eddies,} \end{cases}$$

and this scaling is motivated by experiments with central difference approximations made on linear convection diffusion problems.

Another scaling, again motivated by the interface between models and higher order numerical methods, was proposed in [25]. In 3 dimensions and using a numerical method with accuracy of order $O(h^{p-1})$, a possible choice is

$$\nu_T = C_{S,p}\,|\log(\delta)|^{-\frac{2(p-1)}{3}}\,\delta^{\frac{3(p-1)}{2}}\,|\nabla^s\overline{u}|^{p-2}, \qquad \text{with} \quad p \geq \frac{2}{3}r+1.$$

As p increases, these formulas concentrate the EV more and more in the regions in which the gradient is large. These regions include the smallest resolved eddies and also regions with large shears.

A third rescaling has been proposed from interpreting the turbulent viscosity coefficient ν_T micro-locally in K-41 theory. Thus, the K-41 theory suggests the higher order Smagorinsky-type model

$$\nu_T = (C_{S,p}\delta)^{p-\frac{2}{3}}\,|\nabla^2\overline{u}|^{p-2} \approx \begin{cases} \mathcal{O}(\delta^{p-\frac{2}{3}}) & \text{in smooth regions,} \\ \mathcal{O}(\delta^{\frac{4}{3}}) & \text{in the smallest resolved eddies.} \end{cases}$$

which is consistent with K-41 prediction that the smallest persistent eddy is $\mathcal{O}(\nu^{\frac{3}{4}})$.

We observe that different rescaling have been derived from different motivations and with different goals. So we do not claim that our scaling is "the correct one." It turns out that our scaling is the most natural if one assumes the mathematical hypotheses which are at the basis of the statistical theory of fluids, and this seems the most promising way to attack the problem of description of turbulent flows.

In order to validate the choice of our method we observe that in the classical Smagorinsky model it turns out that

$$\nu_T = \mathcal{O}\left(\delta^{\frac{4}{3}}\right). \tag{15}$$

In fact (this argument is elaborated with more details in Sect. 3.5), K-41 theory implies also that $E(k)$, the spectral amplitude of kinetic energy (defined as the integral over surfaces of spheres in wave-number space parameterized by the radius k) decays as $k^{-\frac{5}{3}}$ in the inertial subrange. This implies, with some guessing (cf. also Eq. (17)), that $|\nabla^s\overline{u}| \simeq \overline{k}^{\frac{2}{3}}$, where $\overline{k}$ corresponds to the spectral resolution limit. If the smallest resolved scale is proportional to $\delta = \overline{k}^{-1}$, then it follows (15). If we apply the same computations to our EV term (2) we get, independently of p,

$$\nu_T = 2\left(C_{S,p}\delta\right)^{\frac{2}{3}p}\left|\sqrt{2}\nabla^s\overline{u}\right|^{p-2} = \mathcal{O}\left(\delta^{\frac{2}{3}p}\delta^{-\frac{2}{3}(p-2)}\right) = \mathcal{O}\left(\delta^{\frac{4}{3}}\right)$$

and this is the main consistency with K-41 theory that the method we propose has. Other details and also some consideration on the possible nature of the over-damping introduced by p-models, in connection with turbulent flows, are examined in Sect. 3.4.

3.3 Is $\overline{u}$ a Large Scale Approximation of u?

In this section we try to give an heuristic justification (from the point of view of statistical fluid mechanics) that the velocity $\overline{u}$ could be a good approximation of the large scales of u.

Let us suppose that on the torus T_L are given a time-stationary solution $\overline{u}$ of (7) and a time-stationary solution u of (1), both with external force $f = W$. Let us fix some $x_0 \in T_L$ that without loss of generality we can take $x_0 = 0$. Next, given an unitary vector e, consider the increment (at any time):

$$\overline{u}(\lambda e) - \overline{u}(0).$$

The aim of this section is to give a reasonable argument for the following two claims:

1. The quantity $\overline{u}(\lambda e) - \overline{u}(0)$ is a statistically an approximation of the increment $u(\lambda e) - u(0)$ for $\delta \ll \lambda \leq L$;
2. The quantity $\overline{u}(\lambda e) - \overline{u}(0)$ is very small for $\lambda \ll \delta$.

The argument requires a number of conditions and (unproved) assumptions, for instance the relative smallness of δ and ν and the cascade properties of the 3D equations, that will be described step by step.

Suppose that L and $\frac{\sigma^2}{2}$ are of order one. Then, the rescaled fields

$$\begin{pmatrix} \overline{u}^{\lambda}(t,x) := \lambda^{-\frac{1}{3}}\overline{u}\left(\lambda^{\frac{2}{3}}t, \lambda x\right) & \overline{\pi}^{\lambda}(t,x) := \lambda^{-\frac{2}{3}}\overline{\pi}\left(\lambda^{\frac{2}{3}}t, \lambda x\right) \\ u^{\lambda}(t,x) := \lambda^{-\frac{1}{3}}u\left(\lambda^{\frac{2}{3}}t, \lambda x\right) & \pi^{\lambda}(t,x) := \lambda^{-\frac{2}{3}}\pi\left(\lambda^{\frac{2}{3}}t, \lambda x\right) \end{pmatrix},$$

satisfy the equations

$$\begin{cases} \dfrac{\partial \overline{u}^{\lambda}}{\partial t} + \nabla\cdot\left(\overline{u}^{\lambda}\otimes\overline{u}^{\lambda}\right) - \nabla\cdot\left(\lambda^{-\frac{4}{3}}\nu + 2\left(C_{S,p}\dfrac{\delta}{\lambda}\right)^{\frac{2}{3}p}\left|\sqrt{2}\nabla^{s}\overline{u}^{\lambda}\right|^{p-2}\right)\nabla\overline{u}^{\lambda} \\ \qquad\qquad\qquad\qquad\qquad\qquad\qquad\qquad + \nabla\overline{\pi}^{\lambda} = \dot{W}^{\lambda}, \\ \\ \dfrac{\partial u^{\lambda}}{\partial t} + \nabla\cdot\left(u^{\lambda}\otimes u^{\lambda}\right) - \nabla\cdot\left(\lambda^{-\frac{4}{3}}\nu\right)\nabla u^{\lambda} + \nabla\pi^{\lambda} = \dot{W}^{\lambda}. \end{cases}$$

First, let us consider the case: $\delta \ll \lambda \leq L$.

If we assume $\nu > 0$ sufficiently small with respect to λ (in order to have $\lambda^{-\frac{4}{3}}\nu \ll 1$), we are considering two Navier-Stokes-type equations (in possibly large domains) but with energy injected per unit volume of order one, and very small viscosity coefficients.

We assume that the energy is transferred, by a cascade mechanism, from large scales (those of the direct action of the noise) to smaller and smaller scales, without essential dissipation until a certain scale, where the dominant effect is that of dissipation. This fact is at the basis of the derivation of K-41 theory, but it has been introduced for the first time by the meteorologist Richardson [38, p. 66], recall his famous verse on big whirls and lesser whirls:

Big whirls have little whirls what feed on their velocity,
little whirls have lesser whirls, and so on to viscosity.

We may conjecture that the statistical properties of $\overline{u}^{\lambda}(e) - \overline{u}^{\lambda}(0)$ and $u^{\lambda}(e) - u^{\lambda}(0)$ are similar. Let us stress that this result would not be true if the injected energy per unit volume of the noise would be of order different from one or also if the viscosity would not be very small, since the difference in viscosities between the two equations could make a difference on the solutions already at scale one. The approximate equality in law

$$\overline{u}^{\lambda}(e) - \overline{u}^{\lambda}(0) \stackrel{\mathcal{L}}{\simeq} u^{\lambda}(e) - u^{\lambda}(0)$$

means

$$\overline{u}(\lambda e) - \overline{u}(0) \stackrel{\mathcal{L}}{\simeq} u(\lambda e) - u(0).$$

We have proved the first part of our claims. In fact, the range of scales λ to which the previous argument applies could be very narrow: not only the viscosity coefficients $\lambda^{\alpha-1}\nu$ and $2\left(C_{S,p}\frac{\delta}{\lambda}\right)^{\frac{2}{3}p}$ should be sufficiently small, but the full coefficient $2\left(C_{S,p}\frac{\delta}{\lambda}\right)^{\frac{2}{3}p}\left|\sqrt{2}\nabla^{s}\overline{u}^{\lambda}\right|^{p-2}$ should be small too. This could be the origin of the over-damping observed in numerical simulations performed with the classical ($p = 3$) Smagorinsky equation as sub-grid-scale model. We shall argue in the next section that this phenomenon could be less strong if p is large and also if there is some degree of *intermittency.*

Consider now the case $\lambda \ll \delta$.

The coefficient $2\left(C_{S,p}\frac{\delta}{\lambda}\right)^{\frac{2}{3}p}$ becomes very large (even if $\lambda^{\alpha-1}\nu$ may still be small). The density of energy injected by the noise is always of order one. We thus conjecture that at scales of order one the solution $\overline{u}^{\lambda}$ is already very smooth, namely $\overline{u}^{\lambda}(e) - \overline{u}^{\lambda}(0)$ is small, i.e., $\overline{u}(\lambda e) - \overline{u}(0)$ is small. This is the second part of our claim. Note that $\lambda^{\alpha-1}\nu$ may still be small, so that $u^{\lambda}(e) - u^{\lambda}(0)$ (and thus $u(\lambda e) - u(0)$) is not necessarily small. So the small scale structures approximately disappear in the Smagorinsky model.

Notice that these arguments are independent of p, hence they also apply to $p = 3$, namely they are a (new) explanation of the classical Smagorinsky approximation.

3.4 Over-Damping and the Size of $\left|\sqrt{2}\nabla^s \overline{u}^\lambda\right|^{p-2}$

As the reader may have noticed, the previous arguments may be affected by a non-unitary size of $\left|\sqrt{2}\nabla^s \overline{u}^\lambda\right|^{p-2}$ and this observation could be used to deduce an explanation of the over-damping observed in numerical simulations, for $p = 3$. Let us try to guess the typical size of $\left|\sqrt{2}\nabla^s \overline{u}^\lambda\right|^{p-2}$ and show that the over-damping could be less strong if p is large and also if there is some "degree of intermittency." In this context the word intermittency means that the flow may have some non regular bursts, which affect the prediction of the K-41 theory, see Frisch [17]. In some sense it can be seen as an irregularity issue, but also as a peculiar and non-standard scaling of the equations at some point, excluding the pure homogeneity.

We use again the balance law (11). Let us assume we are in the case $\delta \ll \lambda \leq L$ and $\lambda^{\alpha-1}\nu \ll 1$ and rewrite (11) for $\overline{u}^\lambda$:

$$\nu\,\mathbb{E}\left[\int_{T_{L/\lambda}} \left|\nabla \overline{u}^\lambda\right|^2 dx\right] + \left(C_{S,p}\frac{\delta}{\lambda}\right)^{\frac{2}{3}p} \mathbb{E}\left[\int_{T_{L/\lambda}} \left|\sqrt{2}\nabla^s \overline{u}^\lambda\right|^p dx\right] = \left(\frac{L}{\lambda}\right)^3 \frac{\sigma^2}{2}.$$

Assume that $\nu > 0$ is small enough that the second term is not infinitesimal with respect to the first one. For space-homogeneous solutions (to simplify the exposition) this implies that

$$\left(C_{S,p}\frac{\delta}{\lambda}\right)^{\frac{2}{3}p} \mathbb{E}\left[\left|\sqrt{2}\nabla^s \overline{u}^\lambda\right|^p\right] \text{ is of order one} \tag{16}$$

(we are always assuming that L and $\frac{\sigma^2}{2}$ are of order one). Very roughly this gives the indication

$$\left|\nabla^s \overline{u}^\lambda\right| \sim \left(\frac{\lambda}{\delta}\right)^{\frac{2}{3}}, \tag{17}$$

and this indication comes also from the standard derivation of the largeness in turbulent viscosity coefficients, as can be exactly evaluated for $p = 3$ and for Gaussian fields, see Lilly [29–31]. This means that $\left|\nabla^s \overline{u}^\lambda\right|$ would not be of order one and the eddy viscosity satisfies

$$\nu_T = 2\left(C_{S,p}\frac{\delta}{\lambda}\right)^{\frac{2}{3}p} \left|\sqrt{2}\nabla^s \overline{u}^\lambda\right|^{p-2} \gg 2\left(C_{S,p}\frac{\delta}{\lambda}\right)^{\frac{2}{3}p}.$$

In fact, as proposed as a consistency test, the turbulent viscosity ν_T turns out to be of the order of $\left(\frac{\delta}{\lambda}\right)^{\frac{4}{3}}$ *independently* of the choice of p. Hence, both for the classical Smagorinsky model and the p-modifications introduced here, the EV is much larger than expected and thus it damps fluctuations of the fluid more than wanted. To be more precise, given $\delta > 0$, the scales $\lambda > 0$ at which the previous arguments work (we mean the argument yielding $\overline{u}(\lambda e) - \overline{u}(0) \overset{\mathcal{L}}{\simeq} u(\lambda e) - u(0)$), are not those for which $\left(\frac{\delta}{\lambda}\right)^{\frac{2}{3}p}$ is sufficiently small, but those for which $\left(\frac{\delta}{\lambda}\right)^{\frac{4}{3}}$ is sufficiently small. Since in numerical simulations the resolved scales δ cannot be very small, this imposes a too strong restriction on λ and this may be the reason we observe over-damping even at large scales.

The picture would be different if there is some degree of intermittency. In our context this means that the random variable $\left|\nabla^s \overline{u}^\lambda\right|$ is not rather homogeneous, statistically speaking, but that:

> The random variable $\left|\nabla^s \overline{u}^\lambda\right|$ assumes relatively small values with large probability and relatively large values with small probability.
>
> $$\left|\nabla^s \overline{u}^\lambda\right| = \begin{cases} r_\lambda & \text{with probability } 1 - \theta_\lambda, \\ R_\lambda & \text{with probability } \quad \theta_\lambda, \end{cases}$$
>
> where θ_λ is small compared to $1, r_\lambda$ is of order one, and R_λ is large.

From (16) we now deduce

$$\left(\frac{\delta}{\lambda}\right)^{\frac{2}{3}p} \left((1 - \theta_\lambda) r_\lambda^p + \theta_\lambda R_\lambda^p\right) \text{ is of order one.}$$

Take p so large that $(1 - \theta_\lambda) r_\lambda^p + \theta_\lambda R_\lambda^p \sim \theta_\lambda R_\lambda^p$, and such that from $\theta_\lambda R_\lambda^p \sim \left(\frac{\delta}{\lambda}\right)^{-\frac{2}{3}p}$ we may deduce

$$R_\lambda \sim \left(\frac{\lambda}{\delta}\right)^{\frac{2}{3}}. \tag{18}$$

This replaces (17) and has the consequence that $2\left(C_{S,p} \frac{\delta}{\lambda}\right)^{\frac{2}{3}p} \left|\sqrt{2}\nabla^s \overline{u}^\lambda\right|^{p-2}$ is of the order $\left(\frac{\delta}{\lambda}\right)^{\frac{4}{3}}$ only with probability θ_λ, while it is of order $\left(\frac{\delta}{\lambda}\right)^{\frac{2}{3}p}$ with probability $(1 - \theta_\lambda)$. The over-damping affects the fluid only rarely and thus the large scale structures in the Smagorinsky approximation, continuously re-created by the noise and the cascade, are observed most of the time as for the original fluid.

As a final comment, one may argue that intermittency, often observed in fluids, is depleted by an EV with very large power p of the symmetric gradient, because of smoothness properties of solutions. In fact, regularity measured in terms of integrability exponents of Sobolev spaces increases as p increases. Therefore, it is not natural to think that the p-modifications of Smagorinsky model behave better and better as p increases. One could just hope that these models behave better than the classical Smagorinsky model ($p = 3$) for certain large (but not too large) values of p. Numerical simulations are needed to throw some light on this issue and we are starting a research project in order to perform accurate simulations aimed at understanding if (moderate) large exponents may lead to better numerical simulations, with respect to those obtained with the Smagorinsky model with $p = 3$.

3.5 Modification of Lilly's Argument for General p

In this section we show how to reproduce for the p-modifications of Smagorinsky model (7) the computations of Lilly [29–31] used to evaluate the constant C_S. Let us denote by ε the rate of kinetic-energy dissipation which, being equal to the rate of injected energy, in the above stochastic model must be equal to $\sigma^2/2$. In (11) we assume that the viscosity is so small that we essentially have

$$\left(C_{S,p}\delta\right)^{\frac{2}{3}p}\,\mathbb{E}\left[\int_{T_L}\left|\sqrt{2}\nabla^s\overline{u}\right|^p dx\right] = L^3\frac{\sigma^2}{2}.$$

Assume also space homogeneity (and write ε for $\frac{\sigma^2}{2}$), so that

$$\left(C_{S,p}\delta\right)^{\frac{2}{3}p}\,\mathbb{E}\left[\left|\sqrt{2}\nabla^s\overline{u}\right|^p\right] = \varepsilon,$$

at any space-time point (x, t). Assume that $\overline{u}$, being a large scale approximation, contains only scales larger than δ (or in Fourier variables only frequencies which are smaller than $k_c = \frac{\pi}{\delta}$):

$$\frac{1}{2}\mathbb{E}\left[\left|\sqrt{2}\nabla^s\overline{u}\right|^2\right] = \int_0^{\frac{\pi}{\delta}} k^2 E(k)\, dk.$$

Now, by following Lilly's argument [30], we assume Kolmogorov scaling law for the spectrum of the kinetic energy $E(k) = \alpha\,\varepsilon^{\frac{2}{3}}k^{-\frac{5}{3}}$, for k in the inertial subrange. The universal constant α is evaluated by means of experiments and it has a value around 1.4. In this way we obtain that

$$\mathbb{E}\left[\left|\sqrt{2}\nabla^s\overline{u}\right|^2\right] = \frac{3}{2}\alpha\,\varepsilon^{\frac{2}{3}}\left(\frac{\pi}{\delta}\right)^{\frac{4}{3}}.$$

As in [29] for $p = 3$, we introduce a very rough approximation

$$\mathbb{E}\left[\left|\sqrt{2}\nabla^s\overline{u}\right|^p\right] \simeq \mathbb{E}\left[\left|\sqrt{2}\nabla^s\overline{u}\right|^2\right]^{\frac{p}{2}}, \tag{19}$$

which nevertheless it is not too bad in the inertial subrange, and for moderate values of p. Then, we obtain

$$
\begin{aligned}
\varepsilon &= (C_{S,p}\delta)^{\frac{2}{3}p}\,\mathbb{E}\left[\left|\sqrt{2}\nabla^s\overline{u}\right|^p\right] \\
&\simeq (C_{S,p}\delta)^{\frac{2}{3}p}\left[\frac{3}{2}\alpha\,\varepsilon^{\frac{2}{3}}\left(\frac{\pi}{\delta}\right)^{\frac{4}{3}}\right]^{\frac{p}{2}} \\
&= \left(\frac{3\alpha}{2}\right)^{\frac{p}{2}}\pi^{\frac{2p}{3}}C_{S,p}^{\frac{2p}{3}}\,\varepsilon^{\frac{p}{3}}.
\end{aligned}
$$

Remarkable is that this relation does not include the cut-off scale δ. We finally get

$$
C_{S,p} = \varepsilon^{\frac{3-p}{2p}}\frac{1}{\pi}\left(\frac{3\alpha}{2}\right)^{-\frac{3}{4}}.
$$

For $p = 3$ it reduces to $C_{S,3} = C_S$ evaluated by Lilly, which is approximately 0.18. It is important to observe that the value of $C_{S,p}$ is independent of ε if and only if $p = 3$. Moreover, as described by Deardorff [11], Lilly's value of the coefficient works well when applied to turbulence produced by buoyant instabilities. For shear-driven turbulence, however, Deardorff and others found it necessary to use a smaller coefficient. These discrepancies have been verified by other investigators, as pointed out in the introduction. A priori tests by McMillan et al. on homogeneous turbulence confirmed that C_S decreases with increasing strain rate.

The above calculations show why the Smagorinsky model is very special in the class of shear-dependent viscosities. Moreover, we know that $\varepsilon = \frac{\sigma^2}{2}$ hence we can finally write

$$
C_{S,p} = \frac{2^{\frac{5}{4}-\frac{3}{2p}}}{\sigma^{\frac{p-3}{p}}}\frac{1}{\pi}(3\alpha)^{-\frac{3}{4}}.
$$

Therefore, in the p-generalizations of the Smagorinsky EV term, the generalized Lilly's constant $C_{S,p}$ depends also on the rate of energy injection (or dissipation). In particular, it is not a universal constant, but it still depends in a precise way on the experiment we are trying to simulate.

Concerning the assumption (19) we observe that for large p the approximation can be very bad. In fact, measurements of the probability distribution function of the gradient of velocity made in the atmospheric boundary layer (hence at a very high Reynolds number) have been performed. The tails of the distribution (beyond four standard deviations) decay as simple exponentials. This decay is much slower than that of the standardized Gaussian (On the other hand the velocity in isotropic turbulence cannot be Gaussian.) Then, the contribution of the tails to the normalized velocity derivative moments

$$M_n = \frac{\mathbb{E}\left[\left|\frac{\partial u_1}{\partial x_1}\right|^n\right]}{\mathbb{E}\left[\left|\frac{\partial u_1}{\partial x_1}\right|^2\right]^{\frac{n}{2}}}$$

increases very rapidly with n. For instance M_6 is about 15 times the corresponding moment for a Gaussian variable. For a discussion see Pope [37, Sect. 6.7].

3.6 On a Wall Bounded Problem

In this section we want to give some ideas of what can be done in presence of some kind of space-anisotropy. First we recall that the first attempt to generalize the Smagorinsky model to more complex geometries dates back to Van Driest [12], even if his studies had different motivations (and they are also dated before appearance of LES!).

The simplest situation with boundaries is the channel flow. For this very simple geometric situation an *ad hoc* generalization of the Smagorinsky model have been proposed in [12], with damping of the turbulent stress tensor near the walls determined by a suitable exponential. Beside being purely empirical and being based on consistency with the *mixing length hypothesis*, this approach provides good representation of the data.

A more recent attempt to extend the problem to more complex geometries has been taken into account by Scotti, Meneveau, and Lilly [41]. In presence of discretization grids with aspect ratios $a_1 = \delta_1/\delta_3$ and $a_2 = \delta_2/\delta_3$ (which are different in the various directions) it has been shown that the term $(C_S\delta)^2$ may be replaced by

$$C_S(\delta_1\delta_2\delta_3)^{\frac{1}{3}} f(a_1, a_2),$$

where the function f can be determined by using an approach based again on theoretical arguments for isotropic turbulence. The function f is approximated by

$$f(a_1, a_2) \simeq \cosh\sqrt{\frac{4}{27}\big[\log^2(a_1) - \log(a_1)\log(a_2) + \log^2(a_2)\big]},$$

and also dynamic versions have been considered. This approach considers the LES method as a computational discrete method, hence it tries to adapt the method to the grid. For instance the flow past a bluff-body needs a big refinement in the streamwise direction. Hence, in the far wake region one can have a very anisotropic grid to simulate a turbulent flow which can be not very far from isotropic.

In this section we want to use a different approach: we do not consider the problem as a discretized problem (as in [41] and further works) but we want to say something on a non-isotropic problem, starting from the point of view of statistical analysis and scaling transformations. Hence, we try to adapt the previous techniques based on scaling to the flow bounded by two rigid walls. In particular, we suppose that the flow takes place in the domain

$$D = \left\{(x, y, z) : x,\ y \in \mathbb{R}^2,\ 0 < z < 1\right\}, \tag{20}$$

with periodicity in the x-y directions. We consider the scale invariant transformations (only in x, y, and t variables) that are allowed for the velocity $u = (u_1, u_2, u_3)$ and the pressure π. (We use now a notation which is a little bit different from the previous sections, because we need to distinguish the various components of the space variables and of the velocity). Since no scaling is possible along the (vertical) z-axis direction, we define the following scaled quantities:

$$\begin{pmatrix} u_1^\lambda(t,x,y,z) = \lambda^\alpha u_1(\lambda^\beta t, \lambda x, \lambda y, z) & u_2^\lambda(t,x,y,z) = \lambda^\alpha u_2(\lambda^\beta t, \lambda x, \lambda y, z) \\ \\ u_3^\lambda(t,x,y,z) = \lambda^\gamma u_3(\lambda^\beta t, \lambda x, \lambda y, z) & \pi^\lambda(t,x,y,z) = \lambda^\delta \pi(\lambda^\beta t, \lambda x, \lambda y, z) \end{pmatrix}.$$

Simple calculations show that necessarily

$$\beta = \gamma = \alpha + 1 \qquad \text{and} \qquad \delta = 2\alpha, \tag{21}$$

if we want to keep the material derivative $\frac{D}{Dt}$ appropriately scaled. Hence, we plug the functions (u^λ, π^λ) with such α, β, γ, and δ in the Navier-Stokes equations and we obtain (here given any differential operator L, the symbol L' denotes the same operator restricted to the first two variables, e.g., Δ' is the Laplacian in the x-y variables, while $\nabla' = (\partial_x, \partial_y, 0)$)

$$\begin{cases} \dfrac{Du_1^\lambda}{Dt} - \nu\lambda^{\alpha-1}\Delta' u_1^\lambda - \nu\lambda^{\alpha+1}\partial_{zz}^2 u_1^\lambda + \partial_x \pi^\lambda = 0, \\ \dfrac{Du_2^\lambda}{Dt} - \nu\lambda^{\alpha-1}\Delta' u_2^\lambda - \nu\lambda^{\alpha+1}\partial_{zz}^2 u_2^\lambda + \partial_y \pi^\lambda = 0, \\ \dfrac{Du_3^\lambda}{Dt} - \nu\lambda^{\alpha-1}\Delta' u_3^\lambda - \nu\lambda^{\alpha+1}\partial_{zz}^2 u_3^\lambda + \lambda^2\partial_z \pi^\lambda = 0. \end{cases} \tag{22}$$

If we assume now that an external force $\dot{W}$ is present and if we use the exponent $\alpha = -\frac{1}{3}$ (for the same reasons explained before) we get

$$\begin{cases} \dfrac{Du_1}{Dt} - \nu\lambda^{-\frac{4}{3}}\Delta' u_1 - \nu\lambda^{\frac{2}{3}}\partial_{zz}^2 u_1 + \partial_x \pi = \dot{W}^\lambda, \\ \dfrac{Du_2}{Dt} - \nu\lambda^{-\frac{4}{3}}\Delta' u_2 - \nu\lambda^{\frac{2}{3}}\partial_{zz}^2 u_2 + \partial_y \pi = \dot{W}^\lambda, \\ \dfrac{Du_3}{Dt} - \nu\lambda^{-\frac{4}{3}}\Delta' u_3 - \nu\lambda^{\frac{2}{3}}\partial_{zz}^2 u_3 + \lambda^2\partial_z \pi = \dot{W}^\lambda. \end{cases} \tag{23}$$

Disregarding the terms that are of smaller order (as $\lambda \to 0$), and calling u^λ (with a slight abuse of notation) again u, we get the following *anisotropic* Navier-Stokes

$$\frac{Du}{Dt} - \nu\lambda^{-\frac{4}{3}}\Delta' u + \nabla'\pi = \dot{W}.$$

Again the structure of the equations allows to find, in the limit of small viscosity, an expression for the energy dissipation involving the term

$$\nu\mathbb{E}\left[\int_{T_L} |\nabla' u|^2 dx\right] = \frac{L^3\sigma^2}{2}.$$

Note that, since the effects of the dissipation in the z-variables are much smaller, the corresponding terms can be disregarded. This can be seen in the light of geostrophic models with Ekman Layers, see Chemin et al. [8].

We now use the same approach, but we suppose that the equations that govern the fluid are those of Smagorinsky (4) (but the same argument applies as well also to generalized p-models). To employ the same procedure, we first need to evaluate the scaling transformation for $\nabla^s\overline{u}^\lambda$

$$\nabla^s\overline{u}^\lambda(t, x, y, z) =$$

$$\begin{pmatrix} \lambda^{\alpha+1}\partial_x\overline{u}_1 & \lambda^{\alpha+1}\frac{\partial_x\overline{u}_2 + \partial_y\overline{u}_2}{2} & \lambda^\alpha\frac{\partial_z\overline{u}_1}{2} + \lambda^{\alpha+2}\frac{\partial_x\overline{u}_3}{2} \\ * & \lambda^{\alpha+1}\partial_y\overline{u}_2 & \lambda^\alpha\frac{\partial_z\overline{u}_2}{2} + \lambda^{\alpha+2}\frac{\partial_y\overline{u}_3}{2} \\ * & * & \lambda^{\alpha+1}\partial_z\overline{u}_3 \end{pmatrix}(\lambda^{\alpha+1}t, \lambda x, \lambda y, z),$$

where $*$ is put just to recall that the matrix is symmetric and we need to mirror terms off from the diagonal. Hence, we can write that

$$|\nabla^s\overline{u}|(\lambda^{\alpha+1}t, \lambda x, \lambda y, z) =$$
$$\lambda^{-\alpha}J_1(t, x, y, z) + \lambda^{-(\alpha+1)}J_2(t, x, y, z) + \lambda^{-(\alpha+2)}J_3(t, x, y, z),$$

with (some factor 1/2 is present, but inessential)

$$J_1(t, x, y, z) = |\partial_z\overline{u}_1^\lambda|(t, x, y, z) + |\partial_z\overline{u}_2^\lambda|(t, x, y, z),$$
$$J_2(t, x, y, z) = |\nabla'\overline{u}_1^\lambda|(t, x, y, z) + |\nabla'\overline{u}_2^\lambda|(t, x, y, z) + |\partial_z\overline{u}_3^\lambda|(t, x, y, z),$$
$$J_3(t, x, y, z) = |\nabla'\overline{u}_3^\lambda|(t, x, y, z).$$

Plugging this expressions into (4) we get the following equations

$$\begin{cases} \dfrac{D\overline{u}_1^\lambda}{Dt} - \lambda^{\alpha-1}\left[\nu\Delta'\overline{u}_1^\lambda + \nabla'\cdot(C_S^2\delta^2|\nabla^s\overline{u}^\lambda|\nabla'\overline{u}_1^\lambda)\right] \\ \qquad\qquad - \lambda^{\alpha+1}\left[\nu\partial_{zz}^2\overline{u}_1^\lambda + \partial_z(C_S^2\delta^2|\nabla^s\overline{u}^\lambda|\partial_z\overline{u}_1^\lambda)\right] + \partial_x\pi^\lambda = \dot{W}, \\ \dfrac{D\overline{u}_2^\lambda}{Dt} - \lambda^{\alpha-1}\left[\nu\Delta'\overline{u}_2^\lambda + \nabla'\cdot(C_S^2\delta^2|\nabla^s\overline{u}^\lambda|\nabla'\overline{u}_2^\lambda)\right] \\ \qquad\qquad - \lambda^{\alpha+1}\left[\nu\partial_{zz}^2\overline{u}_2^\lambda + \partial_z(C_S^2\delta^2|\nabla^s\overline{u}^\lambda|\partial_z\overline{u}_2^\lambda)\right] + \partial_y\pi^\lambda = \dot{W}, \\ \dfrac{D\overline{u}_3^\lambda}{Dt} - \lambda^{\alpha+1}\left[\nu\Delta'\overline{u}_3^\lambda + \nabla'\cdot(C_S^2\delta^2|\nabla^s\overline{u}^\lambda|\nabla'\overline{u}_3^\lambda)\right] \\ \qquad\qquad - \lambda^{\alpha-1}\left[\nu\partial_{zz}^2\overline{u}_3^\lambda + \partial_z C_S^2\delta^2|\nabla^s\overline{u}^\lambda|\partial_z\overline{u}_3^\lambda\right] + \lambda^2\partial_z\pi^\lambda = \dot{W}. \end{cases} \tag{24}$$

At this point to understand which are the "relevant" terms in $\nabla^s\overline{u}^\lambda$, we observe that

$$\delta^2\nabla^s\overline{u}^\lambda = \delta^2 J_1 + \frac{\delta^2}{\lambda}J_2 + \frac{\delta^2}{\lambda^2}J_3,$$

hence for $\delta \simeq \lambda$, and in the limit of asymptotically small λ, the only term that survives is J_3. This observation and setting $\alpha = -\frac{1}{3}$, allows us to consider (up to the leading order) the following system of partial differential equations for $\overline{u}^\lambda$, which we call again $\overline{u}$:

$$\frac{D\overline{u}}{Dt} - \nu\lambda^{-\frac{4}{3}}\Delta'\overline{u} - C_S^2\delta^2\nabla'(|\nabla'\overline{u}_3|\nabla'\overline{u}) + \nabla'\overline{\pi} = \dot{W}.$$

In the limit of small ν we get, for stationary solutions,

$$C_S^2\delta^2\,\mathbb{E}\left[\int_{T_L}|\nabla'\overline{u}_3|\nabla'\overline{u}|^2dx\right] = \frac{L^3\sigma^2}{2}.$$

The resulting equations are similar to certain proposed in order to study gravity waves involving fluids with large scales in the horizontal direction as in global circulation models. Thus, despite the increase in computational power, not all scales in the ocean circulation can be resolved simultaneously. Basin models are configured for $\mathcal{O}(1000\,\text{km})$ to $\mathcal{O}(10\,\text{km})$, and regional or coastal models from $\mathcal{O}(100\,\text{km})$ to $\mathcal{O}(1\text{km})$, requiring both sub-grid-scale parametrization and extra-domain forcing. There exist, however, small-scale ocean flows (which take place below this inherently coarse numerical resolution) that often play a significant role in an accurate representation of the large ocean scales: The entrainment of ambient waters into overflows has a significant impact on the global balance of the thermohaline circulation, and affects the transport of pollutants, sediments, and biological species.

It is then a challenging problem to propose LES models (also based on suitable modifications of the Smagorinsky model) for this problems. Hence, a numerical method based on Smagorinsky acting only in the horizontal variables may be derived also by using our approach and it turns out to be similar to those tested in Özgökmen et al. [36].

4 Conclusions

We reviewed some well-known results on eddy-viscosity models for LES and on stochastic Navier-Stokes equations. Moreover, we provided a new justification, based on a statistical approach, of the derivation of some EV and we used tools from stochastic partial differential equations to estimate relevant parameters. In addition, we proposed a new modeling for equations in thin domains. The presence of a Smagorinsky-like term acting only in the horizontal directions is one of the most promising technique to attack numerically problems of geophysics or more generally with very different scales in different directions. In future work we shall test the generalized models we are proposing and we also shall start the analysis of the well-posedness of the systems of partial differential equations for thins domains we introduced.

References

1. Beirão da Veiga, H.: On the regularity of flows with Ladyzhenskaya shear-dependent viscosity and slip or nonslip boundary conditions. Comm. Pure Appl. Math. **58**, 552–577 (2005)
2. Beirão da Veiga, H.: Navier-Stokes equations with shear-thickening viscosity. Regularity up to the boundary. J. Math. Fluid Mech. (2008) *http://dx.doi.org/10.1007/s00021-008-0257-2*
3. Bensoussan, A., Temam, R.: Équations stochastiques du type Navier-Stokes. J. Functional Analysis **13**, 195–222 (1973)
4. Berselli, L.C., Iliescu, T., Layton, W.J.: *Mathematics of Large Eddy Simulation of Turbulent Flows*. Scientific Computation. Springer-Verlag, Berlin (2006)
5. Boussinesq, J.: Theorie de l'écoulement tourbillant. Mém. prés par div. savants à la Acad. Sci. **23**, 46–50 (1877)
6. Breuer, M., Jovicic, J.: Separated flow around a flat plate at high incidence: An LES investigation. J. Turbulence **2**, 18 (2001)
7. Chalot, F., Marquez, B., Ravachal, M., Ducros, F., Nicoud, F., Poinsot, T.: A consistent finite element approach to Large Eddy Simulation. Tech. Rep. 98-2652, 29th AIAA Fluid Dynamics Conference, Albuquerque, New Mexico, June 15–18 (1998)
8. Chemin, J.Y., Desjardins, B., Gallagher, I., Grenier, E.: Fluids with anisotropic viscosity. M2AN Math. Model. Numer. Anal. **34**, 315–335 (2000). Special issue for R. Temam's 60th birthday
9. Cheskidov, A., Constantin, P., Friedlander, S., Shvydkoy, R.: Energy conservation and Onsager's conjecture for the Euler equations. Nonlinearity **21**, 1233–1252 (2008)
10. Cottet, G.H., Jiroveanu, D., Michaux, B.: Vorticity dynamics and turbulence models for Large Eddy Simulations. M2AN Math. Model. Numer. Anal. **37**, 187–207 (2003)
11. Deardorff, J.W.: On the magnitude of the subgrid scale eddy coefficient. J. Comput. Phys. **7**, 120–133 (1971)
12. Van Driest, E.: On turbulent flow near a wall. J. Aerospace Sci. **23**, 1007–1011 (1956)
13. Du, A., Duan, J.: A stochastic approach for parameterizing unresolved scales in a system with memory. J. Algorithms Comput. Technol. **3**, 393–405 (2009)

14. Duan, J., Nadiga, B.T.: Stochastic parameterization for large Eddy simulation of geophysical flows. Proc. Amer. Math. Soc. **135**, 1187–1196 (2007)
15. Flandoli, F.: An introduction to stochastic 3D fluids. In: *SPDE in Hydrodynamics: Recent Progress and Prospects*, Lecture Notes in Math., Vol. **1942**, 51–148, Springer-Verlag, Berlin (2008). Lectures from the C.I.M.E.-E.M.S. Summer School held in Cetraro, August 29–September 3, (2005)
16. Flandoli, F., Gubinelli, M., Hairer, M., Romito, M.: Rigorous remarks about scaling laws in turbulent fluids. Comm. Math. Phys. **278**, 1–29 (2008)
17. Frisch, U.: *Turbulence*, The Legacy of A.N. Kolmogorov. Cambridge University Press, Cambridge (1995)
18. Galdi, G.P.: An introduction to the Navier-Stokes initial-boundary value problem. In: *Fundamental Directions in Mathematical Fluid Mechanics*. Adv. Math. Fluid Mech., 1–70. Birkhäuser, Basel (2000)
19. Galdi, G.P.: Mathematical Problems in Classical and non-Newtonian Fluid Mechanics. Oberwolfach Reports (2008). To appear
20. Germano, M., Piomelli, U., Moin, P., Cabot, W.: A dynamic subgrid-scale eddy viscosity model. Phys. Fluids A **3**, 1760–1765 (1991)
21. Iliescu, T.: Genuinely nonlinear models for convection-dominated problems. Comput. Math. Appl. **48**, 1677–1692 (2004)
22. Kolmogorov, A.: The local structure of turbulence in incompressible viscous fluids for very large Reynolds number. Dokl. Akad. Nauk SSR **30**, 9–13 (1941)
23. Kupiainen, A.: Statistical theories of turbulence. In: *Advances in Mathematical Sciences and Applications*, Gakkotosho, Tokyo, (2003)
24. Ladyžhenskaya, O.: New equations for the description of motion of viscous incompressible fluids and solvability in the large of boundary value problems for them. Proc. Stek. Inst. Math. **102**, 95–118 (1967)
25. Layton, W.J.: A nonlinear, subgridscale model for incompressible viscous flow problems. SIAM J. Sci. Comput. **17**, 347–357 (1996)
26. Layton, W.J., Neda, M.: A similarity theory of approximate deconvolution models of turbulence. J. Math. Anal. Appl. **333**, 416–429 (2007)
27. Layton, W.J., Neda, M.: Truncation of scales by time relaxation. J. Math. Anal. Appl. **325**, 788–807 (2007)
28. Lesieur, M., Métais, O., Comte, P.: *Large-eddy Simulations of Turbulence*. Cambridge University Press, New York (2005). With a preface by James J. Riley
29. Lilly, D.K.: On the application of the eddy viscosity concept in the inertial subrange of turbulence. NCAR Manuscript (1966). Boulder, Co.
30. Lilly, D.K.: The representation of small scale turbulence in numerical simulation experiments. In: H. Goldstine (ed.) *Proc. IBM Sci. Computing Symp. on Environmental Sciences*. Yorktown Heights NY, 195–210 (1967)
31. Lilly, D.K.: The length scale for subgrid-scale parametrization with anisotropic resolution. Center for Turbulence Research, Stanford University, NASA Ames Research Center, CTR Annual Research Briefs (1988)
32. Lions, J.L.: *Quelques méthodes de résolution des problèmes aux limites non linéaires*. Dunod (1969)
33. Málek, J., Nečas, J., Rokyta, M., Růžička, M.: *Weak and Measure-valued Solutions to Evolutionary PDEs*. Appl. Math. and Math. Comp., Vol. 13. Chapman & Hall, London (1996)
34. Moin, P., Kim, J.: Numerical investigation of turbulent channel flow. J. Fluid Mech. **114**, 343–359 (1982)
35. Øksendal, B.: *Stochastic Differential Equations: An Introduction with Applications*, sixth edn. Universitext. Springer-Verlag, Berlin (2003)
36. Özgökmen, T., Iliescu, T., Fischer, P., Srinivasan, A., Duan, J.: Large eddy simulation of stratified mixing in two-dimensional dam-break problem in a rectangular enclosed domain. Ocean Modelling **16**, 106–140 (2007)

37. Pope, S.: *Turbulent Flows.* Cambridge University Press, Cambridge (2000)
38. Richardson, L.: *Weather Prediction by Numerical Process.* Cambridge University Press, Cambridge (1922)
39. Rodi, W., Ferziger, J., Breuer, M., Pourquié, M.: Status of large-eddy simulation. workshop on LES of flows past bluff bodies (Rottach-Egern, Tegernsee, 1995). ASME J. Fluid Engng. **119**, 248–262 (1997)
40. Sagaut, P.: *Large Eddy Simulation for Incompressible Flows.* Scientific Computation. Springer-Verlag, Berlin (2001). With an introduction by Marcel Lesieur, Translated from the 1998 French original by the author
41. Scotti, A., Meneveau, C., Lilly, D.K.: Generalized Smagorinsky model for anisotropic grids. Phys. Fluids **5**, 2306 (1993)
42. Smagorinsky, J.: General circulation experiments with the primitive equations. Monthly Weather Review **91**, 99–164 (1963)

Numerical Study of the Significance of the Non-Newtonian Nature of Blood in Steady Flow Through a Stenosed Vessel

Tomáš Bodnár and Adélia Sequeira

Abstract In this paper we present a comparative numerical study of non-Newtonian shear-thinning and viscoelastic blood flow models through an idealized stenosis. Three-dimensional numerical simulations are performed using a finite volume semi-discretization in space, on structured grids, and a multistage Runge-Kutta scheme for time integration, to investigate the influence of combined effects of inertia, viscosity and viscoelasticity in this particular geometry. This work lays the foundation for future applications to pulsatile flows in stenosed vessels using constitutive models capturing the rheological response of blood, under relevant physiological conditions.

Keywords Non-Newtonian fluids · Blood rheology · Stenosis · Numerical simulations

1 Introduction

One of the most frequent abnormalities of the vascular system is the partial occlusion of blood vessels due to stenotic obstruction (lumen area reduction) related to atherosclerosis. There is strong evidence that hemodynamical factors such as flow separation, flow recirculation, low and oscillatory wall shear stress, play a major role in the development and progression of atherosclerotic plaques and other arterial lesions (see e.g. [3, 8]) but their specific role is not completely understood. The mathematical and numerical study of meaningful constitutive models, that can accurately capture the rheological response of blood over a range of physiological flow conditions, is recognized as an invaluable tool for the interpretation and analysis of the circulatory system functionality, in both physiological and pathological situations [18].

A. Sequeira (✉)
Department of Mathematics and CEMAT, Instituto Superior Técnico,
Technical University of Lisbon, 1049-001 Lisbon, Portugal
e-mail: adelia.sequeira@math.ist.utl.pt

R. Rannacher, A. Sequeira (eds.), *Advances in Mathematical Fluid Mechanics*,
DOI 10.1007/978-3-642-04068-9_6,

Blood is a concentrated suspension of formed cellular elements including red blood cells (RBCs or erythrocytes), white blood cells (WBCs or leukocytes) and platelets (thrombocytes). These cellular elements are suspended in an aqueous polymeric and ionic solution of low viscosity, the plasma, containing electrolytes and organic molecules such as metabolites, hormones, enzymes, antibodies and other proteins. The formed elements are produced in the bone marrow and represent approximately 45% by volume of the normal human blood [8].

The study of blood flow in the vascular system is complicated in many respects and thus simplifying assumptions are often made. Plasma behaves as a Newtonian fluid but whole blood exhibits marked non-Newtonian properties, like shear thinning viscosity, thixotropy, viscoelasticity and possibly a yield stress. This is largely explained by erythrocyte behavior, mainly their ability to aggregate into three-dimensional microstructures (*rouleaux*) at low shear rates, their deformability (or breakup) and their tendency to align with the flow field at high shear rates [12]. In particular, at rest or at low shear rates (below $1\,s^{-1}$) blood seems to have a high apparent viscosity, while at high shear rates there is a reduction in the blood's viscosity. Attempts to recognize the shear-thinning nature of blood were initiated by Chien et al. [10, 11] in the 1960s. Empirical models like the power-law, Cross, Carreau or W-S generalized Newtonian fluid models (see [4, 32]) have been obtained by fitting experimental data in one dimensional flows. More recently, Vlastos et al. [31] proposed a modified Carreau equation to capture the shear dependence of blood viscosity.

Experiments on blood at low shear rates are extremely difficult to perform and consequently a controversy remains on the behavior of blood at the limit of zero shear rate. Despite this controversy, it is commonly accepted that blood displays a yield stress. Namely, there is a critical value of stress (the yield stress) below which blood does not flow. The treatment of yield stress as a material parameter should be independent of experimental factors and of yielding criteria and this is not the case for blood. In fact there exists a large variation in yield stress values for blood reported in the literature (e.g [22]). The finite time required for the changes in blood microstructure is related to blood yield stress and thixotropy. Charm et al. [9] found that Casson's model gives the best fit to blood data. Casson's and Herschel-Bulkley models [27] are generalizations of the Bingham model that can capture both the yield stress and the shear-thinning behavior of blood.

None of the previous homogenized models can predict the viscoelastic response of blood. Blood cells are essentially elastic membranes filled with a fluid and it seems reasonable, at least under certain flow conditions, to expect blood to behave like a viscoelastic fluid. At low shear rates, erythrocytes aggregate and store elastic energy that accounts for the memory effects in blood. At high shear rates, they disaggregate forming smaller rouleaux, and later individual cells, that are characterized by distinct relaxation times. They lose their ability to store elastic energy and the dissipation is primarily due to the internal friction. Upon cessation of shear, the entire rouleaux network is randomly arranged and may be assumed to be isotropic with respect to the current natural configuration. Thurston [28] was among the earliest to recognize the viscoelastic nature of blood and that the viscoelastic behavior is less prominent with increasing shear rate. He proposed a generalized Maxwell model that was applicable to one dimensional flow simulations and observed later that, beyond a critical shear rate, the non-linear behavior is related to the microstructural changes that occur in blood [29]. Thurston's work was suggested to be more applicable to venous or low shear unhealthy blood flow than to arterial flows. Recently, a generalized Maxwell model related to the microstructure of blood, inspired on the behavior of transient networks in polymers, and exhibiting shear-thinning, viscoelasticity and thixotropy, has been derived by Owens [21].

Other viscoelastic constitutive models for describing blood rheology have been proposed in the recent literature. The empirical three constant generalized Oldroyd-B model studied in [33] belongs to this class. It has been obtained by fitting experimental data in one dimensional flows and generalizing such curve fits to three dimensions. This model captures the shear-thinning behavior of blood over a large range of shear rates but it has its limitations, given that the relaxation times do not depend on the shear rate, which does not agree with experimental observations. The model developed by Anand and Rajagopal [1] in the general thermodynamic framework stated in [23] includes relaxation times depending on the shear rate and gives good agreement with experimental data in steady Poiseuille flow and oscillatory flow.

Non-Newtonian homogeneous continuum models are very significant in hemodynamics and hemorheology. However, it should be emphasized that blood flow is Newtonian in most parts of the arterial system and attention should be drawn to flow regimes and clinical situations where non-Newtonian effects of blood can probably be observed. These include, for normal blood, regions of stable recirculation like in the venous system and parts of the arterial vasculature where geometry has been altered and RBC aggregates become more stable, like downstream a stenosis, inside a saccular aneurysm or in some cerebral anastomoses. In addition, several pathologies are accompanied by significant changes in the mechanical properties of blood and this results in alterations in blood viscosity and viscoelastic properties, as reported in the recent review articles [25, 26].

In what follows we present a comparative numerical study of non-Newtonian fluid models capturing shear-thinning and viscoelastic effects of blood flow in a smooth idealized stenosed vessel. Section 2 is devoted to the description of a number of constitutive models, namely the equations of generalized Oldroyd-B flows with shear dependent viscosity. The numerical methods and the adopted stabilization techniques are briefly outlined in Sect. 2. Preliminary results of the three-dimensional simulations predicted by the constitutive models under physiologically relevant conditions are presented in Sect. 4, showing combined effects of inertia, viscosity and viscoelasticity. The paper ends with concluding remarks.

2 Constitutive Models for Blood

In this section we discuss basic macroscopic constitutive models suitable to capture both shear-thinning and viscoelastic properties of blood, under certain flow conditions. We recall the equations for the conservation of linear momentum and mass (incompressibility condition) for isothermal viscous flows

$$\varrho \frac{D\boldsymbol{u}}{Dt} = \text{div}\,\mathbf{T} - \nabla p \quad (1)$$

$$\text{div}\,\boldsymbol{u} = 0. \quad (2)$$

Here, $\boldsymbol{u}$ is the velocity field, p is the pressure, ϱ is the density, and $D(\cdot)/Dt$ denotes the material time derivative. To close the system of equations we require an equation relating the extra stress tensor $\mathbf{T}$ to the kinematic variables.

The simplest constitutive model for incompressible viscous fluids is based on the assumption that the extra stress tensor is proportional to the symmetric part of the velocity gradient,

$$\mathbf{T} = 2\mu\mathbf{D} \quad (3)$$

where μ is a (constant) viscosity and $\mathbf{D} = (\nabla\boldsymbol{u} + \nabla\boldsymbol{u}^T)/2$ is the rate of deformation tensor. Substitution of (3) in the linear momentum equation (1) leads to the well known Navier-Stokes system. As already discussed, this set of equations is commonly used to describe blood flow in the heart and healthy arteries but, particularly at low shear rates, blood exhibits relevant non-Newtonian characteristics and more complex constitutive models should be used.

2.1 Generalized Newtonian Models

The most general constitutive model of the form $\mathbf{T} = \mathbf{T}(\nabla\boldsymbol{u})$ which satisfies invariance requirements [2] can be written as

$$\mathbf{T} = \varphi_1(II_D, III_D)\mathbf{D} + \varphi_2(II_D, III_D)\mathbf{D}^2 \quad (4)$$

where II_D and III_D are the second and third principal invariants of $\mathbf{D}$

$$II_D = \frac{1}{2}\left((tr\mathbf{D})^2 - tr\left(\mathbf{D}^2\right)\right), \quad III_D = det\mathbf{D} \quad (5)$$

and $tr\mathbf{D} \equiv 0$ for isochoric motions. Incompressible fluids of the form (4) are called Reiner-Rivlin fluids. They include Newtonian fluids as a particular case, corresponding to φ_1 constant and $\varphi_2 \equiv 0$.

The behavior of real fluids impose some restrictions on the material functions φ_1 and φ_2. In fact, there is no evidence of real fluids with non-zero values of φ_2 and the dependance on the value of III_D is often neglected [2]. As a result, attention is usually restricted to a special class of Reiner-Rivlin fluids called generalized Newtonian fluids

$$\mathbf{T} = 2\mu(\dot{\gamma})\mathbf{D} \quad (6)$$

where $\dot{\gamma}$ is the shear rate (a measure of the rate of deformation)[1] defined by

$$\dot{\gamma} \equiv \sqrt{2tr(\mathbf{D}^2)} = \sqrt{-4II_D} \tag{7}$$

and $\mu(\dot{\gamma})$ is a shear dependent viscosity function.

One of the simplest generalized Newtonian fluids is the *power-law*, for which the viscosity function is given by

$$\mu(\dot{\gamma}) = K\dot{\gamma}^{(n-1)} \tag{8}$$

where the positive constants n and K are termed the power-law index and consistency, respectively. This model includes, as a particular case, the constant viscosity fluid (Newtonian) when $n = 1$. For $n < 1$ is leads to a monotonic decreasing function of the shear rate (shear-thinning fluid) and for $n > 1$ the viscosity increases with shear rate (shear thickening fluid). The shear-thinning power-law model is often used for blood, due to the analytical solutions easily obtained for its governing equations, but it predicts an unbounded viscosity at zero shear rate and zero viscosity when $\dot{\gamma} \to \infty$, which is unphysical.

Viscosity functions with bounded and non-zero limiting values of viscosity can be written in the general form

$$\mu(\dot{\gamma}) = \mu_\infty + (\mu_0 - \mu_\infty)F(\dot{\gamma}) \tag{9}$$

or, in non-dimensional form as

$$\frac{\mu(\dot{\gamma}) - \mu_\infty}{\mu_0 - \mu_\infty} = F(\dot{\gamma}). \tag{10}$$

Here μ_0 and μ_∞ are the asymptotic viscosity values at zero and infinite shear rates and $F(\dot{\gamma})$ is a shear dependent function, satisfying the following natural limit conditions

$$\lim_{\dot{\gamma}\to 0^+} F(\dot{\gamma}) = 1 \qquad \text{and} \qquad \lim_{\dot{\gamma}\to\infty} F(\dot{\gamma}) = 0$$

Different choices of function $F(\dot{\gamma})$ correspond to different models for blood flow, with material constants quite sensitive and depending on a number of factors including hematocrit, temperature, plasma viscosity, age of RBCs, exercise level, gender or disease state. The generalized *Cross* model given by

$$\mu(\dot{\gamma}) = \mu_\infty + \frac{\mu_0 - \mu_\infty}{\left(1 + (\lambda\dot{\gamma})^b\right)^a} \tag{11}$$

[1] For isochoric motions II_D is not a positive quantity.

contains other models as special cases and has been adopted in our numerical simulations. Parameters λ, a and b have been obtained by nonlinear regression analysis. Commonly used values found in literature are [17]:

$$\mu_0 = 1.6 \cdot 10^{-1} Pa \cdot s \qquad \mu_\infty = 3.6 \cdot 10^{-3} Pa \cdot s$$
$$a = 1.23, b = 0.64 \qquad \lambda = 8.2\, s$$

2.2 Viscoelastic Models

One of the simplest rate type models accounting for the viscoelasticity of blood is the *Maxwell* model

$$\mathbf{T} + \lambda_1 \frac{\delta \mathbf{T}}{\delta t} = 2\mu \mathbf{D} \tag{12}$$

where λ_1 is the relaxation time and $\delta(\cdot)/\delta t$ stands for the so-called *convected derivative*, a generalization of the material time derivative, chosen so that $\delta \mathbf{T}/\delta t$ is objective under a superposed rigid body motion and the resulting second-order tensor is symmetric [24].

A more general class of rate type models, called *Oldroyd type* models, can be defined by

$$\mathbf{T} + \lambda_1 \frac{\delta \mathbf{T}}{\delta t} = 2\mu \left(\mathbf{D} + \lambda_2 \frac{\delta \mathbf{D}}{\delta t} \right) \tag{13}$$

where the material coefficient λ_2, denotes the retardation time. and is such that $0 \leq \lambda_2 < \lambda_1$. The Oldroyd type fluids can be considered as Maxwell fluids with additional viscosity. These models contain the previous two models (3) and (12) as particular cases.

In order to better understand the theory of viscoelasticity it is instructive and useful to illustrate typical behaviors of viscoelastic materials by simple mechanical models, where a dashpot (piston moving inside a cylinder filled with liquid) represents a viscous (Newtonian) fluid and a spring stands for an elastic (Hookean) solid. These elements can be connected in series or in parallel and their combinations can represent various deformation-stress models to analyze the behavior of different viscoelastic materials [19, 13, 7]. The one-dimensional mechanical analogue to (12) can be represented by an elastic spring and a dashpot in series, as shown in Fig. 1. Here, the speed of movement γ_V is an analogue of the rate of deformation, the coefficient of proportionality μ (for the viscous element) is an analogue of viscosity, γ_E can be treated as a relative deformation, G as the elastic modulus and the force $\boldsymbol{\tau}$ is an analogue of the extra stress $\mathbf{T}$ in (12)). The ratio between the viscosity μ and elastic modulus G is hidden in the relaxation time parameter λ_1.

The combination of the Newtonian model and the Maxwell model joined in parallel is shown in Fig. 2 which represents the mechanical analogue to the Oldroyd

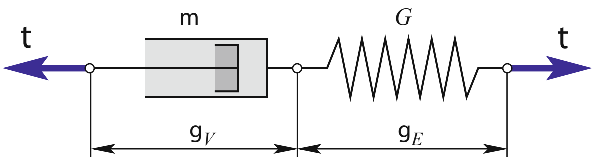

Fig. 1 Mechanical analogue of the Maxwell model

model (13). Here the total viscosity μ is defined as $\mu = \mu_s + \mu_e$, where μ_s and μ_e are the solvent and the elastic viscosity coefficients. Moreover, parameters $\lambda_1, \ \lambda_2$ are defined by

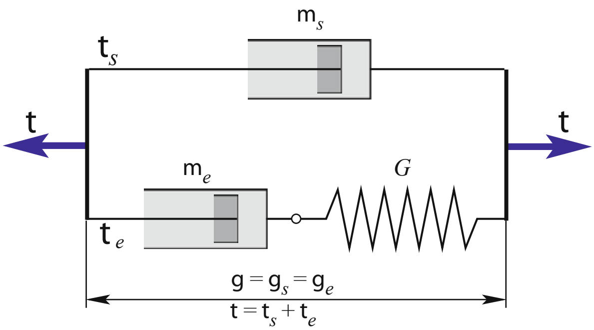

Fig. 2 Mechanical analogue of an Oldroyd-type model

$$\lambda_1 = \frac{\mu_e}{G}, \qquad \lambda_2 = \lambda_1 \frac{\mu_s}{\mu_s + \mu_e} \tag{14}$$

and are such that $0 \le \lambda_2 < \lambda_1$ (assuming μ_e is not zero).

The total force τ can be expressed as the sum of the Newtonian solvent contribution τ_s and its viscoelastic counterpart τ_e. In a similar manner, the extra stress tensor $\mathbf{T}$ in Eq. (13) is decomposed into its Newtonian part $\mathbf{T}_s$ and its elastic part $\mathbf{T}_e$, $\mathbf{T} = \mathbf{T}_s + \mathbf{T}_e$, such that $\mathbf{T}_s = 2\mu_s\mathbf{D}$ and $\mathbf{T}_e$ satisfies a constitutive equation of Maxwell type, namely

$$\mathbf{T}_e + \lambda_1 \frac{\delta \mathbf{T}_e}{\delta t} = \mathbf{2}\mu_e\mathbf{D} \tag{15}$$

2.2.1 Convected Derivatives and Oldroyd-B Model

The general expression for a one-parameter family of convected derivatives of a tensor $\mathbf{M}$ is given by[2]

[2] This is sometimes referred as Gordon-Schowalter derivative with parameter $a = \xi - 1$ where ξ is called slip parameter.

$$\left(\frac{\delta \mathbf{M}}{\delta t}\right)_a = \frac{DM}{Dt} - \mathbf{WM} + \mathbf{MW} + a(\mathbf{DM} + \mathbf{MD}), \qquad a \in [-1, 1] \tag{16}$$

where $\mathbf{W}$ represents the anti-symmetric part of the velocity gradient. The idea of objective derivatives is to take the time derivative with respect to a reference frame suitably fixed to the body. Different choices of body-fixed frames will yield different objective derivatives. A few classical examples of possible objective convected derivatives $\frac{\delta \mathbf{M}}{\delta t}$ are shown in Table 1 ($\mathbf{L} = \mathbf{2D}$).

Table 1 Commonly used convected derivatives

Name	Notation	Definition	Parameter a
Lower-convected	$\overset{\triangle}{\mathbf{M}}$	$\frac{D\mathbf{M}}{Dt} + \mathbf{L}^T\mathbf{M} + \mathbf{ML}$	1
Upper-convected	$\overset{\triangledown}{\mathbf{M}}$	$\frac{D\mathbf{M}}{Dt} - \mathbf{LM} - \mathbf{ML}^T$	−1
Co-rotational (Jaumann)	$\overset{\circ}{\mathbf{M}}$	$\frac{D\mathbf{M}}{Dt} - \mathbf{WM} + \mathbf{MW}$	0

The particular values $a = 1,\ 0$ and -1 correspond respectively to the lower-convected, co-rotational and upper-convected Maxwell or Oldroyd-type (Oldroyd-A and *Oldroyd-B*) models. When $-1 < a < 1$, the Maxwell and Oldroyd-type fluids are often referred to as nonlinear Maxwell and Oldroyd fluids, or Johnson-Segalman fluids [16]. For the upper-convected Maxwell and Oldroyd-B fluids the second normal stress difference is equal to zero. It turns out that this is not observed in viscometric experiments with many real fluids but, since this coefficient has been found to be small, upper-convected Maxwell and Oldroyd-B are often used to model the viscoelastic behavior of real fluids, like blood. However, these models do not account for shear-thinning viscosity. A number of models have already been considered that include both shear-thinning and viscoelastic effects, as mentioned above.

We now recall Eq. (15) for the elastic part of the extra stress tensor. It can be rewritten as

$$\frac{\delta \mathbf{T}_e}{\delta t} = \frac{2\mu_e}{\lambda_1}\mathbf{D} - \frac{1}{\lambda}\mathbf{T}_e \tag{17}$$

or, in terms of the classical material time-derivative, as

$$\frac{D\mathbf{T}_e}{Dt} + \left(\frac{\delta \mathbf{T}_e}{\delta t} - \frac{D\mathbf{T}_e}{Dt}\right) = \frac{2\mu_e}{\lambda_1}\mathbf{D} - \frac{1}{\lambda_1}\mathbf{T}_e, \tag{18}$$

with the term in brackets representing a kind of "objective correction" of the material time-derivative. Moving this term to the right-hand side and expanding the remaining time-derivative on the left, we get the following transport equation for $\mathbf{T}_e$

$$\frac{\partial \mathbf{T}_e}{\partial t} + (\boldsymbol{u} \cdot \nabla)\, \mathbf{T}_e = \frac{2\mu_e}{\lambda_1}\mathbf{D} - \frac{1}{\lambda_1}\mathbf{T}_e - \left(\frac{\delta \mathbf{T}_e}{\delta t} - \frac{D\mathbf{T}_e}{Dt}\right). \tag{19}$$

Using Eq. (16) with $a = -1$, corresponding for the upper-convected derivative (Table 1), transport equation (19) becomes

$$\frac{\partial \mathbf{T}_e}{\partial t} + (\boldsymbol{u} \cdot \nabla)\, \mathbf{T}_e = \frac{2\mu_e}{\lambda_1}\mathbf{D} - \frac{1}{\lambda_1}\mathbf{T}_e + (\mathbf{W}\mathbf{T}_e - \mathbf{T}_e\mathbf{W}) + (\mathbf{D}\mathbf{T}_e + \mathbf{T}_e\mathbf{D}) \tag{20}$$

This is the constitutive equation for an Oldroyd-B fluid. It has one source term and one sink term. The sink term corresponds to an exponential time decay of $\mathbf{T}_e$ at the time-scale related to *relaxation time* λ_1. The parameter λ_1 can thus be regarded as a kind of the "memory time-scale" of the fluid, i.e. the measure of time for which the fluid particle "remembers" that it was previously exposed to a shear stress. The shear stress contributes to the $\mathbf{T}_e$ via the source term, which is proportional to $\mu_e\mathbf{D}$.

Qualitative changes in the model response to variations of λ_1 could be deduced from two limit cases. As $\lambda_1 \to 0$, the first two terms on the righ-hand side of Eq. (20) become dominant. They balance each other and therefore in this case we have $\mathbf{T}_e = 2\mu_e\mathbf{D}$. It means the fluid has no "memory" and behaves like a simple Newtonian fluid. In the opposite case, when $\lambda_1 \to \infty$, both source and sink terms disappear from Eq. (20) and thus $\delta\mathbf{T}_e/\delta t = 0$. The extra stress $\mathbf{T}_e$ is conserved, i.e. it is only advected by the flow, and is decoupled from the momentum equations.

Remark 1 An important non-dimensional parameter characterizing the viscoelastic effects in the flow is the *Weissenberg number* defined as $We = \frac{\lambda_1 U}{L}$, where U denotes a characteristic velocity and L is a characteristic length of the flow. In this case the Weissenberg number can be interpreted as the ratio between "memory" and advection time-scales. It relates the relaxation time to the time the fluid particle needs to pass the distance L while advected at speed U.

2.3 Models Summary

The basic conservation laws for linear momentum (1) and mass (2) are used with the following constitutive equations

$$\mathbf{T} = \mathbf{T}_s + \mathbf{T}_e \tag{21}$$

$$\mathbf{T}_s = 2\mu_s(\dot{\gamma})\mathbf{D} \tag{22}$$

$$\frac{\partial \mathbf{T}_e}{\partial t} + (\boldsymbol{u} \cdot \nabla)\, \mathbf{T}_e = \frac{2\mu_e}{\lambda_1}\mathbf{D} - \frac{1}{\lambda_1}\mathbf{T}_e + (\mathbf{W}\mathbf{T}_e - \mathbf{T}_e\mathbf{W}) + (\mathbf{D}\mathbf{T}_e + \mathbf{T}_e\mathbf{D}), \tag{23}$$

where the constant viscosity μ can be replaced by the shear dependent viscosity $\mu_s(\dot{\gamma})$ given by (11), with parameters listed in Sect. 2.1.

Summarizing the above discussion, four specific models with special parameter settings will be used in the simulations:

Newtonian	$\mu_s(\dot{\gamma}) = \mu_\infty$	$\mathbf{T}_e \equiv \mathbf{0}$
Generalized Newtonian	$\mu_s(\dot{\gamma})$	$\mathbf{T}_e \equiv \mathbf{0}$
Oldroyd-B	$\mu_s(\dot{\gamma}) = \mu_\infty$	$\mathbf{T}_e$
Generalized Oldroyd-B	$\mu_s(\dot{\gamma})$	$\mathbf{T}_e$

Experimental parameter choices will be presented in Sect. 4.1.

These equations can be solved for the variables velocity, pressure and shear stress, provided the viscosity function, flow parameters and appropriate boundary conditions are given.

With respect to boundary conditions for the Navier-Stokes and generalized Navier-Stokes equations, it is necessary to prescribe either the velocity or the surface traction force (Dirichlet or Neumann boundary conditions, respectively) at the inflow boundary. Usually, physiological data are not available and a fully developed Poiseuille velocity profile (or the Womersley solution, in the unsteady case) can be prescribed. This is an acceptable idealization of the inflow condition in relatively long straight vessel segments. At the vessel wall, the no-slip condition, expressing that the velocity at the wall boundary is the wall velocity, is appropriate. At the outflow boundary, a condition prescribing surface traction force can be applied.

The Oldroyd-B and generalized Oldroyd-B models are of mixed elliptic-hyperbolic type (or parabolic-hyperbolic, in the unsteady case). The extra stresses behave hyperbolic, which means that they are only determined by past time. For these models the boundary conditions are the same as for the Navier-Stokes and generalized Navier-Stokes equations, supplemented by the specification of all the stress components representing the fluid memory at the inlet boundary [16].

3 Numerical Methods

The numerical solutions of the above described models are obtained using a three-dimensional code based on a finite-volume semi-dicretization in space, and an explicit Runge-Kutta time integration scheme (see also [6]. We search for steady solutions by a time-marching approach, i.e. the unsteady governing systems are solved with steady boundary conditions and stationary solutions are recovered when $t \to \infty$.

An artificial compressibility formulation [30], often used in steady flow simulations, is applied to resolve pressure and to enforce the divergence-free constraint. The continuity equation (2) is modified by adding the time-derivative of pressure properly scaled by the artificial speed of sound $\mathfrak{c}$, as follows:

$$\frac{1}{\mathfrak{c}^2}\frac{\partial p}{\partial t} + \operatorname{div} \boldsymbol{u} = 0 \tag{24}$$

3.1 Space Discretization

The computational mesh is structured, consisting of hexahedral primary control volumes. To evaluate the viscous fluxes also dual finite volumes are needed. They have octahedral shape and are centered around the corresponding primary cell faces. Figure 3 shows a schematic representation of this configuration. The same grid is used for the calculation of both, flow field and stress tensor. Thus it is natural to use the same method for solving the Navier-Stokes (or generalized Navier-Stokes) equations and the transport equation for the extra stress tensor. The algorithm described below for the flow variables $\mathbf{W}$, is directly applied to the calculation of the extra stress tensor $\mathbf{T}_e$.

System of Eqs. (1) and (24) can be rewritten in vector form, namely[3]

$$\tilde{R}\mathbf{W}_t + \mathbf{F}_x + \mathbf{G}_y + \mathbf{H}_z = \mathbf{R}_x + \mathbf{S}_y + \mathbf{T}_z \tag{25}$$

where $\mathbf{W} = (0, u, v, w)^T$, the inviscid flux vectors are denoted

$$\mathbf{F} = (u, u^2 + p, uv, uw)^T, \quad \mathbf{G} = (v, uv, v^2 + p, vw)^T, \quad \mathbf{H} = (w, uw, vw, w^2 + p)^T,$$

and the viscous fluxes by

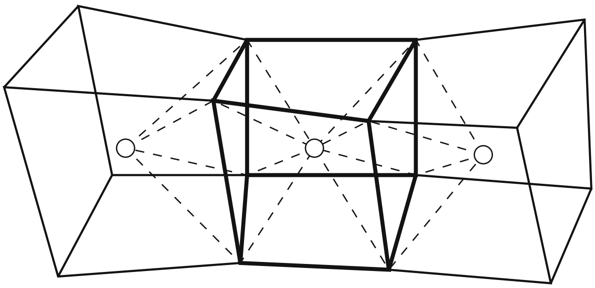

Fig. 3 Finite-volume grid in 3D

$$\mathbf{R} = (0, \mu u_x, \mu v_x, \mu w_x)^T, \quad \mathbf{S} = (0, \mu u_y, \mu v_y, \mu w_y)^T, \quad \mathbf{T} = (0, \mu u_z, \mu v_z, \mu w_z)^T.$$

Here $\tilde{R} = diag(0, 1, 1, 1)$ is a diagonal matrix. Due to the artificial compressibility used in our model (24), $\tilde{R}$ is modified and replaced by $R = diag(1/\mathbf{c}^2, 1, 1, 1)$.[4]

Using this notation, the spatial finite-volume semi-discretization can be written as

---

[3] Subscripts $_{txyz}$ denote partial derivatives with respect to time and x, y, z coordinates

[4] Here, for simplicity, the artificial speed of sound $\mathbf{c}$ is equal to 1 and therefore the matrices R and $\tilde{R}$ do not appear in the equations

$$\frac{\partial \mathbf{W}_{ijk}}{\partial t} = -\frac{1}{|D|}\oint_{\partial D}\Big[(\mathbf{F}-\mathbf{R}), (\mathbf{G}-\mathbf{S}), (\mathbf{H}-\mathbf{T})\Big]\cdot \hat{\boldsymbol{\nu}}\, dS. \tag{26}$$

Here D denotes the computational cell, $\hat{\boldsymbol{\nu}}$ is the outer unit normal vector to the cell boundary and dS is the surface element of this boundary. The operator on the right hand side is still exact at this stage and should be properly discretized replacing the fluxes by their numerical approximations.

The inviscid flux integral can be approximated using centered cell fluxes, e.g. the value of the flux $\mathbf{F}$ on each cell face is computed as the average of cell-centered values from both sides of this face, and the contribution of inviscid fluxes is finally summed up over the cell faces. The discretization of viscous fluxes (appearing in the generalized Newtonian or generalized Oldroyd-B model (Sect. 2.3)) is more complicated since vectors $\mathbf{R}$, $\mathbf{T}$ involve the derivatives of the velocity components that need to be approximated at cell faces. This can be done using a dual finite-volume grid, with octahedral cells, centered around the corresponding faces. The evaluation of the velocity gradient components is then replaced by the evaluation of the surface integral over the dual volume boundary. Finally, this surface integral is approximated by a discrete sum over the dual cell faces. The values of the velocity components in the middle nodes of these faces are taken as an average of the values in the corresponding vertices.

3.2 Time Advancing Scheme

After the discretization with respect to the space variables, and since we are solving a transient problem, we need to consider the time discretization as well. We obtain a system of ordinary differential equations of the form

$$\frac{d\mathbf{W}_{ijk}}{dt} = -\mathcal{L}\,\mathbf{W}_{i,j,k}. \tag{27}$$

For simplicity, as for the discretization in space, the same time integration scheme is used for both the flow field $\mathbf{W}$ and the extra stress tensor $\mathbf{T}_e$. System (27) is solved by an efficient and robust modified Runge-Kutta four-stage method (outlined in [15] and further refined in [14]). The idea behind this modified approach lies in splitting the space discretization operator into its inviscid and viscous parts. The momentum operator is evaluated at each RK stage, while the viscous operator is evaluated in just a few more stages. This corresponds to the use of different RK coefficients for time integration of momentum and viscous fluxes. The modified algorithm can be written in the form

$$\begin{aligned}
\mathbf{W}^{(0)}_{i,j,k} &= \mathbf{W}^{n}_{i,j,k}\\
\mathbf{W}^{(r)}_{i,j,k} &= \mathbf{W}^{(0)}_{i,j,k} - \alpha_{(r)}\Delta t\left(\mathcal{Q}^{(r-1)} + \mathcal{D}^{(r-1)}\right) \qquad r = 1,\dots,s\\
\mathbf{W}^{n+1}_{i,j,k} &= \mathbf{W}^{(s)}_{i,j,k}
\end{aligned} \tag{28}$$

Here the space discretization operator at stage (r) is split as follows

$$\mathcal{L}\mathbf{W}^{(r)}_{i,j,k} = \mathcal{Q}^{(r)} + \mathcal{D}^{(r)}. \tag{29}$$

The momentum flux $\mathcal{Q}$ is evaluated in the usual way at each stage

$$\mathcal{Q}^{(r)} = \mathcal{Q}\mathbf{W}^{(r)}_{i,j,k} \qquad \text{with} \qquad \mathcal{Q}^{(0)} = \mathcal{Q}\mathbf{W}^{n}_{i,j,k}, \tag{30}$$

and the viscous flux $\mathcal{D}$ uses a blended value from the previous stage and the actual stages, according to the rule

$$\mathcal{D}^{(r)} = \beta_{(r)}\mathcal{D}\mathbf{W}^{(r)}_{i,j,k} + (1-\beta_{(r)})\mathcal{D}^{(r-1)} \qquad \text{with} \qquad \mathcal{D}^{(0)} = \mathcal{D}\mathbf{W}^{n}_{i,j,k}. \tag{31}$$

Coefficients $\alpha_{(r)}$ and $\beta_{(r)}$ are chosen to guarantee a large enough stability region for the Runge-Kutta method. The following set of coefficients was used in this study

$$\begin{array}{ll} \alpha_{(1)} = 1/3 & \beta_{(1)} = 1 \\ \alpha_{(1)} = 4/15 & \beta_{(1)} = 1/2 \\ \alpha_{(1)} = 5/9 & \beta_{(1)} = 0 \\ \alpha_{(4)} = 1 & \beta_{(4)} = 0 \end{array}$$

When this four-stage method is used, only two evaluations of the dissipative terms are needed. This saves a significant amount of calculations while retaining the advantage of a large stability region. Further admissible sets of coefficients and remarks on the efficiency and robustness of these methods can be found in [15, 14] and references therein.

3.3 Numerical Stabilization

A well known property of central schemes is the existence of non-physical oscillations in the solution, mainly due to the presence of strong gradients. Several procedures may be considered to avoid these phenomena. A pressure stabilization technique, widespread in finite elements, is used in the present simulations to prevent oscillations in the pressure, and to stabilize the whole numerical method (see e.g. [30]). It consists in adding a pressure dissipation term (Laplacian) into the right-hand side of the modified continuity equation (24), which takes the form

$$\frac{\partial p}{\partial t} + \mathbf{c}^2 \mathrm{div}\, \boldsymbol{u} = \varepsilon \Delta p \tag{32}$$

This type of numerical stabilization has some advantages over the classical artificial diffusion applied to the velocity components. First, the artificial effects induced by the pressure dissipation term do not interfere with the physical constant or shear dependent viscosity. Moreover, this stabilization term contains only second derivatives of the pressure and will vanish if pressure is a linear function of space coordinates, which is for example the case of Poiseuille flow with linear pressure decay along the flow axis. Details can be found in [5]. See also [20] for other stabilization techniques.

4 Numerical Simulations and Results

4.1 Computational Domain and Model Parameters

In this study numerical simulations are performed to model blood flow in a three-dimensional geometric idealized non-symmetric (with respect to the bulk flow direction) cosine-shaped stenosed vessel shown in Fig. 4. The vessel is axisymmetric, rigid-walled, with length $L = 10R = 31\,\text{mm}$ and diameter $D = 2R = 6.2\,\text{mm}$. The diameter is reduced to one half in the stenosed region, which leads to a $4:1$ cross-sectional area reduction and thus to a significant speed-up of the local flow.

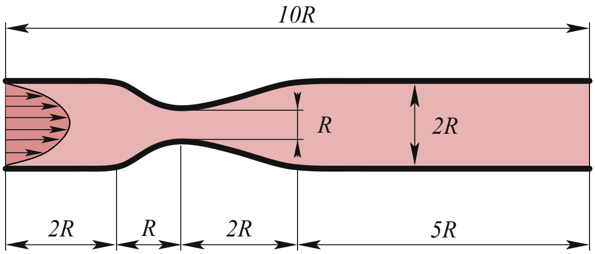

Fig. 4 Stenosis

The whole domain is discretized using a structured multiblock mesh with hexahedral cells. To avoid high cells distortion, the mesh is wall fitted with uniform axial cell spacing, as shown in Fig. 5. The outer mesh block has $40 \times 16 \times 80$ cells, while the central mesh block has $10 \times 10 \times 80$ control volumes.

Numerical simulations have been obtained under physiological conditions, using the values already introduced in Sect.2.1 for the Cross model, as well as the following parameters used for blood flow in the carotid artery (see [17]):

$$\begin{array}{ll} U_0 = 6.62\,\text{cm} \cdot s^{-1} & L_0 = 2R = 0.0062\,\text{m} \\ \mu_e = 4.0 \cdot 10^{-4} Pa \cdot s & \mu_s = 3.6 \cdot 10^{-3} Pa \cdot s \\ \mu_0 = \mu = \mu_s + \mu_e & \mu_\infty = \mu_s \\ \lambda_1 = 0.06\,s & \varrho = 1050\,\text{kg} \cdot \text{m}^{-3} \\ Re \doteq \frac{\varrho U_0 L_0}{\mu_0} = 100 & We \doteq \frac{\lambda_1 U_0}{L_0} = 0.6 \end{array}$$

Using these data fully developed Poiseuille velocity profile is prescribed at the inlet (Dirichlet condition) and the flow rate is set to $Q = 2\,\text{cm}^3\,\text{s}^{-1}$. At the outlet

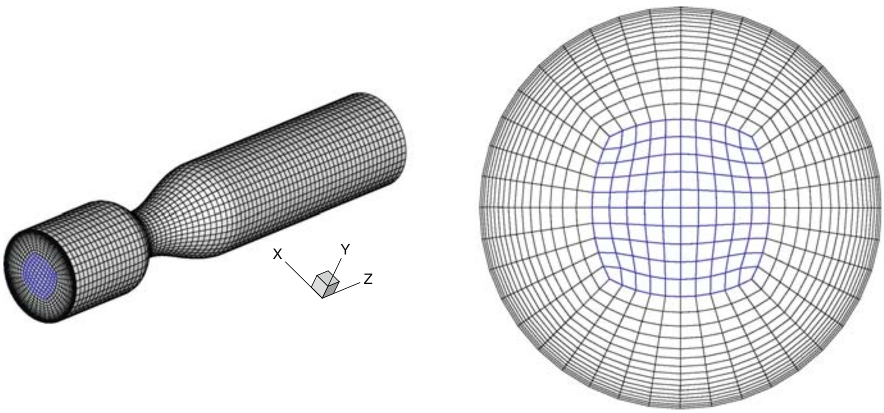

Fig. 5 Computational grid structure

we impose homogeneous Neumann conditions for the velocity components and a constant pressure. On the vessel walls no-slip homogeneous Dirichlet conditions are prescribed for the velocity field. In the case of the Oldroyd-B and generalized Oldroyd-B models, homogeneous Neumann conditions are imposed for the components of the extra stress tensor at all boundaries.

4.2 Numerical Results

Using the different models described in Sect. 2 we investigate the influence of shear-thinning and viscoelastic effects on the qualitative behavior of blood flow in a stenosed idealized three-dimensional vessel.

Figure 6, 7, 8 and 9 show the axial velocity contours corresponding to the models described above, using the same color scale (units in m/s) as in Fig. 6. To emphasize the flow separation behind the stenosis, the regions of reversal flow (with respect to axial direction) are marked with grey color. Upstream the stenosis, separated flow can be seen, with a faster axial velocity for the Newtonian flow (Fig. 6) than for the non-Newtonian flows (Fig. 7, 8 and 9). The slowest axial velocity corresponds to the generalized Oldroyd-B flow (Fig. 9).

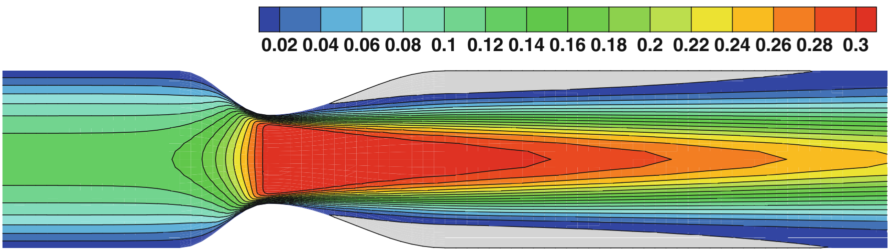

Fig. 6 Axial velocity contours for the Newtonian flow with viscosity $\mu = \mu_\infty$

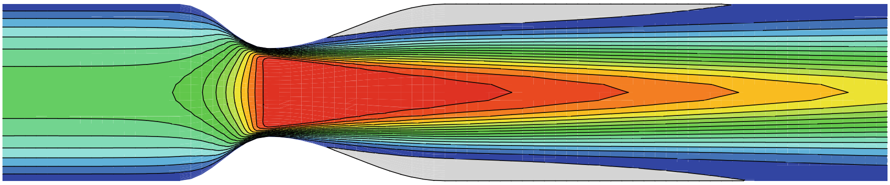

Fig. 7 Axial velocity contours for the Oldroyd-B flow

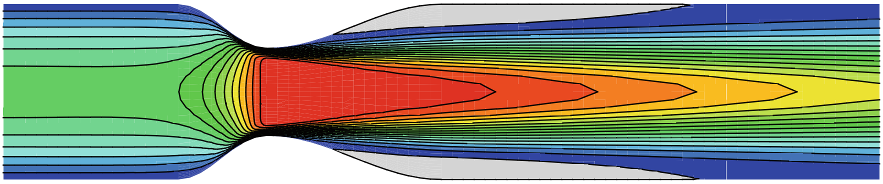

Fig. 8 Axial velocity contours for the generalized Newtonian flow (with shear-thinning viscosity)

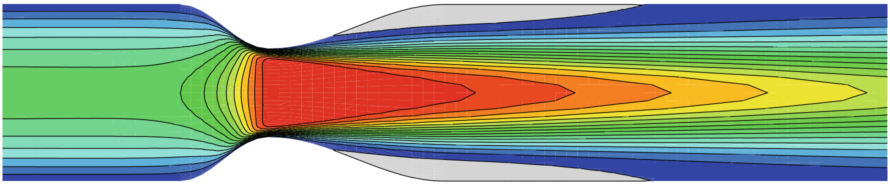

Fig. 9 Axial velocity contours for the generalized Oldroyd-B flow (with shear-thinning viscosity)

The behavior is similar at the stenosis site but, downstream the stenosis and near the wall, it becomes different due to the appearance of the recirculation phenomena. This is better observed in Fig. 10, 11, 12 and 13, showing not only the velocity vectors and streamlines, but also the recirculation fow patterns downstream the stenosis. In the four test cases the flow structure is similar but the impact of the non-Newtonian effects is non-negligible. The axial velocity close to the wall is negative, developing a backflow, and the Newtonian flow is slower than the non-Newtonian ones. The recirculating region is larger for the Newtonian flow (Fig. 10), and we also observe that the shear-thinning and viscoelastic fluid behavior have a

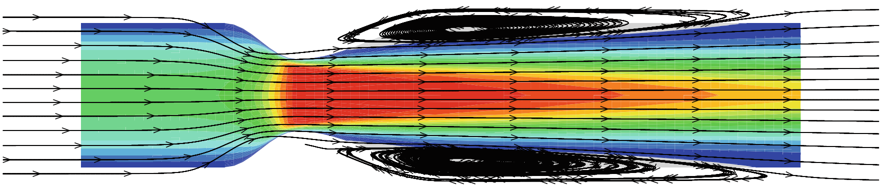

Fig. 10 Streamlines and velocity vectors for the Newtonian flow with viscosity $\mu = \mu_\infty$

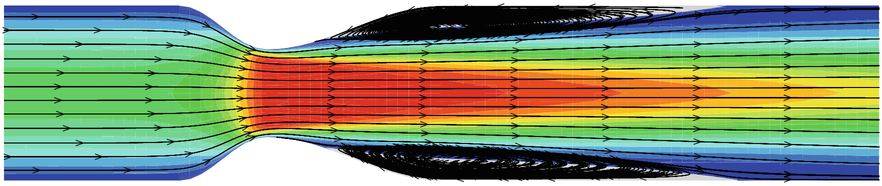

Fig. 11 Streamlines and velocity vectors for the Oldroyd-B flow

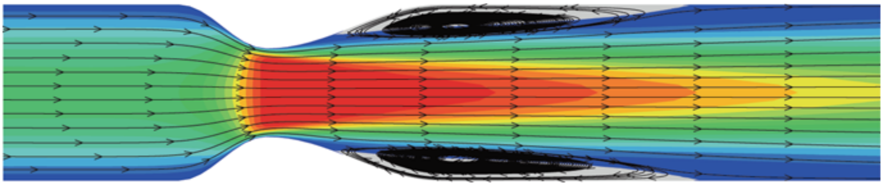

Fig. 12 Streamlines and velocity vectors for the generalized Newtonian flow (with shear-thinning viscosity)

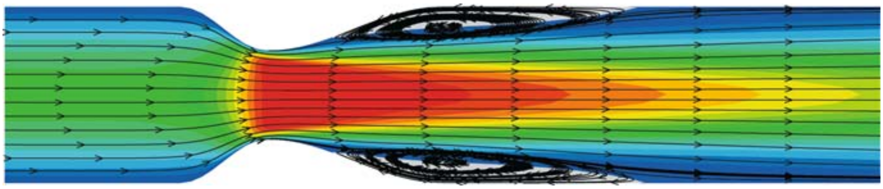

Fig. 13 Streamlines and velocity vectors for the generalized Oldroyd-B flow (with shear-thinning viscosity)

similar influence reducing the recirculating region (Fig. 11 and 12), which becomes remarkably shorter when both effects are added (Fig. 13).

The comparison of pressure distributions relative to the four test cases (Fig. 14, 15, 16 and 17) exhibits visible differences. As expected, the pressure drop between inlet and outlet is higher for shear-thinning flows due to the local increase of the viscosity with respect to the Newtonian flow. Similar effect is observed in the viscoelastic flow simulations, where the additional term (extra stress) appearing in the momentum equations needs to be balanced by an appropriate pressure gradient.

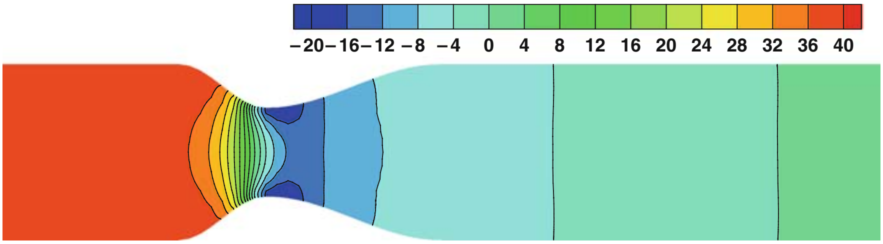

Fig. 14 Pressure contours for Newtonian flow with viscosity $\mu = \mu_\infty$

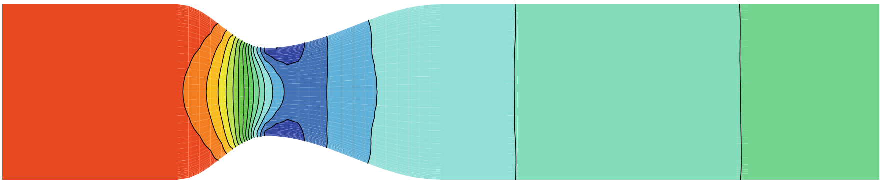

Fig. 15 Pressure contours for the Oldroyd-B flow

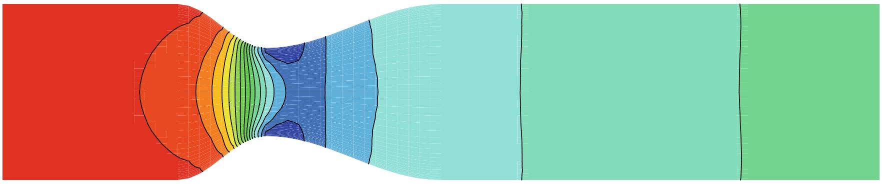

Fig. 16 Pressure contours for the generalized Newtonian flow (with shear-thinning viscosity)

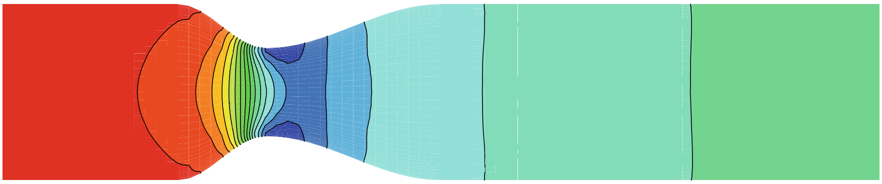

Fig. 17 Pressure contours for the generalized Oldroyd-B flow (with shear-thinning viscosity)

A more complete study of the shear-thinning and viscoelastic effects on the axial velocity contours is shown in Fig. 18, 19 and 20, displaying the differences between solutions of each pair of Newtonian and non-Newtonian flows considered as test cases. Color scale (in physical units m/s) is used to emphasize the set of flow regions ranging from those where differences of solutions are similar (grey color) to regions of the most significant distinctive flow regime. The axial velocity is slower in the central part of the stenosis (region of low shear rate) and faster near the wall (region of high shear rate) due to the shear-thinning behavior of the fluid viscosity (Fig. 18). Viscoelastic effects can be observed in Fig. 19 and the shear-thinning

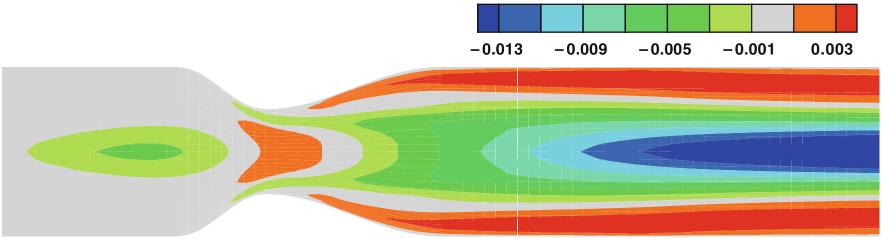

Fig. 18 Axial velocity contours: Difference between the generalized Newtonian and the Newtonian solutions

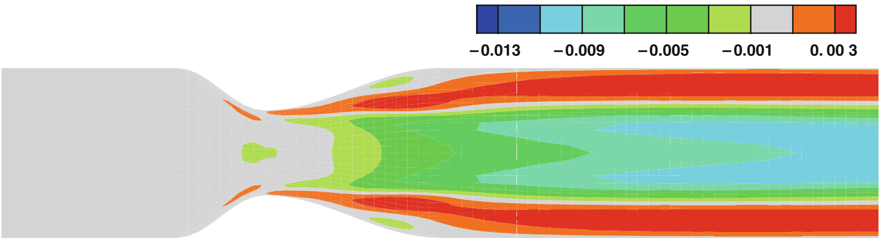

Fig. 19 Axial velocity contours: Difference between the Oldroyd-B the Newtonian solutions

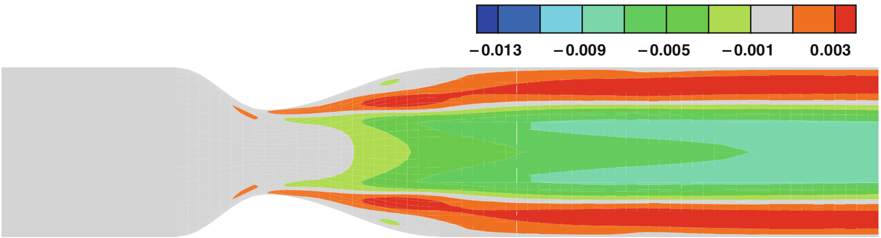

Fig. 20 Axial velocity contours: Difference between the generalized Oldroyd-B the generalized Newtonian solutions

impact in the viscoelastic flow behavior can be detected comparing Fig. 19 and 20. Examining these figures we conclude that flow changes induced by shear-thinning and viscoelastic effects are comparable in magnitude, but differ significantly in their structure.

The viscoelastic fluid behavior is represented in the equations of linear momentum by the divergence of the extra stress tensor $\mathbf{T}_e$. The above described differences between the Oldroyd-B and the Navier-Stokes solutions are therefore a direct consequence of the presence of this term. The magnitude and sign of div $\mathbf{T}_e$ are related to the flow acceleration and deceleration. The contours shown in Fig. 21 and 22 can be interpreted as a measure of the flow acceleration in the axial direction due to the viscoelastic effects in the stenotic region. Axial acceleration distribution suffers large variations in this region, and the fluid is exposed to higher stresses and wall shear stresses, with the greatest values at the point of maximum stenosis As a consequence, viscoelastic effects are enhanced in the stenosis, they are advected by

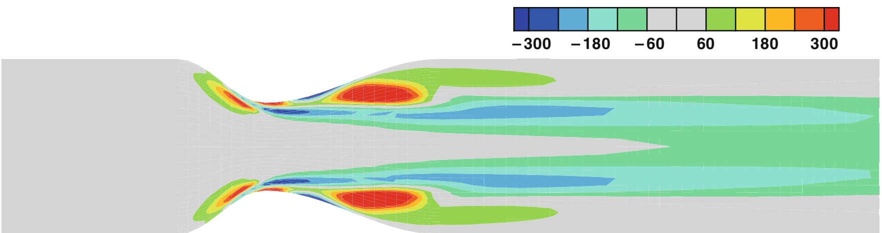

Fig. 21 Contours of the axial component of the extra stress tensor for the Oldroyd-B model

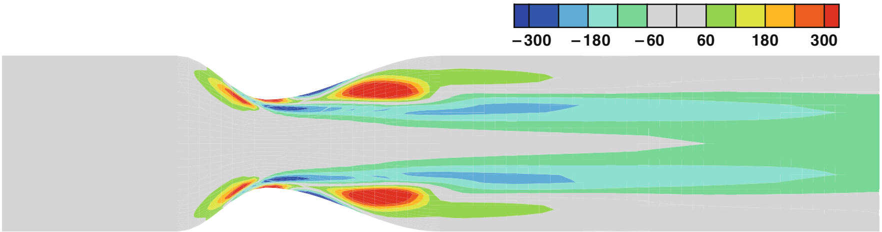

Fig. 22 Contours of the axial component of the extra stress tensor for the generalized Oldroyd-B model

the flow along the vessel and decay in time. Grey color is used in areas where the viscoelastic effects are relatively small.

5 Conclusions and Remarks

The numerical results have shown important non-Newtonian effects for steady flow in a stenosed vessel, related to the rheological models used for blood under the chosen experimental data (Sect. 2.3).

Differences of solutions have been compared for these models, showing that the shear-thinning effect is more pronounced than the viscoelastic one and is mainly localized in the proximity of the stenosed region (Fig. 18, 19 and 20). Deceleration (with respect to Newtonian flow) in the central part of the vessel, downstream the stenosis, gives a flatter velocity profile and results in a marked flow acceleration near the vessel wall. This is a typical behavior of shear-thinning flows that can be neglected for very low or very high shear rates, where the asymptotic viscosity values can be considered.

Concerning the evaluation of the impact of viscoelasticity in the flow, we need to emphasize that the elastic component of the extra stress tensor $\mathbf{T_e}$ is generated in regions with high velocity gradients, then it is advected by the flow and decays in time. In fact, as we can observe comparing Fig. 18 and Fig. 19 and 20 is that a significant influence of the viscoelastic behavior related to flow acceleration/deceleration is only evident dowstream the stenosis. In the present simulation test cases it is clear that the computational domain was not long enough to allow for the full relaxation of the extra stress and thus the differences between viscoelastic and non-viscoelastic solutions are still present at the outlet. On the other hand, it should be noted that the elastic extra stress contributes to the flow acceleration/deceleration through its divergence (equation of linear momentum (1)) and thus it is not the magnitude of the stress that counts, but the magnitude of the "space variation" of the extra stress that influences the flow. This is shown in Fig. 21 and 22 where the contours of the axial component of the extra stress are depicted. It is clearly visible that the highest flow acceleration/deceleration appears in regions of flow recirculation and drops very quickly otherwise.

To gain further insight into some of the problems discussed above, unsteady flow on different stenotic geometries and hemodynamical control quantities such as the wall shear stress (WSS) distribution and the oscillatory shear index (OSI) could be considered (see e.g. [3, 8]) to provide some understanding of the significance of the non-Newtonian characteristics of blood on the genesis of atherosclerosis and other arterial lesions.

Acknowledgments The authors would like to thank Prof. Anne M. Robertson of the Department of Mechanical Engineering and Materials Science at the University of Pittsburgh for helpful discussions and valuable suggestions. This work has been partially supported by the *Czech Science Foundation* under the *Grant No.201/09/0917*, *The Grant Agency of the Academy of Sciences of the CR* under the *Grant No. IAA100190804*, and by the Research Plan *MSM 6840770010* of the Ministry of Education of Czech Republic. Financial support from the Project PTDC/MAT/68166/2006 and from the Center of Mathematics and its Applications – CEMAT/IST through FCT's Funding Program is also acknowledged.

References

1. Anand, M., Rajagopal, K.R.: A shear-thinning viscoelastic fluid model for describing the flow of blood. Intern. J. Cardiovasc. Med. Sci. **4**(2), 59–68 (2004)
2. Astarita, G., Marrucci, G.: *Principles of Non-Newtonian Fluid Mechanics*. McGraw Hill, London (1974)
3. Berger, S.A., Jou, L.D.: Flows in stenotic vessels. Ann. Rev. Fluid Mech. **32**, 347–382 (2000)
4. Bird, R., Armstrong, R., Hassager, O.: *Dynamics of Polymeric Liquids*, vol. 1, second edn. John Willey & Sons, New York (1987)
5. Bodnár, T., Sequeira, A.: Shear-thinning effects of blood flow past a formed clot. WSEAS Transactions on Fluid Mechanics **1**(3), 207–214 (2006)
6. Bodnár, T., Sequeira, A.: Numerical simulation of the coagulation dynamics of blood. Comput. Math. Methods Med. **9**(2), 83–104 (2008)
7. Boyer, F., Chupin, L., Fabrie, P.: Numerical study of viscoelastic mixtures through a cahn-hilliard flow model. Eur. J. Mech. B Fluids **23(5)**, 759–780 (2004)
8. Caro, C.G., Pedley, T.J., Schroter, R.C., Seed, W.A.: *The Mechanics of the Circulation*. Oxford University Press, Oxford (1978)
9. Charm, S.E., Kurland, G.S.: *Blood Flow and Microcirculation*. John Wiley & Sons, New York (1974)
10. Chien, S., Usami, S., Dellenback, R.J., Gregersen, M.I.: Blood viscosity: Influence of erythrocyte aggregation. Science **157**(3790), 829–831 (1967)
11. Chien, S., Usami, S., Dellenback, R.J., Gregersen, M.I.: Blood viscosity: Influence of erythrocyte deformation. Science **157**(3790), 827–829 (1967)
12. Chien, S., Usami, S., Dellenback, R.J., Gregersen, M.I.: Shear-dependent deformation of erythrocytes in rheology of human blood. Am. J. Physiol. **219**, 136–142 (1970)
13. Ferry, J.D.: *Viscoelastic Properties of Polymers*. John Wiley & Sons, New York (1980)
14. Jameson, A.: Time dependent calculations using multigrid, with applications to unsteady flows past airfoils and wings. In: AIAA 10th Computational Fluid Dynamics Conference, Honolulu (1991). AIAA Paper 91-1596
15. Jameson, A., Schmidt, W., Turkel, E.: Numerical solutions of the Euler equations by finite volume methods using Runge-Kutta time-stepping schemes. In: AIAA 14th Fluid and Plasma Dynamic Conference, Palo Alto (1981). AIAA paper 81-1259
16. Joseph, D.D.: *Fluid Dynamics of Viscoelastic Liquids*. Springer-Verlag, New York (1990)

17. Leuprecht, A., Perktold, K.: Computer simulation of non-Newtonian effects of blood flow in large arteries. Computer Methods in Biomechanics and Biomechanical Engineering **4**, 149–163 (2001)
18. Lowe, D.: *Clinical Blood Rheology*, Vol.I, II. CRC Press, Boca Raton, Florida (1998)
19. Maxwell, J.C.: On the dynamical theory of gases. Phil. Trans. Roy. Soc. London **A157**, 26–78 (1866)
20. Nägele, S., Wittum, G.: On the influence of different stabilisation methods for the incompressible Navier–Stokes equations. J. Comp. Phys. **224**, 100–116 (2007)
21. Owens, R.G.: A new microstructure-based constitutive model for human blood. J. Non-Newtonian Fluid Mech. **140**, 57–70 (2006)
22. Picart, C., Piau, J.M., Galliard, H., Carpentier, P.: Human blood shear yield stress and its hematocrit dependence. J. Rheol. **42**, 1–12 (1998)
23. Rajagopal, K., Srinivasa, A.: A thermodynamic frame work for rate type fluid models. J. Non-Newtonian Fluid Mech. **80**, 207–227 (2000)
24. Robertson, A.M.: Review of relevant continuum mechanics. In: G. Galdi, R. Rannacher, A.M. Robertson, S. Turek (eds.) *Hemodynamical Flows: Modeling, Analysis and Simulation* (Oberwolfach Seminars), vol. 37, pp. 1–62. Birkhäuser Verlag, Basel, Boston (2008)
25. Robertson, A.M., Sequeira, A., Kameneva, M.V.: Hemorheology. In: G. Galdi, R. Rannacher, A.M. Robertson, S. Turek (eds.) *Hemodynamical Flows: Modeling, Analysis and Simulation* (Oberwolfach Seminars), vol. 37, pp. 63–120. Birkhäuser Verlag, Basel, Boston (2008)
26. Robertson, A.M., Sequeira, A., Owens, R.G.: Rheological models for blood. In: L. Formaggia, A. Quarteroni, A. Veneziani (eds.) *Cardiovascular Mathematics. Modeling and simulation of the circulatory system* (MS&A, Modeling, Simulations & Applications), vol. 1, pp. 211–241. Springer - Verlag, New York (2009)
27. Sankar, D.S., Hemalatha, K.: Pulsatile flow of herschel-bulkley fluid through catheterized arteries - a mathematical model. Appl. Math. Model. **31 (8)**, 1497–1517 (2007)
28. Thurston, G.B.: Viscoelasticity of human blood. Biophys. J. **12**, 1205–1217 (1972)
29. Thurston, G.B.: Non-Newtonian viscosity of human blood: Flow induced changes in microstructure. Biorheology **31(2)**, 179–192 (1994)
30. Vierendeels, J., Riemslagh, K., Dick, E.: A multigrid semi-implicit line-method for viscous incompressible and low-mach-number flows on high aspect ratio grids. J. Comput. Phys. **154**, 310–344 (1999)
31. Vlastos, G., Lerche, D., Koch, B.: The superposition of steady on oscillatory shear and its effect on the viscoelasticity of human blood and a blood-like model fluid. Biorheology **34**, 19–36 (1997)
32. Walburn, F.J., Schneck, D.J.: A constitutive equation for whole human blood. Biorheology **13**, 201–210 (1976)
33. Yeleswarapu, K.K., Kameneva, M.V., Rajagopal, K.R., Antaki, J.F.: The flow of blood in tubes: Theory and experiment. Mech. Res. Comm. **25**, 257–262 (1998)

A Priori Convergence Estimates for a Rough Poisson-Dirichlet Problem with Natural Vertical Boundary Conditions

Eric Bonnetier, Didier Bresch, and Vuk Milišić

Abstract Stents are medical devices designed to modify blood flow in aneurysm sacs, in order to prevent their rupture. Some of them can be considered as a locally periodic rough boundary. In order to approximate blood flow in arteries and vessels of the cardio-vascular system containing stents, we use multi-scale techniques to construct boundary layers and wall laws. Simplifying the flow we turn to consider a 2-dimensional Poisson problem that conserves essential features related to the rough boundary. Then, we investigate convergence of boundary layer approximations and the corresponding wall laws in the case of Neumann type boundary conditions at the inlet and outlet parts of the domain. The difficulty comes from the fact that correctors, for the boundary layers near the rough surface, may introduce error terms on the other portions of the boundary. In order to correct these spurious oscillations, we introduce a vertical boundary layer. Trough a careful study of its behavior, we prove rigorously decay estimates. We then construct complete boundary layers that respect the macroscopic boundary conditions. We also derive error estimates in terms of the roughness size ε either for the full boundary layer approximation and for the corresponding averaged wall law.

Keywords Wall-laws · Rough boundary · Laplace equation · Multi-scale modelling · Boundary layers · Error estimates

1 Introduction

A common therapeutic treatment to prevent rupture of aneurysms, in large arteries or in blood vessels in the brain, consists in placing a device inside the aneurysm sac. The device is designed to modify the blood flow in this region, so that the blood contained in the sac coagulates and the sac can be absorbed into the surrounding tissue. The traditional technique consists in obstructing the sac with a long coil. In a more recent procedure, a device called *stent*, that can be seen as a second artery

V. Milisic (✉)
LJK-IMAG, UMR 5523 CNRS, 38041 Grenoble cedex 9, France
e-mail: Vuk.Milisic@imag.fr

R. Rannacher, A. Sequeira (eds.), *Advances in Mathematical Fluid Mechanics*,
DOI 10.1007/978-3-642-04068-9_7,

wall, is placed so as to close the inlet of the sac. We are particularly interested in stents produced by a company called Cardiatis, which are designed as multi-layer wired structures. Clinical tests show surprising bio-compatibility features of these particular devices and one of our objectives is to understand how the design of these stents affect their effectiveness. As stent thicknesses are small compared to the characteristic dimensions of the flow inside an artery, studying their properties is a challenging multi-scale problem.

In this work we focus on the fluid part and on the effects of the stent rugosity on the fluid flow. We simplify the geometry to that of a 2-dimensional box Ω^ε, that represents a longitudinal cut through an artery: the rough base represents the shape of the wires of the stent (see Fig. 2, left). We also simplify the flow model and consider a Poisson problem for the axial component of the velocity. Our objective is to analyze precisely multi-scale approximations of this simplified model, in terms of the rugosity.

In [4] we considered periodic inflow and outflow boundary conditions on the vertical sides $\Gamma_{in} \cup \Gamma_{out}$ of Ω^ε. Here, we study the case of more realistic Neumann conditions on these boundaries, which are consistent with the modelling of a flow of blood.

As a zeroth order approximation to u^ε, we consider the solution $\tilde{u}^0$ of the same PDE, posed on a smooth domain Ω^0 strictly contained in Ω^ε. We introduce boundary layer correctors β and τ that correct the incompatibilities between the domain and $\tilde{u}^0$. These correctors induce in turn perturbations on the vertical sides $\Gamma_{in} \cup \Gamma_{out}$ of Ω^ε. We therefore consider additional correctors ξ_{in} and ξ_{out}, that should account for these perturbations (see Fig. 1). We also introduce a first order approximation, defined in Ω^0, that satisfies a mixed boundary condition (called Saffman-Joseph wall law) on a fictitious interface Γ^0 located inside Ω^ε.

For the case of Navier-Stokes equations and the Poiseuille flow the problem was already considered in Jäger et al. [11, 10] but the authors imposed Dirichlet boundary conditions on $\Gamma_{in} \cup \Gamma_{out}$ for the vertical velocity and pressure. Their approach provided a localized vertical boundary layer in the ε-close neighborhood of $\Gamma_{in} \cup \Gamma_{out}$. A convergence proof for the boundary layer approximation and the

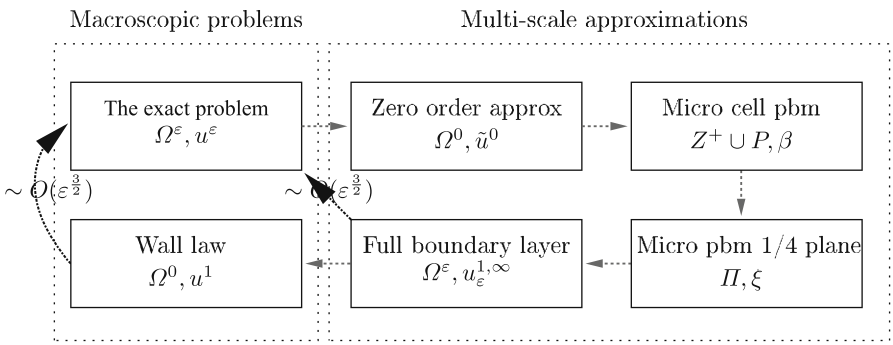

Fig. 1 The exact solution, the multi-scale framework and wall laws

wall law was given wrt to ε, the roughness size. These arguments are specific to the case of Poiseuille flow and differ from the general setting given in the homogenization framework [19]. In this work, we address the case of Neumann boundary conditions, where the above methods do not apply. The difficulty in this case, stems from the "pollution" on the vertical sides due to the bottom boundary layer correctors.

From our point of view, the originality of this work emanate from the following aspects :

- the introduction of a general quarter-plane corrector ξ that reduces the oscillations of the periodic boundary layer approximations on a specific region of interest. Changing the type of boundary conditions implies only to change the boundary conditions of the quarter-plane corrector on a certain part of the microscopic domain.
- the analysis of decay properties of this new corrector: indeed we use techniques based on weighted Sobolev spaces to derive some of the estimates and we complete this description by integral representation and Fragmen-Lindelöf theory in order to derive sharper L^∞ bounds.
- we show new estimates based on duality on the traces and provide a weighted correspondence between macro and micro features of test functions of certain Sobolev spaces.

The error between the wall-law and the exact solution is evaluated on Ω^0, the smooth domain above the roughness, in the $L^2(\Omega^0)$ norm. This relies on very weak estimates [18] that moreover improve a priori estimates by a $\sqrt{\varepsilon}$ factor. While this work focuses on the precise description of vertical boundary layer correctors in the a priori part, a second article extends our methods to the very weak context [16] in order to obtain optimal rates of convergence also for this step.

The paper is organized as follows: in Sect. 2, we present the framework (including notations, domains characteristics and the toy PDE model under consideration), in Sect. 3, we give a brief summary of what is already available from the periodic context [4] that should serve as a basis for what follows, in Sect. 4 we present a microscopic vertical boundary layer and its careful analysis in terms of decay at infinity, such decay properties will be used in Sect. 5 in the convergence proofs for the full boundary layer approximation as well as in the corresponding wall law analysis.

2 The Framework

In this work, Ω^ε denotes the rough domain in $\mathbb{R}^2$ depicted in Fig. 2, Ω^0 denotes the smooth one, Γ^ε is the rough boundary and Γ^0 (resp. Γ^1) the lower (resp. upper) smooth one (see Fig. 2). The rough boundary Γ^ε is described as a periodic repetition at the microscopic scale of a single boundary cell P^0. The latter can be parameterized as the graph of a Lipschitz function $f : [0, 2\pi[\rightarrow] -1 : 0[$, the boundary is then defined as

$$P^0 = \{y \in [0, 2\pi]\times] - 1 : 0[\text{ s.t. } y_2 = f(y_1)\}. \tag{1}$$

Moreover we suppose that f is bounded and negative definite, i.e. there exists a positive constant δ such that $1-\delta < f(y_1) < \delta$ for all $y_1 \in [0, 2\pi]$. The lower bound of f is arbitrary and it is useful only in order to define some weight function see Sect. 4. We assume that the ratio between L (the width of Ω^0) and $2\pi\varepsilon$ (the width of the periodic cell) is always a positive integer. We consider a simplified setting that avoids theoretical difficulties and non-linear complications of the full Navier-Stokes equations. Starting from the Stokes system, we consider a Poisson problem for the

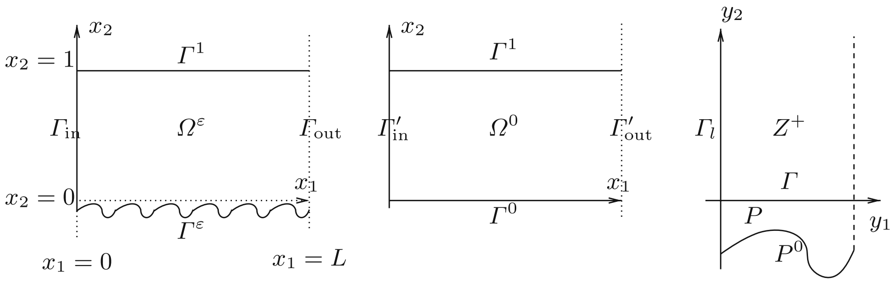

Fig. 2 Rough, smooth and cell domains

axial component of the velocity. The axial component of the pressure gradient is assumed to reduce to a constant right hand side C. If we set periodic inflow and outflow boundary conditions, the simplified formulation reads : find u^ε such that

$$\begin{cases} -\Delta u^\varepsilon_\# = C, \text{ in } \Omega^\varepsilon, \\ u^\varepsilon_\# = 0, \text{ on } \Gamma^\varepsilon \cup \Gamma^1, \\ u^\varepsilon_\# \text{ is } x_1 \text{ periodic.} \end{cases} \tag{2}$$

In Sect. 3 we should give a brief summary of the framework already introduced in [4]. Nevertheless the main concern of this work is to consider the non periodic setting (see Sect. 4) where we should consider an example of a more realistic inlet and outlet boundary conditions. Namely, we look for approximations of the problem: find u^ε such that

$$\begin{cases} -\Delta u^\varepsilon = C, \text{ in } \Omega^\varepsilon, \\ u^\varepsilon = 0, \text{ on } \Gamma^\varepsilon \cup \Gamma^1, \\ \dfrac{\partial u^\varepsilon}{\partial \mathbf{n}} = 0, \text{ on } \Gamma_{\text{in}} \cup \Gamma_{\text{out}}. \end{cases} \tag{3}$$

In what follows, functions that do depend on $y = x/\varepsilon$ should be indexed by an ε (e.g. $\mathcal{U}_\varepsilon = \mathcal{U}_\varepsilon(x, x/\varepsilon)$).

3 Summary of the Results Obtained in the Periodic Case

3.1 The Cell Problems

3.1.1 The First Order Cell Problem

The rough boundary is periodic at the microscopic scale and this leads to solve the microscopic cell problem [4]: find β s.t.

$$\begin{cases} -\Delta\beta = 0, \text{ in } Z^+ \cup \Gamma \cup P, \\ \beta = -y_2, \text{ on } P^0, \\ \beta \text{ is } y_1 - \text{periodic} . \end{cases} \tag{4}$$

We define the microscopic average along the fictitious interface $\Gamma : \overline{\beta} = \frac{1}{2\pi}\int_0^{2\pi} \beta(y_1, 0)dy_1$. As $Z^+ \cup \Gamma \cup P$ is unbounded in the y_2 direction, we define also

$$D^{1,2} = \{v \in L^1_{\text{loc}}(Z^+ \cup \Gamma \cup P)/\ Dv \in L^2(Z^+ \cup \Gamma \cup P)^2,\ v \text{ is } y_1 - \text{periodic}\},$$

then one has the result:

Theorem 1 *Suppose that P^0 is sufficiently smooth (f is Lipschitz) and does not intersect Γ. Let β be a solution of (4), then it belongs to $D^{1,2}$. Moreover, there exists a unique periodic solution $\eta \in H^{\frac{1}{2}}(\Gamma)$, of the problem*

$$< S\eta, \mu >=< 1, \mu >, \quad \forall \mu \in H^{\frac{1}{2}}(\Gamma),$$

where $<,>$ is the $(H^{-\frac{1}{2}}(\Gamma), H^{\frac{1}{2}}(\Gamma))$ duality bracket, and S the inverse of the Steklov-Poincaré operator. One has the correspondence between β and the interface solution η :

$$\beta = H_{Z^+}\eta + H_P\eta,$$

where $H_{Z^+}\eta$ (resp. $H_P\eta$) is the y_1-periodic harmonic extension of η on Z^+ (resp. P). The solution in Z^+ can be written explicitly as a power series of Fourier coefficients of η and reads:

$$H_{Z^+}\eta = \beta(y) = \sum_{k=-\infty}^{\infty} \eta_k e^{iky_1 - |k|y_2}, \quad \forall y \in Z^+, \quad \eta_k = \int_0^{2\pi} \eta(y_1)e^{-iky_1}dy_1,$$

In the macroscopic domain Ω^0 this representation formula gives

$$\left\| \beta\left(\frac{\cdot}{\varepsilon}\right) - \overline{\beta} \right\|_{L^2(\Omega^0)} \le K\sqrt{\varepsilon}\|\eta\|_{H^{\frac{1}{2}}(\Gamma)}. \tag{5}$$

3.1.2 The Second Order Cell Problem

The second order error on Γ^ε should be corrected thanks to a new cell problem: find $\gamma \in D^{1,2}$ solving

$$\begin{cases} -\Delta\tau = 0, \quad \forall y \in Z^+ \cup \Gamma \cup P, \\ \tau = -y_2^2, \quad \forall y_2 \in P^0, \\ \tau \text{ periodic in } y_1. \end{cases} \tag{6}$$

Again, the horizontal average is denoted $\overline{\tau}$. In the same way as for the first order cell problem, one can obtain a similar result:

Proposition 1 *Let P^0 be smooth enough and do not intersect Γ. Then there exists a unique solution τ of* (6) *in $D^{1,2}(Z^+ \cup \Gamma \cup P)$.*

3.2 Standard Averaged Wall Laws

3.2.1 A First Order Approximation

Using the averaged value $\overline{\beta}$ defined above, one can construct a first order approximation u^1 defined on the smooth interior domain Ω^0 that solves :

$$\begin{cases} -\Delta u^1 = C, \quad \forall x \in \Omega^0, \\ u^1 = \varepsilon\overline{\beta}\dfrac{\partial u^1}{\partial x_2}, \quad \forall x \in \Gamma^0, \quad u^1 = 0, \quad \forall x \in \Gamma^1, \\ u^1 \text{ is } x_1 - \text{periodic on } \Gamma_{\text{in}} \cup \Gamma_{\text{out}}, \end{cases} \tag{7}$$

whose explicit solution reads :

$$u^1(x) = -\frac{C}{2}\left(x_2^2 - \frac{x_2}{1+\varepsilon\overline{\beta}} - \frac{\varepsilon\overline{\beta}}{1+\varepsilon\overline{\beta}}\right). \tag{8}$$

Under the hypotheses of Theorem 1, one derives error estimates for the first order wall law

$$\left\| u_\#^\varepsilon - u^1 \right\|_{L^2(\Omega^0)} \leq K\varepsilon^{\frac{3}{2}}.$$

3.2.2 A Second Order Approximation

In the same way one should derive second order averaged wall law u^2 satisfying the boundary value problem:

$$\begin{cases} -\Delta u^2 = C, \quad \forall x \in \Omega^0, \\ u^2 = \varepsilon\overline{\beta}\dfrac{\partial u^2}{\partial x_2} + \dfrac{\varepsilon^2}{2}\overline{\tau}\dfrac{\partial^2 u^2}{\partial x_2^2}, \quad \forall x \in \Gamma^0, \\ u^2 = 0, \quad \forall x \in \Gamma^1, u^2 \text{ is } x_1 - \text{periodic on } \Gamma_{\text{in}} \cup \Gamma_{\text{out}}, \end{cases} \tag{9}$$

whose solution exists, is unique [4] and writes :

$$u^2(x) = -\frac{C}{2}\left(x_2^2 - \frac{x_2(1+\varepsilon^2\overline{\tau})}{1+\varepsilon\overline{\beta}} - \frac{\varepsilon(\overline{\beta}-\varepsilon\overline{\tau})}{1+\varepsilon\overline{\beta}}\right). \tag{10}$$

Now, error estimates do not provide second order accuracy, namely we only obtain

$$\left\| u_{\#}^{\varepsilon} - u^2 \right\|_{L^2(\Omega^0)} \leq K\varepsilon^{\frac{3}{2}},$$

which essentially comes from the influence of microscopic oscillations that this averaged second order approximation neglects. Thanks to estimates (5), one sees easily that these oscillations account as $\varepsilon^{\frac{3}{2}}$ if not included in the wall law approximation.

3.3 Compact Form of the Full Boundary Layer Ansatz

Usually in the presentation of wall laws, one first introduces the full boundary layer approximation. This approximation is an asymptotic expansion defined on the whole rough domain Ω^ε. In a further step one averages this approximation in the axial direction over a fast horizontal period and derives in a second step the corresponding standard wall law.

Thanks to various considerations already exposed in [4], the authors showed that actually a reverse relationship could be defined that expresses the full boundary layer approximations as functions of the wall laws. Obviously this works because the wall laws (defined only on Ω^0) are explicit and thus easy to extend to the whole domain Ω^ε. Indeed we re-define

$$u^1(x) = \frac{C}{2}\left((1-x_2)x_2\chi_{[\Omega^0]} + x_2\chi_{[\Omega^\varepsilon \setminus \Omega^0]}\right) - \frac{\varepsilon\beta}{1+\varepsilon\overline{\beta}}(1-x_2), \quad \forall x \in \Omega^\varepsilon \tag{11}$$

while we simply extend u^2 using the formula (10) over the whole domain. This leads to write:

$$
\begin{aligned}
u_{\#}^{1,\infty} &= u^1 + \varepsilon \frac{\partial u^1}{\partial x_2}(x_1, 0)\left(\beta\left(\frac{x}{\varepsilon}\right) - \overline{\beta}\right), \\
u_{\#}^{2,\infty} &= u^2 + \varepsilon \frac{\partial u^2}{\partial x_2}(x_1, 0)\left(\beta\left(\frac{x}{\varepsilon}\right) - \overline{\beta}\right) + \frac{\varepsilon^2}{2}\frac{\partial^2 u^2}{\partial x_2^2}(x_1, 0)\left(\tau\left(\frac{x}{\varepsilon}\right) - \overline{\tau}\right).
\end{aligned}
\tag{12}
$$

For these first order and second order full boundary layer approximations one can set the error estimates [4]:

$$
\left\| u_{\#}^{\varepsilon} - u_{\varepsilon}^{1,\infty} \right\|_{L^2(\Omega^0)} \leq K\varepsilon^{\frac{3}{2}}, \quad \left\| u_{\#}^{\varepsilon} - u_{\varepsilon}^{2,\infty} \right\|_{L^2(\Omega^0)} \leq K e^{-\frac{1}{\varepsilon}}.
$$

Note that the second order full boundary layer approximation is very close to the exact solution in the periodic case, an important step that this work was aiming to reach is to show how far this can be extended to a more realistic boundary conditions considered in (3). Actually, convergence rates provided hereafter and in [16] show that only first order accuracy can be achieved trough the addition of a vertical boundary layer (see below). For this reason we study in the rest of this paper only the first order full boundary layer and its corresponding wall law.

4 The Non Periodic Case: A Vertical Corrector

The purpose of what follows is to extend above results to the practical case of (3). We should show a general method to handle such a problem. It is inspired in a part from the homogenization framework already presented in [19, 17] for a periodic media in all directions. The approach below uses some arguments exposed in [3] for another setting.

4.1 Microscopic Decay Estimates

In what follows we mainly need to correct oscillations of the normal derivative of the first order boundary layer corrector β on the inlet and outlet $\Gamma_{in} \cup \Gamma_{out}$. For this sake, we define the notations $\Pi := \cup_{k=0}^{+\infty}[Z^+ \cup \Gamma \cup P + 2\pi k \mathbf{e}_1]$, the vertical boundary will be denoted $E := \{0\} \times]f(0), +\infty[$ and the bottom $B := \{y \in P^0 \pm 2k\pi \mathbf{e}_1\}$ (cf. Fig. 3). In what follows we should denote $\Pi' := \mathbb{R}_+^2$, $B' := \mathbb{R}_+ \times \{0\}$ and $E' := \{0\} \times \mathbb{R}_+$.

On this domain, we introduce the problem: find ξ such that

$$
\begin{cases}
-\Delta \xi = 0, & \text{in } \Pi, \\
\dfrac{\partial \xi}{\partial \mathbf{n}}(0, y_2) = \dfrac{\partial \beta}{\partial \mathbf{n}}(0, y_2), & \text{on } E, \\
\xi = 0, & \text{on } B.
\end{cases}
\tag{13}
$$

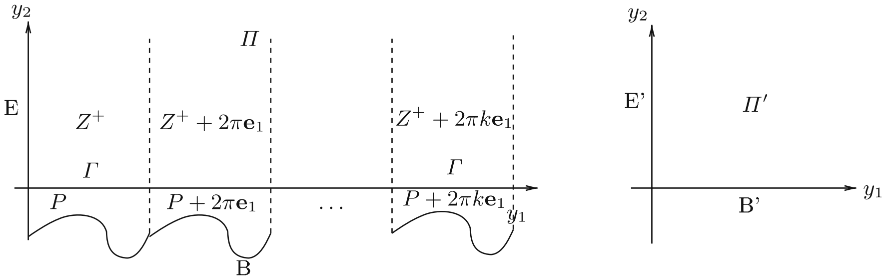

Fig. 3 Semi infinite microscopic domains: Π, the rough quarter-plane and Π', the smooth one

We define the standard weighted Sobolev spaces : for any given integers (n, p) and a real α set

$$W_\alpha^{n,p}(\Omega) := \left\{ v \in \mathcal{D}'(\Omega) \,/\, |D^\lambda v|(1+\varrho^2)^{\frac{\alpha+|\lambda|-n}{2}} \in L^p(\Omega),\ 0 \leq |\lambda| \leq n \right\}$$

where $\varrho := \sqrt{y_1^2 + (y_2+1)^2}$. In what follows we should distinguish between properties depending on ϱ which is a distance to a point exterior to the domain Π and $r = \sqrt{y_1^2 + y_2^2}$ the distance to the interior point $(0, 0)$. These weighted Sobolev spaces are Banach spaces for the norm

$$\|\xi\|_{W_\alpha^{m,p}(\Omega)} := \left(\sum_{0 \leq |\lambda| \leq m} \left\| (1+\varrho^2)^{\frac{\alpha-m+|\lambda|}{2}} D^\lambda u \right\|_{L^p(\Omega)}^p \right)^{\frac{1}{p}},$$

the semi-norm being

$$|\xi|_{W_\alpha^{m,p}(\Omega)} := \left(\sum_{|\lambda| = m} \left\| (1+\varrho^2)^{\frac{\alpha-m+|\lambda|}{2}} D^\lambda u \right\|_{L^p(\Omega)}^p \right)^{\frac{1}{p}}.$$

We refer to [9, 15, 1] for detailed study of these spaces. We introduce a specific subspace

$$\dot{W}_\alpha^{p,n}(\Pi) = \left\{ v \in W_\alpha^{p,n}(\Pi) \text{ s.t. } v \equiv 0 \text{ on B} \right\}.$$

We begin by some important properties satisfied by ξ that will be used to prove convergence Theorems 3, 4 and 5. Such estimates will be obtained by a careful study of the weighted Sobolev properties of ξ as well as its integral representation through a specific Green function.

Theorem 2 *Under the hypotheses of Theorem 1, there exists ξ, a unique solution of problem* (13)*. Moreover $\xi \in \dot{W}_\alpha^{1,2}(\Pi)$ with $\alpha \in]-\alpha_0, \alpha_0[$ where $\alpha_0 := (\sqrt{2}/\pi)$ and*

$$|\xi(y)| \leq \frac{K}{\varrho(y)^{1-\frac{1}{2M}}}, \ \forall y \in \mathbb{R}^2_+ \ s.t. \ \varrho > 1,$$
$$\int_0^\infty \left| \frac{\partial \xi}{\partial y_1}(y_1, y_2) \right|^2 dy_1 \leq \frac{K}{y_2^{1+2\alpha}}, \ \forall y_2 \in \mathbb{R}_+,$$

where M is a positive constant such that $M < 1/(1-2\alpha) \sim 10$.

The proof follows as a consequence of every result claimed until the end of Sect. 4.1.

Lemma 1 *In* $\dot{W}^{1,2}_\alpha(\Pi)$ *the semi-norm is a norm, moreover one has*

$$\|\xi\|_{W^{1,2}_\alpha(\Pi)} \leq \frac{1}{2\alpha_0} |\xi|_{W^{1,2}_\alpha(\Pi)}, \quad \forall \alpha \in \mathbb{R}.$$

On the vertical boundary E one has the continuity of the trace operator

$$\|\xi\|_{W^{\frac{1}{2},2}_\alpha(E)} \leq K \|\xi\|_{W^{1,2}_\alpha(\Pi)}, \quad \forall \alpha \in \mathbb{R},$$

the weighted trace norm being defined as

$$W^{\frac{1}{2},2}_0(\partial\Pi) = \Bigg\{ u \in \mathcal{D}'(\partial\Pi) \ s.t. \ \frac{u}{(1+\varrho^2)^{\frac{1}{4}}} \in L^2(\partial\Pi), \\ \int_{\partial\Pi_l^2} \frac{|u(y) - y(y')|^2}{|y-y'|^2} ds(y) ds(y') < +\infty \Bigg\},$$

and

$$u \in W^{\frac{1}{2},2}_\alpha(\partial\Pi) \iff (1+\varrho^2)^{\frac{\alpha}{2}} u \in W^{\frac{1}{2},2}_0(\partial\Pi).$$

The proof is omitted: the homogeneous Dirichlet condition on B allows to establish Poincaré Wirtinger estimates ([6], vol. I page 56) in a quarter-plane containing Π. Nevertheless, similar arguments are also used in the proof of Lemma 4.

Lemma 2 *The normal derivative* $g := \frac{\partial \beta}{\partial y_1}(0, y_2)$ *is a linear form on* $\dot{W}^{1,2}_\alpha(\Pi)$ *for every* $\alpha \in \mathbb{R}$.

Proof In Z^+, the upper part of the cell domain, the harmonic decomposition of β allows to characterize its normal derivative explicitly on E'. Indeed

$$g = \mathrm{Re} \left\{ \sum_{\mathrm{k}=-\infty}^{+\infty} \mathrm{ik}\eta_{\mathrm{k}} \mathrm{e}^{-|\mathrm{k}|\mathrm{y}_2} \right\} \chi_{[\mathrm{E}']} + \mathrm{g}_- =: \mathrm{g}_+ + \mathrm{g}_-$$

where g_- is a function whose support is located in $y_2 \in [f(0), 0]$. One has for the upper part

$$\int_{E'} g_+^2 y_2^\alpha dy_2 \leq K \|\eta\|^2_{H^{\frac{1}{2}}(\Gamma)}, \quad \forall \alpha \in \mathbb{R},$$

thus g_+ is in the weighted L^2 space for any power of $(1+\varrho^2)^{\frac{1}{2}}$, it is a linear form on $W^{\frac{1}{2},2}_{-\alpha}(E)$. For g_-, we have no explicit formulation. We analyze the problem (4) but restricted to the bounded sublayer P. We define β_- to be harmonic in P satisfying $\beta_- = \eta$ on Γ, where η is the trace on the fictitious interface obtained in Theorem 1 and $\beta_- = -y_2$ on P^0. Note that thanks to standard regularity results $\eta \in C^2(\Gamma)$ because Γ is strictly included in $Z^+ \cup \Gamma \cup P$, [7]. So β solves a Dirichlet y_1-periodic problem in P with regular data. As the boundary is Lipschitz $\beta \in H^1(P)$ and so on the compact interface $E_c := \{0\} \times [f(0), 0]$, $\partial_{\mathbf{n}}\beta$ is a linear form on $H^{\frac{1}{2}}$ functions. Then because E_c is compact :

$$\int_{Ec} \frac{\partial \beta}{\partial \mathbf{n}} v dy_2 \leq \left\| \frac{\partial \beta}{\partial \mathbf{n}} \right\|_{H^{-\frac{1}{2}}(E_c)} \|v\|_{H^{\frac{1}{2}}(E_c)} \leq K \|v\|_{W^{\frac{1}{2},2}_\alpha(E_c)}, \quad \forall \alpha \in \mathbb{R}$$

□

Lemma 3 *If* $\alpha \in]-\alpha_0 : \alpha_0[$ *there exists* $\xi \in \dot{W}^{1,2}_\alpha(\Pi)$ *a unique solution of problem* (13).

Proof The weak formulation of problem (13) reads

$$(\nabla \xi, \nabla v)_\Pi = (g, v)_E\,, \quad \forall\, v \in C^\infty(\Pi),$$

leading to check hypothesis of the abstract inf-sup extension of the Lax-Milgram Theorem [18, 2], for

$$a(u, v) = \int_{\Pi_+} \nabla u \cdot \nabla v \, dy, \quad l(v) = \int_{f(0)}^{+\infty} \frac{\partial \beta}{\partial \mathbf{n}} v \, dy_2.$$

By Lemma 2, l is a linear form on $W^{1,2}_\alpha(\Pi)$. It remains to prove the inf-sup like condition on the bilinear form a. For this purpose we set $v = u\varrho^{2\alpha}$ and we look for a lower estimate of $a(u, v)$.

$$a(u, u\varrho^{2\alpha}) = \int_{\Pi_+} \nabla u \cdot \nabla \left(u\varrho^{2\alpha}\right) dy = |u|^2_{W^{1,2}_\alpha(\Pi)} + 2\alpha \int_{\Pi_+} \varrho^{2\alpha-1} u \nabla u \cdot \nabla \varrho \, dy$$

Using Hölder estimates one has

$$\begin{aligned} \int_{\Pi_+} \varrho^{2\alpha-1} u \nabla u \cdot \nabla \varrho dy &\leq \left(\int_{\Pi_+} \varrho^{2\alpha} \left(\frac{u}{\varrho}\right)^2 dy \right)^{\frac{1}{2}} \left(\int_{\Pi_+} \varrho^{2\alpha} |\nabla u|^2 dy \right)^{\frac{1}{2}} \\ &\leq \frac{1}{2\alpha_0} |u|^2_{W^{1,2}_\alpha(\Pi)} \end{aligned}$$

In this way one gets

$$a(u, u\varrho^{2\alpha}) \geq (1 - \frac{\alpha}{\alpha_0})|u|^2_{W^{1,2}_\alpha(\Pi)}$$

and if $\alpha < \alpha_0$ the inf-sup condition is fulfilled, the rest of the proof is standard and left to the reader [2]. □

Thanks to the Poincaré inequality in $\Pi \setminus \Pi'$ with $\alpha = 0$, we have

Corollary 1 *If a function ξ belongs to $\dot{W}^{1,2}_0(\Pi)$ it satisfies $\xi \in L^2(B')$.*

To characterize the weighted behavior of ξ on B' we set

$$\omega_\alpha(y_1) = (y_1^2 + 1)^{\frac{2\alpha-1}{2}} y_1$$

and we give

Lemma 4 *If ξ in $\dot{W}^{1,2}_\alpha(\Pi)$ then $\xi \in L^2(B', \omega_\alpha) := \{u \in \mathcal{D}'(B') : \int_{B'} \xi^2 \omega_\alpha dy_1 < \infty\}$.*

Proof Π is contained in a set $\mathbb{R}_+ \times \{-1, +\infty\}$. We map the latter with cylindrical coordinates (ϱ, θ). Every function of $\dot{W}^{1,2}_0(\Pi)$, extended by zero on the complementary set of Π, belongs to the space of functions vanishing on the half-line $\theta = 0$. Using Wirtinger estimates, one has for every such a function.

$$\begin{aligned}\int_1^{+\infty} \xi^2 \left(\varrho, \arcsin\left(\frac{1}{\varrho}\right)\right) \varrho^{2\alpha} d\varrho &\leq \int_1^\infty \int_0^{\frac{\pi}{2}} \varrho^{2\alpha-1} \arcsin\left(\frac{1}{\varrho}\right) \left|\frac{\partial \xi}{\partial \theta}\right|^2 \varrho d\theta d\varrho \\ &\leq K \|\xi\|^2_{W^{1,2}_\alpha(\Pi)}\end{aligned}$$

because on B', $\varrho d\varrho = y_1 dy_1$, one gets the desired result. □

In order to derive local and global L^∞ estimates we introduce in this part a representation formula of ξ on Π'. As long as we use the representation formula below, x will be the symmetric variable to the integration variable y. Until the end of Proposition 2 both x and y are microscopic variables living in Π.

Lemma 5 *The solution of problem* (13) *satisfies $\xi(y) \leq K\varrho^{-1+\frac{1}{2M}}$ for every $y \in \Pi'$ such that $\varrho(y) \geq 1$. The constant M can be chosen such that $M < 1/(1-2\alpha) \sim 10$.*

Proof We set the representation formula

$$\xi(x) = \int_{E'} \Gamma_x g(y_2) dy_2 + \int_{B'} \frac{\partial \Gamma_x}{\partial \mathbf{n}} \xi(y_1, 0) dy_1 =: N(x) + D(x), \quad \forall x \in \Pi', \quad (14)$$

where the Green function for the quarter-plane is

$$\Gamma_x(y) = \frac{1}{4\pi} \left(\ln|x-y| + \ln|x^* - y| - \ln|x_* - y| - \ln|\overline{x} - y|\right),$$

with $x = (x_1, x_2)$, $x^* = (-x_1, x_2)$, $x_* = (x_1, -x_2)$, $\overline{x} = (-x_1, -x_2)$.

The Neumann part $N(x)$.

We make the change of variables $x = (r\cos\vartheta, r\sin\vartheta)$ which gives

$$\begin{aligned}
N &:= \lim_{m\to\infty} \sum_{k=0}^{m} \eta_k N_k \\
&= \lim_{m\to\infty} \sum_{k=0}^{m} \frac{\eta_k}{2\pi} \int_0^\infty k e^{-ky_2} \left(\ln(x_1^2 + (y_2 - x_2)^2) - \ln(x_1^2 + (y_2 + x_2)^2)\right) dy_2 \\
&= \lim_{m\to\infty} \frac{1}{2\pi} \sum_{k=1}^{m} \eta_k \int_0^\infty k e^{-ky_2} \left(\ln\left(1 - \frac{2sy_2}{r} + \left(\frac{y_2}{r}\right)^2\right)\right. \\
&\qquad\qquad\qquad\qquad \left. -\ln\left(1 + \frac{2sy_2}{r} + \left(\frac{y_2}{r}\right)^2\right)\right) dy_2,
\end{aligned}$$

where $c = \cos\vartheta$, $s = \sin\vartheta$. Now we perform the second change of variables $t_k = e^{-ky_2}$ and get

$$N_k \le \frac{1}{\pi}\int_0^1 \ln\left(1 - \frac{2s\ln t_k}{r} + \left(\frac{\ln t_k}{r}\right)^2\right) dt_k \le \frac{1}{\pi}\int_0^1 \ln\left(\left(1 - \frac{\ln t}{r}\right)^2\right) dt$$

The last rhs is independent of k; one easily estimates it using the change of variables $y = -\ln t/r$, indeed:

$$\int_0^1 \ln\left(\left(1 - \frac{\ln t}{r}\right)^2\right) dt = \int_0^\infty \ln(1+y) e^{-ry} r\,dy = \int_0^\infty \frac{e^{-ry}}{1+y} dy \le \frac{1}{r}$$

Now because the fictitious interface $\varGamma$ is strictly included in $S := Z^+ \cup \Gamma \cup P$, $\beta \in H^2_{\text{loc}}(S)$ and thus $\|\eta\|_{H^1(\varGamma} := \sum_{k=1}^\infty |\eta_k|^2 k^2 < +\infty$, one has for every finite m

$$\sum_{k=1}^{m} |\eta_k N_k| \le \left(\sum_{k=1}^{\infty} |\eta_k|^2 k^2\right)^{\frac{1}{2}} \left(\sum_{k=1}^{\infty} \frac{1}{k^2}\right)^{\frac{1}{2}} \le C\|\eta\|_{H^1(\varGamma)} \frac{1}{r}$$

the estimate being uniform wrt m one has that $N \le C\|\eta\|_{H^1(\varGamma)}/r$.

The Dirichlet part $D(x)$.

We have, by the same change of variable as above $(x := r(\cos(\vartheta), \sin\vartheta) := r(c, s)$:

$$\begin{aligned}
D(x) &= -\frac{x_2}{2\pi}\int_0^\infty \left(\frac{1}{(y_1 - x_1)^2 + x_2^2} + \frac{1}{(y_1 + x_1)^2 + x_2^2}\right) \xi(y_1, 0) dy_1 \\
&\le \frac{s}{\pi r}\int_0^\infty \frac{1}{1 - 2c\frac{y_1}{r} + \left(\frac{y_1}{r}\right)^2} |\xi| dy_1 = \frac{s}{\pi r}\int_0^\infty \frac{1}{(1 - c^2) + \left(c - \frac{y_1}{r}\right)^2} |\xi| dy_1,
\end{aligned}$$

where we suppose that $c < 1$. We divide this integral in two parts, we set $m > 1$

$$D(x) \leq \frac{s}{\pi r}\left[\int_0^m \frac{1}{(1-c^2)+\left(c-\frac{y_1}{r}\right)^2}|\xi|dy_1 + \int_m^\infty \frac{1}{(1-c^2)+\left(c-\frac{y_1}{r}\right)^2}|\xi|dy_1\right]$$
$$=: (I_1+I_2)(x).$$

For I_1 one uses the L^p_{loc} inclusions :

$$I_1 \leq \frac{s}{\pi r}\frac{K}{1-c^2}\|\xi(\cdot,0)\|_{L^1(0,m)} \leq \frac{2}{\pi x_2}K\|\xi\|_{L^2(B')},$$

while for I_2 one uses the weighted norm established in Lemma 4

$$I_2 \leq \frac{s}{\pi r}\left(\int_m^\infty \left(\frac{1}{(1-c^2)+\left(c-\frac{y_1}{r}\right)^2}\right)^2 \frac{(y_1^2+1)^{\frac{1-2\alpha}{2}}}{y_1}dy_1\right)^{\frac{1}{2}} \|\xi\|_{L^2(B',\omega_\alpha)}$$
$$\leq \frac{2s}{\pi r}\left(\int_m^\infty \left(\frac{1}{(1-c^2)+\left(c-\frac{y_1}{r}\right)^2}\right)^2 y_1^{-2\alpha}dy_1\right)^{\frac{1}{2}} \|\xi\|_{L^2(B',\omega_\alpha)}$$
$$\leq \frac{2s}{\pi r}\left(\left(\int_m^\infty\left(\frac{1}{(1-c^2)+\left(c-\frac{y_1}{r}\right)^2}\right)^{2M}dy_1\right)^{\frac{1}{M}}\left(\int_m^\infty y_1^{-2\alpha M'}dy_1\right)^{\frac{1}{M'}}\right)^{\frac{1}{2}}\|\xi\|_{L^2(B',\omega_\alpha)},$$

where M and M' are Hölder conjugates. We choose $M'2\alpha > 1$ such that the weight contribution provided by ξ is integrable, this implies that $M < 1/(1-2\alpha) \sim 10$. One then recovers easily

$$I_2 \leq \frac{2sK}{\pi r}\left(\frac{\pi r}{(1-c^2)^{2M-\frac{1}{2}}}\right)^{\frac{1}{2M}} = \frac{2K}{(\pi x_2)^{1-\frac{1}{2M}}}.$$

We could shift the fictitious interface Γ to $\Gamma - \delta e_2$ and repeat again the same arguments because the rough boundary does not intersect it. Note that in this case we could establish again the explicit Fourier representation formula for β and its derivative as in Theorem 1. Thus we can obtain that $\xi \leq c(x_2+\delta)^{1-1/(2M)}$ which shows that ξ is bounded in Π'. So that on E', one has $|\xi|\varrho^{1-\frac{1}{2M}} = |\xi|(1+x_2)^{1-\frac{1}{2M}} \leq c'$. Here one applies the Fragmèn-Lindelöf technique (see [3], Lemma 4.3, p. 12). We restrict the domain to a sector, defining $\Pi_S = \Pi \cap S$, where $S = \{(\varrho,\theta) \in [1,\infty]\times[0,\pi/2]\}$. On Π_S, we define $\varpi := -1+1/(2M)$ and $v := \varrho^{\varpi}\sin(\varpi\theta)$ the latter is harmonic definite positive, we set $w = \xi/v$ which solves

$$\Delta w + \frac{2}{v}\nabla v \cdot \nabla w = 0, \text{ in } S_\Pi,$$

with $w = 0$ on $B_S = \partial S \cap B$, whereas w is bounded uniformly on $E_S := E \cap S$. Because by standard regularity arguments $\xi \in C^2(\Pi)$, w is also bounded when $\varrho = 1$. Then by the Hopf maximum principle, we have

$$\sup_{\Pi_S} |w| \leq \sup_{\partial \Pi_S} w \leq K$$

which extends to the whole domain Π_S, the radial decay of ξ. □

Deriving the representation formula (14), one gets for all x strictly included in Π' that

$$\partial_{x_1}\xi(x) = \int_{E'} \partial_{x_1}\Gamma_x\, g dy_2 + \int_{B'} \frac{\partial}{\partial x_1}\frac{\partial \Gamma_x}{\partial y_2}\xi(y_1, 0)dy_1 =: N_{x_1}(x) + D_{x_1}(x), \forall x \in \Pi'$$

Lemma 6 *For any $x \in \Pi'$, the Neumann part of the normal derivative $\partial_{x_1}\xi$ satisfies $N_{x_1}(x) \leq K r^{-2}$ for all x in Π'*

Proof On E' the derivative wrt x_1 of the Green kernel reads

$$\partial_{x_1}\Gamma_x = x_1 \left(\frac{1}{x_1^2 + (x_2 - y_2)^2} - \frac{1}{x_1^2 + (x_2 + y_2)^2} \right)$$

thus using the cylindrical coordinates to express $x = (r \cos \vartheta, r \sin \vartheta) =: r(c, s)$ for $0 \leq s < 1$ one gets

$$\begin{aligned} N_{x_1}(x) &= \frac{c}{r}\int_0^\infty \left(\frac{1}{1 - 2s\frac{y_2}{r} + \left(\frac{y_2}{r}\right)^2} - \frac{1}{1 + 2s\frac{y_2}{r} + \left(\frac{y_2}{r}\right)^2} \right) g(y_2)dy_2 \\ &= \sum_k \frac{c}{r}\int_0^\infty \frac{4s\frac{y_2}{r}}{4s^2(1-s^2) + \left(1 - 2s^2 - \left(\frac{y_2}{r}\right)^2\right)^2} e^{-|k|y_2}dy_2 \\ &\leq 4\sum_k \frac{1}{x_1 x_2}\int_0^\infty y_2 e^{-|k|y_2}dy_1 \leq \frac{1}{x_1 x_2}\sum_k \frac{4}{k^2}|\eta_k|^2 \leq \frac{4}{x_1 x_2}\|\eta\|_{H^{-1}(\Gamma)}. \end{aligned} \tag{15}$$

This estimate is not optimal since it is singular near $x_1 = 0$ or $x_2 = 0$. But it provides useful decay estimates inside Π'.

It's easy to check that N_{x_1} is harmonic, $N_{x_1} = g$ on E', and that it vanishes on B'. Because on E' g is bounded, by the maximum principle N_{x_1} is bounded. We divide $\Pi' \setminus B(0, 1)$ in three angular sectors :

$$S_i = \{(r, \vartheta) \text{ s.t. } r > 1,\ \vartheta \in [\vartheta_{i-1}, \vartheta_i]\},\ (\vartheta_i)_{i=0}^3 = \left\{0, \frac{\pi}{6}, \frac{\pi}{3}, \frac{\pi}{2}\right\}$$

For S_1 and S_3 we define $v_i := \pm\varrho^{-2}\cos(2\vartheta)$, $i = 1, 2$ which is positive definite and harmonic, while for S_2, we set $v_i := \varrho^{-2}\sin(2\vartheta)$, thatshares the same properties. For each sector we define $w_i = N_{x_1}/v_i$, it solves

$$\Delta w_i + \frac{2}{v_i}\nabla v_i \cdot \nabla w_i = 0, \text{ in } S_i, \quad i = 1, \dots, 3$$

The estimate (15) shows that on each interior boundary ∂S_i, w is bounded while on $E' \cup B'$ it is bounded by the boundary conditions that N_{x_1} satisfies. By the Hopf maximum principle [7], one shows that

$$\sup_{S_1} w_1 \leq \sup_{\vartheta=\frac{\pi}{6}} w_1 < \infty, \sup_{S_2} w_2 \leq \sup_{\vartheta=\frac{\pi}{6},\vartheta=\frac{\pi}{3}} w_2 < \infty, \sup_{S_3} w_3 \leq \sup_{\vartheta=\frac{\pi}{3},\vartheta=\frac{\pi}{2}} w_3 < \infty$$

which implies that $N_{x_1} \leq K r^{-2}$ for every $y \in \Pi'_S := \Pi' \cap S$. □

In order to estimate D_{x_1} the latter term of the derivative, we introduce the lemma inspired by proofs of weighted Sobolev embeddings in [13, 14].

Lemma 7 *If* $\xi \in W^{1,2}_\alpha(\Pi)$ *with* $\alpha \in [0, 1/2[$ *then its trace on a horizontal interface satisfies*

$$I(\xi) = \int_0^\infty \int_0^\infty \frac{|\xi(y_1 + h, 0) - \xi(y_1, 0)|^2}{h^{2-2\alpha}}\, dy_1\, dh \leq \|\xi\|_{W^{1,2}_\alpha(\Pi)} \tag{16}$$

The proof follows ideas of Theorem 2.4' in [14] p. 235, we give it for sake of self-containtness.

Proof We make a change of variables $x_1 = r \cos\vartheta$, $x_2 = r \sin\vartheta$, $\vartheta = 0$, leading to rewrite I as

$$I = \int_0^\infty \int_0^\infty \frac{|\xi(r + h, 0) - \xi(r, 0)|^2}{h^{2-2\alpha}}\, dr\, dh,$$

note that the second space variable for ξ is now $\vartheta = 0$. We insert intermediate terms inside the domain, namely

$$I \leq K \left\{ \int \int_0^\infty \frac{\left|\xi(r + h, 0) - \xi\left(r + h, \operatorname{atan}\frac{h}{r}\right)\right|^2}{h^{2-2\alpha}} \right.$$
$$+ \frac{\left|\xi\left(r + h, \operatorname{atan}\frac{h}{r}\right) - \xi\left(r, \operatorname{atan}\frac{h}{r}\right)\right|^2}{h^{2-2\alpha}} dr\, dh$$
$$\left. + \int_0^\infty \int_0^\infty \frac{\left|\xi\left(r, \operatorname{atan}\frac{h}{r}\right) - \xi(r, 0)\right|^2}{h^{2-2\alpha}} dr\, dh \right\} =: I_1 + I_2 + I'_1$$

Obviously the terms I_1 and I'_1 are treated the same way. We make a change of variable $(r, h = r \tan\vartheta)$

$$I_1 = \int_0^{\frac{\pi}{2}} \int_0^{\infty} \frac{|\xi(r(1+\tan\vartheta),0) - \xi(r(1+\tan\vartheta),\vartheta)|^2}{(r\tan\vartheta)^{2-2\alpha}} \frac{r}{1+\vartheta^2} dr\, d\vartheta.$$

In order to eliminate the dependence on ϑ in the first variable of ξ, we then make the change of variable $(r = \tilde{r}/(1+\tan\vartheta), \vartheta)$ which gives

$$\begin{aligned} I_1 &= \int_0^{\frac{\pi}{2}} \int_0^{\infty} \frac{|\xi(\tilde{r},0) - \xi(\tilde{r},\vartheta)|^2}{\tilde{r}^{2-2\alpha}} \tilde{r} d\tilde{r} \frac{(1+\tan\vartheta)^{2\alpha}}{\tan^{2-2\alpha}\vartheta(1+\vartheta^2)} d\vartheta \\ &\le \int_0^{\infty} \int_0^{\frac{\pi}{2}} \frac{|\xi(\tilde{r},0) - \xi(\tilde{r},\vartheta)|^2}{\tilde{r}^{2-2\alpha}} \tilde{r} d\tilde{r}\, \frac{d\vartheta}{\vartheta^{2-2\alpha}}. \end{aligned}$$

We are in the hypotheses of the Hardy inequality (see for instance [13], p. 203 estimate (7)), thus we have

$$\begin{aligned} I_1 &\le \frac{4}{(1-2\alpha)^2} \int_0^{\infty} \int_0^{\frac{\pi}{2}} \left| \frac{\partial \xi}{\partial \vartheta}(\tilde{r},\vartheta) \right|^2 \vartheta^{2\alpha} d\vartheta\, \tilde{r}^{2\alpha-1} d\tilde{r} \\ &\le K \int_0^{\infty} \tilde{r}^{2\alpha} \int_0^{\frac{\pi}{2}} \frac{1}{\tilde{r}^2} \left| \frac{\partial \xi}{\partial \vartheta}(\tilde{r},\vartheta) \right|^2 d\vartheta\, \tilde{r} d\tilde{r} \le \|\xi\|^2_{W^{1,2}_\alpha(\Pi)}, \end{aligned}$$

in the last estimate we used that in Π', the distance to the fixed point $(0,-1)$ can be estimated as $\varrho^{2\alpha} := (y_1^2 + (y_2+1)^2)^\alpha \ge (y_1^2 + y_2^2)^\alpha =: \tilde{r}^{2\alpha}$, this explains why we need a positive α in the hypotheses. In the same manner

$$\begin{aligned} I_2 &\le \int_0^{\frac{\pi}{2}} \int_0^{\infty} \frac{|\xi(r(1+\tan\vartheta),\vartheta) - \xi(r,\vartheta)|^2}{(r\tan\vartheta)^{2-2\alpha}} r dr\, d\vartheta, \\ &= \int_0^{\frac{\pi}{2}} \int_0^{\infty} \left| \int_0^{r\tan\theta} \frac{\partial \xi}{\partial r}(r+s,\vartheta) ds \right|^2 r^{2\alpha-1} dr \frac{d\vartheta}{\tan^{2-2\alpha}\vartheta}, \\ &\le \int_0^{\frac{\pi}{2}} \left\{ \int_0^{\tan\vartheta} \left[\int_0^{\infty} \left| \frac{\partial \xi}{\partial r} \right|^2 (r(1+\sigma),\vartheta) r^{1+2\alpha} dr \right]^{\frac{1}{2}} d\sigma \right\}^2 \frac{d\vartheta}{\tan^{2-2\alpha}\vartheta}, \end{aligned}$$

where we made the change of variables $s = rt$ and applied the generalized Minkowski inequality ([13], p. 203 estimate (6)). Now we set $\tilde{r} = r(1+t)$ inside the most interior integral above

$$I_2 \le \int_0^{\frac{\pi}{2}} \left\{ \int_0^{\tan\vartheta} \frac{dt}{(1+t)^{1+\alpha}} \left[\int_0^{\infty} \left| \frac{\partial \xi}{\partial r} \right|^2 (\tilde{r},\vartheta) \tilde{r}^{1+2\alpha} d\tilde{r} \right]^{\frac{1}{2}} \right\}^2 \frac{d\vartheta}{\tan^{2-2\alpha}\vartheta}.$$

Now, we have separated the integrals in t and r, the part depending on t is easy to integrate. Thus we obtain

$$I_2 \le \int_0^{\frac{\pi}{2}} \mathcal{S}(\vartheta) \int_0^{\infty} \left|\frac{\partial \xi}{\partial r}\right|^2 (\tilde{r}, \vartheta)\tilde{r}^{1+2\alpha} d\tilde{r} d\vartheta,$$

where $\mathcal{S}(\vartheta) = \dfrac{1}{\tan^{2-2\alpha}\vartheta}\left[\dfrac{1}{(1+\tan\vartheta)^{\alpha}} - 1\right]^2$.

Distinguishing whether $\tan\vartheta$ is greater or not than 1, it is possible to show that $\mathcal{S}$ is uniformly bounded wrt ϑ. This gives the desired result. □

We follow similar arguments as in the proof of Theorem 8.20 p. 144 in [12] to claim:

Proposition 2 *Set ξ a function belonging to $W^{1,2}_{\alpha}(\Pi)$, and*

$$D_{x_1}(x) := \int_0^{\infty} G(x, y_1)\xi(y_1, 0)dy_1, \forall x \in \Pi', \ \text{where } G(x, y_1) = \left.\frac{\partial}{\partial x_1}\frac{\partial \Gamma_x}{\partial y_2}\right|_{y \in B'},$$

then it satisfies for every fixed positive h

$$\int_0^{\infty} |D_{x_1}(x_1, h)|^2 dx_1 \le \frac{K}{h^{1+2\alpha}},$$

where the constant K is independent on h.

Proof We recall that

$$G := -x_2\left(\frac{x_1 - y_1}{((x_1 - y_1)^2 + x_2^2)^2} + \frac{x_1 + y_1}{((x_1 + y_1)^2 + x_2^2)^2}\right).$$

Because $\int_0^{\infty} G(x, y_1)dy_1 = 0$ for every $x \in \Pi'$ we have

$$D_{x_1}(x) = \int_0^{\infty} G(x, y_1)\,(\xi(y_1, 0) - \xi(x_1, 0))\,dy_1, \quad \forall x \in \Pi',$$

we underline that $G(x, \cdot)$ is evaluated at $x \in \Pi'$ while $\xi(x_1, 0)$ is taken on B'. By Hölder estimates in y_1 with $p = 2$, $p' = 2$, we have :

$$|D_{x_1}|^2 \le \int_0^{\infty} G^2 |y_1 - x_1|^{2-2\alpha} dy_1 \int_0^{\infty} \frac{|\xi(y_1, 0) - \xi(x_1, 0)|^2}{|y_1 - x_1|^{2-2\alpha}} dy_1 \tag{17}$$

integrating in x_1 and using Hölder estimates with $p = \infty$, $p' = 1$ then

$$\begin{aligned} I_3 &:= \int_0^{\infty} |D_{x_1}|^2 dx_1 \\ &\le \sup_{x_1 \in \mathbb{R}_+} \int_{\mathbb{R}_+} G^2 |y_1 - x_1|^{2-2\alpha}\, dy_1 \int_0^{\infty}\int_0^{\infty} \frac{|\xi(y_1, 0) - \xi(x_1, 0)|^2}{|y_1 - x_1|^{2-2\alpha}} dy_1 dx_1 \end{aligned}$$

Thanks to Proposition 7 we estimate the last integral in the rhs above

$$I_3 \leq K \sup_{x_1 \in \mathbb{R}_+} I_4(x_1, x_2) \|\xi\|_{W^{1,2}_\alpha(\Pi)},$$

where $I_4(x_1, x_2) := \int_{\mathbb{R}_+} G^2 |y_1 - x_1|^{2-2\alpha} \, dy_1$. Considering I_4 one has

$$\begin{aligned} I_4(x) &\leq K \int_0^\infty \frac{x_2^2 (y_1 - x_1)^{4-2\alpha}}{((x_1 - y_1)^2 + x_2^2)^4} dy_1 + \frac{x_2^2 (y_1 + x_1)^2 (y_1 - x_1)^{2-2\alpha}}{((x_1 + y_1)^2 + x_2^2)^4} dy_1 \\ &\leq K \int_0^\infty \frac{x_2^2 (y_1 - x_1)^{4-2\alpha}}{((x_1 - y_1)^2 + x_2^2)^4} dy_1 + \frac{x_2^2 (y_1 + x_1)^{4-2\alpha}}{((x_1 + y_1)^2 + x_2^2)^4} dy_1 =: I_5 + I_6 \end{aligned}$$

Both terms in the last rhs are treated the same, namely

$$I_5 \leq x_2^{2+5-2\alpha-8} \int_{-\infty}^\infty \frac{z^{4-2\alpha}}{(z^2+1)^4} dz \leq \frac{K}{x_2^{1+2\alpha}}$$

which ends the proof. □

Remark 1 This is one of the key point estimates of the paper. One could think of using weighted properties of ξ of Lemma 4 instead of the fractional Sobolev norm introduced from Proposition 7, in the Hölder estimates (17). This implies to transfer the x_1-integral on G, then it seems impossible to conclude because

$$\int_0^\infty \int_0^\infty G^2 \omega_\alpha(y_1) dy_1 dx_1 = \infty,$$

which is easy to show if one performs the change of variables $z_1 = y_1 - x_1$, $y_1 = y_1$.

In this part we study the convergence properties of the normal derivative of ξ on vertical interfaces far from E. For this sake we call

$$\Pi_l = \{y \in \Pi : y_1 > l\}, E_l = \{y_1 = l, \ y_2 \in [f(0), +\infty[\}, B_l = \{y \in B, y_1 > l\},$$

here we redefine the weighted trace spaces of Sobolev type

$$\begin{aligned} W^{\frac{1}{2},2}_{0,\sigma}(\partial\Pi_l) = \Bigg\{ u \in \mathcal{D}'(\partial\Pi_l) \text{ s.t. } \frac{u}{(1+\sigma^2)^{\frac{1}{4}}} \in L^2(\partial\Pi_l), \\ \int_{\partial\Pi_l^2} \frac{|u(y) - y(y')|^2}{|y - y'|^2} ds(y) ds(y') < +\infty \Bigg\} \end{aligned}$$

where we define $\sigma := |y - (0, f(0))| = \sqrt{y_1^2 + (y_2 - f(0))^2}$. Note that the weight is a distance to the fixed point $(0, f(0))$ independent on l.

Proposition 3 *Suppose that $v \in W^{\frac{1}{2},2}_{0,\sigma}(\partial \Pi_l)$ with $v = 0$ on B_l then there exists an extension denoted $R(v) \in \mathcal{D}'(\Pi_l)$ s.t.*

$$|\nabla R(v)|_{L^2(\Pi_l)} \leq K \|v\|_{W^{\frac{1}{2},2}_{0,\sigma}(\partial \Pi_l)},$$

where K depends only on $\left\| f' \right\|_\infty$.

Proof We lift the domain in a first step in order to transform Π_l in a quarter-plane $\hat{\Pi}_l$.

$$y = \varphi(Y) := \begin{pmatrix} Y_1 \\ Y_2 + f(Y_1) \end{pmatrix}, \quad Y \in \hat{\Pi}_l := (\mathbb{R}_+)^2,$$

if we set $\hat{v}(Y_2) = v(Y_2 + f(0)) = v(y_2)$ then the L^2 part of the weighted norm above reads

$$\int_{E_l} \frac{v^2}{(1+\sigma^2)^{\frac{1}{2}}} dy_2 = \int_{E_l} \frac{v^2}{(1 + l^2 + (y_2 - f(0))^2)^{\frac{1}{2}}} dy_2$$
$$= \int_{\{l\}\times\mathbb{R}_+} \frac{\hat{v}^2}{(1 + l^2 + Y_2^2)^{\frac{1}{2}}} dY_2 = \int_{\{l\}\times\mathbb{R}_+} \frac{\hat{v}^2}{(1+\hat{\sigma}^2)^{\frac{1}{2}}} dY_2,$$

where $\hat{\sigma}^2 = Y_1^2 + Y_2^2$. If $v \in W^{\frac{1}{2},2}_{0,\sigma}(\partial \Pi_l)$ and $v = 0$ on B_l we know that ([8], p. 43 Theorem 1.5.2.3)

$$\int_0^\delta |\hat{v}(Y_2)|^2 \frac{dY_2}{Y_2} < +\infty,$$

which authorizes us to extend v by zero on $\hat{E}_l := \{Y_1 = l\} \times \mathbb{R}$, this extension still belongs to $W^{\frac{1}{2},2}_{0,\hat{\sigma}}(\hat{E}_l)$. Arguments above allow obviously to write for every v vanishing on B and $\hat{v}$ defined above

$$\|v\|_{W^{\frac{1}{2},2}_{0,\sigma}(\partial \Pi_l)} = \|\hat{v}\|_{W^{\frac{1}{2},2}_{0,\hat{\sigma}}(\hat{E}_l)}.$$

Here we use trace Theorems II.1 and II.2 of Hanouzet [9], they follow exactly the same in our case except that the weight is not a distance to a point on the boundary (as in [9]) but it is a distance to a point exterior to the domain. So in order to define an extension ([9] p. 249), we set

$$\begin{cases} V(Y) = \displaystyle\int_{|s|<1} \mathcal{K}(s)\hat{v}(Y_1 s + Y_2) ds, \quad s \in \mathbb{R}, \quad \forall Y \in \hat{\Pi}_l, \\ \Psi(Y) = \Phi\left(\dfrac{Y_1 - l}{(1 + Y_2^2 + l^2)^{\frac{1}{2}}}\right), \end{cases}$$

where Φ is a cut-off function such that

$$\mathrm{Supp}\Phi \in [0:1/4[\,,\quad \Phi(0)=1,\quad \Phi \in C^{\infty}\left([0,1/4[\right),$$

and $\mathcal{K}$ is a regularizing kernel i.e. $\mathcal{K} \in C_0^{\infty}(]-1:1[)$ and $\int_{\mathbb{R}} \mathcal{K}(s)ds = 1$. Then the extension in the quarter-plane domain reads

$$w(Y) = (\Psi V)(Y_1, Y_2) - (\Psi V)(Y_1, -Y_2), \quad Y \in \hat{\Pi}_l,$$

which allows to have $w(Y_1, 0) = 0$ for all $Y_1 \in \mathbb{R}_+$. According to Theorems II.1 and II.2 in [9], one then gets

$$\left\| \frac{w}{(1+\hat{\sigma}^2)^{\frac{1}{2}}} \right\|_{L^2(\hat{\Pi}_l)} \leq K \|\hat{v}\|_{W^{\frac{1}{2},2}_{0,\sigma}(\hat{E}_l)}, \quad \|\nabla w\|_{L^2(\hat{\Pi}_l)} \leq K \|\hat{v}\|_{W^{\frac{1}{2},2}_{0,\sigma}(\hat{E}_l)}.$$

Turning back to our starting domain Π_l, we set

$$R(v) = w(\varphi^{-1}(y)) = w(y_1, y_2 - f(y_1)), \quad \forall y \in \Pi_l.$$

We focus on the properties of the gradient

$$\int_{\Pi_l} (A\nabla_y R(v), \nabla_y R(v))dy = \int_{\hat{\Pi}_l} |\nabla_Y w|^2 dY, \text{ where } A = \begin{pmatrix} 1 & f' \\ f' & 1+(f')^2 \end{pmatrix},$$

but the eigenvalues of A are

$$\lambda_{\pm} = \frac{2+(f')^2 \pm \sqrt{2+(f')^2}|f'|}{2},$$

the lowest eigenvalue is positive and tends to zero as $|f'|$ increases. The boundary is Lipschitz so that $\|f'\|_{\infty}$ is bounded. Thus there exists a minimum value of λ_-. All this guarantees the existence of a constant $\delta'(\|f'\|_{\infty}) > 0$ such that

$$\delta' \int_{\Pi_l} \left|\nabla_y R(v)\right|^2 dy \leq K \|\hat{v}\|_{W^{\frac{1}{2},2}_{0,\hat{\sigma}}(\hat{E}_l)},$$

which ends the proof. □

Thanks to the existence of a lift $R(v)$, we are able to estimate a sort of weak weighted Sobolev norm for the normal derivative on vertical interfaces located at $y_1 = L/\varepsilon$.

Proposition 4 *If $v \in W^{\frac{1}{2},2}_{0,\sigma}(\partial \Pi_{\frac{L}{\varepsilon}})$ and $v = 0$ on $B_{\frac{L}{\varepsilon}}$ then one has*

$$\int_{E_{\frac{L}{\varepsilon}}} \frac{\partial \xi}{\partial \mathbf{n}}\left(\frac{L}{\varepsilon}, y_2\right) v(y_2) dy_2 \leq K \varepsilon^{\alpha} \|v\|_{W^{\frac{1}{2},2}_{0,\sigma}(\partial \Pi_{\frac{L}{\varepsilon}})}$$

Proof The function v given in the hypotheses belongs to the adequate spaces in order to apply Proposition 3, thus there exists a lift $R(v) \in W_0^{1,2}(\Pi_{\frac{L}{\varepsilon}})$ s.t. $R(v) = v$ on $\partial \Pi_{\frac{L}{\varepsilon}}$. Because ξ is harmonic and belongs to $W_0^{1,2}(\Pi)$, for any $\varphi \in \partial(\overline{\Pi_{\frac{L}{\varepsilon}}})$ and $\varphi_{|B_{\frac{L}{\varepsilon}}} = 0$, one writes the variational form:

$$\int_{\Pi_{\frac{L}{\varepsilon}}} \nabla\xi \cdot \nabla\varphi dy = \int_{\partial\Pi_{\frac{L}{\varepsilon}}} \frac{\partial \xi}{\partial \mathbf{n}} \varphi d\sigma(y) = \int_{E_{\frac{L}{\varepsilon}}} \frac{\partial \xi}{\partial \mathbf{n}} \varphi dy_2$$

Then by density and continuity arguments one extends this formula to every test functions in $\varphi \in W_{0,\sigma}^{1,2}(\Pi_{\frac{L}{\varepsilon}})$ such that $\varphi = 0$ on $B_{\frac{L}{\varepsilon}}$. As the specific lift $R(v)$ belongs to this space one has

$$\begin{aligned}\int_{E_{\frac{L}{\varepsilon}}} \frac{\partial \xi}{\partial \mathbf{n}} v dy_2 = \int_{\Pi_{\frac{L}{\varepsilon}}} \nabla\xi \nabla R(v) dy &\le \left(\sup_{\Pi_{\frac{L}{\varepsilon}}} \frac{1}{\varrho^{2\alpha}} \int_{\Pi_l} |\nabla \xi|^2 \varrho^{2\alpha} dy \right)^{\frac{1}{2}} \|\nabla R(v)\|_{L^2(\Pi_{\frac{L}{\varepsilon}})} \\ &\le K\varepsilon^\alpha \|\xi\|_{W_\alpha^{1,2}(\Pi_{\frac{L}{\varepsilon}})} \|\nabla R(v)\|_{L^2(\Pi_{\frac{L}{\varepsilon}})} \le K'\varepsilon^\alpha \|v\|_{W_{0,\sigma}^{\frac{1}{2},2}(\partial\Pi_{\frac{L}{\varepsilon}})}\end{aligned}$$

which ends the proof. □

4.2 Test Functions: From Macro to Micro and Vice-Versa

We suppose that $v \in H_D^1(\Omega^\varepsilon) := \{u \in H^1(\Omega^\varepsilon), u = 0 \text{ on } \Gamma^\varepsilon \cup \Gamma^1\}$ then $\gamma(v) \in H^{\frac{1}{2}}(\partial\Omega^\varepsilon)$ which implies that $v \in H^{\frac{1}{2}}(\Gamma_{\text{in}} \cup \Gamma_{\text{out}})$ and that for any corner

$$\int_0^\delta |v(x(t))|^2 \frac{dt}{t} < \infty,$$

where $x(t) \in \Gamma_{\text{in}} \cup \Gamma_{\text{out}}$ is a mapping of the neighborhood of the corners. To the trace of v on Γ_{in} or Γ_{out}, we associate a trace of a function defined on $\partial\Pi_{\frac{L}{\varepsilon}}$ which is zero on $B_{\frac{L}{\varepsilon}}$ s.t.

$$\tilde{v}\left(\frac{L}{\varepsilon}, y_2\right) := v(0, \varepsilon y_2) = v(0, x_2), \forall x_2 \in [\varepsilon f(0), 1] \text{ and } \tilde{v}\left(\frac{L}{\varepsilon}, y_2\right) := 0, y_2 > \frac{1}{\varepsilon},$$

then one has the following connexion between the macroscopic trace norm and the microscopic weighted one.

Proposition 5 *Under the hypotheses above on functions v and $\tilde{v}$,*

$$\|v\|_{H^{\frac{1}{2}}(\Gamma_{\text{in}} \cup \Gamma^\varepsilon \cup \Gamma^1)} \sim \|\tilde{v}\|_{W_{0,\sigma}^{\frac{1}{2},2}(\partial\Pi_{\frac{L}{\varepsilon}})},$$

if $v = 0$ *on* $\Gamma^\varepsilon \cup \Gamma^1$ *(resp.* $\tilde{v} = 0$ *on* $B_{\frac{L}{\varepsilon}}$*).*

Proof Thanks to the change of variables $x_2 = \varepsilon y_2$ we have that

$$\begin{aligned}\int_{\varepsilon f(0)}^{1} v^2(0, x_2) dx_2 &= \varepsilon \int_{f(0)}^{\frac{1}{\varepsilon}} \tilde{v}^2 \left(\frac{L}{\varepsilon}, y_2\right) dy_2 \\ &\leq K\varepsilon \sup_{E_{\frac{L}{\varepsilon}}} (1+\sigma^2)^{\frac{1}{2}} \int_{E_{\frac{L}{\varepsilon}}} \frac{\tilde{v}^2}{(1+\sigma^2)^{\frac{1}{2}}} dy_2, \\ &\leq K\varepsilon \frac{L}{\varepsilon} \|\tilde{v}\|^2_{W^{\frac{1}{2},2}_{0,\sigma}(\partial\Pi_{\frac{L}{\varepsilon}})}.\end{aligned}$$

Conversely

$$\begin{aligned}\int_{E_{\frac{L}{\varepsilon}}} \frac{\tilde{v}^2}{(1+\sigma^2)^{\frac{1}{2}}} dy_2 = \int_{f(0)}^{\frac{1}{\varepsilon}} \frac{\tilde{v}^2}{(1+\sigma^2)^{\frac{1}{2}}} dy_2 \leq \sup_{E_{\frac{L}{\varepsilon}}} \frac{1}{(1+\sigma^2)^{\frac{1}{2}}} \int_{f(0)}^{\frac{1}{\varepsilon}} \tilde{v}^2 dy_2 \\ \leq K\varepsilon \|\tilde{v}\|^2_{L^2(f(0),\frac{1}{\varepsilon})} = K\|v\|^2_{L^2(\Gamma_{\text{in}})}.\end{aligned}$$

For the semi-norm the same change of variable provides an equality due to the homogeneity in ε i.e.

$$|v|^2_{H^{\frac{1}{2}}(\Gamma_{\text{in}})} = \int\int_{\Gamma^2_{\text{out}}} \frac{|v(x_2) - v(x_2)|^2}{|x_2 - x_2'|^2} dx_2 dx_2' = |\tilde{v}|^2_{W^{\frac{1}{2},2}_{0,\sigma}(E_{\frac{L}{\varepsilon}})}$$

□

Remark 2 We insist on the fact that one can associate traces of v either from Γ_{in} or Γ_{out} to $\tilde{v}$, the weight that one gains in the microscopic norm comes from the scaling from macro to micro and not from the vertical position of the macroscopic interface wrt the origin of the domain Ω^ε.

5 A New Proof of Convergence for Standard Averaged Wall Laws

5.1 *The Full First Order Boundary Layer Approximation: Error Estimates*

The periodic boundary layer approximations given in (12) introduce some microscopic oscillations on the inlet and outlet boundaries $\Gamma_{in} \cup \Gamma_{out}$. We define a new full boundary layer approximation

$$u_\varepsilon^{1,\infty} = u^1 + \varepsilon \frac{\partial u^1}{\partial x_2}(x_1, 0) \left(\beta - \overline{\beta} - \xi_{\text{in}} - \xi_{\text{out}}\right) \left(\frac{x}{\varepsilon}\right) \tag{18}$$

where we define

$$\xi_{\mathrm{in}}\left(\frac{x}{\varepsilon}\right)=\xi\left(\frac{x}{\varepsilon}\right),\quad \xi_{\mathrm{out}}\left(\frac{x}{\varepsilon}\right)=\tilde{\xi}\left(\frac{x_1-L}{\varepsilon},\frac{x_2}{\varepsilon}\right),$$

and ξ is the solution of problem (13), and $\tilde{\xi}$ solves the symmetric problem for Γ_{out}:

$$\begin{cases} -\Delta\tilde{\xi}=0, \quad \text{in } \Pi_- := \cup_{k=1}^{\infty}\{Z^+\cup\Gamma\cup P-2\pi k e_1\} \\ \dfrac{\partial\tilde{\xi}}{\partial\mathbf{n}}=\dfrac{\partial\beta}{\partial\mathbf{n}}, \text{ on } E \\ \tilde{\xi}=0, \text{ on } B_- := \cup_{k=1}^{\infty}\{P^0-2\pi k e_1\} \end{cases}$$

Every result shown for ξ in sections above holds equally for $\tilde{\xi}$. One easily checks that

$$\left.\frac{\partial\xi_{\mathrm{in}}}{\partial\mathbf{n}}\right|_{\Gamma_{\mathrm{out}}}=\frac{1}{\varepsilon}\frac{\partial\xi}{\partial\mathbf{n}}\left(\frac{L}{\varepsilon},\frac{x_2}{\varepsilon}\right) \text{ and } \frac{\partial\xi_{\mathrm{out}}}{\partial\mathbf{n}}|_{\Gamma_{\mathrm{in}}}=\frac{1}{\varepsilon}\frac{\partial\tilde{\xi}}{\partial\mathbf{n}}\left(-\frac{L}{\varepsilon},\frac{x_2}{\varepsilon}\right)$$

We estimate the error of this new boundary layer approximation. We denote $r_\varepsilon^{1,\infty}:=u^\varepsilon-u_\varepsilon^{1,\infty}$, it solves

$$\begin{cases} -\Delta r_\varepsilon^{1,\infty}=C\chi_{[\Omega^\varepsilon\setminus\Omega^0]}, \text{ on } \Omega^\varepsilon, \\ \dfrac{\partial r_\varepsilon}{\partial\mathbf{n}}^{1,\infty}=\dfrac{\partial\xi}{\partial\mathbf{n}}\left(\dfrac{L}{\varepsilon},\dfrac{x_2}{\varepsilon}\right) \text{ on } \Gamma_{\mathrm{out}},\ \dfrac{\partial r_\varepsilon}{\partial\mathbf{n}}^{1,\infty}=\dfrac{\partial\tilde{\xi}}{\partial\mathbf{n}}\left(\dfrac{L}{\varepsilon},\dfrac{x_2}{\varepsilon}\right) \text{ on } \Gamma_{\mathrm{in}}, \\ r_\varepsilon^{1,\infty}=\varepsilon\dfrac{\partial u^1}{\partial x_2}(x_1,0)\left(\beta-\overline{\beta}-\xi_{\mathrm{in}}-\xi_{\mathrm{out}}\right)\left(\dfrac{x_1}{\varepsilon},\dfrac{1}{\varepsilon}\right)=:b\left(\dfrac{x_1}{\varepsilon},\dfrac{1}{\varepsilon}\right) \text{ on } \Gamma^1, \\ r_\varepsilon^{1,\infty}=0, \text{ on } \Gamma^\varepsilon \end{cases} \tag{19}$$

As $u_\varepsilon^{1,\infty}$ is only a first order approximation, a second order error remains in $\Omega^\varepsilon\setminus\Omega^0$. This explains the constant source term on the rhs of the first equation in the system above. We then have

Theorem 3 *Under the hypotheses of Theorem 1, $r_\varepsilon^{1,\infty}$ satisfies*

$$\left\|r_\varepsilon^{1,\infty}\right\|_{H^1(\Omega^\varepsilon)}\leq\varepsilon$$

Proof We separate various sources of errors, we set r^1 the solution of the Neumann part of the errors, it solves:

$$\begin{cases} -\Delta r_1=0, \text{ in } \Omega^\varepsilon, \\ \dfrac{\partial r_1}{\partial\mathbf{n}}=\dfrac{\partial\xi}{\partial\mathbf{n}}\left(\dfrac{L}{\varepsilon},\dfrac{x_2}{\varepsilon}\right) \text{ on } \Gamma_{\mathrm{out}},\ \dfrac{\partial r_1}{\partial\mathbf{n}}=\dfrac{\partial\tilde{\xi}}{\partial\mathbf{n}}\left(\dfrac{L}{\varepsilon},\dfrac{x_2}{\varepsilon}\right) \text{ on } \Gamma_{in}, \\ r_1=0 \quad \text{on } \Gamma^\varepsilon\cup\Gamma^1, \end{cases} \tag{20}$$

then the rest r_2 satisfies

$$\begin{cases} -\Delta r_2 = C\chi_{[\Omega^\varepsilon \setminus \Omega^0]}, \text{ in } \Omega^\varepsilon, \\ \dfrac{\partial r_2}{\partial \mathbf{n}} = 0 \text{ on } \Gamma_{in} \cup \Gamma_{out}, \\ r_2 = b\left(\dfrac{x_1}{\varepsilon}, \dfrac{1}{\varepsilon}\right) \quad \text{ on } \Gamma^1, r_2 = 0 \text{ on } \Gamma^\varepsilon, \end{cases} \tag{21}$$

which is the Dirichlet part of the errors and should be evaluated in a second step thanks to appropriate extensions and lifts.

5.1.1 The Neumann Part

The variational form of the problem (20) reads

$$\int_{\Omega^\varepsilon} \nabla r_1 \cdot \nabla v \, dx = \int_{\Gamma_{\text{out}}} \frac{\partial r_1}{\partial \mathbf{n}} \gamma(v) dx_2, \quad \forall v \in H^1_D(\Omega^\varepsilon),$$

dividing this expression by $\|\nabla v\|_{L^2(\Omega^\varepsilon)}$ we first obtain the equivalence:

$$\sup_{v \in H^1_D(\Omega^\varepsilon)} \frac{\int_{\Omega^\varepsilon} \nabla r_1 \cdot \nabla v \, dx}{\|\nabla v\|_{L^2(\Omega^\varepsilon)}} \equiv \|\nabla r_1\|_{L^2(\Omega^\varepsilon)}.$$

Indeed, by Cauchy-Schwartz one has easily that the L^2 norm is greater than the supremum while a specific choice of $v = r_1$ gives the reverse estimate. Thanks to this, one has

$$\|\nabla r_1\|_{L^2(\Omega^\varepsilon)} = \sup_{v \in H^1_D(\Omega^\varepsilon)} \frac{\int_{\Gamma_{\text{out}}} \frac{\partial r_1}{\partial \mathbf{n}} \gamma(v) dx_2}{\|\nabla v\|_{L^2(\Omega^\varepsilon)}}.$$

We underline that we kept the properties of the traces of $H^1_D(\Omega^\varepsilon)$ functions inside the sup that we aim to evaluate. This norm is lower that the simple $H^{-\frac{1}{2}}(\Gamma_{\text{out}})$ which authorizes different behaviors of test functions near the corners of Γ_{out} ([8], p 43, Theorem 1.5.2.3).

Now the integral in the rhs of the last expression reads in fact :

$$\int_{\Gamma_{\text{out}}} \frac{\partial r_1}{\partial \mathbf{n}} \gamma(v) dx_2 = \int_{\Gamma_{\text{out}}} \frac{\partial \xi}{\partial \mathbf{n}} \left(\frac{L}{\varepsilon}, \frac{x_2}{\varepsilon}\right) \gamma(v) dx_2 = \varepsilon \int_{f(0)}^{\frac{1}{\varepsilon}} \frac{\partial \xi}{\partial \mathbf{n}} \left(\frac{L}{\varepsilon}, y_2\right) \gamma(\tilde{v}) dy_2,$$

where we constructed $\tilde{v}$ as in Sect. 4.2 i.e. $\tilde{v}$ has the same trace as v but $\tilde{v}$ is expressed as a microscopic trace function. Thanks to Proposition 5 the corresponding microscopic trace $\tilde{v}$ belongs to $W^{\frac{1}{2},2}_{0,\sigma}(\partial \Pi_{\frac{L}{\varepsilon}})$ and Propositions 4 and 5 give that

$$\int_{f(0)}^{\frac{1}{\varepsilon}} \frac{\partial \xi}{\partial \mathbf{n}} \left(\frac{L}{\varepsilon}, y_2 \right) \gamma(\tilde{v}) dy_2 \leq \varepsilon^{\alpha} \|\tilde{v}\|_{W_{0,\sigma}^{\frac{1}{2},2}(\partial \Pi_{\frac{L}{\varepsilon}})}$$
$$\leq K \varepsilon^{\alpha} \|v\|_{H^{\frac{1}{2}}(\partial \Omega^{\varepsilon})} \leq K' \varepsilon^{\alpha} \|v\|_{H^1(\Omega^{\varepsilon})}.$$

The same analysis and convergence rates hold on Γ_{in} with the normal derivative of ξ_{out}. All together one obtains

$$\|\nabla r_1\|_{L^2(\Omega^{\varepsilon})} \leq \varepsilon^{1+\alpha}.$$

5.1.2 The Dirichlet Part

We should lift b, the non homogeneous Dirichlet boundary conditions on Γ^1 defined in (19), so we set

$$\varsigma := b\left(\frac{x_1}{\varepsilon}, \frac{1}{\varepsilon} \right) x_2^2 \chi_{[\Omega^0]}, \text{ and } \tilde{r}_2 := r_2 - \varsigma.$$

Standard *a priori* estimates give

$$\|\nabla \tilde{r}_2\|_{L^2(\Omega^{\varepsilon})} \leq \|\nabla \varsigma\|_{L^2(\Omega^{\varepsilon})} + \varepsilon,$$

where the ε in the last rhs comes when estimating the constant source term C localized in $\Omega^{\varepsilon} \setminus \Omega^0$, indeed :

$$(C, v)_{\Omega^{\varepsilon}\setminus\Omega^0} \leq \|C\|_{L^2(\Omega^{\varepsilon}\setminus\Omega^0)} \|v\|_{L^2(\Omega^{\varepsilon}\setminus\Omega^0)} \leq \sqrt{\varepsilon} \|C\|_{L^2(\Omega^{\varepsilon}\setminus\Omega^0)} \|\nabla v\|_{L^2(\Omega^{\varepsilon}\setminus\Omega^0)}$$
$$\leq \varepsilon C \|\nabla v\|_{L^2(\Omega^{\varepsilon})}$$

thanks to a Poincaré inequality in the sub-layer. Hereafter we estimate the gradient of the lift,

$$\begin{aligned}
\|\nabla \varsigma\|_{L^2(\Omega^{\varepsilon})} &\leq \varepsilon K \left\| \beta\left(\frac{\cdot}{\varepsilon}, \frac{1}{\varepsilon} \right) - \overline{\beta} \right\|_{L^2(\Gamma^1)} + K \left\| \partial_{x_1} \beta\left(\frac{\cdot}{\varepsilon}, \frac{1}{\varepsilon} \right) \right\|_{L^2(\Gamma^1)} \\
&\quad + \varepsilon \|\xi_{\text{in}}\|_{L^2(\Gamma^1)} + \varepsilon \left\| \partial_{x_1} \xi_{\text{in}} \right\|_{L^2(\Gamma^1)} + \varepsilon \|\xi_{\text{out}}\|_{L^2(\Gamma^1)} + \varepsilon \left\| \partial_{x_1} \xi_{\text{out}} \right\|_{L^2(\Gamma^1)} \\
&\leq K \varepsilon^{\frac{3}{2}} + 2 \left[\varepsilon \left\| \xi\left(\frac{\cdot}{\varepsilon}, \frac{1}{\varepsilon} \right) \right\|_{L^2(\Gamma^1)} + \left\| \frac{\partial \xi}{\partial y_1} \left(\frac{\cdot}{\varepsilon}, \frac{1}{\varepsilon} \right) \right\|_{L^2(\Gamma^1)} \right] \\
&\leq K \left[\varepsilon^{\frac{3}{2}} + \varepsilon^{2 - \frac{1}{2M}} + \varepsilon^{1+\alpha} \right] \leq K \varepsilon^{1+\alpha}
\end{aligned}$$

where we used the second estimate of Theorem 2 describing the decay properties of ξ. This ends the proof: the main error is still made when linearizing the Poiseuille profile in $\Omega^{\varepsilon} \setminus \Omega^0$. As $r_{\varepsilon}^{1,\infty} := r_1 + r_2$ one gets the desired estimate. □

Here comes the error estimate in the L^2 norm that add approximately an $\sqrt{\varepsilon}$ factor to the *a priori* estimates above.

Theorem 4 *Under the hypotheses of Theorem 1, $r_\varepsilon^{1,\infty}$, the solution of system* (19) *satisfies*

$$\left\| r_\varepsilon^{1,\infty} \right\|_{L^2(\Omega^0)} \le K\varepsilon^{1+\alpha},$$

where the constant K is independent on ε and $\alpha < \sqrt{2}/\pi \sim 0.45$.

Proof We define v a regular solution on the "smooth" domain Ω^0 (in the sense: not rough, in particular, Ω^0 is a rectangle) of the problem

$$\begin{cases} -\Delta v = F, \text{ in } \Omega^0, \\ \dfrac{\partial v}{\partial \mathbf{n}} = 0, \text{ on } {\Gamma_{\text{in}}}' \cup \Gamma'_{\text{out}} \\ v = 0, \text{ on } \Gamma^0 \cup \Gamma^1 \end{cases}$$

where the function F is in $L^2(\Omega^0)$. Thanks to [8] Theorem 4.3.1.4 p. 198, one has that there are no singularities near the corners i.e. $v \in H^2(\Omega^0) \cap H^1_D(\Omega^0)$ and

$$\|v\|_{H^2(\Omega^0)} \le K\|F\|_{L^2(\Omega^0)}.$$

Testing $r_\varepsilon^{1,\infty}$ against F, one gets

$$(r_\varepsilon^{1,\infty}, F)_{\Omega^0} = \left\langle \frac{\partial r_\varepsilon^{1,\infty}}{\partial \mathbf{n}}, v \right\rangle - \left(r_\varepsilon^{1,\infty}, \frac{\partial v}{\partial \mathbf{n}} \right)_{\Gamma^1 \cup \Gamma^\varepsilon}$$

where the brackets stand for the duality pairing between $H^{-1}({\Gamma_{\text{in}}}' \cup \Gamma'_{\text{out}})$ and $H^1_0({\Gamma_{\text{in}}}' \cup \Gamma'_{\text{out}})$, whereas the left bracket denotes the standard $L^2(\Gamma^0 \cup \Gamma^1)$ scalar product. This leads to write :

$$\left\| r_\varepsilon^{1,\infty} \right\|_{L^2(\Omega^0)} \le \left\| \frac{\partial r_\varepsilon^{1,\infty}}{\partial \mathbf{n}} \right\|_{H^{-1}({\Gamma_{\text{in}}}' \cup \Gamma'_{\text{out}})} + \left\| r_\varepsilon^{1,\infty} \right\|_{L^2(\Gamma^0 \cup \Gamma^1)} \quad =: I_1 + I_2$$

the latter term of the rhs is classically estimated through Poincaré on the sublayer and the *a priori* estimates above for the Γ^0 part :

$$\left\| r_\varepsilon^{1,\infty} \right\|_{L^2(\Gamma^0)} \le \sqrt{\varepsilon} \left\| r_\varepsilon^{1,\infty} \right\|_{H^1(\Omega^\varepsilon \setminus \Omega^0)} \le \sqrt{\varepsilon} \left\| r_\varepsilon^{1,\infty} \right\|_{H^1(\Omega^\varepsilon)} \le \varepsilon^{\frac{3}{2}}.$$

On Γ^1 there is an exponentially small contribution of the periodic boundary layer and an almost ε^2 term coming from the vertical correctors ξ_{in} and ξ_{out} :

$$\left\| r_\varepsilon^{1,\infty} \right\|_{L^2(\Gamma^1)} \le K\varepsilon \left\| \xi \left(\frac{\cdot}{\varepsilon}, \frac{1}{\varepsilon} \right) \right\|_{L^2(0,L)} \le \varepsilon^{2-\frac{1}{2M}}.$$

I_1 follows using the same arguments as in the proof of the *a priori* estimates. The astuteness resides in the fact that

$$I_1 \leq \sup_{v \in H_0^{\frac{1}{2}}(\Gamma_{\text{out}})} \frac{\left\langle \frac{\partial r_\varepsilon^{1,\infty}}{\partial \mathbf{n}}, v \right\rangle}{\|v\|_{H^{\frac{1}{2}}(\Gamma_{\text{out}})}} \leq K\varepsilon^{1+\alpha}$$

Indeed $H_0^1(\Gamma'_{\text{out}})$ functions when extended by zero on Γ_{out} are a particular subset of $H^{\frac{1}{2}}(\Gamma_{\text{out}})$ functions vanishing on $\partial\Gamma_{\text{out}}$. At this point one uses the same estimates as in the previous proof to obtain the last term in the rhs. □

5.2 The Standard Averaged Wall Law: New Error Estimates

We use the full boundary layer approximation above as an intermediate step to prove error estimates for the wall law. We denote $r_\varepsilon^1 := u^\varepsilon - u^1$.

Theorem 5 *Under the hypotheses of Theorem 1 , one has*

$$\|r_\varepsilon^1\|_{L^2(\Omega^0)} \leq \varepsilon^{1+\alpha}$$

Proof We insert the full boundary layer approximation between u^ε and u^1

$$\begin{aligned} r_\varepsilon^1 &:= u^\varepsilon - u^1 = u^\varepsilon - u_\varepsilon^{1,\infty} + u_\varepsilon^{1,\infty} - u^1 \\ &= r_\varepsilon^{1,\infty} + \varepsilon \frac{\partial u^1}{\partial x_2}(x_1, 0)\left(\beta - \overline{\beta} - \xi_{\text{in}} + \xi_{\text{out}}\right)\left(\frac{x}{\varepsilon}\right) =: r_\varepsilon^{1,\infty} + \frac{\partial u^1}{\partial x_2}(x_1, 0) I_1 \end{aligned}$$

We evaluate the $L^2(\Omega^0)$ norm of I_1

$$\begin{aligned} I_1 &\leq K\left\{\varepsilon \left\|\beta\left(\frac{\cdot}{\varepsilon}\right) - \overline{\beta}\right\|_{L^2(\Omega^0)} + \varepsilon\left\|\xi\left(\frac{\cdot}{\varepsilon}\right)\right\|_{L^2(\Omega^0)}\right\} \\ &\leq K\left\{\varepsilon^{\frac{3}{2}} + \varepsilon\left\|\xi\left(\frac{\cdot}{\varepsilon}\right)\right\|_{L^2(\Omega^0)}\right\} \end{aligned}$$

while the first term is classical and the estimate comes from (5), for what concerns the second term, we use the L^∞ estimates of Theorem 2 and get

$$\begin{aligned} \int_{\Omega^0} \xi^2\left(\frac{x}{\varepsilon}\right) dx &= \varepsilon^2 \int_0^{\frac{L}{\varepsilon}} \int_0^{\frac{1}{\varepsilon}} \xi^2 dy \leq \varepsilon^2 \int_0^{\frac{L}{\varepsilon}} \int_0^{\frac{1}{\varepsilon}} \frac{1}{\varrho^{2-\frac{1}{M}}} dy \\ &\leq \varepsilon^2 \sup_{[0,\frac{L}{\varepsilon}]\times[0,\frac{1}{\varepsilon}]} \varrho^{\frac{1}{M}+\delta''} \int_{[0,\frac{L}{\varepsilon}]\times[0,\frac{1}{\varepsilon}]} \frac{1}{\varrho^{2+\delta''}} dy \leq K\varepsilon^{2-\frac{1}{M}-\delta''} \end{aligned}$$

where δ'' is a positive constant as small as desired. This ends the proof. □

6 Conclusion

In this work we established error estimates for a new boundary layer approximation and for the standard wall law with respect to the exact solution of a rough problem set with non periodic lateral boundary conditions. The final order of approximation is of $\varepsilon^{1+\alpha}$ where $1 + \alpha \sim 1.45$ which is compatible and comparable to results obtained in the periodic case (see [5, 4] and references there in).

Establishing estimates in the spirit of very weak solution [18] but in the weighted context improves the $L^2(\Omega^0)$ estimates but requires an extra amount of work not presented here. This is done in [16], we perform also a numerical validation illustrating the accuracy of our theoretical results.

Acknowledgments The authors would like to thank C. Amrouche for his advises and support, as well as S. Nazarov for fruitful discussions and clarifications. This research was partially funded by Cardiatis,[1] an industrial partner designing and commercializing metallic wired stents.

References

1. Amrouche, C., Girault, V., Giroire, J.: Weighted sobolev spaces and laplace's equation in $\mathbb{R}^n$. J. Math. Pur. Appl. **73**, 579–606 (1994)
2. Babuška, I.: Solution of interface problems by homogenization. Parts I and II. SIAM J. Math. Anal. **7**(5), 603–645 (1976)
3. Bonnetier, E., Vogelius, M.: An elliptic regularity result for a composite medium with "touching" fibers of circular cross-section. SIAM J. Math. Anal. **31**, 651–677 (2000)
4. Bresch, D., Milišić, V.: High order multi-scale wall laws: Part i, the periodic case. Accepted for publication in Quart. Appl. Math. (2008)
5. Bresch, D., Milišić, V.: Towards implicit multi-scale wall laws C.R. Math. **346** (15–16), 833–838 (2008)
6. Galdi, P.: *An Introduction to the Mathematical Theory of the NS Equations,* vol. I & II. Springer, New York (1994)
7. Gilbarg, D., Trudinger, N.S.: *Elliptic Partial Differential Equations of Second Order.* Classics in Mathematics. Springer-Verlag, Berlin (2001). Reprint of the 1998 edition
8. Grisvard, P.: *Elliptic Problems in Nonsmooth Domains*. Monographs and Studies in Mathematics, vol. 24. Pitman (Advanced Publishing Program), Boston, MA (1985)
9. Hanouzet, B.: Espaces de Sobolev avec poids application au problème de Dirichlet dans un demi espace. Rend. Sem. Mat. Univ. Padova **46**, 227–272 (1971)
10. Jäger, W., Mikelić, A.: On the interface boundary condition of Beavers, Joseph, and Saffman. SIAM J. Appl. Math. **60**(4), 1111–1127 (2000)
11. Jäger, W., Mikelić, A.: On the roughness-induced effective boundary condition for an incompressible viscous flow. J. Diff. Eqns. **170**, 96–122 (2001)
12. Kress, R.: *Linear Integral Equations.* Appl. Math. Sci., vol. 82, second edn. Springer-Verlag, New York (1999)
13. Kudrjavcev, L.D.: An imbedding theorem for a class of functions defined in the whole space or in the half-space. I. Mat. Sb. (N.S.) **69**(111), 616–639 (1966)
14. Kudrjavcev, L.D.: Imbedding theorems for classes of functions defined in the whole space or in the half-space. II. Mat. Sb. (N.S.) **70**(112), 3–35 (1966)

[1] www.cardiatis.com

15. Kufner, A.: *Weighted Sobolev Spaces.* Teubner-Texte zur Mathematik edn. BSB B. G. Teubner Verlagsgesellschaft (1980)
16. Milišić, V.: Very weak estimates for a rough Poisson-Dirichlet problem with natural vertical boundary conditions. Meth. Appl. Anal. **16**(2), 157–186 (2009)
17. Moskow, S., Vogelius, M.: First-order corrections to the homogenised eigenvalues of a periodic composite medium. A convergence proof. Proc. Roy. Soc. Edinburgh Sect. **127**(6), 1263–1299 (1997)
18. Nečas, J.: *Les Méthodes Directes en Théorie des Équations Elliptiques.* Masson et Cie, Éditeurs, Paris (1967)
19. Sánchez-Palencia, E.: *Nonhomogeneous Media and Vibration Theory.* Lecture Notes in Physics, vol. 127. Springer-Verlag, Berlin (1980)

Vortex Induced Oscillations of Cylinders at Low and Intermediate Reynolds Numbers

Roberto Camassa, Bong Jae Chung, Philip Howard, Richard McLaughlin, and Ashwin Vaidya

Abstract We study the orientational behavior of a hinged cylinder suspended in a water tunnel in the presence of an incompressible flow with Reynolds number (Re), based on particle dimensions, ranging between 100 and 6000 and non-dimensional inertia of the body(I^*) in the range 0.1–0.6. The cylinder displays four unique features, which include: steady orientation, random oscillations, periodic oscillations and autorotation. We illustrate these features displayed by the cylinder using a phase diagram which captures the observed phenomena as a function of Re and I^*. We identify critical Re and I^* to distinguish the different behaviors of the cylinders. We used the hydrogen bubble flow visualization technique to show vortex shedding structure in the cylinder's wake which results in these oscillations.

Keywords Vortex Induced Oscillation · Autorotation · Vortex Shedding

1 Introduction

This paper deals with a fundamental question of orientation of a symmetric rigid body in a fluid. The orientation behavior of cylinder, for instance, shows several transitions, depending upon the inertia of the fluid in which it is immersed and the inertia of the body. These include (i) steady state orientation, (ii) random oscillations, (iii) periodic oscillations and in some extreme cases, even (iv) autorotation.

The question of orientation bodies in fluids dates back to Kirchoff [7] who examined the dynamics of falling paper. The steady state orientation of bodies with certain classes of symmetries has been long known. A sedimenting cylinder, for instance, is known to fall with its axis of symmetry perpendicular to gravity in a Newtonian fluid when its length exceeds its diameter d. However, in the case of a disk, when the length of the cylinder is less than the diameter, the disk falls with its axis of rotation parallel to gravity. Several more recent systematic studies have experimentally, theoretically and numerically explored the steady state dynamics of

A. Vaidya (✉)
Department of Mathematics, University of North Carolina, Chapel Hill, NC 27599, USA
e-mail: avaidya@email.unc.edu

R. Rannacher, A. Sequeira (eds.), *Advances in Mathematical Fluid Mechanics*,
DOI 10.1007/978-3-642-04068-9_8,

falling bodies (see [4, 6, 8, 14] for instance) in the Stokes and low inertial regimes. The orientational dynamics becomes even more interesting in the unsteady regime, vortex shedding effects become significant and gives rise to oscillations of the body. In the context of sedimentation, several relevant studies have been conducted, both experimental and numerical to document the highly nonlinear dynamics of disk like bodies, i.e. bodies whose aspect ratios (length to diameter ratio, denoted τ) are much less than 1, which are typically represent disks or flat plates. See for instance [2, 3, 16, 19] and references therein. It is seen that a sedimenting disk or flat plate can exhibit (i) fluttering, (ii) tumbling and (iii) chaotic motions. Attempts have been made to classify these different phenomena by means of non-dimensional parameters such as particle aspect ratio, reduced inertia, Froude number, Strouhal number and Reynolds number.

The bulk of previous studies have focused upon translational motions of disks, vibrational motions of bodies or response of disks in aerodynamic flows [2, 5, 21, 19, 18]. The literature on the first two of these studies is far too vast to be discussed here. The more relevant of these studies is the last one. Willmarth et al. [19] have studied the free and forced oscillations of disks of diameters ranging from 15 cms to about 30 cms in a wind tunnel with Reynolds numbers in the range 68000–636000. The aspect ratio in these experiments were $0.014 < \tau < 0.125$. The particles were seen to oscillate periodically with increasing fluid inertia and eventually displaying autorotation at sufficiently large wind speeds. Perhaps the work that comes closest to our study is due to Mittal et al. [12] who perform some interesting two dimensional numerical simulations for uniform flow past a hinged plate which is free to rotate about its central axis and compare it to the dynamics of falling bodies. They examine the effects of varying Re and I^*. The Reynolds number is defined here as $\mathrm{Re} = \frac{U\,l}{\nu}$, where U is the centerline velocity in the absence of the body and l is the maximum of the length or diameter of the cylinder. The second non-dimensional parameter, namely the reduced inertia, is define by $I^* = \frac{I}{\varrho_f d^5}$, where I is the moment of inertia of the body with respect to the symmetry axis and ϱ_f stands for the fluid density. The Re achieved in this experiment ranges from about 100–6000 while the values of I^* typically range from 0.1 to 0.6. In the previous literature, the appearance of *autorotation* is identified in terms of critical values of Re and I^*.

Our study is carried out in a horizontal water tunnel, whereby the effects of gravity do not matter by hinging the cylinder. The advantage of this experiment is that it allows for very long observation times when compared to the case of sedimentation where a falling body is restricted by the height of the tank. We also wish to explore if, neglecting gravity and also translational motions, makes the problem under investigation any different from the free fall experiments. A rigorous quantification of the varying dynamics of the body is missing in the literature, which explores for the most part, merely qualitative aspects of the phenomena. We use a wider range of aspect ratios in our study which has not previously been examined leading us further into the three dimensional effects of vortex induced wake flows. One of our central contribution in this paper lies in the discussion of the effect of autorotation. Autorotation is a phenomena, primarily observed in aerodynamics and defined by Lugt [10] as:

... any continuous rotation of a body in a parallel flow without external sources of energy ...

Autorotation is rather well studied in aerodynamic applications, it has not been documented in the literature for three dimensional liquid flows. In this article, we fill this gap in the literature; we capture the phenomena of autorotation for symmetric, cylindrical bodies and also discuss their dependence upon τ, Re and I^*.

Our specific objectives include: (i) construction of a phase diagram to classify the particle behavior, (ii) obtaining dominant frequency of periodic oscillations and (iii) visualization of the vortex shedding structure. The paper begins with a brief description of the experimental setup and methodology. This is followed in Sect. 3 with an analysis of the particle motion and also a discussion of the wake structure. The concluding Sect. 4 summarizes the central contributions of this paper to the field of vortex induced vibrations and also briefly recounts the additional work being carried out.

It must be said at the outset that the study is still in its preliminary stages. Several questions regarding the experimental setup still need to be addressed which may contribute to errors in our observations. These include a more elaborate study of: (i) friction caused by the suspension, (ii) the pump frequency of the water tunnel, (iii) the effect of varying the tension of the suspension, (iv) flow profile in the water tunnel as a function of increasing flow velocity and (v) the disturbance to the flow in the tank due to the presence on the hydrogen bubble setup. We are continuing to address these issues currently.

2 Experimental Setup

The experimental setup consists of plastic cylinders of diameter (d) 0.635 cm and lengths ranging from 0.32 to 1.27 cms. The aspect ratio, τ, therefore ranged from 0.5 to 2.0. The cylinders were made of *ABS, Lexan and Delrin* (plastics) with densities 1.05, 1.18 and 1.4 g/cc, respectively. The cylinders were held at the center of a water tunnel (Engineering Laboratory Design Inc., Model 502) with range of flow rates between 0.1 and 1.0 fps at 0.5HP. The dimensions of the test section of the water tunnel are $6 \times 6 \times 18$ inches. The cylinder was suspended by means of a stainless steel wire of thickness 0.023 cms passing through a hole of diameter 0.04 cms at the center of the tank. The cylinder was suspended in such a way as to allow it to oscillate freely along the flow direction alone. Figure 1 shows a schematic of the general setup. The dynamics of the cylinder were recorded using a 72 mm SONY HDR FX1 camera fitted with +6 diopter zoom lens (Hoya Inc.). The operational speed of the camera was set at 30 frames per second and the resulting videos were analyzed using the Video Spot Tracker V.5.20 program [17].

Previous studies suggest that the specific motions displayed by the body depend upon the vortex shedding process in the wake of the body which is visualized using the hydrogen bubble technique. The setup involves a copper wire of diameter 0.01 cms mounted vertically at a distance of 12 cms from the cylinder as shown in Fig. 1. A copper rod was used as the anode. Four 9 V batteries in parallel were used to generate the bubbles.

3 Results

This section focuses on the analysis of the particle motion. Our analysis reveals that the cylindrical particle displays the following types of motions:

- *Steady Orientation (S)*: the particles position remains unchanged with time.
- *Oscillations (O)*: defined to represent particle motion which displays time dependent fluctuations in orientation, but not in a systematic manner. Our criterion for defining a motion as being an oscillation is that the average fluctuation with respect to time for the particle be at least 0.1 radians.
- *Periodic Oscillations (P)*: particles oscillate in a steady periodic manner.
- *Autorotation (A)*: represents particles that rotate completely (by an angle of 2π) and periodically around the axis of suspension.

Figure 2 displays some sample plots of angle versus time showing each of the cases discussed above for different I^* and Re. The plots in Fig. 2 were made based upon analysis performed on the Spot Tracker program. The program follows the motion of a dark spot marked on the body and computes the x and y coordinates of the dark spot in each frame. From this data, we can evaluate the angle versus time. The Spot Tracker analysis was applied to all the cases (i.e. recorded movies) except the steady and autorotation case. The former of these cases was not analyzed since there is no motion to speak of while focusing issues due the rapid speed of the auto rotating bodies caused difficulties in the Spot Tracker analysis.

Using the phase diagram adopted by Fields et al. [3], we create a diagram of I^* versus Re for the four different features observed in our experiments. The Fig. 3 shows the four features plotted as distinct points marked by the symbols X, filled circle, open circle and filled triangle which stand for S,O,P and A respectively. To identify clear patterns in the phase diagram, we make a contour diagram using four different color schemes to distinguish clustering of the various features (see Fig. 4). The plot shows four distinctive regions depending upon the values of Re and I^*. Our data indicates: (i) the steady behavior falls along regions of lower values Re (ii) the oscillations predominantly fall in the regions above $I^* = 0.29$ and $1800 < \text{Re} < 4000$ (and possibly larger Re corresponding to the higher I^* values), (iii) the features

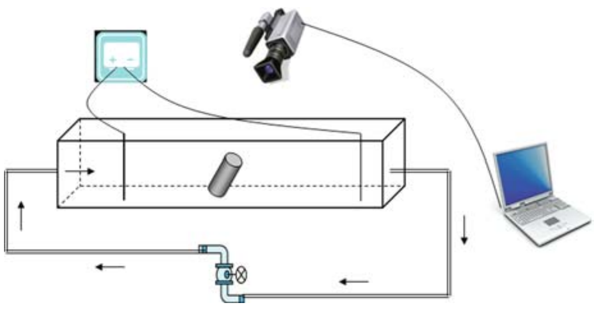

Fig. 1 A schematic of the experimental setup

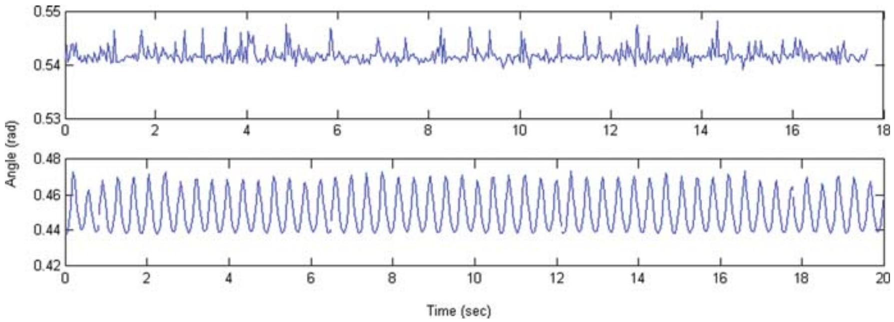

Fig. 2 Angle versus time variations showing representative sample data for the cases of (**a**) oscillation and (**b**) periodic behavior

of periodic behavior is shown to occur approximately for 1600 $<$ Re and in an expanding I^* region contained between 0.15 and 0.35 and finally, (iv) autorotation is densely packed in regions of large Re, exceeding 3000 and for some intermediate values of $0.19 < I^* < 0.29$. To characterize the patterns more clearly, we would like to have a larger range of data with higher Re. Interestingly, the particles can display periodic oscillations even at relatively low Re, as long as I^* is limited to a certain value.

Based upon Fig. 4, we can analyze how the frequency of the periodic oscillations are affected by Re and I^*. This analysis is performed by the Power Spectral Density method using the Matlab software which plots part of the power of the signal within some frequency bins. The results of this analysis are shown in the Figs. 5, 6. The frequency chosen in these plots correspond to the maximum power in the spectrum and only for particles that exhibit periodic motion. These dominant frequencies, denoted f, seem to lie in the range 0.7–5.2 Hz. In our graphs, we chose to work

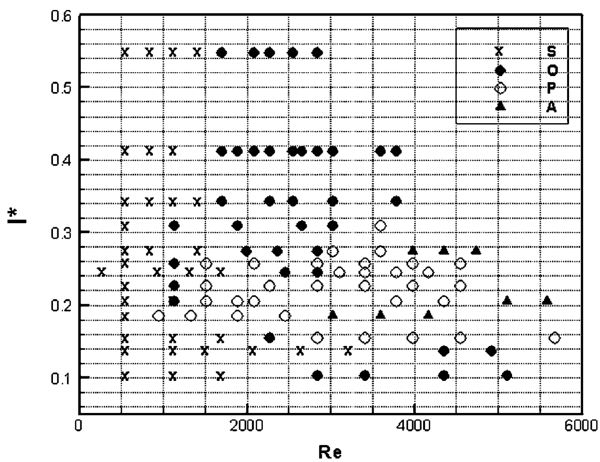

Fig. 3 A phase diagram showing where the different features displayed by the particles lie as a function of I^* and Re

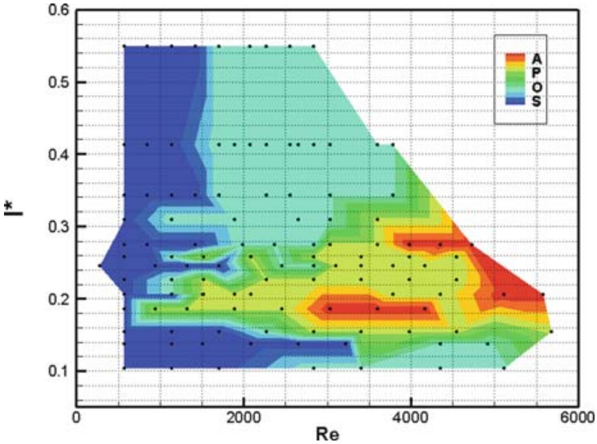

Fig. 4 A contour plot of the phase diagram showing where the different features displayed by the particles lie as a function of I^* and Re

with the non dimensional parameter, given by $\frac{fL}{U}$, which can also be interpreted as the particle Strouhal number.

The Fig. 5 shows the dimensionless frequency versus Re while the Fig. 6 shows the dimensionless frequency versus I^*. A linear fit to the non-dimensional frequency is also displayed on the plots as a dashed line but shows a very low R^2 value making it difficult to discern any explicit correlations between the frequency and Re or I^* at this stage. We need several more data at higher I^* and Re values to be able to capture any possible trends. The non dimensional frequency values in Fig. 5 for all of these cases lie between 0.03 and 0.14 for $1000 < \text{Re} < 6000$.

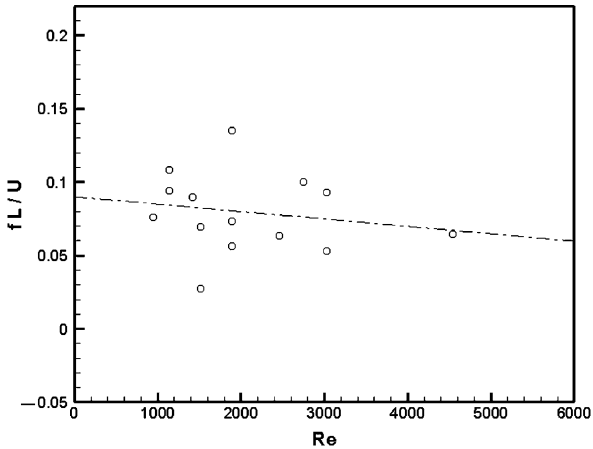

Fig. 5 The non-dimensional frequency versus Reynolds number

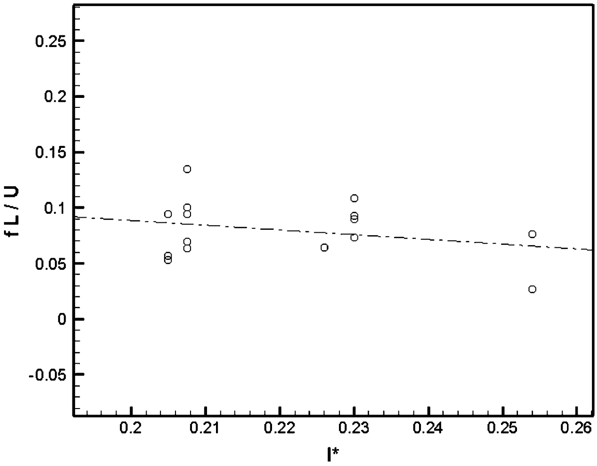

Fig. 6 The dominant non-dimensional frequency versus reduced inertia

The shedding of vortices in the wake of bodies is a very well studied problem. The classical Karman vortex patterns have been previously documented [20, 21]. It is also well established that in the case of free falling bodies (or hinged bodies as in our case), the asymmetric vortex shedding gives rise to oscillatory behavior [2, 12, 3]. The shedding behavior merits some attention although our observations in this regard remains very preliminary. The Strouhal number $Sr = \frac{fL}{U}$ is used to quantify the vortex shedding phenomena, where, f represents the frequency of the vortex shedding, L is the characteristic length which we take to be the maximum of the length or diameter of the cylinder and U is the velocity of the fluid. The dependence of Sr upon Re is well known for the case of spheres and circular cylinders [1, 13] and also known to be sensitive to the geometry of the body. In the low Re range, namely for $40 < \text{Re} < 6000$, the value of $0.17 < Sr < 0.21$.

Visualizations using hydrogen bubble were performed, both for the case of a fixed cylinder and also for a body free to oscillate, for sake of comparison. A visual comparison of the two cases is made in the Figs. 7, 8 below ($\text{Re} \approx 3000$, $I^* \approx 0.3$) for six different times. The first of these, Fig. 7 shows a sequence of images showing variations in the wake structure with time when the cylinder oscillates. Although details of the vortex shedding patterns due to the largeness of the Re and the three dimensional effects are difficult to visualize, one can clearly see the variations in the wake. In the second Fig. 8 for a fixed cylinder, the wake structure shows no dramatic changes over time in the field of view. A quantitative comparison has also been made. Using our flow visualization images, we are able to visually track the emergence of vortex patterns in the wake of a fixed cylinder and then determine its frequency. Similarly, we were, in a few cases, able to determine the vortex shedding frequency past an oscillating cylinder. Our objective in this case was to verify if the Sr number for the two cases (fixed and oscillating) was significantly different. Our estimates are summarized in the Table 1.

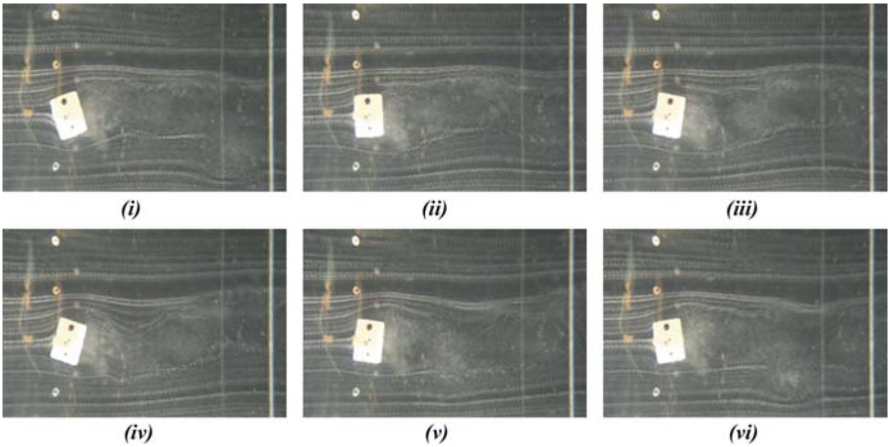

Fig. 7 Flow visualization for vortex shedding past an oscillating cylinder

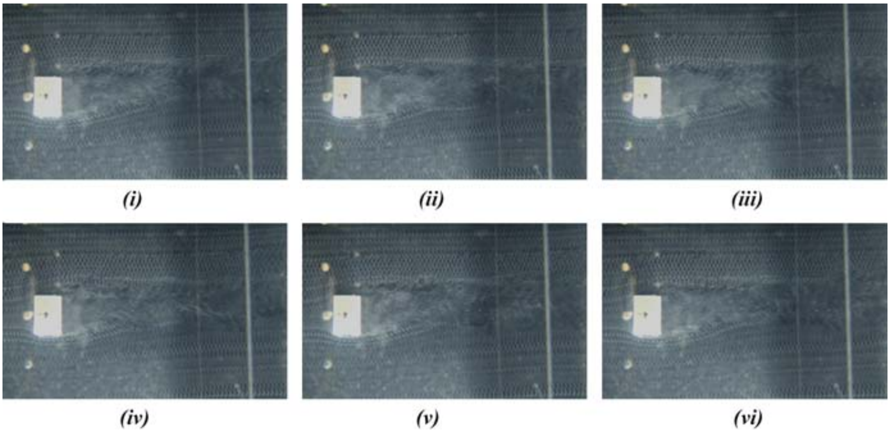

Fig. 8 Flow visualization for vortex shedding past a fixed cylinder

Our analysis thus far reveals a significant difference in the values of Sr versus Re for the case of the fixed cylinder when compared to the oscillating one. The Sr for the former case lie in the neighborhood of 0.21–0.28 as observed in the literature, however for the oscillating cylinders, the Sr is almost half of the previous values and seems to be much less sensitive to Re. Further, the Sr values, based on particle oscillation frequencies, reported in Fig. 6, lie in the same range as Sr due to the

Table 1 A comparison of Sr versus Re for the case of fixed versus oscillating cylinders

Re	568	946	1325	1514	3029	3408
Sr_{fixed}	0.21	0.25	–	0.21	0.26	0.28
Sr_{osc}	–	–	0.12	–	0.105	0.108

vortex shedding past the oscillating cylinders. To conclude this discussion, while our study of the vortex shedding process deserves further attention, there seems enough evidence to suggest that the oscillatory behavior displayed by the particles are driven by vortex shedding.

4 Discussion

Our experiments on hinged cylindrical bodies in a water tunnel reveals four different behavioral characteristics. We have characterized these orientational features of the body as a function of the Reynolds number and reduced inertia. We present a phase diagram which localizes the orientational features of the cylinders in distinct zones. Our analysis indicates that in the range explored, the transition from oscillation to autorotation is highly sensitive to the value of Re and I^*. Autorotation lies in the approximate range $0.19 < I^* < 0.29$ and for $\text{Re} > 3000$. Similarly, periodic oscillation can be said to effectively lie in some region enclosed within $\text{Re} > 1000$ and $0.15 < I^* < 0.35$. We make comparisons with the work of Willmarth et al. They report the oscillation amplitude increases with Re until the body eventually begins to auto rotate. As in our experiments (see Fig. 4), they also note that cylinders with aspect ratio in the neighborhood of $\tau = 1$, have a tendency to oscillate periodically or even auto rotate sooner than others. Our experiments also reveal that in the presence of an obstacle placed downstream and close to the particle, the cylinder has a tendency to auto rotate for values of Re and I^* at which it otherwise does not. This phenomena also merits future study.

The critical non dimensional parameters that we report here vary from those in the literature [2, 3, 11] since these studies are primarily for much smaller disks or for thin filaments. A summary of the different critical values in the literature can be found in the paper by Mittal et al. [12]. The two dimensional numerical results of Mittal et al. are performed for cylinders with $0 < \tau < 0.5$, $I^* > 0.17$ $\text{Re} < 600$ in order to keep the vortex structure essentially two dimensional. Their investigation also reveals a distinctive separation of the oscillation versus autorotation data based on some critical values of I^* and Re.

Our calculation of the Strouhal number indicates a marked difference in the values of Sr for fixed versus oscillating cylinders; Sr in the case of oscillations dropping to almost half of the fixed case. Further the ratio Sr_p/Sr_s, where Sr_p is the particle Strouhal number and Sr_s is the shedding Strouhal number is nearly 1, indicating a *lock-on* phenomena.

Our work at this stage being the only three dimensional study with aspect ratios exceeding 1 cannot be compared effectively to any other study in the literature. It needs to be pointed out that our study is marred by some drawbacks. Our phase diagram, though contains several data points, is lacking in data in regions where perhaps some effective comparisons to the literature can be made, especially for $\tau \ll 1$ and $\text{Re} > 6000$. More data for the power spectrum analysis would yield better possibilities of discerning a correlation between the oscillating frequency and

Re or I^*. Errors, frictional for instance, coming from the suspension mechanism must be reduced. Also a quantification of the flow in the tank and also the vortex shedding is needed. We provide no quantitative data on the vortex shedding mechanism at this stage. However, a quantification of the shedding frequency is currently being looked into using a constant temperature anemometer. We hope to report these results and a detailed comparison of the shedding frequency to that of the oscillating bodies in a soon to follow article. It has been pointed out [9] that bodies with sharp corners such as cylinders, display noticeably different vortex shedding patterns compared to smooth bodies. A next step would therefore to repeat these experiments for spheroidal bodies to study the effect of changing geometry. We are also carrying out three dimensional numerical simulations of this phenomena using the Chimera grid method which is based on a finite volume approach.

Acknowledgments We acknowledge the help of several folks in this project. Among them, Angele Freeman, Dr. Arvind Santhanakrishnan, Neal Johnson, Dr. Laura Miller and Vivek Menon. RMM is partially supported by NSF DMS-030868 and RC is partially supported by DMS-0509423 and NSF DMS-0620687. PH and AV are supported by an NSF Research Training Grant, RTG NSF DMS-0502266.

References

1. Aachenbach, E.: Vortex shedding from a Sphere. J. Fluid Mech., **62** (2), 209–221 (1974)
2. Belmonte, A., Eisenberg, H. and Moses, E.: From flutter to tumble: Inertial drag and Froude similarity in falling paper. Phys. Rev. Lett., **81** (2) 345–349 (1998)
3. Fields, S.B., Klaus, M., Moore, M.G. and Nori, F.: Chaotic dynamics of falling disks. Nature, **388**, 252–254 (1997)
4. Galdi, G., P.: *On the Motion of a Rigid Body in a Viscous Fluid:* A Mathematical Analysis with Applications. Handbook of Mathematical Fluid Mechanics, Elsevier Science, Amsterdam, 653–791 (2002)
5. Hover, F.S., Tvedt, H. and Triantafyllou, M.S.: Vortex induced vibrations of a cylinder with tripping wires. J. Fluid Mech., **448**, 175–195 (2001)
6. Howard, H.H., Joseph, D.D. and Fortes, A.F.: Experiments and direct simulations of fluid particle motions. Int. Video J. Eng. Res., **2**, 17–24 (1992)
7. Kirchoff, G.: Über die Bewegung enines Rotationskorpers in einer Flüssigkeit. J. Reine Ang. Math. Soc., **71**, 237–281 (1869)
8. Leal, L.G.: Particle motion in a viscous fluid. Ann. Rev. Fluid Mech., **12**, 435–476 (1980)
9. Lugt, H.: Autorotation of an elliptic cylinder about an axis perpendicular to the flow. J. Fluid Mech., **99**, 817–840 (1980)
10. Lugt, H.: Autorotation. Annu. Rev. Fluid Mech., **15**, 123–147 (1983)
11. Mittal, R., Seshadri, V. and Udaykumar, H.S.: Flutter, tumble and vortex induced oscillations. Theoret. Comput. Fluid Dynamics, **17**(3), 165–170 (2004)
12. Okajima, A.: Strouhal numbers of rectangular cylinders. J. Fluid Mech., **123**, 379–398 (1982)
13. Pan T.W., Glowinski R., and Galdi G.P.: Direct simulation of a settling ellipsoid in a Newtonian fluid. J. Comp. Appl. Math., **149**, 71–82 (2002)
14. Seshadri, V., Mittal, R. and Udaykumar, H.S.: Vortex induced oscillations of a hinged plate: a computational study. Proceedings of ASME, 4th ASME JSME Joint Fluids Engineering Conference, July 6–10 (2003)
15. Skews, B.W.: Autorotation of rectangular plates. J. Fluid Mech., **217**, 33–40 (1990)

16. Tanabe, Y. and Kaneko, K.: Behavior of falling paper, Phys. Rev. Lett., **73**(10), 1372–1376 (1994)
17. Taylor, R.M.: http://www.cs.unc.edu/cismm/download/spottracker/video_spot_ tracker.html (2005)
18. Vandenberghe, N., Zhang, J. and Childress, S.: Symmetry breaking leads to forward flapping flight. J. Fluid Mech., **506**, 147–155 (2004)
19. Williamson, C.H.K.: Vortex dynamics in the cylinder wake. Ann. Rev. Fluid Mech., **28**, 477–539 (1996)
20. Williamson, C.H.K., Goverdhan, R.: Vortex-induced vibrations. Ann. Rev. Fluid Mech., **36**, 413–455 (2004)
21. Willmarth, W.W., Hawk, N.E., Galloway, A.J. and Roos, F.W.: Aerodynamics of oscillating disks and a right-circular cylinder. J. Fluid Mech., **27**(1), 177–207 (1967)

One-dimensional Modelling of Venous Pathologies: Finite Volume and WENO Schemes

Nicola Cavallini and Vincenzo Coscia

Abstract An efficient and accurate numerical scheme, based on Finite Volumes and WENO (Weighted Essentially Non-Oscillatory) techniques, is used to implement a one-dimensional model of the venous network of the inferior limb, that includes a suitable modelling of venous valves. The model is applied to the physiological as well as to the pathological situation, with data obtained experimentally using an Echo-Color Doppler device.

Keywords One-dimensional blood flow models · Finite volume numerical methods · Phlebologic diseases

1 Introduction

The human circulatory system has become, in the last decades, the focus of a number of studies both on the modelling point of view and on the mathematical and numerical analysis of models [4, 10, 40, 11]. The physiology and the pathology of the circulatory system is very complex [32]. A significant number of vascular diseases are related to mechanical and/or fluid dynamical disfunctions. For this reason the methods of biomechanics, largely based on continuum mechanics, are used in the modelling in order to describe the main issues of the cardiovascular system and give a way to quantify physical processes governing blood and vessels motion [28].

The system build up by vessels and inside blood leads, when considered from a mechanical point of view, to a typical fluid-structure interaction problem whose analysis can be performed in different ways and at different detail levels [15, 17, 26, 18, 38].

One dimensional modelling of the vascular system has attracted a great interest as it results in a good compromise between information achievable, structure detail and computational cost [8, 35]. Integrating the velocity distribution over the vessel's cross section, introducing an empirical velocity profile and a wall constitutive law,

V. Coscia (✉)
Department of Mathematics, University of Ferrara, 44100 Ferrara, Italy
e-mail: cos@unife.it

R. Rannacher, A. Sequeira (eds.), *Advances in Mathematical Fluid Mechanics*, 147
DOI 10.1007/978-3-642-04068-9_9, © Springer-Verlag Berlin Heidelberg 2010

the coupled system of the Navier-Stokes equations and of the equations of motion of the blood vessel is reduced to a second order nonlinear hyperbolic system of partial differential equations. One of the earliest numerical implementation of this model is due to Noseda [23] which uses the characteristics method as proposed by Barnard [2]. Finite differences techniques is applied by Olufsen et al. [24] and Smith et al. [33], while finite elements integration is performed in [1, 8, 30]. Finally, Sherwin et al. [30] accurately examine the modelling of vessels branching.

Because they greatly simplify the complexity of the flow and its interaction with the walls, one-dimensional models are not able to capture the details of blood and vessel motions, details whose investigation is relevant in localized situations and pathologies along the circulatory tree. Recently, Robertson and Sequeira [29] introduced a model of the arterial tree based on the Cosserat curves that gives interesting results when benchmarked versus one-dimensional models in specific flow geometries.

The large part of the literature on the mathematical modelling of the circulatory system concerns the arterial side of it. On the other hand the venous system has its own specificities that force the modelling to stress more on the gross flow properties as they are very well described in the one-dimensional approach [10, 36]. In the systemic circulation, deoxygenated blood from capillaries is returned to the heart's right atrium via the venous tree through collecting venules to small veins to the large veins, following the directions going from superficial to deep and from distal to proximal circulation. With the exception of the largest veins (vena cava, great pulmonary veins) and the smallest venules, veins have valves whose primary function is to facilitate the return of blood to the heart and prevent backflow. From the structural point of view, veins have the same histological components as arteries, but the different content and thickness (veins' walls are much thinner than arteries' ones) resulting in a high venous compliance. Veins are rich in smooth muscle, which responds to to neural and mechanical stimuli. This is very important in physiology, because the veins contain 75% or more of the total blood volume [9]. Because they are thin walled and have a low elastic modulus, veins are very sensitive to variations of transmural pressure (they are highly collapsible). Many interesting phenomena, as well as many common diseases, occur in venous blood flow because of this. In particular, backflows in some vein of the inferior limbs (typically saphenous or collateral veins) due to valves incontinence result, in the clinical practice, in a symptom that can evolve toward diseases such as varicose veins and, more serious, varicose ulcers. Usually surgeons, using their clinical experience, occlude or remove one or more veins in such a way to restore the overall right superficial-deep and low-high flow direction [3].

Aims of a clinically-oriented modelling of the venous tree of the inferior limb (say) can be summarized as follows:

- design a venous system's map of the circulatory district based on anatomic images (CT, NMR and similar);
- choose a mathematical model of the system that is able to describe the main features (flow rates, pressure waves) of the flow;

- design a numerical scheme that permits to solve the model efficiently and fast;
- acquire, for each single patient, the necessary clinical data and introduce them into the model;
- run numerically the model and optimize with respect to the occlusion of different branches in view of a prescribed "target" function (the right flow direction, for example).

In this paper we concentrate, in particular, on the third of the above mentioned steps. A Finite Volume scheme, whose application is well established in the numerical treatment of gas dynamics and shallow water equations [6], is adopted in the integration of a one-dimensional blood flow model. In particular, we show how it is possible to introduce in the model, in a simple but rigorous way, the presence of valves and how to take account of their possible malfunction. The paper is organized as follows. In Sect. 1 we derive a nonlinear hyperbolic one-dimensional model for the blood motion integrating over the the vessel section and using a suitable flow-wall interaction as well as a constitutive relation for the wall. In Sect. 2, following[7], we introduce the numerical scheme to solve the model's equations. Boundary cell fluxes are approximated by the Lax-Friedrichs formulation and boundary cell values are reconstructed using WENO (Weighted Essentially Non-Oscillatory) approximations. The time integration is performed by a strong stability preserving Runge-Kutta five steps scheme, fourth order accurate. The numerical integration is completed with a suitable treatment of the source terms and by the introduction of proper boundary conditions. The source term is integrated by a standard Gauss-Lobatto quadrature, while boundary conditions are accurately described and a non-reflecting boundary flux function is formulated. In Sect. 3 we give an accuracy study of the scheme and apply the model to a venous network of the thigh. It is worth to stress that, even though we consider a small portion of the whole thigh's venous tree the approach is completely generalizable and the data we use in the model are obtained experimentally using the diagnostic facilities available in any good phlebology department or private office. Finally, in Sect. 4 we draw some conclusions and suggest possible research perspectives.

2 Mathematical Modelling

A simple, largely used mathematical modelling of blood flow in the vascular system [2, 33, 8, 1] is based on the two-dimensional Navier-Stokes equations in a cylindrical, axially symmetric geometry [33]. Considering the coordinate system (x, r), where the x is the abscissa along the vessel's axis and r is the vessel's radius, we write the two momentum equations:

$$\frac{\partial V_x}{\partial t} + V_r \frac{\partial V_x}{\partial r} + V_x \frac{\partial V_x}{\partial x} + \frac{1}{\varrho}\frac{\partial p}{\partial x} = \nu \left[\frac{\partial^2 V_x}{\partial r^2} + \frac{1}{r}\frac{\partial V_x}{\partial r} + \frac{\partial^2 V_x}{\partial x^2} \right], \tag{1}$$

$$\frac{\partial V_r}{\partial t} + V_r \frac{\partial V_r}{\partial r} + V_x \frac{\partial V_r}{\partial x} + \frac{1}{\varrho}\frac{\partial p}{\partial r} = \nu \left[\frac{\partial^2 V_r}{\partial r^2} + \frac{1}{r}\frac{\partial V_r}{\partial r} - \frac{V_r}{r^2} + \frac{\partial^2 V_r}{\partial x^2} \right], \tag{2}$$

where V_x and V_r are the axial and radial components of the velocity, respectively, p is the pressure (including the gravity force potential), ϱ is the blood density (assumed constant) and ν the kinematic viscosity. The equations above are completed by the mass conservation equation:

$$\frac{\partial V_x}{\partial x} + \frac{1}{r}\frac{\partial (r V_r)}{\partial r} = 0. \tag{3}$$

Following [2], we write this system in non-dimensional form. If V_0 and U_0 represent typical velocities in the axial and radial directions and R_0 a representative vessel's radius, a characteristic length L_0 is defined as:

$$L_0 = R_0 \frac{U_0}{V_0}.$$

As a consequence, we get the full set of non-dimensional quantities:

$$\tilde{r} = \frac{r}{R_0},\ \tilde{x} = \frac{x}{L_0},\ \tilde{t} = \frac{tU_0}{L_0},\ \tilde{V}_x = \frac{V_x}{U_0},\ \tilde{V}_r = \frac{V_r}{V_0},\ \tilde{p} = \frac{p}{\varrho U_0^2}.$$

The maximum value of U_0 coincide with the radial velocity of the wall. Thus, unless the latter is very flexible, the non-dimensional parameter $\varepsilon = \frac{U_0}{V_0}$ is small [2]. Under this assumption, retaining only terms of order ε, Eq. (1) reads:

$$\frac{\partial}{\partial \tilde{t}}(\tilde{r}\tilde{V}_x) + \frac{\partial}{\partial \tilde{r}}(\tilde{r}\tilde{V}_x\tilde{V}_r) + \frac{\partial}{\partial \tilde{x}}(\tilde{r}\tilde{V}_x^2) + \frac{\partial \tilde{p}}{\partial \tilde{x}} = \frac{\nu L_0}{V_0 R_0^2}\left[\frac{\partial}{\partial \tilde{r}}\left(\tilde{r}\frac{\partial \tilde{V}_x}{\partial \tilde{r}}\right)\right],$$

while Eq. (2) becomes:

$$\frac{\partial \tilde{p}}{\partial \tilde{r}} = 0,$$

so that the pressure is constant across the vessel's 3. In order to write the previous equations in terms of averaged quantities, the mean velocity:

$$U = \frac{1}{A}\int_A 2\pi r V_x \,\mathrm{d}r, \tag{4}$$

is introduced. Together with the stream line condition for the wall, we write the continuity and the first momentum equation as a system of partial differential equations in dimensional form:

$$\frac{\partial A}{\partial t} + \frac{\partial q}{\partial x} = 0 \tag{5}$$

$$\frac{\partial q}{\partial t} + \frac{\partial}{\partial x}\left(\hat{\alpha}\frac{q^2}{A}\right) + \frac{A}{\varrho}\frac{\partial p}{\partial x} = 2\pi\nu R\left[\frac{\partial V_x}{\partial r}\right]_{r=R}, \tag{6}$$

where $q = UA$ and $\hat{\alpha}$ is the momentum correction coefficient:

$$\hat{\alpha} = \frac{1}{A \cdot U^2} \int_0^R 2\pi r V_x^2 \, \mathrm{d}r.$$

The value $\hat{\alpha} = 1$ is a common choice (see for example [8]). Equations (5) and (6) represent the undefined (without initial and boundary conditions) one-dimensional model for blood flow in large vessels and is frequently adopted in literature [2, 23, 24, 33, 8, 38, 1].

In order to close the system, a wall model and an assumption on the velocity profile are needed. To express the interaction between the fluid an the vessel structure we use a simple Laplace's law for the transmural pressure $p(x,t)$, with a Poisson's coefficient equal to 0.5, as mentioned in [24]:

$$p(x,t) - p_0 = \frac{4}{3}\frac{Eh}{r_0}\left(1 - \sqrt{\frac{A_0}{A}}\right), \tag{7}$$

where E represents the Young modulus, h the wall thickness, r_0, A_0 and p_0 the radius, the section area and pressure in diastolic condition, respectively. These coefficients allow to define the quantity $s_t = \frac{4}{3}\frac{Eh}{r_0}$. The velocity profile frequently used (see e.g. [1, 8, 33]) is:

$$V_x = \frac{\gamma + 2}{\gamma} U \left[1 - \left(\frac{r}{R}\right)^{\gamma}\right], \tag{8}$$

with $\gamma = 9$. Equations (7) and (8) are used to write (6) in conservative form:

$$\frac{\partial q}{\partial t} + \frac{\partial}{\partial x}\left(\frac{q^2}{A} + k\sqrt{A}\right) = -2\pi\nu(\gamma+2)U - \frac{1}{\varrho}A\left(1 - 2\sqrt{\frac{A_0}{A}}\right)\frac{\partial s_t}{\partial x} + \frac{2s_t}{\varrho}\sqrt{A}\,\frac{\partial\sqrt{A_0}}{\partial x} \tag{9}$$

where:

$$k = \frac{s_t}{\varrho}\sqrt{A_0}.$$

Equations (5) and (9) give the system of hyperbolic equations we shall study. It can be written in vector form as:

$$\mathbf{U}_t + \mathbf{F}(\mathbf{U})_x = \mathbf{S}(\mathbf{U}) \tag{10}$$

where $\mathbf{U} = [A, q]^T$ represents the conserved variables,

$$\mathbf{F}(\mathbf{U}) = [q, q^2/A + k\sqrt{A}]^T,$$

the corresponding fluxes and

$$\mathbf{S}(\mathbf{U}) = \left[0, -2\pi\nu(\gamma+2)U - \frac{1}{\varrho}A\left(1-2\sqrt{\frac{A_0}{A}}\right)\frac{\partial s_t}{\partial x} + \frac{2s_t}{\varrho}\sqrt{A}\,\frac{\partial\sqrt{A_0}}{\partial x}\right]^T$$

the source term. Equation (10) has to be complemented with proper initial and/or boundary conditions. This issue will be addressed in detail in the following section relating the numerical formulation of (10). Following the procedure sketched in [37], we evaluate the eigenstructure of (10),which is needed in the sequel. The Jacobian matrix is written as:

$$\mathbf{dJ} = \begin{bmatrix} 0 & 1 \\ \frac{k}{2}A^{-\frac{1}{2}} - \frac{q^2}{A^2} & \frac{2q}{A} \end{bmatrix}. \tag{11}$$

From the above definition, we get the eigenvalues:

$$\lambda = \frac{q}{A} - \sqrt{k/2}\cdot A^{-\frac{1}{4}},$$
$$\mu = \frac{q}{A} + \sqrt{k/2}\cdot A^{-\frac{1}{4}},$$

as well as the corresponding right eigenvectors:

$$r_\lambda = \begin{bmatrix} 1 \\ \lambda \end{bmatrix}, \quad r_\mu = \begin{bmatrix} 1 \\ \mu \end{bmatrix}. \tag{12}$$

From (12) and (12) it is easy to show that the field is genuinely nonlinear. To complete the problem characterization, we write down the Riemann invariants as:

$$w(A,q) = \frac{q}{A} - 4\sqrt{k/2}\,A^{-\frac{1}{4}}, \tag{13}$$
$$z(A,q) = \frac{q}{A} + 4\sqrt{k/2}\,A^{-\frac{1}{4}}. \tag{14}$$

3 Numerical Modelling

The model presented in the previous section, is intended to be intensively applied to clinical problems. Since it is not always possible to analytically solve the problem we proceed to discretize equations (10) and find a suitable computational solution. In this case we chose a finite volume discretization with Lax-Friedrichs fluxes approximation, WENO boundary cell values reconstructions and Runge-Kutta strong stability preserving time integration. Several reasons lead to such a choice. First, the Lax-Friedrichs approximation is chosen to keep the fluxes expression as simple as possible. A possible the drawback is that this formulation has the most dissipative behavior among other possible choices: Godunov flux or Enquist flux, [31]. This dissipative behavior is well balanced implying a fifth order accurate WENO reconstruction of border cell values. This spatial integration together with the five steps fourth order accurate Runge-Kutta time integration scheme performs a fifth order accuracy, (see Table 1).

One-dimensional models are often used in biomedical multiscale modelling to connect areas modelled with 3D fluid-structure interaction schemes [27]. Complete schemes are most of the times first or second order accurate, [26, 19, 13, 12], it is then essential that this areas are linked by the lowest possible numerical dissipation. The need of interfacing complete and reduced models [20] leads to choose numerical schemes simple to implement, and WENO represents an ideal solution to such an issue.

WENO schemes where developed to numerically solve problems characterized by discontinuous solutions, for example shallow water equations [6], traffic flow [16] or gas dynamics problems [5]. In the case of bio-fluid mechanics the great pressure and flow-rate gradients can give spurious oscillations we wish to avoid. On the other hand the developed model should apply to certain pathological situations such as heart attack or the opening of an arteriovenous fistula.

Moving to the actual integration of Eq. (10), following the treatment proposed in [14, 37], we discretize system (10) on the domain $\mathcal{D} = \{x \in [0, L]\}$ using $N - 1$ uniformly spaced cells of amplitude:

$$\Delta x = \frac{L}{N-1}.$$

We associate to each cell its center x_i and its edges $x_{i-\frac{1}{2}}$ and $x_{i+\frac{1}{2}}$. Conservation equations are then integrated on each cell extension [14, 37]:

$$\int_{x_{i-\frac{1}{2}}}^{x_{i+\frac{1}{2}}} \mathbf{U}_t \,\mathrm{d}x + \int_{x_{i-\frac{1}{2}}}^{x_{i+\frac{1}{2}}} \mathbf{F}(\mathbf{U})_x \,\mathrm{d}x = \int_{x_{i-\frac{1}{2}}}^{x_{i+\frac{1}{2}}} \mathbf{S}(\mathbf{U}) \,\mathrm{d}x.$$

If we consider a simple fourth-order accurate Gauss-Lobatto quadrature the source term integration becomes:

$$\int_{x_{i-\frac{1}{2}}}^{x_{i+\frac{1}{2}}} \mathbf{S}(\mathbf{U}) \,\mathrm{d}x \approx \mathbf{S}(\mathbf{U}_{i-\frac{1}{2}})\, \omega_{i-\frac{1}{2}} + \mathbf{S}(\mathbf{U}_i)\, \omega_i + \mathbf{S}(\mathbf{U}_{i+\frac{1}{2}})\, \omega_{i+\frac{1}{2}},$$

where ω_k represents the specific Gauss-Lobatto weight. Defining the mean value $\bar{\mathbf{U}}_i$ over the cell extension:

$$\bar{\mathbf{U}} = \frac{1}{\Delta x} \int_{x_{i-\frac{1}{2}}}^{x_{i+\frac{1}{2}}} \mathbf{U} \,\mathrm{d}x;$$

the following ordinary differential equation can be written:

$$\frac{\mathrm{d}\bar{\mathbf{U}}}{\mathrm{d}t} = -\frac{1}{\Delta x}(\mathbf{F}_{i+\frac{1}{2}} - \mathbf{F}_{i-\frac{1}{2}}) + \mathbf{S}(\mathbf{U}_{i-\frac{1}{2}})\, \omega_{i-\frac{1}{2}} + \mathbf{S}(\mathbf{U}_i)\, \omega_i + \mathbf{S}(\mathbf{U}_{i+\frac{1}{2}})\, \omega_{i+\frac{1}{2}}, \quad (15)$$

By this approach we are able to reduce a system of partial differential equations to an ordinary differential equations one, separating spatial and time integration.

As outlined in the lines above we choose the Lax-Friedrichs flux approximation because of its simple expression when compared to other possible choices [31]:

$$\hat{\mathbf{F}}_{i+\frac{1}{2}} = \frac{1}{2}\left[\mathbf{F}(\mathbf{U}^{-}_{i+\frac{1}{2}}) + \mathbf{F}(\mathbf{U}^{+}_{i+\frac{1}{2}}) - \psi(\mathbf{U}^{+}_{i+\frac{1}{2}} - \mathbf{U}^{-}_{i+\frac{1}{2}})\right]$$

where ψ is the maximum right eigenvalue in the significant range of $\mathbf{U}$. The dissipative behavior of the flux is balanced by a fifth-order WENO reconstruction for the border cell values. Such a technique will be only briefly presented in the sequel. The interested reader can find exhaustive reviews on this topic in [31, 25].

Center, left and right approximation of both the border cell values is similar; we, for this reason outline the technique focusing our attention on $\mathbf{U}^{-}_{i+\frac{1}{2}}$. Point values of $\mathbf{U}^{-}_{i+\frac{1}{2}}$ are reconstructed through a suitable polynomial $R_i(x)$ defined over the domain $I_i = [x_{i-\frac{1}{2}} x_{i+\frac{1}{2}}]$. In this domain, *conservation, accuracy* and *non-oscillatory* requirements must be satisfied, in such a way that:

$$\mathbf{U}^{-}_{i+\frac{1}{2}} = R_i(x_{i+\frac{1}{2}}).$$

The requirements we need to satisfy are:

1. *Conservation requirement:* The conservative character of the reconstruction is preserved by the following relation:

$$\frac{1}{\Delta x}\int_{x_{i-\frac{1}{2}}}^{x_{i+\frac{1}{2}}} R_i(x)\,\mathrm{d}x = \bar{\mathbf{U}}_i.$$

2. *Accuracy requirement:* The reconstruction is fifth-order accurate if the following relation holds:

$$R_i(x_{i+\frac{1}{2}}) = \mathbf{U}(x_{i+\frac{1}{2}}, t) + \mathcal{O}(\Delta x^5).$$

3. *Non-oscillation requirement:* Fifth-order accurate WENO reconstructions require that oscillations closed to discontinuities decay as $\mathcal{O}(\Delta x^5)$

The requirements above are fulfilled selecting three *stencils*, sets of three cells, $\mathcal{P}_{i+k} = \cup_{l=-1}^{l=+1} I_{i+k+l}$, with $k = -1, 0, 1$; each $P_{i+k}(x)$ is associated to a polynomial of degree 2. The coefficients of each polynomial $P_{i+k}(x)$ are uniquely determined imposing the conservation requirement on each cell of the stencil $\mathcal{P}_{i+k}$:

$$\frac{1}{\Delta x}\int_{I_{i+k-j}} P_{i+k}(x)\,\mathrm{d}x = \bar{\mathbf{U}}_{i+k-j} \qquad k = -1, 0, 1 \quad j = -1, 0, 1 \qquad (16)$$

For further considerations, we select a bigger stencil, $\mathcal{Q}_i = \cup_{m=-2}^{m=+2} I_{i+m}$, and the corresponding polynomial $Q_i(x)$ of degree 4, whose coefficients are uniquely determined imposing the conservation requirement:

$$\frac{1}{\Delta x}\int_{I_{i+m}} Q_i(x)\,\mathrm{d}x = \bar{\mathbf{U}}_{i+m} \qquad m = -2, 0, 2\,.$$

In case of a smooth reconstructed function, it is easy to prove [25] the following accuracy property of $Q_i(x)$:

$$Q_i(x_{i+\frac{1}{2}}) = \mathbf{U}(x_{i+\frac{1}{2}}, t) + \mathcal{O}(\Delta x^5). \tag{17}$$

Accuracy and the non-oscillatory properties of the reconstruction are achieved writing the polynomial $R_i(x)$ as a convex combination of the three polynomials $P_{i+k}(x)$, using suitable variables *weights*, w_i^k $(k = -1, 0, 1)$:

$$R_i(x) = \sum_{k=-1}^{1} w_i^k \; P_{i+k}(x). \tag{18}$$

Such weights are functions of the solution regularity on each stencil $\mathcal{P}_{i+k}$. They are computed through the definitions of *linear weights* d_k and *index of smoothness* function IS_i^k [25]. The linear weights are chosen in such a way that the reconstruction satisfies the accuracy requirement where the solution is smooth. For $\mathbf{U}^+_{i-\frac{1}{2}}$ and $\mathbf{U}^-_{i+\frac{1}{2}}$ we get:

$$d_{-1} = \frac{1}{10}, \quad d_0 = \frac{3}{5}, \quad d_1 = \frac{3}{10}.$$

In the case of $\mathbf{U}_i$, to avoid coefficients becoming negative, we prefer a fourth-order accurate reconstruction [22]:

$$d_{-1} = \frac{1}{4}, \quad d_0 = \frac{1}{2}, \quad d_1 = \frac{1}{4}.$$

The index of smoothness function allows the optimal weighting of polynomials $P_{i+k}(x)$ in Eq. (18), where the solution is characterized by high gradients or discontinuities. In this paper we quantify the index of smoothness using the L^2 norm of the polynomial derivatives $P_{i+k}^{(l)}(x)$ on the cell I_i:

$$IS_i^k = \sum_{l=1}^{2} \int_{I_i} \Delta x^{2l-1} \left(P_{i+k}^{(l)}\right)^2 \mathrm{d}x. \tag{19}$$

as suggested in [31]. The evaluation of (19) gives:

$$
\begin{aligned}
IS_i^{-1} &= \frac{13}{12}\left(\bar{\mathbf{U}}_{i-2} - 2\bar{\mathbf{U}}_{i-1} + \bar{\mathbf{U}}_i\right)^2 + \frac{1}{4}\left(\bar{\mathbf{U}}_{i-2} - 4\bar{\mathbf{U}}_{i-1} + 3\bar{\mathbf{U}}_i\right)^2, \\
IS_i^0 &= \frac{13}{12}\left(\bar{\mathbf{U}}_{i-1} - 2\bar{\mathbf{U}}_i + \bar{\mathbf{U}}_{i+1}\right)^2 + \frac{1}{4}\left(\bar{\mathbf{U}}_{i-1} - \bar{\mathbf{U}}_{i+1}\right)^2, \\
IS_i^1 &= \frac{13}{12}\left(\bar{\mathbf{U}}_i - 2\bar{\mathbf{U}}_{i+1} + \bar{\mathbf{U}}_{i+2}\right)^2 + \frac{1}{4}\left(3\bar{\mathbf{U}}_i - 4\bar{\mathbf{U}}_{i+1} + \bar{\mathbf{U}}_{i+2}\right)^2.
\end{aligned}
$$

Finally, the indices of smoothness are used into the final expressions for the weights:

$$
\alpha_i^k = \frac{d_k}{\left(\varepsilon + IS_i^k\right)^2}; \qquad w_i^k = \frac{\alpha_i^k}{\sum_{l=-1}^{l=1} \alpha_i^l}, \tag{20}
$$

where ε is equal to 10^{-6} to avoid the denominator to vanish.

Shu in [25] proves that, if the solution is smooth, weights w_i^k tend to d_k and the convex combination (18), evaluated in $x_{i+\frac{1}{2}}$, tends to:

$$
\sum_{k=-1}^{1} d_k \; P_{i+k}(x_{i+\frac{1}{2}}) = Q_i(x_{i+\frac{1}{2}}). \tag{21}
$$

Therefore, considering the Eqs. (17) and (21) it is easy to understand how the fifth-order accuracy is achieved. It is also demonstrated [31] that the weights w_i^k are $\mathcal{O}(\Delta x^4)$ or $\mathcal{O}(1)$ if the solution, inside $P_{i+k}(x)$, is discontinuous or smooth, respectively. As a consequence, the reconstruction $\mathbf{U}^-_{i+\frac{1}{2}}$ is basically based on the polynomials associated to stencils in which the solution is continuous. This behavior of the weights avoids the Gibbs phenomena development.

Time integration is preformed through a strong stability preserving Runge-Kutta five-steps fourth-order accurate scheme (SSPRK(5,4)). Highlighting time integration in Eq. (15) we can focus on the following ordinary differential equation:

$$
\dot{\mathbf{U}} = L(\mathbf{U}).
$$

Runge-Kutta can be briefly described as a linear combination of forward Euler steps:

$$
\begin{aligned}
\mathbf{U}^{(0)} &= \mathbf{U}^n, \\
\mathbf{U}^{(i)} &= \sum_{k=0}^{i-1}(\alpha_{ik}\mathbf{U}^{(k)} + \Delta t \beta_{ik} L(\mathbf{U}^{(k)})), \quad i = 1, 2, \ldots, s \\
\mathbf{U}^{n+1} &= \mathbf{U}^{(s)},
\end{aligned}
$$

where α_{ik} and β_{ik} are the linear coefficients, Δt is the time step and s is the number of steps between t^n and t^{n+1}. The superscript in the above expression indicates the relative time level. Details on the scheme derivation and performances can be found in [34], as well as details about α and β coefficients and Courant-Friedrichs-Lewy (CFL) condition.

3.1 Numerical Treatment of Boundary Conditions

In this subsection we address the treatment of the boundary conditions needed in the numerical formulation of the model. Each vessel in the vascular system interacts with the surrounding apparatus through an appropriate setting of boundary conditions. In the applications explored in Sect. 3 we will model different segments of the venous system. When studying limited sections of the vascular apparatus it is essential to introduce non reflecting boundary conditions in order to avoid reflections the model is not expected to show [21, 8]. In the case of a finite volume discretization the assignment of boundary conditions consists in writing a flux term at the upstream and downstream sections of the domain, namely, *border cell flux values*.

In [7] we introduced highly accurate absorbing boundary conditions. Here we explain the imposition of the flow rate at the inlet and the area, bijectively related to the pressure, at the outlet; the converse situation can be easily derived. We first consider the Riemann invariants definition and write area and mean velocity at the inlet:

$$\begin{cases} U_{\text{in}} = \frac{1}{2}\left(z_{sx} + w_{dx}\right) \\ A_{\text{in}} = \left(\dfrac{8\sqrt{k/2}}{z_{sx} - w_{dx}}\right)^4 \end{cases}, \tag{22}$$

(details of the notation in Fig. 1). Absorbing boundary conditions are achieved introducing an undisturbed state $\mathcal{U} = (q_{\mathcal{U}}, A_{\mathcal{U}})$ and defining the correct w_{dx} which satisfies the imposed $q(t) = q_{\text{in}}$ and preserves $\mathcal{U}$:

$$q_{\text{in}} = 512\frac{k^2(w_{dx} + z_{\mathcal{U}})}{(z_{\mathcal{U}} - w_{dx})^4}. \tag{23}$$

Getting from equation (23) an appropriate value of w_{dx} and stating the conservation z_{sx} from the interior it is possible to use relation (22) and evaluate the inlet expression of the flux:

$$\mathbf{F}_{\text{in}} = \begin{bmatrix} A_{\text{in}} \\ U_{\text{in}}^2 \cdot A_{\text{in}} + k\sqrt{A_{\text{in}}} \end{bmatrix}. \tag{24}$$

The same technique is used with the area (pressure) prescription at the outlet section. Using the Riemann invariants and the undisturbed state definitions the following area expression holds:

$$z_{sx} = w_{\mathcal{U}} + 8\sqrt{k/2} \cdot A_{\text{out}}^{-\frac{1}{4}}. \tag{25}$$

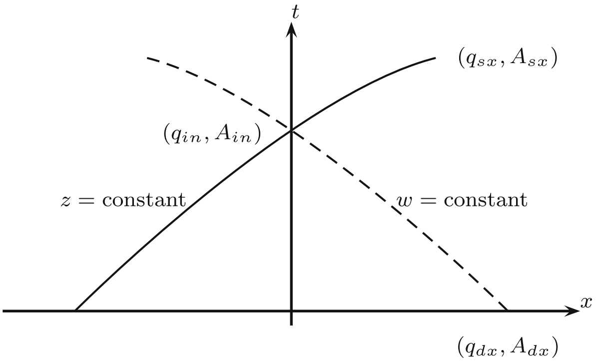

Fig. 1 Riemann invariants represented in the kinematical plane (see [7, 14] for detailed reference)

Then we state the conservation of w_{dx} from the interior and, using the Riemann invariants expressions (22) at the outlet too, we can write the flux $\mathbf{F}_{\text{out}}$.

The tree-type morphology of the vascular system network implies that suitable conditions have to be imposed at the branching of a vessel. In this work we follow a classical approach in fluid mechanics [39] and state the conservation of mass and the continuity of pressure. First the mass conservation holds:

$$\sum_{i=1}^{3} q_i = 0, \tag{26}$$

where the geometry setting is sketched in Fig. 2. Then, imposing $p_i = \bar{p}\ \forall i$ and requiring the conservation of proper Riemann invariants, we can write the following non linear system:

$$\begin{cases} U_1 \cdot k_1^2 \cdot (s_{t1} - \bar{p})^{-2} - U_2 \cdot k_2^2 \cdot (s_{t2} - \bar{p})^{-2} - U_3 \cdot k_3^2 \cdot (s_{t3} - \bar{p})^{-2} = 0 \\ U_1 - 2\sqrt{2}/\varrho\, (s_{t1} - \bar{p})^{\frac{1}{2}} - w_1 = 0 \\ U_2 + 2\sqrt{2}/\varrho\, (s_{t2} - \bar{p})^{\frac{1}{2}} - z_2 = 0 \\ U_3 + 2\sqrt{2}/\varrho\, (s_{t3} - \bar{p})^{\frac{1}{2}} - z_3 = 0. \end{cases} \tag{27}$$

System (27) solution brings values for U_1, U_2, U_3 and $\bar{p}$ letting us evaluating the outlet flux for vessel 1 and the inlet flux for vessels 2 and 3. On the venous side of the apparatus it is essential to model the behavior of the valves. They are essentially non-return valves which prevent the inversion of the blood motion with respect to its physiological direction: from the periphery to the heart and from the superficial to the deep circulation. In the case of one dimensional modelling we are interested in the effect that the valve plays on the whole network. For this reason we do not consider the fluid structure problem, describing how the blood and the leaflets motion affect each other; the whole valve is modelled as a non-return valve. In the present study we evaluate the valve behavior applying the momentum theorem. The result of this original application is simple, but gives a rigorous interpretation of the

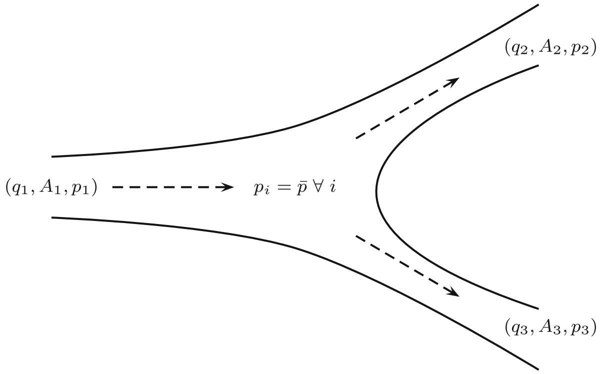

Fig. 2 Branching scheme

physical phenomena. Since in the applications we will consider a test case relative to a patient in supine position we get rid, in the sequel, of the possible presence of the gravity force, for the latter is orthogonal to the vessels' axes. This assumption does not affect the generality of the model's formulation. The momentum theorem derivation is standard, in the next few lines the main steps will be summarized, while the interested reader can refer to [39] for a detailed explanation. The equation of motion for a fluid in a domain Ω with surface Γ states the balance of volume and surface forces, versus the fluid acceleration (the total time derivative of the velocity field):

$$\int_\Omega \varrho \mathbf{f}\, \mathrm{d}\Omega + \int_\Gamma \tau\ \mathrm{d}\Gamma = \frac{\mathrm{D}}{\mathrm{Dt}} \int_\Omega \varrho \mathbf{v}\, \mathrm{d}\Omega,$$

where $\mathbf{f}$ are the volume forces, τ are the internal stresses and $\mathbf{v}$ is the velocity field. With $\mathbf{v}$ and $\varrho \in C^1$ we can write:

$$\int_\Omega \varrho \mathbf{f}\, \mathrm{d}\Omega + \int_\Gamma \tau\ \mathrm{d}\Gamma = \int_\Omega \frac{\partial(\varrho \mathbf{v})}{\partial t}\, \mathrm{d}\Omega - \int_\Gamma \varrho \mathbf{v}(\mathbf{v} \cdot \mathbf{n})\, \mathrm{d}\Gamma,$$

with $\mathbf{n}$ the inward unit normal at volume surface. Putting:

$$\boldsymbol{M}_i = \int_{\Gamma_i} \varrho \mathbf{v}(\mathbf{v} \cdot \mathbf{n})\, \mathrm{d}\Gamma_i,$$
$$\boldsymbol{I} = \int_\Omega \frac{\partial(\varrho \mathbf{v})}{\partial t}\, \mathrm{d}\Omega,$$
$$\boldsymbol{G} = \int_\Omega \varrho \mathbf{f}\, \mathrm{d}\Omega,$$
$$\mathbf{\Pi} = \int_\Gamma \tau\ \mathrm{d}\Gamma,$$

we get:

$$\boldsymbol{G} + \boldsymbol{\Pi} = \boldsymbol{I} + \boldsymbol{M}_{\text{out}} - \boldsymbol{M}_{\text{in}}. \tag{28}$$

Assuming the velocity time derivative bounded and $\Omega \to 0$, in the sense of a lumped treatment of the valve modelling, we can drop $\boldsymbol{I}$. Such a consideration holds also for $\boldsymbol{G}$, in addition the vessels' axes are orthogonal to the gravity direction (see Fig. 3). Projecting Eq. (28) along vessel's axis the surface forces are:

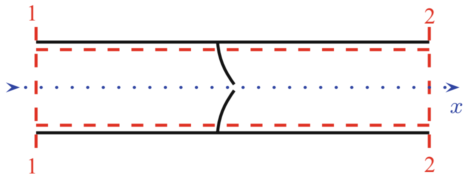

Fig. 3 Control volume used in the momentum theorem application

$$\boldsymbol{\Pi}_x = p_1 \cdot A_1 - p_2 \cdot A_2 - \pi_f,$$

where π_f, our unknown, is the force that the fluid applies on the valve structure. The linear momentum at the outlet and inlet sections is given by:

$$\boldsymbol{M}_{\text{out},x} = \varrho \cdot \frac{q_2^2}{A_2}, \quad \boldsymbol{M}_{\text{in},x} = \varrho \cdot \frac{q_1^2}{A_1}.$$

For the detailed derivation of such quantities in a one dimensional model see [39]. Finally, the surface force on the valve is:

$$\pi_f = \left(p_1 \cdot A_1 + \varrho \frac{q_1^2}{A_1} \right) - \left(p_2 \cdot A_2 + \varrho \frac{q_2^2}{A_2} \right). \tag{29}$$

The term $p_i \cdot A_i + \varrho q_i^2 / A_i$ is to be addressed as *specific hydraulic force*. In the case of the present applications we consider a perfect valve, then, if $\pi_f < 0$, the valve is closed and a reflecting boundary condition $q(t)$ is prescribed. Otherwise if $\pi_f \geq 0$ the valve is opened and the continuity of the fluxes is required: $\mathbf{F}_1 = \mathbf{F}_2$. It is immediate to notice that different levels of valve efficiency can be obtained modifying the reacting value of π_f. Reflecting boundary conditions are achieved with standard techniques [14]. Referring to the outlet condition for the upstream vessel we write:

$$\begin{cases} q_{\text{out}} = 0 \\ w_{\text{out}} = w_{dx} \end{cases} \Rightarrow A_{\text{out}} = \left(-\frac{4\sqrt{k/2}}{w_{dx}} \right)^4,$$

analogous is the result for the inlet condition for the downstream vessel.

4 Applications

In this section we will explore several applications of the model developed in this paper. We first present the model accuracy analysis, in order to demonstrate the required accuracy and dissipative characteristics. Then we develop a test case to validate the valve modelling. Finally we apply the developed model to the investigation of the leg veins network. In particular we consider the perfectly closing and the perfectly non-closing valve. In every application the patient is considered in supine position.

4.1 Accuracy Analysis

As outlined in Sect. 2, we choose a finite-volume fifth-order accurate scheme due to its low-dissipative and high-accurate character; by this accuracy analysis we intend to test such performances. One of the test cases most extensively used to test hyperbolic non-linear numerical models (see for example [31]) is the inviscid Burgers equation:

$$u_t + f(u)_x = 0, \quad \text{with} \quad f(u) = \frac{u^2}{2}; \tag{30}$$

with initial condition $u(x,0) = 1/2 + \sin(\pi \cdot x)$, for $0 \le x \le L = 2$. Fig. 4 presents the comparison between analytical and numerical solutions of such a test, plotting both a continuous and a shocked solution of problem (30); the complete accuracy analysis is reported in Table 1. Analyzing Fig. 4b we observe that the scheme is substantially non-dissipative, on the other hand Table 1 proves the high order of accuracy performed by the scheme.

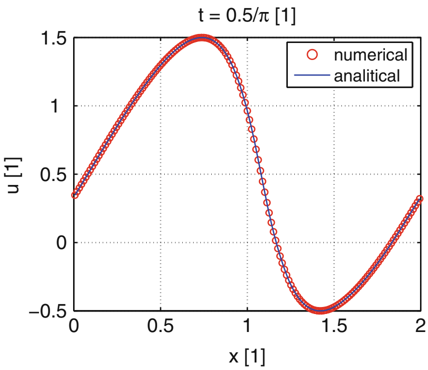

(a) Continuous Burgers solution.

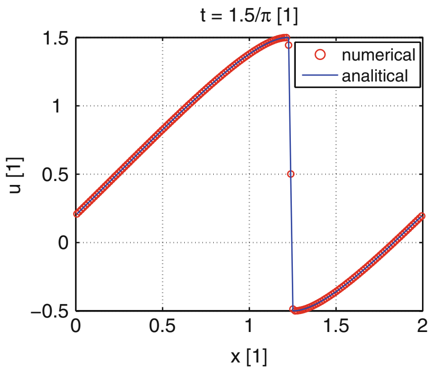

(b) Shocked Burgers solution.

Fig. 4 Continuous and shocked Burgers equation solution

Table 1 Accuracy analysis results

N	L_1 error	L_1 order	L_∞ error	L_∞ order
10	9.525468e-03	–	1.388366e-02	–
20	1.286307e-03	2.68	3.218273e-03	1.96
40	8.532353e-05	3.77	2.889721e-04	3.35
80	3.847901e-06	4.39	1.635095e-05	4.07
160	1.607156e-07	4.54	1.155735e-06	3.79
320	4.835067e-09	5.03	4.609006e-08	4.63
640	1.398019e-10	5.10	4.894403e-10	6.54

4.2 Valve Test Case

Venous valves can be defined as non-return valves of the venous apparatus. In this section we present a test case to verify the modelling of the non-return valve presented in Sect. 2.1. The behavior of the non-return valve is tested taking into account the network structure in Fig. 5 characterized by the physiological geometrical and material properties in Table 2. For sake of clearness Table 2 explains the boundary condition setting too. Here upstream and downstream conditions refer to the physiological conditions where the blood flows from the superficial to the deep apparatus (Fig. 7).

All the boundary conditions, both in the form $A(t)$ or $q(t)$ are non reflecting, to avoid oscillations our model is not supposed to show. At the outlet section of vessel 1 we impose $q(t) = 0 \; \forall t$; at the inlet of vessel 4 we have:

$$A(t) = \begin{cases} 0.9A_0 \text{ for } t \leq t_{\max} \\ \quad 0 \quad \text{ for } t > t_{\max}; \end{cases} \tag{31}$$

and at the inlet of vessel 7 we impose:

$$q(t) = \begin{cases} 20(0.5 - 0.5\cos\left(\frac{2\pi t}{t_{\max}}\right) \text{ [cm}^3\text{/s] for} \quad t_{\max} < t \leq 2t_{\max} \\ \qquad 0 \qquad\qquad\qquad \text{for } t \leq t_{\max}, \; t > 2t_{\max}. \end{cases} \tag{32}$$

In Fig. 6, vessels 6 and 5 are plotted on the same abscissa. Fig. 6a reports the time variation of area (pressure) while Fig. 6b shows the time variation of flow rate. Equation (32) represents a positive pressure drop wave, when it reaches the node among vessels 7, 6 and 2 it is in part reflected, in part transmitted [7, 30]. When it gets into vessel 6, Fig. 6a, it is a pressure drop traveling with negative celerity, but characterized by a positive flow rate and, as a consequence, it passes through the valve without being affected. On the other hand, in vessel 4, we have a pressure drop wave with positive celerity but negative flow rate; as a matter of fact it is transmitted to vessel 5 as positive celerity wave and negative flow rate, then it is reflected. Such a behavior is satisfying and reproduces a correct modelling of non-return valves.

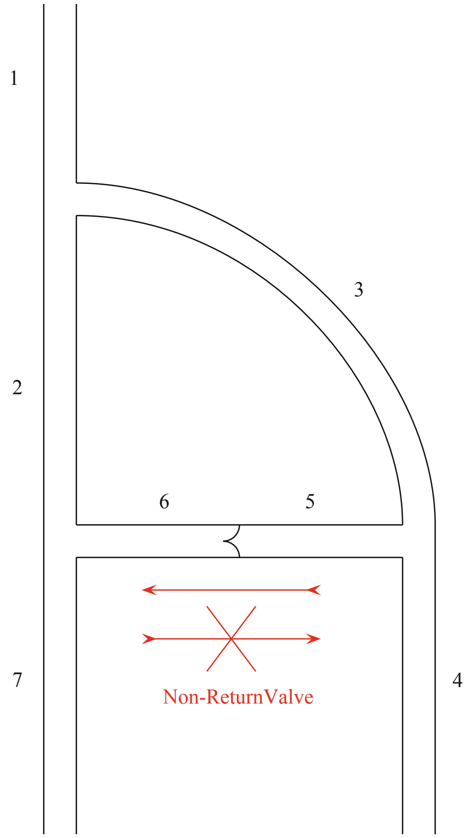

Fig. 5 Scheme of the network employed in the venous valve test case. The valve allows flow from vessel 5 to vessel 6 but not vice versa

Table 2 Boundary conditions, geometrical and structural properties implied in the valve test case

Vessel	Length cm	k cm^2/s^2	r_0 cm	Upstream BC	Downstream BC
1	100	$6.84 \cdot 10^5$	0.35	Branching	$q(t)$
2	100	$6.31 \cdot 10^5$	0.32	Branching	Branching
3	100	$5.97 \cdot 10^5$	0.30	Branching	Branching
4	100	$5.65 \cdot 10^5$	0.28	$q(t)$	Branching
5	50	$5.51 \cdot 10^5$	0.27	Branching	Valve
6	50	$5.51 \cdot 10^5$	0.27	Valve	Branching
7	100	$5.65 \cdot 10^5$	0.28	$A(t)$	Branching

4.3 Leg Veins Network

Phlebology is the clinical science that studies veins diseases. In this area a great role is played by fluid mechanics and fluid-structure interaction to ensure an optimal blood return to the heart. A lot of illnesses are caused by structural damages to the vein network in its vessels or, usually, to the vein valves. In the clinical practice, the

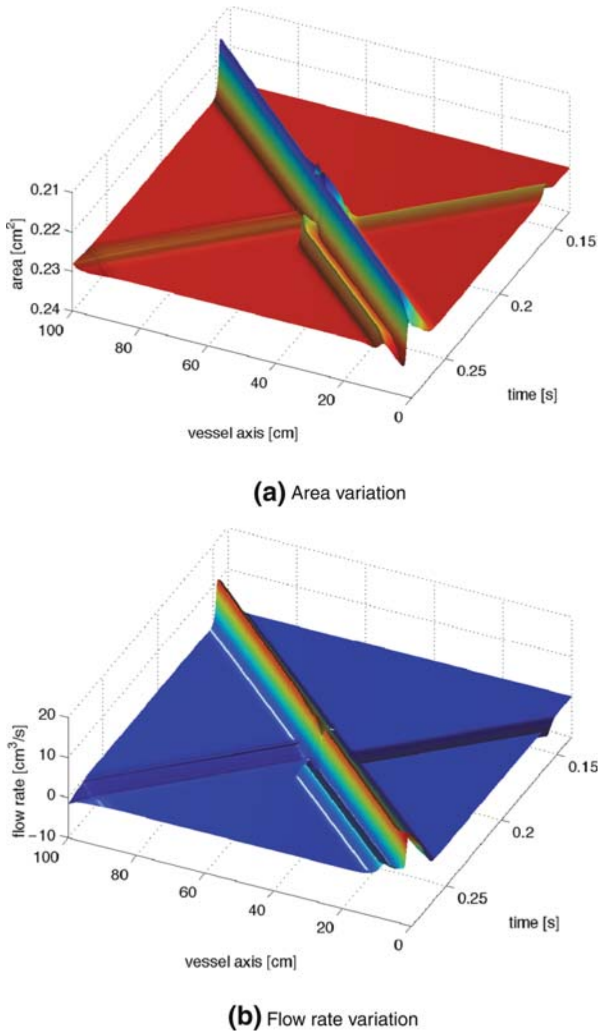

Fig. 6 Non-return valve tests: vessel 5 and 6 are plotted on the same abscissa, area 6a and flow rate 6b time variation are presented

main investigation tool is Echo-Doppler imaging because of low costs and no x-rays or magnetic field exposition.

For the reasons listed above in this section we design the left leg veins network structure of an healthy 26 year old male employing Echo-Doppler imaging. We measure blood velocities using the calf squeezing technique in order to reproduce the muscular pump effect. The structure schematized in Fig. 7 and geometrical properties, reported Table 3, are achieved using images such as Figs. 8a, b, acquired by Echo-Doppler techniques. Valve position is imposed at mid-point of the interested

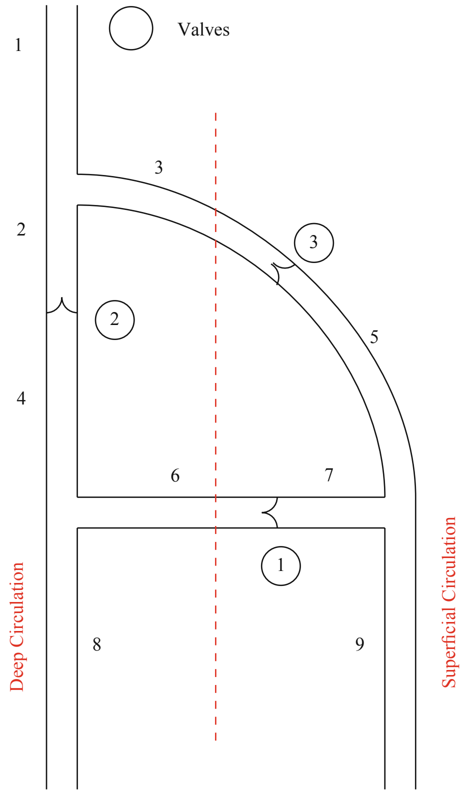

Fig. 7 Physiological scheme of the leg veins

vessel, this assumption simplifies the empirical data achievement without affecting significantly the clinical reliability of the model. The inlet flow rate function at the femoral vein is the mean value of three different calf-squeezing actions in order to get a physiologically reliable average data. No more than three repetitions were possible due to the limited amount of blood stored in the calf. The result is presented in Fig. 9. Structural properties can be achieved from [4, 9] and show: $h = 0.05$ cm and $E = 3.5 \cdot 10^6$ Pa.

Table 3 Geometrical properties of a 26 year old, 183 cm tall male left leg veins

Vessel name	Length cm	Diameter cm	Vessel number
Common femoral vein	4.00	1.580	1
Common femoral vein	7.50	1.400	2–4
Grand saphenous vein	8.00	0.729	3–5
Dodd	1.20	0.127	6–7
Grand saphenous vein	5.00	0.472	9
Common femoral vein	5.00	1.400	4

(a) Femoral diameter.

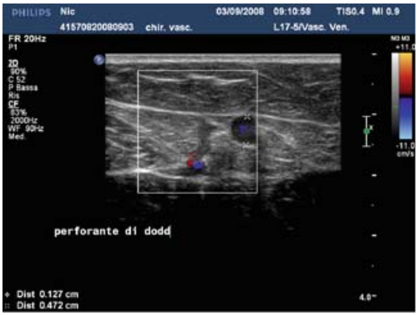

(b) Dodd configuration.

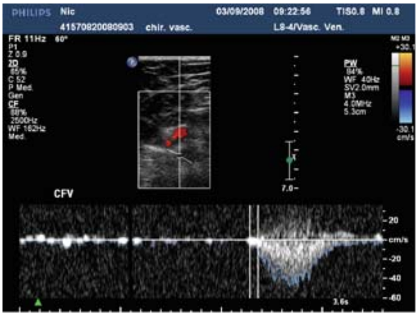

(c) Blood velocity measure at the femoral.

(d) A second velocity measure at the femoral.

Fig. 8 Experimental evaluation by Echo-Doppler imaging of geometrical and flow properties of patient's left leg thigh

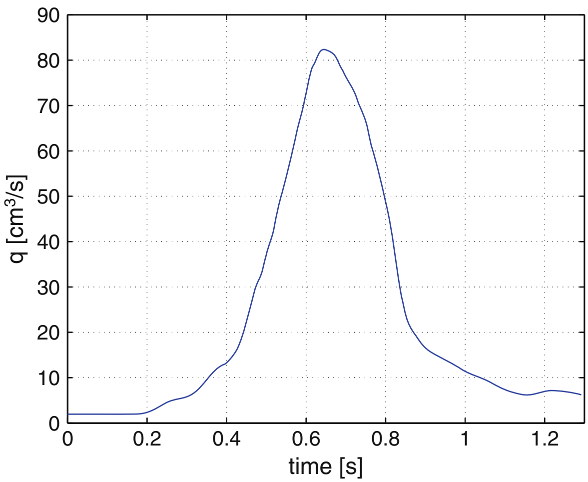

Fig. 9 Averaged femoral inflow (flow rate)

Figure 10 presents the results of the simulation reproducing the muscular pump in two clinically relevant cases. The first one is the physiological case, where the whole structure performs correctly, addressed as *healthy test case*.

In a second test we assumed a dysfunction of valve 3 that does not close at all. This case is named as *pathological test case*. In the healthy case we notice that the wave produced by the muscular pump travels through the femoral vein without affecting the superficial circulation. In the pathological case the disfunction of valve 3 causes the blood to flow into the grand saphenous vein, Fig. 10e and 10f. Moreover the saphenous vein shows a flow inversion, from deep to the superficial circulation, which is a clinically observed behavior in such cases. The high frequency oscillations are due the reflections between the network nodes and they are not to be addressed to numerical instabilities, as Fig. 4 demonstrates. This two test cases are the fist attempt to conjugate a mathematically rigorous model of the leg vein network and the clinical equipment used in every day practice. This are the reasons why a low computational cost model, such as one-dimensional ones, and echo-doppler imaging are used.

5 Conclusions

In this paper we outline the development of an accurate numerical scheme to treat an one-dimensional model of the vascular system. One-dimensional models cannot describe the details of blood flow and of the vessel motion, but they are characterized by simplicity and a relative easiness of implementation. Among the advantages of one-dimensional models we recall that they are often used to link local three-dimensional complete models characterized by low orders of accuracy. In this perspective, it is essential that the one-dimensional link has the lowest dissipative character as possible. Moreover the interface should be as simple as possible to be realized. Both these issues are taken into account in the development of the model and scheme presented in this paper and the results, mainly represented in Fig. 4 and Table 1, prove the achievement of the desired performances.

In the application section we exploit the model and the numerical scheme to develop one of the earliest investigations of the venous apparatus. In that section we investigate the physiological effect of the veins valves. There, the valves are modelled by a simple but rigorous application of the momentum theorem. In this work we limit ourselves to the perfectly physiological or totally pathological situation, but there is no limitation in principle to the modelling of different levels of valve efficiency. In this application the mathematical modelling is coupled with Echo-Color Doppler imaging. The coupling of these two "techniques" represents, to our opinion, an important integration that interfaces the diagnostic apparatus most extensively used in clinical practice with a mathematical vascular modelling with an optimized balance between computational cost and achievable information.

The results presented in this paper are part of a large project, developed in collaboration with vascular surgeons, radiologists and bioengineers funded by the Italian

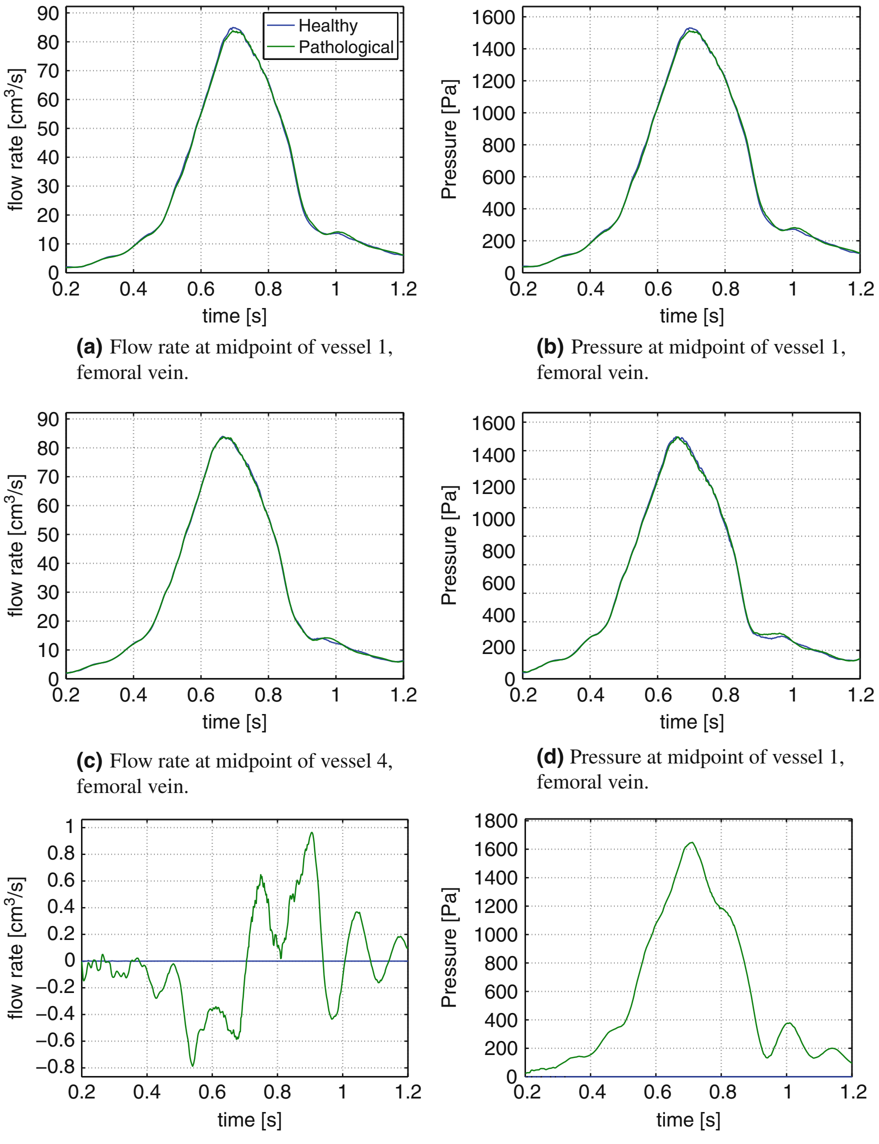

(a) Flow rate at midpoint of vessel 1, femoral vein.

(b) Pressure at midpoint of vessel 1, femoral vein.

(c) Flow rate at midpoint of vessel 4, femoral vein.

(d) Pressure at midpoint of vessel 1, femoral vein.

(e) Flow rate at midpoint of vessel 5, saphenous vein.

(f) Pressure at midpoint of vessel 5, saphenous vein

Fig. 10 Pathological and healthy simulation of the leg vein network

Ministry of Scientific Research. Presently, we are studying the way in which the results given by the model when applied to a large network in pathological conditions can be optimized to suggest the best surgical approach in the outpatient treatment of venous insufficiency.

Acknowledgments We wish to express our gratitude to V. Gasbarro and E. Gresta for giving us access and assistance to the Echo-Color Doppler facilities of the Unit of Vascular Surgery of the University of Ferrara and to V. Caleffi for useful discussions. This work has been partially supported by the Italian National Research Project PRIN "Systems of Virtual Bioengineering" and by TSEM S.p.A.

References

1. Amadori, D., Ferrara, S., Formaggia, L.: Derivation and analysis of a fluid-dynamical model in thin and long elastic vessels. Netw. Heterog. Media **2**(1), 99–125 (2007)
2. Barnard, A.C.L., Hunt, W.A., Timlacke, W.P., Varley, E.: A theory for fluid flow in compliant tubes. Biophys. J. **6**, 717–724 (1966)
3. Bergan, J.J., ed.: *The Vein Book.* Elsevier Academic Press, Burlington, San Diego, London (2007)
4. Bergel, D.H.: *Cardioavascular Fluid Dynamics.* Academic Press, New York, London (1972)
5. Brio, M., Zakharian, A.R., Webb, G.M.: Two-dimensional Riemann solver for euler equations of gas dynamics. J. Comput. Phys. **167**(1), 177–195 (2001)
6. Caleffi, V., Valiani, A., Bernini, A.: Fourth-order balanced source term treatment in central WENO schemes for shallow water equations. J. Comput. Phys. **218**(1), 228–245 (2006)
7. Cavallini, N., Caleffi, V., Coscia, V.: Finite volume and WENO scheme in one-dimensional vascular system modelling. Comput. Math. Appl. **56**, 2382–2397 (2008)
8. Formaggia, L., Lamponi, D., Quarteroni, A.: One-dimensional models for blood flow in arteries. J. Engrg. Math. **47**, 251–276 (2003)
9. Fung, Y.C.: *Biomechanics: Mechanical Properties of Living Tissues*. 2nd ed., Springer, New York (1993)
10. Fung, Y.C.: *Biomechanics: Circulation*. 2nd ed., Springer, New York (1997)
11. Galdi, G.P., Rannacher, R., Robertson, A.M., Turek, S.: *Hemodynamical Flows. Modeling, Analysis and Simulation.* Birkhäuser, Basel-Boston-Berlin (2008)
12. Guidoboni, G., Glowinski, R., Cavallini, N., Canic, S.: Stable loosely-coupled-type algorithm for fluid-structure interaction in blood flow. J. Comput. Phys. **228**, 6916–6937 (2009)
13. Guidoboni, G., Glowinski, R., Cavallini, N., Canic, S., Lapin, S.: A kinematically coupled time-splitting scheme for the fluid-structure interaction in blood flow. Appl. Math. Lett. **22**, 684–688 (2009)
14. Leveque, R.J.: *Finite Volume Methods for Hyperbolic Problems.* Cambridge University Press, Cambridge, United Kingdom (2002)
15. Maurits, N.M., Loots, G.E., Veldman, A.E.P.: The influence of vessel wall elasticity and peripheral resistance on the carotid artery flow wave form: A cfd model compared to in vivo ultrasound measurements. J. Biomech. **80**(2), 427–436 (2007)
16. Menping, Z., Shu, C.W., K., George, C.K., Wong, S.C.: A weighted essentially non-oscillatory numerical scheme for a multi-class Lighthill-Whitham-Richards traffic flow model. J. Comput. Phys. **191**(1), 639–659 (2003)
17. Nadau, L., Sequeira, A.: Numerical simulations of shear dependent viscoelastic flows with a combined finite element-finite volume method. Comput. Math. Appl. **53**(3–4), 547–568 (2007).

18. Nicosia, S., Pezzinga, G.: Mathematical models of blood flow in the arterial network. J. Hydraul. Res. **45**(2), 188–201 (2007)
19. Nobile, F.: Numerical approximation of fluid-structure interaction problems with application to haemodynamics. Ph.D. thesis, Ecole Polytechnique Fédérale de Lausanne (2001)
20. Nobile, F.: Coupling strategies for the numerical simulation of blood flow in deformable arteries by 3d and 1d models. Math. Comput. Mod. **49**(11–12), 2152–2160 (2008)
21. Nobile, F., Vergara, C.: An effective fluid-structure interaction formulation for vascular dynamics by generalized Robin conditions. SIAM J. Sci. Comp. **30/2**, 731–763 (2008)
22. Noelle, S., Pankratz, N., Puppo, G., Natvig, J.: Well-balanced finite volume schemes of arbitrary order of accuracy for shallow water flows. J. Comput. Phys. **213**(2), 474–499 (2006)
23. Noseda, G.: A mathematical model of the arterial system. Meccanica **IX**, 179–193 (1974)
24. Olufsen, M.S., Peskin, C.S., Kim, W.Y., Nadim, E.M.P.A., Larsen, J.: Numerical simulation and experimental validation of blood flow in arteries with structured-tree out flow conditions. Ann. Biomed. Eng. **28**, 1281–1299 (2000)
25. Qiu, J., Shu, C.W.: On the construction, comparison, and local characteristic decomposition for high-order central weno schemes. J. Comput. Phys. **183**, 187–209 (2002)
26. Quaini, A., Quarteroni, A.: A semi-implicit approach for fluid-structure interaction based on algebraic fractional step methods. Mat. Mod. Meth. Appl. Sci. **17**, 957–983 (2007)
27. Quarteroni, A., Ragni, S., Veneziani, A.: Coupling between lumped and distributed models for blood flow problems. Comput. Visual. Sci. **4**, 111–124 (2001)
28. Quarteroni, A., Tuveri, M., Veneziani, A.: Computational vascular fluid dynamics: problems. Models and methods. Comput. Visual. Sci. **2**, 163–197 (2000)
29. Robertson, A.M., Sequeira, A.: A director theory approach for modeling blood flow in the arterial system: An alternative to classical 1d models. Math. Mod. Meth. Appl. Sci. **15**, 871–906 (2005)
30. Sherwin, S., Franke, V., Ppeiró, J., Parker, K.: One-dimensional modelling of a vascular network in space-time variables. J. Engrg. Math. **47**, 217–250 (2003)
31. Shu, C.W.: Essentially Non-Oscillatory and Weighted Essentially Non-Oscillatory Schemes for Hyperbolic Conservation Laws. Institute for Computer Applications in Science and Engineering (1997). Technical Report NASA CR-201746 ICASE Report No. 97-51
32. Smith, J.J., Kampine, J.T.: *Circulatory Physiology: The Essentials*. 3rd ed., Williams and Wilkins, Baltimore (1990)
33. Smith, N.P., Pullan, A.J., Hunter, P.J.: An anatomically based model of transient coronary blood flow in the heart. SIAM J. Appl. Math. **62**, 990–1018 (2002)
34. Spitery, R.J., Ruuth, S.J.: A new class of optimal high-order strong-stability-preserving time discretization methods. SIAM J. Numer. Anal. **40**(2), 469–491 (2002)
35. Steele, B.N., Wan, J., Ku, J.P., Hughes, T.J.R., Taylor, G.A.: In-vivo validation of a one-dimensional finite-element method for predicting blood flow in cardiovascular bypass grafts. IEEE Trans. Biomed. Engrg. **50**, 649–656 (2003)
36. Thiriet, M.: *Biology and Mechanics of Blood Flows, Part II: Mechanics and Medical Aspects*. CRM Series in Mathematical Physics, Springer, New York (2008)
37. Toro, E.F.: *Riemann Solvers and Numerical Methods for Fluid Dynamics.* Springer-Verlag, Berlin, Germany (1999)
38. Čanić, S., Hartley, C.J., Rosenstrauch, D., Tambača, J., Guidoboni, G., Mikelić, A.: Blood flow in compliant arteries: An effective viscoelastic reduced model, numerics, and experimental validation. Ann. Biomed. Eng. **34**(4), 575–592 (2006)
39. White, F.W.: *Fluid Mechanics.* McGraw-Hill, New York, USA (2006)
40. Zamir, M.: *The Physics of Coronary Blood Flow.* Springer, New York (2005)

On the Energy Equality for Weak Solutions of the 3D Navier-Stokes Equations

Alexey Cheskidov, Susan Friedlander, and Roman Shvydkoy

Abstract We prove that the energy equality holds for weak solutions of the Navier-Stokes equations in the functional class $L^3([0,T);\mathcal{D}(A^{5/12}))$, where $\mathcal{D}(A^{5/12})$ is the domain of the fractional power of the Stokes operator.

Keywords Navier-Stokes equations · Weak solutions · Energy equality

1 Introduction

We consider weak solutions to the three dimensional 3D incompressible Navier-Stokes equations (NSE)

$$\begin{cases} \partial_t u - \nu \Delta u + (u \cdot \nabla) u + \nabla p = f, \\ \nabla \cdot u = 0 \end{cases} \tag{1}$$

on a smooth bounded domain $\Omega \subset \mathrm{R}^3$ subject to the Dirichlet boundary condition. We assume $f \in L^1([0,T);L^2(\Omega))$. The classical Leray-Hopf solutions to (1) that belong to $u \in L^\infty L^2_x \cap L^2_t H^1_x$ are known to only satisfy the energy inequality

$$|u(t)|_2^2 + 2\nu \int_{t_0}^t |\nabla u(s)|_2^2 ds \le |u(t_0)|_2^2 + 2 \int_{t_0}^t (f(s) \cdot u(s)) ds, \tag{2}$$

for all $t \in [0,T)$ and almost all $t_0 \in [0,t)$ including $t_0 = 0$ (see [2]). The problem of proving exact energy equality for such solutions is an open problem. In a sequence of papers by Serrin [8], Lions [7], Shinbrot in [9], and more recently, Kukavica [6] it was settled in a stricter regularity class for velocity or pressure. Namely, $u \in L^r_t L^s_x$, with $2/s + 2/r \le 1$ and $s \ge 4$, or $p \in L^2_{t,x}$. The main technical obstacle in proving

S. Friedlander (✉)
Department of Mathematics, Statistics and Computer Science, University of Illinois,
Chicago, IL 60607, USA
e-mail: susan@math.northwestern.edu

R. Rannacher, A. Sequeira (eds.), *Advances in Mathematical Fluid Mechanics*,
DOI 10.1007/978-3-642-04068-9_10,

energy equality is to show vanishing of the energy flux due to the nonlinear term. In context of the related question of energy conservation for weak solutions of the Euler equation ($\nu = 0$, $f = 0$) the optimal regularity of u has been found in terms of Besov-type spaces (see [1, 3–5]):

$$\lim_{y\to 0} \frac{1}{|y|} \int_{\Omega\times[0,T]} |u(x-y,t) - u(x,t)|^3 dxdt = 0. \tag{3}$$

where $\Omega = \mathbb{R}^3$ or $\mathbb{T}^3$. The differential dimension of this space is equivalent to that of $L_t^3 L_x^{9/2}$, which breaks the previously known scaling. On the Sobolev scale the corresponding space is $H^{5/6}$. For Navier-Stokes equation with Dirichlet boundary conditions more practical spaces to use are fractional domains of the Stokes operator A (see [2]). In the scale of those spaces $H^{5/6}$ corresponds to $D(A^{5/12})$. We note that the methods used previously for proving the energy equality in the case of $\mathbb{R}^3$ or $\mathbb{T}^3$ are not applicable to Dirichlet boundary conditions. For such boundary conditions the following theorem is proved in this present paper.

Theorem 1 *Every weakly continuous weak solution* $u : [0,T) \to L^2(\Omega)$ *to* (1) *which belongs to the regularity class* $L_t^3 \mathcal{D}(A^{5/12})_x \cap L_t^2 H_x^1$ *satisfies the energy equality.*

We remark that the energy inequality (2) is not needed in the proof of Theorem 1.

2 Preliminaries

In this section we briefly recall some standard facts (see [2] for details). Let us denote

$$H = \{u \in L^2(\Omega) : \nabla \cdot u = 0, u \cdot n|_{\partial\Omega} = 0\}, \tag{4}$$

and let $\mathbb{P} : L^2(\Omega) \to H$ be the L^2-orthogonal projection. Let A be the Stokes operator defined by

$$Au = -\mathbb{P}\Delta u. \tag{5}$$

The Stokes operator is a self-adjoint positive vectorial operator with a compact inverse. Hence, there exists an orthonormal basis of eigenvectors $\{w_n\}$ in H, and a sequence of positive eigenvalues

$$\lambda_1 \le \lambda_2 \le \ldots \le \lambda_n \to \infty,$$

such that

$$Aw_n = \lambda_n w_n, \qquad w_n \in \mathcal{D}(A), \tag{6}$$

Henceforth we will use the notation $u_n = (u, w_n)$. For $s > 0$ we define the operator A^s by

$$A^s u = \sum_{n=1}^{\infty} \lambda_n^s u_n w_n, \tag{7}$$

and the space

$$V^s = \{u \in H : u = \sum_{n=1}^{\infty} u_n w_n,\ \|u\|_s^2 = \sum_{n=1}^{\infty} \lambda_n^s |u_n|^2 < \infty\}, \tag{8}$$

which is exactly the domain $\mathcal{D}(A^{s/2})$. We denote $V = V^1$ and V' its dual. Let us put $B(u, v) := \mathbb{P}(u \cdot \nabla v) \in V'$ for $u, v \in V$. We can rewrite (1) as the following differential equation in V':

$$\partial_t u + \nu A u + B(u, u) = g, \tag{9}$$

where u is a V-valued function of time and $g = \mathbb{P} f$. Finally, we denote $b(u, v, w) = \langle B(u, v), w\rangle$. This trilinear form is anti-symmetric:

$$b(u, v, w) = -b(u, w, v), \qquad u, v, w \in V,$$

in particular, $b(u, v, v) = 0$ for all $u, v \in V$.

3 The Proof of Theorem 1

Define

$$P_\kappa u = \sum_{n:\lambda_n \le \kappa^2} u_n w_n, \qquad u \in H. \tag{10}$$

Let $u \in V^\beta$ and denote $u_\kappa^{\mathrm{l}} = P_\kappa u$, $u_\kappa^{\mathrm{h}} = u - u_\kappa^{\mathrm{l}}$. Observe the following inequalities:

$$\begin{aligned} \|u_\kappa^{\mathrm{l}}\|_\beta &\le \kappa^{\beta-\alpha} \|u_\kappa^{\mathrm{l}}\|_\alpha \\ \|u_\kappa^{\mathrm{h}}\|_\alpha &\le \kappa^{\alpha-\beta} \|u_\kappa^{\mathrm{h}}\|_\beta, \end{aligned} \tag{11}$$

whenever $\beta > \alpha$.

Lemma 1 *Let* $u : [0, T) \to H$ *be a weakly continuous weak solution of* (1) *on* $[0, T)$. *Then*

$$|u(t)|^2 + 2\nu \int_{t_0}^{t} \|u\|^2\, ds = |u(t_0)|^2 + 2 \int_{t_0}^{t} (g, u)\, ds + 2 \lim_{\kappa \to \infty} \int_{t_0}^{t} b(u, u_\kappa^{\mathrm{l}}, u)\, ds,$$

for all $0 \le t_0 \le t < T$.

Proof One can see from our assumption that $u_\kappa^{\mathrm{l}} \in C([0,T);V)$ and $\partial_t u_\kappa^{\mathrm{l}} \in L^2([0,T);V)$. Thus, using u_κ^{l} as a test function (allowed by the standard approximation argument) we obtain

$$|u_\kappa^{\mathrm{l}}(t)|^2 - |u_\kappa^{\mathrm{l}}(t_0)|^2 + 2\nu \int_{t_0}^{t} \|u_\kappa^{\mathrm{l}}\|^2\, ds - 2\int_{t_0}^{t} (g, u_\kappa^{\mathrm{l}})\, ds$$
$$= 2\int_{t_0}^{t} b(u, u_\kappa^{\mathrm{l}}, u)\, ds. \tag{12}$$

From this we see that the limit of the right hand side exists as $\kappa \to \infty$, which completes the proof of the lemma. □

Let u_κ^{l} and u_κ^{h} be defined as before. In view of Lemma 1, it suffices to show that

$$\lim_{\kappa\to\infty} \int_0^T |b(u, u_\kappa^{\mathrm{l}}, u)|\, ds = 0. \tag{13}$$

To this end let us write

$$b(u, u_\kappa^{\mathrm{l}}, u) = b(u_\kappa^{\mathrm{h}}, u_\kappa^{\mathrm{l}}, u_\kappa^{\mathrm{h}}) + b(u_\kappa^{\mathrm{l}}, u_\kappa^{\mathrm{l}}, u_\kappa^{\mathrm{h}}) + b(u_\kappa^{\mathrm{h}}, u_\kappa^{\mathrm{l}}, u_\kappa^{\mathrm{l}}) + b(u_\kappa^{\mathrm{l}}, u_\kappa^{\mathrm{l}}, u_\kappa^{\mathrm{l}}).$$

The last two terms vanish, so it suffices to estimate only the first two. We use the standard estimate found, for example, in [2]:

$$|b(u, v, w)| \le \|u\|_{s_1}\|v\|_{s_2+1}\|w\|_{s_3} \tag{14}$$

where $s_1 + s_2 + s_3 \ge 3/2$. To estimate the first term let us set $s_1 = s_2 = s_3 = 1/2$, then

$$|b(u_\kappa^{\mathrm{h}}, u_\kappa^{\mathrm{l}}, u_\kappa^{\mathrm{h}})| \le \|u_\kappa^{\mathrm{h}}\|_{1/2}^2 \|u_\kappa^{\mathrm{l}}\|_{3/2},$$

and by (11) we have

$$\|u_\kappa^{\mathrm{h}}\|_{1/2} \le \kappa^{-1/3}\|u_\kappa^{\mathrm{h}}\|_{5/6} \tag{15}$$
$$\|u_\kappa^{\mathrm{l}}\|_{3/2} \le \kappa^{2/3}\|u_\kappa^{\mathrm{l}}\|_{5/6}. \tag{16}$$

So,

$$|b(u_\kappa^{\mathrm{h}}, u_\kappa^{\mathrm{l}}, u_\kappa^{\mathrm{h}})| \le \|u_\kappa^{\mathrm{h}}\|_{5/6}^2 \|u_\kappa^{\mathrm{l}}\|_{5/6},$$

which tends to zero a.e. in t as $\kappa \to \infty$. Since in addition,

$$|b(u_\kappa^{\mathrm{h}}, u_\kappa^{\mathrm{l}}, u_\kappa^{\mathrm{h}})| \le \|u\|_{5/6}^3$$

for all t, by the Dominated Convergence Theorem,

$$|b(u_\kappa^{\mathrm{h}}, u_\kappa^{\mathrm{l}}, u_\kappa^{\mathrm{h}})| \to 0, \qquad \text{as} \qquad \kappa \to \infty,$$

in $L^1([0, T])$. As to the second term, similar estimates with $s_1 = 5/6$, $s_2 = 0$, $s_3 = 2/3$, yield

$$|b(u_\kappa^{\mathrm{l}}, u_\kappa^{\mathrm{l}}, u_\kappa^{\mathrm{h}})| \leq \|u_\kappa^{\mathrm{l}}\|_{5/6}^2 \|u_\kappa^{\mathrm{h}}\|_{5/6},$$

which also tends to zero in $L^1([0, T])$ as $\kappa \to \infty$. This finishes the proof of (13) and the theorem.

Acknowledgments The work of AC was partially supported by NSF PHY grant 0555324, the work of SF by NSF DMS grant 0503768, and the work of RS by NSF DMS grant 0604050.

References

1. Cheskidov, A., Constantin, P., Friedlander, S., Shvydkoy, R.: Energy conservation and Onsager's conjecture for the Euler equations. Nonlinearity, **21**, 1233–1252 (2008)
2. Constantin., P. and Foias, C.: *Navier-Stokes Equations.* Chicago Lect. Math., Univ. of Chicago Press., Chicago (1988)
3. Constantin, P., Weinan, E., Titi, E.S.: Onsager's conjecture on the energy conservation for solutions of Euler's equation. Comm. Math. Phys., **165**(1), 207–209 (1994)
4. Duchon, J., Robert. R.: Inertial energy dissipation for weak solutions of incompressible Euler and Navier-Stokes equations. Nonlinearity, **13**(1), 249–255 (2000)
5. Eyink, G.L.: Energy dissipation without viscosity in ideal hydrodynamics. I. Fourier analysis and local energy transfer. Phys. D, **78**(3–4), 222–240 (1994)
6. Kukavica, I.: Role of the pressure for validity of the energy equality for solutions of the Navier-Stokes equation. J. Dyn. Differ. Equations, **18**(2), 461–482 (2006)
7. Lions, J. L. Sur la régularité et l'unicité des solutions turbulentes des équations de Navier Stokes. Rend. Sem. Mat. Univ. Padova, **30**, 16–23 (1960)
8. Serrin, J.: The initial value problem for the Navier-Stokes equations. In: Nonlinear Problems. Proc. Sympos. Madison, pp. 69–98 (1963)
9. Shinbrot, M.: The energy equation for the Navier-Stokes system. SIAM J. Math. Anal., **5** pp. 948–954 (1974)

The $(p-q)$ Coupled Fluid-Energy Systems

Luisa Consiglieri

Abstract We investigate the nonlinear coupled system of elliptic partial differential equations which describes the fluid motion and the energy transfer what we call *the* $(p-q)$ *coupled fluid-energy system* due to p and q coercivity parameters correlated to the motion and heat fluxes, respectively. Due to the simultaneous action of the convective-radiation effects on a part of the boundary, such system leads to a boundary value problem. We present existence results of weak solutions under different constitutive laws for the Cauchy stress tensor with $p > 3n/(n+2)$, in a n-dimensional space. If the Joule effect is neglected in the energy equation, the existence result is stated for a broader class of fluids such that $p > 2n/(n+1)$, and related q-coercivity parameter to the heat flux.

Keywords Non-Newtonian fluids · Convective-radiative heat transfer · Joule effect · Weak solution · Convex analysis

1 The Formulation of the Problem

Let Ω be an open bounded set of $\mathbb{R}^n$ $(n > 1)$ with a sufficiently smooth boundary $\partial\Omega$. The equations governing the heat transport in incompressible viscous fluids at steady-state consist of

$$(\mathbf{u}\cdot\nabla)\mathbf{u} - \nabla\cdot\tau = -\nabla\pi + \mathbf{f} \text{ in } \Omega \tag{1}$$

$$\nabla\cdot\mathbf{u} = \sum_{i=1}^{n}\frac{\partial u_i}{\partial x_i} = 0 \text{ in } \Omega \tag{2}$$

$$\mathbf{u}\cdot\nabla e - \nabla\cdot(\chi(\cdot,e)\mathbf{a}(\nabla e)) = \tau : D\mathbf{u} + g \text{ in } \Omega. \tag{3}$$

L. Consiglieri (✉)
Department of Mathematics and CMAF, Sciences Faculty, University of Lisbon,
1749-016 Lisboa, Portugal,
e-mail: lcconsiglieri@fc.ul.pt

R. Rannacher, A. Sequeira (eds.), *Advances in Mathematical Fluid Mechanics*,
DOI 10.1007/978-3-642-04068-9_11,

Here $\mathbf{u}$ and e are unknown functions denoting the fluid velocity vector and the specific (i.e., per unit mass) internal energy, respectively, the density ϱ is assumed equal to one, $\mathbf{f}$ and g represent the external and the heat forces, respectively, π denotes the pressure, and $D = (\nabla + \nabla^T)/2$ denotes the symmetrized velocity gradient. We suppose the generalized Fourier law for heat flux, where χ denotes the diffusity,

$$\mathbf{q} = -\chi(\cdot, e)\mathbf{a}(\nabla e)$$

to be consistent with the following constitutive relations between the deviator stress tensor τ and the kinematical and thermal quantities [14].

The differentiable flux. The Cauchy stress tensor σ for the class of non-Newtonian fluids considered here as dependent on the temperature is defined by

$$\sigma = -\pi I + \nu(\cdot, \theta)\tau(D\mathbf{u}), \tag{4}$$

where I is the identity matrix, ν the viscosity, θ the temperature, and $\tau : \mathbb{M}^{n\times n}_{\text{sym}} \to \mathbb{M}^{n\times n}_{\text{sym}}$ is a continuous function which satisfies the conditions of p-coercivity

$$\exists \tau_1 > 0\, \exists \varphi_1 \in L^1(\Omega): \quad \tau(\varkappa) : \varkappa \geq \tau_1 |\varkappa|^p - \varphi_1, \tag{5}$$

of polynomial growth of the power $p - 1$

$$\exists \tau_2 > 0\, \exists \varphi_2 \in L^{p/(p+1)}(\Omega): \quad |\tau(\varkappa)| \leq \tau_2 |\varkappa|^{p-1} + \varphi_2, \tag{6}$$

and of strict monotonicity

$$\Big(\tau(\zeta) - \tau(\varkappa)\Big) : (\zeta - \varkappa) > 0, \tag{7}$$

for any symmetric matrix $\zeta, \varkappa \in \mathbb{M}^{n\times n}_{\text{sym}}$, $\zeta \neq \varkappa$, and taking into account the convention on implicit summation over repeated indices $\zeta : \varkappa = \zeta_{ij}\varkappa_{ij}$.

The non-differentiable flux. The deviator stress tensor τ is defined as a subgradient, i.e.,

$$\tau \in \nu(\cdot, \theta)\partial F(D\mathbf{u}), \tag{8}$$

where ∂ denotes the subdifferential of F at the point $D\mathbf{u}$ with F a convex functional known as superpotential. Indeed $F : \mathbb{M}^{n\times n}_{\text{sym}} \to \mathbb{R}^+_0$ is a continuous and strictly convex function such that $F(0) = 0$, and for some $p > 1$

$$\exists \tau_1, \tau_2 > 0 : \; \tau_1 |\zeta|^p \leq F(\zeta) \leq \tau_2(|\zeta|^p + 1), \; \forall \zeta \in \mathbb{M}^{n\times n}_{\text{sym}}, \tag{9}$$

with $|\zeta| = (\zeta : \zeta)^{1/2}$.

Considering that the specific heat capacity at constant volume is

$$c_v(\theta) = \frac{de}{d\theta}(\theta) > 0,$$

we assume invertible the nonlinear relation between the specific internal energy e and the temperature θ

$$e = e(\theta) \Leftrightarrow \theta = \theta(e).$$

Then the viscosity is given by $\mu(\cdot, e) = \nu(\cdot, \theta(e))$.

Definition 1 We say that (1), (2) and (3) is a $(p-q)$ *coupled fluid-energy system* if τ obeys (4), (5), (6) and (7) or (8) and (9) and $\mathbf{a}$ corresponds to a nonlinear generalization related with the $p-$growth of the constitutive law for the flow, that is, $\mathbf{a} : \mathbb{R}^n \to \mathbb{R}^n$ is a continuous function which satisfies the conditions

$$\exists \alpha_1 > 0 \, \exists \psi_1 \in L^1(\Omega): \quad \mathbf{a}(\varkappa) \cdot \varkappa \geq \alpha_1 |\varkappa|^q - \psi_1 \tag{10}$$

$$\exists \alpha_2 > 0 \, \exists \psi_2 \in L^{q/(q+1)}(\Omega): \quad |\mathbf{a}(\varkappa)| \leq \alpha_2 |\varkappa|^{q-1} + \psi_2, \quad \forall \varkappa \in \mathbb{R}^n \tag{11}$$

$$\Big(\mathbf{a}(\zeta) - \mathbf{a}(\varkappa)\Big) \cdot (\zeta - \varkappa) > 0, \quad \forall \zeta, \varkappa \in \mathbb{R}^n, \ \zeta \neq \varkappa. \tag{12}$$

The application of the developed theory allows to avoid the study of the free boundaries between the different flow regions (e.g. rigid/plastic zones). The $(p-q)$ coupled fluid-energy system includes the Navier-Stokes fluid coupled with Fourier law ($p = q$), namely when $\tau \equiv id$ ($p = 2$), $\mathbf{a} \equiv \mathbf{id}$ ($q = 2$) and the thermal conductivity given by

$$k(\cdot, \theta) = \chi(\cdot, e(\theta)) c_v(\theta).$$

This model also includes the generalized Newtonian fluids (see, for instance, [1, 2, 13, 16] and the references therein) in particular the power-law fluid and its variants describing as the shear thinning and shear thickening behaviors, the modified Navier-Stokes system introduced by Ladyzenskaya [11], and the p-Laplacian. Otherwise the Bingham viscoplastic fluid does not flow at all unless acted on by at least some critical shear stress (the plasticity threshold) dependent on the temperature θ which can be modeled by (8).

The Lipschitz continuous boundary $\partial\Omega$ is assumed to consist of two disjoint open parts Γ_0 and Γ such that $\partial\Omega = \bar{\Gamma}_0 \cup \bar{\Gamma}$ and $\mathrm{meas}(\Gamma_0) > 0$. For p and $q > 1$ correlated one each other, we present a solution $(\mathbf{u}, e) \in \mathbf{W}^{1,p}(\Omega) \times W^{1,q}(\Omega)$ satisfying what we call *the* $(p-q)$ *coupled fluid-energy system* under the following boundary conditions

$$\mathbf{u} = \mathbf{0} \text{ on } \partial\Omega \tag{13}$$

$$e = e_0 \text{ on } \Gamma_0, \ \chi(\cdot, e)\mathbf{a}(\nabla e) \cdot \mathbf{n} + \gamma(\cdot, e) = h \text{ on } \Gamma := \partial\Omega \setminus \bar{\Gamma}_0, \tag{14}$$

where $\mathbf{n} = (n_i)$ denotes the unit outward normal to Γ. For the sake of clarity we assume that $e_0 \equiv 0$.

Traditionally the radiation effects have been described by Stefan-Boltzmann law, which represents 'radiation-to-infinity'. The radiative heat flux is given by $q_r = \varepsilon\sigma(\theta^4 - \theta_0^4)$, where ε represents the emissivity coefficient, σ the Stefan-Boltzmann constant, θ the temperature which satisfies $\theta = \theta(e)$, and θ_0^4 the effective external radiation temperature. Hence, γ and h denote the outgoing radiation, $\gamma(e) = \varepsilon\sigma\theta^4(e)$, and the incoming radiation, $h = \varepsilon\sigma\theta_0^4$, respectively. This emission reflects the radiative flux on a convex Γ [10].

However industrial devices such as furnaces with surfaces which permit emitted as well as incident radiation require convective-radiation effect coupled with a nonlocal boundary condition. Thus, when the surface Γ is not convex, the outgoing radiation is a combination of emission and reflected fraction of incoming radiation which receives radiation from other parts of itself (see [5, 6] and the references therein). Moreover, since Γ is not an enclosure, then $\gamma : \Gamma \times \mathbb{R} \to \mathbb{R}$ is a Carathéodory function such that

$$\exists l \geq 1, \ \exists \gamma_1 > 0, \qquad \gamma(x,e)\operatorname{sign} e \geq \gamma_1 |e|^l, \tag{15}$$

$$\exists \gamma_2 > 0, \qquad |\gamma(x,e)| \leq \gamma_2 (1 + |e|)^l, \tag{16}$$

$$(\gamma(x,e) - \gamma(x,\xi))\operatorname{sign}(e - \xi) > 0, \ \text{a.e. } x \in \Gamma, \ \forall e, \xi \in \mathbb{R}, \tag{17}$$

for limited physical values of the emissivity, $0 \leq \varepsilon(x) \leq 1 (\varepsilon \not\equiv 0)$. When $l = 1$, (14) corresponds to a convection condition. In the case $l = 4$, it corresponds to the radiative heat transfer condition.

We refer to the work [3] where the class of non-Newtonian fluids has a non-differentiable velocity-stress flux but a Fourier law of heat conduction to the heat flux, under a convective boundary condition, that is, $\gamma(\cdot, e) = h(\cdot, e)e$ with a bounded Carathéodory function h. In the work [5] the Navier-Stokes-Fourier fluid is studied under a convective-radiative boundary condition, but the exponent l is restricted undirectly by the exponents couple $(p - q)$. The reader can find in [7] the study for the coupled fluid-energy system when slip boundary conditions are also taken into account. The existence of solution to the coupled system for $2n/(n+1) < p \leq 3n/(n+2)$ based on the $L^\infty-$ truncation method can be found in [6]. The unsteady-state case on the $(p - q)$ coupled fluid-energy systems has been studied since [4].

The outline of the paper is as follows: in next section we establish the appropriate functional framework and we state the main results. Section 3 is devoted to the proofs of the existence of a solution for the coupled fluid-energy system when the Joule effect is neglected, in Sect. 3.1 for $q > 2n/(n+1)$ if $p \geq n$, and $q > 2np/(p(n+2) - n)$ if $3n/(n+2) < p < n$ (see Fig. 1), in Sect. 3.2 for $q > np/(p(n+1) - n)$ if $2n/(n+1) < p \leq 3n/(n+2)$, and in Sect. 3.3 when the external forces involve the energy. In Sect. 4 we prove the existence of a weak solution provided that $q > 2 - 1/n$ if $p \geq n$, and $q > n(2p-1)/(p(n+1) - n)$

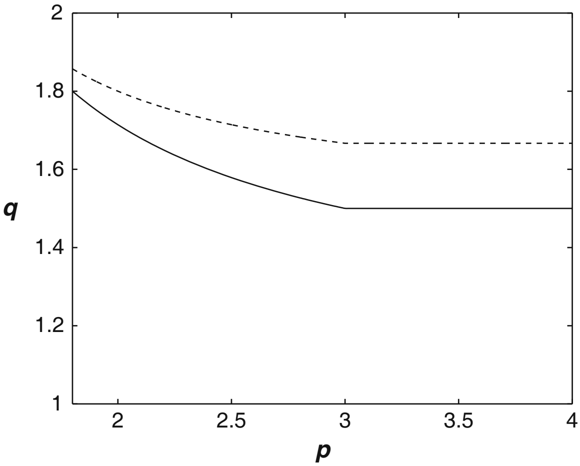

Fig. 1 In 3D, the relations $(p-q)$: $q = 6p/(5p-3)$ if $9/5 < p < 3$, $q = 3/2$ if $p \geq 3$ (*solid line*) and $q = (6p-3)/(4p-3)$ if $9/5 < p < 3$, $q = 5/3$ if $p \geq 3$ (*dashed line*)

if $3n/(n+2) < p < n$ (see Fig. 1), when the Joule effect is taken into account. We apply different fixed point arguments.

The problem of finding a weak solution for the larger range to the coercivity parameter $2n/(n+2) < p \leq 2n/(n+1)$ is still an open problem for coupled fluid-energy systems.

2 Existence Results

In the framework of Lebesgue and Sobolev spaces, we introduce the Banach spaces, for $p, q > 1$, $l \geq 1$ and $p' = p/(p-1)$,

$$\begin{aligned} \mathcal{V} &= \{\mathbf{v} \in \mathbf{C}_0^\infty(\Omega) : \ \nabla \cdot \mathbf{v} = 0 \text{ in } \Omega\} \\ H_p = \overline{\mathcal{V}}^{\|\cdot\|_{p,\Omega}} &= \{\mathbf{v} \in \mathbf{L}^p(\Omega) : \ \nabla \cdot \mathbf{v} = 0 \text{ in } \Omega, \ v_N = 0 \text{ on } \partial\Omega\} \\ V_p = \overline{\mathcal{V}}^{\|\cdot\|_{1,p,\Omega}} &= \{\mathbf{v} \in \mathbf{W}_0^{1,p}(\Omega) : \ \nabla \cdot \mathbf{v} = 0 \text{ in } \Omega\} \\ Y_{p'} &= \{\tau = (\tau_{ij}) : \ \tau_{ij} = \tau_{ij} \in L^{p'}(\Omega), \ \nabla \cdot \tau \in (V_p)'\} \\ X_{q,l} &= \{e \in W^{1,q}(\Omega) \cap L^l(\Gamma) : \ e = 0 \text{ on } \Gamma_0\}, \end{aligned}$$

where X' means the dual space of the Banach space X and it is implicit that the symbol $\cap$ represents the function and its trace. Applying the Trace Theorem, it follows

$$X_{q,l} \equiv W_q := \{e \in W^{1,q}(\Omega) : \ e = 0 \text{ on } \Gamma_0\}$$

if $q \geq nl/(n+l-1)$ or equivalently $l \leq q(n-1)/(n-q)$ for $q < n$. Considering the Poincaré inequality, we can endow the above spaces with the standard norms

$$\|\mathbf{v}\|_{V_p} = \|D\mathbf{v}\|_{p,\Omega}, \quad \|e\|_{X_{q,l}} := \|\nabla e\|_{q,\Omega} + \|e\|_{l,\Gamma}, \quad \|e\|_{W_q} = \|\nabla e\|_{q,\Omega}.$$

2.1 The Differentiable Flux

If we neglect the source term in the energy equation due to the Joule effect, the coupling behavior is due to the fact that physical parameters depend on the temperature. Indeed, these parameters depend not only on the temperature but on the position as well and this prevents us from using Kirchoff transformation to eliminate the nonlinearity in the conductive term of the energy equation. We assume that $\mu, \chi : \Omega \times \mathbb{R} \to \mathbb{R}^+$ are Carathéodory functions, that is, measurable with respect to $x \in \Omega$ for every $e \in \mathbb{R}$, and continuous with respect to $e \in \mathbb{R}$ for almost every $x \in \Omega$ such that

$$\exists \mu_1, \mu_2 > 0: \ \mu_1 \leq \mu(\cdot, e) \leq \mu_2, \quad \forall e \in \mathbb{R}, \text{ a.e. in } \Omega; \tag{18}$$

$$\exists \chi_1, \chi_2 > 0: \ \chi_1 \leq \chi(\cdot, e) \leq \chi_2, \quad \forall e \in \mathbb{R}, \text{ a.e. in } \Omega. \tag{19}$$

Let us state the following results.

Theorem 1 *Under the assumptions (5), (6) and (7), (10), (11) and (12), (15) and (16) and (18) and (19), for*

$$q > \frac{2np}{p(n+2)-n} \quad \text{and} \quad \frac{3n}{n+2} < p < n\ , \tag{20}$$

or $q > 2n/(n+1)$ and $p \geq n$, let

$$\mathbf{f} \in (V_p)', \quad g \in \left(W^{1,q}(\Omega)\right)' \quad \text{and } h \in L^{(l+1)/l}(\Gamma). \tag{21}$$

Then the (p – q) coupled fluid-energy system has a weak solution $(\mathbf{u}, e) \in V_p \times X_{q,l+1}$ in the following sense

$$\int_\Omega \mu(\cdot, e)\tau(D\mathbf{u}) : D\mathbf{v}dx + \int_\Omega \mathbf{u} \otimes \mathbf{v} : D\mathbf{u}dx = \langle \mathbf{f}, \mathbf{v}\rangle, \quad \forall \mathbf{v} \in V_p, \tag{22}$$

$$\int_\Omega \chi(\cdot, e)\mathbf{a}(\nabla e) \cdot \nabla\varphi dx + \int_\Omega \varphi\mathbf{u} \cdot \nabla e dx + \int_\Gamma \gamma(\cdot, e)\varphi d\Gamma =$$
$$= \langle g, \varphi\rangle + \int_\Gamma h\varphi d\Gamma, \quad \forall \varphi \in X_{q,l+1}, \tag{23}$$

where the symbol $\langle \cdot, \cdot \rangle$ denotes a generic duality pairing, not distinguished between scalar and vector fields.

Remark 1 The convective term $\int_\Omega \mathbf{w}\otimes\mathbf{v} : D\mathbf{u}dx$ is well defined for $\mathbf{u}, \mathbf{v},\ \mathbf{w}\in V_p$ if $p\geq 3n/(n+2)$ [11, 12]. For $q > 2n/(n+1)$ arbitrary, the convective term $\int_\Omega \varphi\mathbf{u}\cdot\nabla e dx$ is well defined for $\mathbf{u}\in H_t$ and $e,\varphi\in W^{1,q}(\Omega)$, if

$$\begin{cases} t\geq nq/(q(n+1)-2n) \\ q<n \end{cases} \text{ or } \begin{cases} t>n'=n/(n-1) \\ q=n \end{cases} \text{ or } \begin{cases} t\geq q' \\ q>n. \end{cases} \tag{24}$$

Moreover, both terms satisfy the anti-symmetry property due to the incompressibility condition (2) and the Dirichlet condition (13). Notice that the restriction $p > 3n/(n+2)$ is a sufficient condition to the existence of $t \in]pn/(p(n+1)-2n), pn/(n-p)[$. The restriction $q > 2pn/(p(n+2)-n)$ is a sufficient condition to the existence of $t < pn/(n-p)$ verifying (24).

Theorem 2 *Under all assumptions in Theorem 1 except (20) consider*

$$\frac{2n}{n+1} < p \leq \frac{3n}{n+2} \quad \textit{and} \quad q > \frac{np}{p(n+1)-n}\,. \tag{25}$$

Then there exists a solution to the problem (22) and (23), for $\mathbf{v}\in\mathcal{V}$ *and* $\varphi\in C_0^\infty(\Omega)$.

Remark 2 The convective terms $\int_\Omega \mathbf{w}\otimes\mathbf{v} : D\mathbf{u}dx$ and $\int_\Omega \varphi\mathbf{u}\cdot\nabla e dx$ are still meaningful for $\mathbf{v}\in\mathcal{V}$ and $\mathbf{w},\mathbf{u}\in V_p$ for $p\geq 2n/(n+1)$; and for $\varphi\in L^\infty(\Omega)$, $e\in W^{1,q}(\Omega)$, considering $q > np/(p(n+1)-n)$ which means $nq/(n-q) > p'$ or equivalently $np/(n-p) > q'$. However the anti-symmetry properties are no more valid.

When the external body forces are dependent on the specific internal energy in the form $\mathbf{f}=(e-\bar{e})\mathbf{b}$, for some given functions $\bar{e}$ and $\mathbf{b}$, the coupled system is motivated by the buoyancy driven flow, also known as free or natural convection flow. The motion of a viscous fluid driven by buoyancy forces is in fact generated by density gradients which are not aligned with the gravitational acceleration vector $\mathbf{g}$ and the variation of density is usually provoked by some external heat source, that means, $\mathbf{b}=-\beta\mathbf{g}$ with β denoting the volumetric factor of thermal expansion. Assuming that the variation in density is negligible which corresponds to the constraint of incompressibility (2), we can state the following result.

Theorem 3 *There exists a solution in the conditions of Theorems 1 and 2, if* $\mathbf{f}=\mathbf{b}e$, *with* $\mathbf{b}\in\mathbf{L}^\infty(\Omega)$.

2.2 *The Nondifferentiable Flux*

The minimization problem related to (1), (2) and (8) in its weak formulation (29) follows from the property of subdifferentiability

$$\partial F(D\mathbf{u}) = (-\nabla\cdot)\partial(F\circ D)(\mathbf{u}), \tag{26}$$

for a continuous convex functional F. Indeed, using the definition of subdifferential ∂ in (8) and considering (26) and (1), we find

$$\langle \mathbf{f} - (\mathbf{u}\cdot\nabla)\mathbf{u}, \mathbf{v}-\mathbf{u}\rangle \leq J(e, D\mathbf{v}) - J(e, D\mathbf{u}), \quad \forall \mathbf{v}\in V_p,$$

which corresponds to (29), where $J : L^1(\Omega)\times V_p \to \mathbb{R}_0^+$ is such that

$$J(e,\mathbf{v}) = \int_\Omega \mu(\cdot, e)F(D\mathbf{v})dx.$$

Finally we assume that

$$\mathbf{f}\in (V_p)', \quad g\in L^1(\Omega) \quad \text{and} \quad h\in L^1(\Gamma). \tag{27}$$

Theorem 4 *Suppose that the assumptions (9), (10), (11) and (12), (15), (16), (17), (18) and (19) and (27) are fulfilled. For*

$$q > \frac{n(2p-1)}{p(n+1)-n} \quad \text{and} \quad \frac{3n}{n+2} < p < n \tag{28}$$

or $q > 2 - 1/n$ *and* $p \geq n$*, then the (p – q) coupled fluid-energy system has a weak solution* $(\mathbf{u}, \tau, e) \in V_p \times Y_{p'} \times X_{r,l}$*, for all* $1 < r < (q-1)n/(n-1)$*, in the following sense*

$$J(e,\mathbf{v}) - J(e,\mathbf{u}) - \int_\Omega (\mathbf{u}\otimes\mathbf{u}) : D(\mathbf{v}-\mathbf{u})dx \geq \langle \mathbf{f}, \mathbf{v}-\mathbf{u}\rangle, \quad \forall \mathbf{v}\in V_p; \tag{29}$$

$$\int_\Omega (\chi(e)\mathbf{a}(\nabla e) - e\mathbf{u})\cdot\nabla\varphi dx + \int_\Gamma \gamma(\cdot, e)\varphi d\Gamma =$$
$$= \int_\Omega (\tau : D\mathbf{u} + g)\varphi dx + \int_\Gamma h\varphi d\Gamma, \quad \forall\varphi\in W_{r/(r-q+1)}, \tag{30}$$

and (8) is satisfied.

The convective term in (30) is meaningful for $\mathbf{u}\in H_t$, $e\in W^{1,r}(\Omega)$ and $\varphi\in W^{1,r/(r-q+1)}(\Omega)$ if $t\geq r'$. Thus the requirement

$$\max(pn/(p(n+1)-2n), r') \leq t < pn/(n-p)$$

leads to the restriction (28). Then all the terms on (30) have sense, since $\varphi\in W^{1,r/(r-q+1)}(\Omega)\hookrightarrow C(\bar{\Omega})$ for $r/(r-q+1) > n$, that is, $r < (q-1)n/(n-1)$.

3 The Differentiable Flux

Let us recall the Tychonoff extension to weak topologies of the Schauder fixed point theorem [17, pp. 452].

Theorem 5 *Let K be a nonempty closed bounded convex subset of a reflexive separable Banach space X. Let $\mathcal{L} : K \to K$ be a weakly sequential continuous operator. Then $\mathcal{L}$ has at least one fixed point.*

3.1 Proof of Theorem 1

The proof of Theorem 1 is based on the following fixed point argument (cf. Theorem 5): defining

$$K := \{(\mathbf{w}, \xi) \in V_p \times X_{q,l+1} : \|\mathbf{w}\|_{V_p} \le R_1, \|\xi\|_{X_{q,l+1}} \le R_2\},$$

with R_1 and R_2 given as in (32) and (34), respectively, and the operator $\mathcal{L}$ by $\mathcal{L}(\mathbf{w}, \xi) = (\mathbf{u}, e)$, where $\mathbf{u}$ and e are the following fluid velocity and energy solutions, respectively.

FLUID VELOCITY SOLUTION. For a fixed $\mathbf{w} \in H_t$, for t verifying (24), and $\xi \in L^1(\Omega)$ the existence of the solution $\mathbf{u} = \mathbf{u}(\mathbf{w}, \xi)$ for the problem

$$\int_\Omega (\mu(\cdot, \xi)\tau(D\mathbf{u}) - \mathbf{w} \otimes \mathbf{u}) : D\mathbf{v} dx = \langle \mathbf{f}, \mathbf{v} \rangle, \quad \forall \mathbf{v} \in V_p , \tag{31}$$

holds in V_p for all $p \ge 3n/(n+2)$. Choosing $\mathbf{v} = \mathbf{u} \in V_p$ as a test function in (31), we can state the following result.

Lemma 1 *Under the assumptions (5), (18) and (21), the solution $\mathbf{u}$ of (31) is such that:*

$$\|\mathbf{u}\|_{V_p} \le \left(\frac{\|\mathbf{f}\|^{p'}_{(V_p)'}}{(\mu_1\tau_1)^{p'}} + \frac{p'\mu_2}{\mu_1\tau_1}\|\varphi_1\|_{1,\Omega} \right)^{1/p} := R_1. \tag{32}$$

ENERGY SOLUTION. The existence of the solution $e = e(\mathbf{u}, \xi)$ for the problem

$$\int_\Omega (\chi(\cdot, \xi)\mathbf{a}(\nabla e) - e\mathbf{u}) \cdot \nabla\varphi dx + \int_\Gamma \gamma(\cdot, e)\varphi d\Gamma = \\ = \langle g, \varphi \rangle + \int_\Gamma h\varphi d\Gamma, \quad \forall \varphi \in X_{q,l+1} , \tag{33}$$

holds in $X_{q,l+1}$ for q satisfying (20). Choosing $\varphi = e \in X_{q,l+1}$ as a test function in (33), we obtain the following result.

Lemma 2 *Under the conditions (10), (15), (19) and (21), the solution e of (33) satisfies the estimate*

$$\|e\|_{X_{q,l+1}} \le C \left[\|g\|^{q'}_{(W^{1,q}(\Omega))'} + \|h\|^{(l+1)/l}_{(l+1)/l,\Gamma} + \chi_2\|\psi_1\|_{1,\Omega} \right]^\lambda := R_2, \tag{34}$$

where $C = C(q, l, \Omega, \chi_1\alpha_1, \gamma_1)$ and $\lambda = \lambda(q, l)$.

Henceforth we denote by C every positive constant depending on n, p, q, l, the domain Ω, and the constants τ_i, α_i, μ_i, χ_i, γ_i $(i = 1, 2)$.

The operator $\mathcal{L}$ is well defined, since from classical theory of monotone operators (see for example [11, 12]), there exist $\mathbf{u} = \mathbf{u}(\mathbf{w}, \xi) \in V_p$ a unique solution to the system (31) as well as $e = e(\mathbf{u}, \xi) \in X_{q,l+1}$ a unique solution to the problem (33). Lemmas 1 and 2 guarantee that $\mathcal{L}$ maps K into itself. Since that, for $(p-q)$ verifying (20), $\mathbf{w}_m \rightharpoonup \mathbf{w}$ in V_p and $\xi_m \rightharpoonup \xi$ in $X_{q,l+1}$ imply that $\mathbf{u}_m \rightharpoonup \mathbf{u}$ in V_p and $e_m \to e$ in $W^{1,q}(\Omega)-$weak, $L^1(\Omega)-$strong and $L^l(\Gamma)-$strong, the proof of Theorem 1 holds (for details see [6]).

3.2 *Proof of Theorem 2*

The proof is based on a fixed point argument for the following approximate problem (cf. [6]). For $M \in \mathbb{N}$ and

$$t > \max\left(\frac{2p}{p-1}, \frac{nq}{q(n+1)-2n}\right),$$

find $(\mathbf{u}_M, e_M)$ satisfying

$$\int_\Omega \mu(\cdot, e_M)\tau(D\mathbf{u}_M) : D\mathbf{v}dx + \int_\Omega \mathbf{u}_M \otimes \mathbf{v} : D\mathbf{u}_M dx + \\ + \frac{1}{M}\int_\Omega |\mathbf{u}_M|^{t-2}\mathbf{u}_M \cdot \mathbf{v}dx = \langle \mathbf{f}, \mathbf{v}\rangle, \quad \forall \mathbf{v} \in \mathcal{V}; \tag{35}$$

$$\int_\Omega \chi(\cdot, e_M)\mathbf{a}(\nabla e_M)\cdot\nabla\varphi dx + \int_\Omega \varphi\mathbf{u}_M\cdot\nabla e_M dx + \int_\Gamma \gamma(\cdot, e_M)\varphi d\Gamma = \\ = \langle g, \varphi\rangle + \int_\Gamma h\varphi d\Gamma, \quad \forall\varphi \in C_0^\infty(\Omega). \tag{36}$$

In order to apply Theorem 5, let $\mathcal{L} : K \to K$ be the operator defined by

$$\mathcal{L} : (\mathbf{w}, \xi) \in V_p \times X_{q,l+1} \mapsto (\mathbf{u}_M, e_M),$$

where $\mathbf{u}_M = \mathbf{u}_M(\mathbf{w}, \xi) \in V_p \cap H_t$ is the solution to the system

$$\int_\Omega (\mu(\cdot, \xi)\tau(D\mathbf{u}_M) - \mathbf{w}\otimes\mathbf{u}_M) : D\mathbf{v}dx + \frac{1}{M}\int_\Omega |\mathbf{u}_M|^{t-2}\mathbf{u}_M\cdot\mathbf{v}dx = \\ = \langle \mathbf{f}, \mathbf{v}\rangle, \quad \forall \mathbf{v} \in V_p \tag{37}$$

and $e_M = e_M(\mathbf{u}_M, \xi) \in X_{q,l+1}$ is the solution to the equation

$$\int_\Omega (\chi(\cdot, \xi)\mathbf{a}(\nabla e_M) - e_M\mathbf{u}_M)\cdot\nabla\varphi dx + \int_\Gamma \gamma(\cdot, e_M)\varphi d\Gamma = \\ = \langle g, \varphi\rangle + \int_\Gamma h\varphi d\Gamma, \quad \forall\varphi \in X_{q,l+1}. \tag{38}$$

The existence and uniqueness of solutions to (37) and (38) arises as in the proof of Theorem 1. Note that $2p/(p-1) \geq pn/(n-p)$ (the critical value of Sobolev-Rellich embedding) for $p \leq 3n/(n+2)$. Moreover, the following uniform estimate holds

$$\|D\mathbf{u}_M\|_{p,\Omega}^p + \frac{1}{M}\|\mathbf{u}_M\|_{t,\Omega}^t \leq R_1^p$$

as well as (34). Thus $\mathcal{L}$ is a well defined operator that maps K into itself, and it is weakly sequential continuous. Hence Theorem 5 guarantees the existence of a weak solution $(\mathbf{u}_M, e_M)$ to the approximate problem (35) and (36). Passing to the limit as M tends to infinity we conclude the proof of Theorem 2 (for details see [6]).

3.3 Proof of Theorem 3

The proof is similar to the proofs of Theorems 1 and 2 freezing the term $\mathbf{f} = \mathbf{b}\xi \in L^{qn/(n-q)}(\Omega)$ in (31) and in (37), respectively, and defining R_2 by (34) and

$$R_1 := \left(\frac{R_2\|\mathbf{b}\|_{\infty,\Omega}^{p'}}{(\mu_1\tau_1)^{p'}} + \frac{p'\mu_2}{\mu_1\tau_1}\|\varphi_1\|_{1,\Omega} \right)^{1/p}.$$

For these suitable $R_1, R_2 > 0$, the operator $\mathcal{L}$ is well defined. Its weakly sequential continuity holds by compactness arguments.

4 The Nondifferentiable Flux

Proof of Theorem 4

First we recall the fixed point result for multivalued mappings due to Ky Fan and Glicksberg [17, pp. 452, Generalized Theorem of Kakutani].

Theorem 6 *Let K be a nonempty compact convex subset of a locally convex linear topological vector space X. Let $\mathcal{L} : K \to \mathcal{P}(K)$ be a multivalued upper semi-continuous operator such that the set $\mathcal{L}(z)$ is nonempty closed and convex for all $z \in K$. Then $\mathcal{L}$ has at least one fixed point.*

The proof of Theorem 4 is based on the following fixed point argument. Let us consider the space $X := V_p \times L^1(\Omega) \times X_{r,l}$ endowed with the product of weak topologies. Thus X becomes a locally convex Hausdorff topological vector space, and the ball

$$K = \{(\mathbf{w}, \upsilon, \xi) \in X : \|\mathbf{w}\|_{V_p} \leq R_1, \|\upsilon\|_{1,\Omega} \leq R_2, \|\xi\|_{X_{r,l}} \leq R_3\}$$

is a nonempty convex compact set in X, considering R_i $(i = 1, 2, 3)$ the chosen below positive constants. The operator $\mathcal{L}$ defined by

$$\mathcal{L}(\mathbf{w}, \upsilon, \xi) = \{(\mathbf{u}, \tau : D\mathbf{u}, e)\} \subset \mathcal{P}(K)$$

verifies the fixed point argument (cf. Theorem 6). This proof is slip in the following steps. For details, see [3] and [7].

FLUID VELOCITY SOLUTION. For every $\mathbf{w} \in H_t$, for t verifying (24), and $\xi \in L^1(\Omega)$ there exists a unique solution $\mathbf{u} = \mathbf{u}(\mathbf{w}, \xi)$ to the variational inequality

$$J(\xi, \mathbf{v}) - J(\xi, \mathbf{u}) - \int_\Omega (\mathbf{w} \otimes \mathbf{u}) : D(\mathbf{v} - \mathbf{u}) dx \geq \langle \mathbf{f}, \mathbf{v} - \mathbf{u} \rangle, \quad \forall \mathbf{v} \in V_p. \tag{39}$$

The existence and uniqueness of a solution are consequences of classical results (see [12], for instance) on variational inequalities with convex continuous functionals. Choosing $\mathbf{v} = \mathbf{0}$ as a test function in (39) the following estimate holds

$$\|\mathbf{u}\|_{V_p} \leq \left(\frac{\|\mathbf{f}\|_{(V_p)'}}{\mu_1 \tau_1} \right)^{1/(p-1)} := R_1.$$

STRESS SUBGRADIENT SOLUTIONS. Let $\mathbf{u}$ be the fluid velocity solution. From the duality theory of convex analysis [9, pp. 50–52], there exists a Lagrange multiplier $\varsigma = \varsigma(\xi, \mathbf{u}) \in Y_{p'}$ and from the Rham Theorem (see, for instance, [12]) there exists a pressure $\pi \in L^{p'}(\Omega)$ such that

$$\langle -\varsigma, D\mathbf{u} \rangle = J(\xi, D\mathbf{u}) + \int_\Omega \mu(\cdot, \xi) F^* \left(\left| \frac{\varsigma}{\mu(\cdot, \xi)} \right| \right) dx$$
$$(\mathbf{w} \cdot \nabla)\mathbf{u} - \nabla \pi + \nabla \cdot \varsigma = \mathbf{f} \text{ in } \Omega,$$

where F^* represents the conjugate functional of F. The estimates

$$\|\varsigma\|_{p',\Omega} \leq C(\|D\mathbf{u}\|_{p,\Omega}^{p-1} + 1)$$
$$\|\varsigma : D\mathbf{u}\|_{1,\Omega} \leq C(\|D\mathbf{u}\|_{p,\Omega}^{p-1} + 1)\|D\mathbf{u}\|_{p,\Omega} \leq C(R_1^p + R_1) := R_2$$

hold. We set the stress subgradient $\tau = -\varsigma$. Note that we have no uniqueness of τ. However it is known that the subdifferential of the convex functional F (the set of the subgradient solutions) is a convex set.

ENERGY SOLUTION. For each $M \in \mathbb{N}$, define

$$g_M = \frac{M(\upsilon + g)}{M + |\upsilon + g|} \in L^\infty(\Omega) \quad \text{and} \quad h_M = \frac{Mh}{M + |h|} \in L^\infty(\Gamma).$$

From classical elliptic theory, there exists a unique solution $e_M \in X_{q,l+1}$ to the following variational equality

$$\int_\Omega (\chi(\xi)\mathbf{a}(\nabla e_M) - e_M \mathbf{w}) \cdot \nabla \varphi dx + \int_\Gamma \gamma(e_M)\varphi d\Gamma = \int_\Omega g_M \varphi dx + \int_\Gamma h_M \varphi d\Gamma,$$

for all $\varphi \in X_{q,l+1}$. Using L^1−data theory [8, 15], a unique solution $e = e(\mathbf{w}, \upsilon, \xi) \in X_{r,l}$ is obtained as the limit approximation of e_M and the estimate holds, independently on $\mathbf{w}$ and ξ,

$$\|e\|_{X_{r,l}} \leq C(\|\upsilon + g\|_{1,\Omega} + \|h\|_{1,\Gamma})^{\lambda} \leq C(R_2 + \|g\|_{1,\Omega} + \|h\|_{1,\Gamma})^{\lambda} := R_3,$$

with $\lambda = \lambda(n, r, q)$ some positive constant.

CONTINUOUS DEPENDENCE. Let $\{(\mathbf{w}_m, \upsilon_m, \xi_m)\}$ be a sequence in K and $\mathbf{u}_m = \mathbf{u}(\mathbf{w}_m, \xi_m)$, $\tau_m = \tau(\xi_m, \mathbf{u}_m)$ and $e_m = e(\mathbf{w}_m, \upsilon_m, \xi_m)$ be solutions given by the above steps, respectively. Then, there exists $(\mathbf{u}, \tau, e)$ solution to (29), (30) and (8) verifying

$$\begin{aligned} \mathbf{w}_m \rightharpoonup \mathbf{w},\ \mathbf{u}_m \rightharpoonup \mathbf{u} \text{ in } V_p \hookrightarrow\hookrightarrow H_t \cap \mathbf{L}^p(\Gamma); \\ \upsilon_m \rightharpoonup \upsilon,\ \tau_m : D\mathbf{u}_m \rightharpoonup \tau : D\mathbf{u} \text{ in } L^1(\Omega); \\ \xi_m \rightharpoonup \xi,\ e_m \rightharpoonup e \text{ in } X_{r,l} \hookrightarrow\hookrightarrow L^1(\Omega) \cap L^1(\Gamma). \end{aligned}$$

We conclude that the conditions of Theorem 6 are fulfilled and then Theorem 4 holds. For details see [7].

Acknowledgments Partially supported by FEDER and FCT-Plurianual 2007.

References

1. Amann, H.: Heat-conducting incompressible viscous fluids. In: Sequeira, A. (ed.) *Navier-Stokes Equations and Related Nonlinear Problems*, pp. 231–243. Plenum Press, New York (1995)
2. Bird, R.B., Armstrong, R.C., Hassager, O.: *Dynamics of Polymeric Liquids*. Wiley, New York (1977)
3. Consiglieri, L.: Stationary weak solutions for a class of non-Newtonian fluids with energy transfer. Int. J. Non-Linear Mech. **32**, 961–972 (1997)
4. Consiglieri, L.: Weak solutions for a class of non-Newtonian fluids with energy transfer. J. Math. Fluid Mech. **2**, 267–293 (2000)
5. Consiglieri, L.: Thermal radiation in a steady Navier-Stokes flow. Mat. Contemp. **22**, 55–66 (2002)
6. Consiglieri, L.: Steady-state flows of thermal viscous incompressible fluids with convective-radiation effects. Math. Mod. Meth. Appl. Sci. **16**(12), 2013–2027 (2006)
7. Consiglieri, L.: A $(p-q)$ coupled system in elliptic nonlinear problems with nonstandard boundary conditions. J. Math. Anal. Appl. **340** (1), 183–196 (2008)
8. Dall'Aglio, A.: Approximated solutions of equations with L^1 data. Application to the H-convergence of quasi-linear parabolic equations. Ann. Mat. Pura Appl. **170**, 207–240 (1996)
9. Ekeland, I., Temam, R.: *Analyse convexe et problèmes variationnels*. Dunod et Gauthier-Villars, Paris (1974)
10. Kreith, F.: Principles of heat transfer. In: *Intext Series in Mech. Eng., Univ. of Wisconsin* Harper and Row Publ. Madison, (1973)
11. Ladyzenskaya, O.A.: *Mathematical Problems in the Dynamics of a Viscous Incompressible Fluid.* 2nd rev. aug. ed., Nauka, Moscow (1970) English transl. of 1st ed., *The mathematical Theory of Viscous Incompressible Flow.* Gordon and Breach, New York (1969)

12. Lions, J.L.: *Quelques Méthodes de Résolution des Problèmes aux Limites Non Linéaires*. Dunod et Gauthier-Villars, Paris (1969)
13. Naumann, J.: On the existence of weak solutions to the equations of non-stationary motion of heat-conducting incompressible viscous fluids. Math. Meth. Appl. Sci. **29**, 1883–1906 (2006)
14. Panagiotopoulos, P.D.: *Inequality problems in mechanics and applications*. Convex and non-convex energy functions. Birkhäuser, Boston (1985)
15. Prignet, A.: Conditions aux limites non homogènes pour des problèmes elliptiques avec second membre mesure. Ann. Fac. Sci. Toulouse Math. **6**, 297–318 (1997)
16. Rodrigues, J.F.: Thermoconvection with dissipation of quasi-Newtonian fluids in tubes. In: Sequeira, A. (ed.) *Navier-Stokes Equations and Related Nonlinear Problems*, pp. 279–288. Plenum Press, New York (1995)
17. Zeidler, E.: *Nonlinear Functional Analysis and its Applications I: Fixed-Point Theorems*. Springer-Verlag, NY (1986)

A Potential-Theoretic Approach to the Time-Dependent Oseen System

Paul Deuring

Abstract We consider an initial-boundary value problem for the time-dependent Oseen system in a 3D exterior domain. This problem is reduced to an integral equation for the single layer potential related to the the Oseen system. The resolution of this integral equation, in turn, is reduced to a result by Shen, American Journal of Mathematics, 113, 293–373, 1991 on the nonstationary Stokes system.

Keywords Time dependent Oseen system · Single layer potential · Integral equation

1 Introduction

Let $\Omega \subset \mathbb{R}^3$ be a bounded Lipschitz domain with connected boundary, and let U denote the exterior domain $\mathbb{R}^3 \backslash \overline{\Omega}$. Take $T \in (0, \infty]$. Then we consider the time-dependent Oseen system on $Z_T := U \times (0, T)$,

$$\partial_t u - \Delta_x u + \tau \cdot \partial_{x_1} u + \nabla_x p = f, \quad \text{div}_x u = 0 \quad \text{in } Z_T, \tag{1}$$

with a Dirichlet boundary condition on $\partial\Omega$ and zero velocity at infinity,

$$u \mid S_T = b, \quad u(x,t) \to 0 \ \ (|x| \to \infty) \ \text{ for } \ t \in (0, T), \tag{2}$$

where $S_T := \partial\Omega \times (0, T)$. In addition, we impose an initial condition,

$$u(x, 0) = a(x) \ \text{ for } \ x \in U. \tag{3}$$

Our aim is to solve this initial-boundary value problem by means of potential theory. As usual with this access, the given problem will be split into two subproblems. The first is the Cauchy problem

P. Deuring (✉)
Univ Lille Nord de France, F-59000 Lille, France; ULCO, LMPA, F-62228 Calais, France
e-mail: Paul.Deuring@lmpa.univ-littoral.fr

R. Rannacher, A. Sequeira (eds.), *Advances in Mathematical Fluid Mechanics*,
DOI 10.1007/978-3-642-04068-9_12, © Springer-Verlag Berlin Heidelberg 2010

$$\partial_t v - \Delta_x v + \tau \cdot \partial_{x_1} v + \nabla_x \varrho = f, \quad \operatorname{div}_x v = 0 \quad \text{in } \mathbb{R}^3 \times (0, T), \tag{4}$$
$$v(x,t) \to 0 \ \ (|x| \to \infty) \ \text{ for } \ t \in (0,T), \tag{5}$$
$$v(x,0) = a(x) \ \text{ for } \ x \in \mathbb{R}^3, \tag{6}$$

and the second the ensuing initial-boundary value problem:

$$\partial_t w - \Delta_x w + \tau \cdot \partial_{x_1} w + \nabla_x \pi = 0, \quad \operatorname{div}_x w = 0 \quad \text{in } Z_T, \tag{7}$$
$$w \mid S_T = b - v|S_T, \quad w(x,t) \to 0 \ \ (|x| \to \infty) \ \text{ for } \ t \in (0,T), \tag{8}$$
$$w(x,0) = 0 \ \text{ for } \ x \in \Omega. \tag{9}$$

The function v in (8) is the velocity part of the solution to (4), (5) and (6). Under suitable assumptions on the functions a and f, a solution of the Cauchy problem (4), (5) and (6) is given by the convolution of an Oseen fundamental solution with f and a, respectively. The convolution with f is performed with respect to the space and the time variables and will be denoted by $\mathfrak{R}^{(\tau)}(f)$. The convolution with a only involves the space variables; we will denote it by $\mathfrak{I}^{(\tau)}(a)$. (Precise definitions will be given in Sect. 2.) The function $\mathfrak{R}^{(\tau)}(f)$ solves (4), (5) and (6) with $a = 0$, and $\mathfrak{I}^{(\tau)}(a)$ is a solution of (4), (5) and (6) with $f = 0$, so the sum $\mathfrak{R}^{(\tau)}(f) + \mathfrak{I}^{(\tau)}(a)$ satisfies (4), (5) and (6) without f or a necessarily vanishing. (Here and in the rest of this introduction, when we discuss a solution of the Oseen system, we actually consider only the velocity part of such a solution. Regarding the pressure part, we refer to the main body of the paper.)

As concerns the second subproblem, that is, (7), (8) and (9), we want to solve it by a single layer potential $\mathfrak{V}^{(\tau)}(\varphi)$ with a suitable layer function $\varphi \in L^2(S_T)^3$. The potential $\mathfrak{V}^{(\tau)}(\varphi)$ is defined as a Volterra integral in time and as a surface integral on $\partial\Omega$ in space (see (19)), and satisfies (7) and (9) for any $\varphi \in L^2(S_T)^3$. That latter function is determined by the remaining condition (8), which takes the form

$$\mathfrak{V}^{(\tau)}(\varphi) \mid S_T = b - \big(\mathfrak{R}^{(\tau)}(f) + \mathfrak{I}^{(\tau)}(a)\big) \mid S_T. \tag{10}$$

This is an integral equation on S_T with φ as unknown. Thus we are led to study the integral equation

$$\mathfrak{V}^{(\tau)}(\varphi) \mid S_T = c, \tag{11}$$

where c is given and φ is looked for. It is the main purpose of the work at hand to solve this problem.

To this end, we start from a result by Shen [19] involving the single layer potential $\mathfrak{V}^{(0)}(\varphi)$ associated to the time-dependent Stokes system (Eq. (1) with $\tau = 0$). Shen shows that the equation $\mathfrak{V}^{(0)}(\varphi) \mid S_T = c$ admits a unique solution in the space $L^2_n(S_T)$ of L^2-vector fields on S_T having zero flux on $\partial\Omega$ for a. e. $t \in (0,T)$, provided the data c belongs to a certain Sobolev space H_T involving a fractional derivative with respect to the time variable. It is not straightforward to generalize this result to the Oseen system because if $T = \infty$, the mapping $\varphi \mapsto \big(\mathfrak{V}^{(\tau)}(\varphi) - \mathfrak{V}^{(0)}(\varphi)\big) \mid S_T$ does not seem to be compact as an operator from $L^2_n(S_T)$ into H_T.

Instead of compactness, our argument uses the theory of Fredholm operators. With this theory in mind, we show that the term $\big(\mathfrak{V}^{(\kappa)}(\varphi) - \mathfrak{V}^{(0)}(\varphi)\big) \,|\, S_T$, considered as a function of the Reynolds number $\kappa \in [0, \tau]$, is continuous with respect to the norm of operators from $L^2(S_T)$ into H_T (Theorem 4). The proof of this result is the main difficulty we have to handle in order to solve (11).

Still there is another point which requires some effort, namely the proof of uniqueness of the operator $\mathfrak{V}^{(\tau)}(\varphi) \,|\, S_T$ if φ is taken from $L^2_n(S_T)$ (Theorem 6). Although the general approach for obtaining this result is well known, in the present context we have to deal with the problem of giving a sense to certain surface integrals.

Once these two crucial points are settled, it may be shown by Fredholm theory that $\mathfrak{V}^{(\tau)}(\varphi) \,|\, S_T$ as an operator from $L^2_n(S_T)$ into H_T is bijective. Thus, for any $c \in H_T$, there is a unique solution $\varphi \in L^2_n(S_T)$ to equation (11); see Corollary 3. This is the main result of the present article.

However, this result is not sufficient to solve equation (10). In fact, in order to apply our theory for (11) to (10), we first have to make sure that $\big(\mathfrak{R}^{(\tau)}(f) + \mathfrak{I}^{(\tau)}(a)\big) \,|\, S_T$ belongs to H_T. If we do not want to restrict ourselves to smooth functions, this relation is by no means obvious, in particular if $T = \infty$, and will be discussed in another paper [6]. Actually already in [4] we showed that $\mathfrak{R}^{(\tau)}(f) \,|\, S_T \in H_T$ if the function f belongs to certain L^p-spaces. But the criterion in that reference is not well adapted to an eventual application to the nonlinear case (Navier-Stokes system with Oseen term) and should be considered as preliminary. The result we prove in [6] should be more useful in this respect, although we did not yet study the nonlinear case. Also in [6], we show that $\mathfrak{I}^{(\tau)}(a) \,|\, S_T \in H_T$ if $a \in H^\sigma(U)^3$ for some $\sigma \in (1/2, 1]$. Thus, in reference [6], we are in a position to solve the integral equation (10) by applying Corollary 3 below to (11) with $c = b - \big(\mathfrak{R}^{(\tau)}(f) + \mathfrak{I}^{(\tau)}(a)\big) \,|\, S_T$. This means the function $\big(\mathfrak{R}^{(\tau)}(f) + \mathfrak{I}^{(\tau)}(a) + \mathfrak{V}^{(\tau)}(\varphi)\big) \,|\, Z_T$ is a solution of (1), (2) and (3). In [6], we further show this solution to belong to a function space in which the usual weak solution of (1), (2) and (3) is looked for. Since this space is a uniqueness space for (1), (2) and (3), we may conclude that weak solutions may be represented by the sum $\big(\mathfrak{R}^{(\tau)}(f) + \mathfrak{I}^{(\tau)}(a) + \mathfrak{V}^{(\tau)}(\varphi)\big) \,|\, Z_T$ ([6, Corollary 5.1]), at least if the data f, a and b verify the assumptions we require in our theory. This representation formula, in turn, is exploited in [6] in order to derive estimates of the spatial decay of solutions to (1), (2) and (3) ([6, Corollary 5.2]).

The preceding indications, some of which will be made precise in Sect. 2 (Theorem 1, Lemma 6, Theorem 2, Lemma 7, Corollary 1), should serve to convince the reader that the resolution of Eq. (11) – the subject of the work at hand – is an important element in a wider theory, and thus is worthwhile to be studied. We remark that in [3], we already sketched the approach we present in the following in order to solve (11). But reference [3] does not give a proof of the two crucial result mentioned above (continuous dependence from the Reynolds number and uniqueness of the single layer potential). What we did prove in [3], however, was a useful estimate of the Oseen fundamental solution, although a term was forgotten when this estimate was stated in [3, Lemma 3]. A correct formulation may be found below in Lemma 5. We finally remark that estimates of $\mathfrak{R}^{(\tau)}(f)$ were derived in [12, 13] in a different context. For other studies, based on different methods, of the time-dependent Oseen system or of the resolvent problem associated to the Oseen system, we refer to [8, 9, 15, 16, 20].

2 Notations, Definitions, Auxiliary Results

Recall the bounded Lipschitz domain Ω and the notations $U := \mathbb{R}^3 \backslash \overline{\Omega}$, $Z_T := U \times (0, T)$, $S_T := \partial\Omega \times (0, T)$ $(T \in (0, \infty])$ introduced in Sect. 1. The set Ω was supposed to have a connected boundary, so Ω and U are connected. Let $n^{(\Omega)}$ denote the outward unit normal to Ω. We choose a non-tangential vector field $m^{(\Omega)} \in C_0^\infty(\mathbb{R}^3)^3$ to Ω. This means that $m^{(\Omega)}(x) = 1$ for x from a neighbourhood of $\partial\Omega$, and there are constants $\mathfrak{D}_1, \mathfrak{D}_2 \in (0, \infty)$ with

$$|x + \delta \cdot m^{(\Omega)}(x) - x' - \delta' \cdot m^{(\Omega)}(x')| \geq \mathfrak{D}_1 \cdot \big(|x - x'| + |\delta - \delta'| \big) \tag{12}$$

for $x, x' \in \partial\Omega$, $\delta, \delta' \in [-\mathfrak{D}_2, \mathfrak{D}_2]$, and

$$x + \delta \cdot m^{(\Omega)}(x) \in U, \quad x - \delta \cdot m^{(\Omega)}(x) \in \Omega \quad \text{for } x \in \partial\Omega, \ \delta \in (0, \mathfrak{D}_2]. \tag{13}$$

Some indications on how to construct such a field are given in [18, p. 246]. Since Ω is only Lipschitz bounded, the relations in (12) and (13) do not hold in general when $m^{(\Omega)}$ is replaced by the outward unit normal to Ω.

As explained in the proof of [5, Lemma 3.4], the relations in (12) and (13) imply there is a constant $\mathfrak{D}_3 > 0$ only depending on Ω such that

$$\begin{aligned} |x - y - \kappa \cdot m^{(\Omega)}(y)| &\geq \mathfrak{D}_3 \cdot (|x - y| + \kappa), \\ |z - y + \kappa \cdot m^{(\Omega)}(y)| &\geq \mathfrak{D}_3 \cdot (|z - y| + \kappa) \end{aligned} \tag{14}$$

for $\kappa \in (0, \mathfrak{D}_2]$, $y \in \partial\Omega$, $x, z \in \mathbb{R}^3$ with $\operatorname{dist}(x, \Omega) < \mathfrak{D}_1 \cdot \kappa/2$ and $\operatorname{dist}(z, U) < \mathfrak{D}_1 \cdot \kappa/2$.

Put $B_r := \{y \in \mathbb{R}^3 : |y| < r\}$ for $r \in (0, \infty)$. We fix some $R_0 > 0$ with $\overline{\Omega} \subset B_{R_0/2}$. We further define $|\alpha| := \alpha_1 + \alpha_2 + \alpha_3$ (length of α) for multi-indices $\alpha \in \mathbb{N}_0^3$. Put $e_1 := (1, 0, 0)$ and $s(x) := |x| - x_1$ for $x \in \mathbb{R}^3$.

Let $A \subset \mathbb{R}^3$ be open. Then we write $H^1(A)$ for the usual Sobolev space of order 1 and exponent 2. This space is to be equipped with its standard norm. Denote by V the closure of the set $\big\{ v \in C_0^\infty(U)^3 : \operatorname{div} v = 0 \big\}$ with respect to that norm (with $A = U$). The Sobolev spaces $H^{1/2}(\partial\Omega)$ and $H^1(\partial\Omega)$ are to be defined in the standard way; see [11, Chapter III.6], for example. Let $\| \ \|_{1/2, 2}$ and $\| \ \|_{1, 2}$, respectively, denote their usual norm with respect to some local coordinates of $\partial\Omega$ ([11, Section III.6.7]). Put

$$L_n^2(\partial\Omega) := \{v \in L^2(\partial\Omega)^3 : \int_{\partial\Omega} v \cdot n^{(\Omega)} \, d\Omega = 0\}.$$

Let $T \in (0, \infty]$. (Note that the case $T = \infty$ is admitted.) Then we put

$$L^2_n(S_T) := \{v \in L^2(S_T)^3 \;:\; v(\,\cdot\,, t) \in L^2_n(\partial\Omega) \;\text{ for almost every }\; t \in (0, T)\},$$
$$\widetilde{H}_T := \{v \,|\, S_T \;:\; v \in C_0^\infty(\mathbb{R}^4)^3,\; v \,|\, \mathbb{R}^3 \times (-\infty, 0] = 0\}.$$

For $v \in C^1\big((-\infty, T)\big)$ with $v \,|\, (-\infty, 0] = 0$, and for $t \in (0, T)$, we put

$$\partial_t^{1/2} v(t) := \Gamma(1/2)^{-1} \cdot \partial_t \Big(\int_0^t (t - r)^{-1/2} \cdot v(r)\, dr \Big)$$

("fractional derivative of v"), where Γ denotes the usual gamma function. We further define for $v \in \widetilde{H}_T$:

$$\partial_4^{1/2} v(x, t) := \partial_t^{1/2}\big(v(x, \,\cdot\,)\big)(t) \quad \text{for} \;\; (x, t) \in \partial\Omega \times (0, T).$$

For any $v \in L^2(S_T)$, we may define $F_v \in L^2\big(0, T, H^1(\partial\Omega)'\big)$ by setting

$$F_v(t)(\sigma) := \int_{\partial\Omega} v(x, t) \cdot \sigma(x)\, dx \quad \text{for} \;\; \sigma \in H^1(\partial\Omega) \;\; \text{and for a. e.} \;\; t \in (0, T).$$

We will write v instead of F_v. For $v \in \widetilde{H}_T$, set

$$\|v\|_{H_T} := \Big(\int_0^T \Big(\|v(\,\cdot\,, t) \,|\, \partial\Omega\|^2_{1,2} + \int_{\partial\Omega} \big| \partial_4^{1/2} v(x, t) \big|^2 \, d\Omega(x) + \|\partial_t v(\,\cdot\,, t) \cdot n^{(\Omega)}\|^2_{H^1(\partial\Omega)'} \Big)\, dt \Big)^{1/2}.$$

The mapping $\|\;\|_{H_T}$ is a norm on $\widetilde{H}_T$. Let the space H_T consist of all functions $v \in L^2_n(S_T)$ such that there exists a sequence (w_n) in $\widetilde{H}_T$ with the property that $\|v - w_n \,|\, S_T\|_2 \to 0$, and such that $(w_n \,|\, S_T)$ is a Cauchy sequence with respect to the norm $\|\;\|_{H_T}$. This means in particular that the sequence $\big(\|w_n \,|\, S_T\|_{H_T}\big)$ is convergent. Its limit value does not depend on the choice of the sequence (w_n) with the above properties. Thus, for $v \in H_T$, we may define the quantity $\|v\|_{H_T}$ in an obvious way. The mapping $\|\;\;\|_{H_T}$ is a norm on H_T, and the pair $\big(H_T, \|\;\;\|_{H_T}\big)$ is a Banach space.

Let us present some auxiliary results.

Lemma 1 *([10, Lemma 4.3]) Let $\beta \in (1, \infty)$. Then there is a constant $C = C(\beta)$ such that $\int_{\partial B_r} \big(1 + s(x)\big)^{-\beta}\, do_x \le C \cdot r \quad for \;\; r \in (0, \infty)$.*

Lemma 2 *([7, Lemma 4.8]) There is $C > 0$ such that for $x, y \in \mathbb{R}^3$, $\kappa \in (0, \infty)$, the following inequality holds:*

$$\big(1 + \kappa \cdot s(x - y)\big)^{-1} \;\le\; C \cdot \max\{1, \kappa\} \cdot (1 + |y|) \cdot \big(1 + \kappa \cdot s(x)\big)^{-1}.$$

Lemma 3 *(Compare [2, Lemma 4.9]) Let $\mathfrak{A}$, $\mathfrak{B}$ be measurable spaces equipped with the measure μ and ν, respectively. Let $F,\ F_1,\ F_2 : \mathfrak{A} \times \mathfrak{B} \mapsto [0, \infty),\ \ f : \mathfrak{B} \mapsto [0, \infty)$ be measurable functions. Suppose that $F = F_1 \cdot F_2$. Then*

$$\Big(\int_{\mathfrak{A}} \Big(\int_{\mathfrak{B}} F(x, y) \cdot f(y)\, d\nu(y) \Big)^2 d\mu(x) \Big)^{1/2} \ \le\ C \cdot \|f\|_2, \tag{15}$$

with

$$C := \Big(\sup_{x \in \mathfrak{A}} \Big\{ \int_{\mathfrak{B}} F_1(x, y)^2\, d\nu(y) \Big\} \cdot \sup_{y \in \mathfrak{B}} \Big\{ \int_{\mathfrak{A}} F_2(x, y)^2\, d\mu(x) \Big\} \Big)^{1/2}.$$

Proof Hölder's inequality yields that the left-hand side of (15) is bounded by

$$\Big(\int_{\mathfrak{A}} \Big(\int_{\mathfrak{B}} F_1(x, y)^2\, d\nu(y) \Big) \cdot \Big(\int_{\mathfrak{B}} F_2(x, y)^2 \cdot f(y)^2\, d\nu(y) \Big)\, d\mu(x) \Big)^{1/2}.$$

Thus the lemma follows after an application of Fubini's theorem. □

Next we introduce the fundamental solutions we will consider in what follows. Let $\mathfrak{H}$ denote the usual fundamental solution of the heat equation in $\mathbb{R}^3$, that is,

$$\mathfrak{H}(z, t) := (4 \cdot \pi \cdot t)^{-3/2} \cdot e^{-|z|^2/(4 \cdot t)} \quad \text{for } \ (z, t) \in \mathbb{R}^3 \times (0, \infty),$$
$$\mathfrak{H}(z, t) := 0 \ \text{ for } \ (z, t) \in \big(\mathbb{R}^3 \times (-\infty, 0] \big) \backslash \{0\}.$$

We further introduce a fundamental solution of the time-dependent Stokes system by setting as in [19]

$$\begin{aligned} \Gamma_{jk}(z, t) &:= \delta_{jk} \cdot \mathfrak{H}(z, t) + \int_t^\infty \partial_j \partial_k \mathfrak{H}(z, s)\, ds, \\ E_k(x) &:= (4 \cdot \pi)^{-1} \cdot x_k \cdot |x|^{-3} \end{aligned} \tag{16}$$

for $(z, t) \in G := \big(\mathbb{R}^3 \times [0, \infty) \big) \backslash \{0\},\ \ x \in \mathbb{R}^3 \backslash \{0\},\ \ 1 \le j, k \le 3$. Finally we define the velocity part of a fundamental solution of the time-dependent Oseen system (with Reynolds number κ) by putting

$$\Lambda_{jk}(z, t, \kappa) := \Gamma_{jk}(z - \kappa \cdot t \cdot e_1, t) \quad \text{for } \ (z, t) \in G,\ \ j, k \in \{1,\ 2,\ 3\}.$$

An associated pressure part is given by the functions E_k introduced in (16).

Lemma 4 *The relations $\mathfrak{H} \in C^\infty(\mathbb{R}^4 \backslash \{0\}),\ \ \Gamma_{jk} \in C^\infty(G)$ and $E_k \in C^\infty(\mathbb{R}^3 \backslash \{0\})$ hold for $1 \le j, k \le 3$. Moreover, for $l \in \mathbb{N}_0,\ \alpha \in \mathbb{N}^3$, there is $C = C(l, \alpha) > 0,\ \ \widetilde{C} = \widetilde{C}(\alpha) > 0$ with*

$$\big| \partial_t^l \partial_z^\alpha \mathfrak{H}(z, t) \big| + \big| \partial_t^l \partial_z^\alpha \Gamma_{jk}(z, t) \big| \le C \cdot (|z|^2 + t)^{-3/2 - |\alpha|/2 - l},$$

$$|\partial_x^\alpha E_k(x)| \leq \widetilde{C} \cdot |x|^{-2-|\alpha|}$$

for $z \in \mathbb{R}^3,\ t \in (0,\infty),\ x \in \mathbb{R}^3 \backslash \{0\},\ 1 \leq j,k \leq 3.$

For the Oseen fundamental solution, the following estimate holds:

Lemma 5 *The function* $\Lambda_{jk}(\cdot\,,\,\cdot\,,\kappa)$ *belongs to the space* $C^\infty(G)$*, for* $\kappa > 0,\ 1 \leq j,k \leq 3$. *For any* $K > 0,\ \alpha \in \mathbb{N}_0^3,\ l \in \mathbb{N}_0$*, there is some* $C(K,\alpha,l) > 0$ *with*

$$\begin{aligned}&\left|\, \partial_t^l \partial_z^\alpha \Lambda_{jk}(z,t,\kappa) \,\right| \\ &\leq C(K,\alpha,l) \cdot \max\{1,\kappa\}^{\frac{3}{2}+\frac{|\alpha|}{2}+l} \cdot \left(\gamma(z,t)^{-\frac{3}{2}-\frac{|\alpha|}{2}-l} + \gamma(z,t)^{-\frac{3}{2}-\frac{|\alpha|}{2}-\frac{l}{2}} \right),\end{aligned}$$

for $z,\ t,\ j,\ k$ *as in Lemma 4, and for* $\kappa \in (0,\infty)$*, where*

$$\gamma(z,t) := |z|^2 + t \ \text{ if } \ |z| \ \leq \ K, \quad \gamma(z,t) := |z| \cdot \big(1 + \kappa \cdot s(z)\big) + t \ \text{ if } \ |z| > K.$$

Proof Reference [3, Lemma 2], Lemma 4. □

Let us now fix a Reynolds number $\tau \in (0,\infty)$. In the following, the symbol $\mathfrak{C}$ will always denote constants only depending on $\Omega,\ R_0$ and τ. We write $\mathfrak{C}(\gamma_1,\ \ldots,\ \gamma_n)$ for constants depending additionally on other parameters $\gamma_1,\ \ldots,\ \gamma_n \in (0,\infty)$, for some $n \in \mathbb{N}$.

Let us introduce the volume potentials mentioned in Sect. 1. Take $f \in C_0^\infty\big(\mathbb{R}^3 \times (0,\infty)\big)^3$. Then, for $x \in \mathbb{R}^3,\ t \in [0,\infty),\ j \in \{1,\ 2,\ 3\}$, we put

$$\mathfrak{R}_j^{(\tau)}(f)(x,t) := \int_0^t \int_{\mathbb{R}^3} \sum_{k=1}^3 \Lambda_{jk}(x-y, t-\sigma, \tau) \cdot f_k(y,\sigma)\, dy\, d\sigma, \qquad (17)$$

$$\mathfrak{P}(f)(x,t) := \int_{\mathbb{R}^3} \sum_{k=1}^3 E_k(x-y) \cdot f_k(y,t)\, dy.$$

Let $a \in C_0^\infty(U)^3$. Then we define

$$\mathfrak{I}_j^{(\tau)}(a)(x,t) := \int_U \mathfrak{H}(x - \tau \cdot t \cdot e_1 - y, t) \cdot a_j(y)\, dy, \qquad (18)$$

for $x,\ t$ and j as above.

These potentials solve the Cauchy problem (4), (5) and (6):

Theorem 1 *Take* f *and* a *as in (17), (18). Then the functions* $\mathfrak{R}_j^{(\tau)}(f)$, $\mathfrak{P}(f)$ *and* $\mathfrak{I}_j^{(\tau)}(a)$ *belong to* $C^\infty\big(\mathbb{R}^3 \times [0,\infty)\big)$*, for* $1 \leq j \leq 3$. *Moreover,* $\mathfrak{R}_j^{(\tau)}(f)$ *and* $\mathfrak{I}_j^{(\tau)}(a)$ *verify (5), and the following relations hold for* $x \in \mathbb{R}^3,\ t \in (0,\infty)$*:*

$$\partial_t \mathfrak{R}^{(\tau)}(f)(x,t) - \Delta_x \mathfrak{R}^{(\tau)}(f)(x,t) + \tau \cdot \partial_{x_1} \mathfrak{R}^{(\tau)}(f)(x,t)$$

$$+ \nabla_x \mathfrak{P}(f)(x,t) = f(x,t),$$
$$div_x \mathfrak{R}^{(\tau)}(f)(x,t) = 0, \quad \mathfrak{R}^{(\tau)}(f)(x,0) = 0, \quad \mathfrak{I}^{(\tau)}(a)(x,0) = a(x),$$
$$\partial_t \mathfrak{I}^{(\tau)}(a)(x,t) - \Delta_x \mathfrak{I}^{(\tau)}(a)(x,t) + \tau \cdot \partial_{x_1} \mathfrak{I}^{(\tau)}(a)(x,t) = 0.$$

If $div\, a = 0$, then $div_x \mathfrak{I}^{(\tau)}(a)(x,t) = 0$ for $x \in \mathbb{R}^3,\ t \in (0,\infty)$.

This theorem follows from Lebesgue's theorem on dominated convergence and from some standard properties of $\mathfrak{H}$ (like the equation $\int_{\mathbb{R}^3} \mathfrak{H}(x,t)\, dx = 1$ for $t \in (0,\infty)$). The details of a proof are tedious but simple.

Next we define the single layer potentials mentioned in Sect. 1. For $T \in (0,\infty],\ \varphi \in L^2(S_T)^3,\ \kappa \in (0,\infty),\ x \in \mathbb{R}^3,\ t \in [0,\infty)$, we put

$$\mathfrak{V}^{(0)}(\varphi)(x,t) := \Big(\int_0^t \int_{\partial\Omega} \sum_{k=1}^3 \Gamma_{jk}(x-y, t-\sigma) \cdot \widetilde{\varphi}_k(y,\sigma)\, d\Omega(y)\, d\sigma \Big)_{1 \le j \le 3},$$
$$\mathfrak{V}^{(\kappa)}(\varphi)(x,t) := \Big(\int_0^t \int_{\partial\Omega} \sum_{k=1}^3 \Lambda_{jk}(x-y, t-\sigma, \kappa) \cdot \widetilde{\varphi}_k(y,\sigma)\, d\Omega(y)\, d\sigma \Big)_{1 \le j \le 3},$$

where $\widetilde{\varphi}$ denotes the zero extension of φ from S_T to S_∞ if $T < \infty$, and $\widetilde{\varphi} := \varphi$ else. We further set

$$Q(\varphi)(x,t) := \int_{\partial\Omega} \sum_{k=1}^3 E_k(x-y) \cdot \widetilde{\varphi}_k(y,t)\, d\Omega(y)$$

for $\varphi \in L^2(S_T)^3,\ x \in \mathbb{R}^3 \backslash \partial\Omega,\ t \in (0,\infty)$. We call the function pairs $\big(\mathfrak{V}^{(0)}(\varphi), Q(\varphi)\big)$ and $\big(\mathfrak{V}^{(\kappa)}(\varphi),\ Q(\varphi)\big)$ the "single layer potential related to the time-dependent Stokes and Oseen system", respectively.

The following lemma holds:

Lemma 6 *Let $T \in (0,\infty],\ \kappa \in [0,\infty),\ \varphi \in L^2(S_T)^3$. Abbreviate*

$$w := \mathfrak{V}^{(\kappa)}(\varphi) \,|\, (\mathbb{R}^3 \backslash \partial\Omega) \times [0,\infty), \quad \pi := Q(\varphi).$$

Then $w_j(\,\cdot\,,t),\ \pi(\,\cdot\,,t) \in C^\infty(\mathbb{R}^3 \backslash \partial\Omega)$ for $1 \le j \le 3,\ t \in [0,\infty)$. For $\alpha \in \mathbb{N}_0^3$, the partial derivative $\partial_x^\alpha w(x,t)$ as a function of $x \in \mathbb{R}^3 \backslash \partial\Omega$ and $t \in [0,\infty)$ is continuous. The partial derivative $\partial_t w(x,t)$ exists for $x \in \mathbb{R}^3 \backslash \partial\Omega$ and for a.e. $t \in (0,\infty)$. This derivative also is the weak derivative of w with respect to t on $(\mathbb{R}^3 \backslash \partial\Omega) \times (0,\infty)$, and the weak derivative of $w(x,\ \cdot\,)$ on $(0,\infty)$, for $x \in \mathbb{R}^3 \backslash \partial\Omega$. The equations (7) (with τ replaced by κ) and (9) are satisfied.

We mention a regularity result on $\mathfrak{V}^{(\tau)}(\varphi)$ established in [5].

Theorem 2 $\mathfrak{V}^{(\tau)}(\varphi) \,|\, Z_T \in L^\infty(0,T,L^2(U)^3) \cap L^2(0,T,V) \cap H^1(0,T,V')$ *for* $T \in (0,\infty),\ \varphi \in L^2(S_\infty)^3$.

We note another result proved in [5], and which shows that the restriction of $\mathfrak{V}^{(\kappa)}(\varphi)$ to S_T may be considered as the boundary value of $\mathfrak{V}^{(\kappa)}(\varphi) \mid Z_T$ on S_T:

Lemma 7 *Let $\varphi \in L^2(S_\infty)^3$. Then the trace of $\big(\mathfrak{V}^{(\tau)}(\varphi)(\,\cdot\,,t)\big) \mid U$ coincides with $\mathfrak{V}^{(\tau)}(\varphi)(\,\cdot\,,t) \mid \partial\Omega$, for a. e. $t \in (0,\infty)$.*

Now we can state how the problem of finding a solution to (1), (2) and (3) reduces to an integral equation on S_∞, as indicated in Sect. 1. Since this result is only mentioned in order to motivate the study of Eq. (11), we did not make an effort to weaken the assumptions on f and a.

Corollary 1 *Let f, a be given as in (17), (18), and suppose that* $\operatorname{div} a = 0$. *Let $b \in L^2(S_\infty)^3$, and suppose there is $\varphi \in L^2(S_\infty)^3$ with*

$$\mathfrak{V}^{(\tau)}(\varphi) \mid S_\infty = b - \big(\mathfrak{R}^{(\tau)}(f) + \mathfrak{I}^{(\tau)}(a)\big) \mid S_\infty. \tag{19}$$

Put

$$u := \big(\mathfrak{R}^{(\tau)}(f) + \mathfrak{I}^{(\tau)}(a) + \mathfrak{V}^{(\tau)}(\varphi)\big) \mid Z_\infty, \quad p := \big(\mathfrak{P}(f) + Q(\varphi)\big) \mid Z_\infty. \tag{20}$$

Then $u_j(\,\cdot\,,t),\ p(\,\cdot\,,t) \in C^\infty(U)$ for $t \in (0,\infty)$, $1 \le j \le 3$, the derivative $\partial_t u(x,t)$ exists for $x \in U$ and for a. e. $t \in (0,\infty)$, and the pair (u,p) verifies (1), (2) and (3).

3 Solving Integral Equation (11)

We start by stating a result from [19].

Theorem 3 *For $T \in (0,\infty]$, the operator $\mathfrak{F}_T^{(0)} : L_n^2(S_T) \ni \varphi \mapsto \mathfrak{V}^{(0)}(\varphi) \mid S_T \in H_T$ is well defined, linear, bounded and bijective. In particular, $\mathfrak{F}_T^{(0)}$ is Fredholm with index 0.*

Proof See [19, pp. 365–367]. Note that the arguments given there also hold for $T = \infty$, although only the case $T < \infty$ is considered. □

The ensuing theorem will allow to reduce the invertibility of the Oseen single layer potential to Theorem 3.

Theorem 4 *Let $T \in (0,\infty]$. Then $\big(\mathfrak{V}^{(\kappa_2)}(\varphi) - \mathfrak{V}^{(\kappa_1)}(\varphi)\big) \mid S_T \in H_T$ and*

$$\big\| \big(\mathfrak{V}^{(\kappa_2)}(\varphi) - \mathfrak{V}^{(\kappa_1)}(\varphi)\big) \mid S_T \big\|_{H_T} \le C(\kappa_2) \cdot (\kappa_2 - \kappa_1)^{1/2} \cdot \|\varphi\|_2 \tag{21}$$

for $\varphi \in L^2(S_T)^3$, $\kappa_1, \kappa_2 \in [0,\infty)$ with $\kappa_1 < \kappa_2$, where the constant $C(\kappa)$, for $\kappa \in (0,\infty)$, depends on Ω and κ, and is an increasing function of κ. In view of Theorem 3, this means in particular that the operator

$$\mathfrak{F}_T^{(\kappa)} : L_n^2(S_T) \ni \varphi \mapsto \mathfrak{V}^{(\kappa)}(\varphi) \mid S_T \in H_T$$

is well defined, linear and bounded. Abbreviate $\varepsilon_p := min\,\{1,\ \mathfrak{D}_2\}/p\ \ for\ \ p \in \mathbb{N}$,

$$v := v(\kappa_1, \kappa_2, \varphi) := \big(\mathfrak{V}^{(\kappa_2)}(\varphi) - \mathfrak{V}^{(\kappa_1)}(\varphi)\big)\,|\,(\mathbb{R}^3 \backslash \partial\Omega) \times (0, T),$$

where $\kappa_1, \kappa_2 \in [0, \infty),\ \varphi \in L^2(S_T)^3$. *Then the relation*

$$\partial_l v\big(x + \varepsilon_p \cdot m^{(\Omega)}(x),\ t\big) - \partial_l v\big(x - \varepsilon_p \cdot m^{(\Omega)}(x),\ t\big) \to 0 \text{ for } \ p \to \infty \tag{22}$$

holds for $l \in \{1,\ 2,\ 3\},\ x \in \partial\Omega$ *and* $t \in (0, T)$.

Finally, if $T < \infty$*, the operator* $\mathfrak{F}_T^{(\kappa_2)} - \mathfrak{F}_T^{(\kappa_1)} : L_n^2(S_T) \mapsto H_T$ *is compact for* $\kappa_1, \kappa_2 \in [0, \infty)$.

Proof For $\varrho_1, \varrho_2 \in [0, \infty)$ with $\varrho_1 < \varrho_2,\ z \in \mathbb{R}^3,\ s \in (0, \infty),\ j, k \in \{1,\ 2,\ 3\}$, put

$$K_{jk}^{(\varrho_1, \varrho_2)}(z, s) := \Lambda_{jk}(z, s, \varrho_2) - \Lambda_{jk}(z, s, \varrho_1) \quad \text{if } \varrho_1 > 0.$$

In the case $\varrho_1 = 0$, the term $\Lambda_{jk}(z, t, \varrho_1)$ is replaced by $\Gamma_{jk}(z, t)$.

Let $\kappa_1,\ \kappa_2 \in [0, \infty)$ with $\kappa_1 < \kappa_2$. We will write K_{jk} instead of $K_{jk}^{(\kappa_1, \kappa_2)}$ in what follows. All the constants appearing in the estimates in this proof and depending on κ_2 are increasing functions of κ_2.

Lemma 4 and 5 with $K = 2 \cdot R_0$ yield

$$|\partial_t^l \partial_z^\alpha K_{jk}(z, t)| \ \le\ \mathfrak{C}(\kappa_2) \cdot \Big((|z|^2 + t)^{-\frac{3}{2} - \frac{|\alpha|}{2} - \frac{l}{2}} + (|z|^2 + t)^{-\frac{3}{2} - \frac{|\alpha|}{2} - l} \Big) \tag{23}$$

for $l \in \{0, 1\},\ \alpha \in \mathbb{N}_0^3$ with $|\alpha| + l \le 2,\ z \in B_{2 \cdot R_0},\ t \in (0, \infty),\ j, k \in \{1,\ 2,\ 3\}$. Moreover

$$\begin{aligned} &|\partial_t^l \partial_z^\alpha K_{jk}(z, t)| \qquad (24)\\ &= \Big| \int_0^1 \Big[\partial_z^\alpha \partial_1^{l+1} \Lambda_{jk}\big(z, t, \kappa_1 + \vartheta \cdot (\kappa_2 - \kappa_1)\big) \cdot \big(-\kappa_1 - \vartheta \cdot (\kappa_2 - \kappa_1)\big)^l \cdot t \\ &\qquad + \delta_{l1} \cdot \partial_z^\alpha \partial_1 \partial_4 \Lambda_{jk}\big(z, t, \kappa_1 + \vartheta \cdot (\kappa_2 - \kappa_1)\big) \cdot t \\ &\qquad + \delta_{l1} \cdot \partial_z^\alpha \partial_1 \Lambda_{jk}\big(z, t, \kappa_1 + \vartheta \cdot (\kappa_2 - \kappa_1)\big) \Big] d\vartheta \ \Big| \cdot (\kappa_2 - \kappa_1) \\ &\le\ \mathfrak{C}(\kappa_2) \cdot (\kappa_2 - \kappa_1) \cdot \big((|z|^2 + t)^{-1 - |\alpha|/2 - l/2} + (|z|^2 + t)^{-1 - |\alpha|/2 - l} \big). \end{aligned}$$

By taking the average of the right-hand side of (23) and (24), we get for $l,\ \alpha,\ z,\ t,\ j,\ k$ as before,

$$\begin{aligned} &|\partial_t^l \partial_z^\alpha K_{jk}(z, t)| \qquad (25)\\ &\le \mathfrak{C}(\kappa_2) \cdot (\kappa_2 - \kappa_1)^{1/2} \cdot \big((|z|^2 + t)^{-5/4 - |\alpha|/2 - l/2} + (|z|^2 + t)^{-5/4 - |\alpha|/2 - l} \big). \end{aligned}$$

We further remark that for $z \in \mathbb{R}^3 \backslash \{0\},\ j, k \in \{1,\ 2,\ 3\},\ \alpha \in \mathbb{N}_0^3,\ l \in \mathbb{N}_0$, we have

$$\partial_t^l \partial_z^\alpha K_{jk}(z,t) \to 0 \quad \text{for} \;\; t \downarrow 0. \tag{26}$$

For $\delta \in (0, \mathfrak{D}_2]$, let $\varphi^{(\delta)} \in C_0^\infty(\mathbb{R}^3)$ be such that $\varphi^{(\delta)}(x) = 1$ for $x \in \mathbb{R}^3$ with $\text{dist}(x, \overline{\Omega}) \leq \mathfrak{D}_1 \cdot \delta/4$, and $\varphi^{(\delta)}(x) = 0$ if $dist(x, \overline{\Omega}) \geq 3 \cdot \mathfrak{D}_1 \cdot \delta/8$. Next choose $\zeta \in C^\infty(\mathbb{R})$ with $\zeta \,|\, (-\infty, 1] = 1$ and $\zeta \,|\, [2, \infty) = 0$. Put $\zeta^{(\delta)}(t) := \zeta(\delta \cdot t)$ for $t \in \mathbb{R},\; \delta \in (0,\, \min\{1, \mathfrak{D}_2\}\,]$. Then $supp(\zeta^{(\delta)}) \subset (-\infty,\, 2/\delta]$ and $\zeta^{(\delta)} \,|\, (-\infty,\, 1/\delta] = 1$, hence

$$|\zeta^{(\delta)\prime}(t)| \;\leq\; \mathfrak{C} \cdot \chi_{(1/\delta,\, 2/\delta)}(t) \cdot t^{-1} \;\leq\; \mathfrak{C} \cdot \chi_{(1,\infty)}(t) \cdot t^{-1} \;\leq\; \mathfrak{C} \tag{27}$$

for $t \in (0, \infty)$, $\delta \in (0, \mathfrak{D}_2]$ with $\delta \leq 1$. Using the number ε_p introduced in Theorem 4, we define

$$\begin{aligned} w_{p,j}^{(\varrho_1,\varrho_2)}(\varphi)(x,t) &:= \varphi^{(\varepsilon_p)}(x) \cdot \zeta^{(\varepsilon_p)}(t) \\ &\quad \cdot \int_0^t \int_{\partial\Omega} \sum_{k=1}^3 K_{jk}^{(\varrho_1,\varrho_2)}(x - y - \varepsilon_p \cdot m^{(\Omega)}(y),\; t-\sigma) \cdot \varphi_k(y,\sigma)\, d\Omega(y)\, d\sigma \end{aligned}$$

for $p \in \mathbb{N},\; 1 \leq j \leq 3,\; \varphi \in L^2(S_T)^3,\; x \in \mathbb{R}^3,\; t \in [0,T] \cap \mathbb{R},\; \varrho_1, \varrho_2 \in [0, \infty)$ with $\varrho_1 < \varrho_2$. In the following, we will write $w_p(\varphi)$ instead of $w_p^{(\kappa_1,\kappa_2)}(\varphi)$. Due to (13), (14), (26) and the choice of $\varphi^{(\varepsilon_p)}$ and $\zeta^{(\varepsilon_p)}$, we have $w_p \,|\, S_T \in \widetilde{H}_T \cap L_n^2(S_T)$.

It was shown in the proof of [3, Lemma 9] that $(\mathfrak{F}_T^{(\varrho)} - \mathfrak{F}_T^{(0)})(\varphi) \in H_T$ and

$$\| w_p^{(\varrho,0)}(\varphi) - (\mathfrak{F}_T^{(\varrho)} - \mathfrak{F}_T^{(0)})(\varphi) \|_{H_T} \to 0 \;\; (p \to \infty) \tag{28}$$

for $\varphi \in L^2(S_T)^3,\; \varrho \in (0, \infty)$. We note that the term $\mathfrak{C} \cdot \gamma(x,t)^{-3/2-|\alpha|/2-l/2}$ is lacking on the right-hand side of the estimate in [3, Lemma 3], which corresponds to Lemma 5 here. As a consequence of this oversight, inequality [3, (18)] in the proof of [3, Lemma 9] is incomplete; the term $\mathfrak{C} \cdot (|z|^2 + t)^{-3/2-|\alpha|/2-l/2}$ has to be added on the right-hand side. This modification, in turn, means that the function H_2 in [3, p. 123] has to be changed: the integral over $\big(0,\, (t-\sigma)/2\big)$ in the definition of H_2 should apply to the function

$$r^{-\frac{1}{2}} \cdot \big[\, \chi_{(1,\infty)}(t) \cdot t^{-1} \cdot (|x-y|^2 + t - \sigma - r)^{-\frac{3}{2}} + (|x-y|^2 + t - \sigma - r)^{-2} \,\big].$$

(Distinguish the cases $|x-y|^2 + t - \sigma - r \leq 1$ and $|x-y|^2 + t - \sigma - r \geq 1$.) The rest of the proof of [3, Lemma 9] remains valid with a modification of the upper bound of $H_2(x, y, t, \sigma)$, which may be chosen as

$$\begin{aligned} &\mathfrak{C} \cdot \chi_{(0,1)}(t-\sigma) \cdot |x-y|^{-\frac{15}{8}} \cdot \big(\, \chi_{(1,\infty)}(t) \cdot t^{-1} \cdot (t-\sigma)^{-\frac{1}{16}} + (t-\sigma)^{-\frac{9}{16}} \,\big) \\ &\quad + \mathfrak{C} \cdot \chi_{(1,\infty)}(t-\sigma) \cdot |x-y|^{-\frac{1}{8}} \cdot \big(\, \chi_{(1,\infty)}(t) \cdot t^{-1} \cdot (t-\sigma)^{-\frac{15}{16}} + (t-\sigma)^{-\frac{23}{16}} \,\big). \end{aligned}$$

Since $w_p(\varphi) = w_p^{(\kappa_2,0)}(\varphi) - w_p^{(\kappa_1,0)}(\varphi)$ for $p \in \mathbb{N},\ \varphi \in L^2(S_T)^3$, we may conclude from (28) that

$$\|w_p(\varphi) - (\mathfrak{F}_T^{(\kappa_2)} - \mathfrak{F}_T^{(\kappa_1)})(\varphi)\|_{H_T} \to 0 \ \ (p \to \infty), \quad \text{for } \ \varphi \in L^2(S_T)^3. \tag{29}$$

Let $\varphi \in L^2(S_T)^3,\ \ p \in \mathbb{N}$. We are going to estimate $\|w_p(\varphi)\|_{H_T}$. To this end, using the abbreviation

$$\beta_p(x, y) := x - y - \varepsilon_p \cdot m^{(\Omega)}(y) \quad \text{for } \ x \in \overline{\Omega},\ \ y \in \partial\Omega, \tag{30}$$

we define for $j, k, m \in \{1,\ 2,\ 3\},\ x \in \overline{\Omega},\ y \in \partial\Omega,\ t \in (0, \infty),\ \sigma \in (0, t)$,

$$\mathfrak{K}_{p,j,k,0}(x, y, t, \sigma) := \zeta^{(\varepsilon_p)}(t) \cdot K_{jk}\big(\beta_p(x, y),\ t - \sigma\big),$$
$$\mathfrak{K}_{p,j,k,m}(x, y, t, \sigma) := \zeta^{(\varepsilon_p)}(t) \cdot \partial_{x_m} K_{jk}\big(\beta_p(x, y),\ t - \sigma\big),$$
$$\begin{aligned}\mathfrak{L}_{p,j,k}(x, y, t, \sigma) := &\int_0^{(t-\sigma)/2} r^{-1/2} \cdot \big[\zeta^{(\varepsilon_p)\prime}(t - r) \cdot K_{jk}\big(\beta_p(x, y),\ t - \sigma - r\big)\\ &+\zeta^{(\varepsilon_p)}(t - r) \cdot \partial_t K_{jk}\big(\beta_p(x, y),\ t - \sigma - r\big)\big]\, dr\\ &+ 2^{1/2} \cdot (t - \sigma)^{-1/2} \cdot \zeta^{(\varepsilon_p)}\big((t + \sigma)/2\big) \cdot K_{jk}\big(\beta_p(x, y),\ (t - \sigma)/2\big)\\ &- (1/2) \cdot \int_{(t-\sigma)/2}^{t-\sigma} r^{-3/2} \cdot \zeta^{(\varepsilon_p)}(t - r) \cdot K_{jk}\big(\beta_p(x, y),\ t - \sigma - r\big)\, dr,\end{aligned}$$
$$\begin{aligned}\mathfrak{M}_{p,j,k}(x, y, t, \sigma) := &\ \zeta^{(\varepsilon_p)\prime}(t) \cdot K_{jk}\big(\beta_p(x, y),\ t - \sigma\big)\\ &+\zeta^{(\varepsilon_p)}(t) \cdot \partial_t K_{jk}\big(\beta_p(x, y),\ t - \sigma\big).\end{aligned}$$

Inequalities (23), (27) and (14) imply

$$|\,\partial_t^l \partial_x^\alpha\big[\zeta^{(\varepsilon_p)}(t) \cdot K_{jk}\big(\beta_p(x, y),\ t - \sigma\big)\big]| \le \mathfrak{C}(\kappa_2) \cdot \varepsilon_p^{-3/2-|\alpha|/2-l} \tag{31}$$

for $x \in \overline{\Omega},\ \ y \in \partial\Omega,\ \ t \in (0, T),\ \ \sigma \in (0, t)$, and for $\alpha \in \mathbb{N}_0^3,\ l \in \mathbb{N}_0$ with $|\alpha| + l \le 1$. Thus we see that the functions $\mathfrak{K}_{p,j,k,m}$ and $\mathfrak{M}_{p,j,k}$ are bounded, and

$$|\mathfrak{L}_{p,j,k}(x, y, t, \sigma)| \le \mathfrak{C}(\varepsilon_p, \kappa_2) \cdot \big((t - \sigma)^{1/2} + (t - \sigma)^{-1/2}\big) \tag{32}$$

for $x, y \in \partial\Omega,\ \ t \in (0, \infty),\ \ \sigma \in (0, t),\ \ 1 \le j, k \le 3$. As a consequence, we may define

$$\mathfrak{A}_{p,j,k,m}(\psi)(x, t) := \int_0^t \int_{\partial\Omega} \mathfrak{K}_{p,j,k,m}(x, y, t, \sigma) \cdot \psi(y, \sigma)\, d\Omega(y)\, d\sigma$$

for $j, k \in \{1,\ 2,\ 3\},\ \ m \in \{0,\ 1,\ 2,\ 3\},\ \ x \in \partial\Omega,\ \ t \in (0, T),\ \ \psi \in L^2(S_T)$. In addition, we may introduce $\mathfrak{B}_{p,j,k}(\psi)$ and $\mathfrak{C}_{p,j,k}(\psi)$ in the same way as $\mathfrak{A}_{p,j,k,m}(\psi)$, but with the kernel $\mathfrak{K}_{p,j,k,m}$ replaced by $\mathfrak{L}_{p,j,k}$ and $\mathfrak{M}_{p,j,k}$, respectively, and with

$x \in \Omega$ instead of $x \in \partial\Omega$ in the case of $\mathfrak{C}_{p,j,k}(\psi)$. By referring to (26), it may be shown that

$$\begin{aligned}
&\partial_t\Big(\int_0^t (t-r)^{-1/2} \cdot w_{p,j}(\varphi)(x,r)\,dr\Big) \qquad (33)\\
&= \sum_{k=1}^{3} \int_{\partial\Omega} \partial_t\Big(\int_0^t \varphi_k(y,\sigma) \cdot \int_\sigma^t (t-r)^{-1/2} \cdot \zeta^{(\varepsilon_p)}(r)\\
&\qquad\qquad \cdot K_{jk}\big(\beta_p(x,y),\, r-\sigma\big)\,dr\,d\sigma\Big)\,d\Omega(x)\\
&= \sum_{k=1}^{3} \int_0^t \int_{\partial\Omega} \mathfrak{L}_{p,j,k}(x,y,t,\sigma) \cdot \varphi_k(y,\sigma)\,d\Omega(y)\,d\sigma = \sum_{k=1}^{3} \mathfrak{B}_{p,j,k}(\varphi_k)(x,t)
\end{aligned}$$

for $j \in \{1, 2, 3\}$, $x \in \partial\Omega$, $t \in (0,T)$. Let $E : H^{1/2}(\partial\Omega) \mapsto H^1(\Omega)$ be a linear bounded extension operator. Using the equation $\operatorname{div}_x w_p(\varphi)(x,t) = 0$ $\big(x \in \Omega,\ t \in (0,T)\big)$, we get for $t \in (0,T)$, $v \in H^1(\partial\Omega)$,

$$\begin{aligned}
&\int_{\partial\Omega} \big(\partial_t w_p(\varphi)(x,t) \cdot n^{(\Omega)}(x)\big) \cdot v(x)\,d\Omega(x) \qquad (34)\\
&= \sum_{j=1}^{3} \int_\Omega \partial_t w_{p,j}(\varphi)(x,t) \cdot \partial_j E(v)(x)\,dx\\
&= \sum_{j,k=1}^{3} \int_\Omega \int_0^t \int_{\partial\Omega} \mathfrak{M}_{p,j,k}(x,y,t,\sigma) \cdot \varphi_k(y,\sigma)\,d\Omega(y)\,d\sigma \cdot \partial_j E(v)(x)\,dx\\
&= \sum_{j,k=1}^{3} \int_\Omega \mathfrak{C}_{p,j,k}(\varphi_k)(x,t) \cdot \partial_j E(v)(x)\,dx\\
&\le \sum_{j,k=1}^{3} \|\mathfrak{C}_{p,j,k}(\varphi_k)(\,\cdot\,,t)\|_2 \cdot \|v\|_{1/2,2}.
\end{aligned}$$

Since $\|v\|_{1/2,2} \le \mathfrak{C} \cdot \|v\|_{1,2}$ for $v \in H^1(\partial\Omega)$, and in view of (33) and (34), we may conclude

$$\begin{aligned}
&\|w_p(\varphi)\,|\,S_T\|_{H_T} \qquad (35)\\
&\le \mathfrak{C} \cdot \sum_{j,k=1}^{3} \Big(\sum_{m=0}^{3} \|\mathfrak{A}_{p,j,k,m}(\varphi_k)\|_2 + \|\mathfrak{B}_{p,j,k}(\varphi_k)\|_2 + \|\mathfrak{C}_{p,j,k}(\varphi_k)\|_2\Big).
\end{aligned}$$

Next we indicate an observation which follows from (25) and (14), and which holds for $x, y \in \partial\Omega$, $t \in (0,T)$, $\sigma \in (0,t)$, $j,k \in \{1, 2, 3\}$ and $\alpha \in \mathbb{N}_0^3$ with $|\alpha| \le 1$:

$$|\partial_x^\alpha K_{jk}\big(\beta_p(x,y),\ t-\sigma)| \le \mathfrak{C}(\kappa_2)\cdot(\kappa_2-\kappa_1)^{1/2}\cdot H_1(x-y,t-\sigma), \tag{36}$$

with

$$H_1(z,r) := \chi_{(0,1)}(r)\cdot r^{-15/16}\cdot|z|^{-13/8} + \chi_{(1,\infty)}(r)\cdot r^{-5/4}$$

for $r \in (0,\infty)$, $z \in \mathbb{R}^3\backslash\{0\}$. By referring to (25), (27), (14), we obtain for x, y, t, σ, j, k as in (36),

$$\begin{aligned}
&|\mathfrak{L}_{jk}(x,y,t,\sigma)| \le \mathfrak{C}(\kappa_2)\cdot(\kappa_2-\kappa_1)^{1/2}\\
&\quad\cdot\Big(\int_0^{(t-\sigma)/2} r^{-1/2}\cdot\big[\,\chi_{(1,\infty)}(t-r)\cdot(t-r)^{-1}\cdot(|x-y|^2+t-\sigma-r)^{-5/4}\\
&\quad+(|x-y|^2+t-\sigma-r)^{-7/4}+(|x-y|^2+t-\sigma-r)^{-9/4}\,\big]\,dr\\
&\quad+(t-\sigma)^{-1/2}\cdot(|x-y|^2+t-\sigma)^{-5/4}\\
&\quad+\int_{(t-\sigma)/2}^{t-\sigma} r^{-3/2}\cdot(|x-y|^2+t-\sigma-r)^{-5/4}\,dr\Big)\\
&\le \mathfrak{C}(\kappa_2)\cdot(\kappa_2-\kappa_1)^{1/2}\cdot\Big(\big[\,(t-\sigma)^{-1}\cdot(|x-y|^2+t-\sigma)^{-5/4}\\
&\quad+(|x-y|^2+t-\sigma)^{-7/4}+(|x-y|^2+t-\sigma)^{-9/4}\,\big]\cdot\int_0^{(t-\sigma)/2} r^{-1/2}\,dr\\
&\quad+(t-\sigma)^{-1/2}\cdot(|x-y|^2+t-\sigma)^{-5/4}\\
&\quad+(t-\sigma)^{-3/2}\cdot\int_{(t-\sigma)/2}^{t-\sigma}(|x-y|^2+t-\sigma-r)^{-5/4}\,dr\Big)\\
&\le \mathfrak{C}(\kappa_2)\cdot(\kappa_2-\kappa_1)^{1/2}\cdot\Big(\big(1+(t-\sigma)^{-1/2}\big)\cdot(|x-y|^2+t-\sigma)^{-5/4}\\
&\quad+\chi_{(1,\infty)}(t-\sigma)\cdot(t-\sigma)^{-3/2}\cdot|x-y|^{-1/2}\\
&\quad+\chi_{(0,1)}(t-\sigma)\cdot(t-\sigma)^{-3/2}\cdot|x-y|^{-13/8}\cdot\int_{(t-\sigma)/2}^{t-\sigma}(t-\sigma-r)^{-7/16}\,dr\Big)\\
&\le \mathfrak{C}(\kappa_2)\cdot(\kappa_2-\kappa_1)^{1/2}\cdot H_2(x-y,t-\sigma),
\end{aligned}\tag{37}$$

where we used the following notation, for $z \in \mathbb{R}^3\backslash\{0\}$, $r \in (0,\infty)$,

$$H_2(z,r) := \chi_{(1,\infty)}(r)\cdot r^{-5/4}\cdot|z|^{-1/2} + \chi_{(0,1)}(r)\cdot r^{-15/16}\cdot|z|^{-13/8}.$$

Moreover, due to (24), (25), (27) and (14), we get for $x \in \Omega$ and for y, t, σ, j, k as in (36),

$$\begin{aligned}
&|\mathfrak{M}_{p,j,k}(x,y,t,\sigma)| \\
&\le \mathfrak{C}\cdot\big(\,|\zeta^{(\varepsilon_p)\prime}(t)|\cdot|K_{jk}\big(\beta_p(x,y),\ t-\sigma)|+|\partial_t K_{jk}\big(\beta_p(x,y),\ t-\sigma)|\,\big)
\end{aligned}\tag{38}$$

$$\leq \mathfrak{C}(\kappa_2) \cdot (\kappa_2 - \kappa_1)^{1/2} \cdot \big[(|x-y|^2 + t - \sigma)^{-5/4} + (|x-y|^2 + t - \sigma)^{-3/2} + (|x-y|^2 + t - \sigma)^{-2} \big]$$
$$\leq \mathfrak{C}(\kappa_2) \cdot (\kappa_2 - \kappa_1)^{1/2} \cdot H_3(x-y, t-\sigma),$$

with

$$H_3(z, r) := \chi_{(1,\infty)}(r) \cdot r^{-5/4} + \chi_{(0,1)}(r) \cdot r^{-15/16} \cdot |z|^{-17/8}$$

for $z \in \mathbb{R}^3 \backslash \{0\}$, $r \in (0, \infty)$. Applying Lemma 3 with $\mathfrak{A} = \mathfrak{B} = S_T$, $F_1 = F_2 = F^{1/2}$, we get in the case $i \in \{1, 2\}$ that

$$\Big(\int_0^T \int_{\partial\Omega} \Big(\int_0^T \int_{\partial\Omega} H_i(x-y, t-\sigma) \cdot |\varphi(y,\sigma)| \, d\Omega(y) \, d\sigma \Big)^2 \, d\Omega(x) \, dt \Big)^{1/2} \leq \mathfrak{C} \cdot \|\varphi\|_2. \tag{39}$$

Also by Lemma 3, this time with $\mathfrak{A} = \Omega \times (0, T)$, $\mathfrak{B} = S_T$, $F_1 = F_2 = F^{1/2}$,

$$\Big(\int_0^T \int_{\Omega} \Big(\int_0^T \int_{\partial\Omega} \chi_{(1,\infty)}(t-\sigma) \cdot (t-\sigma)^{-5/4} \cdot |\varphi(y,\sigma)| \, d\Omega(y) \, d\sigma \Big)^2 \, dx \, dt \Big)^{1/2} \leq \mathfrak{C} \cdot \|\varphi\|_2. \tag{40}$$

When we apply Lemma 3 with $\mathfrak{A} = \Omega \times (0, T)$, $\mathfrak{B} = S_T$,

$$F_1(x, t, y, \sigma) := \chi_{(0,1)}(t-\sigma) \cdot (t-\sigma)^{-15/32} \cdot |x-y|^{-7/8}$$

for $x \in \Omega$, $y \in \partial\Omega$, $t, \sigma \in (0, \infty)$, and with F_2 defined in the same way as F_1, except that the exponent $-7/8$ is replaced by $-5/4$, we arrive at the estimate

$$\Big(\int_0^T \int_{\Omega} \Big(\int_0^T \int_{\partial\Omega} \chi_{(0,1)}(t-\sigma) \cdot (t-\sigma)^{-15/16} \cdot |x-y|^{-17/8} \cdot |\varphi(y,\sigma)| \, d\Omega(y) \, d\sigma \Big)^2 \, dx \, dt \Big)^{1/2} \leq \mathfrak{C} \cdot \|\varphi\|_2. \tag{41}$$

Inequalities (40) and (41) imply

$$\Big(\int_0^T \int_{\Omega} \Big(\int_0^T \int_{\partial\Omega} H_3(x-y, t-\sigma) \cdot |\varphi(y,\sigma)| \, d\Omega(y) \, d\sigma \Big)^2 \, dx \, dt \Big)^{1/2} \leq \mathfrak{C} \cdot \|\varphi\|_2. \tag{42}$$

Combining (35), (36), (37), (38), (39) and (42) yields $\|w_p(\varphi) \,|\, S_T\|_{H_T} \leq \mathfrak{C}(\kappa_2) \cdot (\kappa_2 - \kappa_1)^{1/2} \cdot \|\varphi\|_2$. This is true for any $p \in \mathbb{N}$. Thus inequality (21) follows with (29). An obvious application of (24), (14) and the mean value theorem yields

$$\Big|\sum_{k=1}^{3}\Big(\partial_i K_{jk}(x-y+\varepsilon\cdot m^{(\Omega)}(x),t-\sigma)-\partial_i K_{jk}(x-y-\varepsilon\cdot m^{(\Omega)}(x),t-\sigma)\Big)\Big|$$
$$\le \mathfrak{C}(\kappa_2)\cdot \min\big\{(|x-y|^2+t-\sigma)^{-3/2},\ \varepsilon\cdot(|x-y|^2+t-\sigma)^{-2}\big\}$$
$$\le \mathfrak{C}(\kappa_2)\cdot\varepsilon^{1/4}\cdot(|x-y|^2+t-\sigma)^{-13/8}$$

for $x, y \in \partial\Omega,\ t\in(0,T),\ \sigma\in(0,t),\ 1\le i,j\le 3,\ \varepsilon\in(0,\mathfrak{D}_2]$. Now the relation in (22) follows after an integration over S_t, for $t\in(0,T)$.

Let us finally suppose that $T<\infty$. Recalling the abbreviation introduced in (30), we may conclude from (23), (24), (14) that for $x\in\overline{\Omega},\ y\in\partial\Omega,\ t\in(0,T),\ p,q\in\mathbb{N},\ j,k\in\{1,2,3\},\ l\in\mathbb{N},\ \alpha\in\mathbb{N}_0^3$ with $|\alpha|+l\le 1$,

$$\begin{aligned}
&|\partial_t^l\partial_x^\alpha K_{jk}\big(\beta_p(x,y),\,t\big)-\partial_t^l\partial_x^\alpha K_{jk}\big(\beta_q(x,y),\,t\big)|\\
&\le \sum_{\nu\in\{p,q\}}|\partial_t^l\partial_x^\alpha K_{jk}\big(\beta_\nu(x,y),\,t\big)|^{7/8}\\
&\quad\cdot|\partial_t^l\partial_x^\alpha K_{jk}\big(\beta_p(x,y),\,t\big)-\partial_t^l\partial_x^\alpha K_{jk}\big(\beta_q(x,y),\,t\big)|^{1/8}\\
&\le \mathfrak{C}(\kappa_2,T)\cdot(\kappa_2-\kappa_1)^{7/8}\cdot(|x-y|^2+t)^{7\cdot(-1-|\alpha|/2-l)/8}\\
&\quad\cdot\Big|\int_0^1\sum_{i=1}^{3}\partial_t^l\partial_x^\alpha\partial_i K_{jk}\big(x-y-(\varepsilon_q+\vartheta\cdot(\varepsilon_p-\varepsilon_q))\cdot m^{(\Omega)}(y),\,t\big)\\
&\quad\cdot(\varepsilon_p-\varepsilon_q)\cdot m_i^{(\Omega)}(y)\,d\vartheta\,\Big|^{1/8}\\
&\le \mathfrak{C}(T,\kappa_2)\cdot(|x-y|^2+t)^{\frac{7}{8}(-1-\frac{|\alpha|}{2}-l)}\cdot\\
&\quad|\varepsilon_p-\varepsilon_q|^{\frac18}\cdot(|x-y|^2+t)^{(-2-\frac{|\alpha|}{2}-\frac{l}{8})}\\
&\le \mathfrak{C}(T,\kappa_2)\cdot|\varepsilon_p-\varepsilon_q|^{1/8}\cdot(|x-y|^2+t)^{-9/8-|\alpha|/2-l}.
\end{aligned}\tag{43}$$

Now it is easy to show with (24) and (27) that in the situation of (43), with $\sigma\in(0,t)$,

$$|\partial_t^l\partial_x^\alpha\big[\zeta^{(\varepsilon_p)}(t)K_{jk}\big(\beta_p(x,y),\,t-\sigma\big)\big]-\partial_t^l\partial_x^\alpha\big[\zeta^{(\varepsilon_q)}(t)K_{jk}\big(\beta_q(x,y),\,t-\sigma\big)\big]|$$
$$\le \mathfrak{C}(T,\kappa_2)|\varepsilon_p-\varepsilon_q|^{1/8}(|x-y|^2+t-\sigma)^{-9/8-|\alpha|/2-l}.$$

Due to this inequality, one may use similar arguments as in the proof of (21), but with simplifications because of the assumption $T<\infty$, to obtain

$$\|\big(w_p(\varphi)-w_q(\varphi)\big)\,|\,S_T\|_{H_T}\le \mathfrak{C}(T,\kappa_2)\cdot|\varepsilon_p-\varepsilon_q|^{1/8}\cdot\|\varphi\|_2\quad\text{for}\quad p,q\in\mathbb{N}.$$

It follows with (29) that

$$\sup\big\{\,\|w_p(\varphi)-(\mathfrak{F}_T^{(\kappa_2)}-\mathfrak{F}_T^{(\kappa_1)})(\varphi)\|_{H_T}/\|\varphi\|_2\,:\,\varphi\in L^2_n(S_T)\backslash\{0\}\big\}\longrightarrow 0\tag{44}$$

for $n \to \infty$. On the other hand, take $p \in \mathbb{N}$. Since $T < \infty$ and the functions $\mathfrak{K}_{p,j,k,m}$ and $\mathfrak{M}_{p,j,k}$ are bounded (see (31)), and because of (32), we may conclude that $\mathfrak{A}_{p,j,k,m}$, $\mathfrak{B}_{p,j,k}$ and $\mathfrak{C}_{p,j,k}$ are compact as operators from $L^2(S_T)$ into $L^2(S_T)$. Thus, due to (35), it follows that the operator $W_p : L^2_n(S_T) \ni \psi \mapsto w_p(\psi) \,|\, S_T \in H_T$ is compact. In view of (44), this means that $\mathfrak{F}_T^{(\kappa_2)} - \mathfrak{F}_T^{(\kappa_1)} : L^2_n(S_T) \mapsto H_T$ is compact. □

Theorem 5 (jump relations) *Let* $T \in (0, \infty]$, $\kappa \in [0, \infty)$, $\varphi \in L^2(S_T)^3$, $j \in \{1, 2, 3\}$, *and put* $V := \mathfrak{V}^{(\kappa)}(\varphi) \,|\, (\mathbb{R}^3 \backslash \partial\Omega) \times (0, T)$. *Then*

$$Q(\varphi)\big(x + \varepsilon \cdot m^{(\Omega)}(x),\, t\big) - Q(\varphi)\big(x - \varepsilon \cdot m^{(\Omega)}(x),\, t\big) \longrightarrow n^{(\Omega)}(x) \cdot \varphi(x, t),$$

$$\sum_{k=1}^{3}\Big(\big(\partial_k V_j - \delta_{jk} \cdot Q(\varphi)\big)\big(x + \varepsilon \cdot m^{(\Omega)}(x),\, t\big)\Big) \cdot n_k^{(\Omega)}(x)$$
$$- \sum_{k=1}^{3}\Big(\big(\partial_k V_j - \delta_{jk} \cdot Q(\varphi)\big)\big(x - \varepsilon \cdot m^{(\Omega)}(x),\, t\big)\Big) \cdot n_k^{(\Omega)}(x) \longrightarrow -\varphi_j(x, t)$$

for $\varepsilon \downarrow 0$, *for a. e.* $x \in \partial\Omega$, $t \in (0, T)$.

Proof See (13) and [19, Lemma 2.3.4] in the case $\kappa = 0$. The statement for $\kappa > 0$ follows with (22). □

Now we may establish a result which serves to prove uniqueness of a solution to the integral equation (11). The general approach for proving this result is standard, but in our particular situation, the problem consists in interpreting all the integrals involved in a rigorous way.

Theorem 6 *Let* $T \in (0, \infty]$, $\kappa \in [0, \infty)$ $\varphi \in L^2_n(S_T)$ *with* $\mathfrak{F}_T^{(\kappa)}(\varphi) = 0$. *Then* $\varphi = 0$.

Proof Let $\widetilde{T} \in (0, T)$. For $p \in \mathbb{N}$, we put $\varepsilon_p := \min\{1, \mathfrak{D}_2\}/p$, and we set for $j \in \{1, 2, 3\}$, $x \in \mathbb{R}^3$ with $\operatorname{dist}(x, U) < \mathfrak{D}_1 \cdot \varepsilon_p/2$, $t \in [0, \widetilde{T}]$,

$$V_j^{(p)}(x, t) := \int_0^t \int_{\partial\Omega} \sum_{k=1}^{3} \Lambda_{jk}\big(x - y + \varepsilon_p \cdot m^{(\Omega)}(y),\, t - \sigma,\, \kappa\big) \cdot \varphi_k(y, \sigma)\, d\Omega(y)\, d\sigma, \tag{45}$$

$$Q^{(p)}(x, t) := \int_{\partial\Omega} \sum_{k=1}^{3} E_k\big(x - y + \varepsilon_p \cdot m^{(\Omega)}(y)\big) \cdot \varphi_k(y, t)\, d\Omega(y). \tag{46}$$

By (13), (14) and Lemma 5, we have for $1 \le j, k \le 3$, $p \in \mathbb{N}$, $t \in [0, \widetilde{T}]$ that

$$V_j^{(p)}(\,\cdot\,, t),\ Q^{(p)}(\,\cdot\,, t) \in C^\infty(U_p), \quad \partial_k V^{(p)},\ V^{(p)} \in C^0\big(U_p \times [0, \widetilde{T}]\big)^3$$

with $U_p := \{x \in \mathbb{R}^3 : \operatorname{dist}(x, U) < \mathfrak{D}_1 \cdot \varepsilon_p/2\}$. It further follows that the derivative $\partial_t V^{(p)}(x, t)$ exists for $x \in U_p$ and for a. e. $t \in (0, \widetilde{T})$, with

$$\partial_t V_j^{(p)}(x,t) = \int_0^t \int_{\partial\Omega} \sum_{k=1}^{3} \partial_t \Lambda_{jk}\big(x-y+\varepsilon_p \cdot m^{(\Omega)}(y),\ t-\sigma, \kappa\big) \tag{47}$$
$$\cdot \varphi_k(y,\sigma)\, d\Omega(y)\, d\sigma \ -\ \partial_{x_j} Q^{(p)}(x,t),$$
$$\partial_t V_j^{(p)}(x,t) - \Delta_x V_j^{(p)}(x,t) + \tau \cdot \partial_{x_1} V_j^{(p)}(x,t) + \partial_{x_j} Q^{(p)}(x,t) = 0. \tag{48}$$

We may conclude from (47) and (14) that

$$|\partial_t V_j^{(p)}(x,t)| \le \mathfrak{C}(\widetilde{T}, p) \cdot \|\varphi(\,\cdot\,,t)\|_2 \quad \text{for } x \in U_p,\ t \in (0,\widetilde{T}). \tag{49}$$

This means in particular the function $\partial_t V^{(p)}(x,\ \cdot\ )$ is square integrable on $(0,\widetilde{T})$. On the other hand, this function is not only the pointwise, but also the weak derivative of $V^{(p)}(x,\ \cdot\ )$ on $(0,\widetilde{T})$. Since $V^{(p)}(x,\ \cdot\ )$ is continuous on $[0,\widetilde{T}]$, we thus have $V^{(p)}(x,\ \cdot\ ) \in H^1\big((0,\widetilde{T})\big)^3$. Moreover, for $p, q \in \mathbb{N},\ R \in [R_0,\infty)$, we get from (48) that

$$0 = \int_0^{\widetilde{T}} \int_{B_R\setminus\overline{\Omega}} \big(\partial_t V^{(p)} - \Delta_x V^{(p)} + \tau \cdot \partial_{x_1} V^{(p)} + \nabla_x Q^{(p)}\big) \cdot V^{(q)}\, dx\, dt,$$

hence by partial integration and the equation $\operatorname{div}_x V^{(p)} = 0$,

$$\begin{aligned} 0 &= \int_0^{\widetilde{T}}\int_{\partial B_R \cup \partial\Omega} \sum_{j,k=1}^{3} \Big((-\partial_k V_j^{(p)} + \delta_{jk} Q^{(p)}\big) V_j^{(q)}\Big)(x,t) N_k^{(R)}(x)\, do_x\, dt \\ &+ \int_0^{\widetilde{T}}\int_{\Omega_R} \Big((\nabla_x V^{(p)} \nabla_x V^{(q)}) + \tau(\partial_{x_1} V^{(p)} V^{(q)}) + (\partial_t V^{(p)} V^{(q)})\Big)(x,t)\, dx\, dt, \end{aligned} \tag{50}$$

where $N^{(R)} : \partial\Omega_R \mapsto \mathbb{R}^3$ denotes the outward unit normal to $\Omega_R := B_R\setminus\overline{\Omega}$, that is, $N^{(R)}(x) := R^{-1} \cdot x$ for $x \in \partial B_R,\ N^{(R)} := -n^{(\Omega)}(x)$ for $x \in \partial\Omega$. Now abbreviate $\mathfrak{V} := \mathfrak{V}^{(\tau)}(\varphi)$. As explained in the proof of [5, Theorem 2.4], we have

$$\begin{aligned} \|\big(V^{(p)} - \mathfrak{V}\big) \,|\, \Omega_R \times (0,\widetilde{T})\|_{1,2} \to 0, \quad (p \to \infty) \\ \|(V^{(p)} - \mathfrak{V}) \,|\, S_{\widetilde{T}}\|_2 \to 0, \quad (p \to \infty). \end{aligned} \tag{51}$$

Recalling that $\mathfrak{V}|S_T = \mathfrak{F}_T^{(\kappa)}(\varphi) = 0$ by the choice of φ, and noting that the function $\mathfrak{V} \,|\, \Omega_R \times (0,T)$ belongs to $L^2(0,T,\ H^1(\Omega_R)^3)$ by Theorem 2, we may thus deduce from (50) and (49), by first letting q, and then p, tend to zero,

$$0 = \int_0^{\widetilde{T}}\int_{\partial B_R} \Big(\sum_{j,k=1}^{3} \Big((-\partial_{x_k} \mathfrak{V}_j(x,t) + \delta_{jk} Q(\varphi)(x,t)\big)\mathfrak{V}_j(x,t)\Big) x_k/R\, do_x\, dt$$
$$+ \int_0^{\widetilde{T}} \int_{\Omega_R} \big(|\nabla_x \mathfrak{V}(x,t)|^2 + \tau \partial_{x_1} \mathfrak{V}(x,t)\mathfrak{V}(x,t)\big)\, dx\, dt$$

$$+ \lim_{p\to\infty} \int_0^{\widetilde{T}} \int_{\Omega_R} \partial_t V^{(p)}(x,t) \mathfrak{V}(x,t)\, dx\, dt. \tag{52}$$

On the other hand, referring to (51) and the relation $\mathfrak{V}|S_T = \mathfrak{F}_T^{(\kappa)}(\varphi) = 0$, we get

$$\begin{aligned}
&\int_0^{\widetilde{T}} \int_{\Omega_R} \partial_{x_1} \mathfrak{V}(x,t) \cdot \mathfrak{V}(x,t)\, dx\, dt \qquad (53)\\
&= \lim_{p\to\infty} \int_0^{\widetilde{T}} \int_{\Omega_R} \partial_{x_1} V^{(p)}(x,t) \cdot V^{(p)}(x,t)\, dx\, dt\\
&= \lim_{p\to\infty} \int_0^{\widetilde{T}} \int_{\partial B_R \cup \partial\Omega} (1/2) \cdot |V^{(p)}(x,t)|^2 \cdot N^{(R)}(x)\, do_x\, dt\\
&= \int_0^{\widetilde{T}} \int_{\partial B_R} (1/2) \cdot |\mathfrak{V}(x,t)|^2 \cdot x_1/R\, do_x\, dt.
\end{aligned}$$

Let us determine the remaining limit in (52). To this end, we first observe that for $j \in \{1, 2, 3\},\ p \in \mathbb{N},\ x \in \Omega_R,\ t \in (0, \widetilde{T})$, the following relations are valid:

$$\begin{aligned}
&|V^{(p)}(x,t) - \mathfrak{V}(x,t)|\\
&= \Big| \int_0^t \int_{\partial\Omega} \sum_{k,l=1}^3 \int_0^1 \partial_l \Lambda_{jk}\big(x - y + \vartheta \cdot \varepsilon_p \cdot m^{(\Omega)}(y),\ t-\sigma,\ \kappa\big)\, d\vartheta \cdot \varepsilon_p\\
&\qquad \cdot m_l^{(\Omega)}(y) \cdot \varphi_k(y,\sigma)\, d\Omega(y)\, d\sigma \Big|\\
&\le \mathfrak{C}(\kappa, R) \cdot \varepsilon_p \cdot \int_0^t \int_{\partial\Omega} (|x-y|^2 + t - \sigma)^{-2} \cdot |\varphi(y,\sigma)|\, d\Omega(y)\, d\sigma,
\end{aligned}$$

where we used Lemma 5 with $K = 2 \cdot R$ and (14) in the last estimate. By Lemma 3 with $\mathfrak{A} = \Omega_R \times (0, \widetilde{T}),\ \mathfrak{B} = S_{\widetilde{T}}$,

$$\begin{aligned}
F_1(x,t,y,\sigma) &:= \chi_{(0,\infty)}(t-\sigma) \cdot (|x-y|^2 + t - \sigma)^{-7/8},\\
F_2(x,t,y,\sigma) &:= \chi_{(0,\infty)}(t-\sigma) \cdot (|x-y|^2 + t - \sigma)^{-9/8}
\end{aligned}$$

for $x \in \Omega_R,\ y \in \partial\Omega,\ t, \sigma \in (0, \widetilde{T})$, we get

$$\|(V^{(p)} - \mathfrak{V})\,|\,\Omega_R \times (0, \widetilde{T})\|_2 \le \mathfrak{C}(\kappa, \widetilde{T}, R) \cdot \varepsilon_p \cdot \|\varphi\|_2 \quad \text{for } p \in \mathbb{N}. \tag{54}$$

On the other hand, we refer to (14), (47), Lemma 5 with $K = 2 \cdot R$, and to Lemma 3 with $\mathfrak{A}$, $\mathfrak{B}$, $F_2,\ F_1$ as above, except that the exponent $-7/8$ in the definition of F_1 is replaced by $-15/16$. It follows for $p \in \mathbb{N},\ 1 \le j \le 3$,

$$\Big(\int_0^{\widetilde{T}} \int_{\Omega_R} |\partial_t V_j^{(p)}(x,t) + \partial_{x_j} Q^{(p)}(x,t)|^2\, dx\, dt \Big)^{1/2}$$

$$\leq \Big(\int_0^{\widetilde{T}} \int_{\Omega_R} \Big| \int_0^t \int_{\partial\Omega} \sum_{k=1}^{3} \partial_t \Lambda_{jk}\big(x - y + \varepsilon_p m^{(\Omega)}(y),\ t - \sigma, \kappa \big)$$

$$\cdot\ \varphi_k(y,\sigma)\, d\Omega(y)\, d\sigma \Big|^2 dx\, dt \Big)^{1/2}$$

$$\leq \mathfrak{C}(R) \cdot$$

$$\cdot \Big(\int_0^{\widetilde{T}} \int_{\Omega_R} \Big(\int_0^t \int_{\partial\Omega} \leq \big((|x-y| + \varepsilon_p)^2 + t - \sigma \big)^{-5/2} |\varphi(y,\sigma)|\, d\Omega(y)\, d\sigma \Big)^2 dx\, dt \Big)^{1/2}$$

$$\leq \mathfrak{C}(R)\varepsilon_p^{-7/8} \cdot$$

$$\cdot \Big(\int_0^{\widetilde{T}} \int_{\Omega_R} \Big(\int_0^t \int_{\partial\Omega} (|x-y|^2 + t - \sigma)^{-33/16} \cdot |\varphi(y,\sigma)|\, d\Omega(y)\, d\sigma \Big)^2 dx\, dt \Big)^{1/2} \tag{55}$$

$$\leq \mathfrak{C}(\kappa, \widetilde{T}, R) \cdot \varepsilon_p^{-7/8} \cdot \|\varphi\|_2.$$

A similar argument yields

$$\begin{aligned} &\Big(\int_0^{\widetilde{T}} \int_{\Omega_R} |\partial_{x_j} Q^{(p)}(x,t)|^2\, dx\, dt \Big)^{1/2} \\ &\leq \mathfrak{C} \cdot \varepsilon_p^{-7/8} \cdot \Big(\int_0^{\widetilde{T}} \int_{\Omega_R} \Big(\int_{\partial\Omega} |x-y|^{-17/8} \cdot |\varphi(y,t)|\, d\Omega(y) \Big)^2 dx\, dt \Big)^{1/2} \\ &\leq \mathfrak{C}(\widetilde{T}, R) \cdot \varepsilon^{-7/8} \cdot \|\varphi\|_2 \end{aligned}$$

for $p \in \mathbb{N},\ 1 \leq j \leq 3$. Due to (54), (55), (47) and the preceding estimate, we may conclude for $p \in \mathbb{N}$ that

$$\Big| \int_0^{\widetilde{T}} \int_{\Omega_R} \partial_t V^{(p)} \cdot (\mathfrak{V} - V^{(p)})\, dx\, dt \Big| \leq \mathfrak{C}(\kappa, \widetilde{T}, R) \cdot \varepsilon_p^{1/8} \cdot \|\varphi\|_2^2.$$

Thus we get

$$\begin{aligned} &\lim_{p\to\infty} \int_0^{\widetilde{T}} \int_{\Omega_R} \partial_t V^{(p)} \cdot \mathfrak{V}\, dx\, dt = \lim_{p\to\infty} \int_0^{\widetilde{T}} \int_{\Omega_R} \partial_t V^{(p)} \cdot V^{(p)}\, dx\, dt \\ &= \lim_{p\to\infty} \int_{\Omega_R} \big(|V^{(p)}(x,\widetilde{T})|^2 - |V^{(p)}(x,0)|^2 \big)/2\, dx = \int_{\Omega_R} |\mathfrak{V}(x,\widetilde{T})|^2/2\, dx. \end{aligned} \tag{56}$$

We note that the partial integration in (56) is justified because the function $V^{(p)}(x,\ \cdot\ )$ belongs to $C^0([0,\widetilde{T}])^3$ and to $H^1\big((0,\widetilde{T})\big)^3$, for $x \in U_p,\ p \in \mathbb{N}$, as observed above. The last equation in (56) follows from (14) and Lebesgue's theorem on dominated convergence; compare the proof of [5, Theorem 2.4], in particular [5, (33)]. Also note that $V^{(p)}(x,0) = 0$ for $p \in \mathbb{N}$, $x \in U_p$. Equation (52), (53) and (56) yield

$$0 = \int_0^{\widetilde{T}} \int_{\partial B_R} \Big(\sum_{j,k=1}^{3} -\partial_{x_k} \mathfrak{V}_j(x,t) \mathfrak{V}_j(x,t) x_k / R \tag{57}$$

$$+ (\tau/2) |\mathfrak{V}(x,t)|^2 x_1/R \; + \; Q(\varphi)(x,t) R^{-1} \big(x \mathfrak{V}(x,t) \big) \Big) \, do_x \, dt$$

$$+ \int_0^t \int_{\Omega_R} |\nabla_x \mathfrak{V}(x,t)|^2 \, dx \, dt \; + \; (1/2) \int_{\Omega_R} |\mathfrak{V}(x,\widetilde{T})|^2 \, dx.$$

We have $\int_0^{\widetilde{T}} \int_U |\nabla_x \mathfrak{V}(x,t)|^2 \, dx \, dt < \infty$ and $\int_U |\mathfrak{V}(x,\widetilde{T})|^2 \, dx < \infty$, according to [5, Corollary 3.1]. Moreover, by Lemma 5 with $K = R_0/2$,

$$|\partial^\alpha \mathfrak{V}(x,t)| \le \mathfrak{C}(\kappa, \widetilde{T}, R_0) \cdot \|\varphi\|_2 \cdot |x|^{-3/2-|\alpha|/2},$$
$$|Q(\varphi)(x,t)| \le \mathfrak{C}(\kappa, \widetilde{T}) \|\varphi\|_2 \cdot |x|^{-2}$$

for $x \in B^c_{R_0}$, $t \in (0,\widetilde{T})$, $\alpha \in \mathbb{N}_0^3$ with $|\alpha| \le 1$. Thus, letting R tend to infinity in (57), we obtain

$$0 = \int_0^{\widetilde{T}} \int_U |\nabla_x \mathfrak{V}(x,t)|^2 \, dx \, dt + (1/2) \int_U |\mathfrak{V}(x,\widetilde{T})|^2 \, dx. \tag{58}$$

Since $\widetilde{T}$ is an arbitrary number in $(0,T)$, and because $\mathfrak{V}|Z_T$ is continuous, we may conclude that $\mathfrak{V}|Z_T = 0$. Therefore Eq. (7) (verified according to Lemma 6), the assumption that U is connected, and the decay of $Q(\varphi)(x,t)$ for $|x| \to \infty$ imply that $Q(\varphi)(x,t) = 0$ for $x \in U$ and for a. e. $t \in (0,T)$.

Next we define $V^{(-p)}(x,t)$ and $Q^{(-p)}(x,t)$ in the same way as respectively $V^{(p)}(x,t)$ and $Q^{(p)}(x,t)$ in (45) and (46), but for $x \in \mathbb{R}^3$ with $\operatorname{dist}(x,\overline{\Omega}) < \mathfrak{D}_1 \cdot \varepsilon_p/2$ instead of $x \in U_p$, and with the term $-y + \varepsilon_p \cdot m^{(\Omega)}(y)$ replaced by $-y - \varepsilon_p \cdot m^{(\Omega)}(y)$. By a reasoning analogous to (but somewhat simpler than) the one which led to (58), we may show that $\mathfrak{V} \mid \Omega \times (0,T) = 0$ and that for a. e. $t \in (0,T)$, there is $c_{in}(t) \in \mathbb{R}$ with $Q(\varphi)(x,t) = c_{in}(t)$ for $x \in \Omega$. It follows that

$$Q(\varphi)(x + \varepsilon_p \cdot m^{(\Omega)}(x),\ t) - Q(\varphi)(x - \varepsilon_p \cdot m^{(\Omega)}(x),\ t) \;\to\; -c_{in}(t) \quad (p \to \infty)$$

for $x \in \partial\Omega$ and for a. e. $t \in (0,T)$. Thus we may conclude from Theorem 5 that $-c_{in}(t) = n^{(\Omega)}(x) \cdot \varphi(x,t)$ for a. e. $x \in \partial\Omega$, $t \in (0,T)$, hence

$$-c_{in}(t) \cdot \int_{\partial\Omega} d\Omega(x) = \int_{\partial\Omega} n^{(\Omega)}(x) \cdot \varphi(x,t) \, d\Omega(x) \quad \text{for a. e. } t \in (0,T).$$

Since $\varphi \in L^2_n(\partial\Omega)$, we arrive at the equation $c_{\text{in}}(t) = 0$ for a. e. $t \in (0, T)$. But $\mathfrak{V} \,|\, (\mathbb{R}^3 \backslash \partial\Omega) \times (0, T) = 0$, as proved above, so we have

$$\sum_{k=1}^{3} \Big(\partial_k(\mathfrak{V}_j|\mathfrak{O}) - \delta_{jk} \cdot Q(\varphi) \Big)\Big(x + \varepsilon_p \cdot m^{(\Omega)}(x),\ t \Big) \cdot n_k^{(\Omega)}(x) -$$
$$\sum_{k=1}^{3} \Big(\partial_k(\mathfrak{V}_j|\mathfrak{O}) - \delta_{jk} \cdot Q(\varphi) \Big)\Big(x - \varepsilon_p \cdot m^{(\Omega)}(x),\ t \Big) \cdot n_k^{(\Omega)}(x) \ \to 0 \quad (p \to \infty)$$

for $1 \le j \le 3$, a. e. $x \in \partial\Omega,\ \ t \in (0, T)$, where we used the abbreviation $\mathfrak{O} := (\mathbb{R}^3 \backslash \partial\Omega) \times (0, T)$. Now Theorem 5 yields $\varphi = 0$. □

At this point we may prove the invertibility of the operator $\mathfrak{F}_T^{(\tau)}$.

Corollary 2 *Let* $T \in (0, \infty]$. *Then the operator* $\mathcal{F}_T^{(\tau)} : L^2_n(S_T) \mapsto H_T$ *is linear, bounded and bijective.*

Proof Let $\kappa \in (0, \infty)$. For any $T' \in (0, \infty)$, the operator $\mathfrak{F}_{T'}^{(\kappa)} - \mathfrak{F}_{T'}^{(0)}$ is linear, bounded and compact; see Theorem 4. Theorem 3 now implies that $\mathfrak{F}_{T'}^{(\kappa)}$ is linear, bounded and closed range for $T' \in (0, \infty)$. Since $\mathfrak{F}_{T'}^{(\kappa)}(\varphi|S_{T'}) = \mathfrak{F}_T^{(\kappa)}(\varphi) \,|\, S_{T'}$ for $T' \in (0, T),\ \varphi \in L^2_n(S_T)$, it is not difficult to conclude that $\mathfrak{F}_T^{(\kappa)}$ is also closed-range even if $T = \infty$. A detailed argument may be found in the proof of [3, Lemma 12]. On the other hand, we know by Theorem 6 that the operator $\mathfrak{F}_T^{(\kappa)}$ is one-to-one, and by Theorem 3 and 4 that it is bounded. Thus this operator is linear, bounded and semi-Fredholm. This is true for any $\kappa \in (0, \infty)$. Due to inequality (21), the index of this operator is stable with respect to κ. In this respect, we refer to [17, Theorem I.3.11], where Fredholm operators are considered. But the result stated there also holds for semi-Fredholm operators. To see this, it suffices to replace the reference to [17, Theorem I.3.5] in [17] by a reference to [14, p. 235, Theorem 5.17] (stability of the index of semi-Fredholm operators with respect to small perturbations). But by Theorem 3, the index of $\mathfrak{F}_T^{(0)}$ equals zero. Thus we may conclude that the operator $\mathfrak{F}_T^{(\tau)}$ also has index zero. Recalling that the latter operator is one-to-one (Theorem 6), we thus obtain that it is even bijective. □

The preceding corollary means that we may solve the integral equation in (11) if its right-hand side is in H_T:

Corollary 3 *Let* $T \in (0, \infty],\ \ c \in H_T$. *Then there is a unique function* $\varphi \in L^2_n(S_T)$ *which solves (11). There is* $C = C(\tau, \Omega) > 0$ *such that* $\|\varphi\|_2 \le C \cdot \|\mathfrak{F}_T^{(\tau)}(\varphi)\|_{H_T}$ *for* $\varphi \in L^2_n(S_T)$.

Proof We still have to show that the constant C does not depend on $T \in (0, \infty]$. To this end, suppose that $T \in (0, \infty)$. For $b \in H_T,\ \ x \in \partial\Omega,\ \ t \in (0, \infty)$, define

$$G_T(b)(x, t) := b(x, t) \ \text{ if } t \le T, \quad G_T(b)(x, t) := b(x, 2T - t) \ \text{ if } \ t \in (T,\ 2T],$$
$$G_T(b)(x, t) := 0 \ \text{ if } \ t > 2 \cdot T.$$

Then $G_T(b) \in H_T$ and

$$\|G_T(b)\|_{H_\infty} \le \mathfrak{C} \cdot \|b\|_{H_T} \quad \text{for } \; b \in H_T. \tag{59}$$

The proof of this result is not trivial; we refer to [1] for details. To indicate a possible way to proceed, we mention that for $x \in \mathbb{R}^3, \; t \in [0, T], \; v \in \widetilde{H}_T$,

$$v(x,t) = B(1/2, 1/2)^{-1/2} \cdot \int_0^t (t-s)^{-1/2} \cdot \partial_4^{1/2} v(x,s)\, ds, \tag{60}$$

where B denotes the usual beta function. By applying (60) to $v(x,t)$ for $t \le T$ and to $v(x, 2 \cdot T - t)$ for $t \in (T, \; 2 \cdot T)$, it is possible to prove that

$$\|\partial_4^{1/2} G_T(v|S_T)\|_2 \le \mathfrak{C} \cdot \left(\|v|S_T\|_2 + \|\partial_4^{1/2} v|S_T\|_2 \right) \quad \text{for } \; v \in \widetilde{H}_T.$$

Then inequality (59) may be established by some obvious additional estimates. Once an extension operator G_T from H_T to H_∞ with (59) is available, the corollary follows from Corollary 2 with $T = \infty$. □

References

1. Brown, R. M.: Layer Potentials and Boundary Value Problems for the Heat Equation in Lipschitz Domains. Thesis, University of Minnesota (1987)
2. Deuring, P.: *The Stokes System in an Infinite Cone.* Akademie Verlag, Berlin (1994)
3. Deuring, P.: The single-layer potential associated with the time-dependent Oseen system. Proceedings of the 2006 IASME/WSEAS International Conference on Continuum Mechanics. Chalkida, Greeece, May 11–13, 117–125 (2006)
4. Deuring, P.: On volume potentials related to the time-dependent Oseen system. WSEAS Trans. Math. **5**, 252–259 (2006)
5. Deuring, P.: On boundary-driven time-dependent Oseen flows. Banach Center Publ. **81**, 119–132 (2008)
6. Deuring, P.: Spatial decay of time-dependent Oseen flows. SIAM J. Math. Anal. **41**, 886–922 (2009)
7. Deuring, P., Kračmar, S.: Exterior stationary Navier-Stokes flows in 3D with non-zero velocity at infinity: approximation by flows in bounded domains. Math. Nachr. **269–270**, 86–115 (2004)
8. Enomoto, Y., Shibata, Y.: Local energy decay of solutions to the Oseen equation in the exterior domain. Indiana Univ. Math. J. **53**, 1291–1330 (2004)
9. Enomoto, Y., Shibata, Y.: On the rate of decay of the Oseen semigroup in exterior domains and its application to Navier-Stokes equation. J. Math. Fluid Mech. **7**, 339–367 (2005)
10. Farwig, R.: The stationary exterior 3D-problem of Oseen and Navier-Stokes equations in anisotropically weighted Sobolev spaces. Math. Z. **211**, 409–447 (1992)
11. Fučik, S., John, O., Kufner, A.: *Function Spaces.* Noordhoff, Leyden (1977)
12. Galdi, G. P., Silvestre, A. S.: Strong solutions to the Navier-Stokes equations around a rotating obstacle. Arch. Rat. Mech. Appl. **176**, 331–350 (2005)
13. Galdi, G. P., Silvestre, S. A.: The steady motion of a Navier-Stokes liquid around a rigid body. Arch. Rat. Mech. Appl. **184**, 371–400 (2007)
14. Kato, T.: *Perturbation Theory of Linear Operators.* Springer, Berlin e.a. (1996)

15. Knightly, G. H.: Some decay properties of solutions of the Navier-Stokes equations. In: R. Rautmann (ed.), *Approximation Methods for Navier-Stokes Problems.* Lecture Notes in Math. **771**, 287–298, Springer (1979)
16. Kobayashi, T., Shibata, Y.: On the Oseen equation in three dimensional exterior domains. Math. Ann. **310**, 1–45 (1998)
17. Mikhlin, S. G., Prössdorf, S.: *Singular Integral Operators.* Springer, Berlin e.a. (1986)
18. Nečas, J.: *Les Méthodes Directes en Théorie des Équations Elliptiques.* Masson, Paris (1967)
19. Shen, Z.: Boundary value problems for parabolic Lamé systems and a nonstationary linearized system of Navier-Stokes equations in Lipschitz cylinders. Am. J. Math. **113**, 293–373 (1991)
20. Shibata, Y.: On an exterior initial boundary value problem for Navier-Stokes equations. Quarterly Appl. Math. **57**, 117–155 (1999)

Regularity of Weak Solutions for the Navier-Stokes Equations Via Energy Criteria

Reinhard Farwig, Hideo Kozono, and Hermann Sohr

Abstract Consider a weak solution u of the instationary Navier-Stokes system in a bounded domain of $\mathbb{R}^3$ satisfying the strong energy inequality. Extending previous results by Farwig et al., J. Math. Fluid Mech. 11, 1–14 (2008), we prove among other things that u is regular if either the kinetic energy $\frac{1}{2}\|u(t)\|_2^2$ or the dissipation energy $\int_0^t \|\nabla u(\tau)\|_2^2\, d\tau$ is (left-side) Hölder continuous as a function of time t with Hölder exponent $\frac{1}{2}$ and with sufficiently small Hölder seminorm. The proofs use local regularity results which are based on the theory of very weak solutions and on uniqueness arguments for weak solutions.

Keywords Navier-Stokes equations · Weak solutions · Regularity criteria · Energy criteria · Hölder continuity

1 Introduction and Main Results

Given a bounded domain $\Omega \subset \mathbb{R}^3$ with boundary $\partial\Omega$ of class $C^{1,1}$ and a time interval $[0, T)$, $0 < T \leq \infty$, let $u_0 \in L^2_\sigma(\Omega)$ be some initial value and f an external force. In the space-time cylinder $[0, T) \times \Omega$ we consider a weak solution u of the Navier-Stokes system

$$\begin{aligned} u_t - \nu\Delta u + u \cdot \nabla u + \nabla p = f, \quad \operatorname{div} u = 0 \\ u\big|_{\partial\Omega} = 0, \quad u\big|_{t=0} = u_0 \end{aligned} \tag{1}$$

with viscosity $\nu > 0$ as follows.

Definition 1 Let $u_0 \in L^2_\sigma(\Omega)$ and $f = \operatorname{div} F$, $F \in L^2\big(0, T; L^2(\Omega)\big)$. A vector field

$$u \in L^\infty\big(0, T; L^2_\sigma(\Omega)\big) \cap L^2\big(0, T; W_0^{1,2}(\Omega)\big) \tag{2}$$

R. Farwig (✉)
Department of Mathematics, Darmstadt University of Technology, 64283 Darmstadt, Germany
e-mail: farwig@mathematik.tu-darmstadt.de

R. Rannacher, A. Sequeira (eds.), *Advances in Mathematical Fluid Mechanics*,
DOI 10.1007/978-3-642-04068-9_13,

is called a *weak solution* of the system (1) if the relation

$$-\langle u, w_t\rangle_{\Omega,T} + \nu\langle\nabla u, \nabla w\rangle_{\Omega,T} - \langle uu, \nabla w\rangle_{\Omega,T} = \langle u_0, w(0)\rangle_{\Omega} - \langle F, \nabla w\rangle_{\Omega,T} \quad (3)$$

is satisfied for all test functions $w \in C_0^\infty([0,T); C_{0,\sigma}^\infty(\Omega))$.

In this definition $\langle\cdot,\cdot\rangle_\Omega$ and $\langle\cdot,\cdot\rangle_{\Omega,\,T}$ mean the usual pairing of functions on Ω and on $[0,T)\times\Omega$, respectively. For further notations we refer to §2.

As is well known, there exists a weak solution u additionally satisfying the *strong energy inequality*

$$\frac{1}{2}\,\|u(t)\|_2^2 + \nu\int_{t'}^{t}\|\nabla u\|_2^2\,d\tau \le \frac{1}{2}\,\|u(t')\|_2^2 - \int_{t'}^{t}\langle F, \nabla u\rangle_\Omega\,d\tau \quad (4)$$

for almost all $t' \in [0,T)$, including $t' = 0$, and all $t \in [t', T)$, see [22, Theorem V.3.6.2]. Moreover, we may assume in Definition 1 that

$$u : [0,T) \to L_\sigma^2(\Omega) \quad \text{is weakly continuous} \quad (5)$$

with $u(0) = u_0$. Finally, there exists a distribution p, called an *associated pressure*, such that

$$u_t - \nu\Delta u + u\cdot\nabla u + \nabla p = f \quad (6)$$

holds in the sense of distributions, see e.g. [22, Chap. V.1].

Definition 2 A weak solution u of (1) is called *regular* in some interval $(a,b)\subseteq(0,T)$ if *Serrin's condition*

$$u \in L_{\mathrm{loc}}^s\big(a,b;L^q(\Omega)\big) \quad \text{with } 2 < s < \infty,\ 3 < q < \infty,\ \frac{2}{s} + \frac{3}{q} = 1, \quad (7)$$

is satisfied. A time $t \in (0,T)$ is called a *regular point* of u if u is regular in some interval $(a,b)\subseteq(0,T)$ with $a < t < b$.

Condition (7) means that $\|u\|_{L^s(a',b';L^q(\Omega))} < \infty$ for each interval (a',b') with $a < a' < b' < b$. Obviously, for a bounded domain, the identity $\frac{2}{s}+\frac{3}{q} = 1$ may be replaced by the inequality $\frac{2}{s}+\frac{3}{q} \le 1$. If $\partial\Omega$ is of class C^∞ and $f \in C_0^\infty\big((a,b)\times\overline{\Omega}\big)$, then (7) implies that

$$u \in C^\infty\big((a,b)\times\overline{\Omega}\big), \quad p \in C^\infty\big((a,b)\times\overline{\Omega}\big), \quad (8)$$

see e.g. [22, Theorem V.1.8.2]. The limit cases $s = 2$, $q = \infty$ and $s = \infty$, $q = 3$ are much harder to deal with. If $u \in L^\infty\big(a,b;L^3(\Omega)\big)$, then $u \in C^\infty\big((a,b)\times\overline{\Omega}\big)$, see [3, 17–20]. Finally, if $\Omega = \mathbb{R}^3$ and $u \in L^2\big(a,b;L^\infty(\mathbb{R}^3)\big)$ or only $u \in$

$L^2\big(a,b;\mathrm{BMO}(\mathbb{R}^3)\big)$, then the same conclusion holds, see [15]. Concerning criteria based on the kinetic energy $\frac{1}{2}\,\|u(t)\|_2^2$, $t\in(0,T)$, or on the dissipation energy $\int_0^t \|\nabla u(\tau)\|_2^2\,d\tau$ we cite the following result.

Theorem 1 [7, 8] *Let $\Omega\subset\mathbb{R}^3$ be a bounded domain with boundary $\partial\Omega$ of class $C^{2,1}$. Consider a weak solution u of the Navier-Stokes system* (1) *with $u_0\in L^2_\sigma(\Omega)$, $\nu=1$ and vanishing external force f, satisfying the strong energy inequality* (4).

Suppose that at time $t\in(0,T)$ the kinetic energy is left-side Hölder continuous with exponent $\alpha\in(\frac{1}{2},1)$ in the sense that

$$\varlimsup_{\delta\to 0+}\frac{\left|\frac{1}{2}\,\|u(t-\delta)\|_2^2-\frac{1}{2}\,\|u(t)\|_2^2\right|}{\delta^\alpha}<\infty. \tag{9}$$

Then u is regular at t. The same conclusion holds when the dissipation energy satisfies at $t\in(0,T)$ the left-side Hölder condition

$$\varlimsup_{\delta\to 0+}\frac{1}{\delta^\alpha}\int_{t-\delta}^t \|\nabla u\|_2^2\,d\tau<\infty\,. \tag{10}$$

Note that Theorem 1 can easily be generalized to the case of a nonvanishing external force f, see [9].

However, the limit case $\alpha=\frac{1}{2}$ was left open in [8]. The aim of this paper is to extend Theorem 1 to the cases $\alpha=\frac{1}{2}$ and $f\neq 0$, $0<\nu\neq 1$. Note that in this case we do need a smallness condition on the local left-side Hölder seminorm. Actually, it is known, see [12, Theorem 6.4], that if $(0,t)$, $t\in(0,T)$, is a maximal regularity interval of a weak solution u, then necessarily

$$\|\nabla u(\tau)\|_2\geq c(t-\tau)^{-1/4},\quad 0<\tau<t,$$

with some $c=c(\Omega)>0$. Hence (10) with $\alpha=\frac{1}{2}$ fails to imply regularity in general if such a maximal regularity interval exists. Moreover, the estimate

$$2c^2\leq\frac{1}{\delta^{\frac{1}{2}}}\int_{t-\delta}^t\|\nabla u(\tau)\|_2^2\,d\tau\leq\frac{1}{2\delta^{\frac{1}{2}}}\Big|\|u(t)\|_2^2-\|u(t-\delta)\|_2^2\Big|$$

(for a.a. $\delta\in(0,t)$, see (4)) shows in this case that also the condition (9) with $\alpha=\frac{1}{2}$ does not imply regularity in general. Thus the smallness condition (11) in our following main result is essential.

Theorem 2 *Let $\Omega\subset\mathbb{R}^3$ be a bounded domain with boundary $\partial\Omega$ of class $C^{1,1}$. Consider a weak solution u of the Navier-Stokes system* (1) *on* $(0,T)$ *with initial value $u_0\in L^2_\sigma(\Omega)$ and external force $f=\operatorname{div}F$, $f\in L^2\big(0,T;L^2(\Omega)\big)$, $F\in L^4\big(0,T;L^2(\Omega)\big)$, satisfying the strong energy inequality* (4). *Then there exists a constant $\varepsilon_*>0$ independent of ν, u_0 and f with the following property:*

(i) If the kinetic energy is left-side Hölder continuous at time $t\in(0,T)$ with exponent $\alpha=\frac{1}{2}$ in the sense that

$$\varlimsup_{\delta\to 0+} \frac{\left|\frac{1}{2}\,\|u(t-\delta)\|_2^2 - \frac{1}{2}\,\|u(t)\|_2^2\right|}{\delta^{\frac{1}{2}}} \le \varepsilon_* \nu^{5/2}\,, \tag{11}$$

then u is regular at t.

(ii) The same conclusion holds when the dissipation energy satisfies at t the left-side Hölder condition

$$\varlimsup_{\delta\to 0+} \frac{1}{\delta^{\frac{1}{2}}} \int_{t-\delta}^{t} \|\nabla u\|_2^2\, d\tau \le \varepsilon_* \nu^{5/2}\,. \tag{12}$$

Note that the assumptions (9) and (10) immediately imply (11) and (12). Therefore, Theorem 1 is a corollary of Theorem 2. Moreover, $\frac{2}{s} + \frac{3}{2} = -\alpha + \frac{3}{2} = 1$ in Theorem 2. Since

$$\frac{1}{\delta^{\frac{1}{2}}} \int_{t-\delta}^{t} \|\nabla u\|_2^2\, d\tau \le \Big(\int_{t-\delta}^{t} \|\nabla u\|_2^4\, d\tau\Big)^{1/2}$$

we see that condition (12) is weaker than the $L^4(0, T; L^2(\Omega))$-condition on ∇u in [2], which uses Serrin's criterion $\frac{2}{s} + \frac{3}{q} = 2$ for the gradient of the velocity.

We do not know whether there exists any maximal regularity interval $(0, t)$ with $0 < t < T$. However, if it does exist, then Theorem 2 cannot be improved replacing "$\le \varepsilon_* \nu^{5/2}$" by "$< \infty$". Therefore, this result is optimal in a certain sense.

For results on regularity of weak solutions satisfying criteria even beyond Serrin's condition [21] we refer to [6, 9].

2 Proof

Let $\Omega \subset \mathbb{R}^3$ and $0 \le a < b \le T$ be as in Sect. 1. We need the well-known Lebesgue spaces $L^q(\Omega)$, $1 \le q \le \infty$, with norm $\|\cdot\|_{L^q(\Omega)} = \|\cdot\|_q$ and pairing $\langle v, w\rangle_\Omega = \langle v, w\rangle = \int_\Omega v \cdot w\, dx$ for $v \in L^q(\Omega)$, $w \in L^{q'}(\Omega)$, $q' = \frac{q}{q-1}$. Further we use the Bochner spaces $L^s\big(a, b; L^q(\Omega)\big)$, $1 \le s \le \infty$, with norm $\|\cdot\|_{L^s(a,\, b;\, L^q(\Omega))} = \|\cdot\|_{L^s(L^q)} = \big(\int_a^b \|\cdot\|_q^s\, dt\big)^{1/s}$ (and the usual modification when $s = \infty$) and corresponding pairing $\langle v, w\rangle_{\Omega,(a,\, b)}$ for $v \in L^s\big(a, b; L^q(\Omega)\big)$, $w \in L^{s'}\big(a, b; L^{q'}(\Omega)\big)$, $s' = \frac{s}{s-1}$. If $(a, b) = (0, T)$ we write $\langle\cdot,\cdot\rangle_{\Omega,(a,\, b)} = \langle\cdot,\cdot\rangle_{\Omega,\, T}$. We also need the function spaces $C_0^\infty(\Omega)$, $C_{0,\,\sigma}^\infty(\Omega) = \{v \in C_0^\infty(\Omega);\ \operatorname{div} v = 0\}$ of smooth compactly supported functions (vector fields), and $L^q_\sigma(\Omega) = \overline{C_{0,\sigma}^\infty(\Omega)}^{\|\cdot\|_q}$. Let $W^{k,q}(\Omega)$, $k \in \mathbb{N}_0$, $1 \le q \le \infty$ denote the usual Sobolev spaces, and let $W_0^{1,q}(\Omega) = \overline{C_0^\infty(\Omega)}^{\|\cdot\|_{W^{1,q}}}$, $1 \le q < \infty$. For $q = 2$ we also write $W^{1,2}(\Omega) = H^1(\Omega)$ etc.

The proof of Theorem 2 rests on a local existence result of regular solutions, which has been developed in the theory of very weak solutions, see [1, 5]. In this context we use the Helmholtz projection $P_q : L^q(\Omega) \to L^q_\sigma(\Omega)$, $1 < q < \infty$, and the Stokes operator

$$A_q = -P_q\Delta :\ \mathcal{D}(A_q) \to L^q_\sigma(\Omega), \quad \mathcal{D}(A_q) = L^q_\sigma(\Omega) \cap W_0^{1,q}(\Omega) \cap W^{2,q}(\Omega).$$

See [4, 10–14, 23] concerning the following properties of these operators and of the Stokes semigroup $e^{-tA_q} : L^q_\sigma(\Omega) \to L^q_\sigma(\Omega),\ t \geq 0$.

Lemma 1 *Let $\Omega \subset \mathbb{R}^3$ be a bounded domain with boundary of class $C^{1,1}$ and let $1 < q < \infty$.*

1. *The Stokes operator is a closed bijective operator from $\mathcal{D}(A_q) \subset L^q_\sigma(\Omega)$ onto $L^q_\sigma(\Omega)$. If $u \in \mathcal{D}(A_q) \cap \mathcal{D}(A_\varrho)$ for $1 < \varrho < \infty$, then $A_q u = A_\varrho u$.*
2. *For $0 \leq \alpha \leq 1$ the fractional powers $A^\alpha_q : \mathcal{D}(A^\alpha_q) \subset L^q_\sigma(\Omega \to L^q_\sigma(\Omega)$ are well-defined, closed, bijective operators. In particular, the inverses $A^{-\alpha}_q := (A^\alpha_q)^{-1}$ are bounded operators on $L^q_\sigma(\Omega)$ with range $\mathcal{R}(A^{-\alpha}_q) = \mathcal{D}(A^\alpha_q)$. The space $\mathcal{D}(A^\alpha_q)$ endowed with the graph norm $\|u\|_q + \|A^\alpha_q u\|_q$, which is equivalent to $\|A^\alpha_q u\|_q$, is a Banach space. Moreover, for $1 > \alpha > \beta > 0$,*

$$\mathcal{D}(A_q) \subset \mathcal{D}(A^\alpha_q) \subset \mathcal{D}(A^\beta_q) \subset L^q_\sigma(\Omega)$$

   with strict dense inclusions, and $(A^\alpha_q)^* = A^\alpha_{q'}$ is the adjoint to A^α_q.
3. *The norms $\|u\|_{W^{2,q}}$ and $\|A_q u\|_q$ are equivalent for $u \in \mathcal{D}(A_q)$. Analogously, the norms $\|\nabla u\|_q$, $\|u\|_{W^{1,q}}$ and $\|A^{1/2}_q u\|_q$ are equivalent for $u \in \mathcal{D}(A^{1/2}_q) = W^{1,q}_0(\Omega) \cap L^q_\sigma(\Omega)$. More generally, the embedding estimate*

$$\|u\|_q \leq c\|A^\alpha_\gamma u\|_\gamma\,, \quad 1 < \gamma \leq q,\ 2\alpha + \frac{3}{q} = \frac{3}{\gamma}, \tag{13}$$

   holds for every $u \in \mathcal{D}(A^\alpha_\gamma)$; here $c = c(q, \gamma, \Omega) > 0$.
4. *There exists constants $\delta_0 = \delta_0(q, \Omega) > 0$ and $c = c(q, \alpha, \Omega) > 0$ such that*

$$\|A^\alpha_q e^{-tA_q} u\|_q \leq ce^{-\delta_0 t} t^{-\alpha}\, \|u\|_q \quad \text{for } u \in L^q_\sigma(\Omega),\ t > 0. \tag{14}$$

5. *Given $f \in L^s\big(0, T; L^q(\Omega)\big)$, $1 < s,\ q < \infty$, the instationary Stokes system*

$$\begin{aligned} u_t - \nu\Delta u + \nabla p = f,\ \operatorname{div} u = 0 \text{ in } (0, T) \times \Omega,\\ u = 0 \text{ on } (0, T) \times \partial\Omega,\ u(0) = 0 \ \text{ at } t = 0 \end{aligned} \tag{15}$$

   or, equivalently, the abstract evolution equation in $L^q_\sigma(\Omega)$,

$$u_t + \nu A_q u = P_q f, \quad u(0) = 0,$$

   has a unique solution u satisfying the maximal regularity estimate

$$\|u_t\|_{L^s(0,\ T;\ L^q(\Omega))} + \|\nu A_q u\|_{L^s(0,\ T;\ L^q(\Omega))} \leq c\|f\|_{L^s(0,\ T;\ L^q(\Omega))}. \tag{16}$$

   Moreover, there exists a function $p \in L^s\big(0, T; W^{1,q}(\Omega)\big)$ such that (u, p) satisfies (15) *and the estimate*

$$\|(u_t, \nabla p, \nu\nabla^2 u)\|_{L^s(0,\,T;\,L^q(\Omega))} \le c\|f\|_{L^s(0,\,T;\,L^q(\Omega))}. \tag{17}$$

In both estimates $c = c(q, s, \Omega) > 0$ *is independent of* ν, T *and* f.

The following key lemma is an extension and generalization of a similar result, Lemma 2.1 in [6], and essentially a consequence of [5, Theorem 1], the basic theorem on the existence of very weak solutions to the Navier-Stokes equations (see Definition 3 and Lemma 3 below). Here we only need the case $0 < T < \infty$.

Lemma 2 *Given a bounded domain* $\Omega \subset \mathbb{R}^3$ *with boundary* $\partial\Omega \in C^{1,1}$ *and some* $0 < T < \infty$, *consider data*

$$f = \operatorname{div} F,\ \ F \in L^2\big(0, T; L^2(\Omega)\big) \cap L^{\max(s_*,4)}\big(0, T; L^{\max(\varrho,2)}(\Omega)\big)$$

and $u_0 \in L^{q_*}_\sigma(\Omega)$, *where*

$$2 < s_* < \infty, \quad 3 < q_* < \infty, \quad \frac{2}{s_*} + \frac{3}{q_*} = 1, \quad \frac{1}{3} + \frac{1}{q_*} = \frac{1}{\varrho}. \tag{18}$$

Then there exists a constant $\varepsilon_* = \varepsilon_*(q_*, \Omega) > 0$ *independent of* u_0, f *and* ν *with the following property: If*

$$\int_0^T \|F\|_\varrho^{s_*}\, d\tau \le \varepsilon_* \nu^{2s_*-1} \quad \text{and} \quad \int_0^T \|e^{-\nu\tau A_{q_*}} u_0\|_{q_*}^{s_*}\, d\tau \le \varepsilon_* \nu^{s_*-1}, \tag{19}$$

then the Navier-Stokes system (1) *has a unique weak solution u satisfying Serrin's condition* $u \in L^{s_*}\big(0, T; L^{q_*}(\Omega)\big)$ *and moreover the energy inequality* (4).

Before proving Lemma 2 we introduce the notion of very weak solutions (simplified and adapted to our application) and recall the main theorem on their existence and uniqueness. For further results on the theory of very weak solutions to the (Navier-)Stokes equations see [1, 5, 9, 16].

Definition 3 Let $\Omega \subset \mathbb{R}^3$ be a bounded domain with $C^{1,1}$-boundary, let $f = \operatorname{div} F$, $F \in L^2\big(0, T; L^2(\Omega)\big) \cap L^{s_*}\big(0, T; L^\varrho(\Omega)\big)$, $0 < T \le \infty$, and $u_0 \in L^{q_*}_\sigma(\Omega)$, where s_*, q_*, ϱ satisfy (18). Then a vector field $u \in L^{s_*}\big(0, T; L^{q*}(\Omega)\big)$ is called a *very weak solution* of the instationary Navier-Stokes system (1) if

$$-\langle u, w_t\rangle_{\Omega,\,T} - \nu\langle u, \Delta w\rangle_{\Omega,\,T} - \langle uu, \nabla w\rangle_{\Omega,\,T} = \big(u_0, w(0)\big) - \langle F, \nabla w\rangle_{\Omega,\,T} \tag{20}$$

for all test fields $w \in C^1_0\big([0, T);\, C^2_{0,\sigma}(\overline{\Omega})\big)$, and additionally

$$\operatorname{div} u = 0 \quad \text{in } (0, T) \times \Omega, \quad u \cdot N = 0 \quad \text{on } (0, T) \times \partial\Omega. \tag{21}$$

Here $C^2_{0,\sigma}(\overline{\Omega}) = \{w \in C^2(\overline{\Omega}); \operatorname{div} w = 0,\ w = 0 \text{ on } \partial\Omega\}$, and $N = N(x)$ denotes the exterior normal vector at $x \in \partial\Omega$.

Note that $u \cdot N = 0$ on $(0, T) \times \partial\Omega$ is well-defined in the sense of distributions since $\operatorname{div} u = 0$, see [5].

Lemma 3 [5, Theorem 1] *Given data F, u_0 as in Definition 3, there exists some $T' = T'(\nu, F, u_0) \in (0, T]$ and a unique very weak solution $u \in L^{s_*}\big(0, T'; L^{q_*}(\Omega)\big)$ of the Navier-Stokes system* (1)*. The interval of existence,* $[0, T')$*, is determined by the condition*

$$\Big(\int_0^{T'} \|\nu e^{-\nu t A_{q_*}} u_0\|_{q_*}^{s_*}\, dt\Big)^{1/s_*} + \|F\|_{L^{s_*}(0,T';L^{\varrho})} \le \varepsilon_* \nu^{2-1/s_*}. \tag{22}$$

Moreover, the solution u has the representation $u(t) = \gamma(t) + \tilde{u}(t)$ where

$$\gamma \in L^\infty\big(0, T; L^2(\Omega)\big) \cap L^2\big(0, T; H_0^1(\Omega)\big) \tag{23}$$

is the weak solution of the instationary Stokes system with data u_0, f in $(0, T) \times \Omega$*, i.e.*

$$\gamma(t) = e^{-\nu t\, A_{q*}} u_0 + \int_0^t A_{q_*} e^{-\nu(t-\tau)A_{q*}}\, A_{q_*}^{-1} P_{q_*} \operatorname{div} F(\tau)\, d\tau, \tag{24}$$

and where $\tilde{u}$ satisfies

$$\tilde{u}(t) = -\int_0^t A_{q_*/2}^{1/2}\, e^{-\nu(t-\tau)A_{q*/2}} A_{q_*/2}^{-1/2} P_{q_*/2} \operatorname{div}(uu)\, d\tau. \tag{25}$$

Note that $v = A_{q_*/2}^{-1/2}\tilde{u}$ solves the nonlinear system

$$v_t + A_{q_*/2} v = -A_{q_*/2}^{-1/2} P_{q_*/2} \operatorname{div}(uu), \quad v(0) = 0,$$

in the strong sense.

At this point we will explain the meaning of terms such as $A_q^{-1} P_q \operatorname{div} F$ and $A_q^{-1/2} P_q \operatorname{div} F$, cf. (24), (25). Let $0 < \alpha \le 1$, $1 < q < \infty$, and let ψ be a functional on $C_{0,\sigma}^\infty(\Omega)$ satisfying the estimate

$$|\langle \psi, \varphi\rangle| \le c_\psi \|A_{q'}^\alpha \varphi\|_{q'} \quad \text{for all} \quad \varphi \in \mathcal{D}(A_{q'}^\alpha)$$

with constant $c_\psi \ge 0$. Then there exists a unique element $\Psi \in L_\sigma^q(\Omega)$, denoted by $A_q^{-\alpha} P_q \psi$, such that

$$\langle \psi, \varphi\rangle = \langle A_q^{-\alpha} P_q \psi, A_{q'}^\alpha \varphi\rangle \quad \text{for all} \quad \varphi \in \mathcal{D}(A_{q'}^\alpha)$$

and $\|A_q^{-\alpha} P_q \psi\|_q \le c_\psi$.

In particular, if $\frac{1}{3} + \frac{1}{q} = \frac{1}{\varrho}$, then the embedding $W^{1,\varrho}(\Omega) \subset L^q(\Omega)$ implies the estimate

$$\|A_q^{-1} P_q \mathrm{div}\, F\|_q \le c\|F\|_\varrho \quad \text{for all} \quad F \in L^\varrho(\Omega) \tag{26}$$

with $c = c(\Omega, q) > 0$. Correspondingly, it holds

$$\|A_\varrho^{-1/2} P_\varrho \mathrm{div}\, F\|_\varrho \le c\|F\|_\varrho \tag{27}$$

with $c = c(\Omega, q) > 0$. For further details on the operator $A_q^{-\alpha} P_q$ we refer to [5].

Proof of Lemma 2 Given the smallness condition (22), Lemma 3 yields a unique very weak solution $u \in L^{s_*}\big(0, T; L^{q_*}(\Omega)\big)$ of (1). In view of (23) it suffices to prove the property

$$\tilde{u} \in L^\infty\big(0, T; L^2(\Omega)\big) \cap L^2\big(0, T; H_0^1(\Omega)\big) \tag{28}$$

so that $u = \gamma + \tilde{u} \in L^{s_*}\big(0, T; L^{q_*}(\Omega)\big)$ is seen to be a weak solution as well. Hence u satisfies the energy (in-)equality and Serrin's uniqueness condition, see e.g. [22, Theorem V.1.5.1]. This shows that u is the unique weak solution with these properties.

To prove (28) we recall from (27) that

$$\|A_{q_*/2}^{-1/2} P_{q_*} \mathrm{div}\,(uu)\|_{q_*/2} \le c\|uu\|_{q_*/2} \le c\|u\|_{q_*}^2 \quad \text{for a.a. } t \in (0, T). \tag{29}$$

Consequently, (25) implies the identity

$$A_{q_*/2}^{1/2} \tilde{u}(t) = -A_{q_*/2}\Big(\int_0^t e^{-\nu(t-\tau)A_{q_*/2}} A_{q_*/2}^{-1/2} P_{q_*/2}\, \mathrm{div}\,(uu)\, d\tau\Big). \tag{30}$$

Now Lemma 1, in particular the maximal regularity estimate (16), and (29) yield the estimate

$$\begin{aligned} \nu\|\nabla \tilde{u}\|_{L^{s_*/2}(L^{q_*/2})} &\le c\nu\|A_{q_*/2}^{1/2}\tilde{u}\|_{L^{s_*/2}(L^{q_*/2})} \\ &\le c\|uu\|_{L^{s_*/2}(L^{q_*/2})} \le c\|u\|_{L^{s_*}(L^{q_*})}^2 \end{aligned} \tag{31}$$

with $c = c(q_*, \Omega) > 0$, so that

$$\nabla \tilde{u} \in L^{s_*/2}\big(0, T; L^{q_*/2}(\Omega)\big). \tag{32}$$

We will consider four cases concerning the exponent s_*, starting with the case $s_* = 4$, $q_* = 6$ needed to prove Theorem 2. In this case (32) immediately yields $\nabla \tilde{u} \in L^2\big(0, T; L^2(\Omega)\big)$, and (31) shows that $uu \in L^2\big(0, T; L^2(\Omega)\big)$. Now the identity (30) implies that $\tilde{u}$ is the weak solution of an instationary Stokes system with vanishing initial value and external force $\mathrm{div}\, \tilde{F}$ where $\tilde{F} = uu \in L^2\big(0, T; L^2(\Omega)\big)$ so that

$$\tilde{u} \in L^\infty\big(0, T; L^2(\Omega)\big) \cap L^2\big(0, T; H_0^1(\Omega)\big),$$

see e.g. [22, Theorem IV.2.3.1]. Hence also

$$u \in L^\infty\big(0,T;L^2(\Omega)\big) \cap L^2\big(0,T;H_0^1(\Omega)\big).$$

An elementary calculation shows that u is not only a very weak solution, but also a weak one satisfying the energy (in-)equality. Furthermore, the uniqueness assertion follows from Serrin's uniqueness condition.

Next we consider the case $2 < s_* < 4$ (and $q_* > 6$) which has not been considered in [6, 8]. Let $s_1 = s_*$, $q_1 = q_*$. Then (25) and (14) (with $\alpha = \frac{1}{2}$) imply that

$$\|\tilde{u}(t)\|_{q_1/2} \le \frac{c}{\sqrt{\nu}} \int_0^t \frac{1}{(t-\tau)^{1/2}}\, \|uu\|_{q_1/2}\, d\tau,$$

where $\|uu(\tau)\|_{q_1/2} \in L^{s_1/2}(0,T)$. Hence the Hardy-Littlewood inequality proves with

$$\frac{1}{s_2} = \frac{1}{s_1/2} - \frac{1}{2}, \quad q_2 = \frac{q_1}{2}$$

that

$$\tilde{u} \in L^{s_2}\big(0,T;L^{q_2}(\Omega)\big).$$

Here $\frac{2}{s_2} + \frac{3}{q_2} = 1$ since $\frac{2}{s_1} + \frac{3}{q_1} = 1$, and $s_2 > s_1$, $q_2 < q_1$. To get the same result for γ, note that

$$\gamma_1(t) := e^{-\nu t A_{q_*}} u_0 \in L^\infty\big(0,T;L^{q_*}(\Omega)\big) \subset L^{s_2}\big(0,T;L^{q_2}(\Omega)\big).$$

Concerning $\gamma_2(t) = \gamma(t) - \gamma_1(t)$, the second term on the right-hand side of (24), we use (13) with $\alpha = \frac{1}{s_1}$ and conclude, since $A_\varrho^{-1/2} P_\varrho \operatorname{div} F(\tau) \in L^\varrho(\Omega)$ for a.a. τ, see (27), that

$$v := A_\varrho^{-1/s_1} A_\varrho^{-1/2} P_\varrho \operatorname{div} F \in L^{s_1}\big(0,T;L^{q_2}(\Omega)\big).$$

Hence $\gamma_2(t)$ satisfies the estimate

$$\|\gamma_2(t)\|_{q_2} \le c \int_0^t \frac{1}{(t-\tau)^{1/2+1/s_1}}\, \|v(\tau)\|_{q_2}\, d\tau,$$

$c = c(\nu, \Omega, q_2) > 0$, from which we deduce by the Hardy-Littlewood inequality that $\gamma_2 \in L^{s_2}\big(0,T;L^{q_2}(\Omega)\big)$; here we used that $\frac{1}{2} + \frac{1}{s_1} = 1 - \big(\frac{1}{s_1} - \frac{1}{s_2}\big)$.

Summarizing the results for γ_1 and γ_2 we get that $\gamma \in L^{s_2}\big(0,T;L^{q_2}(\Omega)\big)$ so that also $u \in L^{s_2}\big(0,T;L^{q_2}(\Omega)\big)$ and, due to (32),

$$\nabla\tilde{u} \in L^{s_2/2}\big(0,T;L^{q_2/2}(\Omega)\big).$$

Repeating this step finitely many times, we finally arrive at exponents $s_k \in [4,\infty)$, $q_k \in (3,6]$, $k \in \mathbb{N}$. The case of exponents $s_* > 4$, $q_* < 6$ has already been considered in [6, 8], but its proof will be repeated for the convenience of the reader.

Let $4 < s_* \le 8$ (and $4 \le q_* < 6$) so that (32) yields $\nabla\tilde{u} \in L^2\big(0,T;L^2(\Omega)\big)$ and $\tilde{u} \in L^2\big(0,T;H_0^1(\Omega)\big)$. Applying (14) and (29) to (25), Hölder's inequality implies the estimate

$$\begin{aligned}
\|\tilde{u}(t)\|_2 &\le \frac{c}{\sqrt{\nu}}\int_0^t \frac{1}{(t-\tau)^{1/2}}\, e^{-\nu\delta_0(t-\tau)}\,\|uu\|_2\,d\tau\\
&\le \frac{c}{\sqrt{\nu}}\int_0^t \frac{1}{(t-\tau)^{1/2}} e^{-\nu\delta_0(t-\tau)}\,\|uu\|_{q_*/2}\,d\tau\\
&\le c\,\|uu\|_{L^{s_*/2}(0,T;L^{q_*/2}(\Omega))}\\
&\le c\,\|u\|^2_{L^{s_*}(0,T;L^{q_*}(\Omega))},
\end{aligned}$$

where $c = c(\nu,T) > 0$. Consequently, $\tilde{u}$ and even u belong to $L^\infty\big(0,T;L^2(\Omega)\big)$. Now we complete the proof as in the previous case.

Finally assume that $8 < s_* < \infty$ (and $3 < q_* < 4$). Now we need finitely many steps to reduce this case to the former one. Let $s_1 = s_*$ and $q_1 = q_*$. Then $\nabla\tilde{u} \in L^{s_1/2}\big(0,T;L^{q_1/2}(\Omega)\big)$ by (32). Defining $s_2 < s_1$, $q_2 > q_1$ by

$$s_2 = \frac{s_1}{2}\,, \qquad \frac{1}{3} + \frac{1}{q_2} = \frac{2}{q_1}$$

we get by Sobolev's embedding theorem that $\tilde{u} \in L^{s_2}\big(0,T;L^{q_2}(\Omega)\big)$. By Lemma 1 we conclude that also $\gamma \in L^{s_2}\big(0,T;L^{q_2}(\Omega)\big)$ so that

$$u \in L^{s_2}\big(0,T;L^{q_2}(\Omega)\big)$$

where again $\frac{2}{s_2} + \frac{3}{q_2} = 1$. Repeating this step finitely many times, if necessary, we arrive at exponents $s_k \in (4,8]$, $q_k \in [4,6)$, i.e. in the previous case.

Now Lemma 2 is completely proved. □

In the next more technical lemma we will use the notation

$$⨍_a^b h(\tau)\,d\tau = \frac{1}{b-a}\int_a^b h(\tau)\,d\tau$$

for the mean integral value of an integrable function h on (a,b).

Lemma 4 *Under the assumptions of Lemma 2, and for any* $s \in [1,s_*]$, *there exists a constant* $\varepsilon_* = \varepsilon_*(q_*,s,\Omega) > 0$ *with the following property:*

Assume $0 < t_0 < t \le t_1 < T$, $0 \le \beta \le \frac{s}{s_*}$ *and that* $f = \operatorname{div} F$ *and the weak solution* u *of* (1) *satisfy the integrability conditions*

$$\int_{t_0}^{t_1} \|F\|_{\varrho}^{s_*}\, d\tau \le \varepsilon_* \nu^{2s_*-1} \quad \text{and} \quad \fint_{t_0}^{t} (t_1-\tau)^{\beta}\, \|u\|_{q_*}^{s}\, d\tau \le \varepsilon_* \nu^{s-\beta}\,. \tag{33}$$

Moreover, u *is supposed to satisfy the strong energy inequality* (4). *Then* u *is regular in the interval* $(t-\delta, t_1)$ *for some* $0 < \delta < t$ *in the sense that* $u \in L^{s_*}\big(t-\delta, t_1; L^{q_*}(\Omega)\big)$. *In particular, if* $t_1 > t$, *then* t *is a regular point of* u. *If* $\beta = 0$, *then* $t_1 = T \le \infty$ *is allowed.*

Proof From the second condition in (33) and the fact that u satisfies the strong energy inequality we find a null set $N \subset (t_0, t)$ such that for each $\tau_0 \in (t_0, t)\backslash N$

$$\frac{1}{2}\|u(\tau_1)\|_2^2 + \nu \int_{\tau_0}^{\tau_1} \|\nabla u\|_2^2\, d\tau \le \frac{1}{2}\|u(\tau_0)\|_2^2 - \int_{\tau_0}^{\tau_1} \langle F, \nabla u\rangle d\tau, \quad \tau_0 < \tau_1 < T, \tag{34}$$

and $u(\tau_0) \in L^{q_*}_{\sigma}(\Omega)$.

Next we claim the existence of $\tau_0 \in (t_0, t)\backslash N$ such that

$$\int_0^{t_1-\tau_0} \|e^{-\nu\tau A_{q_*}} u(\tau_0)\|_{q_*}^{s_*}\, d\tau \le \varepsilon_* \nu^{s_*-1}\,. \tag{35}$$

Actually, the second condition in (33) yields the existence of $\tau_0 \in (t_0, t)\backslash N$ such that

$$(t_1-\tau_0)^{\beta}\, \|u(\tau_0)\|_{q_*}^{s} \le \fint_{t_0}^{t} (t_1-\tau)^{\beta}\, \|u(\tau)\|_{q_*}^{s}\, d\tau \le \varepsilon_* \nu^{s-\beta}\,; \tag{36}$$

otherwise $(t_1-\tau)^{\beta}\, \|u(\tau)\|_{q_*}^{s}$ is strictly larger than its integral mean on (t_0, t) for every $\tau \in (t_0, T)\backslash N$, and we are led to a contradiction. Now, by Lemma 1, Hölder's inequality and (36),

$$\begin{aligned}
\int_0^{t_1-\tau_0} \|e^{-\nu\tau A_{q_*}} u(\tau_0)\|_{q_*}^{s_*}\, d\tau &\le \int_0^{t_1-\tau_0} e^{-\delta_0 \nu s_* \tau}\, d\tau\, \|u(\tau_0)\|_{q_*}^{s_*} \\
&\le c(t_1-\tau_0)^{\beta s_*/s}\, \nu^{-1+\beta s_*/s} \|u(\tau_0)\|_{q_*}^{s_*} \\
&\le c\, \varepsilon_*^{s_*/s}\, \nu^{s_*-1}
\end{aligned}$$

where $c = c(q, \Omega) > 0$. Hence, with a new constant $\varepsilon_* = \varepsilon_*(q_*, s, \Omega) > 0$, (35) is proved. If $\beta = 0$, then even $t_1 = T \le \infty$ is admitted.

Given τ_0 as in (35) and using (33), Lemma 2 will yield a unique weak solution $v \in L^{s_*}([\tau_0, t_1); L^{q_*}_{\sigma}(\Omega))$ to the Navier-Stokes system (1) with initial value $v(\tau_0) = u(\tau_0)$ at τ_0. Then Serrin's uniqueness theorem shows that

$$u = v \in L^{s_*}\big(\tau_0, t_1; L^{q_*}_{\sigma}(\Omega)\big)$$

which completes the proof. □

Proof of Theorem 2 The proof is based on Lemma 4 with $t \in (0, T)$, $t_0 = t - \delta$, $t_1 = t + \delta$, $\delta > 0$ sufficiently small, and exponents $s = 2,\ q_* = 6,\ s_* = 4,\ \beta = \frac{1}{2}$ (and $\varrho = 2$) so that $u \in L^s\big(0, T; L^{q_*}(\Omega)\big)$. To control the second term in (33) note that

$$I(\delta) := \int_{t_0}^{t} (t_1 - \tau)^{\frac{1}{2}} \|u\|_6^2 \, d\tau \le 2^{\frac{1}{2}} \delta^{-\frac{1}{2}} \int_{t-\delta}^{t} \|u\|_6^2 \, d\tau \le c\, \delta^{-\frac{1}{2}} \int_{t-\delta}^{t} \|\nabla u\|_2^2 \, d\tau\,, \tag{37}$$

where $c = c(\Omega) > 0$. Since u is supposed to satisfy the strong energy inequality, we may assume without loss of generality that

$$I(\delta) \le \frac{c}{\nu}\frac{1}{2} \left(\frac{\big|\|u(t-\delta)\|_2^2 - \|u(t)\|_2^2\big|}{\delta^{\frac{1}{2}}} + \left| \frac{1}{\delta^{\frac{1}{2}}} \int_{t-\delta}^{t} \langle f, u\rangle \, d\tau \right| \right). \tag{38}$$

By the inequality of Cauchy-Schwarz the assumption $f \in L^2\big(0, T; L^2(\Omega)\big)$ implies that $\delta^{-\frac{1}{2}} \int_{t-\delta}^{t} \langle f, u\rangle \, d\tau \to 0$ as $\delta \to 0+$. Moreover, the term

$$\frac{c}{2} \frac{\big|\|u(t-\delta\|_2^2 - \|u(t)\|_2^2\big|}{\nu\, \delta^{\frac{1}{2}}}$$

is bounded by $c\,\varepsilon_* \nu^{3/2}$ for a sequence (δ_j), $0 < \delta_j \to 0$ as $j \to \infty$, due to the assumption on the kinetic energy. Hence the continuity of $I(\delta)$, $\delta > 0$, proves that $(33)_2$ can be satisfied. Finally, since $F \in L^4(0, T; L^2(\Omega)\big)$, $(33)_1$ can be guaranteed for all sufficiently small $\delta > 0$.

Looking at (37), condition (12) allows the same reasoning.

Now Theorem 2 is completely proved. □

References

1. Amann, H.: *Nonhomogeneous Navier-Stokes Equations with Integrable Low-Regularity Data*. Int. Math. Ser., pp. 1–26. Kluwer Academic/Plenum Publishing, New York (2002)
2. Beirão da Veiga, H.: A new regularity class for the Navier-Stokes equations in $\mathbb{R}^n$. Chinese Ann. Math., Ser. B **16**, 407–412 (1995)
3. Escauriaza, L., Seregin, G., Šverák, V.: Backward uniqueness for the heat operator in half space. IMA Preprint Series 1878, Minneapolis (2002)
4. Farwig, R., Sohr, H.: Generalized resolvent estimates for the Stokes system in bounded and unbounded domains. J. Math. Soc. Japan **46**, 607–643 (1994)
5. Farwig, R., Galdi, G.P., Sohr, H.: A new class of weak solutions of the Navier-Stokes equations with nonhomogeneous data. J. Math. Fluid Mech. **8**, 423–444 (2006)
6. Farwig, R., Kozono, H., Sohr, H.: Local in time regularity properties of the Navier-Stokes equations. Indiana Univ. Math. J. **56**, 2111–2132 (2007)

7. Farwig, R., Kozono, H., Sohr, H.: Criteria of local in time regularity of the Navier-Stokes equations beyond Serrin's condition. Banach Center Publ., Warszawa **81/1**, 175–184 (2008)
8. Farwig, R., Kozono, H., Sohr, H.: Energy-based regularity criteria for the Navier-Stokes equations. FB Mathematik, TU Darmstadt, Preprint no. 2521 (2007). J. Math. Fluid Mech. **11**, 1–14 (2008)
9. Farwig, R., Kozono, H., Sohr, H.: Very weak, weak and strong solutions to the instationary Navier-Stokes system. Topics on partial differential equations. J. Nečas Center for Mathematical Modeling, Lecture Notes, Vol. 2, pp. 15–68, ed. by P. Kaplický, Prague (2007)
10. Friedman, A.: *Partial Differential Equations.* Holt, Rinehart and Winston, New York (1969)
11. Galdi, G.P.: *An Introduction to the Mathematical Theory of the Navier-Stokes Equations; Linearized Steady Problems*. Springer Tracts in Nat. Philos., Vol. 38, Springer-Verlag, New York (1998)
12. Galdi, G.P.: An introduction to the Navier-Stokes initial-boundary value problem. Galdi, G.P., et al. (eds.), *Fundamental Directions in Mathematical Fluid Mechanics*, pp. 1–70. Birkhäuser, Basel (2000)
13. Giga, Y.: Analyticity of the semigroup generated by the Stokes operator in L_r-spaces. Math. Z. **178**, 287–329 (1981)
14. Giga, Y., Sohr, H.: Abstract L^q-estimates for the Cauchy problem with applications to the Navier-Stokes equations in exterior domains. J. Funct. Anal. **102**, 72–94 (1991)
15. Kozono, H., Taniuchi, Y.: Bilinear estimates in BMO and the Navier-Stokes equations. Math. Z. **235**, 173–194 (2000)
16. Schumacher, K.: The Navier-Stokes equations with low regularity data in weighted function spaces. Dissertation, FB Mathematik, TU Darmstadt (2007) Online: http://elib.tu-darmstadt.de/diss/000815/
17. Seregin, G.A.: Local regularity of suitable weak solutions to the Navier-Stokes equations near the boundary. J. Math. Fluid Mech. **4**, 1–29 (2002)
18. Seregin, G.A.: On smoothness of $L_{3,\infty}$-solutions to the Navier-Stokes equations up to boundary. Math. Ann. **332**, 219–238 (2005)
19. Seregin, G.A., Shilkin, T.N., Solonnikov, V.A.: Boundary partial regularity for the Navier-Stokes equations. Zap. Nauchn. Sem. S.-Peterburg. Otdel. Mat. Inst. Steklov (POMI) **310**, 158–190 (2004)
20. Seregin, G.A., Šverák, V.: The Navier-Stokes equations and backward uniqueness. IMA Preprint Series 1852, Minneapolis (2002)
21. Serrin, J.: The initial value problem for the Navier-Stokes equations. Nonlinear problems, pp. 69–98. Proc. Sympos. Madison (1962), ed. R.E. Langer (1963)
22. Sohr, H.: *The Navier-Stokes Equations. An Elementary Functional Analytic Approach*. Birkhäuser Advanced Texts, Birkhäuser Verlag, Basel (2001)
23. Solonnikov, V.A.: Estimates for solutions of nonstationary Navier-Stokes equations. J. Soviet Math. **8**, 467–529 (1977)

Looking for the Lost Memory in Diffusion-Reaction Equations

José Augusto Ferreira and Paula de Oliveira

Abstract The paper studies the analytical and numerical behaviours of some non Brownian models for diffusion phenomena. These models have been introduced in the literature to overcome the gap between experimental data and numerical simulations. From analytical point of view stability results leading to the well-posedness in the Hadamard sense of the initial boundary value problems are established. From numerical point of view some numerical methods are analysed. Applications within the fields of drug release, heat conduction and reaction diffusion phenomena are addressed.

Keywords Fick's law for the flux · Reaction-diffusion equations · Integro-differential equations · Stability · Numerical methods

1 Introduction

Diffusion is a mechanism by which the components of a mixture are transported around it by means of a random molecular motion with no preferred movement. In 1827 the english botanist Robert Brown was the first to notice that pollen grains suspended in water performed a chaotic dance, like random fluctuation, that he initially explained as pollen vitality. He soon realised that the process had a physical nature.

Assuming the so called Brownian motion of particles Adolf Fick addressed the problem of diffusion when studying the way that water and nutrients travel through membranes establishing the classical diffusion equation

$$\frac{\partial u}{\partial t}(x,t) = D\frac{\partial^2 u}{\partial x^2}(x,t),\ x \in (0,L), t > 0, \tag{1}$$

where $u(x,t)$ denotes the probability of a diffusing particle in $(0, L)$ be at position x at time t. This model is based on the assumptions that the motion of different

J.A. Ferreira (✉)
CMUC-Department of Mathematics, University of Coimbra, Coimbra, Portugal
e-mail: ferreira@mat.uc.pt

R. Rannacher, A. Sequeira (eds.), *Advances in Mathematical Fluid Mechanics*,
DOI 10.1007/978-3-642-04068-9_14,

particles is independent, there exists a time interval β such that the displacement of the same particle during different β intervals is independent and there exists a mean square displacement during such a β interval.

Equation (1) is obtained by combining Fick's law

$$J(x,t) = -D\frac{\partial u}{\partial x}(x,t) \tag{2}$$

with the mass conservation law

$$\frac{\partial u}{\partial t}(x,t) + \frac{\partial J}{\partial x}(x,t) = 0, \tag{3}$$

where in (2) and (3) J stands for the flux. However experimental evidence of diffusing phenomena within different field of applications shows that (1) is not an accurate model. In fact Fick's law for the flux establishing a simultaneously occurrence of the cause and of the effect does not describe accurately the transport mechanism.

The aim of this paper is to explain this lack of accuracy in different fields focussing three different problems : drug release from polymeric matrices, heat propagation and reaction-diffusion systems.

For instance in the drug release context in [7, 14, 22, 25–27] it is shown a lack of agreement between the theoretical results obtained by the Brownian models and the experimental data. The explanation for this relies on the fact that the polymeric matrix reacts to the presence of the penetrant molecules with a certain delay that is the flux at time t is related to the gradient of the concentration at a time $t - \tau$. In [2, 13, 20] mathematical models to overcome the discrepancies between the results obtained by simulation of the Brownian models and the experimental data are studied.

Heat propagation phenomena in a homogeneous and isotropic bar are also generally modeled by Eq. (1). It is well known that this equation has the unphysical property that if a sudden change in the temperature is made at some point of the bar, it will be felt instantly everywhere. We say that diffusion equation gives rise to infinite speeds of propagation. The problem that unphysical infinite speeds of propagation are generated by diffusion was firstly treated in [9] and considered later in [29]. Modifications of the classical heat equation (1) which avoid the pathological behaviour of the solution are studied in [5, 10–12, 15, 23].

Reaction diffusion systems were traditionally modeled by (1) with a reaction term f, that is by the Fick's law (2) with the mass conservation law

$$\frac{\partial u}{\partial t}(x,t) + \frac{\partial J}{\partial x}(x,t) = f(u(x,t)), \tag{4}$$

(see [6, 21, 24]). This equation, known as Fisher-Kolmogorov-Petrovski-Piskunov equation (FKPP), presents, however, a serious drawback – which is related to its parabolic character – that can be roughly defined as an "infinite speed of heat/mass transfer". As a consequence the propagation rate of traveling wave solutions, given by $\sqrt{4DU}$ for $f(u) = U(1-u)u$, exhibits the unphysical property of becoming arbitrarily large when U goes to infinity. To overcome this difficulty several modifications of (4) have been proposed in the literature. A first modification takes into account the boundness of the transport process by introducing a relaxation parameter τ which represents the waiting time between two successive jumps of the particles whose movement we want to describe [16, 17]. Recently those models were studied in [3, 4, 8, 19].

The alternative models to Brownian ones introduced in the previous papers are obtained modifying at a macroscopic level Fick's law for the flux. Nevertheless they can be established modifying at a microscopic level assumptions for the random walk as for instance in [1, 30, 28].

In this paper we present an overview on some results on non Brownian models obtained recently by the authors in [3, 5, 8, 19, 20]. The results are presented without proofs which can be found in the previous papers. Section 2 focuses on the analysis of the simplest model which takes into account the non Brownian motion of diffusing particles in a domain. Mathematical models for physical phenomena whose fluxes present Brownian and non Brownian contributions are studied in Sect. 3. Finally Sect. 4 addresses non Brownian diffusion-reaction systems.

2 The Simplest Non Brownian Model

2.1 Introduction

To overcome the incompatibility between the numerical simulation of the Brownian model (1) and the experimental data in the drug release context we define the flux J by

$$J(x, t+\tau) = -D\frac{\partial u}{\partial x}(x, t), \tag{5}$$

where τ is a delay parameter. Assuming that τ is small enough we have from (5)

$$\frac{\partial J}{\partial t} + \frac{1}{\tau}J(x, t) = -\frac{D}{\tau}D\frac{\partial u}{\partial x}(x, t)$$

and integrating this first order equation we obtain

$$J(x, t) = -\frac{D}{\tau}\int_0^t e^{-\frac{t-s}{\tau}}\frac{\partial u}{\partial x}(x, s)\,ds. \tag{6}$$

With this new definition for the flux, mass conservation law (3) leads to an integro-differential equation

$$\frac{\partial u}{\partial t}(x, t) = \frac{D}{\tau}\int_0^t e^{-\frac{t-s}{\tau}}\frac{\partial^2 u}{\partial x^2}(x, s)\,ds,\ x \in (0, L), t \in (0, T], \tag{7}$$

coupled with initial and boundary conditions

$$u(x, 0) = u_0(x), x \in (0, L), u(0, t) = u_\ell, u(L, t) = u_R, t \in (0, T]. \tag{8}$$

In Sect. 2.2 we establish the well-posedness of the initial boundary value problem (IBVP) (7), (8), in Hadamard's sense. As (7) depends on the delay parameter τ, the asymptotic behaviour of this model is also studied. In Sect. 2.3 we establish that the solution of the delayed model converges to the solution of the classical diffusion model (1) with the initial and boundary conditions (8). The asymptotic behaviour of the total amount of diffusing substance defined by the integro-differential model is also addressed in this section.

2.2 Well-Posedness in Hadamard's Sense

In this section we establish the existence of a solution of the IBVP (7), (8) and its stability with respect to perturbations of the initial condition. By $L^2(0, L)$ we denote the vector space of all function v defined in $[0, L]$ such that $\int_0^L v^2(x)\,dx < \infty$. In $L^2(0, L)$ we consider the usual L^2 inner product $(.,.)$ and by $\|.\|_{L^2(0,L)}$ we denote the corresponding norm.

Due to its particular structure it is possible to compute the solution of (7), (8) by using Fourier analysis.

Theorem 1 *([20]) If $u_0(0) = u_\ell$, $u_0(L) = u_R$ and $u_0''' \in L^2(0, L)$, then*

$$u(x,t) = \sum_{n=1}^{[\frac{L}{2\pi\sqrt{D\tau}}]} A_n\Big(\frac{1+\delta_n(\tau)}{2\delta_n(\tau)}e^{\frac{t}{2\tau}\left(-1+\delta_n(\tau)\right)} + \frac{-1+\delta_n(\tau)}{2\delta_n(\tau)}e^{\frac{t}{2\tau}\left(-1-\delta_n(\tau)\right)}\Big)sin(\frac{n\pi}{L}x)$$
$$+\sum_{[\frac{L}{2\pi\sqrt{D\tau}}]+1}^{\infty} A_n e^{-\frac{t}{2\tau}}\Big(cos(\frac{t\delta(n\tau)}{2\tau}) + \frac{1}{\delta_n(\tau)}sin(\frac{t\delta(n\tau)}{2\tau})\Big)sin(\frac{n\pi}{L}x) + \frac{u_R-u_\ell}{L}x + u_\ell \quad (9)$$

for $x \in [0, L]$, $t \in [0, T]$, where $[\frac{L}{2\pi\sqrt{D\tau}}]$ represents the integer part of $\frac{L}{2\pi\sqrt{D\tau}}$ and

$$A_n = \frac{2}{L}\int_0^L u_0(x)sin(\frac{n\pi}{L}x)\,dx + \frac{2}{n\pi}\big(u_R(-1)^n - u_\ell\big), n \in \mathbb{N}, \quad (10)$$

$$\delta_n(\tau) = \begin{cases} \sqrt{1-4D\frac{n^2\pi^2}{L^2}\tau}, \ n \le [\frac{L}{2\pi\sqrt{D\tau}}] \\ \sqrt{-1+4D\frac{n^2\pi^2}{L^2}\tau}, \ n \ge [\frac{L}{2\pi\sqrt{D\tau}}]+1. \end{cases} \quad (11)$$

Solution (9) is composed by three terms: a sum with a finite number of terms, a sum with an infinite number of terms and a third term coming from the boundary conditions. We note that the terms in the finite sum recall the terms in the solution of the parabolic IBVP (1), (8) and the terms in the infinite sum recall the solution of a wave type hyperbolic equation. From a formal view point as $\tau \to 0$ we have $\frac{L}{2\pi\sqrt{D\tau}} \to \infty$ and consequently the infinite sum disappears. In this case the solution $u(x,t)$ given by (9) converges formally to the solution of (1),(8). We postpone for a later theorem the establishment of a convergence result for $u(x,t)$.

For the delayed IBVP (7), (8) the stability is based on the following estimate for the energy functional

$$E(u)(t) = \|u(t)\|^2_{L^2(0,L)} + \frac{D}{\tau}\|\int_0^t e^{-\frac{t-s}{\tau}}\frac{\partial u}{\partial x}(s)\,ds\|^2_{L^2(0,L)},\ t \geq 0. \tag{12}$$

The proof of this result is based on the energy method.

Theorem 2 *([20]) Let u be a solution of the delayed IBVP (7), (8) with homogeneous boundary conditions. Then*

$$E(u)(t) \leq \|u_0\|^2_{L^2(0,L)},\ t \geq 0. \tag{13}$$

As a corollary of Theorem 2 we conclude the stability of model (7), (8) in Corollary 1.

Corollary 1 *Let u and $\tilde{u}$ be solutions of the delayed IBVP (7), (8) with initial conditions u_0 and $\tilde{u}_0$ respectively. Then $w = u - \tilde{u}$ satisfies*

$$\|w(t)\|^2_{L^2(0,L)} + \frac{D}{\tau}\|\int_0^t e^{-\frac{t-s}{\tau}}\frac{\partial w}{\partial t}(s)\,ds\|^2_{L^2(0,L)} \leq \|u_0 - \tilde{u}_0\|^2_{L^2[0,L]},\ t \geq 0. \tag{14}$$

By Corollary 1 the delayed IBVP (7), (8) is stable with respect to perturbations of the initial condition. The uniqueness of the solution, established by a constructive approach in Theorem 1, can also be concluded as a consequence of Corollary 1. From the previous we conclude that the integro-differential model (7), (8) is well-posed in Hadamard sense.

The energy estimate (13) gives information on the spatial behaviour of the "average" in time of the gradient of the solution of the IBVP (7), (8).

2.3 Asymptotic Behaviour of the Model

In this section we study the dependence of the solution u of (7), (8) on the parameter τ. In what follows we represent such solution by $u(x,t,\tau)$ and the solution of (1), (8) by $u_F(x,t)$. The solution u can be written in the equivalent form

$$u(x,t,\tau) = \frac{u_R - u_\ell}{L}x + u_\ell + \sum_{n=1}^{\infty} u_n(x,t,\tau)$$

with

$$u_n(x,t,\tau) = A_n\Big(e^{\frac{t}{2\tau}\left(-1+\delta_n(\tau)\right)}\frac{1+\delta_n(\tau)}{2\delta_n(\tau)} + e^{\frac{t}{2\tau}\left(-1-\delta_n(\tau)\right)}\frac{-1+\delta_n(\tau)}{2\delta_n(\tau)}\Big)$$

for $n \leq [\frac{L}{2\pi\sqrt{D\tau}}]$ and

$$u_n(x,t,\tau) = A_n e^{-\frac{t}{2\tau}}\Big(cos\big(\frac{t\delta_n(\tau)}{2\tau}\big) + \frac{1}{\delta_n(\tau)}sin\big(\frac{t\delta_n(\tau)}{2\tau}\big)\Big)$$

for $n \geq [\frac{L}{2\pi\sqrt{D\tau}}] + 1$, where A_n and $\delta_n(\tau)$ are defined by (10) and (11) respectively.

Theorem 3 *([20]) If $u_0(0) = u_\ell, u_0(L) = u_R$ and $u_0' \in L^2(0,L)$ then $u(x,t,\tau)$ is τ-continuous and*

$$\lim_{\tau\to 0} u(x,t,\tau) = u_F(x,t), x \in [0,L], t \in (0,T], \tag{15}$$

where u and u_F are the solutions of IBVPs (7), (8) and (1),(8) respectively.

In Fig. 1 are plotted the graphics of the solution of (7), (8) for $D = 0.05, t = 1$ and for different values of τ. Boundary conditions $u_R = u_\ell = 0$ and initial condition $u_0(x) = 4(1-x)x$ have been considered. The delay effect of parameter τ is clearly observed. As τ decreases the concentration within [0, 1] also decreases. We remark that the Fickian solution u_F of (1),(8)-corresponding to $\tau = 0$ - and the plots of non Fickian solutions corresponding to $\tau = 0.05$ and $\tau = 0.125$ are very close. As a consequence the convergence (15) is also illustrated in this figure.

The delayed IBVP (7), (8) can be used to model sorption or desorption diffusion phenomena depending on the relation between the concentrations at the boundary points and the initial distribution. In this model a time memory effect was introduced to delay the diffusion phenomenon. Consequently, it should be observed a delayed effect on the sorpted or desorpted mass computed by using IBVP (7), (8).

Let $M(t,\tau)$ be the total amount of diffusing substance at time t defined by

$$M(t,\tau) = \int_0^L u(x,t,\tau)dx.$$

As u is given by (9) we obtain

$$M(t,\tau) = \frac{u_R + u_\ell}{2}L + \sum_{n=1}^{\infty} M_n(t,\tau)$$

where $M_n(t,\tau)$ is defined by

$$M_n(t,\tau) = A_n\frac{L((-1)^{n+1}+1)}{n\pi}\Big(e^{\frac{t}{2\tau}\left(-1+\delta_n(\tau)\right)}\frac{1+\delta_n(\tau)}{2\delta_n(\tau)} +$$

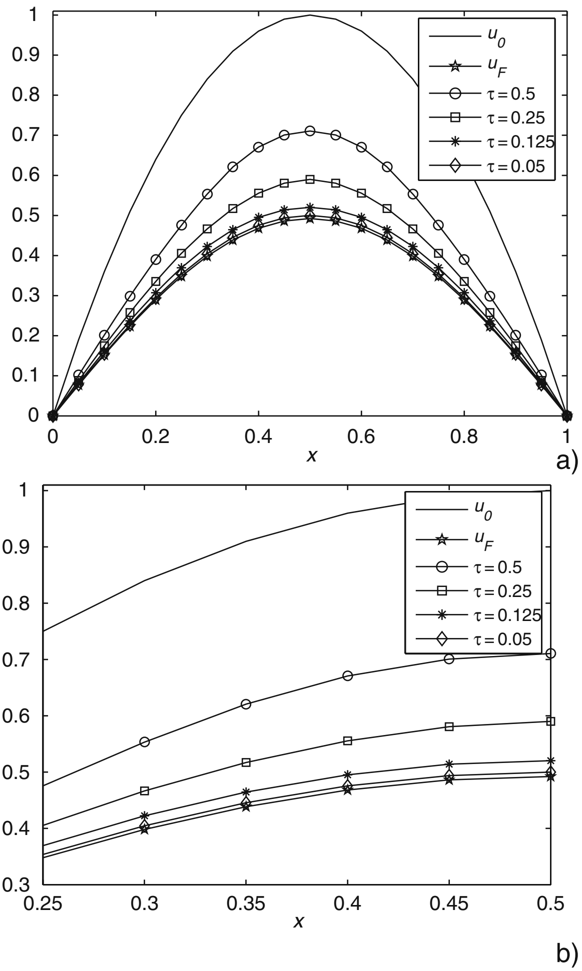

Fig. 1 The effect of τ on the solution of (7), (8)

$$e^{\frac{t}{2\tau}\left(-1-\delta_n(\tau)\right)}\frac{-1+\delta_n(\tau)}{2\delta_n(\tau)}\Big)$$

for $n \leq [\frac{L}{2\pi\sqrt{D\tau}}]$, and

$$M_n(t,\tau) = A_n\frac{L((-1)^{n+1}+1)}{n\pi}e^{-\frac{t}{2\tau}}\Big(cos\big(\frac{t\delta_n(\tau)}{2\tau}\big)+\frac{1}{\delta_n(\tau)}sin\big(\frac{t\delta_n(\tau)}{2\tau}\big)\Big)$$

for $n \geq [\frac{L}{2\pi\sqrt{D\tau}}]+1$, with A_n and $\delta_n(\tau)$ defined by (10) and (11) respectively.

It can be shown ([20]) that if $u_0 \in L^2(0, L)$, then

$$M(t, \tau) \to M_F(t) \text{ as } \tau \to 0, \text{for } t \in (0, T], \tag{16}$$

where $M_F(t)$ is the total amount of diffusing substance at time t defined by the classical diffusion model (1), (8).

The behaviour of $M(t, \tau)$ when $t \in [0, 10]$, is illustrated in Fig. 2 for $u_0(x) = 4(1 - x)x, x \in [0, 1]$, $u_\ell = u_R = 0$ and $D = 0.05$. Convergence (16) is also illustrated by Fig. 2.

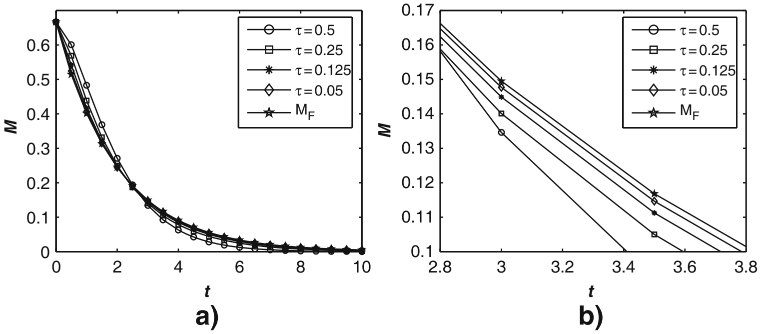

Fig. 2 The effect of τ on the total amount of diffusing substance defined by (7)

3 An Hybrid Method for Diffusion: Brownian and Non Brownian Character

3.1 Introduction

Heat conduction phenomena were traditionally modeled by Eq. (1) where $u(x, t)$ represents the temperature at (x, t) and D represents in this case the effective thermal conductivity. This model gives rise to an infinite speed of propagation. In order to avoid this serious drawback it has been proposed by Cattaneo in [9] to define the flux by using all the history of the temperature gradient, that is,

$$J_1(x, t) = -\frac{D}{\tau} \int_{-\infty}^{t} e^{-\frac{t-s}{\tau}} \frac{\partial u}{\partial x}(x, s)\, ds \tag{17}$$

where D represents the thermal conductivity. The asymptotic behaviour observed for the non Fickian flux (6) with respect to the delay parameter τ can be also established for (17) that is the flux (17) converges to the Fourier flux defined by (2) when $\tau \to 0$.

Considering (17), it can be shown that the temperature u at (x, t) satisfies the integro-differential equation

$$\frac{\partial u}{\partial t}(x,t) = \frac{D}{\gamma\tau}\int_{-\infty}^{t} e^{-\frac{t-s}{\tau}} \frac{\partial^2 u}{\partial x^2}(x,s)\, ds\,, \tag{18}$$

where γ is the heat capacity. This equation, known as Cattaneo's equation, was considered by several authors. For instance Vernotte, in [29], considered Cattaneo's equation as the simplest one that gives rise to finite speed of propagation. However, as pointed out in the engineering literature (see for example [24]), there are no real conductors which exhibit the wave propagation behaviour of Cattaneo's model. In Fig. 3 are plotted the solutions of the heat equation and Cattaneo's equation with a Dirac delta initial condition. The plots have been obtained from a discretization with a standard numerical method in a very fine mesh. Neither of the plots represent accurately the heat propagation: heat equation produces a very "dissipative solution", Cattaneo's equation exhibits a too "conservative behaviour". This last remark suggest that a compromise between the two flux definitions should be considered.

In [23] a such compromise is presented. A kernel of Jeffrey's type was then considered by replacing in (17) the exponential kernel by

$$Q(s) = D_1\delta(s) + \frac{D_2}{\tau}e^{-\frac{s}{\tau}}, \tag{19}$$

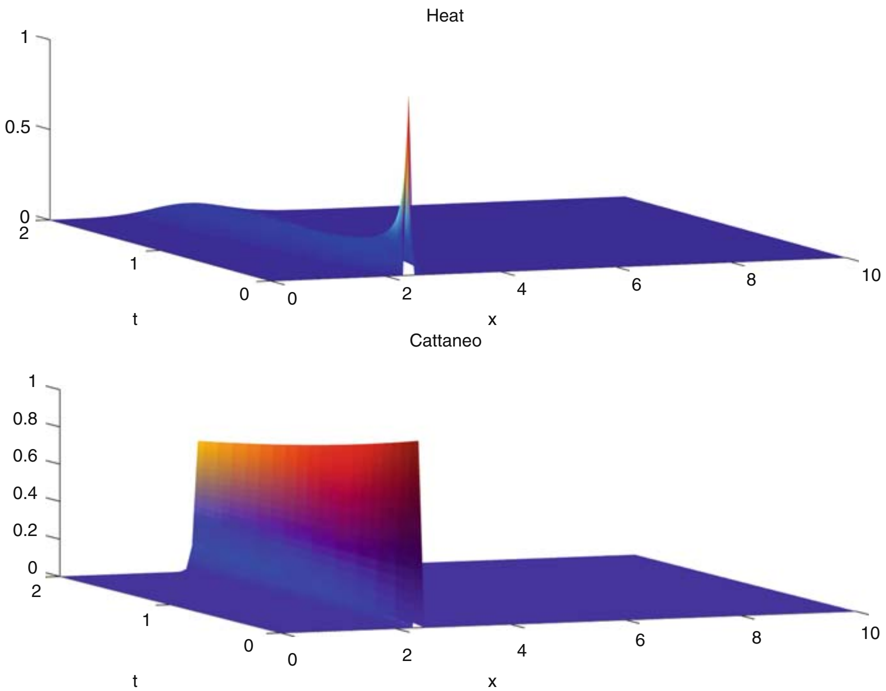

Fig. 3 Solutions of the heat equation and Cattaneo's equation with a Dirac delta initial condition

where $\delta(s)$ is a Dirac delta function, and D_1 and D_2 represent, respectively, the effective thermal conductivity and the elastic conductivity. In this case the flux J has two contributions, $J = J_1 + J_2$, being J_1 defined by (2) with D replaced by the effective thermal conductivity coefficient D_1 and J_2 defined by (17) with D replaced by the elastic conductivity coefficient D_2. It can be shown that the temperature, in this case, satisfies Jeffrey's integro-differential equation

$$\frac{\partial u}{\partial t}(x,t) = \frac{D_1}{\gamma}\frac{\partial^2 u}{\partial x^2}(x,t) + \frac{D_2}{\gamma\tau}\int_{-\infty}^{t} e^{-\frac{t-s}{\tau}}\frac{\partial^2 u}{\partial x^2}(x,s)\,ds\,. \tag{20}$$

For $D_2 = 0$ we have the classical diffusion equation while for $D_1 = 0$ we obtain Cattaneo's equation. As shown in Fig. 4 a solution that represents a compromise between Fickian and Cattaneo model is obtained from this model.

The rest of the section is organized as follows. In Sect. 3.2 we study the stability behaviour of the solution of Jeffrey's model (20). In Sect. 3.3 is proposed a numerical method for (20) using a splitting technique. Numerical simulations are included.

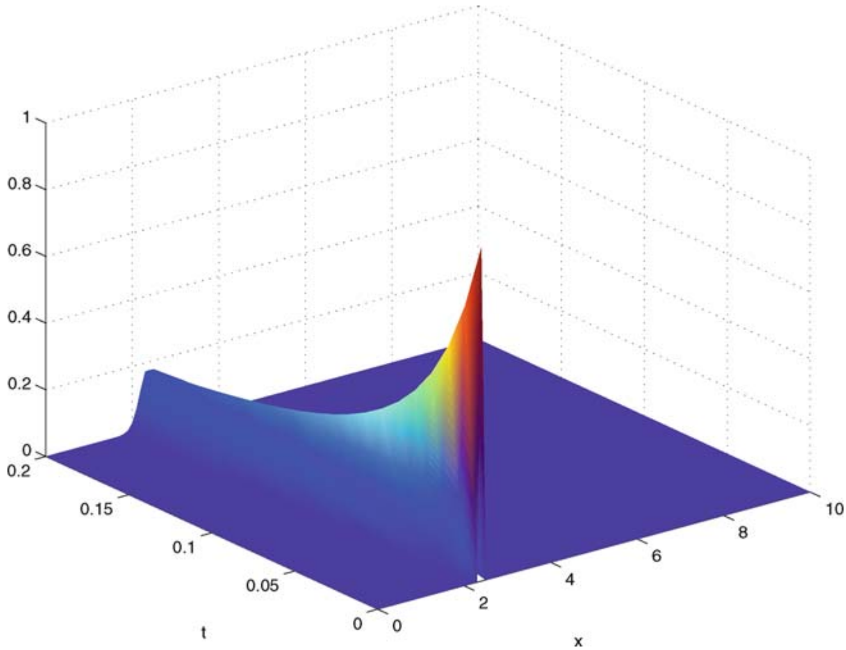

Fig. 4 Numerical solution of Jeffrey's equation obtained using method (24) with $\frac{D_i}{\gamma} = 0.1, \tau = 1, h = 0.1, \Delta t = 0.03$

3.2 An Energy Estimate for the Jeffrey's Equation

We consider in what follows the IBVP associated with (20) but where the integral is computed in $(0, t)$, that is

$$\frac{\partial u}{\partial t}(x,t) = \frac{D_1}{\gamma}\frac{\partial^2 u}{\partial x^2}(x,t) + \frac{D_2}{\gamma\tau}\int_0^t e^{-\frac{t-s}{\tau}}\frac{\partial^2 u}{\partial x^2}(x,s)\,ds,\ \ x\in(0,L), t>0, \quad (21)$$

associated with initial and boundary conditions (8) with $u_\ell = u_R = 0$.

In the following theorem, an estimate for the energy functional (12) with D replaced by $\frac{D_2}{\gamma}$ that is

$$E(u)(t) = \|u\|_{L^2(0,L)} + \frac{D_2}{\gamma\tau}\|\int_0^t e^{-\frac{t-s}{\tau}}\frac{\partial u}{\partial x}(s)\,ds\|^2_{L^2(0,L)},$$

for $t > 0$, is established. Such estimate is obtained by using the energy method and the Poincaré-Friedrichs inequality in the term $-\frac{D_1}{\gamma}\|\frac{\partial u}{\partial x}(t)\|^2_{L^2(0,L)}$.

Theorem 4 *([5]) Let u be a solution of (21), (8) with $u_\ell = u_R = 0$. Then*

$$E(u)(t) \le e^{-2min\,\{\frac{D_1}{\gamma L^2},\frac{1}{\tau}\}t}\|u_0\|^2_{L^2(0,L)}\,,\ t\ge 0. \quad (22)$$

Nevertheless, if we do not use the Poincaré-Friedrichs inequality, then the following energy estimate

$$\|u\|_{L^2(0,L)} + \frac{2D_1}{\gamma}\int_0^t \|\frac{\partial u}{\partial x}(s)\|^2_{L^2(0,L)}\,ds + \frac{D_2}{\gamma\tau}\|\int_0^t e^{-\frac{t-s}{\tau}}\frac{\partial u}{\partial x}(s)\,ds\|^2_{L^2(0,L)} \le \|u_0\|^2_{L^2(0,L)}, \quad (23)$$

can be established using $-\frac{D_1}{\gamma}\|\frac{\partial u}{\partial x}(t)\|^2_{L^2(0,L)} = -\frac{D_1}{\gamma}\frac{d}{dt}\int_0^t\|\frac{\partial u}{\partial x}(s)\|^2_{L^2(0,L)}$.

We remark that estimate (22) gives information on the behaviour in time of solution u and of the "average" in time of its gradient. Estimate (23) gives also information on the evolution in time of the "average" in space of the solution u. From both estimates we conclude the following

$$\|u(t)\|_{L^2(0,L)} \to 0,\ \|\int_0^t e^{-\frac{t-s}{\tau}}\frac{\partial u}{\partial x}(s)\,ds\|^2_{L^2(0,L)} \to 0$$

and $\int_0^t \|\frac{\partial u}{\partial x}(s)\|^2_{L^2(0,L)}\,ds$ remains bounded as $t\to\infty$.

Let us now consider the stability of Jeffrey's model. Let $\tilde{u}$ be the solution corresponding to the initial condition $\tilde{u}_0$. As for $w = u - \tilde{u}$ holds the estimate

$$\|w\|_{L^2(0,L)}^2 + \frac{D_2}{\gamma\tau}\|\int_0^t e^{-\frac{t-s}{\tau}}\frac{\partial w}{\partial x}(s)\,ds\|_{L^2(0,L)}^2 \leq e^{-2\min\{\frac{D_1}{\gamma L^2},\frac{1}{\tau}\}t}\|u_0 - \tilde{u}_0\|_{L^2(0,L)}^2$$

if (22) is used and

$$\|w\|_{L^2(0,L)} + \frac{2D_1}{\gamma}\int_0^t \|\frac{\partial w}{\partial x}(s)\|_{L^2(0,L)}^2\,ds + \frac{D_2}{\gamma\tau}\|\int_0^t e^{-\frac{t-s}{\tau}}\frac{\partial w}{\partial x}(s)\,ds\|_{L^2(0,L)}^2$$
$$\leq \|u_0 - \tilde{u}_0\|_{L^2(0,L)}^2.$$

if (23) is considered, we conclude that

$$\|w\|_{L^2(0,L)}^2 \to 0,\ \|\int_0^t e^{-\frac{t-s}{\tau}}\frac{\partial w}{\partial x}(s)\,ds\|_{L^2(0,L)}^2 \to 0$$

as $t \to \infty$ independently of $\|u_0 - \tilde{u}_0\|_{L^2(0,L)}^2$ and $\int_0^t \|\frac{\partial u}{\partial x}(s)\|_{L^2(0,L)}^2\,ds$ remains arbitrarily small as t increases provided that $\|u_0 - \tilde{u}_0\|_{L^2(0,L)}^2$ is arbitrarily small.

3.3 A Splitting Method

The solution u of the Jeffrey's IBVP (21), (8) can be computed by using the approach introduced in Sect. 2. As this approach gives u as the sum of a series, we present in this section a family of numerical methods to compute an approximation for u.

We consider a spatial uniform grid x_i such that $x_{i+1} - x_i = h$ and a uniform temporal grid t_n such that $t_{n+1} - t_n = \Delta t$. By $u_h^n(x_j)$ we denote a numerical approximation of $u(x_j, t_n)$.

Let us consider Eq. (21) at (x_j, t_n). Using the trapezoidal rule in the discretization of the integral term and discretizing the partial derivative with respect to t with backward differences and the partial derivative with respect to the space variable with second order centered differences we obtain

$$\frac{u_h^n(x_j) - u_h^{n-1}(x_{j-1})}{\Delta t} = \frac{D_1}{\gamma} D_{2,x} u_h^{n-1}(x_j)$$
$$+\frac{k_2 \Delta t}{2\gamma\tau}\left(e^{-\frac{t_{n-1}}{\tau}} D_{2,x} u_h^0(x_j) + 2\sum_{\ell=1}^{n-2} e^{-\frac{t_{n-1}-t_\ell}{\tau}} D_{2,x} u_h^\ell(x_j) + D_{2,x} u_h^{n-1}(x_j)\right), \quad (24)$$

where $j = 1, \ldots, N-1$, and

$$D_{2,x} v_h(x_j) = \frac{1}{h^2}(v_h(x_{j+1}) - 2v_h(x_j) + v_h(x_{j-1})).$$

The numerical solution obtained with method (24) is plotted in Fig. 4. Experimentally we observed an unstable behaviour of this method for reasonable values of stepsizes h and Δt. This behaviour is illustrated in Fig. 5. To overcome this drawback we consider in what follows a splitting method.

The splitting method that we propose is based on a functional splitting suggested by the decomposition of Jeffrey's heat flux J into two parts: Fourier's heat flux J_1 and modified heat flux J_2 where the first one is updated by the second one. This assumption is equivalent to consider the IBVP (21) in the interval $[t, t+\Delta t]$ splitted into the two subproblems:

$$\begin{cases} \dfrac{\partial v_1}{\partial t} = \dfrac{D_1}{\gamma} \dfrac{\partial^2 v_1}{\partial x^2} \text{ in } (0, L) \times (t, t + \Delta t]\,, \\ v_1(x, t) = u(x, t)\,, x \in (0, L), \end{cases} \tag{25}$$

$$\begin{cases} \dfrac{\partial v_2}{\partial t}(x, t) = \dfrac{D_2}{\gamma \tau} \displaystyle\int_0^t e^{-\frac{t-s}{\tau}} \dfrac{\partial^2 v_2}{\partial x^2}(s)\, ds \text{ in } (0, L) \times (t, t + \Delta t], \\ v_2(x, t) = v_1(x, t + \Delta t)\,, x \in (0, L). \end{cases} \tag{26}$$

The temperature $u(x, t + \Delta t)$ is approximated by $v_2(x, t + \Delta t)$.

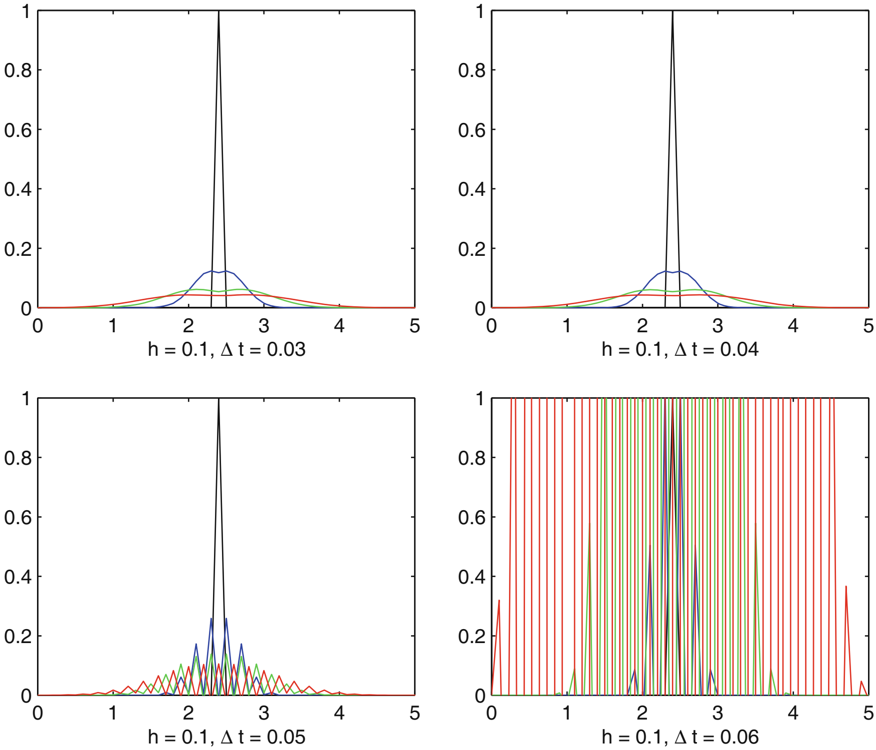

Fig. 5 Stability behaviour of method (24) with $\dfrac{D_i}{\gamma} = 0.1, i = 1, 2, \tau = 1, h = 0.1$ at $T = 2$

In order to replace the integro-differential equation in (26) by an equivalent partial differential equation, we remark that such equation is equivalent to the telegraph equation

$$\frac{\partial^2 v_2}{\partial t^2} + \frac{1}{\tau}\frac{\partial v_2}{\partial t} = \frac{D_2}{\gamma\tau}\frac{\partial^2 v_2}{\partial x^2}. \tag{27}$$

This last assertion follows immediately for Theorem 5.

Theorem 5 *([5]) Let u be the solution of (21) with initial condition* $u(x,0) = u_0(x)$, $x \in (0,L)$, *and v be the solution of*

$$\frac{\partial^2 v}{\partial t^2} + \frac{1}{\tau}\frac{\partial v}{\partial t} = \frac{D_1}{\gamma}\frac{\partial^3 v}{\partial t\partial x^2} + \frac{D_2}{\gamma\tau}\frac{\partial^2 v}{\partial x^2} \tag{28}$$

with initial conditions $\frac{\partial v}{\partial t}(x,0) = f(x),\ x \in (0,L),\ v(x,0) = v_0(x),\ x \in (0,L).$ *Then* $u = v$ *if and only if* $u_0 = v_0$ *and* $f = \frac{D_1}{\gamma}u_0''$.

We consider in $[0,L]$ a spatial uniform grid x_i such that $x_{i+1} - x_i = h$ and a uniform temporal grid t_n such that $t_{n+1} - t_n = \Delta t$. By $u_h^n(x_j)$ we denote a numerical approximation of $u(x_j, t_n)$.

Discretizing (25) and (27) we obtain

$$\begin{cases} D_t v_{h,1}^n(x_j) = \dfrac{D_1}{\gamma} D_{2,x} v_{h,1}^{n+1}(x_j), & j = 1,\ldots,N-1, \\ v_{h,1}^n(x_j) = u_h^n(x_j), \quad j = 1,\ldots,N-1, \end{cases} \tag{29}$$

$$\begin{cases} D_t w_h^n(x_j) = \dfrac{D_2}{\gamma\tau} D_{2,x} v_{h,2}^n - \dfrac{1}{\tau} w_h^n(x_j), & j = 1,\ldots,N-1, \\ D_t v_{h,2}^n(x_j) = w_h^{n+1}(x_j), \quad j = 1,\ldots,N-1, \end{cases}$$
$$\begin{cases} v_{h,2}^n(x_j) = v_{h,1}^{n+1}(x_j), & j = 1,\ldots,N-1, \\ w_h^n(x_j) = \dfrac{D_1}{\gamma} D_{2,x} v_{h,1}^{n+1}(x_j), & j = 1,\ldots,N-1, \end{cases} \tag{30}$$

where $u(x_j, t^{n+1}) \simeq v_{h,2}^{n+1}(x_j)$, $j = 1,\ldots,N-1$. In (29), (30) D_t represents the backward finite difference operator with respect to time variable.

Using matrix notation, the splitting method (29), (30) has the form

1. $(I - \frac{D_1}{\gamma}\Delta t A_2)v_{h,1}^{n+1} = u_h^n$,
2. $w_h^{n+1} = \left(\frac{D_1}{\gamma} + \frac{\Delta t}{\tau}\frac{D_2 - D_1}{\gamma}\right) A_2 v_{h,1}^{n+1}$,
3. $u_h^{n+1} = v_{h,1}^{n+1} + \Delta t w_h^{n+1}$,

which lead to

$$u_h^{n+1} = \left(I + \Delta t \left(\frac{D_1}{\gamma} + \frac{\Delta t}{\tau} \frac{D_2 - D_1}{\gamma} \right) A_2 \right) \left(I - \frac{D_1}{\gamma} \Delta t A_2 \right)^{-1} u_h^n, \tag{31}$$

where A_2 is the matrix associated with $D_{2,x}$.

In the next result we establish the stability of the splitting method (29), (30) with respect to the L^2- discrete norm.

Theorem 6 *([5]) Let u_h^n and u_h^{n+1} be the numerical approximations at time levels n and $n+1$ defined by the splitting method (29), (30). If $\varepsilon \in (0, 1)$ and Δt and h are such such that*

$$4\frac{\Delta t}{h^2} \left(\frac{D_1}{\gamma} + \frac{\Delta t}{\tau} \frac{|D_2 - D_1|}{\gamma} \right) \leq \varepsilon, \tag{32}$$

then

$$\|u_h^{n+1}\|_{L^2} \leq \frac{1 - \varepsilon}{1 + \frac{D_1}{\gamma} \frac{\Delta t}{L^2 \tau}} \|u_h^n\|_{L^2}. \tag{33}$$

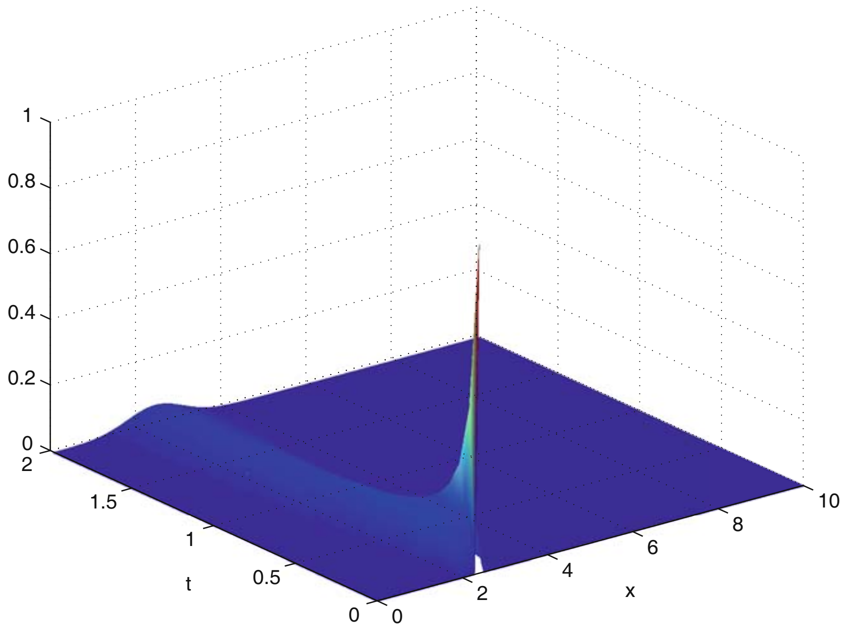

Fig. 6 Numerical approximation for the solution of Jeffrey's equation obtained using the splitting method (29), (30) ($\frac{k_i}{\gamma} = 0.1, i = 1, 2, \tau = 1,\ h = 0.1, \Delta t = 0.06$)

We note that taking $D_1 = D_2$ and $\tau \to 0$ Eq. (20) leads to heat equation with a diffusion coefficient $\frac{2D_1}{\gamma}$. Stability condition (32) is then equivalent to Courant-Friedrichs-Lewy condition.

By using the consistency of the splitting method and the stability established in Theorem 6, the convergence can be easily proved.

An energy estimate for (29), (30) which looks like a discretized version of (22) could not be obtained. Nevertheless the method is computationally efficient because the use of telegraph equation avoids the discretization of the integral. However a splitting method presenting stability properties analogous to the continuous one is studied in [3]. From a computational point of view this method is more time-consuming.

A numerical simulation obtained using the splitting method is plotted in Fig. 6 considering a Dirac delta initial condition.

4 A Non Brownian Model for a Quasi-linear Reaction-Diffusion Problem

4.1 Introduction

A huge number of biological and physical phenomena are modeled by reaction-diffusion equation (2), (4). In certain cases, as we mentioned before, the solution of this equation presents a pathological behaviour. In order to avoid such behaviour the integro-differential equation

$$\frac{\partial u}{\partial t}(x,t) = \frac{D}{\tau}\int_0^t e^{-\frac{t-s}{\tau}}\frac{\partial^2 u}{\partial x^2}(x,s)\,ds + f(u(x,t)),\ x \in (0,L), t > 0, \tag{34}$$

is introduced in [16–18]. Equation (34) is known as a generalized Fisher-Kolmogorov-Petrovskii-Piskunov equation, FKPP, and it is coupled with initial and boundary conditions

$$u(x,0) = u_0(x),\ x \in (0,L),\ u(0,t) = u_\ell(t),\ u(L,t) = u_R(t), t > 0\,. \tag{35}$$

Equation (34) is established combining the conservation law (4) with the non Fickian flux (6). The parameter τ is a relaxation parameter and when $\tau \to 0$, the FKPP equation is replaced by (2),(4).

The existence and the behaviour of solutions of Eq. (34) with $f(u) = Uu(1-u)$, $U > 0$, and a Heaviside initial condition is considered in [16].

We point out that in [4] some qualitative properties of the non Brownian model (34) are studied. Moreover reaction transport systems with memory and long range interaction with a transport process described by a non Brownian random walk model and a memory term induced by a waiting time distribution of the gamma type is considered in [19].

In Sect. 4.2 we focus on the stability analysis of the integro-differential model. In Sect. 4.3, we study numerical methods to compute approximations for the solution of (34), (35). Numerical experiments illustrating the theoretical results presented are also included.

4.2 Energy Estimates for the PDE

In this section we study the stability of the solution of (34), (35) when the initial condition is perturbed. Attending to this fact we assume in Theorem 7 homogeneous Dirichlet boundary conditions.

We establish in what follows an estimate for the energy functional (12) by using the energy method.

Theorem 7 *([8]) Let u be a solution of (34), (35) with $u_\ell(t) = u_R(t) = 0, t > 0$, satisfying for each $t \in [0, T]$*

$$u(x,t) \in [c,d], \ \ x \in [0,L], \tag{36}$$

where c, d are constants. If f is continuously differentiable and $f(0) = 0$, then the energy $E(u)$ is such that

$$E(u)(t) \leq e^{2\max\{-\frac{1}{\tau}, f'_{\max}\}t} \ \|u_0\|^2_{L^2(0,L)} \tag{37}$$

for each $t \in (0, T]$, where $f'_{\max} = max_{|u|\leq max\{|c|,|d|\}} f'(u)$.

Under the assumptions of Theorem 7, a solution u of (34), (35) exists then u is unique. Moreover u satisfies

$$\|u(t)\|_{L^2(0,L)} \leq e^{\max\{-\frac{1}{\tau}, f'_{\max}\}t} \|u_0\|_{L^2(0,L)}, \tag{38}$$

and

$$\frac{D}{\tau}\| \int_0^t e^{-\frac{t-s}{\tau}} \frac{\partial u}{\partial x}(s)\, ds \|_{L^2(0,L)} \leq e^{\max\{-\frac{1}{\tau}, f'_{\max}\}t} \|u_0\|_{L^2(0,L)}\,. \tag{39}$$

Let us consider now the classical Fisher equation (2), (4). It can be shown that

$$\|u(t)\|_{L^2(0,L)} \leq e^{f'_{\max}t} \|u_0\|_{L^2(0,L)}. \tag{40}$$

and no information is available about $\dfrac{\partial u}{\partial x}$. But if u represents the solution of (34), we conclude from (39) a stronger result that is the "average in time" of the gradient is bounded by $e^{\max\{-\frac{1}{\tau}, f'_{\max}\}t} \|u_0\|_{L^2(0,L)}$, for each time $t \in (0, T]$.

In what follows the stability behaviour of u under perturbations in the initial condition u_0 is considered. Let u and $\tilde{u}$ be solutions of (34) satisfying the same boundary conditions (not necessarily homogenous) and initial conditions u_0 and $\tilde{u}_0$ respectively. For $u - \tilde{u}$ holds the following stability result.

Theorem 8 *([8]) Let u and $\tilde{u}$ be solutions of (34), (35) with initial conditions u_0 and $\tilde{u}_0$, respectively. If for u, $\tilde{u}$ assumption (36) holds and the source function f is continuously differentiable with $f(0) = 0$, then*

$$E(u - \tilde{u})(t) \leq e^{2\max\{-\frac{1}{\tau}, f'_{\max}\}t} \|u_0 - \tilde{u}_0\|^2_{L^2(0,L)}. \tag{41}$$

4.3 Energy Estimates for the Fully Discrete Approximation

Let us consider in $[0, L]$ a grid $I_h = \{x_j,\ j = 0, \dots, N\}$ with $x_0 = 0, x_N = L$ and $x_j - x_{j-1} = h$. We denote by $L^2(I_h)$ the space of grid functions v_h defined in I_h such that $v_h(x_0) = v_h(x_N) = 0$. In $L^2(I_h)$ we consider the discrete inner product

$$(v_h, w_h)_h = h \sum_{i=1}^{N-1} v_h(x_i) w_h(x_i),\ v_h, w_h \in L^2(I_h). \tag{42}$$

We denote by $\|.\|_{L^2(I_h)}$ the norm induced by the above inner product. For grid functions w_h and v_h defined in I_h we introduce the notations

$$(D_{-x} w_h, D_{-x} v_h)_{h,+} = \sum_{i=1}^{N} h D_{-x} w_h(x_i) D_{-x} v_h(x_i),$$

$$|D_{-x} w_h\|_{L^2(I_h^+)} = \left(\sum_{i=1}^{N} h (D_{-x} w_h(x_i))^2 \right)^{1/2},$$

where D_{-x} denotes the backward finite-difference operator.

We remark that $(.,.)_h + (D_{-x}., D_{-x}.)_{h,+}$ is a natural discretization of the usual inner product in $H^1(0, L)$.

In the following we establish an estimate for the fully discrete version of the energy $E(u)(t)$ defined by (12):

$$E(u_h^{n+1}) = \|u_h^{n+1}\|^2_{L^2(I_h)} + \frac{D}{\tau} \|\Delta t \sum_{\ell=1}^{n+1} e^{-\frac{t_{n+1} - t_j}{\tau}} D_{-x} u_h^{\ell}\|^2_{L^2(I_h^+)},$$

where u_h^j is the numerical approximation defined in what follows.

Implicit discretization of the reaction term: In this case the fully discrete approximation of (34) is defined by the system of nonlinear equations

$$\frac{u_h^{n+1}(x_j) - u_h^n(x_j)}{\Delta t} = \frac{D}{\tau}\Delta t \sum_{\ell=1}^{n+1} e^{-\frac{t_{n+1}-t_\ell}{\tau}} D_{2,x} u_h^\ell(x_j) + f(u_h^{n+1}(x_j)), \quad j = 1, \dots, N-1, \tag{43}$$

where

$$u_h^\ell(x_0) = u_\ell(t_\ell),\ u_h^\ell(x_N) = u_R(t_\ell),\ \ell = 1, \dots, M-1,\ u_h^0(x_j) = u_0(x_j), \quad j = 1, \dots, N-1. \tag{44}$$

The discrete version of Theorem 7 holds for the solution of (43), (44).

Theorem 9 *([8]) Let u_h^ℓ be defined by (43), (44) with $u_\ell(t) = u_R(t) = 0, t > 0$, such that $u_h^\ell(x_i) \in [c, d]$, for $i = 0, \dots, N$, and $\ell = 0, \dots, M$. If the source function f is continuously differentiable and $f(0) = 0$, then*

$$E(u_h^{n+1}) \le \left(\frac{1}{min\{1, 1 - 2\Delta t f'_{\max}\}}\right)^{n+1} \|u_h^0\|^2_{L^2(I_h)} \tag{45}$$

provided that $1 - 2\Delta t f'_{\max} > 0$.

The factor $S_I = \dfrac{1}{\min\{1, 1 - 2\Delta t f'_{\max}\}}$ represents the stability amplification factor. If $f'_{\max} < 0$ then $S_I = 1$ and from (45) we obtain

$$E(u_h^{n+1}) \le \|u_h^0\|^2_{L^2(I_h)}.$$

Otherwise if $f'_{\max} > 0$, then

$$E(u_h^{n+1}) \le e^{\beta(n+1)\Delta t} \|u_h^0\|^2_{L^2(I_h)} \tag{46}$$

for $\Delta t \le \Delta t_0$ with $\beta = \dfrac{2 f'_{\max}}{1 - 2\Delta t_0 f'_{\max}}$.

Explicit discretization of the reaction term: Let us consider now the implicit-explicit (IMEX) scheme obtained by replacing in (43) $f(u_h^{n+1})$ by $f(u_h^n)$, that is,

$$\frac{u_h^{n+1}(x_j) - u_h^n(x_j)}{\Delta t} = \frac{D}{\tau}\Delta t \sum_{\ell=1}^{n+1} e^{-\frac{t_{n+1}-t_\ell}{\tau}} D_{2,x} u_h^\ell(x_j) + f(u_h^n(x_j)),\ j = 1, \dots, N-1. \tag{47}$$

In this case we can establish a result analogous to Theorem 9 where the stability coefficient S_I is replaced by the stability coefficient S_{IMEX} defined by $S_{\text{IMEX}} = \dfrac{1 + \Delta t}{1 - \Delta t (f'_{\max})^2}$ provided that $1 - \Delta t (f'_{\max})^2 > 0$. As we have $S_{\text{IMEX}} \le 1 + \dfrac{1 + (f'_{\max})^2}{1 - \Delta t_0 (f'_{\max})^2}\Delta t$, we can prove (46) with $\beta = \dfrac{1 + (f'_{\max})^2}{1 - \Delta t_0 (f'_{\max})^2}$.

4.4 Convergence

Let us study now the convergence of the approximation defined by (43), (44). Let $e_h^\ell(x_i) = u_h^\ell(x_i) - u(x_i, t_\ell)$ be the global error of the approximation $u_h^\ell(x_i)$ computed using (43), (44), and let $T_h^\ell(x_i)$ be the corresponding truncation error. These two errors are related by

$$e_h^{n+1}(x_i) = e_h^n(x_i) + \frac{D}{\tau}\Delta t^2 \sum_{j=1}^{n+1} e^{-\frac{t_{n+1}-t_j}{\tau}} D_{2,x} e_h^j(x_i) + f(u_h^{n+1}(x_i)) - f(u(x_i, t_{n+1})) + \Delta t T_h^{n+1}(x_i),\ i = 1, \ldots, M-1 \tag{48}$$

with

$$e_h^0(x_i) = 0,\ i = 1, \ldots, N-1,\ e_h^\ell(x_0) = e_h^\ell(x_N) = 0,\ \ell = 1, \ldots, M.$$

The next convergence result can be proved.

Theorem 10 *([8]) Let u_h^ℓ be defined by (43), (44) and such that $u_h^\ell(x_i) \in [c, d]$, for all i and for all ℓ. If the solution u of (34), (35) satisfies (36) and the source function f is continuously differentiable with $f(0) = 0$, then*

$$E(e_h^{n+1}) \leq \sum_{j=0}^{n} \hat{S}_I^{j+1} \Delta t \| T_h^{n+1-j} \|^2_{L^2(I_h)} \tag{49}$$

with $\hat{S}_I = \dfrac{1}{min\,\{1, 1-(1+2f'_{\max})\Delta t\}}$.

Considering that (43) is defined approximating the second-order spatial derivative using centered differences, the integral term using the rectangular rule and the integration in time using the Euler implicit method, we have

$$\|T_h\|_\infty = \max_\ell \|T_h^\ell\|_\infty \leq C \max_{t\in(0,T]} \left(\Delta t + h^2\right). \tag{50}$$

In the last inequality C denotes a positive constant independent of h and Δt. Using (50) in Theorem 10 we conclude:

Corollary 2 *([8]) Under the assumptions of Theorem 10 and assuming* $f'_{\max} \leq -\dfrac{1}{2}$ *then*

$$E(e_h^n) \leq C \|T_h\|^2_\infty. \tag{51}$$

If $f'_{\max} > -\dfrac{1}{2}$ *then*

$$E(e_h^{n+1}) \leq C e^{\beta n \Delta t} \|T_h\|^2_\infty, \tag{52}$$

with

$$\beta = \frac{1 + 2f'_{\max}}{1 - (1 + 2f'_{\max})\Delta t_0}.$$

Analogous convergence results can be established for the IMEX method.

We present in what follows some numerical results that illustrate the qualitative and stability properties of methods (43) and (47). The computational experiments were obtained with a reaction term of type $f(u) = U(1-u)u$, and with the initial condition

$$u_0(x) = \begin{cases} 1, & x \in [0, 50] \\ 0, & x \in]50, 100] \, . \end{cases}$$

In Fig. 7 we plot the numerical approximations obtained using method (43) and method (47) with $U = 1, \tau = 0.1 = D = 0.1$ and $\Delta t = h = 0.1$. The two numerical solutions exhibit the same stability behaviour, but as it can be observed the speed of the numerical solution obtained with method (43) is greater.

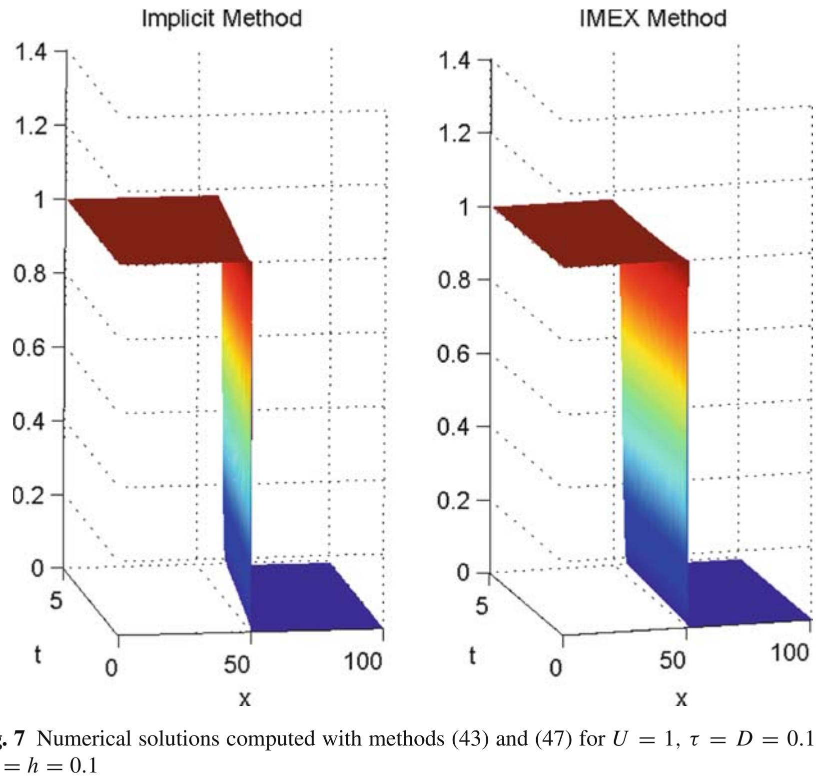

Fig. 7 Numerical solutions computed with methods (43) and (47) for $U = 1$, $\tau = D = 0.1$ and $\Delta t = h = 0.1$

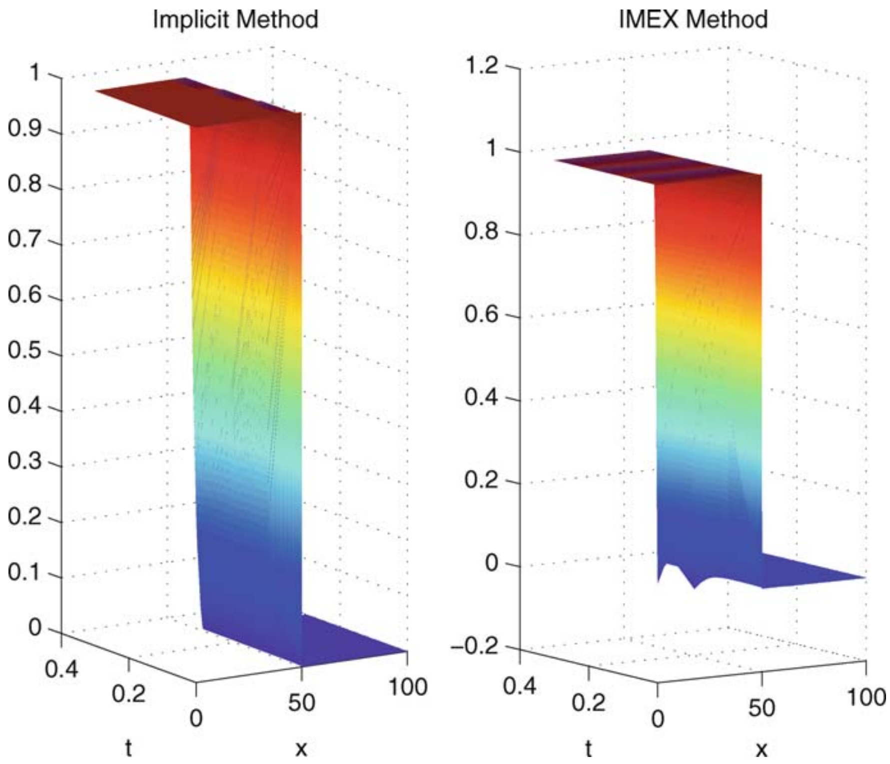

Fig. 8 Numerical solutions computed with methods (43) and (47) for $D = \tau = 0.1 = \Delta t = h = 0.1$ and $U = -25$

We shown that if the reaction term f is stiff, then method (43) is more stable then method (47). This behaviour is illustrated in Fig. 8 where we plot the numerical solution obtained with the previous methods for $U = -25$ and $h = \Delta t = \tau = D = 0.1$. As can be observed, the numerical solution obtained with method (47) presents an unstable behaviour.

Acknowledgments This work was supported by CMUC through FCT's funding program and project PTDC/MAT/74548/2006

References

1. Abe S., Thurner S.: Anomalous diffusion in view of Einstein's 1905 theory of Brwonian motions. Phys. A. **356**, 403–407 (2005)
2. Aoki K.: Diffusion-controlled current with memory. J. Electroanal Chem. **592**, 31–36 (2006)
3. Araújo A., Branco J.R., Ferreira J.A.: On the stability of a class of splitting methods for integro-differential equations. Appl. Num. Math. (2008) doi:10.1016/j.apnum.2008.03.005
4. Araújo A., Ferreira J.A., Oliveira P.: Qualitative behaviour of numerical traveling waves solutions for reaction diffusion equations with memory. Appl. Anal. **84**, 1231–1246 (2005)

5. Araújo A., Ferreira J.A., Oliveira P.: The effect of memory terms in the qualitative behaviour of the solution of the diffusion equations. J. Comput. Math. **24**, 91–102 (2006)
6. Aronson D.G., Weinberger H.F.: Multidimensional nonlinear diffusion in population genetics. Adv. Math. **30**, 33–76 (1978)
7. Bernik D.L., Zubiri D., Monge M.E., Negri R.M.: New kinetic model of drug release from swollen gels under non-sink conditions. Colloid. Surf. A: Physicochem. Eng. Asp. **273**, 165–173 (2006)
8. Branco J.R., Ferreira J.A., Oliveira P.: Numerical methods for generalized Fisher-Kolmogorov-Petrovskii-Piskunov equation. Appl. Numer. Math. **57**, 89–102 (2007)
9. Cattaneo C.: Sulla conduzione del calore. Atti del Seminario Matematico e Fisico dell' Università di Modena **3**, 3–21 (1948)
10. Carillo S.: Some remarks on material with memory: heat conduction and viscoelasticity. J. Nonlinear. Math. Phys. **12**(Supp. 1), 163–178 (2005)
11. Chang J.C.: Solutions to non-autonomous integrodifferential equations with infinite delay. J. Math. Anal. Appl. **331**, 137–151 (2007)
12. Chang J.C.: Local existence of retarded Volterra integrodifferential equations with Hille-Yosida operators. Nonlinear Anal. **66**, 2814–2832 (2007)
13. Chen H.-T., Liu K.-C.: Analysis of non-Fickian diffusion problems in a composite medium. Comput. Phys. Commun. **150**, 31–42 (2003)
14. Coutts-Lendon C.A., Wright N.A.: The use of FT-IR imaging as an analytical tool for the characterization of drug delivery systems. J. Control. Release. **93**, 223–248 (2003)
15. Fabrizio M., Gentili G., Reynolds D. W.: On rigid heat conductors with memory. Int. J. Eng. Sci. **36**, 765–782 (1998)
16. Fedotov S.: Traveling waves in a reaction – diffusion system: diffusion with finite velocity and Kolmogorov-Petrovski-Piskunov kinectics. Phys. Rev. E. **5**(4), 5143–5145 (1998)
17. Fedotov S.: Nonuniform reaction rate distribution for the generalized Fisher equation: Ignition ahead of the reaction front. Phys. Rev. E. **60**(4), 4958–4961 (1999)
18. Fedotov S.: Front propagation into an unstable state of reaction - transport systems. Phys. Rev. Lett. **86** (5), 926– 929 (2001)
19. Ferreira J.A., de Oliveira P.: Memory effects and random walks in reaction-transport systems. Appl. Anal. **86**, 99–118 (2207)
20. Ferreira J.A., de Oliveira P.: Qualitative Analysis of a Delayed non Fickian model. App. Anal. **87**, 873–886 (2008)
21. Fisher R.A.: The wave of advance of advantageous genes. Ann. Eugen **7**, 353–369 (1937)
22. Iordanskii A.L., Feldstein M.M., Markin V.S., Hadgraft J., Plate N.A.: Modeling of the drug delivery from a hydrophilic transdermal therapeutic system across polymer membrane. Eur. J. Pharm. Biopharm. **49**, 287–293 (2000)
23. Joseph D., Preziosi L.: Heat waves. Rev. Mod. Phys. **61**, 41–73 (1989)
24. Kolmogorov A., Petrovskii I., Piskunov N.S.: Étude de l'equation de la diffusion avec croissance de la matière et son application à un problème biologique. Mosc. Univ. Bull. Math. **1**, 1–25 (1937)
25. Ouriemchi E.M., Ghosh T.P., Vergnaud J.M.: Transdermal drug transfer from a polymer device: study of the polymer and the process. Polym. Test. **19**, 889–897 (2000)
26. Ouriemchi E.M., Vergnaud J.M.: Process of drug transfer with three different polymeric systems with transdermal drug delivery. Comput. Theor. Polym. Sci. **10**, 391–401 (2000)
27. Serra E.M., Doménech J., Peppas N.A.: Drug transport mechanisms and release kinetics from molecularly designed poly(acrylic acid-g-ethylene glycol) hydrogels. Biomaterials **27**, 5440–5451 (2006)
28. Sokolov I.M.: From diffusion to anomalous diffusion: A century ater Einstein's Brownian motion. Chaos **15**, 026103 (2005)
29. Vernotte P.: La véritable equation de la chaleur. C. R. Hebd. Séances Acad. Sci. Paris **247**, 2103–2105 (1958)
30. Zauderer E.: *Partial Differential Equations of Applied Mathematics*. John Wiley & Sons, N Y (1983)

Maximum Principle and Gradient Estimates for Stationary Solutions of the Navier-Stokes Equations: A Partly Numerical Investigation

Robert Finn, Abderrahim Ouazzi, and Stefan Turek

Abstract We calculate numerically the solutions of the stationary Navier-Stokes equations in two dimensions, for a square domain with particular choices of boundary data. The data are chosen to test whether bounded disturbances on the boundary can be expected to spread into the interior of the domain. The results indicate that such behavior indeed can occur, but suggest an estimate of general form for the magnitudes of the solution and of its derivatives, analogous to classical bounds for harmonic functions.

The qualitative behavior of the solutions we found displayed some striking and unexpected features. As a corollary of the study, we obtain two new examples of non-uniqueness for stationary solutions at large Reynolds numbers.

Keywords Navier-Stokes equations · Maximum Principle · Gradient estimates

1 Introduction

Two cornerstones of the theory of the Laplace equation

$$\triangle u = 0 \tag{1}$$

are the *a priori* bound on the solution, and the *a priori* bound on the gradient ∇u; see, e.g., [3], Chap. VIII, Theorems X and XII. The former bound states that if $u(x)$ is a solution of (1) in a bounded domain Ω and continuous up to $\Gamma = \partial\Omega$, then

$$\sup_{\Omega} |u| \leq M \doteq \max_{\Gamma} |u| \tag{2}$$

The latter bound states that there exists a function $\mathcal{F}(d; M)$ such that if d is distance from $p \in \Omega$ to Γ then

R. Finn (✉)
Department of Mathematics, Stanford University, Stanford, CA, USA
e-mail: finn@math.stanford.edu

R. Rannacher, A. Sequeira (eds.), *Advances in Mathematical Fluid Mechanics*,
DOI 10.1007/978-3-642-04068-9_15,

$$|\nabla u(p)| < \mathcal{F}(d; M). \tag{3}$$

The linearized (Stokes) equations of hydrodynamics

$$\begin{aligned} \triangle \boldsymbol{w} &= \nabla p \\ \operatorname{div} \boldsymbol{w} &= 0 \end{aligned} \tag{4}$$

for slow stationary viscous fluid flow, with velocity field $\boldsymbol{w}$ and pressure p, bear a formal resemblance to (1); this was exploited in a beautiful way by Odqvist [5] who showed that much of the classical Fredholm theory for (1) can be extended to solutions of (4). As a consequence, Odqvist was led to a bound

$$|\nabla \boldsymbol{w}(p)| < \mathcal{F}_{\Omega}(d; M) \tag{5}$$

analogous to (3), although Odqvist imposed also smoothness requirements on Γ that are not needed for (3). The subscript Ω in (5) indicates an additional distinction that occurs, that was not explicitly observed in [5]: *the functional dependence of* Φ *on* d *and on* M *can vary greatly, depending on the particular domain*. That was exhibited in [2], as a property of an explicitly known family of Couette flows, considered in expanding domains.

Given a domain Ω, the results of Odqvist lead to construction of a "Green's tensor" for the system (4) in Ω, and then to an integral equation for solutions of the Navier-Stokes equations

$$\begin{aligned} \triangle \boldsymbol{w} - \mathrm{Re}\, \boldsymbol{w} \cdot \nabla \boldsymbol{w} &= \nabla p \\ \operatorname{div} \boldsymbol{w} &= 0 \end{aligned} \tag{6}$$

in Ω, with prescribed boundary data subject to an outflow condition on Γ. Leray [4] studied the integral equation, and by an ingenious reasoning obtained an *a priori* bound for the Dirichlet integral for any solution and in consequence a bound for the gradient analogous to that of Odqvist; however the bound depends additionally on the Reynolds number Re and on the tangential derivatives of the data on Γ up to third order; see, e.g., the comments in [1]. Using that bound in the integral equation, Leray was able to prove the existence of a smooth solution of (6), in any domain bounded by smooth components, corresponding to sufficiently smooth data having zero outflow on each boundary component. It is a remarkable result that had not been predicted and certainly was unexpected, in view of the known instabilities that arise with increasing Re.

The question, whether for a specific domain there is a gradient bound for (6) fully analogous to that of Odqvist (i.e., depending only on Re and on M and not on smoothness of the boundary data), remains open. Such a bound would remove the differentiability requirements imposed by Leray on the data, and would also be of independent interest, in many contexts. Partial information was supplied by Finn and Solonnikov [2], who obtained a result of somewhat different character, weakening the requirements imposed by Leray but not yet including the specific estimate that is sought. Those authors offered a suggestive reasoning (short of a proof) that in two dimensions the indicated estimate may fail.

In the present note, we put the matter to an initial experimental test in the two dimensional case, using numerical calculations. We take as domain Ω a square, and impose data on the sides Γ that are uniformly bounded but successively more oscillatory, to determine whether the rapid disturbances on the boundary will spread into the interior. We do that for two ranges of data that are tangential on Γ, so that no fluid enters Ω but for which the tangential direction oscillates. We do it also for two ranges of data that are orthogonal on Γ, with rapid oscillation between entering Ω and leaving it. Each calculation was performed for three different Reynolds numbers, in a range from 1 to 10000, and for five different oscillation rates, determined by a parameter k. We use the computer calculations to estimate the magnitudes $|\boldsymbol{w}|$ in Ω. The corresponding bounds on $|\nabla \boldsymbol{w}|$ are then inferred from Theorem 1 in [2].

2 Test Configurations

Specifically, the data were as follows, for velocities $\boldsymbol{w} = (u, v)$ on the sides $x = \pm 1$, $y = \pm 1$ of a square of side length 2:

(A) Tangential data

A1) $\boldsymbol{w} = ((x^2 - 1)\sin kx, 0)$ on $y = \pm 1$, $\boldsymbol{w} = (0, 0)$ on $x = \pm 1$
AC) $\boldsymbol{w} = ((x^2 - 1)\sin kx, 0)$ on $y = +1$, $\boldsymbol{w} = (0, (y^2 - 1)\sin ky)$ on $x = +1$ and
$\boldsymbol{w} = (0, 0)$ on the remaining sides

$$k = 1, \cdots, 120; \ \mathrm{Re} = 1, \cdots, 10000.$$

(B) Normal data

B1) $\boldsymbol{w} = (0, (x^2 - 1)\sin kx)$ on $y = \pm 1$, $\boldsymbol{w} = (0, 0)$ on $x = \pm 1$
BC) $\boldsymbol{w} = (0, (x^2 - 1)\sin kx)$ on $y = 1$, $\boldsymbol{w} = (-(y^2 - 1)\sin ky, 0)$ on $x = 1$ and
$\boldsymbol{w} = (0, 0)$ on the remaining sides

$$k = 1, \cdots, 120; \ \mathrm{Re} = 1, \cdots, 10000.$$

We examined also the question, whether a local jump discontinuity in boundary data can spread into the interior as an unbounded disturbance. In the view that such behavior could be dependent on the magnitude of the jump, we made the choices:

(C) Tangential data

$\boldsymbol{w} = (K, 0)$ on $y = \pm 1$, $-0.9\,eps < x < +0.9$; $\boldsymbol{w} = (0, 0)$ elsewhere on the boundary

(D) Normal data

$\boldsymbol{w} = (0, K)$ on $y = \pm 1$, $-0.9 < x < +0.9$; $\boldsymbol{w} = (0, 0)$ elsewhere on the boundary

$$K = 1, \cdots, 60; \text{ Re} = 1, \cdots, 10,000.$$

3 Numerical Methods

In our numerical studies with the open source CFD package FEATFLOW (`www.featflow.de`), we mainly focus on low order Stokes elements with nonconforming finite element approximations for the velocity and piecewise constant pressure functions which satisfy the LBB condition [7]. Moreover, in the case of nonstationary flow simulations, second order time stepping schemes are used which can be applied in a fully coupled as well as operator-splitting, resp., pressure correction framework. However, in these studies, we directly solved the stationary Navier-Stokes equations by applying a Newton-like method to the fully coupled discretized system while the auxiliary linear problems are solved via multigrid techniques.

There are well-known situations for standard FEM methods when severe numerical problems may arise, namely in the case of convection dominated problems. Then, numerical difficulties arise for instance for medium and high Re numbers since the standard Galerkin formulation usually fails and may lead to numerical oscillations and to convergence problems of the iterative solvers. Among the stabilization methods existing in the literature for these types of problems, we use the proposed one in [6, 8] which is based on the penalization of the gradient jumps over element boundaries. In 2D, the additional stabilization term $\mathbf{J}\boldsymbol{u}$, acting only on the velocity $\boldsymbol{u}$ in the momentum equations, takes the following form (with $h_E = |E|$)

$$< \mathbf{J}\boldsymbol{u}, \boldsymbol{v} > \to = \sum_{\text{edge E}} \max(\gamma \frac{1}{\text{Re}} h_E, \gamma^* h_E^2) \int_E [\nabla \boldsymbol{u}] : [\nabla \boldsymbol{v}] \, ds, \tag{7}$$

and can simply added to the original bilinear form. Summarizing, in the underlying test cases which require the solution of stationary problems, efficient Newton-type and multigrid solvers can be easily applied for such highly accurate stabilization techniques (see [8] for more details) which are the basis of the subsequent numerical analysis.

4 Results and Analysis

In the data for cases **A** and **B**, the factors of the form $\left(x^2 - 1\right)$ are inserted to impose continuity with zero data at the corner points, thus ameliorating eventual singularities that could arise from the corner boundary discontinuities. Although the presence of these discontinuities causes both the domain and the data to be outside the range

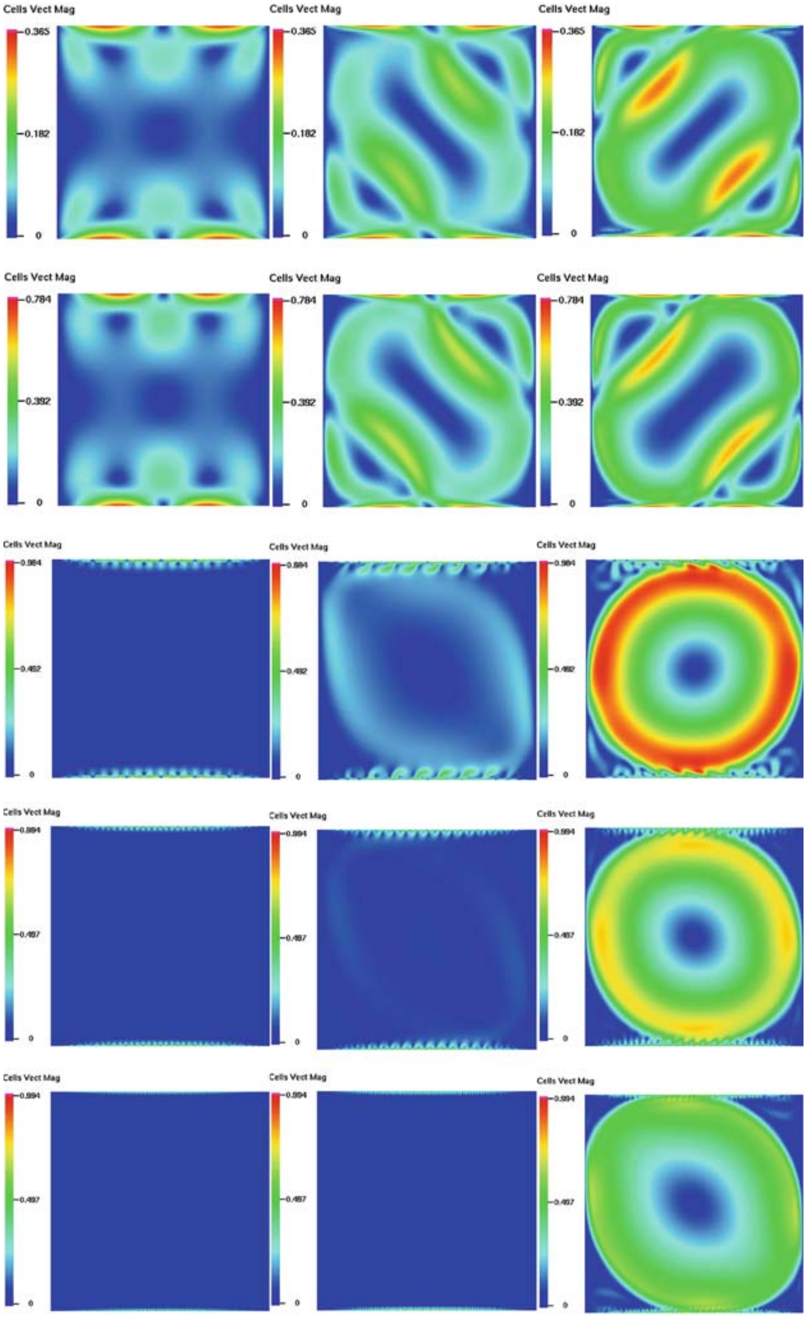

Fig. 1 The tangential data A1: Velocity magnitude for $k = 1$, $k = 3$, $k = 30$, $k = 60$ and $k = 120$ and Reynolds numbers Re $= 1$, Re $= 1000$ and Re $= 10000$. Reynolds number increases from left to right and k increases from top to bottom

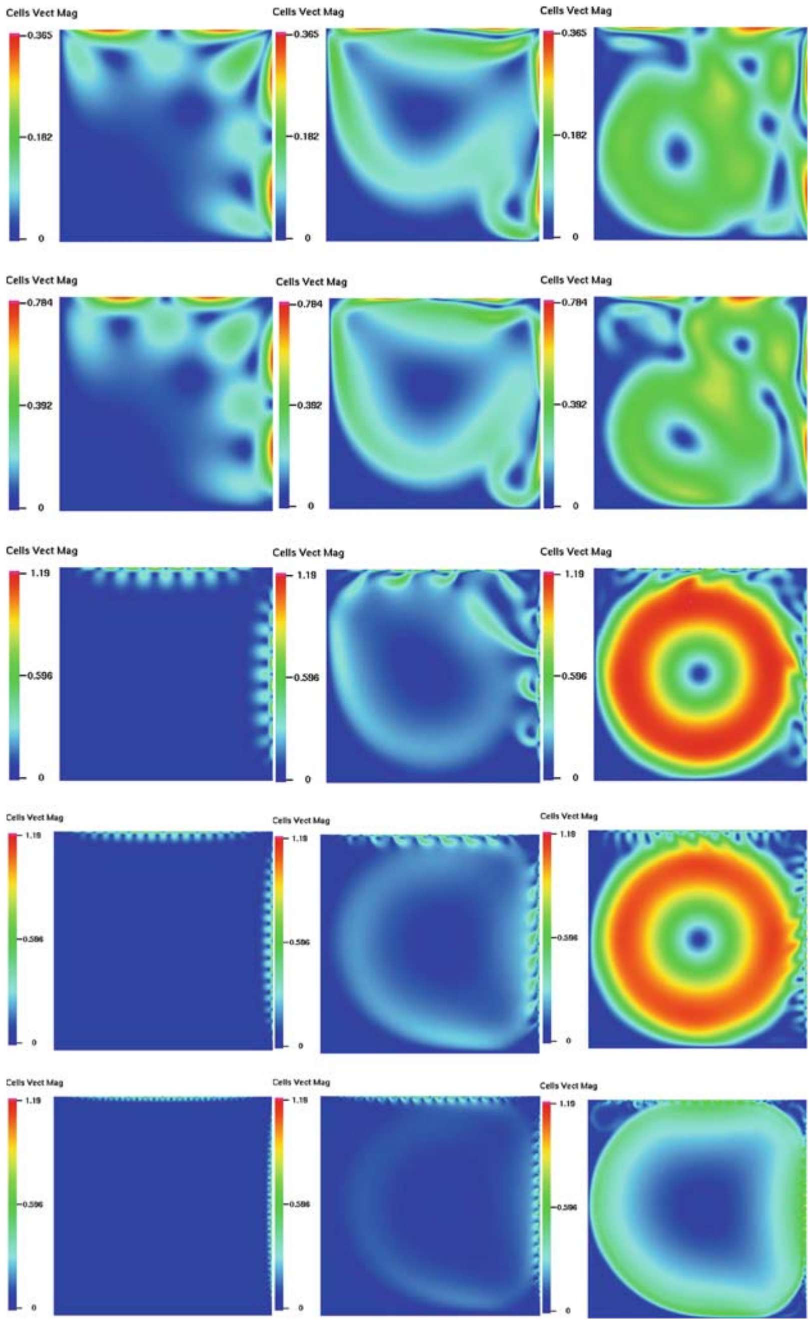

Fig. 2 The tangential data AC: Velocity magnitude for $k = 1$, $k = 3$, $k = 15$, $k = 30$ and $k = 60$ and Reynolds numbers Re $= 1$, Re $= 1000$ and Re $= 10000$. Reynolds number increases from left to right and k increases from top to bottom

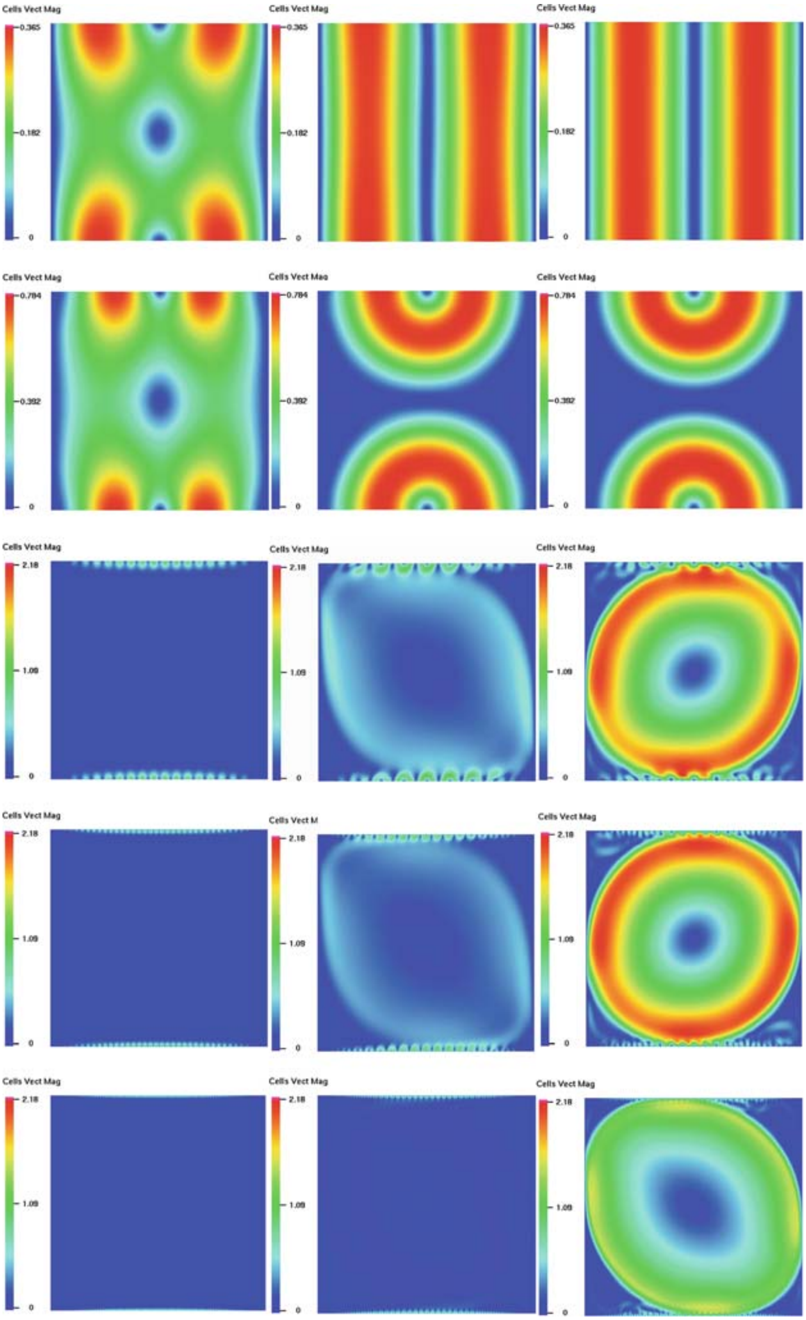

Fig. 3 The normal data B1: Velocity magnitude for $k = 1$, $k = 3$, $k = 30$, $k = 60$ and $k = 120$ and Reynolds numbers Re $= 1$, Re $= 1000$ and Re $= 10000$. Reynolds number increases from left to right and k increases from top to bottom

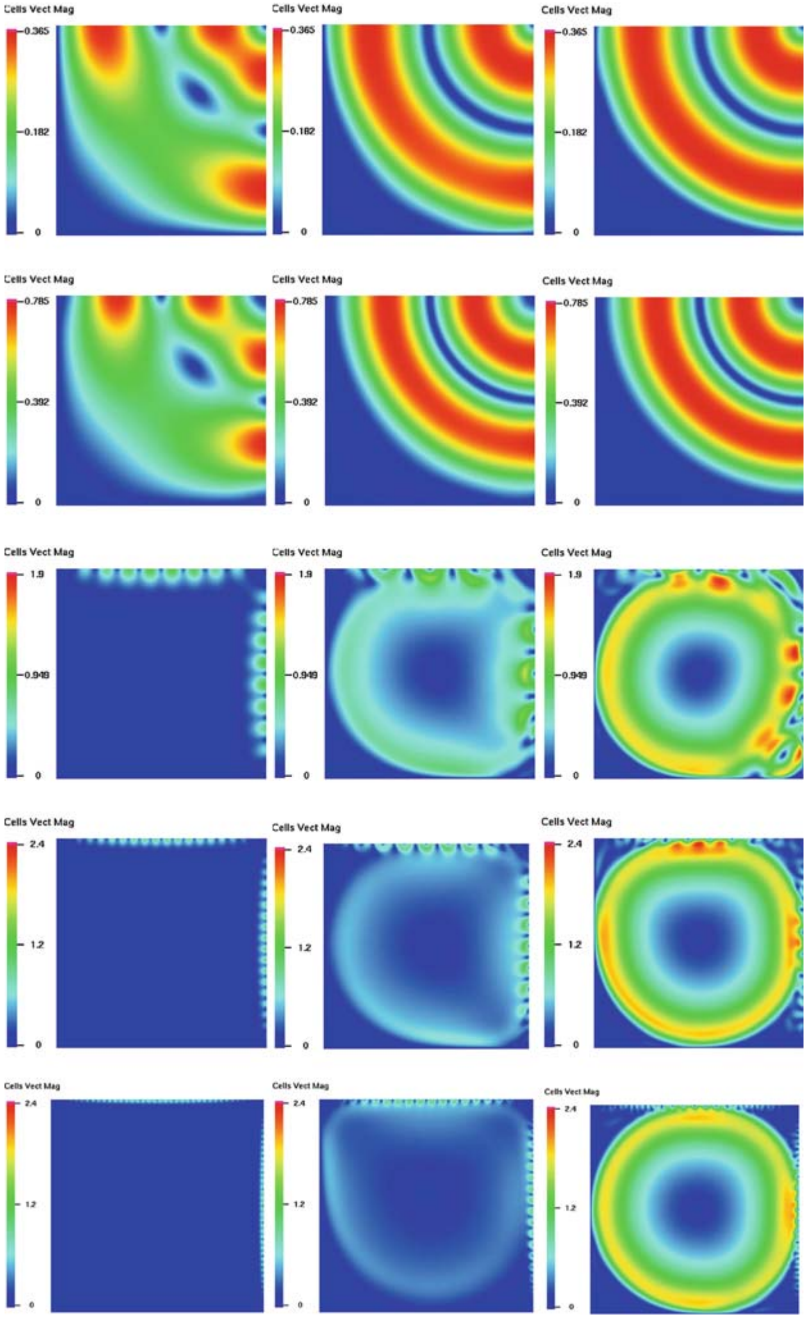

Fig. 4 The normal data BC: Velocity magnitude for $k = 1$, $k = 3$, $k = 15$, $k = 30$ and $k = 60$ and Reynolds numbers Re $= 1$, Re $= 1000$ and Re $= 10000$. Reynolds number increases from left to right and k increases from top to bottom

for Leray's existence theorem, the choice made was considered preferable from the point of view of programming data for the computer procedures. No indication was observed of any difficulty in finding at least one solution of the boundary problem in all cases, and in some instances multiple solutions could be identified, see the discussion below. The choice $k = 120$, which appears only in Figs. 1 and 3, was not originally contemplated; it is outside the range for which the computation procedures can be trusted to be reliable, and so the inferences we make from that case must be considered provisional; however the results obtained for it are consistent with other observations, and point to trends that we feel are worth noting.

An initial comment is in order on the choice of scaling for the figures, which display interior velocity magnitudes on a color scale ranging from blue (small) to red (large). One is tempted as a "natural" choice to make the highest scale point in each figure the maximum velocity magnitude in the figure. Such a procedure is well suited for examining what happens in that figure, but can be misleading when comparing one figure with another. In consideration of the behavior features that we felt most important to emphasize, and with a view to minimize confusion in interpretation, we decided to choose the highest scale point for each row to be the maximum of the two numbers: (a) the maximum velocity magnitude achieved in that row, and (b) the maximum velocity magnitude achieved in any row that is above that one. The reader should keep that choice in mind when interpreting the figures; a change in scale in any figure can produce a very different appearance of the figure. In the relevant (groups of) Figs. 1, 2, 3 and 4, k increases with row from top to bottom, Re increases with column from left to right. Thus in our choice of scaling, the highest scale point is the same for all figures in a row, and is non-decreasing from top to bottom.

It should be noted that the maximum boundary velocity magnitude is the same for all figures in a row. For reference, the values for this quantity are: $k = 1 : .365; k = 3 : .784; k = 15 : .989; k = 30 : .997; k = 60 : .999; k = 120 : 1.000$. For the data as chosen, this maximum magnitude is usually achieved at only a single point. In some of the figures, the highest scale points will be slightly less than these values; that is because the computer mesh points in general differ from those special extremal points.

We organize our interpretations of the figures according to Roman numerals.

I. Figure 1 displays the velocity magnitudes $|\boldsymbol{w}|$ in case A1 corresponding to five values of k and three values of Re, arising from oscillating tangential data on the sides $y = \pm 1$ for which no fluid enters or leaves the square Ω. The value $k = 15$ is not included in the figure, however the $k = 15$ fluid patterns are similar to those for $k = 1$ and $k = 3$ cases. The maximum magnitudes interior to Ω for some of the cases are roughly comparable to those on Γ, and in that sense one sees that the boundary disturbances do transmit into the interior.

   With increasing k and small Re, the oscillations in data are dissipated rapidly by frictional forces within the fluid; there appears to be no focusing of energy, and to the extent visible in the figures, one can not even discern that the boundary data are achieved, although the oscillations in data are detectable near the

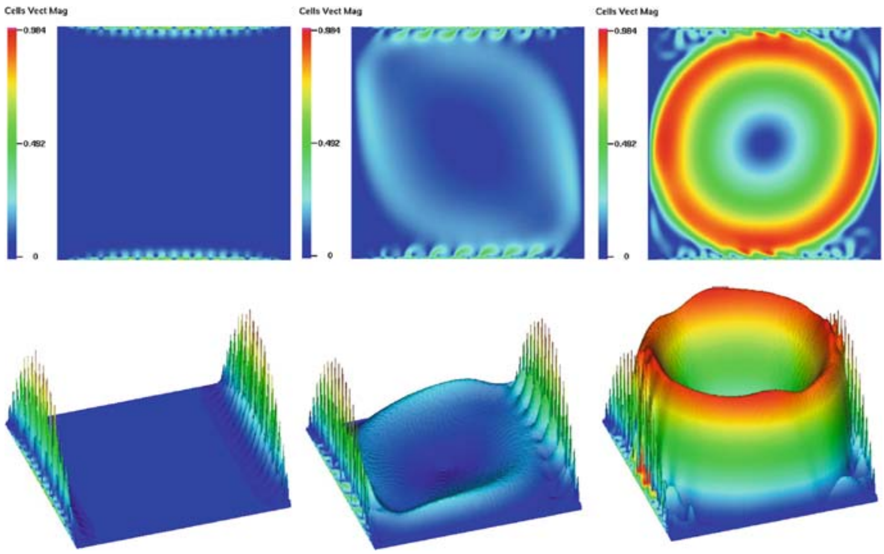

Fig. 5 The tangential data A1: Solution (*top*) and corresponding three dimensional view of the solution (*bottom*) for $k = 30$ and $\text{Re} = 1$, $\text{Re} = 1000$ and $\text{Re} = 10000$. Reynolds number increases from left to right

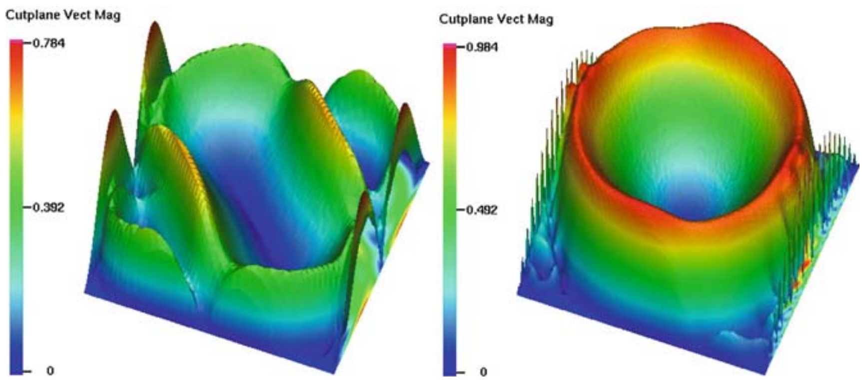

Fig. 6 The tangential data A1: A three dimension of the norm of the velocity for $k = 3$ and $k = 30$ for $\text{Re} = 10000$

boundary. We have suppressed the case $\text{Re} = 100$ in the interest of more clarity for the remaining cases, but we remark that the behavior does not differ greatly from that of $\text{Re} = 1$.

For large Re this behavior changes dramatically, and a ring of relatively large kinetic energy appears with increasing k when Re is large enough. For fixed Re and further increasing k, the effect fades and for $\text{Re} \leq 1000$ disappears. Presumably it will eventually disappear also for larger Re, as suggested in the figure. Thus, for large Re a rotational symmetry not apparently connected with

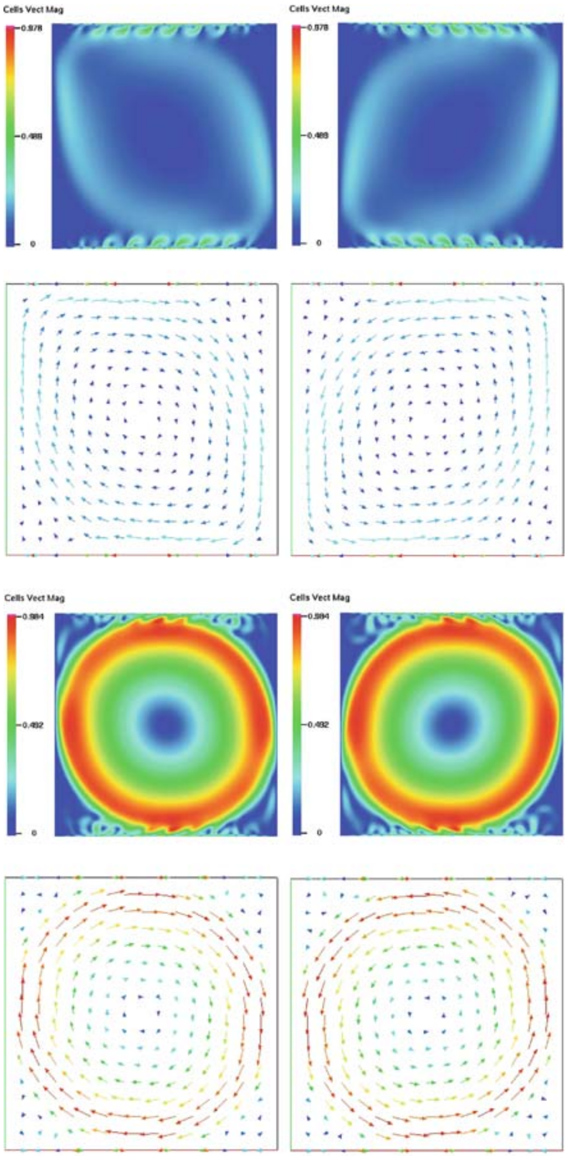

Fig. 7 The tangential data A1: Solution and the corresponding vector plot for $k = 30$ and $\mathrm{Re} = 1000$, and $\mathrm{Re} = 10000$, arising from changes in detail of the calculation procedure for case A (Fig. 1). Reynolds number increases from top to bottom

the boundary data at first occurs with increasing k, but as k increases further the effect then is overwhelmed by dissipation and washes out. It should be noted that throughout this development, the magnitudes interior to Ω do not exceed the maximum on the boundary.

We examine the effect in further detail in Figs. 5 and 6, which offer relief figures for the magnitudes, with the particular choices $k = 3$ and $k = 30$, with increasing Re. The "spikes" on opposite sides are the prescribed boundary data.

The flow within the rings is roughly rotational, and can be produced in either rotation sense, depending on details of the computational procedure. Thus *we obtain a new example of non-uniqueness for stationary solutions of (6) at large Reynolds number*. The two solutions are illustrated in Fig. 7, for $k = 30$ and for $\mathrm{Re} = 1000$ and 10000.

II. In order to determine the extent to which the symmetry of the data affected the results, the same oscillating data were imposed on two adjacent sides. Results are shown in Fig. 2, The same qualitative behavior occurs, with somewhat larger magnitudes appearing, presumably since the boundary data are imposed on sides that are closer together.

III. Figure 3 results from identical data normal to the boundary, imposed on the top and bottom of the square, with $k = 1, 3, 30, 60, 120$, and $\mathrm{Re} = 11000, 10000$. A notable event occurs when k changes from 1 to 3, with $\mathrm{Re} = 10000$. Presumably due to more rapidly changing data and larger magnitudes, the entering flow for $k = 3$ does not succeed in crossing to the opposite side as does the flow for $k = 1$, but instead enters and then leaves again on the same side. It is for this reason that we decided to retain the case $k = 1$ for display, despite that no full oscillation occurs. It exhibits an initial step in a behavior that seems to exert a controlling influence on the further developments.

The change to $k = 30$ in that column is again dramatic, with the development of a circular flow as in the tangential data case. What appears to be happening is that flow enters the square and then departs in adjacent boundary segments. For large k these segments are close together and most of that motion occurs close to the boundary, as indicated by the succession of half-rings in the figure. Space then appears in the central part of the square for development of the observed large circular motion, with larger velocities than occur near the boundary. The magnitudes in the central ring become for normal data notably larger than occurs for tangential data. There is clear evidence of energy focusing, with magnitudes in the ring more than double those of the (isolated) boundary peaks.

For each k the top and bottom boundary segments are divided into an even number $2j = 2(1 + [k/\pi])$ of subsegments, in each of which flow either enters or exits, and such that for each subsegment on either half of the boundary in which flow is entering, there is a corresponding one on the other half in which flow is leaving. Flow alternately enters and leaves in adjacent subsegments. If j is odd, then a predominantly left oriented flow near the upper boundary will be created, as will a predominantly right oriented flow near the lower boundary, see Fig. 8a. The reverse orientation occurs when j is even, see Fig. 8b.The flows

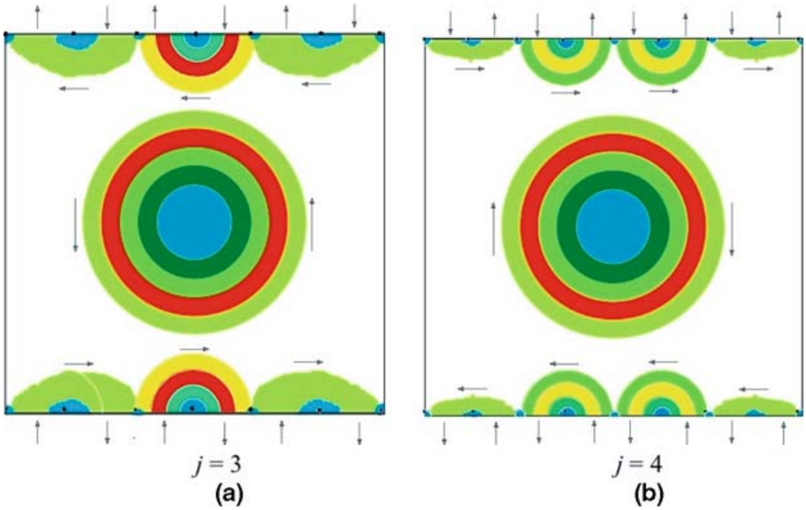

Fig. 8 The normal data B1: Projected explanation for development of rotation interior to the square, in Case B1. The *arrows* exterior to the square indicate the directions of applied data in the intervals separated by dots on the sides. Fluid enters between two dots and exits in an adjacent interval. Identical data are prescribed on the *top* and *bottom* of the square. The boundary motions combine to induce rotation in the center. Note that orientation reverses from j = 3 to j = 4. These numbers were chosen for illustration; they may be too small for actual development of interior rotation

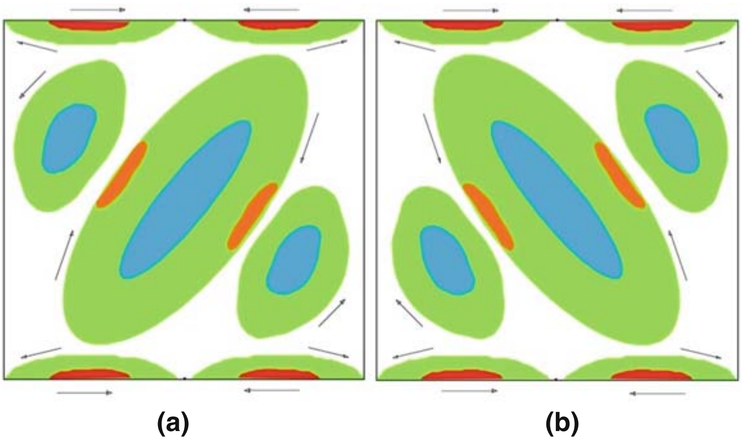

Fig. 9 The tangential data A1: Development of large-scale interior rotation in case k = 1 or 3, as result of instability of symmetric flow. Two distinct configurations with opposite flow orientations appear, in addition to a presumed symmetric solution

thus occasioned provide an explanation for the development of the circular flow in the central region. The determination of orientation just described is reasonable when k is not large. As k increases, the subsegments near the vertices lose their influence in view of the factor $(x^2 - 1)$, and the actual flow could be established in either direction, determined by circumstances having nothing to do with the equations. That could be an explanation for non-uniqueness of computed solutions. In fact, in Fig. 3 with $\mathrm{Re} = 10000$ the computed flow orientation reverses from $k = 30$–60, although j is even in both cases, and again from 60 to 120, when j reverses parity.

We note however that the non-uniqueness we have already observed under I above occurred for tangential data, for which a corresponding reasoning does not at first seem available to us. In that case the data and also the figures seem to suggest a succession of symmetrically placed small eddies at the boundary in alternating orientations; these lead formally to symmetric influence on a symmetrically placed interior circle, which would not induce rotation.

In fact, we believe the interior rotation arises in the tangential data case from quite different causes, than for the normal data case.

The clue to what happens for tangential data can be found in the upper two rows of Fig. 1. The behavior in the $\mathrm{Re} = 10000$ column of those rows is sketched in Fig. 9a, where flow directions are shown. One sees there that a large-scale rotational motion in the interior of the square is indeed supported by the data, and occurs as the result of an instability of the symmetric solution. This can happen in either rotation sense, as indicated in Fig. 9b, and as can be seen by comparing the second and third columns for the upper two rows of Fig. 3. With increasing k, the effects become more complicated, and combine to lead at large k and Re to a nearly circular configuration.

Thus, we must expect in this situation the existence of at least three distinct solutions: a solution exhibiting the symmetries of the symmetric data but which is unstable to skew-symmetric rotational disturbances, and then two rotational solutions with opposite flow orientations, as there is no reason to prefer one orientation to the other. It is these two rotational solutions that give rise to the non-uniqueness observed in item I above.

IV. Again for normal data we reduced the symmetry by placing the data on adjacent sides instead of opposite sides. Again the same kind of behavior appeared, with larger interior magnitudes presumably occasioned by the sides being closer together.

V. We consider Figs. 10 and 11, arising from successively increasing constant data on fixed subsegments of opposite boundary segments, with a jump to zero data at the endpoints. Here the behavior yielded clearly less dramatic events. Interior magnitudes in some instances exceeded those of the boundary data, but not by large amounts. This is noteworthy, especially as the boundary data are identically their maxima on intervals close to the entire sides in length, rather than at a few isolated points as in the earlier cases. On comparing behavior in the two situations, it becomes clear that rapid boundary oscillations do propagate into

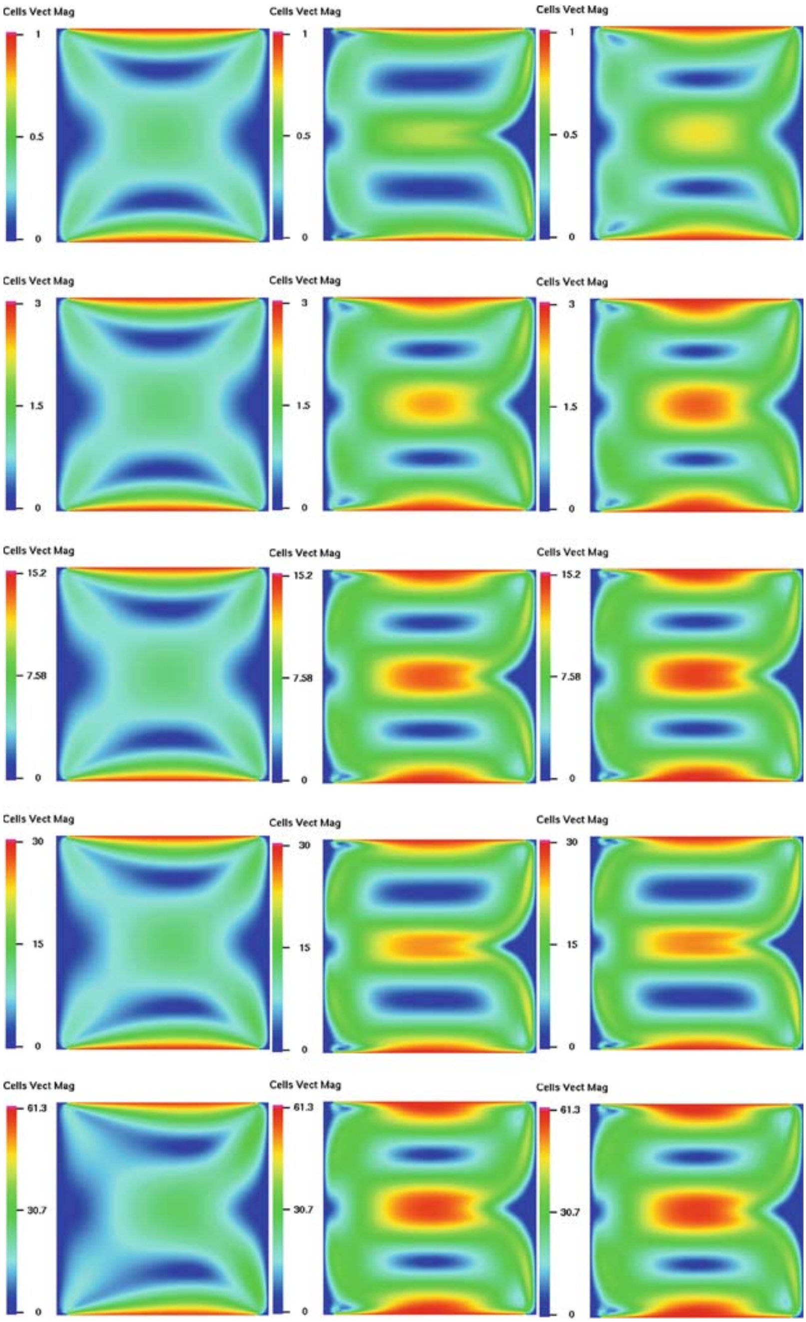

Fig. 10 The tangential data C: Velocity magnitude for $K = 1$, $K = 3$, $K = 15$, $K = 30$ and $K = 60$ and Reynolds numbers $\mathrm{Re} = 1$, $\mathrm{Re} = 1000$ and $\mathrm{Re} = 10000$. Reynolds number increases from left to right and K increases from top to bottom

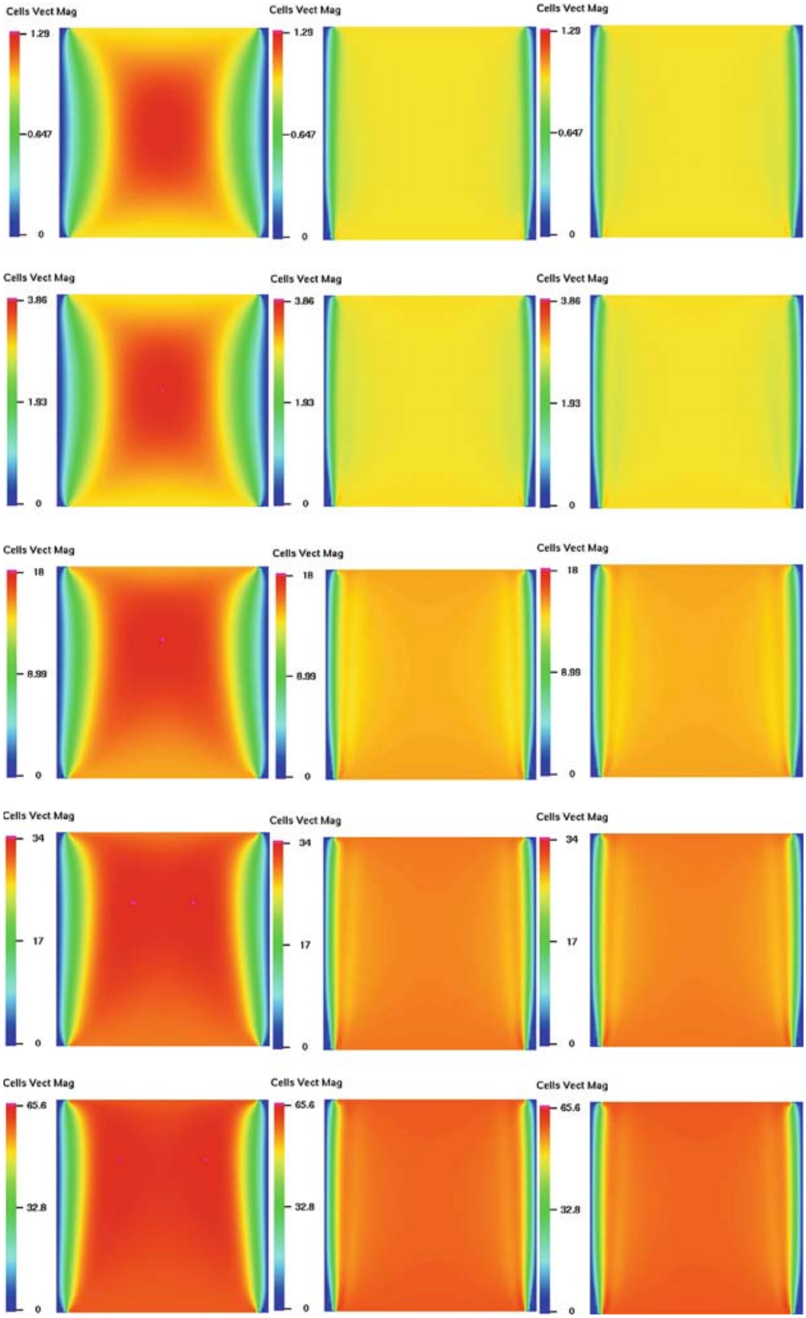

Fig. 11 The normal data D: Velocity magnitude for $K = 1$, $K = 3$, $K = 15$, $K = 30$ and $K = 60$ and Reynolds numbers $\mathrm{Re} = 1$, $\mathrm{Re} = 1000$ and $\mathrm{Re} = 10000$. Reynolds number increases from left to right and K increases from top to bottom

the interior and cause disturbances that can be large in relation to the boundary magnitudes.

5 Some Conclusions

We may interpret the figures from the point of view of the a priori estimates discussed in the Introduction. Looking at Figs. 2, 4, 10 and 11 we see immediately that *the estimate* $|\boldsymbol{w}| < M$ *does not extend without change from solutions of (1) to solutions of (6)*; larger values can be attained throughout large interior sets, including even the midpoint of the square. However, from Figs. 10 and 11 we see no evidence that even a large jump discontinuity in data will induce arbitrarily large magnitudes in the interior. The calculations suggest that with increasing k, oscillating disturbances may initially spread into the interior and even exhibit some focusing behavior, but as k becomes large enough, the focusing dampens out due to frictional dissipation. Thus, we are inclined to expect an *a priori* estimate of the form $|\boldsymbol{w}| < \Phi_{\Omega}(\mathrm{Re}\,;\mathrm{M})$. From Theorem 1 of [2] would then follow an estimate $|\nabla \boldsymbol{w}| < \mathcal{G}_{\Omega}(d;\mathrm{Re}\,;\mathrm{M})$.

We emphasize again that although our calculations suggest such estimates, we have not proved them.

Acknowledgments We are indebted to John Heywood for helpful comments. This work was supported by the German Research Association (DFG) through the collaborative research center SFB/TRR 30 and through the grants TU 102/21-1. The initial author thanks the Max-Planck-Institut für Mathematik in den Naturwissenschaften, in Leipzig, for its hospitality during preparation of the work.

References

1. Finn, R.: On the steady-state solutions of the Navier-Stokes equations, III. Acta Mathematica **105**, 197–244 (1961)
2. Finn, R., Solonnikov, V. A.: Gradient estimates for solutions of the Navier-Stokes equations. Top. Meth. Nonl. Anal. **9**, 29–39 (1997)
3. Kellogg, O. D.: *Foundations of Potential Theory*. Ungar Publishing Co, New York (1929)
4. Leray, J.: Étude de diverses équations intégrales non linéaires et de quelquess problèmes que pose l'hydrodynamique. J. Math. Pures Appl. **12**, 329–375 (1933)
5. Odqvist, F. K. G.: Über die Randwertaufgaben der Hydrodynamik zäher Flüssigkeiten. Math. Z. **32**, 1–82 (1930)
6. Ouazzi, A.: Finite Element Simulation of Nonlinear Fluids. Application to Granular Material and Powder. Shaker Verlag, Achen (2006) ISBN 3-8322-5201-0
7. Rannacher, R., Turek, S.: A simple nonconforming quadrilateral Stokes element. Numerical Methods for Partial Differential Equations **8**, 97–112 (1992)
8. Turek, S., Ouazzi, A.: Unified edge–oriented stabilization of nonconforming FEM for incompressible flow problems: Numerical investigations. J. Numer. Math. **15**, 299–322 (2007)

A Study of Shark Skin and Its Drag Reducing Mechanism

Elfriede Friedmann, Julia Portl, and Thomas Richter

Abstract In this paper we will give an overview of our studies on turbulent flow over rough surfaces such as shark skin, which have a drag reducing effect known as shark-skin effect. Our mathematical model is restricted to the flow in the viscous sublayer. Here, the turbulences which occur in the flow above this layer enter through a boundary condition. The flow equations are the steady state Navier-Stokes equations with a Couette flow profile given through two boundary conditions: a diagonal flow on the top and the no-slip condition on the rough surface. Direct simulations are performed via stabilized finite elements. For a better approximation of the boundary isoparametric finite elements are used. Our first calculations give a drag reduction of rough surfaces up to 8% whereas 15% is obtained with an improved model. We will discuss this amount of drag reduction and how it can be compared with experimental results. For gaining insight in the details of the flow, how it is influenced by the different shapes of microstructures, and how their drag reducing mechanism can be explained, we used scientific flow visualization. We will present a short overview of the methods employed.

Keywords Boundary layers · Navier-Stokes equations · Direct simulations · Drag reduction · Flow visualization

1 Introduction

Microstructures on surfaces influence the flow at first only in a small region around the surface but this small influences can have a great importance, e.g. for the drag. The golf ball flies 2.5 times further than a smooth ball of the same size would do. The lotus flower is always clean because of its special structure, and sharks are so fast because of their rough skin. In this paper we will describe the so-called shark

E. Friedmann (✉)
Department of Applied Mathematics, University Heidelberg, Im Neuenheimer Feld 293, 69120 Heidelberg, Germany
e-mail: friedmann@iwr.uni-heidelberg.de

R. Rannacher, A. Sequeira (eds.), *Advances in Mathematical Fluid Mechanics*,
DOI 10.1007/978-3-642-04068-9_16,

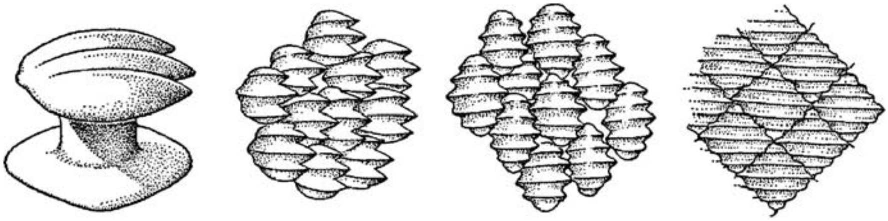

Fig. 1 The skin of sharks is made up of so-called placoidal scales (0.1-few mm). The shape of these scales depends on the species and on the position along the body. The microstructures on the crown form riblets in the main stream direction (Fig. from [16])

skin effect, i.e. the drag reducing mechanism of the small riblets found on the skin of sharks. Sharks live since more than 350 million years, so that they had a long period of time during evolution to adapt optimally in their environment. They are very fast swimmers and can reach velocities up to 60 km/h. W.E. Reif discovered in the 80s that fast swimming sharks are covered with very fine and sharp riblets which are streamlined on the body (see Fig. 1). This kind of riblets were observed on contemporary sharks but also on petrified pieces of skin which were 100 million years old. This observation signaled the importance of these structures so that a detailed study was innitated. The main result of these studies was that riblets do reduce the drag. They work only in turbulent flow which has in addition to the main stream velocity component also a cross flow velocity component which is dampened by the riblets, and so the magnitude of turbulence is reduced. This theory sounds very promising for engineers, and this so-called shark skin effect found many applications where the contribution of the turbulent skin friction to the total drag is high, e.g. swimming suits ($\approx 39\%$), airplanes ($\leq 50\%$), submarine vehicles ($\leq 70\%$) and long distance pipelines ($\leq 100\%$). Tested in wind and water channels all these applications showed a drag reduction of 7–8%. In the case of airplanes it corresponds to a fuel saving of 3% per long distance flight.

2 Modeling of Shark Skin

Due to the high burst velocity of sharks (around 70 km/h), their length and the viscosity of water, the Reynolds number of the flow around a shark is high: It lies between 10^6 and 10^7. One of the difficulties of modeling the flow around a shark is that analysis of turbulent flow is out of reach until now, and the other difficulty is the fact that the microstructures are very small (0.01–0.2 mm). To build up a suitable model we have to restrict ourself only to a small region of the flow: We will zoom into the flow (see Fig. 2) until we obtain the part which can be described by a suitable model. For describing a small part of a turbulent flow we have to know something about its structure.

Around 1904 Prandtl found out that the flow over a body of high Reynolds number can be decomposed firstly in a thin layer near the wall, the so-called boundary layer, and secondly in a potential flow. The so-called boundary layer is the domain of

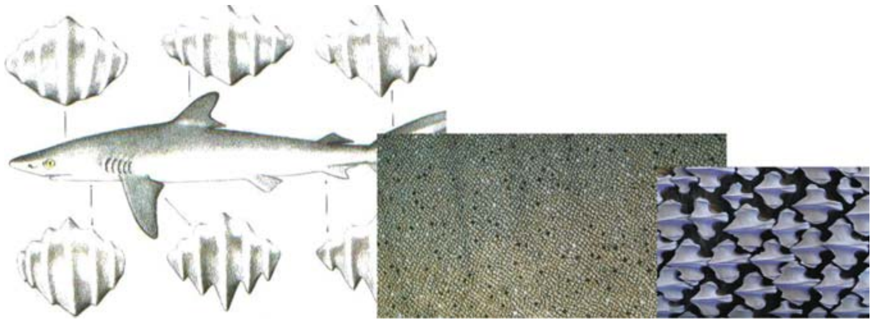

Fig. 2 Our model of flow around sharks describes only a small part of the real situation (Fig. from [5, 13]). This figure shows a duplex zooming into the skin of a shark

influence of the viscosity on the flow. In this region the velocity profile shows values from 0 (no-slip boundary condition) to U_∞ (the frictionless external velocity). This deceleration of the fluid is the cause of the drag which seems to be a pure boundary layer phenomena. Dependent on the flow situation the boundary layer can be laminar or turbulent. In the case of fast swimming sharks we have a turbulent boundary layer. A turbulent boundary layer can not be described analytically. Following the boundary layer theory of Schlichting (see [15]) we observe following structure (see Fig. 3): the viscous sublayer is a thin layer of fluid (thickness: $0 < y^+ \leq 5$, where y^+ is the dimensionless characteristic wall coordinate) which is slowed down near the wall through friction forces. Here we have a linear velocity profile. The buffer layer is the region near the wall (thickness $5 < y^+ \leq 25$) where the friction can be neglected. There the velocity profile is unknown because the flow is turbulent. The last sublayer is called logarithmic layer because of the logarithmic velocity profile, it is the frictionless layer far away from the wall (thickness $25 < y^+$). From Schlichting we know that as long as the riblets stay within the viscous sublayer of the turbulent flow, they do not induce additional drag and are considered as a hydraulic smooth surface. Let δ be the thickness of the viscous sublayer and h be the height of the microstructures: if $h < 0.6\delta$ then the riblets do not influence the thickness of the viscous boundary layer for Re $\approx 10^6$ (for higher Re they must be slightly smaller). If we zoom into the flow around a swimming shark until we see only the viscous sublayer we are able to formulate a suitable model. The flow equations are the incompressible stationary Navier-Stokes equations with a Couette profile prescribed through the no-slip boundary condition on the rough skin and a velocity U on the upper boundary. The Reynolds number here is very small (Re ≈ 1). The turbulent character of our original model enters only through the boundary condition $U = (U_1, U_2, 0)$ which indicates that we have a mean flow velocity U_1 and a cross flow velocity U_2 which is induced by the vortices in the turbulent flow above the modeled area.

The so-called canonical cell of roughness is denoted by $Z = (0, b_1) \times (0, b_2) \times (0, b_3)$ which is plotted in Fig. 5. The rough boundary is denoted by $\gamma(y_1, y_2)$, where $y_1, y_2 \in (0, b_1) \times (0, b_2)$ are the macroscopic variables. The fluid part of this cell is denoted by $Y = \{y \in Z |\ b_3 > y_3 > \max\{0, \gamma(y_1, y_2)\}\}$. Then the bottom of

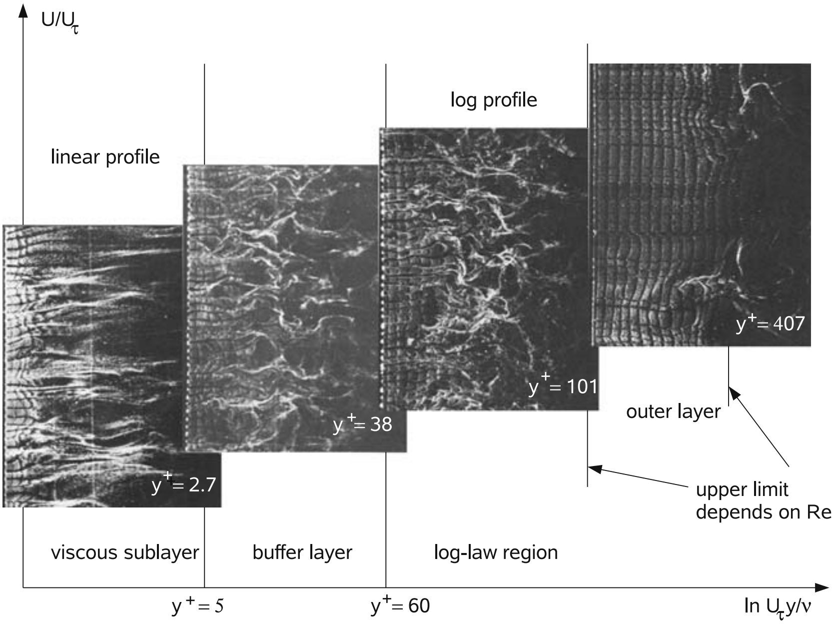

Fig. 3 In this figure we see the structure of a turbulent boundary layer. In each sublayer the velocity has a different profile. Here, photographs from [18] are inserted in the corresponding layers to get a better impression of the flow behavior

our three-dimensional channel consists of the layer of roughness given through the periodical repetition of one basic cell of roughness scaled with our scaling parameter ε to obtain the microscopical description. Mathematically the layer of roughness is $\mathcal{R}^\varepsilon = (\cup\varepsilon(Y + (k_1, k_2, -b_3))) \cap ((0, L_1) \times (0, L_2) \times (-\varepsilon b_3, 0))$. We recall the connection between the macroscopic and microscopic variables: $y_i = \frac{x_i}{\varepsilon}$, with $i = 1, 2, 3$. The rough boundary $\mathcal{B}^\varepsilon = \varepsilon(\cup\gamma + (k_1, k_2, -b_3))$ consists of a large number of periodically distributed humps of characteristic length ε but variable height εh with $h \in [0, 1]$. The region above the layer of roughness is the cuboid $P = (0, L_1) \times (0, L_2) \times (0, L_3)$, and the interface which separates this region from the layer of roughness is denoted by $\Sigma = (0, L_1) \times (0, L_2) \times (0)$. Thus the region where the fluid flows is $\Omega^\varepsilon = P \cup \Sigma \cup \mathcal{R}^\varepsilon$ (see Fig. 4). With Σ_2 we denote the upper interface $(0, L_1) \times (0, L_2) \times \{L_3\}$, where the velocity is prescribed.

The steady state incompressible Navier-Stokes equation for the three-dimensional viscous sublayer reads as follows:

$$\begin{cases} -\nu\Delta v^\varepsilon + v^\varepsilon \cdot \nabla v^\varepsilon + \nabla p^\varepsilon = 0, & \text{in } \Omega^\varepsilon \\ \operatorname{div} v^\varepsilon = 0, & \text{in } \Omega^\varepsilon \\ v^\varepsilon = 0, & \text{on } \mathcal{B}^\varepsilon \\ v^\varepsilon = U, & \text{on } \Sigma_2 \\ \{v^\varepsilon, p^\varepsilon\} - (x_1, x_2) \text{ periodic.} \end{cases} \tag{1}$$

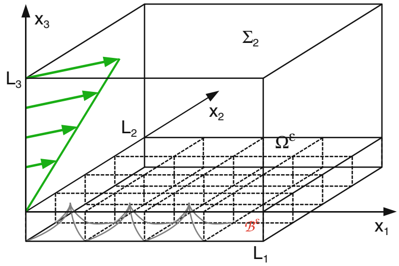

Fig. 4 The three-dimensional viscous sublayer

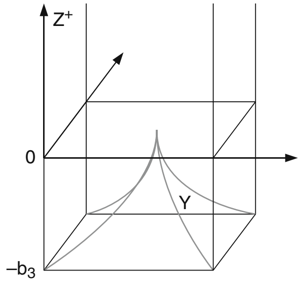

Fig. 5 The three-dimensional canonical cell of roughness

Due to the rough boundary the system (1) is difficult to solve. Jäger and Mikelić proved in [11] that if $|U|\delta < 2\nu$, there exists a unique solution $\{u^\varepsilon, p^\varepsilon\} \in H^2(\Omega^\varepsilon) \times H^1(\Omega^\varepsilon)$.

Further in this paper we are interested in the numerical solution of (1) and especially on the numerical evaluation of the drag force in order to analyze the effect of different roughness to it. The drag which is the force that resists the movement of a solid object through a fluid is made up of friction forces, which act in the direction parallel to the surface, plus pressure forces, which act in the direction perpendicular to the surface. In our case the surface of the object is the oscillating boundary $\mathcal{B}^\varepsilon$ with normal n. In the three-dimensional case the drag force on the rough boundary is a two-dimensional vector:

Definition 1 The longitudinal drag component of our shark skin model is defined by

$$\begin{aligned}(\mathcal{F}_{\mathrm{t}}^\varepsilon)_1 &= \frac{1}{L_1 L_2}\int_{\mathcal{B}^\varepsilon} \nu\sigma n e_1 dx_1 dx_2 \\ &= \frac{\nu}{L_1 L_2}\int_{\mathcal{B}^\varepsilon} \Big(2\frac{\partial v_1^\varepsilon}{\partial x_1} - p\Big)n_1 + \Big(\frac{\partial v_1^\varepsilon}{\partial x_2} + \frac{\partial v_2^\varepsilon}{\partial x_1}\Big)n_2 + \Big(\frac{\partial v_1^\varepsilon}{\partial x_3} + \frac{\partial v_3^\varepsilon}{\partial x_1}\Big)n_3\end{aligned} \tag{2}$$

and the cross drag component by

$$
\begin{aligned}
\left(\mathcal{F}_{\mathrm{t}}^{\varepsilon}\right)_2 &= \frac{1}{L_1 L_2} \int_{\mathcal{B}^\varepsilon} \nu \sigma n e_2 dx_1 dx_2 \\
&= \frac{\nu}{L_1 L_2} \int_{\mathcal{B}^\varepsilon} \Big(\frac{\partial v_2^\varepsilon}{\partial x_1} + \frac{\partial v_1^\varepsilon}{\partial x_2}\Big) n_1 + \Big(2\frac{\partial v_2^\varepsilon}{\partial x_2} - p\Big) n_2 + \Big(\frac{\partial v_2^\varepsilon}{\partial x_3} + \frac{\partial v_3^\varepsilon}{\partial x_2}\Big) n_3 .
\end{aligned} \tag{3}
$$

We will calculate the two components of the drag where the drag in the longitudinal flow direction is of main interest (denoted by drag - x_1 in the tables). The values were obtained after a transformation of the boundary integral into a domain integral to obtain a more accurate evaluation.

3 Direct Simulations

Numerical simulations for (1) are very difficult especially for the three-dimensional flow problem with very small microstructures. To capture the microstructures with a sufficient accuracy, we need a very fine mesh which requires a huge amount of data.

The direct simulations of the oscillating incompressible steady state Navier-Stokes equation (1) were performed using one of the powerful codes developed by the numerical group of R. Rannacher called GASCOIGNE. Here error control, adaptive mesh refinement and a fast solution algorithm based on multigrid methods are combined (see [2] and [4]). A stabilized Finite Element formulation is used with a local projection stabilization (LPS). For details on this local projection stabilization method see [3]. Since we are interested in the evaluation of functionals directly on the rough surface we have to use isoparametric finite elements to achieve a higher order boundary approximation. More details about the direct simulations of flow over a shark skin one can find in [8].

Under some assumptions like the periodicity of the microstructures and their smallness we can reduce the calculation costs by using homogenization. In [6] and [7] we showed how the oscillating drag force given in (2) and (3) can be approximated by the so-called effective drag force using a homogenization process. In this process the rough surface will be replaced by an artificial smooth surface situated above the microtructures on which the effect of these enter through a different boundary condition (the Navier slip condition). The solution of (1) is than constructed analytically as a correction of the Couette flow with the no-slip boundary condition on this smooth surface. The correction terms include the solution of an auxiliary boundary layer problem. In [11] convergence results are proved for this asymptotic expansion of the velocity, for the mass-flow and for the drag force. The computation costs for the effective drag are drastically smaller: the unknown (Navier matrix) is obtained by solving the boundary layer equation, i.e. a Stokes type system on the cell of roughness Y (see Fig. 5) and another fluid cell above it instead of the complete Navier Stokes system on the whole rough channel (see Fig. 4).

Table 1 The amount of drag reduction of rough surfaces

	Drag - x_1	Drag - x_2	Skin friction - x_1	Skin friction - x_2
$\mathcal{F}_{\text{t}}^{\text{smooth}}$	1.1765	1.1765	1.1765	1.1765
$\mathcal{F}_{\mathcal{B}^\varepsilon}^{\varepsilon}$ n-o. rib.	1.122 (4.6%)	1.146 (2.5%)	1.122 (4.6%)	0.37 (69%)
$\mathcal{F}_{\mathcal{B}^\varepsilon}^{\varepsilon}$ o. rib.	1.111 (5.5%)	1.142 (2.9%)	0.764 (35%)	–0.023 (102%)
$\mathcal{F}_{\mathcal{B}^\varepsilon}^{\varepsilon}$ thorns	1.086 (7.7%)	1.086 (7.7%)	0.7 (40%)	0.7 (40%)

We made firstly direct calculations on a channel of size $1.2 \times 1.2 \times 1$ with two different shapes of microstructures: riblets and a thorn like structure which was observed on the skin of slow swimming sharks. The results for the drag are listed in Table 1.

We expected a higher contribution to drag reduction in the case of riblets. Instead of that we obtained 7.7% drag reduction for the thorn like structure. In [9] we analyzed different models with different channel lengths, different in- and outflow conditions and different evaluation positions of the drag to get comparable values. For that we could use information from the homogenized model concerning the correct in-and outflow conditions: We used the effective Couette flow. The conclusion of this comparison was to choose a longer channel for our model of shark skin and evaluate the drag on a smaller domain from inside to avoid the disturbances from the in- and outflow. The evaluation of the drag on the domain $[2.4..3] \times [2.4..3]$ inside a channel of size $3.6 \times 3.6 \times 1$ gave us different values (see Table 2) but the drag for the thorn-like structure is again lower than the drag for riblets.

For better understanding of the differences between the two structures we compared the amount of in- and outflow (see Table 3). Because we have a diagonal inflow we have two inflow and two outflow faces. We also considered two different models, one model with free overflow and no-slip condition on the rough surface and the other one with prescribed Dirichlet boundary conditions. A detailed description of the models are in [9].

We observe that in the case of riblets we have a total in- and outflow of 1.055 for the model with free overflow and a total in- and outflow of 1.08 for our model with prescribed in-and outflow, i.e. 2.5% higher. In the case of the thorn-like microstructure we have a total in- and outflow of 1.114 for the model with free overflow and a total in- and outflow of 1.08 for our model with prescribed in-and outflow, i.e. 3% less. These calculations explain the different results in the amount of drag reduction of the two models (see Sect. 5).

Another point of interest in our work was to evaluate the vorticity and the stabilization terms for the two models (see Table 4). The L_2-norm of the vorticity, $||\nabla \times u^\varepsilon||^2$, is for all models in the same range, only slightly higher for the

Table 2 The drag and its components compared on the two geometries

	Drag - x_1	Fric - x_1	Press. - x_2	Drag - x_2	Fric - x_2	Press. - x_2
Thorns	0.361	0.224	0.132	0.361	0.224	0.132
Riblets	0.419	0.411	0	0.471	0.123	0.327

Table 3 The amount of in- and outflow compared on the two geometries

		In-flow		Out-flow	
		Left	Front	Right	Back
Riblets	Free overflow & no-slip	−0.52	−0.535	0.52	0.535
Riblets	D.b.c.	−0.54	−0.5398	0.533	0.547
Thorns	Free overflow & no-slip	−0.553	−0.553	0.553	0.553
Thorns	D.b.c.	−0.54	−0.54	0.54	0.54

Table 4 The amount of vorticity and of the stabilization term

		Norm of vorticity	Vorticity range	Stabilization
Riblets	Free overflow & no-slip	8.82502	0..26	0.000550819
Riblets	D.b.c.	10.3983	0..26	0.00182755
Thorns	Free overflow & no-slip	8.54718	0..130	0.000651022
Thorns	D.b.c.	8.28226	0..119	0.000579329

riblet-model with Dirichlet boundary conditions. But if we look at the vorticity in each gridpoint, we see a higher difference (see Fig. 6). Due to the small Reynolds number the vorticity is nearly zero in the greatest part of the channel. It is not zero only near the rough surface. Directly on the top of the microstructures we find the highest value. In case of the riblets the top value is 26 whereas for the thorn-like structure it can reaches 130 but only in a singular point so that it has not a great effect to the total value.

The values in the last column of Table 4 comes from the following stabilization term: $\int_{\Omega^\varepsilon} \alpha_K |\nabla(p_h - i_{2h} p_h)|^2$, where i_{2h} denotes the interpolation on the grid with double grid size and $\alpha_K = 0.5 * h_K^2$ in our case of very viscous flow. The stabilization term is small and if we look at its distribution in the rough channel (see Fig. 7) we see two clearly defined positions, where this term acts: in front and after the highest point of the microstructures.

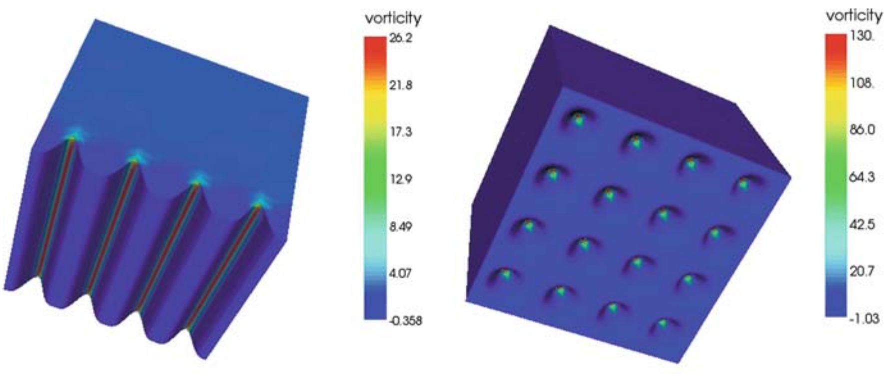

Fig. 6 The vorticity is zero far away from the microstructures. The high values are concentrated directly on the tip of the microstructures

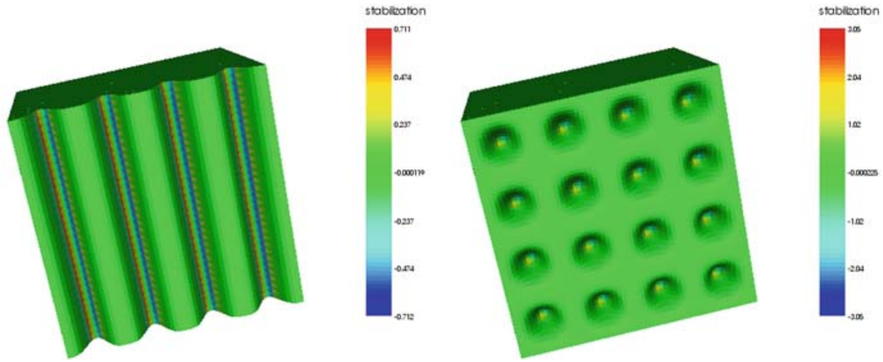

Fig. 7 The stabilization term used for the direct simulations is very small almost everywhere. The extreme values are concentrated directly in front and back of the tip of the microstructures, there where the pressure has higher values

4 Scientific Visualization of our Flow Data

Virtual flow visualization is largely influenced by traditional experimental techniques of visualization, like smoke or dye injection, as well as by the existing data types, typically vector fields. Because there exists no natural visual representation of three-dimensional vector fields we have to use simplified representations which we can understand more easily. In this section we will give a short description of the techniques we used with the software COVISE.

COVISE is a visualization system developed at the High Performance Computing Center Stuttgart (HLRS), advanced and distributed by VISENSO. Originally designed for applications of fluid mechanics, it has been extended by many other application areas. Via an amount of various modules a work flow for the data to pass can be built. Those modules are precast programs, so that the intrinsic programming work can be avoided by linking the needed modules together. COVISE gives a fully scalable and rotatable model of the input data. There is also the possibility to develop some new modules to extend the range of the program or to fit it to own circumstances respectively.

4.1 The Visualization Pipeline

Generally scientific visualizations pass some specified work steps, known as visualization pipeline: read/compute → filter → map → render → display.

Our work steps can be collocated in this pipeline like this:

To read the data generated by GASCOIGNE we needed a Visualization Toolkit (vtk) data reading module. Such a module had been developed by M. Winckler and D. Neumayer in 2001, but it did not match neither our data nor our current HLRS-COVISE. So we had to match this module to our conditions.

To get just some specific data from our source file, we had to filter it. COVISE offers some different filter modules, we used them e. g. for cutting of parts of a geometry to see inside, extracting a cutting plane or for computing an outer surface of a grid.

For mapping we can choose between a large number of visualization methods where everyone has its assets and drawbacks. We used arrow plot which is one of the oldest visualization techniques. It is a so-called direct visualization technique used for immediate investigation of the flow data. Here arrows are drawn in each sample point in the field oriented according to the flow with length proportional to the flow velocity (see Fig. 10 and 9). Often there is a problem that the arrows will overlap in a two dimensional view, so that it is difficult to gain further insights. At this point the advantage of COVISE is to display the model not only on a conventional monitor, but with a stereo projection installation. So it is possible to study the model with a realistic depth effect and additionally the plane with the arrows can be moved within the stream. The module `CuttingSurface` (see also Fig. 10) describes a technique where a plane is extracted from the data, often colored e. g. by velocity or pressure values. A very common technique for flow visualization is a geometric technique based on integral objects such as streamlines which can be obtained with the module `Tracer` (see Fig. 11, 12, 13). This visualization is based on making streams visible in a wind tunnel by injecting smoke. Streamlines result from integration of flow vectors over a longer time. They are a natural extension of the arrow plot-based technique and for the user it is easier to understand that flow evolves along integral objects. The velocity of the stream is displayed at the respective location by the coloration of the streamlines. Problems could appear in finding an adequate starting point for the integration so that no essential effects are missed (see Fig. 12 and 14). A more dynamic visualization can be obtained with the module `Tracer` with the moving points option. Here single particles are rendered among the stream as animated points, or, for better cognition, spheres. It is also important to chose an adequate start position, otherwise some areas of the volume might not be reached by particles. To avoid this, we had chosen more then only one starting plane (see Fig. 15). With the filter module `DomainSurface` the sharkskin could be illustrated (see Fig. 11). It computes the outer surface of the grid. To obtain a smooth surface, we used the additional module `GenNormals` before rendering, which creates normals for the surface (see Fig. 16).

The last component of the visualization pipeline is rendering and displaying. If the computing is extensive it might be necessary to separate them: the rendering can be distributed to different processors having the display only on one screen. But that was not requested in our case. Besides the monitor display COVISE also supports the output through a stereo projection installation with tracking of the line of sight and interactive operations (with a 3d pointer), so that a full three dimensional impression of the model can be provided. For more details on visualization techniques for flow data see e.g. [12] and [14], for more informations about COVISE see [19] or visit the web page [20].

4.2 A Small Album on the Visualization of Flow over Shark Skin

In this section we present some figures which visualize the flow over shark skin. The techniques described in the former subsection help to understand how the microstructures act.

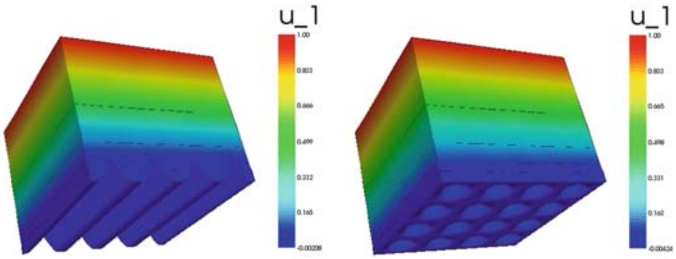

Fig. 8 Here we see a simple visualization of the computed data obtained by plotting the values of the first component of the velocity using VisuSimple. In generally it is sufficient for the first evaluation of the computations. But we get no informations for the flow insight and can not compare the two models

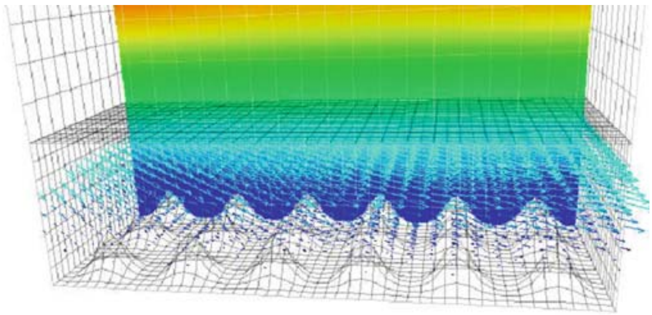

Fig. 9 In this figure the three-dimensional velocity is represented by a vectorfield using VisuSimple. The evaluation of the data is quiet difficult if we want to see the differences of the flow over the two different shapes of microstructures

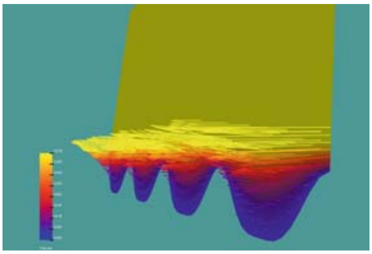

Fig. 10 Here we used the module `VectorField` on a cut surface to avoid overlapping of the arrows. One can see the linear profile of the Couette flow contouring the arrows

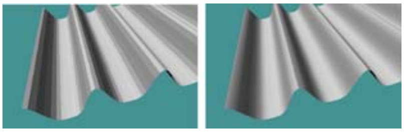

Fig. 11 This figure presents a part of our modeled shark skin visualized using the module `DomainSurface`. The smoother surface was obtained by using the additional module `GenNormals`

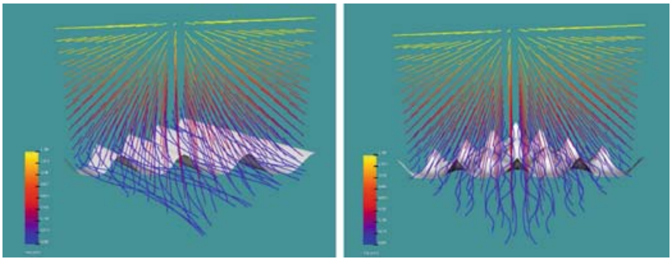

Fig. 12 This figure gives us the main insights of the flow of our computation model. We see the shark skin visualized using `DomainSurface` and `GenNormals` and the complete flow by streamlines. We get a realistic impression of how the microstructures effect the flow and we can clearly see the differences

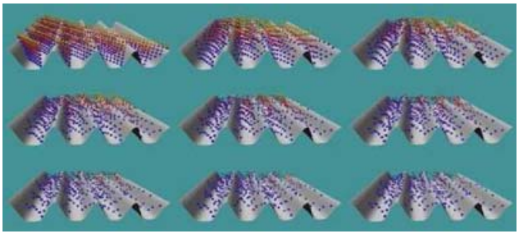

Fig. 13 This figure shows a series of snapshots from our movie which represents the flow over shark skin visualized by moving spheres traced from five parallel planes. If it is displayed on the stereo projection installation a realistic three-dimensional impression of the flow model is provided

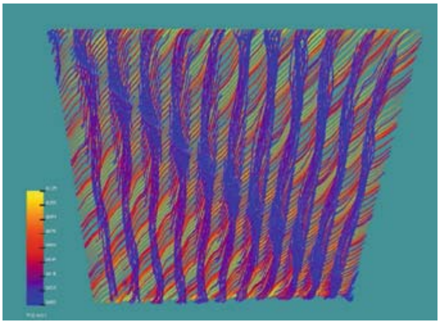

Fig. 14 In this figure we filtered the velocity data and visualized them only in the part of interest, i.e. around the microstructures, using streamlines traced forward and backwards from a diagonal plane parallel to the in-flow situated in the middle of the geometry

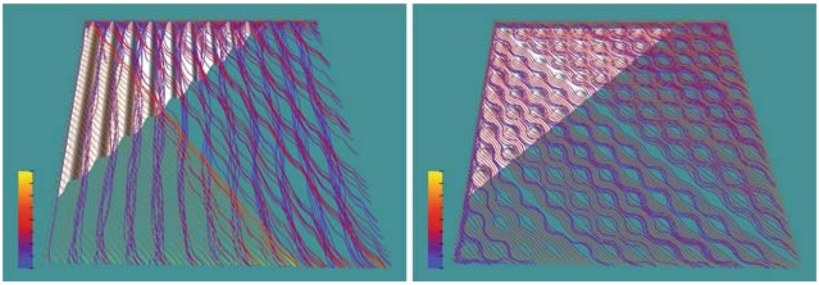

Fig. 15 Here the streamlines were traced from the two in-flow planes (front and back), so that we can see only where the incoming particles are distributed

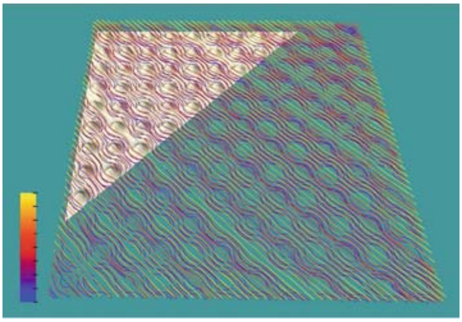

Fig. 16 This figure stays in direct comparison with Fig. 14, i.e. we used the same visualization tools in order to explain the drag reduction mechanism of shark skin

5 Drag Reduction Mechanism of Shark Skin

Our direct calculations in three dimensions showed a drag reduction of rough surfaces up to 15% compared with a smooth surface situated on the top of the microstructures and up to 10% compared with a smooth surface situated at the origin of the effective flow. This position can be calculated using homogenization. In experiments it is estimated by engineers. If we want to compare the results from our calculations with results from experiments (e.g. Deutsches Zentrum für Luft und Raumfahrt (DLR), see [10, 17]) then we should compare the drag of the rough surfaces with the drag of a smooth surface situated at this position. From [6], where we solved a shape optimization problem in order to find the optimal microstructure which minimizes the drag, we know how to change the riblets to get a higher contribution to drag reduction: they must be very sharp and their height must be twice their spacing. Considering only riblets, we can explain the drag reducing mechanism after applying homogenization as follows: The effective drag which we explained in Sect. 3 depends only on the Navier Matrix. Due to the simple geometry (constant in one direction) this matrix is diagonal and its components can be calculated from the boundary layer equations which are of Stokes type. This three dimensional flow equations can be decomposed in two two-dimensional systems: the longitudinal and the cross flow. In both cases the velocity profile of the flow is linear, two Couette flows with different origins. The riblets work like fences: they impede the cross flow and redirect it into the longitudinal direction (see Fig. 12). This effect is characterized mathematically through the fact that the origin of the cross flow lies always higher than the one of the longitudinal flow. Physically it means that the grade of turbulence of the flow above the viscous sublayer is dampened. Through this redirecting very slow rotating spirals are formed in the riblet valleys (see Fig. 12). Because we modeled only the viscous sublayer which has a small viscosity it is possible that we obtained a smaller contribution to drag reduction for the riblets than for the thorn-like structure. In Fig. 15 we can observe that the particles above the riblets flow away with the stream with higher velocity (colored by yellow and red) whereas the particles in the riblet valleys rotate slowly inside (colored by blue) while new particles come and slip over them. This means that riblets work also as an anti-friction coating (lubricant): Are the riblet valleys once filled up with water the flow slips more easily over the shark skin.

In the case of thorn-like microstructures (see Fig. 13) there are no slow rotating spirals formed and there is no redirecting of the flow (see Fig. 11). Therefore the flow channels between the structures and is a little bit faster than the flow over riblets.

The different amount of drag reduction from the different models can also be explained by analyzing the amount of in- and outflow (see Sect. 3). In our first model with free overflow and no-slip boundary condition on the rough surface (see Fig. 11) we had a discrepancy between the amount of inflow in the cross flow direction (see Table 1): In case of the riblets the geometry started with a hill so that we had a smaller inflow than in the case of the thorn-like structure. By choosing the effective Couette flow as Dirichlet boundary conditions for the in- and outflow we obtained an improved model witch shows the same amount of inflow for both structures. In the case of thorns we have no redirecting of the flow, we have the same amount of in- and outflow whereas in the case of riblets the outflow of the cross flow is slightly reduced and the outflow of the longitudinal flow slightly increased.

We conclude that in our case where we modeled only the viscous sublayer of the turbulent flow over a rough shark skin a thorn-like structure showed higher contribution to drag reduction than riblets. We will enlarge our model in future and will see if riblets will be as good as they are in nature on the skin of fast swimming sharks.

Acknowledgments R. Ranacher for bringing together modeling and analysis with numerical calculations, P. Penel who recommended us at this conference to look at the vorticity, M. Ridinger who came out with the idea to visualize the shark skin in our virtual reality and his time consuming effort to keep it running, S. Krömker for the graphical support and E. Michel for discussions.

References

1. D.W. Bechert, M. Bruse, and W. Hage, Experiments with three-dimensional riblets as an idealized model of shark skin, Experiments in Fluids **28**, 403–412 (2000)
2. R. Becker, and R. Rannacher, A feed-back approach to error control in finite element methods: Basic analysis and examples, East-West J. Numer. Math **4**(4),237–264 (1996)

3. R. Becker, and M. Braack, A finite element pressure gradient stabilization for the Stokes equation based on Local Projections, Calcolo **38**(4), 173–199 (2001)
4. R. Becker, and R. Rannacher, An optimal control approach to a posteriori error estimation in finite element methods, Acta Numerica 2001 (2001)
5. K.G. Blüchel, and F. Malik, *Faszination Bionik. Die Intelligenz der Schöpfung*, Mcb Verlag (2006)
6. E. Friedmann, Riblets in the viscous sublayer. Optimal Shape Design of Microstructures, PhD thesis, Ruprecht - Karls - University Heidelberg (2005)
7. E. Friedmann, The optimal shape of riblets in the viscous sublayer, J. Math. Fluid Mech., Birkhäuser Basel, 2008. DOI 10.1007/s00021-008-0284-Z
8. E. Friedmann, and Th. Richter, Optimal microstructures. Drag reducing mechanism of riblets, J. Math. Fluid Mech., submitted (2007)
9. E. Friedmann, and Th. Richter, The effect of different in- and outflow conditions modeled on a microscopic flow problem on the macroscopic drag force, Nonlinear Anal.: Real World Applications, Multiscale Problems in Science and Technology: Challenges to Mathematical Analysis and Perspectives, submitted (2008)
10. W. Hage, *Zur Widerstandsverminderung von dreidimensionalen Riblet-Strukturen und anderen Oberflächen*, Mensch & Buch, Verlag (2005)
11. W. Jäger, and A. Mikelić, Couette flows over a rough boundary and drag reduction, Comm. Math. Phys. **232**, 429–455 (2003)
12. F.H. Post, T. van Walsum, W.C. de Leeuw, A.J.S. Hin, Visualization Techniques for Vector Fields with Applications to Flow Data, CWI Quarterly **7**(2), 131–146 (1994)
13. A. Mojetta, *Haie - Biografie eines Räubers*, Jahr Verlag GmbH & Co (1997)
14. F.H. Post, B. Vrolijk, H. Hauser, R.S. Laramee and H. Doleisch, Feature Extraction and Visualization of Flow Fields, Eurographics 2002 State-of-the-Art Reports (2002)
15. H. Schlichting, and K. Gersten, *Boundary-Layer Theory*, 8th revised and enlarged edition, Springer-Verlag, Berlin (2000)
16. K. Sch. Steuben and G. Krefft, *Die Haie der Sieben Meere*, Verlag Paul Parey (1995)
17. P. Thiede, *Aerodynamic Drag Reduction Technologies* Proceedings of the CEAS/DragNet European Drag Reduction Conference, 19–21 June 2000, Potsdam, Germany
18. M. Van Dyke, *An Album of Fluid Motion*, Parabolic Pr. (1988)
19. A. Wierse, R. Lang, U. Lang, H. Nebel, D. Rantzau, The Performance of a Distributed Visualization System, Visualization Methods in High Performance Computing and flow Visualization (1996)
20. http://www.HLRS.de Cited 29th April 2008

Stability of Poiseuille Flow in a Porous Medium

Antony A. Hill and Brian Straughan

Abstract We study the linear instability and nonlinear stability of Poiseuille flow in a porous medium of Brinkman type. The equivalent of the Orr-Sommerfeld eigenvalue problem is solved numerically. Difficulties with obtaining the spectrum of the porous Orr-Sommerfeld equation are discussed. The nonlinear energy stability eigenvalue problems are solved for x, z and y, z disturbances.

Keywords Poiseuille flow · Porous media · Orr-Sommerfeld equation · Nonlinear stability

1 Introduction

The classical hydrodynamic problem of stability of Poiseuille flow in a channel is a major one in fluid dynamics, see e.g. Joseph [7], Chap. 3, Straughan [10], Chap. 8. As these texts point out there are major problems in trying to develop a meaningful nonlinear energy stability theory for such flows since the nonlinear energy stability threshold is inevitably far away from the linear instability one. Additionally, the eigenvalue problems associated with this class of flows are numerically very difficult, see e.g. Dongarra et al. [2], Yecko [13]. Nevertheless, this area continues to attract much attention in the fluid dynamics literature. In particular, we draw attention to the nonlinear energy stability work of Kaiser and Mulone [8], the analyses of time - dependent and time - periodic Poiseuille flows by Galdi and Robertson [4], Galdi et al. [3], the work on the problem with slip boundary conditions by Webber and Straughan [12], the problem of Poiseuille flow of a fluid overlying a porous medium, see Chang et al. [1], Hill and Straughan [6], and the Poiseuille problem for flow in a channel with one fluid overlying another, see Yecko [13]. These papers contain many other pertinent references.

The focus of attention here is on the problem of Poiseuille flow in a channel which is filled with a porous medium saturated with a linear viscous fluid. Due to

B. Straughan (✉)
Department of Mathematical Sciences, Durham University, Durham, DH1 3LE, UK
e-mail: brian.straughan@durham.ac.uk

R. Rannacher, A. Sequeira (eds.), *Advances in Mathematical Fluid Mechanics*,
DOI 10.1007/978-3-642-04068-9_17,

the invention of man-made materials such as metallic foams which have a porosity close to one, and are of much use in the heat transfer industry, the porous – Poiseuille problem is of practical interest. To the best of our knowledge, this problem was first addressed by Nield [9] who developed a linearised instability analysis. Straughan [11], Sect. 5.8.1 shows that the analysis of Nield [9] is incomplete in that he omits a term from one equation. We here present a numerical solution of the corrected system of equations. However, we stress that the fundamental model is due to Nield [9].

2 Linear Instability

The basic equations are given in Nield [9], again in Straughan [11], Sect. 5.8.1, and for completeness and readability we include them here. We suppose the saturated porous medium is one of Brinkman type and occupies the spatial domain $\{(x, y) \in \mathbb{R}^2\} \times \{z \in (-L/2, L/2)\}$. The basic equations are

$$\begin{aligned} \varrho\Big(\frac{\partial v_i}{\partial t} + v_j \frac{\partial v_i}{\partial x_j}\Big) &= -\frac{\partial p}{\partial x_i} + \mu \Delta v_i - \frac{\varphi\mu}{K} v_i, \\ \frac{\partial v_i}{\partial x_i} &= 0. \end{aligned} \tag{1}$$

In these equations (v_i, p) denote the velocity field and pressure, ϱ is the density, μ is the equivalent viscosity (for a Brinkman model), φ is the porosity, and K is the permeability.

With the scalings of L, V and L/V for length, velocity, and time, Eqs. (1) may be rewritten in non-dimensional form as

$$\begin{aligned} \mathrm{R}\Big(\frac{\partial v_i}{\partial t} + v_j \frac{\partial v_i}{\partial x_j}\Big) &= -\frac{\partial p}{\partial x_i} + \Delta v_i - M^2 v_i, \\ \frac{\partial v_i}{\partial x_i} &= 0, \end{aligned} \tag{2}$$

where R is the Reynolds number and M^2 is a non-dimensional (porous) quantity, given by

$$\mathrm{R} = \frac{\varrho V L}{\mu}, \qquad M^2 = \frac{\varphi L^2}{K}.$$

The spatial domain is now $\{(x, y) \in \mathbb{R}^2\} \times \{z \in (-1, 1)\}$.

With no-slip boundary conditions

$$v_i = 0, \qquad z = \pm 1,$$

and the flow driven by a constant pressure gradient in the $x-$direction, $G = -\partial p/\partial x > 0$, the basic solution whose stability we are interested in is, cf. Nield [9], Straughan [11], Sect. 5.8.1,

$$\mathbf{U} = (U(z), 0, 0),$$
$$U = \frac{G}{M^2}\left(1 - \frac{\cosh Mz}{\cosh M}\right).$$

The non-dimensional perturbation equations are then

$$\begin{aligned} &\mathrm{R}(u_{i,t} + u_j U_{i,j} + U_j u_{i,j} + u_j u_{i,j}) = -\pi_{,i} + \Delta u_i - M^2 u_i, \\ &u_{i,i} = 0. \end{aligned} \tag{3}$$

where (u_i, π) is the velocity, pressure perturbation. If we linearize and use Squire's theorem to reduce to a two-dimensional spatial perturbation we may show, see Straughan [11], Eqs. (5.117), that the $(u, w, \pi) \equiv (u_1, u_3, \pi)$ perturbations satisfy the system of equations

$$\begin{aligned} &[\mathcal{L} - ia\mathrm{R}(U - c)]u = \mathrm{R}U'w + ia\pi, \\ &[\mathcal{L} - ia\mathrm{R}(U - c)]w = D\pi, \\ &iau + Dw = 0, \end{aligned} \tag{4}$$

where $D = d/dz$, $\mathcal{L} = D^2 - a^2 - M^2$, and a and c are a wavenumber and growth rate which arise from a representation $u = u(z)\exp[ia(x - ct)]$ with similar forms for w and π. Straughan [11], Sect. 5.8.1, notes that equation $(4)_2$ differs from that of Nield [9] in that he has $D^2 - a^2$ instead of $\mathcal{L}$. By eliminating u and π one then derives the analogue of the Orr-Sommerfeld equation for the Brinkman porous theory. This is, cf. Straughan [11], Eq. (5.119),

$$\mathcal{D}^2 w - M^2 \mathcal{D} w = ia\mathrm{R}(U - c)\mathcal{D} w - ia\mathrm{R}U'' w, \tag{5}$$

where $\mathcal{D} = D^2 - a^2$, $z \in (-1, 1)$, and the boundary conditions are

$$w = Dw = 0, \qquad z = \pm 1. \tag{6}$$

3 Numerical Results

We have solved (5), (6) by using a D^2-Chebyshev tau method, cf. Dongarra et al. [2]. The neutral curves for $M = 0$ to 10 are given in Fig. 1 below.

Actually, there is very little variation with the critical Reynolds numbers observed by Nield [9], as is shown in Table 1.

The spectrum of (5), (6) behaves very like that of the Orr-Sommerfeld problem for classical Poiseuille flow. For example, for higher Reynolds numbers we witnessed mode crossing of eigenvalues. For example, for $M = 0, 0.5, 1.0$, the first and second eigenvalues interchange places for R between 80822 and 80828, 86852 and 86854, and 106618 and 106620, respectively, with the previous first eigenvalue moving down the list as R increases. This behaviour is very similar to that observed

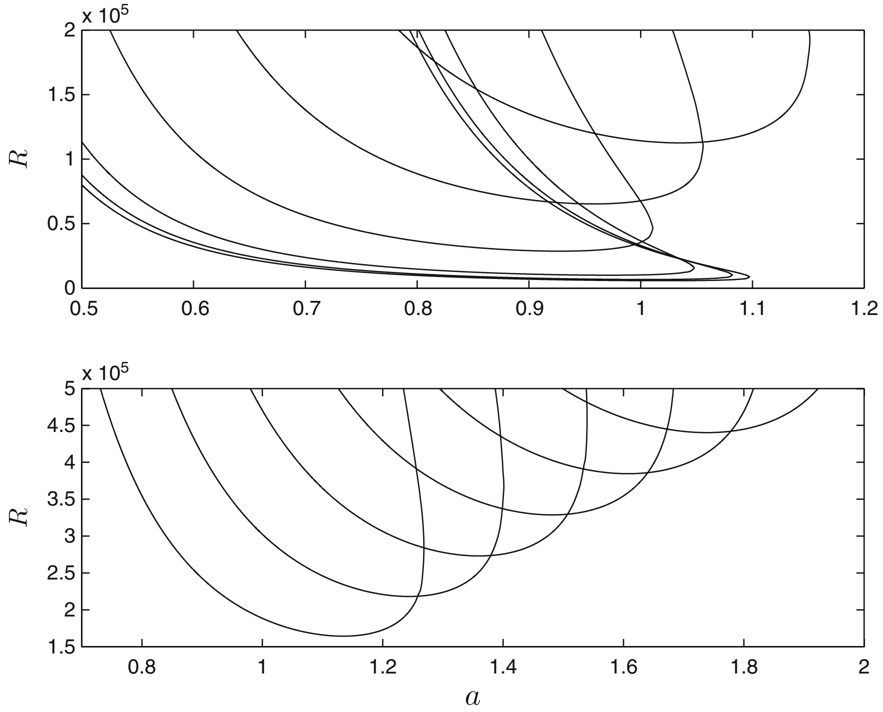

Fig. 1 Critical Reynolds number R against wavenumber a. The thresholds in the *upper* graph correspond to $M = 0$–4 from bottom to top, and in the *lower* graph for $M = 5$–10

Table 1 Comparison between the critical Reynolds numbers (minimised over the wavenumber) of Nield [9] and this paper for a selection of M values

M	R_{crit} (Nield [9])	R_{crit}
0	5772	5772
0.5	6706	6710
1	10016	10033
2	28604	28663
5	164090	164298
10	439818	440223

by Dongarra et al. [2]. Additionally the spectrum is very sensitive and care must be taken with the number of polynomials used in the numerical approximation, and in the arithmetical precision used in the calculation (those presented here are all in 64 bit arithmetic). Figure 2 show the spectrum for $R = 3 \times 10^4$, $M = 1$.

The split in the "tail", evident in Fig. 2 (i) (ii), is removed by increasing the number of polynomials but the inexactness at the branch of the "Y" increases, cf. Fig. 2 (iii) (iv). Again, this is analogous to what is observed by Dongarra et al. [2], and by Yecko [13].

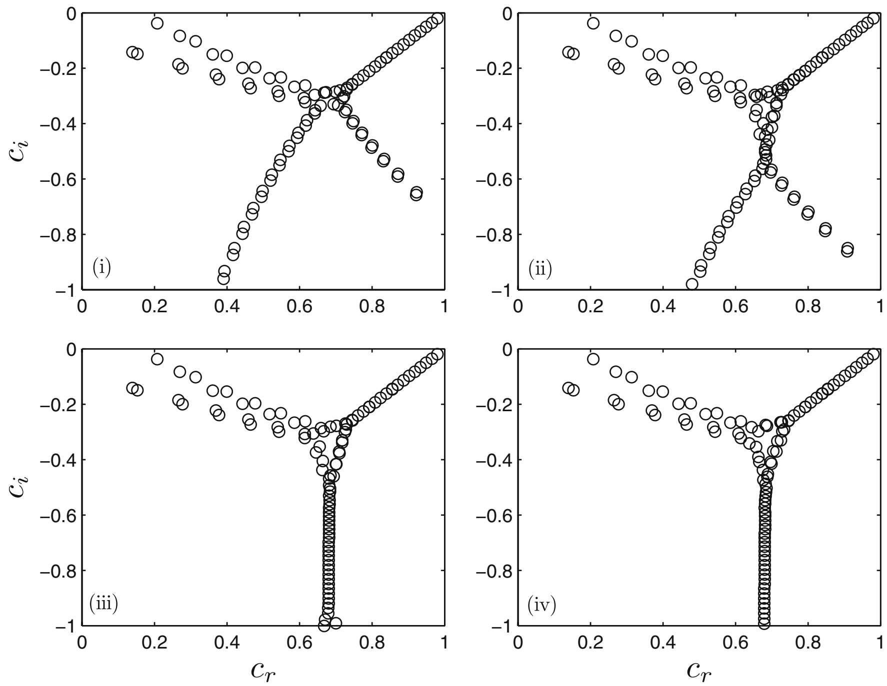

Fig. 2 Spectra of growth rate $c = c_r + ic_i$, with $R = 3 \times 10^4$ and $M = 1$. The number of polynomials used in the numerical approximation correspond to (i) 150, (ii) 170, (iii) 200, (iv) 400

4 Nonlinear Energy Stability Theory

We briefly discuss the employment of the energy method on the full system of Eq. (3). Since the linear operator is far from symmetric we do not expect the linear instability results to necessarily be close to the nonlinear stability ones. If the linear operator is symmetric they are the same, Galdi and Straughan [5]. For the classical Poiseuille problem they are far apart, cf. Joseph [7], Straughan [10], Chap. 8.

To investigate energy theory for the porous Poiseuille problem, multiply $(3)_1$ by u_i and integrate over a period cell for the disturbance. With $\|\cdot\|$ denoting the L^2 norm on the period cell V we find

$$\frac{R}{2}\frac{d}{dt}\|\mathbf{u}\|^2 = -R\int_V U'wu\,dV - \|\nabla\mathbf{u}\|^2 - M^2\|\mathbf{u}\|^2.$$

One may then use variational energy theory to derive a nonlinear global stability threshold, R_E, cf. Galdi and Straughan [5]. The Euler-Lagrange equations which arise are not in a form such that Squire's theorem may be applied. Thus, we here investigate the cases of (x, z) and (y, z) dependent solutions (this has been done in the non-porous case, cf. Joseph [7], Kaiser and Mulone [8], Webber and Straughan [12]).

For a perturbation u, w dependent on x, z the equivalent energy Orr-Sommerfeld equation may be shown to be

$$\mathcal{D}\mathcal{L}w + iaR(U'Dw + \frac{1}{2}U''w) = 0, \tag{7}$$

where $z \in (-1, 1)$ and w satisfies the boundary conditions

$$w = Dw = 0 \qquad \text{at} \quad z = \pm 1. \tag{8}$$

For the case of y, z dependent solutions the Euler-Lagrange equations reduce to

$$\begin{aligned} &2\mathcal{L}\mathcal{D}w + RU'a^2u = 0, \\ &2\mathcal{L}u - RU'w = 0, \end{aligned} \tag{9}$$

$z \in (-1, 1)$, with

$$u = 0, \quad w = Dw = 0 \qquad \text{at} \quad z = \pm 1. \tag{10}$$

Here a is again a wavenumber, but now $u = u(z)e^{iay}$, $w = w(z)e^{iay}$ in the derivation of (9).

Numerical results for the critical value of R_E in the nonlinear energy stability theory are presented in Fig. 3.

Again, as in the non-porous case, we find there is a large gap between the linear instability and nonlinear stability boundaries. This does raise the issue as to whether strong nonlinear subcritical instabilities exist.

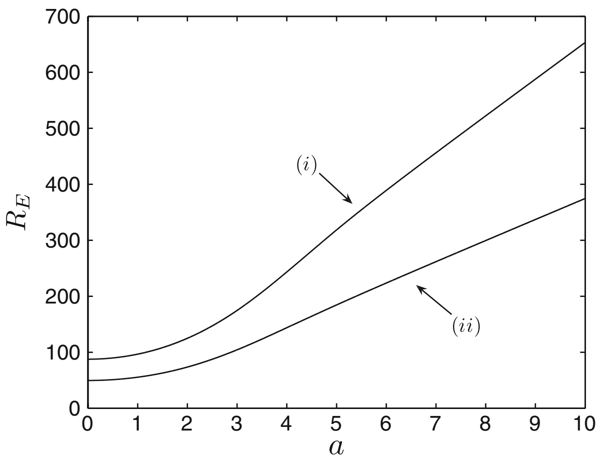

Fig. 3 Critical Reynolds number R_E against wavenumber a. Thresholds (i) and (ii) refer to the (x, z) and (y, z) dependent solutions respectively

Acknowledgments This work was supported by a Research Project Grant of the Leverhulme Trust - Grant Number F/00128/AK.

References

1. Chang, M.H., Chen, F., Straughan, B.: Instability of Poiseuille flow in a fluid overlying a porous layer. J. Fluid Mech. **564**, 287–303 (2006)
2. Dongarra, J.J., Straughan, B., Walker, D.W.: Chebyshev tau – QZ algorithm methods for calculating spectra of hydrodynamic stability problems. Appl. Numer. Math. **22**, 399–435 (1996)
3. Galdi, G.P., Pileckas, K., Silvestre, A.L.: On the unsteady Poiseuille flow in a pipe. ZAMP **58**, 994–1007 (2007)
4. Galdi, G.P., Robertson, A.M.: The relation between flow rate and axial pressure gradient for time-periodic Poiseuille flow in a pipe. J. Math. Fluid Mech. **7**, S211–S223 (2005)
5. Galdi, G.P., Straughan, B.: Exchange of stabilities, symmetry and nonlinear stability. Arch. Rational Mech. Anal. **89**, 211–228 (1985)
6. Hill, A.A., Straughan, B.: Poiseuille flow of a fluid overlying a porous layer. J. Fluid Mech. **603**, 137–149 (2008)
7. Joseph, D.D.: *Stability of Fluid Motions I.* Springer, New York (1976)
8. Kaiser, R., Mulone, G.: A note on nonlinear stability of plane parallel shear flows. J. Math. Anal. Appl. **302**, 543–556 (2005)
9. Nield, D.A.: The stability of flow in a channel or duct occupied by a porous medium. Int. J. Heat Mass Transfer **46**, 4351–4354 (2003)
10. Straughan, B.: Explosive Instabilities in Mechanics. Springer, Heidelberg (1998)
11. Straughan, B.: Stability and wave motion in porous media. Appl. Math. Sci. Ser. 165, Springer, New York (2008).
12. Webber, M., Straughan, B.: Stability of pressure driven flow in a microchannel. Rend. Circolo Matem. Palermo **78**, 343–357 (2006)
13. Yecko, P.: Disturbance growth in two-fluid channel flow. The role of capillarity. Int. J. Multiphase Flow **34**, 272–282 (2008)

Towards a Geometrical Multiscale Approach to Non-Newtonian Blood Flow Simulations

João Janela, Alexandra Moura, and Adélia Sequeira

Abstract In this paper we address some problems that arise when modelling the human cardiovascular system. On one hand, blood is a complex fluid and in many situations Newtonian models may not be capable of capturing important aspects of blood rheology, for example its shear-thinning viscosity, viscoelasticity or yield stress. On the other hand, the geometric complexity of the cardiovascular system does not permit the use of full three-dimensional (3D) models in large regions. We deal with these problems by using a relatively simple non-Newtonian model capturing the shear-thinning behaviour of blood in a confined region of interest, and coupling it with a zero dimensional (0D) model (also called lumped parameters model) accounting for the remaining circulatory system. More specifically, the 0D system emulates the global circulation, providing proper boundary conditions to the 3D model.

Keywords Blood rheology · Geometrical multiscale approach · Lumped parameters models · Numerical coupling strategies

1 Introduction

Over the past few years the mathematical modelling and numerical simulation of the cardiovascular system has gained great importance in the study of cardiovascular diseases, helping to understand the blood flow dynamics in specific patients without using invasive techniques. The research activity in this field has been very active, and mainly driven by the research needs in biology and medicine. Ultimately, the objective is to help medical decisions in the prevention and treatment of cardiovascular pathologies. However, there are still many problems to resolve. Indeed, the enormous complexity and variability of the human circulatory system make its modelling and simulation a very difficult and challenging task.

A. Sequeira (✉)
Department of Mathematics and CEMAT/IST, 1049-001 Lisboa, Portugal
e-mail: adelia.sequeira@math.ist.utl.pt

R. Rannacher, A. Sequeira (eds.), *Advances in Mathematical Fluid Mechanics*,
DOI 10.1007/978-3-642-04068-9_18,

Precisely, blood is a multi-component mixture with complex rheological characteristics. It consists of multiple particles such as red blood cells - RBCs, white blood cells - WBCs and platelets, suspended in an aqueous polymer solution, the plasma (Newtonian fluid). Because of its composition, blood exhibits non-Newtonian properties, such as shear-thinning viscosity, thixotropy and viscoelasticity [13, 12]. For this reason, the Navier-Stokes equations are not always appropriate to simulate blood flow, and non-Newtonian fluid models should be used. Indeed, even in large vessels, blood viscosity can vary up to two orders of magnitude, thus considering a constant viscosity can be a too rough approximation and simplification, specially in some disease situations or in parts of the venous system. Another difficulty is that the cardiovascular system is extremely heterogeneous, both geometrically, and in what concerns the physical and mechanical characteristics, being at the same time highly integrated. In order to deal with this heterogeneity a whole hierarchy of models for the simulation of blood flow in the vascular system has been developed, giving rise to the so-called *geometrical multiscale modelling* of the cardiovascular system [9, 3]. It consists in coupling different models operating at different space scales involving local and systemic dynamics. To that scope, apart from the 3D detailed model, composed by the 3D equations for incompressible non-Newtonian fluids, reduced 1D and 0D models are considered. These reduced models are obtained from the 3D detailed one, by making simplifying assumptions and averaging procedures [3]. Namely, 0D models, also called lumped parameters models, describe the variation in time of the mean pressure and flow rate. They are able to represent large compartments of the cardiovascular system, having at the same time a very low computational cost. This approach provides a way of accounting for the entire cardiovascular system, by resorting to reduced models, while using 3D detailed models on selected parts of interest.

Very little can be found in the literature regarding the coupling of reduced blood flow models with 3D non-Newtonian ones. In fact, the geometrical multiscale approach has not yet been applied to the study of the non-Newtonian behaviour of blood. In this work we provide a first step in that direction. We consider the coupling between a 3D incompressible generalized Newtonian model with a 0D model, representing the systemic circulation. We perform the coupling, demonstrating that it can be extended to the non-Newtonian case.

In Sect. 2 we describe the models, providing the 3D generalized Newtonian equations for incompressible fluids, the description of the lumped parameters model, and the coupling strategy between them both. In Sect. 3 we introduce the numerical methods to solve both models and their coupling. We also supply a technique to obtain semi-analytical solutions of the generalized Newtonian 3D problem, in order to guarantee the accuracy of the fluid solver. In Sect. 4 we present the numerical results, and Sect. 5 is devoted to the conclusions.

2 The Mathematical Models

The mathematical model describing local blood flow in 3D regions of the cardiovascular system consists of the 3D equations of fluid dynamics for incompressible fluids (see for instance [10, 12]). The application of such model and its

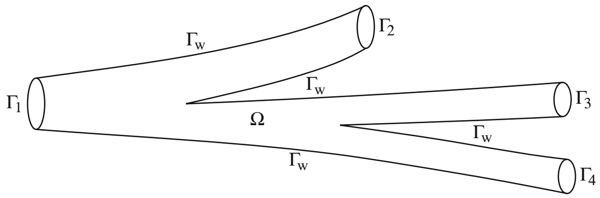

Fig. 1 Generic vascular region Ω

numerical resolution requires a bounded domain. Also, the geometrical complexity of the human circulatory system makes it unfeasible to discretize large geometrical domains. The truncation of the 3D regions into specific regions of interest generates *artificial sections* that do not correspond to any physical interface (see Fig. 1).

Consider a bounded domain $\Omega \subset \mathbb{R}^3$, representing a portion of an arterial vessel. We denote by Γ_w the part of the boundary corresponding to the physical artery wall. In this work we assume that the vessel is rigid, thus Γ_w does not change in time. We denote by Γ_i, $i = 1, \dots, n$, the *artificial boundaries* (Fig. 1).

The equations of fluid dynamics, consisting in the equations of the conservation of the momentum and mass, read as follows

$$\begin{cases} \varrho \left(\dfrac{\partial \mathbf{u}}{\partial t} + \mathbf{u} \cdot \nabla \mathbf{u} \right) - \operatorname{div} \boldsymbol{\sigma}(\mathbf{u}, P) = 0, & \text{in } \Omega \\ \operatorname{div} \mathbf{u} = 0, & \text{in } \Omega. \end{cases} \tag{1}$$

Here the unknowns are the velocity $\mathbf{u}$ and the pressure P; ϱ is the blood density, which is considered constant and equal to $1g/\mathrm{cm}^3$, and $\boldsymbol{\sigma}(\mathbf{u}, P)$ is the Cauchy stress tensor. To close system (1) a constitutive law, relating the Cauchy stress tensor with the kinematic quantities, velocity and pressure, must be provided. The constitutive law characterizes the rheology of the fluid at study. Very often in literature [10, 8, 14], blood is considered as a Newtonian fluid: $\boldsymbol{\sigma}(\mathbf{u}, P) = -P\mathbf{I} + 2\mu\mathbf{D}(\mathbf{u})$, where μ is the blood dynamical viscosity and $\mathbf{D}$ is the strain rate tensor, given by

$$\mathbf{D}(\mathbf{u}) = \frac{1}{2}\left(\nabla \mathbf{u} + \nabla \mathbf{u}^T\right).$$

However, as referred, the complex rheological behaviour of blood is difficult to describe and is still a subject of active research (see for instance [13, 12] as recent review papers on mathematical models of blood rheology). One of the consensual non-Newtonian properties exhibited by blood is the shear-thinning viscosity. Precisely, blood viscosity depends on the shear rate $\dot{\gamma}$:

$$\dot{\gamma} = \sqrt{\frac{1}{2}\left(\nabla \mathbf{u} + \nabla \mathbf{u}^T\right) : \left(\nabla \mathbf{u} + \nabla \mathbf{u}^T\right)}.$$

In particular, the shear-thinning behaviour is characterized by the decreasing of the apparent viscosity, while the shear rate increases.

The *generalized Newtonian* fluid models account for this dependence of viscosity on shear rate:

$$\boldsymbol{\sigma}(\mathbf{u}, P) = -P\mathbf{I} + 2\mu(\dot{\gamma})\mathbf{D}(\mathbf{u}). \tag{2}$$

They represent a wide class of fluid models which can be shear-thinning or shear-thickening. For instance, for the classical Power-Law model the viscosity is given by $\mu(\dot{\gamma}) = k\dot{\gamma}^{n-1}$, where $n \in \mathbb{R}$ is the so called power-law index. In this model the flow is shear-thinning if $n < 1$ and shear-thickening if $n > 1$. Another generalized Newtonian model is the Carreau-Yasuda, where the viscosity is given by

$$\mu(\dot{\gamma}) = \mu_\infty + (\mu_0 - \mu_\infty) \times (1 + (\lambda\dot{\gamma})^a)^{\frac{n-1}{a}},$$

with $\mu_0 > \mu_\infty > 0, \lambda > 0$, and $n, a \in \mathbb{R}$. In the particular case of $a = 2$ we obtain the so-called Carreau model. The coefficient μ_∞ corresponds to the viscosity at higher shear rates, that is for the highest pressure drop, and μ_0 is the viscosity for the lower shear rates, which corresponds to the lowest pressure drop. Notice that if $\lambda = 0$ or $n = 1$, the viscosity is constant and we have the Newtonian case, with a constant viscosity equal to μ_0.

The fluid equations (1) must be endowed with initial and boundary conditions. We consider the initial condition $\mathbf{u} = \mathbf{u}_0$, for $t = 0$ in Ω. Regarding the boundary conditions on the physical wall Γ_w, we impose the no-slip condition which, for a viscous flow in a fixed domain, is given by the Dirichlet boundary condition $\mathbf{u} = \mathbf{0}$ in Γ_w, for $t \in I$, with $I = (0, T]$ the time interval where we solve the Eqs. (1) and (2).

The prescription of boundary conditions on artificial sections is a much more complex task. While on physical interfaces the boundary conditions are imposed through physical arguments, like the no-slip condition, this is not the case in artificial sections. Moreover, standard Neumann or Dirichlet boundary conditions are rather unphysical. In fact, in order to have reliable simulations, the boundary conditions on these sections need to take into account the remaining parts of the cardiovascular system (see for instance [8] for an illustrative example where the prescription of physiological boundary conditions on the artificial sections is critical). This is not the case if Neumann or Dirichlet boundary conditions are used. We solve this difficulty by resorting to the *geometrical multiscale approach* [9, 3].

2.1 The Geometrical Multiscale Approach

The geometrical multiscale approach has been introduced to address the complexity and heterogeneity of the human cardiovascular system [3, 9]. It consists in using models of different dimensions, 3D, 1D and 0D, with different levels of complexity, accuracy, and computational cost, and to put them together by means of suitable coupling strategies [9].

The reduced 1D and 0D models can be derived from the 3D fluid-structure interaction model, of which the fluid equations were introduced in the previous section, by making simplifying assumptions and averaging procedures [3]. Although they represent simplified descriptions of blood flow, they are able to describe the presence of the remaining parts of the cardiovascular system, providing appropriate boundary conditions when coupled to the 3D fluid equations (1) at the artificial boundaries. In this work we consider the coupling of the fluid equations with a 0D, also called lumped parameters model.

2.1.1 The Lumped Parameters Model

Lumped parameters models can be derived from the 3D model, starting by integrating over the cross section after considering simplifying hypotheses, and by further integrating in space (see for instance [3]). They are expressed in terms of a system of ODEs, and describe the variation in time of the averaged pressure and flow rate in specific compartments of the cardiovascular system, such as the heart, the venous bed, or the pulmonary circulation. Since they do not account for variations in space, they are also called 0D models.

In general, a lumped parameters model describing blood flow in a cylindrical vessel can be written as (see [3, 11])

$$\begin{cases} C\dfrac{dP}{dt} + Q_{\text{out}} - Q_{\text{in}} = 0, \\ L\dfrac{dQ}{dt} + RQ + P_{\text{out}} - P_{\text{in}} = 0, \end{cases}$$

where the state variables are the flow rate Q and the mean pressure P. The coefficients R, L and C correspond to the lumped parameters which summarize the geometrical and physical features of the 3D model:

$$R = \frac{\varrho \mu l}{\pi R_0^4}, \qquad L = \frac{\varrho l}{A_0}, \qquad C = \frac{3 l A_0 R_0}{2Eh}, \tag{3}$$

being ϱ the fluid density, l the vessel length, μ the viscosity, A_0 the section area at rest, R_0 the section radius at rest, E the vessel wall Young modulus, and h the vessel wall thickness. The values Q_{in}, Q_{out}, P_{in} and P_{out} are obtained from the values of the velocity and pressure at the upstream (in) and downstream (out) sections of the initial 3D cylinder. Two of these values are derived from the boundary conditions of the 3D fluid equations which originated the 0D model: from a Dirichlet condition we obtain the value of the flow rate, while a Neumann condition provides the pressure value. The two remaining values are set equal to the state variables, which is a reasonable approximation since a single cylindrical vessel is sufficiently small.

We remark the analogy between the lumped parameters model and the electric networks, where the flow rate can be thought as the electric current and the mean pressure as the voltage. In this context the lumped parameters are the resistance R, related with blood viscosity, the inductance L, related with blood inertia, and the capacitance C, related with the wall compliance.

Joining together the lumped description of single vessels, we are able to build complex systems. We can also include terms such as diodes, to describe the presence of valves. By combining all these components, we are lead to an ODEs system of the type [3, 8]

$$\begin{cases} \dfrac{d\mathbf{y}(t)}{dt} = \mathbf{A}(t)\mathbf{y}(t) + \mathbf{r}(t), \quad t > 0, \\ \\ \mathbf{y}(0) = \mathbf{y}_0, \end{cases} \tag{4}$$

where $\mathbf{y}$ is the vector of the state variables, which are the flow rate and the mean pressure at the different compartments. $\mathbf{A}$ is the matrix of parameters (possibly depending on time), $\mathbf{r}(t)$ accounts for the forcing term (for instance, the heart action) and some components like the diodes, and $\mathbf{y}_0$ is the initial data.

2.1.2 Coupling the 3D and the 0D Model

To couple the 3D fluid equations (1) and (2) and the 0D model (4) we impose, at the coupling interfaces, the continuity of the mean pressure and of the flow rate. This coupling is accomplished by means of boundary conditions on the 3D model and forcing conditions on the 0D one.

In an iterative frame to the solution of the coupled problem, the 3D model provides pointwise information on the velocity and pressure, which are integrated to obtain the averaged data to be given to the 0D model as a forcing term. In turn, the 0D model provides average data to be prescribed as boundary conditions at the artificial sections of the 3D model (see [2, 11]).

In this work we perform the coupling based on the prescription of pressure at all artificial boundaries of the 3D model, while the 0D model receives the 3D flow rate as input. Let us notice that in this case we have mean pressure boundary conditions for the 3D fluid equations. These are defective boundary conditions for Eq. (1), since they require pointwise boundary conditions. This is one of the difficulties of using the geometrical multiscale approach [3, 9], which is due to the different mathematical nature of the models to be coupled.

The defective boundary conditions are not sufficient to the well posedness of the 3D problem, since in that case there is no uniqueness of the solution, and require a special treatment. In [4] a variational formulation has been proposed for this problem where, if the boundary interface Γ_i is a plane section perpendicular to a cylindrical pipe, imposing the mean pressure P_i is equivalent to prescribe the following condition

$$-\boldsymbol{\sigma}(\mathbf{u}, P) \cdot \mathbf{n} = P_i, \quad \text{on } \Gamma_i, \forall t \in I, \tag{5}$$

where $\mathbf{n}$ is the unit normal vector to Γ_i. We will follow this approach to carry out the coupling strategy. Although in real vascular geometries we do not have artificial sections exactly perpendicular to a cylindrical pipe, this technique has proved to be a good approximation for blood flow simulations [2, 9, 8].

3 The Numerical Methods

In order to perform the numerical simulations on the 3D problem, we start by discretizing in space the equations of motion, using the finite element method. This method requires that the differential problem (1) and (2) is written in a weak form. First, we rewrite the fluid equations (1) and (2) in the following form:

$$\begin{cases} \dfrac{\partial \mathbf{u}}{\partial t} + \mathbf{u} \cdot \nabla \mathbf{u} + \nabla p - \dfrac{1}{\varrho} \operatorname{div} \boldsymbol{\tau} = \mathbf{0}, & \text{in } \Omega \\ \operatorname{div} \mathbf{u} = 0, & \text{in } \Omega, \end{cases} \tag{6}$$

where $p = \dfrac{P}{\varrho}$ and $\boldsymbol{\tau} = \boldsymbol{\tau}(\mathbf{u})$ is the extra stress tensor $\boldsymbol{\tau} = 2\mu(\dot{\gamma})\mathbf{D}(\mathbf{u})$.

Let us define the Hilbert spaces $V = \boldsymbol{H}_0^1(\Omega)$ and $Q = L^2(\Omega)$. The weak form of the equations of motion is obtained by multiplying Eqs. (6) by suitable test functions and integrating by parts. Namely, the weak formulation of Eqs. (6) is given by

$$\int_\Omega \left(\frac{\partial \mathbf{u}}{\partial t} + \mathbf{u} \cdot \nabla \mathbf{u} \right) \cdot \mathbf{v} + \frac{1}{\varrho} \int_\Omega \boldsymbol{\tau} : \nabla \mathbf{v} - \int_\Omega p \operatorname{div} \mathbf{v} = \int_\Omega \boldsymbol{f} \cdot \mathbf{v} + \int_\Gamma (\boldsymbol{\sigma} \cdot \boldsymbol{n}) \cdot \mathbf{v}, \forall \mathbf{v} \in V$$

$$\int_\Omega q \operatorname{div} \mathbf{v} = 0, \qquad \forall q \in Q.$$

The finite element method corresponds to substitute the functional spaces V and Q by suitable sequences of finite dimensional subspaces $\{V_h | h > 0\}$ and $\{Q_h | h > 0\}$ in which we can compute an approximate solution $(\mathbf{u}_h, p_h)$. A proper choice of these subspaces ensures that the problem is solvable in the finite dimensional spaces and the approximate solutions converge to the solution of (7) when $h \to 0$. More precisely, we have used a space discretization of problem (7) that corresponds to use $\mathbf{P}_1 - \mathbf{P}_1$ finite elements with interior penalty (IP) stabilization [1] for the approximation of $\mathbf{u}$ and p.

The discretization in time is performed with a standard backward Euler method, and the convective term is linearized in a semi-implicit way, by considering that at time step t^{k+1} we have $\mathbf{u}^{k+1} \cdot \nabla \mathbf{u}^{k+1} \approx \mathbf{u}^k \cdot \nabla \mathbf{u}^{k+1}$. Finally, in order to fully linearize the discrete problem, we use the following approximation

$$\boldsymbol{\tau}^{k+1} = \mu(\dot{\gamma}^{k+1})(\nabla \mathbf{u}^{k+1} + (\nabla \mathbf{u}^{k+1})^T) \approx \mu(\dot{\gamma}^{k})(\nabla \mathbf{u}^{k+1} + (\nabla \mathbf{u}^{k+1})^T).$$

The fully discrete problem then reads: Find $(\mathbf{u}_h, p_h) \in V_h \times Q_h$ such that

$$\int_\Omega \left(\frac{1}{\delta t}\mathbf{u}_h^{k+1} + \mathbf{u}_h^k \cdot \nabla \mathbf{u}_h^{k+1}\right) \cdot \mathbf{v}_h + \frac{1}{\varrho}\int_\Omega \mu(\dot{\gamma}^k)(\nabla \mathbf{u}_h^{k+1} + (\nabla \mathbf{u}^{k+1})) : \nabla \mathbf{v}_h$$
$$- \int_\Omega p_h^{k+1} \operatorname{div} \mathbf{v}_h = \int_\Omega \left(\boldsymbol{f} + \frac{1}{\delta t}\mathbf{u}_h^k\right) \cdot \mathbf{v}_h + \int_\Gamma (\boldsymbol{\sigma} \cdot \boldsymbol{n}) \cdot \mathbf{v}_h, \qquad \forall \mathbf{v}_h \in V_h$$

and

$$\int_\Omega q_h \operatorname{div} \mathbf{u}_h^{k+1} = 0, \qquad \forall q_h \in Q_h.$$

The computational effort necessary to perform the numerical simulation of the previous equations is of the same order of magnitude as for the Navier-Stokes equations. The extra computational load is related to the necessity, at each time step, of computing the shear rate. In the simulations we used the *LifeV* (`lifev.org`) solver, that we have adapted to support the simulation of generalized Newtonian fluids.

The 0D model system of ODEs is discretized by means of the explicit Euler method. In what concerns the 3D-0D coupling, its approximation is based on a splitting strategy, where each model is solved separately at each time step, providing the necessary data to the other one (see Fig. 2). Since the time discretization of the 0D model is explicit, the computation of the two discretized models is completely independent at each time step, with no need for subiterations [2, 11].

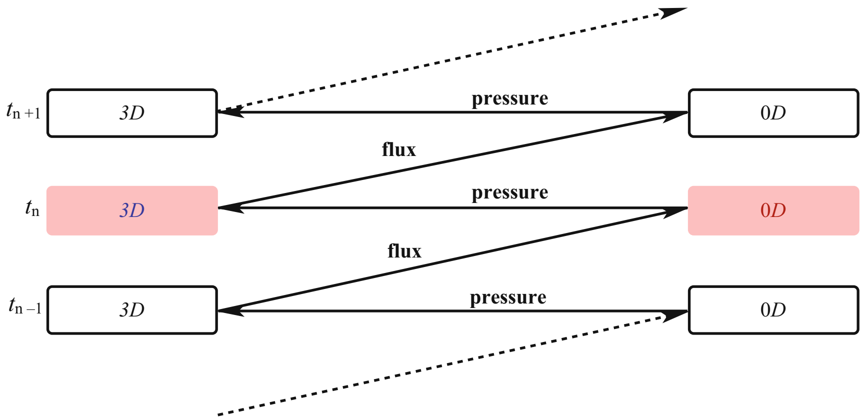

Fig. 2 Explicit coupling between the 3D and 0D models

3.1 Solution of a Reduced Problem

In the case of Newtonian fluids, for some particular geometries and flow conditions, it is possible to derive closed form analytical solutions for the velocity and pressure fields. This supplies natural benchmark solutions against which we can test our numerical solvers. However, for generalized Newtonian fluids no such solutions were available in the literature, apart from the classical technique where we fix a priori the solution and boundary conditions, and then compute the forcing term that yields that solution.

In order to fill this gap, we next present a method that can provide benchmark solutions, with arbitrary precision, to a particular viscometric flow of generalized Newtonian fluids (for details see [5, 6]). More precisely, we consider the steady fully developed flow of a generalized Newtonian fluid in an infinite cylinder of radius R, that we suppose aligned with the z axis. Rewriting the equations of motion in cylindrical coordinates (r, θ, z) and looking for solutions for the velocity field of the form $(0, 0, v_z(r))$, we recognize that the pressure gradient must be constant $\nabla p = (0, 0, G)$, the shear rate is given by $\dot{\gamma} = -\partial_r v_z$ and the only nonzero components of the extra-stress tensor are

$$\tau_{rz} = \tau_{zr} = \mu(\dot{\gamma})\partial_r v_z.$$

In addition, since we can derive the explicit formula $\tau_{rz} = Gr/2$, the velocity field can be computed as the solution of

$$\mu\left(-\partial_r v_z\right)\partial_r v_z = \frac{Gr}{2}. \tag{7}$$

Although this implicit ordinary differential equation could be directly solved to obtain a solution for the velocity profile v_z, we will take a different direction because of the difficulty in justifying the accuracy of the numerical methods. Instead, we will first solve the equation for $\varphi = -\partial_r v_z$, determining for each $r \in [0, R]$ the corresponding value of the shear rate φ_r as the solution of

$$\mu(\varphi_r)\varphi_r = \frac{|G|r}{2} \Leftrightarrow \varphi_r = \frac{|G|r}{2\mu(\varphi_r)}.$$

Defining the mapping $H : C[0, R] \to C[0, R]$ such that $H(\psi) = |G|r/\mu(\psi)$, we realize that the shear rate profile is precisely a fixed point of H. The Banach fixed point theorem gives a straightforward way of computing $\varphi(r)$.

Proposition 1 *Let* $\mu : \mathbb{R}_+ \to \mathbb{R}$ *be a continuous decreasing function for which there exist constants* μ_0, μ_∞ *such that* $0 < \mu_\infty \leq \mu_0 < +\infty$. *Let also* $H : C[0, R] \to C[0, R]$ *be the mapping defined by* $\psi \mapsto |G|r/\mu(\psi)$. *Then, if the pressure gradient is such that* $G < \mu_\infty^2/R$, *the mapping* H *has a unique fixed point* φ *that can be approximated by the fixed point iteration*

$$\begin{cases} \varphi_0 \\ \varphi_{n+1} = H(\varphi_n) \end{cases}$$

where $\varphi_0 \in C[0, R]$ *is some initial approximation and* $\varphi = \lim_{n\to\infty} \varphi_n$. *Furthermore, the function defined by*

$$v_z(r) = \int_r^R \varphi(s)\, ds \tag{8}$$

is a solution of Eq. (7).

Using this result, it is possible to compute the velocity profile with any prescribed accuracy. Since the fixed point iteration allows to compute φ at any point in $[0, R]$, the integral (8) can be computed with any accuracy using any efficient adaptive quadrature rule. Tests conducted with the truncated power-law viscosity model, for which we have an analytical closed form solution, reveal that in fact we can compute the velocity profiles, up to machine precision, in a fast way.

We next present the so-called semi-analytical solution given by (8), in the case of the fluid model we are using to describe blood flow, the Carreau model, with parameters $\mu_0 = 0.56Pas, \mu_\infty = 0.0345Pas, \lambda = 3.313s$ and $n = 0.3568$, taken from [7]. The domain is a cylinder of radius $R = 0.5cm$ and the flow is driven by a constant pressure gradient $|G| = 2$. In Fig. 3 we show a graphic of the "exact" velocity profile, together with the velocity values for selected radial distances.

Having access to the semi-analytical solution, we can also provide relevant data like the relation between the volume flow rate and pressure gradient (see Fig. 4) or the equivalent Newtonian viscosity (see Fig. 5). The later is especially useful

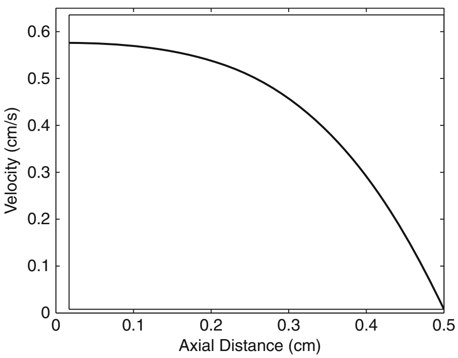

(a)

Axial Distance	Velocity
0.0	0.588092117019
0.1	0.578655021642
0.2	0.543245708447
0.3	0.456881623945
0.4	0.285320092239
0.5	0.000000000000

(b)

Fig. 3 (**a**) Exact velocity profile obtained for a Carreau fluid with parameters $\mu_0 = 0.56Pas, \mu_\infty = 0.0345Pas, \lambda = 3.313s$ and $n = 0.3568$ driven by a constant pressure gradient $|G| = 2$ in a cylinder of radius $R = 0.5$ cm. (**b**) Values of the velocity [cm/s] for several axial distances when comparing Newtonian and generalized Newtonian models. The curve shown in Fig. 5 gives, for each value of the pressure gradient, the viscosity of the Newtonian model that would yield the same volume flow rate. As expected, for low pressure gradient the equivalent Newtonian viscosity approaches μ_0, and for high pressure gradient approaches μ_∞.

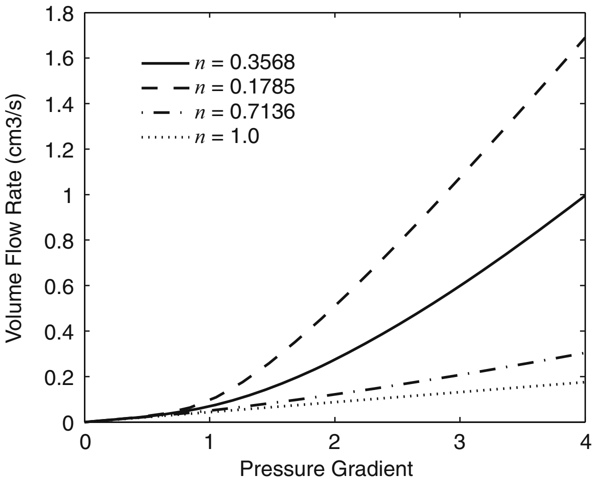

Fig. 4 Relation between pressure gradient and volume flow rate for the Carreau model with the set of parameters taken from [7] (*solid line*) and for other values of *n*

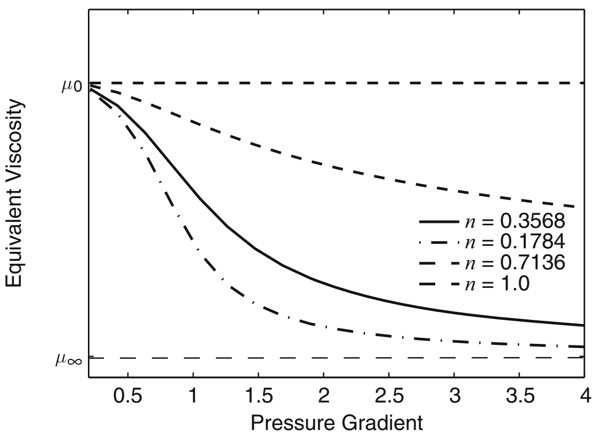

Fig. 5 Equivalent Newtonian viscosity for the Carreau model with the set of parameters taken from [7] (*solid line*) and for other values of *n*

4 Numerical Results

We consider the coupling of a straight 3D rigid wall cylinder with $5cm$ length and a radius of $0.5cm$, with a lumped parameters network. The lumped parameters model is composed by four RCL elements, as shown in Fig. 6. We impose on the 0D model a pressure source of the type $\mathbf{U}(t) = c + \cos(2\pi t)$, representing a periodic action. Notice that although not physiologic, this source term captures the characteristic periodicity of the heart beat.

The results presented here were obtained using the Carreau generalized Newtonian model on the 3D cylinder with the coefficients previously mentioned: $\mu_0 = 0.56Pas$, $\mu_\infty = 0.0345Pas$, $\lambda = 3.313s$ and $n = 0.3568$, taken from [7].

We compare the numerical results of the 3D-0D coupling with the results obtained by substituting the 3D model with its equivalent lumped parameters description (see Fig. 6). Since the 3D cylinder is rigid, its 0D equivalent is composed only by an inductance and a resistance, without any compliance. We remark that, due to the fact that we are using a generalized Newtonian model on the 3D cylinder, and recalling that the lumped parameters reflect the geometrical and physical properties of the 3D model, the 0D equivalent must take into account the variability of the viscosity, namely in the computation of the parameter R as in (3). As mentioned in Sect. 2, the 0D model is a system of ODEs, thus in this case it is relevant the variability of the viscosity in time. In the present numerical test, since we are applying a sinusoidal impulse, the mean value of the mean pressure drop along time is equal to zero. In this case, although we are using the Carreau generalized Newtonian model, it is sufficient for the equivalent 0D model to consider the viscosity equal to μ_0, corresponding to the lowest pressure drop.

In Fig. 7 are depicted the flow rate and mean pressure drop values of the difference between the 3D-0D coupling and its 0D equivalent network. We can observe that the differences between the two simulations are small, and the maximum differences are attained for the maximum absolute values of the flow rate and mean pressure drop.

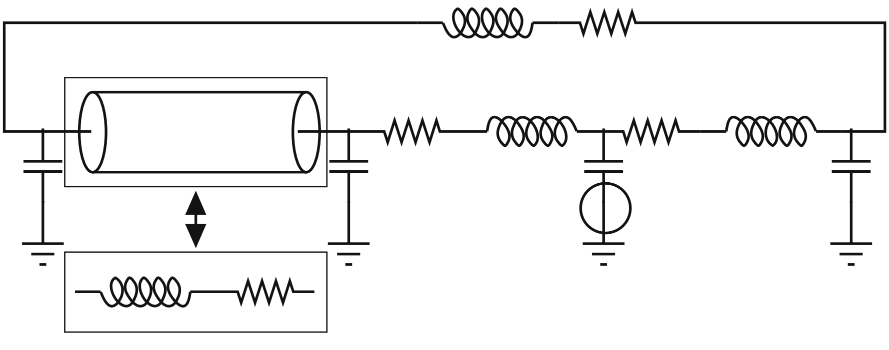

Fig. 6 Scheme of the 3D-0D coupling, with the RCL representation of the 0D network

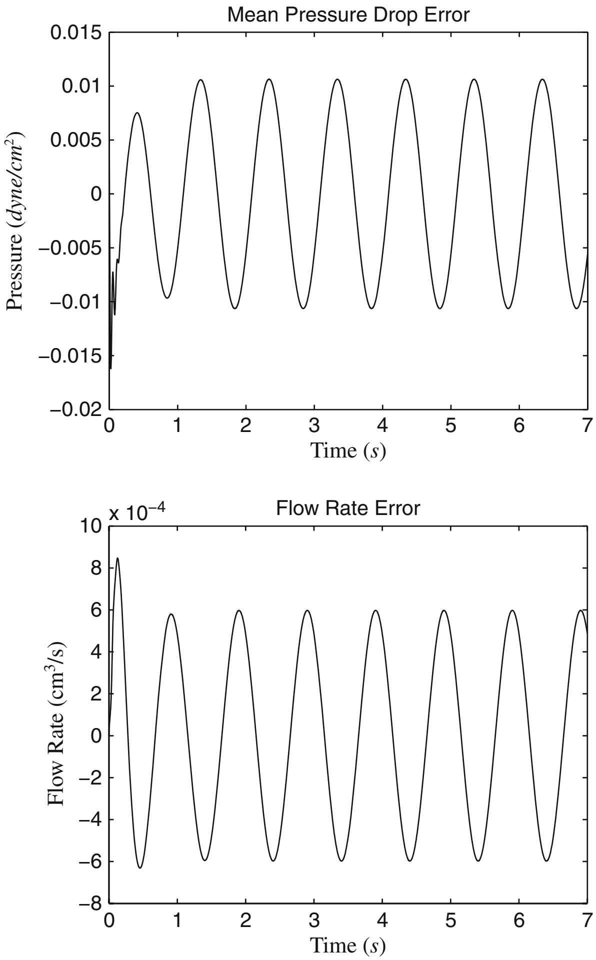

Fig. 7 Differences between the 3D-0D coupling and the equivalent 0D network values of the mean pressure drop (*top*) and the flow rate (*bottom*)

Figure 8 presents the graphics of the mean pressure drop and flow rate values for both the 3D-0D coupled and the equivalent 0D model. From these graphics we can see that the results of both simulations are very close to each other.

The absolute errors and the graphical comparison results demonstrate that the coupling strategy works very well, the 3D model capturing the impulse input of the 0D model. We can conclude that, although with very different mathematical natures, these models can be coupled in an effective way. These results demonstrate that the 0D-3D coupling can be extended to non-Newtonian flows.

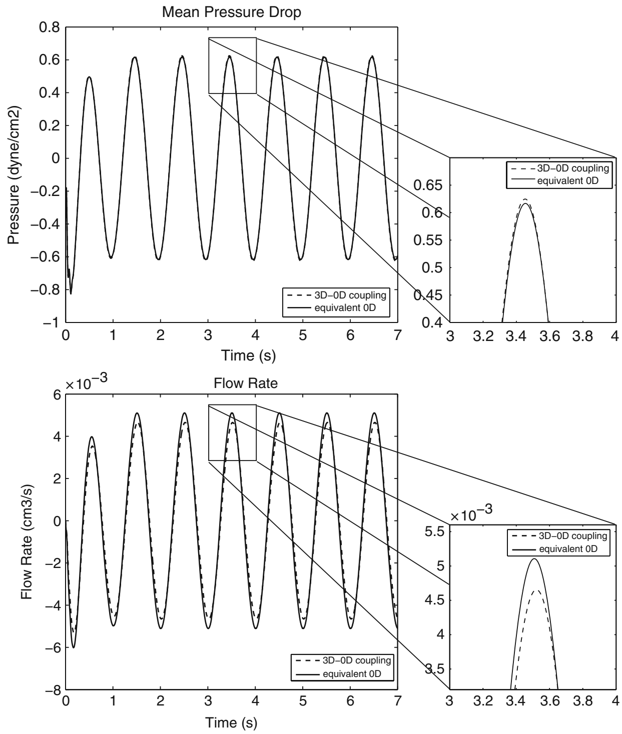

Fig. 8 Comparison between the 3D-0D coupling and the equivalent 0D network values of the mean pressure drop (*top*) and the flow rate (*bottom*), for whole time interval (*left*), and in detail (*right*)

5 Conclusions

In this work we have coupled a 3D model for blood flow, consisting of the 3D equations for incompressible generalized Newtonian fluids, with a 0D model describing blood flow in wide compartments. We have used a coupling strategy where the 0D model provides the mean pressure drop to the 3D model, which in turn gives the flow rate to the 0D network.

We have guaranteed the accuracy of the generalized Newtonian solver applied through the use of semi-analytical solutions, which are obtained by means of a reduced problem.

In order to assess the quality of the coupling, we have compared the 3D-0D coupling with its equivalent 0D network. Here we took into account into the lumped parameters model the shear-rate dependent viscosity of the non-Newtonian constitutive law. The derivation of a fully 0D model in which the viscosity, at each compartment, varies in time, is a work in progress.

From the numerical results obtained so far, we have seen that the quantitative and qualitative behaviour of the mean pressure drop and the flow rate are similar for both 3D-0D coupling and 0D models. This means that the 3D-0D coupling works very well, since the quantities were not affected by the coupling. These results also show that the 3D-0D coupling, now extended to generalized Newtonian models, might be extended to more complex non-Newtonian flows. The coupling between a physiological 0D network and a 3D realistic geometry is a work in progress.

Acknowledgments This work has been partially supported by the research center CEMAT/IST through FCT's (Portuguese Foundation for Science and Technology) funding program and by the project FCT/PTDC/MAT/68166/2006. The second author is funded by FCT through grant SFRH/BPD/34273/2006.

References

1. Burman, E., Fernández, M.: Continuous interior penalty finite element method for the time-dependent Navier-Stokes equations: space discretization and convergence. Numerische Mathematik **107**(1), 39–77 (2007)
2. Fernández, M., Moura, A., Vergara, C.: Defective boundary conditions applied to multiscale analysis of blood flow. In: E. Cancès, J.F. Gerbeau (eds.) CEMRACS 2004 – Mathematics and applications to biology and medicine, Marseille, France, July 26 – September 3, 2004, vol. 14, pp. 89–100. ESAIM: Proceedings (2005)
3. Formaggia, L., Veneziani, A.: Reduced and multiscale models for the human cardiovascular system. Lecture notes VKI Lecture Series 2003–07, Brussels (2003)
4. Heywood, J., Rannacher, R., Turek, S.: Artificial boundaries and flux and pressure conditions for the incompressible Navier-Stokes equations. Int. J. Num. Meth. Fluids **22**, 325–352 (1996)
5. Janela, J.: Mathematical and Numerical Modelling in Hemodynamics and Hemorheology. Ph.D. thesis, Instituto Superior Técnico (2008)
6. Janela, J., Sequeira, A.: High accuracy semi-analytical solutions for generalized Newtonian flows. In: Proc. of the Conf. on Topical problems in Fluid Mech., Inst. Thermomechanics, Prague (2007)
7. Kim, S., Cho, Y.I., Jeon, A.H., Hogenauer, B., Kensey, K.R.: A new method for blood viscosity measurements. J. non-Newtonian Fluid Mech. **94**, 47–56 (2000)
8. Laganà, K., Dubini, G., Migliavacca, F., Pietrabissa, R., Pennati, G., Veneziani, A., Quarteroni, A.: Multiscale modelling as a tool to prescribe realistic boundary conditions for the study of surgical procedures. Biorheology **39**, 359–364 (2002)
9. Moura, A.: The geometrical multiscale modelling of the cardiovascular system: coupling 3D and 1D models. Ph.D. thesis, Politecnico di Milano (2007)
10. Quarteroni, A., Formaggia., L.: *Handbook of Numerical Analysis*, vol. XII, chap. Mathematical modelling and numerical simulation of the cardiovascular system. Elsevier, Amsterdam (2002)
11. Quarteroni, A., Ragni, S., Veneziani, A.: Coupling between lumped and distributed models for blood flow problems. Comput. Vis. Sci. **4**, 111–124 (2001)
12. Robertson, A., Sequeira, A., Kameneva, M.: Hemorheology. In: G.P. Galdi, R. Rannacher, A. Robertson, S. Turek (eds.) *Haemodynamical Flows: Modelling Analysis and Simulation*, *Oberwolfach Seminars*, vol. 37, pp. 63–120. Birkhauser Basel, Switzerland (2008)
13. Robertson, A., Sequeira, A., Owens, R.G.: Rheological models for blood. In: A. Quarteroni, L. Formaggia, A. Veneziani (eds.) *Cardiovascular Mathematics*: *Modelling and simulation of the cardiovascular system,* pp. 211–241. Springer-Verlag, Italia (2009)
14. Steinman, D., Vorp, D., Ethier, C.: Computational modeling of the arterial biomechanics: insights into pathogenesis and treatment of vascular disease. J. Vasc. Surg. **37**, 1118–1128 (2003)

The Role of Potential Flow in the Theory of the Navier-Stokes Equations

Daniel D. Joseph

Abstract Solutions of the Navier-Stokes equations for flows of incompressible fluids satisfying no-slip boundary conditions are discussed in the frame of the Helmholtz decomposition. The focus is on the steady flow of a body in an unbounded fluid. The decomposition of the velocity into rotational and irrotational parts can be uniquely determined as the velocity generated by the vorticity in the Biot-Savart law plus a harmonic velocity in which the body and boundary conditions are identified. It is shown that contribution of the rotational velocity to the drag is larger than the total which includes a negative contribution from the irrotational velocity, The dissipation due to the potential flow cannot be neglected in any exact theory as it is in the conventional boundary layer theory and elsewhere.

Keywords Rotational · Irrotational · Biot-Savart law · Uniqueness · Dissipation · Drag · Stokes flow

1 Helmholtz Decomposition

Here I will derive some results which extend those derived by Joseph [1] and extended by Joseph et al. [2]. The Helmholtz decomposition says that every vector field $\boldsymbol{u}$ can be decomposed into a rotational part $\boldsymbol{v}$ and an irrotational part $\nabla\varphi$,

$$\boldsymbol{u} = \boldsymbol{v} + \nabla\varphi \tag{1}$$

where

$$\nabla \times \boldsymbol{u} = \nabla \times \boldsymbol{v} + \nabla^2\varphi \tag{2}$$

$$\nabla \times \boldsymbol{u} = \nabla \times \boldsymbol{v}. \tag{3}$$

D.D. Joseph (✉)
University of Minnesota and University of California, Irvine, CA, USA
e-mail: joseph@aem.umn.edu

R. Rannacher, A. Sequeira (eds.), *Advances in Mathematical Fluid Mechanics*, 311
DOI 10.1007/978-3-642-04068-9_19, © Springer-Verlag Berlin Heidelberg 2010

If the field is solenoidal, then

$$\nabla \times \boldsymbol{u} = \nabla \times \boldsymbol{v} = 0,\ \nabla^2 \varphi = 0. \tag{4}$$

This decomposition leads to the theory of the vector potential which I did not pursue in my earlier work but I do consider here. The decomposition is unique on unbounded domains without boundaries and explicit formulas for the vector potential are well known. The sense of the decomposition (1) is that is entirely rotational with no irrotational component. Uniqueness of the decomposition is not guaranteed by (1) since $\boldsymbol{v}$ could have an additional irrotational component. However, the condition (3) annihilates irrotational components; if (4) holds, then (3) can also be written as

$$\nabla^2 \boldsymbol{u} = \nabla^2 \boldsymbol{v} = 0. \tag{5}$$

In our previous publications [1, 2] we showed that unique decompositions can be easily identified in explicit solutions.

2 Irrotational Viscous Stress and the Irrotational Viscous Dissipation

The irrotational viscous stress is given by

$$\tau = 2\mu \nabla \otimes \nabla \varphi, \left(\tau_{ij} = 2\mu \frac{\partial^2 \varphi}{\partial x_i \partial x_j} \right) \tag{6}$$

The irrotational viscous stress $\tau_I = 2\mu \nabla \otimes \nabla \varphi$ does not give rise to a force density term in (5). The divergence of vanishes on each and every point in the domain V of flow. Even though an irrotational viscous stress exists, it does not produce a net force to drive motions. Moreover,

$$\int \operatorname{div} \tau_I \, dV = \int n \times \tau_I \, dS = 0. \tag{7}$$

The traction vectors $n \times \tau_I$ have no net resultant on each and every closed surface in the domain V of flow. We say that the irrotational viscous stresses, which do not drive motions, are self-equilibrated. Equation (1), (2), (3), (4), (5), (6) and (7) were given in our earlier work. An implication of (7) is that *no force can be produced on a body in steady flow by the viscous irrotational stresses*. This can be called a generalized D'Alembert Paradox which is usually presented as valid for inviscid fluids. Irrotational viscous torques on bodies also vanish because

$$\int \varepsilon_{ijk} x_j \tau_{kl} n_l \, dS = \int \frac{\partial \varepsilon_{ijk} x_j \tau_{kl}}{\partial x_l} \, dV = 0. \tag{8}$$

The key to understanding purely irrotational flows is that even though the irrotational stresses are self-equilibrated the power of these irrotational stresses is positive

$$\int \nabla\varphi \cdot (n \cdot \tau)\, dS = \int \frac{\partial \varphi}{\partial x_i} \tau_{ij} n_j \, dS = 2\mu \int \frac{\partial^2 \varphi}{\partial x_i \partial x_j} \frac{\partial^2 \varphi}{\partial x_i \partial x_j} \, dV. \tag{9}$$

3 Navier-Stokes Equations and Viscous Dissipation in Decomposed Form

The Navier-Stokes equations in decomposed form may be written as

$$\frac{\partial}{\partial x_i}(\varrho \frac{\partial \varphi}{\partial t} + \frac{\varrho}{2} |\nabla\varphi|^2 + p) + \varrho \frac{\partial}{\partial x_j} \left(v_j \frac{\partial \varphi}{\partial x_i} + v_i \frac{\partial \varphi}{\partial x_j} + v_i v_j \right) = \mu \nabla^2 v_i \tag{10}$$

These equations, together with $\nabla^2 \varphi = 0$, are five equations for the three components of velocity, the potential and the pressure. The boundaries conditions for $\boldsymbol{v}$ and φ are determined by the prescribed values for the velocity $\boldsymbol{u}$; for example, for the problem of drag on a body moving to the left in steady flow $\mathbf{U} = -\mathbf{e}_x U$ without rotation, we have

$$-\mathbf{e}_x U = \boldsymbol{v} + \nabla\varphi \tag{11}$$

The dissipation function evaluated on the decomposed field (1) sorts out into rotational, mixed and irrotational terms given by

$$\begin{aligned} \Phi &= \int 2\mu D_{ij} D_{ij} \, dV \\ &= \int 2\mu D_{ij}[\boldsymbol{v}] D_{ij}[\boldsymbol{v}] dV + 4\mu \int D_{ij} \frac{\partial^2 \varphi}{\partial x_i \partial x_j} dV \\ &\quad + 2\mu \int \frac{\partial^2 \varphi}{\partial x_i \partial x_j} \frac{\partial^2 \varphi}{\partial x_i \partial x_j} dV. \end{aligned} \tag{12}$$

Equation (12) can be greatly simplified; we have

$$\begin{aligned} &\int D_{ij}[\boldsymbol{v}] \frac{\partial^2 \varphi}{\partial x_i \partial x_j} dV + 2\mu \int \frac{\partial^2 \varphi}{\partial x_i \partial x_j} \frac{\partial^2 \varphi}{\partial x_i \partial x_j} dV = \\ &\frac{1}{2} \int \left(\frac{\partial v_i}{\partial x_j} + \frac{\partial v_j}{\partial x_i} \right) \frac{\partial^2 \varphi}{\partial x_i \partial x_j} dV = \int v_i \frac{\partial^2 \varphi}{\partial x_i \partial x_j} n_j dS \end{aligned} \tag{13}$$

where v_i is given by (11) and

$$\int \frac{\partial^2\varphi}{\partial x_i \partial x_j}\frac{\partial^2\varphi}{\partial x_i \partial x_j} dV = \int \frac{\partial\varphi}{\partial x_i}\frac{\partial^2\varphi}{\partial x_i \partial x_j} dS. \tag{14}$$

Hence, using (7), we have

$$\int v_i \frac{\partial^2\varphi}{\partial x_i \partial x_j} n_j dS = \int \left(U_i - \frac{\partial\varphi}{\partial x_i}\right)\frac{\partial^2\varphi}{\partial x_i \partial x_j} n_j dS = -\int \frac{\partial\varphi}{\partial x_i}\frac{\partial^2\varphi}{\partial x_i \partial x_j} n_j dS. \tag{15}$$

Combining now (15) and (12), we have

$$\Phi = \int 2\mu D_{ij} D_{ij} dV = \int 2\mu D_{ij}[\boldsymbol{v}] D_{ij}[\boldsymbol{v}] dV = -\int \frac{\partial\varphi}{\partial x_i}\frac{\partial^2\varphi}{\partial x_i \partial x_j} n_j dS. \tag{16}$$

Not only is potential flow necessary to satisfy no-slip boundary conditions but the potential flow terms enter into the dissipation.

4 Computation of Drag from Dissipation

It is not generally true that drag on a body in steady rectilinear motions can be computed from the dissipation integral. Joseph and Liao [3], (Eqs. (2.6) and (2.7)) showed that the drag could be computed from the dissipation if no-slip conditions on a solid or no-shear conditions on a bubble are required. In the case of a solid body moving the left with a steady velocity $-\mathbf{e}_x U$, we have $F_x U = \Phi$ where Φ is given by (12) or (16).

5 Stokes Flow Around a Sphere of Radius *a* in a Uniform Stream U

Rotational and irrotational velocities in many exact solutions were identified by Joseph [1] and Joseph et al. [2]. The problem of Stokes flow around a sphere is a good example in which all the main features of the general theory can exhibited. The solution for Stokes flow around a sphere of radius a in a uniform stream U is given in decomposed form

$$\begin{aligned}
\boldsymbol{u} = (u_r,\, u_\theta) &= \left(v_r + \frac{\partial\varphi}{\partial r},\, v_\theta + \frac{\partial\varphi}{r\partial\theta}\right),\\
u_r &= U\left(1 - \frac{3a}{2r} + \frac{a^3}{2r^3}\right)\cos\theta,\\
u_\theta &= -U\left(1 - \frac{3a}{4r} - \frac{a^3}{4r^3}\right)\sin\theta,
\end{aligned}$$

$$\begin{aligned}
\nabla \times \boldsymbol{u} &= U\left(0, 0, -\frac{3a}{2r^2}\sin\theta\right),\\
v_r &= -\frac{3a}{2r}U\cos\theta,\\
v_\theta &= \frac{3a}{4r}U\sin\theta,\\
\frac{\partial\varphi}{\partial r} &= U\left(1+\frac{a^3}{2r^3}\right]\cos\theta,\\
\frac{1}{r}\frac{\partial\varphi}{\partial\theta} &= -\left(1-\frac{a^3}{4r^3}\right)\sin\theta.
\end{aligned} \tag{17}$$

This problem is Galilean invariant; the sphere moves to the left with a velocity U and the fluid at infinity is at rest. In the usual approach, the drag $F_x = 6\pi\mu aU$ is computed directly; two thirds of the drag arises from the pressure and 1/3 from shear stress. Of course, the drag on the moving sphere is equal to the drag on the stationary sphere. The decomposed form of the strain rates are

$$[D_{rr}, D_{\theta\theta}, D_{\varphi\varphi}, D_{r\theta}] = U[(2, 1, 1)(P - V)\cos\theta, -P\sin\theta] \tag{18}$$

where $P = 3a^3/(4r^4)$ is the irrotational part computed from φ and $V = 3a/r^2$ is the irrotational part computed from $\boldsymbol{v}$. The stresses are proportional to the strain rate. At $r = a$, $P = V$ and all the stresses except the shear stress vanish. The shear stress is entirely from the irrotational flow proportional to P. The drag on the moving sphere, following (12), is given by

$$\begin{aligned}
F_x U &= 2\mu \int_0^\pi d\theta \int_a^\infty [D_{rr}^2 + D_{\theta\theta}^2 + D_{\varphi\varphi}^2 + D_{r\theta}^2] 2\pi\, r^2 \sin\theta\, dr\\
&= (9-3)\pi\mu a U^2 = 6\pi a\mu U^2.
\end{aligned} \tag{19}$$

The factor 9 arises from the purely rotational velocity $\boldsymbol{v}$ and the factor 3 from the irrotational velocity $\nabla\varphi$.

6 Biot-Savart Law

The Biot-Savart law gives a recipe for the calculation of velocity from a given distribution of vorticity. It is understood that the vorticity is a smooth function defined on all of R^3 and vanishes at infinity. The velocity generated from the Biot-Savart integral

$$\boldsymbol{v} = \int \frac{\omega \times \mathbf{r}}{4\pi\mathbf{r}}\, dV' \tag{20}$$

where $\mathbf{r} = \mathbf{x} - \mathbf{x}'$ and $\omega = \omega(\mathbf{x}') = \nabla \times \mathbf{v}(\mathbf{x}')$, is rotational. The irrotational contribution to the velocity cannot give rise to vorticity and cannot enter on the left of (20) and hence, an irrotational component of velocity cannot be generated by the Biot-Savart integral.

$$\boldsymbol{v} + \nabla\varphi = \int \frac{curl(\boldsymbol{v} + \nabla\varphi)}{4\pi\mathbf{r}} dV' = \int \frac{curl\,\boldsymbol{v} \times \mathbf{r}}{4\pi\mathbf{r}} dV' = \boldsymbol{v}. \tag{21}$$

No body is recognized in the Biot-Savart law. Suppose we are interested in the steady motion of a sphere in R^3 ; we prescribe the velocity $\mathbf{U}$ of the sphere and require that the no-slip boundary condition be satisfied. To use (20) in this problem we would have to know the vorticity and require no-slip there. But $\boldsymbol{v}$ on the sphere could not in general be U. We can add $\nabla\varphi$ to $\boldsymbol{v}$ and try to find a φ such that

$$\mathbf{U} = \nabla\varphi + \int \frac{curl\,\boldsymbol{v} \times \mathbf{r}}{4\pi\mathbf{r}} dV'. \tag{22}$$

We cannot satisfy (22) because only one boundary condition can be satisfied by a solution of the Laplace equation. This problem was considered by Lamb ([4], Chap. vii), who has shown that, for any given solenoidal distribution of vorticity outside the body whose motion is prescribed, one and only one solenoidal velocity exists, tending to zero at infinity and with zero normal relative velocity at the solid surface. This form of the Helmholtz decomposition was considered by Lighthill [5]. In general, $\boldsymbol{u}$ does not satisfy the boundary condition for $\boldsymbol{v}$. However, the difference $\boldsymbol{u} - \boldsymbol{v}$ must be irrotational (since curl $\boldsymbol{u} = \boldsymbol{u}'$), and hence equal to $\nabla\varphi$ for some potential φ. On the body surface

$$\frac{\partial\varphi}{\partial n} = U_n - v_n \tag{23}$$

is prescribed. The normal component of the velocity $\mathbf{U}$ can be balanced but the tangential component cannot. It is instructive to consider the example of Stokes flow over a sphere (17). The rotational component $\boldsymbol{v}$ gives rise to the vorticity. It is a smooth function on R^3 and satisfies (20). The irrotational components are required to satisfy the no-slip boundary condition. The irrotational flow does not have a zero normal component; rather the irrotational flow satisfies a Robin condition in which a linear combination of the tangential and normal components has equal weight. The role of Robin boundary conditions for the Laplace equation in the Helmholtz decomposition of the Navier-Stokes equations is under-studied.

References

1. Joseph, D.D.: Helmholtz decomposition coupling rotational to irrotational flow of a viscous fluid. PNAS **103**, 14272–14277 (2006)
2. Joseph, D.D., Funada, T., Wang, J.: Potential flows of viscous and viscoelastic liquids. Cambridge University Press, UK (2007)

3. Joseph, D.D., Liao, T.Y.: Viscous and viscoelastic potential flow. In *Trends and Perspectives in Applied Mathematics*, Applied mathematical sciences. L Sirovich, ed. Springer-Verlag Berlin, Chap. 5, 109–154 (1994)
4. Lamb, H.: *Hydrodynamics.* 6th ed. Cambridge University Press (1932)
5. Lighthill M.J.: Introduction. Boundary layer theory. In *Laminar Boundary Layers*, L. Rosenhad, ed. Oxford University Press (1963)

Small Perturbations of Initial Conditions of Solutions of the Navier-Stokes Equations in the L^3-Norm and Applications

Petr Kučera

Abstract In this paper, we solve two problems. We prove a theorem on stability of a strong solution with respect to the norm $\| \,.\, \|_{L^2} + \| \,.\, \|_{L^3}$ in Sect. 2. Then, in Sect. 3, we show that there exist strong solutions of the Navier-Stokes initial-boundary value problem such that their initial values are arbitrarily large (in the norm of $\mathcal{D}(A^{1/4})$) and they belong to an arbitrarily chosen open set $U \subset \mathcal{D}(A^{1/2})$ at a time instant $\xi > 0$ which can be as small as we wish (We denote by A the Stokes operator.)

Keywords Navier-Stokes equations · Stokes operator

1 Introduction

Let $T > 0$, $T \leq \infty$, $Q_T = R^3 \times (0, T)$. The classical formulation of the considered initial-value problem is as follows:

$$\frac{\partial \mathbf{u}}{\partial t} - \nu \Delta \mathbf{u} + (\mathbf{u} \cdot \nabla)\mathbf{u} + \nabla \mathcal{P} = \mathbf{0} \quad \text{in } Q_T, \tag{1}$$

$$\nabla \cdot \mathbf{u} = 0 \quad \text{in } Q_T, \tag{2}$$

$$\mathbf{u}(0) = \mathbf{u}_0 \quad \text{in } R^3. \tag{3}$$

$\mathbf{u} = (u_1, u_2, u_3)$ denotes the velocity, $\mathcal{P}$ represents the pressure and ν is the kinematic coefficient of viscosity. For simplicity we suppose that $\nu = 1$.

Let $\mathcal{V} = \mathcal{C}_0^\infty(R^3)^3 \cap \{\mathbf{v};\ \nabla \cdot \mathbf{v} = 0\}$. As usual in literature, H and V denote the closures of $\mathcal{V}$ in the norms of $L^2(R^3)^3$ and $W_0^{1,2}(R^3)^3$. We denote by $\|.\|_2$, $\|.\|_3$ and $((.,.))$, respectively, the norms in $L^2(R^3)^3$, $L^3(R^3)^3$ and the scalar product in $L^2(R^3)^3$. Let $A = -P\Delta$, where P is the Helmholtz projection of $L^2(R^3)^3$ onto H. The Stokes operator A has the domain $\mathcal{D}(A) \equiv W^{2,2}(R^3)^3 \cap V$. It is well known that

P. Kučera (✉)
Department of Mathematics, Faculty of Civil Engineering, Czech Technical University, Prague 6, 16629, Czech Republic
e-mail: kucera@mat.fsv.cvut.cz

R. Rannacher, A. Sequeira (eds.), *Advances in Mathematical Fluid Mechanics*,
DOI 10.1007/978-3-642-04068-9_20,

A is self-adjoint and non-negative. Therefore it is possible to define its fractional powers. $\mathcal{D}(A)$ is a Banach space with the norm $\|\mathbf{u}\|_{\mathcal{D}(A)} = \|A\mathbf{u}\|_2 + \|\mathbf{u}\|_2$. This norm is equivalent to the norm $\|.\|_{W^{2,2}(R^3)^3}$ (see e.g. [6], Chap. III, Theorem 2.1.1). Similarly, $\mathcal{D}(A^\alpha)$ is a Banach space with the norm $\|\mathbf{u}\|_{\mathcal{D}(A^\alpha)} = \|A^\alpha \mathbf{u}\|_2 + \|\mathbf{u}\|_2$ for $\alpha > 0$. The space V can now be identified with $\mathcal{D}(A^{1/2})$ (see e.g. [6], Chap. III, Lemma 2.2.1).

Definition 1 Let $\mathbf{u}_0 \in H$. We call a function $\mathbf{u} \in L^\infty_{\text{loc}}(0, T;\, H) \cap L^2_{\text{loc}}(0, T;\, V)$ a weak solution of the problem (1), (2) and (3) if

$$\int_0^T \int_{R^3} \left[-\mathbf{u} \cdot \frac{\partial \boldsymbol{\varphi}}{\partial t} + \nabla \mathbf{u} \cdot \nabla \boldsymbol{\varphi} + (\mathbf{u} \cdot \nabla)\mathbf{u} \cdot \boldsymbol{\varphi} \right] = \int_{R^3} \mathbf{u}_0 \cdot \boldsymbol{\varphi}(0)$$

for all $\boldsymbol{\varphi} \in \mathcal{C}_0{}^\infty([0, T); \mathcal{V})$ such that $\nabla \cdot \boldsymbol{\varphi} = 0$ in Q_T.

We use the notion of a strong solution of the Navier-Stokes equations as it is defined in ([6], Chap. V, Definition 4.1.1):

Definition 2 Let $\mathbf{u}$ be a weak solution of the system (1), (2) and (3) with an initial velocity $\mathbf{u}_0 \in V$. Then $\mathbf{u}$ is called a strong solution of the problem (1), (2) and (3) if there exist real numbers $q,\ s$ such that $3 < q < \infty,\ 2 < s < \infty,\ \frac{3}{q} + \frac{2}{s} = 1$ and

$$\mathbf{u} \in L^s_{\text{loc}}(0, T;\, L^q(R^3)^3).$$

It is well known that if $\mathbf{u}$ is a strong solution of the problem (1), (2) and (3) then

$$\mathbf{u} \in L^2_{\text{loc}}(0, T;\, W^{2,2}(R^3)^3) \cap L^\infty_{\text{loc}}(0, T;\, V), \tag{4}$$
$$\mathbf{u}' \in L^2_{\text{loc}}(0, T;\, H)$$

and

$$\mathbf{u} \in \mathcal{C}([0, T);\, V)$$

(see. e.g. [6], Chap. V, Theorem 1.8.1).

In [3], G. Ponce et al. proved a theorem on stability of a strong solution $\mathbf{u}$ of the Navier-Stokes problem (1), (2) and (3) with respect to perturbation of the initial velocity in the norm $\|A^{1/2}.\|_2$.

In [4] and [5], B. Scarpellini constructed strong global solutions of the Navier-Stokes equations in a bounded sufficiently smooth domain Ω with an arbitrary large initial conditions in the norm of $\mathcal{D}(A^{1/2})$. He proved that to a given nonempty open set U in $\mathcal{D}(A^\gamma)$ (for $\frac{3}{4} < \gamma < 1$), $\chi > 0$ (arbitrarily small) and $K > 0$ (arbitrarily large), there exist $\mathbf{u}_0 \in \mathcal{D}(A)$ and real numbers κ and ξ such that $\|A^{1/2}\mathbf{u}_0\|_2 > K$ and $0 < \xi < \kappa < \chi$ and the solution $\mathbf{u}$ of the Navier-Stokes equations with the initial velocity $\mathbf{u}_0$ that is strong on the time interval $(0, \kappa)$ and satisfies the condition $\mathbf{u}(\xi) \in U$.

In the next section we prove Theorem 1 which extends the mentioned result from [3]. We prove a theorem on stability of a strong solution $\mathbf{u}$ of the Navier-Stokes problem (1), (2) and (3) with respect to perturbation of the initial velocity in the norm $\|.\|_2 + \|.\|_3$ instead of $\|A^{1/2}.\|_2$. In the last Sect. 3, we use this result and we improve the above cited Scarpellini's theorem in the sense that the size of the initial value $\mathbf{u}_0$ is measured by the norm $\|A^{1/4}.\|_2$. Moreover, we consider U to be an open subset of $\mathcal{D}(A^{1/2})$ instead of $\mathcal{D}(A^{\gamma})$.

2 Small Perturbations of the Initial Velocity in the Norm $\|.\|_2 + \|.\|_3$

The goal of this section is to prove the theorem on stability of a strong solution $\mathbf{u}$ of the problem (1), (2) and (3) with respect to the norm $\|.\|_2 + \|.\|_3$.

We shall denote by c_1 a generic constant, i.e. a constant whose value may change from one line to the next. On the other hand, c will be used to denote a constant depending on certain number ε whose exact value will be specified later. Numbered constants $C_1, \ldots, C_4$ will have fixed values throughout the whole paper.

Remark 1 We often deal with functions $\boldsymbol{\psi}$ satisfying

$$\boldsymbol{\psi} \in L^2(0, T;\ W^{2,2}(R^3)^3) \cap L^\infty(0, T;\ V) \tag{5}$$

in this paper. The sense of this remark is to recall other integrability properties of $\boldsymbol{\psi}$ that can be directly derived from (5) by means of Hölder's inequality or embedding inequalities. Naturally, (5) implies that

$$|\nabla\boldsymbol{\psi}| \in L^2(0, T;\ L^6(R^3)) \cap L^2(0, T;\ L^2(R^3)) \cap L^\infty(0, T;\ L^2(R^3)). \tag{6}$$

Consequently,

$$\boldsymbol{\psi} \in L^2(0, T;\ W^{1,3}(R^3)) \cap L^4(0, T;\ W^{1,3}(R^3)). \tag{7}$$

By analogy, one can derive that

$$(\boldsymbol{\psi} \cdot \nabla)\boldsymbol{\psi} \cdot \boldsymbol{\psi} \in L^1(0, T;\ L^1(R^3)), \tag{8}$$

$$(\boldsymbol{\psi} \cdot \nabla)\boldsymbol{\psi} \in L^2(0, T;\ L^2(R^3)^3), \tag{9}$$

$$\boldsymbol{\psi} \in L^3(0, T;\ L^9(R^3)^3). \tag{10}$$

Lemma 1 *Let* $\mathbf{u}$ *and* $\mathbf{v}$ *be strong solutions of (1), (2) and (3) with the initial velocities* $\mathbf{u}(0) = \mathbf{u}_0 \in V$ *and* $\mathbf{v}(0) = \mathbf{v}_0 \in V$*, satisfying the stronger variant of (4), i.e.*

$$\mathbf{u}, \mathbf{v} \in L^2(0, T;\ W^{2,2}(R^3)^3) \cap L^\infty(0, T;\ V). \tag{11}$$

Denote $\mathbf{w} = \mathbf{v} - \mathbf{u}$*. Then there exists* $C_3 = C_3(\mathbf{u}) > 0$ *such that*

$$\|\mathbf{w}(t)\|_2^2 + \int_0^t \|\nabla\mathbf{w}\|_2^2 \ \le\ C_3\, \|\mathbf{w}(0)\|_2^2 \tag{12}$$

for almost all $t \in (0, T)$.

Proof Equations (7), (8) and (9) imply that

$$\begin{aligned} &\mathbf{u}, \mathbf{w} \in L^2(0, T;\ W^{1,3}(R^3)), \\ &(\mathbf{w} \cdot \nabla)\mathbf{w} \cdot \mathbf{w} \in L^1(0, T;\ L^1(R^3)), \\ &(\mathbf{w} \cdot \nabla)\mathbf{w} \in L^2(0, T;\ L^2(R^3)^3), \qquad (13) \\ &(\mathbf{w} \cdot \nabla)\mathbf{u} \cdot \mathbf{w},\ (\mathbf{u} \cdot \nabla)\mathbf{w} \cdot \mathbf{w} \in L^1(0, T;\ L^1(R^3)), \\ &(\mathbf{w} \cdot \nabla)\mathbf{u},\ (\mathbf{u} \cdot \nabla)\mathbf{w} \in L^2(0, T;\ L^2(R^3)^3). \qquad (14) \end{aligned}$$

It is easy to see that

$$2 \int_{R^3} \left|(\mathbf{w} \cdot \nabla)\mathbf{u} \cdot \mathbf{w}\right| \ \le\ \|\nabla \mathbf{w}\|_2^2 + C_1\, \|\nabla \mathbf{u}\|_3^2\, \|\mathbf{w}\|_2^2 \tag{15}$$

for almost every $t \in (0, T)$. Using inclusions (13), (14) and applying projection P to the equation for the difference $\mathbf{w} = \mathbf{v} - \mathbf{u}$, we get

$$\mathbf{w}' + A\mathbf{w} + P\big((\mathbf{w} \cdot \nabla)\mathbf{w} + (\mathbf{u} \cdot \nabla)\mathbf{w} + (\mathbf{w} \cdot \nabla)\mathbf{u}\big) \ =\ 0. \tag{16}$$

Equation (16) is the operator equation in space H, satisfied for almost all $t \in (0, T)$. Multiplying (16) by $2\mathbf{w}(t)$ and using (15) we obtain

$$\frac{d}{dt}\|\mathbf{w}\|_2^2 + 2\|\nabla \mathbf{w}\|_2^2 \ \le\ 2\int_{R^3} \left|(\mathbf{w} \cdot \nabla)\mathbf{u} \cdot \mathbf{w}\right| \le \|\nabla \mathbf{w}\|_2^2 + C_1\, \|\nabla \mathbf{u}\|_3^2\, \|\mathbf{w}\|_2^2. \tag{17}$$

Hence

$$\frac{d}{dt}\|\mathbf{w}\|_2^2 \ \le\ C_1\, \|\nabla \mathbf{u}\|_3^2\, \|\mathbf{w}\|_2^2.$$

Put $C_2 := C_1 \cdot \int_0^T \|\nabla \mathbf{u}\|_3^2$. Then

$$\|\mathbf{w}(t)\|_2^2 \ \le\ \mathrm{e}^{C_2}\, \|\mathbf{w}(0)\|_2^2 \tag{18}$$

for almost all $t \in (0, T)$. Integrating (17) on $(0, t)$ $(0 < t \le T)$ and using (18) we get

$$\|\mathbf{w}(t)\|_2^2 + \int_0^t \|\nabla \mathbf{w}\|_2^2 \ \le\ \big(1 + C_2\, \mathrm{e}^{C_2}\big)\, \|\mathbf{w}(0)\|_2^2.$$

Denoting $C_3 := 1 + C_2\, \mathrm{e}^{C_2}$, we complete the proof. □

Theorem 1 *Let*

$$\mathbf{u} \in L^2(0, T;\ W^{2,2}(R^3)^3) \cap L^\infty(0, T;\ V)$$

be a strong solution of (1), (2) and (3) with the initial velocity $\mathbf{u}(0) = \mathbf{u}_0 \in V$. *Then there exists* $\delta > 0$ *such that if* $\mathbf{v}_0 \in V$ *satisfies*

$$\|\mathbf{u}(0) - \mathbf{v}_0\|_2 + \|\mathbf{u}(0) - \mathbf{v}_0\|_3 < \delta \tag{19}$$

then there exists a unique strong solution $\mathbf{v}$ *of (1), (2) and (3) with the initial velocity* $\mathbf{v}_0$.

Proof Let

$$\sigma \ := \ \sup\big\{\varsigma \in (0, T);\ \mathbf{v} \text{ is a strong solution on the time interval } (0, \varsigma)\big\}. \tag{20}$$

Since $\mathbf{v}(0) \in V$, $\sigma > 0$. Then $\mathbf{w} = \mathbf{v} - \mathbf{u}$ satisfies the equation

$$\mathbf{w}' + A\mathbf{w} + P\big[(\mathbf{w} \cdot \nabla)\mathbf{w} + (\mathbf{u} \cdot \nabla)\mathbf{w} + (\mathbf{w} \cdot \nabla)\mathbf{u}\big] \ = \ 0 \tag{21}$$

on $(0, \sigma)$. This follows in the same way as (16). Since $\Omega = R^3$, we have $A = -\Delta$ on $\mathcal{D}(A)$ (see [6], Chapter III, Lemma 2.3.2). Hence

$$\big(\!\big(A\mathbf{w},\ P(\mathbf{w}\,|\mathbf{w}|)\big)\!\big) = \ \big(\!\big(-\Delta\mathbf{w},\ \mathbf{w}|\mathbf{w}|\big)\!\big) = \ -\int_{R^3} \Delta\mathbf{w} \cdot \mathbf{w}|\mathbf{w}|. \tag{22}$$

Multiplying (21) by $P(\mathbf{w}\,|\mathbf{w}|)$, using (22) and integrating over R^3, we obtain

$$\begin{aligned} &\frac{1}{3}\frac{d}{dt}\int_{R^3} |\mathbf{w}|^3 + \int_{R^3} |\nabla\mathbf{w}|^2|\mathbf{w}| + \frac{4}{9}\int_{R^3} \big|\nabla|\mathbf{w}|^{3/2}\big|^2 = \\ &-\big(\!\big((\mathbf{w} \cdot \nabla)\mathbf{w},\ P(\mathbf{w}\,|\mathbf{w}|)\big)\!\big) - \big(\!\big((\mathbf{u} \cdot \nabla)\mathbf{w},\ P(\mathbf{w}\,|\mathbf{w}|)\big)\!\big) \\ &-\big(\!\big((\mathbf{w} \cdot \nabla)\mathbf{u},\ P(\mathbf{w}\,|\mathbf{w}|)\big)\!\big). \end{aligned} \tag{23}$$

We will now estimate the integrals in (23). We shall use the Helmholtz decomposition and the embedding $\mathcal{D}(A^{1/2}) \hookrightarrow L^6(R^3)^3$ (see [6], Chap. III, Lemma 2.4.1). At first, the inequality

$$\begin{aligned} \Big|\big(\!\big((\mathbf{w} \cdot \nabla)\mathbf{w},\ P(\mathbf{w}\,|\mathbf{w}|)\big)\!\big)\Big| \ &= \ \Big|\int_{R^3} (\mathbf{w} \cdot \nabla)\mathbf{w} \cdot P(\mathbf{w}\,|\mathbf{w}|)\Big| \ \le \\ &\le \varepsilon \left(\int_{R^3} |\nabla\mathbf{w}|^2|\mathbf{w}|\right) + \left(\varepsilon \ + \ c(\varepsilon) \int_{R^3} |\mathbf{w}|^3\right)\left(\int_{R^3} \big|\nabla|\mathbf{w}|^{3/2}\big|^2\right) \end{aligned} \tag{24}$$

holds on $(0, \sigma)$ (see the inequality (24) in [2]) and for every $\varepsilon > 0$. Furthermore,

$$\begin{aligned}
&\Big|\big(\!\big((\mathbf{u}\cdot\nabla)\mathbf{w},\,P(\mathbf{w}\,|\mathbf{w}|)\big)\!\big)\Big| \;=\; \Big|\int_{R^3}(\mathbf{u}\cdot\nabla)\mathbf{w}\cdot P(\mathbf{w}\,|\mathbf{w}|)\Big| \;\le\\
&\le c_1\Big(\int_{R^3}|\mathbf{u}|^6\Big)^{1/6}\Big(\int_{R^3}|\nabla\mathbf{w}|^2\Big)^{1/2}\Big(\int_{R^3}|P(\mathbf{w}\,|\mathbf{w}|)|^3\Big)^{1/3} \;\le\\
&\le c_1\Big(\int_{R^3}|\mathbf{u}|^6\Big)^{1/6}\Big(\int_{R^3}|\nabla\mathbf{w}|^2\Big)^{1/2}\Big(\int_{R^3}|\mathbf{w}|^6\Big)^{1/3} \;\le\\
&\le c_1\,\|A^{1/2}\mathbf{u}\|_2\Big(\int_{R^3}|\mathbf{w}|^3\Big)^{1/6}\Big(\int_{R^3}|\mathbf{w}|^9\Big)^{1/6}\Big(\int_{R^3}|\nabla\mathbf{w}|^2\Big)^{1/2} \;\le\\
&\le \varepsilon\,\|A^{1/2}\mathbf{u}\|_2^2\Big(\int_{R^3}|\mathbf{w}|^3\Big)^{1/3}\Big(\int_{R^3}\big|\nabla|\mathbf{w}|^{3/2}\big|^2\Big) \;+\; c(\varepsilon)\Big(\int_{R^3}|\nabla\mathbf{w}|^2\Big) \qquad (25)
\end{aligned}$$

and

$$\begin{aligned}
&\Big|\big(\!\big((\mathbf{w}\cdot\nabla)\mathbf{u},\,P(\mathbf{w}\,|\mathbf{w}|)\big)\!\big)\Big| \;=\; \Big|\int_{R^3}(\mathbf{w}\cdot\nabla)\mathbf{u}\cdot P(\mathbf{w}\,|\mathbf{w}|)\Big| \;\le\\
&\le c_1\Big(\int_{R^3}|\nabla\mathbf{u}|^3\Big)^{1/3}\Big(\int_{R^3}|\mathbf{w}|^3\Big)^{1/3}\Big(\int_{R^3}|P(\mathbf{w}\,|\mathbf{w}|)|^3\Big)^{1/3} \;\le\\
&\le c_1\Big(\int_{R^3}|\nabla\mathbf{u}|^3\Big)^{1/3}\Big(\int_{R^3}|\mathbf{w}|^3\Big)^{1/3}\Big(\int_{R^3}|\mathbf{w}|^6\Big)^{1/3} \;\le\\
&\le c_1\Big(\int_{R^3}|\nabla\mathbf{u}|^3\Big)^{1/3}\Big(\int_{R^3}|\mathbf{w}|^3\Big)^{1/2}\Big(\int_{R^3}|\mathbf{w}|^9\Big)^{1/6} \;\le\\
&\le c_1\Big(\int_{R^3}\big|\nabla|\mathbf{w}|^{3/2}\big|^2\Big)^{1/2}\Big(\int_{R^3}|\nabla\mathbf{u}|^3\Big)^{1/3}\Big(\int_{R^3}|\mathbf{w}|^3\Big)^{1/2} \;\le\\
&\le \varepsilon\,\Big(\int_{R^3}\big|\nabla|\mathbf{w}|^{3/2}\big|^2\Big) \;+\; c(\varepsilon)\Big(\int_{R^3}|\nabla\mathbf{u}|^3\Big)^{2/3}\Big(\int_{R^3}|\mathbf{w}|^3\Big). \qquad (26)
\end{aligned}$$

The two latter inequalities also hold on $(0,\sigma)$ and for every $\varepsilon > 0$. Using (23), (24), (25) and (26), we obtain

$$\begin{aligned}
&\frac{1}{3}\frac{d}{dt}\int_{R^3}|\mathbf{w}|^3 + (1-\varepsilon)\int_{R^3}|\nabla\mathbf{w}|^2|\mathbf{w}| +\\
&+\Big[\frac{4}{9} - 2\varepsilon - c(\varepsilon)\int_{R^3}|\mathbf{w}|^3 - \varepsilon\,\|A^{1/2}\mathbf{u}\|_2^2\Big(\int_{R^3}|\mathbf{w}|^3\Big)^{1/3}\Big]\Big(\int_{R^3}\big|\nabla|\mathbf{w}|^{3/2}\big|^2\Big) \;\le\\
&\le c(\varepsilon)\Big(\int_{R^3}|\nabla\mathbf{u}|^3\Big)^{2/3}\Big(\int_{R^3}|\mathbf{w}|^3\Big) \;+\; c(\varepsilon)\Big(\int_{R^3}|\nabla\mathbf{w}|^2\Big). \qquad (27)
\end{aligned}$$

Choose $\varepsilon > 0$ such that $\frac{4}{9} - 2\varepsilon > \frac{1}{3}$ and fix ε and $c = c(\varepsilon)$. Denote

$$\begin{aligned}
h(t) &:= \int_{R^3}|\mathbf{w}(.,t)|^3,\\
\theta(t) &:= 3c\Big(\int_{R^3}|\nabla\mathbf{u}(.,t)|^3\Big)^{2/3},
\end{aligned}$$

$$\vartheta(t) := 3c \int_{R^3} |\nabla \mathbf{w}(.,t)|^2,$$
$$\varphi(t) := \int_{R^3} \left|\nabla |\mathbf{w}(.,t)|^{3/2}\right|^2$$

and

$$\eta(t) \;:=\; 3\Big(\frac{4}{9} - 2\varepsilon - c\; h(t) - \varepsilon\,\|A^{1/2}\mathbf{u}(.,t)\|_2^2\; h^{1/3}(t)\Big).$$

In the definitions of functions h, θ, ϑ, φ and η we use notation $\mathbf{w}(.,t)$ and $\mathbf{u}(.,t)$ instead of $\mathbf{u}$ and $\mathbf{w}$ in order to emphasize that h, θ, ϑ, φ and η depend only on t and we integrate over R^3 in their definition. Clearly, $\theta, \vartheta \in L^1((0,T))$. The inequality (27) now reads

$$h'(t) + \eta(t)\varphi(t) \le \theta(t)h(t) + \vartheta(t). \tag{28}$$

Note that there exists $\kappa > 0$ such that if $h(t) = \int_{R^3} |\mathbf{w}|^3 < \kappa$, then $\eta(t) > \frac{1}{4}$. Suppose that such κ is fixed from now. Let us compare function $h(t) = \int_{R^3} |\mathbf{w}|^3$ with function φ such that $\varphi(0) = h(0) = \|\mathbf{w}(0)\|_3^3$ and φ satisfies the estimate

$$\varphi'(t) = \theta(t)\varphi(t) + \vartheta(t). \tag{29}$$

Obviously,

$$h(t) \le \varphi(t) \tag{30}$$

on each interval $(0,\sigma^*)$, $\sigma^* < \sigma$, provided that

$$\eta(t) > \frac{1}{4} \tag{31}$$

also holds on $(0,\sigma^*)$. Integrating (29), we get

$$\varphi(t) \le e^{\int_0^T \theta(s)}\Big(\varphi(0) + \int_0^T \vartheta(s)\Big). \tag{32}$$

Lemma 1, (19) and (32) yield the existence of $\delta > 0$ (see (19)) sufficiently small such that the inequality $\varphi(0) < \delta$ implies that

$$\varphi(t) < \kappa \tag{33}$$

on $(0,T)$. Thus, (31), and consequently (30), hold on $(0,\sigma)$. Using (27), (31) and (33) we obtain the inequalities

$$\|\mathbf{w}(t)\|_3^3 + \frac{1}{2}\int_0^t \int_{R^3} |\nabla \mathbf{w}|^2 |\mathbf{w}| + \frac{1}{4}\int_0^t \int_{R^3} \big|\nabla |\mathbf{w}|^{3/2}\big|^2 \le$$
$$\le \|\mathbf{w}(0)\|_3^3 + 3c\kappa \int_0^t \Big(\int_{R^3} |\nabla \mathbf{u}|^3\Big)^{2/3} + 3c\int_0^t \int_{R^3} |\nabla \mathbf{w}|^2 \le$$
$$\le \|\mathbf{w}(0)\|_3^3 + 3c\kappa \int_0^T \Big(\int_{R^3} |\nabla \mathbf{u}|^3\Big)^{2/3} + 3c\int_0^T \int_{R^3} |\nabla \mathbf{w}|^2 < +\infty$$

which hold for every $t \in (0, \sigma)$. Therefore

$$\int_0^\sigma \int_{R^3} \big|\nabla |\mathbf{w}|^{3/2}\big|^2 < \infty.$$

Since

$$\nabla |\mathbf{w}|^{3/2} \in L^2(0, \sigma;\ L^2(R^3)^3),$$

we obtain $|\mathbf{w}|^{3/2} \in L^2(0, \sigma;\ L^6(R^3))$. Thus

$$\int_0^\sigma \Big(\int_{R^3} |\mathbf{w}|^9\Big)^{1/3} < \infty. \tag{34}$$

(10) and (34) yield $\mathbf{v} = \mathbf{u} + \mathbf{w} \in L^3(0, \sigma;\ L^9(R^3)^3)$. We want to prove that $\sigma = T$. Suppose that $\sigma < T$. Hence $\mathbf{v} \in \mathcal{C}([0, \sigma];\ V)$ (see [1], Lemma 5.4). Using the well known theorem on the local in time existence of a strong solution (see e.g. [1], Theorem 6.2) we obtain the contradiction with (20). Therefore $\sigma = T$ and the theorem is proved. □

3 Strong Solution of the Navier-Stokes Equations with Large Initial Conditions

In this section, we show that Theorem 1 enables us to show, relatively easily, that there exist strong solutions of the Navier-Stokes initial-boundary value problem such that their initial values are arbitrarily large (in the norm of $\mathcal{D}(A^{1/4})$) and they belong to an arbitrarily chosen open set $U \subset \mathcal{D}(A^{1/2})$ at a time instant $\xi > 0$ which can be as small as we wish.

Remark 2 Let Ω be a bounded domain. Let us denote by $\mathcal{B}$ the operator of restriction from $L^2(R^3)^3$ into $L^2(\Omega)^3$ by setting $(\mathcal{B}\boldsymbol{\psi})(x) := \boldsymbol{\psi}(x)$ for $x \in \Omega$. Obviously, $\mathcal{B}$ is bounded and linear. Let A_Ω be the Stokes operator for Ω. (It is the operator analogous to A, which is derived from the Stokes problem with the homogeneous Dirichlet boundary conditions; see [6], Chap. II, 2.1). Applying Lemma 2.4.2 in [6, Chap. III], we can deduce that to given $K > 0$ arbitrarily large, there exists a function $\boldsymbol{\psi} \in \mathcal{C}_0^\infty(R^3)^3$ such that $\nabla \cdot \boldsymbol{\psi} \equiv 0$ in R^3, $\operatorname{Supp} \boldsymbol{\psi} \subset \Omega$,

$$\|\boldsymbol{\psi}\|_2 + \|\boldsymbol{\psi}\|_3 \le 1,$$
$$\|A_\Omega^{1/4}\mathcal{B}\boldsymbol{\psi}\|_2 \ge K.$$

Using the Heinz lemma (see [6], Chap. II, Lemma 3.2.3) we obtain

$$\|A^{1/4}\boldsymbol{\psi}\|_2 \ge C_4 K,$$

where $C_4 > 0$ is independent of a concrete function $\boldsymbol{\psi}$.

The goal of this section is to prove the following theorem.

Theorem 2 *Let* U *be a nonempty open set in* $\subset \mathcal{D}(A^{1/2})$. *Given* $K > 0$ *(arbitrarily large),* $\chi > 0$ *(arbitrarily small), there exists a weak solution* $\mathbf{v}$ *of the problem (1), (2) and (3) with initial value* $\mathbf{v}(0) = \mathbf{v}_0 \in \mathcal{D}(A^{1/2})$ *and real numbers* κ *and* ξ *such that* $0 < \xi < \kappa < T,\ \kappa < \chi$ *and*

$$\|A^{1/4}(\mathbf{v}_0)\|_2 \ge K, \tag{35}$$
$$\mathbf{v}(\xi) \in U, \tag{36}$$
$$\mathbf{v} \in \mathcal{C}([0,\kappa);\ \mathcal{D}(A^{1/2})). \tag{37}$$

Proof Since U is an open set in $\mathcal{D}(A^{1/2})$, there exist $\mu > 0$, $\kappa > 0$ and a weak solution $\mathbf{u}$ of the problem (1), (2) and (3) with the initial value $\mathbf{u}(0) \in U$ such that $\mathbf{u} \in \mathcal{C}([0,\kappa], \mathcal{D}(A^{1/2}))$ and $B_\mu(\mathbf{u}(t)) \subset U$ for every $t \in [0,\kappa]$ (where$\mathcal{B}_\mu(\mathbf{u}(t))$ denotes the ball of radius μ with the center at the point $u(t)$.) By Theorem 1 there exists $\delta > 0$ such that if

$$\|\mathbf{u}(0) - \mathbf{v}_0\|_2 + \|\mathbf{u}(0) - \mathbf{v}_0\|_3 < \delta \tag{38}$$

for some $\mathbf{v}_0 \in \mathcal{D}(A^{1/2})$, then there exists a solution $\mathbf{v}$ of the problem (1), (2) and (3) with the initial velocity $\mathbf{v}_0$ which is strong on the time interval $(0,\kappa)$. Moreover, applying Lemma 1, inequality (12), we can derive that if $\delta > 0$ is chosen to be sufficiently small, there exists $\xi \in (0, \kappa/2)$ such that

$$\|\mathbf{u}(\xi) - \mathbf{v}(\xi)\|_2 + \|A^{1/2}(\mathbf{u}(\xi) - A^{1/2}(\mathbf{v}(\xi))\|_2 = \|\mathbf{w}(\xi)\|_2 + \|A^{1/2}(\mathbf{w}(\xi)\|_2 < \mu.$$

Then $\xi \in (0,\kappa)$ and $\mathbf{v}(\xi) \in U$. Due to Remark 2, $\mathbf{v}_0$ can be considered such that in addition to (38), it also satisfies (35). The theorem is proved. □

Acknowledgments The research was supported by the Grant Agency of the Czech Academy of Sciences (grant No. IAA100190612) and by the research plan of the Ministry of Education of the Czech Republic No. MSM 6840770010.

References

1. Galdi, G.P.: An Introduction to the Navier-Stokes initial-boundary value problem. In *Fundamental Directions in Math. Fluid Mechanics*, G. P. Galdi, J. Heywood and R. Rannacher eds. series "Advances in Mathematical Fluid Mechanics", Birkhauser, Basel, 1–98 (2000)
2. Neustupa, J.: Partial regularity of weak solutions to the Navier-Stokes equations in the Class $L^\infty(0, T; L^3(R^3)^3)$. J. Math. Fluid Mech. **1**, 309–325 (1999)
3. Ponce, G., Racke, R., Sideris T.C., Titi E.S.: Global stability of large solutions to the 3D Navier-Stokes equations. Commun. Math. Phys. **159**, 329–341 (1994)
4. Scarpellini, B.: On a family of large solutions of Navier-Stokes. Houston J. Math. **28**(3), 621–647 (2002)
5. Scarpellini, B.: Fast decaying solutions of the Navier-Stokes equations and asymptotic properties. J. Math. Fluid Mech. **6**, 103–120 (2004)
6. Sohr, H.: *The Navier-Stokes Equations.* An elementary functional analytic approach. Birkhäuser advanced texts, Basel-Boston-Berlin (2001)

Streaming Flow Effects in the Nearly Inviscid Faraday Instability

Elena Martín and José M. Vega

Abstract We study the weakly nonlinear evolution of Faraday waves in a two dimensional container that is vertically vibrated. It is seen that the surface wave evolves to a drifting standing wave, namely a wave that is standing in a moving reference frame. In the small viscosity limit, the evolution of the surface waves is coupled to a non-oscillatory mean flow that develops in the bulk of the container. A system of equations is derived for the coupled slow evolution of the spatial phase of the surface wave and the streaming flow. These equations are numerically integrated to show that the simplest reflection symmetric steady state (the usual array of counter-rotating eddies below the surface wave) becomes unstable for realistic values of the parameters. The new states include limit cycles, drifted standing waves and some more complex attractors. We also consider the effect of surface contamination, modelled by Marangoni elasticity with insoluble surfactant, in promoting drift instabilities in spatially uniform standing Faraday waves. It is seen that contamination enhances drift instabilities that lead to various steadily propagating and (both standing and propagating) oscillatory patterns. In particular, steadily propagating waves appear to be quite robust, as in the experiment by Douady et al., Europhysics Letters, pp. 309–315, 1989.

Keywords Faraday waves · Weakly nonlinear evolution · Hydrodynamic instabilities · Surface contamination · Marangoni elasticity · Navier-Stokes numerical simulation

1 Introduction

We consider the parametric excitation of waves at the free surface of a liquid that is being vertically vibrated with a forcing amplitude that exceeds a threshold value. The surface waves that appear (named after Faraday [3]) have attracted a great deal of attention because of the rich variety of non-linear pattern forming phenomena

E. Martín (✉)
E. T. S. Ingenieros Industriales, Universidad de Vigo, Spain
e-mail: emortega@uvigo.es

R. Rannacher, A. Sequeira (eds.), *Advances in Mathematical Fluid Mechanics*,
DOI 10.1007/978-3-642-04068-9_21,

that the Faraday instability exhibits (see [8] and references herein) and that current theoretical approaches fail to explain, particularly in the singular limit of small viscosity. The usual nonlinear amplitude equations used to described this weakly nonlinear regime are obtained from a strictly inviscid formulation and corrected a posteriori by adding some linear dissipation terms [8, 1]. This formulation ignores the presence of the slow non oscillatory mean flow that is driven by the boundary layers at the container walls and free surface and, in the case of a monochromatic wave only predicts standing waves (SW) after onset and fails to reproduce the drifting SWs that have been observed experimentally in annular containers [2, 9]. This paper is organized as follows: in $\mathbb{S}2$ we shall present the systems of equations for the slow time evolution of the surface waves and the mean flow, derived from the full Navier-Stokes equations that described the problems assuming a clean free surface and a contaminated one (surface contamination is likely to be present in water, as in [2], unless care is taken in the experimental set-up); the relevant large-time patterns resulting from the primary bifurcations will be described in $\mathbb{S}3$ as well as the main conclusions.

2 Coupled Amplitude-Mean Flow Equations

We consider a horizontal 2-D liquid layer supported by a vertically vibrating plate (Fig. 1), and use the container's depth h and the gravitational time $\sqrt{h/g}$ for nondimensionalization. The governing equations are the following

$$u_x + v_y = 0, \tag{1}$$

$$u_t + v(u_y - v_x) = -q_x + C(u_{xx} + u_{yy}), \tag{2}$$

$$v_t - u(u_y - v_x) = -q_y + C(v_{xx} + v_{yy}), \tag{3}$$

$$u = v = 0 \quad \text{at} \quad y = -1, \tag{4}$$

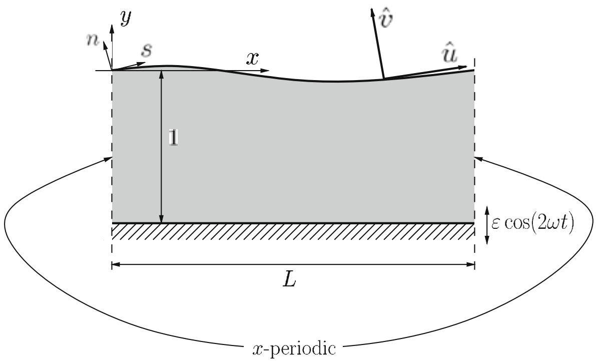

Fig. 1 Sketch of the fluid domain

$$v = f_t + uf_x \text{ (a)}, \quad C^{1/2}(\hat{u}_n + \hat{v}_s + \kappa\hat{u}) = 0 \text{ (b)},$$

$$q - \frac{u^2 + v^2}{2} + 4\omega^2\varepsilon f\cos(2\omega t) - f + T\kappa = 2C\hat{v}_n \text{ (c)} \quad \text{at } y = f, \tag{5}$$

$$u,\ v,\ q \text{ and } f \text{ are } L\text{-periodic in } x, \tag{6}$$

where

$$s = \int_0^x \sqrt{1 + f_x^2}\,dx \quad \text{and} \quad \kappa = \frac{f_{xx}}{(1 + f_x^2)^{3/2}} \tag{7}$$

are an arch length parameter and the curvature of the free surface (defined as $y = f$), respectively, and n is a coordinate along the upward unit normal to the free surface; $\hat{u}$ and $\hat{v}$ are the tangential and normal velocity components at the free surface $y = f$, which are related to the horizontal and vertical components u and v by

$$\hat{u} = \frac{u + f_x v}{\sqrt{1 + f_x^2}}, \quad \hat{v} = \frac{v - f_x u}{\sqrt{1 + f_x^2}}. \tag{8}$$

Equations (1), (2), (3), (4), (5) and (6) formulate the problem when dealing with a clean free surface, with no contamination. Nevertheless, surface contamination is likely to be present in water. The only difference between the equations for a clean surface and the formulation that takes into account the presence of surfactant contamination is the boundary condition (5b), whose right hand side was zero for the clean surface and now accounts for the presence of contaminating surfactants (9), modelled in the simplest way, where the resulting tangential stress includes Marangoni elasticity effects produced by a variation of surface tension with surfactant concentration

$$C^{1/2}(\hat{u}_n + \hat{v}_s + \kappa\hat{u}) = -\gamma\zeta_s. \tag{9}$$

A linear law for the variation of the surface tension T^* with the surfactant concentration ζ^* is assumed $T^*(\zeta^*) = T_0^* + (dT^*/d\zeta_0^*)(\zeta^* - \zeta_0^*)$, where the derivative is calculated at the equilibrium value of the surfactant concentration ζ^*, denoted as ζ_0^*.

The nondimensional surfactant concentration $\zeta = (\zeta^* - \zeta_0^*)/\zeta_0^*$ is given by the conservation equation for an insoluble surfactant

$$\zeta_t + [(1 + \zeta)u]_s = 0 \quad \text{in } 0 < s < s_L, \qquad \zeta(s + s_L, t) = \zeta(s, t). \tag{10}$$

Here, s_L is the length of the free surface in one period and we are neglecting both cubic terms and surface diffusion of the surfactant.

Both dimensionless problems (1), (2), (3), (4), (5) and (6) and (1), (2), (3), (4) and (5a), (5c) and (6), (9), (10) depend on the following nondimensional parameters: the forcing frequency $2\omega = 2\omega^*\sqrt{h/g}$ and amplitude $\varepsilon = \varepsilon^*/h$, the ratio of viscous to gravitational effects $C = \mu/(\varrho\sqrt{gh^3})$ (ϱ = density, μ = viscosity), the Bond number $T^{-1} = \varrho gh^2/T_0^*$ (T_0^* = surface tension at equilibrium), the horizontal aspect ratio $L = L^*/h$ (L^* = horizontal length of the domain), and only for the contaminated free surface problem, the Marangoni elasticity number $\gamma = \zeta_0^*(dT^*/d\zeta_0^*)C^{1/2}/(\mu\sqrt{gh})$.

We shall consider small, nearly-resonant solutions at small viscosity and conveniently rescaled Marangoni elasticity, i.e.,

$$|u|+|v|+|q|+|f|+|\zeta| \ll 1, \quad \varepsilon \ll 1, \quad |\omega-\omega_0| \ll 1, \quad C \ll 1, \quad \gamma \sim 1. \tag{11}$$

The assumption that $C \ll 1$ is reasonable for not too viscous fluids in not too thin layers. The assumption $\gamma \sim 1$ is made for the Marangoni elasticity to have a significant effect both in the damping ratio of the surface waves and in the streaming flow (see [7] for more details). Frequency ω_0 in (11) is a natural frequency in the inviscid limit ($C = 0$). As explained in [6] and [5], the solution can be expanded as an oscillating first part caused by the oscillatory inviscid modes (with a $\mathcal{O}(1)$ frequency and a $\mathcal{O}(\sqrt{C})$ decay rate) and a slow non-oscillatory secondary part generated by the viscous modes (with a $\mathcal{O}(C)$ decay rate), that produce the mean flow. The solution in the bulk region, outside the boundary layers that appear at the free surface and the bottom plate, is written as follows

$$\begin{aligned}
u &= U_0(y)e^{i\omega t}[A(t)e^{ikx} - B(t)e^{-ikx}] + c.c. + u^m(x,y,t) + \cdots, \\
v &= iV_0(y)e^{i\omega t}[A(t)e^{ikx} + B(t)e^{-ikx}] + c.c. + v^m(x,y,t) + \cdots, \\
q &= Q_0(y)e^{i\omega t}[A(t)e^{ikx} + B(t)e^{-ikx}] + c.c. + q^m(x,y,t) + \cdots, \\
f &= e^{i\omega t}[A(t)e^{ikx} + B(t)e^{-ikx}] + c.c. + f^m(x,t) + \cdots, \\
\zeta &= \Xi_0 e^{i\omega t}[A(t)e^{ikx} + B(t)e^{-ikx}] + c.c. + \zeta^m(x,t) + \cdots,
\end{aligned} \tag{12}$$

where $c.c$ stands for the complex conjugate, $k = 2m\pi/L$ (with m a positive integer) is the horizontal wave number and U_0, V_0 and Q_0 are the corresponding inviscid eigenfunctions

$$U_0 = -\frac{kQ_0}{\omega_0}, \quad V_0 = \frac{Q_{0y}}{\omega_0}, \quad Q_0 = \frac{\omega_0^2 \cosh k(y+1)}{k \sinh k}, \tag{13}$$

$$\omega_0^2 = k(1+Tk^2)\tanh k. \tag{14}$$

Note that the expansion for the surfactant concentration variable (12e) is only necessary for the contaminated problem, where

$$\Xi_0 = (k\omega_0\sqrt{i\omega_0})/(\tanh k(\omega_0\sqrt{i\omega_0} - ik^2\gamma)) \tag{15}$$

can not be obtained in the inviscid approximation. The terms displayed above correspond to the only surface mode that is sub-harmonically excited by the external forcing and the mean flow, that will be denoted hereinafter by the superscript m. Dependence of the complex amplitudes A and B on x is ignored for simplicity, see [10] and [4] for a more complicated analysis including spatial wave modulations. The weakly nonlinear analysis requires the amplitudes A and B to be small and depend slowly on time $|A'| \ll |A| \ll 1$, $|B'| \ll |B| \ll 1$

If we insert expansions (12a), (12b), (12c) and (12d) into the governing equations for the clean free surface case, and (12a), (12b), (12c), (12d) and (12e) into the equations for the contaminated free surface problem, take into account the boundary layers at the free surface and the bottom of the container and apply solvability conditions, the following equations for the evolution of the complex amplitudes are obtained

$$A' = [-d_1 - id_2 + \mathrm{i}\alpha_3|A|^2 - \mathrm{i}\alpha_4|B|^2 - \mathrm{i}\frac{\alpha_6}{L}\int_{-1}^{0}\int_{0}^{L} g(y)u^m\,dxdy]A + \mathrm{i}\varepsilon\alpha_5\bar{B}, \tag{16}$$

$$B' = [-d_1 - id_2 + \mathrm{i}\alpha_3|B|^2 - \mathrm{i}\alpha_4|A|^2 + \mathrm{i}\frac{\alpha_6}{L}\int_{-1}^{0}\int_{0}^{L} g(y)u^m\,dxdy]B + \mathrm{i}\varepsilon\alpha_5\bar{A}, \tag{17}$$

and depend on the mean flow through a non local term. See [6] and [7] for a more detailed derivation of the equations above and for the expressions of the coefficients and the function $g(y)$ in the non contaminated and contaminated case, respectively.

The solution of Eqs. (16) and (17) always relaxes to a standing wave ($|A| = |B| = R_0$) of the form

$$f(x,t) = 4R_0\cos(\omega t + \varphi_0)\cos[k(x - \psi)] \tag{18}$$

with constant amplitude R_0 (which depends on the amplitude of the applied forcing) and spatial phase $\psi(t)$ that remains coupled to the streaming flow through the equation

$$\psi' = \frac{\alpha_6}{kL}\int_{-1}^{0}\int_{0}^{L} g(y)u^m\,dxdy. \tag{19}$$

Ignoring the initial transient, taking into account the last result in expansions (12a), (12b), (12c), (12d) and (12e) and introducing these expressions in the two cases, we obtain the following equations for the mean flow outside the two boundary layers

$$\tilde{u}_x + \tilde{v}_y = 0, \tag{20}$$

$$\frac{\partial\tilde{u}}{\partial\tau} + \tilde{v}(\tilde{u}_y - \tilde{v}_x) = -\tilde{q}_x + Re^{-1}(\tilde{u}_{xx} + \tilde{u}_{yy}), \tag{21}$$

$$\frac{\partial\tilde{v}}{\partial\tau} - \tilde{u}(\tilde{u}_y - \tilde{v}_x) = -\tilde{q}_y + Re^{-1}(\tilde{v}_{xx} + \tilde{v}_{yy}), \tag{22}$$

$$\tilde{u},\ \tilde{v} \text{ and } \tilde{q} \quad \text{are } x\text{-periodic, of period } L = 2m\pi/k, \tag{23}$$

$$\frac{d\psi}{d\tau} = \frac{1}{L}\int_{-1}^{0}\int_{0}^{L} G(y)\tilde{u}(x,y,\tau)dxdy, \quad G(y) = \frac{2k\cosh 2k(y+1)}{\sinh 2k} \tag{24}$$

where the bottom and free surface horizontal velocities are determined from one of the following additional conditions, (25) and (26) for the clean free surface case and (27) and (28) for the contaminated free surface problem

$$\tilde{u} = -\sin[2k(x-\psi)], \qquad \tilde{v} = 0 \quad \text{at } y = -1, \tag{25}$$

$$\tilde{u}_y = 0, \quad \tilde{v} = 0, \quad \text{at } y = 0, \tag{26}$$

$$\tilde{u} = -(1-\Gamma)\sin[2k(x-\psi)], \qquad \tilde{v} = 0 \quad \text{at } y = -1, \tag{27}$$

$$\tilde{u} = -\Gamma \sin[2k(x-\psi)] + \tilde{u}_0(\tau), \quad \tilde{v} = 0, \quad \int_0^L \tilde{u}_y \, dx = 0, \quad \text{at } y = 0, \tag{28}$$

where, for convenience, we have rescale time and mean flow variables as

$$\tau = ReCt, \quad \tilde{u} = \frac{u^m}{ReC}, \quad \tilde{v} = \frac{v^m}{ReC}, \quad \tilde{q} = \frac{q^m}{(ReC)^2}, \tag{29}$$

with the effective mean flow Reynolds number defined as follows

$$Re = \frac{2R_0^2}{C}(\alpha_7 + \alpha_8), \tag{30}$$

with

$$\alpha_7 = \frac{3\omega_0 k}{\sinh^2 k}, \quad \alpha_8 = \frac{\omega_0 k}{\tanh^2 k}\left(\frac{4\gamma k^2}{\omega_0\sqrt{i\omega_0} - i\gamma k^2} + c.c + \frac{3\gamma^2 k^4}{|\omega_0\sqrt{i\omega_0} - i\gamma k^2|^2}\right). \tag{31}$$

where, for the clean surface case, γ must be substituted by 0 in expression (31). Equations for the clean case (20), (21), (22), (23), (24), (25) and (26), hereinafter referred to as MFClean, depend on the values of the 3 parameters (Re, k, m), while the contaminated free surface problem defined by (20), (21), (22), (23) and (24), (27) and (28), hereinafter MFContam, depends on an additional contamination parameter Γ that measures the relative effect of contamination in the generation of the streaming flow

$$\Gamma = \Gamma(k, T, \gamma) \equiv \frac{\alpha_8}{\alpha_7 + \alpha_8}, \tag{32}$$

and is plotted *vs.* the wavenumber k in Fig. 2(a) for the indicated values of γ for $T = 7.42 \cdot 10^{-4}$, that corresponds to the inverse of the Bond number for a 10 cm depth water container. It can be seen that for deep water problems, namely $k > \pi$, the contamination parameter is of the order of 1, even for quite small values of the Marangoni number γ. The maximum values of Γ are plotted in Fig. 2(b).

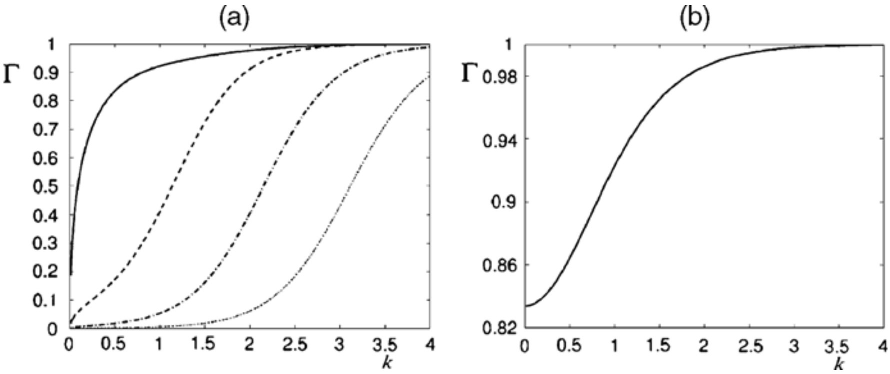

Fig. 2 The contamination parameter Γ. (**a**) Γ vs. k for $T = 7.42 \cdot 10^{-4}$ and: (——) $\gamma = 1$, (− − −) $\gamma = 0.1$, (− · − · −) $\gamma = 0.01$, and (· · · · ·) $\gamma = 10^{-3}$. (**b**) The maximum value of Γ vs. k for $T = 7.42 \cdot 10^{-4}$ and varying γ

3 Results and Conclusions

Problems MFClean and MFContam are both numerically solved to show that for small values of the effective mean flow Reynolds number Re, the solution relaxes to the usual standing wave (SW) with $\psi' = 0$ and for the mean flow corresponds to pairs of steady counterrotating eddies as the ones plotted in Fig. 3(a) for the clean free surface problem and (4a), (4b) and (4c) for the contaminated free surface case and the indicated values of the contamination parameter Γ. These steady solutions are $L/2$-symmetric and since they are also reflection symmetric in x, the integral (24) vanishes and the streaming flow does not affect the surface SW.

For the MFClean problem, if Re exceeds a threshold value, indicated in Fig. 5(a), this steady solution becomes unstable always through a Hopf bifurcation and a branch of time periodic solutions (PSW) appears, that produces a time periodic drift of the SW with no net drift on the free surface. These periodic solutions resemble the so called compression modes that have been observed in annular containers [2, 9] and cannot be obtained with the usual amplitude equations that ignore the coupling with the streaming flow. For some values of k and L there are some additional

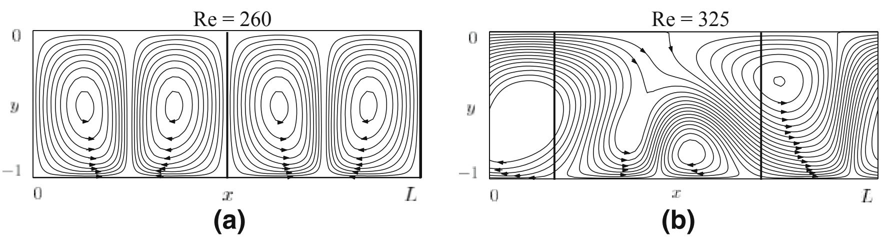

Fig. 3 Streamlines of the streaming flow of MFClean for $k = 2.37$, $L = 2.65$ ($m = 1$) and (**a**) Re = 260 and (**b**) Re = 325 (in moving axes $x - \psi'\tau$ with constant drift velocity). Thick vertical lines correspond to the nodes of the surface waves given by (18)

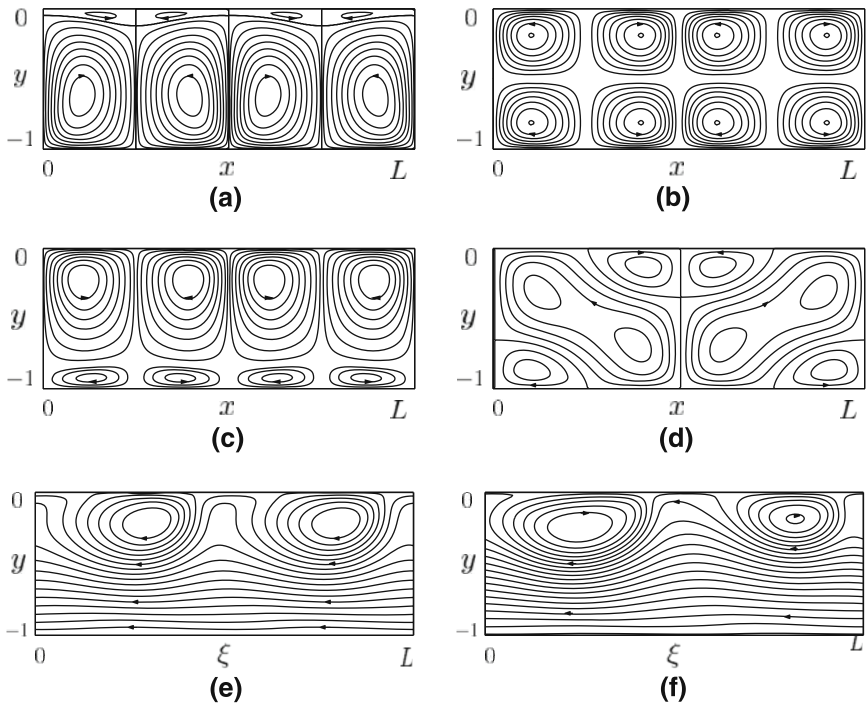

Fig. 4 Streamlines of MFContam, for $k = 2.37$, $L = 2.65$ $(m = 1)$, and (Re, Γ): (**a**) (200, 0.1), (**b**) (160, 0.5), (**c**) (60, 0.9), (**d**) (200, 0.5), (**e**) (200, 0.9) in moving axes $\xi = x - \psi'\tau$ with constant drift velocity $\psi' = 0.32$ and $\tilde{u_0} = 0.49$, (**f**) (600, 0.9) in moving axes with constant drift velocity $\psi' = 0.27$ and $\tilde{u_0} = 0.53$

bifurcations to drifted SWs, namely travelling waves TWs, that move at a constant speed like the one shown in Fig. 3(b), and more complex oscillatory attractors, but these depend strongly on k and L (see [6] for more details). However, drift instabilities were quite robust in the experiment of Douady et. al. [2] (Fauve, personal communication, 2003) and the MFclean problem does not seem to reproduce this feature.

In order to mimic the behaviour of tap water (used in the experiment [2]) the MFContam problem is solved to obtain that the primary instability of the basic SW (SW($L/2$)) depends on the value of the contamination parameter. In Fig. 5(b) it can be seen that for small values of Γ the instability takes place through a Hopf bifurcation and for quite small values of Γ the contamination effect seems to stabilize the basic SWs (note that the critic Reynolds number for the clean case for the same values of k and L is marked with a large point in the horizontal axis of Fig. 5(b)).

This is because the only effect of contamination in this regime on the mean flow is to replace the free stress boundary condition at the free surface by a no-slip boundary condition, which reduces the strength of the mean flow. For an intermediate value of Γ a symmetry breaking bifurcation to another type of SW no longer $L/2$ symmetric

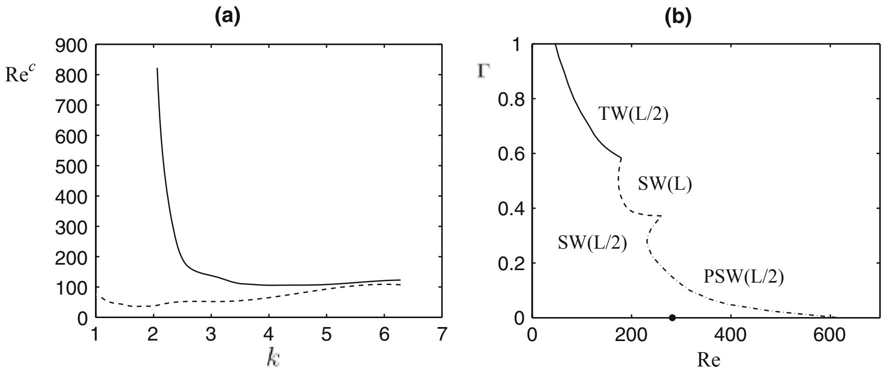

Fig. 5 The primary instability of the basic SW for: (a) MFClean for different wave numbers k and (b) MFContam, for $k = 2.37$, $L = 2.65$ ($m = 1$). Figure 5(**a**): The bifurcation is always a Hopf bifurcation (——) ((— — —) shows the parity breaking bifurcation that takes place only if the coupling between the surface wave and the mean flow (24) it is ignored). Figure 5(**b**): The bifurcation is either a Hopf bifurcation (— · — · —) if $0 < \Gamma < 0.372$, a ($L/2$)-symmetry breaking bifurcation (— — —) if $0.372 < \Gamma < 0.584$, or a parity breaking bifurcation (——) if $0.584 < \Gamma < 1$

(SW(L)) occurs, see Fig. 4(d) as an example. For larger values of the contamination parameter Γ the basic SW($L/2$) destabilizes through a parity breaking bifurcation that leads to TWs (TW($L/2$)) whose streamlines for the mean flow in a moving reference frame are similar to the one plotted in 4(e). Note that the mean flow is still $L/2$-symmetric. In contrast with the clean case, these TWs appear in a primary bifurcation and are quite robust (remain unchanged for larger domains and appear for all values of the wave number we have checked). Thus, contamination effects seem to play an important role in the surface waves dynamics. For bigger values of the Reynolds number Re different secondary instabilities are obtained, among them another type of TWs with no $L/2$-symmetric mean flow (Fig. 4(f)), pulsating travelling waves and even complex attractors ([7]). For all these states which are not steady SW, the coupling with the mean flow is an essential ingredient that should not be ignored.

Acknowledgments This work was supported by the National Aeronautics and Space Administration (Grant NNC04GA47G) and the Spanish Ministry of Education (Grant MTM2004-03808)

References

1. Cross, M. and Hohenberg, P.C.: Pattern formation outside of equilibrium. Rev. Mod. Phys., **65**, pp. 851–1112 (1993)
2. Douady, S. Fauve, S. and Thual, O.: Oscillatory phase modulation of parametrically forced surface waves. Europhys. Lett., **10**, pp. 309–315 (1989)
3. Faraday, M.: On the forms and states assumed by fluids in contact with vibrating elastic surfaces. Phil. Trans. R. Soc. Lond., **121**, pp. 319–340 (1831)

4. Lapuerta, V., Martel, C. and Vega, J.M.: Interaction of nearly-inviscid Faraday waves and mean flows in 2-D containers of quite large aspect ratio. Physica D, **173**, pp. 178–203 (2002)
5. Martel C. and Knobloch, E.: Damping of nearly-inviscid water waves. Phys. Rev. E, **56**, pp. 5544–5548 (1997)
6. Martín, E., Martel, C. and Vega, J.M.: Drift instability of standing Faraday waves. J. Fluid Mech., **467**, pp. 57–79 (2002)
7. Martín, E. and Vega, J.M.: The effect of surface contamination on the drift instability of standing Faraday waves. J. Fluid Mech., **546**, pp. 203–225 (2006)
8. Miles, J. and Henderson D.: On the forms and states assumed by fluids in contact with vibrating elastic surfaces. Annu. Rev. Fluid Mech., **22**, pp. 143–165 (1990)
9. Thual, O., Douady, S. and Fauve, S.: Intabilities and Nonequilibrium Structures II. Ed. Tirapegui, E. and Villaroel, D., Kluwer, Dordrecht p. 227 (1989)
10. Vega, J.M., Knobloch, E. and Martel, C.: Nearly inviscid Faraday waves in annular containers of moderately large aspect ratio. Physica D, **154**, pp. 147–171 (2001)

The Dirichlet Problems for Steady Navier-Stokes Equations in Domains with Thin Channels

Yuliya V. Namlyeyeva, Šarka Nečasová, and Igor Igorievich Skrypnik

Abstract We consider a sequence of the Dirichlet problems for steady Navier-Stokes equations in domains perforated with channels $\Omega_s = \Omega \setminus \bigcup_{i=1}^{I(s)} \mathcal{F}_i^{(s)}$, where $\mathcal{F}_i^{(s)}$, $i = 1, \ldots, I(s)$, are closed subsets of bounded domain $\Omega \subset \mathbf{R}^3$ contained in small neighborhoods of some lines. While the number $I(s)$ of channels tends to infinity as $s \to \infty$, these small sets $\mathcal{F}_i^{(s)}$ are becoming thinned. We study the asymptotic behavior of solutions $u_s(x)$ to problems in domains with thin channels as $s \to \infty$. We find conditions on perforated domains under which sequence of solutions $\{u_s(x)\}_{s=1}^{\infty}$ converges to solution of homogenized problem as $s \to \infty$. The proof is based on the asymptotic expansion of $u_s(x)$ and on pointwise and integral estimates of auxiliary functions which are solutions of model boundary value problems.

Keywords Homogenization · Navier-Stokes equations · Perforated domains

1 Introduction and Formulation of the Problem

Processes in locally inhomogeneous media, the local properties of which are subject to sharp small scale changes in the space, are of great interest in various fields of science. Various methods were applied to the investigation of such problems. We mention one of the most famous micro-macro approach which was used for homogenization of processes in porous periodic media, [21]. In particular, there were constructed the asymptotic expansions for flow in small channels of solid porous body and for moving of composite of solid elastic bodies and viscous fluids. It is known that it is possible to get **Darcy's law** in the limit. By the Darcy's law a slow fluid flowing through a rigid medium can be modelled. Ene and Sanchez-Palencia seems to be first to give a derivation of it, from the Stokes system, using multiscale expansion [8]. This derivation was made rigorously by Tartar in [24]. This result was generalized by many authors and we mention one generalization, which was done

Š. Nečasová (✉)
Mathematical Institute of Academy of Sciences, 11567 Prague 1, Czech Republic
e-mail: matus@math.cas.cz

R. Rannacher, A. Sequeira (eds.), *Advances in Mathematical Fluid Mechanics*,
DOI 10.1007/978-3-642-04068-9_22,

by Allaire [1] and to random statistically porous medium by Beliaev and Kozlov [3]. Also we would like to mention the fundamental work of Jikov, Kozlov and Oleinik [12] and several fundamental works which were done by Jäger, Mikelic [11], Mikelic at el. [10, 5]. If a rigid part of the porous medium Ω has the critical size, much smaller than $O(1)$, then it is possible to get **Brinkman's law**, (in detail, see [2]). In many applications the solid part is supposed to be elastic. In this case the effective filtration law is known as **Biot's law** [7].

Different problems in perforated domains with non periodic structure, corresponding to the case of Brinkman's law, were considered in [17, 18, 22]. Firstly, elliptic systems of higher order in domains with fine-grained boundary were studied in [17] using potential theory and variational methods. This approach was applied, in particular, to the Dirichlet problems for Navier-Stokes equations in domains with fine-grained boundary (see [13, 14]). Another approach was developed by I.V.Skrypnik for nonlinear elliptic and parabolic equations (see, for example, [22, 23] and reference therein). This situation is essentially different from the study of linear problems. It is necessary to have some strong convergence of gradients of solutions of nonlinear problems in perforated domains to construct the homogenized boundary value problem. The proof of such strong convergence is based on the special asymptotic expansion. In this case solutions of nonlinear problems in perforated domains are approximated by solution of appropriate model nonlinear problems near small sets of perforation. The main role in construction of the homogenized boundary value problems is played by pointwise and integral estimates of solutions to model problems. This approach, which gives us possibility to show the strong convergence of gradients of solutions, was applied to the homogenization of the Navier-Stokes equation with Dirichlet's condition in domains with fine-grained boundary ([19]). In this paper we consider the problem of homogenization of the Navier-Stokes equations with the Dirichlet boundary condition in sequence of domains with thin channels.

To begin with we formulate the state of the problem. Let $\varrho(x, G)$ be the distance from a point x to a set $G \subset \mathbf{R}^3$. Let us define the ε-neighborhood $\mathcal{U}(G, \varepsilon)$ of the set G by

$$\mathcal{U}(G, \varepsilon) := \{x \in \mathbf{R}^3 : \varrho(x, G) < \varepsilon\},$$

for every $\varepsilon > 0$. Let Ω be a bounded domain in $\mathbf{R}^3$. For every fixed number $s \in \mathbf{N}$ we consider a finite number $I(s)$ of lines $l_i^{(s)} \subset \overline{\Omega}$, positive numbers $d_i^{(s)}$, and closed domains $\mathcal{F}_i^{(s)}$, such that

$$\mathcal{F}_i^{(s)} \subset \mathcal{U}(l_i^{(s)}, d_i^{(s)}), \quad i = 1, \dots, I(s).$$

The number $I(s)$ tends to infinity as $s \to \infty$. Let us denote by Ω_s, $s \in \mathbf{N}$, the following sequence of perforated domains

$$\Omega_s = \Omega \setminus \bigcup_{i=1}^{I(s)} \mathcal{F}_i^{(s)}.$$

In the sequence of domains Ω_s, perforated with channels, we study the following problems

$$\begin{gathered} \nu \Delta \mathbf{u}^{(s)} - (\mathbf{u}^{(s)} \cdot \nabla)\, \mathbf{u}^{(s)} = \nabla p^{(s)} + \mathbf{f}, \\ \operatorname{div} \mathbf{u}^{(s)} = 0, \quad x \in \Omega_s, \\ \mathbf{u}^{(s)}|_{\partial\Omega_s} = 0, \end{gathered} \tag{1}$$

where $p^{(s)}(x)$ is a pressure, $\mathbf{f}(x) \in L_2(\Omega)^3$ is a force, $\nu \in \mathbf{R}^1_+$.
In study of this problem the following questions arise:

- How to establish conditions under which the solutions of the problem (1) converge as $s \to \infty$?
- How to determine a boundary value problem for the limit function?

Let us introduce the following spaces

$$\begin{gathered} H(\Omega_s) := \{\mathbf{u}_s \in W_0^{1,2}(\Omega_s)^3 : \operatorname{div} \mathbf{u}_s = 0,\ x \in \Omega_s\}, \\ H(\Omega) := \{\mathbf{u} \in W_0^{1,2}(\Omega)^3 : \operatorname{div} \mathbf{u} = 0,\ x \in \Omega\}. \end{gathered}$$

Denote by $\mathbf{D}[u]$ the symmetrized gradient of the velocity

$$\mathbf{D}[u] = \frac{1}{2}\left(\frac{\partial u_i}{\partial x_j} + \frac{\partial u_j}{\partial x_i}\right).$$

We introduce a weak formulation of problem (1).

Definition 1 We say that $\mathbf{u}^{(s)} \in H(\Omega_s)$ is a weak solution of problem (1) if the following integral identity

$$\int_{\Omega_s} \left(\nu \mathbf{D}[\mathbf{u}^{(s)}] \cdot \mathbf{D}[\boldsymbol{\varphi}^{(s)}] - (\mathbf{u}^{(s)} \cdot \nabla)\boldsymbol{\varphi}^{(s)} \cdot \mathbf{u}^{(s)}\right) dx = -\int_{\Omega_s} (\mathbf{f}, \boldsymbol{\varphi}^{(s)}) dx \tag{2}$$

is satisfied for every $\boldsymbol{\varphi}^{(s)} \in H(\Omega_s)$.

Analogously to [16] it is possible to show the existence of the solution to problem (1) and to prove the following a priory estimate

$$\|\mathbf{u}^{(s)}\|_{H(\Omega_s)} \le C_0 \|\mathbf{f}\|_{L_2(\Omega_s)^3},$$

with a positive constant C_0 not depending on s. Extending the function $\mathbf{u}^{(s)} \in H(\Omega_s)$ into $\bigcup_{i=1}^{I(s)} \mathcal{F}_i^{(s)}$ by zero and keeping the same notation, we obtain the function $\mathbf{u}^{(s)} \in H(\Omega)$ which satisfies the following estimate

$$\|\mathbf{u}^{(s)}\|_{H(\Omega)} \le C_0 \|\mathbf{f}\|_{L_2(\Omega)^3}.$$

Then, there exists a subsequence of the sequence $\{\mathbf{u}^{(s)}\}_{s=1}^{\infty}$ converging to a function from $H(\Omega)$ weakly in $H(\Omega)$ and strongly in $L_p(\Omega)^3$ ($p < 6$) as $s \to \infty$. We denote this weak limit by $\mathbf{u}^{(0)} \in H(\Omega)$.

Remark 1 Hereafter we denote by $C,\ C_j,\ K_j,\ j = 0, 1, \ldots,$ different positive constants depending on Ω and not depending on i and s.

2 Assumptions on the Sequence of Perforated Domains $\{\Omega_s\}_{s=1}^{\infty}$ and Formulation of the Main Result

We denote by $B(x, r)$ a ball of a radius r with center at a point x. We suppose that there exist positive constants $\lambda,\ C_1,\ C_2$, not depending on i and s, and positive numbers $r_i^{(s)},\ s \in \mathbf{N},\ i = 1, \ldots, I(s)$, such that the following conditions are satisfied:

- (**i**) $\lim\limits_{s\to\infty} r^{(s)} = 0$, *where* $r^{(s)} = \max\limits_{1\le i\le I(s)} r_i^{(s)}$,
  $(2 + C_1)d_i^{(s)} \le r_i^{(s)},\ \forall s \in \mathbf{N},\ i = 1, \ldots, I(s)$,
  $$\sum_{i=1}^{I(s)} \frac{\ln^{-2}\frac{1}{d_i^{(s)}}}{(r_i^{(s)})^2} \le C_2;$$
- (**ii**) *there exists a finite number* $\mathcal{P}(i, s)$ *of points* $z_{i,p}^{(s)},\ l = 1, \ldots, \mathcal{P}(i, s)$, *such that for every* $t_i^{(s)} \in [d_i^{(s)}, r_i^{(s)}]$ *the inclusion*
  $$\mathcal{U}\left(T_i^{(s)}(\{t_i^{(s)}\}), t_i^{(s)}\right) \subset \bigcup_{p=1}^{\mathcal{P}(i,s)} B(z_{i,p}^{(s)}, \lambda t_i^{(s)}),$$
  holds for every $s \in \mathbf{N},\ i = 1, \ldots, I(s)$, *where*
  $$T_i^{(s)}(\{t_i^{(s)}\}) = \mathcal{U}(l_i^{(s)}, t_i^{(s)}) \bigcap \left\{ \bigcup_{j\neq i} \mathcal{U}(l_j^{(s)}, t_j^{(s)}) \bigcup \partial\Omega \right\},$$
  $$\mathcal{U}(l_i^{(s)}, r_i^{(s)}) \subset \Omega, \quad B(z_{i,p}^{(s)}, \lambda r_i^{(s)}) \subset \Omega;$$
- (**iii**) *there exists a number* $p_0 \in \mathbf{N}$ *such that for every* $s \in \mathbf{N}$ *the orders of families of sets*
  $$\{\mathcal{U}(l_i^{(s)}, \ln^{-1}\frac{1}{r_i^{(s)}}), \quad i = 1, \ldots, I(s)\},$$
  $$\{B(z_{i,p}^{(s)}, \lambda \ln^{-1}\frac{1}{r_i^{(s)}}), \quad i = 1, \ldots, I(s), \quad p = 1, \ldots, \mathcal{P}(i, s)\},$$
  do not exceed p_0.

The order p_0 of families of sets in condition (**iii**) we understand in such sense that p_0 is the largest positive number for which $(p_0 + 1)$ sets from these families with common points exist.

We suppose the following conditions on regularity of the lines $l_i^{(s)}$, $s \in \mathbf{N}$, $i = 1, \dots, I(s)$, also:

- (**iv**) *there exists a diffeomorphisms* $g_i^{(s)} : \mathcal{U}(l_i^{(s)}, 1) \to g_i^{(s)}(\mathcal{U}(l_i^{(s)}, 1)) \subset \mathbf{R}^3$ *from class* C^1*, such that the following inclusion holds*

$$g_i^{(s)}(l_i^{(s)}) \subset \{y \in \mathbf{R}^3 : \; y_1 = y_2 = 0\};$$

- (**v**) *there exists a positive constant* κ*, not depending on* i *and* s*, such that the following inequalities*

$$\left| \frac{\partial g_i^{(s)}(x)}{\partial x} \right| \le \kappa, \quad det \frac{D g_i^{(s)}(x)}{Dx} \ge \kappa^{-1},$$

are satisfied for every $x \in \mathcal{U}(l_i^{(s)}, 1)$*, where* $\frac{D g_i^{(s)}(x)}{Dx}$ *is the Jacobi matrix of* $g_i^{(s)}(x)$ *at a point* x.

Remark 2 From condition (**v**) we derive that there exists a positive constant C_3, depending on n and κ only, such that the following inequality

$$\frac{1}{C_3}|x_1 - x_2| \le |g_i^{(s)}(x_1) - g_i^{(s)}(x_2)| \le C_3|x_1 - x_2| \tag{3}$$

is valid for every $x_1, x_2 \in \mathcal{U}(l_i^{(s)}, 1)$.

To formulate an additional condition for the sets $\mathcal{F}_i^{(s)}$ that guarantees the possibility to construct an averaged problem, we define auxiliary functions which are solutions of an appropriate model problem in every domain $B(0, 1)\backslash \mathcal{F}_i^{(s)}$, $i = 1, \dots, I(s)$. We define $\mathbf{v}^k(x; G, \mathcal{F})$ as a solution of the following problem

$$\begin{gathered} \Delta \mathbf{v}^k(x) = \nabla p^k(x), \\ \operatorname{div} \mathbf{v}^k(x) = 0, \;\; x \in \mathcal{U}(G, 1/2) \setminus \mathcal{F}, \\ \mathbf{v}^k(x)|_{\partial \mathcal{F}} = \mathbf{e}^k, \;\; \mathbf{v}^k(x)|_{\partial \mathcal{U}(G,1/2)} = 0, \end{gathered} \tag{4}$$

for every open set $G \subset \mathbf{R}^3$ and a closed set $\mathcal{F} \subset G$ where $\mathbf{e}^k$ is the unit vector of axis $0X_k$, $k = 1, 2, 3$.

We suppose that for every $s \in \mathbf{N}$ the inequality $r^{(s)} \le 1/2$ is valid. We define sequences of numbers $\{\lambda_s\}$, $\{\mu_s\}$

$$\lambda_s = \ln^{-1} \frac{1}{r^{(s)}}, \;\; \mu_s = \ln \ln \frac{1}{r^{(s)}}. \tag{5}$$

These sequences satisfy the following properties

$$\lim_{s\to\infty} \lambda_s = 0,\ \lim_{s\to\infty} \mu_s = \infty,\ \lim_{s\to\infty} \lambda_s^2 \mu_s = 0$$

which were shown in [22]. For $s \in \mathbf{N}, \dots,\ i = 1, \dots, I(s)$, we introduce subsets of indices

$$I'(s) := \left\{ i : i = 1, \dots, I(s),\ \ln^{-1} \frac{1}{d_i^{(s)}} \geq [r_i^{(s)}]^2 \mu_s \right\},$$
$$I''(s) := \left\{ i : i = 1, \dots, I(s), \ln^{-1} \frac{1}{d_i^{(s)}} < [r_i^{(s)}]^2 \mu_s \right\},$$

and a sequence of numbers $\varepsilon_i^{(s)}$ by the following relations

$$\varepsilon_i^{(s)} := 2C_3^2 [r_i^{(s)}]^2 \mu_s \ \text{ if } \ i \in I''(s), \tag{6}$$

where C_3 is the constant from (3). For every $s \in \mathbf{N},\ i \in I''(s)$, we consider the following sets

$$L_i^{(s)} := \left\{ x \in l_i^{(s)} :\ \varrho \left(x, T_i^{(s)}(\{2\varepsilon_i^{(s)}\}) \right) \geq 2\varepsilon_i^{(s)} \right\} = L_{i,1}^{(s)} \bigcup L_{i,2}^{(s)}.$$

We denote by $L_{i,1}^{(s)}$ the union of all connected sets from $L_i^{(s)}$ which lengths are not less than $\lambda_s^{-1}\varepsilon_i^{(s)}$. The closed set $L_{i,2}^{(s)}$ consists of all curve segments of $l_i^{(s)}$ such that their lengths are less or equal $\lambda_s^{-1}\varepsilon_i^{(s)}$. We divide every curvilinear segment from the set $L_{i,1}^{(s)}$ on the finite number $\mathcal{M}(i, s)$ of segments with equal lengths such that

$$L_{i,1}^{(s)} = \bigcup_{m=1}^{\mathcal{M}(i,s)} L_i^{(s)}(m),\ \ (2\lambda_s)^{-1}\varepsilon_i^{(s)} \leq |L_i^{(s)}(m)| \leq \lambda_s^{-1}\varepsilon_i^{(s)},$$

where $|L_i^{(s)}(m)|$ is the length of curvilinear segment $L_i^{(s)}(m)$. Let $\alpha_{i,m}^{(s)},\ \beta_{i,m}^{(s)}$ be endings of curvilinear piece $L_i^{(s)}(m)$, for every $s = 1, 2, \dots,\ i \in I''(s),\ m = 1, \dots, \mathcal{M}(i, s)$. For some constant γ we use the following notations:

$$G_{i,m}^{(s)}(\gamma) := \mathcal{U}(L_i^{(s)}(m), 2\varepsilon_i^{(s)}) \setminus \overline{\{B(\alpha_{i,m}^{(s)}, \gamma\varepsilon_i^{(s)}) \bigcup B(\beta_{i,m}^{(s)}, \gamma\varepsilon_i^{(s)})\}}, \tag{7}$$
$$\mathbf{v}_{k,i,m}^{(s)}(x) := \mathbf{v}^k(x; G_{i,m}^{(s)}(\gamma), \mathcal{F}_i^{(s)} \bigcap G_{i,m}^{(s)}(\gamma)),$$
$$C_m^{k\ell}(\mathcal{F}_i^{(s)}) := \int\limits_{\mathcal{U}(G_{i,m}^{(s)}(\gamma),1/2)} \mathbf{D}[\mathbf{v}_{k,i,m}^{(s)}] \cdot \mathbf{D}[\mathbf{v}_{\ell,i,m}^{(s)}]\, dx, \quad k, \ell = 1, \dots, n,$$

for every $s \in \mathbf{N}, i = 1, \ldots, I(s), m = 1, \ldots, \mathcal{M}(i, s)$. We assume that the following additional condition is satisfied:

- (**vi**) *There exists a continuous nonnegative matrix* $||c^{k\ell}(x)||_{k,\ell=1}^n$ *such that for every ball* $B \subset \Omega$ *we have*

$$\lim_{s\to\infty} \sum_{(i,m)\in I_s(B)} C_m^{k\ell}(\mathcal{F}_i^{(s)}) = \int_B c^{k\ell}(x)\,dx.$$

By $I_s(B)$ *we denote the set of all pairs* $(i, m),\ i \in I''(s),\ m = 1, \ldots, \mathcal{M}(i, s)$, *such that* $x_{i,m}^{(s)} \in B$, *where* $x_{i,m}^{(s)}$ *is middle of the curvilinear piece* $L_i^{(s)}(m)$.

Under conditions (**i**)–(**vi**) on the sequence of perforated domains, it is constructed the following averaged problem in a domain Ω

$$\begin{gathered} \nu\Delta\mathbf{u}(x) - (\mathbf{u}\cdot\nabla)\,\mathbf{u} - \nu c(x)\mathbf{u}(x) = \nabla p(x) + \mathbf{f}(x), \\ \operatorname{div}\mathbf{u}(x) = 0, \quad x \in \Omega, \\ \mathbf{u}(x)|_{\partial\Omega} = 0, \end{gathered} \tag{8}$$

where $c(x) = \|c^{kl}(x)\|_{k,l=1}^n$ is the continuous nonnegative matrix from condition (**vi**).

A weak solution of the problem (8) we understand in the sense of the following definition:

Definition 2 We say that $\mathbf{u}(x) \in H(\Omega)$ is a weak solution of problem (8), if the integral identity

$$\int_\Omega (\nu\nabla\mathbf{u}\nabla\boldsymbol{\varphi} - (\mathbf{u}\cdot\nabla)\boldsymbol{\varphi}\cdot\mathbf{u})\,dx + \int_\Omega \nu c(x)\mathbf{u}\boldsymbol{\varphi}\,dx = -\int_\Omega (\mathbf{f},\boldsymbol{\varphi})\,dx$$

is satisfied for every $\boldsymbol{\varphi} \in H(\Omega)$.

The main result of this paper is the following:

Theorem 1 *Suppose that conditions (***i***)–(***vi***) are satisfied. Then the subsequence of solutions* $\{\mathbf{u}^{(s)}\}_{s=1}^\infty$ *of problems (1) converges to function* $\mathbf{u}^{(0)}$ *strongly in* $W^{1,\vartheta}(\Omega)^3$ *for any* $0 < \vartheta < 2$ *as* $s \to \infty$ *and the function* $\mathbf{u}^{(0)}$ *is a weak solution of problem (8).*

3 Pointwise and Integral Estimates of the Auxiliary Functions

To construct a homogenized problem (8) we investigate the qualitative asymptotic behavior of the solution to model problems type (4).

We denote by $Q_a^h,\ a > 0$, the following cylinder with a base a and a height $2h$:

$$Q_a^h = \{x \in R^n;\ x = (x', x_n),\ x' = (x_1, x_2),\ |x'| < a,\ |x_3| < h\}.$$

Let $\mathcal{F}$ be a closed set such that $\mathcal{F} \subset Q_d^H$ and $0 < d < h < H < 1/4$.

Without loss of generality, we assume that $\nu = 1$. We consider the main model problem in $B(0, 1) \setminus \mathcal{F}$:

$$\begin{gathered} \Delta \mathbf{v}^k(x) = \nabla p^k(x), \\ \operatorname{div} \mathbf{v}^k(x) = 0,\ x \in B(0,1) \setminus \mathcal{F}, \\ \mathbf{v}^k(x)|_{\partial\mathcal{F}} = \mathbf{e}^k, \quad \mathbf{v}^k(x)|_{\partial B(0,1)} = 0. \end{gathered} \tag{9}$$

We extend $\mathbf{v}^k(x)$ by $\mathbf{e}^k$ for $x \in \mathcal{F}$ and keep for the extended function the same notation. Let us define by $H_k(\mathcal{F})$ the following class of functions

$$H_k(\mathcal{F}) := \{\mathbf{v}^k(x) \in W_0^{1,2}(B(0,1))^3 :\ \text{div } \mathbf{v}^k = 0,\ x \in B(0,1),\ \mathbf{v}^k = \mathbf{e}^k,\ x \in \mathcal{F}\}.$$

Definition 3 We say that $\mathbf{v}^k \in H_k(\mathcal{F})$ is a weak solution of problem (9) if the following integral identity

$$\int_{B(0,1)} \mathbf{D}[\mathbf{v}^k] \cdot \mathbf{D}[\boldsymbol{\varphi}^k]\, dx = 0 \tag{10}$$

is satisfied for every $\boldsymbol{\varphi}^k \in H_k(\mathcal{F})$.

The existence and uniqueness of the weak solution $\mathbf{v}^k(x, t)$ to problem (9) follows from [16]. The solution $\mathbf{v}^k(x, t)$ can be found as a minimizer of the following functional

$$J(\mathbf{v}^k) = \int_{B(0,1)} |\mathbf{D}[\mathbf{v}^k]|^2 dx = \int_{B(0,1)} \sum_{l,p=1}^{n} \left|\frac{\partial v_l^k}{\partial x_p}\right|^2 dx$$

in the class of functions $H_k(\mathcal{F})$.

Pointwise and integral estimates of solution to model problem (9) play the key role in study of the homogenization of problems (1) in sequence of domains with channels. We obtain this estimates using methods of [13, 14].

Theorem 2 *There exists a positive constant C_4 not depending on d, such that the following estimates for the solutions $\mathbf{v}^k(x, t)$, $k = 1, 2, 3$, of problem (9) are satisfied*

$$|D^\alpha v_i^k(x)| \le \frac{C_4}{|x'|^{|\alpha|}} \ln^{-1}\frac{1}{d},\ |\alpha| = 0, 1, 2, \tag{11}$$

for every $x \in B(0,1) \setminus Q_a^1$, *where* $a \geq 2b$, $4d < b < 2\sqrt{d}$, *for every* $i = 1, 2, 3$. *Here* $D^\alpha = \frac{\partial^{|\alpha|}}{\partial^{\alpha_1} x_1 \partial^{\alpha_2} x_2 \partial^{\alpha_3} x_3}$, $|\alpha| = \alpha_1 + \alpha_2 + \alpha_3$.

Moreover, there exists a positive constant C_5 *such that the following integral estimates are valid*

$$\int\limits_{B(0,1)\setminus\mathcal{F}} |\mathbf{v}^k|^2 \, dx \leq C_5 (b^2 \ln^{-1} \frac{1}{d} + \ln^{-2} \frac{1}{d}), \tag{12}$$

$$\int\limits_{B(0,1)} |\mathbf{D}[\mathbf{v}^k]|^2 \, dx \leq C_5 H \ln^{-1} \frac{1}{d}, \tag{13}$$

for every $b \in [4d, 1]$.

Proof Denote by $\mathbf{U}(x, y) = \|U_{ij}(x, y)\|_{i,j=1}^3$ the velocity part of the Green function to the Dirichlet problem for the Stokes system in the whole space R^3

$$\Delta_x U_{ij}(x-y) - \frac{\partial}{\partial x_i} q_j(x-y) = \Delta^2 \varphi(x-y)\delta_{ij},$$
$$\sum_{i=1}^3 \frac{\partial}{\partial x_i} U_{ij}(x-y) = 0, \;\; x \neq y,$$

where $\varphi(x-y) = \frac{|x-y|}{8\pi}$ is a fundamental solution to the biharmonic equation. This solution has the following explicit form

$$U_{ij}(x-y) = -\frac{1}{8\pi}\left(\frac{\delta_{ij}}{|x-y|} - \frac{(x_i - y_i)(x_j - y_j)}{|x-y|^3}\right),$$
$$q_j(x-y) = \frac{1}{4\pi}\frac{(x_j - y_j)}{|x-y|^3}.$$

To construct Green's tensor for the Stokes problem in an arbitrary bounded domain Ω we follow the tools from Galdi [9]. We consider functions $H_{ij}(x, y)$ and $a_i(x, y)$, $i, j = 1, 2, 3$, such that they are solutions to the following problems

$$\begin{gathered} \Delta_x H_{ij}(x,y) + \frac{\partial a_j(x,y)}{\partial x_i} = 0, \;\; x \in \Omega, \\ \sum_{i=1}^3 \frac{\partial}{\partial x_i} H_{ij}(x,y) = 0, \;\; x \in \Omega, \\ H_{ij}(x,y) = U_{ij}(x-y), \;\; x \in \partial\Omega. \end{gathered} \tag{14}$$

Then we define

$$G_{ij}(x,y) = U_{ij}(x-y) - H_{ij}(x,y),$$
$$g_i(x,y) = q_i(x-y) - a_i(x,y),$$

where $H_{ij}(x, y)$ is a solution of problem (14) for $\Omega = B(0, 1)$. Functions $G_{ij}(x, y)$ satisfy the symmetry condition

$$G_{ij}(x, y) = G_{ji}(x, y).$$

Also the following derivatives

$$D_x^\alpha D_y^\beta G_{ij}(x, y) = \mathcal{A}(x, y)|x - y|^{-1-|\alpha|-|\beta|}, \; x \neq y,$$

exist and are continuous. Here the functions $\mathcal{A}(x, y)$ are bounded for $x \neq y$.

Due to Theorem 6 from Appendix there exist functions $\tilde{\mathbf{G}}_{\mathbf{j}}(x, y)$ such that

$$\mathbf{G}_j(x, y) = \mathrm{curl}_x \tilde{\mathbf{G}}_{\mathbf{j}}(x, y),$$

where

$$\tilde{\mathbf{G}}_{\mathbf{j}}(x, y) := \tilde{\mathbf{U}}_{\mathbf{j}}(x, y) + \tilde{\mathbf{H}}_{\mathbf{j}}(x, y),$$
$$\tilde{\mathbf{U}}_{\mathbf{j}}(x, y) = \mathrm{curl}_x \left(\frac{1}{8\pi} |x - y| \mathbf{e}^j \right), \; \mathbf{H}_{\mathbf{j}}(x, y) = \mathrm{curl}_x \tilde{\mathbf{H}}_{\mathbf{j}}(x, y).$$

Here

$$D_x^\alpha D_y^\beta \tilde{G}_{ij}(x, y) = \mathcal{B}(x, y)|x - y|^{-|\alpha|-|\beta|}, \; x \neq y,$$

and $\mathcal{B}(x, y)$ are bounded functions.

Let $\mathbf{u}$, $\mathbf{v}$ be smooth solenoidal functions in $B(0, 1)$. We use Green's formulas in the next consideration:

$$\int\limits_{B(0,1)\setminus\mathcal{F}} \Big(\Delta\mathbf{v} - \nabla p, \mathbf{u}\Big) dx = \int\limits_{B(0,1)\setminus\mathcal{F}} \mathbf{D}[\mathbf{v}] \cdot \mathbf{D}[\mathbf{u}] dx$$
$$+ \int\limits_{\partial B(0,1)} \left(\frac{\partial \mathbf{v}}{\partial n_1} - p\mathbf{n}_1, \mathbf{u} \right) ds + \int\limits_{\partial\mathcal{F}} \left(\frac{\partial \mathbf{v}}{\partial n_2} - p\mathbf{n}_2, \mathbf{u} \right) ds, \tag{15}$$

$$\int\limits_{B(0,1)\setminus\mathcal{F}} \Big\{(\Delta\mathbf{v} - \nabla p, \mathbf{u}) - (\Delta\mathbf{u} - \nabla q, \mathbf{v})\Big\} dx$$
$$= \int\limits_{\partial B(0,1)} \Big\{(\tfrac{\partial \mathbf{v}}{\partial n_1} - p\mathbf{n}_1, \mathbf{u}) - (\tfrac{\partial \mathbf{u}}{\partial n_1} - q\mathbf{n}_1, \mathbf{v})\Big\} ds$$
$$+ \int\limits_{\partial\mathcal{F}} \Big\{(\tfrac{\partial \mathbf{v}}{\partial n_2} - p\mathbf{n}_2, \mathbf{u}) - (\tfrac{\partial \mathbf{u}}{\partial n_2} - q\mathbf{n}_2, \mathbf{v})\Big\} ds, \tag{16}$$

where $\mathbf{n}_1$ is the outer normal vector to $B(0, 1)$, $\mathbf{n}_2$ is the interior vector to $\mathcal{F}$.

Let in (16) $\mathbf{u} := \mathbf{G}_j(x, y)$ and $\mathbf{v} := \mathbf{v}^k(x)$ be a solution of (9), then

$$\int\limits_{B(0,1)\setminus\mathcal{F}} \Big\{(\Delta \mathbf{v}^k - \nabla p^k, \mathbf{G}_j(x,y)) - (\Delta_x \mathbf{G}_j(x,y) - \nabla q, \mathbf{v}^k)\Big\} dx$$
$$= \int\limits_{\partial B(0,1)} \Big\{(\tfrac{\partial \mathbf{v}^k}{\partial n_1} - p^k \mathbf{n}_1, \mathbf{G}_j(x,y)) - (\tfrac{\partial_x \mathbf{G}_j(x,y)}{\partial n_1} - q_j \mathbf{n}_1, \mathbf{v}^k)\Big\} d_x s$$
$$+ \int\limits_{\partial\mathcal{F}} \Big\{(\tfrac{\partial \mathbf{v}^k}{\partial n_2} - p^k \mathbf{n}_2, \mathbf{G}_j(x,y)) - (\tfrac{\partial_x \mathbf{G}_j(x,y)}{\partial n_2} - q_j \mathbf{n}_2, \mathbf{v}^k)\Big\} d_x s. \quad (17)$$

We use the following properties of functions $\mathbf{v}^k(x),\ \mathbf{G}_j(x,y)$:

$$\nabla \mathbf{v}^k(x) = \nabla_x \mathbf{G}_j(x,y) = 0 \ \text{ if } x \in \partial B(0,1),$$
$$\mathbf{v}^k(x) = \mathbf{e}^k,\ \frac{\partial \mathbf{v}^k}{\partial n_2} = 0 \ \text{ if } x \in \partial\mathcal{F},$$
$$\int\limits_{B(0,1)\setminus\mathcal{F}} (\Delta_x \mathbf{G}_j(x,y) - \nabla q_j, \mathbf{v}^k) dx = \int\limits_{B(0,1)\setminus\mathcal{F}} \delta(x,y) v_j^k(x) dx = v_j^k(y),$$

if $(x,y) \in B(0,1) \times B(0,1)$. Then from (17) we derive

$$v_j^k(y) = -\int\limits_{\partial\mathcal{F}} \bigg(\Big(\frac{\partial \mathbf{v}^k}{\partial n_2} - p^k \mathbf{n}_2, \mathbf{G}_j(x,y)\Big) - \Big(\frac{\partial_x \mathbf{G}_j(x,y)}{\partial n_2} - q_j \mathbf{n}_2, \mathbf{e}^k\Big)\bigg) d_x s \quad (18)$$

for all $y \in B(0,1)$. To prove that

$$\int\limits_{\partial\mathcal{F}} \Big(\frac{\partial_x \mathbf{G}_j(x,y)}{\partial n} - q_j \mathbf{n}_2, \mathbf{e}^k\Big) d_x s = 0, \quad (19)$$

we use formula (15) with $\mathbf{v} := \mathbf{G}_j(x,y),\ \mathbf{u} := \mathbf{e}_k,\ y \in \mathcal{F}$, and the domain of integration $\mathcal{F} \setminus \partial\mathcal{F}$. Then we obtain

$$\int\limits_{\mathcal{F}\setminus\partial\mathcal{F}} \Big(\Delta_x \mathbf{G}_j(x,y) - \nabla q_j, \mathbf{e}_k\Big) dx$$
$$= \int\limits_{\mathcal{F}\setminus\partial\mathcal{F}} \mathbf{D}_x[\mathbf{G}_j(x,y)] \cdot \mathbf{D}[\mathbf{e}_k] dx + \int\limits_{\partial\mathcal{F}} \Big(\tfrac{\partial \mathbf{G}_j(x,y)}{\partial n_2} - q_j(x)\mathbf{n}_2, \mathbf{e}_k\Big) d_x s. \quad (20)$$

From (20) we have (19). Using (18) and (19), we derive

$$D^\alpha v_j^k(y) = -\int\limits_{\partial\mathcal{F}} \Big(\frac{\partial \mathbf{v}^k}{\partial n_2} - p^k \mathbf{n}, D_y^\alpha \mathbf{G}_j(x,y)\Big) d_x s \ \forall y \in B(0,1), \quad (21)$$

with $|\alpha| = 0, 1, 2$.

Now we introduce cut-off functions φ and ψ:

- $\varphi(|x'|) \in C_0^\infty(B(0,b))$, $\varphi(|x'|) = 1$ if $|x'| \le d$, $\varphi(|x'|) = 0$ if $|x'| \ge b$, and such that $\|\nabla\varphi(|x'|)\|^2_{L_2(B(0,b))} \le C_6 \ln^{-1}\frac{b}{2d}$, where C_6 is a positive constant;
- $\psi(t) \in C^\infty(\mathbf{R}^1)$, is such that $\psi(t) = 1$ if $|t| \le \frac{1}{2}$, $\psi(t) = 0$ if $|t| \ge 1$.

By $\mathbf{u}_j^\alpha(x,y)$, $|\alpha| = 0, 1$, we define the following function

$$\mathbf{u}_j^\alpha(x,y) := \mathrm{curl}_x\left(D_y^\alpha \tilde{\mathbf{G}}_j(x,y)\varphi(|x'|)\psi\left(\frac{y_3 - x_3}{h}\right)\right)$$

$\forall (x,y) \in B(0,1) \times B(0,1)$, $h < H$. This type of functions was used in [4]. It is easy to see that

$$\mathbf{u}_j^\alpha(x,y) = D_y^\alpha \mathbf{G}_j(x,y),\ \forall x \in \partial\mathcal{F} \subset Q_a^h.$$

Moreover,

$$\mathbf{u}_j^\alpha(x,y) \in C^\infty(Q_a^h),\ \text{if } |y'| \ge 2b,$$

and

$$\mathbf{u}_j^\alpha(x,y) = 0 \text{ if } |x'| \ge b.$$

Let in (15) $\mathbf{u} := \mathbf{u}_j^\alpha(x,y)$, $\mathbf{v} := \mathbf{v}^k$ be a solution of (9), then we deduce

$$\int\limits_{B(0,1)\setminus\mathcal{F}} \left(\Delta\mathbf{v}^k - \nabla p^k, \mathbf{u}_j^\alpha(x,y)\right)dx = \int\limits_{B(0,1)\setminus\mathcal{F}} \mathbf{D}[\mathbf{v}^k]\cdot\mathbf{D}_x[\mathbf{u}_j^\alpha(x,y)]dx$$
$$+ \int\limits_{\partial B(0,1)} \left(\frac{\partial\mathbf{v}^k}{\partial n_1} - p^k\mathbf{n}_1, \mathbf{u}_j^\alpha(x,y)\right) d_x s + \int\limits_{\partial\mathcal{F}} \left(\frac{\partial\mathbf{v}^k}{\partial n_2} - p^k\mathbf{n}_2, \mathbf{u}_j^\alpha(x,y)\right) d_x s.$$

From the last identity we derive

$$\int\limits_{\partial\mathcal{F}} \left(\frac{\partial\mathbf{v}^k}{\partial n_2} - p^k\mathbf{n}_2, D_y^\alpha\mathbf{G}_j(x,y)\right) d_x s = -\int\limits_{B(0,1)\setminus\mathcal{F}} \mathbf{D}[\mathbf{v}^k]\cdot\mathbf{D}_x[\mathbf{u}_j^\alpha(x,y)]dx. \quad (22)$$

Finally, from (21) and (22) we have

$$D_y^\alpha v_j^k(y) = \int\limits_{B(0,1)\setminus\mathcal{F}} \mathbf{D}[\mathbf{v}^k]\cdot\mathbf{D}_x[\mathbf{u}_j^\alpha(x,y)]dx,$$

for $|y'| \ge 2b$. From this identity, using Hölder's inequality, we derive

$$|D_y^\alpha v_j^k(y)| \le \left(\int\limits_{B(0,1)\setminus\mathcal{F}} |\mathbf{D}[\mathbf{v}^k]|^2 dx\right)^{\frac{1}{2}} \left(\int\limits_{B(0,1)\setminus\mathcal{F}} |\mathbf{D}_x[\mathbf{u}_j^\alpha(x,y)]|^2 dx\right)^{\frac{1}{2}}. \quad (23)$$

By $\boldsymbol{\omega}^k(x) \in H_k(\mathcal{F})$ we denote a function

$$\boldsymbol{\omega}^k(x) := \text{curl}\{\tilde{\mathbf{e}}_k(x)\varphi(|x'|)\psi\left(\frac{x_3}{2h}\right)\},$$

where $\tilde{\mathbf{e}}_k$ is such that curl $\tilde{\mathbf{e}}_k(x) = \mathbf{e}_k$, that is, $\tilde{\mathbf{e}}_1(x) = \{0, 0, x_2\}$, $\tilde{\mathbf{e}}_2(x) = \{x_3, 0, 0\}$, $\tilde{\mathbf{e}}_3(x) = \{0, x_1, 0\}$. Using the fact that minimum of the functional $J(\mathbf{v}^k)$ in class $H_k(\mathcal{F})$ is reached on $\mathbf{v}^k$, we obtain

$$\begin{aligned}\int\limits_{B(0,1)\setminus\mathcal{F}} |\mathbf{D}[\mathbf{v}^k]|^2 dx \leq C \int\limits_{B(0,1)} |\mathbf{D}[\boldsymbol{\omega}^k]|^2 dx = \\ \sum_{i,j=1}^{n} \int\limits_{B(0,1)} \left|\frac{\partial \omega_i^k}{\partial x_j}\right|^2 dx \leq C_7 h \ln^{-1}\frac{b}{2d},\end{aligned} \tag{24}$$

hereafter C are generic constants not depending of d.

We consider the second integral in the right-hand side of (23). Using properties of the cut-off functions φ and ψ, we derive the following estimate

$$\begin{aligned}\int\limits_{B(0,1)\setminus\mathcal{F}} \left|\mathbf{D}_x[\text{curl}_x \left(D_y^\alpha \tilde{\mathbf{G}}_j(x,y)\varphi(|x'|)\psi\left(\frac{y_3 - x_3}{h}\right)\right)]\right|^2 dx \leq \\ \frac{C}{|y'|^{2|\alpha|+1}} \ln^{-1}\frac{b}{2d}.\end{aligned} \tag{25}$$

Here we used that $|y'| \geq 2b$, $|x'| \leq b$, and $|y'| - |x'| \geq \frac{|y'|}{2}$. Finally, from (23), (24) and (25) we obtain the following preliminary pointwise estimate

$$|D^\alpha v_i^k(x)| \leq C_8 \left(\frac{h}{|y'|}\right)^{\frac{1}{2}} \frac{1}{|y'|^{|\alpha|}} \ln^{-1}\frac{1}{d}, \ |\alpha| = 0, 1, 2, \tag{26}$$

for $4d < b < 2\sqrt{d}$. In this step we apply the auxiliary lemma which is proved using methods from [22, 23].

Lemma 1 *Let* $\mathbf{v}^k$ *be a solution of problem (9) and there exist positive constants* $K_1,\ K_2,\ K_3$, *such that the following estimates*

$$\int\limits_{Q^h_{K_3 h}} |\mathbf{D}[\mathbf{v}^k]|^2 dx \leq K_1 h \ln^{-1}\frac{1}{d}, \tag{27}$$

$$|D^\alpha v_i^k(x)| \leq K_2 \left(\frac{h}{|x'|}\right)^{\frac{1}{2}} \frac{\ln^{-1}\frac{1}{d}}{|x'|^{|\alpha|}}, \ 2b \leq |x'| \leq K_3 h, \tag{28}$$

$$|D^\alpha v_i^k(x)| \leq K_2 \left(\frac{2}{K_3}\right)^{\frac{1}{2}} \frac{\ln^{-1}\frac{1}{d}}{|x'|^{|\alpha|}}, \ K_3 h < |x'| \leq 1, \tag{29}$$

are valid for a fixed $h < H$ *and* $|\alpha| = 0, 1, 2$. *Then the following estimates are satisfied*

$$\int\limits_{Q^{\frac{h}{2}}_{K_3\frac{h}{2}}} |\mathbf{D}[v^k]|^2 dx \leq K_1 \frac{h}{2} \ln^{-1} \frac{1}{d}, \tag{30}$$

$$|D^\alpha v_i^k(x)| \leq K_2 \left(\frac{h}{2|x'|}\right)^{\frac{1}{2}} \frac{\ln^{-1}\frac{1}{d}}{|x'|^{|\alpha|}},\ 2b \leq |x'| \leq K_3 \frac{h}{2}, \tag{31}$$

$$|D^\alpha v_i^k(x)| \leq K_2 \left(\frac{2}{K_3}\right)^{\frac{1}{2}} \frac{\ln^{-1}\frac{1}{d}}{|x'|^{|\alpha|}},\ K_3 \frac{h}{2} < |x'| \leq 1, \tag{32}$$

for $|\alpha| = 0, 1, 2$.

Let $R = \min\{K_3 H, 1\}$. We define a sequence of numbers $h_i = 2^{-i+1}H$, $i = 1, \ldots, I$, such that $2^{-I}R < 2b < 2^{-I+1}R$. Then the following inequalities are valid

$$\int\limits_{Q^{h_i}_{K_3 h_i}} |\mathbf{D}[v^k]|^2 dx \leq K_1 h_i \ln^{-1} \frac{1}{d}, \tag{33}$$

$$|D^\alpha v_i^k(x)| \leq K_2 \left(\frac{h_i}{|x'|}\right)^{\frac{1}{2}} \frac{\ln^{-1}\frac{1}{d}}{|x'|^{|\alpha|}},\ 2b \leq |x'| \leq K_3 h_i, \tag{34}$$

$$|D^\alpha v_i^k(x)| \leq K_2 \left(\frac{2}{K_3}\right)^{\frac{1}{2}} \frac{\ln^{-1}\frac{1}{d}}{|x'|^{|\alpha|}},\ K_3 h_i < |x'| \leq 1, \tag{35}$$

for every $i = 1, \ldots, I$, and $|\alpha| = 0, 1, 2$. Let $i = 1$. Then inequalities (34), (35) follow from preliminary estimate (26) with $K_2 \geq C_7$. Integral estimate (33) is a consequence of (24) for $K_1 \geq C_8$. Estimates (34), (35) hold for $i = i_1 \leq I - 1$, this means that they are valid for $i = i_1 + 1$ due to Lemma 1. It implies that estimates (33), (34) and (35) are satisfied for every $i = 1, \ldots, I$.

Let $x_0 \in Q_1^1 \backslash \mathcal{F}$ be an arbitrary point. For x_0 satisfying the following estimate

$$K_3 h_I < |x_0'| \leq R,$$

we define a number $i_0 = i_0(|x_0'|)$ such that

$$K_3 h_{i_0+1} < |x_0'| \leq K_3 h_{i_0}.$$

In this case we apply pointwise estimate (34) for $i = i_0$

$$|D^\alpha v_i^k(x_0)| \le K_2 \left(\frac{h_{i_0}}{|x_0'|}\right)^{\frac{1}{2}} \frac{\ln^{-1}\frac{1}{d}}{|x_0'|^{|\alpha|}} \le K_2 \left(\frac{h_{i_0}}{K_3 h_{i_0+1}}\right)^{\frac{1}{2}} \frac{\ln^{-1}\frac{1}{d}}{|x_0'|^{|\alpha|}} \le \tag{36}$$
$$2K_2 K_3^{-\frac{1}{2}} \frac{\ln^{-1}\frac{1}{d}}{|x_0'|^{|\alpha|}}.$$

For the case $|x_0'| > R$ we use preliminary pointwise estimate (26). From the choice of R we obtain

$$|D^\alpha v_i^k(x_0)| \le C_8 \left(\frac{H}{R}+1\right)^{\frac{1}{2}} \frac{\ln^{-1}\frac{1}{d}}{|x_0'|^{|\alpha|}} \le C\left(K_3^{-1}+1\right)^{\frac{1}{2}} \frac{\ln^{-1}\frac{1}{d}}{|x_0'|^{|\alpha|}} \tag{37}$$

for $|\alpha| = 0, 1, 2$. From (36) and (37) we derive (11).

Now we will show the integral estimates for the solution of the model problem. Estimate (13) is obtained analogously to (24), with the help of cut-off function $\psi(\frac{x_3}{2H})$. Let us prove (12). We divide the domain of integration $B(0,1)$ into two parts

$$B(0,1) = \left(B(0,1) \setminus Q_{2b}^H\right) \bigcup Q_{2b}^H.$$

Integral over $B(0,1) \setminus Q_{2b}^H$ we estimate using pointwise estimate (11):

$$\int\limits_{B(0,1)\setminus Q_{2b}^H} |v_i^k(x)|^2 dx \le C\ln^{-2}\frac{1}{d}. \tag{38}$$

Now we estimate the integral over the cylinder Q_{2b}^H. For $x \in Q_{2b}^H$ we denote by $x_t' = x'\frac{t}{|x'|}$, then

$$v_i^k(x) = v_i^k(x_{2b}', x_3) - \int\limits_{|x'|}^{2b} \frac{dv_i^k(x_t', x_3)}{dt} dt.$$

Using Hölder's inequality, we derive

$$|v_i^k(x)|^2 = 2|v_i^k(x_{2b}', x_3)|^2 + 2\left(\int\limits_{|x'|}^{2b} \left|\frac{dv_i^k(x_t', x_3)}{dt}\right| dt\right)^2$$
$$\le 2|v_i^k(x_{2b}', x_3)|^2 + 2\int\limits_{|x'|}^{2b} dt \int\limits_0^{2b} |\nabla v_i^k|^2\, dt.$$

Integrating the last inequality over the cylinder Q_{2b}^H, we obtain

$$\int\limits_{Q_{2b}^H} |v_i^k(x)|^2 dx \le 2 \int\limits_{Q_{2b}^H} |v_i^k(x'_{2b}, x_3)|^2\, dx + 4b \int\limits_{Q_{2b}^H} \int\limits_0^{2b} |\nabla v_i^k(x'_t, x_3)|^2\, dt dx.$$

The first integral on the right-hand side we estimate using (11), the second integral is estimated analogously to (24). Then we get (13). The proof is completed. □

Remark 3 Using integral estimate of solution to problem (9) one obtains the following estimate

$$\int\limits_{Q_1^h} |\mathbf{D}[\mathbf{v}^k]|^2\, dx \le C_9 h \ln^{-1}\frac{1}{d}, \quad \forall\, h \le H. \tag{39}$$

4 Auxiliary Statements and Cut-off Functions

To specify some geometrical properties of perforated domains Ω_s, we formulate the additional statements which can be found in [22]. The following inclusion is valid for $i \in I''$

$$\mathcal{U}(l_i^{(s)}, 2\varepsilon_i^{(s)}) \subset \mathcal{U}(L_{i,1}^{(s)}, 2\varepsilon_i^{(s)}) \bigcup \mathcal{U}(T_i^{(s)}(\{2\varepsilon_i^{(s)}\}), 2\varepsilon_i^{(s)}(2 + \frac{1}{\lambda_s})).$$

The following results were proved in [22].

Lemma 2 *There exists a number γ, not depending on s and i, such that*

(I) *the sets $G_{i,m}^{(s)}(\gamma)$, $m = 1, \dots, \mathcal{M}(i, s)$, are disjoint for every fixed s, i. Here the sets $G_{i,m}^{(s)}(\gamma)$ are defined by (7);*

(II) *the following inclusion holds*

$$\mathcal{U}(l_i^{(s)}, 2\varepsilon_i^{(s)}) \subset \Big\{ \bigcup_{p=1}^{P(i,s)} B(z_{i,p}^{(s)}, 2\lambda_s \varepsilon_i^{(s)}(2 + 1/\lambda_s))\Big\} \bigcup$$
$$\Big\{ \bigcup_{m=1}^{\mathcal{M}(i,s)} \Big\{ G_{i,m}^{(s)}(\gamma + 1/3) \bigcup B(\alpha_{i,m}^{(s)}, (\gamma + 2/3)\varepsilon_i^{(s)}) \bigcup B(\beta_{i,m}^{(s)}, (\gamma + 2/3)\varepsilon_i^{(s)})\Big\}\Big\}.$$

The covering of set $\mathcal{U}(l_i^{(s)}, 2\varepsilon_i^{(s)})$ introduced in (**II**) is used for the construction of asymptotic expansion of solutions $\{\mathbf{u}^{(s)}(x)\}_{s=1}^{\infty}$ to problem (1).

If $i \in I'(s)$ we divide the curve onto the finite number of curvilinear segments with equal length such that it belongs to the segment $[\frac{d_i^{(s)}}{2}, d_i^{(s)}]$. Then we have

$$l_i^{(s)} = \bigcup_{r=1}^{\mathcal{R}(i,s)} l_i^{(s)}(r), \qquad \frac{d_i^{(s)}}{2} \le |l_i^{(s)}(r)| \le d_i^{(s)},$$

$$\mathcal{U}(l_i^{(s)}, 2d_i^{(s)}) = \bigcup_{r=1}^{\mathcal{R}(i,s)} \mathcal{U}(l_i^{(s)}(r), 2d_i^{(s)}), \quad i \in I'(s).$$

Now we define the cut-off functions in a different way for indices $i \in I'(s)$, $i \in I''(s)$. Let $m = 1, \dots, \mathcal{M}(i, s)$, $p = 1, \dots, \mathcal{P}(i, s)$, $j \in I'(s)$, $r = 1, \dots, \mathcal{R}(j, s)$, then we denote:

$$B_{i,m}^{(s,1)} = B(\alpha_{i,m}, (\gamma + 1)\varepsilon_i^{(s)}), \quad B_{i,m}^{(s,2)} = B(\beta_{i,m}^{(s)}, (\gamma + 1)\varepsilon_i^{(s)}),$$
$$B_{i,m}^{(s,3)} = B\Big(x_{i,m}^{(s)}, \Big(2 + \frac{1}{\lambda_s}\Big)\varepsilon_i^{(s)}\Big), \quad \bar{B}_{i,m}^{(s)} = B\Big(z_{i,m}^{(s)}, 2\lambda\varepsilon_i^{(s)}\Big(3 + \frac{1}{\lambda_s}\Big)\Big),$$
$$D_{j,r}^{(s)} = \mathcal{U}(l_j^{(s)}(r), 2d_j^{(s)}), \quad G_{i,m}^{(s)} = G_{i,m}^{(s)}(\gamma),$$

where $x_{i,m}^{(s)}$ is the middle of the curve segment $L_i^{(s)}(m)$. Numbers λ_s and $\varepsilon_i^{(s)}$ are defined in (5) and (6) accordingly, and $\alpha_{i,m}^{(s)}, \beta_{i,m}^{(s)}, \gamma$, take the same values as in (7).

We define for $i \in I''(s)$, $m = 1, \dots, \mathcal{M}(i, s)$, $p = 1, \dots, \mathcal{P}(i, s)$, $j \in I'(s)$, $r = 1, \dots, \mathcal{R}(j, s)$, the sequences of cut-off functions

$$\{\varphi_{i,m}^{(s)}(x)\}, \ \{\psi_{i,m}^{(s,1)}(x)\}, \ \{\psi_{i,m}^{(s,2)}(x)\}, \ \{\chi_{i,p}^{(s)}(x)\}, \ \{\omega_{j,r}^{(s)}(x)\}$$

from $C^\infty(\mathbf{R}^3)$ with values in [0, 1], such that the following properties are satisfied:

(a) $\operatorname{supp} \varphi_{i,m}^{(s)}(x) \subset G_{i,m}^{(s)}$, $\operatorname{supp} \psi_{i,m}^{(s,1)}(x) \subset B_{i,m}^{(s,1)}$, $\operatorname{supp} \psi_{i,m}^{(s,2)}(x) \subset B_{i,m}^{(s,2)}$,

$$\operatorname{supp} \chi_{i,p}^{(s)}(x) \subset \bar{B}_{i,p}^{(s)}, \quad \operatorname{supp} \omega_{j,r}^{(s)}(x) \subset D_{j,r}^{(s)};$$

(b) $\sum\limits_{j \in I'(s)} \omega_j^{(s)}(x) + \sum\limits_{j \in I''(s)} \sigma_i^{(s)}(x) = 1, \quad$ for $x \in \bigcup\limits_{i=1}^{I(s)} \mathcal{U}(l_i^{(s)}, \varrho_i)$,

where $\qquad \omega_j^{(s)}(x) = \sum\limits_{r=1}^{\mathcal{R}(j,s)} \omega_{j,r}^{(s)}(x)$,

$$\sigma_i^{(s)}(x) = \sum_{m=1}^{\mathcal{M}(i,s)} \big[\varphi_{i,m}^{(s)}(x) + \psi_{i,m}^{(s,1)}(x) + \psi_{i,m}^{(s,2)}(x)\big] + \sum_{p=1}^{\mathcal{P}(i,s)} \chi_{i,p}^{(s)}(x);$$

(c) $\varphi_{i,m}^{(s)}(x) = 1$ for $x \in \mathcal{U}(l_i^{(s)}, \varrho_i^{(s)}) \cap G_{i,m}^{(s)}(\gamma + 1)$;

(d) there exists a constant C_{10} not depending on i, s, such that

$$|\nabla\varphi_{i,m}^{(s)}(x)| + |\nabla\psi_{i,m}^{(s,1)}(x)| + |\nabla\psi_{i,m}^{(s,2)}(x)| + |\nabla\chi_{i,p}^{(s)}(x)| \le \frac{C_{10}}{\varepsilon_i^{(s)}} \quad \text{for } i \in I_s'',$$

$$|\nabla\omega_{i,r}^{(s)}(x)| \le \frac{C_{10}}{d_i^{(s)}} \quad \text{for } i \in I'_s;$$

(e) the order of the following families of sets

$$\{\operatorname{supp}\varphi_{i,m}^{(s)},\ \operatorname{supp}\psi_{i,m}^{(s,1)},\ \operatorname{supp}\psi_{i,m}^{(s,2)},\ \operatorname{supp}\chi_{i,p}^{(s)},\ \operatorname{supp}\omega_{j,r}^{(s)}\},$$

for every $i \in I''(s)$, $m = 1, \dots, \mathcal{M}(i,s)$, $p = 1, \dots, \mathcal{P}(i,s)$, $j \in I'(s)$, $r = 1, \dots, \mathcal{R}(j,s)$, is less or equal than a constant not depending of s.

These functions were constructed in [22] and it was shown that

$$\{\operatorname{supp}\varphi_{i',m'}^{(s)}(x)\} \cap \{\operatorname{supp}\varphi_{i'',m''}^{(s)}(x)\} = \emptyset \quad \text{if} \quad (i',m') \ne (i'',m'')$$

for every fixed number s. We recall the asymptotic properties which were proved in [22]:

$$\mathcal{M}(i,s)\frac{\varepsilon_i^{(s)}}{\lambda_s} \le C_{11},\ \mathcal{R}(i,s)d_i^{(s)} \le C_{11},\ \sum_{i=1}^{I(s)}\mathcal{P}(i,s)(r_i^{(s)})^3 \le C_{11},$$
$$\sum_{i=1}^{I(s)}(r_i^{(s)})^2 \le C_{12},\ \sum_{i=1}^{I(s)}\ln^{-1}\frac{1}{d_i^{(s)}} \le C_{12}. \tag{40}$$

Using definitions of $\varepsilon_i^{(s)}$, λ_s, μ_s, and inequalities (40) it can be shown that

$$\lim_{s\to\infty}\sum_{i\in I''(s)}\frac{\mathcal{M}(i,s)}{\lambda_s}(\varepsilon_i^{(s)})^3 = 0,\ \lim_{s\to\infty}\sum_{i\in I'(s)}\mathcal{R}(i,s)(\varepsilon_i^{(s)})^2 = 0,$$
$$\lim_{s\to\infty}\sum_{i\in I''(s)}\mathcal{M}(i,s)(\varepsilon_i^{(s)})^2 = 0,\ \lim_{s\to\infty}\sum_{i\in I''(s)}\mathcal{P}(i,s)(\varepsilon_i^{(s)})^2 = 0. \tag{41}$$

5 Asymptotic Expansion of Solutions and Proof of the Main Result

The construction of asymptotic expansion of solutions to problems (1) is connected with the separation of leading terms which are constructed by means of solutions of local boundary value problems. We need Theorem 6 (see Appendix) about the representation of solenoidal vectors from the space $L_2(\Omega)^3$ in the form of rotors [6]. Let $G = B(x_0, R)$, then from this theorem and using a scaling argument, the following estimates can be obtained:

$$\|\tilde{\mathbf{u}}\|_{L_2(G)^3} \le C_{13}R\|\mathbf{u}\|_{L_2(G)^3},\ \|D\tilde{\mathbf{u}}\|_{L_2(G)^3} \le C_{13}\|\mathbf{u}\|_{L_2(G)^3}, \tag{42}$$

where the constant C_{13} does not depend on R and $\mathbf{u}(x)$.

For an arbitrary function $\mathbf{g}(x) = (g_1(x), g_2(x), g_3(x)) \in L_1(\Omega)^3$ we define:

$$M_{i,m}^{(s)}[g_k] = \frac{1}{meas\, B_{i,m}^{(s,3)}} \int\limits_{B_{i,m}^{(s,3)}} g_k(x)\, dx, \quad M_{i,m}^{(s,t)}[g_k] = \frac{1}{meas\, B_{i,m}^{(s,t)}} \int\limits_{B_{i,m}^{(s,t)}} g_k(x)\, dx,$$

$$\bar{M}_{i,p}^{(s)}[g_k] = \frac{1}{mes\, \bar{B}_{i,p}^{(s)}} \int\limits_{\bar{B}_{i,p}^{(s)}} g_k(x)\, dx, \quad \hat{M}_{j,r}^{(s)}[g_k] = \frac{1}{meas\, D_{j,r}^{(s)}} \int\limits_{D_{j,r}^{(s)}} g_k(x)\, dx,$$

where $i \in I''(s),\ m = 1, \dots, \mathcal{M}(i,s),\ t = 1, 2,\ p = 1, \dots, \mathcal{P}(i,s),\ j \in I'(s),\ r = 1, \dots, \mathcal{R}(i,s),\ k = 1, 2, 3.$

Let $\{u^{(\delta)}\}_{\delta=1}^{\infty}$ be a uniformly bounded sequence of functions from $C^\infty(\Omega)$ which converges to $u^{(0)}$ in $W^{1,2}(\Omega)^3$ as $\delta \to \infty$. Let us define the following vectors:

$$\begin{aligned}
\mathbf{u}_{i,m}^{(s,\delta)} &= \big(M_{i,m}^{(s)}[u_1^{(\delta)}],\, M_{i,m}^{(s)}[u_2^{(\delta)}],\, M_{i,m}^{(s)}[u_3^{(\delta)}]\big),\\
\mathbf{u}_{i,m}^{(s,\delta,t)} &= \big(M_{i,m}^{(s,t)}[u_1^{(\delta)}],\, M_{i,m}^{(s,t)}[u_2^{(\delta)}],\, M_{i,m}^{(s,t)}[u_3^{(\delta)}]\big),\\
\bar{\mathbf{u}}_{i,p}^{(s,\delta)} &= \big(\bar{M}_{i,p}^{(s)}[u_1^{(\delta)}],\, \bar{M}_{i,p}^{(s)}[u_2^{(\delta)}],\, \bar{M}_{i,p}^{(s)}[u_3^{(\delta)}]\big),\\
\mathbf{f}_{i,m}^{(s)} &= \big(M_{i,m}^{(s)}[f_1],\, M_{i,m}^{(s)}[f_2],\, M_{i,m}^{(s)}[f_3]\big),\\
\hat{\mathbf{u}}_{j,r}^{(s,\delta)} &= \big(\hat{M}_{j,r}^{(s)}[u_1^{(\delta)}],\, \hat{M}_{j,r}^{(s)}[u_2^{(\delta)}],\, \hat{M}_{j,r}^{(s)}[u_3^{(\delta)}]\big),\\
\mathbf{f}_{i,m}^{(s,t)} &= \big(M_{i,m}^{(s,t)}[f_1],\, M_{i,m}^{(s,t)}[f_2],\, M_{i,m}^{(s,t)}[f_3]\big),\\
\bar{\mathbf{f}}_{i,p}^{(s)} &= \big(\bar{M}_{i,p}^{(s)}[f_1],\, \bar{M}_{i,p}^{(s)}[f_2],\, \bar{M}_{i,p}^{(s)}[f_n]\big),\\
\hat{\mathbf{f}}_{j,r}^{(s)} &= \big(\hat{M}_{j,r}^{(s)}[f_1],\, \hat{M}_{j,r}^{(s)}[f_2],\, \hat{M}_{j,r}^{(s)}[f_3]\big).
\end{aligned}$$

We denote by $\bar{\mathbf{v}}_{k,i,r}^{(s)},\ \mathbf{v}_{k,i,m}^{(s,t)},\ \hat{\mathbf{v}}_{k,i,p}^{(s)}$, the following solutions of the model problem (4) in different domains:

$$\begin{aligned}
\bar{\mathbf{v}}_{k,i,r}^{(s)}(x) &:= \mathbf{v}^k(x; D_{i,r}^{(s)}, D_{i,r}^{(s)} \cap [F^{(s)} \cap \partial\Omega]),\\
\mathbf{v}_{k,i,m}^{(s,t)}(x) &:= \mathbf{v}^k(x; B_{i,m}^{(s,t)}, B_{i,m}^{(s,t)} \cap [F^{(s)} \cap \partial\Omega]),\\
\hat{\mathbf{v}}_{k,i,p}^{(s)}(x) &:= \mathbf{v}^k(x; \hat{B}_{i,p}^{(s)}, \hat{B}_{i,p}^{(s)} \cap [F^{(s)} \cap \partial\Omega]).
\end{aligned}$$

With the help of Theorem 6, we define the rotations of these solutions to the model problems with the mentioned properties

$$\mathbf{v}_{k,i,m}^{(s)} = \operatorname{curl} \tilde{\mathbf{v}}_{k,i,m}^{(s)},\ \mathbf{v}_{k,i,m}^{(s,t)} = \operatorname{curl} \tilde{\mathbf{v}}_{k,i,m}^{(s,t)},\ \bar{\mathbf{v}}_{k,i,r}^{(s)} = \operatorname{curl} \tilde{\bar{\mathbf{v}}}_{k,i,r}^{(s)},\ \hat{\mathbf{v}}_{k,i,p}^{(s)} = \operatorname{curl} \tilde{\hat{\mathbf{v}}}_{k,i,p}^{(s)}.$$

By $\tilde{\mathbf{u}}_{i,m}^{(s,\delta)}(x),\ \tilde{\mathbf{u}}_{i,m}^{(s,\delta,t)}(x),\ \tilde{\bar{\mathbf{u}}}_{i,r}^{(s,\delta)}(x),\ \tilde{\hat{\mathbf{u}}}_{i,r}^{(s,\delta)}(x)$, we denote functions satisfying the following relations

$$\mathbf{u}_{i,m}^{(s,\delta)} - \mathbf{u}^{(\delta)}(x) = \operatorname{curl} \tilde{\mathbf{u}}_{i,m}^{(s,\delta)}(x), \quad \mathbf{u}_{i,m}^{(s,\delta,t)} - \mathbf{u}^{(\delta)}(x) = \operatorname{curl} \tilde{\mathbf{u}}_{i,m}^{(s,\delta,t)}(x),$$
$$\bar{\mathbf{u}}_{i,r}^{(s,\delta)} - \mathbf{u}^{(\delta)}(x) = \operatorname{curl} \tilde{\bar{\mathbf{u}}}_{i,r}^{(s,\delta)}(x), \quad \hat{\mathbf{u}}_{i,p}^{(s)} - \mathbf{u}^{(\delta)}(x) = \operatorname{curl} \tilde{\hat{\mathbf{u}}}_{i,p}^{(s,\delta)}(x).$$

We use the following ansatz for the asymptotic expansion of the solution to problem (1)

$$\mathbf{u}^{(s,\delta)}(x) = \mathbf{u}^{(\delta)}(x) + \mathbf{r}^{(s,\delta)}(x) + \sum_{j=1}^{4} \mathbf{r}_j^{(s,\delta)}(x) + \mathbf{w}_{s,\delta}(x), \tag{43}$$

where

$$\mathbf{r}^{(s,\delta)}(x) = -\sum_{i\in I_s''} \sum_{m=1}^{\mathcal{M}(i,s)} \operatorname{curl}\Big\{\sum_{k=1}^{3} \tilde{\mathbf{v}}_{k,i,m}^{(s)}(x)\, \mathbf{u}_{i,m,k}^{(s,\delta)} \varphi_{i,m}^{(s)}(x)\Big\},$$

$$\mathbf{r}_1^{(s,\delta)}(x) = \sum_{i\in I_s'} \sum_{r=1}^{\mathcal{R}(i,s)} \operatorname{curl}\big\{\tilde{\tilde{\mathbf{u}}}_{i,r}^{(s,\delta)}(x)\omega_{i,r}^{(s)}\big\} + \sum_{i\in I_s''} \sum_{p=1}^{\mathcal{P}(i,s)} \operatorname{curl}\big\{\tilde{\tilde{\mathbf{u}}}_{i,p}^{(s,\delta)}(x)\chi_{i,p}^{(s)}\big\}$$

$$+ \sum_{i\in I_s''} \sum_{m=1}^{\mathcal{M}(i,s)} \left(\operatorname{curl}\big\{\tilde{\mathbf{u}}_{i,m}^{(s,\delta)}(x)\varphi_{i,m}^{(s)}\big\} + \sum_{t=1}^{2} \operatorname{curl}\big\{\tilde{\mathbf{u}}_{i,m}^{(s,\delta,t)}(x)\psi_{i,m}^{(s,t)}\big\}\right),$$

$$\mathbf{r}_2^{(s,\delta)}(x) = -\sum_{i\in I_s'} \sum_{r=1}^{\mathcal{R}(i,s)} \operatorname{curl}\Big\{\sum_{k=1}^{3} \tilde{\tilde{\mathbf{v}}}_{k,i,r}^{(s)}(x)\, \mathbf{u}_{i,r,k}^{(s,\delta)} \omega_{i,r}^{(s)}(x)\Big\},$$

$$\mathbf{r}_3^{(s,\delta)}(x) = -\sum_{i\in I_s''} \sum_{m=1}^{\mathcal{M}(i,s)} \sum_{t=1}^{2} \operatorname{curl}\Big\{\sum_{k=1}^{3} \tilde{\mathbf{v}}_{k,i,m}^{(s,t)}(x)\, \mathbf{u}_{i,m,k}^{(s,\delta,t)} \psi_{i,m}^{(s,t)}(x)\Big\},$$

$$\mathbf{r}_4^{(s,\delta)}(x) = -\sum_{i\in I''(s)} \sum_{p=1}^{\mathcal{P}(i,s)} \operatorname{curl}\Big\{\sum_{k=1}^{3} \tilde{\tilde{\mathbf{v}}}_{k,i,p}^{(s)}(x)\, \tilde{\mathbf{u}}_{i,p,k}^{(s,\delta)} \chi_{i,p}^{(s)}(x)\Big\},$$

and $\mathbf{w}_{s,\delta} \in H(\Omega_s)$ is the remainder term of asymptotic expansion.

In order to investigate the behavior of $\mathbf{r}^{(s,\delta)}(x)$ and $\mathbf{r}_j^{(s,\delta)}(x)$ as $s \to \infty$ from asymptotic expansion (43) we use the pointwise and integral estimates from Theorem 2, definition and properties of the cut-off functions. In such way we prove the following results:

Theorem 3 *Suppose that conditions (i)–(v) are satisfied. Then the sequences of functions* $\{\mathbf{r}_j^{(s,\delta)}\}_{s=1}^{\infty}$, $j = 1, 2, 3, 4$, *converge to zero strongly in* $H(\Omega)$ *as* $s \to \infty$.

Theorem 4 *Suppose that conditions (i)–(v) are satisfied. Then the sequence of solutions* $\{\mathbf{r}^{(s,\delta)}\}_{s=1}^{\infty}$ *converges to zero strongly in* $W^{1,\vartheta}(\Omega)^3$ *for any* $0 < \vartheta < 2$ *and weakly in* $H(\Omega)$ *as* $s \to \infty$.

Proofs of these theorems are similar to the proofs of analogous results in [22] and they are omitted here.

In the next theorem we obtain the behavior of the reminder term $\mathbf{w}_{s,\delta}(x)$ of asymptotic expansion (43).

Theorem 5 *Suppose that conditions (**i**)–(**v**) are satisfied. Then the sequence of functions* $\{\mathbf{w}_{s,\delta}\}_{s=1}^{\infty}$ *converges to zero strongly in* $H(\Omega)$ *as* $s \to \infty$.

Proof It follows from definition (43) of function $\mathbf{u}^{(s,\delta)}$, and from Theorems 3, 4, that $\mathbf{w}_{s,\delta}$ converges to zero weakly as $s \to \infty$. We will prove that $\mathbf{w}_{s,\delta}$ converges to zero strongly in $H(\Omega)$. Plugging the function $\boldsymbol{\varphi}_s = \mathbf{w}_{s,\delta} \in H(\Omega_s)$ into integral identity (2), we have

$$\int_{\Omega_s} \nu \mathbf{D}[\mathbf{u}^{(s,\delta)}] \cdot \mathbf{D}[\mathbf{w}_{s,\delta}]\, dx - \int_{\Omega_s} (\mathbf{u}^{(s,\delta)} \cdot \nabla)\mathbf{w}_{s,\delta} \cdot \mathbf{u}^{(s,\delta)} dx = - \int_{\Omega_s} \mathbf{f}\mathbf{w}_{s,\delta}\, dx. \tag{44}$$

From the weak convergence $\mathbf{w}_{s,\delta}$ to zero in $H(\Omega)$ as $s \to \infty$ we derive

$$\lim_{s\to\infty} \int_{\Omega_s} \mathbf{f}\mathbf{w}_{s,\delta} dx = 0.$$

Let us consider the second integral on the left-hand side of (44). From the definition of the function $u^{(s,\delta)}$ we have

$$\int_{\Omega_s} (\mathbf{u}^{(s,\delta)} \cdot \nabla)\mathbf{w}_{s,\delta} \cdot \mathbf{u}^{(s,\delta)} dx$$

$$= \int_{\Omega_s} ((\mathbf{u}^{(\delta)} + \mathbf{r}^{(s,\delta)} + \sum_{j=1}^{4} \mathbf{r}_j^{(s,\delta)} + \mathbf{w}_{s,\delta}) \cdot \nabla)\mathbf{w}_{s,\delta} \cdot (\mathbf{u}^{(\delta)} + \mathbf{r}^{(s,\delta)} + \sum_{j=1}^{4} \mathbf{r}_j^{(s,\delta)} + \mathbf{w}_{s,\delta}) dx.$$

Then, from the weak convergence of function $\mathbf{w}_s$ to zero in $H(\Omega)$, it is simple to see that

$$\lim_{s\to\infty} \int_{\Omega_s} (\mathbf{u}^{(\delta)} \cdot \nabla)\mathbf{w}_{s,\delta} \cdot \mathbf{u}^{(\delta)} dx = 0.$$

From the strong convergence of $(\mathbf{r}^{(s,\delta)} + \sum_{j=1}^{4} \mathbf{r}_j^{(s,\delta)})$ and $\mathbf{w}_{s,\delta}$ in $L_q(\Omega)^3,\ q < 6$, to zero as $s \to \infty$, and from the boundedness of $\|\mathbf{u}^{(\delta)}\|_{L_2(\Omega)^3}$ and $\|\nabla \mathbf{w}_{s,\delta}\|_{L_2(\Omega)^3}$ by a constant not depending of s, we derive

$$\lim_{s\to\infty} \int_{\Omega_s} (\mathbf{w}_{s,\delta} \cdot \nabla)\mathbf{w}_{s,\delta} \cdot \mathbf{w}_{s,\delta} dx \le C \lim_{s\to\infty} \Big(\int_{\Omega_s} |\mathbf{w}_{s,\delta}|^4\, dx \Big)^{\frac{1}{2}} \Big(\int_{\Omega_s} |\nabla \mathbf{w}_{s,\delta}|^2\, dx \Big)^{\frac{1}{2}} = 0,$$

$$\lim_{s\to\infty} \int_{\Omega_s} (\mathbf{w}_{s,\delta} \cdot \nabla)\mathbf{w}_{s,\delta} \cdot \mathbf{u}^{(\delta)}\, dx = \lim_{s\to\infty} \int_{\Omega_s} (\mathbf{u}^{(\delta)} \cdot \nabla)\mathbf{w}_{s,\delta} \cdot \mathbf{w}_{s,\delta} dx$$

$$\le C \lim_{s\to\infty} \Big(\int_{\Omega_{s,\delta}} |\mathbf{w}_{s,\delta}|^4\, dx \Big)^{\frac{1}{4}} \Big(\int_{\Omega_s} |\mathbf{u}^{(\delta)}|^4\, dx \Big)^{\frac{1}{4}} \Big(\int_{\Omega_s} |\nabla \mathbf{w}_{s,\delta}|^2\, dx \Big)^{\frac{1}{2}} = 0,$$

$$\lim_{s\to\infty}\int\limits_{\Omega_s}(\mathbf{u}^{(\delta)}\cdot\nabla)\mathbf{w}_{s,\delta}\cdot(\mathbf{r}^{(s,\delta)}+\sum_{j=1}^{4}\mathbf{r}_j^{(s,\delta)})dx$$

$$\leq C\lim_{s\to\infty}\Big(\int\limits_{\Omega_s}|\mathbf{r}^{(s,\delta)}+\sum_{j=1}^{4}\mathbf{r}_j^{(s,\delta)}|^4\,dx\Big)^{\frac{1}{4}}\Big(\int\limits_{\Omega_s}|\nabla\mathbf{w}_{s,\delta}|^2\,dx\Big)^{\frac{1}{2}}\Big(\int\limits_{\Omega_s}|\mathbf{u}^{(\delta)}|^4\,dx\Big)^{\frac{1}{4}}=0,$$

$$\lim_{s\to\infty}\int\limits_{\Omega_s}(\mathbf{w}_{s,\delta}\cdot\nabla)\mathbf{w}_{s,\delta}\cdot(\mathbf{r}^{(s,\delta)}+\sum_{j=1}^{4}\mathbf{r}_j^{(s,\delta)})dx$$

$$=\lim_{s\to\infty}\int\limits_{\Omega_s}((\mathbf{r}^{(s,\delta)}+\sum_{j=1}^{4}\mathbf{r}_j^{(s,\delta)})\cdot\nabla)\mathbf{w}_{s,\delta}\cdot\mathbf{w}_{s,\delta}dx$$

$$\leq C\lim_{s\to\infty}\Big(\int\limits_{\Omega_s}|\mathbf{r}^{(s,\delta)}+\sum_{j=1}^{4}\mathbf{r}_j^{(s,\delta)}|^4\,dx\Big)^{\frac{1}{4}}\Big(\int\limits_{\Omega_s}|\nabla\mathbf{w}_{s,\delta}|^2\,dx\Big)^{\frac{1}{2}}\Big(\int\limits_{\Omega_s}|\mathbf{w}_{s,\delta}|^4\,dx\Big)^{\frac{1}{4}}=0,$$

$$\lim_{s\to\infty}\int\limits_{\Omega_s}((\mathbf{r}^{(s,\delta)}+\sum_{j=1}^{4}\mathbf{r}_j^{(s,\delta)})\cdot\nabla)\mathbf{w}_{s,\delta}\cdot\mathbf{u}^{(\delta)}dx$$

$$\leq C\lim_{s\to\infty}\Big(\int\limits_{\Omega_s}|\mathbf{r}^{(s,\delta)}+\sum_{j=1}^{4}\mathbf{r}_j^{(s,\delta)}|^4\,dx\Big)^{\frac{1}{4}}\Big(\int\limits_{\Omega_s}|\nabla\mathbf{w}_{s,\delta}|^2\,dx\Big)^{\frac{1}{2}}\Big(\int\limits_{\Omega_s}|\mathbf{u}^{(\delta)}|^4\,dx\Big)^{\frac{1}{4}}=0,$$

$$\lim_{s\to\infty}\int\limits_{\Omega_s}((\mathbf{r}^{(s,\delta)}+\sum_{j=1}^{4}\mathbf{r}_j^{(s,\delta)})\cdot\nabla)\mathbf{w}_s\cdot(\mathbf{r}^{(s,\delta)}+\sum_{j=1}^{4}\mathbf{r}_j^{(s,\delta)})dx$$

$$\leq C\lim_{s\to\infty}\Big(\int\limits_{\Omega_s}|\mathbf{r}^{(s,\delta)}+\sum_{j=1}^{4}\mathbf{r}_j^{(s,\delta)}|^4\,dx\Big)^{\frac{1}{2}}\Big(\int\limits_{\Omega_s}|\nabla\mathbf{w}_{s,\delta}|^2\,dx\Big)^{\frac{1}{2}}=0.$$

This gives us

$$\lim_{s\to\infty}\int\limits_{\Omega_s}(\mathbf{u}^{(s,\delta)}\cdot\nabla)\mathbf{w}_{s,\delta}\cdot\mathbf{u}^{(s,\delta)}dx=0. \tag{45}$$

Now we consider the first integral on the left-hand side of (44)

$$\int\limits_{\Omega_s}\mathbf{D}[\mathbf{u}^{(s,\delta)}]\cdot\mathbf{D}[\mathbf{w}_{s,\delta}]\,dx$$

$$\leq C\int\limits_{\Omega_s}\bigg(\mathbf{D}[\mathbf{u}^{(\delta)}]+\mathbf{D}[\mathbf{r}^{(s,\delta)}]+\mathbf{D}[\sum_{j=1}^{4}\mathbf{r}_j^{(s,\delta)}]+\mathbf{D}[\mathbf{w}_{s,\delta}]\bigg)\mathbf{D}[\mathbf{w}_{s,\delta}]\,dx.$$

Since $\|\mathbf{D}[\mathbf{u}^{(\delta)}]\|_{L_2(\Omega)^3}$ is bounded, $\nabla(\sum_{j=1}^4 \mathbf{r}_j^{(s,\delta)})$ converges strongly to zero, and $\nabla \mathbf{w}_{s,\delta}(x)$ converges weakly to zero in $L_2(\Omega)^3$ as $s \to \infty$, we obtain

$$\lim_{s\to\infty} \int\limits_{\Omega_s} \mathbf{D}[\mathbf{u}^{(\delta)}] \cdot \mathbf{D}[\mathbf{w}_{s,\delta}]\, dx = 0, \quad \lim_{s\to\infty} \int\limits_{\Omega_s} \mathbf{D}[\sum_{j=1}^{4} \mathbf{r}_j^{(s,\delta)}] \cdot \mathbf{D}[\mathbf{w}_{s,\delta}]\, dx = 0.$$

Let us prove that

$$\lim_{s\to\infty} \int\limits_{\Omega_s} \mathbf{D}[\mathbf{r}^{(s,\delta)}] \cdot \mathbf{D}[\mathbf{w}_{s,\delta}]\, dx = 0. \tag{46}$$

Using that $\varphi_{i,m}^{(s)} \frac{\partial w_{s,\delta,\xi}}{\partial x_\xi} = \frac{\partial}{\partial x_\xi}(\varphi_{i,m}^{(s)} w_{s,\delta,\xi}) - w_{s,\delta,\xi} \frac{\partial \varphi_{i,m}^{(s)}}{\partial x_\xi}$, $\xi = 1, 2, 3$, and definition of the function $\mathbf{v}_{k,i,m}^{(s)}(x)$, we obtain

$$\Big|\int\limits_{\Omega_s} \mathbf{D}[\mathbf{r}^{(s,\delta)}] \cdot \mathbf{D}[\mathbf{w}_{s,\delta}]\, dx\Big| = \Big|\int\limits_{\Omega_s} \mathbf{D}[\sum_{i\in I_s''} \sum_{m=1}^{\mathcal{M}(i,s)} \operatorname{curl}\{\sum_{k=1}^{3} \tilde{\mathbf{v}}_{k,i,m}^{(s)} \mathbf{u}_{i,m,k}^{(s,\delta)} \varphi_{i,m}^{(s)}\}]$$
$$\cdot \mathbf{D}[\mathbf{w}_{s,\delta}]\, dx\Big| \le$$
$$\sum_{i\in I_s''} \sum_{m=1}^{\mathcal{M}(i,s)} \sum_{k=1}^{3} |\mathbf{u}_{i,m,k}^{(s,\delta)}| \Big|\int\limits_{\Omega_s} \mathbf{D}[\mathbf{v}_{k,i,m}^{(s)} \varphi_{i,m}^{(s)}] \cdot \mathbf{D}[\mathbf{w}_{s,\delta}]\, dx + \int\limits_{\Omega_s} \mathbf{D}[\nabla \varphi_{i,m}^{(s)} \times \tilde{\mathbf{v}}_{k,i,m}^{(s)}]$$
$$\cdot \mathbf{D}[\mathbf{w}_{s,\delta}]\, dx\Big| \le$$
$$C \sum_{i\in I_s''} \sum_{m=1}^{\mathcal{M}(i,s)} \sum_{k=1}^{3} |\mathbf{u}_{i,m,k}^{(s,\delta)}| \Big(\Big|\int\limits_{\Omega_s} \mathbf{D}[\mathbf{v}_{k,i,m}^{(s)}] \cdot \mathbf{D}[\mathbf{w}_{s,\delta} \varphi_{i,m}^{(s)}]\, dx\Big|$$
$$+ \Big|\int\limits_{\Omega_s} \mathbf{D}[\nabla \varphi_{i,m}^{(s)} \times \tilde{\mathbf{v}}_{k,i,m}^{(s)}] \cdot \mathbf{D}[\mathbf{w}_{s,\delta}]\, dx\Big| + \int\limits_{\Omega_s} |\mathbf{D}[\mathbf{v}_{k,i,m}^{(s)}]| |\mathbf{w}_{s,\delta}| |\nabla \varphi_{i,m}^{(s)}|\, dx$$
$$+ \int\limits_{\Omega_s} |\mathbf{v}_{k,i,m}^{(s)}| |\mathbf{D}[\mathbf{w}_{s,\delta}]| |\nabla \varphi_{i,m}^{(s)}|\, dx\Big). \tag{47}$$

We consider every integral on the right-hand side of the last inequality, using the pointwise and integral estimates of solutions to model problems and definition of the cut-off functions. For the first integral on the right-hand side of (47) we derive

$$\lim_{s\to\infty} \sum_{i\in I_s''} \sum_{m=1}^{\mathcal{M}(i,s)} \sum_{k=1}^{3} \Big|\int_{\Omega_s} \mathbf{D}[\mathbf{v}_{k,i,m}^{(s)}] \cdot \mathbf{D}[\mathbf{w}_{s,\delta} \varphi_{i,m}^{(s)}]\, dx\Big|$$

$$\leq C \lim_{s\to\infty} \left(\int\limits_{G_{i,m}^{(s)}} \left(\frac{\varepsilon_i^{(s)}}{|x'|} \right)^2 dx \right)^{\frac{1}{2}} \left(\int\limits_{G_{i,m}^{(s)}} |\mathbf{w}_{s,\delta}|^2 \, dx \right)^{\frac{1}{2}} = 0,$$

since $\mathbf{w}_{s,\delta}$ converges to zero strongly in $L_2(\Omega)^3$ as $s \to \infty$. From condition (**i**) and definition of $\varepsilon_i^{(s)}$ we obtain

$$\lim_{s\to\infty} \sum_{i\in I_s''} \sum_{m=1}^{\mathcal{M}(i,s)} \sum_{k=1}^{3} \int\limits_{\Omega_s} |\mathbf{v}_{k,i,m}^{(s)}||\mathbf{D}[\mathbf{w}_{s,\delta}]||\nabla\varphi_{i,m}^{(s)}| \, dx \leq$$

$$C \lim_{s\to\infty} \sum_{m=1}^{\mathcal{M}(i,s)} \sum_{k=1}^{3} \left(\int\limits_{\Omega} |\mathbf{D}[\mathbf{w}_{s,\delta}]| dx \right)^{\frac{1}{2}} \left(\sum_{i\in I_s''} \frac{1}{(\varepsilon_i^{(s)})^2} \int\limits_{F_{i,m}^{(s,1)}} |\mathbf{v}_{k,i,m}^{(s)}|^2 \, dx \right)^{\frac{1}{2}} = 0,$$

where $F_{i,m}^{(s,1)} := G_{i,m}^{(s)} \setminus (\mathcal{U}(l_i^{(s)}, \varepsilon_i^{(s)}) \bigcap G_{i,m}^{(s)}(\gamma + 1))$.

Analogously, using inequality (42) and the integral estimate of solutions $\mathbf{v}_{k,i,m}^{(s)}$ of the model problems, we have

$$\lim_{s\to\infty} \sum_{m=1}^{\mathcal{M}(i,s)} \sum_{k=1}^{3} \sum_{i\in I_s''} \left| \int\limits_{\Omega_s} \mathbf{D}[\nabla\varphi_{i,m}^{(s)} \times \tilde{\mathbf{v}}_{k,i,m}^{(s)}] \cdot \mathbf{D}[\mathbf{w}_{s,\delta}] \, dx \right| = 0.$$

For estimation of the third integral on the right-hand side of (47) we use the following inequalities for the function $\mathbf{w}_{s,\delta}$

$$\sum_{m=1}^{\mathcal{M}(i,s)} \int\limits_{E_{i,m}^{(s,\zeta)}} |\mathbf{w}_{s,\delta}|^2 \, dx \leq$$

$$C(\varepsilon_i^{(s)})^2 \left(\frac{1}{(r_i^{(s)})^2} \int\limits_{\mathcal{U}(l_i^{(s)}, r_i^{(s)})} |\mathbf{w}_{s,\delta}|^2 \, dx + \ln \frac{1}{\varepsilon_i^{(s)}} \int\limits_{\mathcal{U}(l_i^{(s)}, r_i^{(s)})} |\mathbf{D}[\mathbf{w}_{s,\delta}]|^2 \, dx \right) \qquad (48)$$

where $\zeta = 1, 2$, and

$$E_{i,m}^{(s,1)} := \{\mathcal{U}(l_i^{(s)}, 2\varepsilon_i^{(s)}) \setminus \mathcal{U}(l_i^{(s)}, \varepsilon_i^{(s)})\} \bigcap G_{i,m}^{(s)}(\gamma + 2),$$
$$E_{i,m}^{(s,2)} := G_{i,m}^{(s)}(\gamma) \setminus G_{i,m}^{(s)}(\gamma + 2).$$

To prove this inequality we use the change of variables $y = g_i^{(s)}(x)$ where $g_i^{(s)}$ are the diffeomorphisms from condition (**v**). The following estimates are valid

$$|D^\alpha v_i^k(x)| \le \frac{C_{14}}{\varrho^{|\alpha|}(x, l_i^{(s)})}\ln^{-1}\frac{1}{d_i^{(s)}},\ |\alpha| = 0, 1, 2,\ \forall\, x \in E_{i,m}^{(s,1)}, \tag{49}$$

$$\int\limits_{E_{i,m}^{(s,2)}} |\mathbf{D}[\mathbf{v}^k]|^2\, dx \le C_{15}\varepsilon_i^{(s)}\ln^{-1}\frac{1}{d_i^{(s)}}. \tag{50}$$

Using (48), (49), (50), we obtain

$$\lim_{s\to\infty} \sum_{i\in I_s''} \sum_{m=1}^{\mathcal{M}(i,s)} \sum_{k=1}^{3} \int_{\Omega_s} |\mathbf{D}[\mathbf{v}_{k,i,m}^{(s)}]||\mathbf{w}_{s,\delta}||\nabla\varphi_{i,m}^{(s)}|\, dx$$

$$\le \lim_{s\to\infty} C \sum_{\zeta=1,2} \sum_{i\in I_s''} \sum_{k=1}^{3} \left(\sum_{m=1}^{\mathcal{M}(i,s)} \int\limits_{E_{i,m}^{(s,\zeta)}} |\mathbf{D}[\mathbf{v}_{k,i,m}^{(s)}]|^2\, dx \right)^{\frac{1}{2}}$$

$$\times \left(\sum_{m=1}^{\mathcal{M}(i,s)} \frac{1}{(\varepsilon_i^{(s)})^2} \int\limits_{E_{i,m}^{(s,\zeta)}} |\mathbf{D}[\mathbf{w}_{s,\delta}]|^2\, dx \right)^{\frac{1}{2}} = 0.$$

From (45) and (46) we derive

$$\lim_{s\to\infty} \int\limits_{\Omega_s} |\mathbf{D}[\mathbf{w}_{s,\delta}]|^2\, dx = 0.$$

From Korn's inequality (see [15, 20]) and the last equality we obtain the convergence of $\nabla\mathbf{w}_{s,\delta}$ in $L_2(\Omega)^3$ to zero as $s \to \infty$. Theorem 5 is proved. □

Now we present the method how to construct a boundary value problem for the limit function $\mathbf{u}^{(0)}$. Let $\mathbf{h}$ be an arbitrary function of class $C_0^\infty(\Omega)$. Let us introduce a sequence of functions

$$\mathbf{h}_s(x) = \mathbf{h}(x) + \mathbf{q}^{(s)}(x) + \sum_{j=1}^{4} \mathbf{q}_j^{(s)}(x),\ s \in \mathbf{N}, \tag{51}$$

where

$$\mathbf{q}^{(s)}(x) = -\sum_{i\in I_s''} \sum_{m=1}^{\mathcal{M}(i,s)} \operatorname{curl}\Big\{ \sum_{k=1}^{n} \tilde{v}_{k,i,m}^{(s)}(x)\, \mathbf{h}_{i,m,k}^{(s)}\varphi_{i,m}^{(s)}(x)\Big\},$$

$$\mathbf{q}_1^{(s)}(x) = \sum_{i\in I_s'} \sum_{r=1}^{\mathcal{R}(i,s)} \operatorname{curl}\big\{\tilde{\tilde{\mathbf{h}}}_{i,r}^{(s)}(x)\omega_{i,r}^{(s)}(x)\big\} + \sum_{i\in I_s''} \sum_{p=1}^{\mathcal{P}(i,s)} \operatorname{curl}\big\{\hat{\tilde{\mathbf{h}}}_{i,p}^{(s)}(x)\chi_{i,p}^{(s)}(x)\big\}$$

$$+ \sum_{i\in I_s''} \sum_{m=1}^{\mathcal{M}(i,s)} \left(\operatorname{curl}\big\{\tilde{\mathbf{h}}_{i,m}^{(s)}(x)\varphi_{i,m}^{(s)}(x)\big\} + \sum_{t=1}^{2} \operatorname{curl}\big\{\tilde{\mathbf{h}}_{i,m}^{(s,t)}(x)\psi_{i,m}^{(s,t)}(x)\big\} \right)$$

$$\mathbf{q}_2^{(s)}(x) = -\sum_{i\in I'_s}\sum_{r=1}^{\mathcal{R}(i,s)} \operatorname{curl}\Big\{\sum_{k=1}^{n} \tilde{\bar{v}}_{k,i,r}^{(s)}(x)\bar{h}_{i,r,k}^{(s)}\omega_{i,r}^{(s)}(x)\Big\},$$

$$\mathbf{q}_3^{(s)}(x) = -\sum_{i\in I''_s}\sum_{m=1}^{\mathcal{M}(i,s)}\sum_{t=1}^{2} \operatorname{curl}\Big\{\sum_{k=1}^{n} \tilde{v}_{k,i,m}^{(s,t)}(x)h_{i,m,k}^{(s,t)}\psi_{i,m}^{(s,t)}(x)\Big\},$$

$$\mathbf{q}_4^{(s)}(x) = -\sum_{i\in I''(s)}\sum_{p=1}^{\mathcal{P}(i,s)} \operatorname{curl}\Big\{\sum_{k=1}^{n} \tilde{\hat{v}}_{k,i,p}^{(s)}(x)\tilde{h}_{i,p,k}^{(s)}\chi_{i,p}^{(s)}(x)\Big\},$$

here we keep for the function $\mathbf{h}(x)$ all notations as in (43) and

$$\mathbf{h}_{i,m}^{(s)} - \mathbf{h}(x) = \operatorname{curl}\tilde{\mathbf{h}}_{i,m}^{(s)}(x),\ \ \mathbf{h}_{i,m}^{(s,t)} - \mathbf{h}(x) = \operatorname{curl}\tilde{\mathbf{h}}_{i,m}^{(s,t)}(x),$$
$$\bar{\mathbf{h}}_{i,r}^{(s)} - \mathbf{h}(x) = \operatorname{curl}\tilde{\bar{\mathbf{h}}}_{i,r}^{(s)}(x),\ \ \hat{\mathbf{h}}_{i,p}^{(s)} - \mathbf{h}(x) = \operatorname{curl}\tilde{\hat{\mathbf{h}}}_{i,p}^{(s)}(x).$$

Substituting the function $\boldsymbol{\varphi}^{(s)}(x) = \mathbf{h}_s(x) \in W_0^{1,2}(\Omega)^3$ into integral identity (2), we get:

$$\int_\Omega (\nu\mathbf{D}[\mathbf{u}^{(0)}]\cdot\mathbf{D}[\mathbf{h}] - (\mathbf{u}^{(0)}\cdot\nabla)\mathbf{h}\cdot\mathbf{u}^{(0)})\,dx + \int_\Omega (\mathbf{f},\mathbf{h})\,dx$$
$$+\nu\sum_{i\in I''_s}\sum_{m=1}^{M(i,s)}\sum_{k,\ell=1}^{n} \mathbf{h}_{i,m,k}^{(s)}\mathbf{u}_{i,m,\ell}^{(s)}\int_\Omega \mathbf{D}[\mathbf{v}_{k,i,m}^{(s)}]\cdot\mathbf{D}[\mathbf{v}_{\ell,i,m}^{(s)}]\,dx = \Upsilon(\delta,s), \tag{52}$$

where

$$|\Upsilon(\delta,s)| \le \gamma_1^{(s)} + \gamma_2^{(\delta)},$$

and sequences $\gamma_1^{(s)}$, $\gamma_2^{(\delta)}$ are such that $\lim_{s\to\infty}\gamma_1^{(s)} = 0$, $\lim_{\delta\to\infty}\gamma_2^{(\delta)} = 0$. Finally, using the condition (**vi**) on the left-hand side of (52) and passing to the limit as $s\to\infty$, $\delta\to\infty$, we obtain that the limit function $\mathbf{u}^{(0)}(x)$ is a weak solution of averaged problem (8) in the sense of Definition 2. Theorem 1 is proved completely.

6 Appendix

Theorem 6 *(see [6]) Let G be a domain of $\mathbf{R}^3$ which is a diffeomorphic image of ball. Let $J(G)$ be the closure of linear smooth solenoidal functions from $L_2(G)^3$. Then for every $\mathbf{u}(x)\in J(G)$ the following representation is valid*

$$\mathbf{u}(x) = \operatorname{curl}\widetilde{\mathbf{u}}(x),$$

where $\tilde{\mathbf{u}}(x)\in W^{1,2}(G)^3,\ div\,\tilde{\mathbf{u}}(x) = 0,\ \frac{\partial\tilde{\mathbf{u}}}{\partial\mathbf{n}}|_{\partial G} = 0,$

$$\|\tilde{\mathbf{u}}\|_{W^{1,2}(G)^3} \leq K\|\mathbf{u}\|_{L_2(G)^3},$$

where $K = K(G)$ is a positive constant. The vector-function $\widetilde{\mathbf{u}}$ is defined by these conditions in a unique way.

Acknowledgments The work of Š. N. was supported by project n.201/08/0012 of GACR and also in the framework of the general research programme of the Academy of Sciences of the Czech Republic, Institutional Plan AV0Z10190503. The works of Yu.V.N., Š.N., and I.I.S. were supported by joint project between Czech Academy of Sciences and National Academy of Sciences of Ukraine. Also we would like to thank the referee for his very stimulating remarks.

References

1. Allaire, G.: Homogenization of the Stokes flow in a connected porous medium. Asymptot. Anal. **2**, 203–222 (1989)
2. Allaire, G.: One-phase newtonian flow. In *Homogenization and Porous Media*, ed. U.Hornung, pp. 45–68. Springer, New York (1997)
3. Beliaev, A.Yu, Kozlov, S.M.: Darcy equation for random porous media. Comm. Pure Appl. Math. **49**, 1–34 (1995)
4. Berezhnyi, M., Berlyand L., Khruslov E.: Homogenized models of complex fluids, Networks and heterogeneous media. **3** (4), 831–862 (2008)
5. Bourgeaut, A., Mikelic, A.: Note on the Homogenization of Bingham Flow through Porous Medium. J. Math. Pures Appl. **72**, 405–414 (1993)
6. Byhovskij, E.B., Smirnov, N.V.: Orthogonal decomposition of the space of vector functions square-summable on a given domain, and the operators of vector analysis. Works of Steklov Institute of Mathematics AN SSSR, M.-L. 59, 5–35 (1960)
7. Clopeau, Th., Ferrin, Gilbert, R. P., Mikelic, A.: Homogenizing the acoustic properties of the Seabed, II, Math. Comp. Model. **32**, 821–841, (2001)
8. Ene, H.I., Sanchez-Palencia, E.: Equations et phénomenènes de surface pour l'écoulement dans un modèle de milieu poreux. J. Mécan. **14**, 73–108 (1975)
9. Galdi, G. P.: *An Introduction to the Mathematical Theory of the Navier-Stokes Equations.* Volume I, Linearized steady problems, Springer Tracts in Nat. Philos., Vol. 38 (1994)
10. Gilbert, R.P., Mikelic, A.: Homogenizing the acoustic properties of the seabed, Part I. Nonlinear Anal. **40**, 185–212 (2000)
11. Jäger, W., Mikelic, A.: On the effective equations for a viscous incompressible fluid flow through a filter of finite thickness. Commun. Pure Appl. Math. **LI**, 1073–1121 (1998)
12. Jikov, V.V., Kozlov, S., Oleinik, O.: *Homogenization of Differential Operators and Integral Functionals.* Springer Verlag, New York (1994)
13. Khruslov, E.Ya., Lvov, V.A.: Boundary problems for the linearized Navier-Stokes system in domains with a fine-grained boundary (Russian). Vestn. Khar'kov. Univ. **119**, Mat. Mekh. **40**, 3–22 (1975)
14. Khruslov, E.Ya., Lvov, V.A.: Boundary problems for the general Navier-Stokes system in domains with a fine-grained boundary (Russian). Vestn. Khar'kov. Univ. **119**. Mat. Mekh. **40**, 23–36 (1975)
15. Kondratiev, V.A., Oleinik, O.A.: On Korn's inequalities. C.R. Acas. Sci. Paris **308**, Serie I, 483–487 (1989)
16. Ladyzhenskaya, O.A.: *Mathematical Problems of the Dynamics of Viscous Incompressible Fluids.* Nauka, Moscow (1970)
17. Marchenko, V.A., Khruslov, E.Ya.: Kraevye zadaci v oblastjah s melkozernistoi granicei (Russian). Kiev, "Naukova Dumka" (1974)

18. Marchenko, V.A., Khruslov, E.Ya.: Homogenization of Partial Differential Equations. Series: Prog. Math. Phys., **XII**, Vol. 46 (2006)
19. Namlyeyeva, Yu., Nečasová, Š.: Homogenization of the steady Navier-Stokes equations in domains with a fine-grained boundary. Proceedings of the Conference "Topical problems of the fluid mechanics 2006. Institute of Thermomechanics AS CR 2006, 103–106 (2006)
20. Nitsche, J.A.: On Korn's second inequality. R.A.I.R.O., Analyse Numerique **15**(3) 237–248 (1981)
21. Sanchez-Palencia, E.: *Non-Homogeneous Media and Vibration Theory.* Lecture Notes in Physics, **127**, Springer, IX (1980)
22. Skrypnik, I.V.: *Methods for Analysis of Nonlinear Elliptic Boundary Value Problems.* American Mathematical Society, Providence, RI (1994)
23. Skrypnik, I.V.: Averaging of quasilinear parabolic problems in domains with fine-grained boundaries. Diff. Equ. **31**(2), 327–339 (1995)
24. Tartar, L.: *Navier- Stokes Equations.* Elsevier Science Publishers B. V., Amsterdam (1984)

Existence of Weak Solutions to the Equations of Natural Convection with Dissipative Heating

Joachim Naumann and Jörg Wolf

Abstract In this paper, we prove the existence of a weak solution to a system of PDE's which model the non-stationary motion of a heat-conducting incompressible viscous fluid including the effects of dissipative and adiabatic heating. Our method of proof consists in approximating these heat sources by bounded nonlinearities.

Keywords Heat conducting fluid · Dissipative heating · Conservation of internal energy

1 Introduction

In this paper, we consider the following system of PDE's modeling the motion of a heat-conducting incompressible viscous fluid:

$$\operatorname{div}\mathbf{u} = 0 \tag{1}$$

$$\frac{\partial \mathbf{u}}{\partial t} + (\mathbf{u}\cdot\nabla)\mathbf{u} - \operatorname{div}\Big(\nu(\theta)D(\mathbf{u})\Big) + \nabla p = (1-\alpha_0\theta)\mathbf{f} \tag{2}$$

$$\frac{\partial \theta}{\partial t} + \mathbf{u}\cdot\nabla\theta - \operatorname{div}\Big(\kappa(\theta)\nabla\theta\Big) = \nu(\theta)D(\mathbf{u}) : D(\mathbf{u}) + \alpha_1\theta\mathbf{f}\cdot\mathbf{u} + g,\ ^{1} \tag{3}$$

where the unknowns are: $\mathbf{u}$ = velocity, p = mechanical pressure and θ = temperature. $D(\mathbf{u}) = \frac{1}{2}\Big(\nabla\mathbf{u} + (\nabla\mathbf{u})^\top\Big)$ denotes the rate of strain tensor. System (1), (2) and (3) represents the laws of conservation of mass, momentum and internal energy, respectively, of a fluid with constitutive relations

J. Naumann (✉)
Mathematical Institute, Humboldt University Berlin, 10099 Berlin
e-mail: jnaumann@math.hu-berlin.de

R. Rannacher, A. Sequeira (eds.), *Advances in Mathematical Fluid Mechanics*,
DOI 10.1007/978-3-642-04068-9_23,

$$\sigma = \nu(\theta)D(\mathbf{u}) - pI \quad \text{stress tensor } (I = \text{unit tensor}),$$

$$\mathbf{q} = -\kappa(\theta)\nabla\theta \quad \text{heat flux},$$

$$e = C_0\theta \quad \text{internal energy} \quad (C_0 = \text{const} > 0),$$

where

$$\nu(\theta) = \text{viscosity}, \quad \kappa(\theta) = \text{heat conductivity}$$

(for notational simplicity, in what follows we set $C_0 = 1$). The density of the fluid is treated as a constant in all terms of the equations of conservation of momentum except the one in the external force $\mathbf{f}$. Accordingly, α_0 is the coefficient of linearized density variation with respect to the temperature (see, e. g., [3]).

The term $\nu(\theta)D(\mathbf{u}) : D(\mathbf{u})$ on the right hand side of (3) models viscous dissipation of internal energy. The terms $\alpha_1\theta\mathbf{f} \cdot \mathbf{u}$ and g represent an adiabatic and an external heat source, respectively.

If $\nu(\theta)D(\mathbf{u}) : D(\mathbf{u})$ and $\alpha_1\theta\mathbf{f} \cdot \mathbf{u}$ are neglected in (3), the resulting system for the unknowns $\mathbf{u}$, p and θ is usually referred to as the Boussinesq approximation of the general system of conservation laws governing the motion of a heat-conducting incompressible viscous fluid (see [3] for details). The above version of (1), (2) and (3) has been derived in [6], however, with $\nu = \text{const}$ (see (2.21) there). This approach is closely related to the Oberbeck-Boussinesq approximation presented in [10]. □

We consider system (1), (2) and (3) in the cylinder $Q = \Omega\times]0, T[$, where Ω is a bounded domain in $\mathbb{R}^3$. We restrict our discussion of (1), (2) and (3) to the case of three space dimensions for the same reasons as in [7, 8]. Namely, in contrast to the case of two space dimensions, the well-known integrability properties of $\mathbf{u} \cdot (\nabla\mathbf{u})$ in $Q = \Omega\times]0, T[\quad (\Omega \subset \mathbb{R}^3)$ produce serious difficulties when handling the term $\nu(\theta)D(\mathbf{u}) : D(\mathbf{u})$ in (3) by approximation methods within the standard weak formulation. This leads to a defect measure in the weak formulation of (3).

To complete the formulation of the problem that we shall consider, assume

$$\partial\Omega \text{ is Lipschitz,}$$
$$\partial\Omega = \Gamma_0 \cup \Gamma_1, \quad \Gamma_0 \cap \Gamma_1 = \emptyset.$$

The boundary and initial conditions on $\mathbf{u}$ and θ are then as follows:

$$\begin{cases} \mathbf{u} = \mathbf{0} \quad \text{on} \quad \partial\Omega\times]0, T[, \\ \theta = 0 \quad \text{on} \quad \Gamma_0\times]0, T[, \quad \kappa(\theta)\dfrac{\partial\theta}{\partial n} = 0 \quad \text{on} \quad \Gamma_1\times]0, T[, \end{cases} \tag{4}$$

[1] By $A : B = A_{ij}B_{ij}$ we denote the trace of the matrices $A = \{A_{ij}\}$, $B = \{B_{ij}\}$ (throughout repeated Latin subscripts imply summation on $1, 2, 3$). - For $\mathbf{u} = (u_1, u_2, u_3)$ we have $D(\mathbf{u}) = \{D_{ij}(\mathbf{u})\}$, $D_{ij}(\mathbf{u}) = \frac{1}{2}\left(\frac{\partial u_i}{\partial x_j} + \frac{\partial u_j}{\partial x_i}\right)$.

$$\mathbf{u} = \mathbf{u}_0, \quad \theta = \theta_0 \quad \text{on} \quad \Omega \times \{0\} \tag{5}$$

(n = exterior unit normal along $\partial\Omega$). Here, $\mathbf{u}_0$ and θ_0 are given data. □

The equations of non-stationary motion of heat-conducting incompressible viscous fluids with temperature dependent material coefficients and viscous energy dissipation have attracted much interest in recent time.

Amann [1] investigated the conservation laws for mass, momentum and internal energy for large classes of constitutive laws $\sigma = \nu(\theta, D_{II})D - pI$ ($D_{II} = \frac{1}{2}D : D$) and $\mathbf{q} = \mathbf{q}(\theta, \nabla\theta)$, with dissipative heating and certain additional heat sources. Under smallness assumptions on the initial values $\mathbf{u}_0$ and θ_0 he proved the existence of a strong solution to the problem considered. Feireisl/Màlek [5] (ν depending on θ, $\alpha_0 = \alpha_1 = 0$) and Kagai; Růžička; Thäter [6] ($\nu = \text{const} > 0$) proved the existence of weak resp. strong solutions to (1), (2) and (3) under space periodic boundary conditions on $\mathbf{u}$ and θ. Buliček; Feireisl; Málek [2] investigated (1), (2) and (3) with ν depending on θ, $\alpha_0 = \alpha_1 = 0$ and slip boundary conditions. This paper contains a profound discussion the thermodynamical aspects of (1), (2) and (3). Nečas; Roubiček [9] studied the system of conservation laws for mass, momentum and internal energy with dissipative heating and $\alpha_0 \neq 0$, $\alpha_1 \neq 0$, but with a power law type constitutive assumption on the stress tensor σ which excludes the case of Navier-Stokes equations that we consider in the present paper.

In Sect. 2 we introduce the notations and present the main result of our paper. It states the existence of a weak solution to (1), (2), (3), (4) and (5) with a defect measure in 3. The concept of a defect measure occurs in Feireisl [4] in the field of compressible fluids, and has been subsequently developed by this author and his collaborators. We note that in [1, 5, 6, 9] the weak formulation of the equation of conservation of internal energy does not involve a defect measure. Sect. 3 is devoted to the proof of our main result. It makes use of techniques developed by the authors in [7, 8, 11].

2 Notations. Statement of the Main Result

Let $W^{1,q}(\Omega)$ $(1 \le q \le +\infty)$ denote the usual Sobolev space. Define

$$W^{1,q}_{\Gamma_0}(\Omega) := \{\varphi \in W^{1,q}(\Omega);\ \varphi = 0 \text{ a. e. on } \Gamma_0\},$$

$$V_q := \{\mathbf{v} \in [W^{1,q}(\Omega)]^3;\ \mathbf{v} = 0 \text{ a. e. on } \partial\Omega, \quad \operatorname{div}\mathbf{v} = 0 \text{ a. e. in } \Omega\},$$

$$H := \Big\{\mathbf{h} \in [L^2(\Omega)]^3;\ \int_\Omega \mathbf{h} \cdot \nabla\varphi dx = 0 \ \forall\, \varphi \in C_c^\infty(\Omega)\Big\}.$$

If $\Gamma_0 = \partial\Omega$, we write $W^{1,q}_0(\Omega) := W^{1,q}_{\Gamma_0}(\Omega)$.

Next, given a normed space X with norm $\|\cdot\|$, we denote by X^* the dual space of X and by $\langle x^*, x\rangle_X$ the value of $x^* \in X^*$ at $x \in X$. $C_w([0,T];X)$ stands for the vector space of all mappings $z : [0,T] \to X$ such that for every $x^* \in X^*$ the function

$$t \mapsto \langle x^*, z(t)\rangle$$

is continuous in $[0,T]$. By $L^q(0,T;X)$ $(1 \le q \le +\infty)$ we denote the vector space of all equivalence classes of Bochner measurable functions $z : [0,T] \to X$ such that

$$\int_0^T \|z(t)\|^q dt < +\infty \text{ if } 1 \le q < +\infty, \quad \operatorname*{ess\,sup}_{t\in[0,T]} \|z(t)\| < +\infty \text{ if } q = +\infty.$$

Finally, let $\mathcal{M}(\bar{Q})$ be the set of all Radon measures in $\bar{Q}$.

For notational simplicity, in what follows we write

$$D(\mathbf{u},\mathbf{v}) := D(\mathbf{u}) : D(\mathbf{v}) = D_{ij}(\mathbf{u})D_{ij}(\mathbf{v}).$$

Without further reference, throughout we assume

$$\begin{gathered}
\nu \in C(\mathbb{R}), \quad \kappa \in C(\mathbb{R}),\\
0 < \nu_1 \le \nu(\xi) \le \nu_2 < +\infty \quad \forall\, \xi \in \mathbb{R} \quad (\nu_1, \nu_2 = \text{const}),\\
0 < \kappa_1 \le \kappa(\xi) \le \kappa_2 < +\infty \quad \forall\, \xi \in \mathbb{R} \quad (\kappa_1, \kappa_2 = \text{const}).
\end{gathered}$$

The main result of our paper is the following

Theorem 1 *Assume*

$$\mathbf{f} \in [L^\infty(Q)]^3, \quad g \in L^1(Q),\ g \ge 0 \quad \text{a. e. in} \quad Q, \tag{6}$$

$$\mathbf{u}_0 \in H, \quad \theta_0 \in L^1(\Omega),\ \theta_0 \ge 0 \quad \text{a. e. in} \quad \Omega, \tag{7}$$

$$\alpha_0, \alpha_1 \in \mathbb{R}. \tag{8}$$

Then there is an $\varepsilon_0 > 0$ such that if

$$(|\alpha_0| + |\alpha_1|)^2 \|\mathbf{f}\|^2_{L^\infty} T^{1/3} \le \varepsilon_0,$$

there exists a triple $\{\mathbf{u}, \theta, \mu\}$ such that

$$\begin{cases}
\mathbf{u} \in C_w([0,T];H) \cap L^2(0,T;V_2),\ \mathbf{u}' \in L^{4/3}(0,T;V_2^*),\\[2ex]
\theta \in L^\infty(0,T;L^1(\Omega)) \cap \bigcap\limits_{1\le r<\frac{5}{4}} L^r(0,T;W^{1,r}_{\Gamma_0}(\Omega)), \quad \theta \ge 0 \quad a.\,e.\ in \quad Q,\\[2ex]
\mu \in \mathcal{M}(\bar{Q})
\end{cases} \tag{9}$$

and

$$
\begin{cases}
\int\limits_0^T \langle \mathbf{u}', \mathbf{v}\rangle_{V_2} dt - \int\limits_Q u_i u_j \frac{\partial v_i}{\partial x_j} dxdt + \int\limits_Q \nu(\theta) D(\mathbf{u}, \mathbf{v}) dxdt = \\
= \int\limits_Q (1 - \alpha_0 \theta) \mathbf{f} \cdot \mathbf{v} \, dxdt \quad \forall\, \mathbf{v} \in L^4(0, T; V_2),
\end{cases}
\tag{10}
$$

$$
\begin{cases}
- \int\limits_Q \theta \frac{\partial \varphi}{\partial t} dxdt - \int\limits_Q u_i \theta \frac{\partial \varphi}{\partial x_i} dxdt + \int\limits_Q \kappa(\theta) \nabla\theta \cdot \nabla\varphi \, dxdt = \\
= \int\limits_\Omega \theta_0(x) \varphi(x, 0) dx \\
\quad + \int\limits_Q \Big(\nu(\theta) D(\mathbf{u}, \mathbf{u}) + \alpha_1 \theta \mathbf{f} \cdot \mathbf{u} + g \Big) \varphi dxdt + \int\limits_{\bar{Q}} \varphi d\mu \\
\forall\, \varphi \in C^1(\bar{Q}), \varphi = 0 \;\; on \;\; \Gamma_0 \times]0, T[, \quad \varphi(x, T) = 0 \quad \forall\, x \in \Omega,
\end{cases}
\tag{11}
$$

$$
\begin{cases}
\mathbf{u}(0) = \mathbf{u}_0 \quad a.\,e.\, in \quad \Omega, \\
\lim\limits_{t \to 0} \int\limits_\Omega \theta(x, t) \zeta(x) dx \geq \int\limits_\Omega \theta_0(x) \zeta(x) dx \quad \forall\, \zeta \in C^1(\bar{\Omega}), \quad \zeta \geq 0 \;\; in \;\; \Omega.
\end{cases}
\tag{12}
$$

If $\Gamma_0 = \emptyset$, *then*

$$
\lim_{t \to 0} \int\limits_\Omega \theta(x, t) dx = \int\limits_\Omega \theta_0(x) dx,
\tag{13}
$$

$$
\begin{cases}
\int\limits_\Omega \left(\frac{1}{2} |\mathbf{u}(t)|^2 + \theta(t) \right) dx = \\
= \int\limits_\Omega \left(\frac{1}{2} |\mathbf{u}_0|^2 + \theta_0 \right) dx + \int\limits_0^t \int\limits_\Omega \Big(\mathbf{f} \cdot \mathbf{u} + (\alpha_1 - \alpha_0) \theta \mathbf{f} \cdot \mathbf{u} + g \Big) dxds \\
for \; a.\,e.\;\; t \in]0, T[.
\end{cases}
\tag{14}
$$

3 Proof of the Main Theorem

3.1 Approximate Solutions

Let $\Phi \in C([0, +\infty[)$ be a fixed, non-increasing function such that

$$
0 \leq \Phi \leq 1 \quad \text{in} \quad [0, +\infty[,
$$

$$\Phi = 1 \quad \text{in} \quad [0,1], \qquad \Phi = 0 \quad \text{in} \quad [2,+\infty[.$$

For $\varepsilon > 0$ and $\xi \geq 0$, define

$$\Phi_\varepsilon(\xi) := \Phi(\varepsilon\xi).$$

The following properties of Φ_ε are readily verified:

- $\xi\Phi_\varepsilon(\xi) \leq \dfrac{2}{\varepsilon} \quad \forall\, \xi \geq 0, \quad \forall\, \varepsilon > 0;$
- $\lim\limits_{\varepsilon\to 0} \Phi_\varepsilon(\xi) = 1$ uniformly for all ξ in a bounded interval of $[0,+\infty[$;
- $\displaystyle\int\limits_\Omega w_i w_j \Phi_\varepsilon(|\mathbf{w}|^2)\frac{\partial w_i}{\partial x_j}dx = 0 \quad \forall\, \mathbf{w} \in V_2, \quad \forall\, \varepsilon > 0.$

The function Φ_ε is used for a cut-off procedure of the quadratic term $u_i u_j$ which occurs in the second integral on the left hand side in (10). More specifically, we replace this integral by

$$\int\limits_Q u_i u_j \Phi_\varepsilon(|\mathbf{u}|^2)\frac{\partial v_i}{\partial x_j}dxdt.$$

Then the term $u_i u_j \Phi_\varepsilon(|\mathbf{u}|^2)$ gives rise to a uniformly bounded nonlinearity which is easy to handle when proving the existence of an approximate solution. The passage to the limit $\varepsilon \to 0$ is then straightforward (see Sect. 3.3 below).

The method of approximation of $u_i u_j$ by $u_i u_j \Phi_\varepsilon(|\mathbf{u}|^2)$ has been developed in [11]. □

The following result forms the point of departure for the proof of our main result.

Proposition 1 *Assume* $\mathbf{f}, g$ *satisfy* (6), $\mathbf{u}_0 \in V_6$, $\theta_0 \in W_0^{1,2}(\Omega)$, $\theta_0 \geq 0$ *a. e. in* Ω, α_0, α_1 *satisfy* (8). *Then, for every* $0 < \varepsilon \leq 1$, $0 < \delta \leq 1$ *there exists a pair* $\{\mathbf{u},\theta\}$ *(*$\mathbf{u} = \mathbf{u}_{\varepsilon,\delta}, \theta = \theta_{\varepsilon,\delta}$*) such that*

$$\begin{cases} \mathbf{u} \in L^6(0,T;V_6) \cap C([0,T];H), \quad \mathbf{u}' \in L^{6/5}(0,T;V_6^*), \\ \theta \in L^2(0,T;W^{1,2}_{\Gamma_0}) \cap C([0,T];L^2), \quad \theta' \in L^2(0,T;(W^{1,2}_{\Gamma_0})^*), \\ \theta \geq 0 \quad a.\,e.\,in \quad Q, \end{cases} \tag{15}$$

and

$$\begin{cases} \int_0^t \langle \mathbf{u}', \mathbf{v} \rangle_{V_6} ds + \int_Q^t \int_\Omega [\nu(\theta) + \delta(D(\mathbf{u}, \mathbf{u}))^2] D(\mathbf{u}, \mathbf{v}) dxds - \\ - \int_0^t \int_\Omega u_i u_j \Phi_\varepsilon(|\mathbf{u}|^2) \frac{\partial v_i}{\partial x_j} dxds = \int_0^t \int_\Omega \Big(1 - \frac{\alpha_0 \theta}{1 + \varepsilon\theta^2}\Big) \mathbf{f} \cdot \mathbf{v}\, dxds \\ \forall\, t \in [0, T], \quad \forall\, \mathbf{v} \in L^6(0, T; V_6), \end{cases} \tag{16}$$

$$\begin{cases} \int_0^t \langle \theta', \varphi \rangle_{W^{1,2}_{\Gamma_0}} ds + \delta \int_0^t \int_\Omega \theta\varphi dxds + \int_0^t \int_\Omega \kappa(\theta) \nabla\theta \cdot \nabla\varphi dxds - \\ - \int_0^t \int_\Omega u_i \theta \frac{\partial \varphi}{\partial x_i} dxds \\ = \int_0^t \int_\Omega \Big(\nu(\theta) D(\mathbf{u}, \mathbf{u}) + \frac{\alpha_1 \theta}{1 + \varepsilon\theta^2} \mathbf{f} \cdot \mathbf{u} + \frac{g}{1 + \varepsilon g}\Big)\, \varphi\, dxds \\ \forall\, t \in [0, T], \quad \forall\, \varphi \in L^2(0, T; W^{1,2}_{\Gamma_0}), \end{cases} \tag{17}$$

$$\mathbf{u}(0) = \mathbf{u}_0, \quad \theta(0) = \theta_0 \quad a.\,e.\,in \quad \Omega. \tag{18}$$

The proof of this proposition follows the same lines as those of [7; Prop. 1]. To see this, it suffices to note the elementary inequalities

$$\frac{\xi}{1 + \varepsilon\xi^2} \le \frac{1}{2\sqrt{\varepsilon}}, \quad \frac{\xi^2}{1 + \varepsilon\xi^2} \le \frac{1}{\varepsilon} \quad \forall\, \xi \in [0, +\infty[.$$

Hence the integrals

$$-\alpha_0 \int_0^t \int_\Omega \frac{\theta}{1 + \varepsilon\theta^2}\, \mathbf{f} \cdot \mathbf{v} dxds \quad \text{in (16)},$$

$$\alpha_1 \int_0^t \int_\Omega \frac{\theta}{1 + \varepsilon\theta^2} \mathbf{f} \cdot \mathbf{u}\varphi\, dxds \quad \text{in (17)}$$

give rise to compact perturbations which can be easily included into the context of [8]. Therefore we dispense with further details.

Remark 1 The assumption $\mathbf{u}_0 \in V_6,\ \theta_0 \in W^{1,2}_0(\Omega)$, $\theta_0 \ge 0$ a. e. in Ω, we made for reducing the weak formulation of (1), (2), (3), (4) and (5) to zero initial conditions (see [8] for details).

3.2 A-priori Estimates

We derive estimates on $\mathbf{u}=\mathbf{u}_{\varepsilon,\delta}$ and $\theta=\theta_{\varepsilon,\delta}$ which are independent of $0<\varepsilon,\delta\le 1$.
1st step. Inserting $\mathbf{v}=\mathbf{u}$ into (16) gives

$$\frac{1}{2}\|\mathbf{u}(t)\|^2_{L^2}+\int\limits_0^t\int\limits_\Omega[\nu(\theta)+\delta(D(\mathbf{u},\mathbf{u}))^2]D(\mathbf{u},\mathbf{u})dxds$$
$$\le\frac{1}{2}\|\mathbf{u}_0\|^2_{L^2}+\|\mathbf{f}\|_{L^\infty}\int\limits_0^t\int\limits_\Omega|\mathbf{u}|dxds+|\alpha_0|\|\mathbf{f}\|_{L^\infty}\int\limits_0^t\int\limits_\Omega\theta|\mathbf{u}|dxds$$

for all $t\in[0,T]$. Observing that $0<\nu_1\le\nu(\theta)$ a. e. in Q we obtain by the aid of Korn's inequality

$$\|\mathbf{f}\|_{L^\infty}\int\limits_0^t\int\limits_\Omega|\mathbf{u}|dxds\le\frac{1}{4}\int\limits_0^t\int\limits_\Omega\nu(\theta)D(\mathbf{u},\mathbf{u})dxds+c\|\mathbf{f}\|^2_{L^\infty}T\text{ mes }\Omega.$$

Thus

$$\frac{1}{2}\|\mathbf{u}(t)\|^2_{L^2}+\frac{3}{4}\int\limits_0^t\int\limits_\Omega\nu(\theta)D(\mathbf{u},\mathbf{u})dxds+\delta\int\limits_0^t\int\limits_\Omega(D(\mathbf{u},\mathbf{u}))^3dxds\le$$
$$\le\frac{1}{2}\|\mathbf{u}_0\|^2_{L^2}+c\|\mathbf{f}\|^2_{L^\infty}T\text{ mes }\Omega+|\alpha_0|\|\mathbf{f}\|_{L^\infty}\int\limits_0^t\int\limits_\Omega\theta|\mathbf{u}|dxds \tag{19}$$

for all $t\in[0,T]$.

Next, for $0<\sigma<1$ define

$$\Psi_\sigma(\xi):=\xi+\frac{1}{1-\sigma}\Big(1-(1+\xi)^{1-\sigma}\Big),\qquad 0\le\xi<+\infty.$$

Clearly,

$$\frac{\xi}{2}-\frac{2^{(1-\sigma)/\sigma}}{1-\sigma}\le\Psi_\sigma(\xi)\le\xi,\quad \Psi'_\sigma(\xi)=1-\frac{1}{(1+\xi)^\sigma}\quad\forall\,\xi\in[0,+\infty[.$$

Consider $\varphi=\Psi'_\sigma(\theta)$ a. e. in Q. We have

$$\frac{\partial\varphi}{\partial x_i}=\frac{\sigma}{(1+\theta)^{1+\sigma}}\cdot\frac{\partial\theta}{\partial x_i}\quad\text{a. e. in }Q\quad(\text{thus }\varphi\in L^2(0,T;W^{1,2}_{\Gamma_0}))$$

$$\int_0^t \langle \theta', \varphi \rangle_{W^{1,2}_{\Gamma_0}} ds = \int_\Omega \Psi_\sigma(\theta(t))dx - \int_\Omega \Psi_\sigma(\theta_0)dx \quad \forall\, t \in [0, T],$$

$$\int_\Omega u_i \theta \frac{\partial \varphi}{\partial x_i} dx = -\int_\Omega u_i \frac{\partial}{\partial x_i} \Psi_\sigma(\theta)dx = 0 \quad \text{for a. e.} \quad t \in [0, T].$$

Inserting φ into (17) gives

$$\frac{1}{2}\int_\Omega \theta(t)dx + \sigma \int_0^t \int_\Omega \kappa(\theta)\frac{|\nabla\theta|^2}{(1+\theta)^{1+\sigma}} dxds \le$$
$$\le \frac{2^{(1-\sigma)/\sigma}}{1-\sigma}\text{mes}\Omega + \int_\Omega \theta_0 dx + \int_0^t\int_\Omega \Big(\nu(\theta)D(\mathbf{u},\mathbf{u}) + |\alpha_1|\|\mathbf{f}\|_{L^\infty}\theta|\mathbf{u}| + g\Big)dxds$$

for all $t \in [0, T]$. We now multiply this inequality by $\frac{1}{4}$ and add it to (19). Again using Korn's inequality we find

$$\|\mathbf{u}(t)\|^2_{L^2} + \|\theta(t)\|_{L^1} + \int_0^t\int_\Omega \Big(|\nabla\mathbf{u}|^2 + \delta|\nabla\mathbf{u}|^6\Big)dxds + \sigma\int_0^t\int_\Omega \frac{|\nabla\theta|^2}{(1+\theta)^{1+\sigma}}dxds$$
$$\le c_1\Big(1 + \|\mathbf{u}_0\|^2_{L^2} + \|\theta_0\|_{L^1} + \|\mathbf{f}\|^2_{L^\infty} + \|g\|_{L^1}\Big) + \tag{20}$$
$$+ c_2(|\alpha_0| + |\alpha_1|)\|\mathbf{f}\|_{L^\infty}\int_0^t\int_\Omega \theta|\mathbf{u}|dxds \text{ [2]}$$

for all $t \in [0, T]$.

For the sake of notational simplicity, in what follows we use the notation

$$\Lambda := 1 + \|\mathbf{u}_0\|^2_{L^2} + \|\theta_0\|_{L^1} + \|\mathbf{f}\|^2_{L^\infty} + \|g\|_{L^1}.$$

We estimate the last integral on the right hand side of (20). By Hölder's inequality and Sobolev's embedding theorem,

[2] In what follows, we denote by $c_1, c_2, \ldots$ positive constants which may change their numerical value from line to line, but depend neither on ε nor on δ.

$$\int_0^t \int_\Omega \theta|\mathbf{u}|dxds \le c_3\Big(\int_0^t \|\theta\|^2_{L^{6/5}}ds\Big)^{1/2}\Big(\int_0^t \int_\Omega |\nabla \mathbf{u}|^2 dxds\Big)^{1/2}$$
$$\le c_3\Big\{\Big(\int_0^t \|\theta\|^4_{L^1}ds\Big)^{1/3}\Big(\int_0^t \|\theta\|_{L^2}ds\Big)^{2/3}\Big\}^{1/2}\Big(\int_0^t \int_\Omega |\nabla \mathbf{u}|^2 dxds\Big)^{1/2}$$

($t \in [0,T]$). Inserting this estimate into (19) and applying Young's inequality gives

$$\|\mathbf{u}(t)\|^2_{L^2} + \|\theta(t)\|_{L^1} + \int_0^t\int_\Omega \big(|\nabla \mathbf{u}|^2 + \delta|\nabla \mathbf{u}|^6\big)\,dxds + \sigma\int_0^t\int_\Omega \frac{|\nabla\theta|^2}{(1+\theta)^{1+\sigma}}\,dxds$$
$$\le c_4\Lambda + c_5(|\alpha_0| + |\alpha_1|)^2\|\mathbf{f}\|^2_{L^\infty}\Big(\int_0^t \|\theta\|^4_{L^1}ds\Big)^{1/3}\Big(\int_0^t \|\theta\|_{L^2}ds\Big)^{2/3} \tag{21}$$

for all $t \in [0,T]$.

2nd step. From (21) we derive a-priori estimates on $\mathbf{u}$ and θ. To begin with, we estimate the last integral on the right hand side of (21).

Firstly, let $t \in]0,T]$. From Hölder's inequality we obtain, for every $s \in [0,t]$,

$$\|\theta(s)\|_{L^2} \le \|\theta(s)\|^{1/6}_{L^1}\|\theta(s)\|^{5/6}_{L^{5/2}} \le \|\theta\|^{1/6}_{C([0,t];L^1)}\|\theta(s)\|^{5/6}_{L^{5/2}}. \tag{22}$$

Secondly, for $0 < \sigma < 1$ define

$$\eta := \frac{\theta}{(1+\theta)^{(1+\sigma)/2}} \quad \text{a. e. in} \quad Q.$$

Clearly,

$$(1+\theta)^{(1-\sigma)/2} \le 1+\eta, \quad |\nabla\eta| \le \frac{|\nabla\theta|}{(1+\theta)^{(1+\sigma)/2}} \quad \text{a. e. in } Q. \tag{23}$$

Take $\sigma = \dfrac{1}{6}$. Then the first inequality in (23) implies

$$\|\theta(s)\|^{5/6}_{L^{5/2}} \le c_6(1 + \|\eta(s)\|^2_{L^6}) \quad \text{for a. e.} \quad s \in [0,t].$$

From (22) we thus obtain

$$\int_0^t \|\theta\|_{L^2}ds \le c_6\|\theta\|^{1/6}_{C([0,t];L^1)}\Big(t + \int_0^t \|\eta\|^2_{L^6}ds\Big) \tag{24}$$

for all $t \in [0, T]$.

To continue, define

$$\phi(t) := \|\theta\|_{C([0,t];L^1)} + \|\eta\|^2_{L^2(0,t;L^6)}, \quad t \in [0, T].$$

The function ϕ is continuous and non-decreasing on $[0, T]$. Inserting (24) into (21) (with $\sigma = \frac{1}{6}$), using Sobolev's embedding theorem and the second inequality in (23) gives

$$\begin{aligned}
\phi(t) &\leq \|\theta\|_{C([0,t];L^1)} + c_7 \int_0^t \int_\Omega |\nabla\eta|^2 dx ds \\
&\leq \|\theta\|_{C([0,t];L^1)} + c_7 \int_0^t \int_\Omega \frac{|\nabla\theta|^2}{(1+\theta)^{7/6}} dx ds \\
&\leq c_8 \Lambda + c_9(|\alpha_0| + |\alpha_1|)^2 \|\mathbf{f}\|^2_{L^\infty} \times \\
&\quad \times \left(t\|\theta\|^4_{C([0,t];L^1)}\right)^{1/3} \left(\|\theta\|^{1/6}_{C([0,t];L^1)} \left(t + \|\eta\|^2_{L^2(0,t;L^6)}\right)\right)^{2/3}
\end{aligned}$$

for all $t \in [0, T]$.

Thus, for every $t \in [0, T]$,

$$t + \phi(t) \leq K_0 + c_9(|\alpha_0| + |\alpha_1|)^2 \|\mathbf{f}\|^2_{L^\infty} T^{1/3} (t + \phi(t))^{19/9},$$

where

$$K_0 := T + c_8 \Lambda.$$

Without loss of generality we may assume that $\phi(0) \leq K_0$.

Define

$$\varepsilon_0 := \frac{1}{3c_9} (2K_0)^{-10/9}.$$

We now apply Lemma 1 (Appendix) to the function $\Psi(t) := t + \phi(t)$ ($t \in [0, T]$). It follows that if

$$(|\alpha_0| + |\alpha_1|)^2 \|\mathbf{f}\|^2_{L^\infty} T^{1/3} \leq \varepsilon_0, \tag{25}$$

then

$$\phi(t) \leq 2K_0 \quad \forall\, t \in [0, T].$$

We obtain

$$\int_0^T \|\theta\|_{L^1}^4 ds \le (2K_0)^4 T,$$

$$\int_0^T \|\theta\|_{L^2} ds \le c_6 \|\theta\|_{C([0,T];L^1)}^{1/6} (T + \|\eta\|_{L^2(0,T;L^6)}^2) \quad \text{[cf. (24)]}$$

$$\le c_6 (T + 2K_0)^{7/6}.$$

Inserting these estimates into (21) gives

$$\|\mathbf{u}(t)\|_{L^2}^2 + \|\theta(t)\|_{L^1} + \int_0^t \int_\Omega (|\nabla \mathbf{u}|^2 + \delta |\nabla \mathbf{u}|^6) dx ds + \int_0^t \int_\Omega \frac{|\nabla \theta|^2}{(1+\theta)^{1+\sigma}} dx ds \le c_{10} \Lambda \tag{26}$$

for all $t \in [0, T]$, provided the smallness condition (25) is satisfied. The constant c_{10} depends on $\nu_1, \nu_2, \kappa_1, \kappa_2, |\alpha_0|, |\alpha_1|, \sigma$, mes Ω and T, but is independent of ε and δ (note that $c_{10} \to +\infty$ as $\sigma \to 1$). □

Recall that $\mathbf{u}_0 \in V_6$, $\theta_0 \in W_0^{1,2}(\Omega)$, $\theta_0 \ge 0$ a. e. in Ω (see the remark above). By the definition of Λ, it is clear that estimate (26) continues to hold when these initial data are replaced by sequences $(\mathbf{u}_{0,\varepsilon}) \subset V_6$ and $(\theta_{0,\varepsilon}) \subset W_0^{1,2}(\Omega)$, $\theta_{0,\varepsilon} \ge 0$ a. e. in Ω, respectively, such that $\mathbf{u}_{0,\varepsilon} \to \mathbf{u}_0$ in H and $\theta_{\theta,\varepsilon} \to \theta_0$ in $L^1(\Omega)$ as $\varepsilon \to 0$. □

By an elementary application of Hölder's inequality, from (26) it follows that

$$\|\theta\|_{L^{r(\sigma+1)/(2-r)}} + \|\nabla \theta\|_{L^r} \le c_{11} \Lambda \tag{27}$$

for all $1 \le r < \frac{5}{4}$ and all $0 < \sigma < 1$ $\left(\text{clearly, } \sigma + 1 \le \frac{r(\sigma+1)}{2-r} < \frac{5}{3}(\sigma+1) \right)$.

3rd step. From (16), (17) and (26), (27) we derive estimates on $\mathbf{u}'$ and θ'.

Firstly, the last integral on the right hand side of (16) can be estimated as follows. For every $\mathbf{v} \in L^2(0, T; V_2)$,

$$\left| \int_Q \frac{\theta}{1+\varepsilon\theta^2} \mathbf{f} \cdot \mathbf{v} dx dt \right| \le \|\mathbf{f}\|_{L^\infty} \int_0^T \left(\int_\Omega \theta^{6/5} dx \right)^{5/6} \left(\int_\Omega |\mathbf{v}|^6 dx \right)^{1/6} dt$$
$$\le c_{12} \|\mathbf{f}\|_{L^\infty} \|\theta\|_{L^{4/3}} \|\nabla \mathbf{v}\|_{L^2}$$
$$\le c_{13}(1+\Lambda^2) \|\mathbf{v}\|_{L^2(0,T;V_2)} \quad \left[\text{by (27) with } \frac{r(\sigma+1)}{2-r} = \frac{4}{3} \right] \tag{28}$$

The estimation of the other terms in (16) follows that in [8] word by word. Therefore

$$\|\mathbf{u}'\|_{L^{6/5}(0,T;V_6^*)} \le c_{14}(1+\Lambda^2). \tag{29}$$

Secondly, as in [8], let $\frac{6}{5} < r < \frac{5}{4}$ and define $\rho := \frac{8r}{5r-6}$ (clearly, $\rho > 3$). Then the second integral on the right hand side of (17) can be estimated as follows. For a. e. $t \in [0, T]$ and all $\psi \in W^{1,\varrho}_{\Gamma_0}(\Omega)$, we have

$$\left| \int_\Omega \frac{\theta(x,t)}{1+\varepsilon\theta^2(x,t)} \mathbf{f}(x,t)\cdot\mathbf{u}(x,t)\psi(x)dx \right| \leq \|\mathbf{f}\|_{L^\infty} \int_\Omega \theta(x,t)|\mathbf{u}(x,t)|dx \max_{\bar{\Omega}} |\psi|$$

$$\leq c_{15}\|\mathbf{f}\|_{L^\infty}\|\theta(t)\|_{L^2}\|\mathbf{u}\|_{L^\infty(0,T;H)}\|\nabla\psi\|_{L^\varrho}.$$

Then the same arguments as in [8] give

$$\|\theta'\|_{L^1(0,T;(W^{1,\varrho}_{\Gamma_0})^*)} \leq c_{16}(1+\Lambda^3). \tag{30}$$

□

3.3 Passage to the Limit

(i) *Passage to the limit* $\delta \to 0$ $(0 < \varepsilon \leq 1$ *fixed*). From (26), (27) and (29), (30) it follows that there exists a subsequence of $\{\mathbf{u}_{\varepsilon,\delta}, \theta_{\varepsilon,\delta}\}$ (not relabeled, $0 < \varepsilon \leq 1$ fixed) such that

$\mathbf{u}_{\varepsilon,\delta} \to \mathbf{u}_\varepsilon$ *weakly in* $L^2(0,T;V_2)$, *strongly in* $L^2(Q)$, *a. e. in* Q,

and, for every $1 \leq r < \frac{5}{4}$ and $0 < \sigma < 1$,

$\theta_{\varepsilon,\delta} \to \theta_\varepsilon$ *weakly in* $L^r(0,T;W^{1,r}_{\Gamma_0})$, *weakly in* $L^{r(\sigma+1)/(2-r)}(Q)$, *strongly in* $L^r(Q)$, *a. e. in* Q

as $\delta \to 0$. In addition,

$$\nabla\mathbf{u}_{\varepsilon,\delta} \to \nabla\mathbf{u}_\varepsilon \textit{ strongly in } [L^2(Q)]^9 \textit{ as } \delta \to 0,$$
$$\int_Q \frac{|\nabla\theta_\varepsilon|^2}{(1+\theta_\varepsilon)^{1+\sigma}}\,dxdt \leq \varliminf_{\delta\to 0}\int_Q \frac{|\nabla\theta_{\varepsilon,\delta}|^2}{(1+\theta_{\varepsilon,\delta})^{1+\sigma}}\,dxdt$$

(see [8] for more details).

Now, the passage to the limit $\delta \to 0$ in (16), (17), (18) and (26), (27) is straightforward. Indeed, given $\mathbf{w} \in V_6$, we set $\mathbf{v}(t) = \mathbf{w}$ for a. e. $t \in [0,T]$. Inserting this $\mathbf{v}$ into (16), integrating by parts

$$\int_0^t \langle \mathbf{u}'_{\varepsilon,\delta}(s), \mathbf{w}\rangle_{V_6} ds, \qquad t \in [0,T]$$

and passing to the limit $\delta \to 0$ in (16) gives

$$\int\limits_{\Omega} \mathbf{u}_\varepsilon(x,t)\cdot\mathbf{w}(x)dx + \int\limits_0^t\int\limits_{\Omega} \nu(\theta_\varepsilon)D(\mathbf{u}_\varepsilon,\mathbf{w})dxds - \int\limits_0^t\int\limits_{\Omega} u_{\varepsilon i}u_{\varepsilon j}\Phi(|\mathbf{u}_\varepsilon|^2\frac{\partial w_i}{\partial x_j}dxds$$
$$= \int\limits_{\Omega} \mathbf{u}_{0,\varepsilon}(x)\cdot\mathbf{w}(x)dx + \int\limits_0^t\int\limits_{\Omega}\Big(1-\frac{\alpha_0\theta_\varepsilon}{1+\varepsilon\theta_\varepsilon^2}\Big)\mathbf{f}\cdot\mathbf{w}\,dxds$$
$$\text{for a. e. } t\in[0,T],\quad \forall\,\mathbf{w}\in V_2. \tag{31}$$

Here we approximated $\mathbf{w}\in V_2$ by functions from V_6.

Analogously, given $\psi\in W^{1,\varrho}_{\Gamma_0}(\Omega)$, we set $\varphi(t)=\psi$ for a. e. $t\in[0,T]$. Inserting this φ into (17), integrating the first integral on the left hand side by parts and passing to the limit $\delta\to 0$ gives

$$\begin{cases} \displaystyle\int\limits_{\Omega}\theta_\varepsilon(x,t)\psi(x)dx + \int\limits_0^t\int\limits_{\Omega}\kappa(\theta_\varepsilon)\nabla\theta_\varepsilon\cdot\nabla\psi\,dxds - \int\limits_0^t\int\limits_{\Omega}u_{\varepsilon i}\theta_\varepsilon\frac{\partial\psi}{\partial x_i}dxds = \\ \displaystyle = \int\limits_{\Omega}\theta_{0,\varepsilon}(x)\psi(x)dx + \\ \displaystyle\quad + \int\limits_0^t\int\limits_{\Omega}\Big(\nu(\theta_\varepsilon)D(\mathbf{u}_\varepsilon,\mathbf{u}_\varepsilon) + \frac{\alpha_1\theta_\varepsilon}{1+\varepsilon\theta_\varepsilon^2}\mathbf{f}\cdot\mathbf{u}_\varepsilon + \frac{g}{1+\varepsilon g}\Big)\psi\,dxds \\ \text{for a. e. } t\in[0,T],\quad\forall\,\psi\in W^{1,\varrho}_{\Gamma_0}(\Omega) \end{cases} \tag{32}$$

$\Big($ note that $\delta\int\limits_0^t\int\limits_{\Omega}\theta_{\varepsilon,\delta}(s)\psi dxds\to 0$ as $\delta\to 0\Big)$.

The passage to the limit in (18) and (26), (27) gives

$$\mathbf{u}_\varepsilon(0)=\mathbf{u}_{0,\varepsilon},\quad \theta_\varepsilon(0)=\theta_{0,\varepsilon}\quad a.\ e.\ in\ \Omega, \tag{33}$$

and

$$\begin{cases} \displaystyle\|\mathbf{u}_\varepsilon(t)\|^2_{L^2} + \|\theta_\varepsilon(t)\|_{L^1} + \int\limits_0^t\int\limits_{\Omega}\Big(|\nabla\mathbf{u}_\varepsilon|^2 + \frac{|\nabla\theta_\varepsilon|^2}{(1+\theta_\varepsilon)^{1+\sigma}}\Big)dxds \\ \le c_{10}\Lambda\quad for\ a.\ e.\ t\in[0,T]\qquad \text{[by Lemma 2, Appendix]}, \end{cases} \tag{34}$$

$$\|\theta_\varepsilon\|_{L^{r(\sigma+1)/(2-r)}} + \|\nabla\theta_\varepsilon\|_{L^r} \le c_{11}\Lambda\quad\forall\,1\le r<\frac{5}{4},\quad\forall\,0<\sigma<1, \tag{35}$$

respectively. We recall that $\mathbf{u}_{0,\varepsilon} \in V_6$ and $\theta_{0,\varepsilon} \in W_0^{1,2}(\Omega)$, $\theta_{0,\varepsilon} \geq 0$ a. e. in Ω, are such that $\mathbf{u}_{0,\varepsilon} \to \mathbf{u}_0$ in H and $\theta_{0,\varepsilon} \to \theta_0$ in $L^1(\Omega)$, respectively, as $\varepsilon \to 0$.

Next, by a routine argument, from (31) it follows that

$$\frac{1}{2}\int_\Omega |\mathbf{u}_\varepsilon(x,t)|^2 dx + \int_0^t \int_\Omega \nu(\theta_\varepsilon) D(\mathbf{u}_\varepsilon, \mathbf{u}_\varepsilon) dxds$$

$$= \frac{1}{2}\int_\Omega |\mathbf{u}_{0,\varepsilon}(x)|^2 dx + \int_0^t \int_\Omega \Big(1 - \frac{\alpha_0 \theta_\varepsilon}{1+\varepsilon\theta_\varepsilon^2}\Big) \mathbf{f}\cdot \mathbf{u}_\varepsilon \, dxds \tag{36}$$

for a. e. $t \in [0,T]$. Let $\Gamma_0 = \emptyset$. Then $\psi = 1$ is an admissible test function in (32). We add (36) and (32) with $\psi = 1$ therein, and obtain

$$\int_\Omega \Big(\frac{1}{2}|\mathbf{u}_\varepsilon(x,t)|^2 + \theta_\varepsilon(x,t)\Big) dx =$$

$$= \int_\Omega \Big(\frac{1}{2}|\mathbf{u}_{0,\varepsilon}(x)|^2 + \theta_{0,\varepsilon}(x)\Big) dx + \int_0^t \int_\Omega \Big(\mathbf{f}\cdot\mathbf{u}_\varepsilon + (\alpha_1 - \alpha_0)\theta \mathbf{f}\cdot \mathbf{u}_\varepsilon + g\Big) dxds \tag{37}$$

for a. e. $t \in [0,T]$.

Finally, from (31) it follows that there exists $\mathbf{u}'_\varepsilon \in L^{4/3}(0,T;V_2^*)$, there holds

$$\langle \mathbf{u}'_\varepsilon(t), \mathbf{w}\rangle_{V_2} + \int_\Omega \nu(\theta_\varepsilon(t)) D(\mathbf{u}_\varepsilon(t), \mathbf{w}) dx - \int_\Omega u_{\varepsilon i}(t) u_{\varepsilon j}(t) \Phi\Big(|\mathbf{u}_\varepsilon(t)|^2\Big) \frac{\partial w_i}{\partial x_j} dx =$$

$$= \int_\Omega \Big(1 - \frac{\alpha_0\theta_\varepsilon(t)}{1+\varepsilon\theta_\varepsilon^2(t)}\Big) \mathbf{f}(t)\cdot \mathbf{w} dx \quad \textit{for a. e.} \quad t \in [0,T], \quad \forall\, \mathbf{w} \in V_2$$

and

$$\|\mathbf{u}'_\varepsilon\|_{L^{4/3}(0,T;V_2^*)} \leq c_{17}(1+\Lambda^2), \quad \text{for all } 0 < \varepsilon \leq 1. \tag{38}$$

Analogously, (32) implies the existence of $\theta'_\varepsilon \in L^1(0,T;(W_{\Gamma_0}^{1,\rho})^*)$ and

$$\|\theta'_\varepsilon\|_{L^1(0,T;(W_{\Gamma_0}^{1,\rho})^*)} \leq c_{18}(1+\Lambda^3) \quad \forall\, 0 < \varepsilon \leq 1 \tag{39}$$

$\Big(\text{recall } \frac{6}{5} < r < \frac{5}{4}, \rho = \frac{8r}{5r-6}\Big)$.

□

(ii) Passage to the limit $\varepsilon \to 0$.

From (34), (35) and (38), (39) we obtain the existence of a subsequence of $\{\mathbf{u}_\varepsilon, \theta_\varepsilon\}$ (not relabeled) such that
$\mathbf{u}_\varepsilon \to \mathbf{u}$ *weakly in* $L^2(0,T;V_2)$, *strongly in* $L^2(Q)$, *a. e. in* Q,

$$\mathbf{u}'_\varepsilon \to \mathbf{u}' \textit{ weakly in } L^{4/3}(0,T;V_2^*),$$

and, for every $1 \le r < \dfrac{5}{4}$ and $0 < \sigma < 1$,
$\theta_\varepsilon \to \theta$ *weakly in* $L^r(0,T;W^{1,r}_{\Gamma_0})$, *weakly in* $L^{r(\sigma+1)/(2-r)}(Q)$,

$$\textit{strongly in } L^r(Q),\ \textit{a. e. in } Q$$

as $\varepsilon \to 0$. In addition,

$$\int\limits_Q \frac{|\nabla\theta|^2}{(1+\theta)^{1+\sigma}}\,dxdt \le \underline{\lim} \int\limits_Q \frac{|\nabla\theta_\varepsilon|^2}{(1+\theta_\varepsilon)^{1+\sigma}}\,dxdt.$$

By routine arguments,

$$\lim_{\varepsilon\to 0}\int\limits_Q \Big(\frac{\theta_\varepsilon}{1+\varepsilon\theta_\varepsilon^2} - \theta\Big)\mathbf{f}\cdot\mathbf{v}\,dxdt = 0 \quad \forall\, \mathbf{v} \in [L^2(Q)]^3,$$

$$\lim_{\varepsilon\to 0}\int\limits_Q \Big(\frac{\theta_\varepsilon}{1+\varepsilon\theta_\varepsilon^2}\mathbf{f}\cdot\mathbf{u}_\varepsilon - \theta\mathbf{f}\cdot\mathbf{u}\Big)\varphi\,dxdt = 0 \quad \forall\, \varphi \in L^\infty(Q).$$

Using all the above convergence properties, we deduce (9), (10), (11) and (12) from (31)-(29), (36) and (38) by passing to the limit $\varepsilon \to 0$ with the help of the same arguments as in [8].

Finally, let $\Gamma_0 = \emptyset$. Then the passage to the limit $\varepsilon \to 0$ in (37) gives (14) Observing that

$$\lim_{t\to 0}\|\mathbf{u}(t)\|_{L^2} = \|\mathbf{u}_0\|_{L^2}$$

one easily deduces (13) from (14). □

Appendix

Lemma 1 *Let* $\Psi : [0,T] \to [0,+\infty[$ *be a continuous non-decreasing function such that*

$$\Psi(0) \le K_0,$$
$$\Psi(t) \le K_0 + \beta(\Psi(t))^\gamma \quad \forall\, t \in [0,T],$$

where $K_0 = \text{const} > 0$, $\gamma = \text{const} > 1$ *and*

$$\beta = \frac{1}{3}(2K_0)^{1-\gamma}.$$

Then

$$\Psi(t) \le 2K_0 \quad \forall\, t \in [0, T].$$

Proof Define

$$T_* := \sup\{t \in [0, T[; \quad \Psi(s) \le 2K_0 \quad \forall\, s \in [0, t]\}.$$

Clearly, $0 < T^* \le T$. If $T^* = T$, we have finished.

Assume $T_* < T$. For every $t \in [0, T_*[$, there holds $\Psi(t) \le 2K_0$. The continuity of Ψ implies $\Psi(T_*) \le 2K_0$. On the other hand, again by the continuity of Ψ, since $T_* < T$ we find $\Psi(T_*) \ge 2K_0$. Thus, $\Psi(T_*) = 2K_0$. It now follows

$$2K_0 = \Psi(T_*) \le K_0 + \beta(\Psi(T_*))^\gamma = \frac{5}{3}K_0,$$

a contradiction.

Whence the claim. □

The following result can be easily proved by routine arguments from measure and integration theory.

Lemma 2 *Let* $(w_\varepsilon) \subset L^\infty(0, T; L^1(\Omega)) \cap L^r(Q)$ $(1 < r < +\infty)$ *be a sequence such that*

$$w_\varepsilon \to w \text{ weakly in } L^r(Q) \text{ as } \varepsilon \to 0,$$
$$\|w_\varepsilon\|_{L^\infty(0,T;L^1)} \le C_0 = \text{const} \quad \forall\, \varepsilon > 0.$$

Then

$$w \in L^\infty(0, T; L^1), \quad \|w\|_{L^\infty(0,T,L^1)} \le C_0.$$

References

1. Amann, H.: Heat-conducting incompressible viscous fluids. In *Navier-Stokes Equations and Related Nonlinear Problems*. Proceedings 3rd Inter. Conf. Navier-Stokes Equs., Funchal, Madeira 21–27 May 1994; A. Sequeira (ed.), Plenum Press, New York, pp. 231–243 (1995)
2. Buliček, M., Feireisl, E., Málek, J.: Navier-Stokes-Fourier system for incompressible fluids with temperature dependent material coefficients. Nonlinear Anal. Real World Appl. **10**, 992–1015 (2009)
3. Chandrasekhar, S.: *Hydrodynamic and Hydromagnetic Stability*. Clarendon Press, Oxford (1961)

4. Feireisl, E.: *Dynamics of Viscous Compressible Fluids.* Oxford Univ. Press, Oxford (2004)
5. Feireisl, E., Málek, J.: On the Navier-Stokes equations with temperature dependent transport coefficients. Differ. Equ. Nonlinear Mech. (2006) Art. ID 90616 (electronic).
6. Kagei, Y., Růžička, M., Thäter, G.: Natural convection with dissipative heating. Commun. Math. Phys. **214**, 287–313 (2000)
7. Naumann, J.: On the existence of weak solutions to the equations of non-stationary motion of heat-conducting incompressible viscous fluids. Math. Meth. Appl. Sci. **29**, 1883–1906 (2006)
8. Naumann J.: An existence theorem for weak solutions to the equations of non-stationary motion of heat-conducting incompressible viscous fluids. J. Nonlin. Convex Anal. **7**, 483–497 (2006)
9. Nečas, J., Roubiček, T.: Bouyancy-driven viscous flow with L^1-data. Nonlin. Analysis **46**, 737–755 (2001)
10. Rajagopal, K. R., Růžička, M., Srinivasa, A. R.: On the Oberbeck-Boussinesq approximation. Math. Models Meth. Appl. Sci. **6**, 1157–1167 (1996)
11. Wolf, J.: Existence of weak solutions to the equations of non-stationary motion of non-Newtonian fluids with shear rate dependent viscosity. J. Math. Fluid Mech. **8**, 1–35 (2006)

A Weak Solvability of the Navier-Stokes Equation with Navier's Boundary Condition Around a Ball Striking the Wall

Jiří Neustupa and Patrick Penel

Abstract We assume that B^t is a closed ball in $\mathbb{R}^3_+ := \{(x_1, x_2, x_3) \in \mathbb{R}^3;\ x_3 > 0\}$, striking the wall (= the x_1, x_2–plane) at time $t_c \in (0, T)$. The speed of the ball at the instant of the collision need not be zero. Although a weak solution to the Navier-Stokes equation with Dirichlet's no-slip boundary condition in $(\mathbb{R}^3_+ \smallsetminus B^t) \times (0, T)$ does not exist if the speed of the stroke is non-zero, we prove that such a solution may exist if Dirichlet's boundary condition is replaced by Navier's slip boundary condition.

Keywords Navier-Stokes equations · Weak solution · Navier's boundary condition

1 Motivation, Introduction and Notation

The existence of a weak solution to the Navier-Stokes equation in a fixed domain $\Omega \subset \mathbb{R}^3$ on a given time interval $(0, T)$ belongs to fundamental results of the qualitative theory of the Navier-Stokes equation. (See e.g. J. Leray [17], E. Hopf [15], O. A. Ladyzhenskaya [16], J. L. Lions [18], R. Temam [22] or G. P. Galdi [10].)

Of all results on the existence of the weak solution in domains with given moving boundaries, we cite the papers by H. Fujita and N. Sauer [7] (the boundary of a variable domain Ω^t consists of a finite number of moving simple closed surfaces of the class C^3, the distance of any two of these surfaces is never less than $d_0 > 0$) and J. Neustupa [19] (Ω^t has an arbitrary shape and smoothness, the assumptions on Ω^t involve simulation of collisions of bodies moving in a fluid).

There exists a series of other works dealing with flows in time varying domains that concern the motion of one or more bodies in a fluid. The fluid and the bodies are studied as an interconnected system so that the position of the bodies in the fluid is not apriori known. The weak solvability of such a problem, provided the bodies do not touch each other or they do not strike the boundary, was proved by B. Desjardins and M. J. Esteban [4, 5], K. H. Hoffmann and V. N. Starovoitov [13] (the 2D case),

J. Neustupa (✉)
Mathematical Institute of the Czech Academy of Sciences, 115 67 Praha 1, Czech Republic
e-mail: neustupa@math.cas.cz

R. Rannacher, A. Sequeira (eds.), *Advances in Mathematical Fluid Mechanics*,
DOI 10.1007/978-3-642-04068-9_24, © Springer-Verlag Berlin Heidelberg 2010

C. Conca et al. [2] and M. D. Gunzburger et al. [12]. The analogous result, without the assumption on the lack of collisions, was proved by J. San Martín et al. [20] (the 2D case), K. H. Hoffmann and V. N. Starovoitov [14] (the motion of a "small" ball in a fluid filling a "large ball") and E. Feireisl 2003 [6] (in a 3D bounded domain, the author uses the contact condition that once two bodies touch one another, they remain stuck together forever).

All the mentioned authors consider the homogeneous Dirichlet boundary condition for velocity on the boundary of Ω^t. The motion of the so called "self-propelled bodies" (which produce certain velocity profile on their surface), together with the motion of the fluid around them, was studied except others by G. P. Galdi, see the survey paper [11].

None of the mentioned papers provides the existence of a weak solution to the Navier-Stokes equation at the geometrical configuration when the fluid fills a domain Ω^t around a solid ball striking a wall with a finite non-zero speed. Moreover, it follows from results of V. N. Starovoitov 2003 [21] that the weak solution with the no-slip Dirichlet boundary condition in such a situation cannot exist. Reference [19], where the no-slip boundary condition is also considered, provides the weak solution only if the ball strikes the wall with the speed that tends to zero as time approaches the instant of the collision. (With a non-zero speed, the body must have another shape than the ball, see [19].)

This state motivated us to study the Navier-Stokes equation in the described domain Ω^t with boundary conditions that enable the fluid to slip on the boundary. We assume that the motion of the ball is given. We use Navier's boundary condition and we prove the global in time existence of a weak solution under the restriction that the speed of the ball is "sufficiently small" at times close to the instant of the collision – see Theorem 1. The considered case of a ball moving in a fluid and striking perpendicularly the wall represents a sample example. We actually prepare a generalization concerning flow around moving bodies of various shapes which may collide one with another. Nevertheless, the basic techniques is developed in the present paper. It is based on the construction of Rothe approximations.

A series of steps require a different approach than in the case of homogeneous Dirichlet's boundary condition. For instance, Sobolev's embedding inequalities cannot be used in a standard fashion because the constants in these inequalities now depend on time. Other difficulties appear in the part where we treat the limit transition in the nonlinear term and we therefore need an information on a strong convergence of a sequence of approximations in an appropriate norm. (The argument based on the Lions–Aubin lemma cannot be used in a usual way – see Sect. 6.)

The time-variable domain Ω^t. We suppose that $(0, T)$ is a bounded time interval and $t_c \in (0, T)$. We denote by $\mathbb{R}^3_+$ the half-space $\{\mathbf{x} = (x_1, x_2, x_3) \in \mathbb{R}^3;\ x_3 > 0\}$, by $\overline{\mathbb{R}}^3_+$ the closure of $\mathbb{R}^3_+$ and by $\partial\mathbb{R}^3_+$ the boundary of $\mathbb{R}^3_+$ (= the $x_1,\ x_2$-plane).

Further, we denote by B^t the closed ball in $\overline{\mathbb{R}}^3_+$ with radius R and center $S^t = (0,\ 0,\ \delta^t + R)$. We suppose that δ^t (the distance of the ball B^t from $\partial\mathbb{R}^3_+$) is a continuous function of t for $t \in [0, T]$ such that $\delta^{t_c} = 0$ and

(i) δ^t is decreasing on $[0, t_c]$ and increasing on $[t_c, T]$,
(ii) $\dot{\delta}^t$ (the derivative of δ^t) is bounded on the intervals $[0, t_c)$ and $(t_c, T]$,
(iii) $\ddot{\delta}^t$ (the second derivative of δ^t) is integrable on $(0, T)$.

We put $\Omega^t := \mathbb{R}^3_+ \smallsetminus B^t$. The boundary of Ω^t is denoted by Γ^t. Ω^t represents the space filled by the fluid and B^t represents the solid ball which moves in the fluid and strikes the fixed wall $\partial\mathbb{R}^3_+$ at time $t = t_c$. We assume, for simplicity, that the ball B^t does not rotate and all its particles have only translational velocity. Thus, the velocity of "material points" on the boundary Γ^t of Ω^t is

$$\mathbf{V}^t(\mathbf{x}) := \begin{cases} (0, 0, \dot{\delta}^t) & \text{for } t \neq t_c \text{ and } \mathbf{x} \in \partial B^t, \\ \mathbf{0} & \text{for } t \neq t_c \text{ and } \mathbf{x} \in \partial\mathbb{R}^3_+. \end{cases}$$

Notation of norms and function spaces.

- $(\,.\,,\,.\,)_{2;\,\Omega^t}$ is the scalar product and $\|\,.\,\|_{2;\,\Omega^t}$ is the norm in $L^2(\Omega^t)$ or in $L^2(\Omega^t)^3$ or in $L^2(\Omega^t)^9$, respectively. The meaning of $(\,.\,,\,.\,)_{2;\,\Gamma^t}$ and $\|\,.\,\|_{2;\,\Gamma^t}$ is analogous.
- $\|\,.\,\|_{q;\,\Omega^t}$ is the norm in $L^q(\Omega^t)$ or in $L^q(\Omega^t)^3$ or in $L^q(\Omega^t)^9$, respectively.
- $C^\infty_\sigma(\Omega^t)$ is the space of infinitely differentiable divergence-free vector-functions in $\overline{\Omega}^t$ with a compact support in $\overline{\Omega}^t$ and zero normal component on Γ^t.
- $W^{1,2}_\sigma(\Omega^t)$ is the closure of $C^\infty_\sigma(\Omega^t)$ in $W^{1,2}(\Omega^t)^3$.
- $C^\infty_{0,\sigma}(\Omega^t)$ is a subspace of $C^\infty_\sigma(\Omega^t)$, containing functions with a compact support in Ω^t.
- $L^q_\sigma(\Omega^t)$ is the closure of $C^\infty_{0,\sigma}(\Omega^t)$ in $L^q(\Omega^t)^3$ (for $1 \le q < +\infty$).

If $t \in (0, T) \smallsetminus \{t_c\}$ then $W^{1,2}_\sigma(\Omega^t) \hookrightarrow L^q(\Omega^t)^3$ for $2 \le q \le 6$. Using the characterization of $L^q_\sigma(\Omega^t)$ (see [8, p. 111]), we can verify that $W^{1,2}_\sigma(\Omega^t) \hookrightarrow L^q_\sigma(\Omega^t)$.

The initial-boundary value problem. Put $Q_{(0,T)} := \{(\mathbf{x}, t);\ 0 < t < T,\ \mathbf{x} \in \Omega^t\}$ and $\Gamma_{(0,T)} := \{(\mathbf{x}, t);\ 0 < t < T,\ \mathbf{x} \in \Gamma^t\}$.

Our aim is to prove the existence of a weak solution of the problem

$$\partial_t\mathbf{v} + \mathbf{v}\cdot\nabla\mathbf{v} + \nabla p = \nu\Delta\mathbf{v} + \mathbf{f} \quad \text{in } Q_{(0,T)}, \tag{1}$$

$$\operatorname{div}\mathbf{v} = 0 \quad \text{in } Q_{(0,T)}, \tag{2}$$

$$\mathbf{v}\cdot\mathbf{n} = \mathbf{V}^t\cdot\mathbf{n} \quad \text{in } \Gamma_{(0,T)}, \tag{3}$$

$$[\mathbb{T}_\mathrm{d}(\mathbf{v})\cdot\mathbf{n}]_\tau + K(\mathbf{v} - \mathbf{V}^t) = \mathbf{0} \quad \text{in } \Gamma_{(0,T)}, \tag{4}$$

$$\mathbf{v} = \mathbf{v}_0 \quad \text{in } \Omega^0 \times \{0\}. \tag{5}$$

The Eqs. (1) and (2) describe the motion of a viscous incompressible fluid in domain Ω^t. The symbols $\mathbf{v}$, p, ν, $\mathbf{f}$, $\mathbf{n}$ and $\mathbb{T}_\mathrm{d}(\mathbf{v})$ successively denote the velocity of the fluid, the pressure, the kinematic coefficient of viscosity, the specific external body force, the outer normal vector on the boundary of Ω^t and the dynamic stress tensor associated with the flow $\mathbf{v}$. The density of the fluid is supposed to be one. The subscript τ denotes the tangential component to Γ^t. Since the considered fluid is Newtonian, the dynamic stress tensor has the form $\mathbb{T}_d(\mathbf{v}) = 2\nu\,(\nabla\mathbf{v})_s$ where $(\nabla\mathbf{v})_s$ is the symmetrized gradient of $\mathbf{v}$. Condition (3) expresses the impermeability of Γ^t. Condition (4) is due to H. Navier, who proposed in 1824 that the tangential component of the stress acting on the boundary should be proportional to the velocity of the fluid (relative with respect to the material boundary). We suppose (in accordance with physical arguments) that $K \geq 0$.

Introduction of function $\mathbf{a}^t$. In order to transform the inhomogeneous boundary condition (3) to the homogeneous one, we look for solution $\mathbf{v}$ in the form $\mathbf{v} = \mathbf{a}^t + \mathbf{u}$ where $\mathbf{a}^t$ is considered to be a known function satisfying the condition

$$\mathbf{a}^t \cdot \mathbf{n} \;=\; \mathbf{V}^t \cdot \mathbf{n} \qquad \text{a.e. in } \Gamma_{(0,T)} \tag{6}$$

and $\mathbf{u}$ is a new unknown function. The construction of an appropriate function $\mathbf{a}^t$ is presented in Sect. 2. We shall see that for $t \in (0, T)$, $t \neq t_c$, function $\mathbf{a}^t$ can be defined a.e. in $\mathbb{R}^3_+$ so that it is divergence-free and, in addition to condition (6), it also satisfies the series of estimates

$$\|\nabla\mathbf{a}^t\|^2_{2;\,\Omega^t} \;\leq\; c_1\,(\dot{\delta}^t)^2 \ln\Big(1 + \frac{R}{\delta^t}\Big), \tag{7}$$

$$\big|\big(\partial_t\mathbf{a}^t,\, \boldsymbol{\varphi}\big)_{2;\,\Omega^t}\big| \;\leq\; c_2\,(\dot{\delta}^t)^2\,\|\nabla\boldsymbol{\varphi}\|_{2;\,\Omega^t} + c_3\,|\ddot{\delta}^t|\,\|\boldsymbol{\varphi}\|_{2;\,\Omega^t}, \tag{8}$$

$$\big|\big(\mathbf{a}^t\cdot\nabla\mathbf{a}^t,\, \boldsymbol{\varphi}\big)_{2;\,\Omega^t}\big| \;\leq\; c_4\,(\dot{\delta}^t)^2\,\|\nabla\boldsymbol{\varphi}\|_{2;\,\Omega^t}, \tag{9}$$

$$\|\mathbf{a}^t\|_{5;\,\Omega^t} \;\leq\; c_5\,\frac{|\dot{\delta}^t|}{(\delta^t)^{1/10}}, \tag{10}$$

$$\big|\big(\boldsymbol{\varphi}\cdot\nabla\mathbf{a}^t,\, \boldsymbol{\varphi}\big)_{2;\,\Omega^t}\big| \;\leq\; c_6\,|\dot{\delta}^t|\,\|\nabla\boldsymbol{\varphi}\|^2_{2;\,\Omega^t}, \tag{11}$$

$$K\,\big|\big(\mathbf{a}^t - \mathbf{V}^t,\, \boldsymbol{\varphi}\big)_{2;\,\Gamma^t}\big| \;\leq\; \tfrac{1}{16}\nu\,\|\nabla\boldsymbol{\varphi}\|^2_{2;\,\Omega^t} + c_7 \tag{12}$$

for $t \neq t_c$, all $\boldsymbol{\varphi} \in W^{1,2}_\sigma(\Omega^t)$, with constants c_1–c_7 which are independent of $\boldsymbol{\varphi}$ and t. Obviously, the right hand side of (7) is integrable on $(0, T)$ with any power $\alpha \geq 0$ and the right hand side of (10) is integrable on $(0, T)$ with any power $\alpha \in [1, 10)$.

If $t \neq t_c$ then domain Ω^t has the cone property and consequently, $W^{1,2}(\Omega^t)^3$ is continuously embedded into $L^6(\Omega^t)^3$. Thus, we can also derive the estimate

$$\begin{aligned}\big|\big(\boldsymbol{\varphi}\cdot\nabla\mathbf{a}^t,\, \boldsymbol{\varphi}\big)_{2;\,\Omega^t}\big| &\leq \|\nabla\mathbf{a}^t\|_{2;\,\Omega^t}\,\|\boldsymbol{\varphi}\|^{1/2}_{2;\,\Omega^t}\,\|\boldsymbol{\varphi}\|^{3/2}_{6;\,\Omega^t} \\ &\leq c_8\,a(t)\,\|\boldsymbol{\varphi}\|^2_{2;\,\Omega^t} + \tfrac{1}{16}\nu\,\|\nabla\boldsymbol{\varphi}\|^2_{2;\,\Omega^t},\end{aligned} \tag{13}$$

valid for $t \neq t_c$, where $a(t) := \|\nabla\mathbf{a}^t\|^4_{2;\,\Omega^t}$. Constant c_8 depends on ν and it also generally depends on t through the cone parameters appearing in the definition of the cone property of Ω^t, see e.g. [1, p. 103]. However, if we use (13) only at times t such that $|t - t_c| > \kappa_0$ then c_8, although dependent on κ_0, can be considered to be independent of t. The value of κ_0 will be fixed by condition (iv) in Lemma 1.

We shall also see in Sect. 2 that the initial-value problem

$$\frac{\mathrm{d}}{\mathrm{d}t}\mathbf{X}(t;\, t_0, \mathbf{x}_0) \;=\; \mathbf{a}^t\big(\mathbf{X}(t;\, t_0, \mathbf{x}_0)\big), \qquad \mathbf{X}(t_0;\, t_0, \mathbf{x}_0) = \mathbf{x}_0 \tag{14}$$

has a unique solution $X(t;\, t_0, \mathbf{x}_0)$, defined for a.a. $t_0 \in (0, T)$, all $t \in [0, T]$ and all $\mathbf{x}_0 \in \mathbb{R}^3_+$. The mapping $\mathbf{x}_0 \mapsto \mathbf{X}(t;\, t_0, \mathbf{x}_0)$ is a 1–1 transformation of $\Omega^{t_0} \smallsetminus \ell^{t_0}$ onto $\Omega^t \smallsetminus \ell^t$ (where ℓ^{t_0} and ℓ^t are certain sets of measure zero), whose Jacobian equals one due to the incompressibility of the flow $\mathbf{a}^t$. This mapping can be used in order to transform volume integrals on Ω^{t_0} to volume integrals on Ω^t.

2 A Formal Study of the Initial-Boundary Value Problem (1)–(5) and the Main Theorem

A formal derivation of the weak formulation. The weak formulation of the problem (1), (2), (3), (4), and (5) can be formally derived from the classical formulation if we multiply Eq. (1) by an appropriate test function $\boldsymbol{\varphi}$, integrate in $Q_{(0,T)}$ and use all the conditions (2), (3), (4), and (5). Thus, assume that $\boldsymbol{\varphi}$ is an infinitely differentiable divergence-free vector-function in $\overline{\mathbb{R}}^3_+ \times [0, T]$ that has a compact support in $\overline{\mathbb{R}}^3_+ \times [0, T)$ and satisfies the condition $\boldsymbol{\varphi} \cdot \mathbf{n} = 0$ on $\Gamma_{(0,T)}$. Assume that $\mathbf{v}$ is a "sufficiently smooth" solution of (1)–(5) of the form $\mathbf{v} = \mathbf{a}^t + \mathbf{u}$ where $\mathbf{a}^t$ has all the properties named in the last paragraph of Sect. 1 and $\mathbf{u} \in L^2_\sigma(\Omega^t)$ for a.a. $t \in (0, T)$. The product $\{\partial_t \mathbf{v} + (\mathbf{v}^t \cdot \nabla)\mathbf{v}\} \cdot \boldsymbol{\varphi}$ equals the sum of $\{\partial_t \mathbf{v} + (\mathbf{a}^t \cdot \nabla)\mathbf{v}\} \cdot \boldsymbol{\varphi}$ and $\mathbf{u} \cdot \nabla\mathbf{v} \cdot \boldsymbol{\varphi}$. The integral of the first term can be treated as follows:

$$\begin{aligned}
&\int_0^T\!\!\int_{\Omega^t} \big\{\partial_t \mathbf{v}(\mathbf{x}, t) + \mathbf{a}^t(\mathbf{x}) \cdot \nabla\mathbf{v}(\mathbf{x}, t)\big\} \cdot \boldsymbol{\varphi}(\mathbf{x}, t)\, \mathrm{d}\mathbf{x}\, \mathrm{d}t + \int_{\Omega^0} \mathbf{v}_0(\mathbf{x}_0) \cdot \boldsymbol{\varphi}(\mathbf{x}_0, 0)\, \mathrm{d}\mathbf{x}_0 \\
&= \int_0^T\!\!\int_{\Omega^0} \frac{\mathrm{d}}{\mathrm{d}t}\, \mathbf{v}\big(\mathbf{X}(t; 0, \mathbf{x}_0), t\big) \cdot \boldsymbol{\varphi}\big(\mathbf{X}(t; 0, \mathbf{x}_0), t\big) \mathrm{d}\mathbf{x}_0 \mathrm{d}t + \int_{\Omega^0} \mathbf{v}_0(\mathbf{x}_0) \cdot \boldsymbol{\varphi}(\mathbf{x}_0, 0) \mathrm{d}\mathbf{x}_0 \\
&= -\int_0^T \int_{\Omega^t} \big\{\partial_t \boldsymbol{\varphi}(\mathbf{x}, t) + \mathbf{a}^t(\mathbf{x}) \cdot \nabla\boldsymbol{\varphi}(\mathbf{x}, t)\big\} \cdot \mathbf{v}(\mathbf{x}, t)\, \mathrm{d}\mathbf{x}\, \mathrm{d}t.
\end{aligned} \tag{15}$$

The integral of $\mathbf{u} \cdot \nabla\mathbf{v} \cdot \boldsymbol{\varphi}$ in Ω^t can be transformed to the negative integral of $\mathbf{u} \cdot \nabla\boldsymbol{\varphi} \cdot \mathbf{v}$ by means of the integration by parts. Further, we have

$$\begin{aligned}
&\int_{\Omega^t} \nu \Delta\mathbf{v} \cdot \boldsymbol{\varphi}\, \mathrm{d}\mathbf{x} \;=\; \int_{\Omega^t} \nu \Delta\mathbf{a}^t \cdot \boldsymbol{\varphi}\, \mathrm{d}\mathbf{x} + \int_{\Gamma^t} \nu \frac{\partial \mathbf{u}}{\partial \mathbf{n}} \cdot \boldsymbol{\varphi}\, \mathrm{d}S - \int_{\Omega^t} \nu \nabla\mathbf{u} : \nabla\boldsymbol{\varphi}\, \mathrm{d}\mathbf{x} \\
&= \int_{\Gamma^t} \nu \big[2\mathbf{n} \cdot (\nabla\mathbf{u})_s - \mathbf{n} \cdot \nabla\mathbf{u}\big] \cdot \boldsymbol{\varphi}\, \mathrm{d}S + \int_{\Omega^t} \big[\nu \Delta\mathbf{a}^t \cdot \boldsymbol{\varphi} - \nu \nabla\mathbf{u} : \nabla\boldsymbol{\varphi}\big]\, \mathrm{d}\mathbf{x} \\
&= \int_{\Gamma^t} \mathbf{n} \cdot [2\nu(\nabla\mathbf{v})_s - 2\nu(\nabla\mathbf{a}^t)_s] \cdot \boldsymbol{\varphi}\, \mathrm{d}S + \int_{\Omega^t} \big[\nu \Delta\mathbf{a}^t \cdot \boldsymbol{\varphi} - 2\nu(\nabla\mathbf{u})_s : \nabla\boldsymbol{\varphi}\big]\, \mathrm{d}\mathbf{x} \\
&= -\int_{\Gamma^t} K(\mathbf{v} - \mathbf{V}^t) \cdot \boldsymbol{\varphi}\, \mathrm{d}S - \int_{\Omega^t} 2\nu(\nabla\mathbf{v})_s : \nabla\boldsymbol{\varphi}\, \mathrm{d}\mathbf{x}.
\end{aligned} \tag{16}$$

We have used the identities

$$\int_{\Gamma^t} \mathbf{n} \cdot 2\nu(\nabla\mathbf{v})_s \cdot \boldsymbol{\varphi} \, \mathrm{d}S = \int_{\Gamma^t} [\mathbf{n} \cdot \mathbb{T}_{\mathrm{d}}(\mathbf{v})]_\tau \cdot \boldsymbol{\varphi} \, \mathrm{d}S = -\int_{\Gamma^t} K(\mathbf{v} - \mathbf{V}^t) \cdot \boldsymbol{\varphi} \, \mathrm{d}S,$$

$$\int_{\Gamma^t} \mathbf{n} \cdot \nabla\mathbf{u} \cdot \boldsymbol{\varphi} \, \mathrm{d}S = \int_{\Omega^t} (\nabla\mathbf{u})^T : \nabla\boldsymbol{\varphi} \, \mathrm{d}\mathbf{x},$$

$$\int_{\Omega^t} \nu\Delta\mathbf{a}^t \cdot \boldsymbol{\varphi} \, \mathrm{d}\mathbf{x} = \int_{\Gamma^t} 2\nu \, \mathbf{n} \cdot (\nabla\mathbf{a}^t)_s \cdot \boldsymbol{\varphi} \, \mathrm{d}S - \int_{\Omega^t} 2\nu \, (\nabla\mathbf{a}^t)_s : \nabla\boldsymbol{\varphi} \, \mathrm{d}\mathbf{x},$$

the first of whose follows from (4). The integral of $\nabla p \cdot \boldsymbol{\varphi}$ on Ω^t equals zero because the subspace of gradients of scalar functions is orthogonal to $L^2_\sigma(\Omega^t)$ in $L^2(\Omega^t)^3$. Thus, using (15) and (16), we obtain the integral identity

$$\int_0^T \int_{\Omega^t} \Big\{ -\mathbf{v} \cdot \partial_t\boldsymbol{\varphi} - \mathbf{v} \cdot \nabla\boldsymbol{\varphi} \cdot \mathbf{v} + 2\nu(\nabla\mathbf{v})_s : \nabla\boldsymbol{\varphi} \Big\} \, \mathrm{d}\mathbf{x} \, \mathrm{d}t +$$

$$+ \int_0^T \int_{\Gamma^t} K(\mathbf{v} - \mathbf{V}^t) \cdot \boldsymbol{\varphi} \, \mathrm{d}S \, \mathrm{d}t = \int_0^T \int_{\Omega^t} \mathbf{f} \cdot \boldsymbol{\varphi} \, \mathrm{d}\mathbf{x} \, \mathrm{d}t + \int_{\Omega^0} \mathbf{v}_0 \cdot \boldsymbol{\varphi}(.\,,0) \, \mathrm{d}\mathbf{x}.$$

Replacing $\mathbf{v}$ by the sum $\mathbf{a}^t + \mathbf{u}$, we arrive at the definition:

Definition (the weak solution of (1), (2), (3), (4), and (5)) *Suppose that* $\mathbf{u}_0 \in L^2_\sigma(\Omega^0)$ *and* $\mathbf{f} \in L^2(0, T; L^2(\Omega^t)^3)$. *The function* $\mathbf{v} \equiv \mathbf{a}^t + \mathbf{u}$ *is called a weak solution of the problem (1)–(5) if* $\mathbf{u} \in L^2(0, T; W^{1,2}_\sigma(\Omega^t)) \cap L^\infty(0, T; L^2_\sigma(\Omega^t))$ *satisfies*

$$\int_0^T \int_{\Omega^t} \Big\{ -(\mathbf{a}^t + \mathbf{u}) \cdot \partial_t\boldsymbol{\varphi} - (\mathbf{a}^t + \mathbf{u}) \cdot \nabla\boldsymbol{\varphi} \cdot (\mathbf{a}^t + \mathbf{u}) + 2\nu[\nabla(\mathbf{a}^t + \mathbf{u})]_s : \nabla\boldsymbol{\varphi} \Big\} \, \mathrm{d}\mathbf{x} \, \mathrm{d}t$$

$$+ \int_0^T \int_{\Gamma^t} K(\mathbf{a}^t + \mathbf{u} - \mathbf{V}^t) \cdot \boldsymbol{\varphi} \, \mathrm{d}S \, \mathrm{d}t = \int_0^T \int_{\Omega^t} \mathbf{f} \cdot \boldsymbol{\varphi} \, \mathrm{d}\mathbf{x} \, \mathrm{d}t + \int_{\Omega^0} [\mathbf{a}^0 + \mathbf{u}_0] \cdot \boldsymbol{\varphi}(.\,,0) \, \mathrm{d}\mathbf{x} \quad (17)$$

for all divergence-free vector-functions $\boldsymbol{\varphi} \in C_0^\infty\big(\overline{\mathbb{R}^3_+} \times [0, T)\big)$, *that satisfy the condition* $\boldsymbol{\varphi} \cdot \mathbf{n} = 0$ *on* $\Gamma_{(0,T)}$.

The readers can verify that this definition enables us the "backward calculation", i.e. to show that if the weak solution $\mathbf{v}$ is "sufficiently smooth" and all other input data are also "sufficiently smooth" then there exists a pressure p so that the pair $\mathbf{v}$, p is a classical solution of (1), (2), (3), (4), and (5).

We shall refer to the problem defined above as to the weak problem (17).

A formal derivation of the energy inequality. The energy inequality is a fundamental apriori estimate of a solution of the problem (1), (2), (3), (4), and (5). An analogous estimate can be rigorously derived for appropriate approximations of the solution. However, in order to abstract from technical details connected with the approximations and to explain how we use the boundary conditions and apply estimates (7), (8), (9), (10), (11), (12), and (13), we include the formal derivation of the energy inequality already in this section.

Lemma 1 *Suppose that*

(iv) there exists $\kappa_0 > 0$ so that $c_6\,|\dot{\delta}^t| < \frac{1}{4}\nu$ for $t_c - \kappa_0 < t < t_c + \kappa_0$.

Then there exists a non–negative integrable function G on $(0, T)$ such that if $(\mathbf{v}, p) \equiv (\mathbf{a}^t + \mathbf{u}, p)$ is a smooth solution of the initial-boundary value problem (1)–(5) and $t \in (0, T)$ then

$$\|\mathbf{u}(.\,,t)\|^2_{2;\,\Omega^t} + \nu \int_0^t \|\nabla\mathbf{u}(.\,,s)\|^2_{2;\,\Omega^s}\,\mathrm{d}s + 2K \int_0^t \|\mathbf{u}(.\,,s)\|^2_{2;\,\Gamma^s}\,\mathrm{d}s$$
$$\leq \|\mathbf{u}_0\|^2_{2;\,\Omega^0} + \int_0^t \omega(s)\,\|\mathbf{u}(.\,,s)\|^2_{2;\,\Omega^s}\,\mathrm{d}s + G(t), \tag{18}$$

where $\omega(t) = 2c_3\,|\ddot{\delta}^t| + 2c_8\,a(t) + 1$. (Recall that c_6 and c_8 are the constants from inequalities (11), (13) and $a(t) = \|\nabla\mathbf{a}^t\|^4_{2;\Omega^t}$.)

Proof Assume that $t \neq t_c$, multiply Eq. (1) (where $\mathbf{v} = \mathbf{a}^t + \mathbf{u}$) by $\mathbf{u}$ and integrate in Ω^t. We obtain

$$\int_{\Omega^t} \big\{[\partial_t(\mathbf{a}^t + \mathbf{u}) + \mathbf{a}^t\cdot\nabla(\mathbf{a}^t + \mathbf{u})]\cdot\mathbf{u} + \mathbf{u}\cdot\nabla\mathbf{a}^t\cdot\mathbf{u} - \nu\Delta\mathbf{v}\cdot\mathbf{u}\big\}\,\mathrm{d}\mathbf{x} = \int_{\Omega^t} \mathbf{f}\cdot\mathbf{u}\,\mathrm{d}\mathbf{x}. \tag{19}$$

Now we estimate or rewrite the terms in (19):

- Following (16), we have

$$-\nu \int_{\Omega^t} \Delta\mathbf{v}\cdot\mathbf{u}\,\mathrm{d}\mathbf{x} = K \int_{\Gamma^t} |\mathbf{u}|^2\,\mathrm{d}S + K \int_{\Gamma^t} (\mathbf{a}^t - \mathbf{V}^t)\cdot\mathbf{u}\,\mathrm{d}S +$$
$$+\nu \int_{\Gamma^t} \mathbf{n}\cdot\nabla\mathbf{u}\cdot\mathbf{u}\,\mathrm{d}S + \nu \int_{\Omega^t} |\nabla\mathbf{u}|^2\,\mathrm{d}\mathbf{x} + 2\nu \int_{\Omega^t} (\nabla\mathbf{a}^t)_s : \nabla\mathbf{u}\,\mathrm{d}\mathbf{x}.$$

- Using the identity $\nabla(\mathbf{u}\cdot\mathbf{n})\cdot\mathbf{u} = 0$ (valid a.e. on Γ^t) and the negative semi-definiteness of the tensor $\nabla\mathbf{n}$ a.e. on Γ^t (following from the special geometry of Ω^t), we observe that $\int_{\Gamma^t} \mathbf{n}\cdot\nabla\mathbf{u}\cdot\mathbf{u}\,\mathrm{d}S \geq 0$. Therefore, using (12), we get

$$\int_{\Gamma^t} \mathbf{n}\cdot\nabla\mathbf{u}\cdot\mathbf{u}\,\mathrm{d}S + K \int_{\Gamma^t} (\mathbf{a}^t - \mathbf{V}^t)\cdot\mathbf{u}\,\mathrm{d}S \geq -\tfrac{1}{16}\nu\,\|\nabla\mathbf{u}\|^2_{2;\,\Omega^t} - c_7,$$
$$-\nu\int_{\Omega^t} \Delta\mathbf{v}\cdot\mathbf{u}\,\mathrm{d}\mathbf{x} \geq K\,\|\mathbf{u}\|^2_{2;\,\Gamma^t} + \tfrac{14}{16}\nu\int_{\Omega^t} |\nabla\mathbf{u}|^2\,\mathrm{d}\mathbf{x} - 16\nu \int_{\Omega^t} |\nabla\mathbf{a}^t|^2\,\mathrm{d}\mathbf{x} - c_7. \tag{20}$$

- Due to (8) and (9), we obtain (with $c_9 = [8(c_2^2 + c_4^2)/\nu]\cdot\operatorname{ess\,sup}(\dot{\delta}^t)^4$)

$$\left|\int_{\Omega^t} [\partial_t\mathbf{a}^t + \mathbf{a}^t\cdot\nabla\mathbf{a}^t]\cdot\mathbf{u}\,\mathrm{d}\mathbf{x}\right| \leq c_3\,|\ddot{\delta}^t|\,\|\mathbf{u}\|^2_{2;\,\Omega^t} + \tfrac{1}{4}\,c_3\,|\ddot{\delta}^t| + \tfrac{1}{16}\nu\,\|\nabla\mathbf{u}\|^2_{2;\,\Omega^t} + c_9.$$

- Using the transformation $\mathbf{x} \mapsto \mathbf{y} = \mathbf{X}(t+h;\, t, \mathbf{x})$ of $\Omega^t \setminus \ell^t$ onto $\Omega^{t+h} \setminus \ell^{t+h}$, we can rewrite the next integral as follows:

$$\int_{\Omega^t} \big[\partial_t \mathbf{u} + \mathbf{a}^t \cdot \nabla \mathbf{u}\big] \cdot \mathbf{u}\, \mathrm{d}\mathbf{x} \;=\; \left[\int_{\Omega^t} \frac{\mathrm{d}}{\mathrm{d}\vartheta}\, \frac{1}{2}\, \big|\mathbf{u}\big(\mathbf{X}(\vartheta;\, t, \mathbf{x}), \vartheta\big)\big|^2\, \mathrm{d}\mathbf{x}\right]_{\vartheta = t}$$
$$= \lim_{h \to 0} \frac{1}{2h} \left[\int_{\Omega^t} \Big(\big|\mathbf{u}\big(\mathbf{X}(t+h;\, t, \mathbf{x}), t+h\big)\big|^2 - \big|\mathbf{u}\big(\mathbf{X}(t;\, t, \mathbf{x}), t\big)\big|^2\Big)\, \mathrm{d}\mathbf{x}\right]$$
$$= \lim_{h \to 0} \frac{1}{2h}\left[\int_{\Omega^{t+h}} |\mathbf{u}(\mathbf{y}, t+h)|^2\, \mathrm{d}\mathbf{y} - \int_{\Omega^t} |\mathbf{u}(\mathbf{x}, t)|^2\, \mathrm{d}\mathbf{x}\right] = \frac{\mathrm{d}}{\mathrm{d}t}\, \frac{1}{2} \int_{\Omega^t} |\mathbf{u}|^2\, \mathrm{d}\mathbf{x}.$$

- Now, due to inequalities (11) and (13) and denoting by χ_0 the characteristic function of the interval $(t_c - \kappa_0, t_c + \kappa_0)$, we can estimate

$$\left|\int_{\Omega^t} \mathbf{u} \cdot \nabla \mathbf{a}^t \cdot \mathbf{u}\, \mathrm{d}\mathbf{x}\right| \le c_6\, \chi_0(t)\, |\dot{\delta}^t|\; \|\nabla \mathbf{u}\|^2_{2;\, \Omega^t} + \tfrac{1}{16} \nu\, \|\nabla \mathbf{u}\|^2_{2;\, \Omega^t} + c_8\, a(t)\, \|\mathbf{u}\|^2_{2;\, \Omega^t}\, .$$

- Finally, by means of condition (iv) of the smallness of $|\dot{\delta}^t|$ on the interval $(t_c - \kappa_0, t_c + \kappa_0)$, the term $c_6\, \chi_0(t)\, |\dot{\delta}^t|\; \|\nabla \mathbf{u}\|^2_{2;\, \Omega^t}$ can also be absorbed by $\frac{14}{16} \nu\, \|\nabla \mathbf{u}\|^2_{2;\, \Omega^t}$ (see (20)).
- Substituting now all previous estimates or identities to (19) and using inequality (7), we obtain

$$\frac{\mathrm{d}}{\mathrm{d}t}\; \|\mathbf{u}\|^2_{2;\, \Omega^t} + \nu\, \|\nabla \mathbf{u}\|^2_{2;\, \Omega^t} + 2K\, \|\mathbf{u}\|^2_{2;\, \Gamma^t} \;\le\; \|\mathbf{f}\|^2_{2;\, \Omega^t} + \omega(t)\, \|\mathbf{u}\|^2_{2;\, \Omega^t}$$
$$+\; \tfrac{1}{2} c_3\, |\ddot{\delta}^t| + 16 c_1\, (\dot{\delta}^t)^2 \ln\left(1 + \frac{R}{\delta^t}\right) + c_7 + c_9.$$

To complete the proof, we integrate this inequality on the time interval $(0, t)$. □

Our main theorem, whose proof is given in Sect. 4, 5 and 6, reads:

Theorem 1 *Suppose that function δ^t satisfies conditions (i)–(iii) and also the condition of smallness (iv). Then the weak problem (17) has a solution.*

3 Construction of the Auxiliary Function $\mathbf{a}^t$ and its Properties

The purpose of this section is to define a divergence-free function $\mathbf{a}^t$ in $\mathbb{R}^3_+ \times [0, T]$ which has the properties named and used in Sect. 1: identity (6), essentially $\mathbf{a}^t \cdot \mathbf{n} = (0, 0, \dot{\delta}^t) \cdot \mathbf{n}$ in ∂B^t for $t \neq t_c$, and inequalities (7)–(13).

Except for the Cartesian coordinates x_1, x_2, x_3, we shall also use the cylindrical coordinates r, φ and x_3. Thus, $r^2 = x_1^2 + x_2^2$. The lower half of the surface of B^t coincides with the graph of the function

$$x_3 \;=\; g^t(r) \;:=\; \delta^t + R - \sqrt{R^2 - r^2}; \qquad 0 \le r \le R.$$

Domains $\Omega^t(r_0)$, $\Omega_{\rm ext}$ *and* $\Omega_{\rm int}$. Let us fix $r_0 := \frac{3}{4}R$. The crucial sub-domain of Ω^t, where the collision occurs, is (see Fig. 1)

$$\Omega^t(r_0) \;:=\; \big\{\mathbf{x} = (r, \varphi, x_3) \in \Omega^t;\; r < r_0, \;\; x_3 < g^t(r)\big\}. \tag{21}$$

We also denote by $\Omega_{\rm ext}$ the set of points $\mathbf{x} = (r, \varphi, x_3) \in \mathbb{R}^3_+$ such that either $r > \frac{21}{20}R$ or $x_3 > \max\{\delta^0; \delta^T\}$. The complementary set $\Omega_{\rm int}$ is defined as $\mathbb{R}^3_+ \setminus \overline{\Omega}_{\rm ext}$.

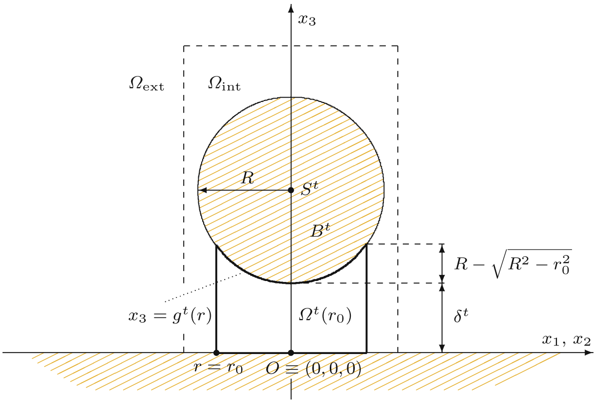

Fig. 1 Structure of domain Ω^t

An auxiliary function $\mathbf{b}^t$. Suppose that $t \in (0, T) \setminus \{t_c\}$. We define

$$\begin{aligned}
\beta^t &= (\beta^t_r, \beta^t_\varphi, \beta^t_3) \;:=\; \Big(0,\; \frac{r x_3}{2g^t(r)},\; 0\Big)\,\dot{\delta}^t, \\
\mathbf{b}^t &= (b^t_r, b^t_\varphi, b^t_3) \;:=\; \textbf{curl}\,\beta^t \;=\; \Big(-\frac{r}{2g^t(r)},\; 0,\; -\frac{x_3 r\,\partial_r g^t(r)}{2g^t(r)^2} + \frac{x_3}{g^t(r)}\Big)\,\dot{\delta}^t
\end{aligned} \tag{22}$$

in the cylinder $r < r_0$, $0 < x_3 < \delta^t + R$. The derivative of $g^t(r)$ with respect to r is $\partial_r g^t(r) = r/\sqrt{R^2 - r^2}$. The function $\mathbf{b}^t$ is divergence–free and it satisfies the conditions of impermeability, $\mathbf{b}^t \cdot \mathbf{n} = -b^t_3 = 0$ for $x_3 = 0$, and for $x_3 = g^t(r)$,

$$\mathbf{b}^t \cdot \mathbf{n} \;=\; \Big(-\frac{r}{2g^t(r)},\; 0,\; -\frac{r\,\partial_r g^t(r)}{2g^t(r)} + 1\Big)\,\dot{\delta}^t \cdot \frac{\big(-\partial_r g^t(r),\; 0,\; 1\big)}{\sqrt{[g^t(r)]^2 + 1}} \;=\; (0,\; 0,\; \dot{\delta}^t) \cdot \mathbf{n}$$

Thus, $\mathbf{b}^t \cdot \mathbf{n} = \mathbf{V}^t \cdot \mathbf{n}$ on the lower and upper parts of the boundary of $\Omega^t(r_0)$.

Two auxiliary cut-off functions. We shall use two cut-off functions: η_1 is an infinitely differentiable cut–off function of one variable such that

$$\eta_1(s) := \begin{cases} 1 & \text{for} \quad s < R, \\ 0 & \text{for} \quad \frac{21}{20}R < s, \\ \in [0,1] & \text{for} \quad R \le s \le \frac{21}{20}R \end{cases}$$

and η_2^t is an infinitely differentiable cut-off function in $\overline{\mathbb{R}}^3_+$ whose support is a subset of $\{\mathbf{x} = (r, \varphi, x_3);\ r \le r_0,\ x_3 \le \delta^t + R\}$ and $\eta_2^t(\mathbf{x}) = 1$ for $r < \frac{1}{2}R$ and $0 \le x_3 < g^t(r)$.

Let $\mathbf{e}_\varphi$ denote the unit vector in the direction of φ. Then $\mathbf{curl}\left[\frac{1}{2}r\dot{\delta}^t\,\mathbf{e}_\varphi\right] = (0, 0, \dot{\delta}^t)$. Furthermore, $\mathbf{curl}\left[\eta_1\big(|\mathbf{x} - S^t|\big)\,\frac{1}{2}r\dot{\delta}^t\,\mathbf{e}_\varphi\right]$ coincides with $(0, 0, \dot{\delta}^t)$ in B^t and it equals zero if $|\mathbf{x} - S^t| > \frac{21}{20}R$.

Definition of function $\mathbf{a}^t$. We put

$$\mathbf{a}^t(\mathbf{x}) := \mathbf{curl}\left[\eta_2^t(\mathbf{x})\,\beta^t(\mathbf{x}) + \left[1 - \eta_2^t(\mathbf{x})\right]\eta_1(|\mathbf{x} - S^t|)\,\tfrac{1}{2}r\dot{\delta}^t\,\mathbf{e}_\varphi\right]. \tag{23}$$

Then, in the important regions,

$$\mathbf{a}^t(\mathbf{x}) = \begin{cases} \mathbf{b}^t(\mathbf{x}) & \text{for } \mathbf{x} \in \Omega^t(r_1) \text{ with } r_1 := \frac{1}{2}R = \frac{2}{3}r_0, \\ (0,0,\dot{\delta}^t) & \text{for } \mathbf{x} \in B^t_+ := \left\{\mathbf{x} \in \mathbb{R}^3_+;\ |\mathbf{x} - S^t| \le R,\ x_3 > R + \delta^t\right\}, \\ \mathbf{0} & \text{for } \mathbf{x} \in \Omega_{\text{ext}}. \end{cases}$$

Obviously, $\mathbf{a}^t$ is divergence-free and satisfies identity (6). It can be proved that it also satisfies all the estimates (7)–(13) named in Sect. 1: since $\mathbf{a}^t$ is smooth outside the critical region $\Omega^t(r_1)$, where the collision of the ball B^t with the x_1, x_2-plane occurs, and $\mathbf{a}^t = 0$ in Ω_{ext}, we can focus only on the behavior of $\mathbf{a}^t$ in $\Omega^t(r_1)$, where $\mathbf{a}^t = \mathbf{b}^t$.

Using the explicit form of $\mathbf{b}^t$, given by (22), one can show that $\mathbf{b}^t$ indeed satisfies the same estimates as (7), (8), (9), (10), (11), (12), and (13). We only have to consider the norms or scalar products in $\Omega^t(r_1)$ instead of Ω^t on the left hand sides of (7)–(11). Similarly, $\mathbf{b}^t$ satisfies an estimate analogous to (12) with $\Gamma^t \cap \partial\Omega^t(r_1)$ instead of Γ^t.

We verify only two of the estimates in the rest of this section.

An estimate of $\left|\left(\boldsymbol{\varphi}\cdot\nabla\mathbf{b}^t,\ \boldsymbol{\varphi}\right)_{2;\,\Omega^t(r_1)}\right|$ *with* $\boldsymbol{\varphi} \in W^{1,2}_\sigma(\Omega^t)$. We consider this estimate to be crucial, because although domain $\Omega^t(r_1)$ is time-dependent, it provides an estimate with constant C independent of t.

Let us begin with the integral of $(\partial_r b_r^t)\,\varphi_r^2$, where we can easily check that $|\partial_r b_r^t| = \left|\partial_r\big(r\dot{\delta}^t/2g^t(r)\big)\right| \le C\,|\dot{\delta}^t|/g^t(r)$. We put $\tilde{\varphi}_r(r, x_3) := \int_0^{2\pi}\varphi_r(r, \varphi, x_3)\,\mathrm{d}\varphi$. Since the flow $\boldsymbol{\varphi}$ is incompressible and it also satisfies the condition of impermeability $\boldsymbol{\varphi}\cdot\mathbf{n} = 0$ on Γ^t, we have

$$\int_0^{g^t(r)}\tilde{\varphi}_r\,\mathrm{d}x_3 = \int_0^{g^t(r)}\int_0^{2\pi}\varphi_r\,\mathrm{d}\varphi\,\mathrm{d}x_3 = \int_{\partial\Omega^t(r)}\boldsymbol{\varphi}\cdot\mathbf{n}\,\mathrm{d}S = \int_{\Omega^t(r)}\operatorname{div}\boldsymbol{\varphi}\,\mathrm{d}\mathbf{x} = 0 \tag{24}$$

(where $0 < r \leq r_1$). This implies that to each $r \in (0, r_1)$ there exists $x_3(r)$ between 0 and $g^t(r)$ such that $\tilde{\varphi}_r(r, x_3(r)) = 0$. Using also the inequality $r^2 \leq 2R\, g^t(r)$ and applying Poincaré's inequality (see e.g. [3, R. Dautray and J. L. Lions, p. 127]) to the integral $\int_0^{2\pi} \varphi_r^2\, \mathrm{d}\varphi$, we obtain

$$
\begin{aligned}
&\left| \int_{\Omega^t(r_1)} (\partial_r b_r^t)\, \varphi_r^2\, \mathrm{d}\mathbf{x} \right| \;\leq\; C\, |\dot{\delta}^t| \int_0^{r_1} \frac{r\, \mathrm{d}r}{g^t(r)} \int_0^{g^t(r)} \mathrm{d}x_3 \left(\int_0^{2\pi} \varphi_r^2\, \mathrm{d}\varphi \right) \\
&\leq C\, |\dot{\delta}^t| \int_0^{r_1} \frac{r\, \mathrm{d}r}{g^t(r)} \int_0^{g^t(r)} \mathrm{d}x_3 \left(4\pi \int_0^{2\pi} (\partial_\varphi \varphi_r)^2\, \mathrm{d}\varphi + \frac{1}{2\pi} \left[\int_0^{2\pi} \varphi_r\, \mathrm{d}\varphi \right]^2 \right) \\
&= C\, |\dot{\delta}^t| \int_0^{r_1} \frac{r\, \mathrm{d}r}{g^t(r)} \int_0^{g^t(r)} \mathrm{d}x_3 \int_0^{2\pi} (\partial_\varphi \varphi_r)^2\, \mathrm{d}\varphi + C\, |\dot{\delta}^t| \int_0^{r_1} \frac{r\, \mathrm{d}r}{g^t(r)} \int_0^{g^t(r)} |\tilde{\varphi}_r|^2\, \mathrm{d}x_3 \\
&\leq C\, |\dot{\delta}^t| \int_0^{r_1} \frac{r^3\, \mathrm{d}r}{g^t(r)} \int_0^{g^t(r)} \mathrm{d}x_3 \int_0^{2\pi} \frac{1}{r^2} \left[\partial_\varphi \varphi_r(r, \varphi, x_3) \right]^2 \mathrm{d}\varphi \\
&\quad + C\, |\dot{\delta}^t| \int_0^{r_1} \frac{r\, \mathrm{d}r}{g^t(r)} \int_0^{g^t(r)} \left[\int_{x_3(r)}^{x_3} \partial_y \tilde{\varphi}_r(r, y)\, \mathrm{d}y \right]^2 \mathrm{d}x_3 \\
&\leq C\, |\dot{\delta}^t| \int_0^{r_1} r\, \mathrm{d}r \int_0^{g^t(r)} \mathrm{d}x_3 \int_0^{2\pi} \frac{1}{r^2} \left[\partial_\varphi \varphi_r(r, \varphi, x_3) \right]^2 \mathrm{d}\varphi \\
&\quad + C\, |\dot{\delta}^t| \int_0^{r_1} g^t(r)\, r\, \mathrm{d}r \int_0^{g^t(r)} \left| \partial_{x_3} \tilde{\varphi}_r(r, x_3) \right|^2 \mathrm{d}x_3 \;\leq\; C\, |\dot{\delta}^t| \int_{\Omega^t(r_1)} |\nabla \varphi_r|^2\, \mathrm{d}\mathbf{x}.
\end{aligned}
$$

The generic constant C is always independent of t. The integrals of $(\partial_3 b_3^t)\, \varphi_3^2$ and $(\partial_r b_3^t)\, \varphi_r\, \varphi_3$ can be treated similarly. (Here we can use the identity $\varphi_3(r, \varphi, 0) = 0$.) Thus, we finally estimate the modulus of $\big(\boldsymbol{\varphi} \cdot \nabla \mathbf{b}^t,\ \boldsymbol{\varphi}\big)_{2;\, \Omega^t(r_1)}$ by $C\, |\dot{\delta}^t|\ \|\nabla \boldsymbol{\varphi}\|_{2;\, \Omega^t(r_1)}^2$.

An estimate of the surface integral of $(\mathbf{b}^t - \mathbf{V}^t) \cdot \boldsymbol{\varphi}$. We estimate the product $(\mathbf{b}^t - \mathbf{V}^t) \cdot \boldsymbol{\varphi}$ on the "lower part" $\Gamma_0^t(r_1) := \{\mathbf{x} = (r, \varphi, x_3) \in \Gamma^t;\ r < r_1,\ x_3 = 0\}$ and on the "upper part" $\Gamma_1^t(r_1) := \{\mathbf{x} = (r, \varphi, x_3) \in \Gamma^t;\ r < r_1,\ x_3 = g^t(r)\}$ of $\Gamma^t \cap \partial \Omega^t(r_1)$. Using the explicit forms of $\mathbf{b}^t - \mathbf{V}^t$ on $\Gamma_0^t(r_1)$ and $\Gamma_1^t(r_1)$ and the identity $\varphi_3 = \partial_r g^t(r)\, \varphi_r$ on $\Gamma_1^t(r_1)$ (following from the condition $\boldsymbol{\varphi} \cdot \mathbf{n} = 0$), we get

$$
\begin{aligned}
&\left| \int_{\Gamma_0^t(r_1)} (\mathbf{b}^t - \mathbf{V}^t) \cdot \boldsymbol{\varphi}\, \mathrm{d}S + \int_{\Gamma_1^t(r_1)} (\mathbf{b}^t - \mathbf{V}^t) \cdot \boldsymbol{\varphi}\, \mathrm{d}S \right| \\
&= \left| \frac{\dot{\delta}^t}{2} \int_0^{r_1} \!\! \int_0^{2\pi} \! \left[\frac{r^2}{g^t(r)}\, \varphi_r(r, \varphi, 0) + \frac{r^2}{g^t(r)} \left(1 + \left[\partial_r g^t(r) \right]^2 \right) \varphi_r\big(r, \varphi, g^t(r)\big) \right] \mathrm{d}\varphi \mathrm{d}r \right| \\
&= \left| \frac{\dot{\delta}^t}{2} \int_0^{r_1} \left[\frac{r^2}{g^t(r)}\, \tilde{\varphi}_r(r, 0) + \frac{r^2}{g^t(r)} \left(1 + \left[\partial_r g^t(r) \right]^2 \right) \tilde{\varphi}_r\big(r, g^t(r)\big) \right] \mathrm{d}r \right| \\
&\leq C \left| \int_0^{r_1} \frac{r^2}{g^t(r)} \left(\int_{x_3(r)}^0 \partial_\sigma \tilde{\varphi}_r(r, \sigma)\, \mathrm{d}\sigma \right) \mathrm{d}r \right| \\
&\quad + C \left| \int_0^{r_1} \frac{r^2}{g^t(r)} \left(1 + \left[\partial_r g^t(r) \right]^2 \right) \left(\int_{x_3(r)}^{g^t(r)} \partial_\sigma \tilde{\varphi}_r(r, \sigma)\, \mathrm{d}\sigma \right) \mathrm{d}r \right|
\end{aligned}
$$

$$\leq \left| \int_0^{r_1} r \int_0^{g^t(r)} \left(\varepsilon \left| \partial_{x_3} \tilde{\varphi}_r(r, x_3) \right|^2 + C(\varepsilon) \right) \mathrm{d}x_3 \; \mathrm{d}r \right|.$$

The generic constant again C does not depend on t. Choosing sufficiently small $\varepsilon > 0$, we obtain an inequality that further enables us to arrive at (12).

The initial-value problem (14). Suppose that $t_0 \in [0, T]$ and $\mathbf{x}_0 \in \Omega^{t_0} \smallsetminus l^{t_0}$ (where l^{t_0} is the open line segment in Ω^{t_0} with the end points $(0, 0, 0)$ and $(0, 0, \delta^{t_0})$). Then the initial-value problem (14) has a unique solution $\mathbf{X}(t;\, t_0, \mathbf{x}_0)$ defined for $t \in [0, T]$ by the Carathéodory theorem. The trajectory of the solution stays in $\Omega^t \smallsetminus \ell^t$ (where ℓ^t is defined by analogy with ℓ^{t_0}) due to the condition $\mathbf{a}^t \cdot \mathbf{n} = \mathbf{V}^t \cdot \mathbf{n}$ satisfied by function $\mathbf{a}^t$ on Γ^t. The mapping $\mathbf{x}_0 \mapsto \mathbf{X}(t;\, t_0, \mathbf{x}_0)$ is a 1–1 regular mapping of $\Omega^{t_0} \smallsetminus \ell^{t_0}$ onto $\Omega^t \smallsetminus \ell^t$, whose Jacobian equals one. Note that if $\mathbf{x}_0 \in \Omega_{\mathrm{ext}}$ then $\mathbf{X}(t;\, t_0, \mathbf{x}_0) = \mathbf{x}_0$ independently of t and t_0 because $\mathbf{a}^t(\mathbf{x}_0, t) = 0$ for all $0 \leq t \leq T$.

4 The Time Discretized Boundary Value Problems

The time-discretization. Let $n \in \mathbb{N}$ and $k \in \{0; 1; \ldots; n\}$. We put $h := T/n$, $t_k := kh$, $\Omega_k := \Omega^{t_k}$ and $\Gamma_k := \Gamma^{t_k}$. We can assume without loss of generality that the critical time t_c of the collision differs from all the time instants t_k.

The stationary boundary value problems. We put $\mathbf{U}_0 := \mathbf{u}_0$. We successively solve, for $k = 1, \ldots, n$, a sequence of these stationary boundary value problems: given $\mathbf{U}_{k-1} \in L^2_\sigma(\Omega_{k-1})$ and $\mathbf{f}_k \in L^2(\Omega_k)^3$, we look for $\mathbf{U}_k$, P_k such that

$$\begin{aligned} \mathbf{U}_k(\mathbf{x}) - \mathbf{U}_{k-1}\big(\mathbf{X}(t_{k-1};\, t_k, \mathbf{x})\big) + h\mathbf{U}_k(\mathbf{x}) \cdot \big\{[\nabla \mathbf{a}]_k(\mathbf{x}) + \nabla \mathbf{U}_k(\mathbf{x})\big\} + h \nabla P_k(\mathbf{x}) \\ = \nu h \big\{ \mathrm{Div}[\nabla \mathbf{a}]_k(\mathbf{x}) + \Delta \mathbf{U}_k(\mathbf{x}) \big\} + \mathbf{A}_k(\mathbf{x}) + h \mathbf{f}_k(\mathbf{x}) \quad \text{in } \Omega_k, \end{aligned} \tag{25}$$

$$\mathrm{div}\, \mathbf{U}_k(\mathbf{x}) = 0 \quad \text{in } \Omega_k, \tag{26}$$

$$\mathbf{U}_k \cdot \mathbf{n} = 0 \quad \text{in } \Gamma_k, \tag{27}$$

$$\big[(\mathbb{T}_{\mathrm{d}})_k \cdot \mathbf{n}\big]_\tau + K\,(\mathbf{a}_k + \mathbf{U}_k - \mathbf{V}_k) = \mathbf{0} \quad \text{in } \Gamma_k, \tag{28}$$

The meaning of the functions $\mathbf{A}_k$, $[\nabla \mathbf{a}]_k$, $\mathbf{f}_k$, $\mathbf{a}_k$, $\mathbf{V}_k$ and $(\mathbb{T}_{\mathrm{d}})_k$ is explained below:

$$\mathbf{A}_k(\mathbf{x}) := -\mathbf{a}^{t_k}(\mathbf{x}) + \mathbf{a}^{t_{k-1}}\big(\mathbf{X}(t_{k-1};\, t_k, \mathbf{x})\big) = -\int_{t_{k-1}}^{t_k} \frac{\mathrm{d}}{\mathrm{d}t} \mathbf{a}^t\big(\mathbf{X}(t;\, t_k, \mathbf{x})\big)\, \mathrm{d}t,$$

$$[\nabla \mathbf{a}]_k(\mathbf{x}) := \frac{1}{h} \int_{t_{k-1}}^{t_k} \nabla \mathbf{a}^t(\mathbf{x})\, \mathrm{d}t, \qquad \mathbf{f}_k(\mathbf{x}) := \frac{1}{h} \int_{t_{k-1}}^{t_k} \mathbf{f}(\mathbf{x}, t)\, \mathrm{d}t$$

for $\mathbf{x} \in \Omega_k$ and $(\mathbb{T}_{\mathrm{d}})_k := 2\nu \big\{[\nabla \mathbf{a}]_k + \nabla \mathbf{U}_k\big\}_s$ on Γ_k. Denoting by $\mathbf{e}_3$ the unit vector $(0, 0, 1)$, we define for $\mathbf{x} \in \Gamma^s$ and $t,\ s \in [0, T]$ (such that $s \leq t$)

$$\mathbf{Y}(t;\, s, \mathbf{x}) := \begin{cases} \mathbf{x} + \big(\delta^t - \delta^s\big)\, \mathbf{e}_3 & \text{if } \mathbf{x} \in \partial B^s, \\ \mathbf{x} & \text{if } \mathbf{x} \in \text{the } x_1, x_2\text{–plane.} \end{cases} \tag{29}$$

The mapping $\mathbf{x} \mapsto \mathbf{Y}(t;\, s, \mathbf{x})$ represents the shift of the "material point" $\mathbf{x}$ on the boundary of the flow field in the time interval $[s, t]$. Now we denote for $\mathbf{x} \in \Gamma_k$

$$\mathbf{a}_k(\mathbf{x}) \;:=\; \frac{1}{h}\int_{t_{k-1}}^{t_k} \mathbf{a}^t\big(\mathbf{Y}(t;\, t_k, \mathbf{x})\big)\, \mathrm{d}t, \qquad \mathbf{V}_k(\mathbf{x}) \;:=\; \frac{1}{h}\int_{t_{k-1}}^{t_k} \mathbf{V}^t\big(\mathbf{Y}(t;\, t_k, \mathbf{x})\big)\, \mathrm{d}t.$$

Note that the term $\mathbf{a}^t \cdot \nabla\mathbf{u}$, which appears in Eq. (1) if we write $\mathbf{v}$ in the form $\mathbf{v} = \mathbf{a}^t + \mathbf{u}$, is now related to the difference at the beginning of (25):

$$\mathbf{U}_k(\mathbf{x}) - \mathbf{U}_{k-1}\big(\mathbf{X}(t_{k-1};\, t_k, \mathbf{x})\big) \;=\; \int_{t_{k-1}}^{t_k} \nabla\mathbf{U}_k\big(\mathbf{X}(t;\, t_k, \mathbf{x})\big) \cdot \mathbf{a}^t\big(\mathbf{X}(t;\, t_k, \mathbf{x})\big)\, \mathrm{d}t.$$

The weak formulation of the BV problem (25)–(28). We can get rid of pressure P_k in the classical formulation (25)–(28) if we formally multiply Eq. (25) by a test function $\boldsymbol{\Phi}_k$ from $W^{1,2}_\sigma(\Omega_k)$. Furthermore, we integrate by parts in the "viscous term" and we use boundary conditions (27) and (28) in the same way as the conditions (3) and (4) were used in (16). Thus, we arrive at the weak formulation: *we look for* $\mathbf{U}_k \in W^{1,2}_\sigma(\Omega_k)$ *such that*

$$\begin{aligned}
&\int_{\Omega_k}\Big\{\mathbf{U}_k(\mathbf{x}) - \mathbf{U}_{k-1}\big(\mathbf{X}(t_{k-1}; t_k, \mathbf{x})\big) + h\mathbf{U}_k(\mathbf{x})\cdot\big\{[\nabla\mathbf{a}]_k(\mathbf{x}) + \nabla\mathbf{U}_k(\mathbf{x})\big\}\Big\}\cdot\boldsymbol{\Phi}_k(\mathbf{x})\, \mathrm{d}\mathbf{x} \\
&\qquad + \int_{\Omega_k} 2\nu h\big\{[\nabla\mathbf{a}]_k(\mathbf{x}) + \nabla\mathbf{U}_k(\mathbf{x})\big\}_s : \nabla\boldsymbol{\Phi}_k(\mathbf{x})\, \mathrm{d}\mathbf{x} \\
&\qquad + \int_{\Gamma_k} K\, h\big[\mathbf{a}_k(\mathbf{x}) + \mathbf{U}_k(\mathbf{x}) - \mathbf{V}_k(\mathbf{x})\big]\cdot\boldsymbol{\Phi}_k(\mathbf{x})\, \mathrm{d}S \\
&= \int_{\Omega_k} h\,\mathbf{f}_k(\mathbf{x})\cdot\boldsymbol{\Phi}_k(\mathbf{x})\, \mathrm{d}\mathbf{x} + \int_{\Omega_k} \mathbf{A}_k(\mathbf{x})\cdot\boldsymbol{\Phi}_k(\mathbf{x})\, \mathrm{d}\mathbf{x}
\end{aligned} \tag{30}$$

for all $\boldsymbol{\Phi}_k \in W^{1,2}_\sigma(\Omega_k)$. The solvability of this nonlinear elliptic problem can be proved by standard methods, particularly of theory of the steady Navier-Stokes equation. We refer e.g. to the book [9] by G. P. Galdi for the corresponding techniques. The coerciveness of an associated quadratic form follows from the next estimates.

Apriori estimates of solutions of the BV problem (30). Using $\boldsymbol{\Phi}_k = \mathbf{U}_k$ in (30), we obtain:

$$\begin{gathered}
\frac{1}{2}\,\|\mathbf{U}_k\|^2_{2;\,\Omega_k} + \frac{1}{2}\int_{\Omega_k}\big|\mathbf{U}_k(\mathbf{x}) - \mathbf{U}_{k-1}\big(\mathbf{X}(t_{k-1};\, t_k\mathbf{x})\big)\big|^2\, \mathrm{d}\mathbf{x} \\
+\nu h\int_{\Omega_k}(\nabla\mathbf{U}_k)_s : \nabla\mathbf{U}_k\, \mathrm{d}\mathbf{x} + \int_{\Gamma_k} K\, h\, |\mathbf{U}_k|^2\, \mathrm{d}S \;\le \\
\frac{1}{2}\,\|\mathbf{U}_{k-1}\|^2_{2;\,\Omega_{k-1}} + \left|h\int_{\Omega_k}\mathbf{f}_k\cdot\mathbf{U}_k\, \mathrm{d}\mathbf{x}\right| + \left|h\int_{\Omega_k}\mathbf{U}_k\cdot[\nabla\mathbf{a}]_k\cdot\mathbf{U}_k\, \mathrm{d}\mathbf{x}\right|
\end{gathered}$$

$$\left|\int_{\Omega_k} \mathbf{A}_k \cdot \mathbf{U}_k \, \mathrm{d}\mathbf{x}\right| + \left|\nu h \int_{\Omega_k} \big([\nabla \mathbf{a}]_k\big)_s : \nabla \mathbf{U}_k \, \mathrm{d}\mathbf{x}\right| + \left|\int_{\Gamma_k} K\,(\mathbf{a}_k - \mathbf{V}_k)\cdot \mathbf{U}_k \, \mathrm{d}S\right|.$$

The integral of $(\nabla \mathbf{U}_k)_s : \nabla \mathbf{U}_k$ can be estimated from below by $\frac{1}{2}\,\|\nabla \mathbf{U}_k\|^2_{2;\,\Omega_k}$ by means of the integration by parts, the identity $\nabla(\mathbf{n}\cdot\mathbf{U}_k)\cdot\mathbf{U}_k = 0$ (valid on Γ_k) and the negative semi-definiteness of $\nabla\mathbf{n}$ on Γ_k. The integrals on the right hand side can F be treated by analogy with the procedure explained in Sect. 1, which now leads us to a discrete variant of the energy inequality (18):

$$\|\mathbf{U}_j\|^2_{2;\,\Omega_j} + \sum_{k=1}^{j} \int_{\Omega_k} \big|\mathbf{U}_k(\mathbf{x}) - \mathbf{U}_{k-1}\big(\mathbf{X}(t_{k-1};\, t_k, \mathbf{x})\big)\big|^2 \, \mathrm{d}\mathbf{x} + \nu h \sum_{k=1}^{j} \|\nabla \mathbf{U}_k\|^2_{2;\,\Omega_k}$$
$$+\, 2K h \sum_{k=1}^{j} \|\mathbf{U}_k\|^2_{2;\,\Gamma_k} \;\le\; \|\mathbf{U}_0\|^2_{2;\,\Omega_0} + \sum_{k=1}^{j} \omega_k\, \|\mathbf{U}_k\|^2_{2;\,\Omega_k} + \sum_{k=1}^{j} g_k \qquad (31)$$

for $j = 1, \dots, n$, where ω_k, g_k are certain positive numbers, depending on the same quantities as functions ω and G in (18), and satisfying the estimates $\sum_{k=1}^{n} \omega_k \le c_{11}$ and $\sum_{k=1}^{n} g_k \le c_{12}$ (with appropriate constants c_{11} and c_{12} independent of n).

5 The Non-stationary Approximations, Their Estimates and Weak Convergence

We define for $t_{k-1} < t \le t_k$ (where $k = 1, \dots, n$)

$$\mathbf{u}^n(\mathbf{x}, t) := \begin{cases} \mathbf{U}_k(\mathbf{x}) & \text{if } \mathbf{x} \in \overline{\Omega}_k, \\ \mathbf{0} & \text{if } \mathbf{x} \in \mathbb{R}^3_+ \setminus \overline{\Omega}_k, \end{cases}$$

$$\mathbb{U}^n(\mathbf{x}, t) := \begin{cases} \nabla \mathbf{U}_k(\mathbf{x}) & \text{if } \mathbf{x} \in \Omega_k, \\ \mathbb{O} & \text{if } \mathbf{x} \in \mathbb{R}^3_+ \setminus \Omega_k, \end{cases}$$

$$\mathbf{u}^n_*(\mathbf{x}, t) := \mathbf{u}^n\big(\mathbf{Y}(t_k;\, t, \mathbf{x}), t\big) \;=\; \mathbf{U}_k\big(\mathbf{Y}(t_k;\, t, \mathbf{x})\big) \quad \text{if } \mathbf{x} \in \Gamma^t.$$

Estimates of the sequences $\{\mathbf{u}^n\}$, $\{\mathbb{U}^n\}$ *and* $\{\mathbf{u}^n_*\}$. Inequality (31) implies that there exist $c_{13}(h) > 0$ and $c_{14}(h) > 0$ such that both $c_{13}(h)$ and $c_{14}(h)$ tend to zero as $h \to 0+$ and

$$\big[1 - c_{13}(h)\big]\, \|\mathbf{u}^n(.\,, t)\|^2_{2;\,\mathbb{R}^3_+} + \nu \int_0^t \|\mathbb{U}^n(.\,, s)\|^2_{2;\,\mathbb{R}^3_+} \, \mathrm{d}s + 2K \int_0^t \|\mathbf{u}^n_*(.\,, s)\|^2_{2;\,\Gamma^s} \, \mathrm{d}s$$
$$\le\; \|\mathbf{u}_0\|^2_{2;\,\Omega^0} + \int_0^t \lambda_n(s)\, \|\mathbf{u}^n(.\,, s)\|^2_{2;\,\mathbb{R}^3_+} \, \mathrm{d}s + c_{12} + c_{14}(h) \qquad (32)$$

where $\lambda_n(s) := \omega_k$ for $t_{k-1} < s \le t_k$. Applying Gronwall's lemma, we deduce that there exists $c_{15} > 0$ (depending on c_{11}, c_{12} and $\|\mathbf{u}_0\|_{2;\,\Omega^0}$) such that for all $n \in \mathbb{N}$ so large that $c_{13}(h) \le \frac{1}{2}$ and for all $t \in (0, T)$, we have

$$\|\mathbf{u}^n(.\,,t)\|_{2;\mathbb{R}^3_+} \;\leq\; c_{15}\,. \tag{33}$$

Using this estimate in (32), we observe that there exist c_{16} and c_{17} independent of n and such that

$$\int_0^T \|\mathbb{U}^n(.\,,s)\|^2_{2;\mathbb{R}^3_+}\,\mathrm{d}s \;\leq\; c_{16}\,, \qquad \int_0^T \|\mathbf{u}^n_*(.\,,s)\|^2_{2;\Gamma^s}\,\mathrm{d}s \;\leq\; c_{17}\,. \tag{34}$$

Inequalities (33) and (34) conversely yield:

$$\|\mathbf{U}_k\|_{2;\Omega_k} \leq c_{15} \quad (k=1,\ldots,n) \qquad \text{and} \qquad h\sum_{k=1}^{n} \|\nabla\mathbf{U}_k\|^2_{2;\Omega_k} \leq c_{16}\,. \tag{35}$$

Weak convergence of selected subsequences. Estimates (33) and (34) imply that there exist subsequences of $\{\mathbf{u}^n\}$, $\{\mathbb{U}^n\}$ and $\{\mathbf{u}^n_*\}$ (we shall denote them again by $\{\mathbf{u}^n\}$, $\{\mathbb{U}^n\}$ and $\{\mathbf{u}^n_*\}$ in order not to complicate the notation) and functions $\mathbf{u} \in L^\infty(0,T;\,L^2(\mathbb{R}^3_+)^3)$, $\mathbb{U} \in L^2(0,T;\,L^2(\mathbb{R}^3_+)^9)$ and $\mathbf{u}_* \in L^2(\Gamma_{(0,T)})^3$ such that

$$\mathbf{u}^n \rightharpoonup \mathbf{u} \qquad \text{weakly–}{*}\text{ in } L^\infty(0,T;\,L^2(\mathbb{R}^3_+)^3) \qquad \text{for } n\to+\infty, \tag{36}$$

$$\mathbb{U}^n \rightharpoonup \mathbb{U} \qquad \text{weakly in } L^2(0,T;\,L^2(\mathbb{R}^3_+)^9) \qquad \text{for } n\to+\infty, \tag{37}$$

$$\mathbf{u}^n_* \rightharpoonup \mathbf{u}_* \qquad \text{weakly in } L^2(\Gamma_{(0,T)})^3 \qquad \text{for } n\to+\infty \tag{38}$$

with the following relations between $\mathbf{u}$, $\mathbb{U}$ and $\mathbf{u}_*$:

Lemma 2 *(a)* $\mathbb{U} = \nabla\mathbf{u}$ *in the sense of distributions in* $Q_{(0,T)}$*,*
(b) $\mathbf{u} \in L^2(0,T;\,W^{1,2}_\sigma(\Omega^t))$*,*
(c) $\mathbf{u}_* = \mathbf{u}$ *on* $\Gamma_{(0,T)}$ *(here* $\mathbf{u}$ *denotes the trace of function* $\mathbf{u}\big|_{Q_{(0,T)}}$ *on* $\Gamma_{(0,T)}$*).*

The proof can be made by standard techniques.

6 The Limit Function u: A Solution of the Weak Problem (17)

Suppose that $\boldsymbol{\varphi}$ is a fixed infinitely differentiable divergence-free vector-function in $\overline{\mathbb{R}}^3_+ \times [0,T]$ with a compact support in $\overline{\mathbb{R}}^3_+ \times [0,T)$, such that $\boldsymbol{\varphi}\cdot\mathbf{n} = 0$ on $\Gamma_{[0,T]}$.

Using the relation between $\mathbf{u}^n$ and the solutions of the steady weak problem (30), one can verify that $\mathbf{u}^n$ (with $\mathbb{U}^n$ standing for $\nabla\mathbf{u}^n$ and $\mathbf{u}_*$ standing for the trace on $\Gamma_{(0,T)}$) satisfies the non-steady weak problem (17), up to a correction which tends to zero as $n\to+\infty$. (The intermediate step is to use (30) with $\boldsymbol{\Phi}_k = \boldsymbol{\varphi}(.\,,t_k)$.)

Applying (36), (37), and (38), we can pass to the limit as $n\to+\infty$ in all the linear terms. Thus, the limit of the nonlinear term (the integral of $\mathbf{u}^n\cdot\mathbb{U}^n\cdot\boldsymbol{\varphi}$) also exists. So we obtain:

$$\int_0^T\!\!\int_{\Omega^t}\Big\{-[\partial_t\boldsymbol{\varphi} + \mathbf{a}^t\cdot\|\nabla\boldsymbol{\varphi}]\cdot(\mathbf{a}^t+\mathbf{u}) - \mathbf{u}\cdot\nabla\boldsymbol{\varphi}\cdot\mathbf{a}^t + 2\nu\,[\nabla(\mathbf{a}^t+\mathbf{u})]_s : \nabla\boldsymbol{\varphi}\Big\}\mathrm{d}\mathbf{x}\,\mathrm{d}t$$

$$+ \lim_{n\to+\infty} \int_0^T \int_{\Omega^t} \mathbf{u}^n \cdot \mathbb{U}^n \cdot \boldsymbol{\varphi} \, \mathrm{d}\mathbf{x}\, \mathrm{d}t + \int_0^T \int_{\Gamma^t} K\, [\mathbf{a}^t + \mathbf{u} - \mathbf{V}^t] \cdot \boldsymbol{\varphi} \, \mathrm{d}S\, \mathrm{d}t$$
$$= \int_0^T \int_{\Omega^t} \mathbf{f} \cdot \boldsymbol{\varphi} \, \mathrm{d}\mathbf{x}\, \mathrm{d}t + \int_{\Omega^0} (\mathbf{a}^0 + \mathbf{u}_0) \cdot \boldsymbol{\varphi}(.\,, 0) \, \mathrm{d}\mathbf{x}. \qquad (39)$$

Comparing (39) with (17), we observe that in order to verify that $\mathbf{u}$ is a solution of the weak problem (17), it is sufficient to show that there exists a subsequence of $\{\mathbf{u}^n\}$ (we shall denote it again by $\{\mathbf{u}^n\}$) such that

$$\lim_{n\to+\infty} \int_0^T \int_{\Omega^t} \mathbf{u}^n \cdot \mathbb{U}^n \cdot \boldsymbol{\varphi} \, \mathrm{d}\mathbf{x}\, \mathrm{d}t \;=\; \int_0^T \int_{\Omega^t} \mathbf{u} \cdot \nabla\mathbf{u} \cdot \boldsymbol{\varphi} \, \mathrm{d}\mathbf{x}\, \mathrm{d}t. \qquad (40)$$

This limit procedure is not standard because of the variability of domain Ω^t and the choice of the test function $\boldsymbol{\varphi}$, which generally has only the normal component equal to zero on $\Gamma_{(0,T)}$. We explain it in greater detail in the next six paragraphs.

Cutting-off function $\boldsymbol{\varphi}$. Let $\varepsilon_1 > 0$ be given. Then, due to (33) and (34), there exists $\kappa_1 > 0$ so small that

$$\left| \int_{t_c-\kappa_1}^{t_c+\kappa_1} \int_{\Omega^t} \mathbf{u}^n \cdot \mathbb{U}^n \cdot \boldsymbol{\varphi} \, \mathrm{d}\mathbf{x}\, \mathrm{d}t \right| \leq$$
$$c_{18} \left[\operatorname*{ess\,sup}_{0<t<T} \|\mathbf{u}^n(.,t)\|_{2;\,\Omega^t} \right] \int_{t_c-\kappa_1}^{t_c+\kappa_1} \|\mathbb{U}^n(.,t)\|_{2;\,\Omega^t} \mathrm{d}\mathbf{x} \leq c_{18}\, c_{15}\, \sqrt{2\kappa_1 c_{16}} \;<\; \varepsilon_1 \qquad (41)$$

for all $n \in \mathbb{N}$ sufficiently large. (Here c_{18} is the maximum of $|\boldsymbol{\varphi}|$ on $\mathbb{R}^3_+ \times [0, T]$.) Let η_3 be an infinitely differentiable cut-off function of variable t defined on the interval $[0, T]$, with values in $[0, 1]$, such that

$$\eta_3(t) \;:=\; \begin{cases} 1 \text{ for} & t \in [0, t_c - \kappa_1] \cup [t_c + \kappa_1, T], \\ 0 \text{ for} & t \in \left[t_c - \frac{1}{2}\kappa_1, t_c + \frac{1}{2}\kappa_1\right], \end{cases}$$

The function $\boldsymbol{\varphi}^*(\mathbf{x}, t) := \eta_3(t)\, \boldsymbol{\varphi}(\mathbf{x}, t)$ equals zero for $t_c - \frac{1}{2}\kappa_1 \leq t \leq t_c + \frac{1}{2}\kappa_1$ and

$$\left| \int_{t_c-\kappa_1}^{t_c+\kappa_1} \int_{\Omega^t} \mathbf{u}^n \cdot \mathbb{U}^n \cdot (\boldsymbol{\varphi} - \boldsymbol{\varphi}^*) \, \mathrm{d}\mathbf{x}\, \mathrm{d}t \right| \;<\; \varepsilon_1$$

due to (41). Since ε_1 can be chosen arbitrarily small, it is sufficient to prove (40) with function $\boldsymbol{\varphi}^*$ instead of $\boldsymbol{\varphi}$.

Approximation of function $\boldsymbol{\varphi}^*$. Since each of the domains Ω_k (for $k = 1, \ldots, n$) has the cone property (because all the time instants t_k differ from t_c), inequalities (35) and the Sobolev embedding theorem imply that $\mathbf{U}_k \in L^6(\Omega_k)^3$. This means that $\mathbf{u}^n(.\,, t) \in L^6(\mathbb{R}^3_+)^3$ for all $t \in (0, T)$. Moreover, if we restrict ourselves to times $t \in I(\kappa_1)$, where

$$I(\kappa_1) \;:=\; \big[0, t_c - \tfrac{1}{2}\kappa_1\big) \cup \big(t_c + \tfrac{1}{2}\kappa_1, T\big],$$

then the cone parameters in the definition of the cone property of domain Ω^t can be chosen to be independent of t. Hence the constants in the embedding inequalities also become independent of t and we obtain the uniform estimate $\|\mathbf{u}^n(.\,,t)\|_{6;\mathbb{R}^3_+} \leq C\,(\|\mathbf{u}^n(.\,,t)\|_{2;\mathbb{R}^3_+} + \|\mathbb{U}^n(.\,,t)\|_{2;\mathbb{R}^3_+})$ for all $t \in I(\kappa_1)$. From this information and from (34), we can deduce that the product $\mathbf{u}^n \cdot \mathbb{U}^n$ belongs to $L^2\big(I(\kappa_1);\, L^1(\mathbb{R}^3_+)^3\big) \cap L^1\big(I(\kappa_1);\, L^{3/2}(\mathbb{R}^3_+)^3\big)$. By interpolation, we obtain the inclusion $\mathbf{u}^n \cdot \mathbb{U}^n \in L^r\big(I(\kappa_1);\, L^s(\mathbb{R}^3_+)^3\big)$ for $r \geq 1$, $s \geq 1$ such that $2/r + 3/s = 4$. Particularly, $\mathbf{u}^n \cdot \mathbb{U}^n \in L^{5/4}\big(I(\kappa_1);\, L^{5/4}(\mathbb{R}^3_+)^3\big)$.

Function $\boldsymbol{\varphi}^*$ can be approximated by infinitely differentiable divergence–free vector-functions that have a compact support in $Q_{[0,T)}$ with an arbitrary accuracy in the norm of the space $L^5\big(I(\kappa_1);\, L^5(\Omega^t)^3\big)$. Hence, given $\varepsilon_2 > 0$, there exists such a vector–function $\boldsymbol{\varphi}^{**}$ which satisfies

$$\bigg| \int_0^T \int_{\Omega^t} \mathbf{u}^n \cdot \mathbb{U}^n \cdot \boldsymbol{\varphi}^*\, \mathrm{d}\mathbf{x} - \int_0^T \int_{\Omega^t} \mathbf{u}^n \cdot \mathbb{U}^n \cdot \boldsymbol{\varphi}^{**}\, \mathrm{d}\mathbf{x} \bigg| \;<\; \varepsilon_2$$

for all $n \in \mathbb{N}$ sufficiently large. Since ε_2 can be chosen to be arbitrarily small, we can prove (40) only with the function $\boldsymbol{\varphi}^{**}$ instead of $\boldsymbol{\varphi}$ (respectively instead of $\boldsymbol{\varphi}^*$).

Partition of function $\boldsymbol{\varphi}^{**}$. Let $m \in \mathbb{N}$. We denote $\tau_j = jT/m$ (for $j = 0, \dots, m$). There exist $m+1$ infinitely differentiable functions $\theta_0, \dots, \theta_m$ on $[0, T]$ with their values in the interval $[0, 1]$ such that $\operatorname{supp}\theta_0 \subset I_0 := [\tau_0, \tau_1)$, $\operatorname{supp}\theta_j \subset I_j := (\tau_{j-1}, \tau_{j+1})$ (for $j = 1, \dots, m-1$), $\operatorname{supp}\theta_m \subset I_m := (\tau_{m-1}, \tau_m]$ and $\sum_{j=0}^m \theta_j(t) = 1$ for $0 \leq t \leq T$. Now we put $\boldsymbol{\varphi}_j^{**} := \theta_j\, \boldsymbol{\varphi}^{**}$ (for $j = 0, 1, \dots, m$). The functions $\boldsymbol{\varphi}_j^{**}$ are divergence–free, they have compact supports in Q_{I_j} (where $Q_{I_j} = \big\{(\mathbf{x}, t) \in \mathbb{R}^3 \times [0, T];\;\; t \in I_j,\;\; \mathbf{x} \in \Omega^t\big\}$) and

$$\sum_{j=0}^m \boldsymbol{\varphi}_j^{**} \;=\; \boldsymbol{\varphi}^{**} \qquad \text{in } \; Q_{[0,T]}.$$

Denote by K_j be the orthogonal projection of $\operatorname{supp}\boldsymbol{\varphi}_j^{**}$ into $\mathbb{R}^3$. If m is large enough then the distance between K_j and Γ^t is greater than one half of the distance between $\operatorname{supp}\boldsymbol{\varphi}^{**}$ and $\Gamma_{[0,T]}$ for all $t \in I_j$. Thus, there exists a bounded open set Ω_j^* in $\mathbb{R}^3$ with the boundary of the class $C^{1,1}$ such that $K_j \subset \Omega_j^* \subset \overline{\Omega_j^*} \subset \Omega^t$ for all $t \in I_j$. So, we conclude that in order to prove (40), it is sufficient to treat (40) separately with $\boldsymbol{\varphi} = \boldsymbol{\varphi}_j^{**}$ (for $j = 0, 1, \dots, m$) and to show that

$$\lim_{n \to +\infty} \int_{I_j} \int_{\Omega_j^*} \mathbf{u}^n \cdot \nabla \mathbf{u}^n \cdot \boldsymbol{\varphi}_j^{**}\, \mathrm{d}\mathbf{x}\, \mathrm{d}t \;=\; \int_{I_j} \int_{\Omega_j^*} \mathbf{u} \cdot \nabla \mathbf{u} \cdot \boldsymbol{\varphi}_j^{**}\, \mathrm{d}\mathbf{x}\, \mathrm{d}t. \tag{42}$$

The local Helmholtz decomposition of function $\mathbf{u}^n$. We denote by P_σ^j the Helmholtz projection in $L^2(\Omega_j^*)^3$. Put $\mathbf{w}_n^j := P_\sigma^j \mathbf{u}^n$. The function $(I - P_\sigma^j)\mathbf{u}^n$ has the form $\nabla\varphi_n^j$ for an appropriate scalar function φ_n^j. Equation (42) can now be written as

$$\lim_{n\to+\infty}\int_{I_j}\int_{\Omega_j^*}\Big[\mathbf{w}_n^j\cdot\nabla\mathbf{w}_n^j\cdot\boldsymbol{\varphi}_j^{**}+\mathbf{w}_n^j\cdot\nabla^2\varphi_n^j\cdot\boldsymbol{\varphi}_j^{**}+\nabla\varphi_n^j\cdot\nabla\mathbf{w}_n^j\cdot\boldsymbol{\varphi}_j^{**}$$
$$+\nabla\varphi_n^j\cdot\nabla^2\varphi_n^j\cdot\boldsymbol{\varphi}_j^{**}\Big]\,\mathrm{d}\mathbf{x}\,\mathrm{d}t\;=\;\int_{I_j}\int_{\Omega_j^*}(\mathbf{u}\cdot\nabla)\mathbf{u}\cdot\boldsymbol{\varphi}_j^{**}\,\mathrm{d}\mathbf{x}\,\mathrm{d}t. \tag{43}$$

Since $\nabla\varphi_n^j\cdot\nabla^2\varphi_n^j=\nabla\big(\frac{1}{2}|\nabla\varphi_n^j|^2\big)$ and $\boldsymbol{\varphi}_j^{**}(.\,,t)\in L^2_\sigma(\Omega_j^*)$, the integral of $\nabla\varphi_n^j\cdot\nabla^2\varphi_n^j\cdot\boldsymbol{\varphi}_j^{**}$ on Ω_j^* equals zero.

The convergence (36) and (37), the coincidence of $\mathbb{U}^n$ with $\nabla\mathbf{u}^n$ on $\Omega_j^*\times I_j$ and the boundedness of operator P_σ^j in $L^2(\Omega_j^*)^3$ and in $W^{1,2}(\Omega_j^*)^3$ imply that

$$\mathbf{w}_n^j\rightharpoonup\mathbf{w}^j=P_\sigma^j\mathbf{u},\quad\text{and}\quad\nabla\varphi_n^j\rightharpoonup\nabla\varphi^j=(I-P_\sigma^j)\mathbf{u}\quad\text{for }n\to+\infty \tag{44}$$

weakly in $L^2(I_j;\,W^{1,2}(\Omega_j^*)^3)$ and weakly–$*$ in $L^\infty(I_j;\,L^2_\sigma(\Omega_j^*))$.

Strong convergence of a subsequence of $\{\mathbf{w}_n^j\}$. We are going to show that there exists a subsequence of $\{\mathbf{w}_n^j\}$ that tends to $\mathbf{w}^j$ strongly in $L^2(I_j;\,L^2_\sigma(\Omega_j^*))$ as $n\to+\infty$. We shall therefore use the next lemma, see J. L. Lions [18, Theorem 5.2].

Lemma 3 *Let* $0<\gamma<\frac{1}{2}$ *and let* H_0, H *and* H_1 *be Hilbert spaces such that* $H_0\hookrightarrow\hookrightarrow H\hookrightarrow H_1$. *Let* $\mathcal{H}^\gamma(\mathbb{R};\,H_0,\,H_1)$ *denote the Banach space* $\big\{w\in L^2(\mathbb{R};\,H_0);\ |\vartheta|^\gamma\,\hat{w}(\vartheta)\in L^2(\mathbb{R};\,H_1)\big\}$ *with the norm*

$$|||w|||_{\gamma;\mathbb{R}}\;:=\;\big(\|w\|^2_{L^2(\mathbb{R};\,H_0)}+\|\,|\vartheta|^\gamma\,\hat{w}(\vartheta)\|^2_{L^2(\mathbb{R};\,H_1)}\big)^{1/2}.$$

(Here $\hat{w}(\vartheta)$ *is the Fourier transform of* $w(t)$*.) Let* $\mathcal{H}^\gamma(a,b;\,H_0,\,H_1)$ *further denote the Banach space of restrictions of functions from* $\mathcal{H}^\gamma(\mathbb{R};\,H_0,\,H_1)$ *onto the interval* (a,b)*, with the norm*

$$|||w|||_{\gamma;(a,b)}\;:=\;\inf\;|||z|||_{\gamma;\mathbb{R}}$$

where the infimum is taken over all $z\in\mathcal{H}^\gamma(\mathbb{R};\,H_0,\,H_1)$ *such that* $z=w$ *a.e. in* (a,b)*. Then* $\mathcal{H}^\gamma(0,T;\,H_0,\,H_1)\hookrightarrow\hookrightarrow L^2(a,b;\,H)$.

Consider $j\in\{1;\ldots;m\}$ fixed. We shall use Lemma 3 with $(a,b)=I_j$, $H_0=W^{1,2}_\sigma(\Omega_j^*)$, $H=L^2_\sigma(\Omega_j^*)$ and $H_1=W^{-1,2}_{0,\sigma}(\Omega_j^*)$. (Here $W^{-1,2}_{0,\sigma}(\Omega_j^*)$ denotes the dual to $W^{1,2}_{0,\sigma}(\Omega_j^*)$ where $W^{1,2}_{0,\sigma}(\Omega_j^*)$ is the closure of $C^\infty_{0,\sigma}(\Omega_j^*)$ in $W^{1,2}(\Omega_j^*)^3$. The space $W^{1,2}_{0,\sigma}(\Omega_j^*)$ can be characterized as the space of functions from $W^{1,2}_\sigma(\Omega_j^*)$ that have the trace on $\partial\Omega_j^*$ equal to zero.) We claim that $\{\mathbf{w}_n^j\}$ is bounded in the space $\mathcal{H}^\gamma(I_j;\,H_0,\,H_1)$. The boundedness of $\{\mathbf{w}_n^j\}$ in $L^2(I_j;\,H_0)$ follows from (33), (34), from the coincidence of $\mathbb{U}^n$ with $\nabla\mathbf{u}^n$ on $\Omega_j^*\times I_j$ and from the boundedness of operator P_σ^j in $L^2(\Omega_j^*)^3$ and in $W^{1,2}(\Omega_j^*)^3$. Thus, we only need to verify that $\{|\vartheta|^\gamma\,\hat{\mathbf{w}}_n^j\}$ is bounded in the space $L^2(I_j;\,H_1)$, i.e. in $L^2(I_j;\,W^{-1,2}_{0,\sigma}(\Omega_j^*))$. Let $\mathbf{z}_n^j$ be an extension by zero of $\mathbf{w}_n^j$ from the time interval I_j onto $\mathbb{R}$. Then

$$\hat{\mathbf{z}}_n^j(\vartheta) = \int_{-\infty}^{+\infty} \mathrm{e}^{-2\pi\,\mathrm{i}\,t\vartheta}\, \mathbf{w}_n^j(t)\,\mathrm{d}t = \sum_{k\in\Lambda_j^n} \int_{t_{k-1}}^{t_k} \mathrm{e}^{-2\pi\,\mathrm{i}\,t\vartheta}\, P_\sigma^j \mathbf{U}_k\,\mathrm{d}t \tag{45}$$

where Λ_j^n is the set of such indices $k \in \{1;\dots;n\}$ that $[\mathbb{R}^3 \times (t_{k-1}, t_k)] \cap \operatorname{supp} \boldsymbol{\varphi}_j^{**} \neq \emptyset$. Λ_j^n has the form $\Lambda_j^n = \{l; l+1; \dots; q\}$ where $1 \leq l \leq q \leq n$. Calculating the integrals in (45), we obtain

$$\begin{aligned}\hat{\mathbf{z}}_n^j(\vartheta) &= \sum_{k=l}^{q} \frac{1}{2\pi\,\mathbf{rir}\vartheta} \left[\mathrm{e}^{-2\pi\,\mathrm{i}\,t_{k-1}\vartheta} - \mathrm{e}^{-2\pi\,\mathrm{i}\,t_k\vartheta}\right] P_\sigma^j \mathbf{U}_k \\ &= \frac{1}{2\pi\,\mathbf{rir}\vartheta} \left[\mathrm{e}^{-2\pi\,\mathrm{i}\,t_{l-1}}\, P_\sigma^j \mathbf{U}_l - \mathrm{e}^{-2\pi\,\mathrm{i}\,t_q}\, P_\sigma^j \mathbf{U}_q\right] \\ &\quad + \frac{1}{2\pi\,\mathbf{rir}\vartheta} \sum_{k=l+1}^{q} \mathrm{e}^{-2\pi\,\mathrm{i}\,t_{k-1}\vartheta}\, [P_\sigma^j \mathbf{U}_k - P_\sigma^j \mathbf{U}_{k-1}].\end{aligned}$$

Since $\Omega_j^* \subset \Omega^s$ for all $s \in I_j$, we also have $\Omega_j^* \subset \Omega_k$ for all $k \in \Lambda_j^n$ (if n is large enough). If $|\vartheta| \leq 1$ then, using (45) and (35), we can estimate the norm of $|\vartheta|^\gamma\, \hat{\mathbf{z}}_n^j(\vartheta)$ in $W_{0,\sigma}^{-1,2}(\Omega_j^*)$ as follows:

$$\big\|\, |\vartheta|^\gamma\, \hat{\mathbf{z}}_n^j(\vartheta) \big\|_{-1,2;\,\Omega_j^*} \leq C(\Omega_j^*)\, |\vartheta|^\gamma \sum_{k=l}^{q} h\, \|\mathbf{U}_k\|_{2:\,\Omega_j^*} \leq C(\Omega_j^*)\, |\vartheta|^\gamma. \tag{46}$$

If $|\vartheta| > 1$ then we must proceed more subtly:

$$\begin{aligned}&\big\|\, |\vartheta|^\gamma\, \hat{\mathbf{z}}_n^j(\vartheta) \big\|_{-1,2;\,\Omega_j^*} \leq \frac{|\vartheta|^{\gamma-1}}{2\pi} \left(\|P_\sigma^j \mathbf{U}_l\|_{-1,2;\,\Omega_j^*} + \|P_\sigma^j \mathbf{U}_q\|_{-1,2;\,\Omega_j^*}\right) \\ &\quad + \frac{|\vartheta|^{\gamma-1}}{2\pi} \sum_{k=l+1}^{q} \|P_\sigma^j \mathbf{U}_k - P_\sigma^j \mathbf{U}_{k-1}\|_{-1,2;\,\Omega_j^*} \\ &\leq C(\Omega_j^*)\, |\vartheta|^{\gamma-1} \left(\|\mathbf{U}_l\|_{2:\,\Omega_j^*} + \|\mathbf{U}_q\|_{2:\,\Omega_j^*}\right) \\ &\quad + \frac{|\vartheta|^{\gamma-1}}{2\pi} \sum_{k=l+1}^{q} \sup_{\psi_k} \frac{1}{\|\boldsymbol{\psi}_k\|_{1,2;\,\Omega_j^*}} \left| \int_{\Omega_j^*} (\mathbf{U}_k - \mathbf{U}_{k-1}) \cdot \boldsymbol{\psi}_k\,\mathrm{d}\mathbf{x} \right|\end{aligned} \tag{47}$$

where the supremum is taken over all $\boldsymbol{\psi}_k \in W_{0,\sigma}^{1,2}(\Omega_j^*)$ such that $\|\boldsymbol{\psi}_k\|_{1,2;\,\Omega_j^*} > 0$. The sum in (47) can be estimated by $\mathcal{S}_1 + \mathcal{S}_2$ where

$$\begin{aligned}\mathcal{S}_1 &= \sum_{k=l+1}^{q} \sup_{\psi_k} \frac{1}{\|\boldsymbol{\psi}_k\|_{1,2;\,\Omega_j^*}} \left| \int_{\Omega_j^*} \left[\mathbf{U}_k(\mathbf{x}) - \mathbf{U}_{k-1}\big(\mathbf{X}(t_{k-1};\, t_k, \mathbf{x})\big)\right] \cdot \boldsymbol{\psi}_k(\mathbf{x})\,\mathrm{d}\mathbf{x} \right|, \\ \mathcal{S}_2 &= \sum_{k=l+1}^{q} \sup_{\psi_k} \frac{1}{\|\boldsymbol{\psi}_k\|_{1,2;\,\Omega_j^*}} \left| \int_{\Omega_j^*} \left[\mathbf{U}_{k-1}(\mathbf{x}) - \mathbf{U}_{k-1}\big(\mathbf{X}(t_{k-1};\, t_k, \mathbf{x})\big)\right] \cdot \boldsymbol{\psi}_k(\mathbf{x})\,\mathrm{d}\mathbf{x} \right|.\end{aligned}$$

The function $\boldsymbol{\psi}_k$, extended by zero to $\mathbb{R}^3_+ \smallsetminus \Omega^*_j$, belongs to $W^{1,2}_\sigma(\Omega_k)$. Hence the integral of $\big[\mathbf{U}_k(\mathbf{x}) - \mathbf{U}_{k-1}\big(\mathbf{X}(t_{k-1};\, t_k, \mathbf{x})\big)\big] \cdot \boldsymbol{\psi}_k(\mathbf{x})$ on Ω^*_j equals the integral of the same function in Ω_k and it can be therefore expressed by means of (30). Thus, $\mathcal{S}_1$ can be estimated:

$$\begin{aligned}\mathcal{S}_1 \leq \sum_{k=l+1}^{q} \sup_{\psi_k} \frac{1}{\|\boldsymbol{\psi}_k\|_{1,2;\,\Omega^*_j}} \bigg| &-h \int_{\Omega_k} \mathbf{U}_k(\mathbf{x}) \cdot [\nabla \mathbf{a}]_k(\mathbf{x}) \cdot \boldsymbol{\psi}_k(\mathbf{x})\, \mathrm{d}\mathbf{x} \\ &- h \int_{\Omega_k} \mathbf{U}_k(\mathbf{x}) \cdot \nabla \mathbf{U}_k(\mathbf{x}) \cdot \boldsymbol{\psi}_k(\mathbf{x})\, \mathrm{d}\mathbf{x} \\ &- h \int_{\Omega_k} \nu \big\{[\nabla \mathbf{a}]_k(\mathbf{x}) + \nabla \mathbf{U}_k(\mathbf{x})\big\}_s : \nabla \boldsymbol{\psi}_k(\mathbf{x})\, \mathrm{d}\mathbf{x} \\ &- \int_{\Gamma_k} K \big[\mathbf{a}_k(\mathbf{x}) + \mathbf{U}_k(\mathbf{x}) - \mathbf{V}_k(\mathbf{x})\big] \cdot \boldsymbol{\psi}_k(\mathbf{x})\, \mathrm{d}S \\ &+ \int_{\Omega_k} h\, \mathbf{f}_k(\mathbf{x}) \cdot \boldsymbol{\psi}_k(\mathbf{x})\, \mathrm{d}\mathbf{x} + \int_{\Omega_k} \mathbf{A}_k(\mathbf{x}) \cdot \boldsymbol{\psi}_k(\mathbf{x})\, \mathrm{d}\mathbf{x} \bigg|.\end{aligned}$$

The surface integral on Γ_k equals zero because the function $\boldsymbol{\psi}_k$ is zero on Γ_k. The right hand side can be estimated by $C(\Omega^*_j)$ by means of (7) and (35), standard inequalities based on the Sobolev embedding theorem (applied in Ω^*_j) and the Hölder inequality. Let us show the procedure in greater detail, for example, in the case of the terms containing the product $\mathbf{U}_k \cdot \nabla \mathbf{U}_k \cdot \boldsymbol{\psi}_k$:

$$\begin{aligned}&\sum_{k=l+1}^{q} \sup_{\psi_k} \frac{1}{\|\boldsymbol{\psi}_k\|_{1,2;\,\Omega^*_j}} \bigg| h \int_{\Omega_k} \mathbf{U}_k \cdot \nabla \mathbf{U}_k \cdot \boldsymbol{\psi}_k\, \mathrm{d}\mathbf{x} \bigg| \\ &\leq C(\Omega^*_j) \bigg(\sum_{k=l+1}^{q} h \int_{\Omega_k} |\nabla \mathbf{U}_k|^2\, \mathrm{d}\mathbf{x} \bigg)^{1/2} \bigg(\sum_{k=l+1}^{q} h \int_{\Omega_k} |\mathbf{U}_k|^3\, \mathrm{d}\mathbf{x} \bigg)^{1/3} \\ &\leq C(\Omega^*_j) \bigg(h \sum_{k=l+1}^{q} \|\nabla \mathbf{U}_k\|^{3/2}_{2;\,\Omega_k}\, \|\mathbf{U}_k\|^{3/2}_{6;\,\Omega_k} \bigg)^{1/3} \\ &\leq C(\Omega^*_j) \bigg[h \sum_{k=l+1}^{q} \|\nabla \mathbf{U}_k\|^{3/2}_{2;\,\Omega_k} \Big(\|\mathbf{U}_k\|^{3/2}_{2;\,\Omega_k} + \|\nabla \mathbf{U}_k\|^{3/2}_{2;\,\Omega_k} \Big) \bigg]^{1/3} \\ &\leq C(\Omega^*_j) \bigg[1 + \bigg(h \sum_{k=1}^{n} \|\nabla \mathbf{U}_k\|^2_{2;\,\Omega_k} \bigg)^{3/4} \bigg]^{1/3} \leq\; C(\Omega^*_j).\end{aligned}$$

Here the constant $C(\Omega^*_j)$ also depends on the right hand sides of (7) and (35). In order to estimate $\mathcal{S}_2$, we use the identities

$$\mathbf{U}_{k-1}(\mathbf{x}) - \mathbf{U}_{k-1}\big(\mathbf{X}(t_{k-1};\, t_k, \mathbf{x})\big) \;=\; \int_{t_{k-1}}^{t_k} \frac{\mathrm{d}}{\mathrm{d}\xi}\, \mathbf{U}_{k-1}\big(\mathbf{X}(\xi;\, t_k, \mathbf{x})\big)\, \mathrm{d}\xi$$

$$= \int_{t_{k-1}}^{t_k} \mathbf{a}^\xi \big(\mathbf{X}(\xi;\, t_k, \mathbf{x})\big) \cdot \nabla \mathbf{U}_{k-1}\big(\mathbf{X}(\xi;\, t_k, \mathbf{x})\big)\, \mathrm{d}\xi.$$

Then the sum $\mathcal{S}_2$ can be estimated by means of (10) and (35) as follows:

$$\begin{aligned}
\mathcal{S}_2 \leq\; & C(\Omega_j^*) \sup_{\psi_k} \frac{\|\boldsymbol{\psi}_k\|_{6;\,\Omega_j^*}}{\|\boldsymbol{\psi}_k\|_{1,2;\,\Omega_j^*}} \sum_{k=l+1}^{q} \bigg[\int_{t_{k-1}}^{t_k} \int_{\Omega_j^*} \big|\nabla \mathbf{U}_{k-1}\big(\mathbf{X}(\xi;\, t_k, \mathbf{x})\big)\big|^2\, \mathrm{d}\mathbf{x}\, \mathrm{d}\xi \bigg]^{1/2} \\
& \cdot \bigg[\int_{t_{k-1}}^{t_k} \bigg(\int_{\Omega_j^*} \big|\mathbf{a}^\xi \big(\mathbf{X}(\xi;\, t_k, \mathbf{x})\big)\big|^3\, \mathrm{d}\mathbf{x} \bigg)^{2/3} \mathrm{d}\xi \bigg]^{1/2} \\
\leq\; & C(\Omega_j^*) \bigg[\sum_{k=l+1}^{q} \int_{t_{k-1}}^{t_k} \int_{\Omega_{k-1}} \big|\nabla \mathbf{U}_{k-1}(\mathbf{x})\big|^2\, \mathrm{d}\mathbf{x}\, \mathrm{d}\xi \bigg]^{1/2} \bigg[\int_0^T \int_{\Omega^\xi} \big|\mathbf{a}^\xi(\mathbf{x})\big|^5\, \mathrm{d}\mathbf{x}\, \mathrm{d}\xi \bigg]^{1/5} \\
\leq\; & C(\Omega_j^*).
\end{aligned}$$

Substituting the estimates of $\mathcal{S}_1$ and $\mathcal{S}_2$ to (47), we finally obtain

$$\big\| |\vartheta|^\gamma\, \hat{\mathbf{z}}_n^j(\vartheta) \big\|_{-1,2;\,\Omega_j^*} \;\leq\; C(\Omega_j^*)\, |\vartheta|^{\gamma-1}. \tag{48}$$

The constant $C(\Omega_j^*)$ is independent of n. Recall that inequality (48) holds for $|\vartheta| > 1$. Since the exponent γ satisfies $0 < \gamma < \frac{1}{2}$, the right hand side of (48) is integrable on $(-\infty, -1) \cup (1, +\infty)$ with power 2. This, together with (46), implies that the sequence $\{|\vartheta|^\gamma\, \hat{\mathbf{z}}_n^j(\vartheta)\}$ is bounded in $L^2(\mathbb{R};\, W_{0,\sigma}^{-1,2}(\Omega_j^*))$. Consequently, the sequence $\{\mathbf{w}_n^j\}$ is bounded in $\mathcal{H}^\gamma\big(I_j;\, W_\sigma^{1,2}(\Omega_j^*),\, W_{0,\sigma}^{-1,2}(\Omega_j^*)\big)$. This space is reflexive, hence there exists a subsequence (we denote it again by $\{\mathbf{w}_n^j\}$) which converges weakly in $\mathcal{H}^\gamma\big(I_j;\, W_\sigma^{1,2}(\Omega_j^*),\, W_{0,\sigma}^{-1,2}(\Omega_j^*)\big)$. Due to (44), the limit must be $\mathbf{w}^j$. Applying now Lemma 3, we have: $\mathbf{w}_n^j \longrightarrow \mathbf{w}^j = P_\sigma^j \mathbf{u}$ strongly in $L^2\big(I_j;\, L^2(\Omega_j^*)^3\big)$. This strong convergence, together with the weak convergence (44), enables us to pass to the limit in the first three terms on the left hand side of (43). The procedure is standard (see e.g. J. L. Lions [18] or R. Temam [22]), therefore we omit the details. Using also the equation

$$\int_{\Omega_j^*} (\nabla\varphi \cdot \nabla)\nabla\varphi \cdot \boldsymbol{\varphi}_j^{**}\, \mathrm{d}\mathbf{x} \;=\; 0,$$

following from the inclusion $\boldsymbol{\varphi}_j^{**} \in L_\sigma^2(\Omega_j^*)$ and from the identity $(\nabla\varphi \cdot \nabla)\nabla\varphi = \nabla\big(\frac{1}{2}|\nabla\varphi|^2\big)$, we can verify the validity of (43), and consequently also the validity of (40). This confirms that $\mathbf{u}$ is a weak solution of the weak problem (17). The proof of Theorem 1 is thus completed.

7 Concluding Remarks

Energy inequality for the weak solution. The limit processes (36), (37) and (38) and Lemma 2 imply that the limit function **u**, which is a solution of (17), satisfies the same estimates (33) and (34) as the approximations. Inequality (33) thus provides an estimate of the kinetic energy associated with the flow **u** at a.a. times $t \in (0, T)$ and the first inequality in (34) estimates the dissipation of this energy in the time interval $(0, T)$. The question whether **u** also satisfies the energy inequality (18), formally derived in Sect. 2 (see Lemma 1), is open. To obtain (18), it would be necessary to make the limit transition in inequality (32) (which is the discrete equivalent of (18)). Here we need an information on the strong convergence of a subsequence of $\{\mathbf{u}^n\}$ in $L^2(0, T; L^2_\sigma(\Omega^t))$ in order to control the second term on the right hand side of (32). However, we do not have such an information: we have only obtained the strong convergence of appropriate local interior Helmholtz projections of $\mathbf{u}^n$ in Sect. 6. It was sufficient for the limit transition (40), but it does not enable us to treat the integral on the right hand side of (32) in a similar way.

The condition of smallness (iv). Condition (iv) (see Lemma 1) requires a sufficient smallness of the speed of the ball B^t at times close to the critical instant t_c of the collision of the ball with the wall. We need this condition because estimate (13), based on the continuous embedding $W^{1,2}(\Omega^t)) \hookrightarrow L^6(\Omega^t)$, cannot be used in order to estimate the approximations at times close to t_c. (The constant in the embedding inequality increases "too rapidly" to infinity as $t \to t_c$.) Thus, we use estimate (11) instead of (13) at times close to t_c and since we need the right hand side to be absorbed by the "viscous term", it must be "sufficiently small".

Flow around a body of a general shape striking the wall. We have mainly used the information on the shape of B^t (i.e. that it is a ball) in the region close to the point of the collision of B^t with the wall. (Particularly, the shape of B^t influences the form of function g^t in Sect. 2. With another function g^t, we would obtain other inequalities than (7), (8), (9), (10), (11), (12), and (13) for function $\mathbf{a}^t$.) Thus, Theorem 1 could be generalized in such a way that instead of the ball B^t we would speak on a compact body of another (however sufficiently smooth) shape, which coincides with a ball in the neighborhood of the point of the collision.

Acknowledgments The research was supported by the Grant Agency of the Czech Academy of Sciences (Grant No. IAA100190612), by the Academy of Sciences of the Czech Republic, Institutional Research Plan No. AV0Z10190503, and by the University of Sud Toulon–Var.

References

1. Adams R.: *Sobolev Spaces.* Academic Press, New York, San Francisco, London (1975)
2. Conca C., San Martín J., Tucsnak M.: Existence of solutions for the equations modelling the motion of a rigid body in a viscous fluid. Comm. Part. Diff. Equat. **25** (5&6), 1019–1042 (2000)
3. Dautray R., Lions M.J.: *Mathematical Analysis and Numerical Methods for Science and Technology II.* Springer, Berlin, Heidelberg (2000)

4. Desjardins B., Esteban M.J.: Existence of weak solutions for the motion of rigid bodies in a viscous fluid. Arch. Rat. Mech. Anal. **146**, 59–71 (1999)
5. Desjardins B., Esteban M.J.: On weak solutions for fluid-rigid structure interaction: compressible and incompressible models. Comm. Part. Diff. Equat. **25** (7&8), 1399–1413 (2000)
6. Feireisl E.: On the motion of rigid bodies in a viscous incompressible fluid. J. Evol. Equat. **3**, 419–441 (2003)
7. Fujita H., Sauer N.: On existence of weak solutions of the Navier-Stokes equations in regions with moving boundaries. J. Fac. Sci. Univ. Tokyo, Sec. 1A, **17**, 403–420 (1970)
8. Galdi G.P.: *An Introduction to the Mathematical Theory of the Navier-Stokes Equations, Vol. I, Linear Steady Problems.* Springer Tracts in Natural Philosophy **38** (1998)
9. Galdi G.P.: *An Introduction to the Mathematical Theory of the Navier-Stokes Equations, Vol. II, Nonlinear Steady Problems.* Springer Tracts in Natural Philosophy **39** (1998)
10. Galdi G.P.: An Introduction to the Navier–Stokes initial–boundary value problem. In *Fundamental Directions in Mathematical Fluid Mechanics,* ed. G.P.Galdi, J.Heywood, R.Rannacher, series "Advances in Mathematical Fluid Mechanics", Vol. 1, Birkhauser–Verlag, Basel, 1–98 (2000)
11. Galdi G.P.: On the motion of a rigid body in a viscous fluid: a mathematical analysis with applications. In *Handbook of Mathematical Fluid Dynamics I*, Ed. S. Friedlander and D. Serre, Elsevier (2002)
12. Gunzburger M.D., Lee H.C., Seregin G.: Global existence of weak solutions for viscous incompressible flows around a moving rigid body in three dimensions. J. Math. Fluid Mech. **2**, 219–266 (2000)
13. Hoffmann K.H., Starovoitov V.N.: On a motion of a solid body in a viscous fluid. Two–dimensional case. Adv. Math. Sci. Appl. **9**, 633–648 (1999)
14. Hoffmann K.H., Starovoitov V.N.: Zur Bewegung einer Kugel in einen zähen Flüssigkeit. Documenta Mathematica **5**, 15–21 (2000)
15. Hopf E.: Über die Anfangswertaufgabe für die Hydrodynamischen Grundgleichungen. Math. Nachr. **4**, 213–231 (1950)
16. Ladyzhenskaya O.A.: *The Mathematical Theory of Viscous Incompressible Flow.* Gordon and Breach, New York (1969)
17. Leray J.: Sur le mouvements d'un liquide visqueux emplissant l'espace. Acta Mathematica **63**, 193–248 (1934)
18. Lions J.L.: *Quelques Méthodes de Résolution des Problèmes aux Limites Non Linéaires.* Dunod, Gauthier–Villars, Paris (1969)
19. Neustupa J.: Existence of a weak solution to the Navier-Stokes equation in a general time–varying domain by the Rothe method. Preprint (2007)
20. San Martín J., Starovoitov V.N., Tucsnak M.: Global weak solutions for the two–dimensional motion of several rigid bodies in an incompressible viscous fluid. Arch. Rat. Mech. Anal. **161**, 113–147 (2002)
21. Starovoitov V.N.: Behavior of a rigid body in an incompressible viscous fluid near a boundary. Int. Series of Num. Math. **147**, 313–327 (2003)
22. Temam R.: *Navier-Stokes Equations.* North-Holland, Amsterdam–New York–Oxford (1977)

On the Influence of an Absorption Term in Incompressible Fluid Flows

Hermenegildo B. de Oliveira

Abstract This work is concerned with a mathematical problem derived from the Ellis model used in Fluid Mechanics to describe the response of a great variety of generalized fluid flows. For pseudoplastic fluids, it is well-known that the weak solutions to that problem extinct in a finite time. In order to obtain the same property for Newtonian and dilatant fluids, we modify the problem by introducing an absorption term in the momentum equation. The proof relies on a suitable energy method, Sobolev type interpolation inequalities and also on a generalized Korn's inequality. Then we extend our results for several cases: slip boundary conditions, anisotropic absorption and non-homogeneous fluid flows. We also discuss existence and uniqueness of weak solutions for the modified problem.

Keywords Non-Newtonian fluids · Ellis model · Absorption · Existence · Uniqueness · Extinction in time

1 Introduction

In Fluid Mechanics, the most widely used constitutive relation to model the response of incompressible and homogeneous fluids is

$$\mathbf{T} = -p\mathbf{I} + \mathbf{F}(\mathbf{D}), \quad \mathbf{F}(\mathbf{D}) = \alpha_1(\mathbb{I}_{\mathbf{D}})\mathbf{D}, \quad \mathbf{D} = \frac{1}{2}\left(\nabla \mathbf{u} + \nabla \mathbf{u}^T\right). \tag{1}$$

The notation is well known: $\mathbf{u}$ is the velocity field, p is the pressure, $\mathbf{T}$ is the Cauchy stress tensor, $\mathbf{I}$ is the unit tensor, $\mathbf{D}$ is the stretching tensor which mathematically corresponds to the symmetric part of the velocity gradient $\nabla \mathbf{u}$, usually denominated in Fluid Mechanics as the shear rate, and $\mathbb{I}_{\mathbf{D}} = 1/2|\mathbf{D}|^2$ is the first invariant of $\mathbf{D}$. In this work, we assume the extra stress tensor $\mathbf{F}$ and the stretching tensor $\mathbf{D}$ are related by the following rheological flow law

H.B. de Oliveira (✉)
FCT – Universidade do Algarve, Campus de Gambelas 8005-139 Faro, Portugal
e-mail: holivei@ualg.pt

R. Rannacher, A. Sequeira (eds.), *Advances in Mathematical Fluid Mechanics*,
DOI 10.1007/978-3-642-04068-9_25,

$$\mathbf{F} = \left(\mu_0 + \mu_1 |\mathbf{D}|^{q-2}\right) \mathbf{D}\,. \tag{2}$$

Parameters μ_0, μ_1 and q are non-negative, being the first two related with the fluid viscosity and the latter characterizing the flow. Equations (1) and (2) are known in the literature as the Ellis model and describe the response of a great variety of generalized fluids. For $q >> 1$ and small values of $|\mathbf{D}|$, (1) and (2) tend to approximate the Stokes model for Newtonian fluids. On the contrary, for $q << 1$ and great values of $|\mathbf{D}|$, they approximate the Ostwald-de Waele model for power law fluids, very often used to model non-Newtonian fluids. Therefore many fluid models can be obtained from the Ellis law (1) and (2) by combining the parameters μ_0, μ_1 and q as follows:

$$\begin{cases} \text{Newtonian} & \text{if } \mu_0 > 0 \wedge \mu_1 = 0 \\ \text{Ostwald-de Waele} & \text{if } \mu_0 = 0 \wedge \mu_1 > 0 \end{cases} \quad \begin{cases} \text{Bingham} & \text{if } q = 1 \\ \text{pseudoplastic} & \text{if } 1 < q < 2 \\ \text{Newtonian} & \text{if } q = 2 \\ \text{dilatant} & \text{if } q > 2\,. \end{cases}$$

Examples of such fluids are water solutions, gasoline, vegetal and mineral oils (Newtonian), drilling muds used in petroleum industry, toothpaste and face creams (Bingham), milk fluids, varnishes, shampoo and blood fluids (pseudoplastic), polar ice, glaciers, volcano lava and sand (dilatant). It is well known that a pseudoplastic fluid is characterized by a viscosity that decreases with shear rate and a dilatant fluid by a viscosity that increases with shear rate. As a consequence, many authors rather use to denote them as shear thinning and shear thickening fluids, respectively. Bingham fluid is similar to a pseudoplastic fluid, but it exhibits a yield point. The existence of a yield point means fluid flow is prevented below a critical stress level, but flow occurs when the critical stress level is exceeded. Other names found in the literature for Bingham fluids are plastic fluids and sometimes viscoplastic fluids to avoid confusion with the word plastic as applied to solid polymers. See Schowalter [18] and the references therein for the models more often used in non-Newtonian Fluid Mechanics.

From the basic principles of Fluid Mechanics, it is well known that, in motions of incompressible fluids modeled by the Ellis law (1) and (2) (with neither inner mass sources nor sinks), the velocity field and pressure are determined by:

- the incompressibility condition

$$\operatorname{div} \mathbf{u} = 0; \tag{3}$$

- the conservation of mass

$$\frac{\partial \varrho}{\partial t} + \operatorname{div}(\varrho \mathbf{u}) = 0; \tag{4}$$

- the conservation of momentum

$$\varrho\left(\frac{\partial \mathbf{u}}{\partial t}+(\mathbf{u}\cdot\nabla)\mathbf{u}\right)=\varrho\,\mathbf{f}-\nabla p+\operatorname{div}\left[\left(\mu_0+\mu_1|\mathbf{D}|^{q-2}\right)\mathbf{D}\right]. \tag{5}$$

Again in (3), (4), and (5), ϱ is the density and $\mathbf{f}$ is the forcing term. For homogeneous fluids, the density is regarded as constant. Therefore, in that case, we can replace the continuity equation (4) by its incompressible form (3). System (3), (4), and (5) must be supplemented with boundary conditions characterizing the flow on the boundary of the domain occupied by the fluid and by initial conditions determining the initial state of the flow at the beginning of the time interval.

2 The Modified Ellis Problem

In this section, we shall introduce the main problem we are going to work with. Let us consider a general cylinder

$$Q_T := \Omega\times(0,T)\subset\mathbb{R}^N\times\mathbb{R}^+,$$

where Ω is a bounded domain whose boundary $\partial\Omega$ is assumed to be smooth enough. The boundary of Q_T is defined by

$$\Gamma_T := (0,T)\times\partial\Omega\,.$$

The dimensions of physical interest are $N=2$ and $N=3$, but the results to be presented here extend to any dimension $N\geq 2$. In this paper we shall consider the following modified Ellis problem (MEP) for homogeneous fluids

$$\operatorname{div}\mathbf{u}=0 \tag{6}$$

$$\frac{\partial \mathbf{u}}{\partial t}+(\mathbf{u}\cdot\nabla)\mathbf{u}-\operatorname{div}\left[\left(\nu_0+\nu_1|\mathbf{D}|^{q-2}\right)\mathbf{D}\right]+\alpha|\mathbf{u}|^{\sigma-2}\mathbf{u}=\mathbf{f}-\nabla p \tag{7}$$

supplemented by the initial condition

$$\mathbf{u}=\mathbf{u}_0 \quad \text{when} \quad t=t_0 \tag{8}$$

and by the adherence boundary condition

$$\mathbf{u}=\mathbf{0} \quad \text{on} \quad \Gamma_T\,. \tag{9}$$

In (7), we have set $p=p/\varrho$, and $\nu_0=\mu_0/\varrho$ and $\nu_1=\mu_1/\varrho$ are non-negative parameters related to the kinematics viscosity, $\alpha=\alpha/\varrho$ is a non-negative constant and, for the time being, σ is a constant such that $\sigma\geq 1$. The term $|\mathbf{u}|^{\sigma-2}\mathbf{u}$ is understood as an absorption and, as we shall see, it behaves like a sink inside the flow domain. Its motivation is purely mathematical and goes back to the works of Benilan, Brezis and Crandall, Díaz and Herrero, and Bernis (see Antontsev et al. [5] and Díaz [11]) Of particular importance to this work is the Dirichlet problem

$$-\mathrm{div}\,\left(|\nabla u|^{q-2}\nabla u\right)+|u|^{\sigma-2}u\ = f \text{ in } \Omega\subset\mathbb{R}^N\,,\quad q\geq 1,\ \sigma>1\,,\qquad u\ = h \text{ on } \partial\Omega \tag{10}$$

presented in Díaz [11] as modeling a stationary non-Newtonian fluid. When (10) is linear, i.e. with $p=\sigma=2$, the solution u of (10) corresponding to data, say $f\geq 0$ and $h\geq 0$, is such that $u>0$ in Ω. When (10) is nonlinear, entirely different behavior may appear. Roughly speaking, the effective power of the diffusion term div $\left(|\nabla u|^{p-2}\nabla u\right)$ and of the absorption term $|u|^{\sigma-2}u$ vary with p and σ, generating new phenomena. If $\sigma\geq p$, Ω is an unbounded open domain and f and h have compact support, then the support of the solution contains the whole domain Ω and if $\sigma<p$ the solution u has compact support and so $u=0$ in an unbounded region of Ω. With this motivation, the purpose of this work is to study the asymptotic behavior of the weak solutions to the MEP problem (6), (7), (8), and (9). Specifically we want to know if these solutions extinct in a finite time and if so, what is the relation between the parameter q which characterizes the flow and the absorption constants α and σ. The problem of the solutions vanishing in some space region is much more difficult and we address the reader to Antontsev et al. [3, 4], where 2D stationary Navier-Stokes problems were studied. It should be remarked that these issues have been studied by many authors, either in time or in space. There exists an extensive literature on decay rates for the solutions of the Navier-Stokes problem (see Oliveira [10] and the references cited therein). For the non-Newtonian setting, the literature is scarce, although many techniques of the Navier-Stokes model can be used. In Bae [6] it was proved that the L^2 norm of weak solutions to the homogeneous problem (6), (7), (8), and (9) with $\alpha=0$, decreases with rate $t^{-1/(q-2)}$ as t tends to infinity for the dilatant case ($q>2$) and vanishes in a finite time for the pseudoplastic case ($1<q<2$). The same problem was solved by Guo and Zhu [12] and by Ňečasová and Penel [17], but only for the dilatant case ($q>2$). As regards to the non-homogeneous problem (6), (7), (8), and (9), with $\alpha=0$, and to the best of our knowledge, there is no references where such kind of decays are studied.

3 Notation and Auxiliary Results

The notation used throughout this paper is largely standard in Mathematical Fluid Mechanics – see, e.g., Lions [15]. We distinguish vectors from scalars by using boldface letters. For functions and function spaces we will use this distinction as well. The symbol C will denote a generic constant – generally a positive one, whose value will not be specified; it can change from one inequality to another by subscripting different numbers and it can be related to an important result by subscripting initial letters of that result. The dependence of C on other constants or parameters will always be clear from the exposition. In this article, the notation Ω stands always for a domain, i.e., a connected open subset of $\mathbb{R}^N$, whose compact boundary is denoted by $\partial\Omega$.

Let $1 \leq p \leq \infty$ and $\Omega \subset \mathbb{R}^N$ be a domain. We shall use the classical Lebesgue spaces $\mathrm{L}^p(\Omega)$, whose norm is denoted by $\|\cdot\|_{\mathrm{L}^p(\Omega)}$. $\mathrm{W}^{1,p}(\Omega)$ denotes the Sobolev space of all functions $u \in \mathrm{L}^p(\Omega)$ such that the weak derivatives $\mathrm{D}u$ exist, in the generalized sense, and are in $\mathrm{L}^p(\Omega)$. Given $T > 0$ and a Banach space X, $\mathrm{L}^p(0,T;X)$ is the Bochner space used in evolutive problems. The corresponding spaces of vector-valued functions are denoted by boldface letters. All these spaces are Banach spaces and the Hilbert framework corresponds to $p = 2$. In the last case, we use the abbreviation $\mathrm{W}^{1,2} = \mathrm{H}^1$.

To prove the main results of this paper, it will be of the utmost importance some Sobolev type inequalities established in lemmas below.

Lemma 1 (Korn) *Assume $1 < p < \infty$ and let Ω be a domain of $\mathbb{R}^N$, $N \geq 2$, with a locally compact boundary $\partial\Omega$. Then for any $\mathbf{u} \in \mathbf{W}_0^{1,p}(\Omega)$,*

$$C_K \|\nabla \mathbf{u}\|_{\mathbf{L}^p(\Omega)} \leq \|\mathbf{D}(\mathbf{u})\|_{\mathbf{L}^p(\Omega)}\,, \qquad C_K = C(p,\Omega). \tag{11}$$

This is the so-called second Korn's inequality and it extends to suitable unbounded domains (see e.g. Ladyzhenskaya et al. [14]).

Lemma 2 (Interpolation Embedding) *Let Ω be a domain of $\mathbb{R}^N$, $N \geq 1$, with a locally compact boundary $\partial\Omega$. Assume that $u \in \mathrm{W}_0^{1,p}(\Omega)$. Then, for every fixed number $r \geq 1$ there exists a constant C_{GN} depending only on N, p, r such that*

$$\|u\|_{\mathrm{L}^q(\Omega)} \leq C_{GN} \|\nabla u\|^{\theta}_{\mathrm{L}^p(\Omega)} \|u\|^{1-\theta}_{\mathrm{L}^r(\Omega)}, \tag{12}$$

where p, $q \geq 1$, are linked by $\theta = \left(\frac{1}{r} - \frac{1}{q}\right)\left(\frac{1}{N} - \frac{1}{p} + \frac{1}{r}\right)^{-1}$, and their admissible range is:

(1) If $N = 1$, $q \in [r,\infty]$, $\theta \in \left[0, \frac{p}{p+r(p-1)}\right]$, $C_{GN} = [1+(p-1)/pr]^{\theta}$;
(2) If $p < N$, $q \in \left[\frac{Np}{N-p}, r\right]$ if $r \geq \frac{Np}{N-p}$ and $q \in \left[r, \frac{Np}{N-p}\right]$ if $r \leq \frac{Np}{N-p}$, $\theta \in [0,1]$ and $C_{GN} = [(N-1)p/(N-p)]^{\theta}$;
(3) If $p \geq N > 1$, $q \in [r,\infty)$, $\theta \in \left[0, \frac{Np}{Np+r(p-N)}\right)$ and $C_{GN} = \max\{q(N-1)/N, 1+(p-1)pr\}^{\theta}$.

The interpolation inequality (12) is known in the literature as Gagliardo-Nirenberg inequality. This result is valid whether the domain Ω is bounded or not and notice the constant C_{GN} does not depend on Ω (see e.g. Ladyzhenskaya et al. [14]). Notice also that in the particular case of $\theta = 1$, (12) reduces to the well-known Sobolev's inequality and, in this case, the constant will be denoted by C_S.

4 Weak Formulation

The mathematical analysis of incompressible fluid problems is commonly done in the context of divergence free function spaces. Working in this context, we introduce the following function spaces:

$$\mathcal{V} := \{\mathbf{v} \in \mathbf{C}_0^\infty(\Omega) : \operatorname{div} \mathbf{v} = 0\} ;$$
$$\mathbf{H} := \text{closure of } \mathcal{V} \text{ in } \mathbf{L}^2(\Omega) ;$$
$$\mathbf{V}_q := \text{closure of } \mathcal{V} \text{ in } \mathbf{W}^{1,q}(\Omega) .$$

It is worth to recall that $\mathbf{H}$ is endowed with the $\mathbf{L}^2(\Omega)$ inner product and norm, and $\mathbf{V}_q$ is a Banach space whose norm is inherited from the Sobolev space $\mathbf{W}^{1,q}(\Omega)$. For a bounded domain Ω, $\mathbf{V}_2 \subset \mathbf{V}_q$ if $q < 2$ and $\mathbf{V}_q \subset \mathbf{V}_2$ if $q > 2$. Below we define the notion of weak solutions we shall work with.

Definition 1 Let Ω be a bounded domain in $\mathbf{R}^N$, $N \geq 2$, with a Lipschitz boundary $\partial\Omega$, and let $q\,,\ \sigma > 1$. A vector field $\mathbf{u}$ is a weak solution to the MEP problem (6), (7), (8), and (9), if:

1. $\mathbf{u} \in \mathrm{L}^2(0, T; \mathbf{V}) \cap \mathrm{L}^q(0, T; \mathbf{V}_q) \cap \mathrm{L}^\sigma(Q_T) \cap \mathrm{L}^\infty(0, T; \mathbf{H})$;
2. The following identity

$$-\int_{Q_T} \mathbf{u} \cdot \varphi_t \, d\mathbf{z} - \int_{Q_T} \mathbf{u} \otimes \mathbf{u} : \nabla\varphi \, d\mathbf{z} + \int_{Q_T} \left(\mu_0 + \mu_1 |\mathbf{D}(\mathbf{u}|^{q-2}\right) \mathbf{D}(\mathbf{u}) : \nabla\varphi \, d\,\mathbf{z}$$
$$+ \alpha \int_{Q_T} |\mathbf{u}|^{\sigma-2}\mathbf{u} \cdot \varphi \, d\,\mathbf{z} = \int_{Q_T} \mathbf{f} \cdot \varphi \, d\,\mathbf{x} + \int_{\Omega} \mathbf{u}_0 \cdot \varphi(0) \, d\mathbf{x}$$

holds for all $\varphi \in \mathbf{C}^\infty(Q_T)$ with $\operatorname{div}\varphi = 0$ and $\operatorname{supp}\varphi \subset\subset \Omega \times [0, T)$, and where $\mathbf{z} = (\mathbf{x}, t)$.

To the best of our knowledge, the MEP problem (6), (7), (8), and (9) is new and there are no references to it in the literature. On the other hand, for the problem (6), (7), (8), and (9) with $\alpha = 0$ there are some important works. The first results on existence and uniqueness of weak solutions were achieved by Ladyzhenskaya [13] for $N = 2$ and $N = 3$. Lions [15] has extended her results to a general dimension $N \geq 2$. Combining monotone operator theory and compactness arguments, he has proved the existence of weak solutions for $q > (3N + 2)/(N + 2)$ and their uniqueness for $q \geq (N + 2)/2$. For the success of those proofs, it was of the utmost importance the embedding

$$\mathrm{L}^q(0, T; \mathbf{V}_q) \cap \mathrm{L}^\infty(0, T; \mathbf{H}) \hookrightarrow \mathrm{L}^{q\frac{N+2}{N}}(Q_T)$$

to prove that $\mathbf{u} \otimes \mathbf{u} : \mathbf{D}(\varphi) \in \mathrm{L}^1(Q_T)$ for all $\mathbf{u}$, $\varphi \in \mathrm{L}^q(0, T; \mathbf{V}_q) \cap \mathrm{L}^\infty(0, T; \mathbf{H})$ (see Lions [15]). For $2 \leq q \leq 11/5$ and $N = 3$, the existence of weak solutions has been proved by Málek et al. [16] under the restrictive assumption that $\partial\Omega \in \mathrm{C}^3$.

Moreover, they have proved a uniqueness result for any $q > 20/9$. Without any restriction on Ω, Wolf [19] has proved the existence of weak solutions in the space $\mathrm{L}^q(0,T;\mathbf{V}_q)\cap \mathrm{C}_w(0,T;\mathbf{H})$ for $q > 2(N+1)/(N+2)$. For the existence results of Málek et al. [16] and Wolf [19], were very important the q-coercivity condition

$$\mathbf{F}:\mathbf{D} \geq C|\mathbf{D}|^q\,, \quad C = constant > 0 \tag{13}$$

and the q-growth condition

$$|\mathbf{F}| \leq C\,(1+|\mathbf{D}|)^{q-1}\,, \quad C = constant > 0\,.$$

Although the results of Wolf [19] extend to some values $q < 2$, so far it is an open problem to prove the existence of weak solutions for all $q > 1$. The main obstacle is the fact that one is unable to construct the pressure as a measurable function in $(\mathbf{x},t) \in Q_T$, but only as a distribution with regard to $t \in (0,T)$. On the contrary, for the space periodic problem, the full existence result is proved for any $q > 1$ (see Bae and Choe [7]).

Theorem 1 *Assume that $q > 2N/(N+2)$, $\sigma > 1$ and $\mathbf{u}_0 \in \mathbf{H}$. Then, there exists, at least, a weak solution to the MEP problem (6), (7), (8), and (9) in the sense of Definition 1.*

The proof can be adapted from Wolf [19] by using the arguments of Bernis [9] to deal with the absorption term if $\sigma > 2$. For $1 < \sigma \leq 2$, we use the Sobolev embedding $\mathbf{H}^1(\Omega) \hookrightarrow \mathbf{L}^{\sigma}(\Omega)$ valid for $1 \leq \sigma \leq 2N/(N-2)$ if $N \geq 3$ and for any $\sigma \geq 1$ if $N = 2$. In this case and in order to prove the convergence of the approximate solutions, it is also important the inequality (14), established in the Lemma below, to deal with the absorption term, where we have to take $p = \sigma$ and $\delta = 2 - \sigma$, which in turn implies $\sigma \leq 2$.

Lemma 3 *For all $p \in (1,\infty)$ and $\delta \geq 0$, there exist constants C_1 and C_2, depending on p and N, such that for all $\boldsymbol{\xi},\ \boldsymbol{\eta} \in \mathbb{R}^N$, $N \geq 1$,*

$$\left||\xi|^{p-2}\xi - |\eta|^{p-2}\eta\right| \leq C_1|\xi-\eta|^{1-\delta}\,(|\xi|+|\eta|)^{p-2+\delta} \tag{14}$$

and

$$\left(|\xi|^{p-2}\xi - |\eta|^{p-2}\eta\right)\cdot(\xi-\eta) \geq C_2|\xi-\eta|^{2+\delta}\,(|\xi|+|\eta|)^{p-2-\delta} \tag{15}$$

Proof See Barret and Liu [8]. □

Below we present a result about uniqueness which, for $N = 3$, can be improved by using the results of the same kind of Málek et al. [16].

Theorem 2 *Assume that $q > 2N/(N+2)$, $\sigma > 1$, $\mathbf{f} \in \mathrm{L}^{q'}(Q_T)$ and $\mathbf{u}_0 \in \mathbf{H}$. Then the weak solution of the MEP problem (6), (7), (8), and (9) is unique.*

For $q \geq (N+2)/2$, the uniqueness result can be derived from Lions [15]. Here, the problem lies in proving that the difference of absorptions from two weak solutions is non-negative. But this follows directly from (15) by taking $p = \sigma$ and $\delta = 0$.

Shortly, existence and uniqueness of weak solutions to the MEP problem (6), (7), (8), and (9) hold for any $\sigma > 1$ as far as the same results hold for the problem (6), (7), (8), and (9) with $\alpha = 0$. If one can improve these results for any $q > 1$, then the same results for the MEP problem (6), (7), (8), and (9) can be obtained.

5 Extinction in Time

In this section, we are interested in weak solutions for the MEP problem (6), (7), (8), and (9) such that

$$E(t) + \int_\Omega \left(|\nabla \mathbf{u}(t)|^2 + |\nabla \mathbf{u}(t)|^q\right) d\mathbf{x} < \infty, \quad E(t) := \frac{1}{2}\int_\Omega |\mathbf{u}(t)|^2 \, d\mathbf{x}. \tag{16}$$

We denote by $E(t)$ the energy associated with the MEP problem (6), (7), (8), and (9), which in Fluid Mechanics is usually denoted as the kinetic energy.

Theorem 3 *Assume that* $1 < \sigma < 2$, $\mathbf{u}_0 \in \mathbf{H}$ *and let* $\mathbf{u}$ *be a weak solution to the MEP problem (6), (7), (8), and (9) in the sense of Definition 1.*

1. If $\mathbf{f} = \mathbf{0}$ a.e. in Q_T, then there exists $t^* > 0$ such that $\mathbf{u}(\mathbf{x}, t) = \mathbf{0}$ a.e. in Ω and for almost all $t \geq t^*$.
2. Let $\mathbf{f} \neq \mathbf{0}$ and assume that there exist positive constants ε and θ and that there exists a positive time $t_\mathbf{f}$ such that, for almost all $t \in [0, T]$,

$$\|\mathbf{f}(t)\|_{\mathbf{L}^{q'}(\Omega)} \leq \varepsilon \left(1 - \frac{t}{t_\mathbf{f}}\right)_+^\theta \quad \text{if} \quad \frac{Nq}{N-q} \leq q < 2\,, \quad (\theta \textit{ is given by (30)})\,, \tag{17}$$

or

$$\|\mathbf{f}(t)\|_{\mathbf{L}^{q'}(\Omega)} \leq \varepsilon \left(1 - \frac{t}{t_\mathbf{f}}\right)_+^\theta \quad \text{if} \quad q > 2\,, \quad (\theta \textit{ is given by (38)})\,. \tag{18}$$

Then there exists a constant $\varepsilon_0 > 0$ (defined by *(30)* for *(17)* and by *(39)* for *(18))* such that $\mathbf{u} = 0$ a.e. in Ω and for almost all $t \geq t_\mathbf{f}$ provided $0 < \varepsilon \leq \varepsilon_0$.

Notice that, although the property is the same, the constants ε, θ, $t_\mathbf{f}$ and ε_0 can be distinct in the different cases (17) and (18). The notation u_+ means the positive part of u, *i.e.* $u = \max(u, 0)$.

Proof We formally multiply (7) by $\mathbf{u}$, a weak solution to the MEP problem (6), (7), (8), and (9), integrate over Ω and use (6), (9) and the symmetry of $\mathbf{D}$. Then we use Korn's inequality (11) to obtain the following energy relation

$$\frac{d}{dt}E(t) + \int_\Omega \left(C_0|\nabla \mathbf{u}(t)|^2 + C_1|\nabla \mathbf{u}(t)|^q + \alpha|\mathbf{u}(t)|^\sigma\right) d\mathbf{x} \\ \leq \int_\Omega \mathbf{u}(t)\cdot\mathbf{f}(t)\,d\mathbf{x} \quad \text{for a.a. } t \in [0,T]\,, \tag{19}$$

where $C_0 = C_K^2\nu_0$ and $C_1 = C_K^q\nu_1$, being C_K the Korn's inequality constant. Applying successively Schwarz's, Young's and Sobolev's (12) inequalities, the latter with $p = q$, we obtain

$$\left|\int_\Omega \mathbf{u}(t)\cdot\mathbf{f}(t)\,d\mathbf{x}\right| \leq \varepsilon C_S^q\|\nabla\mathbf{u}(t)\|^q_{\mathbf{L}^q(\Omega)} + C(\varepsilon)\|\mathbf{f}(t)\|^{q'}_{\mathbf{L}^{q'}(\Omega)} \text{ for a.a. } t \in [0,T]\,, \tag{20}$$

where C_S is the Sobolev inequality constant. Choosing $\varepsilon : 0 < \varepsilon < C_1/C_S^q$, we obtain from (19) and (20)

$$\frac{d}{dt}E(t) + \left(\int_\Omega \left(C_0|\nabla \mathbf{u}(t)|^2 + C_2|\nabla \mathbf{u}(t)|^q + \alpha|\mathbf{u}(t)|^\sigma\right) d\mathbf{x}\right) \\ \leq C_3\int_\Omega |\mathbf{f}(t)|^{q'}\,d\mathbf{x} \quad \text{for a.a. } t \in [0,T]\,, \tag{21}$$

where $C_2 = C_1 - \varepsilon C_S^q$ and $C_3 = C(\varepsilon)$. To be precise, (21) is first established for the approximations of the weak solutions to the MEP problem (6), (7), (8), and (9) and then is shown to be true for the limit function.

Case $2N/(N+2) \leq q < 2$. Using a vector version of Sobolev's inequality (12), we obtain

$$E(t) \leq C_4\left(\int_\Omega |\nabla\mathbf{u}(t)|^q\,d\mathbf{x}\right)^{\frac{2}{q}} \quad \text{for a.a. } t \in [0,T]\,, \quad q \geq \frac{2N}{N+2}\,, \tag{22}$$

where $C_4 = C_S^2/2$. Taking into account that C_0 and α are non-negative constants, we obtain from (19) and (22) that

$$\frac{d}{dt}E(t) + C_5E(t)^{\frac{q}{2}} \leq C_3\int_\Omega |\mathbf{f}(t)|^{q'}d\mathbf{x} \quad \text{for a.a. } t \in [0,T]\,, \tag{23}$$

where $C_5 = C_2C_4^{-q/2}$. If $\mathbf{f} = \mathbf{0}$, then we obtain the following homogeneous ordinary differential inequality for the energy function $E(t)$

$$\frac{d}{dt}E(t) + C_5E(t)^{\frac{q}{2}} \leq 0 \quad \text{for a.a. } t \in [0,T]. \tag{24}$$

Knowing that $2N/(N+2) \leq q < 2$, an explicit integration of (24) between $t = 0$ and t leads us to

$$E(t) \leq \left(E(0)^{\frac{2-q}{2}} - \frac{2-q}{2} C_3 t \right)^{\frac{2}{2-q}} \quad \text{for a.a. } t \in [0, T]. \tag{25}$$

The right-hand side of (25) vanishes for $t \geq t^* := 2E(0)^{(2-q)/2}/[C_5(2-q)]$ and the first assertion is then proved.

If **f** satisfies to (17), then from (23), we obtain the following non-homogeneous ordinary differential inequality

$$\frac{d}{d\,t} E(t) + C_5 E(t)^{\frac{q}{2}} \leq C_3 \varepsilon^{q'} \left(1 - \frac{t}{t_{\mathbf{f}}} \right)_+^{q'\theta} . \tag{26}$$

To analyze (26), we need the following result.

Lemma 4 *Let* $\delta > 0$ *such that* $\left(t_f - \delta, t_f + \delta\right) \subset [0, T]$ *and assume* $E \in \mathrm{W}^{1,1}\left(t_f - \delta,\ t_f + \delta\right)$ *satisfies the differential inequality*

$$\frac{d}{dt} E(t) + \varphi(E(t)) \leq F\left(\left(1 - \frac{t}{t_f} \right)_+ \right) \quad \textit{a.e. in } \left(t_f - \delta, t_f + \delta\right), \tag{27}$$

where φ *is a continuous non-decreasing function such that*

$$\varphi(0) = 0 \quad \textit{and} \quad \int_{0^+} \frac{ds}{\varphi(s)} < \infty , \tag{28}$$

and the function F *satisfies, for some* $\overline{k} \in (0, 1)$*, to*

$$F(s) \leq (1 - \overline{k}) \varphi(\eta_{\overline{k}}(s)) \quad \textit{in } (0, t_{\mathbf{f}}) , \tag{29}$$

where

$$\eta_k(s) = \theta_k^{-1}(s) \quad \textit{and} \quad \theta_k(s) = \int_0^s \frac{d\tau}{k\varphi(\tau)} .$$

Then $E(t) = 0$ *for all* $t \geq t_{\mathbf{f}}$.

Proof See Antontsev et al. [5]. □

In order to read (26) in the form (27), we define

$$\varphi(s) := C_5 s^{\frac{q}{2}} \quad \text{and} \quad F(s) := C_3 \varepsilon^{q'} s^{\theta q'} .$$

Then clearly (28) is satisfied and we have

$$\theta_k(s) = \frac{2}{kC_5(2-q)} s^{\frac{2-q}{2}} \quad \text{and} \quad \eta_k(s) = \left(\frac{kC_5(2-q)}{2} s \right)^{\frac{2}{2-q}} .$$

Moreover, (29) is satisfied if

$$\theta := \frac{q-1}{2-q} \quad \text{and} \quad \varepsilon \leq \varepsilon_0 := \frac{(1-k)C_5}{C_3}\left(\frac{kC_5(2-q)}{2}\right)^{\frac{q}{2-q}} \tag{30}$$

for a certain $k \in (0, 1)$, e.g. $k = q/2$. Then Lemma 4 proves the second assertion. *Case* $q \geq 2$. Using a vector version of the interpolation embedding inequality (12) with $q = 2$, $p = q$ and $r = \sigma$, and the algebraic inequality $A^{\alpha}B^{\beta} \leq (A+B)^{\alpha+\beta}$ valid for every $\alpha, \beta \in \mathbb{R}$ and every $A, B \geq 0$, we obtain

$$E(t) \leq C_6\left(\int_{\Omega}\left(|\nabla \mathbf{u}(t)|^q + |\mathbf{u}(t)|^{\sigma}\right) d\mathbf{x}\right)^{\mu} \quad \text{for a.a. } t \in [0, T], \tag{31}$$

where $C_6 = C_{GN}^2/2$, being C_{GN} the interpolation embedding inequality constant, and

$$\mu := 1 + \frac{q(2-\sigma)}{q(N+\sigma) - N\sigma}. \tag{32}$$

The analysis of (32) shows us that

$$q \geq 2 \quad \Rightarrow \quad \mu > 1 \text{ iff } \sigma < 2. \tag{33}$$

Taking into account that C_0 is a non-negative constant, we obtain from (21) and (31),

$$\frac{d}{dt}E(t) + C_7 E(t)^{\frac{1}{\mu}} \leq C_3 \int_{\Omega} |\mathbf{f}(t)|^{q'}\, d\mathbf{x} \quad \text{for a.a. } t \in [0, T], \tag{34}$$

where $C_7 = \min(C_2, \alpha)C_6^{-1/\mu}$ and C_3 is given in (21). If $\mathbf{f} = 0$, then (34) leads us to the homogeneous ordinary differential inequality

$$\frac{d}{dt}E(t) + C_7 E(t)^{1/\mu} \leq 0. \tag{35}$$

An explicit integration of (35) between $t = 0$ and t, where we use (32) and (33), leads us to

$$E(t) \leq \left(E(0)^{\frac{\mu-1}{\mu}} - \frac{C_7(\mu-1)}{\mu}t\right)^{\frac{\mu}{\mu-1}} \tag{36}$$

and $E(t)$ vanishes for $t \geq t^* := \mu E(0)^{\frac{\mu-1}{\mu}}/[C_7(\mu-1)]$. This proves the first assertion.

Assume now that (18) is satisfied. Then, using (18) and (34), we obtain the following non-homogeneous ordinary differential inequality

$$\frac{d}{dt}E(t) + C_7 E(t)^{1/\mu} \leq C_3 \varepsilon^{q'} \left(1 - \frac{t}{t_{\mathbf{f}}}\right)_+^{\theta} \qquad \text{for a.a. } t \in [0, T], \tag{37}$$

where C_7 is given in (34) and C_3 in (21). In order to use Lemma 4, let

$$\varphi(s) = C_7 s^{\frac{1}{\mu}} \quad \text{and} \quad F(s) = C_3 \varepsilon^{q'} s^{\frac{1}{\mu-1}} .$$

Then clearly (28) is satisfied,

$$\theta_k(s) = \frac{\mu}{C_7 k(\mu - 1)} s^{\frac{\mu-1}{\mu}} , \qquad \eta_k(s) = \left(\frac{C_7 k(\mu - 1)}{\mu} s\right)^{\frac{\mu}{\mu-1}}$$

and (29) holds provided

$$\theta := \frac{q-1}{q(\mu - 1)} , \qquad (32) \quad \Rightarrow \quad \theta = \frac{(q-1)[q(N+\sigma) - N\sigma]}{q^2(2-\sigma)} \tag{38}$$

and

$$\varepsilon \leq \varepsilon_0 := \left\{ \frac{C_7(1-k)}{C_3} \left[\frac{k(\mu - 1)}{\mu}\right]^{\frac{1}{\mu-1}} \right\}^{\frac{q-1}{q}} , \tag{39}$$

the latter for some $k \in (0, 1)$, e.g. $k = \mu/2$. Second assertion is thus proved and this concludes the proof. □

Remark 1 Theorem 3 still holds for unbounded domains Ω as far as the used Sobolev type inequalities hold.

Remark 2 We could also have considered non-homogeneous boundary conditions, say $\mathbf{u}_*$, on Γ_T. But then, in order to carry out the results of Theorem 3, we would have to assume the existence of a time $t_* > 0$ such that $\mathbf{u}_* = \mathbf{0}$ for all $t \geq t_*$ and $E(t_*) < \infty$. In the above proof we only would have to replace the time $t = 0$ by $t = t_*$.

Remark 3 For the 2D stationary version of the MEP problem (6), (7), (8), and (9), we are able to prove that its weak solutions have compact support in Ω. This is obtained by using the arguments of Antontsev et al. [3, 4] and reducing the original problem to a fourth-order non-linear one for the stream function, where the pressure term does not appear anymore.

6 Discussion and Extensions

In the previous section, we have shown the weak solutions to the MEP problem (6), (7), (8), and (9) extinct in a finite time whether $2N/(N+2) \leq q < 2$ or $q \geq 2$. In both cases the diffusion term $|\nabla \mathbf{u}|^2$ does not play any role in the obtained results. Therefore, we may simplify the exposition by saying, at the beginning, that the extra stress tensor should satisfy to the q-coercivity condition (13), instead of (2). This is certainly the case if $\mathbf{F}$ is given by (2). In such situation, the energy relation (19) would come in the form

$$\frac{d}{dt}E(t) + \int_\Omega \left(C_1|\nabla \mathbf{u}(t)|^q + \alpha|\mathbf{u}(t)|^\sigma\right) d\mathbf{x} \leq \int_\Omega \mathbf{u}(t)\cdot\mathbf{f}(t)\,d\mathbf{x} \quad \text{for a.a. } t \in [0,T]\,,$$

where now $C_1 = C_K^q C$, being C the constant resulting from (13). The analysis of the case when $2N/(N+2) \leq q < 2$ takes only into account the q-diffusion term $|\nabla \mathbf{u}|^q$. Not only the diffusion term, but also the absorption term $|\mathbf{u}|^\sigma$ is neglected. Therefore, in this case, the extinction in a finite time property holds for all fluid problems governed by the Eqs. (3), (4), and (5), with $2N/(N+2) \leq q < 2$, supplemented with the initial-boundary conditions (8) and (9). Moreover, once the diffusion term $|\nabla \mathbf{u}|^2$ is useless for the obtained properties, we may also consider the q-coercivity condition (13), instead of (2), and the energy relation (19) would come in the form

$$\frac{d}{dt}E(t) + C_1\int_\Omega |\nabla \mathbf{u}(t)|^q\, d\mathbf{x} \leq \int_\Omega \mathbf{u}(t)\cdot\mathbf{f}(t)\,d\mathbf{x} \quad \text{for a.a. } t \in [0,T]\,.$$

We thus can say that for a pseudoplastic fluid the structure of the stress tensor is able to stop the flow in a finite time. For $q \geq 2$, the analysis of the previous case is no longer valid, because in (23) we have now $q/2 \geq 1$. If $\mathbf{f} = 0$, then (24) comes with $q/2 \geq 1$. An explicit integration of (24) between $t = 0$ and t leads us to

$$E(t) \leq \left(C_3\frac{q-2}{2}t + E(0)^{-(q-2)/2}\right)^{-2/(q-2)} \qquad \text{for a.a. } t \in [0,T]\,, \quad q > 2\,.$$

If $q = 2$, then (24) is linear and the same integration procedure leads us to

$$E(t) \leq E(0)e^{-C_3 t} \quad \text{for a.a. } t \in [0,T].$$

Then $E(t)$ decays to zero at the rate $t^{-2/(q-2)}$ if $q > 2$ and with an exponential decay if $q = 2$. This means that dilatant fluid flows tend to extinct with the fractional time rate $t^{-2/(q-2)}$ and Newtonian fluid flows with the exponential time rate e^{-t}. If, $\mathbf{f} \neq 0$, we obtain analogous results as for $\mathbf{f} = 0$ (see Bae [6], Guo and Zhu [12] and Nečasová and Penel [17]). As a consequence, for $q \geq 2$, if we want to obtain an analogous property as for the case $2N/(N+2) \leq q < 2$, we need to modify the momentum equation (5) by introducing there the absorption term $|\mathbf{u}|^{\sigma-2}\mathbf{u}$. As we have seen, in this case, the results are valid under the assumption that $\sigma < 2$ (see (32) and (33)). On the other hand for the well-posedness of the MEP problem (6), (7), (8), and (9), one needs to assume that $\sigma > 1$. In the limit case of $\sigma = 1$, the extinction in a finite time property remains valid, because it is still true that $\mu > 1$

(see (32) and (33)). If $\sigma = 2$, then the obtained ordinary differential inequalities become linear and using this framework we can only obtain an exponential decay.

These properties extend for the MEP problem (6), (7), and (8) supplemented with the following slip boundary conditions:

$$\mathbf{u} \cdot \mathbf{n} = 0 \quad \text{and} \quad \mathbf{u} \cdot \tau = \beta^{-1} \mathbf{t} \cdot \tau \quad \text{on} \quad \Gamma_T \,;$$

where $\mathbf{n}$ and τ denote, respectively, unit normal and tangential vectors to the boundary $\partial\Omega$, $\mathbf{t} = \mathbf{n} \cdot \mathbf{T}$ is the stress vector and β is a coefficient with no defined sign. In this case, the energy relation (19) comes in the form

$$\frac{d}{dt} E(t) + \int_\Omega \left(C_0 |\nabla\, \mathbf{u}(t)|^2 + C_1 |\nabla\, \mathbf{u}(t)|^q + \alpha |\mathbf{u}(t)|^\sigma \right) d\mathbf{x} \leq \\ \int_\Omega \mathbf{u}(t) \cdot \mathbf{f}(t)\, d\mathbf{x} + \beta \int_{\partial\Omega} |\mathbf{u}(t)|^2\, d\mathbf{x} \quad \text{for a.a. } t \in [0, T]\,.$$

The last term on the right-hand side is estimated by using an interpolation trace inequality (see Antontsev and Oliveira [2] and Ladyzhenskaya et al. [14]). Proceeding in an analogous way, we can prove that, regardless the sign of β, the weak solutions to this problem extinct in a finite time if $q < 2$ or if $1 < \sigma < 2$.

We can also consider the MEP problem (6), (7), (8), and (9) with an anisotropic absorption, i.e. if we replace the modified momentum equation (7) by the following one

$$\frac{\partial\, \mathbf{u}}{\partial\, t} + (\mathbf{u} \cdot \nabla)\mathbf{u} - \operatorname{div} \left[\left(\nu_0 + \nu_1 |\mathbf{D}|^{q-2} \right) \mathbf{D} \right] + \\ \left(\alpha_1 |u_1|^{\sigma_1 - 2} u_1, \ldots, \alpha_N |u_N|^{\sigma_N - 2} u_N \right) = \mathbf{f} - \nabla p\,,$$

where $\alpha_1, ..., \alpha_N$ are non-negative constants. For the weak solutions to this problem, we are able to obtain the same properties if, at most, $\alpha_i = 0$ for only one i and if the domain Ω is convex in that direction x_i, where $i \in \{1, \ldots, N\}$. If that direction is $i = N$, then the energy relation (19) comes in the form

$$\frac{d}{dt} E(t) + \int_\Omega \left(C_0 |\nabla\, \mathbf{u}(t)|^2 + C_1 |\nabla\, \mathbf{u}(t)|^q + \sum_{i=1}^{N-1} \alpha_i |u_i(t)|^{\sigma_i} \right) d\mathbf{x} \leq \\ \int_\Omega \mathbf{u}(t) \cdot \mathbf{f}(t)\, d\mathbf{x} \quad \text{for a.a. } t \in [0, T]\,.$$

We prove the extinction in a finite time property by using the same techniques of the previous section to estimate all the components u_i, with $i = 1, \ldots, N-1$, and the incompressibility condition (6) to estimate u_N (see Antontsev and Oliveira [1]).

The main results established in this paper can be generalized to non-homogeneous fluid flows. In this case, we only need to assume that the density function ϱ is bounded as follows

$$\frac{1}{C_\varrho} \leq \varrho\,,\ \varrho_0 \leq C_\varrho\,,$$

where C_ϱ is a positive constant and ϱ_0 is the initial density. The energy function is now defined by

$$E(t) := \frac{1}{2}\int_\Omega \varrho(t)|\mathbf{u}(t)|^2\,d\mathbf{x}$$

and the energy relation comes such as in (23) and in (34), with the constants appearing there depending also on C_ϱ. See Antontsev et al. [5] where this property was obtained for fluid problems with the extra stress tensor satisfying to the q-coercivity condition (13) with $1 < q < 2$, i.e. pseudoplastic fluids.

Acknowledgments This work was partially supported by the Portuguese research project POCI/MAT/61576/2004/FCT/MCES and by FEDER and FCT-Plurianual 2007.

References

1. S.N. Antontsev and H.B. de Oliveira, Finite time localized solutions of fluid problems with anisotropic dissipation. Internat. Ser. Numer. Math., Birkhäuser **154**, 23–32 (2007)
2. S.N. Antontsev and H.B. de Oliveira, Navier-Stokes equations with absorption under slip boundary conditions: existence, uniqueness and extinction in time. RIMS Kôkyûroku Bessatsu, **B1**, University of Kyoto, Kyoto 21–42 (2007)
3. S.N. Antontsev, J.I. Díaz and H.B. de Oliveira, Stopping a viscous fluid by a feedback dissipative field. I. The stationary Stokes problem. J. Math. Fluid Mech., **6**(4), 439-461 (2004)
4. S.N. Antontsev, J.I. Díaz and H.B. de Oliveira, Stopping a viscous fluid by a feedback dissipative field. II. The stationary Navier-Stokes problem. Atti Accad. Naz. Lincei Cl. Sci. Fis. Mat. Natur. Rend. Lincei (9) Mat. Appl. **15**(3-4), 257–270 (2004)
5. S.N. Antontsev, J.I. Díaz and S.I. Shmarev, Energy methods for free boundary problems. *Progr. Nonlinear Differential Equations Appl.*,Birkhäuser **48**, (2002)
6. H.-O. Bae, Existence, regularity, and decay rate of solutions of non-Newtonian flow. J. Math. Anal. Appl. **231**(2), 467–491 (1999)
7. H.-O. Bae and H.J. Choe, Existence of weak solutions to a class of non-Newtonian flows. Houston J. Math. **26**(2), 387–408 (2000)
8. J.W. Barret and W.B. Liu, Finite element approximation of the parabolic p-Laplacian. SIAM J. Numer. Anal. **31**(2), 413–428 (1994)
9. F. Bernis, Elliptic and parabolic semilinear problems without conditions at infinity. Arch. Rat. Mech. Anal. **106**(3), 217–241 (1989)
10. H.B. de Oliveira, The Navier-Stokes problem modified by an absorption term. To appear.
11. J.I. Díaz, *Nonlinear Partial Differential Equations and Free Boundaries: Elliptic Equations*. Research Notes in Mathematics, **106**, Pitman, London, 1985.
12. B. Guo and P. Zhu, Algebraic L^2 decay for the solution to a class system of non-Newtonian fluid in $\mathbb{R}^n$. J. Math. Phys. **41**(1), 349–356 (2000)
13. O.A. Ladyzhenskaya, New equations for the description of motion of viscous incompressible fluids and solvability in the large of boundary value problem for them. Proc. Steklov Inst. Math. **102**, 95–118 (1967)

14. O.A. Ladyzhenskaya, V.A. Solonnikov and N.N. Uraltseva. Linear and quasilinear equations of parabolic type. Translations of Mathematical Monographs **23**, American Mathematical Society, Providence R.I., (1967)
15. J.-L. Lions, *Quelques Méthodes de Résolution des Problèmes aux Limites Non Linéaires*. Dunod, Paris (1969)
16. J. Málek, J. Ňečas and M. Rȯžička, On weak solutions to a class of non-Newtonian incompressible fluids in bounded three-dimensional domains: the case $p \geq 2$. Adv. Diff. Eqns. **6**(3), 257–302 (2001)
17. Š. Nečasová, P. Penel, L^2 decay for weak solution to equations of non-Newtonian incompressible fluids in the whole space. Nonlin. Anal. **47**, 4181–4192 (2001)
18. W.R. Schowalter, *Mechanics of Non-Newtonian Fluids*. Pergamon, Oxford (1978)
19. J. Wolf, Existence of weak solutions to the equations of non-stationary motion of non-Newtonian fluids with shear rate dependent viscosity. J. Math. Fluid Mech. **9**(1), 104–138 (2007)

Adaptive FE Eigenvalue Computation with Applications to Hydrodynamic Stability

Rolf Rannacher

Abstract We present an adaptive finite element method for the solution of eigenvalue problems associated with the linearized stability analysis of non-linear operators in the context of hydrodynamic stability theory. The goal is to obtain a posteriori information about the location of critical eigenvalues, their possible degeneration and the corresponding pseudo-spectrum. The general framework is the Dual Weighted Residual (DWR) method for local mesh adaptation which is driven by residual- and sensitivity-based information. The basic idea is to embed the eigenvalue approximation into the general framework of Galerkin methods for nonlinear variational equations for which the DWR method is already well developed. The evaluation of these error representations results in a posteriori error bounds for approximate eigenvalues reflecting the errors by discretization of the eigenvalue problem as well as those by linearization about an only approximately known base solution. From these error estimates local error indicators are derived by which economical meshes can be constructed.

Keywords Navier-Stokes equations · Hydrodynamic stability · Linearized stability analysis · Perturbation analysis

1 Introduction

We consider the Galerkin finite element approximation of eigenvalue problems arising in the linearized stability theory of nonlinear variational equations particularly in hydrodynamic stability theory. Some parts of the underlying theory will be developed within a more abstract setting suggesting the application to other kinds of nonlinear problems. On a bounded domain $\Omega \subset \mathbb{R}^d$, $d = 2$ or $d = 3$, with boundary $\partial\Omega = \Gamma_{\text{rigid}} \cup \Gamma_{\text{in}} \cup \Gamma_{\text{out}}$, we consider the typical eigenvalue problem occurring in hydrodynamic stability theory:

R. Rannacher (✉)
Institute of Applied Mathematics, University of Heidelberg, D-69120 Heidelberg, Germany
e-mail: rannacher@iwr.uni-heidelberg.de

R. Rannacher, A. Sequeira (eds.), *Advances in Mathematical Fluid Mechanics*,
DOI 10.1007/978-3-642-04068-9_26,

$$
\begin{aligned}
&-\nu\Delta v+\hat{v}\cdot\nabla v+v\cdot\nabla\hat{v}+\nabla q=\lambda v,\quad \nabla\cdot v=0,\quad \text{in }\ \Omega,\\
&v|_{\Gamma_{\text{rigid}}}=0,\quad v|_{\Gamma_{\text{in}}}=0,\quad \nu\partial_n v-pn|_{\Gamma_{\text{out}}}=0.
\end{aligned}
\tag{1}
$$

Here, $\hat{u}:=\{\hat{v},\hat{p}\}$ is a stationary "base flow", i.e. a stationary solution of the corresponding Navier-Stokes equations

$$
\begin{aligned}
&-\nu\Delta v+v\cdot\nabla v+\nabla p=f,\quad \nabla\cdot v=0,\quad \text{in }\ \Omega,\\
&v|_{\Gamma_{\text{rigid}}}=0,\quad v|_{\Gamma_{\text{in}}}=v^{\text{in}},\quad \nu\partial_n v-pn|_{\Gamma_{\text{out}}}=P,
\end{aligned}
\tag{2}
$$

where v is the velocity vector field of the flow, p its hydrostatic pressure, ν the kinematic viscosity (density $\varrho\equiv 1$), P a prescribed mean pressure, and f a prescribed volume force. The goal is to investigate the stability of this base flow under small perturbations, which leads us to consider the eigenvalue problem (1). If an eigenvalue of (1) has $\operatorname{Re}\lambda<0$, the base flow is unstable, otherwise it is said to by "linearly stable". That means that the solution of the linearized nonstationary perturbation problem

$$
\partial_t w-\nu\Delta w+\hat{v}\cdot\nabla w+w\cdot\nabla\hat{v}+\nabla q=0,\quad \nabla\cdot w=0,\quad \text{in }\ \Omega,
\tag{3}
$$

corresponding to some initial perturbation $w_{|t=0}=w^0$ satisfies a bound of the form

$$
\sup_{t\geq 0}\|w(t)\|\leq c\|w^0\|,
\tag{4}
$$

for some constant $c\geq 1$, where $\|\cdot\|$ denotes the L^2-norm over Ω. However, *linear* stability does not guarantee full *nonlinear* stability due to effects caused by the "non-normality" of the operator governing problem (1), which may make the constant A large. This is related to the possible "deficiency" (discrepancy of geometric and algebraic multiplicity) or a large "pseudo-spectrum" (range of large resolvent norm) of the critical eigenvalue.

The finite element discretization of the stability eigenvalue problem is based on its variational formulation. It uses finite element spaces V_h consisting of piecewise polynomial functions on certain decompositions $\mathbb{T}_h$ of the domain $\bar{\Omega}$ into cells $T\in\mathbb{T}_h$ of width $h_T:=\operatorname{diam}(T)$. Our primal goal is to derive an *a posteriori* estimate for the eigenvalue error $\lambda-\lambda_h$ in terms of the "cell residuals" of the computed approximations $\hat{v}_h$, $\{v_h,\lambda_h\}$, and a practical criterion for the degeneracy of λ. In Heuveline & Rannacher [10] nonsymmetric eigenvalue problems of the kind (1) have been treated by employing duality techniques from optimal control theory. In this approach one simultaneously considers the approximation of the "primal" eigenvalue problem $\mathcal{A}u=\lambda u$ and its associated "dual" analogue $\mathcal{A}^*u^*=\lambda^*u^*$. The combined problem is embedded into the general optimal-control framework of Galerkin approximations of nonlinear variational equations developed in Becker and Rannacher [5, 4]. In this paper, we use this approach for the case of nonsymmetric stability eigenvalue problems with special emphasis on non-normality effects and coefficient perturbation. The result is an *a posteriori* error estimate of the form

$$|\lambda - \lambda_h| \approx \sum_{T \in \mathbb{T}_h} h_T^2 \left\{ \hat{\varrho}_T(\hat{u}_h)\hat{\varrho}_T^*(\hat{u}_h^*) + \varrho_T(u_h, \lambda_h)\, \varrho_T^*(u_h^*, \lambda_h^*) \right\}, \tag{5}$$

involving the cell residuals $\hat{\varrho}_T$, $\hat{\varrho}_T^*$, and ϱ_T , ϱ_T^* of the computed primal and dual base solutions $\hat{u}_h$, $\hat{u}_h^*$, and eigenpairs $\{u_h, \lambda_h\}$, $\{u_h^*, \lambda_h^*\}$, respectively. This error estimate accomplishes simultaneous control of the error in the linearization, $\hat{v} - \hat{v}_h$, and the error in the resulting eigenvalues, $\lambda - \lambda_h$. The cell-wise error indicators can then guide the mesh refinement process. Further, we devise a simple computational criterion based on the inner products (v_h, v_h^*) which can detect possible instability caused by non-normality effects.

The a priori error analysis for nonsymmetric eigenvalue problems is well developed in the literature, e.g., Babuska and Osborn [1]. Particularly to mention is Osborn [18], where the eigenvalue problem of the linearized Navier-Stokes equations is considered, though neglecting the additional error due to the approximative linearization. These studies usually employ the heavy machinery of resolvent integral calculus. In contrast to that the *a posteriori* error analysis only needs arguments from elementary calculus since it is based on the assumption that the approximation is sufficiently accurate on the considered meshes. In turn, this assumption is justified by the a priori error analysis.

The further contents of this paper are as follows. In Sect. 2, we present an example from optimal flow control which illustrates several principle questions arising in numerical stability analysis. Section 3 summarizes some basic facts about the stability eigenvalue problem of the Navier-Stokes equations, particularly the consequences arising from its non-normality. Section 4 recalls the details of the finite element approximation of problems (2) and (1) from Rannacher [19, 20]. Then, Sect. 5 contains an a posteriori error analysis for the finite element approximation of the perturbed stability eigenvalue problem based on the general optimal control approach developed in Heuveline and Rannacher [10–12]. In Sect. 6, we discuss the possible effect of the non-normality of the linearized Navier-Stokes operator and its numerical detection. Finally, Sect. 8 illustrates the theoretical results at some model eigenvalue problems.

2 An Example from Flow Control

We consider the configuration shown in Fig. 1, i.e. flow through a channel around a fixed cylinder with circular cross section and surface S [3]. The mathematical model are the stationary Navier-Stokes equations (2) complemented by Neumann-type boundary conditions at the two openings Γ_Q,

$$\nu\partial_n v - np|_{\Gamma_Q} = P, \tag{6}$$

where P represents mean pressure. The diameter of the cylinder, the viscosity and the mean inflow velocity are chosen such that for $P = 0$ the Reynolds number is moderate, $\mathrm{Re} \sim 40$, corresponding to stable stationary flow.

Fig. 1 Configuration of the drag minimization problem

The goal is to minimize the drag coefficient

$$C_{\text{drag}} := \frac{2}{\bar{U}^2 D} \int_S n \cdot \sigma(v, p) \cdot e_1 \, ds,$$

by varying the mean pressure P. Here, S is the surface of the cylinder, D its diameter, $\bar{U}$ a reference inflow velocity, and $\sigma(v, p) = -pI + \nu(\nabla v + \nabla v^T)$ the stress tensor. For given P the corresponding state $\{v, p\} \in H^1(\Omega) \times L^2(\Omega)$ is determined by the variational equation

$$\nu(\nabla v, \nabla \psi) + (v \cdot \nabla v, \psi) - (p, \nabla \cdot \psi) - (\chi, \nabla \cdot v) = (P, n \cdot \psi)_{\Gamma_Q}, \qquad (7)$$

for all test pairs $\{\psi, \chi\}$, and the appropriate boundary conditions at $\Gamma_{\text{in}} \cup \Gamma_{\text{rigid}}$.

The discretization of this optimization problem is by a standard 2nd-order FE method using equal-order bilinear elements for velocity and pressure with least-squares pressure stabilization (see [19] and [20]). The "goal-oriented" mesh adaptation is done by the "Dual Weighted residual (DWR) Method" (see [3, 5, 2]) which uses local residual information of the computed solution weighted by sensitivity factors obtained from the approximate solution of an associated "dual problem". The results obtained by the DWR method for this optimization problem are shown in Table 1 and Fig. 2. The drag minimization on an adapted mesh with only about $11,000$ cells is as accurate as that on a uniformly refined mesh with about $164,000$ cells. This demonstrates the potential of sensitivity-driven mesh adaptation particularly in solving optimal control problems.

The optimal state shown in Fig. 2 has been computed in a post-processing step on a globally refined mesh from the stationary model by using Newton's method. Its rough pattern races the question of its stability. It is well known that Newton's method may give solutions to stationary models which are actually unstable in the dynamic sense. This question has to be investigated by an accompanying stability analysis, i.e. by solving the associated stability eigenvalue problem (1) for $u := \{v, p\} \in V$ and $\lambda \in \mathbb{C}$,

Table 1 Uniform versus adaptive refinement

Uniform refinement		Adaptive refinement	
N	J_{drag}	N	J_{drag}
10,512	3.31321	1,572	3.28625
41,504	3.21096	4,264	3.16723
164,928	3.11800	11,146	3.11972

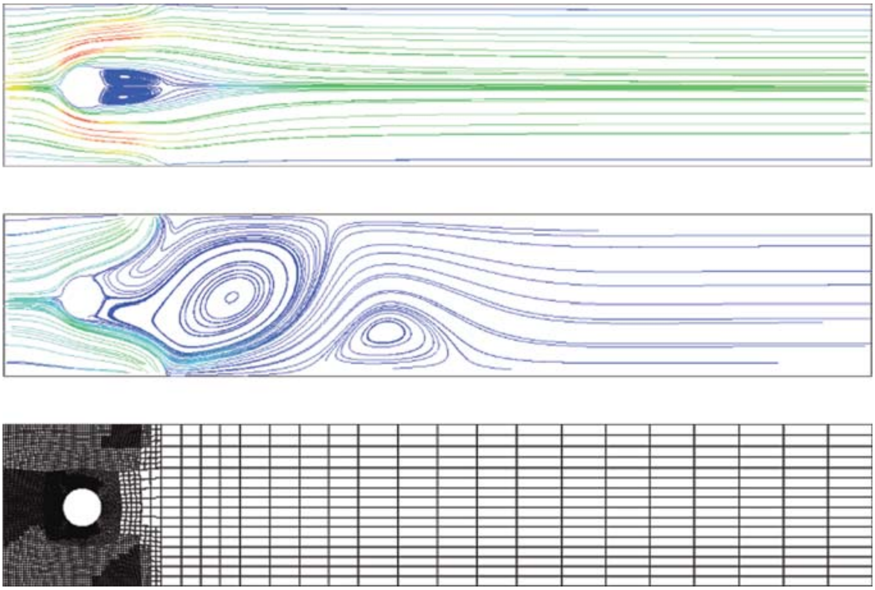

Fig. 2 Streamlines of uncontrolled flow ($P = 0$), controlled flow ($P = P_{\text{opt}}$), and adapted mesh for the optimization cycle

$$-\nu\Delta v + \hat{v}\cdot\nabla v + v\cdot\nabla\hat{v} + \nabla p = \lambda v, \quad \nabla\cdot v = 0.$$

Here, $\hat{u} = \{\hat{v}, \hat{p}\}$ is the stationary optimal state of the drag minimization problem. If all eigenvalues satisfy $\operatorname{Re}\lambda \geq 0$ then the base solution is said to be linearly stable. In this context the following questions occur:

- *Inaccurate model:* The approximate base solution $\hat{u}_h = \{\hat{v}_h, \hat{p}_h\}$ has been computed on a possibly rather coarse mesh, which was just sufficiently fine for the particular needs of the optimization process (see Fig. 2). How large is the deterioration of the eigenvalues for only approximately known base solution used in the coefficients?
- *Efficient solution:* Since solving large nonsymmetric eigenvalue problems is rather expensive the mesh on which this computation is done should be as coarse as possible according to the accuracy requirements of the stability analysis.
- *The effect of non-normality:* The linearized Navier-Stokes operator $\mathcal{A}'(\hat{u})$ is non-normal, i.e., it does not commute with its Hilbert-space adjoint. This has well-known implications for the associated eigenvalue problem (non-trivial algebraic eigenspaces) and the corresponding stability analysis characterized by the key words "non-monotone perturbation growth", "large resolvent norm" and "pseudo-spectrum". How could a simple numerical test look like for indicating that in a particular situation, due to the non-normality, linear (eigenvalue-based) stability analysis may be misleading?

3 The Navier-Stokes Problem and its Stability Analysis

We use the common notation $L^2(\Omega)$ and $H_0^m(\Gamma;\Omega) \subset H^m(\Omega)$ for the Lebesgue and Sobolev spaces on Ω, with the corresponding norms denoted by $\|\cdot\|$ and $\|\cdot\|_m$, respectively. Spaces of $\mathbb{R}^d$-valued functions $v = (v_1,\dots,v_d)$ are denoted by boldface-type, but no distinction is made in the notation of norms and inner products; thus $\mathbf{H}_0^1(\Gamma;\Omega) = H_0^1(\Gamma;\Omega)^d$ has norm $\|v\|_1 = (\sum_{i=1}^d \|v_i\|_1^2)^{1/2}$, etc. All other notation are self-evident, e.g., $\partial_t u = \partial u/\partial t$ and $\partial_n v = n\cdot\nabla v$, where n is an outer normal unit vector. We assume $\partial\Omega = \Gamma_{\text{in}} \cup \Gamma_{\text{out}} \cup \Gamma_{\text{rigid}}$, where Γ_{in}, Γ_{out}, and Γ_{rigid} denote the inlet, the outlet and the rigid part of the boundary, respectively. We introduce the abbreviation $L := L^2(\Omega)$, $\bar{\mathbf{H}} := \mathbf{H}^1(\Omega)$, $\mathbf{H} := \{v \in \bar{\mathbf{H}},\ v_{|\Gamma_{\text{in}}\cup\Gamma_{\text{rigid}}} = 0\}$, $\bar{\mathbf{V}} := \bar{\mathbf{H}}\times L$ and $\mathbf{V} := \mathbf{H}\times L$. In the case $\Gamma_{\text{out}} = \emptyset$, we use $L := L_0^2(\Omega) = \{q \in L^2(\Omega) : (q,1) = 0\}$. For pairs $u = \{v,p\}$ and $\varphi = \{\varphi^v,\varphi^p\} \in \mathbf{V}$, we define the semilinear form

$$a(u;\varphi) := \nu(\nabla v, \nabla\varphi^v) + (v\cdot\nabla v, \varphi^v) - (p, \nabla\cdot\varphi^v) + (\varphi^p, \nabla\cdot v),$$

and the functional $F(\varphi) := (f,\varphi^v)$. With a solenoidal extension $\bar{v}^{\text{in}} \in \bar{\mathbf{H}}$ of the inflow data v^{in}, we consider a solution $\hat{u} = \{\hat{v},\hat{p}\} \in \mathbf{V} + \{\bar{v}^{\text{in}},0\}$ of the equation

$$a(\hat{u};\varphi) = F(\varphi) \quad \forall \varphi \in \mathbf{V}, \tag{8}$$

or $\mathcal{A}(\hat{u}) = F$ in operator notation. In the following, we do not need H^2-regularity of this problem therefore allowing for general domains which may even be non-convex polygonal or polyhedral. For theoretical analysis it is convenient to introduce spaces of solenoidal functions in order to formally eliminate the pressure from the discussion, $\mathbf{J}_1 := \{v \in \mathbf{H},\ \nabla\cdot v = 0\}$ and $\mathbf{J}_0 := \overline{\mathbf{J}}_1^{\|\cdot\|}$ (see Galdi [7]). We assume that the solution $\hat{u} = \{\hat{v},\hat{p}\}$ is (locally) unique and that the derivative of $a(\cdot;\cdot)$ at $\hat{v}$,

$$a'(\hat{v};\psi,\varphi) := \nu(\nabla\psi,\nabla\varphi) + (\hat{v}\cdot\nabla\psi,\varphi) + (\psi\cdot\nabla\hat{v},\varphi), \qquad \varphi,\psi \in \mathbf{J}_1,$$

is regular on $\mathbf{V}$, i.e., it satisfies the "inf-sup condition"

$$\inf_{\psi\in\mathbf{J}_1}\left(\sup_{\varphi\in\mathbf{J}_1} \frac{a'(\hat{v};\psi,\varphi)}{\|\nabla\psi\|\,\|\nabla\varphi\|}\right) \geq \beta > 0.$$

The corresponding linearized stability analysis considers the nonstationary linearized perturbation equation

$$(\partial_t v,\varphi) + a'(\hat{v};v,\varphi) = 0 \quad \forall\varphi \in \mathbf{J}_1, \qquad v(0) = v_0. \tag{9}$$

The stability of $\hat{u}$ under "small" perturbations is then characterized by the growth property of the corresponding solution operator $S(t) : \mathbf{J}_0 \to \mathbf{J}_0$,

$$\|S(t)\| \approx A e^{-\mathrm{Re}\lambda\, t}, \tag{10}$$

where $A \geq 1$ and λ is the most critical eigenvalue of the stability eigenvalue problem, i.e. that with the smallest real part,

$$-\nu \Delta v + \hat{v} \cdot \nabla v + v \cdot \nabla \hat{v} + \nabla p = \lambda v, \quad \nabla \cdot v = 0. \tag{11}$$

If one of the eigenvalues has negative real part, then the base solution is unstable. The variational formulation of this eigenvalue problem reads

$$a'(\hat{v}; v, \varphi) = \lambda\, (v, \varphi) \quad \forall \varphi \in \mathbf{J}_1, \tag{12}$$

or $\mathcal{A}'(\hat{v})v = \lambda v$ in operator notation, with the normalization condition $\|v\| = 1$. Since the domain Ω is bounded, the classical Riesz-Schauder theorem (see Kato [16]) implies that this eigenvalue problem possesses a countably infinite set $\Sigma(\mathcal{A}'(\hat{v})) := \{\lambda_i\}_{i=1}^{\infty} \subset \mathcal{C}$ of isolated eigenvalues with finite (algebraic) multiplicities which have no finite accumulation points. The difference between the algebraic and geometric multiplicity of an eigenvalue λ, its so-called "defect", is denoted by $\alpha \in \mathbb{N}_0$ and corresponds to the largest integer such that $N((\mathcal{A}'(\hat{v}) - \lambda \mathcal{I})^{\alpha+1}) \neq N((\mathcal{A}'(\hat{v}) - \lambda \mathcal{I})^{\alpha})$. For the following discussion, we assume that the eigenvalue of interest, λ, has *geometric multiplicity one*. The case of higher geometric multiplicity requires some minor technical modifications. Associated to the primal eigenfunction $v \in \mathbf{J}_1$, there is a "dual" (left) eigenfunction $v^* \in \mathbf{J}_1 \setminus \{0\}$ corresponding to λ, that is determined by the "dual" eigenvalue problem

$$a'(\hat{v}; \varphi, v^*) = \lambda\, (\varphi, v^*) \quad \forall \varphi \in \mathbf{J}_1, \tag{13}$$

or $\mathcal{A}'(\hat{v})^* v^* = \lambda^* v^*$ in operator notation. Here, $\lambda^* = \bar{\lambda}$ and the dual eigenfunction may be normalized by $(v, v^*) = 1$. If $(v, v^*) = 0$, then (and only then) the problem

$$a'(\hat{v}; v^1, \varphi) - \lambda\, (v^1, \varphi) = (u, \varphi) \quad \forall \varphi \in \mathbf{J}_1, \tag{14}$$

possesses a solution $u^1 \in \mathbf{J}_1$, a "generalized eigenfunction", satisfying $(v^1, v) = 0$. In this case the eigenvalue λ has defect $\alpha \geq 1$ and the solution operator $S(t)$ has the growth property

$$\|S(t)\| \approx t^{\alpha} e^{-\mathrm{Re}\lambda\, t}. \tag{15}$$

For more details, we refer to Heuveline and Rannacher [11]. The effect of degeneracy on the numerical approximation of the Navier-Stokes equations has been addressed in Johnson et al. [15].

4 The Galerkin Finite Element Approximation

The discretization of the variational problem (8) and of its associated eigenvalue problem uses a standard second-order finite element method as described in [11] and [12]. Let $\mathbb{T}_h$ be decompositions of $\bar{\Omega}$ into cells T (triangles, quadrilaterals, etc.). The local width of a cell $T \in \mathbb{T}_h$ is h_T, while $h := \max_{T\in\mathbb{T}_h} h_T$ denotes the global mesh size. For simplicity, we consider here only low-order tensor-product elements, that is piecewise d-linear trial and test functions for all unknowns (so-called "Q_1/Q_1-Stokes element"). In order to ease local mesh refinement and coarsening, we allow "hanging" nodes (see Fig. 3), where the corresponding "irregular" nodal values are eliminated from the system by linear interpolation of neighboring regular nodal values. The corresponding finite element subspaces are denoted by $L_h \subset L$, $\bar{\mathbf{H}}_h \subset \bar{\mathbf{H}}$, $\mathbf{H}_h \subset \mathbf{H}$, $\bar{\mathbf{V}}_h := \bar{\mathbf{H}}_h \times L_h$, $\mathbf{V}_h := \mathbf{H}_h \times L_h$, and $\bar{v}_h^{\text{in}} \in \bar{\mathbf{H}}_h$ is a suitable interpolation of the boundary function $\bar{v}^{\text{in}}$. This construction is oriented by the situation of a polygonal domain Ω for which the boundary $\partial\Omega$ is exactly matched by the mesh domain $\Omega_h := \cup\{T \in \mathbb{T}_h\}$. In the case of a curved boundary certain modifications are necessary, which are rather standard in finite element analysis (see Ciarlet [6]).

Since the finite element approximations $v_h \in \mathbf{H}_h$ of $v \in \mathbf{J}_1$ are usually not exactly solenoidal, we have to include the approximate pressures $p_h \in L_h$ in the analysis. Therefore, from now on we will consider approximating pairs $u_h = \{v_h, p_h\} \in \mathbf{V}_h$ to $u = \{v, p\} \in \mathbf{V}$. In order to obtain a stable discretization in these spaces with "equal-order interpolation" of pressure and velocity, we use the least-squares technique proposed by Hughes et al. [14]. Following Hughes and Brooks [13], a similar approach is employed for stabilizing the convection term. We use the approximation

$$\mathcal{S}(\hat{u})\varphi := \hat{v} \cdot \nabla\varphi^v + \nabla\varphi^p, \quad \varphi = \{\varphi^v, \varphi^p\} \in \mathbf{V},$$

to the derivative $\mathcal{A}'(\hat{u})$ for defining the stabilized form

$$a_h(\hat{u};\varphi) := a(\hat{u};\varphi) + (\mathcal{A}(\hat{u}) - f, \mathcal{S}(\hat{u})\varphi)_h,$$

with the mesh-dependent inner product and norm

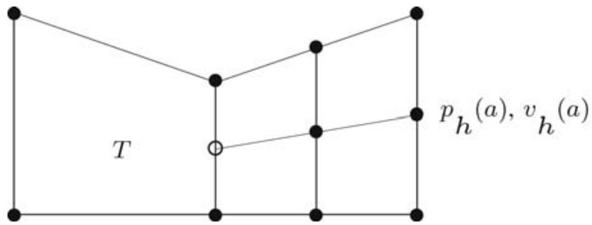

Fig. 3 Quadrilateral mesh patch for the Q_1/Q_1-Stokes element with a "hanging node"

$$(\varphi, \psi)_h := \sum_{T \in \mathbb{T}_h} \delta_T \, (\varphi, \psi)_T, \quad \|\varphi\|_h = (\varphi, \varphi)_h^{1/2}.$$

With this notation the discrete eigenvalue problem (19) uses the sesquilinear form

$$a_h'(\hat{v}_h; u_h, \varphi_h) := a'(\hat{u}; u_h, \varphi) + (\mathcal{A}'(\hat{u})u - \lambda_h v, \mathcal{S}(\hat{u})\varphi)_h$$

which is not the derivative of the stabilized form $a_h(\cdot;\cdot)$, but rather a consistent stabilization of $a'(\hat{u}; \cdot, \cdot)$. Based on theoretical analysis the stabilization parameters δ_T are chosen according to

$$\delta_T = \alpha\big(\nu h_T^{-2}, \beta\, |v_h|_{T;\infty} h_T^{-1}\big)^{-1}, \tag{16}$$

with the heuristic values $\alpha = \frac{1}{12}$, $\beta = \frac{1}{6}$. Then, the discrete Navier-Stokes problem determines $\hat{u}_h := \{\hat{v}_h, \hat{p}_h\} \in V_h + \{\hat{v}_h^{\text{in}}, 0\}$ by

$$a_h(\hat{u}_h; \varphi_h) = F(\varphi_h) \quad \forall \varphi_h \in \mathbf{V}_h. \tag{17}$$

This discretization is fully consistent with (8) in the sense that the continuous solution $\hat{u}$ automatically satisfies (17). This implies “Galerkin orthogonality” what in this case means

$$a_h(\hat{u}; \varphi_h) - a_h(\hat{u}_h; \varphi_h) = 0, \quad \varphi_h \in \mathbf{V}_h. \tag{18}$$

The associated discrete primal and dual eigenvalue problems seek $u_h = \{v_h, p_h\}$ and $u_h^* = \{v_h^*, p_h^*\}$ in $\mathbf{V}\backslash\{0\}$ and $\lambda_h, \lambda_h^* \in \mathcal{C}$, such that

$$a_h'(\hat{u}_h; u_h, \varphi_h) = \lambda_h \, m(u_h, \varphi_h) \quad \forall \varphi_h \in \mathbf{V}_h, \tag{19}$$
$$a_h'(\hat{u}_h; \varphi_h, u_h^*) = \lambda_h^* \, m(\varphi_h, u_h^*) \quad \forall \varphi_h \in \mathbf{V}_h, \tag{20}$$

where $m(u_h, \varphi_h) := (v_h, \varphi_h^v)$ and $m(\varphi_h, u_h^*) := (\varphi_h^v, v_h^*)$. The eigenfunctions are usually normalized by $m(u_h, u_h) = m(u_h, u_h^*) = 1$, assuming non-degeneracy of the approximate eigenvalue λ_h. The question of possibly non-zero defect of this eigenvalue will be addressed below.

For this approximation, we can recall a priori error estimates from the literature. If the problem is H^2-regular, there holds an optimal-order error estimate for the approximation of the base solution (see Girault and Raviart [8] or Rannacher [19]),

$$\|\hat{v}_h - \hat{v}\| = \mathcal{O}(h^2), \tag{21}$$

and for a non-deficient eigenvalue (see Osborn [18]),

$$|\lambda_h - \lambda| = \mathcal{O}(h^2). \tag{22}$$

Further, for normalized discrete primal and dual eigenfunctions $\{u_h, u_h^*\} \in \mathbf{V}_h \times \mathbf{V}_h$, there exists an associated pair of eigenfunctions $\{u^h, u^{h*}\} \in \mathbf{V} \times \mathbf{V}$, such that

$$\|v_h - v^h\| + \|v_h^* - v^{h*}\| = \mathcal{O}(h^2). \tag{23}$$

Here, the superscript in v^h indicates that the continuous eigenfunction associated to v_h may vary with h. For a non-deficient eigenvalue λ with multiplicity m, there are exactly m approximating eigenvalues $\{\lambda_h^i\}_{i=1,\dots,m}$, counted according to their algebraic multiplicities, such that

$$\Big|\sum_{i=1}^m \lambda_h^i - \lambda\Big| = \mathcal{O}(h^2). \tag{24}$$

If λ has non-trivial defect, we have to construct approximations $u_h^{ij} \in \mathbf{V}_h$ to higher-order generalized eigenfunctions of λ. This construction is technically complicated and therefore not presented in this paper. For details, we refer to Heuveline and Rannacher [12].

5 The Perturbed Stability Eigenvalue Problem

In the error estimates (22), (23), and (24) the linearization is assumed to be exact, that is also in the approximate eigenvalue problem (19) the derivative of $a(\cdot;\cdot)$ is taken at the true solution $\hat{u}$. In the following *a posteriori* error analysis, we will treat the full discretization error incorporating also the linearization due to replacing $\hat{u}$ by $\hat{u}_h$. For simplifying the presentation, we will only consider the case of purely homogeneous Dirichlet boundary conditions, $\Gamma_{\text{rigid}} = \partial\Omega$, and will omit the terms related to the stabilization, that is, we will set $\delta = 0$. Then, the general theory for a posteriori error estimation in Galerkin methods developed in Becker and Rannacher [5] (see also Bangerth and Rannacher [2]) yields the following result.

Proposition 1 *With the weighted residuals*

$$\begin{aligned}
\varrho(\hat{u}_h;\cdot) &:= F(\cdot) - a_\delta(\hat{u}_h;\cdot),\\
\varrho^*(\hat{u}_h^*;\cdot) &:= -a_\delta''(\hat{u};\cdot,u_h,u_h^*) - a_\delta'(\hat{u}_h;\cdot,\hat{u}_h^*),\\
\varrho(\{u_h,\lambda_h\};\cdot) &:= \lambda_h\, m(u_h,\cdot) - a_\delta'(\hat{u}_h;u_h,\cdot),\\
\varrho^*(\{u_h^*,\lambda_h\};\cdot) &:= \lambda_h\, m(\cdot,u_h^*) - a_\delta'(\hat{u}_h;\cdot,u_h^*),
\end{aligned}$$

there holds the eigenvalue error representation

$$\begin{aligned}\lambda-\lambda_h \;=\; & \underbrace{\tfrac{1}{2}\varrho(\hat{u}_h;\hat{u}^*-I_h\hat{u}^*)+\tfrac{1}{2}\varrho^*(\hat{u}_h^*;\hat{u}-I_h\hat{u})}_{\textit{base solution residuals}} \\ & +\underbrace{\tfrac{1}{2}\varrho(\{u_h,\lambda_h\};u^*-I_hu^*)+\tfrac{1}{2}\varrho^*(\{u_h^*,\lambda_h\};u-I_hu)}_{\textit{eigenvalue residuals}}+R_h^{(3)},\end{aligned} \tag{25}$$

for arbitrary $I_h\hat{u}^*,\ I_h\hat{u},\ I_hu^*,\ I_hu\in V_h$. *The remainder is given by*

$$R_h^{(3)}=\tfrac{1}{2}e^{\lambda}(e^v,e^{v*})-\tfrac{1}{2}(\hat{e}^v\cdot\nabla\hat{e}^v,\hat{e}^{v*})-\tfrac{1}{2}(\hat{e}^v\cdot\nabla e^v,e^{v*})-\tfrac{1}{2}(e^v\cdot\nabla\hat{e}^v,e^{v*}),$$

where $e^{\lambda}:=\lambda-\lambda_h$, $\hat{e}^v:=\hat{v}-\hat{v}_h$, $\hat{e}^{v*}:=\hat{v}^*-\hat{v}_h^*$, $e^v:=v-v_h$, *and* $e^{v*}:=v^*-v_h^*$.

Proof We only give a brief sketch of the argument; for the details see Heuveline and Rannacher [11, 12]. In order to use the general theory, we have to embed the present situation into the framework of variational equations. To this end, we introduce the product spaces $\mathcal{V}:=V\times V\times\mathcal{C}$ and $\mathcal{V}_h:=V_h\times V_h\times\mathcal{C}$ with elements $U:=\{\hat{u},u,\lambda\}$, $\Phi=\{\hat{\varphi},\varphi,\mu\}$ and $U_h:=\{\hat{u}_h,u_h,\lambda_h\}$, respectively, and the semi-linear form

$$A(U;\Phi):=\underbrace{F(\hat{\varphi})-a_\delta(\hat{u};\hat{\varphi})}_{\text{base solution}}+\underbrace{\lambda\,m(u,\varphi)-a_\delta'(\hat{u};u,\varphi)}_{\text{eigenvalue problem}}+\underbrace{\overline{\mu}\big\{m(u,u)-1\big\}}_{\text{normalization}}.$$

With this notation the stationary Navier-Stokes equations for the base solution and the associated stability eigenvalue problem with its normalization condition as well as the corresponding Galerkin approximations can be written in the following compact variational form:

$$A(U;\Phi)=0\quad\forall\Phi\in\mathcal{V}, \tag{26}$$

$$A(U_h;\Phi_h)=0\quad\forall\Phi_h\in\mathcal{V}_h. \tag{27}$$

The error in this approximation will be measured with respect to the evaluation functional $J(\Phi):=\mu\,m(\varphi,\varphi)$, which is motivated by $J(U)=\lambda m(u,u)=\lambda$. For deriving a representation for the error $J(U)-J(U_h)=\lambda-\lambda_h$, we employ the Euler-Lagrange approach used in optimal control theory. Computing $J(U)$ from the solution of (26) is equivalent to determining stationary points of the Lagrangian functional

$$\mathcal{L}(U;Z):=J(U)-A(U;Z),$$

with the dual variable $Z\in\mathcal{V}$. In this framework, we seek solutions $\{U,Z\}\in\mathcal{V}\times\mathcal{V}$ to the Euler-Lagrange system

$$A(U;\Phi)=0\qquad\forall\Phi\in\mathcal{V}, \tag{28}$$

$$A'(U;\Phi,Z) = J'(U;\Phi) \quad \forall \Phi \in \mathcal{V}. \tag{29}$$

We note that the first equation of this system is just the considered variational equation (26). The Galerkin approximation of system (28), (29) in the subspace $\mathcal{V}_h \subset \mathcal{V}$ seeks pairs $\{U_h, Z_h\} \in \mathcal{V}_h \times \mathcal{V}_h$, satisfying

$$A(U_h;\Phi_h) = 0 \qquad \forall \Phi_h \in \mathcal{V}_h, \tag{30}$$

$$A'(U_h;\Phi_h,Z_h) = J'(U_h;\Phi_h) \quad \forall \Phi_h \in \mathcal{V}_h. \tag{31}$$

To the approximate solutions $U_h \in \mathcal{V}_h$ of (30) and $Z_h \in \mathcal{V}_h$ of (31), we associate the residuals

$$\varrho(U_h;\Phi) := -A(U_h;\Phi), \quad \varrho^*(Z_h;\Phi) := J'(U_h;\Phi) - A'(U_h;\Phi,Z_h),$$

which are defined for $\Phi \in \mathcal{V}$. For $\Phi_h \in \mathcal{V}_h$, we have $\varrho(U_h;\Phi_h) = \varrho^*(Z_h;\Phi_h) = 0$, by definition. For this situation, we have the following fundamental result of Becker and Rannacher [5], which can be proved by elementary analysis:

$$J(U) - J(U_h) = \tfrac{1}{2}\,\varrho(U_h; Z - \Psi_h) + \tfrac{1}{2}\,\varrho^*(Z_h; U - \Phi_h) + R_h^{(3)}, \tag{32}$$

for arbitrary elements $\Psi_h,\ \Phi_h \in \mathcal{V}_h$. The cubic remainder term $R_h^{(3)}$ is given by

$$\begin{aligned} R_h^{(3)} := \tfrac{1}{2}\int_0^1 \big\{ & J'''(U_h + sE_h; E_h, E_h, E_h) \\ & - A'''(U_h + sE_h; E_h, E_h, E_h, Z_h + sE_h^*) \\ & - 3A''(U_h + sE_h; E_h, E_h, E_h^*)\big\}\, s(s-1)\, ds\,, \end{aligned} \tag{33}$$

where $E_h := U - U_h$ and $E_h^* := Z - Z_h$. The residuals $\varrho(U_h;\Psi)$ and $\varrho^*(Z_h;\Phi)$ have the explicit form

$$\varrho(U_h;\Psi) = -A(U_h;\Psi) = a(\hat{u}_h;\hat{\psi}) - f(\hat{\psi}) + a'(\hat{u}_h;u_h,\psi) - \lambda_h\, m(u_h,\psi),$$

and

$$\begin{aligned} \varrho^*(Z_h;\Phi) &= J'(U_h;\Phi) - A'(U_h;\Phi,Z_h) \\ &= a''(\hat{u}_h;\hat{\varphi},u_h,u_h^*) + a'(\hat{u}_h;\hat{\varphi},\hat{u}_h^*) + a'(\hat{u}_h;\varphi,u_h^*) - \lambda_h\, m(\varphi,u_h^*), \end{aligned}$$

for $\Psi = \{\hat{\psi},\psi,\chi\}$ and $\Phi = \{\hat{\varphi},\varphi,\mu\}$. Finally, we have to evaluate the remainder term. By a simple calculation, we have

$$J'''(U_h + sE; E, E, E) = 6(\lambda - \lambda_h)\|v - v_h\|^2,$$

and, since the semilinear form $A(U;\cdot)$ is quadratic in U,

$$A'''(U_h+sE; E, E, E, Z_h+sE^*) = 0.$$

Further, since $a(\hat{u};\cdot)$ is quadratic in $\hat{u}$,

$$\begin{aligned} A''(U;\Phi,\Psi,Z) = &-a''(\hat{u};\hat{\varphi},\hat{\psi},\hat{z}) - a''(\hat{u};\hat{\varphi},\psi,z) - a''(\hat{u};\varphi,\hat{\psi},z) \\ &+ \mu\, m(\psi,z) + \chi\, m(\varphi,z) + 2\bar{\pi}\,\mathrm{Re}\{m(\varphi,\psi)\}, \end{aligned}$$

and consequently,

$$\begin{aligned} -3A''(U_h+sE; E, E, E^*) = &\, 6(\hat{e}^v\cdot\nabla\hat{e}^v, \hat{e}^{v*}) \\ &+ 6(\hat{e}^v\cdot\nabla e^v, e^{v*}) + 6(e^v\cdot\nabla\hat{e}^v, e^{v*}) \\ &- 6(\lambda-\lambda_h)(v-v_h, v^*-v_h^*) \\ &- 6(\lambda-\lambda_h)\|v-v_h\|^2. \end{aligned}$$

Collecting the above results, we obtain

$$R_h^{(3)} = \tfrac{1}{2}e^\lambda\,(e^v, e^{v*}) - \tfrac{1}{2}\big\{(\hat{e}^v\cdot\nabla\hat{e}^v, \hat{e}^{v*}) + (\hat{e}^v\cdot\nabla e^v, e^{v*}) + (e^v\cdot\nabla\hat{e}^v, e^{v*})\big\}.$$

This completes the proof. □

6 The Effect of Non-normality

In general, under discretization an eigenvalue λ with algebraic multiplicity $m\geq 2$ will split into a group of m simple eigenvalues $\{\lambda_h^{(i)},\ i=1,\ldots,m\}$ which may be considered as the approximation to λ. Only in special cases, for instance when the discretization preserves certain symmetry properties of the continuous problem, some of the discrete eigenvalues may have geometric multiplicity greater than one. Further these eigenvalues will usually be non-degenerate because of asymmetries in the discretization. The existence of an eigenvalue with $\mathrm{Re}\lambda<0$ inevitably causes dynamic instability of the base flow $\hat{v}$, i.e., arbitrarily small perturbations may grow without bound. For the solution operator $S:\mathbf{J}_0\to\mathbf{J}_0$ of the linearized perturbation equation

$$(\partial_t w, \varphi) + a'(\hat{v}; w, \varphi) = 0 \quad \forall\varphi\in\mathbf{J}_1, \tag{34}$$

there holds the the growth property

$$\|S(t)\| \approx t^\alpha e^{-\mathrm{Re}\lambda\, t}, \tag{35}$$

where λ is the eigenvalue with smallest $\mathrm{Re}\lambda>0$ and defect $\alpha\geq 0$. This can be shown by standard "energy arguments" and linear algebra (see Gustavsson [9] and Johnson et al. [15]). In the case $\alpha\geq 1$, (35) implies that

$$\sup_{t>0} \|S(t)\| \approx \frac{\alpha}{|\text{Re}\lambda|}, \tag{36}$$

i.e., the amplification constant A in the stability estimate (4) becomes very large and small perturbations may initially be amplified to an extent such that nonlinear instability occurs.

Therefore, we are mainly interested in the case that all eigenvalues have positive real part and want to compute the most "critical" eigenvalues, that is those λ with minimal $\text{Re}\lambda > 0$. The crucial question is how to detect *a posteriori* whether the growth factor in the estimate (35) may become critical or not.

To this end, we may employ the following simple indicator: For any small $h > 0$, let λ_h be one of the approximating eigenvalues of $\mathcal{A}_h'(\hat{v})$ with corresponding right and left eigenvectors v_h and v_h^*, satisfying $\|v_h\| = 1$ and $(v_h, v_h^*) = 1$. By theory, there are associated (normalized) right and left eigenvectors (depending on h), say v and v^*, corresponding to the eigenvalue λ of $\mathcal{A}'(\hat{v})$, such that $\|v_h - v\| \to 0$ and $\|v_h^* - v^*\| \to 0$, as $h \to 0$. If the limit eigenvalue λ is deficient, then there must be an algebraic eigenvector w associated to v, such that

$$\mathcal{A}'(\hat{v})w - \lambda w = v.$$

The condition for the existence of such an algebraic eigenvector is that $(v, v^*) = 0$. Hence, in view of the normalization $\|v_h\| = (v_h, v_h^*) = 1$, we obtain the following result.

Corollary 1 *The blow-up*

$$\|v_h^*\| \to \infty \quad (h \to 0), \tag{37}$$

of the computed normalized adjoint eigenfunction, $(v_h, v_h^*) = \|v_h\| = 1$*, with a certain rate, can be used as an indicator for* $\alpha(\lambda) > 0$.

However, a similar effect is also possible for non-deficient eigenvalues λ. This is related to the concept of the "pseudo-spectrum" described in Trefethen and Embree [22] and the literature cited therein (see also Landahl [17]). For $\varepsilon \in \mathbb{R}_+$ the ε-pseudo-spectrum $\sigma_\varepsilon \subset \mathcal{C}$ of the operator $\mathcal{A}'(\hat{v})$ is defined by

$$\sigma_\varepsilon := \big\{ z \in \mathcal{C},\ \|(\mathcal{A}'(\hat{v}) - z\mathcal{I})^{-1}\| \ge \varepsilon^{-1} \big\}.$$

In the following, we recall a result on the possible size of the amplification constant A which in the finite dimensional case may be obtained from the so-called "Kreiss matrix theorem" (see [22] and the references cited therein). For completeness, we supply a proof by "energy arguments".

Proposition 2 *Let* $z \in \mathcal{C}$ *be a regular point of the operator* $\mathcal{A}'(\hat{v})$ *with* $\text{Re}z < 0$. *Then, for the solution operator* $S(t) : \mathbf{J}_0 \to \mathbf{J}_0$ *of the linear perturbation equation (34), there holds*

$$\sup_{t\geq 0} \|S(t)\| \geq |\mathrm{Re} z|\, \|(\mathcal{A}'(\hat{v}) - z\mathcal{I})^{-1}\|. \tag{38}$$

Proof Notice that, for $z \notin \sigma(\mathcal{A}'(\hat{v}))$, the resolvent $(\mathcal{A}'(\hat{v}) - z\mathcal{I})^{-1}$ is well defined as a bounded operator in $\mathbf{J}_0$, and there holds

$$\|(\mathcal{A}'(\hat{v}) - z\mathcal{I})^{-1}\|^{-1} = \inf_{v\in \mathbf{J}_1} \left(\sup_{\varphi\in \mathbf{J}_1} \frac{|a'(\hat{v}; v, \varphi) - z\,(v, \varphi)|}{\|v\|\,\|\varphi\|} \right). \tag{39}$$

We rewrite the perturbation equation (34) in the form

$$(\partial_t v, \varphi) + z(v, \varphi) + a'(\hat{v}; v, \varphi) - z(v, \varphi) = 0,$$

and multiply by e^{tz}, to obtain

$$\frac{d}{dt}\big[e^{tz}(v, \varphi)\big] + e^{tz}\big(a'(\hat{v}; v, \varphi) - z(v, \varphi)\big) = 0.$$

Next, integrating this with respect to t, we conclude

$$|(v^0, \varphi)| \leq e^{t\mathrm{Re} z}|(v(t), \varphi)| + \sup_{\psi\in \mathbf{J}_1} \frac{a'(\hat{v}; \psi, \varphi) - z(\psi, \varphi)}{\|\psi\|} \int_0^t e^{s\mathrm{Re} z}\|v\|\, ds.$$

Taking $\varphi = v^0$, and observing $\mathrm{Re} z < 0$, we conclude that

$$\|v^0\| \leq \big(e^{t\mathrm{Re} z} + \beta_z(v^0)|\mathrm{Re} z|^{-1}\big) \max_{[0,t]} \|v\|,$$

with the notation

$$\beta_z(v^0) := \sup_{\psi\in \mathbf{J}_1} \frac{a'(\hat{v}; \psi, v^0) - z(\psi, v^0)}{\|\psi\|}.$$

Hence, recalling that $v(t) = S(t)v^0$,

$$1 \leq \left(e^{t\mathrm{Re} z} + \frac{\beta_z(v^0)}{|\mathrm{Re} z|}\right) \max_{[0,t]} \|S\|.$$

Since $\inf_{v^0\in \mathbf{J}_1} \beta_z(v^0) = \|(\mathcal{A}'(\hat{v}) - z\mathcal{I})^{-1}\|^{-1}$, we conclude that

$$|\mathrm{Re} z|\, \|(\mathcal{A}'(\hat{v}) - z\mathcal{I})^{-1}\| \leq \big(e^{t\mathrm{Re} z}|\mathrm{Re} z|\, \|(\mathcal{A}'(\hat{v}) - z\mathcal{I})^{-1}\| + 1\big) \max_{[0,t]} \|S\|,$$

for all $t \geq 0$. From this, the asserted estimate follows. Because, assuming the contrary, we would have

$$\|(\mathcal{A}'(\hat{v}) - z\mathcal{I})^{-1}\| < \big(e^{t\mathrm{Re}z}|\mathrm{Re}z|\,\|(\mathcal{A}'(\hat{v}) - z\mathcal{I})^{-1}\| + 1\big)\|(\mathcal{A}'(\hat{v}) - z\mathcal{I})^{-1}\|,$$

which, since $\mathrm{Re}z < 0$, would result in a contradiction for sufficiently large t.

The next proposition relates the size of the resolvent norm $\|(\mathcal{A}'(\hat{v}) - z\mathcal{I})^{-1}\|$ to easily computable quantities in terms of the eigenvalues and eigenfunctions of the operator $\mathcal{A}'(\hat{v})$.

Proposition 3 *Let* $\lambda \in \mathcal{C}$ *be a non-deficient eigenvalue of the operator* $\mathcal{A}'(\hat{v})$ *with corresponding primal and dual eigenvectors* $v, v^* \in \mathbf{J}_1$ *normalized by* $\|v\| = (v, v^*) = 1$. *Then, there exists a continuous function*

$$\omega(\varepsilon) \to 1 \quad (\varepsilon \to 0),$$

such that for $\lambda_\varepsilon := \lambda - \varepsilon\omega(\varepsilon)\|v^*\|$, *there holds*

$$\|(\mathcal{A}'(\hat{v}) - \lambda_\varepsilon\mathcal{I})^{-1}\| \geq \frac{1}{\varepsilon}. \tag{40}$$

Proof (i) Let $b(\cdot,\cdot)$ be a continuous bilinear form on $\mathbf{J}_0$, such that

$$\sup_{\psi,\varphi\in\mathbf{J}_1} \frac{|b(\psi,\varphi)|}{\|\psi\|\,\|\varphi\|} \leq 1.$$

We consider the perturbed eigenvalue problem, for $\varepsilon \in \mathbb{R}_+$,

$$a'(\hat{v}; v_\varepsilon, \varphi) + \varepsilon b(v_\varepsilon, \varphi) = \lambda_\varepsilon\,(v_\varepsilon, \varphi) \quad \forall \varphi \in \mathbf{J}_1. \tag{41}$$

Since this is a regular perturbation and λ non-deficient, there exist corresponding eigenvalues $\lambda_\varepsilon \in \mathcal{C}$ and associated eigenfunctions $v_\varepsilon \in \mathbf{J}_1$, $\|v_\varepsilon\| = 1$, such that

$$|\lambda_\varepsilon - \lambda| = \mathcal{O}(\varepsilon), \qquad \|v_\varepsilon - v\| = \mathcal{O}(\varepsilon).$$

Furthermore, from the relation

$$a'(\hat{v}; v_\varepsilon, \varphi) - \lambda_\varepsilon(v_\varepsilon, \varphi) = -\varepsilon b(v_\varepsilon, \varphi), \qquad \varphi \in \mathbf{J}_1,$$

we conclude that

$$\sup_{\varphi\in\mathbf{J}_1} \frac{|a'(\hat{v}; v_\varepsilon, \varphi) - \lambda_\varepsilon(v_\varepsilon, \varphi)|}{\|\varphi\|} \leq |\varepsilon| \sup_{\varphi\in\mathbf{J}_1} \frac{|b(v_\varepsilon, \varphi)|}{\|\varphi\|} \leq \varepsilon\,\|v_\varepsilon\|,$$

and from this, if λ_ε is not an eigenvalue of $\mathcal{A}'(\hat{v})$,

$$\|(\mathcal{A}'(\hat{v}) - \lambda_\varepsilon\mathcal{I})^{-1}\|^{-1} = \inf_{\psi\in\mathbf{J}_1} \sup_{\varphi\in\mathbf{J}_1} \frac{|a'(\hat{v}; \psi, \varphi) - \lambda_\varepsilon(\psi, \varphi)|}{\|\psi\|\,\|\varphi\|} \leq \varepsilon.$$

This implies the asserted estimate

$$\|(\mathcal{A}'(\hat{v}) - \lambda_\varepsilon \mathcal{I})^{-1}\| \geq \frac{1}{\varepsilon}. \tag{42}$$

Next, we analyze the dependence of the eigenvalue λ_ε on ε in more detail. Subtracting the equation for v form that for v_ε, we obtain

$$a'(\hat{v}; v_\varepsilon - v, \varphi) + \varepsilon b(v_\varepsilon, \varphi) = (\lambda_\varepsilon - \lambda)(v_\varepsilon, \varphi) + \lambda(v_\varepsilon - v, \varphi).$$

Taking $\varphi = v^*$ yields

$$a'(\hat{v}; v_\varepsilon - v, v^*) + \varepsilon b(v_\varepsilon, v^*) = (\lambda_\varepsilon - \lambda)(v_\varepsilon, v^*) + \lambda(v_\varepsilon - v, v^*)$$

and, using the equation satisfied by v^*,

$$\varepsilon b(v_\varepsilon, v^*) = (\lambda_\varepsilon - \lambda)(v_\varepsilon, v^*).$$

This yields

$$\lambda_\varepsilon = \lambda + \varepsilon\omega(\varepsilon) b(v, v^*),$$

where, observing $v_\varepsilon \to v\, (\varepsilon \to 0)$ and $(v, v^*) = 1$,

$$\omega(\varepsilon) := \frac{b(v_\varepsilon, v^*)}{(v_\varepsilon, v^*) b(v, v^*)} \to 1 \quad (\varepsilon \to 0).$$

(ii) It remains to construct an appropriate perturbation form $b(\cdot,\cdot)$. For technical convenience, we consider the renormalized dual eigenfunction $\tilde{v}^* := v^*\|v^*\|^{-1}$, satisfying $\|\tilde{v}^*\| = 1$. With the function $w := (v - \tilde{v}^*)\|v - \tilde{v}^*\|^{-1}$, we set

$$Tv := v - 2\mathrm{Re}(v, w)w, \qquad b(v, \varphi) := -(Tv, \varphi).$$

The operator $T : \mathbf{J}_0 \to \mathbf{J}_0$ acts like a Householder transformation mapping v into $\tilde{v}^*$. In fact, observing $\|v\| = \|\tilde{v}^*\| = 1$, there holds

$$\begin{aligned} Tv &= v - \frac{2\mathrm{Re}(v, v - \tilde{v}^*)}{\|v - \tilde{v}^*\|^2}(v - \tilde{v}^*) \\ &= \frac{(2 - 2\mathrm{Re}(v, \tilde{v}^*))v - 2\mathrm{Re}(v, v - \tilde{v}^*)(v - \tilde{v}^*)}{2 - 2\mathrm{Re}(v, \tilde{v}^*)} \\ &= \frac{2v - 2\mathrm{Re}(v, \tilde{v}^*)v - 2v + 2\mathrm{Re}(v, \tilde{v}^*)v + (2 - 2\mathrm{Re}(v, \tilde{v}^*))\tilde{v}^*}{2 - 2\mathrm{Re}(v, \tilde{v}^*)} = \tilde{v}^*. \end{aligned}$$

This implies that

$$b(v, v^*) = -(Tv, v^*) = -(\tilde{v}^*, v^*) = -\|v^*\|.$$

Further, observing $\|w\| = 1$ and

$$\|Tv\|^2 = \|v\|^2 - 2\text{Re}(v, w)(v, w) - 2\text{Re}(v, w)(w, v) + 4\text{Re}(v, w)^2\|w\|^2 = \|v\|^2,$$

we have

$$\sup_{v,\varphi\in\mathbf{J}_1} \frac{|b(v, \varphi)|}{\|v\|\,\|\varphi\|} \le \sup_{v,\varphi\in\mathbf{J}_1} \frac{\|Tv\|\,\|\varphi\|}{\|v\|\,\|\varphi\|} = 1.$$

Hence, for this particular choice of the form $b(\cdot, \cdot)$, we have

$$\lambda_\varepsilon = \lambda - \varepsilon\omega(\varepsilon)\|v^*\|, \qquad \lim_{\varepsilon\to 0} \omega(\varepsilon) = 1,$$

as asserted.

Combining the two foregoing propositions, we obtain the following result. Under the assumption that $\text{Re}\lambda_\varepsilon = \text{Re}\lambda - \varepsilon\text{Re}\,\omega(\varepsilon)\|v^*\| < 0$, there holds

$$\sup_{t\ge 0} \|S(t)\| \ge \frac{|\text{Re}\lambda_\varepsilon|}{|\varepsilon|}. \tag{43}$$

Therefore, for $\varepsilon := \text{Re}\lambda > 0$, we have

$$\text{Re}\lambda_\varepsilon = \text{Re}\lambda - \text{Re}\lambda\text{Re}\,\omega(\text{Re}\lambda)\|v^*\| = \text{Re}\lambda\big(1 - \text{Re}\,\omega(\text{Re}\lambda)\|v^*\|\big) < 0,$$

for $\|v^*\|$ sufficiently large. Consequently,

$$\sup_{t\ge 0} \|S(t)\| \ge \big|1 - \text{Re}\,\omega(\text{Re}\lambda)\|v^*\|\big|. \tag{44}$$

This consideration leads us to the following conclusion, which has to be observed in the numerical stability analysis.

Corollary 2 *For small* $\text{Re}\lambda > 0$*, a large value* $\|v^*\| \gg 1$ *indicates a large growth constant* A *and consequently possible nonlinear instability.*

7 Practical Stability Analysis of the Navier-Stokes Equations

In the following, we want to convert the general a posteriori error representation (25) into an a posteriori error estimate which can be used in practice for guiding automatic mesh refinement.

7.1 The Deficiency Test

As described above, first, we have to detect whether the limit eigenvalue λ may be degenerate. To this end, in view of Corollary 1, we construct the normalized dual eigenfunctions $u_h^{i*} \in \mathbf{V}_h$, $m(u_h^i, u_h^i) = m(u_h^i, u_h^{i*}) = 1$, corresponding to the approximate eigenvalues λ_h^i $(i = 1, \dots, m)$ and check whether the blow-up

$$m(u_h^{i*}, u_h^{i*}) \to \infty \quad (h \to 0), \tag{45}$$

with a certain rate is observed for any index i. If

$$\sup_{h \in \mathbb{R}_+} m(u_h^{i*}, u_h^{i*}) \le K \quad (i = 1, \dots, m), \tag{46}$$

with some constant K of moderate size, we can use the a posteriori error representations (25). Otherwise it needs to be refined for the case of a degenerate limit eigenvalue λ, which is complicated and not further considered here. For the details, we refer to Heuveline and Rannacher [11]. However, in view of Corollary 2 also

$$\sup_{h \in \mathbb{R}_+} m(u_h^{i*}, u_h^{i*}) \gg 1 \tag{47}$$

can be taken as indication that the limiting eigenvalue λ satisfying $0 < \mathrm{Re}\lambda \ll 1$, though non-degenerate, may cause a large amplification constant A and consequently nonlinear instability. In the following, we will only consider the case of Proposition 1 in more detail.

7.2 Evaluation of the Error Representation

According to our consistency assumption, that is the convergence $\hat{u}_h \to \hat{u}$, $\hat{u}_h^* \to \hat{u}^*$, $u_h \to u$, and $u_h^* \to u^*$, as $h \to 0$, the higher-order remainder term $R_h^{(3)}$ in the error representation (25) is supposed to be small and is therefore neglected. Let $i_h : \mathbf{H}^2(\Omega) \to \bar{\mathbf{H}}_h$ and $j_h : H^2(\Omega) \to L_h$ denote the generic operators of nodal interpolation in the finite element spaces $\bar{\mathbf{H}}_h$ and L_h, respectively. The evaluation of the residual terms is described only for the prototypical term

$$\varrho(\hat{u}_h; \hat{u}^* - \hat{\psi}_h) = F(\hat{u}^* - \hat{\psi}_h) - a(\hat{u}_h; \hat{u}^* - \hat{\psi}_h).$$

Suppose that the forcing term is given in the form $F(\cdot) = (f, \cdot)$ with some density function f. Splitting the integrals over Ω into the contributions from each cell T, and integrating cell-wise by parts, we obtain for $\hat{w}^* := \{\hat{v}^* - i_h \hat{v}^*, \hat{p}^* - j_h \hat{p}^*\}$:

$$\begin{aligned}\varrho(\hat u_h;\hat w) &= \sum_{T\in\mathbb{T}_h}\big\{(f-\mathcal{A}(\hat u_h),\hat w^{v*})_T-(\nu\partial_n v_h,\hat w^{v*})_{\partial T}-(\hat w^{p*},\nabla\cdot\hat v_h)_T\big\}\\ &= \sum_{T\in\mathbb{T}_h}\big\{(f-\mathcal{A}(\hat u_h),\hat w^{v*})_T-\tfrac12(\nu[\partial_n v_h],\hat w^{v*})_{\partial T}-(\hat w^{p*},\nabla\cdot\hat v_h)_T\big\},\end{aligned}$$

where $[\partial_n v_h]_\Gamma := \partial_n v_{h|\Gamma}+\partial_{n'}v_{h|\Gamma}$ denotes the jump of $\partial_n v_h$ across the common edge of two cells, $\Gamma = T\cap T'$. For cells with an edge Γ on the boundary $\partial\Omega$, we use the convention that $[\partial_n v_h]_{|\Gamma} := 0$, if $\Gamma\subset\Gamma_{\text{rigid}}\cup\Gamma_{\text{in}}$, and $[\partial_n v_h]_{|\Gamma} := \partial_n v_h$, if $\Gamma\subset\Gamma_{\text{out}}$.

While the cell-residual quantities $f-\mathcal{A}(\hat u_h)$, $\nu[\partial_n v_h]$, and $\nabla\cdot\hat v_h$ can be computed exactly, the functions $\hat w^v$ and $\hat w^p$ depend on the unknown dual solution $\hat u^*$ and have to be approximated. However, this approximation does not need to be of very high accuracy since these terms only play the role of "weights" for the residuals in the error representation. Here, we consider patch-wise higher-order interpolation as one of the simplest and cheapest options. Let $\hat u_h^*$ be the approximation computed on the current mesh. On square blocks of 2^d neighboring cells the 3^d nodal values of $\hat v_h$ and $\hat p_h$ are used to define d-quadratic interpolations $i_{2h}^{(2)}\hat v_h^*$ and $j_{2h}^{(2)}\hat p_h^*$, respectively. These are then used in the approximation

$$\hat v^*-i_h\hat v^*\approx i_{2h}^{(2)}\hat v_h^*-\hat v_h^*,\qquad \hat p^*-j_h\hat p_h^*\approx j_{2h}^{(2)}\hat p_h^*-\hat p_h^*.$$

In many applications this approximation has proved to be sufficiently accurate. For a detailed discussion of this crucial aspect of using duality-based a posteriori error representations of the type (25), we refer to Bangerth and Rannacher [2]. The other residual terms $\varrho^*(\hat u_h^*;\hat u-\hat\varphi_h)$, $\varrho(u_h^i,\lambda_h^i;u^{i*}-\psi_h^i)$, and $\varrho^*(u_h^{i*},\lambda_h^{i*};u^i-\varphi_h^i)$ can be treated analogously. This leads us to the following result.

Proposition 4 *With the notation of Proposition 1, we have the a posteriori error estimate:*

$$|\lambda-\lambda_h|\approx\eta(\hat u_h,\hat u_h^*,u_h,u_h^*,\lambda_h):=\sum_{T\in\mathbb{T}_h}\{\hat\eta_T+\eta_T^\lambda\},\qquad(48)$$

with the cell-error indicators

$$\begin{aligned}\hat\eta_T &:= |(f-\mathcal{A}(\hat u_h),\hat w^{v*})_T-\tfrac12(\nu[\partial_n\hat v_h],\hat w^{v*})_{\partial T}-(\hat w^{p*},\nabla\cdot\hat v_h)_T\\ &\qquad +(\hat w^v,g(v_h,v_h^*)+\mathcal{A}'(\hat u_h)\hat u_h^*)_T-\tfrac12(\hat w^v,\nu[\partial_n\hat v_h^*])_{\partial T}-(\nabla\cdot\hat v_h^*,\hat w^p)_T|,\\ \eta_T^\lambda &:= |(\lambda_h v_h-\mathcal{A}'(\hat u_h)u_h,w^{v*})_T-\tfrac12(\nu[\partial_n v_h],w^{v*})_{\partial T}-(w^{p*},\nabla\cdot v_h)_T\\ &\qquad +(w^v,\lambda_h v_h^*-\mathcal{A}'(\hat u_h)u_h^*)_T-\tfrac12(w^v,\nu[\partial_n v_h^*])_{\partial T}-(\nabla\cdot v_h^*,w^p)_T|,\end{aligned}$$

where $\hat w^{v*}:=i_{2h}^{(2)}\hat v_h^*-\hat v_h^*$, $\hat w^{p*}:=j_{2h}^{(2)}\hat p_h^*-\hat p_h^*$, $\hat w^v:=\hat w^v:=i_{2h}^{(2)}\hat v_h-\hat v_h$, $\hat w^p:=j_{2h}^{(2)}\hat p_h-\hat p_h$, $w^{v*}:=i_{2h}^{(2)}v_h^*-v_h^*$, $w^{p*}:=j_{2h}^{(2)}p_h^*-p_h^*$.

In the case $|\eta_T^\lambda|\ll|\hat\eta_T|$ the total error contribution by the cell T is dominated by its component due to the base flow approximation. This would suggest the use of different meshes in computing the base flow and solving the eigenvalue problem in order to decrease costs. The a posteriori error estimate (48) remains valid for such a hybrid discretization.

7.3 Strategies for Mesh Refinement

We briefly discuss our strategy for automatic mesh adaptation based on the approximate a posteriori error estimate (48) derived above. Let TOL be a given error tolerance and $N_{\max}$ the maximum number of mesh cells that can be used due to memory constraints. Then, the mesh adaptation strategy aims to equilibrate the combined indicators

$$\eta_T := |\hat{\eta}_T| + |\eta_T^\lambda|$$

by locally refining or coarsening the mesh.

Starting from a coarse mesh $\mathbb{T}_0 := \mathbb{T}_{h_0}$ with mesh size distribution h_0, let after l refinement cycles the mesh-level $\mathbb{T}_l := \mathbb{T}_{h_l}$ with space $\mathbf{V}_l := \mathbf{V}_{h_l}$ be reached. Let $N_l \approx \dim(\mathbf{V}_l)$ be the number of cells of the mesh $\mathbb{T}_l$. On this mesh the approximate solution $\{\hat{u}_l, \hat{u}_l^*, u_l, u_l^*, \lambda_l\}$ is computed and the associated cell-error indicators $\hat{\eta}_T$ and η_T^λ are evaluated.
Stopping criterion: If the criterion

$$\Big|\sum_{T\in\mathbb{T}_h}\{\hat{\eta}_T + \eta_T^\lambda\}\Big| \le \tfrac{1}{2}\mathrm{TOL}, \qquad \Big|\sum_{T\in\mathbb{T}_h}\hat{\eta}_T\Big| \le \Big|\sum_{T\in\mathbb{T}_h}\eta_T^\lambda\Big| \tag{49}$$

is satisfied on the mesh $\mathbb{T}_l$, then the refinement process is stopped and λ_l is accepted as approximation to λ. Otherwise, the next refinement cycle is started.

Adaptation step: The transition from mesh $\mathbb{T}_l$ to the next mesh $\mathbb{T}_{l+1}$ may follow the so-called "fixed rate" strategy. Here, in each refinement cycle, the goal is to increase the number of mesh cells N_l by a fixed rate or to reduce the error estimator $\eta_l^\lambda(\hat{u}_l, \hat{u}_l^*, u_l, u_l^*, \lambda_l)$ by a fixed rate. First, the cells $T \in \mathbb{T}_l$ are ordered according to the size of the indicator values η_T, $\eta_{T,1} \ge \ldots \ge \eta_{T,i} \ge \eta_{T,i+1} \ge \ldots \ge \eta_{T,N_l}$. For prescribed fractions X and Y the cells are grouped according to

$$\#\{T_i, i = 1, \ldots, N_*\} \approx X\, N_l, \qquad \#\{T_{N_l-i+1}, i = 1, \ldots, N^*\} \approx Y\, N_l.$$

If $N_{l+1} = N_l\big(1 - X - Y + 2^d X + 2^{-d} Y\big) > N_{\max}$, the refinement process is stopped. Otherwise, the cells $T_1, \ldots, T_{N_*}$ are refined and the cells $T_{N_l-N^*+1}, \ldots, N_l$ are coarsened. On the resulting mesh T_{l+1} the adaptation process is continued. By this strategy the number of mesh cells changes with a prescribed rate which is advantageous in using a multigrid solver. In the test calculations discussed below, we have used $X = 20$ and $Y = 0$, i.e., only mesh refinement is performed.

8 Numerical Examples

We present some results of calculations that are intended to illustrate the theoretical statements in this paper.

8.1 Burgers Equation

The first test case is the two-dimensional Burgers equation

$$-\nu\Delta\hat{v} + \hat{v}\cdot\nabla\hat{v} = 0 \quad \text{in } \Omega, \tag{50}$$

on the rectangular domain $\Omega := (0, 10) \times (0, 1) \subset \mathbb{R}^2$, with Dirichlet boundary conditions corresponding to plane shear flow $\hat{v} = (x_2, 0)^T$ along $\{x_1 = 0\}$, $\{x_2 = 0\}$, and $\{x_2 = 1\}$, and Neumann boundary conditions along $\{x_1 = 10\}$. Linearization about this base solution results in the nonsymmetric eigenvalue problem

$$\begin{aligned} -\nu\Delta v_1 + x_2\partial_1 v_1 + v_2 &= \lambda v_1, \\ -\nu\Delta v_2 + x_2\partial_1 v_2 \qquad &= \lambda v_2, \end{aligned} \tag{51}$$

for $v = \{v_1, v_2\}$, with homogeneous boundary conditions. It is easily seen that all eigenvalues have positive real part. Due to the coupling of the second component v_2 into the first equation, the most critical eigenvalue λ^{crit} is expected to have defect $\alpha > 0$. This property persists under discretization because of the particular structure of the problem. We introduce an additional coupling term $h^2 v_1$ in the second equation which makes the discrete eigenvalue λ_h^{crit} split into two simple (real) eigenvalues λ_h^1 and λ_h^2. As suggested by the a priori error analysis, we take $\lambda_h := \frac{1}{2}\{\lambda_h^1 + \lambda_h^2\}$ as our primary approximation to the limit eigenvalue λ. Table 2 presents the corresponding results obtained on a sequence of uniformly refined meshes for the parameter value $\nu = 10^{-2}$. We observe the reduced order $\mathcal{O}(h)$ for the error $|\lambda_h^1 - \lambda|$ and the optimal order $\mathcal{O}(h^2)$ for $|\lambda_h - \lambda|$. The same order is obtained for the error estimator $\eta^{\lambda}_{\text{weight}}$. Furthermore, as predicted, the dual eigenfunctions v_h^*, normalized by $(v_h, v_h^*) = 1$ have norms that blow up with order $\mathcal{O}(h^{-1})$.

8.2 Plane Shear Flow (Couette Flow)

We consider the two-dimensional stationary Navier-Stokes problem (2) on the rectangular domain $\Omega := (0, 10) \times (0, 1) \subset \mathbb{R}^2$, with boundary conditions corresponding to plane shear flow as described in the preceding section. Linearization about this base solution results in the nonsymmetric eigenvalue problem

$$-\nu\Delta v_1 + x_2\partial_1 v_1 + v_2 + \partial_1 p = \lambda v_1,$$

Table 2 Computational results for the most critical eigenvalue $\lambda^{\text{crit}} = 2.1228\ldots$ of the Burgers equation on uniform meshes ($\nu = 10^{-2}$)

h	N	$\lvert\lambda_h^1 - \lambda\rvert$	$\lvert\lambda_h - \lambda\rvert$	η_ω^λ	$\lVert v_h^* \rVert$
2^{-3}	162	3.24e-2	7.07e-3	1.25e-2	19.3
2^{-4}	578	1.79e-2	1.80e-3	2.77e-3	38.8
2^{-5}	2178	9.42e-3	4.55e-4	6.54e-4	77.9
2^{-6}	8450	4.82e-3	1.16e-4	1.39e-4	155.9
2^{-7}	33282	2.43e-3	3.11e-5	3.47e-5	311.9
2^{-8}	132098	1.21e-3	8.02e-6	8.58e-6	623.9
order		$\mathcal{O}(h)$	$\mathcal{O}(h^2)$	$\mathcal{O}(h^2)$	$\mathcal{O}(h^{-1})$

$$
\begin{aligned}
-\nu\Delta v_2 + x_2\partial_1 v_2 \qquad\quad + \partial_2 p &= \lambda v_2,\\
\partial_1 v_1 + \partial_2 v_2 &= 0.
\end{aligned}
$$

for $v = \{v_1, v_2\}$, with homogeneous boundary conditions. Again all eigenvalues have positive real parts (see Landahl [17] and Gustavsson [9]). Hence linearized stability theory would predict stability for any Reynolds number $\text{Re} = 1/\nu$. However, experiments show transition to turbulence for $\text{Re} = 300 - 1,500$ depending on the experimental set-up. Since numerical computations indicate that the critical eigenvalues are non-deficient the explanation of this discrepancy between theory and experiment has to be sought in the possibly large pseudo-spectrum of these critical eigenvalues λ^{crit}. For a more detailed discussion of this aspect see Schmid and Henningson [21] and the literature cited therein.

8.3 Stability of Drag-Minimal Flow

We consider the optimal control configuration described in Sect. 2. The question is that of the stability of the computed stationary optimal flow state $\hat{u} = \{\hat{v}, \hat{p}\}$ shown in Fig. 2. The locally refined mesh for the optimization cycle produced by the adaptive algorithm seems to contradict intuition since the recirculation behind the cylinder is not so well resolved. However, due to the particular structure of the optimal velocity field (most of the flow leaves the domain at the control boundary), it might be clear that this recirculation does not significantly influence the drag value. Instead, a strong local refinement near the cylinder, where the drag is evaluated, as well as near the control boundary is produced. However, the structure of the flow field of the drag-minimal solution, which has actually been calculated in a post-processing step on a finer mesh, indicates that this stationary flow may not be (dynamically) stable and hence not physical. To test this, we consider the corresponding stability eigenvalue problem (1). The state equation (7) has been solved for several values of the control P with mesh adaptation on the basis of the corresponding a posteriori error estimator. Figure 4 displays the real and imaginary parts of the computed critical eigenvalue λ^{crit} as function of the control mean pressure P. The "optimal" control pressure for the stationary model is around $P = 0.5$

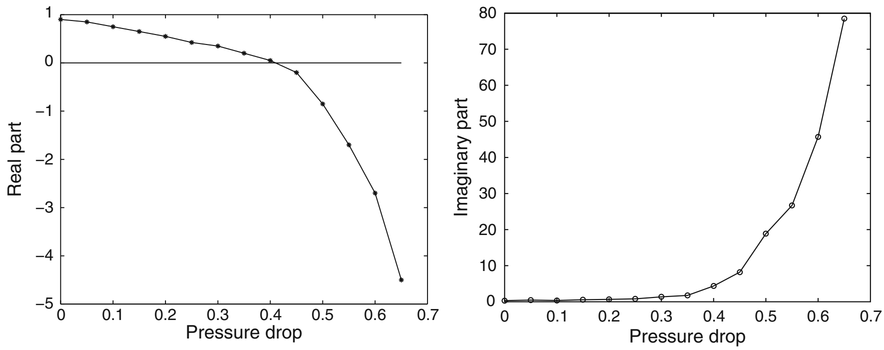

Fig. 4 Real and imaginary parts of the critical eigenvalue as function of the control pressure

and the corresponding flow state actually turns out to be unstable, Heuveline and Rannacher [11].

To test the reliability of this numerical stability analysis, we use the quality criterion (49) stated in Sect. 7.3, i.e., the computed eigenvalue is accepted only if the indicator for the error caused by the inexact computation of the base flow, i.e. the coefficient in the stability eigenvalue problem, is significantly smaller than that due to the discretization of the eigenvalue problem itself. Figure 5 shows the development of these two components in the eigenvalue error estimator $\eta_h^\lambda(\hat{u}_h, \hat{u}_h^*, u_h, u_h^*, \lambda_h)$ within the mesh refinement process. On coarse meshes the error in approximating the base solution dominates while under further mesh refinement this error becomes smaller than that of the eigenvalue approximation. In particular, we see that on the finest mesh shown in Fig. 5, which is adapted in accordance to the drag minimization process, we can reliably predict the instability of the corresponding flow state, Heuveline and Rannacher [11].

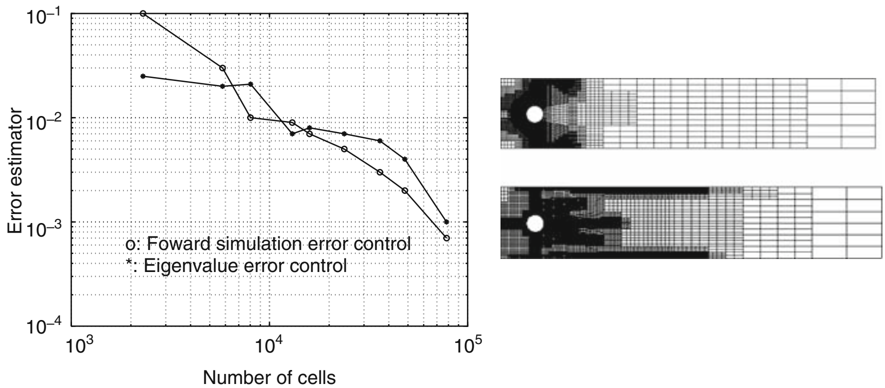

Fig. 5 The size of the two components of the error estimator $\eta_h^\lambda(\hat{u}_h, \hat{u}_h^*, u_h, u_h^*, \lambda_h)$, i.e. the errors in the base solution and the eigenvalue approximation, and automatically adapted meshes for the optimization process (*top*) and the eigenvalue computation (*bottom*)

References

1. I. Babuska and J.E. Osborn, Eigenvalue problems. Finite Element Methods, *Handbook of Numerical Analysis*, Vol. 2, Part 1 (P.G. Ciarlet and J.L. Lions, eds), pp. 641–792, Elsevier, The Netherland (1991)
2. W. Bangerth and R. Rannacher, *Adaptive Finite Element Methods for Differential Equations*. Birkhäuser, Basel-Boston-Berlin (2003)
3. R. Becker, Mesh adaptation for stationary flow control. J. Math. Fluid Mech. **3**, 317–341 (2001)
4. R. Becker, V. Heuveline, and R. Rannacher, An optimal control approach to adaptivity in computational fluid mechanics. Int. J. Numer. Meth. Fluids **40**, 105–120 (2002)
5. R. Becker and R. Rannacher, An optimal control approach to error control and mesh adaptation in finite element methods. *Acta Numerica 2001* (A. Iserles, ed.), Cambridge University Press, Cambridge (2001)
6. P.G. Ciarlet, *Finite Element Methods for Elliptic Problems*. North-Holland, Amsterdam (1978)
7. G.P. Galdi, *An Introduction to the Mathematical Theory of the Navier-Stokes Equations. Vol. 1: Linearized Steady Problems, Vol. 2: Nonlinear Steady Problems*. Springer, Berlin-Heidelberg-New York (1998)
8. V. Girault and P.A. Raviart, *Finite Element Methods for Navier-Stokes Equations*. Springer, Berlin-Heidelberg (1986)
9. H. Gustavsson, Energy growth of three-dimensional disturbances in plane Couette flow. J. Fluid Mech. **98**, 149–159 (1991)
10. V. Heuveline and R. Rannacher, A posteriori error control for finite element approximations of elliptic eigenvalue problems. J. Comput. Math. Appl. **15**, 107–138 (2001)
11. V. Heuveline and R. Rannacher, Adaptive FE eigenvalue approximation with application to hydrodynamic stability analysis. Proceedings of the international conference on Advances in Numerical Mathematics, Moscow, Sept. 16–17, 2005 (W. Fitzgibbon et al., eds), pp. 109–140, Institute of Numerical Mathematics RAS, Moscow, (2006)
12. V. Heuveline and R. Rannacher, *Solution of Stability Eigenvalue Problems by Adaptive Finite Elements with Application in Hydrodynamic Stability Theory*. Institute of Applied Mathematics, University of Heidelberg, Germany Preprint (2007)
13. T.J.R. Hughes and A.N. Brooks, Streamline upwind/Petrov Galerkin formulations for convection dominated flows with particular emphasis on the incompressible Navier-Stokes equation. Comp. Math. Appl. Mech. Eng. **32**, 199–259 (1982)
14. T.J.R. Hughes, L.P. Franca, and M. Balestra, A new finite element formulation for computational fluid dynamics: V. Circumvent the Babuska-Brezzi condition: A stable Petrov-Galerkin formulation for the Stokes problem accomodating equal order interpolation. Comp. Meth. Appl. Mech. Eng. **59**, 89–99 (1986)
15. C. Johnson, R. Rannacher, and M. Boman, Numerics and hydrodynamic stability: Towards error control in CFD. SIAM J. Numer. Anal. **32**, 1058–1079 (1995)
16. T. Kato, *Perturbation Theory for Linear Operators*. Springer, Berlin-Heidelberg-New York (1966)
17. M. Landahl, A note on an algebraic instability of viscous parallel shear flows. J. Fluid Mech. **98**, 243 (1980)
18. J.E. Osborn, Spectral approximation for compact operators. Math. Comp. **29**, 712–725 (1975)
19. R. Rannacher, Finite element methods for the incompressible Navier-Stokes equations. In *Fundamental Directions in Mathematical Fluid Mechanics* (G.P. Galdi, J. Heywood, R. Rannacher, eds), pp. 191–293, Birkhäuser, Basel-Boston-Berlin (2000)
20. R. Rannacher, Lectures on numerical flow simulation: Finite element discretization, numerical boundary conditions and automatic mesh adaptation. In *Hemodynamical Flows: Aspects of Modeling, Analysis and Simulation* (G.P. Galdi et al., eds), Birkhäuser, Basel-Boston-Berlin (2008)

21. P.J. Schmid and D.S. Henningson. *Stability and Transition in Shear Flows*. Springer, New York (2000)
22. L.N. Trefethen and M. Embree. *Spectra and Pseudospectra: The Behavior of Nonnormal Matrices and Operators*. Princeton University Press, Princeton and Oxford (2005)

Numerical Simulation of Laminar Incompressible Fluid-Structure Interaction for Elastic Material with Point Constraints

Mudassar Razzaq, Jaroslav Hron, and Stefan Turek

Abstract We present numerical techniques for solving the problem of fluid structure interaction with a compressible elastic material in a laminar incompressible viscous flow via fully coupled monolithic Arbitrary Lagrangian-Eulerian (ALE) formulation. The mathematical description and the numerical schemes are designed in such a way that more complicated constitutive relations can be easily incorporated. The whole domain of interest is treated as one continuum and we utilize the well known Q_2P_1 finite element pair for discretization in space to gain high accuracy. We perform numerical comparisons for different time stepping schemes, including variants of the Fractional-Step-θ-scheme, Backward Euler and Crank-Nicholson scheme for both solid and fluid parts. The resulting nonlinear discretized algebraic system is solved by a quasi-Newton method which approximates the Jacobian matrices by the divided differences approach and the resulting linear systems are solved by a geometric multigrid approach. In the numerical examples, a cylinder with attached flexible beam is allowed to freely rotate around its axis which requires a special numerical treatment. By identifying the center of the cylinder with one grid point of the computational mesh we prescribe a Dirichlet type boundary condition for the velocity and the displacement of the structure at this point, which allows free rotation around this point. We present numerical studies for different problem parameters on various mesh types and compare the results with experimental values from a corresponding benchmarking experiment.

Keywords Fluid-structure interaction · Monolithic FEM · Incompressible Navier-Stokes equations · ALE · Multigrid

1 Introduction

We consider the problem of viscous fluid flow interacting with an elastic body which is being deformed by the fluid action. Such a problem is encountered in many real life applications of great importance. Typical examples of this type of problem are

S. Turek (✉)
Institute of Applied Mathematics, TU Dortmund, Germany
e-mail: ture@featflow.de

R. Rannacher, A. Sequeira (eds.), *Advances in Mathematical Fluid Mechanics*,
DOI 10.1007/978-3-642-04068-9_27,

the areas of biomedical fluids which include joint lubrication and deformable cartilage and blood flow interaction with implants. The theoretical investigation of fluid structure interaction problems is complicated by the need of a mixed description. While for the solid part the natural view is the material (Lagrangian) description, for the fluid it is the spatial (Eulerian) description. In the case of their combination some kind of mixed description (usually referred to as the Arbitrary Lagrangian-Eulerian description or ALE) has to be used which brings additional nonlinearity into the resulting equations.

A numerical solution of the resulting equations of the fluid structure interaction problem poses great challenges since it includes the features of elasticity, fluid mechanics and their coupling. The easiest solution strategy, mostly used in the available software packages, is to decouple the problem into the fluid part and solid part, for each of those parts using some well established method of solution; then the interaction process is introduced as external boundary conditions in each of the subproblems. This has the advantage that there are many well tested numerical methods for both separate problems of fluid flow and elastic deformation, while on the other hand the treatment of the interface and the interaction is problematic. In contrast, the approach presented here treats the problem as a single continuum with the coupling automatically taken care of as internal interface, which in our formulation does not require any special treatment.

2 Fluid-Structure Interaction Problem Formulation

A general fluid structure interaction problem consists of the description of the fluid and solid fields, appropriate interface conditions at the interface and conditions for the remaining boundaries, respectively. In this paper, we consider the flow of an incompressible Newtonian fluid interacting with an elastic solid. We denote the domain occupied by the fluid by Ω_t^f and the solid by Ω_t^s at the time $t \in [0, T]$. Let $\Gamma_t^0 = \bar{\Omega}_t^f \cap \bar{\Omega}_t^s$ be the part of the boundary where the elastic solid interacts with the fluid.

In the following, the fields and interface conditions are introduced. Furthermore, problem configurations and solution procedure for each of the fields is presented in detail.

2.1 Fluid

The fluid is considered to be *Newtonian, incompressible* and its state is described by the *velocity* and *pressure* fields $\mathbf{v^f}$, p^f respectively. The constant density of the fluid is ϱ^f and the kinematic viscosity is denoted by ν^f. The balance equations are:

$$\varrho^f \frac{D\boldsymbol{v}^f}{Dt} = \operatorname{div} \sigma^f, \quad \operatorname{div} \boldsymbol{v}^f = 0 \quad \text{in} \quad \Omega_t^f \tag{1}$$

In order to solve the balance equations we need to specify the constitutive relations for the stress tensors. For the fluid we use the incompressible Newtonian relation

$$\boldsymbol{\sigma}^f = -p^f \mathbf{I} + \mu(\operatorname{grad} \mathbf{v}^f + (\operatorname{grad} \mathbf{v}^f)^T), \tag{2}$$

where μ represents the dynamic viscosity of the fluid and p^f is the Lagrange multiplier corresponding to the incompressibility constraint in (1). The material time derivative depends on the choice of the reference system. There are basically 3 alternative reference systems: the Eulerian, the Lagrangian, and the Arbitrary Lagrangian Eulerian formulation. The most commonly used description for the fluid structure interaction is the ALE description. For the ALE formulation presented in this paper, discretization techniques are discussed in Sect. 3.

2.2 Structure

The structure is assumed to be *elastic* and *compressible*. Its configuration is described by the displacement $\mathbf{u}^\mathbf{s}$, with velocity field $\mathbf{v}^\mathbf{s} = \frac{\partial \boldsymbol{u}^s}{\partial t}$. The balance equations are:

$$\varrho^s \frac{\partial \boldsymbol{v}^s}{\partial t} + \varrho^s (\nabla \boldsymbol{v}^s)\boldsymbol{v}^s = \operatorname{div} \sigma^s + \varrho^s \mathbf{g}, \quad \text{in} \quad \Omega_t^s. \tag{3}$$

Written in the more common Lagrangian description, i.e. with respect to some fixed reference (initial) state Ω^s, we have

$$\varrho^s \frac{\partial^2 \mathbf{u}^\mathbf{s}}{\partial t^2} = \operatorname{div}(J\sigma^s F^{-T}) + \varrho^s \mathbf{g}, \quad \text{in} \quad \Omega^s. \tag{4}$$

The constitutive relations for the stress tensors for the compressible structure are presented, however, also incompressible structures can be handled in the same way. The density of the structure in the undeformed configuration is ϱ^s. The material elasticity is characterized by a set of two parameters, the Poisson ratio ν^s and the Young modulus E. Alternatively, the characterization is described by the Lamé coefficients λ^s and the shear modulus μ^s. These parameters satisfy the following relations

$$\nu^s = \frac{\lambda^s}{2(\lambda^s + \mu^s)} \qquad E = \frac{\mu^s(3\lambda^s + 2\mu^2)}{(\lambda^s + \mu^s)} \tag{5}$$

$$\mu^s = \frac{E}{2(1 + \nu^s)} \quad \lambda^s = \frac{\nu^s E}{(1 + \nu^s)(1 - 2\nu^s)}, \tag{6}$$

where $\nu^s = 1/2$ for a incompressible and $\nu^s < 1/2$ for a compressible structure. In the large deformation case it is common to describe the constitutive equation using a stress-strain relation based on the Green Lagrangian strain tensor E and the 2.Piola-Kirchhoff stress tensor $S(E)$ as a function of E. The 2.Piola-Kirchhoff stress can be obtained from the Cauchy stress σ^s as

$$S^s = JF^{-1}\sigma^s F^{-T}, \tag{7}$$

and the Green-Lagrange tensor E as

$$E = \frac{1}{2}(F^T F - I). \tag{8}$$

In this paper, the material is specified by giving the Cauchy stress tensor σ^s by the following constitutive law for the *St.Venant-Kirchhoff material* for simplicity

$$\sigma^s = \frac{1}{J}\mathbf{F}(\lambda^s(trE)I + 2\mu^s E)\mathbf{F}^T \qquad \mathbf{S}^s = \lambda^s(trE)I + 2\mu^s E. \tag{9}$$

J denotes the determinant of the deformation gradient tensor F, defined as $F = I + \nabla\mathbf{u^s}$.

2.3 Interaction Condition

The boundary conditions on the fluid solid interface are assumed to be

$$\sigma^f n = \sigma^s n, \quad \mathbf{v}^f = \mathbf{v}^s, \quad \text{on} \quad \Gamma_t^0, \tag{10}$$

where n is a unit normal vector to the interface Γ_t^0. This implies the no-slip condition for the flow and that the forces on the interface are in balance.

3 Discretization and Solution Techniques

The common solution approach is a separate discretization in space and time. We first discretize in time by one of the usual methods known from the treatment of ordinary differential equations, such as the Backward Euler (BE), the Crank-Nicholson (CN), Fractional-Step-θ-scheme (FS) or a new modified Fractional-Step-θ-scheme (GL). Properties of these time stepping schemes applying on incompressible Navier-Stokes equations are described in detail below.

3.1 Time Discretization

We consider numerical solution techniques for the incompressible Navier-Stokes equations

$$\boldsymbol{v}_t - \nu\Delta\boldsymbol{v} + \boldsymbol{v}\cdot\text{grad}\,\boldsymbol{v} + \text{grad}\,p = \mathbf{f}, \quad \text{div}\,\boldsymbol{v} = 0, \quad \text{in} \quad \Omega\times(0,T], \tag{11}$$

for given force $\mathbf{f}$ and viscosity ν, with prescribed boundary values on the boundary $\partial\Omega$ and an initial condition at $t = 0$.

3.1.1 Basic θ-Scheme

Given $\boldsymbol{v}^n$ and $K = t_{n+1} - t_n$, then solve for $\boldsymbol{v} = \boldsymbol{v}^{n+1}$ and $p = p^{n+1}$

$$\frac{\boldsymbol{v} - \boldsymbol{v}^n}{K} + \theta[-\nu\Delta\boldsymbol{v} + \boldsymbol{v}\cdot\operatorname{grad}\boldsymbol{v}] + \operatorname{grad} p = \mathbf{g}^{n+1}, \quad \operatorname{div}\boldsymbol{v} = 0, \quad \text{in} \quad \Omega \tag{12}$$

with right hand side $\mathbf{g}^{n+1} := \theta\mathbf{f}^{n+1} + (1-\theta)\mathbf{f}^n - (1-\theta)[-\nu\Delta\boldsymbol{v}^n + \boldsymbol{v}^n\cdot\operatorname{grad}\boldsymbol{v}^n]$.

The parameter θ has to be chosen depending on the time-stepping scheme, e.g., $\theta = 1$ for the Backward Euler, or $\theta = 1/2$ for the Crank-Nicholson-scheme. The pressure term $\operatorname{grad} p = \operatorname{grad} p^{n+1}$ may be replaced by $\theta \operatorname{grad} p^{n+1} + (1-\theta)\operatorname{grad} p^n$, but, with appropriate post processing, both strategies lead to solutions of the same accuracy. In all cases, we end up with the task of solving, at each time step, a nonlinear saddle point problem of given type which has then to be discretized in space.

In the past, explicit time-stepping schemes have been commonly used in non-stationary flow calculations, but because of the severe stability problems inherent in this approach, the required small time steps prohibit the efficient treatment of long time flow simulations. Due to the high stiffness, one should prefer implicit schemes in the choice of time-stepping methods for solving this problem. Since implicit methods have become feasible thanks to more efficient nonlinear and linear solvers, the schemes most frequently used are still either the simple first-order Backward Euler scheme (BE), with $\theta = 1$, or more preferably the second-order Crank-Nicholson scheme (CN), with $\theta = 1/2$.

These two methods belong to the group of *One-Step-θ-schemes*. The CN scheme occasionally suffers from numerical instabilities because of its only weak damping property (not strongly A-stable), while the BE-scheme is of first order accuracy only (however: it is a good candidate for steady-state simulations). Another method which has proven to have the potential to excel in this competition is the Fractional-Step-θ-scheme (FS). It uses three different values for θ and for the time step K at each time level.

We define a time step with $K = t_{n+1} - t_n$ in the case of the Backward Euler or the Crank-Nicholson scheme, with the same θ ($\theta = 0.5$ or $\theta = 1$) as above. In the following, we use the more compact form for the diffusive and advective part:

$$N(\boldsymbol{v})\boldsymbol{v} = -\nu\Delta\boldsymbol{v} + \boldsymbol{v}\cdot\operatorname{grad}\boldsymbol{v} \tag{13}$$

3.1.2 Backward Euler-Scheme

$$[I + KN(\boldsymbol{v}^{n+1})]\boldsymbol{v}^{n+1} + \operatorname{grad} p^{n+1} = \boldsymbol{v}^n + K\mathbf{f}^{n+1}$$
$$\operatorname{div}\boldsymbol{v}^{n+1} = 0$$

3.1.3 Crank-Nicholson-Scheme

$$\left[I + \frac{K}{2}N(\boldsymbol{v}^{n+1})\right]\boldsymbol{v}^{n+1} + \text{grad}\, p^{n+1} = [I - \frac{K}{2}N(\boldsymbol{v}^{n})]\boldsymbol{v}^{n} + \frac{K}{2}\mathbf{f}^{n+1} + \frac{K}{2}\mathbf{f}^{n}$$
$$\text{div}\, \boldsymbol{v}^{n+1} = 0$$

3.1.4 Fractional-Step-θ-Scheme

For the Fractional-Step-θ-scheme we proceed as follows. Choosing $\theta = 1 - \frac{\sqrt{2}}{2}$, $\theta' = 1-2\theta$, and $\alpha = \frac{1-2\theta}{1-\theta}$, $\beta = 1-\alpha$, the macro time step $t_n \to t_{n+1} = t_n + K$ is split into the three following consecutive sub steps (with $\tilde{\theta} := \alpha\theta K = \beta\theta' K$):

$$[I + \tilde{\theta}N(\boldsymbol{v}^{n+\theta})]\boldsymbol{v}^{n+\theta} + \text{grad}\, p^{n+\theta} = [I - \beta\theta K N(\boldsymbol{v}^{n})]\boldsymbol{v}^{n} + \theta K\mathbf{f}^{n}$$
$$\text{div}\, \boldsymbol{v}^{n+\theta} = 0$$

$$\begin{aligned}[I + \tilde{\theta}N(\boldsymbol{v}^{n+1-\theta})]\boldsymbol{v}^{n+1-\theta} + \text{grad}\, p^{n+1-\theta} &= [I - \alpha\theta' K N(\boldsymbol{v}^{n+\theta})]\boldsymbol{v}^{n+\theta} \\ &\quad +\theta' K\mathbf{f}^{n+1-\theta} \\ \text{div}\, \boldsymbol{v}^{n+1-\theta} &= 0 \\ [I + \tilde{\theta}N(\boldsymbol{v}^{n+1})]\boldsymbol{v}^{n+1} + \text{grad}\, p^{n+1} &= [I - \beta\theta K N(\boldsymbol{v}^{n+1-\theta})]\boldsymbol{v}^{n+1-\theta} \\ &\quad +\theta K\mathbf{f}^{n+1-\theta} \\ \text{div}\, \boldsymbol{v}^{n+1} &= 0\end{aligned}$$

3.1.5 A Modified Fractional-Step-θ-Scheme

Consider an initial value problem of the following form, with $X(t) \in \mathbf{R}^d$, $d \geq 1$:

$$\begin{cases} \dfrac{dX}{dt} = f(X,t) \quad \forall t > 0 \\ X(0) = X_0 \end{cases} \tag{14}$$

Then, a modified θ-scheme (see [1, 2]) with macro time step Δt can be written again as three consecutive sub steps, where $\theta = 1 - 1/\sqrt{2}$, $X^0 = X_0$, $n \geq 0$ and X^n is known:

$$\begin{aligned}\frac{X^{n+\theta} - X^n}{\theta\Delta t} &= f\left(X^{n+\theta}, t^{n+\theta}\right) \\ X^{n+1-\theta} &= \frac{1-\theta}{\theta}X^{n+\theta} + \frac{2\theta - 1}{\theta}X^n \\ \frac{X^{n+1} - X^{n+1-\theta}}{\theta\Delta t} &= f\left(X^{n+1}, t^{n+1}\right)\end{aligned}$$

As shown in [2], the most important properties of this θ-scheme are that

- it is fully implicit;
- it is strongly A-stable;
- it is second order accurate (in fact, it is "nearly" third order accurate [2]).

These properties promise some advantageous behavior, particularly in implicit CFD simulations for nonstationary incompressible flow problems. Applying one step of this scheme to the Navier-Stokes equations, we obtain the following variant of the scheme:

$$1. \quad \begin{cases} \dfrac{\boldsymbol{v}^{n+\theta} - \boldsymbol{v}^{n}}{\theta \Delta t} + N(\boldsymbol{v}^{n+\theta})\boldsymbol{v}^{n+\theta} + \operatorname{grad} p^{n+\theta} = \mathbf{f}^{n+\theta} \\ \operatorname{div} \mathbf{v}^{n+\theta} = 0 \end{cases}$$

$$2. \quad \boldsymbol{v}^{n+1-\theta} = \tfrac{1-\theta}{\theta}\boldsymbol{v}^{n+\theta} + \tfrac{2\theta-1}{\theta}\boldsymbol{v}^{n}$$

$$3. \quad \begin{cases} \dfrac{\boldsymbol{v}^{n+1} - \boldsymbol{v}^{n+1-\theta}}{\theta \Delta t} + N(\boldsymbol{v}^{n+1})\boldsymbol{v}^{n+1} + \operatorname{grad} \widetilde{p}^{n+1} = \mathbf{f}^{n+1} \\ \operatorname{div} \mathbf{v}^{n+1} = 0 \end{cases}$$

$$3b. \quad p^{n+1} = (1-\theta)p^{n+\theta} + \theta\widetilde{p}^{n+1}$$

These 3 substeps build one macro time step and have to be compared with the previous description of the Backward Euler, Crank-Nicholson and the classical Fractional-Step-θ-scheme which all have been formulated in terms of a macro time step with 3 sub steps, too. Then, the resulting accuracy and numerical cost are better comparable and the rating is fair. The main difference to the previous "classical" FS scheme is that substeps 1. and 3. look like a Backward Euler step while substep 2. is an extrapolation step only for previously computed data such that no operator evaluations at previous time steps are required.

Substep 3b. can be viewed as postprocessing step for updating the new pressure which however is not a must. In fact, in our numerical tests [1] we omitted this substep 3b. and accepted the pressure from substep 3. as final pressure approximation, that means $p^{n+1} = \widetilde{p}^{n+1}$.

Summarizing, one obtains that the numerical effort of the modified scheme for each substep is cheaper – at least for "small" time steps (treatment of the nonlinearity) and complex right hand side evaluations while the resulting accuracy is similar. Incidentally, the modified θ-scheme is a *Runge-Kutta* one; it has been derived in [2] as a particular case of the Fractional-Step-θ-scheme.

3.2 Space Discretization

Our treatment of the fluid structure-interaction problem as one system suggests that we use the same finite elements for both the solid part and the fluid region. Since the fluid is incompressible we have to choose a pair of finite element spaces known to be stable for problems with incompressibility constraint.

3.2.1 The Conforming Element $Q_2 P_1$

One possible choice is the conforming biquadratic, discontinuous linear $Q_2 P_1$ pair, see Fig. 1 for the location of the degrees of freedom. This choice results in 39 degrees of freedom per element in the case of displacement, velocity, pressure formulation in two dimensions and 112 degrees of freedom per element in three dimensions. Let us define the following spaces

$$
\begin{aligned}
U &= \{\mathbf{u} \in L^\infty(I, [W^{1,2}(\Omega)]^3), \mathbf{u} = 0 \text{ on } \partial\Omega\},\\
V &= \{\mathbf{v} \in L^2(I, [W^{1,2}(\Omega_t)]^3) \cap L^\infty(I, [L^2(\Omega_t)]^3), \mathbf{v} = 0 \text{ on } \partial\Omega\},\\
P &= \{p \in L^2(I, L^2(\Omega))\},
\end{aligned}
$$

then the variational formulation of the fluid-structure interaction problem is to find $(\mathbf{u}, \mathbf{v}, p) \in U \times V \times P$ such that the equations are satisfied for all $(\boldsymbol{\zeta}, \boldsymbol{\xi}, \gamma) \in U \times V \times P$ including appropriate initial conditions. The spaces U, V, P on an interval $[t^n, t^{n+1}]$ would be approximated in the case of the Q_2, P_1 pair as

$$
\begin{aligned}
U_h &= \{\mathbf{u}_h \in [C(\Omega_h)]^2, \mathbf{u}_h|_T \in [Q_2(T)]^2 \quad \forall T \in \mathcal{T}_h, \mathbf{u}_h = 0 \text{ on } \partial\Omega\},\\
V_h &= \{\mathbf{v}_h \in [C(\Omega_h)]^2, \mathbf{v}_h|_T \in [Q_2(T)]^2 \quad \forall T \in \mathcal{T}_h, \mathbf{v}_h = 0 \text{ on } \partial\Omega\},\\
P_h &= \{p_h \in L^2(\Omega_h), p_h|_T \in P_1(T) \quad \forall T \in \mathcal{T}_h\}.
\end{aligned}
$$

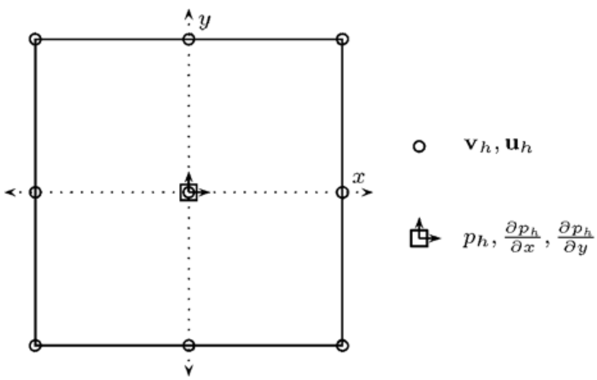

Fig. 1 Location of the degrees of freedom for the $Q_2 P_1$ element

Let us denote by $\mathbf{u}_h^n$ the approximation of $\mathbf{u}(t^n)$, $\mathbf{v}_h^n$ the approximation of $\mathbf{v}(t^n)$ and p_h^n the approximation of $p(t^n)$. Consider for each $T \in T_h$ the bilinear transformation $\psi_T : \hat{T} \to T$ to the unit square T. Then, $Q_2(T)$ is defined as

$$\mathrm{Q}_2(T) = \left\{ q \circ \psi_T^{-1} : q \in span < 1, x, y, xy, x^2, y^2, x^2 y, y^2 x, x^2 y^2 > \right\} \tag{15}$$

with nine local degrees of freedom located at the vertices, midpoints of the edges and in the center of the quadrilateral. The space $P_1(T)$ consists of linear functions defined by

$$\mathrm{P}_1(T) = \left\{ q \circ \psi_T^{-1} : q \in span < 1, x, y > \right\} \tag{16}$$

with the function value and both partial derivatives located in the center of the quadrilateral, as its three local degrees of freedom, which leads to a discontinuous pressure. The inf-sup condition is satisfied (see [3]); however, the combination of the bilinear transformation ψ with a linear function on the reference square $P_1(\widehat{T})$ would imply that the basis on the reference square did not contain the full basis. So, the method can at most be first order accurate on general meshes (see [3, 4])

$$\|p - p_h\| = O(h). \tag{17}$$

The standard remedy is to consider a local coordinate system (ξ, η) obtained by joining the midpoints of the opposing faces of T (see [4–6]). Then, we set on each element T

$$P_1(T) := span < 1, \xi, \eta > . \tag{18}$$

For this case, the inf-sup condition is also satisfied and the second order approximation is recovered for the pressure as well as for the velocity gradient (see [3, 7])

$$\|p - p_h\| = O(h^2) \quad \text{and} \quad \|\nabla(u - u_h)\|_0 = O(h^2). \tag{19}$$

For a smooth solution, the approximation error for the velocity in the L_2-norm is of order $O(h^3)$ which can easily be demonstrated for prescribed polynomials or for smooth data on appropriate domains.

3.3 Solution Algorithm

The system of nonlinear algebraic equations arising from the governing equations prescribed in Sects. 2.1 and 2.2 is

$$\begin{bmatrix} S_{uu} & S_{uv} & 0 \\ S_{vu} & S_{vv} & kB \\ c_u B_s^T & c_v B_f^T & 0 \end{bmatrix} \begin{bmatrix} \boldsymbol{u} \\ \boldsymbol{v} \\ p \end{bmatrix} = \begin{bmatrix} \mathbf{f_u} \\ \mathbf{f_v} \\ f_p \end{bmatrix} \tag{20}$$

which is typical saddle point problem, where S describes the diffusive and convective terms from the governing equations. The above system of nonlinear algebraic equations (20) is solved using Newton method as basic iteration. The basic idea of the Newton iteration is to find a root of a function, $\mathbf{R}(\mathbf{X}) = 0$, using the available known function value and its first derivative, where $\mathbf{X} = (\mathbf{u}_h, \mathbf{v}_h, p_h) \in U_h \times V_h \times P_h$. One step of the Newton iteration can be written as

$$\mathbf{X}^{n+1} = \mathbf{X}^n - \left[\frac{\partial \mathbf{R}}{\partial \mathbf{X}}(\mathbf{X}^n)\right]^{-1} \mathbf{R}(\mathbf{X}^n). \qquad (21)$$

This basic iteration can exhibit quadratic convergence provided that the initial guess is sufficiently close to the solution. To ensure the convergence globally, some improvements of this basic iteration are used. The damped Newton method with line search improves the chance of convergence by adaptively changing the length of the correction vector (Fig. 2). The solution update step in the Newton method (21) is replaced by

1. Let $\mathbf{X}^n$ be some starting guess.
2. Set the residuum vector $\mathbf{R}^n = \mathbf{R}(\mathbf{X}^n)$ and the tangent matrix $\mathsf{A} = \frac{\partial \mathbf{R}}{\partial \mathbf{X}}(\mathbf{X}^n)$.
3. Solve for the correction $\delta \mathbf{X}$
$$\mathsf{A}\delta \mathbf{X} = \mathbf{R}^n.$$
4. Find optimal step length ω.
5. Update the solution $\mathbf{X}^{n+1} = \mathbf{X}^n - \omega \delta \mathbf{X}$.

Fig. 2 One step of the Newton method with line search

$$\mathbf{X}^{n+1} = \mathbf{X}^n - \omega \delta \mathbf{X}, \qquad (22)$$

where the parameter ω is determined such that a certain error measure decreases (see [6, 8] for more details). The Jacobian matrix $\frac{\partial \mathbf{R}(\mathbf{X}^n)}{\partial \mathbf{X}}$ can be computed by finite differences from the residual vector $\mathbf{R}(\mathbf{X})$

$$\left[\frac{\partial \mathbf{R}}{\partial \mathbf{X}}\right]_{ij} (\mathbf{X}^n) \approx \frac{[\mathbf{R}]_i(\mathbf{X}^n + \alpha_j \mathbf{e}_j) - [\mathbf{R}]_i(\mathbf{X}^n - \alpha_j \mathbf{e}_j)}{2\alpha_j}, \qquad (23)$$

where $\mathbf{e}_j$ are the unit basis vectors in $\mathbb{R}^n$ and the coefficients α_j are adaptively taken according to the change in the solution in the previous time step. Since we know the sparsity pattern of the Jacobian matrix in advance, which is given by the used finite element method, this computation can be done in an efficient way so that the linear solver remains the dominant part in terms of the CPU time (see [6, 9] for more details).

3.4 Multigrid Solver

The solution of the linear problems is the most time consuming part of the solution process. A good candidate seems to be a direct solver for sparse systems like UMFPACK (see [10]); while this choice provides very robust linear solvers, its memory and CPU time requirements are too high for larger systems (i.e. more than 20.000 unknowns). Large linear problems can be solved by Krylov space methods (BiCGStab, GMRes, see [11]) with suitable preconditioners. One possibility is the ILU preconditioner with special treatment of the saddle point character of our system, where we allow certain fill-in for the zero diagonal blocks, see [12]. The alternative option for larger systems is the multigrid method presented in this section.

We also utilize a standard geometric multigrid approach based on a hierarchy of grids obtained by successive regular refinement of a given coarse mesh. The complete multigrid iteration is performed in the standard defect-correction setup with the V or F-type cycle. While a direct sparse solver [10] is used for the coarse grid solution, on finer levels a fixed number (2 or 4) of iterations by local MPSC schemes (Vanka-like smoother) [6, 13, 8] is performed. Such iterations can be written as

$$\begin{bmatrix} \boldsymbol{u}^{l+1} \\ \boldsymbol{v}^{l+1} \\ p^{l+1} \end{bmatrix} = \begin{bmatrix} \boldsymbol{u}^{l} \\ \boldsymbol{v}^{l} \\ p^{l} \end{bmatrix} - \omega \sum_{\text{element}\Omega_i} \begin{bmatrix} S_{\boldsymbol{uu}|\Omega_i} & S_{\boldsymbol{uv}|\Omega_i} & 0 \\ S_{\boldsymbol{vu}|\Omega_i} & S_{\boldsymbol{vv}|\Omega_i} & kB_{|\Omega_i} \\ c_{\boldsymbol{u}} B^T_{s|\Omega_i} & c_{\boldsymbol{v}} B^T_{f|\Omega_i} & 0 \end{bmatrix}^{-1} \begin{bmatrix} \mathbf{def}^l_{\boldsymbol{u}} \\ \mathbf{def}^l_{\boldsymbol{v}} \\ def^l_p \end{bmatrix}.$$

The inverse of the local systems (39×39) can be done by hardware optimized direct solvers. The full nodal interpolation is used as the prolongation operator P with its transposed operator used as the restriction $\mathsf{R} = \mathsf{P}^T$ (see [14, 6] for more details).

4 Objectives and Problem Configuration

The main objective of the following numerical investigation is to analyze and to validate our monolithic approach for a configuration with a point constraint ("rigid solid with rotational degree of freedom") for a special experimental set up. In the future, these numerical and experimental studies shall lead to a reliable data basis for the validation and comparison purposes of different numerical methods and code implementations for fluid-structure interaction simulations. These numerical studies are focused on the two-dimensional periodical swiveling motion of a simple flexible structure driven by a prescribed inflow velocity (see [15]). The structure has a linear mechanical behavior and the fluid is considered incompressible and in the laminar regime. The cylinder is fixed only at the center and can rotate freely. To allow for this kind of additional rotational movement in our method, the cylinder has to be included in the mesh in our recent approach. By prescribing zero displacement for

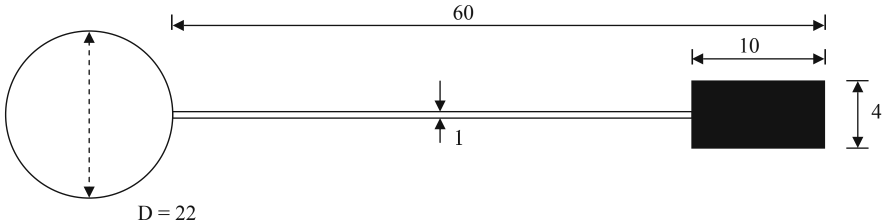

Fig. 3 Structure (dimensions in millimeters)

Table 1 Density values of the structure components

Cylinder	(aluminum)	2.828×10^{-6} kg/mm^3
Beam	(stainless steel)	7.855×10^{-6} kg/mm^3
Rear mass	(stainless steel)	7.800×10^{-6} kg/mm^3

the node located in the center of the cylinder we eliminate the translational degree of freedom of the whole structure but preserve the rotational freedom of the cylinder. Hence, the position of all other nodes located inside the cylinder are taken into account as part of the solution. We divided the numerical tests into two parts corresponding to the thickness of the elastic beam i.e for 1 mm thick beam and for 0.04 mm thick beam attached to an aluminum cylinder. At the trailing edge of the elastic beam a rectangular stainless steel mass is located. Both the rear mass and the cylinder are considered rigid. All the structure is free to rotate around an axis located in the center point of the cylinder. The detailed dimensions of the structure are presented in Fig. 3. The densities of the different materials used in the construction of the model are given in Table 1. The shear modulus of stainless steel is 7.58×10^{13} kg/mms^2 and Poisson ratio of the beam ν^p is taken as 0.3. The Young modulus is measured to be 200 kN/mm^2. As fluid for the tests, a Polyethylene glycol syrup is chosen because of its high viscosity and a density close to water. It has a kinematic viscosity 164 mm^2/s and the density of the fluid is 1.05×10^{-6} kg/mm^3.

4.1 Geometry of the Problem

The geometry of the physical domain coincides with the shape of the facility test function. The co-ordinate system used is centered in the rotating axis of the flexible structure front body. The x-axis is aligned with the incoming flow. Then, the geometric details are as follows:

- The overall dimensions of the physical domain are length $L = 338$ mm and width $W = 240$ mm.
- The center of the cylindrical front body is C which is located 55 mm downstream of the beginning of the physical domain, and the radius r is 11 mm.
- The dimensions of the flow field measuring domain (hatched line) are given by length $L' = 272$ mm and width $W' = 170$ mm. The measuring domain

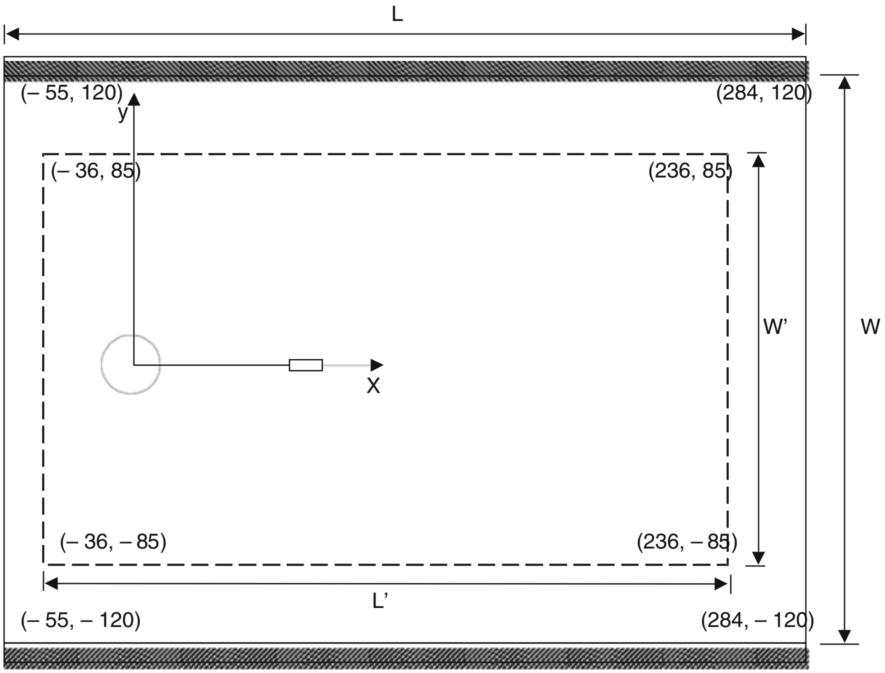

Fig. 4 Physical domain (*continuous line*) and flow field measuring domain (*hatched line*)

begins 19 mm after the beginning of the physical domain as shown in Fig. 4. The Reynolds number is defined by $\mathrm{Re} = \frac{2r\bar{V}}{\nu^f}$ with mean velocity $\bar{\mathbf{V}} = \frac{2}{3}v(0, W/2, t)$, r radius of the cylinder and W height of the channel (see Fig. 4).

4.2 Boundary and Initial Conditions

The velocity profile prescribed at the left channel inflow is defined as approximation of the experimental inflow data

$$\mathbf{v}^f(0, y) = \bar{U}(1 - (y/120)^8)(1 + (y/120)^8), \qquad (24)$$

such that the maximum of the inflow velocity profile is $\bar{U}$. The outflow condition effectively prescribes some reference value for the pressure variable p. While this value could be arbitrarily set in the incompressible case, in the case of a compressible structure this will have influence onto the stress and consequently the deformation of the solid. The no-slip condition is prescribed for the fluid on the other boundary parts, i.e. top and bottom wall, circle and fluid-structure interface Γ_t^0. Suggested starting procedure for the non-steady tests is to use a smooth increase of the velocity profile in time as

$$\mathbf{v}^f(t,0,y) = \begin{cases} \mathbf{v}^f(0,y)\dfrac{1-cos(\pi t/2)}{2} & if \quad t<1 \\ \mathbf{v}^f(0,y) & \text{otherwise} \end{cases} \tag{25}$$

where $\mathbf{v}^f(0, y)$ is the velocity profile given in (24). Since the cylinder is allowed to freely rotate around its axis, we need to incorporate this into our setup. As described before, by identifying the center of the cylinder with one grid point of our mesh we can prescribe a Dirichlet type boundary condition for the velocity and the displacement of the structure at this point. This point constraint effectively fixes the position of the cylinder axis, but still allows the free rotation around this point.

5 Experimental Results

Experimental studies on reference test cases were conducted in laminar flows (Re $\leq$ 200) at the Institute of Fluid Mechanics at University of Erlangen-Nürnberg (see [15]). The structure was defined to be constituted by a 0.04 mm thick stainless steel sheet attached to an 22 mm diameter aluminum cylindrical front body. At the trailing edge of the beam a 10 mm $\times$ 4 mm rectangular stainless steel mass was located. All the structure was free to rotate around an axis located in the center point of the front cylinder. Both the front cylinder and the rear mass were considered rigid. The structure model was tested in a viscous liquid flow at different velocities up to 2000 mm/s. The minimum velocity needed for the movement of the structure slightly varied from test to test. In most of the cases it was already possible to achieve a consistent swiveling motion for velocities slightly smaller than 1000 mm/s. The frequency of the structure movement increased linearly with the velocity of the approaching fluid. For velocity ranging from 1140 to 1300 mm/s, the frequency of oscillations showed a pronounced hysteresis depending on increasing versus decreasing flow velocity. There were two test cases performed using different flow velocity and the corresponding results were as follows: Using velocity 1080 mm/s (Re $\approx$ 145) one measures a frequency of oscillations of the structure $\approx$ 6 Hz, and with velocity 1450 mm/s (Re $\approx$ 195) a frequency of oscillations of the structure $\approx$ 13.58 Hz is observed. At higher velocities the motion of the structure became faster and more complex. At around 1300 mm/s the structure shifted abruptly to a new swiveling mode in which the second deflection mode played an important role.

6 Numerical Investigations

In this section we will present numerical results for the 1 mm thick beam and preliminary calculations for the 0.04 mm thick beam.

6.1 Results for 1 mm Thick Beam

Experimental studies are conducted taking a 0.04 mm thick beam. However, in the first numerical test we set the thickness of the beam 1 mm (see Fig. 3) and also we reduce the rigidity of the beam (i.e., shear modulus) from 7.69×10^{7} to 7.69×10^{4} kg/mms^2 to make the problem numerically easier, all other parameters are from Table 1. We applied the presented time stepping schemes, namely (BE, CN, FS, GL) prescribed in Sect. 3.1 to analyze the behavior for different Δt. For $\Delta t = 0.0005$ almost the identical amplitude of oscillations (≈ 13.84) of rear mass is observed (see Fig. 7) for the higher order schemes (CN, FS, GL) and for the 1st order Backward Euler (BE) the amplitude of oscillations ($\approx$ 12.42) of rear mass shows 10% less accuracy compared to CN, FS and GL. For $\Delta t = 0.00005$ Backward Euler (BE) shows better agreement of the amplitude of oscillations (≈ 13.71) of the rear mass to CN, FS, GL. For larger time step, GL is more damped than CN and FS. We use two different meshes (see Figs. 5 and 6) and also we increase the mesh refinement level from level 1 to level 2. Corresponding plots for two different meshes and different mesh refinement levels are given in Figs. 8 and 9 which shows that our solution is almost independent of mesh type and mesh refinement levels. From experimental results, for velocity 1130 mm/s the structure shows hysteric behavior, but in our simulations no hysteric behavior could be observed so far and resulting frequency of oscillations is $\approx$ 10 Hz for applying all the four time stepping schemes mentioned above as can be seen in the Figs. 10 and 11.

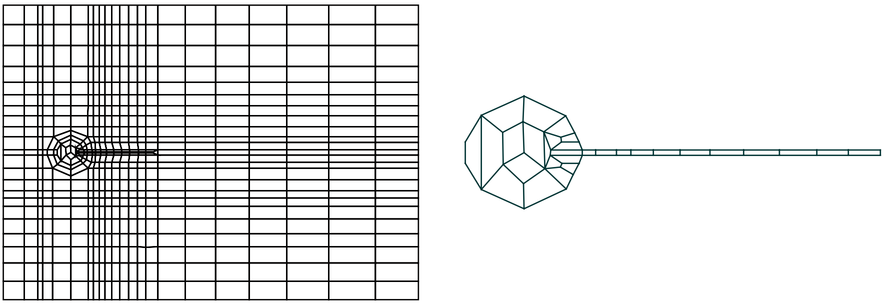

Fig. 5 Coarse mesh1 with 576 elements, 622 nodes and 11308 dof

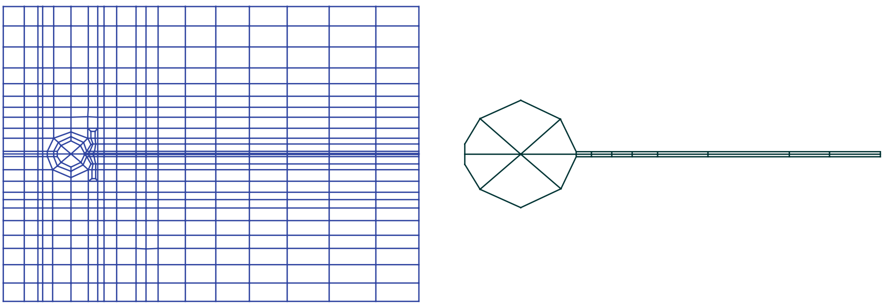

Fig. 6 Coarse mesh2 with 529 elements, 574 nodes and 10407 dof

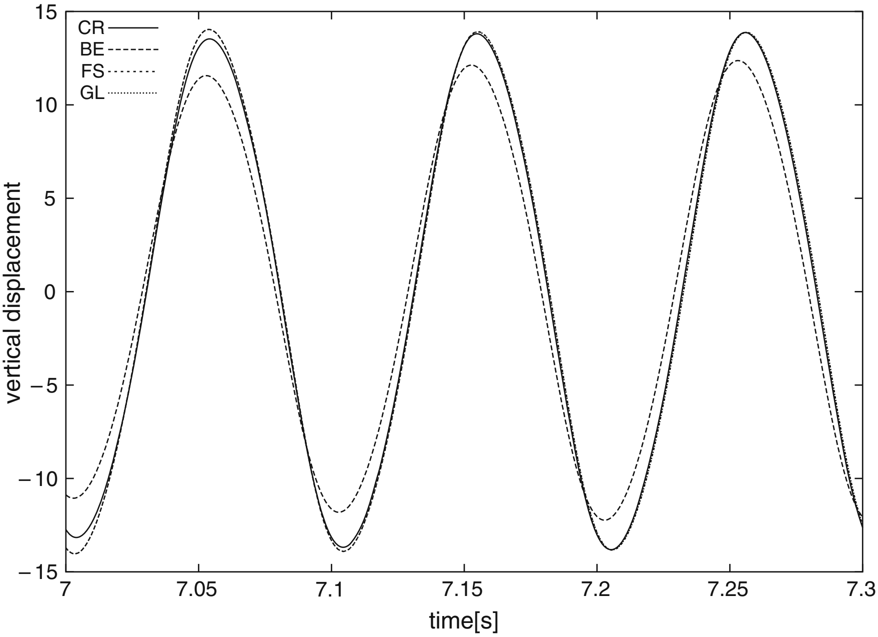

Fig. 7 For $\Delta t = 0.0005$, the amplitude of oscillations of rear mass is almost identical for the different time stepping schemes CN, FS, GL

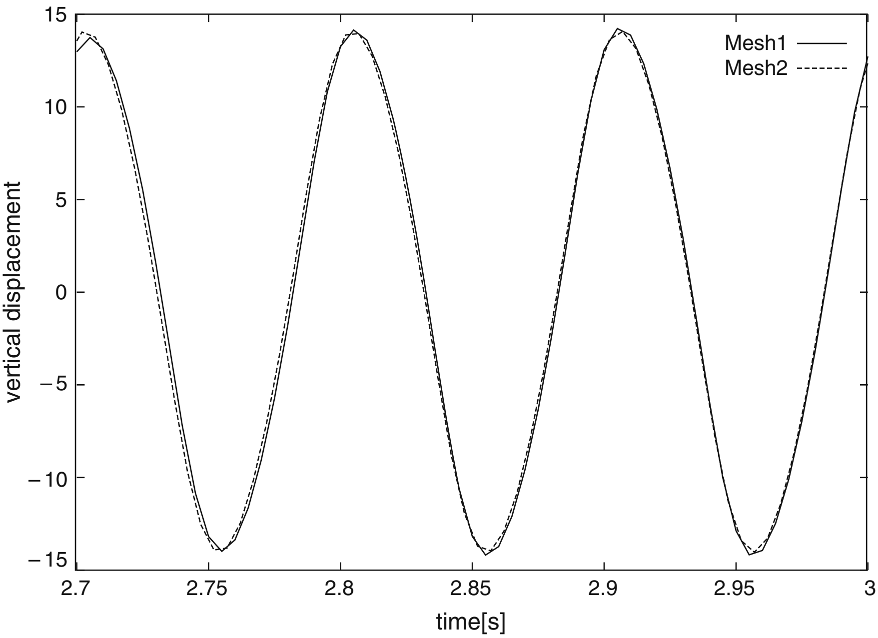

Fig. 8 For the two different meshes, the amplitude of oscillations is almost the same for the Fractional-Step-θ-scheme

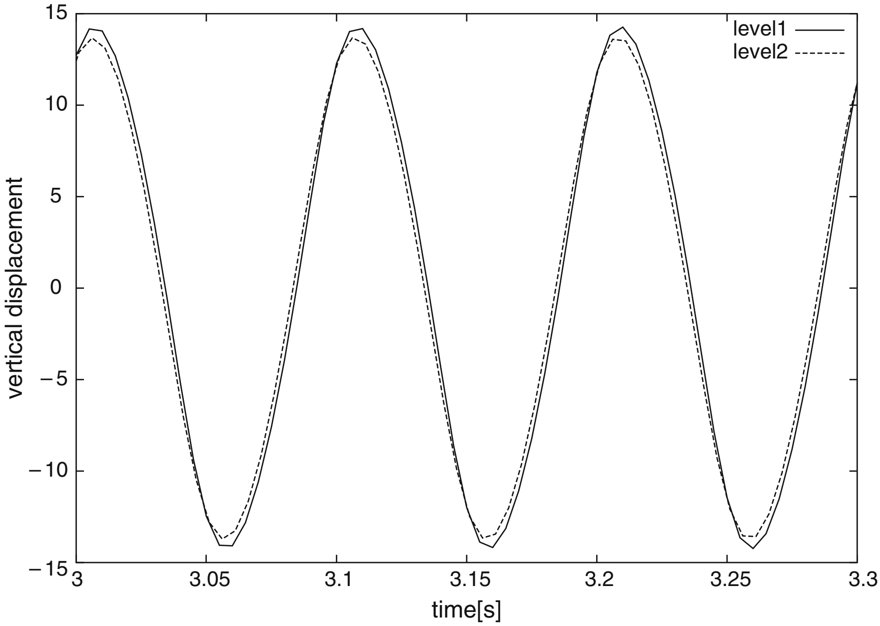

Fig. 9 For refinement level 1 and 2 (mesh1) the amplitude of oscillation is almost identical

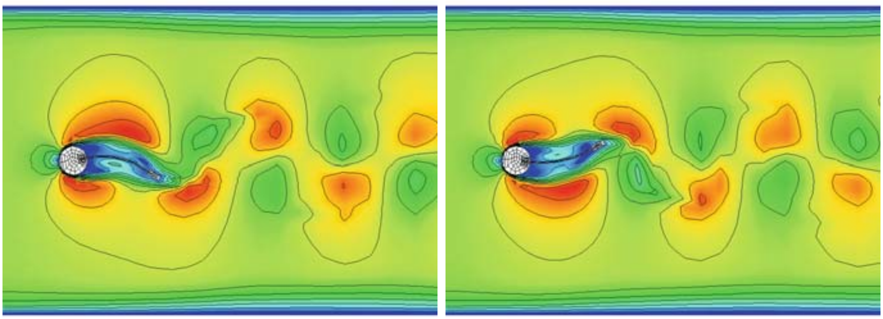

Fig. 10 Snapshots of the vertical displacement of the rear mass with frequency of oscillations ≈ 10 Hz for 1 mm thick beam

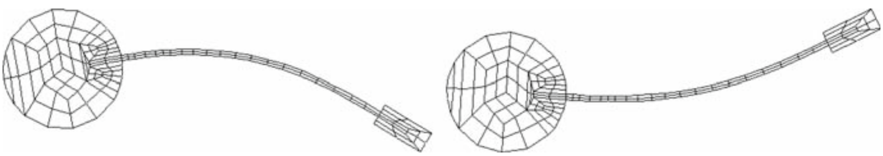

Fig. 11 Zoomed snapshots of the deformed 1 mm thick beam

6.2 Results for 0.04 mm Thick Beam

In this test we keep the thickness of the beam 0.04 mm as described in the experimental set up. The minimum velocity needed to excite the movement of the structure slightly varied from test to test. In our case for velocity 600 mm/s (Re $\approx$ 80) we are able to excite the structure. Frequency of the structure movement increases linearly with the increase of the velocity of the fluid. We used the velocity 600 mm/s (Re $\approx$ 80) at beginning, then switching to 800 mm/s (Re $\approx$ 107) for simplicity, see Figs. 14 and 15. Figure 12 shows the comparison between experimental versus numerical results of the problem. Figure 13 shows the amplitude of oscillations of rear mass attached to the elastic beam for velocity 1080 mm/s and the frequency of oscillation observed is $\approx$ 9.5 Hz. Figure 16 shows resulting mesh deformation. Figures 17 and 18 shows the deformed shape of the beam for velocity 1080 mm/s, and for the velocity 1450 mm/s the deformation of the elastic beam is even more significant, see Figs. 19 and 20.

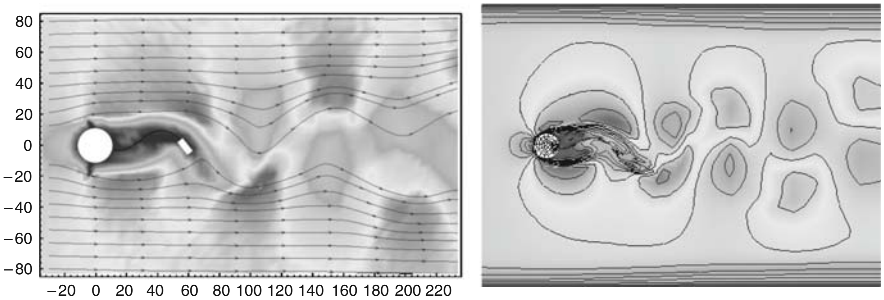

Fig. 12 Experiment from Erlangen (*left*) and numerical result for velocity 1450 mm/s (*right*)

7 Summary and Future Developments

We presented a general ALE formulation of fluid-structure interaction problems suitable for applications with finite deformations of the structure and laminar viscous flows. The resulting discrete nonlinear systems arise from the finite element discretization by using the high order Q_2P_1 FEM pair which are solved monolithically via discrete Newton iteration and special Krylov space and multigrid approaches. We applied the Backward Euler, Crank Nicholson, Fractional-Step-θ-scheme and a new modified Fractional-Step-θ-scheme for time discretization which are numerically examined for several prototypical benchmark configurations. Results have been given that are obtained from a rigid cylinder in laminar flow. The structure consists of a thin elastic beam attached to the cylinder, which is identified by the center of the cylinder with one grid point. This point constraint effectively fixes the position of the cylinder axis, but still allows the free rotation around this point. At the trailing end of the beam a rear mass is attached. We simulated two cases corresponding to the thickness of the beam to be 1 and 0.04 mm, respectively. Addi-

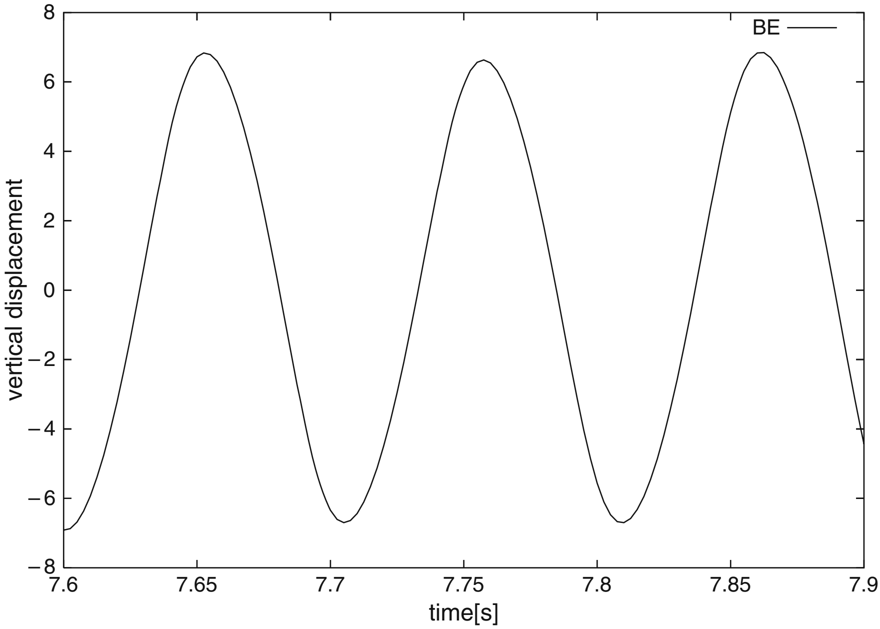

Fig. 13 Frequency of oscillations of the rear mass for velocity 1080 mm/s for the described numerical set up is ≈ 9 Hz

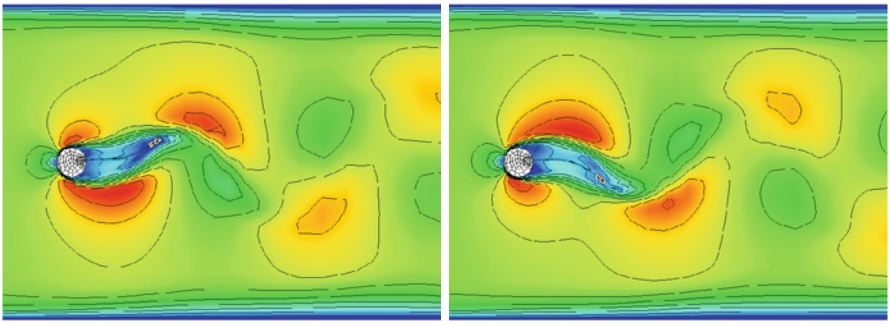

Fig. 14 Snapshots of the vertical displacement of the rear mass with maximum amplitude ≈ 17.0 and frequency ≈ 4.5 Hz and velocity 800 mm/s

tionally, we present numerical studies on different mesh types. Numerical results are provided for all time stepping schemes which show very reproducible symmetrical two-dimensional swiveling motions. These numerical tests show that the solution is independent of the mesh type and mesh refinement level. Preliminary results for the experimental benchmark configuration are shown to see the qualitative behavior of the elastic beam for a high velocity profile fluid. The next steps regarding better efficiency of the solvers include the development of improved multigrid solvers, for instance of global pressure Schur complement type [6], and the combination with

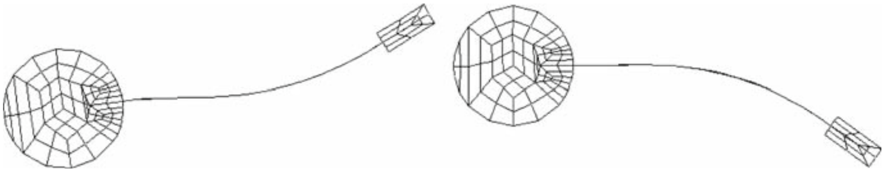

Fig. 15 Zoomed snapshots of the deformed beam for velocity 800 mm/s

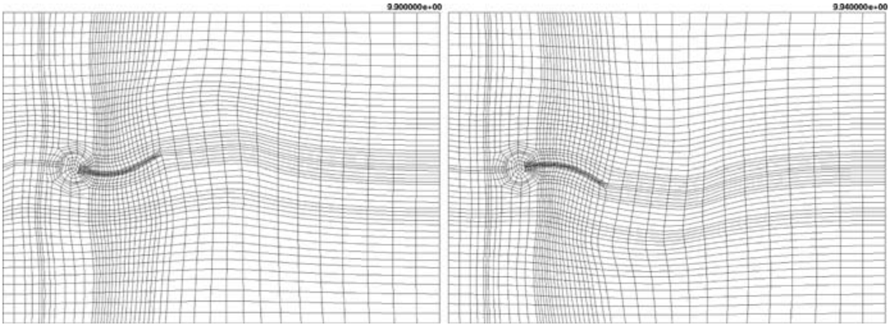

Fig. 16 Snapshot of the complete mesh

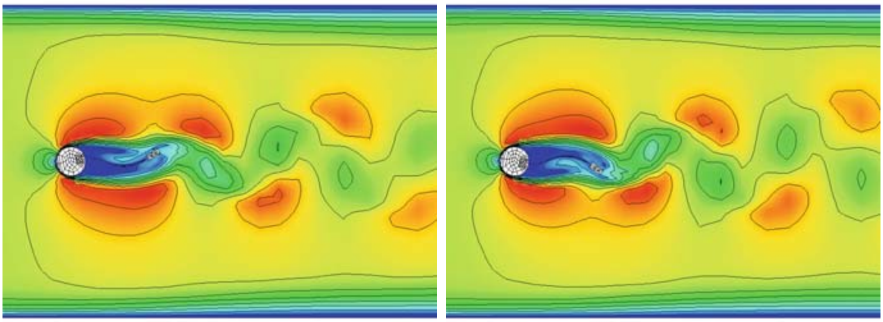

Fig. 17 Snapshots of the vertical displacement of the rear mass for velocity 1080 mm/s

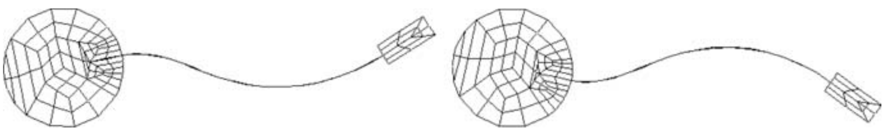

Fig. 18 Zoomed snapshots for deformed thick beam

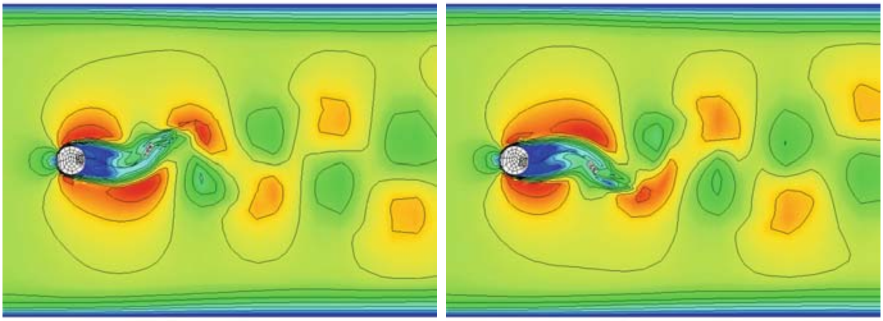

Fig. 19 Snapshots of the vertical displacement of the rear mass and velocity 1450 mm/s

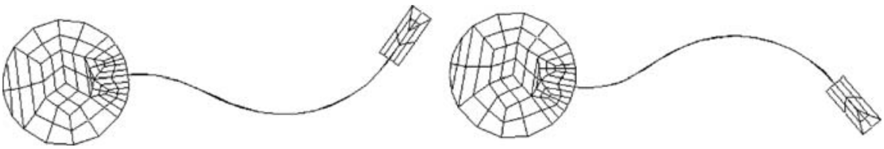

Fig. 20 Zoomed snapshots for the deformed beam

parallel high performance computing techniques in future, particularly towards 3D configurations.

Acknowledgments This work is supported by the German Research Association (DFG), Research unit 493, by the Jindrich Necas Center for Mathematical Modeling, project LC06052 financed by MSMT, and by the Higher Education Commission (HEC) of Pakistan. This support is gratefully acknowledged.

References

1. Turek, S., Rivkind, L., Hron, J., Glowinski, R.: Numerical study of a modified time-steeping theta-scheme for incompressible flow simulations. J. Sci. Comput. **28**, 533–547 (2006)
2. Glowinski, R.: Finite Element Method for Incompressible Viscous Flow. In: *Handbook of Numerical Analysis*, Volume IX, Ciarlet, P. G and Lions, J. L., (Ed.), North-Holland, Amsterdam (2003)
3. Boffi, D. and Gastaldi, L.: On the quadrilateral Q2-P1 element for the stokes problem. Int. J. Numer. Meth. Fluids **39**, 1001–1011, (2002)
4. Arnold, D. N., Boffi, D., and Falk, R. S.: Approximation by quadrilateral finite element. Math. Comput. **71**(239), 909–922, (2002)
5. Rannacher, R. and Turek, S: A simple nonconforming quadrilateral Stokes element. Numer. Meth. Part. Diff. Equ. **8**, 97–111 (1992)
6. Turek, S.: *Efficient Solvers for Incompressible Flow Problems: An Algorithmic and Computational Approach.* ELNCSE 6, Springer-Verlag, New York (1999)
7. Gresho, P. M.: On the theory of semi-implicit projection methods for viscous incompressible flow and its implementation via a finite element method that also introduces a nearly consistent mass matrix, part 1: Theor. Int. J. Numer. Meth. Fluids **11**, 587–620, (1990)

8. Hron, J. and Turek, S.: A monolithic FEM/Multigrid solver for ALE formulation of fluid-structure interaction with application in biomechanics, *Fluid-Structure Interaction: Modelling, Simulation, Optimisation*, Lecture Notes in Computational Science and Engineering, Vol. **53**, 146–170, Bungartz, H.-J., Schafer, M. (Eds.), Springer, New York (2006) ISBN: 3-540-34595-7
9. Turek, S. and Schmachtel, R.: Fully coupled and operator-splitting approaches for natural convection flows. In enclosures, Int. J. Numer. Meth. Fluids 1109–1119 (2002)
10. Davis, T. A. and Duff, I. S.: A combined unifrontal/multifrontal method for unsymmetric sparse matrices. SACM Trans. Math. Software **25**, 1–19 (1999)
11. Barrett, R., Berry, M., Chan, T. F., Demmel, J., Donato, J., Dongarra, J., Eijkhout, V., Pozo, R., Romine, C., and Van der Vorst, H.: Templates for the solution of linear systems: Building blocks for iterative methods, SIAM Philadelphia, PA (1994)
12. Bramley, R. and Wang, X.: *SPLIB: A library of iterative methods for sparse linear systems* Department of Computer Science, Indiana University, Bloomington, IN, `http://www.cs.indiana.edu/ftp/bramley/splib.tar.gz` (1997)
13. Vanka, S. P.: Implicit multigrid solutions of Navier-Stokes equations in primitive variables. J. Comp. Phys. **65**, 138–158 (1985)
14. Hron, J., Quazzi, A., Turek, S.: A Computational Comparison of two FEM Solvers For Nonlinear Incompressible Flow, Bansch, E., LNCSE, 87–109 Challenges in Scientific Computing CISC, Springer (2002) ISBN 3–540–40887-8
15. Gomes J. P. and Lienhart H.: Experimental study on a fluid-structure interaction reference test case, *Fluid-Structure Interaction: Modelling, Simulation, Optimisation*. Lecture Notes in Computational Science and Engineering, Vol. **53**, 356–370, Bungartz, H.-J., Schafer, M. (Eds.), Springer, New York (2006) ISBN: 3-540-34595-7

On Stokes' Problem

Remigio Russo

Abstract We consider the Stokes problem of viscous hydrodynamics in bounded and exterior Lipschitz domains Ω of $\mathbb{R}^m$ (≥ 2) with boundary datum in $L^2(\partial\Omega)$. We show that this problem has a unique very weak solution in bounded domains. As far as exterior domains are concerned, we prove that a very weak solution exists such that $u = \mathfrak{p}_k + O(r^{-1-m-k})$ at infinity, with $\mathfrak{p}_k$ a Stokes's polynomial of degree k, if and only if the data satisfy a suitable compatibility condition. In particular, we derive the well-known Stokes'paradox of hydrodynamics for very weak solutions. We use this results to prove the existence of a very weak solution to the Navier-Stokes problem in bounded and exterior Lipschitz domains of $\mathbb{R}^3$ by requiring that the boundary datum belongs to $L^{8/3}(\partial\Omega)$.

Keywords Stokes problem · Existence and uniqueness theorems · Stokes paradox

1 Introduction

Let Ω be a domain (open connected set) of $\mathbb{R}^m$, $m \geq 2$. As is well-known [33], the *Stokes problem* of stationary viscous hydrodynamics is to find a solution to the equations

$$\begin{aligned} \Delta u - \nabla p = f \quad & \text{in } \Omega, \\ \operatorname{div} u = 0 \quad & \text{in } \Omega, \\ u = a \quad & \text{on } \partial\Omega, \end{aligned} \tag{1}$$

where $u : \Omega \to \mathbb{R}^m$ and $p : \Omega \to \mathbb{R}$ are the (unknown) kinetic field and pressure field respectively, $f : \Omega \to \mathbb{R}^m$ and $a : \partial\Omega \to \mathbb{R}^m$ are the (assigned) body force

R. Russo (✉)
Dipartimento di Matematica, Seconda Università di Napoli, 81100, Caserta, Italy
e-mail: remigio.russo@unina2.it

DOI 10.1007/978-3-642-04068-9_28,

field and boundary datum respectively. If Ω is an exterior domain we require that u satisfies the condition at infinity

$$\lim_{r\to+\infty} u(x) = u_\infty, \tag{2}$$

where u_∞ is an assigned constant vector. In the last hundred years, problem (1) has been the object of many papers. We quote [33] for an historical review and a rich bibliography (see also [18, 26, 49, 52, 74, 80, 81]).

Under suitable regularity assumptions on the data for a Ω bounded or exterior domain and $m > 2$ problems (1) and (2) have a unique weak solution (see, e.g, [3, 10, 33, 41, 49, 74, 75, 80]). If Ω is exterior and $m = 2$, then (1) and (2) is not solvable for arbitrary data even if they are of class C^∞, in view of the Stokes paradox [78, 11, 31, 35, 43, 47] and [33] Chap. V. To see this easily, let us note that for $f = 0$ every weak solution u to (1) is of class C^∞ and a biharmonic vector field in Ω. Therefore, by a classical result of M. Picone [64] if u converges to a constant vector u_0 at infinity, then

$$u_0 = \frac{1}{2\pi}\int_0^{2\pi} u(R,\theta). \tag{3}$$

If $\partial\Omega$ is a disk of radius R_0, then (3) implies that in order (1) and (2) to have a solution a and u_∞ must satisfy the necessary *compatibility condition*

$$u_\infty = \frac{1}{2\pi}\int_0^{2\pi} a(R_0,\theta). \tag{4}$$

In particular, if $a = 0$, then (1) and (2) has no solution. This problem was solved by G.P. Galdi and C.G. Simader [35] (see also [33] Chap. V, and [34]). Assuming Ω of class C^2, $a \in W^{1-1/q,q}(\partial\Omega)$ and $f \in D^{-1,q}(\Omega)$ $(q > 1)$, they first prove that the linear space $\mathfrak{H}$ of solutions to the system

$$\begin{aligned} \Delta h - \nabla Q = 0 \quad & \text{in } \Omega, \\ \operatorname{div} h = 0 \quad & \text{in } \Omega, \\ h = 0 \quad & \text{on } \partial\Omega \end{aligned}$$

has dimension 2, then they conclude that in order (1) and (2) to be solvable it is necessary and sufficient that a, f and and u_∞ satisfy the compatibility condition

$$\int_{\partial\Omega} (a - u_\infty)\cdot T[h,Q]n = \langle f, h\rangle, \quad \forall\, h \in \mathfrak{H}, \tag{5}$$

where

$$T[h,Q] = \nabla h + \nabla h^{\mathrm{T}} - QI$$

is the Cauchy stress tensor. If $\partial\Omega$ is a disk, they observe that $T[h,Q]n$ is a constant vector so that for, $f = 0$, (5) reduces to (4).

In [52] we performed a study of the Stokes problem by the *Fredholm-Riesz-Schauder theory of integral equations* in bounded and exterior domains with Liapounov boundaries and for continuous boundary data. A condition similar to (5) was found for the existence of a classical solution in a plane exterior domain. In [67] we extended these results to Lipschitz domains and boundary data in $L^2(\partial\Omega)$. The purpose of this paper is to present in a reasonably simple way what is, to our knowledge, the state of art for the existence and uniqueness problem for Stokes' equations under nonslip boundary conditions, by following the method of integral equations as developed in [67, 82]. We shall also present simpler proofs of well-known theorems and obtain new results concerning exterior domains. In particular, to (1) we append the condition at infinity

$$u = \mathfrak{p}_k(x) + O(r^{1-m-k}), \tag{6}$$

where $\mathfrak{p}_k$ is an assigned *Stokes polynomial* of degree k and determine a necessary and sufficient condition on the data in order that (1), (6) admits a solution, which generalizes the one found in [35, 52, 67] for $k = 0$.

The plan of the paper is as follows: in Section 2 we recall some general facts concerning Eq. $(1)_{1,2}$ and prove Stokes' formula for exterior domains; in Sect. 3 we summarize the classical potential theory for Liaponouv surfaces and its extension to boundaries of class C^1; in Sect. 4 we describe the L^2–simple layer potential approach to the solvability of (1) in Lipschitz domains, that we use in Sects. 5 and 6 respectively for bounded and exterior regions; in Sect. 7 we show that Stokes' paradox is not confined to the Stokes problem with nonslip boundary conditions; finally, in Sect. 8 we apply the foregoing results to prove an existence theorem for the Navier-Stokes problem in three-dimensional bounded and exterior Lipschitz domains for boundary datum $a \in L^{8/3}(\partial\Omega)$ and small fluxes.

NOTATION – $\mathbb{R}$ is the set of the real numbers; $\mathbb{N}$ is the set of the natural numbers and $\mathbb{N}_0 = \mathbb{N}\cup\{0\}$. A domain (open connected set) Ω of $\mathbb{R}^m$ is said to be of class $C^{k,\alpha}$ ($k \in \mathbb{N}_0$, $\alpha \in [0, 1]$) if for every $\xi \in \partial\Omega$, there exists a neighborhood of ξ in $\partial\Omega$ which can be expressed as a graph of a function of class $C^{k,\alpha}$; for ($k = 0, \alpha = 1$) and ($k = 1, \alpha \in (0, 1)$) Ω is called Lipschitz and Liapounov respectively. Scalar, vector and tensor valued functions are not distinguished in notation; it will be clear from the context when we will refer to a scalar, vector or tensor field in Ω or on $\partial\Omega$: x, y denote points of $\mathbb{R}^3$, (ζ, ξ) points on surfaces and o the origin of the reference frame $(o, \{e_i\})$, with $\{e_i\}_{i=1\dots,m}$ orthonormal basis of $\mathbb{R}^m$; $S_R = \{x : r = |x| < R\}$ and $T_R = S_{2R} \setminus S_R$, $e_r = x/r$, $\Omega_R = \Omega \cap S_R$. The function spaces $C(\Omega)$, $C^{k,\alpha}(\Omega)$, $C(\overline{\Omega})$, $C^{k,\alpha}(\overline{\Omega})$, $C(\partial\Omega)$, $C^{k,\alpha}(\partial\Omega)$, $W^{k,q}(\Omega)$, $W_0^{\alpha,q}(\Omega)$, $W^{k,q}(\partial\Omega)$, $W^{\alpha,q}(\partial\Omega)$ ($\alpha \in (0, 1)$, $k \in \mathbb{N}_0$, $q \in (1, +\infty)$) have their usual meaning and $W^{-\alpha,q}(\Omega)$, $W^{-\alpha,q}(\partial\Omega)$ ($1/q + 1/q' = 1$) are the spaces dual to $W_0^{\alpha,q'}(\Omega)$ and $W^{\alpha,q'}(\partial\Omega)$ respectively; $\mathcal{H}^1(\Omega)$ denotes the space of all $f \in L^1(\Omega)$ whose zero extensions belong to the Hardy space $\mathcal{H}^1(\mathbb{R}^m)$; recall that if $\varphi \in \mathcal{H}^1(\Omega)$, then $\int_\Omega \varphi = 0$. If ϱ is a positive function on Ω, we set $L^q(\Omega, \varrho) = \{\varphi \in L^1_{\text{loc}}(\Omega) : \varrho\varphi \in L^q(\Omega)\}$. To conform notation we express the duality $W^{-\alpha,q}(\mathcal{B}) - W^{\alpha,q'}(\mathcal{B})$ by the symbol

$$\langle \sigma, \varphi \rangle = \int_{\mathcal{B}}^{\star} \varphi \sigma,$$

which must be understood as an usual integral when $\varphi\sigma \in L^1(\mathcal{B})$. Moreover, if Ω is bounded, we set

$$\varphi_{\mathcal{B}} = \frac{1}{|\Omega|} \int_{\Omega}^{\star} \varphi$$

Throughout the paper, we shall use the same symbol to denote a space of scalar, vector and tensor-valued functions. L^1_{loc} is the space of all measurable functions φ such that $\varphi \in L^1(K)$ for every compact K contained in Ω; if V is a subspace of $L^1_{\text{loc}}(\overline{\Omega})$, V_σ stands for the subset of V of all vector fields u such that $\int_\Omega u \cdot \nabla\varphi = 0$, for all $\varphi \in C_0^\infty(\Omega)$. If u is a vector field in $W^{1,q}_{\text{loc}}(\overline{\Omega})$, we denote by $\hat{\nabla} u$ and $\tilde{\nabla} u$ the symmetric and skew parts of ∇u respectively. The symbol c will be reserved to denote positive constants whose numerical values are not essential to our purposes. The Landau symbols $f(x) = o(g(r))$ and $f(x) = O(g(r))$ are used to mean that $\lim_{r\to+\infty} |f(x)|/g(r) = 0$ and $|f(x)| \le cg(r) = 0$, where f is a function defined in $\complement S_R$ and g a positive function in $(0, +\infty)$.

2 The Stokes Formulae

Let Ω_i $(i = 0, 1, \ldots, h \in \mathbb{N})$ be $h + 1$ bounded domains with connected and Lipschitz boundaries such that

$$\Omega' = \bigcup_{i=1}^{h} \Omega_i \subset \Omega_0, \quad \overline{\Omega}_i \cap \overline{\Omega}_j = \varnothing,\ i \neq j.$$

By bounded and exterior domain we mean the sets defined respectively by

$$\Omega = \Omega_0 \setminus \overline{\Omega'}$$

and

$$\Omega = \mathbb{R}^m \setminus \overline{\Omega'}.$$

The direction of the unit normal n to $\partial\Omega$ is chosen in such a way that n is inner for exterior domains and outer for bounded domains.

The equations

$$\begin{aligned} \Delta u - \nabla p = 0, \\ \operatorname{div} u = 0 \end{aligned} \tag{7}$$

admits the *Lorentz fundamental solution* [33, 49]

$$\begin{aligned}\mathbb{S}(x-y) &= \frac{1}{2}\big[\mathcal{U}(x-y)I + (x-y)\otimes\nabla_y\mathcal{U}(x-y)\big],\\ \mathcal{P}(x-y) &= -\nabla_x\mathcal{U}(x-y),\end{aligned}$$

where

$$\mathcal{U}(x-y) = \begin{cases} -\dfrac{1}{(m-2)\omega_m|x-y|^{m-2}}, & m>2,\\[2ex] \dfrac{1}{2\pi}\log|x-y|, & m=2,\end{cases}$$

is the fundamental solution to the Laplacian, I the unit second-order tensor and ω_n the area of the unit sphere in $\mathbb{R}^m$.

Let φ be a field on Ω. We say that φ has a (non tangential) value on $\partial\Omega$, if there is a family of "geometric solids" $\{\gamma_\xi\}_{\xi\in\partial\Omega}$ contained in Ω such that

$$\varphi(\xi) = \lim_{\substack{x\to\xi\\ (x\in\gamma(\xi))}} \varphi(x) \overset{\text{def}}{\Longleftrightarrow} \varphi(x) \overset{\text{nt}}{\longrightarrow} \varphi(\xi)$$

for almost all $\xi\in\partial\Omega$. If $\partial\Omega$ is of class C^1, as γ_ξ we can take a ball tangent to $\partial\Omega$ at ξ. If $\partial\Omega$ is Lipschitz, as γ_ξ we can choose a finite cone whose aperture depends on the *Lipschitz character of* $\partial\Omega$. It φ is defined in $\mathbb{R}^m\setminus\partial\Omega$ and Ω is bounded, then by φ^+ [respect. φ^-] we mean the (non tangential) value of the restriction of φ to Ω [respect. $\complement\overline{\Omega}$]; if Ω is exterior, φ^+ [respect. φ^-] denotes the (non tangential) value of the restriction of φ to Ω' [respect. Ω].

It is well-known that for a bounded Lipschitz domain Ω, if $1/q<\alpha<1+1/q$, $q\in(1,+\infty)$, and $s=\alpha-1/q$, the classical trace operators $\varphi\in C(\overline{\Omega})\to\varphi_{|\partial\Omega}\in C(\partial\Omega)$ and $u\in C(\overline{\Omega})\to(u\cdot n)_{|\partial\Omega}\in C(\partial\Omega)$ extend uniquely to continuous operators from $W^{\alpha,q}(\Omega)$ onto $W^{s,q}(\partial\Omega)$ and from $L^q_{\text{div}}(\Omega)=\{\varphi\in L^q(\Omega:\operatorname{div}\varphi\in L^q(\Omega)\}$ onto $W^{-1/q,q}(\partial\Omega)$, respectively [4, 27, 80]. Moreover, $W^{\alpha,q}(\partial\Omega)\hookrightarrow L^t(\partial\Omega)$, $t=(m-1)q/(m-\alpha q)$, and the Gauss generalized formula holds (see, e.g., [33])

$$\int_\Omega \operatorname{div}(\varphi u) = \int^\star_{\partial\Omega}\varphi u\cdot n$$

for all $\varphi\in W^{1,q}(\Omega)$ and $u\in L^{q'}_{\text{div}}(\Omega)$.

A *distributional* or *weak solution* (*variational solution* for $q=2$) to Eq. $(1)_{1,2}$ is a field $u\in W^{1,q}_{\sigma,\text{loc}}(\Omega)$ ($q>1$) such that

$$\int_\Omega\nabla u\cdot\nabla\varphi + \int^\star_\Omega f\cdot\varphi = 0,\quad \forall\varphi\in C^\infty_{0,\sigma}(\Omega).$$

To every solution $u \in W^{1,q}_{\sigma,\text{loc}}(\Omega)$ to $(1)_{1,2}$ we can associate a pressure field $p \in L^q_{\text{loc}}(\Omega)$ such that the pair (u, p) is a distributional solution to equations $(1)_{1,2}$ (see, e.g., [33]), i.e.,

$$\int_\Omega \nabla u \cdot \nabla\varphi + \int_\Omega^\star f \cdot \varphi = \int_\Omega p \,\operatorname{div}\varphi, \quad \forall\varphi \in C_0^\infty(\Omega).$$

Of course, the pressure p is defined within an arbitrary additive constant. If Ω is bounded, we normalize p by setting $p_\Omega = 0$.

Set (see [49], Chap. 3)

$$T'[\mathbb{S}, \mathcal{P}](x-y) = \mathcal{P}(x-y)I + \nabla_y \mathbb{S}(x-y) + \nabla_y \mathbb{S}^{\mathrm{T}}(x-y).$$

The following result is classical [49, 57].

Lemma 1 *(Stokes' formula for bounded domains) Let Ω be a bounded Lipschitz domain and let $u \in W^{1,q}(\Omega) \times L^q(\Omega)$ be a weak solution to $(1)_{1,2}$. If $f \in \mathcal{H}^1(\Omega)$, then for almost all $x \in \Omega$*

$$\begin{aligned} u(x) &= \int_\Omega \mathbb{S}(x-y) f(y)\,\mathrm{dv}_y + \int_{\partial\Omega} T'[\mathbb{S}, \mathcal{P}](x-\zeta)(u\otimes n)(\zeta)\,\mathrm{da}_\zeta \\ &\quad - \int_{\partial\Omega}^\star \mathbb{S}(x-\zeta)(T[u,p]n)(\zeta)\,\mathrm{da}_\zeta, \\ p(x) &= \int_\Omega \mathcal{P}(x-y) f(y)\,\mathrm{dv}_y - 2\int_{\partial\Omega} u(\zeta)\cdot[\nabla_x \mathcal{P}(x-\zeta)]n(\zeta)\,\mathrm{da}_\zeta \\ &\quad - \int_{\partial\Omega}^\star \mathcal{P}(x-\zeta)\cdot(T[u,p]n)(\zeta)\,\mathrm{da}_\zeta \end{aligned} \tag{8}$$

If $m = 2$, then $(8)_1$ holds for all $x \in \Omega$.

From Lemma 1 it follows that if $f \in C^\infty(\Omega)$, then a weak solution to Eq. $(1)_{1,2}$ and the corresponding pressure are of class C^∞ in Ω.

Let us extend (8) to exterior domains (see also [16, 33]).

Lemma 2 *(Caccioppoli's inequality) Let (u, p) be a solution to (7) in $\mathbb{R}^m$. Then*

$$\int_{S_R} |\nabla u|^2 \le \frac{c}{R^2}\int_{T_R} |u|^2, \tag{9}$$

for all $R > 0$.

Proof Let g be a C^∞ function in $\mathbb{R}^m$, equal to 1 in S_R, to zero outside S_{2R} and such that $|\nabla_k g| \le cR^{-k}$, with c independent of R and

$$\nabla_k g = \underbrace{\nabla\ldots\nabla}_{k-\text{times}} g, \quad \nabla_0 g = g.$$

Let $h \in C_0^\infty(T_R)$ be a solution to the problem [65] (see also [33] Chap. III)

$$\begin{aligned} &\operatorname{div} h = -\operatorname{div}(g^2 u) \quad \text{in } T_R, \\ &\|h\|_{W^{k+1,2}(T_R)} \le c\|\operatorname{div}(g^2 u)\|_{W^{k,2}(T_R)}, \quad k \in \mathbb{N}_0. \end{aligned} \tag{10}$$

Then, a simple integration by parts yields

$$\int_{\mathbb{R}^m} |g\nabla u|^2 = -2\int_{\mathbb{R}^m} g(\nabla u)\nabla g + \int_{\mathbb{R}^m} u \cdot \Delta h. \tag{11}$$

Since by the arithmetic-geometric mean inequality

$$\left|\int_{\mathbb{R}^m} g(\nabla u)\nabla g\right| \le c\left\{\frac{1}{\varepsilon R^2}\int_{T_R} |u|^2 + \varepsilon\int_{\mathbb{R}^m} |g\nabla u|^2\right\}$$
$$\left|\int_{\mathbb{R}^m} u \cdot \Delta h\right| \le c\left\{\frac{1}{\varepsilon R^2}\int_{T_R} |u|^2 + \varepsilon R^2\int_{\mathbb{R}^m} |\Delta h|^2\right\}$$

for every positive ε, and by $(10)_2$ and a rescaling argument

$$\int_{\mathbb{R}^m} |\Delta h|^2 \le c\left\{\frac{1}{R^4}\int_{T_R} |u|^2 + R^2\int_{\mathbb{R}^m} |g\nabla u|^2\right\},$$

(9) follows from (11) by properly choosing ε. □

Lemma 2 was first proved in [39]. The above proof is contained in [51].

Lemma 3 *(Campanato's inequality) Let* (u, p) *be a solution to (7) in* $\mathbb{R}^m$*. Then*

$$\int_{S_\varrho} |\nabla_k u|^2 \le c\left(\frac{\varrho}{R}\right)^m \int_{S_R} |\nabla_k u|^2, \tag{12}$$

for all $k \in \mathbb{N}_0$ *and for all* $R > \varrho > 0$.

Proof We follow [9]. Since any derivatives of (u, p) is a solution to (7) in $\mathbb{R}^m$, from (9) and Sobolev's lemma we get

$$|u|^2(x) \le \frac{c}{R^m}\int_{S_R} |u|^2,$$

for all $x \in S_\varrho$ ($\varrho < R/4$). Hence, integrating over S_ϱ, it follows

$$\int_{S_\varrho} |u|^2 \le c\left(\frac{\varrho}{R}\right)^m \int_{S_R} |u|^2 \tag{13}$$

It is immediate to get (13) for $\varrho \in (R/4, R)$ and (12) is proved. □

By a k-Stokes polynomial we mean a vector polynomial field $\mathfrak{p}_k$ of degree $k \in \mathbb{N}_0$ which satisfies (7) for a suitable associated harmonic polynomial $\mathfrak{q}_{k-1} \in \mathfrak{A}_{k-1}$ of degree $k-1$ (pressure field), if $k \in \mathbb{N}$ and constant if $k = 0$. We denote by $\mathfrak{S}_k$ the whole set of k–Stokes polynomial of degree k. It is well-known that [12]

$$\dim \mathfrak{S}_k = m + m^2 - 1 + \sum_{j=2}^{k} m \left[\binom{m+j-1}{j} - \binom{m+j-3}{j-2} \right]$$

Lemma 4 *(Liouville's theorem) Let* (u, p) *be a solution to (7) in* $\mathbb{R}^m$. *If*

$$u = o(r^{k+1}) \quad \text{as } r \to +\infty, \tag{14}$$

with $k \in \mathbb{N}_0$, *then*

$$(u, p) \in \mathfrak{S}_k \times \mathfrak{A}_{k-1}. \tag{15}$$

Proof From (12) and (9) we have

$$\int_{S_\varrho} |\nabla_{k+1} u|^2 \le \frac{c\varrho^m}{R^{m+2(k+1)}} \int_{S_{2(k+1)R} \setminus S_R} |u|^2.$$

Hence (15) follows, letting $R \to +\infty$ and taking into account (14). □

• In virtue of the *reflexion principle* of R.J. Duffin [21] a solution (u, p) to (7) in the half-space $\mathbb{R}^+_m = \{x : x_m > 0\}$, vanishing on the boundary, can be analytically continued across $\{x_n = 0\}$. Therefore, (u, p) is the restriction to $\mathbb{R}^+_m$ of a solution (u', p') to the Stokes equations in $\mathbb{R}^m$. Moreover, if $u = o(r^{k+1})$, then so does u'. Under this condition, from Lemma 4 it follows that u is a Stokes polynomial of degree k vanishing on the boundary. In particular, if $u = o(r^2)$ and $u_i = o(r)$, $i = 1, \dots m-1$, then $u = 0$. This can also be seen in a direct way by noting that from a Campanato's inequality [39] and (9) written in $S^+_R = \mathbb{R}^+_m \cap S_R$ it follows

$$\int_{S^+_\varrho} \left| \nabla u - (\nabla u)_{S^+_\varrho} \right|^2 \le c \left(\frac{\varrho}{R} \right)^{m+2} \int_{S^+_R} |\nabla u|^2 \le \frac{c\varrho^{m+2}}{R^{m+4}} \int_{S^+_{2R} \setminus S^+_R} |u|^2.$$

Theorem 1 *(Stokes's formula for exterior domains) Let* Ω *be an exterior Lipschitz domain and let* $u \in W^{1,q}_{\sigma,\mathrm{loc}}(\overline{\Omega})$ *be a weak solution to* $(1)_{1,2}$. *If* $f \in \mathcal{H}^1(\Omega)$ *has compact support and* u *satisfies (14), then there is a polynomial* $\mathfrak{p}_k \in \mathfrak{S}_k$ *such that*

$$\begin{aligned} u(x) = \mathfrak{p}_k &+ \int_{\Omega} \mathbb{S}(x-y) f(y)\, \mathrm{dv}_y + \int^{\star}_{\partial\Omega} \mathbb{S}(x-\zeta)(T[u,p]n)(\zeta) \\ &- \int_{\partial\Omega} T'[\mathbb{S}, \mathcal{P}](\zeta - x)](u \otimes n)(\zeta)\, \mathrm{da}_\zeta \end{aligned} \tag{16}$$

holds for almost all $x \in \Omega$. *If* $m = 2$, *then (16) holds everywhere in* Ω.

Proof Writing (8) in Ω_R for large R and recalling our choice of the direction of n, we have

$$u(x) - \int_{\Omega} \mathbb{S}(x-y)f(y) - \int_{\partial\Omega}^{\star} \mathbb{S}(x-\zeta)(T[u,p]n)(\zeta) \\ + \int_{\partial\Omega} T'[\mathbb{S},\mathcal{P}](x-\zeta)](u\otimes n)(\zeta)\,\mathrm{d}a_\zeta = \mathcal{J}(x)$$

with

$$\mathcal{J}(x) = \int_{\partial S_R} T'[\mathbb{S},\mathcal{P}](x-\zeta)(u\otimes e_R)(\zeta)\,\mathrm{d}a_\zeta - \int_{\partial S_R} \mathbb{S}(x-\zeta)(T[u,p]e_R\big)(\zeta)\mathrm{d}a_\zeta .$$

Since $\mathcal{J}(x)$ does not depend on R, $\mathcal{J}(x)$ is a solution equations (7) in $\mathbb{R}^m$ which satisfies (14). Therefore, by Lemma 4 $J(x) \in \mathfrak{S}_k$ and (16) is proved. The last assertion follows from the fact that the first integral in (16) is a continuous function in $\mathbb{R}^2$ [77]. □

The vector

$$\varrho = \int_{\partial\Omega}^{\star} T[u,p]n$$

gives the net force exerted by the fluid on Ω' and (16) can be written

$$u(x) = \mathfrak{p}_k + \mathbb{S}(x)\varrho + \mathcal{J}(x), \tag{17}$$

with

$$\mathbb{S}(x)\varrho = O(\mathcal{U}(x))$$

and

$$\nabla_j \mathcal{J} = O(r^{1-m-j}).$$

Likewise, for the pressure field we have

$$p(x) = \mathfrak{q}_{k-1} + \mathcal{P}(x)\varrho + \mathcal{J}_0(x), \tag{18}$$

with

$$\mathcal{P}(x)\varrho = O(\nabla\mathcal{U}(x))$$

and

$$\nabla_j \mathcal{J}_0 = O(r^{-m-j}).$$

Of course, the decomposition (17) holds for every weak solution to (7) in $\complement S_R$. As a simple consequence of (17), we have the following uniqueness theorems.

Theorem 2 *Let Ω be an exterior Lipschitz domain. If $u \in W^{1,2}_{\mathrm{loc}}(\overline{\Omega})$ is a variational solution to (7) vanishing on $\partial\Omega$ and such that*

$$u = \begin{cases} o(\log r), & m = 2, \\ o(1), & m > 2. \end{cases} \tag{19}$$

as $r \to +\infty$, then $u = 0$ in Ω.

Proof An integration by parts yields

$$2\int_{\Omega_R} |\hat{\nabla} u|^2 = \int_{\partial S_R} u \cdot T[u, p]e_R.$$

Hence the desired result follows, letting $R \to +\infty$ and taking into account (17), (18), and (19). □

Theorem 3 *Let Ω be an exterior Lipschitz domain. If $u \in W^{1,2}_{\mathrm{loc}}(\overline{\Omega})$ is a variational solution to (7) constant on $\partial\Omega$ and such that*

$$u(x) = o(\mathcal{U}(x)) \quad \text{as } r \to +\infty \tag{20}$$

then $u = 0$ in Ω.

Proof From

$$2\int_{\Omega_R} |\hat{\nabla} u|^2 = -\bar{u} \cdot \int^{\star}_{\partial\Omega} T[u, p]n + \int_{\partial S_R} u \cdot T[u, p]e_R,$$

where $\bar{u}$ is the constant value of u on $\partial\Omega$, the assertion of the theorem follows, letting $R \to +\infty$ and noting that (17) and (20) imply that $\varrho = 0$. □

Lemma 5 *Let Ω be a bounded Lipschitz domain. If $(u, p) \in W^{1,2}(\Omega) \times L^2(\Omega)$ is a a variational solution to (7), then*

$$\int_{\Omega} |\nabla u|^2 + \int_{\Omega} |p|^2 \leq c\|u_{|\partial\Omega}\|_{W^{1/2,2}(\partial\Omega)} \tag{21}$$

Lemma 5 is well-known (see, e.g., [33] Chap. IV). The uniqueness of the variational solution is a simple consequence of (21).

Lemma 6 *(Rellich's inequality) – Let Ω be a bounded regular domain. If (u, p) is regular solution to (7), then*

$$\int_{\partial\Omega} |T[u, p]n|^2 \leq c\int_{\partial\Omega} |\partial_t u|^2. \tag{22}$$

where $\partial_t u$ is the tangential derivative of u on $\partial\Omega$.

Lemma 6 is proved in [15, 26]. Starting from (22) and using the argument in [62] Chap. 5, we have

Lemma 7 *(Regularity of weak solutions at the boundary) – Let Ω be a bounded Lipschitz domain. If $(u, p) \in W^{1,2}(\Omega) \times L^2(\Omega)$ is a variational solution to (7) and $u_{|\partial\Omega} \in W^{1,2}(\partial\Omega)$, then $T[u, p]n_{|\partial\Omega} \in L^2(\partial\Omega)$.*

3 The Classical Potential Theory

The volume potential with density $f \in C_0^\infty(\Omega)$ is the pair

$$\mathcal{V}[f](x) = \int_\Omega \mathbb{S}(x-y)f(y)\,dv_y,$$
$$\mathcal{P}[f](x) = \int_\Omega \mathcal{P}(x-y)f(y)\,dv_y.$$

It is a regular solution to $(1)_{1,2}$. The following results are classical (cf., e.g., [27, 77]).

Let Ω be bounded. Then $\mathcal{V}[f]$ is continuous from $W^{s-2,q}(\Omega)$ into $W^{s,q}(\Omega)$, for all $s \in [0, 2]$ and for all $q \in (1, +\infty)$, and $\mathcal{P}[f]$ is continuous from $W^{s-1,q}(\Omega)$ into $W^{s,q}(\Omega)$, for all $s \in [0, 1]$ and for all $q \in (1, +\infty)$; if $f \in W^{-1,q}(\Omega)$, then $(\mathcal{V}, \mathcal{P})$ is a weak solution to $(1)_{1,2}$.

$\nabla_2\mathcal{V}[f]$ and $\nabla\mathcal{P}[f]$ are continuous from $\mathcal{H}^1(\mathbb{R}^m)$ into $L^1(\mathbb{R}^m)$. In particular, if $m = 2$, then $\mathcal{V}[f]$ is continuous in $\mathbb{R}^2$.

The simple and double layer potentials with densities $\psi, \varphi \in L^q(\partial\Omega)$ $(q \geq 1)$ are the pairs defined respectively by

$$\begin{aligned} v[\psi](x) &= -\int_{\partial\Omega} \mathbb{S}(x-\zeta)\psi(\zeta)\,d\sigma_\zeta, \\ P[\psi](x) &= -\int_{\partial\Omega} \mathcal{P}(x-\zeta)\psi(\zeta)\,d\sigma_\zeta \end{aligned} \tag{23}$$

and

$$\begin{aligned} w[\varphi](x) &= \int_{\partial\Omega} T'[\mathbb{S}, \mathcal{P}](x-\zeta)(\varphi \otimes n)(\zeta)\,d\mathrm{a}_\zeta, \\ \varpi[\varphi](x) &= -2\int_{\partial\Omega} \varphi(\zeta)\cdot[\nabla_x\mathcal{P}(x-\zeta)]n(\zeta)\,d\mathrm{a}_\zeta \end{aligned} \tag{24}$$

They are analytical solutions to (7) in $\mathbb{R}^m \setminus \partial\Omega$ and behave at infinity according to:

$$\begin{aligned} &\nabla_k v[\psi] = O(\nabla_k\mathcal{U}), \quad \nabla_k P[\psi] = O(\nabla_{k+1}\mathcal{U}), \\ &\nabla_k w[\varphi] = O(\nabla_{k+1}\mathcal{U}), \quad \nabla_k \varpi[\varphi] = O(\nabla_{k+2}\mathcal{U}), \end{aligned} \tag{25}$$

for all $k \in \mathbb{N}_0$. Moreover,

$$\nabla_k v[\psi] = O(\nabla_{k+1}\mathcal{U}),\ \nabla_k P[\psi] = O(\nabla_{k+2}\mathcal{U}) \Leftrightarrow \int_{\partial\Omega} \psi = 0. \tag{26}$$

If Ω is of class[1] C^2, classical results assure that (see, e.g., [57])

$$v[\psi] \xrightarrow{\text{nt}} \mathcal{S}[\psi]$$

on "both faces" of $\partial\Omega$. Moreover [49],

$$\begin{aligned} w[\varphi]^{\pm}(\xi) &= \pm\tfrac{1}{2}\varphi(\xi) + \int_{\partial\Omega} T'(\mathbb{S}, \mathcal{P})(\xi-\zeta)(\varphi\otimes n)(\zeta)\, d\mathrm{a}_\zeta \\ &= \left(\pm\tfrac{1}{2}I + \mathcal{K}\right)[\varphi](\xi), \end{aligned}$$

and

$$T\big[v[\psi], P[\psi]\big]^{\pm} n(\xi) = \left(\pm\tfrac{1}{2}I - \mathcal{K}^*\right)[\psi](\xi),$$

for almost all $\xi \in \partial\Omega$, where $\mathcal{K}^*$ denotes the adjoint operator to $\mathcal{K}$. If $\varphi \in W^{1,q}(\Omega)$, then the *Liapounov – Tauber* theorem holds [48, 57]

$$T\big[w[\varphi], \varpi[\varphi]\big]^{+} n(\xi) = T\big[w[\varphi], \varpi[\varphi]\big]^{-} n(\xi). \tag{27}$$

for almost all $\xi \in \partial\Omega$. Note that the above relations imply the *jump conditions*

$$\begin{aligned} \psi &= T[v[\psi], P[\psi]]^{+}n - T[[v[\psi], P[\psi]]^{-}n, \\ \varphi &= w[\varphi]^{+} - w[\varphi]^{-}. \end{aligned} \tag{28}$$

It is well-known that $\mathcal{S}$ is continuous from $L^q(\partial\Omega)$ into $W^{1,q}(\partial\Omega)$ and $w^{\pm}$ is continuous from $L^q(\Omega)$ into itself and from $W^{1,q}(\partial\Omega)$ into itself (see, e.g., [16, 56]). Since $\mathcal{K}(L^q(\partial\Omega)) \subset C^{0,\mu}(\partial\Omega)$ [57], by Ascoli–Arzelà's theorem $\mathcal{K} : L^q(\partial\Omega) \to L^q(\partial\Omega)$ is completely continuous. Therefore, one can use the *Fredholm–Riesz–Schauder theory* (see, e.g., [58] Chap. VII) to get the existence of a solution to the Stokes problems (1) and (2) (at least for $m > 2$) [29, 48, 49].

Let Ω be a bounded domain of class C^2, let

$$f \in W^{s-2,t}(\Omega),\ (m-1)t/(m-st) \geq q,\ st > 1 \tag{29}$$

and let $a \in L^q(\partial\Omega)$ satisfies

$$\int_{\partial\Omega} a \cdot n = 0. \tag{30}$$

[1] We made this assumption only for the sake of simplicity. Indeed, for $q > 1$, it is sufficient to assume that $\partial\Omega$ is a Liapounov surface (see [48, 57]).

Note that (29) assures that $\mathcal{V}[f]_{|\partial\Omega} \in L^q(\partial\Omega)$. Consider the homogeneous equation

$$\left(\mathcal{S} + \tfrac{1}{2}I + \mathcal{K}^*\right)[\psi] = 0. \tag{31}$$

If $\psi \in \operatorname{Ker}\left(\mathcal{S} + \frac{1}{2}I + \mathcal{K}^*\right)$, then the pair

$$\begin{aligned} u &= v[\psi], \\ p &= P[\psi] \end{aligned} \tag{32}$$

is a solution to the *Robin Problem*

$$\begin{aligned} \Delta u - \nabla p = 0 \quad &\text{in} \quad \complement\overline{\Omega}, \\ \operatorname{div} u = 0 \quad &\text{in} \quad \complement\overline{\Omega}, \\ u - T[u,p]n = 0 \quad &\text{on} \quad \partial\Omega \end{aligned} \tag{33}$$

The regularity properties of (u, p) allow us to integrate on Ω' to get

$$2\int_{\Omega'} |\hat{\nabla} u|^2 = -\int_{\partial\Omega'} u \cdot T[u,p]n = -\int_{\partial\Omega} |u|^2$$

Hence it follows that $u = 0$, $p = 0$ in Ω'. If $m > 2$ or $\psi_{\partial\Omega} = 0$ for $m = 2$, taking into account that by (26) $u \cdot T[u,p] = O(R^{-m})$, then we can let $R \to +\infty$ in the relation

$$2\int_{\complement\Omega_0 \cap S_R} |\hat{\nabla} u|^2 + \int_{\partial\Omega_0} |u|^2 = \int_{\partial S_R} u \cdot T[u,p]e_R$$

to have that (32) vanish in $\complement\Omega_0$. Bearing in mind the continuity of the simple layer potential through $\partial\Omega$, a simple integration on Ω implies that u vanishes and p is constant in Ω. Therefore, $(28)_1$ yields $\psi = \alpha n$ for some scalar α. From the expression of the simple layer potential with density n we have

$$v[n](x) = -\int_{\partial\Omega} \mathbb{S}(x-\zeta)n(\zeta)\,\mathrm{da}_\zeta = \operatorname{div}\int_{\Omega} \mathbb{S}(x-y)\,dv_y = 0$$

so that $v[n] = 0$ and $P[n]$ is a constant in Ω. On the other hand, by (26) we easily see that $v[n] = 0$ and $P[n] = 0$ in $\complement\Omega_0$. Hence it follows that n is a solution to (31), unique for $m > 2$. If $m = 2$, then, setting

$$\mathfrak{M}' = \operatorname{Ker}\left(\mathcal{S} + \tfrac{1}{2}I + \mathcal{K}^*\right) \setminus \operatorname{sp}\{n\},$$

we have that $\dim \mathfrak{M}' \leq 2$. Indeed, if $\psi (\neq 0) \in \mathfrak{M}'$, then necessarily $\psi_{\partial\Omega} \neq 0$; otherwise, a simple integration and (26) implies that $\psi \in \operatorname{sp}\{n\}$. Also, if $\{\psi_i\}_{i=1,2,3} \subset$

$\mathfrak{M}'$, then the system $\{\int_{\partial\Omega}\psi_i\}_{i=1,2,3}$ is linearly dependent so that there are nonzero scalars α_i such that $\alpha_i\int_{\partial\Omega}\psi_i = 0$. Then the pair $(v[\bar\psi], P[\bar\psi])$, with $\bar\psi = \alpha_i\psi_i$, is a solution to (33) such that $\bar\psi_{\partial\Omega} = 0$. By what we said above we have the absurd $\bar\psi \in \mathrm{sp}\,\{n\}$. Hence

$$\mathrm{Ker}\,(\mathcal{S} + \tfrac{1}{2}I + \mathcal{K}^*) = \begin{cases} \mathrm{sp}\,\{n\}, & m > 2, \\ \mathrm{sp}\,\{n\} \cup \mathfrak{M}' & m = 2. \end{cases}$$

Set

$$\gamma = \begin{cases} 0, & m > 2 \text{ or } \mathfrak{M}' = \{0\}, \\ 1, & \text{otherwise.} \end{cases}$$

Looking for a solution to Eq. (1) expressed by (see, e.g., [48])

$$\begin{aligned} u &= v[\varphi] + w[\varphi] + \mathcal{V}[f] + \gamma\kappa, \\ p &= P[\varphi] + \varpi[\varphi] + \mathcal{P}[f], \end{aligned} \tag{34}$$

with κ constant vector, we are led to find a solution $\varphi \in L^q(\partial\Omega)$ to the functional equation

$$a - \mathcal{V}[f]_{|\partial\Omega} - \gamma\kappa = \big(\mathcal{S} + \tfrac{1}{2}I + \mathcal{K}\big)[\varphi]. \tag{35}$$

Since $\mathcal{S}$ is completely continuous from $L^q(\partial\Omega)$ into itself and $(\frac{1}{2}I + \mathcal{K}) : L^q(\partial\Omega) \to L^q(\partial\Omega)$ is Fredholm with index zero, then also $\mathcal{S} + \frac{1}{2}I + \mathcal{K}$ is Fredholm with index zero, so that to solve (35) we can use *Fredholm's theory*: Eq. (35) has a solution if and only if

$$\int_{\partial\Omega} (a - \mathcal{V}[f]_{|\partial\Omega} - \gamma\kappa)\cdot\psi = 0, \quad \forall\,\psi \in \mathrm{Ker}\,(\mathcal{S} + \tfrac{1}{2}I + \mathcal{K}^*).$$

Therefore, taking into account (30) and choosing κ such that

$$\gamma\kappa \cdot \int_{\partial\Omega}\psi = \int_{\partial\Omega}(a - \mathcal{V}[f]_{|\partial\Omega})\cdot\psi, \quad \psi \in \mathfrak{M}', \tag{36}$$

we have that (35) has a solution $\varphi \in L^q(\partial\Omega)$ and the pair (34) gives the desired solution to the Stokes problem (1). Of course, by the regularity properties of $\mathcal{S}$ and $\mathcal{K}$ over regular surfaces [57], we have that if the data are more regular, then so does the density φ; for instance, if $a \in W^{1,q}(\partial\Omega)$ and $f \in L^t(\Omega)$, with $(m-1)/(m-s) \ge q$, then $\varphi \in W^{1,q}(\partial\Omega)$. Therefore, we can state the following existence theorem.

Theorem 4 *Let Ω be bounded domain of class C^2. If $a, \mathcal{V}[f]_{\partial\Omega} \in W^{\alpha,q}(\partial\Omega)$ ($q \ge 1, \alpha \in [0,1]$) and a satisfies (30), then (1) has a solution expressed by (34), with $\varphi \in W^{\alpha,q}(\partial\Omega)$, κ defined by (36), and if $\mathcal{V}[f] \in C(\overline{\Omega})$, then $u \xrightarrow{\mathrm{nt}} a$. Moreover* *natural estimates hold; in particular, if* $f = 0$ *and* $a \in C^{k,\mu}(\partial\Omega)$, *(*$k = 0, 1,\ \mu \in [0, 1)$*), then*

$$\begin{aligned} \|u\|_{C^{k,\mu}(\overline{\Omega})} &\le c\|a\|_{C^{k,\mu}(\partial\Omega)} \\ \|p\|_{C^{0,\mu}(\overline{\Omega})} &\le c\|a\|_{C^{1,\mu}(\partial\Omega)} \end{aligned} \tag{37}$$

Inequality (37) for $a \in C(\partial\Omega)$:

$$\|u\|_{C(\overline{\Omega})} \le c\|a\|_{C(\partial\Omega)} \tag{38}$$

is known as *maximum modulus theorem* (see, e.g., [54, 60]). If $m = 2$, $a \in C(\partial\Omega)$ and $f \in \mathcal{H}^1(\Omega)$, then we have

$$\|u\|_{C(\overline{\Omega})} \le c\left\{\|a\|_{C(\partial\Omega)} + \|f\|_{\mathcal{H}^1(\Omega)}\right\}. \tag{39}$$

If Ω is an exterior domain of class C^2, then by reproducing the above argument we can prove that

$$\dim \operatorname{Ker}\left(\mathcal{S} + \tfrac{1}{2}I - \mathcal{K}^*\right) = \begin{cases} 0, & m > 2, \\ \le 2, & m = 2. \end{cases}$$

Then a solution to (1) in the form

$$\begin{aligned} u &= v[\varphi] - w[\varphi] + \mathcal{V}[f] + \gamma\kappa, \\ p &= P[\varphi] - \varpi[\varphi] + \mathcal{P}[f], \end{aligned} \tag{40}$$

where now

$$\gamma = \begin{cases} 0, & m > 2 \text{ or } \dim \operatorname{Ker}\left(\mathcal{S} + \tfrac{1}{2}I - \mathcal{K}^*\right) = 0, \\ 1, & \text{otherwise,} \end{cases}$$

exists if and only if φ satisfies the equation

$$a - \mathcal{V}[f]_{|\partial\Omega} - \gamma\kappa = \left(\mathcal{S} + \tfrac{1}{2}I - \mathcal{K}\right)[\varphi] \tag{41}$$

and this is assured by choosing κ such that

$$\gamma\kappa \cdot \int_{\partial\Omega} \psi = \int_{\partial\Omega} (a - \mathcal{V}[f]_{|\partial\Omega}) \cdot \psi, \quad \psi \in \operatorname{Ker}\left(\mathcal{S} + \tfrac{1}{2}I - \mathcal{K}^*\right). \tag{42}$$

Therefore, we proved

Theorem 5 *Let* Ω *be an exterior domain of* $\mathbb{R}^m$ *of class* C^2*. If* $a, \mathcal{V}[f]_{\partial\Omega} \in W^{\alpha,q}(\partial\Omega)$ *(*$q \ge 1, \alpha \in [0, 1]$*) and* f *has compact support, then (1)–(2) has a* *solution expressed by (40), with* $\varphi \in W^{\alpha,q}(\partial\Omega)$ *and* κ *defined by (42). If* $\mathcal{V}[f] \in C(\overline{\Omega})$*, then* $u \xrightarrow{\text{nt}} a$ *and for* $m > 2$ $u \to 0$ *at infinity. Moreover, inequalities (37) hold locally in* $\overline{\Omega}_R$ *and if* $f = 0$*,* $a \in C(\partial\Omega)$ *and* $m > 2$*, then (38) holds.*

To solve (1) and (2) in a plane exterior domain, one first defines the linear space

$$\mathfrak{C}_0 = \{\psi : \mathcal{S}[\psi] = \text{constant}, \ \ P[\psi] = 0 \text{ in } \Omega'\} \tag{43}$$

and shows that

$$\dim \mathfrak{C}_0 = 2.$$

Moreover, if $\{\psi_1, \psi_2\}$ is a basis of $\mathfrak{C}$, then $\{\int_{\partial\Omega} \psi_1, \int_{\partial\Omega} \psi_2\}$ is a basis of $\mathbb{R}^2$ [67]. Then, one observes that the pair

$$\begin{aligned} u' &= v[\varphi + \psi] - w[\varphi] + \mathcal{V}[f] + u_\infty, \\ p' &= P[\varphi + \psi] - \varpi[\varphi] + \mathcal{P}[f] \end{aligned} \tag{44}$$

where φ is density appearing in (34), $u_\infty = -\mathcal{S}[\psi] + \gamma\kappa$ and $\psi \in \mathfrak{C}_0$ is chosen such that

$$\int_{\partial\Omega} (\varphi + \psi) = 0, \tag{45}$$

is again a solution to (1), but now thanks to (26) and (45)

$$\lim_{r\to+\infty} u(x) = u_\infty.$$

Then, since an elementary calculation shows that

$$\int_{\partial\Omega} (a - \mathcal{V}[f]_{|\partial\Omega} - u_\infty) \cdot \psi' = 0, \quad \psi' \in \mathfrak{C}_0, \tag{46}$$

we have

Theorem 6 *Let* Ω *be an exterior domain of* $\mathbb{R}^2$ *of class* C^2*. Let* $a, \mathcal{V}[f]_{\partial\Omega} \in W^{\alpha,q}(\partial\Omega)$ $(q \geq 1, \alpha \in [0, 1])$ *and let* f *have compact support. If (46) holds, then (1) and (2) has a solution expressed by (44), with* $\varphi \in W^{\alpha,q}(\partial\Omega)$*. If* $\mathcal{V}[f] \in C(\overline{\Omega})$*, then* $u \xrightarrow{\text{nt}} a$*.*

Note that:

- Theorems 5, 6 still hold for $a \in L^q(\partial\Omega)$ and $f \in \mathcal{H}^1(\Omega)$.
- if $f = 0$ and $a \in C(\partial\Omega)$, then from (46) it follows

$$|u_\infty| \leq c\|a\|_{C(\partial\Omega)},$$

so that the solution in Theorem 6 satisfies (38). More regular are Ω, a and f, more regular is the corresponding solution. We do not insist on such a problem, quoting [57] for an exhaustive treatment in spaces of regular functions.

- if (u, p) is a weak solution to (1) and (2), then the scalar multiplication of $(1)_1$ by $v[\psi']$, with $\psi' \in \mathfrak{C}_0$, and a simple integration by parts imply that a and u_∞ must satisfy (46), which turns out to be also necessary to the existence of a solution to (1) and (2). Then we recover Galdi–Simader's result [35]. To see that this result keeps holding for more general boundary data and forces (for instance, $a, \mathcal{V}[f]_{|\partial\Omega} \in L^q(\partial\Omega)$) we need some additional considerations about the uniqueness of a (non weak) solution. In general, a solution u to a boundary value problem associated to an elliptic operator like the Stokes one, with boundary data in $L^q(\partial\Omega)$, is not unique [17, 19]. It is in a certain sense necessary to require that u satisfies another condition, like an *integral relation*. We shall discuss this question in the next sections and we shall prove that condition (46) is also necessary to the existence of a solution of Eqs. (1) and (2) with less regular boundary data in reasonable function classes.

By making use of a result of A.P. Calderón about the L^q – boundedness of the Cauchy integral on a curve with a small Lipschitz constant, E.B. Fabes, M. Jodeit Jr. and N.M. Rivière were able to extend (among other things) the classical trace properties of the harmonic layer potentials to surfaces of class C^1 and to show that $\mathcal{S}$ is continuous from $L^q(\partial\Omega)$ into $W^{1,q}(\partial\Omega)$ and $\mathcal{K}$ is completely continuous from $L^q(\partial\Omega)$ into itself and from $W^{1,q}(\partial\Omega)$ into itself. What they proved for harmonic layer potentials can be easily extended to layer potentials that are weakly singular on Liapounov surfaces, as layer hydrodynamical potentials (23) and (24). Then, repeating the above argument we can prove the following theorems.

Theorem 7 *Let Ω be a bounded domain of class C^1. If $a, \mathcal{V}[f]_{\partial\Omega} \in W^{\alpha,q}(\partial\Omega)$ ($q \in (1, +\infty), \alpha \in [0, 1]$) and a satisfies (30), then (1) has a solution expressed by (34), with $\varphi \in W^{\alpha,q}(\partial\Omega)$, and if $\mathcal{V}[f] \in C(\overline{\Omega})$, $u \overset{\text{nt}}{\longrightarrow} a$.*

Theorem 8 *Let Ω be an exterior domain of class C^1. If $a, \mathcal{V}[f]_{\partial\Omega} \in W^{\alpha,q}(\partial\Omega)$ ($q \in (1, +\infty), \alpha \in [0, 1]$) and f has compact support, then (1) has a solution expressed by (40), with $\varphi \in W^{\alpha,q}(\partial\Omega)$. If $\mathcal{V}[f] \in C(\overline{\Omega})$, then $u \overset{\text{nt}}{\longrightarrow} a$ and for $m > 2$ $u \to 0$ at infinity.*

Theorem 9 *Let Ω be an exterior domain of $\mathbb{R}^2$ of class C^2. Let $a, \mathcal{V}[f]_{\partial\Omega} \in W^{\alpha,q}(\partial\Omega)$ ($q \in (1, +\infty), \alpha \in [0, 1]$) and let f have compact support. If (46) holds, then (1) and (2) has a solution expressed by (44), with $\varphi \in W^{\alpha,q}(\partial\Omega)$ and, if $\mathcal{V}[f] \in C(\overline{\Omega})$, then $u \overset{\text{nt}}{\longrightarrow} a$.*

Existence and uniqueness of a solution to the Stokes problem in domains of class C^1 or with a small Lipschitz constant have been obtained in a variational context in [36].

If Ω is of class $C^{2,1}$, then the simple and double layer potentials, with densities in $W^{-1-1/q,q}(\partial\Omega)$ and $W^{-1/q,q}(\partial\Omega)$ respectively, are defined respectively by

$$v[\psi](x) = -\int_{\partial\Omega}^{\star} \mathbb{S}(x-\zeta)\psi(\zeta)\,d\sigma_\zeta,$$
$$P[\psi](x) = -\int_{\partial\Omega}^{\star} \mathcal{P}(x-\zeta)\psi(\zeta)\,d\sigma_\zeta,$$

and

$$w[\varphi](x) = \int_{\partial\Omega}^{\star} T'[\mathbb{S},\mathcal{P}](x-\zeta)(\varphi\otimes n)(\zeta)\,d\mathrm{a}_\zeta,$$
$$\varpi[\psi](x) = -2\int_{\partial\Omega}^{\star} \varphi(\zeta)\cdot[\nabla_x\mathcal{P}(x-\zeta)]n(\zeta)\,d\mathrm{a}_\zeta$$

The boundary trace relations continue to hold as continuous extension of $L^q(\partial\Omega)$ to $W^{-1/q,q}(\partial\Omega)$ and the operator $\mathcal{K}$ is compact [16]. Therefore, we have

Theorem 10 *Let Ω be bounded domain of class $C^{2,1}$. If f satisfies (29) and $a \in W^{-1/q,q}(\partial\Omega)$, $q > 1$, satisfies*

$$\int_{\partial\Omega}^{\star} a\cdot n = 0 \tag{47}$$

then (1) has a solution expressed by (34), with $\varphi \in W^{-1/q,q}(\partial\Omega)$, and

$$\|u\|_{L^q(\Omega)} \le c\{\|a\|_{W^{-1/q,q}(\partial\Omega)} + \|f\|_{W^{2-s,t}(\Omega)}\}.$$

Theorem 11 *Let Ω be an exterior domain of class $C^{2,1}$. If $a \in W^{-1/q,q}(\partial\Omega)$, $q > 1$, f satisfies (29) and has compact support, then (1) has a solution expressed by (40), with $\varphi \in W^{-1/q,q}(\partial\Omega)$, and for $m > 2$ $u \to 0$ at infinity.*

Theorem 12 *Let Ω be an exterior domain of $\mathbb{R}^2$ of class $C^{2,1}$. If $a \in W^{-1/q,q}(\partial\Omega)$, $q > 1$, f satisfies (29) and has compact support and*

$$\int_{\partial\Omega}^{*} (a - \mathcal{V}[f]_{|\partial\Omega} - u_\infty)\cdot\psi' = 0, \quad \psi' \in \mathfrak{C}_0,$$

then (1) and (2) has a solution expressed by (44), with $\varphi \in W^{-1/q,q}(\partial\Omega)$.

Existence and uniqueness of a solution to (1) in domains of class $C^{2,1}$ and boundary data in $W^{-1/q,q}(\partial\Omega)$ have been also studied in [28, 37] (see also [1, 40]).

4 A Variant of G. Verchota's Approach to Potential Theory for Lipschitz Domains

In a seminal paper of 1982 [13] R.R. Coifman, A. McIntosh and Y. Meyer removed the smallness restriction on the Lipschitz constant in Calderón theorem [8] so that the techniques developed in [25] can be used to show that the trace of the layer potentials on Lipschitz surfaces have meaning in the sense of non tangential convergence. Moreover, $\mathcal{S}$ is continuous from $L^q(\partial\Omega)$ into $W^{1,q}(\partial\Omega)$ and $\mathcal{K}$ is continuous from $L^q(\partial\Omega)$ into itself and from $W^{1,q}(\partial\Omega)$ into itself for all $q \in (1, +\infty)$. Nevertheless, since, in general, $\mathcal{K}$ is no longer completely continuous [24], the method in Sect. 3 cannot be used to get invertibility of the functional equations (35) and (41), which is the core of the Fredholm–Riesz–Schauder theory of integral equations. However, what we really need to achieve this goal is that the trace operator we want to invert has closed range and finite index [58]. For instance, if $f = 0$, $a \in L^2(\partial\Omega)$ and we look for a solution expressed by a simple layer potential, it is sufficient to detect whether $\mathcal{S}[W^{-1,2}(\partial\Omega)]$ is a closed subspace of $L^2(\partial\Omega)$ and $\mathrm{Ker}\,\mathcal{S}^* < +\infty$. In such a case the equation

$$\mathcal{S}[\psi] = a \in L^2(\partial\Omega)$$

has a solution $\psi \in W^{-1,2}(\partial\Omega)$ if and only if

$$\int_{\partial\Omega} a \cdot \psi' = 0, \qquad \psi' \in \mathrm{Ker}\,\mathcal{S}^*.$$

Two years after the publication of [13], G. Verchota [82] was able to find another approach to the L^2 – invertibility of the (double layer) harmonic trace integral equation based on some classical inequality of F. Rellich [66] (see also [62], Chap. V). Roughly speaking, if u is a simple layer harmonic potential in $\mathbb{R}^3$ (say) with density in $L^2(\partial\Omega)$, then from the Rellich inequalities

$$\int_{\partial\Omega} |\partial_n u|^2 \le c \left\{ \int_{\partial\Omega} |\partial_t u|^2 + \int_{\partial\Omega} u^2 \right\},$$
$$\int_{\partial\Omega} |\partial_t u|^2 \le c \left\{ \int_{\partial\Omega} |\partial_n u|^2 + \int_{\partial\Omega} u^2 \right\},$$

the jump condition on $\partial_n v_a[\psi]$ and the continuity of $\partial_t u$ across $\partial\Omega$, one shows that the operator $\frac{1}{2} \pm \mathcal{K}^*$ from $L^2(\partial\Omega)$ into itself have closed ranges. Then, starting from this basic property and proceeding in a more classical setting, Verchota proved the solvability of the classical Dirichlet and Neumann problem in bounded or exterior Lipschitz domains with connected boundaries (see also [23] and Chap. 15 of [55]).[2]

[2] The general case of domains with non connected boundaries is considered in [27]

An important feature of Verchota's approach is that it is not confined to the Laplacian but it is sufficiently general to tackle, in principle, any boundary value problem associated to an elliptic operator with constant coefficients in Lipschitz bounded or exterior domains, once one has at disposal inequalities of Rellich type [23]. As a consequence, the great flexibility of Verchota's technique leads to the solvability of important problems of mathematical physics in Lipschitz domains and with boundary data in L^2, like for instance the displacement and the traction problems of homogeneous and isotropic elasticity and the linearized hydrodynamics ([15, 26, 38, 46, 59, 68] and the references therein).

In 2003 [67] in the context of the Stokes problem we propose another approach to the L^2 – invertibility of the (simple layer) trace integral equation, based on the Nečas theory of regularity of variational solutions [62], Chap. V. We first show that $\mathcal{S}$ is Fredholm with index zero in $W^{-1/2,2}(\partial\Omega)$, then thanks to the results in [62] we prove that $\mathcal{S} : L^2(\partial\Omega) \to W^{1,2}(\partial\Omega)$ has closed range and finite index. In this section, we shall prove the above results by a simpler and more direct argument.

Let $\partial\Omega$ be Lipschitz. The operator

$$\mathcal{S} : L^2(\partial\Omega) \to W^{1,2}(\partial\Omega)$$

is linear and continuous [13] and

$$v[\psi] \xrightarrow{\text{nt}} \mathcal{S}^*[\psi],$$

where

$$\mathcal{S}^* : W^{-1,2}(\partial\Omega) \to L^2(\partial\Omega)$$

is the adjoint operator to $\mathcal{S}$, which coincides with the (unique) continuous extension of $\mathcal{S}$ to $W^{-1,2}(\partial\Omega)$. Moreover, (28) holds and, denoting by $\delta(x)$ the distance of x from $\partial\Omega$, for Ω bounded we have [7, 27, 59]

$$\begin{aligned} \|u\|_{W^{1,2}(\Omega,\sqrt{\delta})} + \|p\|_{L^2(\Omega,\sqrt{\delta})} &\le c\|\psi\|_{W^{-1,2}(\partial\Omega)}, \\ \|u\|_{W^{2,2}(\Omega,\sqrt{\delta})} + \|p\|_{W^{1,2}(\Omega,\sqrt{\delta})} &\le c\|\psi\|_{L^2(\partial\Omega)}. \end{aligned}$$

Let

$$n_i = \begin{cases} n, & \text{on } \partial\Omega_i, \\ 0, & \text{on } \partial\Omega \setminus \partial\Omega_i, \end{cases} \qquad i = 1, \dots, m,$$

Lemma 8 *The operator $\mathcal{S}$ is Fredholm with index zero and*

$$\operatorname{Ker}\mathcal{S} = \operatorname{Ker}\mathcal{S}^* = \begin{cases} \operatorname{sp}\{n, n_i\}_{i=1,\dots,h}, & m > 2, \\ \operatorname{sp}\{n, n_i\}_{i=1,\dots,h} \oplus \mathfrak{M}, & m = 2, \end{cases} \tag{48}$$

for Ω bounded, and

$$\operatorname{Ker}\mathcal{S} = \operatorname{Ker}\mathcal{S}^* = \begin{cases} \operatorname{sp}\{n_i\}_{i=1,\dots,h}, & m > 2, \\ \operatorname{sp}\{n_i\}_{i=1,\dots,h} \oplus \mathfrak{M}_0, & m = 2, \end{cases} \tag{49}$$

for Ω exterior, with

$$\dim \mathfrak{M},\ \dim \mathfrak{M}_0 \leq 2. \tag{50}$$

Proof Let Ω be exterior. If $\psi \in W^{-1/2,2}(\partial\Omega)$, then by (28), the trace theorem and Lemma 5

$$\begin{aligned}\|\psi\|_{W^{-1/2,2}(\partial\Omega)} &\leq \|T[v[\psi], P[\psi]]^+ n\|_{W^{-1/2,2}(\partial\Omega)} + \|T[v[\psi], P[\psi]]^- n\|_{W^{-1/2,2}(\partial\Omega)} \\ &\leq c\|\mathcal{S}[\psi]\|_{W^{1/2,2}(\partial\Omega_R)} \leq c\|\mathcal{S}[\psi]\|_{W^{1/2,2}(\partial\Omega)} + \|\text{compact map}\|.\end{aligned}$$

Hence, by a classical theorem of J. Peetre (see, e.g., [58] p. 618), it follows that the self-adjoint operator

$$\mathcal{S}_0 : W^{-1/2,2}(\partial\Omega) \to W^{1/2,2}(\partial\Omega)$$

is Fredholm with index zero. Let $\psi \in \operatorname{Ker}\mathcal{S}_0$. If $m > 2$ a simple computation shows that $v[\psi] = 0$ in $\mathbb{R}^m$, $P[\psi] = c_i$ in Ω_i and $P[\psi] = 0$ in Ω. Hence $\psi \in \operatorname{sp}\{n_i\}$. On the other hand, it is not difficult to see that $n_i \in \operatorname{Ker}\mathcal{S}_0$ and (49) is proved. If $m = 2$, to prove (50) we can proceed as we did above to show that $\dim \mathfrak{M}' \leq 2$. Let $a \in W^{1,2}(\partial\Omega)$ be orthogonal to every $\psi \in \operatorname{Ker}\mathcal{S}_0$; by Fredholm's alternative, there exists $\psi \in W^{-1/2,2}(\partial\Omega)$ such that $\mathcal{S}_0[\psi] = a$. Then $v[\psi]$ is a weak solution to the Stokes problem in $\Omega \cap S_R$ corresponding to boundary value in $W^{1,2}(\partial\Omega \cup \partial S_R)$ so that from Lemma 7 it follows $T[v[\psi], P[\psi]]n^- \in L^2(\partial\Omega)$. Since $v[\psi]$ is also a solution to Stokes system in Ω' corresponding to a, by the same argument we see that $T[v[\psi], P[\psi]]n^+ \in L^2(\partial\Omega)$ and (28) yields $\psi \in L^2(\partial\Omega)$. Hence the operator.

$$\mathcal{S} : L^2(\partial\Omega) \to W^{1,2}(\partial\Omega)$$

has a closed range and its kernel is given by (49). Let $\psi \in \operatorname{Ker}\mathcal{S}^*$. There exists a sequence $\{\psi_k\}_{k\in\mathbb{N}}$ in $L^2(\partial\Omega)$ which converges to ψ in $W^{-1,2}(\partial\Omega)$. Let $\varphi \in C_0^\infty(\Omega)$ be such that for $m = 2$

$$\int_\Omega \varphi = 0, \quad \int_\Omega \varphi \cdot v[\psi'] = 0, \quad \forall\, \psi' \in \mathfrak{C}_0, \tag{51}$$

with $\mathfrak{C}_0$ defined by (43). Since a simple calculation and (51) imply

$$\int_{\partial\Omega} \mathcal{V}[\varphi] \cdot \psi' = 0, \quad \forall\, \psi' \in \operatorname{Ker}\mathcal{S} \setminus \mathfrak{C}_0,$$

the system

$$\begin{aligned} \Delta z - \nabla Q = \varphi \quad & \text{in} \quad \Omega, \\ \operatorname{div} z = 0 \quad & \text{in} \quad \Omega, \\ z = 0 \quad & \text{on} \quad \partial\Omega, \\ \lim_{r \to +\infty} z(x) = 0 & \end{aligned} \tag{52}$$

admits the solution

$$z = v[\bar{\psi}] + \mathcal{V}[\varphi],$$
$$p = P(\bar{\psi}) + \mathcal{P}[\varphi],$$

with $\bar{\psi}_{\partial\Omega} = 0$ for $n = 2$. Then an integration by parts yields

$$\int_{\Omega} v[\psi_k] \cdot \varphi = \int_{\partial\Omega} \mathcal{S}[\psi_k] \cdot T(z, Q)n.$$

Hence, letting $k \to \infty$, it follows

$$\int_{\Omega} v[\psi] \cdot \varphi = 0,$$

forall $\varphi \in C_0^\infty$ satisfying (51). Repeating the above argument, with $\varphi \in C_0^\infty(\Omega')$ and (z, Q) solution to $(52)_{1,2,3}$ in Ω', we easily arrive at

$$\int_{\Omega'} v[\psi] \cdot \varphi = 0,$$

forall $\varphi \in C_0^\infty$. Hence it follows that $\operatorname{Ker} \mathcal{S} = \operatorname{Ker} \mathcal{S}^*$. The proof for Ω bounded follows the same argument. □

Theorem 1 tells us in particular that any solution to the Stokes system $(1)_{1,2}$ which behaves at infinity as $O(r^{k+1})$ can be decomposed as a sum of a solution which goes at infinity as the fundamental solution and a k-Stokes polynomial. In the sequel we shall prove that such a solution actually exists provided $f \in \mathcal{H}^1(\Omega)$ has compact support and $a \in L^2(\partial\Omega)$ satisfies

$$\int_{\partial\Omega_i} a \cdot n = 0$$

Let

$$\mathfrak{C}_j = \{\psi(\neq n_i) : \mathcal{S}[\psi] + \gamma\kappa \in \mathfrak{S}_j\}, \quad j \in \mathbb{N}_0,$$
$$\mathfrak{C}'_j = \left\{\psi \in \mathfrak{C}_j : \int_{\partial\Omega} \underbrace{\xi \otimes \ldots \otimes \xi}_{i-\text{times}} \otimes \psi = 0,\ i = 1, \ldots j-1\right\}, \quad j \in \mathbb{N},$$

where

$$\gamma = \dim \mathfrak{M}_0.$$

Of course $\mathfrak{M}_0 \subseteq \mathfrak{C}_0$. By repeating the argument in the proof of Lemma 3 in [14], we have

Lemma 9 *It holds*

$$\mathfrak{C}_k = \mathfrak{C}_0 \oplus \bigoplus_{j=1}^{k} \mathfrak{C}'_j.$$

and $\dim \mathfrak{C}_k = \dim \mathfrak{S}_k$.

5 Existence, Uniqueness and Regularity of Very Weak Solutions in Bounded Lipschitz Domains

We are now in a position to apply Fredholm's theory to get the existence of a solution to (1) in Lipschitz domains with boundary data in $L^2(\partial\Omega)$. To this end, consider the vector field

$$\sigma(x) = -\sum_{i=1}^{h} \left\{\nabla\mathcal{U}(x - x_i) \int_{\partial\Omega} a \cdot n_i\right\}.$$

where x_i is a (fixed) point in Ω_i, $i = 1, \ldots, h$.

Let Ω be bounded and assume that

$$a \in L^2(\partial\Omega); \quad f \in W^{s-2,t}(\Omega),\ (m - 1 + 2s)t \geq 2m,\ st > 1. \tag{53}$$

Note that $(53)_2$ assures that $\mathcal{V}[f]_{|\partial\Omega} \in L^2(\partial\Omega)$; also, if $f \in L^2(\Omega)$, then $\mathcal{V}[f]_{|\partial\Omega} \in W^{1,2}(\partial\Omega)$ [62]. Looking for a solution to problem (1) expressed by

$$\begin{aligned} u &= v[\psi] + \sigma + \mathcal{V}[f] + \gamma\kappa, \\ p &= P[\psi] + \mathcal{P}[f], \end{aligned} \tag{54}$$

with κ a constant vector, we have to find a solution to the functional equation

$$\mathcal{S}[\psi] = a - (\sigma + \mathcal{V}[\psi])_{|\partial\Omega} - \gamma\kappa. \tag{55}$$

If $a \in L^2(\partial\Omega)$ [respect. $a \in W^{1,2}(\partial\Omega)$ and $f \in L^2(\Omega)$], then, by what we proved in the foregoing section, we have that (55) has a solution $\psi \in W^{-1,2}(\partial\Omega)$ [respect. $\psi \in L^2(\partial\Omega)$] if and only if we choose κ such that

$$\gamma\kappa \cdot \int_{\partial\Omega} \psi' = \int_{\partial\Omega} a \cdot \psi' - \int_{\Omega}^{\star} f \cdot v[\psi'], \quad \psi' \in \mathfrak{M}.$$

It is evident that u satisfies *natural estimates*. For instance [59],

$$\|u\|_{W^{1/2,2}(\Omega)} \le c\left\{\|a\|_{L^2(\Omega)} + \|f\|_{W^{s-2,t}(\Omega)}\right\}. \tag{56}$$

Let $a \in L^2(\partial\Omega)$ and let $\{a_k\}_{k\in\mathbb{N}}$ be a sequence in $W^{1,2}(\partial\Omega)$ which converges strongly in $L^2(\partial\Omega)$ to a. Let (u_k, p_k) be the solution corresponding to data (a_k, f) given by (54). Then, denoting by (z, Q) the solution to $(52)_{1,2,3}$ with $\varphi \in C_0^\infty(\Omega)$, an integration by parts yields

$$\int_\Omega u_k \cdot \varphi = \int_{\partial\Omega} a_k \cdot T[z, Q]n + \int_\Omega^\star f \cdot z$$

Hence, letting $k \to +\infty$ and taking into account (56), it follows that u satisfies the relation

$$\int_\Omega u \cdot \varphi = \int_{\partial\Omega} a \cdot T[z, Q]n + \int_\Omega^\star f \cdot z \tag{57}$$

for all $\varphi \in C_0^\infty(\Omega)$, with (z, Q) solution to $(52)_{1,2,3}$. According to J. Nečas [62], we call *very weak solution* to problem (1) a field $u \in L^2_\sigma(\Omega)$ which satisfies (57).

Therefore, we can state

Theorem 13 *Let Ω be a bounded Lipschitz domain. If a, f satisfy (30) and (53), then (1) has a unique very weak solution expressed by (54) and natural estimates hold; in particular,*

$$\|u\|_{W^{1,2}(\Omega,\sqrt{\delta})} + \|p\|_{L^2(\Omega,\sqrt{\delta})} \le c\Big\{\|a\|_{L^2(\partial\Omega)} + \|f\|_{W^{s-2,t}(\Omega)}\Big\}.$$

Moreover, if $st > m$, then $u \xrightarrow{\text{nt}} a$; if $a \in W^{1,2}(\partial\Omega)$ and $f \in L^2(\Omega)$, then $\psi \in L^2(\partial\Omega)$ and

$$\|u\|_{W^{2,2}(\Omega,\sqrt{\delta})} + \|p\|_{W^{1,2}(\Omega,\sqrt{\delta})} \le c\Big\{\|a\|_{W^{1,2}(\partial\Omega)} + \|f\|_{L^2(\Omega)}\Big\}.$$

In virtue of well-known *stability and interpolation results* (see, e.g., [44, 59]), there is a positive constant ε depending only on m and $\partial\Omega$ such that Theorem 13 can be stated for $a \in W^{\alpha,q}(\partial\Omega)$ and f such that $\mathcal{V}[f]_{|\partial\Omega} \in W^{\alpha,q}(\partial\Omega)$, with $\alpha \in [0,1]$ and $q \in (2-\varepsilon, 2+\varepsilon)$. If $m \leq 4$, then by well–known results of R.M. Brown and Z. Shen [7, 72] we can say much more; for instance, for $m = 2$ and $a \in C(\partial\Omega)$, $f \in \mathcal{H}^1(\Omega)$, that $u \in C(\overline{\Omega})$ and the maximum modulus theorem (39) holds. Therefore, we can state the following

Theorem 14 *If Ω be a bounded Lipschitz domain, then there is a positive constant ε depending on $\partial\Omega$ such that if a, $\mathcal{V}[f]_{|\partial\Omega} \in W^{\alpha,q}(\partial\Omega)$ ($\alpha \in [0,1]$, $q \in (2-\varepsilon, 2+\varepsilon)$) and a satisfies (30), then (1) has a unique very weak solution expressed by (54), natural estimates hold and if $\mathcal{V}[f] \in C(\overline{\Omega})$, then $u \xrightarrow{\text{nt}} a$. Moreover, if $m = 3$, then there are positive constant ε' and μ_0 such that*

- *if $a \in W^{1-1/q,q}(\partial\Omega)$ and $f \in W^{-1,q}(\Omega)$, $q \in [3/2, 3+\varepsilon')$, then*

$$\|u\|_{W^{1,q}(\Omega)} + \|p\|_{L^q(\Omega)} \leq c\left\{\|a\|_{W^{1-1/q,q}(\partial\Omega)} + \|f\|_{W^{-1,q}(\Omega)}\right\};$$

- *if $a \in C^{0,\mu}(\partial\Omega)$, $\mu \in [0,\mu_0)$, $\mu \in [0,\mu_0)$, and $f \in W^{-1,q}(\Omega)$, $q > 3(1-\mu)$, then*

$$\|u\|_{C^{0,\mu}(\overline{\Omega})} \leq c\left\{\|a\|_{C^{0,\mu}(\partial\Omega)} + \|f\|_{W^{-1,q}(\Omega)}\right\};$$

If Ω is of class C^1 we can take $\mu_0 = 1$ andq $\in (1,+\infty)$.

If Ω is of class $C^{2,1}$, f and $a \in W^{-1/q,q}(\partial\Omega)$ ($q > 1$) satisfy (29) and (47) respectively, a field $u \in L^q_\sigma(\Omega)$ is a very weak solution to (1) provided the relation

$$\int_\Omega u \cdot \varphi = \int^\star_{\partial\Omega} a \cdot T[z,Q]n + \int^\star_\Omega f \cdot z$$

holds for all $\varphi \in C_0^\infty(\Omega)$, with (z,Q) solution to $(52)_{1,2,3}$. It is readily seen that system (1) has a unique very weak solution expressed by (54) with $\psi \in W^{-1-1/q,q}(\partial\Omega)$.

6 Existence and Uniqueness of Very Weak Solutions in Lipschitz Exterior Domains

Let Ω be an exterior domain and assume that

$$a \in L^2(\partial\Omega), \quad f \in \mathcal{H}^1(\Omega). \tag{58}$$

It is quite evident that the argument used at the beginning of Sect. 5 can be repeated to prove existence of a solution to (1) in Ω expressed by the pair (54) with

$\psi \in W^{-1,2}(\partial\Omega)$ (and $\psi \in L^2(\partial\Omega)$, if $a \in W^{1,2}(\partial\Omega)$). As far as the uniqueness of this solution is concerned, consider a sequence $\{a_k\}_{k\in\mathbb{N}}$ in $W^{1,2}(\partial\Omega)$ which converges to a strongly in $L^2(\partial\Omega)$. Let (u_k, p_k) be the solution corresponding to data (a_k, f) given by (54). Then, denoting by (z, Q) the solution to (52) with $\varphi \in C_0^\infty(\Omega)$ satisfying (51), then an integration by parts yields

$$\int_{\Omega_R} u_k \cdot \varphi = -\int_{\partial\Omega} a_k \cdot T[z, Q]n + \int_{\Omega_R} f \cdot z + \int_{\partial S_R} e_R \cdot (T[z, Q]u_k - T[u_k, p_k]z).$$

Hence, letting $R \to +\infty$ and taking into account the behavior at infinity of (u_k, p_k) and (z, Q), it follows

$$\int_{\Omega} u_k \cdot \varphi = -\int_{\partial\Omega} a_k \cdot T[z, Q]n + \int_{\Omega} f \cdot z. \tag{59}$$

Letting $k \to +\infty$ in (59) we see that (u, p) satisfies the relation

$$\int_{\Omega} u \cdot \varphi = -\int_{\partial\Omega} a \cdot T[z, Q]n + \int_{\Omega} f \cdot z. \tag{60}$$

Moreover, if $a = 0$, $f = 0$ and $m = 2$, then

$$(u, p) \in \mathfrak{F}_0 = \{(v[\psi'] - \gamma\mathcal{S}[\psi'], P[\psi']),\ \psi' \in \mathfrak{C}_0\}.$$

Therefore, calling very weak solution to (1) in an exterior domain Ω a field $u \in L^2_{\sigma,\mathrm{loc}}(\overline{\Omega})$ which meets (60), with (z, Q) solution to (52) and $\varphi \in C^\infty(\Omega)$ satisfying (51), we can state

Theorem 15 *Let Ω be an exterior Lipschitz domain. If a, f satisfy (58), then (1) has a unique very weak solution expressed by (54) modulo a pair in $\mathfrak{F}_0$ for $m = 2$. Moreover, if $f \in L^t(\Omega)$, $t > m/2$, then $u \xrightarrow{\mathrm{nt}} a$; the regularity results stated in Theorem 14 hold locally and natural estimates hold.*

It is clear that, if f has compact support, then the solution in Theorem 15 behaves at infinity as the function $\mathbb{S}(x)$. Then it is reasonable to look whether there are conditions on the data assuring the corresponding solution to decay at infinity more rapidly than $\nabla_k\mathbb{S}(x)$. To this end, choose $\psi_k \in \mathfrak{C}_k$ such that

$$\int_{\partial\Omega} \underbrace{\xi \otimes \ldots \otimes \xi}_{i \text{ times}} \otimes (\psi + \psi_k) = 0, \quad i = 0, \ldots, k-1.$$

where ψ is the density of the simple layer potential appearing in (54). Then setting $\bar{\psi} = \psi + \psi_k$, the pair

$$
\begin{aligned}
u &= v[\bar{\psi}] + \sigma + \mathcal{V}[f] + \mathfrak{p}_k + \gamma\kappa, \\
p &= P[\bar{\psi}] + \mathcal{P}[f] + \mathfrak{q}_{k-1},
\end{aligned}
\tag{61}
$$

with $\mathcal{S}[\psi_k] = -\mathfrak{p}_k$, is a solution to (1) such that

$$
v[\bar{\psi}] = O(r^{1-m-k})
$$

and we can state the following

Theorem 16 *Let Ω be an exterior Lipschitz domain. If a, f satisfy (58), then there is a density $\psi \in W^{-1,2}(\partial\Omega)$, with*

$$
\int_{\partial\Omega} \underbrace{\xi \otimes \ldots \otimes \xi}_{i-\text{times}} \otimes \psi = 0, \quad i = 0, 1, \ldots k-1,
$$

and a k-Stokes polynomial defined by

$$
\int_{\partial\Omega} (a - \sigma) \cdot \psi' = \int_{\partial\Omega} \mathfrak{p}_k \cdot \psi' + \int_{\Omega} f \cdot v[\psi'], \quad \forall\, \psi' \in \mathfrak{C}_k,
\tag{62}
$$

such that the pair (61) is a solution to (1).

If we assign a Stokes polynomial $\mathfrak{p}_k$ and aim at solving the problem

$$
\begin{aligned}
\Delta u - \nabla p &= f && \text{in} \quad \Omega, \\
\operatorname{div} u &= 0 && \text{in} \quad \Omega, \\
u &= a && \text{on} \quad \partial\Omega, \\
u - \mathfrak{p}_k &= O(r^{1-m-k})
\end{aligned}
\tag{63}
$$

we have to require at least that a, f and $\mathfrak{p}_k$ satisfies a compatibility condition derived from (62).

Let us call very weak solution to (63) a field $u \in L^2_{\sigma,\text{loc}}(\overline{\Omega})$ which satisfies

$$
\int_{\Omega} (u - \mathfrak{p}_k) \cdot \varphi = -\int_{\partial\Omega} (a - \mathfrak{p}_k) \cdot T[z, Q]n + \int_{\Omega} f \cdot z
\tag{64}
$$

for all $\varphi \in C_0^\infty(\Omega)$, with (z, Q) solution to $(52)_{1,2,3}$, $z = o(r^{k+1})$. Set for $k \in \mathbb{N}$

$$
\mathfrak{F}_k = \{(v[\psi'] - \mathcal{S}[\psi'], P[\psi']),\ \psi' \in \mathfrak{C}_k\}.
$$

Starting from Theorem 16 it is not difficult to get

Theorem 17 *Let Ω be an exterior Lipschitz domain. If $a \in L^2(\partial\Omega)$ and $f \in C_0^\infty(\Omega)$ satisfy*

$$\int_{\partial\Omega} a \cdot n_i = 0, \quad \int_\Omega \nabla_j f = 0, \quad j = 0, \ldots k,$$

then (63) has a unique very weak solution up to a field in $\mathfrak{F}_k$ if and only if

$$\int_{\partial\Omega} a \cdot \psi' = \int_{\partial\Omega} \mathfrak{p}_k \cdot \psi' + \int_\Omega f \cdot v[\psi'], \quad \forall\, \psi' \in \mathfrak{C}_k. \tag{65}$$

Proof We have only to prove that condition (65) is necessary. Let u satisfy (64). Since the field $z + v[\psi'] - \mathcal{S}[\psi']$ is a solution to $(52)_{1,2,3}$ for all $\psi' \in \mathfrak{C}_k$, then (65) easily follows from (64). □

A simple consequence of Theorem 17 is the famous *Stokes' paradox.*

Theorem 18 *Let Ω be an exterior Lipschitz domain of $\mathbb{R}^2$. If $a \in L^2(\partial\Omega)$ and $f \in \mathcal{H}^1(\Omega)$, then (1) and (2) has a unique very weak solution $(u, p) \in W^{2,1}_{\rm loc}(\Omega) \times W^{1,1}_{\rm loc}(\Omega)$, $\nabla u, p \in L^2(\Omega, \sqrt{\delta})$, expressed by*

$$\begin{aligned} u &= v[\psi] + \mathcal{V}[f] + \sigma + u_\infty, \\ p &= P[\psi] + \mathcal{P}[f] \end{aligned}$$

with $\psi \in W^{-1,2}(\partial\Omega)$, if and only if

$$\int_{\partial\Omega} a \cdot \psi' = \int_\Omega f \cdot v[\psi'] + u_\infty \cdot \int_{\partial\Omega} \psi', \qquad \forall\, \psi' \in \mathfrak{C}_0. \tag{66}$$

• Even if conditions (66) are necessary and sufficient for the existence of a solution vanishing at infinity as r^{1-m}, nevertheless they are not useful to select the boundary data assuring the desired decay, unless we are able to discover the fields of the linear spaces $\mathfrak{C}_0$. As far as we are aware, this is possible only when $\partial\Omega$ is an ellipsoid (cf., e.g., [42, 52]; see also [6, 14, 69]). Indeed, in such a case we have

$$\mathfrak{C}_0 = \mathrm{sp}\,\{(\xi \cdot n)e_i\}_{i=1,\ldots,m}.$$

7 The Stokes Paradox for the Robin Problem

We aim at noting that the *validity* of Stokes' paradox is not confined to the Stokes equations with nonslip boundary conditions [70]. To avoid unessential formal complications we shall assume $\partial\Omega$ connected and $f = 0$. However, the general case can be treated by the same argument.

In an exterior Lipschitz domain Ω of $\mathbb{R}^2$ consider the *Robin problem*

$$\begin{aligned} \Delta u &= \nabla p \quad && \text{in} \quad \Omega, \\ \operatorname{div} u &= 0 \quad && \text{in} \quad \Omega, \\ \mathcal{R}[u,p] = u - T(u,p)n &= a \quad && \text{on} \quad \partial\Omega, \\ \lim_{r\to+\infty} u(x) &= u_\infty. && \end{aligned} \tag{67}$$

Our aim is to show that (67) admits a solution provided a and u_∞ satisfy a suitable compatibility condition (Stokes' paradox).

Since $\frac{1}{2}I + \mathcal{K}^* : L^2(\partial\Omega) \to L^2(\partial\Omega)$ is Fredholm with index zero [67] and $\mathcal{S}$ is completely continuous as an operator from $L^2(\partial\Omega)$ into itself, also $\mathcal{S} + \frac{1}{2}I + \mathcal{K}^*$ is Fredholm with index zero. It is easy to see that

$$\operatorname{Ker}\big(\mathcal{S} + \tfrac{1}{2}I + \mathcal{K}^*\big) = \operatorname{sp}\{n\} + \mathfrak{M}'_0.$$

with $\dim \mathfrak{M}'_0 \le 2$. Assume only for simplicity $\mathfrak{M}'_0 = \{0\}$. If $\varphi \in \operatorname{Ker}\big(\mathcal{S} + \frac{1}{2}I + \mathcal{K}\big)$, then the pair

$$\begin{aligned} u &= v[\varphi] + w[\varphi], \\ p &= P[\varphi] + \varpi[\varphi] \end{aligned}$$

is a solution to (7) in $\mathbb{R}^2 \setminus \partial\Omega$ such that $u = 0$ and $p = c$ in Ω' and from the jump conditions it follows

$$u^- = -\varphi, \quad T[u,p]^- n = cn - \varphi. \tag{68}$$

If $\varphi_{\partial\Omega} = 0$, then an integration by parts and $(25)_2$, (26) yields

$$2\int_\Omega |\hat{\nabla} u|^2 + \int_{\partial\Omega} |\varphi|^2 = c\int_{\partial\Omega} \varphi\cdot n.$$

Hence necessarily

$$\int_{\partial\Omega} \varphi\cdot n \neq 0.$$

If $\varphi_{\partial\Omega} \neq 0$ and we choose

$$\kappa = \left(\int_{\partial\Omega} a\cdot\varphi\right)\left(\int_{\partial\Omega}\varphi\right)^{-2}\int_{\partial\Omega}\varphi,$$

the equation

$$a - \kappa = \big(\mathcal{S} + \tfrac{1}{2}I + \mathcal{K}^*\big)[\psi]$$

has a solution $\psi \in L^2(\partial\Omega)$. Hence it follows that the pair

$$\begin{aligned} u &= v[\psi] + \kappa, \\ p &= P[\psi], \end{aligned} \tag{69}$$

is a solution to (67). Let $\varphi_{\partial\Omega} = 0$. Let us note that in such a case the constant c in (68) is non zero, otherwise we have $\varphi = 0$. We look for a solution given by

$$\begin{aligned} u &= v[\psi + \varphi] + w[\varphi], \\ p &= P[\psi + \varphi] + \varpi[\varphi], \end{aligned}$$

for some $\varphi \in \operatorname{Ker}\big(\mathcal{S} + \frac{1}{2}I + \mathcal{K}\big)$. Therefore, we consider the equation

$$a - \mathcal{R}\big[v[\varphi] + w[\varphi], P[\varphi] + \varpi[\varphi]\big] = \big(\mathcal{S} + \tfrac{1}{2}I + \mathcal{K}^*\big)[\psi].$$

Of course, the equation

$$\int_{\partial\Omega} \big\{a - \mathcal{R}\big[v[\varphi] + w[\varphi], P[\varphi] + \varpi[\varphi]\big]\big\} \cdot \varphi' = 0, \quad \forall \varphi' \in \operatorname{Ker}\big(\mathcal{S} + \tfrac{1}{2}I + \mathcal{K}\big),$$

is satisfied if and only if the homogeneous equation

$$\int_{\partial\Omega} \varphi' \cdot \mathcal{R}\big[v[\varphi] + w[\varphi], P[\varphi] + \varpi[\varphi]\big] = 0, \quad \forall \varphi' \in \operatorname{Ker}\big(\mathcal{S} + \tfrac{1}{2}I + \mathcal{K}\big), \tag{70}$$

has only the solution $\varphi = 0$. To show this choose $\varphi' = \varphi$ in (70). Then from (68) we have

$$\int_{\partial\Omega} \varphi \cdot n = 0$$

Hence it follows the desired result. In the sequel we shall assume, to fix ideas, that $\varphi_{\partial\Omega} \neq 0$. The case $\varphi_{\partial\Omega} = 0$ is treated by the same argument (with minor modifications).

In general $v[\psi] = O(\log r)$. To find a solution which satisfies condition $(67)_4$ too, define

$$\mathfrak{C}' = \{\psi \in L^2(\partial\Omega) : \mathcal{R}\big[v[\psi], P[\psi]\big] = \text{constant}\}$$

Reasoning as we did for the space $\mathfrak{C}_0$ it is not difficult to see that $\dim \mathfrak{C}' = 2$ and if $\{\psi_1, \psi_2\}$ is a basis of $\mathfrak{C}'$, then $\{\int_{\partial\Omega} \psi_1, \int_{\partial\Omega} \psi_2\}$ is a basis of $\mathbb{R}^2$. Let $\bar{\psi} \in \mathfrak{C}'$ be such that $\int_{\partial\Omega}(\psi + \bar{\psi}) = 0$, where ψ is the density appearing in (69). Moreover, let

$$\mathfrak{B} = \{\varphi \in W^{1,2}(\partial\Omega) : \mathcal{S}[\varphi] + w[\varphi]^+ = \text{constant}, \quad P[\varphi] + \varpi[\varphi] = 0 \text{ in } \Omega'\}.$$

If $\varphi(\neq 0) \in \mathfrak{B}$, then $u = (v[\varphi] + w[\varphi], p = P[\varphi] + \varpi[\varphi])$ is a solution to the Stokes equations, constant in Ω'. Then, taking in account (27) and (28), we have

$$u^- = u^+ - \varphi, \quad T[u, p]^- n = -\varphi$$

where u^+ is constant. If $\varphi_{\partial\Omega} = 0$, then an integration on Ω yields

$$2\int_{\Omega} |\hat{\nabla} u|^2 = -\int_{\partial\Omega} u^- \cdot T[u, p]^- n = -\int_{\partial\Omega} |\varphi|^2 - u^+ \cdot \int_{\partial\Omega} T[u, p]^- n$$

so that we have the absurd $\varphi = 0$. Then, $\varphi_{\partial\Omega} \neq 0$ and, proceeding in the usual way, we have that $\dim \mathfrak{B} = 2$ and if $\{\varphi_1, \varphi_2\}$ is a basis of $\mathfrak{B}$, then $\{\int_{\partial\Omega} \varphi_1, \int_{\partial\Omega} \varphi_2\}$ is a basis of $\mathfrak{B}$.

From what we said above it follows that the pair

$$\begin{aligned} u &= v[\psi + \bar{\psi}] + u_\infty, \\ p &= P[\psi + \bar{\psi}], \end{aligned}$$

with $u_\infty = \kappa - \mathrm{Re}[\mathrm{v}[\bar{\psi}], \mathrm{P}[\bar{\psi}]]$ is a solution to $(67)_{1,2,3}$ which converges to the constant vector u_∞ and a simple computation shows that

$$\int_{\partial\Omega} (a - u_\infty) \cdot \varphi = 0, \quad \varphi \in \mathfrak{B}. \tag{71}$$

By proceeding in the same way as we did for system (1), we can give the definition of the class of the very weak solutions to (67) and prove uniqueness therein. Therefore, we have

Theorem 19 *(Stokes' paradox for the Robin problem) Let Ω be an exterior Lipschitz domain of $\mathbb{R}^2$. If $a \in L^2(\partial\Omega)$, then (67) has a unique very weak solution if and only if a, and u_∞ satisfy the compatibility condition (71).*

The above argument can be also used to treat to the more general case when $a \in W^{-1,2}(\partial\Omega)$ for Lipschitz domains and $a \in W^{\alpha,q}(\partial\Omega)$ ($\alpha \in [-1, 0]$, $q \in (1, +\infty)$) for domains of class C^1. Note that, taking into account that if $\partial\Omega$ is a disk and κ is a constant vector, then $\mathcal{S}[\kappa] + w[\kappa]^+$ is constant in Ω', we can state a sort of Picone's result for system (67).

Corollary 1 *Let Ω be the exterior of a disk. If $a \in L^q(\partial\Omega)$, then (67) has a unique very weak solution if and only if*

$$\frac{1}{2\pi}\int_{\Omega} a = u_\infty$$

Therefore, if $u_\infty \neq 0$ and $a = 0$, then (67) does not admit any solution.

8 An Existence Theorem to the Steady-State Navier-Stokes Problem

In this section we aim at showing how the results in Sect. 5 can be used to obtain the existence of a solution to the Navier-Stokes problem

$$\begin{aligned} \Delta u-(\nabla u)u-\nabla p=f \quad &\text{in} \quad \Omega,\\ \operatorname{div} u=0 \quad &\text{in} \quad \Omega,\\ u=a \quad &\text{on} \quad \partial\Omega \end{aligned} \tag{72}$$

in a bounded or exterior domain Ω of $\mathbb{R}^3$ under weak assumptions on f and a. For exterior domains we also require that

$$\lim_{r\to+\infty} u(x)=u_\infty, \tag{73}$$

with u_∞ assigned constant vector. Let

$$\Phi=\frac{1}{8\pi}\sum_{i=1}^{h}|\Phi_i|\left\{\max_{\partial\Omega}\frac{1}{|x-x_i|}-\min_{\partial\Omega}\frac{1}{|x-x_i|}\right\},\quad \Phi_i=\int_{\partial\Omega_i} a\cdot n,$$

where x_i is a fixed point in Ω_i. The following theorem holds true [67].

Theorem 20 *Let Ω be a bounded Lipschitz domain of $\mathbb{R}^3$. If $f\in\mathcal{H}^1(\Omega)$, $a\in L^{8/3}(\partial\Omega)$ satisfies (30) and*

$$\Phi<1, \tag{74}$$

then there is a pair $(u,p)\in W^{2,1}_{\mathrm{loc}}(\Omega)\times W^{1,1}_{\mathrm{loc}}(\Omega)$ which satisfies $(72)_{1,2}$ pointwise almost everywhere and $(72)_3$ in the sense of the trace in Sobolev's spaces. Moreover,

- *if $a\in L^q(\partial\Omega)$, $q\in[8/3,+\infty]$, then $u\in W^{1/q,q}(\Omega)$ and if $q>4$, $f\in L^s(\Omega)$ $(s>3/2)$ then $u\xrightarrow{\text{nt}}a$;*

and there are positive scalars ε and μ_0 such that

- *if $a\in W^{1-1/q,q}(\partial\Omega)$ and $f\in W^{-1,q}(\Omega)$, $q\in[12/7,3+\varepsilon)$, then $(u,p)\in W^{1,q}(\Omega)\times L^q(\Omega)$;*
- *if $a\in C^{0,\mu}(\partial\Omega)$ and $f\in W^{-1,q}(\Omega)$, $\mu\in[0,\mu_0)$ and $q>3/(1-\mu)$, then $u\in C^{0,\mu}(\overline{\Omega})$.*

If Ω is of class C^1, then we can take $\varepsilon=+\infty$ and $\mu_0=1$.

Proof Let (u_s,p_s) be the solution to the Stokes problem with data (f,a). The operator $\mathcal{V}[(\nabla u)u]$ maps $L^4_\sigma(\Omega)$ into $W^{1,2}_\sigma(\Omega)$. Denote by $(\mathcal{K}[u],\mathcal{Q}[u])$ the solution to the Stokes problem with zero body force and boundary datum $-\mathcal{V}[(\nabla u)u]_{|\partial\Omega}\in W^{1/2,2}(\partial\Omega)$. It is simple to see that the operator

$$\mathcal{N}[u] = \mathcal{K}[u] + \mathcal{V}[(\nabla u)u]$$

is completely continuous from $L^4_\sigma(\Omega)$ into itself and a fixed point of the map

$$u' = u_s + \mathcal{N}[u] \tag{75}$$

gives the desired solution to (72); the corresponding pressure field is expressed by $p_s + \mathcal{Q}[u] + \mathcal{P}[(\nabla u)u]$. If we show that the solutions to the equation

$$u = \lambda(u_s + \mathcal{N}[u])$$

are bounded in $L^4_\sigma(\Omega)$ uniformly for $\lambda \in [0, 1]$, then from the Schaefer theorem (see, e.g., [22] p. 504) it follows that (75) has a fixed point. To this end we follow a classical argument of J. Leray [50] (see also, [5, 33, 49]). The field $w = \mathcal{N}[u]$ is a variational solution to the system

$$\begin{aligned} \Delta w - \lambda[\nabla(u_s + w)](u_s + w) = \nabla Q \quad & \text{in} \quad \Omega, \\ \operatorname{div} w = 0 \quad & \text{in} \quad \Omega, \\ w = 0 \quad & \text{on} \quad \partial\Omega. \end{aligned} \tag{76}$$

If the variational solutions to (76) are not uniformly bounded in $W^{1,2}_0(\Omega)$, then two sequences $(\{\lambda_k\}_{k\in\mathbb{N}}, \{w_k\}_{k\in\mathbb{N}}) \in [0, 1] \times W^{1,2}_{\sigma,0}(\Omega)$ exist such that

$$\lim_{k\to+\infty} \lambda_k = \lambda_0 \in [0, 1], \qquad \lim_{k\to+\infty} \|\nabla w_k\|_{L^2(\Omega)} = +\infty$$

and, setting $w'_k = w_k/J_k$ with $J_k = \|\nabla w_k\|_{L^2(\Omega)}$, by the definition of variational solution w'_k satisfies

$$\frac{1}{J_k}\int_\Omega \nabla\varphi \cdot \nabla w'_k = \lambda_k \int_\Omega \Big(\frac{u_s}{J_k} + w'_k\Big) \cdot (\nabla\varphi)\Big(\frac{u_s}{J_k} + w'_k\Big) \tag{77}$$

for all $\varphi \in W^{1,2}_{\sigma,0}(\Omega)$. Since $\|\nabla w'_k\|_{L^2(\Omega)} = 1$, by Rellich selection theorem from $\{w'_k\}_{k\in\mathbb{N}}$ we can extract a subsequence, still denoted by w'_k, which converges weakly in $W^{1,2}(\Omega)$ and strongly in $L^q(\Omega)$, $q \in [1, 6)$, to a field $w' \in W^{1,2}_{\sigma,0}(\Omega)$, with $\|\nabla w'\|_{L^2(\Omega)} \le 1$. Then, choosing first $\varphi \in C^\infty_{\sigma,0}(\Omega)$, then $\varphi = w_k$ in (77) and letting $k \to +\infty$, it follows that w' is a variational solution to the Euler equations

$$\begin{aligned} \lambda_0(\nabla w')w' + \nabla Q' = 0 \quad & \text{in} \quad \Omega, \\ \operatorname{div} w' = 0 \quad & \text{in} \quad \Omega, \\ w' = 0 \quad & \text{on} \quad \partial\Omega, \end{aligned} \tag{78}$$

for some $Q' \in W^{1,3/2}(\Omega)$, and satisfies the relation

$$1 = \lambda_0 \int_\Omega u_s \cdot (\nabla w')w'. \tag{79}$$

Moreover, Q' is constant on every $\partial\Omega_i$ [2, 45], say Q'_i. Since u_s is expressed by (54), taking into account (78) a simple computation yields

$$\begin{aligned}1 =&\lambda_0 \int_\Omega \sigma \cdot (\nabla w')w' = \lambda_0 \sum_{i=1}^h \Phi_i \int_\Omega \frac{|\hat{\nabla} w'|^2 - |\tilde{\nabla} w'|^2}{|x - x_i|} \\ &+ \lambda_0 \int_\Omega (u_s - \sigma) \cdot (\nabla w')w'\end{aligned}$$

Hence, taking into account that

$$2\|\hat{\nabla} w'\|_{L^2(\Omega)} = 2\|\tilde{\nabla} w'\|_{L^2(\Omega)} = \|\nabla w'\|_{L^2(\Omega)}$$

and

$$\int_{\partial\Omega_i} (u_s - \sigma) \cdot n = 0,$$

it follows

$$1 - \lambda_0 \Phi \le \lambda_0 \int_\Omega (u_s - \sigma) \cdot (\nabla w')w' = -\lambda_0 \sum_{i=1}^h Q'_i \int_{\partial\Omega_i} (u_s - \sigma) \cdot n = 0.$$

Since this contradicts (74) we are in the hypotheses of Schaefer theorem and the proof is completed, by noting that the regularity properties of (u, p) are a consequence of the analogous ones concerning Stokes equations and the regularity properties of the operator $\mathcal{V}[(\nabla u)u]$. □

The solution in Theorem 20 is unique provided $\|u_s\|_{L^4(\Omega)}$ is sufficiently small. Existence of a regular solution to (72) under the hypothesis of small fluxes comes back to R. Finn [30]. For variational solutions and Lipschitz domains the results of [30] were extended in [5] and [32]. In dimensions two and four Theorem 20 can be proved under the assumptions $a \in L^2(\partial\Omega)$ and $a \in L^3(\partial\Omega)$ respectively (see [67]). As far as we are aware, the first existence results for (72) in regular domains under weak assumptions on the boundary datum ($a \in W^{1-1/q,q}(\partial\Omega)$, $q > 3/2$) are due to D. Serre [71]; in this connection see also [53].

Since the operator $\mathbb{N}$ in (75) obeys

$$\|\mathcal{N}[u]\|_{L^3(\Omega)} \le c\|u\|^2_{L^3(\Omega)},$$

if $\|u_s\|_{L^3(\Omega)} < 1/(4c)$, then the map (75) is contractive in the ball $\{u \in L^3_\sigma(\Omega) : \|u\|_{L^3_\sigma(\Omega)}\} < 1/(2c)\}$. Hence existence of a solution to (72) follows for "small" $\|a\|_{L^2(\partial\Omega)} + \|f\|_{\mathcal{H}^1(\Omega)}$ in virtue of Banach contractions' theorem. Moreover, if $f = 0$ and $a \in C(\partial\Omega)$, then one proves a maximum modulus theorem [67] (see also [76]).

The first part of Theorem 20 can be also stated for bounded domains of $\mathbb{R}^m$, provided $a \in L^q(\partial\Omega)$, $q > m-1$, and Ω is of class C^1. Existence of solutions to problem (72) under weak regularity hypotheses on (small) data have proved in [20, 37], Starting from Theorem 20 and making use of Leray's procedure of invading domains [50] (see also [74] Chap. 5) we can prove the following existence theorem for exterior domains.

Theorem 21 *Let Ω be an exterior Lipschitz domain of $\mathbb{R}^3$. If $f \in \mathcal{H}^1(\Omega)$ and $a \in L^{8/3}(\partial\Omega)$ satisfies (74) then there is a pair $(u, p) \in W^{2,1}_{\text{loc}}(\Omega) \times W^{1,1}_{\text{loc}}(\Omega)$ which satisfies $(72)_{1,2}$ pointwise almost everywhere and $(72)_3$ in the sense of trace in Sobolev's spaces. Moreover, the regularity properties in Theorem 20 hold locally in Ω and if $f \in L^q(\Omega)$ $(q > 3/2)$ then (73) is satisfied uniformly.*

Note that the above procedure requires only that $u_s \in L^4_\sigma(\Omega)$. Therefore, Theorems 20 and 21 can also be stated for a boundary datum $a \in W^{-1/4,4}(\partial\Omega)$ and Ω of class $C^{2,1}$.

Let Ω be an exterior Lipschitz domain of $\mathbb{R}^3$ and let $a \in L^\infty(\partial\Omega)$, $f \in C^\infty_0(\Omega)$. Let $\mathcal{C}[u]$ be the solution to the Stokes problem with zero body force and boundary datum $\mathcal{V}[(\nabla u)u]_{|\partial\Omega}$. By classical results about the behavior at infinity of volume potentials (see, e.g., [33], Lemma II.7.2) the operator $\nabla\mathcal{V}[u \otimes u] + \mathcal{C}[u]$ maps boundedly $L^\infty(\Omega, r)$ into itself. Moreover, by the estimates about solutions to the Stokes problem it holds

$$\|\nabla\mathcal{V}[u \otimes u] + \mathcal{C}[u]\|_{L^\infty(\Omega,r)} \le c\|u\|^2_{L^\infty(\Omega,r)},$$

Therefore, for $\|a_\infty\|_{L^\infty(\partial\Omega)}$ sufficiently small the equation

$$u = u_s + \nabla\mathcal{V}[u \otimes u] + \mathcal{C}[u]$$

has a fixed point which is a solution to (72) such that $u = O(r^{-1})$. Moreover, by a result of V. Sverák and T-P Tsai [79], $\nabla_k u = O(r^{-1-k})$ for every $k \in \mathbb{N}$. In this connection see also [61, 63, 73].

References

1. H. Amann, Nonhomogeneous Navier–Stokes equations with integrable low–regularity data, *Int. Math. Ser.* Kluwer Academic/Plenum Publishing, New York, 1–26 (2002)
2. C.J. Amick, Existence of solutions to the nonhomogeneous steady Navier–Stokes equations. Indiana Univ. Math. J. **33**, 817–830 (1984)
3. C. Amrouche and V. Girault, On the existence and regularity of the solution of Stokes problem in arbitrary dimension. Proc. Japan Acad. **67**, 171–175 (1990)

4. J. Bergh and J. Lofstfröm, *Interpolation Spaces. An Introduction*, Springer–Verlag, Berlin (1976)
5. W. Borchers and K. Pileckas, Note on the flux problem for stationary Navier–Stokes equations in domains with multiply connected boundary. Acta Appl. Math. **37**, 21–30 (1994)
6. C. Bortone and G. Starita, On the motion of spheroid in a viscous fluid. Rend. Acc. Sci. Napoli **70**, 119–151 (2003)
7. R.M. Brown and Z. Shen, Estimates for the Stokes operator in Lipschitz domains. Indiana Univ. Math. J. **44**, 1183–1206 (1995)
8. A.P. Calderòn, Cauchy integrals on Lipschitz curves and related operators. Proc. Nat. Acad. Sci. USA **74**, 1324–1327 (1977)
9. S. Campanato, Equazioni Ellittiche del secondo ordine e spazi $\mathcal{L}^{2,\lambda}$. Ann. Mat. Pura Appl. **73**, 321–380 (1965)
10. L. Cattabriga, Su un problema al contorno relativo al sistema di equazioni di Stokes. Rend. Sem. Mat. Padova **31**, 308–340 (1961)
11. I–D Chang and R. Finn, On the solutions of a class of equations occurring in continuum mechanics, with applications to the Stokes paradox. Arch. Rational Mech. Anal. **7**, 388–401 (1961)
12. H. J. Choe and B.J. Jin, Characterization of generalized solutions for the homogeneous Stokes equations in exterior domains. Nonlinear Anal. **48**, 765–779 (2002)
13. R.R. Coifman, A. McIntosh and Y. Meyer, L'intégrale de Cauchy definit un operateur borné sur L^2 pour les courbes Lipschitziennes. Ann. Math. **122**, 361–387 (1982)
14. V. Coscia and R. Russo, Some remarks on the Dirichlet problem in plane exterior domains. Ricerche Mat. **53** (2007)
15. B.J. Dahlberg, C.E. Kenig and G.C. Verchota, Boundary value problems for the systems of elastostatics in Lipschitz domains. Duke Math. J. **57**, 795–818 (1988)
16. R. Dautray and J.L. Lions, *Mathematical Analysis and Numerical Methods for Sciences and Technology*, vol. I, Springer, Berlin (1990)
17. E. De Giorgi, Osservazioni relative ai teoremi di unicità per le equazioni differenziali a derivate parziali di tipo ellittico, con condizioni al contorno di tipo misto. Ricerche Mat. **2**, 183–191 (1954)
18. P. Deuring and W. Von Wahl, Das lineare Stokes system in $\mathbb{R}^3$, I, II. Bayreuth Math. Schr. **27**, 1–252 (1988), **28**, 1–109 (1989)
19. E. De Vito, Sulle funzioni ad integrale di Dirichlet finito. Ann. Sc. Norm. Super. Pisa Cl. Sci. (III) **12**, 55–127 (1958)
20. M. Dindoš and M. Mitrea, The stationary Navier–Stokes system in nonsmooth manifolds: the Poisson problem in Lipschitz domains and C^1 domains. Arch. Rational Mech. Anal. **174**, 1–47 (2004)
21. R.J. Duffin, Analytic continuation in elasticity. J. Rational Mech. Anal. **5**, 939–950 (1956)
22. L.C. Evans, *Partial Differential Equations*, AMS, New York (2002)
23. E.B. Fabes, Layer potential methods for boundary value problems on Lipschitz domains. Lect. Notes Math., Springer–Verlag **1344**, 55–80 (1988)
24. E.B. Fabes, M. Jodeit Jr. ans J. Lewis, Double layer potentials for domains with corners and edges. Indiana U. Math. J. **26**, 95–114 (1977)
25. E.B. Fabes, M. Jodeit Jr. and N.M. Rivière, Potential techniques for boundary value problems on C^1 domains. Acta Math. **141**, 165–185 (1978)
26. E.B. Fabes, C.E. Kenig and G.C. Verchota, The Dirichlet problem for the Stokes system in Lipschitz domains. Duke Math. J. **57**, 769-793 (1988)
27. E.B. Fabes, O. Mendez and M. Mitrea, Boundary layers on Sobolev–Besov spaces and Poisson's equation for the Laplacian in Lipschitz domains. J. Funct. Anal. **159**, 323–368 (1998)
28. R. Farwig, G.P. Galdi and H. Sohr, Very weak solutions and large uniqueness classes of stationary Navier–Stokes equations in bounded domains of $\mathbb{R}^2$. J. Diff. Equat. **227**, 564–580 (2006)
29. G. Fichera, Sull'esistenza e sul calcolo delle soluzioni dei problemi al contorno, relativi all'equilibrio di un corpo elastico. Ann. Sc. Norm. Super. Pisa Cl. Sci. (III) **4**, 35–99 (1950)

30. R. Finn, On the steady-state solutions of the Navier–Stokes equations. III. Acta Math. **105**, 197–244 (1961)
31. R. Finn and W. Noll, On the uniqueness and non-existence of Stokes flows. Arch. Rational Mech. Anal. **1**, 97–106 (1957)
32. G.P. Galdi, On the existence of steady motions of a viscous flow with non-homogeneous conditions. Le Matematiche **66**, 503–524 (1991)
33. G.P. Galdi, *An Introduction to the Mathematical Theory of the Navier–Stokes Equations*, vol. I, II revised edition, Springer Tracts in Natural Philosophy (ed. C. Truesdell) **38**, **39**, Springer–Verlag, New York (1998)
34. G.P. Galdi, Stationary Navier-Stokes problem in a two-dimensional exterior domain. In *Stationary Partial Differential Equations*, vol. I, 71–155, Handb. Differ. Equ., North-Holland, Amsterdam (2004)
35. G.P. Galdi and C.G. Simader, Existence, uniqueness and L^q estimates for the Stokes problem in an exterior domain. Arch. Rational Mech. Anal. **112**, 291–318 (1990)
36. G.P. Galdi, C.G. Simader and H. Sohr, On the Stokes problem in Lipschitz domains. Ann. Mat. Pura Appl. (IV) **167**, 147–163 (1994)
37. G.P. Galdi, C.G. Simader and H. Sohr, A class of solutions of stationary Stokes and Navier–Stokes equations with boundary data in $W^{-1/q,q}(\partial\Omega)$. Math. Ann. **33** 41–74 (2003)
38. W. Gao, Layer potentials and boundary value problems for elliptic systems in Lipschitz domains. J. Funct. Anal. **95**, 377–399 (1991)
39. M. Giaquinta and G. Modica, Nonlinear systems of the type of the stationary Navier-Stokes system. J. Reine Angew. Math. **330**, 173–214 (1982)
40. Y. Giga, Analyticity of the semigroup generated by the Stokes operator in L_r–spaces. Math. Z. **178**, 287–329 (1981)
41. V. Girault and A. Sequeira, A well-posed problem for the exterior Stokes equations in two and three dimensions. Arch. Rational Mech. Anal. **114**, 313–333 (1991)
42. J. Happel and H. Brenner, *Low Reynolds Number Hydrodynamics*, Martin Nijhoff Publishers, Boston (1983)
43. J.G. Heywood, On Some paradoxes concerning two-dimensional Stokes flow past an obstacle. Indiana Univ. Math. J. **24**, 443–450 (1974)
44. N. Kalton and M. Mitrea, Stability results on interpolation scale of quasi-Banach spaces and applications. Trans. Amer. Math. Soc. **350**, 3903–3922 (1998)
45. L.V. Kapitanskii and K. Pileckas, On spaces of solenoidal vector fields and boundary value problems for the Navier–Stokes equations in domains with noncompact boundaries. Trudy Mat. Inst. Steklov **159**, 5–36 (1983); english transl.: *Proc. Math. Inst. Steklov* **159**, 3–34 (1984)
46. C.E. Kenig, Harmonic Analysis techniques for second order elliptic boundary value problems. CBMS Regional Conf. Ser. in Math. **83**, AMS (1994)
47. H. Kozono and H. Sohr, On a new class of generalized solutions for the Stokes equations in exterior domains. Ann. Scuola Norm. Sup. Pisa **19**, 155–181 (1992)
48. V.D. Kupradze, T.G. Gegelia, M.O. Basheleishvili and T.V. Burchuladze, *Three Dimensional Problems of the Mathematical Theory of Elasticity and Thermoelasticity*, North-Holland, Amsterdam (1979)
49. O.A. Ladyzhenskaya, *The Mathematical Theory of Viscous Incompressible Fluid*, Gordon and Breach, London (1969)
50. J. Leray, Étude de diverses équations intégrales non linéaire et de quelques problèmes que pose l'hydrodynamique. J. Math. Pures Appl. **12** , 1–82 (1933)
51. P. Maremonti and R. Russo, On existence and uniqueness of classical solutions of the stationary Navier–Stokes equations and to the traction problem of linear elastostatics. Quad. Mat. **1**, 171–251 (1997)
52. P. Maremonti, R. Russo and G. Starita, On the Stokes equations: the boundary value problem. Quad. Mat. **4**, 69–140 (1999)
53. E. Marušić-Paloka, Solvability of the Navier-Stokes system with L^2 boundary data. Appl. Math. Opt. **41**, 365–375 (2000)

54. V.G. Maz'ya and G.I. Kresin, On the maximum principle for strongly elliptic and parabolic second order systems with constant coefficients. Math. USSR Sbornic **53**, 457–479 (1986)
55. Y. Meyer and R.R. Coifman, *Wavelet. Calderón–Zygmund and Multilinear Operators*, Cambridge University Press, Cambridge (1997)
56. C. Miranda, Sulle proprietà di regolarità di certe trasformazioni integrali. Mem. Acc. Lincei **7**, 303–336 (1965)
57. C. Miranda, *Partial Differential Equations of Elliptic Type*, Springer-Verlag, Berlin (1970)
58. C. Miranda, Istituzioni di analisi funzionale lineare. Unione Matematica Italiana, Oderisi Gubbio Editrice (1978)
59. M. Mitrea and M. Taylor, Navier–Stokes equations on Lipschitz domains in Riemannian manifolds. Math. Ann. **321**, 955–987 (2001)
60. J. Naumann, On a maximum principle for weak solutions of the stationary Stokes system. Ann. Scuola Norm. Sup. Pisa Cl. Sci. **15**(4), 149–168 (1988)
61. S.A. Nazarov and K. Pileckas, On steady Stokes and Navier–Stokes problems with zero velocity at infinity in a three-dimensional exterior domain. J. Math. Kyoto Univ. **40**, 475–492 (2000)
62. J. Nečas, *Les Méthodes Directes en Théorie des Équations Élliptiques*. Masson, Paris and Academie, Prague (1967)
63. A. Novotny and M. Padula, Note on decay of solutions of steady Navier-Stokes equations in 3–D exterior domains. Diff. Integr. Eq. **8**, 1833–1842 (1995)
64. M. Picone, Nuovi indirizzi di ricerca nella teoria e nel calcolo delle soluzioni di talune equazioni lineari alle derivate parziali della fisica–matematica. Ann. Scuola Norm. Sup. Pisa **5**(2), 213–288 (1936)
65. K. Pileckas, On space of solenoidal vectors. Trudy Mat. Inst. Steklov **159**, 137–149 (1983) english tansl.: Proc. Steklov Math. Inst. **159**, 141–154 (1984)
66. F. Rellich, Darstellung der Eigenwerte von $\Delta u + \lambda u$ durch ein randintegral. Math. Z. **46**, 635–646 (1940)
67. R. Russo, On the existence of solutions to the stationary Navier–Stokes equations. Ricerche Mat. **52**, 285–348 (2003)
68. R. Russo and C.G. Simader, A note on the existence of solutions to the Oseen problem in Lipschitz domains. J. Math. Fluid Mech. **8**, 64–76 (2006)
69. R. Russo and A. Tartaglione, On the Robin problem in classical potential theory. Math. Mod. Meth. Appl. Sci. **11**, 1343–1347 (2001)
70. R. Russo and A. Tartaglione, On the Robin problem for Stokes and Navier–Stokes systems. Math. Mod. Meth. Appl. Sci. **16**, 701–716 (2006)
71. D. Serre, Équations de Navier–Stokes stationnaire avec données peu regulières. Ann. Sc. Norm. Sup. Pisa **10**(4), 543–559 (1982)
72. Z. Shen, A note on the Dirichlet problem for the Stokes system in Lipschitz domains. Proc. Amer. Math. Soc. **123**, 801–811 (1995)
73. Y. Shibata and M. Yamazaki, Uniform estimates in the velocity at infinity for stationary solutions to the Navier-Stokes exterior problem. Japanese J. Math. **31**, 225–279 (2005)
74. H. Sohr, *The Navier–Stokes Equations*, Birkhäuser, Basel (2001)
75. V.A. Solonnikov, General boundary value problems for Douglis–Niremberg elliptic system II. Trudy Mat. Inst. Steklov **92**, 233–297 (1966) english transl.: Proc. Steklov Inst. Math. **92**, 212, 272 (1966)
76. V.A. Solonnikov, On an estimate for the maximum modulus of the solution of a stationary problem for Navier-Stokes equations. Zap. Nauchn. Sem. S.-Peterburg. Otdel. Mat. Inst. Steklov (POMI) **249**, 294–302 (1997) english transl.: J. Math. Sci. (New York) **101**, 3563–3569 (2000)
77. E.M. Stein, *Harmonic Analysis, Real-Variable Methods, Orthogonality, and Oscillatory Integrals*, Princeton University Press, Princeton (1993)
78. G.G. Stokes, On the effects of the internal friction of fluids on the motion of pendulus. Trans. Cambridge Phil. Soc. **8**, 8–106 (1851)
79. V. Sverák and T.-P. Tsai, On the spatial decay of 3-D steady-state Navier-Stokes flows. Comm. Part. Diff. Equat. **25**, 2107–2117 (2000)

80. R. Temam, *Navier-Stokes Equations*, North-Holland, Amsterdam (1977)
81. W. Varnhorn, *The Stokes Equations*, Mathematical Research, vol. 76, Akademie Verlag, Berlin (1994)
82. G. Verchota, Layer potentials and regularity for the Dirichlet problem for Laplace's equation in Lipschitz domains. J. Funct. Anal. **59**, 572–611 (1984)

On a C^0 Semigroup Associated with a Modified Oseen Equation with Rotating Effect

Yoshihiro Shibata

Abstract In this paper, we show the unique existence of solutions to the non-stationary problem for the modified Oseen equation with rotating effect in Ω:

$$\begin{aligned} D_t u - \Delta u + kD_3 u + M_a u + \nabla p = 0, \quad \operatorname{div} u = 0 \ \text{ in } \Omega \times (0,\infty), \\ u|_{\partial\Omega} = 0, \quad u|_{t=0} = f, \end{aligned} \tag{OS}$$

where Ω is an exterior domain in $\mathbb{R}^3$, $M_a u = -a(\mathbf{e}_3 \times x)\cdot\nabla u + a\mathbf{e}_3 \times u$, $x = (x_1, x_2, x_3) \in \mathbb{R}^3$ and $\mathbf{e}_3 = (0,0,1)$. This problem arises from a linearization of the Navier Stokes equations describing an incompressible viscous fluid flow past a rotating obstacle. If $1 < q < \infty$ and initial data f satisfies the conditions: $f \in W^2_q(\Omega)$, $\operatorname{div} f = 0$ in Ω, $f|_{\partial\Omega} = 0$ and $M_a f \in L_q(\Omega)$, then problem (OS) admits a unique solution $(u(t), p(t))$ which satisfies the following conditions:

$$u(t) \in C^1([0,\infty), L_q(\Omega)) \cap C^0([0,\infty), W^2_q(\Omega)), \quad p(t) \in C^0([0,\infty), \hat{W}^1_q(\Omega)),$$

$$\|(u(t), t^{1/2}\nabla u(t), t\nabla^2 u(t), \nabla p(t))\|_{L_q(\Omega)} \le C_{a_0,k_0,\gamma}\, \boldsymbol{E}^{\gamma t}\|f\|_{L_q(\Omega)},$$

$$t^{(1/2)(1+(1/q))}\|p(t)\|_{L_q(\Omega_b)} \le C_{a_0,k_0,b,\gamma}\, \boldsymbol{E}^{\gamma t}\|f\|_{L_q(\Omega)},$$

$$\|D_t u(t)\|_{L_q(\Omega)} + \|u(t)\|_{W^2_q(\Omega)} + \|\nabla p(t)\|_{L_q(\Omega)} \le C_{a_0,k_0,\gamma}\, \boldsymbol{E}^{\gamma t}(\|f\|_{W^2_q(\Omega)} + \|M_a f\|_{L_q(\Omega)})$$

for any $t > 0$ and large positive γ, where b is any number such that $B_b \supset \mathbb{R}^3 \setminus \Omega$ and $\Omega_b = B_b \cap \Omega$ with $B_b = \{x \in \mathbb{R}^3 \mid |x| < b\}$. The estimate for pressure term p is new and important for further researches of the corresponding full nonlinear problem. We also prove the generation of a continuous semigroup associated with problem (OS), which has been announced in Shibata [20, Theorem 1.1]. The result

Y. Shibata (✉)
Department of Mathematics, Research Institute of Science and Engineering,
Waseda University, Tokyo 169-8555, Japan
e-mail: yshibata@waseda.jp

R. Rannacher, A. Sequeira (eds.), *Advances in Mathematical Fluid Mechanics*,
DOI 10.1007/978-3-642-04068-9_29, © Springer-Verlag Berlin Heidelberg 2010

obtained in this paper is an extended version of Shibata [20, Theorem 1.1] with more detailed proofs.

Keywords Oseen operator · Rotating effect · Continuous semigroup · L_q framework

1 Introduction and Main Results

Consider a rigid body $\mathcal{R}$ moving through an incompressible viscous fluid that fills the whole three-dimensional space $\mathbb{R}^3$ exterior to $\mathcal{R}$. We assume that with respect to a frame attached to $\mathcal{R}$, the translational velocity u_∞ and the angular velocity ω of $\mathcal{R}$ are both constant vectors. Without loss of generarity we may assume that $\omega = a\mathbf{e}_3$, $\mathbf{e}_3 = {}^T(0, 0, 1)$, ${}^TM$ standing for the transposed of M. If the flow is non-slip at the boundary, then the motion of fluid is described by the following equation:

$$\begin{aligned} &D_t v + v \cdot \nabla v - \Delta v + \nabla \pi = g, \quad \operatorname{div} v = 0 \quad \text{in } \Omega(t) \ \ (t > 0), \\ &v(y, t)|_{\partial\Omega(t)} = \omega \times y|_{\partial\Omega(t)}, \quad \lim_{|y|\to\infty} v(y, t) = u_\infty, \quad v(y, 0) = v_0(y) \end{aligned} \tag{1}$$

in the time-dependent exterior domain: $\Omega(t) = \mathcal{O}(at)\Omega$, where $D_t = \partial/\partial t$, $\nabla = {}^T(D_1, D_2, D_3)$, $D_j = \partial/\partial y_j$, $\Delta = \sum_{j=1}^3 D_j^2$, Ω is a fixed exterior domain in $\mathbb{R}^3$ with $C^{1,1}$ boundary $\partial\Omega$ and $\mathcal{O}(t)$ denotes the orthogonal matrix defined by the formula:

$$\mathcal{O}(t) = \begin{pmatrix} \cos t & -\sin t & 0 \\ \sin t & \cos t & 0 \\ 0 & 0 & 1 \end{pmatrix}.$$

To treat (1) in the time-independent domain Ω, we introduce the change of variables and unknown functions as follows:

$$x = {}^T\mathcal{O}(at)y, \quad u(x, t) = {}^T\mathcal{O}(at)(v(y, t) - u_\infty), \quad p(x, t) = \pi(y, t), \tag{2}$$

and then (u, p) satisfies the modified Navier–Stokes equations:

$$\begin{aligned} &D_t u + u \cdot \nabla u - \Delta u + ({}^T\mathcal{O}(at)u_\infty) + M_a u + \nabla p = f, \ \operatorname{div} u = 0 \quad \text{in } \Omega(t), \\ &u(x, t)|_{\partial\Omega} = (\omega \times x - {}^T\mathcal{O}(t)u_\infty)|_{\partial\Omega}, \quad \lim_{|x|\to\infty} u(x, t) = 0, \quad u(y, 0) = v_0(y). \end{aligned} \tag{3}$$

Here and hereafter, M_a is the operator defined by the formula:

$$M_a u = -a(\mathbf{e}_3 \times x) \cdot \nabla u + a\mathbf{e}_3 \times u. \tag{4}$$

In this paper, we consider only the case where: $u_\infty = k\mathbf{e}_3$, so that ${}^T\mathcal{O}(at)u_\infty = k\mathbf{e}_3$ for any $t > 0$. Therefore, the Eq. (1) leads to the system:

$$
\begin{aligned}
&D_t u + u\cdot\nabla u - \Delta u + kD_3 u + M_a u + \nabla p = f, \quad \operatorname{div} u = 0 \quad \text{in } \Omega \quad (t>0),\\
&u(x,t)|_{\partial\Omega} = (\omega\times x - k\mathbf{e}_3)|_{\partial\Omega}, \quad \lim_{|x|\to\infty} u(x,t) = 0, \quad u(x,0) = v_0(x) - u_\infty.
\end{aligned} \tag{5}
$$

Our purpose of study is to show some stability of stationary solutions when $f = f(x)$, that is $g = g({}^T\mathcal{O}(at)y)$ (time periodic force). Here, $(w(x), \theta(x))$ is called a stationary solution to (5) if $(w(x), \theta(x))$ satisfies the equation:

$$
\begin{aligned}
&w\cdot\nabla w - \Delta w + kD_3 w + M_a w + \nabla\theta = f, \quad \operatorname{div} w = 0 \quad \text{in } \Omega,\\
&w(x)|_{\partial\Omega} = (\omega\times x - k\mathbf{e}_3)|_{\partial\Omega}, \quad \lim_{|x|\to\infty} w(x) = 0.
\end{aligned} \tag{6}
$$

Setting $u(x,t) = w(x) + z(x,t)$ and $p(x,t) = \theta(x) + \kappa(x,t)$ in (5), as equations for new unknown functions (z,κ) we have

$$
\begin{aligned}
D_t z + z\cdot\nabla z + L(w)z - \Delta z + kD_3 z + M_a z + \nabla\kappa &= 0 \quad \text{in } \Omega\times(0,\infty)\\
\operatorname{div} z &= 0 \quad \text{in } \Omega\times(0,\infty),\\
z(x,t)|_{\partial\Omega} = 0, \quad \lim_{|x|\to\infty} z(x,t) &= 0 \quad \text{for } t>0,\\
z(x,0) = v_0(x) - u_\infty - w(x),&
\end{aligned} \tag{7}
$$

where we have set $L(w)z = z\cdot\nabla w + w\cdot\nabla z$. We say that the stationary solution (w,θ) is stable if (7) admits a unique solution (z,κ) globally in time and the L_∞ norm in space of z tends to 0 as t goes to ∞ when $v_0 - u_\infty - w$ is small enough in some sense. Shibata [18] together with Kobayashi and Shibata [14] proved a stability theorem of Finn's physically reasonable solutions in the L_3 framework, that is such stability theorem was known when $a = 0$ (no-rotation) and $k \neq 0$ (cf., also Enomoto and Shibata [2] and Shibata [19]). Recently, Galdi and Silvestre [9, 10] proved some unique existence theorem for the stationary problem (6). Our goal is to extend the result in [18] to the case where $a \neq 0$ and $k \neq 0$. Especially, we are interested in a stability of the Galdi-Silvestre stationary solutions.

In this paper, we will discuss the unique existence theorem of solutions to the linearized equaiton of (7), which is given as a non-stationary problem for the modified Oseen equation with rotating effect in Ω:

$$
\begin{aligned}
D_t u + L_{a,k}u + \nabla p &= 0, \quad \operatorname{div} v = 0 \;\text{ in } \Omega\times(0,\infty),\\
u|_{\partial\Omega} &= 0, \quad u|_{t=0} = f,
\end{aligned} \tag{8}
$$

where we have set $L_{a,k}u = -\Delta u + kD_3 u + M_a u$.

To state our result, at this point we explain several symbols used throughout the paper. For any domain D in $\mathbb{R}^3$, $L_q(D)$ and $W_q^m(D)$ stand for the usual Lebesgue space and Sobolev space, respectively. $\|\cdot\|_{L_q(D)}$ and $\|\cdot\|_{W_q^m(D)}$ stand for their norms. Let $R > 0$ be a fixed constant such that $\mathbb{R}^3 \setminus \Omega \subset B_R$, where $B_L = \{x \in \mathbb{R}^3 \mid |x| < L\}$. For $b > R$, we set $\Omega_b = \Omega \cap B_b$. For $D = \mathbb{R}^3$, Ω or Ω_{R+3}, we define the space $\hat{W}_q^1(D)$ by the formula:

$$\hat{W}_q^1(D) = \{p \in L_{q,\mathrm{loc}}(D) \mid \nabla p \in L_q(D)^3, \int_{\Omega_{R+3}} p(x)\,dx = 0\}. \tag{9}$$

Moreover, we set

$$\begin{aligned} C^\infty_{0,\sigma}(D) &= \{u \in C_0^\infty(D)^3 \mid \operatorname{div} u = 0 \ \text{ in } D\}, \\ J_q(D) &= \text{closure of } C^\infty_{0,\sigma} \text{ in } L_q(\Omega)^3, \\ G_q(D) &= \{\nabla p \mid p \in \hat{W}_q^1(D)\}. \end{aligned}$$

Then, for any $1 < q < \infty$ the Helmholtz decomposition: $L_q(D) = J_q(D) \oplus G_q(D)$ holds. Namely, given $f \in L_q(D)^3$ there exist $g \in J_q(D)$ and $p \in \hat{W}_q^1(D)$ uniquely such that $f = g + \nabla p$. By the formulas: $P_D f = g$ and $Q_D f = p$ we define the operators $P_D : L_q(D)^3 \to J_q(D)$ and $Q_D : L_3(D)^3 \to \hat{W}_q^1(D)$ and then we know that

$$\begin{aligned} f &= P_D f + \nabla Q_D f, \\ \|P_D f\|_{L_q(D)} + \|\nabla Q_D f\|_{L_q(D)} &\leq C_{D,q} \|f\|_{L_q(D)}, \\ (\nabla Q_D f, \nabla\theta)_D &= (f, \nabla\theta)_D \quad \text{for any } \theta \in \hat{W}^1_{q'}(D) \text{ with } q' = q/(q-1) \end{aligned} \tag{10}$$

(cf., Fujiwara and Morimoto [7], Miyakawa [15], Galdi [8] and references therein), where $(u, v)_D = \int_D u(x) \cdot v(x)\,\mathrm{d}x$. Here and hereafter, C stands for a generic constant and $C_{a,b,\ldots}$ denotes a generic constant depending on $a, b, \ldots$.

The following two theorems are our main results in this paper.

Theorem 1 *Let* $1 < q < \infty$ *and* $a_0, k_0 > 0$. *Assume that* $|a| \leq a_0$ *and* $|k| \leq k_0$. *Set*

$$\begin{aligned} \mathcal{D}_q(\Omega) &= \{f \in J_q(\Omega) \cap W_q^2(\Omega) \mid f|_{\partial\Omega} = 0, \quad M_a f \in L_q(\Omega)\}, \\ \|f\|_{\mathcal{D}_q(\Omega)} &= \|f\|_{W_q^2(\Omega)} + \|M_a f\|_{L_q(\Omega)}. \end{aligned}$$

Then, for any $f \in \mathcal{D}_q(\Omega)$ *problem* (8) *admits a unique solution* $(u(t), p(t))$ *which satisfies the following conditions:*

$$\begin{aligned} & u(t) \in C^1([0,\infty), L_q(\Omega)) \cap C^0([0,\infty), W_q^2(\Omega)), \quad p(t) \in C^0([0,\infty), \hat{W}_q^1(\Omega)), \\ & \|(u(t), t^{1/2}\nabla u(t), t\nabla^2 u(t), \nabla p(t))\|_{L_q(\Omega)} \leq C_{a_0,k_0,\gamma}\, \boldsymbol{E}^{\gamma t} \|f\|_{L_q(\Omega)}, \\ & t^{(1/2)(1+(1/q))} \|p(t)\|_{L_q(\Omega_b)} \leq C_{a_0,k_0,b,\gamma}\, \boldsymbol{E}^{\gamma t} \|f\|_{L_q(\Omega)}, \\ & \|D_t u(t)\|_{L_q(\Omega)} + \|u(t)\|_{\mathcal{D}_q(\Omega)} + \|\nabla p(t)\|_{L_q(\Omega)} \leq C_{a_0,k_0,\gamma}\, \boldsymbol{E}^{\gamma t} \|f\|_{\mathcal{D}_q(\Omega)} \end{aligned} \tag{11}$$

for any $\gamma \geq \gamma_0$, $b > R+3$ *and* $t > 0$, *where* γ_0 *is some constant* ≥ 1 *which depends on* a_0 *and* k_0.

Theorem 2 *Let $1 < q < \infty$ and let $\mathcal{D}_q(\Omega)$ be the same as in Theorem 1. Let $\mathcal{L}_{a,k}$ be the operator defined by the following operation:*

$$\mathcal{L}_{a,k}u = P_\Omega L_{a,k}u \quad \text{for } u \in \mathcal{D}_q(\Omega). \tag{12}$$

Then, $-\mathcal{L}_{a,k}$ generates a continuous semigroup $\{T_\Omega(t)\}_{t\geq 0}$ on $J_q(\Omega)$.

Remark 1 Theorem 2 has been already announced in [20, Theorem 1.1]. Theorem 1 is an extended version of Theorem 2. In fact, Theorem 2 immediately follows from Theorem 1. Our purpose of this paper is to give a detailed proof of Theorem 1.

Theorem 2 was proved by Geissert, Heck and Hieber [11] when $k = 0$. Our theorem is an extension of their result to the case where $k \neq 0$. But, our approach is completely different from [11]. In fact, they solved the corresponding resolvent problem along the large positive real axis, escaping the appearance of pressure term in terms of Bogovski lemma, and the semigroup generated by $-\mathcal{L}_{a,0}$ is constructed via the technique of iterated convolutions. But, the core of our approach is to prove that the semigroup $\{T_\Omega(t)\}_{t\geq 0}$ associated with $-\mathcal{L}_{a,k}$ is represented in such a way that

$$T_\Omega(t)f = \lim_{\omega\to\infty} \int_{\gamma-\mathrm{i}\omega}^{\gamma+\mathrm{i}\omega} (\lambda I + \mathcal{L}_{a,k})^{-1} f \, \mathrm{d}\lambda \quad (\gamma \geq 1) \tag{13}$$

when $f \in \mathcal{D}_q(\Omega)$ and the support of f is compact, which follows from some summability properties of the resolvent operator $(\lambda I + \mathcal{L}_{a,k})^{-1}$ when the imaginary part of resolvent parameter λ tends to infinity in the complex plane with positive real part. And such summability properties follow from the investigation of the asymptotic behaviour not only of $(\lambda I + \mathcal{L}_{a,k})^{-1}$ but also of the pressure term with respect to the large resolvent parameter. Without the analysis of the pressure term, we can not get any representation formula like (13). The formula (13) also plays an important role to show so called L_p-L_q decay property of $\{T_\Omega(t)\}_{t\geq 0}$ which is the core of our approach to prove the stability of stationary solutions and will be proved in another paper, because our proof is so long totally. Our main concern of this paper is to prove Theorem 1, which tells us some detailed properties of solutions, especially the estimate for pressure p is new and important in our approach to the stability theorem. Theorem 2 follows almost automatically from Theorem 1. Since the rotation effect implies the hyperbolic aspect of the equation (8), we can not expect any analyticity of our semigroup $\{T_\Omega(t)\}_{t\geq 0}$. In fact, we understand this fact rigorously by the result due to Farwig and Neustupa [5] concerning a spectral property of the operator $\mathcal{L}_{a,k}$.

The paper is orginized as follows: In Sect. 2 we consider the whole space problem and derive several necessary properties of solutions to the nonstationary problem and corresponding resolvent problem by using the concreate representation formula of solutions. In Sect. 3, we consider a problem in a bounded domain. In Sect. 4, using the results obtained in Sects. 2 and 3, we construct a parametrix for the corresponding resolvent problem in Ω assuming that the support of the right member is compact. In Sect. 5, we solve (8) assuming that initial data has a compact support. In

Sect. 6, using the results in Sects. 2 and 5, by cut-off technique we prove Theorem 1. In appendix, we discuss the resolvent problem when the resolvent parameter is a positive number.

2 Analysis of the Resolvent Problem in $\mathbb{R}^3$

In this section, we consider the initial problem for the modified Oseen equation with rotation effect in $\mathbb{R}^3$:

$$v_t + L_{a,k}v + \nabla\theta = 0, \quad \operatorname{div} v = 0 \ \text{ in } \mathbb{R}^3 \times (0,\infty), \quad v|_{t=0} = f, \tag{14}$$

and the corresponding resolvent problem:

$$(\lambda I + L_{a,k})u + \nabla\theta = f, \quad \operatorname{div} u = 0 \ \text{ in } \mathbb{R}^3. \tag{15}$$

If f satisfies the divergence free condition: $\operatorname{div} f = 0$ in $\mathbb{R}^3$, in other words, $f \in J_q(\mathbb{R}^3)$, then by direct calculation we see that a solution (v,θ) to problem (14) is given by the formula:

$$v(x,t) = [S_{a,k}(t)f](x) = {}^T\mathcal{O}(at)(\boldsymbol{E}^{t\mathbb{O}_k} f)(\mathcal{O}(at)x), \quad \theta(x,t) = 0, \tag{16}$$

where $\mathbb{O}_k = -\Delta + kD_3$, and

$$\begin{aligned}[\boldsymbol{E}^{t\mathbb{O}_k} f](x) &= (4\pi t)^{-\frac{3}{2}} \int_{\mathbb{R}^3} \boldsymbol{E}^{-\frac{|x-y-k\mathbf{e}_3 t|^2}{4t}} f(y)\,dy \\ &= \mathcal{F}_\xi^{-1}[\boldsymbol{E}^{-(|\xi|^2+\mathbf{i}k\xi_3)t}\mathcal{F}[f](\xi)](x).\end{aligned} \tag{17}$$

Here and hereafter, $\mathcal{F}$ and $\mathcal{F}_\xi^{-1}$ stand for the Fourier transform and inverse Fourier transform, respectively, which are defined by the formulas:

$$\mathcal{F}[f](\xi) = \hat{f}(\xi) = \int_{\mathbb{R}^3} \boldsymbol{E}^{-\mathrm{i}x\cdot\xi} f(x)\,dx \ \ \text{(Fourier transform)},$$

$$\mathcal{F}_\xi^{-1}[h(\xi)](x) = (2\pi)^{-3} \int_{\mathbb{R}^3} \boldsymbol{E}^{\mathrm{i}x\cdot\xi} h(\xi)\,\mathrm{d}\xi \ \ \text{(inverse Fourier transform)}.$$

By using the Young inequality for the convolution operator, we have the following theorem.

Theorem 3 *Let* $1 < q < \infty$. *Set*

$$\mathcal{D}_q(\mathbb{R}^3) = \{u \in J_q(\mathbb{R}^3) \cap L_3(\mathbb{R}^3)^3 \mid M_a u \in L_q(\mathbb{R}^3)\},$$
$$\|u\|_{\mathcal{D}_q(\mathbb{R}^3)} = \|u\|_{W_q^2(\mathbb{R}^3)} + \|M_a u\|_{L_q(\mathbb{R}^3)}.$$

Then, for any $j \in \mathbb{N}_0$*, multi-index* $\alpha \in \mathbb{N}_0^3$ *with* $|\alpha| \geq j$ *and* $f \in L_q(\mathbb{R}^3)$ *with* $D_x^\beta f \in L_q(\mathbb{R}^3)^3$ $(|\beta| = j)$*, we have*

$$\|D_x^\alpha S_{a,k}(t) f\|_{L_q(\mathbb{R}^3)} \leq C_{\alpha,j,q} t^{-\frac{|\alpha|-j}{2}} \|\nabla^j f\|_{L_q(\mathbb{R}^3)}, \tag{18}$$

where $\nabla^j f = (D_x^\beta f \mid |\beta| = j)$ *and* $\mathbb{N}_0$ *stands for the set of all non-negative integers.*

Moreover, for any $f \in \mathcal{D}_q(\mathbb{R}^3)$ *we have*

$$\|D_t S_{a,k}(t) f\|_{L_q(\mathbb{R}^3)} + \|S_{a,k}(t) f\|_{\mathcal{D}_q(\mathbb{R}^3)} \leq C(1+|k|)\|f\|_{\mathcal{D}_q(\mathbb{R}^3)}. \tag{19}$$

Proof From (16) it follows that there exist 3×3 matrices of polynomials $M_{\alpha,\beta}(A, B)$ with respect to $(A, B) \in \mathbb{R}^2$ such that

$$\begin{aligned} D_x^\alpha v(x,t) &= \sum_{|\beta|=|\alpha|} M_{\alpha,\beta}(\sin at, \cos at)(D_x^\beta \boldsymbol{E}^{t\mathbb{O}_k} f)(\mathcal{O}(at)x) \\ &= \sum_{|\beta|=|\alpha|} M_{\alpha,\beta}(\sin at, \cos at)\Big[\frac{1}{(4\pi t)^{\frac{3}{2}}} D_z^\beta \int_{\mathbb{R}^3} \boldsymbol{E}^{-\frac{|z-y|^2}{4t}} f(y + t\mathbf{e}_3)\, dy\Big]\Big|_{z=\mathcal{O}(at)x}. \end{aligned}$$

Since $\mathcal{O}(at)$ is an orthogonal matrix, the $L_q(\mathbb{R}^3)$ norm does not change under the change of variable: $z = \mathcal{O}(at)x$, so that by the Young inequality
for the convolution operator we have (18). To prove (19), we write

$$\begin{aligned} [S_{a,k}(t)f](x) &= \frac{1}{(2\pi)^3}\int_{\mathbb{R}^3} \boldsymbol{E}^{\mathrm{i}(\mathcal{O}(at)x)\cdot\xi)} \boldsymbol{E}^{-(|\xi|^2+\mathrm{i}k\xi_3)t}\, {}^T\mathcal{O}(at)\hat{f}(\xi)\, d\xi \\ &= \frac{1}{(2\pi)^3}\int_{\mathbb{R}^3} \boldsymbol{E}^{\mathrm{i}x\cdot\xi} \boldsymbol{E}^{-(|\xi|^2+\mathrm{i}k\xi_3)t}\, {}^T\mathcal{O}(at)\hat{f}(\mathcal{O}(at)\xi)\, d\xi. \end{aligned} \tag{20}$$

Setting $X_{\xi,a} = a[(\mathbf{e}_3 \times \xi)\cdot\nabla_\xi - \mathbf{e}_3\times]$, we have

$$D_t[{}^T\mathcal{O}(at)g(\mathcal{O}(at)\xi)] = {}^T\mathcal{O}(at)[X_{\xi,a}g](\mathcal{O}(at)\xi),$$

which implies that

$$\begin{aligned} &D_t[S_{a,k}(t)f](x) = \\ &\quad \frac{-1}{(2\pi)^3}\int_{\mathbb{R}^3} \boldsymbol{E}^{\mathrm{i}x\cdot\xi} \boldsymbol{E}^{-(|\xi|^2+\mathrm{i}k\xi_3)t}\,(|\xi|^2+\mathrm{i}k\xi_3)\, {}^T\mathcal{O}(at)\hat{f}(\mathcal{O}(at)\xi)\, d\xi \\ &\quad + \frac{1}{(2\pi)^3}\int_{\mathbb{R}^3} \boldsymbol{E}^{\mathrm{i}x\cdot\xi} \boldsymbol{E}^{-(|\xi|^2+\mathrm{i}k\xi_3)t}\, {}^T\mathcal{O}(at)(X_{\xi,a}\hat{f})(\mathcal{O}(at)\xi)\, d\xi \\ &\quad = {}^T\mathcal{O}(at)[\boldsymbol{E}^{t\mathbb{O}_k}(\Delta - kD_3)f](\mathcal{O}(at)x) + {}^T\mathcal{O}(at)[\boldsymbol{E}^{t\mathbb{O}_k} M_a f](\mathcal{O}(at)x], \end{aligned}$$

This combined with (18) with $\alpha = 0$ implies that

$$\|D_t S_{a,k}(t)f\|_{L_q(\mathbb{R}^3)} \le C(\|(\Delta - kD_3)f\|_{L_q(\mathbb{R}^3)} + \|M_a f\|_{L_q(\mathbb{R}^3)}). \tag{21}$$

Since $M_a S_{a,k} f = -D_t S_{a,k} f + (\Delta - kD_3)S_{a,k} f$ as follows from (14) with $\theta = 0$, combining (21) with (18) implies (19), which completes the proof of Theorem3. □

Now, we consider the resolvent problem (15). The operators $P_{\mathbb{R}^3}$ and $Q_{\mathbb{R}^3}$ corresponding to the Helmholtz decomposition of $L_q(\mathbb{R}^3)^3$ are given by using the Fourier transform as follows:

$$\begin{aligned} &P_{\mathbb{R}^3} f = \mathcal{F}_\xi^{-1}[P(\xi)\hat{f}(\xi)](x), \quad P(\xi) = (\delta_{jk} - \xi_j\xi_k|\xi|^{-2}) \text{ (3} \times \text{3 matrix)}, \\ &Q_{\mathbb{R}^3} f = \mathcal{F}_\xi^{-1}[\sum_{j=1}^{3} \xi_j \hat{f}_j(\xi)(\mathbf{i}|\xi|)^{-2}](x) + c_0(f) \end{aligned} \tag{22}$$

for $f = {}^T(f_1, f_2, f_3) \in L_q(\mathbb{R}^3)^3$ with $1 < q < \infty$, where $c_0(f)$ is a constant chosen in such a way that

$$\int_{\Omega_{R+3}} Q_{\mathbb{R}^3} f \, dx = 0 \tag{23}$$

and δ_{jk} is the Kronecker delta symbols. From (14) and (16) it follows that if we set $u(x,t) = [S_{a,k}(t)P_{\mathbb{R}^3} f](x)$, then $u(x,t)$ satisfies the equation:

$$u_t + L_{k,a}u = 0, \quad \operatorname{div} u = 0 \quad \text{in } \mathbb{R}^3 \times (0,\infty), \quad u|_{t=0} = P_{\mathbb{R}^3} f. \tag{24}$$

Let us define the operator $\mathcal{A}_{\mathbb{R}^3,a,k}(\lambda)f$ by the formula:

$$\mathcal{A}_{\mathbb{R}^3,a,k}(\lambda)f = \mathcal{L}_t[S_{a,k}(t)P_{\mathbb{R}^3} f](\lambda, x) = \int_0^\infty e^{-\lambda t}[S_{a,k}(t)P_{\mathbb{R}^3} f](x)\,dt \tag{25}$$

where $\mathcal{L}_t$ stands for the Laplace transform. By (24) we have

$$(\lambda I + L_{a,k})\mathcal{A}_{\mathbb{R}^3,a,k}(\lambda)f = P_{\mathbb{R}^3} f, \quad \operatorname{div} \mathcal{A}_{\mathbb{R}^3,a,k}(\lambda)f = 0 \text{ in } \mathbb{R}^3, \tag{26}$$

which combined with (10) with $D = \mathbb{R}^3$ implies that

$$(\lambda I + L_{a,k})\mathcal{A}_{\mathbb{R}^3,a,k}(\lambda)f + \nabla Q_{\mathbb{R}^3} f = f, \quad \operatorname{div} \mathcal{A}_{\mathbb{R}^3,a,k}(\lambda)f = 0 \text{ in } \mathbb{R}^3. \tag{27}$$

Therefore, if we set $(u,\theta) = (\mathcal{A}_{\mathbb{R}^3,a,k}(\lambda)f, Q_{\mathbb{R}^3} f)$, then (u,θ) solves problem (15).

In what follows, we always assume that $|a| \le a_0$ and $|k| \le k_0$. $C_{a_0,k_0,\ldots}$ denotes a generic constant depending on $a_0, k_0, \ldots$, but independent of a and k whenever $|a| \le a_0$ and $|k| \le k_0$. In the following theorem, we shall state several properties of $\mathcal{A}_{\mathbb{R}^3,a,k}(\lambda)$, which will play an essential role in latter sections.

Theorem 4 *Let* $1 < q < \infty$, a_0, k_0, $\sigma > 0$ *and* $0 < \varepsilon < \pi/2$. *Assume that* $|a| \le a_0$ *and* $|k| \le k_0$. *Let* N *be a natural number greater than* 3. *Set*

$$
\begin{aligned}
&\Sigma_\varepsilon = \{\lambda \in \mathbb{C} \setminus \{0\} \mid |\arg \lambda| < \pi - \varepsilon\}, \quad \Sigma_{\varepsilon,\mu} = \{\lambda \in \Sigma_\varepsilon \mid |\lambda| > \mu\},\\
&\mathbb{C}_\gamma = \{\lambda \in \mathbb{C} \mid \operatorname{Re}\lambda > \gamma\}, \quad \lambda_0 = \lambda_0(k_0, \varepsilon) = 2(1 + 2\sin^{-2}(\varepsilon/2))\, k_0^2,\\
&L_{q,R+2}(\mathbb{R}^3) = \{f \in L_q(\mathbb{R}^3) \mid f(x) = 0 \ \textit{for}\ |x| > R + 2\},\\
&\mathcal{L}_R(\mathbb{R}^3) = \mathcal{L}(L_{q,R+2}(\mathbb{R}^3)^3, W_q^2(\mathbb{R}^3)^3).
\end{aligned} \tag{28}
$$

For a domain U *in* $\mathbb{C}$ *and a Banach space* X, $\operatorname{Anal}(U, X)$ *denotes the set of all anayltic functions defined on* U *with their values in* X. *Then, we have*

$$
\mathcal{A}_{\mathbb{R}^3,a,k}(\lambda) \in \operatorname{Anal}(\mathbb{C}_0, \mathcal{L}_R(\mathbb{R}^3)). \tag{29}
$$

Moreover, there exist operator-valued functions

$$
\mathcal{A}^N_{1,a,k}(\lambda),\ \ \tilde{\mathcal{A}}_{1,a,k}(\lambda) \in \operatorname{Anal}(\Sigma_{\varepsilon,\lambda_0}, \mathcal{L}_R(\mathbb{R}^3)),\ \ \mathcal{A}^N_{2,a,k}(\lambda) \in \operatorname{Anal}(\mathbb{C}_0, \mathcal{L}_R(\mathbb{R}^3))
$$

such that

$$
\begin{aligned}
\mathcal{A}_{\mathbb{R}^3,a,k}(\lambda) &= \mathcal{A}^N_{1,a,k}(\lambda) + \mathcal{A}^N_{2,a,k}(\lambda),\\
\mathcal{A}^N_{1,a,k}(\lambda) &= (\lambda I + \mathbb{O}_{k,\mathbb{R}^3})^{-1} P_{\mathbb{R}^3} + \tilde{\mathcal{A}}^N_{1,a,k}(\lambda),
\end{aligned}
$$

$$
\| D^\beta_x \mathcal{A}^N_{1,0,k}(\lambda) f \|_{L_q(\mathbb{R}^3)} \le C_{a_0,k_0,q,R,\varepsilon,N} (|\lambda| + k_0^2)^{-(1-(|\beta|/2))} \| f \|_{L_q(\mathbb{R}^3)}, \tag{30}
$$

$$
\| D^\beta_x \tilde{\mathcal{A}}^N_{1,0,k}(\lambda) f \|_{L_q(\mathbb{R}^3)} \le C_{a_0,k_0,q,R,\varepsilon,N} (|\lambda| + k_0^2)^{-((3/2)-(|\beta|/2))} \| f \|_{L_q(\mathbb{R}^3)} \tag{31}
$$

for any $f \in L_{q,R+2}(\mathbb{R}^3)^3$, $\lambda \in \Sigma_{\varepsilon,\lambda_0}$ *and* $\beta \in \mathbb{N}_0$ *with* $|\beta| \le 2$, *and*

$$
\| D^\beta_x \mathcal{A}^N_{2,a,k}(\lambda) f \|_{L_q(\mathbb{R}^3)} \le C_{a_0,k_0,q,R,N,\sigma} |\lambda|^{-((N/2)-(|\beta|/2))} \| f \|_{L_q(\mathbb{R}^3)} \tag{32}
$$

for any $f \in L_{q,R+2}(\mathbb{R}^3)^3$, $\lambda \in \mathbb{C}_\sigma$, *and* $\beta \in \mathbb{N}_0^n$ *with* $|\beta| \le 2$.

Here, $(\lambda + \mathbb{O}_{k,\mathbb{R}^3})^{-1}$ *denotes the resolvent of the Oseen operator in* $\mathbb{R}^3$ *which is defined by the formula:*

$$
(\lambda + \mathbb{O}_{k,\mathbb{R}^3})^{-1} g = \mathcal{F}^{-1}_\xi [(\lambda + |\xi|^2 + \mathrm{i}k\xi_3)^{-1} \hat{g}(\xi)]. \tag{33}
$$

Proof From (21) we have

$$
\mathcal{A}_{\mathbb{R}^3,a,k}(\lambda) f = \frac{1}{(2\pi)^3} \int_0^\infty \int_{\mathbb{R}^3} \boldsymbol{E}^{-(\lambda+|\xi|^2+\mathrm{i}k\xi_3)t} \boldsymbol{E}^{\mathrm{i}(\mathcal{O}(at)x)\cdot\xi}\ {}^T\mathcal{O}(at) P(\xi) \hat{f}(\xi)\, d\xi\, dt. \tag{34}
$$

First, we shall show the following lemma.

Lemma 1 *Let* $k_0, \sigma > 0$ *and* $0 < \varepsilon < \pi/2$ *and let* λ_0 *and* Σ_ε *be the same as in Theorem 4. Then, there exists a positive number* c *depending on* ε, k_0 *and* σ *such that*

$$|\lambda + |\xi|^2 + ik\xi_3| \geq c(|\lambda| + |\xi|^2 + k_0^2) \tag{35}$$

for any $|k| \leq k_0$, $\xi \in \mathbb{R}^3$, *and* $\lambda \in \Sigma_\varepsilon$ *with* $|\lambda| \geq \lambda_0$, *or* $\lambda \in \mathbb{C}$ *with* $\mathrm{Re}\,\lambda \geq 0$ *and* $|\lambda| \geq \sigma$.

Proof Since

$$|\lambda + |\xi|^2| \geq (\sin(\varepsilon/2))(|\lambda| + |\xi|^2) \tag{36}$$

for any $\xi \in \mathbb{R}^n$ and $\lambda \in \Sigma_\varepsilon$, we have

$$\begin{aligned}
|\lambda + |\xi|^2 + ik\xi_3| &\geq (\sin(\varepsilon/2))(|\lambda| + |\xi|^2) - k|\xi_3| \\
&\geq (\sin(\varepsilon/2))(|\lambda| + |\xi|^2 + k_0^2) - (\sin(\varepsilon/2))k_0^2 - k_0|\xi| \\
&\geq (\sin(\varepsilon/2))(|\lambda| + |\xi|^2 + k_0^2) - (\sin(\varepsilon/2))k_0^2 \\
&\qquad - (1/2)(k_0^2/\sin(\varepsilon/2)) - (1/2)(\sin(\varepsilon/2))|\xi|^2 \\
&\geq (1/2)(\sin(\varepsilon/2))(|\lambda| + |\xi|^2 + k_0^2) + (1/2)(\sin(\varepsilon/2))\lambda_0 \\
&\qquad - (\sin(\varepsilon/2) + (2\sin(\varepsilon/2))^{-1})k_0^2.
\end{aligned}$$

If we set $\lambda_0 = (2 + (\sin(\varepsilon/2)^{-2})k_0^2$, then we have

$$|\lambda + |\xi|^2 + ik\xi_3| \geq (1/2)(\sin(\varepsilon/2))(|\lambda| + |\xi|^2 + k_0^2) \tag{37}$$

for $\lambda \in \Sigma_\varepsilon$ with $|\lambda| \geq \lambda_0$, $|k| \leq k_0$ and $\xi \in \mathbb{R}^3$.

Now, we shall consider the case where $|\lambda| \leq \lambda_0$. If $|\xi|$ is large enough, then

$$\begin{aligned}
|\lambda + |\xi|^2 + ik\xi_3| &\geq |\xi|^2 - \lambda_0 - k_0|\xi| \geq (1/2)|\xi|^2 - \lambda_0 - (1/2)k_0^2 \\
&\geq (1/4)(|\xi|^2 + |\lambda| + k_0^2) + (1/4)|\xi|^2 - (5/4)\lambda_0 - (3/4)k_0^2.
\end{aligned}$$

Choose R so large that $(1/4)R^2 - (5/4)\lambda_0 - (3/4)k_0^2 \geq 0$, we have

$$|\lambda + |\xi|^2 + ik\xi_3| \geq (1/4)(|\xi|^2 + |\lambda| + k_0^2) \tag{38}$$

for any $\xi \in \mathbb{R}^3$ with $|\xi| \geq R$, $\lambda \in \mathbb{C}$ with $|\lambda| \leq \lambda_0$ and $|k| \leq k_0$.

We set $K = \{(\lambda, \xi, k) \in \mathbb{C} \times \mathbb{R}^3 \times \mathbb{R} \mid \mathrm{Re}\,\lambda \geq 0,\ \sigma \leq |\lambda| \leq \lambda_0,\ |\xi| \leq R,\ |k| \leq k_0\}$ to consider the case where $|\xi| \leq R$. To see that $\lambda + |\xi|^2 + ik\xi_3 \neq 0$ for $\lambda \in K$, we observe that

$$\lambda + |\xi|^2 + ik\xi_3 \neq 0 \tag{39}$$

if $\mathrm{Re}\,\lambda + (\mathrm{Im}\,\lambda/k)^2 > 0$ and $k > 0$. In fact, if $\lambda + |\xi|^2 + ik\xi_3 = 0$, then $\mathrm{Re}\,\lambda + |\xi|^2 = 0$ and $\mathrm{Im}\,\lambda + k\xi_3 = 0$, which implies that $\mathrm{Re}\,\lambda + |\xi'|^2 + (\mathrm{Im}\,\lambda/k)^2 = 0$, where $\xi' = (\xi_1, \xi_2)$. Therefore, $\mathrm{Re}\,\lambda + (\mathrm{Im}\,\lambda/k)^2 \leq 0$. By contraposition, we have (39). When $k = 0$, obviously $\lambda + |\xi|^2 \neq 0$ if $\mathrm{Im}\,\lambda \neq 0$ or $\mathrm{Im}\,\lambda = 0$ and $\mathrm{Re}\,\lambda > 0$. Since K is a compact set, from above observations we have

$$\inf\{|\lambda + |\xi|^2 + ik\xi_3| \mid (\lambda, \xi, k) \in K\} = c_0 > 0.$$

Since $|\lambda| + |\xi|^2 + k_0^2 \le \lambda_0 + R^2 + k_0^2$ for $(\lambda, \xi, k) \in K$, we have

$$|\lambda + |\xi|^2 + ik\xi_3| \ge c_0 = c_0(\lambda_0 + R^2 + k_0^2)^{-1}(|\lambda| + |\xi|^2 + k_0^2)$$

for any $(\lambda, \xi, k) \in K$, which combined with (37) and (38) implies the lemma. □

Now, we shall show Theorem 4. Since $(\mathcal{O}(at)x) \cdot \xi = x \cdot ({}^T\mathcal{O}(at)\xi)$, setting

$$\mathcal{O}'(t) = \begin{pmatrix} \cos t & -\sin t \\ \sin t & \cos t \end{pmatrix}, \quad \eta' = \begin{pmatrix} \eta_1 \\ \eta_2 \end{pmatrix}, \quad \xi' = \begin{pmatrix} \xi_1 \\ \xi_2 \end{pmatrix},$$

from (34) we have

$$[\mathcal{A}_{\mathbb{R}^3,a,k}(\lambda)f](x) = \frac{1}{(2\pi)^3}\int_0^\infty\int_{\mathbb{R}^3} \boldsymbol{E}^{-(\lambda+|\eta|^2+ik\eta_3)t}\boldsymbol{E}^{ix\cdot\eta}\, {}^T\mathcal{O}(at)P(\mathcal{O}(at)'\eta', \eta_3)\hat{f}(\mathcal{O}(at)'\eta', \eta_3)\, dt d\eta.$$

For the notational simplicity, we set

$$I_a(t, \eta)f = {}^T\mathcal{O}(at)P(\mathcal{O}(at)'\eta', \eta_3)\hat{f}(\mathcal{O}(at)'\eta', \eta_3).$$

We can write

$$D_t^j I_a(t, \xi)f = a^j \sum_{k=0}^{j} |\xi'|^k \Big(\sum_{|\alpha'|=k} a_{\alpha'}^{jk}(\sin at, \cos at, \xi/|\xi|)(D_{\xi'}^{\alpha'}\hat{f})(\mathcal{O}(at)'\xi', \xi_3)\Big)$$

where $D_{\xi'}^{\alpha'} = D_{\xi_1}^{\alpha_1} D_{\xi_2}^{\alpha_2}$ with $\alpha' = (\alpha_1, \alpha_2) \in \mathbb{N}_0^2$, $a_{\alpha'}^{jk}(A, B, \eta)$ are 3×3 matrices of polynomials with respect to $(A, B, \eta) \in \mathbb{R}^5$. Using these notations, by integration by parts we have

$$\mathcal{A}_{\mathbb{R}^3,a,k}(\lambda)f = \sum_{j=0}^{N-1} \frac{1}{(2\pi)^3} \int_{\mathbb{R}^3} \frac{\boldsymbol{E}^{ix\dot{\xi}} D_t^j I_a(t, \xi)f|_{t=0}}{(\lambda + |\xi|^2 + ik\xi_3)^{j+1}}\, d\xi$$
$$+ \frac{1}{(2\pi)^3} \int_0^\infty \int_{\mathbb{R}^3} \frac{\boldsymbol{E}^{-(\lambda+|\xi|^2+ik\xi_3)t}\boldsymbol{E}^{ix\cdot\xi}}{(\lambda + |\xi|^2 + ik\xi_3)^N} D_t^N I_a(t, \xi)f\, dt d\xi.$$

Since

$$I_a(t, \xi)f|_{t=0} = \hat{f}(\xi),$$
$$D_t^j I_a(t, \xi)f|_{t=0} = a^j \sum_{k=0}^{j} |\xi'|^k \Big(\sum_{|\alpha'|=k} a_{\alpha'}^{jk}(0, 1, \xi/|\xi|) D_{\xi'}^{\alpha'}\hat{f}(\xi)\Big),$$

we have

$$\mathcal{A}_{\mathbb{R}^3,a,k}(\lambda)f = (\lambda + \mathbb{O}_{\mathbb{R}^3,k})f + \tilde{\mathcal{A}}^N_{1,a,k}(\lambda)f + \mathcal{A}^N_{2,a,k}(\lambda)f,$$

where we have set

$$\begin{aligned}
(\lambda + \mathbb{O}_{\mathbb{R}^3,k})f &= \frac{1}{(2\pi)^3}\int_{\mathbb{R}^3} \frac{\boldsymbol{E}^{\mathrm{i}x\cdot\xi}}{\lambda + |\xi|^2 + \mathrm{i}k\xi_3}\hat{f}(\xi)\,\mathrm{d}\xi,\\
\tilde{\mathcal{A}}^N_{1,a,k}(\lambda)f &= \sum_{j=1}^{N-1} a^j \sum_{\ell=0}^{j}\sum_{|\alpha'|=\ell}\frac{1}{(2\pi)^3}\int_{\mathbb{R}^3}\frac{\boldsymbol{E}^{\mathrm{i}x\cdot\xi}|\xi'|^\ell a^{j\ell}_{\alpha'}(0,1,\xi/|\xi|)}{(\lambda+|\xi|^2+\mathrm{i}k\xi_3)^{j+1}}(D^{\alpha'}_{\xi'}\hat{f})(\xi)\,d\xi,\\
\mathcal{A}^N_{2,a,k}(\lambda)f &= \sum_{j=0}^{N} a^j \sum_{\ell=0}^{j}\sum_{|\alpha'|=\ell}\frac{1}{(2\pi)^3}\int_0^\infty\int_{\mathbb{R}^3}\boldsymbol{E}^{-(\lambda+|\xi|^2+\mathrm{i}k\xi_3)t}\boldsymbol{E}^{\mathrm{i}x\cdot\xi}\\
&\qquad \frac{|\xi'|^\ell a^{j\ell}_{\alpha'}(\sin at,\cos at,\xi/|\xi|)}{(\lambda+|\xi|^2+\mathrm{i}k\xi_3)^N}(D^{\alpha'}_{\xi'}\hat{f})(\mathcal{O}(at)'\xi',\xi_3)\,d\xi\,dt.
\end{aligned}$$

We shall show the L_q boundedness of each operators defined above by using the following Fourier multiplier theorem (cf., Triebel [Sect. 2.2.4, Remark 3] [21]).

Theorem 5 *Let* $1 < q < \infty$. *Set* $U = \mathbb{R}^3 \setminus \{\xi \in \mathbb{R}^3 \mid \xi_j = 0$ *for some* $j = 1,2,3\}$. *Then, there exists a positive constant* C_q *such that for every* $P(\xi) \in C^3(U)$ *satisfying the estimate:*

$$\sup_{\xi\in U, |\alpha|\leq 3} |\xi^\alpha D^\alpha_\xi P(\xi)| \leq A$$

the operator $f \mapsto \mathcal{F}^{-1}_\xi[P(\xi)\hat{f}(\xi)]$ *is extended to a bounded linear operator on* $L_q(\mathbb{R}^3)$ *with the estimate:*

$$\|\mathcal{F}^{-1}_\xi[P(\xi)\hat{f}(\xi)]\|_{L_q(\mathbb{R}^3)} \leq C_q A \|f\|_{L_q(\mathbb{R}^3)}.$$

To start with our estimate, first of all we observe that

$$|D^\alpha_\xi(\lambda + |\xi|^2 + \mathrm{i}k\xi_3)^s| \leq C_{\alpha,s,\sigma,\varepsilon,k_0}(|\lambda| + |\xi|^2 + k_0^2)^s|\xi|^{-|\alpha|} \tag{40}$$

for any $s \in \mathbb{R}$, $\alpha \in \mathbb{N}_0^3$, $|k| \leq k_0$, $\xi \in \mathbb{R}^3$, and $\lambda \in \Sigma_\varepsilon$ with $|\lambda| \geq \lambda_0$ or $\lambda \in \mathbb{C}$ with $\mathrm{Re}\,\lambda \geq 0$ and $|\lambda| \geq \sigma$. In fact, let $p(t) = t^s$. By the Bell formula we have

$$\begin{aligned}
D^\alpha_\xi(\lambda + |\xi|^2 + \mathrm{i}k\xi_3)^s &= \sum_{\ell=1}^{|\alpha|} p^{(\ell)}(\lambda + |\xi|^2 + \mathrm{i}k\xi_3)\times\\
&\sum_{\substack{\alpha_1+\cdots+\alpha_\ell=\alpha\\ |\alpha_i|\geq 1}} \Gamma^{\alpha,\ell}_{\alpha_1,\ldots,\alpha_\ell} D^{\alpha_1}_\xi(\lambda + |\xi|^2 + \mathrm{i}k\xi_3)\cdots D^{\alpha_\ell}_\xi(\lambda + |\xi|^2 + \mathrm{i}k\xi_3)
\end{aligned} \tag{41}$$

where $p^{(\ell)}(t) = \mathrm{d}^\ell p/\mathrm{d}t^\ell$ and $\Gamma^{\alpha,\ell}_{\alpha_1,\dots,\alpha_\ell}$ are some constants depending on $\alpha, \ell, \alpha_1, \dots, \alpha_\ell$. Since

$$\begin{aligned}
|\lambda + |\xi|^2 + \mathrm{i}k\xi_3| &\le 2(|\lambda| + |\xi|^2 + k_0^2),\\
|D^\alpha_\xi(\lambda + |\xi|^2 + \mathrm{i}k\xi_3)| &\le 2|\xi| + k \le 2(|\lambda| + |\xi|^2 + k_0^2)^{\frac12} \quad (|\alpha| = 1),\\
|D^\alpha_\xi(\lambda + |\xi|^2 + \mathrm{i}k\xi_3)| &\le 2 = 2(|\lambda| + |\xi|^2 + k_0^2)^0 \quad (|\alpha| = 2),\\
|D^\alpha_\xi(\lambda + |\xi|^2 + \mathrm{i}k\xi_3)| &= 0 \le 2(|\lambda| + |\xi|^2 + k_0^2)^{-\frac{|\alpha|}{2}} \quad (|\alpha| \ge 3),
\end{aligned}$$

we have

$$|D^\alpha_\xi(\lambda + |\xi|^2 + \mathrm{i}k\xi_3)| \le 2(|\lambda| + |\xi|^2 + k_0^2)^{1-\frac{|\alpha|}{2}} \tag{42}$$

for any $\alpha \in \mathbb{N}_0^3$, $\lambda \in \mathbb{C}$, $\xi \in \mathbb{R}^3$ and $0 \le k \le k_0$. Combining (41), (42) and Lemma 1 we have (40).

By (40) with $s = -1$ and Theorem 5 we have

$$\|D^\beta_x(\lambda + \mathbb{O}_{\mathbb{R}^3,k})^{-1}f\|_{L_q(\mathbb{R}^3)} \le C_{q,k_0,\varepsilon}(|\lambda| + k_0^2)^{-(1-\frac{|\beta|}{2})}\|f\|_{L_q(\mathbb{R}^3)}. \tag{43}$$

To estimate $\tilde{\mathcal{A}}^N_{1,a,k}(\lambda)f$, we set

$$\mathcal{B}_{j,\ell,\alpha'}(\lambda)f = \frac{1}{(2\pi)^3}\int_{\mathbb{R}^3} \frac{\boldsymbol{E}^{\mathrm{i}x\cdot\xi}|\xi'|^\ell a^{j,\ell}_{\alpha'}(0,1,\xi/|\xi|)}{(\lambda + |\xi|^2 + \mathrm{i}k\xi_3)^{j+1}}(D^{\alpha'}_{\xi'}\hat{f})(\xi)\,d\xi'.$$

By (40) with $s = -(j+1)$ and Leibniz's rule, we have

$$\begin{aligned}
&\Big|D^\alpha_\xi\Big[\frac{(i\xi)^\beta|\xi'|^\ell a^{j,\ell}_{\alpha'}(0,1,\xi/|\xi|)}{(\lambda + |\xi|^2 + \mathrm{i}k\xi_3)^{j+1}}\Big]\Big|\\
&\quad\le C_{\alpha,j,\ell,k_0,\varepsilon}(|\lambda| + |\xi|^2 + k_0^2)^{-(j+1)}|\xi|^\ell|\xi|^{|\beta|}|\xi|^{-|\alpha|}\\
&\quad\le C_{\alpha,j,k_0,\varepsilon}(|\lambda| + k_0^2)^{-\left(j+1-\frac{\ell+|\beta|}{2}\right)}|\xi|^{-|\alpha|}
\end{aligned}$$

for any $\alpha \in \mathbb{N}_0^3$, $0 \le \ell \le j$, $\beta \in \mathbb{N}_0^3$ with $|\beta| \le 2$, $\xi \in \mathbb{R}^3$, $|k| \le k_0$ and $\lambda \in \Sigma_{\varepsilon,\lambda_0}$. By Theorem 5 we have

$$\|D^\beta_x\mathcal{B}_{j,\ell,\alpha'}(\lambda)f\|_{L_q(\mathbb{R}^3)} \le C_{j,\ell,k_0,\varepsilon}(|\lambda| + k_0^2)^{-\left(j+1-\frac{\ell+|\beta|}{2}\right)}\|(-\mathbf{l}x')^{\alpha'}f\|_{L_q(\mathbb{R}^3)} \tag{44}$$

where $x' = (x_1, x_2)$ and $\alpha' = (\alpha_1, \alpha_2) \in \mathbb{N}_0^2$. Since $f \in L_{q,R+2}(\mathbb{R}^3)$, we have

$$\|(-\mathbf{l}x')^{\alpha'}f\|_{L_r(\mathbb{R}^3)} \le C_{R,r}\|f\|_{L_q(\mathbb{R}^3)} \tag{45}$$

for $r = 1$ and $r = q$ where $(x')^{\alpha'} = x_1^{\alpha_1}x_2^{\alpha_2}$. Combining (45) with (44) implies that

$$\|D_x^\beta \mathcal{B}_{j,\ell,\alpha'}(\lambda)f\|_{L_q(\mathbb{R}^3)} \leq C_{j,\ell,\alpha',k_0,\varepsilon,R}\,(|\lambda|+k_0^2)^{-\left(j+1-\frac{\ell+|\beta|}{2}\right)}\|f\|_{L_q(\mathbb{R}^3)} \tag{46}$$

for any $\lambda \in \Sigma_{\varepsilon,\lambda_0}$ and $0 \leq \ell \leq j \leq N-1$. Since

$$\tilde{\mathcal{A}}^N_{1,a,k}(\lambda)f = \sum_{j=1}^{N-1} a^j \sum_{\ell=0}^{j}\sum_{|\alpha'|=\ell} \mathcal{B}_{j,\ell,\alpha'}f,$$

by (46) and (43) we have (30) and (31).

Now, we shall estimate $\mathcal{A}^N_{2,a,k}(\lambda)f$. By the change of variables: $\mathcal{O}(at)'\xi' = \eta'$ and $\xi_3 = \eta_3$, we have

$$\begin{aligned}
&\frac{1}{(2\pi)^3}\int_{\mathbb{R}^3}\frac{\boldsymbol{E}^{-(|\xi|^2+ik\xi_3)t}\boldsymbol{E}^{ix\cdot\xi}|\xi'|^\ell a^{j,\ell}_{\alpha'}(\sin at, \cos at, \xi/|\xi|)}{(\lambda+|\xi|^2+ik\xi_3)^N}(D^{\alpha'}_{\xi'}\hat{f})(\mathcal{O}(at)'\xi',\xi_3)\,d\xi\\
&= \frac{1}{(2\pi)^3}\int_{\mathbb{R}^3}\frac{\boldsymbol{E}^{-(|\eta|^2+ik\eta_3)t}\boldsymbol{E}^{i(\mathcal{O}(at)x)\cdot\eta}|\eta'|^\ell \tilde{a}^{j,\ell}_{\alpha'}(\sin at, \cos at, \eta/|\eta|)}{(\lambda+|\eta|^2+ik\eta_3)^N}D^{\alpha'}_{\eta'}\hat{f}(\eta)\,d\eta
\end{aligned}$$

where we have set

$$\tilde{a}^{j,\ell}_{\alpha'}(\sin at, \cos at, \eta/|\eta|) = a^{j,\ell}_{\alpha'}(\sin at, \cos at, ({}^T\mathcal{O}(at)'\eta', \eta_3)/|\eta|).$$

For the notational simplicity, we set

$$\begin{aligned}
&[\Phi_{\alpha',j,\ell,N}(t,\lambda)g](x)\\
&\quad= \frac{1}{(2\pi)^3}\int_{\mathbb{R}^3}\frac{\boldsymbol{E}^{-(|\xi|^2+ik\xi_3)t}\boldsymbol{E}^{ix\cdot\xi}|\xi'|^\ell \tilde{a}^{j,\ell}_{\alpha'}(\sin at, \cos at, \xi/|\xi|)}{(\lambda+|\xi|^2+ik\xi_3)^N}\hat{g}(\xi)\,d\xi
\end{aligned}$$

and then we have

$$\mathcal{A}^N_{2,a,k}(\lambda)f = \sum_{j=0}^{N} a^j \sum_{\ell=0}^{j}\sum_{|\alpha'|=\ell}\int_0^\infty e^{-\lambda t}[\Phi_{\alpha',j,\ell,N}(t,\lambda)((-\mathrm{I}x')^{\alpha'}f)](\mathcal{O}(at)x)\,dt. \tag{47}$$

To estimate $\mathcal{A}^N_{2,a,k}(\lambda)f$, we shall use Theorem 5. For this purpose, we shall observe that

$$|D^\alpha_\xi \boldsymbol{E}^{-(|\xi|^2+ik\xi_3)t}| \leq C_\alpha(1+tk_0^2)^{|\alpha|}|\xi|^{-|\alpha|} \tag{48}$$

for any $|k| \leq k_0$, $t > 0$ and $\xi \in \mathbb{R}^3$. In fact, setting $q(s) = \boldsymbol{E}^{-st}$, by the Bell formula and (42) with $\lambda = 0$ we have

$$|D^\alpha_\xi \boldsymbol{E}^{-(|\xi|^2+ik\xi_3)t}| \leq C_\alpha \sum_{\ell=1}^{|\alpha|}|q^{(\ell)}(|\xi|^2+ik\xi_3)|$$

$$\sum_{\substack{\alpha_1+\cdots+\alpha_\ell=\alpha \\ |\alpha_i|\geq 1}} |D_\xi^{\alpha_1}(|\xi|^2 + \mathrm{i}k\xi_3)| \cdots |D_\xi^{\alpha_\ell}(|\xi|^2 + \mathrm{i}k\xi_3)|$$
$$\leq C_\alpha \sum_{\ell=1}^{|\alpha|} t^\ell \boldsymbol{E}^{-|\xi|^2 t}(|\xi|^2 + k_0^2)^\ell |\xi|^{-|\alpha|},$$

which implies (48). Combining (48) with (40) implies that

$$\begin{aligned} &\left| D_\xi^\alpha \left[(\mathrm{i}\xi)^\beta \boldsymbol{E}^{-(|\xi|^2+\mathrm{i}k\xi_3)t} \frac{|\xi'|^\ell \tilde{a}_{\alpha'}^{j,\ell}(\sin at, \cos at, \xi/|\xi|)}{(\lambda + |\xi|^2 + \mathrm{i}k\xi_3)^N} \right] \right| \\ &\quad \leq C_{\alpha,j,\ell,\alpha',k_0}(1 + tk_0^2)^{|\alpha|}(|\lambda| + |\xi|^2 + k_0^2)^{-N}|\xi'|^\ell |\xi|^{|\beta|}|\xi|^{-|\alpha|} \\ &\quad \leq C_{\alpha,j,\ell,\alpha',k_0}(1 + tk_0^2)^{|\alpha|}(|\lambda| + k_0^2)^{-\left(N - \frac{\ell+|\beta|}{2}\right)}|\xi|^{-|\alpha|} \end{aligned} \tag{49}$$

for any $\lambda \in \Sigma_{\varepsilon,\lambda_0}$, $\xi \in \mathbb{R}^3$, $t > 0$, $|k| \leq k_0$, $|\alpha'| = \ell$ and $0 \leq \ell \leq j \leq N$. Therefore, by Theorem 5 we have

$$\|D_x^\beta \Phi_{j,\ell,\alpha'}(t,\lambda)g\|_{L_q(\mathbb{R}^3)} \leq C_{j,\ell,\alpha',k_0}(1 + tk_0^2)^3 |\lambda|^{-\left(\frac{N}{2} - \frac{|\beta|}{2}\right)} \|g\|_{L_q(\mathbb{R}^3)}. \tag{50}$$

Since $\mathcal{O}(at)$ is an orthogonal matrix, the L_q norm does not change under the change of variables: $y = \mathcal{O}(at)x$, and then by (50) and (47) we have

$$\begin{aligned} &\|D_x^\beta \mathcal{A}_{2,a,k}^N(\lambda) f\|_{L_q(\mathbb{R}^3)} \leq \\ &\sum_{j=0}^N |a|^j \sum_{\ell=0}^j \sum_{|\alpha|=\ell} C_{j,\ell,\alpha',k_0} \int_0^\infty e^{-\mathrm{Re}\,\lambda t}(1 + tk_0^2)^3 \, \mathrm{d}t |\lambda|^{-\left(\frac{N}{2} - \frac{|\beta|}{2}\right)} \|(-\mathrm{i}x')^{\alpha'} f\|_{L_q(\mathbb{R}^3)}, \end{aligned}$$

which combined with (45) implies (32), because $\boldsymbol{E}^{-\mathrm{Re}\,\lambda t} \leq \boldsymbol{E}^{-\sigma t}$ provided that $\lambda \in \mathbb{C}_\sigma$ and $t > 0$. This completes the proof of Theorem 4. □

3 Interior Problem

In this section, we consider the following resolvent problem in $\Omega_{R+3} = \Omega \cap B_{R+3}$:

$$(\lambda I + L_{a,k})u + \nabla p = f, \ \ \mathrm{div}\, u = 0 \ \text{ in } \Omega_{R+3}, \ \ u|_{\partial\Omega_{R+3}} = 0 \tag{51}$$

where $\partial\Omega_{R+3} = \partial\Omega \cup S_{R+3}$ and $S_L = \{x \in \mathbb{R}^3 \mid |x| = L\}$. Using the Helmholtz decomposition (cf., (10) with $D = \Omega$), we rewrite (51) as follows:

$$(\lambda I + L_{a,k})v + \nabla(Q_\Omega f + \theta) = f, \ \ \mathrm{div}\, v = 0 \ \text{ in } \Omega, \ \ v|_\Omega = 0. \tag{52}$$

We shall prove the following theorem.

Theorem 6 *Let $1 < q < \infty$, a_0, $k_0 > 0$ and $0 < \varepsilon < \pi/2$. Assume that $|a| \le a_0$ and $|k| \le k_0$. Let $\Sigma_{\varepsilon,\mu}$ be the same as in Theorem 4. Then there exists a constant $\lambda_1 = \lambda(a_0, k_0, \varepsilon)$ and operators*

$$\mathcal{A}_{\Omega,a,k}(\lambda) \in \mathrm{Anal}\,(\Sigma_{\varepsilon,\lambda_1(a_0,k_0,\varepsilon)}, \mathcal{L}(L_q(\Omega)^3, W_q^2(\Omega)^3 \cap J_q(\Omega))),$$
$$\mathcal{B}_{\Omega,a,k}(\lambda) \in \mathrm{Anal}\,(\Sigma_{\varepsilon,\lambda_1(a_0,k_0,\varepsilon)}, \mathcal{L}(L_q(\Omega)^3, \hat{W}_q^1(\Omega)^3))$$

such that $v = \mathcal{A}_{\Omega,a,k}(\lambda)f$ and $\theta = \mathcal{B}_{\Omega,a,k}(\lambda)f$ uniquely solve (52), that is

$$\begin{aligned} (\lambda I + L_a)\mathcal{A}_{\Omega,a}(\lambda)f + \nabla[\mathcal{B}_{\Omega,a}(\lambda)f + Q_\Omega f] = f &\quad \text{in } \Omega, \\ \operatorname{div} \mathcal{A}_{\Omega,a}(\lambda)f = 0 &\quad \text{in } \Omega, \\ \mathcal{A}_{\Omega,a}(\lambda)f = 0 &\quad \text{on } \partial\Omega, \end{aligned} \tag{53}$$

and satisfy the estimate:

$$\begin{aligned} &(1 + |\lambda|)\|v\|_{L_q(\Omega)} + (1 + |\lambda|)^{\frac{1}{2}}\|\nabla v\|_{L_q(\Omega)} + \|v\|_{W_q^2(\Omega)} \\ &\quad + (1 + |\lambda|^{\frac{1}{2}\left(1-\frac{1}{q}\right)}\|\theta\|_{L_q(\Omega)} + \|\nabla\theta\|_{L_q(\Omega)} \le C_{q,a_0,k_0,\varepsilon}\|f\|_{L_q(\Omega)} \end{aligned} \tag{54}$$

with some constant $C_{q,a_0,k_0,\varepsilon}$ for any $f \in L_q(\Omega)^3$ and $\lambda \in \Sigma_{\varepsilon,\lambda_1(a_0,k_0,\varepsilon)}$.

Remark 2 We note that

$$\mathcal{A}_{\Omega_{R+3},a,k}(\lambda) = \mathcal{A}_{\Omega_{R+3},a,k}(\lambda)P_{\Omega_{R+3}}, \quad \mathcal{B}_{\Omega_{R+3},a,k}(\lambda) = \mathcal{B}_{\Omega_{R+3},a,k}(\lambda)P_{\Omega_{R+3}}.$$

Let us define the operator $\mathcal{L}_{\Omega_{R+3},a,k}$ by

$$\begin{cases} \mathcal{D}_q(\mathcal{L}_{\Omega_{R+3},a,k}) = \left\{v \in J_q(\Omega_{R+3}) \cap W_q^2(\Omega_{R+3})^3 \mid v|_{\partial\Omega_{R+3}} = 0\right\}, \\ \mathcal{L}_{\Omega_{R+3},a,k}v = P_{\Omega_{R+3}}L_{a,k}v \qquad \text{for } v \in \mathcal{D}_q(\mathcal{L}_{\Omega_{R+3},a,k}). \end{cases}$$

Then (52) is rewritten as

$$(\lambda I + \mathcal{L}_{\Omega_{R+3},a,k})v = P_{\Omega_{R+3}}f \qquad \text{in } J_q(\Omega_{R+3})$$

and Theorem 6 provides its solution operator

$$\mathcal{A}_{\Omega_{R+3},a,k}(\lambda) = (\lambda I + \mathcal{L}_{\Omega_{R+3},a,k})^{-1}P_{\Omega_{R+3}}.$$

When $f \in J_q(\Omega_{R+3})$, estimate (54) for $v = (\lambda I + \mathcal{L}_{\Omega_{R+3},a,k})^{-1}f$ implies that the operator $-\mathcal{L}_{\Omega_{R+3},a,k}$ generates a bounded analytic semigroup $\{T_{\Omega_{R+3},a,k}(t)\}_{t\geq 0}$ of class C_0 on $J_q(\Omega_{R+3})$. Another important point in Theorem 6 is the structure of the pressure $p = Q_{\Omega_{R+3}}f + \theta$ together with decay property (54) of $\theta = \mathcal{B}_{\Omega_{R+3},a,k}(\lambda)f$ with respect to λ.

Proof To show Theorem 6, we shall use the following fact: For any $f \in L_q(\Omega_{R+3})$ there exists a unique solution $(U, \Xi) \in W_q^2(\Omega)^3 \times \hat{W}_q^1(\Omega)$ to the resolvent equation of the usual Stokes operator:

$$(\lambda I - \Delta)U + \nabla\Xi = f, \ \ \mathrm{div}\, U = 0 \ \text{ in } \Omega, \ U|_{\partial\Omega} = 0 \tag{55}$$

(cf., [6] and references therein). Using such U and Ξ, we define the operators $\mathcal{A}^0_\Omega(\lambda) : L_q(\Omega)^3 \to W_q^2(\Omega)^3$ and $\mathcal{B}^0_\Omega(\lambda) : L_q(\Omega)^3 \to \hat{W}_q^1(\Omega)$ by the relations: $\mathcal{A}^0_\Omega(\lambda)f = U$ and $\mathcal{B}^0_\Omega(\lambda)f = \Xi - Q_\Omega f$, respectively. Using these notations, we rewrite (55) as follows:

$$\begin{aligned}(\lambda I - \Delta)\mathcal{A}^0_\Omega(\lambda)f + \nabla(Q_\Omega + \mathcal{B}^0_\Omega(\lambda))f &= f \quad \text{in } \Omega_{R+3},\\ \mathrm{div}\, \mathcal{A}^0_\Omega(\lambda)f &= 0 \quad \text{in } \Omega_{R+3},\\ \mathcal{A}^0_\Omega(\lambda)f|_{\partial\Omega} &= 0.\end{aligned} \tag{56}$$

From [6] we know the estimate:

$$\begin{aligned}|\lambda|\|\mathcal{A}^0_\Omega(\lambda)f\|_{L_q(\Omega)} &+ |\lambda|^{\frac{1}{2}}\|\nabla\mathcal{A}^0_\Omega(\lambda)f\|_{L_q(\Omega)}\\ &+ \|\mathcal{A}^0_\Omega(\lambda)f\|_{W_q^2(\Omega)} + \|\mathcal{B}^0_\Omega(\lambda)f\|_{W_q^1(\Omega)} \le C_{q,\varepsilon}\|f\|_{L_q(\Omega)}\end{aligned} \tag{57}$$

provided that $f \in L_q(\Omega)^3$ and $\lambda \in \Sigma_\varepsilon \cup \{\lambda \in \mathbb{C} \mid |\lambda| \le \sigma_0\}$ with some $\sigma_0 > 0$. Moreover, by Hishida and Shibata [13] (cf., also Noll and Saal [16] and Geiser-Heck-Hieber [11]) we know that

$$\|\mathcal{B}^0_\Omega(\lambda)f\|_{L_q(\Omega)} \le C_{q,R,\varepsilon}|\lambda|^{-\frac{1}{2}\left(1-\frac{1}{q}\right)}\|f\|_{L_q(\Omega)} \tag{58}$$

for any $f \in L_q(\Omega)^3$ and $\lambda \in \Sigma_\varepsilon$ with $|\lambda| \ge 1$.

Now, we shall solve (51) for $f \in L_q(\Omega)^3$. To solve (51), we set

$$v = \mathcal{A}^0_\Omega(\lambda)g, \ \ p = (Q_\Omega + \mathcal{B}^0_\Omega(\lambda))g,$$

and then we have

$$(\lambda I + L_{a,k})v + \nabla p = g + K_{a,k}(\lambda)g. \tag{59}$$

where $K_{a,k}(\lambda) = (kD_3 + M_a)\mathcal{A}^0_\Omega(\lambda)$. If $(I + K_{a,k}(\lambda))^{-1}$ exists as a bounded linear operator on $L_q(\Omega)^3$, by (59), (57), and (58) $v = \mathcal{A}^0_\Omega(\lambda)(I + K_{a,k}(\lambda))^{-1}f$ and $p = (Q_\Omega + \mathcal{B}^0_\Omega(\lambda))(I + K_{a,k}(\lambda))^{-1}f$ solve problem (51). Therefore, our task is to show the existence of $(I + K_{a,k}(\lambda))^{-1}$. Let us denote the operator norm of the bounded linear operators on $L_q(\Omega)^3$ by $\|\cdot\|_{\mathcal{L}(L_q(\Omega)^3)}$. Since Ω is bounded, in view of (57) we have

$$\|K_{a,k}(\lambda)\|_{\mathcal{L}(L_q(\Omega)^3)} \le C_{q,a_0,k_0,\varepsilon,R}|\lambda|^{-\frac{1}{2}} \quad (\lambda \in \Sigma_\varepsilon, |\lambda| \ge 1). \tag{60}$$

From (60) it follows that there exists a large $\lambda_1 = \lambda_1(a_0, k_0, \varepsilon) > 0$ such that $\|K_{a,k}(\lambda)\|_{\mathcal{L}(L_q(\Omega)^3)} \leq 1/2$ provided that $|\lambda| \geq \lambda_1(a_0, k_0, \varepsilon)$ and $\lambda \in \Sigma_\varepsilon$, and then we have the inverse operator $(I + K_{a,k}(\lambda))^{-1} \in \mathcal{L}(L_q(\Omega)^3)$ and by (60)

$$\|(I + K_{a,k}(\lambda))^{-1} - I\|_{\mathcal{L}(L_q(\Omega)^3)} \leq C_{q,a_0,k_0,\varepsilon,R}|\lambda|^{-\frac{1}{2}} \tag{61}$$

for any $\lambda \in \Sigma_\varepsilon$ with $|\lambda| \geq \lambda_1(\varepsilon, a_0)$. Combining (61), (57), and (58), we have (54), which completes the proof of Theorem 6. □

By (52) and Theorem 6 we have the following corollary.

Corollary 1 *Let* $1 < q < \infty$, a_0, $k_0 > 0$ *and* $0 < \varepsilon < \pi/2$. *Assume that* $|a| \leq a_0$ *and* $|k| \leq k_0$. *Let* $\lambda_1(a_0, k_0, \varepsilon)$, $\Sigma_{\varepsilon,\lambda_1(a_0,k_0,\varepsilon)}$, $\mathcal{A}_{\Omega,a,k}(\lambda)$ *and* $\mathcal{B}_{\Omega,a,k}(\lambda)$ *be the same constant, set and operators as in Theorem 6, respectively. For* $\lambda \in \Sigma_{\varepsilon,\lambda_1(a_0,k_0,\varepsilon)}$ *and* $f \in L_q(\Omega)^3$, *we set* $u_\lambda = \mathcal{A}_{\Omega,a,k}(\lambda)f$ *and* $p_\lambda = \mathcal{B}_{\Omega,a,k}(\lambda)f$. *Then, for any* $m \in \mathbb{N}$ *we have*

$$\|(|\lambda|\partial_\lambda^m u_\lambda, |\lambda|^{\frac{1}{2}}\nabla\partial_\lambda^m u_\lambda)\|_{L_q(\Omega)} + \|\partial_\lambda^m u_\lambda\|_{W_q^2(\Omega)} + \|\nabla\partial_\lambda^m p_\lambda\|_{L_q(\Omega)}$$
$$+ (1 + |\lambda|)^{\frac{1}{2}\left(1-\frac{1}{q}\right)}\|\partial_\lambda^m p_\lambda\|_{L_q(\Omega)} \leq C_k(1 + |\lambda|)^{-m}\|f\|_{L_q(\Omega)}.$$

Proof Differentiating (52) m-times by λ, we have

$$\begin{aligned}(\lambda I + L_{a,k})[\partial_\lambda^m u_\lambda] + \nabla[\partial_\lambda^m p_\lambda] = -m\partial_\lambda^{m-1}u_\lambda, \quad \operatorname{div}[\partial_\lambda^m u_\lambda] = 0 \quad &\text{in } \Omega,\\ \partial_\lambda^m u_\lambda = 0 \quad &\text{on } \partial\Omega.\end{aligned}$$

Since $u_\lambda \in J_q(\Omega)$ and $\|u_\lambda\|_{L_q(\Omega)} \leq C(1 + |\lambda|)^{-1}\|f\|_{L_q(\Omega)}$, by (54) and the mathematical induction on m we have the corollary. □

4 A Preparation for Construction of Parametrix in an Exterior Domain

In this section, we shall construct a solution operator to the equations:

$$(\lambda I + L_{a,k})u + \nabla p = f, \quad \operatorname{div} u = 0 \ \text{ in } \Omega, \quad u|_{\partial\Omega} = 0. \tag{62}$$

Throughout this section, we assume that $|a| \leq a_0$ and $|k| \leq k_0$. To state the main result in this section, we have to prepare several symbols which will be used not only in this section but also in later sections, so that the main result will be stated at the end of this section. We start with the Bogovskiĭ - Pileckas operator, which is used to keep the divergence free condition in the cut-off procedure.

Lemma 2 *Let* $1 < q < \infty$. (1) *Let* D *be a bounded, lipschitzian domain in* $\mathbb{R}^3$. *We set*

$$W^m_{q,0}(D) = \{u \in W^m_q(D) \mid \partial^\alpha_x u|_{\partial D} = 0 \ \textit{for}\ |\alpha| \le m-1\}$$

for any integer $m \ge 1$ *and* $W^0_{q,0}(D) = L_q(D)$. *Then, there exists a bounded linear operator* $\mathbb{B}$ *from* $W^m_{q,0}(D)$ *to* $W^{m+1}_q(\mathbb{R}^3)^3$ *such that* $\operatorname{supp}\mathbb{B}[f] \subset D$ *and* $\|\mathbb{B}[f]\|_{W^{m+1}_q(\mathbb{R}^3)} \le C_{m,q}\|f\|_{W^m_q(D)}$. *Moreover, if* $f \in W^m_{q,0}(D)$ *satisfies the average free condition:* $\int_D f\,\mathrm{d}x = 0$, *then* $\operatorname{div}\mathbb{B}[f] = f_0$ *in* $\mathbb{R}^3$, *where* $f_0(x) = f(x)$ *for* $x \in D$ *and* $f(x) = 0$ *for* $x \notin D$.
(2) *Let* m *be a positive integer and* D *be one of* $\mathbb{R}^3$, Ω *and* Ω. *Let* ψ *be a function in* C^∞ *such that* ψ *or* $1-\psi$ *has a compact support and* $\operatorname{supp}\nabla\psi \subset D_{R+1,R+2} = B_{R+2}\setminus B_{R+1}$. *If* $u \in W^m_q(D)^3$ *satisfies the conditions:* $\operatorname{div} u = 0$ *in* D *and* $\nu\cdot u|_{\partial D} = 0$ *when* D *is* Ω *or* Ω, *then* $(\nabla\psi)\cdot u \in W^m_{q,0}(D_{R+1,R+2})$ *and* $\int_{D_{R+1,R+2}}(\nabla\psi)\cdot u\,\mathrm{d}x = 0$.
(3) *Let* ψ *be the same function as in* (2). *Then, we have for* $j = 1, 2, 3$

$$\begin{aligned}
&\|\mathbb{B}[(\nabla\psi)\cdot(\partial_j v)]\|_{L_q(\mathbb{R}^3)} \le C_{q,R}\|v\|_{L_q(D_{R+1,R+2})}, \qquad v \in W^1_{q,0}(D_{R+1,R+2})^3\\
&\|\mathbb{B}[(\nabla\psi)\cdot(\nabla w)]\|_{L_q(\mathbb{R}^3)} \le C_{q,R}\|w\|_{L_q(D_{R+1,R+2})}, \quad w \in W^1_{q,0}(D_{R+1,R+2}). \qquad (63)
\end{aligned}$$

Proof (1) For the proof of the assertion (1), we refer to [1] (cf., also Galdi [8, Theorem 3.2] and references therein).
(2) Since $\operatorname{supp}\nabla\psi \subset D_{R+1,R+2}$, we trivially see that $(\nabla\psi)\cdot u \in W^m_{q,0}(D_{R+1,R+2})$. To check the average free, we consider the case where $1-\psi$ has a compact support and $D = \Omega$ and observe that

$$\int_{D_{R+1,R+2}}(\nabla\psi)\cdot u\,\mathrm{d}x = -\int_\Omega \operatorname{div}((1-\psi)u)\,\mathrm{d}x = -\int_{\partial\Omega}(1-\psi)\nu\cdot u\,\mathrm{d}\sigma = 0,$$

where $\mathrm{d}\sigma$ denotes the surface element of $\partial\Omega$. In the case where ψ has a compact support, analogously we have $\int_{D_{R+1,R+2}}(\nabla\psi)\cdot u\,dx = 0$.
(3) By employing the same argument as in the proof of [8, Lemma 3.1 in Chap. III], we can prove (63) (more general bounded domain case being treated in [12]). This completes the proof of Lemma 2. □

Now, we shall define a parametrix to (62). Let φ be a cut-off function in $C^\infty_0(\mathbb{R}^3)$ such that $\varphi(x) = 1$ for $|x| \le R+1$ and $\varphi(x) = 0$ for $|x| \ge R+2$. Given $f \in L_{q,R+2}(\Omega)$, $r_{\Omega_{R+3}} f$ denotes the restriction of f on Ω and f_0 is the zero extension of f to the whole space. We set

$$\begin{aligned}
\Phi_{a,k}(\lambda)f &= (1-\varphi)\mathcal{A}_{\mathbb{R}^3,a,k}(\lambda)f_0 + \varphi\mathcal{A}_{\Omega,a,k}(\lambda)r_{\Omega_{R+3}}f + \mathbb{B}[(\nabla\varphi)\cdot\mathcal{C}_{a,k}(\lambda)f],\\
\mathcal{C}_{a,k}(\lambda)f &= \mathcal{A}_{\mathbb{R}^3,a,k}(\lambda)f_0 - \mathcal{A}_{\Omega,a,k}(\lambda)r_{\Omega_{R+3}}f,\\
\Psi_{a,k}(\lambda)f &= (1-\varphi)\mathcal{Q}_{\mathbb{R}^3}f_0 + \varphi(\mathcal{Q}_\Omega r_{\Omega_{R+3}}f + \mathcal{B}_{\Omega,a,k}(\lambda)r_{\Omega_{R+3}}f), \qquad (64)\\
Tf &= -(\nabla\varphi)(\mathcal{Q}_{\mathbb{R}^3}f_0 - \mathcal{Q}_\Omega r_{\Omega_{R+3}}f)\\
&\quad - \mathbb{B}[(\nabla\varphi)\cdot\nabla(\mathcal{Q}_{\mathbb{R}^3}f_0 - \mathcal{Q}_\Omega r_{\Omega_{R+3}}f)], \qquad (65)
\end{aligned}$$

$$\begin{aligned}S_{a,k}(\lambda)f &= 2(\nabla\varphi)\cdot\nabla(\mathcal{C}_{a,k}(\lambda)f) + (\Delta\varphi)\mathcal{C}_{a,k}(\lambda)f - k(D_3\varphi)\mathcal{C}_{a,k}(\lambda)f \\ &\quad + a((\mathbf{e}_3\times x)\cdot\nabla\varphi)\mathcal{C}_{a,k}(\lambda)f + \mathbb{B}[(\nabla\varphi)\cdot\Delta\mathcal{C}_{a,k}(\lambda)f] \\ &\quad - k\mathbb{B}[(\nabla\varphi)\cdot D_3\mathcal{C}_{a,k}(\lambda)f] - \mathbb{B}[(\nabla\varphi)\cdot M_a\mathcal{C}_{a,k}(\lambda)f] \\ &\quad + \mathbb{B}[(\nabla\varphi)\cdot\nabla\mathcal{B}_{\Omega,a,k}(\lambda)r_{\Omega_{R+3}}f] - \Delta\mathbb{B}[(\nabla\varphi)\cdot\mathcal{C}_{a,k}(\lambda)f] \\ &\quad + M_a\mathbb{B}[(\nabla\varphi)\cdot\mathcal{C}_{a,k}(\lambda)f] + (\nabla\varphi)\mathcal{B}_{\Omega,a,k}(\lambda)r_{\Omega_{R+3}}f, \end{aligned} \tag{66}$$

and then we have

$$\begin{aligned}(\lambda I + L_{a,k})\Phi_{a,k}(\lambda)f + \nabla\Psi_{a,k}(\lambda)f &= (I+T)f + S_{a,k}(\lambda)f \quad \text{in } \Omega, \\ \operatorname{div}\Phi_{a,k}(\lambda)f &= 0 \quad \text{in } \Omega, \qquad (67)\\ \Phi_{a,k}(\lambda)f|_{\partial\Omega} &= 0. \qquad (68)\end{aligned}$$

In fact, we observe that

$$\begin{aligned}&(\lambda I + L_{a,k})\Phi_{a,k}(\lambda)f + \nabla\Psi_{a,k}(\lambda)f \\ &= (1-\varphi)f_0 + \varphi(r_{\Omega_{R+3}}f) + 2(\nabla\varphi)\cdot\nabla\mathcal{C}_{a,k}(\lambda)f \\ &\quad + (\Delta\varphi)\mathcal{C}_{a,k}(\lambda)f - k(D_3\varphi)\mathcal{C}_{a,k}(\lambda)f + a((\mathbf{e}_3\times x)\cdot\nabla\varphi)\mathcal{C}_{a,k}(\lambda)f \\ &\quad + \lambda\mathbb{B}[(\nabla\varphi)\cdot\mathcal{C}_{a,k}(\lambda)f] - \Delta\mathbb{B}[(\nabla\varphi)\cdot\mathcal{C}_{a,k}(\lambda)f] + kD_3\mathbb{B}[(\nabla\varphi)\cdot\mathcal{C}_{a,k}(\lambda)f] \\ &\quad + M_a\mathbb{B}[(\nabla\varphi)\cdot\mathcal{C}_{a,k}(\lambda)f] + (\nabla\varphi)\mathcal{B}_{\Omega,a,k}(\lambda)r_{\Omega_{R+3}}f \\ &\quad - (\nabla\varphi)(Q_{\mathbb{R}^3}f_0 - Q_\Omega r_{\Omega_{R+3}}f)\end{aligned} \tag{69}$$

Since $f_0 = r_{\Omega_{R+3}}f$ on supp $\nabla\varphi$, by (27) and (53) we have

$$\begin{aligned}\lambda(\nabla\varphi)\cdot\mathcal{C}_{a,k}(\lambda)f =& (\nabla\varphi)\cdot(\Delta\mathcal{C}_{a,k}(\lambda)f - kD_3\mathcal{C}_{a,k}(\lambda)f - M_a\mathcal{C}_{a,k}(\lambda)f \\ &+ \nabla\mathcal{B}_{\Omega,a,k}(\lambda)r_{\Omega_{R+3}}f - \nabla(Q_{\mathbb{R}^3}f_0 - Q_\Omega r_{\Omega_{R+3}}f))\end{aligned}$$

which inserted into (69) implies (67) with (66).

In what follows, we discuss the existence of $(I+T+S_a(\lambda))^{-1} \in \mathcal{L}(L_{q,R+2}(\Omega))$. Let λ_0 and λ_1 be the same constants as in Theorems 4 and 6, and set $\lambda_2 = \lambda_2(a_0, k_0, \varepsilon) = \max(\lambda_0, \lambda_1, 1)$. Since $\Sigma_{\varepsilon,\lambda_2}\cap\mathbb{C}_{+,0} \supset \mathbb{C}_{\lambda_2}$, by Theorems 4, 6, Lemma 2 and (66), we have

$$\begin{aligned}&S_{a,k}(\lambda) \in \operatorname{Anal}(\mathbb{C}_{\lambda_2}, \mathcal{L}(L_{q,R+2}(\Omega))), \\ &\|S_{a,k}(\lambda)\|_{\mathcal{L}(L_{q,R+2}(\Omega)^3)} \le C_{a_0,k_0,q,R}(1+|\lambda|)^{-(1/2)(1-(1/q))} \quad (\lambda \in \mathbb{C}_{\lambda_2}).\end{aligned} \tag{70}$$

The following lemma was proved by Hishida and Shibata [13].

Lemma 3 *There exists an inverse operator* $(I+T)^{-1} \in \mathcal{L}(L_{q,R+2}(\Omega))$.

Combining (70) and Lemma 3 we see that there exists a large number $\lambda_3 = \lambda(a_0, k_0, \varepsilon) > 0$ such that

$$\|(I+T)^{-1}S_{a,k}(\lambda)f\|_{L_q(\Omega)} \le (1/2)\|f\|_{L_q(\Omega)} \tag{71}$$

for any $f \in L_{q,R+2}(\Omega)$ and $\lambda \in \mathbb{C}_{\lambda_3}$. By (71) and the Neumann series expansion we have

$$\begin{aligned}
&(I+T+S_{a,k}(\lambda))^{-1} \in \mathrm{Anal}\,(\mathbb{C}_{\lambda_3}, \mathcal{L}(L_{q,R+2}(\Omega))),\\
&\|(I+T+S_{a,k}(\lambda))^{-1}f\|_{L_q(\Omega)} \le 2\|(I+T)^{-1}\|_{\mathcal{L}(L_{q,R+2}(\Omega))}\|f\|_{L_q(\Omega)},\\
&(I+T+S_{a,k}(\lambda))^{-1} = (I+T)^{-1} + \sum_{j=1}^{\infty}(-(I+T)^{-1}S_a(\lambda))^j(I+T)^{-1}
\end{aligned} \tag{72}$$

for any $f \in L_{q,R+2}(\Omega)$ and $\lambda \in \mathbb{C}_{\lambda_3}$.

Now, we are in position to show the main result in this section.

Proposition 6 *Let* $1 < q < \infty$, a_0, $k_0 > 0$ *and* $0 < \varepsilon < \pi/2$. *Let* N *be a natural number* > 3. *Assume that* $|a| \le a_0$ *and* $|k| \le k_0$. *Then, there exists a number* $\lambda_3 = \lambda_3(a_0, k_0, \varepsilon) \ge 1$ *such that* $(I+T+S_{a,k}(\lambda))^{-1} \in \mathcal{L}(L_{q,R+2}(\Omega))$ *exists and*

$$\|(I+T+S_{a,k}(\lambda))^{-1}\|_{\mathcal{L}(L_{q,R+2}(\Omega))} \le K \tag{73}$$

with some constant $K > 0$ *for any* $\lambda \in \mathbb{C}_{\lambda_3}$.

Moreover, there exist two operator valued functions

$$U^1_{a,k,N}(\lambda) \in \mathrm{Anal}\,(\Sigma_{\varepsilon,\lambda_3}, \mathcal{L}(L_{q,R+3}(\Omega))), \quad U^2_{a,k,N} \in \mathrm{Anal}\,(\mathbb{C}_{\lambda_3}, \mathcal{L}(L_{q,R+3}(\Omega)))$$

such that

$$\begin{aligned}
&(I+T+S_{a,k}(\lambda))^{-1} = (I+T)^{-1} + U^1_{a,k,N}(\lambda) + U^2_{a,k,N}(\lambda) \quad (\lambda \in \mathbb{C}_{\lambda_3}),\\
&\|U^1_{a,k,N}(\lambda)\|_{\mathcal{L}(L_{q,R+3}(\Omega))} \le C_{a_0,k_0,\varepsilon,q,N}|\lambda|^{-\frac{1}{2}\left(1-\frac{1}{q}\right)} \quad (\lambda \in \Sigma_{\varepsilon,\lambda_3}),\\
&\|U^2_{a,k,N}(\lambda)\|_{\mathcal{L}(L_{q,R+3}(\Omega))} \le C_{a_0,k_0,\varepsilon,q,N}|\lambda|^{-\frac{(N-1)(1-(1/q))}{4}} \quad (\lambda \in \mathbb{C}_{\lambda_3}).
\end{aligned} \tag{74}$$

Proof Equation (73) follows from Lemma 3 and (74), so that we shall prove (74). In view of Theorems 4 and 6, we set

$$\mathcal{C}^1_{a,k}(\lambda)f = r_{\Omega_{R+3}}\mathcal{A}^N_{1,a,k}(\lambda)f - \mathcal{A}_{\Omega,a,k}(\lambda)f, \quad \mathcal{C}^2_{a,k}(\lambda)f = r_{\Omega_{R+3}}\mathcal{A}^N_{2,a,k}(\lambda)f.$$

Let λ_0 and λ_1 be the same constans as in Theorems 4 and 6 and set $\lambda_3 = \max(\lambda_0, \lambda_1, 1)$. By Theorems 4 and 6 we have $\mathcal{C}_{a,k}(\lambda) = \mathcal{C}^1_{a,k}(\lambda) + \mathcal{C}^2_{a,k}(\lambda)$,

$$\begin{aligned}
&\mathcal{C}^1_{a,k}(\lambda) \in \mathrm{Anal}\,(\Sigma_{\varepsilon,\lambda_3}, \mathcal{L}(L_{q,R+3}(\Omega), W^2_q(\Omega)^3)),\\
&\mathcal{C}^2_{a,k}(\lambda) \in \mathrm{Anal}\,(\mathbb{C}_{\lambda_3}, \mathcal{L}(L_{q,R+3}(\Omega), W^2_q(\Omega))),\\
&\|\mathcal{C}^1_{a,k}(\lambda)\|_{\mathcal{L}(L_{q,R+3}(\Omega), W^1_q(\Omega)^3)} \le C_{a_0,k_0,\varepsilon,q,R,N}|\lambda|^{-\frac{1}{2}},\\
&\|\mathcal{C}^2_{a,k}(\lambda)\|_{\mathcal{L}(L_{q,R+3}(\Omega), W^1_q(\Omega)^3)} \le C_{a_0,k_0,\varepsilon,q,R,N}|\lambda|^{-\frac{N-1}{2}}.
\end{aligned} \tag{75}$$

By using $\mathcal{C}^1_{a,k}(\lambda)$ and $\mathcal{C}^2_{a,k}(\lambda)$, we devide $S_{a,k}(\lambda)$ as follows:

$$\begin{aligned}
&S^1_{a,k}(\lambda)f = 2(\nabla\varphi)\cdot\nabla(\mathcal{C}^1_{a,k}(\lambda)f) + (\Delta\varphi)\mathcal{C}^1_{a,k}(\lambda)f - k(D_3\varphi)\mathcal{C}^1_{a,k}(\lambda)f \\
&+ a((\mathbf{e}_3\times x)\cdot\nabla\varphi)\mathcal{C}^1_{a,k}(\lambda)f + \mathbb{B}[(\nabla\varphi)\cdot\Delta\mathcal{C}^1_{a,k}(\lambda)f] - k\mathbb{B}[(\nabla\varphi)\cdot D_3\mathcal{C}^1_{a,k}(\lambda)f] \\
&- \mathbb{B}[(\nabla\varphi)\cdot M_a\mathcal{C}^1_{a,k}(\lambda)f] + \mathbb{B}[(\nabla\varphi)\cdot\nabla\mathcal{B}_{\Omega,a,k}(\lambda)r_{\Omega_{R+3}}f] \\
&- \Delta\mathbb{B}[(\nabla\varphi)\cdot\mathcal{C}^1_{a,k}(\lambda)f] + M_a\mathbb{B}[(\nabla\varphi)\cdot\mathcal{C}^1_{a,k}(\lambda)f] + (\nabla\varphi)\mathcal{B}_{\Omega,a,k}(\lambda)r_{\Omega_{R+3}}f, \\
&S^2_{a,k}(\lambda)f = S_{a,k}(\lambda)f - S^1_{a,k}(\lambda)f.
\end{aligned}$$

By (75) and Theorem 6 we have

$$\begin{aligned}
&S^1_{a,k}(\lambda) \in \mathrm{Anal}\,(\Sigma_{\varepsilon,\lambda_3}, \mathcal{L}(L_{q,R+3}(\Omega), W^2_q(\Omega)^3)), \\
&S^2_{a,k} \in \mathrm{Anal}\,(\mathbb{C}_{\lambda_3}, \mathcal{L}(L_{q,R+3}(\Omega), W^2_q(\Omega))), \\
&\|S^1_{a,k}\|_{\mathcal{L}(L_{q,R+3}(\Omega),W^1_q(\Omega)^3)} \le C_{a_0,k_0,\varepsilon,q,R,N}|\lambda|^{-\frac12\left(1-\frac1q\right)}, \\
&\|S^2_{a,k}\|_{\mathcal{L}(L_{q,R+3}(\Omega),W^1_q(\Omega)^3)} \le C_{a_0,k_0,\varepsilon,q,R,N}|\lambda|^{-\frac{N-1}{2}}.
\end{aligned} \tag{76}$$

In view of (75) and (72), choosing an integer M so large that $M \ge (N-1)/2$, we set

$$\begin{aligned}
U^1_{a,k,N}(\lambda) &= \sum_{j=1}^{M-1}(-(I+T)^{-1}S^1_{a,k}(\lambda))^j(I+T)^{-1}, \\
U^2_{a,k,N}(\lambda) &= (I+T+S_{a,k}(\lambda))^{-1} - (I+T)^{-1} - U^1_{a,k,N}(\lambda),
\end{aligned}$$

and then by (76) we have (74), which completes the proof of Proposition 6. □

Especially, by Theorem 4, Theorem 6, (64), (67) and Proposition 6 we can find the following operators: Set

$$\begin{aligned}
R_{a,k}(\lambda) &= \Phi_{a,k}(\lambda)(I+T+S_{a,k}(\lambda))^{-1}, \\
\Pi_{a,k}(\lambda) &= \Psi_{a,k}(\lambda)(I+T+S_{a,k}(\lambda))^{-1},
\end{aligned} \tag{77}$$

and then for any $f \in L_{q,R+2}(\Omega)$ we have

$$R_{a,k}(\lambda)f \in W^2_q(\Omega)^3, \quad \Pi_{a,k}(\lambda)f \in \hat{W}^1_q(\Omega), \tag{78}$$

and $R_{a,k}(\lambda)f$ and $\Pi_{a,k}(\lambda)f$ satisfy the equations:

$$\begin{gathered}
(\lambda I + L_{a,k})R_{a,k}(\lambda)f + \nabla\Pi_{a,k}(\lambda)f = f, \quad \mathrm{div}\,R_{a,k}(\lambda)f = 0 \quad \text{in } \Omega, \\
R_{a,k}(\lambda)f|_{\partial\Omega} = 0.
\end{gathered} \tag{79}$$

5 On a Unique Existence Theorem to the Nonstationary Problem for the Initial Data in $L_{q,R+2}(\Omega)$

In this section, we shall consider the non-stationary problem:

$$\begin{aligned} u_t + Lu + \nabla p = 0, \quad \operatorname{div} u = 0 \quad & \text{in } \Omega \times (0, \infty), \\ u|_{\partial\Omega} = 0, \quad u|_{t=0} = P_\Omega f \quad & \text{in } \Omega \end{aligned} \tag{80}$$

for $f \in L_{q,R+2}(\Omega)$, and we shall show the following theorem.

Theorem 7 *Let* $1 < q < \infty$, $a_0\ k_0 > 0$ *and let* λ_3 *be the same constant as in Proposition 6. Set* $\mathbb{R}_+ = (0, \infty)$. *Assume that* $|a| \le a_0$ *and* $|k| \le k_0$. *For every* $f \in L_{q,R+2}(\Omega)$, *problem* (80) *admits a unique solution* $(u(t), p(t))$ *such that* $u(t)$ *and* $p(t)$ *satisfy the regularity condition:*

$$\begin{aligned} & u(t) \in C^1(\mathbb{R}_+, L_q(\Omega)^3) \cap C^0(\mathbb{R}_+, W_q^2(\Omega)^3) \cap C^0([0, \infty), L_q(\Omega)^3), \\ & p(t) \in C^0(\mathbb{R}_+, \hat{W}_q^1(\Omega)), \end{aligned} \tag{81}$$

and the following estimates:

$$\begin{aligned} \|(u(t), t^{1/2}\nabla u(t), t\nabla^2 u(t), tu_t(t), t\nabla p(t))\|_{L_q(\Omega)} \le & C_{a_0,k_0,\gamma}\, \boldsymbol{E}^{\gamma t} \|f\|_{L_q(\Omega)}, \\ t^{(1/2)(1+(1/q))} \|p(t)\|_{L_q(\Omega_b)} \le & C_{a_0,k_0,\gamma,b}\, \boldsymbol{E}^{\gamma t} \|f\|_{L_q(\Omega)} \end{aligned} \tag{82}$$

for any $t > 0$, $\gamma > 2\lambda_3$ *and* $b > R + 3$, *where* λ_3 *is the same constant as in Proposition 6, and* $C_{a_0,k_0,\gamma}$ *and* $C_{a_0,k_0,\gamma,b}$ *are constants independent of* $t > 0$.

Moreover, $u(t)$ *is represented by*

$$u(t) = \lim_{\ell \to \infty} \frac{1}{2\pi i} \int_{\gamma - i\ell}^{\gamma + i\ell} \boldsymbol{E}^{\lambda t} R_{a,k}(\lambda) f \, d\lambda \tag{83}$$

for any $f \in L_{q,R+2}(\Omega)$, *where* $R_{a,k}(\lambda)$ *is the operator defined by* (77) *and the right hand side in* (83) *converges strongly in* $W_q^1(\Omega)$ *for any* $t > 0$.

Remark 3 The conditions: $u(t) \in W_q^2(\Omega)^3$, $u_t(t) \in L_q(\Omega)$ and $\nabla p(t) \in L_q(\Omega)^3$ together with the Eq. (80) automatically imply that $M_a u(t) \in L_q(\Omega)^3$, that is $M_a u(t) \in \mathcal{D}_q(\Omega)$.

In the course of our proof of Theorem 7 below, we do not mention the dependence of a_0, k_0, q and ε for generic constants, although constants depend on a_0, k_0, q and ε in almost all the cases. Using the formula (83), we shall construct a solution to (80) with $f \in L_{q,R+2}(\Omega)$. Our idea is to divide $R_{a,k}(\lambda)$ into a sectorial operator and an operator which is analytic only on $\mathbb{C}_{\lambda_3}$ but summable for large λ. More precisely, there exist operators:

$$R^1_{a,k}(\lambda) \in \operatorname{Anal}(\Sigma_{\varepsilon,\lambda_3}, \mathcal{L}(L_{q,R+2}(\Omega), W_q^2(\Omega)^3)),$$

$$\begin{aligned}
&R^2_{a,k}(\lambda) \in \mathrm{Anal}\,(\mathbb{C}_{\lambda_3}, \mathcal{L}(L_{q,R+2}(\Omega), W^2_q(\Omega)^3)),\\
&\Pi^1_{a,k}(\lambda) \in \mathrm{Anal}\,(\Sigma_{\varepsilon,\lambda_3}, \mathcal{L}(L_{q,R+2}(\Omega), \hat{W}^1_q(\Omega))),\\
&\Pi^2_{a,k}(\lambda) \in \mathrm{Anal}\,(\mathbb{C}_{\lambda_3}, \mathcal{L}(L_{q,R+2}(\Omega), \hat{W}^1_q(\Omega))),
\end{aligned} \tag{84}$$

such that

$$\begin{aligned}
R_{a,k}(\lambda)f &= R^1_{a,k}(\lambda)f + R^2_{a,k}(\lambda)f,\\
\Pi_{a,k}(\lambda)f &= \mathcal{Q}f + \Pi^1_{a,k}(\lambda)f + \Pi^2_{a,k}(\lambda)f,\\
\mathcal{Q}f &= (1-\varphi)Q_{\mathbb{R}^3}[(1+T)^{-1}f]_0 + \varphi Q_\Omega r_{\Omega_{R+3}}[(I+T)^{-1}f],
\end{aligned} \tag{85}$$

$$\begin{aligned}
&\|\partial^\alpha_x R^1_{a,k}(\lambda)f\|_{L_q(\Omega)} \le C_{\alpha,q,R}|\lambda|^{-(1-(|\alpha|/2))}\|f\|_{L_q(\Omega)} \ \ (|\alpha|\le 2) && \lambda\in\Sigma_{\varepsilon,\lambda_3},\\
&\|R^2_{a,k}(\lambda)f\|_{W^2_q(\Omega)} \le C_{q,R}\gamma^{-1}|\lambda|^{-3}\|f\|_{L_q(\Omega)} && \lambda\in\mathbb{C}_{\lambda_3},\\
&\|\nabla\Pi^1_{a,k}(\lambda)f\|_{L_q(\Omega)} \le C_{b,q,R,\varepsilon}\|f\|_{L_q(\Omega)} && \lambda\in\Sigma_{\varepsilon,\lambda_3},\\
&\|\Pi^1_{a,k}(\lambda)f\|_{L_q(\Omega_b)} \le C_{b,q,R}|\lambda|^{-(1/2)(1-(1/q))}\|f\|_{L_q(\Omega)} && \lambda\in\Sigma_{\varepsilon,\lambda_3},\\
&\|\nabla\Pi^2_{a,k}(\lambda)f\|_{L_q(\Omega)} + \|\Pi^2_{a,k}(\lambda)f\|_{L_q(\Omega_b)} \le C_{b,q,R}\gamma^{-1}|\lambda|^{-3}\|f\|_{L_q(\Omega)} && \lambda\in\mathbb{C}_{\lambda_3},
\end{aligned} \tag{86}$$

where b is any number $> R+3$.

To prove the above assertions, in view of Theorem 4 choosing N so large that

$$\begin{aligned}
&\|\partial^\beta_x \mathcal{A}^N_{1,a,k}(\lambda)f\|_{L_q(\mathbb{R}^3)} \le C_{q,R}|\lambda|^{-(1-(|\beta|/2))}\|f\|_{L_q(\mathbb{R}^3)} && (\lambda\in\Sigma_{\varepsilon,\lambda_3}, |\beta|\le 2),\\
&\|\mathcal{A}^N_{2,a,k}(\lambda)f\|_{W^2_q(\mathbb{R}^3)} \le C_{q,R}|\lambda|^{-3}\|f\|_{L_q(\mathbb{R}^3)} && (\lambda\in\mathbb{C}_{\lambda_3}),
\end{aligned} \tag{87}$$

we set $\mathcal{A}_{\mathbb{R}^3,a,k}(\lambda) = \mathcal{A}^N_{1,a,k}(\lambda) + \mathcal{A}^N_{2,a,k}(\lambda)$. In view of Proposition 6 we set

$$\begin{aligned}
R^1_{a,k}(\lambda)f = {}&(1-\varphi)\mathcal{A}^N_{1,a,k}(\lambda)[((1+T)^{-1} + U^1_a(\lambda))f]_0\\
&+\varphi\mathcal{A}_{\Omega,a,k}(\lambda)r_{\Omega_{R+3}}[((I+T)^{-1} + U^1_{a,k}(\lambda))f]\\
&+\mathbb{B}[(\nabla\varphi)\cdot\{\mathcal{A}^N_{1,a,k}(\lambda)[((I+T)^{-1} + U^1_{a,k}(\lambda))f]_0\\
&-\mathcal{A}_{\Omega,a,k}(\lambda)r_{\Omega_{R+3}}[((I+T)^{-1} + U^1_{a,k}(\lambda))f]\}],\\
R^2_{a,k}(\lambda)f = {}&R_{a,k}(\lambda)f - R^1_{a,k}(\lambda)f.
\end{aligned} \tag{88}$$

Then, $R^1_{a,k}(\lambda)$ and $R^2_{a,k}(\lambda)$ satisfy the analytic properties in (84) and estimates in (86). Concerning $\Pi_{a,k}(\lambda)$, if we set

$$\begin{aligned}
\Pi^1_{a,k}(\lambda)f = {}&(1-\varphi)Q_{\mathbb{R}^3}[U^1_{a,k}(\lambda)f]_0 + \varphi Q_\Omega r_{\Omega_{R+3}}[U^1_{a,k}(\lambda)f]\\
&+\varphi\mathcal{B}_{\Omega,a,k}(\lambda)r_{\Omega_{R+3}}[((I+T)^{-1} + U^1_{a,k}(\lambda))f],\\
\Pi^2_{a,k}(\lambda)f = {}&(1-\varphi)Q_{\mathbb{R}^3}[U^2_{a,k}(\lambda)f]_0 + \varphi Q_\Omega r_{\Omega_{R+3}}[U^2_{a,k}(\lambda)f]\\
&+\varphi\mathcal{B}_{\Omega,a,k}(\lambda)r_{\Omega_{R+3}}[U^2_{a,k}(\lambda)f],
\end{aligned}$$

then we see that

$$\begin{aligned}\Pi_{a,k}(\lambda)f =&(1-\varphi)Q_{\mathbb{R}^3}[(I+T)^{-1}f]_0 + \varphi Q_\Omega r_{\Omega_{R+3}}[(I+T)^{-1}f]\\ &+ \Pi^1_{a,k}(\lambda)f + \Pi^2_{a,k}(\lambda)f,\end{aligned}$$

and that $\Pi^1_{a,k}(\lambda)$ and $\Pi^2_{a,k}(\lambda)$ satisfy the analytic properties in (84) and the estimates in (86).

Now, we shall define the velocity field $u(t)$ and pressure term $p(t)$ by the Laplace inverse transform of $R_{a,k}(\lambda)f$ and $\Pi_{a,k}(\lambda)f$. For this purpose, we shall use $u_\ell(t)$ and $p_\ell(t)$ which are defined by the relations:

$$u_\ell(t) = \frac{1}{2\pi i}\int_{\gamma-i\ell}^{\gamma+i\ell} \boldsymbol{E}^{\lambda t} R_{a,k}(\lambda)f\,d\lambda, \quad p_\ell(t) = \frac{1}{2\pi i}\int_{\gamma-i\ell}^{\gamma+i\ell} \boldsymbol{E}^{\lambda t}\Pi_{a.k}(\lambda)f\,d\lambda \quad (89)$$

respectively. Given any $\gamma > \lambda_3$, we choose $\theta \in (\pi/2, \pi)$ in such a way that

$$\Gamma = \{\gamma + se^{i\theta} \mid s \geq 0\} \cup \{\gamma + se^{-i\theta} \mid s \geq 0\} \subset \Sigma_{\varepsilon,\lambda_3}. \quad (90)$$

To show the existence of the limits of $u_\ell(t)$ and $p_\ell(t)$ as $\ell \to \infty$ and several properties of their limit functions, we use the following two lemmas which were proved in Hishida and Shibata [13, Lemmas 5.2 and 5.3].

Lemma 4 (1) *Let X and $\|\cdot\|_X$ be a Banach space and its norm, respectively.* (1) *Let $\gamma_0 > 0$ and let $V(\lambda)$ be a function in* $\mathrm{Anal}(\mathbb{C}_{\gamma_0}, X)$ *which satisfies the estimate:*

$$\|V(\lambda)\|_X \leq M_v|\lambda|^{-2}$$

for any $\lambda \in \mathbb{C}_{\gamma_0}$. Set

$$v_\ell(t) = \frac{1}{2\pi i}\int_{\gamma-i\ell}^{\gamma+i\ell} \boldsymbol{E}^{\lambda t} V(\lambda)\,d\lambda, \quad v(t) = \frac{1}{2\pi i}\int_{\gamma-i\infty}^{\gamma+i\infty} \boldsymbol{E}^{\lambda t} V(\lambda)\,d\lambda \quad (\gamma > \gamma_0).$$

Then, $v(t)$ is independent of $\gamma > \gamma_0$, $v(t) \in C^0([0,\infty), X)$ and $v(t)$ possesses the following properties:

$$\begin{aligned}&\lim_{\ell\to\infty}\sup_{0\leq t\leq T}\|v_\ell(t) - v(t)\|_X = 0 && \text{for any } T > 0,\\ &\|v(t)\|_X \leq C_\gamma M_v\,\boldsymbol{E}^{\gamma t} && \text{for any } t > 0 \text{ and } \gamma > \gamma_0,\end{aligned}$$

where $C_\gamma > 0$ is a constant independent of v, V and M_V.
(2) *Let Γ and θ be the same as in* (106). *Let $W(\lambda)$ be a function in* $\mathrm{Anal}(\Sigma_{\varepsilon,\lambda_3}, X)$ *which satisfies the estimate:*

$$\|W(\lambda)\|_X \leq M_w|\lambda|^{-\sigma}$$

for any $\lambda \in \Sigma_{\varepsilon,\lambda_3}$ *with some* $\sigma \leq 1$. *Set*

$$w(t) = \frac{1}{2\pi i}\int_\Gamma \boldsymbol{E}^{\lambda t}W(\lambda)\,\mathrm{d}\lambda.$$

Then, $w(t)$ *is independent of* $\gamma > \lambda_3$, $w(t) \in C^0([0,\infty), X)$ *and* $w(t)$ *satisfies the estimate:*

$$\|w(t)\|_X \leq C_{\gamma,\theta}M_w\,\boldsymbol{E}^{\gamma t}t^{-(1-\sigma)} \quad \text{for any } t > 0,$$

where $C_{\gamma,\theta} > 0$ *is a constant independent of* w, W *and* M_W.

Moreover, when $0 < \sigma \leq 1$, *if we set*

$$w_\ell(t) = \frac{1}{2\pi i}\int_{\gamma-i\ell}^{\gamma+i\ell} \boldsymbol{E}^{\lambda t}W(\lambda)\,d\lambda,$$

then

$$\lim_{\ell\to\infty}\sup_{T_1\leq t\leq T_2}\|w_\ell(t) - w(t)\|_X = 0 \quad \text{for any } 0 < T_1 < T_2.$$

Lemma 5 *Let* $\gamma > 0$. *Then, we have*

$$\frac{1}{2\pi i}\int_{\gamma-i\infty}^{\gamma+i\infty} \boldsymbol{E}^{\lambda t}\,\mathrm{d}\lambda = \delta(t) \quad \text{in } \mathcal{D}'(\mathbb{R}), \tag{91}$$

where $\delta(t)$ *denotes the Dirac delta function. Here and hereafter,* $\mathcal{D}'(D)$ *denotes the space of distributions on a domain* D *equipped with simple topology.*

Remark 4 By Lemma 5 we see easily that

$$\frac{1}{2\pi i}\int_{\gamma-i\infty}^{\gamma+i\infty} \boldsymbol{E}^{\lambda t}\,\mathrm{d}\lambda = 0 \quad \text{for } t > 0 \text{ in the sense of } \mathcal{D}'(\mathbb{R}_+). \tag{92}$$

In view of Lemma 4, Remark 4, (84), (85), and (86), we set

$$\begin{aligned}
u_1(t) &= \frac{1}{2\pi i}\int_\Gamma \boldsymbol{E}^{\lambda t}R^1_{a,k}(\lambda)f\,\mathrm{d}\lambda, & u_2(t) &= \frac{1}{2\pi i}\int_{\gamma-i\infty}^{\gamma+i\infty} \boldsymbol{E}^{\lambda t}R^2_{a,k}(\lambda)f\,d\lambda,\\
p_1(t) &= \frac{1}{2\pi i}\int_\Gamma \boldsymbol{E}^{\lambda t}\Pi^1_{a,k}(\lambda)f\,\mathrm{d}\lambda, & p_2(t) &= \frac{1}{2\pi i}\int_{\gamma-i\infty}^{\gamma+i\infty} \boldsymbol{E}^{\lambda t}\Pi^2_{a,k}(\lambda)f\,d\lambda,\\
u_{j\ell}(t) &= \frac{1}{2\pi i}\int_{\gamma-i\ell}^{\gamma+i\ell} \boldsymbol{E}^{\lambda t}R^j_{a,k}(\lambda)f\,\mathrm{d}\lambda, & p_{j\ell}(t) &= \frac{1}{2\pi i}\int_{\gamma-i\ell}^{\gamma+i\ell} \boldsymbol{E}^{\lambda t}\Pi^j_{a,k}(\lambda),\,d\lambda,\\
u(t) &= u_1(t) + u_2(t), & p(t) &= p_1(t) + p_2(t).
\end{aligned}$$

In view of (84) and (86), we see that $R^1_{a,k}(\lambda)$ and $\Pi^1_{a,k}(\lambda)$ have good properties of sectorial operators, so that $u_1(t)$ and $p_1(t)$ can be treated in the same way as in the theory of analytic semigroup (cf., Pazy [17]). On the other hand, $R^2_{a,k}(\lambda)$ and $\Pi^2_{a,k}(\lambda)$ are summable for large λ, so that we can apply Lemma 4 to treat $u_2(t)$ and $p_2(t)$. By Lemma 4, (84) and (86),

$$\begin{aligned}
&\lim_{\ell\to\infty} \sup_{T_1\leq t\leq T_2} \|u_{j\ell}(t) - u_j(t)\|_{W^1_q(\Omega)} = 0 \ \ (j = 1, 2) && \text{for any } 0 < T_1 < T_2,\\
&\lim_{\ell\to\infty} \sup_{0\leqq t\leq T} \|\partial_t u_{2\ell}(t) - \partial_t u_2(t)\|_{L_q(\Omega)} = 0 && \text{for any } T > 0,\\
&\lim_{\ell\to\infty} \sup_{T_1\leq t\leq T_2} \|\nabla\{p_{2\ell}(t) - p_2(t)\}\|_{L_q(\Omega)} = 0 && \text{for any } 0 < T_1 < T_2,\\
&\lim_{\ell\to\infty} \sup_{T_1\leq t\leq T_2} \|p_{j\ell}(t) - p_j(t)\|_{L_q(\Omega_b)} = 0 \ \ (j = 1, 2) && \text{for any } 0 < T_1 < T_2,
\end{aligned} \tag{93}$$

$$u(t) \in C^1(\mathbb{R}_+, L_q(\Omega)^3) \cap C^0(\mathbb{R}_+, W^2_q(\Omega)^3), \quad p(t) \in C^0(\mathbb{R}_+, \hat{W}^1_q(\Omega)), \tag{94}$$

$$\begin{aligned}
&\|(u_1(t), t^{1/2}\nabla u_1(t), t\nabla^2 u_1(t), t\partial_t u_1(t), t\nabla p_1(t))\|_{L_q(\Omega)} \leq C_{q,\gamma}\, \boldsymbol{E}^{\gamma t}\|f\|_{L_q(\Omega)},\\
&t^{(1/2)(1+(1/q))}\|p_1(t)\|_{L_q(\Omega_b)} \leq C_{q,b,\gamma}\, \boldsymbol{E}^{\gamma t}\|f\|_{L_q(\Omega)},\\
&\|(u_2(t), \partial_t u_2(t), \nabla p_2(t))\|_{W^2_q(\Omega)} \leq C_{q,\gamma}\, \boldsymbol{E}^{\gamma t}\|f\|_{L_q(\Omega)},\\
&\|p_2(t)\|_{L_q(\Omega_b)} \leq C_{q,b,\gamma}\, \boldsymbol{E}^{\gamma t}\|f\|_{L_q(\Omega)}.
\end{aligned} \tag{95}$$

Here and hereafter, b denotes any real number $> R + 3$ and γ is a constant $> \lambda_3$. If we set

$$p_{0\ell}(t) = \frac{1}{2\pi i}\int_{\gamma-i\ell}^{\gamma+i\ell} \boldsymbol{E}^{\lambda t}\, d\lambda\, \mathcal{Q}f$$

then by Remark 4 we have

$$p_{0,\ell}(t) \to 0 \quad \text{in } \mathcal{D}'(\Omega \times \mathbb{R}_+). \tag{96}$$

Since $u_\ell(t) = u_{1\ell}(t) + u_{2\ell}(t)$ and $p_\ell(t) = p_{0\ell}(t) + p_{1\ell}(t) + p_{2\ell}(t)$ as follows from (85), by (93) and (96) we have

$$u_\ell(t) \to u(t) \quad \text{and} \quad p_\ell(t) \to p(t) \quad \text{as } \ell \to \infty \text{ in the sense of } \mathcal{D}'(\Omega \times \mathbb{R}_+). \tag{97}$$

Since

$$\partial_t u_\ell(t) + L_{a,k}u_\ell(t) + \nabla p_\ell(t) = \frac{1}{2\pi i}\int_{\gamma-i\ell}^{\gamma+i\ell} \boldsymbol{E}^{\lambda t}\, d\lambda f \quad \text{in } \Omega \times \mathbb{R}_+$$

as follows from (79), by (97) and Lemma 5 we have

$$u_t + L_{a,k}u + \nabla p = 0 \quad \text{in the sense of } \mathcal{D}'(\Omega \times \mathbb{R}_+).$$

Since $\operatorname{div} u_\ell(t) = 0$ in Ω and $u_\ell(t) = 0$ on $\partial\Omega$ as also follows from (79) and since $u_\ell(t) \to u(t)$ as $\ell \to \infty$ for each $t > 0$ in $W^1_q(\Omega)^3$, we see that $\operatorname{div} u(t) = 0$ in $\Omega \times \mathbb{R}_+$ and $u(t) = 0$ on $\partial\Omega \times \mathbb{R}_+$. Noting that

$$\begin{aligned}
\|(u_2(t), t^{1/2}\nabla u_2(t), t\nabla^2 u_2(t), tu_t(t), t\nabla p_2(t))\|_{L_q(\Omega)} & \\
\le C_{q,\gamma}(1+t)\boldsymbol{E}^{\gamma t}\|f\|_{L_q(\Omega)} &\le C_{q,\gamma}\boldsymbol{E}^{2\gamma t}\|f\|_{L_q(\Omega)} \\
t^{(1/2)(1+(1/q))}\|p_2(t)\|_{L_q(\Omega)} &\le C_{q,b,\gamma} t^{(1/2)(1+(1/q))}\boldsymbol{E}^{\gamma t}\|f\|_{L_q(\Omega)} \\
&\le C_{q,b,\gamma}\boldsymbol{E}^{2\gamma t}\|f\|_{L_q(\Omega)},
\end{aligned}$$

we see that $u(t)$ and $p(t)$ are solutions to (80) and satisfy the conditions (81) and (82).

Our final task is to show that

$$\lim_{t\to 0+} \|u(t) - P_\Omega f\|_{L_q(\Omega)} = 0. \tag{98}$$

For this purpose, in view of Theorem 4, Theorem 6, Proposition 6 and (88), we write

$$R_{a,k}(\lambda)f = R^0_{a,k}(\lambda)f + T^1_{a,k}(\lambda)f + R^2_{a,k}(\lambda)f,$$

where $R^2_{a,k}(\lambda)$ is the same operator as in (88), $R^0_{a,k}(\lambda)$ is the operator defined by the formula:

$$\begin{aligned}
R^0_{a,k}(\lambda)f =&(1-\varphi)(\lambda + \mathbb{O}_{\mathbb{R}^3,k})^{-1}P_{\mathbb{R}^3}[(I+T)^{-1}f]_0 \\
&+ \varphi\mathcal{A}_{\Omega,a,k}(\lambda)r_\Omega(I+T)^{-1}f \\
&+ \mathbb{B}[(\nabla\varphi)\cdot((\lambda + \mathbb{O}_{\mathbb{R}^3,k})^{-1}P_{\mathbb{R}^3}[(I+T)^{-1}f]_0 \\
&- \mathcal{A}_{\Omega,a,k}(\lambda)r_\Omega(I+T)^{-1}f)]
\end{aligned}$$

and $T^1_{a,k}(\lambda)$ is the linear operator possessing the following properties:

$$\begin{aligned}
&T^1_{a,k}(\lambda) \in \mathrm{Anal}(\Sigma_{\varepsilon,\lambda_3}, \mathcal{L}(L_{q,R+2}(\Omega), W^2_q(\Omega)^3)), \\
&\|T^1_{a,k}(\lambda)f\|_{L_q(\Omega)} \le C|\lambda|^{-(1+(1/2)(1-(1/q)))}\|f\|_{L_q(\Omega)} \quad (\lambda \in \Sigma_{\varepsilon,\lambda_3}).
\end{aligned} \tag{99}$$

Since

$$\begin{aligned}
&\frac{1}{2\pi i}\int_\Gamma \boldsymbol{E}^{\lambda t}(\lambda + \mathbb{O}_{\mathbb{R}^3,k})^{-1}P_{\mathbb{R}^3}[(I+T)^{-1}f]_0\,d\lambda \\
&\qquad = (4\pi t)^{-\frac{3}{2}}\int_{\mathbb{R}^3} \boldsymbol{E}^{-\frac{|x-y-t\mathbf{e}_3|^2}{4t}}\,P_{\mathbb{R}^3}[(I+T)^{-1}f]_0(y)\,dy,
\end{aligned}$$

we see easily that

$$\lim_{t\to 0+}\frac{1}{2\pi i}\int_\Gamma \boldsymbol{E}^{\lambda t}(\lambda+\mathbb{O}_{\mathbb{R}^3,k})^{-1}P_{\mathbb{R}^3}[(I+T)^{-1}f]_0\,d\lambda = P_{\mathbb{R}^3}[(I+T)^{-1}f]_0$$

strongly in $L_q(\mathbb{R}^3)^3$. On the other hand, by Theorem 6 together with Remark 2, we have the continuous analytic semigroup

$$T_{\Omega,a}(t)=\frac{1}{2\pi i}\int_\Gamma \boldsymbol{E}^{\lambda t}(\lambda I+\mathcal{L}_{\Omega_{R+3},a})^{-1}\,d\lambda \qquad \text{on } J_q(\Omega),$$

which satisfies

$$\lim_{t\to 0+}\|T_{\Omega,a}(t)g-g\|_{L_q(\Omega)}=0 \quad \text{for any } g\in J_q(\Omega).$$

Therefore, if we set

$$\begin{aligned} u^0(t)=&\frac{1}{2\pi i}\int_\Gamma \boldsymbol{E}^{\lambda t}R^0_{a,k}(\lambda)f\,d\lambda,\\ Wf=&(1-\varphi)P_{\mathbb{R}^3}[(I+T)^{-1}f]_0+\varphi P_\Omega r_{\Omega_{R+3}}[(I+T)^{-1}f]\\ &+\mathbb{B}[(\nabla\varphi)\cdot\{P_{\mathbb{R}^3}[(I+T)^{-1}f]_0-P_\Omega r_{\Omega_{R+3}}[(I+T)^{-1}f]\}], \end{aligned} \tag{100}$$

then from $\mathcal{A}_{\Omega_{R+3},a,k}(\lambda)=(\lambda I+\mathcal{L}_{\Omega_{R+3},a,k})^{-1}P_{\Omega_{R+3}}$ (cf. Remark 2) it follows that

$$\lim_{t\to 0+}\|u^0(t)-Wf\|_{L_q(\Omega)}=0. \tag{101}$$

Set

$$v^1(t)=\frac{1}{2\pi i}\int_\Gamma \boldsymbol{E}^{\lambda t}T^1_{a,k}(\lambda)f\,\mathrm{d}\lambda, \quad v^2(t)=\frac{1}{2\pi i}\int_{\gamma-i\infty}^{\gamma+i\infty}\boldsymbol{E}^{\lambda t}R^2_{a,k}(\lambda)f\,d\lambda$$

and then $u(t)=u^0(t)+v^1(t)+v^2(t)$. To prove

$$\lim_{t\to 0+}\|v^j(t)\|_{L_q(\Omega)}=0 \quad (j=1,2), \tag{102}$$

we use the following lemma which was proved in Hishida and Shibata [13, Lemma 2.3].

Lemma 6 *Let X be a Banach space with norm $\|\cdot\|_X$ and $\gamma>0$. Let $\Psi(\lambda)\in$* $\mathrm{Anal}\,(\mathbb{C}_\gamma,X)$ *such that*

$$\|\Psi(\lambda)\|_X\le C_\gamma|\lambda|^{-1-\sigma} \quad \mathrm{Re}\,\lambda\ge\gamma>0 \tag{103}$$

for some $\sigma>0$. Then, we have

$$\lim_{t\to 0+}\left\|\int_{\gamma-i\infty}^{\gamma+i\infty}\boldsymbol{E}^{\lambda t}\,\Psi(\lambda)\,d\lambda\right\|_X=0. \tag{104}$$

By (99) we can rewrite

$$v^1(t) = \frac{1}{2\pi i}\int_{\gamma-i\infty}^{\gamma+i\infty} \boldsymbol{E}^{\lambda t} T_a^1(\lambda) f \, d\lambda$$

and therefore by (86), (99) and Lemma 6 we have (102). Combining (102) with (101) implies that

$$\lim_{t\to 0+} \|u(t) - Wf\|_{L_q(\Omega)} = 0 \tag{105}$$

By Lemma 5.5 in Hishida and Shibata [13], we know $Wf = P_\Omega f$, which combined with (105) implies

$$\lim_{t\to 0+} \|u(t) - P_\Omega f\|_{L_q(\Omega)} = 0.$$

Summing up, we have proved the existence of required solutions $u(t)$ and $p(t)$ of problem (80), which satisfy (81) and (82). Moreover, from (93) we see that $u(t)$ is given by the formula (83).

Finally, we shall show the uniqueness. Let $u(t)$ and $p(t)$ satisfy (81), (82) and a homogeneous equation:

$$\begin{aligned} u_t + L_{a,k}u + \nabla p = 0,\ \operatorname{div} u = 0 \ \text{ in } \Omega \times (0,\infty), \\ u|_{\partial\Omega} = 0,\ u|_{t=0} = 0 \ \text{ in } \Omega. \end{aligned} \tag{106}$$

Given any $T > 0$, we consider the dual problem:

$$\begin{aligned} -v_t + L_{-a,-k}u + \nabla\theta = 0,\ \operatorname{div} v = 0 \ \text{ in } \Omega \times (-\infty, T), \\ v|_{\partial\Omega} = 0,\ v|_{t=T} = \varphi \ \text{ in } \Omega. \end{aligned} \tag{107}$$

for any $\varphi \in C^\infty_{0,\sigma}(\Omega)$. Then, employing the same argument as in the existence proof of solutions in Theorem 7 which were given above, we can show the existence of v and θ which satisfy the regularity conditions:

$$\begin{aligned} &v(t) \in C^1((-\infty,T), L_{q'}(\Omega)^3) \cap C^0((-\infty,T), W^2_{q'}(\Omega)^3) \cap C^0((-\infty,T], L_{q'}(\Omega)^3), \\ &\theta(t) \in C^0((-\infty,T), \hat{W}^1_{q'}(\Omega)), \end{aligned}$$

where $q' = q/(q-1)$. From Remark 3 we see that $M_a u(t)$ and $M_{-a}v(t)$ belongs to $L_q(\Omega)^3$ and $L_{q'}(\Omega)^3$ for any $0 < t < T$, respectively, so that by integration by parts we have

$$\begin{aligned} (u_t + L_{a,k}u + \nabla p, v)_{\Omega\times(0,T)} &= (u(T),\varphi)_\Omega + (u, -v_t + L_{-a,-k}v + \nabla\theta)_{\Omega\times(0,T)} \\ &= (u(T),\varphi)_\Omega, \end{aligned}$$

where we have set

$$(u, v)_\Omega = \int_\Omega u(x) \cdot v(x)\, dx \quad \text{and} \quad (u, v)_{\Omega \times (0,T)} = \int_0^T (u(t), v(t))_\Omega \, dt.$$

Therefore, we have $(u(T), \varphi)_\Omega = 0$ for any $\varphi \in C^\infty_{0,\sigma}(\Omega)$. Since $u(T) \in J_q(\Omega)$, we have $u(T) = 0$. But, T is also arbitrary positive number, so that $u = 0$, which implies the uniqueness of solutions. This completes the proof of Theorem 7.

6 Proofs of Main Results

In this section, we consider the solvability of problem (8). We start with the following theorem.

Theorem 8 *Let* $1 < q < \infty$ *and* $a_0, k_0 > 0$. *Assume that* $|a| \le a_0$ *and* $|k| \le k_0$. *If* $f \in L_{q,R+2}(\Omega) \cap \mathcal{D}_q(\Omega)$, *then problem* (8) *admits a unique solution* $(u(t), p(t))$ *satisfying not only* (82) *but also conditions:*

$$\begin{aligned} &u(t) \in C^0([0,\infty), W^2_q(\Omega)) \cap C^1([0,\infty), L_q(\Omega)), \\ &\|u_t(t)\|_{L_q(\Omega)} + \|u(t)\|_{\mathcal{D}_q(\Omega)} + \|\nabla p(t)\|_{L_q(\Omega)} \le C_{a_0,k_0,\gamma}\, \boldsymbol{E}^{\gamma t} \|f\|_{W^2_q(\Omega)}, \end{aligned} \tag{108}$$

for any $t \ge 0$ *and* $\gamma > 2\lambda_3$, *where* λ_3 *is the same constant as in Proposition 6.*

Proof By Theorem 7 we know the existence of $(u(t), p(t))$ which solves (8) and satisfies the conditions (81) and (82). Since $f \in L_{q,R+2}(\Omega) \cap \mathcal{D}_q(\Omega)$, we have $L_{a,k} f \in L_{q,R+2}(\Omega)$ and

$$\|P_\Omega L_{a,k} f\|_{L_q(\Omega)} \le C_{a_0,k_0} \|f\|_{W^2_q(\Omega)}. \tag{109}$$

Therefore, by Theorem 7 there exists a $(v(t), \theta(t))$ which solves the equation:

$$\begin{aligned} v_t + L_{a,k} v + \nabla\theta = 0,\ \operatorname{div} v = 0 \quad \text{in } \Omega \times (0,\infty), \\ v|_{\partial\Omega} = 0,\ v|_{t=0} = -P_\Omega L_{a,k} f, \end{aligned} \tag{110}$$

and conditions:

$$\begin{aligned} &v(t) \in C^1(\mathbb{R}_+, L_q(\Omega)^3) \cap C^0(\mathbb{R}_+, W^2_q(\Omega)^3) \cap C^0([0,\infty), L_q(\Omega)^3), \\ &\theta(t) \in C^0(\mathbb{R}_+, \hat{W}^1_q(\Omega)), \\ &\|v(t)\|_{L_q(\Omega)} \le C_{a_0,k_0,\gamma}\, \boldsymbol{E}^{\gamma t} \|P_\Omega L_{a,k} f\|_{L_q(\Omega)} \le C_{a_0,k_0,\gamma}\, \boldsymbol{E}^{\gamma t} \|f\|_{W^2_q(\Omega)} \end{aligned} \tag{111}$$

for any $t > 0$ and $\gamma > 2\lambda_3$. Our task is to show that $u_t = v$. For this purpose we consider

$$w(x,t) = f(x) + \int_0^t v(x,s)\,\mathrm{d}s \tag{112}$$

Given $\varphi \in \mathcal{D}_{q'}(\Omega)$ ($q' = q/(q-1)$), by (112) we have

$$(w_t(t), \varphi)_\Omega = (v(t), \varphi)_\Omega. \tag{113}$$

On the other hand, from Remark 3 we see that $M_a v(t) \in L_q(\Omega)^3$ for any $t > 0$, and therefore by integration by parts we have

$$(v_t(t), \varphi)_\Omega = -(L_{a,k} v(t) + \nabla\theta(t), \varphi)_\Omega = -(v(t), L_{-a,-k}\varphi)_\Omega. \tag{114}$$

Integrating (114) with respect to t and using (110) implies that

$$(v(t), \varphi)_\Omega = (-P_\Omega L_{a,k} f, \varphi)_\Omega - \int_0^t (v(s), L_{-a,-k}\varphi)_\Omega\, ds. \tag{115}$$

Since $f \in \mathcal{D}_q(\Omega)$ and $\varphi \in \mathcal{D}_{q'}(\Omega)$, we have

$$(P_\Omega L_{a,k} f, \varphi)_\Omega = (L_{a,k} f, P_\Omega \varphi)_\Omega = (L_{a,k} f, \varphi)_\Omega = (f, L_{-a,-k}\varphi)_\Omega,$$

and therefore by (112) and (115) we have

$$(w_t(t), \varphi)_\Omega + (w(t), L_{-a,-k}\varphi)_\Omega = 0. \tag{116}$$

From Remark 3 we see that $M_a u(t) \in L_q(\Omega)^3$ for $t > 0$, we have

$$(u_t(t), \varphi)_\Omega = (-L_{a,k} u(t) - \nabla p(t), \varphi)_\Omega = -(u(t), L_{-a,-k}\varphi)_\Omega,$$

which combined with (116) implies that

$$(w_t(t) - u_t(t), \varphi)_\Omega + (w(t) - u(t), L_{-a,-k}\varphi)_\Omega = 0 \tag{117}$$

for any $\varphi \in \mathcal{D}_{q'}(\Omega)$ and $t > 0$. Now, given any $\psi \in C^\infty_{0,\sigma}(\Omega)$ and $T > 0$, by Theorem 7 let (z, τ) be a solutions to the dual problem:

$$\begin{gathered} -z_t + L_{-a,-k} z + \nabla\tau = 0, \ \operatorname{div} z = 0 \quad \text{in } \Omega \times (-\infty, T), \\ z|_{\partial\Omega} = 0, \ z|_{t=T} = \psi, \end{gathered} \tag{118}$$

which satisfies the regularity condition:

$$\begin{gathered} z(t) \in C^1((-\infty,T), L_{q'}(\Omega)^3) \cap C^0((-\infty,T), W^2_{q'}(\Omega)^3) \cap C^0((-\infty,T], L_{q'}(\Omega)^3), \\ \tau(t) \in C^0((-\infty,T), \hat{W}^1_{q'}(\Omega)). \end{gathered} \tag{119}$$

From (119) and (118), $z(t) \in \mathcal{D}_{q'}(\Omega)$ for any $t \in (-\infty, T)$, so that by (117) and (118) we have

$$
\begin{aligned}
0 &= \int_0^T \{(w_t(t) - u_t(t), z(t))_\Omega + (w(t) - u(t), L_{-a,-k}z(t))_\Omega\}\,dt \\
&= (w(T) - u(T), \psi)_\Omega + \int_0^T (w(t) - u(t), -z_t(t) + L_{-a,-k}z(t) + \nabla\tau(t))_\Omega\,dt \\
&= (w(T) - u(T), \psi)_\Omega.
\end{aligned}
$$

Since $\psi \in C^\infty_{0,\sigma}(\Omega)$ is chosen arbitrarily and since $w(T) - u(T) \in J_q(\Omega)$, we have $w(T) = u(T)$, which combined with the arbitrariness of choice of $T > 0$ implies that $w(t) = u(t)$ for any $t > 0$. Therefore, we have $u_t(t) = v(t)$, which combined with (111) implies that $u_t(t) \in C^0([0, \infty), L_q(\Omega)^3)$ and

$$
\|u_t(t)\|_{L_q(\Omega)} \leq C_{a_0,k_0,\gamma}\,\boldsymbol{E}^{\gamma t}\|f\|_{W^2_q(\Omega)} \tag{120}
$$

for any $t \geq 0$ and $\gamma > 2\lambda_3$. Applying Theorem Ap.1 in the appendix below to the equation:

$$
u(t) + L_{a,k}u(t) + \nabla p(t) = -u_t(t) + u(t), \quad \operatorname{div} u(t) = 0 \ \text{ in } \Omega, \quad u(t)|_{\partial\Omega} = 0,
$$

we have $u(t) \in C^0([0, \infty), \mathcal{D}_q(\Omega))$, $p(t) \in C^0([0, \infty), \hat{W}^1_q(\Omega))$ and

$$
\|u(t)\|_{\mathcal{D}_q(\Omega)} + \|\nabla p(t)\|_{L_q(\Omega)} \leq C_{a_0,k_0}(\|u_t(t)\|_{L_q(\Omega)} + \|u(t)\|_{L_q(\Omega)}),
$$

which combined with (120) and (82) completes the proof of Theorem 8. □

Now, we shall give a

Proof of Theorem 1 Let φ be a function such that $\varphi(x) = 1$ for $|x| \leq R + 1$ and $\varphi(x) = 0$ for $|x| \geq R + 2$. Given $f \in \mathcal{D}_q(\Omega)$ we set $g = (1 - \varphi)f + \mathbb{B}[(\nabla\varphi) \cdot f]$, where $\mathbb{B}$ is the Bogovski ǐ-Pileckas operator. Then, $g \in \mathcal{D}_q(\mathbb{R}^3)$ and

$$
\|g\|_{L_q(\mathbb{R}^3)} \leq C\|f\|_{L_q(\Omega)}, \quad \|g\|_{W^2_q(\mathbb{R}^3)} \leq C\|f\|_{W^2_q(\Omega)}, \quad \|g\|_{\mathcal{D}_q(\Omega)} \leq C_{a_0,k_0}\|f\|_{\mathcal{D}_q(\Omega)}. \tag{121}
$$

Recalling the symbol $S_{a,k}(t)$ defined by (16), we set $v_0(t) = S_{a,k}(t)g$. By Theorem 3 and (121) we have

$$
\begin{aligned}
&\|(v_0(t), t^{\frac{1}{2}}\nabla v_0(t), t\nabla^2 v_0(t))\|_{L_q(\mathbb{R}^3)} \leq C\|g\|_{L_q(\mathbb{R}^3)} \leq C\|f\|_{L_q(\Omega)}, \\
&\|(\nabla^2 v_0(t), t^{\frac{1}{2}}\nabla^3 v_0(t))\|_{L_q(\mathbb{R}^3)} \leq C\|\nabla^2 g\|_{W^2_q(\mathbb{R}^3)} \leq C\|f\|_{W^2_q(\Omega)}, \\
&\|D_t v_0(t)\|_{L_q(\mathbb{R}^3)} + \|v_0(t)\|_{W^2_q(\mathbb{R}^3)} \leq C_{a_0,k_0}\|g\|_{\mathcal{D}_q(\mathbb{R}^3)} \leq C_{a_0,k_0}\|f\|_{\mathcal{D}_q(\Omega)}.
\end{aligned} \tag{122}
$$

We set

$$
v(t) = (1 - \varphi)v_0(t) + \mathbb{B}[(\nabla\varphi) \cdot v_0(t)],
$$

and then we have

$$\begin{aligned} v_t + L_{a,k} v = F, \ \ \mathrm{div}\, v = 0 \quad \text{in } \Omega \times (0, \infty), \\ v|_{\partial\Omega} = 0, \ \ v|_{t=0} = h, \end{aligned} \tag{123}$$

where we have set

$$\begin{aligned} F =& 2(\nabla\varphi) \cdot (\nabla v_0(t)) + (\Delta\varphi) v_0(t) - k(D_3\varphi) v_0(t) \\ & - a((\mathbf{e}_3 \times x) \cdot (\nabla\varphi)) v_0(t) g + D_t \mathbb{B}[(\nabla\varphi) \cdot (v_0(t))] + L_{a,k} \mathbb{B}[(\nabla\varphi) \cdot (v_0(t))], \\ h =& (1 - \varphi) g + \mathbb{B}[(\nabla\varphi) \cdot g]. \end{aligned}$$

Observing that

$$D_t \mathbb{B}[(\nabla\varphi) \cdot v_0(t)] = \mathbb{B}[(\nabla\varphi) \cdot D_t v_0(t)] = -\mathbb{B}[(\nabla\varphi) \cdot (L_{a,k} v_0(t)],$$

by Lemma 2, (121) and (122) we have

$$\begin{aligned} & \|(v(t), (1 + t^{-\frac{1}{2}})^{-1} \nabla v(t), (1 + t^{-1})^{-1} \nabla^2 v(t))\|_{L_q(\Omega)} \le C_{a_0,k_0} \|f\|_{L_q(\Omega)}, \\ & \|v_t(t)\|_{L_q(\Omega)} + \|v(t)\|_{\mathcal{D}_q(\Omega)} \le C_{a_0,k_0} \|f\|_{W^2_q(\Omega)}, \end{aligned} \tag{124}$$

and

$$\begin{aligned} & \|F(t)\|_{L_q(\Omega)} \le C_{a_0,k_0} (1 + t^{-\frac{1}{2}}) \|f\|_{L_q(\Omega)}, && \|F(t)\|_{L_q(\Omega)} \le C_{a_0,k_0} \|f\|_{\mathcal{D}_q(\Omega)}, \\ & \|F(t)\|_{\mathcal{D}_q(\Omega)} \le C_{a_0,k_0} (1 + t^{-\frac{1}{2}}) \|f\|_{W^2_q(\Omega)}, && \mathrm{supp}\, F(t) \subset B_{R+2} \setminus B_{R+1}, \\ & \|h\|_{L_q(\Omega)} \le C \|f\|_{L_q(\Omega)}, && \|h\|_{\mathcal{D}^2_q(\Omega)} \le C_{a_0,k_0} \|f\|_{\mathcal{D}_q(\Omega)}. \end{aligned} \tag{125}$$

Now, we shall consider problem:

$$\begin{aligned} w_t + L_{a,k} w = -F, \ \ \mathrm{div}\, w = 0 \quad \text{in } \Omega \times (0, \infty), \\ w|_{\partial\Omega} = 0, \ \ w|_{t=0} = f - h. \end{aligned} \tag{126}$$

Since $f - h = \varphi f = 0$ for $|x| \ge R+2$, $\mathrm{div}\,(f - h) = 0$ in Ω and $\nu \cdot (f - h)|_{\partial\Omega} = \nu \cdot f|_{\partial\Omega} = 0$ as follows from $f \in \mathcal{D}_q(\Omega)$ where ν stands for the unit outer normal to $\partial\Omega$, we have $f - h \in \mathcal{D}_q(\Omega) \cap L_{q,R+2}(\Omega)$ and

$$\|f - h\|_{L_q(\Omega)} \le C \|f\|_{L_q(\Omega)}, \ \ \|f - h\|_{\mathcal{D}_q(\Omega)} \le C \|f\|_{W^2_q(\Omega)}. \tag{127}$$

In view of Theorem 8, for any $g \in L_{q,R+2}(\Omega) \cap \mathcal{D}_q(\Omega)$, problem (8) admits a unique solution $z(t)$ and $\kappa(t)$ and therefore we define the operator $S_\Omega(t)$ and $\Pi_\Omega(t)$ by the formulas: $S_\Omega(t) g = z(t)$ and $\Pi_\Omega(t) g = \kappa(t)$ for the notational simplicity. By Theorem 8, we have

$$
\begin{aligned}
&\|(S_\Omega(t)g, t^{\frac{1}{2}}\nabla S_\Omega(t)g, t\nabla^2 S_\Omega(t)g, \nabla \Pi_\Omega(t)g)\|_{L_q(\Omega)} \le C_{a_0,k_0,\gamma}\,\boldsymbol{E}^{\gamma t}\|g\|_{L_q(\Omega)} \\
&\|\Pi_\Omega(t)g\|_{L_q(\Omega_b)} \le C_{a_0,k_0,b,\gamma}\,\boldsymbol{E}^{\gamma t}\|g\|_{L_q(\Omega)}, \\
&\|D_t S_\Omega(t)g\|_{L_q(\Omega)} + \|S_\Omega(t)g\|_{\mathcal{D}_q(\Omega)} + \|\nabla \Pi_\Omega(t)g\|_{L_q(\Omega)} \le C_{a_0,k_0,\gamma}\,\boldsymbol{E}^{\gamma t}\|g\|_{W^2_q(\Omega)}
\end{aligned} \tag{128}
$$

for any $t > 0$ and $\gamma > 2\lambda_3$, where λ_3 is the same constant as in Proposition 6.

In view of Duhamel's principle, we set

$$
\begin{aligned}
w(t) &= S_\Omega(t)(f-h) - \int_0^t S_\Omega(t-s)F(s)\,ds, \\
p(t) &= \Pi_\Omega(t)(f-h) - \int_0^t \Pi_\Omega(t-s)F(s)\,ds.
\end{aligned}
$$

By (127) and (125) we have

$$
\begin{aligned}
&\|(w(t), t^{\frac{1}{2}}\nabla w(t), t\nabla^2 w(t), \nabla p(t))\|_{L_q(\Omega)} \\
&\le C_{a_0,k_0,\gamma}\Big[\boldsymbol{E}^{\gamma t} + \int_0^t e^{\gamma(t-s)}(1+s^{-\frac{1}{2}})\,ds\Big]\|f\|_{L_q(\Omega)} \le C_{a_0,k_0,\gamma}\,\boldsymbol{E}^{2\gamma t}\|f\|_{L_q(\Omega)}, \\
&\|p(t)\|_{L_q(\Omega_b)} \\
&\le C_{a_0,k_0\gamma}\Big[t^{-\frac{1}{2}\left(1+\frac{1}{q}\right)}\boldsymbol{E}^{\gamma t} + \int_0^t e^{\gamma(t-s)}(t-s)^{-\frac{1}{2}\left(1+\frac{1}{q}\right)}(1+s^{-\frac{1}{2}})\,ds\Big]\|f\|_{L_q(\Omega)} \\
&\le C_{a_0,k_0,b,\gamma}\,t^{-\frac{1}{2}\left(1+\frac{1}{q}\right)}\,\boldsymbol{E}^{2\gamma t}\|f\|_{L_q(\Omega)}, \\
&\|D_t w(t)\|_{L_q(\Omega)} + \|w(t)\|_{\mathcal{D}_q(\Omega)} + \|\nabla p(t)\|_{L_q(\Omega)} \\
&\le C_{a_0,k_0,\gamma}\Big[\boldsymbol{E}^{\gamma t} + \int_0^t e^{\gamma(t-s)}(1+s^{-\frac{1}{2}})\,\mathrm{d}s\Big]\|f\|_{\mathcal{D}_q(\Omega)} \le C_{a_0,k_0,\gamma}\,\boldsymbol{E}^{2\gamma t}\|f\|_{\mathcal{D}_q(\Omega)}.
\end{aligned} \tag{129}
$$

In fact, we observe that

$$
\begin{aligned}
\int_0^t \boldsymbol{E}^{\gamma(t-s)}(1+s^{-\frac{1}{2}})\,\mathrm{d}s &\le \boldsymbol{E}^{\gamma t}\int_0^t \boldsymbol{E}^{-\gamma s}(s^{\frac{1}{2}}+1)s^{-\frac{1}{2}}\,ds \\
&\le (1+t^{\frac{1}{2}})\boldsymbol{E}^{\gamma t}\int_0^t s^{-\frac{1}{2}}\,ds \le 2(\gamma^{-\frac{1}{2}}+1)\boldsymbol{E}^{2\gamma t}
\end{aligned}
$$

Analogously, we have

$$
\begin{aligned}
&\int_0^t \boldsymbol{E}^{\gamma(t-s)}(t-s)^{-\frac{1}{2}\left(1+\frac{1}{q}\right)}(1+s^{-\frac{1}{2}})\,ds \\
&= \boldsymbol{E}^{\gamma t}\int_0^t (t-s)^{-\frac{1}{2}\left(1+\frac{1}{q}\right)}s^{-\frac{1}{2}}(s^{\frac{1}{2}}+1)\boldsymbol{E}^{-\gamma s}\,ds
\end{aligned}
$$

$$\leq \boldsymbol{E}^{\gamma t}(t^{\frac{1}{2}}+1)t^{-\frac{1}{2q}}\int_0^1 (1-\ell)^{-\frac{1}{2}\left(1+\frac{1}{q}\right)}\ell^{-\frac{1}{2}}\,\mathrm{d}\ell \leq C_q(1+\gamma^{-\frac{1}{2}})t^{-\frac{1}{2}\left(1+\frac{1}{q}\right)}\boldsymbol{E}^{2\gamma t}.$$

Since $\lim_{s\to t-0}\|S_\Omega(t-s)F(s)-F(t)\|_{L_q(\Omega)}=0$, $(w(t),\ p(t))$ satisfies (126). If we set $u(t)=v(t)+w(t)$, then by (123), (124), (126), and (129) we see that $(u(t),\ p(t))$ satisfies all the properties stated in Theorem 1 with $\gamma_0=4\lambda_3$, which completes the proof of Theorem 1.

Proof of Theorem 2 In view of Theorem 1, for any $f\in\mathcal{D}_q(\Omega)$ problem (8) admits a unique solution $(u(t),\ p(t))$, and therefore $T_\Omega(t)$ is defined by the formula: $T_\Omega(t)f=u(t)$. From Theorem 1, $T_\Omega(t)f\in\mathcal{D}_q(\Omega)$ for any $t\geq 0$ and

$$\lim_{t\to 0+}\|T_\Omega(t)f-f\|_{L_q(\Omega)}=0 \quad\text{and}\quad \|T_\Omega(t)f\|_{L_q(\Omega)}\leq C_{a_0,k_0,\gamma}\boldsymbol{E}^{\gamma t}\|f\|_{L_q(\Omega)} \tag{130}$$

for any $t\geq 0$ and $\gamma\geq\gamma_0=4\lambda_0$. Moreover, by uniqueness of solutions we have $T(t+s)f=T(t)T(s)f$ for any $t,s>0$ and $f\in\mathcal{D}_q(\Omega)$. $\mathcal{D}_q(\Omega)$ is dense in $J_q(\Omega)$, because $C^\infty_{0,\sigma}(\Omega)\subset\mathcal{D}_q(\Omega)\subset J_q(\Omega)$ and $C^\infty_{0,\sigma}(\Omega)$ is dense in $J_q(\Omega)$. Therefore, in view of (130) we can extend $T_\Omega(t)$ to $J_q(\Omega)$ continuously. We write this extension also by $T_\Omega(t)$. Then, $\{T_\Omega(t)\}_{t\geq 0}$ is a continous semigroup on $J_q(\Omega)$. What we have to show is that $-\mathcal{L}_{a,k}$ is an infinitesimal generator of $\{T_\Omega(t)\}_{t\geq 0}$. To this end, let us define domain $\mathcal{D}_q(\mathcal{M}_{a,k})$ and the operator $\mathcal{M}_{a,k}$ by the formulas:

$$\mathcal{D}_q(\mathcal{M}_{a,k})=\{f\in J_q(\Omega)\mid \lim_{t\to 0+}\frac{T_\Omega(t)f-f}{t}\ \text{exists in}\ J_q(\Omega)\},$$
$$\mathcal{M}_{a,k}f=\lim_{t\to 0+}\frac{T_\Omega(t)f-f}{t}\quad\text{for}\ f\in\mathcal{D}_q(\mathcal{M}_{a,k}).$$

When $f\in\mathcal{D}_q(\Omega)$,

$$\begin{aligned}\lim_{t\to 0+}\frac{T_\Omega(t)f-f}{t}&=\lim_{t\to 0+}\frac{1}{t}\int_0^t D_tT_\Omega(s)f\,ds\\&=-\lim_{t\to 0+}\frac{1}{t}\int_0^t\mathcal{L}_{a,k}T_\Omega(s)f\,\mathrm{d}s=-\mathcal{L}_{a,k}f,\end{aligned}$$

which shows that

$$\mathcal{D}_q(\Omega)\subset\mathcal{D}_q(\mathcal{M}_{a,k}),\quad -\mathcal{L}_{a,k}f=\mathcal{M}_{a,k}f\quad (f\in\mathcal{D}_q(\Omega)). \tag{131}$$

It follows from the Hille-Yosida theorem that there exists a positive number γ_1 such that $\varrho(\mathcal{M}_{a,k})\supset\{\lambda\in\mathbb{R}\mid\lambda>\gamma_1\}$, where $\varrho(\mathcal{M}_{a,k})$ denotes the resolvent set of $\mathcal{M}_{a,k}$. Let $\lambda>1$ be a number in $\varrho(\mathcal{M}_{a,k})$. Let $f\in\mathcal{D}_q(\mathcal{M}_{a,k})$. By Theorem Ap.1 in the appendix below there exists a $u\in\mathcal{D}_q(\Omega)$ such that $(\lambda I-\mathcal{M}_{a,k})f=(\lambda I+\mathcal{L}_{a,k})u$. From (131), $-\mathcal{L}_{a,k}u=\mathcal{M}_{a,k}u$, so that $(\lambda I-\mathcal{M}_{a,k})(f-u)=0$. Since $\lambda\in\varrho(\mathcal{M}_{a,k})$, we have $f=u\in\mathcal{D}_q(\Omega)$, which shows that $\mathcal{D}_q(\mathcal{M}_{a,k})\subset\mathcal{D}_q(\Omega)$. This completes the proof of Theorem 2.

Appendix

In this appendix we consider the following problem:

$$\lambda u + L_{a,k}u + \nabla p = f, \quad \mathrm{div}\, u = 0 \ \text{ in } \Omega, \quad u|_{\partial\Omega} = 0 \tag{132}$$

for any $f \in J_q(\Omega)$. We shall show the following theorem.

Theorem 9 *Let* $1 < q < \infty$ *and* a_0*,* $k_0 > 0$*. Assume that* $|a| \le a_0$ *and* $|k| \le k_0$*. Then, problem* (132) *admits a unique solution* $(u, p) \in \mathcal{D}_q(\Omega) \times \hat{W}^1_q(\Omega)$ *for any* $\lambda \ge 1$ *and* $f \in J_q(\Omega)$*, which satisfies the estimate:*

$$\|u\|_{\mathcal{D}_q(\Omega)} + \|\nabla p\|_{L_q(\Omega)} \le C_{a_0,k_0,\lambda}\|f\|_{L_q(\Omega)}. \tag{133}$$

Proof Since $C^\infty_{0,\sigma}(\Omega)$ is dense in $J_q(\Omega)$, we may assume that $f \in C^\infty_{0,\sigma}(\Omega)$. Since $\mathrm{supp}\, f \subset \Omega$, the zero extension of f belongs to $C^\infty_{0,\sigma}(\mathbb{R}^3)$. We denote the zero extension of f by f again. Let $\mathcal{A}_{\mathbb{R}^3,a,k}(\lambda)$ be the operator defined by (25), and then $u_0(x) = \mathcal{A}_{\mathbb{R}^3,a,k}(\lambda)f$ satisfies the equation:

$$(\lambda I + L_{a,k})u_0 = f, \quad \mathrm{div}\, u_0 = 0 \quad \text{in } \mathbb{R}^3. \tag{134}$$

Applying Theorem 3 to (25), we have

$$\begin{aligned}
\|u_0\|_{L_q(\mathbb{R}^3)} &\le C\int_0^\infty \boldsymbol{E}^{-(\mathrm{Re}\,\lambda)t}\, dt\, \|f\|_{L_q(\mathbb{R}^3)} = C(\mathrm{Re}\,\lambda)^{-1}\|f\|_{L_q(\Omega)}, \\
\|\nabla u_0\|_{L_q(\mathbb{R}^3)} &\le C\int_0^\infty \boldsymbol{E}^{-(\mathrm{Re}\,\lambda)t} t^{-\frac{1}{2}}\, dt\, \|f\|_{L_q(\mathbb{R}^3)} = C\sqrt{\pi}(\mathrm{Re}\,\lambda)^{-\frac{1}{2}}\|f\|_{L_q(\Omega)}.
\end{aligned} \tag{135}$$

Concerning the estimate of second derivatives of u_0, we write (134) as follows:

$$-\Delta u_0 + M_a u_0 = f - \lambda u_0 + kD_3 u_0 \quad \text{in } \mathbb{R}^3,$$

and then by an estimate due to Farwig-Hishida-Müller [4] (cf., also Farwig [3]) and (135) we have

$$\|\nabla^2 u_0\|_{L_q(\Omega)} + \|M_a u_0\|_{L_q(\Omega)} \le C\|f - \lambda u - kD_3 u\|_{L_q(\mathbb{R}^3)} \le C_{a_0,k_0,\lambda}\|f\|_{L_q(\Omega)}. \tag{136}$$

Let φ be a function in $C^\infty_0(\mathbb{R}^3)$ such that $\varphi(x) = 1$ for $|x| \le R + 1$ and $\varphi(x) = 0$ for $|x| \ge R + 2$ and set $u_1 = (1 - \varphi)u_0 + \mathbb{B}[(\nabla\varphi) \cdot u_0]$, where $\mathbb{B}$ is the Bogovskiĭ-Pileckas operator. Then, by (134) and Lemma 2 we have

$$\lambda u_1 + L_{a,k}u_1 = (1 - \varphi)f + F, \quad \mathrm{div}\, u_1 = 0 \ \text{ in } \Omega, \quad u_1|_{\partial\Omega} = 0, \tag{137}$$

where

$$F = 2(\nabla\varphi)\cdot(\nabla u_0) + (\Delta\varphi)u_0 - k(D_3\varphi)u_0 - a((\mathbf{e}_3\times x)\cdot(\nabla\varphi))u_0 \\ + (\lambda I + L_{a,k})\mathbb{B}[(\nabla\varphi)\cdot u_0].$$

By (136) and Lemma 2 we have

$$\|F\|_{L_q(\Omega)} \le C_{a_0,k_0,\lambda}\|f\|_{L_q(\Omega)}. \tag{138}$$

Since $F \in L_{q,R+2}(\Omega)$, in view of (79) we set $v = R_{a,k}(\lambda)(\varphi f - F)$ and $p = \Pi_{a,k}(\lambda)(\varphi f - F)$. Then, we have

$$\lambda v + L_{a,k}v + \nabla p = \varphi f - F, \quad \mathrm{div}\, v = 0 \ \text{ in } \Omega, \quad v|_{\partial\Omega} = 0. \tag{139}$$

Moreover, by (85) and (138) we have

$$\|v\|_{\mathcal{D}_q(\Omega)} + \|\nabla p\|_{L_q(\Omega)} \le C_{a_0,k_0,\lambda}\|f\|_{L_q(\Omega)}, \tag{140}$$

where we have used the relation: $M_a v = f - \lambda v + \Delta v - kD_3 v - \nabla p$. If we set $u(x) = u_1(x) + v(x)$, then from (135), (136), (137), (139), and (140) we see that (u, p) is a required solution to (132) which satisfies (133). The uniqueness follows from the solvability of the dual problem, so that we have the theorem. □

References

1. M. E. Bogovskiĭ, Solution of Some Vector Analysis Problems connected with Operators div and grad (Russian). Trudy Seminar S.L. Sobolev, No. 1, **80**, Akademia Nauk SSR, Sibirskoe Otdelenie Matematiki, Nowosibirsk, 5–40 (1980)
2. Y. Enomoto and Y. Shibata, On the rate of decay of the Oseen semigroup in exterior domains and its application to Navier-Stokes equation. J. Math. Fluid Mech. **7**, 339–367 (2005)
3. R. Farwig, An L^q-analysis of viscous fluid flow past a rotating obstacle. Tôhoku Math. J. **58**, 129–147 (2006)
4. R. Farwig, T. Hishida and D. Müller, L^q-theory of a singular "winding" integral operator arising from fluid dynamics. Pacific. J. Math. **215**, 297–312 (2004)
5. R. Farwig and J. Neustupa, On the Spectrum of an Oseen-type operator arising from flow past a rotating body. Integr. Equat. Operat. Theor. **62**, 169–189 (2008)
6. R. Farwig and H. Sohr, Generalized resolvent estimates for the Stokes operator in bounded and unbounded domains. J. Math. Soc. Japan **46**, 607–643 (1994)
7. D. Fujiwara and H. Morimoto, An L_r-theory of the Helmholtz decomposition of vector fields. J. Fac. Sci. Univ. Tokyo, Sect. Math. **24**, 685–700 (1977)
8. G. P. Galdi, *An Introduction to the Mathematical Theory of the Navier-Stokes Equations, Vol. I: Linear Steady Problems, Vol. II: Nonlinear Steady Problems*. Springer Tracts in Nat. Ph. **38**, **39**, Springer Verlag, New York (1994) 2nd edition (1998)
9. G. P. Galdi and A. L. Silvestre, The steady motion of a Navier-Stokes liquid around a rigid body. Arch. Rational Mech. Anal. **184**, 371–400 (2007).
10. G. P. Galdi and A. L. Silvestre, Further results on steady-state flow of a Navier-Stokes liquid around a rigid body, Existence of the wake. Kyoto Conference on the Navier-Stokes Equations and their applications, RIMS Kokyuroku Bessatsu **B1**, 127–143 (2007)
11. M. Geissert, H. Heck and M. Hieber, L^p-theory of the Navier-Stokes flow in the exterior of a moving or rotating obstacle. J. Reine Angew. Math. **596**, 45–62 (2006)

12. M. Geissert, H. Heck and M. Hieber, On the equation div $u = g$ and Bogovskii's operator in Sobolev spaces of negative order. Operat. Theor. Advan. Appl. **168**, 113–121 (2006)
13. T. Hishida and Y. Shibata, L_p–L_q estimate of the Stokes operator and Navier-Stokes flows in the exterior of a rotating obstacle. Arch. Rational Mech. Anal. **193**, 339–421 (2009)
14. T. Kobayashi and Y. Shibata, On the Oseen equation in the three dimensional exterior domains. Math. Ann. **310**, 1–45 (1998)
15. T. Miyakawa, On non-stationary solutions of the Navier-Stokes equations in an exterior domain. Hiroshima Math. J. **12**, 115–140 (1982)
16. A. Noll and J. Saal, H^∞-calculus for the Stokes operator on L_q-spaces. Math. Z. **244**, 651–688 (2003)
17. A. Pazy, *Semigroups of Linear Operators and Applications to Partial Differential Equations.* Appl. Math. Sci. Springer-Verlag, New York, **44** (1983)
18. Y. Shibata, On the exterior initial boundary value problem for Navier-Stokes equations. Quartely Appl. Math. **LVII**(1), 117–155 (1999)
19. Y. Shibata, Time-global solutions of nonlinear evolution equations and their stability. Amer. Math. Soc. Transl. **211**(2), 87–105 (2003)
20. Y. Shibata, On the Oseen semigroup with rotating effect. *Functional Analysis and Evolution Equations, The Günter Lumer Volume*, H. Amann et al (eds.), Birkhauser Verlag, Basel, 595–611 (2008)
21. H. Triebel, *Interpolation Theory, Function Spaces, Differential Operators.* North Holland, Amsterdam (1978)

A New Approach to the Regularity of Weak L^q-Solutions of Stokes and Similar Equations via the Cosserat Operator

Christian G. Simader

Abstract Throughout this paper let $G \subset \mathbb{R}^n (n \geq 2)$ be a bounded domain with sufficiently smooth boundary. We present a new approach to the problem of higher regularity of weak L^q-solutions to Stokes' equation, Stokes-like equations and the Lamé-Navier equation. The key point is a regularity property of the so-called Cosserat operator Z_q. This can be easily deduced from an estimate due to Weyers. With the help of this regularity result the regularity problem for the equations mentioned above can be reduced to the corresponding results for the Laplacian Δ and the Bilaplacian Δ^2.

Keywords Cosserat operator · Stokes-like equations · Regularity theorems

1 Introduction

For an arbitrary elliptic operator especially of order ≥ 4 the estimates up to the boundary are difficult and technically involved (see e.g. [5, Sect. 9]). But Δ and Δ^2 respectively the associated sesquilinear forms are invariant under orthogonal coordinate transforms of the independent variables. This property allows to use the tangential hyperplane at a point $x_0 \in \partial G$ for local parametrization of ∂G and flattening the boundary. Then the sesquilinear form in the new coordinates is defined in a subset of the upper half-space and it is of the original form plus a suitable "good" perturbation. The estimates for the sesquilinear forms associated with Δ [6] and Δ^2 [4] in a half-space are well known. The usual difference quotient method applies then. For Δ we did this in [6, Sect. II.8]. The same procedure is possible for Δ^2 (see [4, Lemmas III.17 and III.19]).

For the regularity of weak L^q-solutions of Stokes' equation Temam [9] refers to the very general theory of Agmon-Douglis-Nirenberg [1] for elliptic systems (see [9,

C.G. Simader (✉)
Universität Bayreuth, D-95447 Bayreuth, Germany
e-mail: Christian.Simader@uni-bayreuth.de

R. Rannacher, A. Sequeira (eds.), *Advances in Mathematical Fluid Mechanics*, 553
DOI 10.1007/978-3-642-04068-9_30,

Proposition 2.2, p. 33]). A much simpler direct and self-consistent approach is due to Galdi [3, Chap. IV]. A different more recent approach was presented by Beirão da Veiga [2]. We would like to mention that we don't need any results on elliptic systems. If we have a weak L^q-solution $\underline{u}$ of the stationary Navier-Stokes equation, then we have certain information on the integrability properties concerning the non-linear term $\underline{u} \cdot \nabla \underline{u}$. But then we treat it like an external force and apply the results for the Stokes equation. Our method applies to exterior domains too. But because of the presence of a null space of strong solutions things are more complicated and we'll present details separately in a forthcoming paper.

2 Notations

Throughout this paper let $G \subset \mathbb{R}^n$ $(n \geq 2)$ be a bounded domain with at least $\partial G \in C^2$. For $k \in \mathbb{N}$ and $1 < q < \infty$ we consider the usual Sobolev spaces

$$H^{k,q}(G) = \{u \in L^q(G) : \exists D^\alpha u \in L^q(G) \text{ for } |\alpha| \leq k\}$$

where $D^\alpha u$ denotes the weak derivative of u. For $u \in H^{k,q}(G)$ let

$$\|u\|_{k,q} := \left(\sum_{|\alpha| \leq k} \|D^\alpha u\|_q^q \right)^{\frac{1}{q}}$$

where

$$\|f\|_q := \left(\int_G |f(x)|^q dx \right)^{\frac{1}{q}} \quad \text{for } f \in L^q(G)$$

As usual let $H_0^{k,q}(G) := \overline{C_0^\infty(G)}^{\|\cdot\|_{k,q}}$. In case $k = 1$ we use the equivalent norm $\|\nabla u\|_q$ for $u \in H_0^{1,q}(G)$. Further let

$$\underline{H}_0^{1,q}(G) := \left(H_0^{1,q}(G) \right)^n .$$

For $\underline{u} \in \underline{H}_0^{1,q}(G)$, $\underline{\varphi} \in \underline{H}_0^{1,q'}(G)$ $\left(q' := \frac{q}{q-1} \right)$ let

$$\langle \nabla \underline{u}, \nabla \underline{\varphi} \rangle = \sum_{i,k=1}^{n} \int_G \partial_i u_k \partial_i \varphi_k dx$$

and for $f \in L^q(G)$, $g \in L^{q'}(G)$ we set

$$\langle f, g \rangle := \int_G fg\mathrm{d}x.$$

Let

$$L_0^q(G) := \left\{ p \in L^q(G) : \int_G p dx = 0 \right\}.$$

3 Regularity Theorems for Δ, Δ^2 and the Cosserat Operator

We need the following well-known regularity theorems for the operators Δ and Δ^2.

Theorem 1 *Let* $1 < q < \infty$, $j \in \mathbb{N}_0 := \mathbb{N} \cup \{0\}$ *and assume that* $\partial G \in C^{1+j}$. *Let* $\underline{f} \in \underline{H}^{j,q}(G) := [H^{j,q}(G)]^n$ *(where* $H^{0,q}(G) := L^q(G)$*).*

1. *Then there is a unique* $u \in H_0^{1,q}(G) \cap H^{1+j,q}(G)$ *such that*

$$\langle \nabla u, \nabla \varphi \rangle = \langle \underline{f}, \nabla \varphi \rangle \quad \forall \varphi \in H_0^{1,q'}(G) \quad \left(q' = \frac{q}{q-1} \right) \tag{1}$$

and with a constant $C_j := C(j, q, G) > 0$

$$\|u\|_{1+j,q} \leq C_j \|\underline{f}\|_{j,q} \tag{2}$$

2. *If there is* $g \in H^{j-1,q}(G)$ $(j \in \mathbb{N})$, *there exists a unique* $u \in H_0^{1,q}(G) \cap H^{1+j}$ (G) *such that*

$$\langle \nabla u, \nabla \varphi \rangle = \langle g, \varphi \rangle \qquad \forall \varphi \in H_0^{1,q'}(G) \tag{3}$$

and with a constant $C'_j > 0$

$$\|u\|_{1+j,q} \leq C'_j \|g\|_{j-1,q} \tag{4}$$

Theorem 2 *(Compare [4]). Let* $1 < q < \infty$, $j \in \mathbb{N}_0$ *and assume* $\partial G \in C^{2+j}$. *Let* $f \in H^{j,q}(G)$. *Then there is a unique* $u \in H_0^{2,q}(G) \cap H^{2+j,q}(G)$ *satisfying*

$$\langle \Delta u, \Delta \varphi \rangle = \langle f, \Delta \varphi \rangle \qquad \forall \varphi \in H_0^{2,q'}(G) \tag{5}$$

and with a constant $C'_j = C(j, q, G) > 0$

$$\begin{cases} \|u\|_{2+j,q} & \leq C'_j \|f\|_{j,q} \text{ or equivalently} \\ \|\Delta u\|_{j,q} & \leq C'_j \|f\|_{j,q} \end{cases} \tag{6}$$

The following decomposition theorem is an immediate consequence of Theorem 2. Let

$$\begin{cases} A^q(G) & := \{\Delta s : s \in H_0^{2,q}(G)\} \\ B_0^q(G) & := \left\{ p_h \in L^q(G) : \int\limits_G p_h(y)dy = 0, \langle p, \Delta s\rangle = 0 \quad \forall s \in H_0^{2,q'(G)} \right\} \end{cases} \tag{7}$$

Since $C_0^\infty(G)$ is dense in $H_0^{2,q'}(G)$, by means of Weyl's lemma, $B_0^q(G)$ consists of all harmonic $L^q(G)$-functions with vanishing mean value (or more precisely, every equivalence class of $B_0^q(G)$ contains a unique harmonic representative). We need the following approximation theorem.

Theorem 3 *Let* $1 < q < \infty$ *and let*

$$L_0^q(G) := \left\{ f \in L^q(G) : \int\limits_G f(y)dy = 0 \right\}.$$

Let $\partial G \in C^2$. *Then the following direct* ($q = 2$: *orthogonal*) *decomposition holds true:*

$$\begin{aligned} L_0^q(G) &= A^q(G) \oplus B_0^q(G) \\ f &= \Delta s + p_h \end{aligned} \tag{8}$$

In addition with $D_q := (1 + 2C'_0) > 0$ *(with* C'_q *by Theorem 2)*

$$\|\Delta s\|_q + \|p_h\|_q \leq D_q \|\Delta s + p_h\|_q \qquad \forall s \in H_0^{2,q}(G), \quad \forall p_h \in B_0^q(G) \tag{9}$$

If moreover $j \in \mathbb{N}$ *and* $\partial G \in C^{2+j}$ *then for* $f \in H^{j,q}(G)$, $f = \Delta s + p_h$, *it holds* $s \in H_0^{2,q}(G) \cap H^{2+j,q}(G)$, $p_h \in B_0^q(G) \cap H^{j,q}(G)$ *and with* $D_j := (1 + 2C'_j)$

$$\|\Delta s\|_{j,q} + \|p_h\|_{j,q} \leq D_j \|f\|_{j,q} = D_j \|\Delta s + p_h\|_{j,q} \tag{10}$$

Proof 1. If $g \in A^q(G) \cap B_0^q(G)$ then for $\varphi \in C_0^\infty(G)$

$$\langle g, \Delta\varphi\rangle = 0$$

On the other hand $g = \Delta s$, $s \in H_0^{2,q}(G)$ and by density of $C_0^\infty(G)$ in $H_0^{2,q}(G)$ we see for $\varphi \in H_0^{2,q'}(G)$

$$\langle \Delta s, \Delta\varphi \rangle = \langle g, \Delta\varphi \rangle = 0$$

and by (6_2) with $j = 0$: $\Delta s = 0$. Therefore $A^q(G) \cap B_0^q(G) = \{0\}$.

2. Let $f \in L_0^q(G)$. By Theorem 2 there is a unique $s \in H_0^{2,q}(G)$ such that

$$\langle \Delta s, \Delta\varphi \rangle = \langle f, \Delta\varphi \rangle \qquad \forall \varphi \in H_0^{1,q'}(G) \tag{11}$$

There exists a sequence $(s_k) \subset C_0^\infty(G)$ such that $\|\Delta s - \Delta s_k\|_q \to 0$. By Hölder's inequality

$$\|\Delta s - \Delta s_k\|_1 \le \|\Delta s - \Delta s_k\|_q |G|^{\frac{1}{q'}}$$

and therefore by the Gausian theorem

$$\int\limits_G \Delta s dy = \lim_{k\to\infty} \int\limits_G \Delta s_k dy = 0.$$

Therefore $\Delta s \in L_0^q(G)$ and $p_h = f - \Delta s \in L_0^q(G)$, $f = \Delta s + p_h$. Further, by (11) and Weyl's lemma

$$\langle p_h, \Delta\varphi \rangle = \langle f - \Delta s, \Delta\varphi \rangle \qquad \forall \varphi \in C_0^\infty(G)$$

whence $\Delta p_h = 0$ (more precisely, there exists a unique harmonic function in the equivalence class p_h). By (6_2)

$$\|\Delta s\|_q \le C_0' \|f\|_q,$$
$$\|p_h\|_q = \|f - \Delta s\|_q \le (1 + C_0')\|f\|_q$$

and finally

$$\|\Delta s\|_q + \|p_h\|_q \le (1 + 2C_0')\|f\|_q$$

3. If $j \in \mathbb{N}$ and $f \in H^{j,q}(G)$, then by Theorem 2 $s \in H_0^{2,q}(G) \cap H^{2+j,q}(G)$, $p_h = f - \Delta s \in H^{j,q}(G) \cap B_0^q(G)$ and

$$\|\Delta s\|_{j,q} + \|p_h\|_{j,q} \le (1 + 2C_j')\|f\|_{j,q}$$

□

For the proof of Theorem 5 we need an approximation property of *harmonic* $H^{k-1,q}(G)$ functions by *harmonic* $H^{k,q}(G)$ functions ($k \in \mathbb{N}$).

In case $k = 1$ the theorem was proved by Weyers ([10, Theorem 9.1]). If e.g. $G = B_1$ is the unit ball one can consider for $1 < R < \infty$ $p_R(x) := p\left(\frac{1}{R}x\right)$. Then $p_R \in B_0^q(B_R) \cap H^{k-1,q}(B_R)$. Since $p_R |_{\bar{B}_1} \in C^\infty(\bar{B}_1)$, $\Delta p_R = 0$ in $\bar{B}_1$, we see $p_R |_{B_1} \in H^{k,q}(B_1)$. Because of $\|p - p_R |_{B_1} \|_{H^{k-1,q}(B_1)} \to 0$ $(R \to 1)$ we found the desired approximation. In the case of an arbitrary bounded domain with sufficiently smooth boundary we have to proceed more carefully.

Theorem 4 *Let $k \in \mathbb{N}$ and let $1 < q < \infty$. Let $G \subset \mathbb{R}^n$ be a bounded domain with $\partial G \in C^{k+2}$. Then for $p \in B_0^q(G) \cap H^{k-1,q}(G)$ there exists a sequence (p_m) $\in B_0^q(G) \cap H^{k,q}(G)$ such that*

$$\|p - p_m\|_{k-1,q} \to 0 \quad (m \to \infty)$$

Proof Let $k \geq 2$ and let $G \subset\subset G_0 \subset\subset \mathbb{R}^n$. As is well known, since $\partial G \in C^{k+2} \subset C^{k-1}$ there exists an continuous extension operator

$$E : H^{k-1,q}(G) \to H_0^{k-1,q}(G_o) \subset H_0^{k-1,q}(\mathbb{R}^n)$$

such that

$$Ef\,|_G = f \qquad \forall f \in H^{k-1,q}(G)$$

and with a constant $C_1 = C_1(k, q, G) > 0$

$$\|Ef\|_{k-1,q;G_0} \leq C_1 \|f\|_{k-1,q;G} \qquad \forall f \in H^{k-1,q}(G) \tag{12}$$

For $p \in B_0^q(G) \cap H^{k-1,q}(G)$ we consider for $0 < \varepsilon < \infty$ the mollifications $(Ep)_\varepsilon \in C_0^\infty(\mathbb{R}^n)$. Since for $|\alpha| \leq k-1$ it holds $D^\alpha(Ep)_\varepsilon(x) = (D^\alpha Ep)_\varepsilon(x)$ for all $x \in \mathbb{R}^n$ and therefore

$$\|(Ep)_\varepsilon - p\|_{k-1,q;G} \leq \|(Ep)_\varepsilon - Ep\|_{k-1,q;\mathbb{R}^n} \to 0 \quad (\varepsilon \to 0). \tag{13}$$

Clearly, $(Ep)_\varepsilon\,|_G$ is no longer harmonic. Since $(Ep)_\varepsilon\,|_G \in H^{k,q}(G)$ by Theorem 2 there exists a unique $s^{(\varepsilon)} \in H_0^{2,q}(G) \cap H^{2+k,q}(G)$ satisfying

$$\langle \Delta s^{(\varepsilon)}, \Delta\varphi \rangle = \langle (Ep)_\varepsilon, \Delta\varphi \rangle \qquad \forall \varphi \in H_0^{2,q'}(G). \tag{14}$$

Since $p \in B_0^q(G)$, $\langle p, \Delta\varphi \rangle = 0\ \forall \varphi \in H_0^{2,q'}(G)$ and by (14) and estimate (6)

$$\|\Delta s^{(\varepsilon)}\|_{k-1,q} \leq \|(Ep)_\varepsilon - p\|_{k-1,q;G} \to 0 \quad (\varepsilon \to 0) \tag{15}$$

From (14) we conclude by Weyl's lemma that $\left[(Ep)_\varepsilon - \Delta s^{(\varepsilon)}\right]|_G$ is harmonic in G. For $\varepsilon := \frac{1}{m}$ $(m \in \mathbb{N})$ let

$$p_m := \left[(Ep)_{\frac{1}{m}} - \Delta s^{(\frac{1}{m})}\right]|_G\ .$$

Then, by (13) and (15)

$$\|p - p_m\|_{k-1,q;G} \leq \|(Ep)_{\frac{1}{m}} - p\|_{k-1,q;G} + \|\Delta s^{(\frac{1}{m})}\|_{k-1,q;G} \to 0 \qquad (m \to \infty)$$

□

The following result on the solvability of the divergence equation is an easy consequence of Theorem 3.4 from [7, p. 175]. Compare in addition [8, Satz 8.3.3, p. 303]. We use the following notations: Let $p \in L_0^q(G)$ and let $\underline{v} \in \underline{H}_0^{1,q}(G)$ be the unique solution of

$$\langle \nabla \underline{v}, \nabla \underline{\varphi} \rangle = \langle p, \operatorname{div} \underline{\varphi} \rangle \qquad \forall \underline{\varphi} \in \underline{H}_0^{1,q'}(G) \tag{16}$$

Then let

$$\underline{\mathrm{T}}_q : L_0^q(G) \to \underline{H}_0^{1,q}(G), \qquad \mathrm{T}_q p := \underline{v} \tag{17}$$

where $\underline{v}$ is the unique solution of (16). Let

$$\underline{M}_q(G) := \mathrm{T}_q(L_0^q(G)) \tag{18}$$

If moreover $p \in H^{j,q}(G) \cap L_0^q(G)$ ($j \in \mathbb{N}$) and $\partial G \in C^{1+j}$ then by Theorem 1

$$\underline{\mathrm{T}}_q p = \underline{v} \in \underline{H}_0^{1,q}(G) \cap \underline{H}^{1+j,q}(G)$$

Further for $p_h \in B_0^q(G)$ we define the Cosserat operator Z_q by

$$Z_q : B_0^q(G) \to B_0^q(G), \quad Z_q p_h := \operatorname{div} \underline{\mathrm{T}}_q p_h = \operatorname{div} \underline{v} \tag{19}$$

It was proved in [7, Theorem 3.1] that $Z_q : B_0^q(G) \to B_0^q(G)$ is bijektive and Z_q, Z_q^{-1} are bounded.

Theorem 5 *Let $G \subset \mathbb{R}^n$ be a bounded domain with boundary $\partial G \in C^{k+2}$ ($k \in \mathbb{N}$). If $p \in B_0^q(G) \cap H^{k-1,q}(G)$ ($1 < q < \infty$) then*

$$Z_q(p) - \frac{1}{2}p \in B_0^q(G) \cap H^{k,q}(G)$$

and there is a constant $\tilde{C}_k = C(k, q, G) > 0$ such that

$$\left\| Z_q(p) - \frac{1}{2}p \right\|_{k,q} \leq \tilde{C}_k \|p\|_{k-1,q} \qquad \forall p \in B_0^q(G) \cap H^{k-1,q}(G) \tag{20}$$

Proof Estimate (20) was proved by Weyers [10, Lemma 13.3, p. 141] in case $k \geq 2$ under the *additional assumption* that $p \in H^{k,q}(G)$. Observe that Weyers' assumption on ∂G is unnecessarily restrictive. Our assumption $\partial G \in C^{k+2}$ is sufficient.

Let $p \in B_0^q(G) \cap H^{k-1,q}(G)$ and let $k \geq 2$. By Theorem 4 there is a sequence $(p_m) \subset B_0^q(G) \cap H^{k,q}(G)$ such that $\|p - p_m\|_{k-1,q} \to 0$ $(m \to \infty)$. By Weyers' result, (20) holds with $p_j - p_m \in B_0^q(G) \cap H^{k,q}(G)$ in place of p:

$$\left\| Z_q(p_j - p_m) - \frac{1}{2}(p_j - p_m) \right\|_{k,q} \leq \tilde{C}_k \|p_j - p_m\|_{k-1,q} \to 0 \, (j, m \to \infty)$$

By completeness of $H^{k,q}(G)$ there exists a unique $v \in H^{k,q}(G)$ such that

$$\left\| v - (Z_q(p_m)) - \frac{1}{2} p_m \right\|_{k,q} \to 0 \qquad (m \to \infty).$$

On the other hand by (20) with $k - 1$ in place of $k \geq 2$,

$$\left\| Z_q(p_m - p) - \frac{1}{2}(p_m - p) \right\|_{k-1,q} \leq \tilde{C}_{k-1} \|p_m - p\|_{k-2,q} \to 0$$

Since $\left\| v - \left(Z_q(p_m) - \frac{1}{2} p_m\right) \right\|_{k-1,q} \to 0$ we conclude in $H^{k-1,q}(G)$: $v = Z_q(p) - \frac{1}{2}p$. Since $v \in H^{k,q}(G)$, we see $Z_q(p) - \frac{1}{2}p \in B_0^q(G) \cap H^{k,q}(G)$. Now (20) is true with p_m in place of p and passing to the limit $m \to \infty$ (20) follows finally. □

The following theorem tells us that for $p \in B_0^q(G)$ and for the solution $\underline{v} := \mathrm{T}_q p$ of (21) regularity properties of $\operatorname{div} \underline{v} = Z_q(p) \in B_0^q(G)$ are transmitted in those of $\underline{v}$ and p.

Theorem 6 *Let $k \in \mathbb{N}$ and assume that $\partial G \in C^{k+2}$. Let $1 < q < \infty$, let $p \in B_0^q(G)$ and let $\underline{v} = \mathrm{T}_q p \in \underline{H}_0^{1,q}(G)$ be the solution of*

$$\langle \nabla \underline{v}, \nabla \underline{\varphi} \rangle = \langle p, \operatorname{div} \underline{\varphi} \rangle \qquad \forall \underline{\varphi} \in \underline{H}_0^{1,q'}(G). \tag{21}$$

Assume in addition that $\operatorname{div} \underline{v} \in H^{k,q}(G)$. Then $p \in H^{k,q}(G)$ and $\underline{v} \in \underline{H}_0^{1,q}(G) \cap \underline{H}^{1+k,q}(G)$. Further there are constants $C'_k = C'(k, q, G) > 0$ and $D_k = D(k, q, G)$ such that

$$\|p\|_{k,q} \leq C'_k \|Z_q(p)\|_{k,q} = C'_k \|\operatorname{div} \underline{v}\|_{k,q} \tag{22}$$

and

$$\|\underline{v}\|_{1+k,q} \leq D_k \|Z_q(p)\|_{k,q} = D_k \|\operatorname{div} \underline{v}\|_{k,q}. \tag{23}$$

Proof The proof is by induction on $k \in \mathbb{N}$. Let $k = 1$, $\operatorname{div} \underline{v} \in H^{1,q}(G)$. By Theorem 5 $\operatorname{div} \underline{v} - \frac{1}{2}p =: f_1 \in H^{1,q}(G)$ whence $p = 2(\operatorname{div} \underline{v} - f_1) \in H^{1,q}(G)$. Furthermore by (20)

$$\|p\|_{1,q} \leq \left\| 2\left(\frac{1}{2}p - \operatorname{div} \underline{v}\right)\right\|_{1,q} + 2\|\operatorname{div} \underline{v}\|_{1,q} \leq 2\tilde{C}_1\|p\|_q + 2\|\operatorname{div} \underline{v}\|_{1,q}$$

By [7, Theorem 3.2, p. 174] with $C > 0$

$$\|p\|_q \leq C\|\operatorname{div} \underline{v}\|_q \leq C\|\operatorname{div} \underline{v}\|_{1,q}$$

and with $C_1' := 2(\tilde{C}_1 C + 1)$ it follows (22). Because of

$$\langle \nabla v_i, \nabla\varphi\rangle = \langle p, \partial_i\varphi\rangle \qquad \forall\varphi \in H_0^{1,q'}(G), i = 1, \ldots, n$$

we get from (1), (2) with $C_1 > 0$

$$\|\nabla v_i\|_{2,q} \leq C_1\|p\|_{1,q}$$

whence by (22)

$$\|\nabla\underline{v}\|_{2,q} = \left(\sum_{i=1}^{n}\|v_i\|_{2,q}^q\right)^{\frac{1}{q}} \leq n^{\frac{1}{q}}C_1\|p\|_{1,q} \leq n^{\frac{1}{q}}C_1'\|\operatorname{div} \underline{v}\|_{1,q}.$$

With $D_1 := n^{\frac{1}{q}}C_1'$ follows (23). Assume now that the assertion is true for some $k \in \mathbb{N}$ and assume that $\operatorname{div} \underline{v} \in H^{k+1,q}(G) \subset H^{k,q}(G)$. By induction hypothesis $p \in H^{k,q}(G) \cap B_0^q(G)$. By Theorem 5 $\operatorname{div} \underline{v} - \frac{1}{2}p =: f_k \in H^{k+1,q}(G) \cap B_0^q(G)$ and (20) holds true with $k+1$ in place of k. Then

$$p = 2(\operatorname{div} \underline{v} - f_k) \in H^{k+1,q}(G)$$

and by (20) and the induction hypothesis

$$\begin{aligned}\|p\|_{k+1,q} &\leq \left\| 2\left(\frac{1}{2}p - \operatorname{div} \underline{v}\right)\right\|_{k+1,q} + 2\|\operatorname{div} \underline{v}\|_{k+1,q} \leq 2\tilde{C}_k\|p\|_{k,q} + 2\|\operatorname{div} \underline{v}\|_{k+1,q} \leq \\ &\leq 2\tilde{C}_k C_k'\|\operatorname{div} \underline{v}\|_{k,q} + 2\|\operatorname{div} \underline{v}\|_{k+1,q} \leq 2(\tilde{C}_k C_k' + 1)\|\operatorname{div} \underline{v}\|_{k+1,q}\end{aligned}$$

and (22) follows with $C_{k+1}' := 2(\tilde{C}_{k+1}C_k') + 1$. Similarly to the case $k = 1$ we derive (23) from (2) with $D_{k+1} := n^{\frac{1}{q}}C_{k+1}'$. □

4 The Solution of the Equation div $\underline{v} = \pi$ with Prescribed Boundary Values: Applications to Stokes' Equation and Similar Equations

Theorem 7 *Let $1 < q < \infty$, $j \in \mathbb{N}$ and let $\partial G \in C^{2+j}$. Then for $\pi \in H^{j,q}(G) \cap L_0^q(G)$ there is a unique $\underline{u} \in \underline{M}^q(G) \cap H^{1+j,q}(G)$ satisfying* $\operatorname{div} \underline{u} = \pi$. *If $\underline{u} = \mathrm{T}_q p$ with a unique $p \in L_0^q(G)$, then $p \in H^{j,q}(G) \cap L_0^q(G)$. Further with a constant $E_j = E(j,q,G) > 0$*

$$\begin{aligned} \|p\|_{j,q} &\leq E_j \|\operatorname{div} \underline{u}\|_{j,q} = E_j \|\pi\|_{j,q} \\ \|\underline{u}\|_{1+j,q} &\leq E_j \|\pi\|_{j,q}. \end{aligned} \tag{24}$$

Proof We divide $\pi = \pi_0 + \pi_h$, $\pi_0 \in A^q(G)$, $\pi_h \in B_0^q(G)$, where $\pi_0 = \Delta s$, $s \in H_0^{2,q}(G)$ is the unique solution of

$$\langle \Delta s, \Delta\varphi \rangle = \langle \pi, \Delta\varphi \rangle \qquad \forall \varphi \in H_0^{2,q'}(G)$$

By Theorem 2 it follows that $s \in H^{2+j,q}(G)$, whence $\pi_0 = \Delta s \in H^{j,q}(G)$. Let $\pi_h := \pi - \Delta s$. Then $\pi_h \in B_0^q(G) \cap H^{j,q}(G)$ and by (10)

$$\|\Delta s\|_{j,q} + \|\pi_h\|_{j,q} \leq (1 + 2C_j')\|\pi\|_{j,q}. \tag{25}$$

Let now $p_h \in B_0^q(G)$, $\underline{v}_h := \mathrm{T}_q p_h \in \underline{H}_0^{1,q}(G)$ such that $Z_q p_h = \operatorname{div} \underline{v}_h = \pi_h$. By Theorem 4 we see $p_h \in B_0^q(G) \cap H^{j,q}(G)$ and $\underline{v}_h \subset \underline{H}_0^{1,q}(G) \cap \underline{H}^{1+j,q}(G)$ and with constants $C_j' > 0$ resp. $D_j > 0$

$$\begin{aligned} \|p_h\|_{j,q} &\leq C_j' \|\operatorname{div} \underline{v}_h\|_{j,q} \\ \|\underline{v}_h\|_{1+j,q} &\leq D_j \|\operatorname{div} v_h\|_{j,q}. \end{aligned} \tag{26}$$

Let $\underline{v}_0 := \nabla s \in \underline{H}_0^{1,q} \cap \underline{H}^{1+j,q(G)}$.Then $\underline{u} := \underline{v}_0 + \underline{v}_h \in \underline{H}_0^{1,q}(G) \cap \underline{H}^{1+j,q}(G)$, $\operatorname{div} \underline{u} = \Delta s + \operatorname{div} \underline{v}_h = \pi_0 + \pi_h = \pi$. Since $\|s\|_{2+j,q} \leq L\|\Delta s\|_{j,q}$ we get from (25)

$$\begin{aligned} \|\underline{u}\|_{1+j,q} &\leq \|\underline{v}_0\|_{1+j,q} + \|v_h\|_{1+j,q} \leq L\|\Delta s\|_{j,q} + \|v_h\|_{j,q} \\ &\leq \max(1, L)(1 + 2C_j')\|\pi\|_{j,q}. \end{aligned}$$

□

Lemma 1 *Let $1 < q < \infty$, let $j \in \mathbb{N}_0$ and $\partial G \in C^{2+j}$. Then for $\underline{a} \in \underline{H}^{1+j,q}(G)$, $g \in H^{j,q}(G)$ satisfying*

$$\int_G g\,dx = \int_G \operatorname{div} \underline{a}\,dx \tag{27}$$

there exists a unique $\underline{w} \in \underline{H}^{1+j,q}(G)$ such that

$$\operatorname{div} \underline{w} = g \textit{ and } (\underline{w} - \underline{a}) \in \underline{H}_0^{1,q}(G) \cap \underline{H}^{1+j,q}(G). \tag{28}$$

With the constant $E_j > 0$ by (24) it holds

$$\|w\|_{1+j,q} \leq \|a\|_{1+j,q} + E_j \|g - \operatorname{div} \underline{a}\|_{j,q}. \tag{29}$$

Proof Because of (27) $(g - \operatorname{div} \underline{a}) \in L_0^q(G)$. By Theorem 7 there exists a unique $\underline{u} \in \underline{M}^q(G) \cap \underline{H}^{1+j,q}(G)$ such that $\operatorname{div} \underline{u} = g - \operatorname{div} \underline{a}$ and by (24_2)

$$\|\underline{u}\|_{1+j,q} \leq E_j \|g - \operatorname{div} \underline{a}\|_{j,q}. \tag{30}$$

Let $\underline{w} := \underline{a} + \underline{u}$. Then $\underline{w}$ is the desired solution and (29) follows immediately from (30). Suppose now that $\underline{w}_i \in \underline{H}^{1+j,q}(G)$ $(i = 1, 2)$ are solutions of (28). Then $\operatorname{div}(\underline{w}_1 - \underline{w}_2) = 0$ and $\underline{w}_1 - \underline{w}_2 = (\underline{w}_1 - \underline{a}) + (\underline{a} - \underline{w}_2) \in \underline{H}_0^{1,q}(G)$ and by (24_2)

$$\|w_1 - w_2\|_{1,q} \leq E_1 \| \operatorname{div}(\underline{w}_1 - \underline{w}_2)\|_q = 0.$$

□

Theorem 8 *Let $1 < q < \infty$, let $j \in \mathbb{N}_0$ and $\partial G \in C^{2+j}$. Let $\underline{f} \in \underline{H}^{j,q}(G)$, $\underline{a} \in \underline{H}^{2+j,q}(G)$ and $g \in H^{1+j,q}(G)$ be given such that (27) is satisfied. Then there exists a unique $\underline{v} \in \underline{H}^{2+j,q}(G)$ and a unique $p \in H^{1+j,q}(G) \cap L_0^q(G)$ such that for $\mu > 0$*

$$\left\{ \begin{array}{ll} \mu\langle \nabla \underline{v}, \nabla \underline{\varphi} \rangle + \langle p, \operatorname{div} \underline{\varphi} \rangle = \langle \underline{f}, \underline{\varphi} \rangle & \forall \underline{\varphi} \in \underline{H}_0^{1,q'}(G) \\ -\mu \Delta \underline{v} - \nabla p = \underline{f} \text{ in } G & \\ \underline{v} - \underline{a} \in \underline{H}_0^{1,q}(G) & \\ \operatorname{div} \underline{v} = g \text{ in } G & \end{array} \right. \tag{31}$$

Furthermore we get with a constant $F_j = F(j, q, G) > 0$

$$\mu\|\underline{v}\|_{2+j,q} + \|p\|_{j+1,q} \leq F_j \left(\|\underline{f}\|_{j,q} + \mu\|\underline{a}\|_{2+j,q} + \mu\|g - \operatorname{div} \underline{a}\|_{j+1,q} \right). \tag{32}$$

Proof According Lemma 1 there is a unique $\underline{w} \in \underline{H}^{2+j,q}(G)$ such that $\operatorname{div} \underline{w} = g$ and $\underline{w} - \underline{a} \in \underline{H}_0^{1,q}(G) \cap \underline{H}^{2+j,q}(G)$. By (29) we get

$$\|\underline{w}\|_{2+j,q} \leq \|\underline{a}\|_{2+j,q} + E_{j+1}\|g - \operatorname{div} \underline{a}\|_{j+1,q}. \tag{33}$$

Consider the n Dirichlet problems for $\underline{\tilde{z}} \in \underline{H}_0^{1,q}(G)$.

$$\langle \nabla \underline{\tilde{z}}, \nabla \underline{\varphi} \rangle = \langle \underline{f} + \mu \Delta \underline{w}, \underline{\varphi} \rangle = \langle \underline{f}, \underline{\varphi} \rangle - \mu \langle \nabla \underline{w}, \nabla \underline{\varphi} \rangle \qquad \forall \underline{\varphi} \in \underline{H}_0^{1,q'}(G) \tag{34}$$

By Theorem 1 $\underline{\tilde{z}} \in \underline{H}_0^{1,q}(G) \cap \underline{H}^{2+j,q}(G)$ and

$$\|\underline{\tilde{z}}\|_{2+j,q} \leq C'_{j+1}(\|\underline{f}\|_{j,q} + \|\underline{w}\|_{2+j,q}). \tag{35}$$

Let $\underline{z} := \frac{1}{\mu}\underline{\tilde{z}}$. Let $\pi := \operatorname{div}\underline{z} \in L_0^q(G) \cap H^{1+j,q}(G)$. By Theorem 7 there is a unique $\tilde{p} \in L_0^q(G) \cap H^{1+j,q}(G)$, such that with $\underline{u} := \underline{\mathrm{T}}_q \tilde{p} \in \underline{H}_0^{1,q}(G) \cap \underline{H}^{2+j,q}(G) \cap \underline{M}^q(G)$ it holds $\operatorname{div}\underline{u} = \pi$. Furthermore

$$\begin{cases} \mu\|\tilde{p}\|_{j+1,q} & \leq \mu E_{j+1}\|\operatorname{div}\underline{z}\|_{j+1,q} \leq E_{j+1}\|\underline{\tilde{z}}\|_{2+j,q} \\ \mu\|\underline{u}\|_{2+j,q} & \leq \mu E_{j+1}\|\operatorname{div}\underline{z}\|_{j+1,q} \leq E_{j+1}\|\underline{\tilde{z}}\|_{2+j,q}. \end{cases} \tag{36}$$

With $\underline{v} := \underline{z} - \underline{u} + \underline{w} \in \underline{H}^{2+j,q}(G)$ we see $\underline{v} - \underline{a} \in \underline{H}_0^{1,q}(G) \cap \underline{H}^{2+j,q}(G)$, $\operatorname{div}\underline{v} = g$ and we derive from (34)

$$\mu\langle\nabla\underline{v}, \nabla\underline{\varphi}\rangle + \mu\langle\nabla\underline{u}, \nabla\underline{\varphi}\rangle = \langle\underline{f}, \underline{\varphi}\rangle \qquad \forall\underline{\varphi} \in H_0^{1,q'}(G).$$

$\underline{u} = \underline{\mathrm{T}}_q \tilde{p}$ means

$$\langle\nabla\underline{u}, \nabla\underline{\varphi}\rangle = \langle\tilde{p}, \operatorname{div}\underline{\varphi}\rangle \qquad \forall\underline{\varphi} \in \underline{H}_0^{1,q'}(G)$$

Let $p := \mu\tilde{p}$. Then combining last equations leads to (31_1). Then (31_2) follows by partial integration and by density of $C_0^\infty(G)$ in $L^{q'}(G)$. Let $F_j' := \Big[(2E_{j+1} + 1)C_j' + 1\Big]$. Then (32) follows from (33), (35) and (36) with $F_j := F_j' \max(1, E_{j+1})$. □

As a simple corollary we derive from Theorem 8 existence and regularity of the following Stokes-like equation.

Theorem 9 *Same assumptions as in Theorem 8. Let* $\lambda \in \mathbb{R}$. *Then there exists a unique* $\underline{v} \in \underline{H}^{2+j,q}(G)$ *and a unique* $\tilde{p} \in H^{1+j,q}(G) \cap L_0^q(G)$ *such that for* $\mu > 0$

$$\begin{cases} \mu\langle\nabla\underline{v}, \nabla\underline{\varphi}\rangle + \lambda\langle\operatorname{div}\underline{v}, \operatorname{div}\underline{\varphi}\rangle + \langle\tilde{p}, \operatorname{div}\underline{\varphi}\rangle = \langle\underline{f}, \underline{\varphi}\rangle \qquad \forall\underline{\varphi} \in \underline{H}_0^{1,q'}(G) \\ -\mu\Delta\underline{v} - \lambda\nabla\operatorname{div}\underline{v} - \nabla\tilde{p} = f \text{ in } G \\ \underline{v} - \underline{a} \in \underline{H}_0^{1,q}(G) \\ \operatorname{div}\underline{v} = g \text{ in } G \end{cases} \tag{37}$$

Furthermore, with $F_j > 0$ *by (32)*

$$\|\underline{v}\|_{2+j,q} + \|\tilde{p}\|_{j+1,q} \leq F_j\left(\|\underline{f}\|_{j,q} + \|\underline{a}\|_{2+j,q} + \|g - \operatorname{div}\underline{a}\|_{j+1,q}\right) + |\lambda|\|g\|_{j+1,q} \tag{38}$$

Proof Consider the solution of (31) and write

$$\mu\langle\nabla\underline{v}, \nabla\underline{\varphi}\rangle + \lambda\langle\operatorname{div}\underline{v}, \operatorname{div}\underline{\varphi}\rangle + \langle p - \lambda\operatorname{div}\underline{v}, \operatorname{div}\underline{\varphi}\rangle = \langle\underline{f}, \underline{\varphi}\rangle \qquad \forall\underline{\varphi} \in \underline{H}_0^{1,q'}(G).$$

We put $\tilde{p} := (p - \lambda\operatorname{div}\underline{v}) \in H^{1+j,q}(G) \cap L_0^q(G)$. This gives (37_1). (38) follows immediately from (32) since $\operatorname{div}\underline{v} = g$. Let $\underline{v}^{(i)} \in \underline{H}^{2+j,q}(G)$, $\tilde{p}^{(i)} \in H^{1+j,q}(G) \cap$

$L^q_0(G)$ be solutions of (37_1), $i = 1, 2$. Put $\underline{u} := \underline{v}^{(1)} - \underline{v}^{(2)} \in \underline{H}^{2+j,q}(G)$, $\pi := \tilde{p}^{(1)} - \tilde{p}^{(2)} \in H^{1+j,q}(G) \cap L^q_0(G)$. Moreover $\underline{u} = \big(\underline{v}^{(1)} - \underline{a}\big) - \big(\underline{v}^{(2)} - \underline{a}\big) \in \underline{H}^{1,q}_0(G)$ and $\operatorname{div} \underline{u} = 0$. Then we get from (37_1)

$$\mu\langle \nabla \underline{u}, \nabla \underline{\varphi}\rangle + \langle \pi, \operatorname{div} \underline{\varphi}\rangle = 0 \qquad \forall \underline{\varphi} \in \underline{H}^{1,q'}_0(G)$$

whence $\underline{u} \in \underline{H}^{1,q}_0(G) \cap \underline{H}^{2+j,q}(G)$ is a solution of (31) (with $\underline{f} = \underline{a} = 0$, $g = 0$) and therefore $\underline{u} = 0$. □

The next Stokes-like equation was considered by H. Beirão da Veiga [2].

Theorem 10 *Same assumptions as in Theorem 8. Let $\mu > 0$ and let $\lambda \geq 0$. Then there exists a unique $\underline{u}_\lambda \in \underline{H}^{2+j,q}(G)$ and $p_\lambda \in H^{1+j,q}(G) \cap L^q_0(G)$ such that*

$$\begin{cases} \mu\langle \nabla \underline{u}_\lambda, \nabla \underline{\varphi}\rangle + \langle p_\lambda, \operatorname{div} \underline{\varphi}\rangle = \langle \underline{f}, \underline{\varphi}\rangle \qquad \forall \underline{\varphi} \in \underline{H}^{1,q'}_0(G) \\ -\mu\Delta u_\lambda - \nabla p_\lambda = \underline{f} \text{ in } G \\ \operatorname{div} \underline{u}_\lambda - \lambda p_\lambda = g \text{ in } G \\ (\underline{u}_\lambda - \underline{a}) \in \underline{H}^{1,q}_0(G) \end{cases} \tag{39}$$

Furthermore with the constant $F_j > 0$ from (32) and $K_{j+1} = K(j+1, q, G) > 0$

$$\begin{aligned} &\mu\|u_\lambda\|_{2+j,q} + \|p_\lambda\|_{2+j,q} \leq \\ &\qquad \leq F_j(1 + \lambda K_{j+1})\Big(\|\underline{f}\|_{j,q} + \|\underline{a}\|_{2+j,q} + \|g - \operatorname{div} \underline{a}\|_{1+j,q}\Big). \end{aligned} \tag{40}$$

Let $(\underline{v}, p)$ be the solution of (37). Put $\underline{u}_0 := \underline{v}$, $p_0 := p$. Then with

$$K_{j+1} = K(j+1, \mu, q, G)$$

$$\begin{aligned} &\mu\|\underline{u}_\lambda - \underline{u}_0\|_{2+j,q} + \|p_\lambda - p_0\|_{1+j,q} \leq 2K_{j+1}\lambda F_j \cdot \\ &\qquad \cdot \Big(\|\underline{f}\|_{j,q} + \|\underline{a}\|_{2+j,q} + \|g - \operatorname{div} \underline{a}\|_{1+j,q}\Big). \end{aligned} \tag{41}$$

Proof Let $\lambda > 0$. Consider the solution $\underline{v} \in \underline{H}^{2+j,q}(G)$, $p \in H^{1+j,q}(G) \cap L^q_0(G)$ of (31). Let $t \in L^q_0(G)$ be given and let $\underline{w} := \underline{\mathrm{T}}_q t \in \underline{H}^{1,q}_0(G)$, that is

$$\langle \nabla \underline{w}, \nabla \underline{\varphi}\rangle = \langle t, \operatorname{div} \underline{\varphi}\rangle \qquad \forall \underline{\varphi} \in \underline{H}^{1,q'}_0(G).$$

We consider

$$\mu\langle \nabla(\underline{v} + \underline{w}), \nabla \underline{\varphi}\rangle + \langle p - \mu t, \operatorname{div} \underline{\varphi}\rangle = \langle \underline{f}, \underline{\varphi}\rangle \qquad \forall \underline{\varphi} \in \underline{H}^{1,q'}_0(G)$$

We would like to put $\underline{u}_\lambda := \underline{v} + \underline{w}$ and $p_\lambda := p - \mu t$. Then $\operatorname{div} \underline{u} - \lambda p_\lambda = g$ if and only if (observe $\operatorname{div} \underline{v} = g$)

$$\operatorname{div} \underline{w} = \operatorname{div} \underline{\mathrm{T}}_q t = \lambda(p - \mu t). \tag{42}$$

We split according (8)

$$p = p_0 + p_h, \qquad t = t_0 + t_h, \qquad p_0, t_0 \in A^q(G), \qquad p_h, t_h \in B_0^q(G).$$

Let $\underline{w}_0 := \underline{\mathrm{T}}_q t_0$, $\underline{w}_h := \underline{\mathrm{T}}_q t_h$, $\underline{w} = \underline{w}_0 + \underline{w}_h$. Then $\operatorname{div} \underline{w}_0 = t_0$ and because of (42) it must be satisfied $t_0 = \lambda(p_0 - \mu t_0)$ or equivalently

$$t_0 := \frac{\lambda}{1 + \lambda\mu} p_0. \tag{43}$$

Since $\operatorname{div} \underline{w}_h = Z_q t_h$ because of (42) $Z_q t_h = \lambda(p_h - \mu t_h)$ or equivalently

$$(Z_q + \lambda\mu I) t_h = \lambda p_h \tag{44}$$

must be satisfied.

Since $p \in H^{1+j,q}(G) \cap L_0^q(G)$ we get from Theorem 3 that $p = p_0 + p_h$ where $p_0 = \Delta s$, $s \in H_0^{2,q}(G) \cap H^{3+j,q}(G)$, $p_h \in H^{1+j,q}(G) \cap B_0^q(G)$. Then by Theorem 6 $\left(Z_q p_h - \frac{1}{2} p_h\right) \in H^{2+j,q}(G) \cap B_0^q(G)$ and (22, 23) hold true with $k = 2 + j$. Since the embedding of $H^{2+j,q}(G) \cap B_0^q(G)$ in $H^{1+j,q}(G) \cap B_0^q(G)$ is compact, the operator

$$Z_q - \frac{1}{2} I : H^{1+j,q}(G) \cap B_0^q(G) \to H^{1+j,q}(G) \cap B_0^q(G)$$

is compact. Therefore the operator

$$Z_q + \lambda\mu I = \left(Z_q - \frac{1}{2} I\right) + \left(\lambda\mu + \frac{1}{2}\right) I$$

is a Fredholm operator. Suppose now that there is $p \in H^{1+j,q} \cap B_0^q(G) \subset B_0^q(G)$ with $Z_q p + \lambda\mu p = 0$ $(\lambda > 0)$. Let $\underline{v} := \mathrm{T}_q p \in \underline{H}_0^{1,q}(G) \cap \underline{H}^{2+j}(G) \subset \underline{H}_0^{1,q}(G)$ be the weak solution of (16), $\operatorname{div} \underline{v} = Z_q p = -\lambda\mu p$. Then

$$\langle \nabla \underline{v}, \nabla \underline{\varphi} \rangle = -\frac{1}{\lambda\mu} \langle \operatorname{div} \underline{v}, \operatorname{div} \underline{\varphi} \rangle.$$

By [10, Theorem 13.1] we conclude $\underline{v} \in \underline{H}_0^{1,2}(G)$ and $\underline{\varphi} := \underline{v}$ is admissible, whence

$$\|\nabla \underline{v}\|_2^2 = -\frac{1}{\lambda\mu} \|\operatorname{div} \underline{v}\|_2^2 \leq 0.$$

Therefore the kernel of $(Z_q + \lambda\mu I)$ is trivial. With the same arguments used in parts (b) and (c) of the proof of Lemma 4.2 in [7] (replace $B_0^q(G)$ by $B_0^q(G) \cap H^{1+j,q}(G)$) we see for $\varrho > -1$ that the operator

$$\varrho Z_q + I : B_0^q(G) \cap H^{1+j,q}(G) \to B_0^q(G) \cap H^{1+j,q}(G)$$

is bijective and with a constant $C_\varrho > 0$ holds

$$C_\varrho \|p + \varrho Z_q p\|_{1+j,q} \geq \|p\|_{1+j,q} \qquad \forall p \in B_0^q(G) \cap H^{1+j,q}(G).$$

Therefore for $\lambda\mu > 0$ there is $D_\lambda = D(\lambda, \mu, j, q, G) > 0$ such that

$$\|(Z_q + \lambda\mu I)p\|_{1+j,q} \geq D_\lambda \|p\|_{1+j,q} \qquad \forall p \in B_0^q(G) \cap H^{1+j,q}(G).$$

Similarly with the same arguments used in the proof of Theorem 3.2 in [7] there is $D_0 > 0$ such that

$$\|Z_q p\|_{1+j,q} \geq D_0 \|p\|_{1+j,q} \qquad \forall p \in B_0^q(G) \cap H^{1+j,q}(G).$$

Let for $\lambda \geq 0$

$$C(\lambda) := \inf\left\{ \frac{\|(Z_q + \lambda\mu)p\|_{1+j,q}}{\|p\|_{1+j,q}} : 0 \neq p \in B_0^q(G) \cap H^{1+j,q}(G) \right\} \geq D_\lambda > 0.$$

Let $\lambda' \geq 0$. Then

$$\begin{aligned} \|Z_q p + \lambda'\mu p\|_{1+j,q} &= \|Z_q p + \lambda\mu p + (\lambda' - \lambda)\mu p\|_{1+j,q} \geq \\ &\geq \|Z_q p + \lambda\mu p\|_{1+j,q} - |\lambda' - \lambda|\mu\|p\|_{1+j,q} \geq \\ &\geq (C(\lambda) - |\lambda' - \lambda|\mu)\|p\|_{1+j,q} \end{aligned}$$

for all $p \in B_0^q(G) \cap H^{1+j,q}(G)$ and therefore

$$C(\lambda') \geq C(\lambda) - |\lambda' - \lambda|\mu.$$

Interchanging the roles of λ and λ' gives $C(\lambda) \geq C(\lambda') - |\lambda' - \lambda|$ whence

$$|C(\lambda) - C(\lambda')| \leq |\lambda - \lambda'|\mu \qquad \forall \lambda, \lambda' \geq 0.$$

The continuous and positive function $C(.)$ attains its minimum on the compact interval $\left[0, \frac{2}{\mu}\|Z_q\|\right]$. Let

$$d := \min\left\{ C(\lambda) : 0 \leq \lambda \leq \frac{2}{\mu}\|Z_q\| \right\} > 0.$$

For $\lambda \geq \frac{2}{\mu}\|Z_q\|$ we see

$$\|\lambda\mu p + Z_q p\|_{1+j,q} \geq \lambda\mu\|p\|_{1+j,q} - \|Z_q\|\|p\|_{1+j,q} \geq \frac{\lambda\mu}{2}\|p\|_{1+j,q}.$$

Therefore we see

$$\|(Z_q + \lambda\mu I)p\|_{1+j,q} \geq d_0\|p\|_q \qquad \forall\lambda \geq 0, \quad \forall p \in B_0^q(G) \cap H^{1+j,q}(G) \quad (45)$$

where $d_0 := \max\left(d, \frac{\lambda\mu}{2}\right) \geq d$. Let $t_h \in B_0^q(G) \cap H^{1+j,q}(G)$ be the unique solution of (44). By (45) we get

$$\|t_h\|_{1+j,q} \leq d^{-1}\lambda\|p_h\|_{1+j,q}. \qquad (46)$$

By Theorem 1 we see for $\underline{w}_h := \underline{\mathrm{T}}_q t_h \in \underline{H}^{2+j,q}(G)$ and by (2), (10) and (46)

$$\|\underline{w}_h\|_{2+j,q} \leq C_{j+1}\|t_h\|_{1+j,q} \leq C_{j+1}d^{-1}\lambda\|p_h\|_{1+j,q} \leq$$
$$\leq C_{j+1}d^{-1}\lambda(1 + 2C'_{j+1})\|p\|_{1+j,q}. \qquad (47)$$

As noted above, $p_0 = \Delta s$ with $s \in H_0^{2,q}(G) \cap H^{3+j,q}(G)$ and $\underline{\mathrm{T}}_q p_0 = \nabla s \in \underline{H}_0^{1,q}(G) \cap \underline{H}^{2+j,q}(G)$. Then because of (43)

$$\underline{w}_0 := \underline{\mathrm{T}}_q t_0 = \frac{\lambda}{1 + \lambda\mu}\underline{\mathrm{T}}_q p_0 = \frac{\lambda}{1 + \lambda\mu}\nabla s$$

and by (10)

$$\|\underline{w}_0\|_{2+j,q} \leq \frac{\lambda}{1 + \lambda\mu}\|\Delta s\|_{1+j,q} \leq \lambda(1 + 2C'_{j+1})\|p\|_{1+j,q}. \qquad (48)$$

With $K_{j+1} := \max(1, C_{j+1} \cdot d^{-1})(1 + 2C'_{j+1}) > 0$ we derive from (47) and (48) for $\underline{w} := \underline{w}_0 + \underline{w}_h$

$$\|\underline{w}\|_{2+j,q} \leq K_{j+1}\lambda\|p\|_{1+j,q}. \qquad (49)$$

Since by (10)

$$\|t_0\|_{1+j,q} = \frac{\lambda}{1 + \lambda\mu}\|p_0\|_{1+j,q} \leq \lambda(1 + 2C'_{j+1})\|p\|_{1+j,q}$$

we get from (46) and (10) for $t := t_0 + t_h$

$$\|t\|_{1+j,q} \leq K_{j+1}\lambda\|p\|_{1+j,q}. \qquad (50)$$

If we put now $\underline{u}_\lambda := \underline{v} + \underline{w}$ and $p_\lambda := p - \mu t$ we derive from (32), (49) and (50) estimate (40). We put $\underline{u}_0 := \underline{v}$ and $p_0 := p$. Then $\underline{u}_\lambda - \underline{u}_0 = \underline{w}$ and $p_\lambda - p_0 = -\mu t$ and by (49), (50) and (32) we derive (41).

Uniqueness: In case $\lambda = 0$ (37) reduces to (31) and uniqueness follows from Theorem 8. Assume now that $\lambda > 0$ and that $\underline{u}_\lambda^{(i)} \in \underline{H}^{2+j,q}(G)$ and $p_\lambda^{(i)} \in H^{1+j,q}(G) \cap L_0^q(G)$ $(i = 1, 2)$ are solutions of (37). Put $\underline{z} := \underline{u}_\lambda^{(1)} - \underline{u}_\lambda^{(2)} \in \underline{H}^{2+j,q}(G)$ and $\pi := p_\lambda^{(1)} - p_\lambda^{(2)} \in H^{1+j,q}(G) \cap L_0^q(G)$. Further, $\underline{z} = \left(\underline{u}_\lambda^{(1)} - \underline{a}\right) - \left(\underline{u}_\lambda^{(2)} - \underline{a}\right) \in \underline{H}_0^{1,q}(G) \cap \underline{H}^{2+j,q}(G)$, $\operatorname{div} \underline{z} = \lambda\pi$ and

$$\mu\langle\nabla\underline{z}, \nabla\underline{\varphi}\rangle + \langle\pi, \operatorname{div}\underline{\varphi}\rangle = 0 \qquad \forall\underline{\varphi} \in \underline{H}_0^{1,q'}(G). \tag{51}$$

Let now $s \in C_0^\infty(G)$ and $\underline{\varphi} := \nabla s \in \underline{H}^{1,q'}(G)$. Since

$$\langle\nabla\underline{z}, \nabla\underline{\varphi}\rangle = -\langle\underline{z}, \Delta\underline{\varphi}\rangle = -\langle\underline{z}, \Delta\nabla s\rangle = \langle\operatorname{div}\underline{z}, \Delta s\rangle$$

and from (51) we get (observe: $\operatorname{div}\underline{z} = \lambda\pi$)

$$0 = \mu\langle\operatorname{div}\underline{z}, \Delta s\rangle + \langle\underline{\pi}, \Delta s\rangle = \left(\mu + \frac{1}{\lambda}\right)\langle\operatorname{div}\underline{z}, \Delta s\rangle = 0.$$

This is true even for all $s \in H_0^{2,q'}(G)$ which proves $\operatorname{div}\underline{z} \in \underline{B}_0^q(G)$. Further, by (51)

$$\langle\nabla\underline{z}, \nabla\underline{\varphi}\rangle = -\frac{1}{\lambda\mu}\langle\operatorname{div}\underline{z}\operatorname{div}\underline{\varphi}\rangle \qquad \underline{\varphi} \in \underline{H}_0^{1,q'}(G). \tag{52}$$

Since $-\frac{1}{\lambda\mu} \in \mathbb{R} \setminus \{1, 2\}$ by [10, Theorem 1.2], it follows $\underline{z} \in \underline{H}_0^{1,\tilde{q}}(G)$ for all $1 < \tilde{q} < \infty$. For $\underline{\varphi} := \underline{z} \in \underline{H}_0^{1,2}(G)$ by (49)

$$\|\nabla\underline{z}\|_2^2 = -\frac{1}{\lambda\mu}\|\operatorname{div}\underline{z}\|_2^2 \le 0.$$

Therefore $\underline{z} = 0$ and $\lambda\pi = \operatorname{div}\underline{z} = 0$. □

The method of proof of the following theorem is similar to that one used for the proof of Theorem 4.3 in [7].

Theorem 11 *Let* $1 < q < \infty$, *let* $j \in \mathbb{N}_0$ *and* $\partial G \in C^{2+j}$. *Let* $\underline{g} \in \underline{H}^{j,q}(G)$ *and let* $\varrho > -1$. *Then there exists* $\underline{u} \in \underline{H}_0^{1,q}(G) \cap \underline{H}^{2+j,q}(G)$ *such that*

$$\begin{cases} \langle\nabla\underline{u}, \nabla\underline{\varphi}\rangle + \varrho\langle\operatorname{div}\underline{u}, \operatorname{div}\underline{\varphi}\rangle = \langle\underline{g}, \underline{\varphi}\rangle \qquad \forall\underline{\varphi} \in \underline{H}_0^{1,q'}(G) \\ \textit{or equivalently} \\ -\Delta\underline{u} - \varrho\nabla\operatorname{div}\underline{u} = \underline{g} \end{cases} \tag{53}$$

Further, there is a constant $K_j(\varrho) = K(j, \varrho, G) > 0$ *such that*

$$\|\underline{u}\|_{2+j,q} \leq K_j(\varrho)\|g\|_{j,q}. \tag{54}$$

Proof Let $\underline{w} \in \underline{H}_0^{1,q}(G)$ be the solution of

$$\langle\nabla\underline{w}, \nabla\underline{\varphi}\rangle = \langle\underline{g}, \underline{\varphi}\rangle \qquad \forall\underline{\varphi} \in \hat{\underline{H}}_0^{1,q'}(G).$$

By Theorem 1 $\underline{w} \in \underline{H}_0^{1,q}(G)\cap\underline{H}^{2+j,q}(G)$. Applying Theorem 8 with $\underline{f} := -\Delta\underline{w}$, $\mu = 1$, $\underline{a} = 0$, $g = 0$ leads to $\underline{v} \in \underline{H}_0^{1,q}(G) \cap \underline{H}^{2+j,q}(G)$ with $\operatorname{div}\underline{v} = 0$ and $p \in H^{1+j,q}(G) \cap L_0^q(G)$ such that

$$\langle\nabla\underline{v}, \nabla\underline{\varphi}\rangle + \langle p, \operatorname{div}\underline{\varphi}\rangle = \langle -\Delta\underline{w}, \underline{\varphi}\rangle = \langle\nabla\underline{w}, \nabla\underline{\varphi}\rangle = \langle\underline{g}, \underline{\varphi}\rangle \qquad \forall\underline{\varphi} \in \underline{H}_0^{1,q'}(G) \tag{55}$$

By (2)

$$\|\underline{w}\|_{2+j,q} \leq C'_{j+1}\|g\|_{j,q}$$

and by (32)

$$\|\underline{v}\|_{2+j,q} + \|p\|_{1+j,q} \leq F_j\|\Delta\underline{w}\|_{j,q} \leq F_j\|\underline{g}\|_{j,q}. \tag{56}$$

Since $\operatorname{div}\underline{v} = 0$ we see trivially

$$\langle\nabla\underline{v}, \nabla\underline{\varphi}\rangle + \varrho\langle\operatorname{div}\underline{v}, \operatorname{div}\underline{\varphi}\rangle = \langle\nabla\underline{v}, \nabla\underline{\varphi}\rangle \qquad \forall\underline{\varphi} \in \underline{H}_0^{1,q'}(G) \tag{57}$$

According Theorem 3 we split $p \in H^{1+j,q}(G) \cap L_0^q(G)$, $p = p_0 + p_h$, where $p_0 = \Delta s \in A^q(H)$, $s \in H_0^{2,q}(G) \cap H^{3+j,q}(G)$ and $p_h \in B_0^q(G) \cap H^{1+j,q}(G)$. By (10)

$$\|\Delta s\|_{1+j,q} + \|p_h\|_{1+j,q} \leq (1 + 2C'_j)\|p\|_{1+j,q}. \tag{58}$$

Let $\underline{v}_0 := \nabla s \in \underline{H}_0^{1,q}(G) \cap \underline{H}^{2+j,q}(G)$. Then

$$\langle\nabla\underline{v}_0, \nabla\underline{\varphi}\rangle = \langle\operatorname{div}\underline{v}_0, \operatorname{div}\underline{\varphi}\rangle = \langle\Delta s, \operatorname{div}\underline{\varphi}\rangle \qquad \forall\underline{\varphi} \in \underline{H}_0^{1,q'}(G).$$

Therefore

$$\langle\nabla\underline{v}_0, \nabla\underline{\varphi}\rangle + \varrho\langle\operatorname{div}\underline{v}_0, \operatorname{div}\underline{\varphi}\rangle = \langle(1 + \varrho)\Delta s, \operatorname{div}\underline{\varphi}\rangle.$$

We put $\underline{z}_0 := \frac{1}{1+\varrho}\underline{v}_0$. Then

$$\langle\nabla\underline{z}_0, \nabla\underline{\varphi}\rangle + \varrho\langle\operatorname{div}\underline{z}_0, \operatorname{div}\underline{\varphi}\rangle = \langle\Delta s, \operatorname{div}\underline{\varphi}\rangle \qquad \forall\underline{\varphi} \in \underline{H}_0^{1,q'}(G) \tag{59}$$

and by (58)

$$\|\underline{z}_0\|_{2+j,q} \le \frac{1}{1+\varrho}\|\underline{v}_0\|_{2+j,q} \le \frac{1+2C'_{j+1}}{1+\varrho}\|p\|_{1+j,q}. \tag{60}$$

In the proof of Theorem 10 we have shown that $\varrho Z_q + I : B_0^q(G) \cap H^{1+j,q}(G) \to B_0^q(G) \cap H^{1+j,q}(G)$ is bijective and with a constant $C_\varrho > 0$ holds

$$C_\varrho \|p + \varrho Z_q p\|_{1+j,q} \ge \|p\|_{1+j,q} \qquad \forall p \in B_0^q(G) \cap H^{1+j,q}(G). \tag{61}$$

Therefore there is a unique $\pi \in B_0^q(G) \cap H^{1+j,q}(G)$ such that

$$\pi + \varrho Z_q \pi = p_h.$$

Let $\underline{t} := \underline{\mathrm{T}}_q \pi \in \underline{H}_0^{1,q}(G) \cap \underline{H}^{2+j,q}(G)$, that is

$$\langle \nabla \underline{t}, \nabla \underline{\varphi} \rangle = \langle \pi, \operatorname{div} \underline{\varphi} \rangle = -\langle \nabla \pi, \underline{\varphi} \rangle \qquad \forall \underline{\varphi} \in \underline{H}_0^{1,q'}(G).$$

By (2) and (61)

$$\|\underline{t}\|_{2+j,q} \le C'_{j+1}\|\pi\|_{j,q} \le C'_{j+1} C_\varrho \|\pi + \varrho Z_q \pi\|_{1+j,q} = C'_{j+1} C_\varrho \|p_h\|_{1+j,q}. \tag{62}$$

Since $\operatorname{div} \underline{t} = Z_q \pi$ we see

$$\langle \nabla \underline{t}, \nabla \underline{\varphi} \rangle + \varrho \langle \operatorname{div} \underline{t}, \operatorname{div} \underline{\varphi} \rangle = \langle \pi + \varrho Z_q \pi, \operatorname{div} \varphi \rangle = \langle p_h, \operatorname{div} \underline{\varphi} \rangle \qquad \forall \underline{\varphi} \in H_0^{1,q'}(G). \tag{63}$$

Let $\underline{u} := \underline{v} + \underline{z}_0 + \underline{t} \in \underline{H}_0^{1,q}(G) \cap \underline{H}^{2+j,q}(G)$. By (57), (59) and (63) and finally (55) we see

$$\begin{aligned} \langle \nabla \underline{u}, \nabla \underline{\varphi} \rangle + \varrho \langle \operatorname{div} \underline{u}, \operatorname{div} \varphi \rangle &= \langle \nabla \underline{v}, \nabla \underline{\varphi} \rangle + \langle \Delta s, \operatorname{div} \underline{\varphi} \rangle + \langle p_h, \operatorname{div} \underline{\varphi} \rangle = \\ &= \langle \nabla \underline{v}, \nabla \underline{\varphi} \rangle + \langle p, \operatorname{div} \underline{\varphi} \rangle = \langle \nabla \underline{w}, \nabla \underline{\varphi} \rangle = \langle \underline{g}, \underline{\varphi} \rangle \qquad \forall \underline{\varphi} \in \underline{H}_0^{1,q}(G). \end{aligned}$$

Combining (56), (58), (60) and (62) leads to (54). Uniqueness: Let $\underline{u}^{(i)} \in \underline{H}_0^{1,q}(G) \cap \underline{H}^{2+j,q}(G)$ be solutions of (53). Let $\underline{u} := \underline{u}^{(1)} - \underline{u}^{(2)} \in \underline{H}_0^{1,q}(G) \cap \underline{H}^{2+j,q}(G)$. Then

$$\langle \nabla \underline{u}, \nabla \underline{\varphi} \rangle = -\varrho \langle \operatorname{div} \underline{u}, \operatorname{div} \underline{\varphi} \rangle \qquad \forall \underline{\varphi} \in \underline{H}_0^{1,q'}(G). \tag{64}$$

We proceed similarly to the proof of Theorem 10. Let $s \in C_0^\infty(G)$ and $\underline{\varphi} := \nabla s$. Then we see again

$$\langle \operatorname{div} \underline{u}, \Delta s \rangle = \langle \nabla \underline{u}, \nabla \underline{\varphi} \rangle = -\varrho \langle \operatorname{div} \underline{u}, \Delta s \rangle,$$

that is

$$(1+\varrho)\langle \operatorname{div} \underline{u}, \Delta s\rangle = 0 \qquad \forall s \in C_0^\infty(G).$$

Since $1+\varrho > 0$ and $C_0^\infty(G)$ dense in $H_0^{2,q'}(G)$, it follows

$$\langle \operatorname{div} \underline{u}, \Delta s\rangle = 0 \qquad \forall s \in H_0^{2,q'}(G)$$

whence $\operatorname{div} \underline{u} \in B_0^q(G)$. Because of (60) and since $-\varrho \in \mathbb{R}\backslash\{1,2\}$ again by Theorem 1.2 of [10] follows $\underline{u} \in \underline{H}_0^{1,\tilde{q}(G)}$ for all $1 < \tilde{q} < \infty$, especially for $\tilde{q} = 2$. Then, by (60) with $\underline{\varphi} := u$

$$\|\nabla \underline{u}\|_2^2 = -\varrho \| \operatorname{div} \underline{u}\|_2^2 \le 0.$$

□

References

1. S. Agmon, A. Douglis, L. Nirenberg, Estimates near the boundary of solutions of elliptic partial differential equations satisfying general boundary conditions II. Comm. Pure Appl. Math. 17, 35–92 (1964)
2. H. Beirão da Veiga, A new approach to the L^2-regularity theorems for linear stationary non homogeneous Stokes systems. Portugal. Math. 54(3), 271–286 (1997)
3. G. P. Galdi, *An Introduction to the Mathematical Theory of the Navier-Stokes Equations. Vol. I: Linearized Steady Problems*. First ed. Berlin-Heidelberg-New York, Springer (1994)
4. R. Müller, Das schwache Dirichletproblem in L^q für den Bipotentialoperator in beschränkten Gebieten und Aussengebieten. Bayreuth. Math. Schr. 49, 115–211 (1995)
5. C. G. Simader, *On Dirichlet's Boundary Value Problem*. Lecture Notes in Mathematics, vol. 268. Berlin, Heidelberg, New York, Springer-Verlag (1972)
6. C. G. Simader, H. Sohr, *The Dirichlet Problem for the Laplacian in Bounded and Unbounded Domains*. Pitman Research Notes in Mathematics Series, vol. 360, Harlow, Addison Wesley Longman Ltd. (1996)
7. C. G. Simader, St. Weyers, An operator related to the Cosserat spectrum. Applications. Analysis (Munich) 26(1), 169–198 (2006)
8. M. Stark, Das schwache Dirichletproblem in L^q für das Differentialgleichungssystem $\Delta \underline{v} = \nabla p$ und die Lösung der Divergenzgleichung. Bayreuth. Math. Schr. 70, 1–35 (2004)
9. R. Temam, *Navier-Stokes Equations. Theory and Numerical Analysis*. North-Holland Publishing Company, Amsterdam (1977)
10. St. Weyers, L^q-solutions to the Cosserat spectrum in bounded and exterior domains. Analysis (Munich) 26(1), 85–167 (2006)

Large Time Behavior of Energy in Some Slowly Decreasing Solutions of the Navier-Stokes Equations

Zdeněk Skalák

Abstract We study the large time behavior of the energy in some slowly decreasing global strong solutions of the Navier-Stokes equations. We show as the main result of the paper that the energy concentrates in the lowest frequencies, while the middle and high frequencies die out as time goes to infinity.

Keywords Navier-Stokes equations · Strong solution · Asymptotic behavior · Energy concentration

1 Introduction

Let $\Omega \subseteq \mathbf{R}^3$ be uniformly regular of the class C^3 (see [5]) for which the Poincaré inequality does not hold (that is for every $c > 0$ there exists $v \in W_0^{1,2}(\Omega)$ such that $||\nabla v|| \leq c||v||$). We study the large time behavior of global strong solutions of the Navier-Stokes equations in Ω:

$$\frac{\partial u}{\partial t} - \Delta u + u \cdot \nabla u + \nabla p = 0 \quad \text{in } \Omega \times (0, \infty), \tag{1}$$

$$\nabla \cdot u = 0 \quad \text{in } \Omega \times (0, \infty), \tag{2}$$

$$u|_{t=0} = u_0, \tag{3}$$

$$u = 0 \quad \text{on } \partial\Omega \times (0, \infty), \tag{4}$$

where $u = u(x,t) = (u_1(x,t), u_2(x,t), u_3(x,t))$ and $p = p(x,t)$ denote the unknown velocity vector field and the pressure and $u_0 = u_0(x) = (u_{01}(x), u_{02}(x), u_{03}(x))$ is a given initial velocity vector field.

There are plenty of papers dealing with various aspects of the large time behavior of solutions of the Navier-Stokes equations, let us mention, for example, [6, 7, 10, 9]. In this paper we try to contribute to the study of the large time behavior of global

Z. Skalák (✉)
Czech Technical University, 16629, Prague 6, Czech Republic
e-mail: skalak@mat.fsv.cvut.cz

R. Rannacher, A. Sequeira (eds.), *Advances in Mathematical Fluid Mechanics*,
DOI 10.1007/978-3-642-04068-9_31,

strong solutions. Let $u_0 \in D(A^{1/4})$. Then the function $u \in C([0,\infty); D(A^{1/4})) \cap C((0,\infty); D(A)) \cap C^1((0,\infty); L^2_\sigma)$ is called a global strong solution of (1), (2), (3), and (4) if $u(0) = u_0$ and $\mathrm{d}u/\mathrm{d}t + Au + P_\sigma(u\cdot\nabla u) = 0$ for every $t > 0$ (see [5], where the existence and asymptotic decays of global strong solutions were thoroughly studied). We will show as our main result that there exist global strong solutions in which middle and high frequencies disappear for times approaching infinity and so the energy concentrates asymptotically only in the lowest frequencies. More precisely, if Ω is such a domain for which the Poincaré inequality does not hold then there exist global strong solutions u of (1), (2), (3), and (4) such that

$$\lim_{t\to\infty} \frac{||E_\lambda u(t)||}{||u(t)||} = 1 \tag{5}$$

for every $\lambda > 0$, where $\{E_\lambda;\ \lambda \geq 0\}$ is the resolution of identity of the Stokes operator A.

The proof of (5) is based on the results from [5] and [13]: It was proved in [5] that if u is a global strong solution of (1), (2), (3), and (4) then

$$||A^\alpha u(t)|| = O(t^{-\alpha}),\ t \to \infty \tag{6}$$

for every $\alpha \in (0,1]$. The following theorem from [14] describes to some extent the asymptotic behavior of frequencies in global strong solutions of (1), (2),(3), and (4).

Definition 1 Let u be a global strong solution of (1), (2), (3), and (4), $u \neq 0$. Let $\beta \in (0,1)$. We define

$$C(\beta) = \overline{\lim_{t\to\infty}} \frac{\|A^\beta u(t)\|}{\|u(t)\|}, \quad L_\beta = \{\lambda \geq 0;\ \overline{\lim_{t\to\infty}} \frac{|||E_\lambda u(t)|||_\beta}{|||u(t)|||_\beta} > 0\},$$
$$M_\beta = \{\lambda \geq 0;\ \underline{\lim_{t\to\infty}} \frac{|||E_\lambda u(t)|||_\beta}{|||u(t)|||_\beta} > 0\}, \quad B(\beta) = \underline{\lim_{t\to\infty}} \frac{\|A^\beta u(t)\|}{\|u(t)\|},$$
$$M = \{\lambda \geq 0;\ \underline{\lim_{t\to\infty}} \frac{\|E_\lambda u(t)\|}{\|u(t)\|} > 0\}, \quad L = \{\lambda \geq 0;\ \overline{\lim_{t\to\infty}} \frac{\|E_\lambda u(t)\|}{\|u(t)\|} > 0\},$$
$$A_\beta = \inf M_\beta, \quad D_\beta = \inf L_\beta, \quad A = \inf M, \quad D = \inf L.$$

Theorem 1 *Let $\Omega \subseteq \mathbf{R}^3$ be uniformly regular of the class C^3, u be a global strong solution of (1), (2), (3), and (4), $u \neq 0$. Let further $C(\beta_0) < \infty$ for some $\beta_0 \in [1/2, 1)$. Let $\beta \in (0, \beta_0]$. Then $0 \leq D \leq A < \infty$ and*

$$A = A_\beta = C(\beta)^{1/\beta}, \quad D = D_\beta = B(\beta)^{1/\beta}. \tag{7}$$

Further,

$$\lim_{t\to\infty} \frac{|||E_\mu u(t)|||_\beta}{|||u(t)|||_\beta} = \lim_{t\to\infty} \frac{||E_\mu u(t)||}{||u(t)||} = 1, \quad \text{if } \mu > A, \tag{8}$$

$$\overline{\lim_{t\to\infty}} \frac{|||E_\mu u(t)|||_\beta}{|||u(t)|||_\beta} = \overline{\lim_{t\to\infty}} \frac{||E_\mu u(t)||}{||u(t)||} = 1, \quad \text{if } \mu > D, \tag{9}$$

$$\underline{\lim_{t\to\infty}} \frac{|||E_\mu u(t)|||_\beta}{|||u(t)|||_\beta} = \underline{\lim_{t\to\infty}} \frac{||E_\mu u(t)||}{||u(t)||} = 0, \quad \text{if } \mu < A, \tag{10}$$

$$\lim_{t\to\infty} \frac{|||E_\mu u(t)|||_\beta}{|||u(t)|||_\beta} = \lim_{t\to\infty} \frac{||E_\mu u(t)||}{||u(t)||} = 0, \quad \text{if } \mu < D. \tag{11}$$

Moreover, if $\mu \in (D, A)$ and $\varepsilon \in (0, \mu)$, then

$$\overline{\lim_{t\to\infty}} \frac{||(E_{\mu+\varepsilon} - E_{\mu-\varepsilon})u(t)||}{||u(t)||} = \overline{\lim_{t\to\infty}} \frac{|||(E_{\mu+\varepsilon} - E_{\mu-\varepsilon})u(t)|||_\beta}{|||u(t)|||_\beta} = 1. \tag{12}$$

Suppose that the assumptions of Theorem 1 are satisfied. Then only one of the four disjunct possibilities can occur: (1) $0 = D = A$, (2) $0 = D < A$, (3) $0 < D = A$ and (4) $0 < D < A$. There are some open questions connected with Theorem 1, especially, we do not know whether (2) and (4) can occur in some solutions. If it was so, then (as follows from (12)) the particular solution would exhibit a complex asymptotic behavior, at least as far as the asymptotic dynamics of its frequencies is concerned. It was proved in [12] and [11] that if Ω is a smooth bounded domain then for any solution u always $0 < D = A$ and A can be equal only to any eigenvalue of the Stokes operator. So in this case the energy of u concentrates asymptotically in eigenfunctions associated with some eigenvalue of the Stokes operator. If Ω is such a domain for which the Poincaré inequality holds then $E_\lambda = 0$ for all positive sufficiently small λ and using Remark 1 we get that either $0 < D = A$ or $0 < D < A$. However, it is not again clear, if both of these two conditions really occur. If Ω is such a domain for which the Poincaré inequality does not hold then we are not able to exclude any of the possibilities (1)–(4). On the other hand we know for certain that either $0 < D = A$ or $0 < D < A$ occur for and only for exponentially decreasing global strong solutions (as was shown in [14]). To prove our main result, we will show that there exist global strong solutions in which $C(\beta) = D = A = 0$ for every $\beta \in [1/2, 1)$. Equation (5) will then be an immediate consequence of (8).

Remark 1 It is known (see [4]) that $\lambda \in \sigma(A)$ (spectrum of A) if and only if $E_{\lambda-\varepsilon} \neq E_{\lambda+\varepsilon}$ for every positive ε. It follows from (12) that $[D, A] \subseteq \sigma(A)$. Thus, the values D and A cannot be separated by the points belonging to the resolvent set of A.

In the paper we use the standard notations: $L^q = L^q(\Omega)$, $q \geq 1$, denotes the Lebesgue spaces with the norm $\| \cdot \|_q$. If $q = 2$, we denote $\| \cdot \| = \| \cdot \|_2$ and $(\cdot, \cdot)$ is the inner product in L^2. $W^{s,q} = W^{s,q}(\Omega)$, $s \geq 0$, $q \geq 2$, are the usual Sobolev spaces with the norm $\| \cdot \|_{s,q}$. $L^2_\sigma = L^2_\sigma(\Omega)$, resp. $W^{1,2}_{0,\sigma} = W^{1,2}_{0,\sigma}(\Omega)$, is defined as the closure of $C^\infty_{0,\sigma}(\Omega) = \{\varphi \in C^\infty_0(\Omega)^3; \nabla \cdot \varphi = 0\}$ in $L^2(\Omega)^3$, resp. $W^{1,2}(\Omega)^3$. P_σ denotes the orthogonal projection of $L^2(\Omega)^3$ onto L^2_σ. A is the Stokes operator on L^2_σ. A is positive selfadjoint with a dense domain $D(A) \subset L^2_\sigma$. If Ω is a uniform C^2-domain or if $\Omega = \mathbf{R}^3$ then $D(A) = W^{1,2}_{0,\sigma}(\Omega) \cap W^{2,2}(\Omega)^3$ and $Au = -P_\sigma \Delta u$ for every $u \in D(A)$. Let A^α, $\alpha \in \mathbf{R}$, denote the fractional powers of

A and $\{e^{-At}; t \geq 0\}$ be the Stokes semigroup generated by $-A$. $\{E_\lambda; \lambda \geq 0\}$ is the resolution of identity of A. $|||\cdot|||_\beta$, $\beta \geq 0$, denotes the graph norm which is defined as $|||\cdot|||_\beta = \|A^\beta \cdot\| + \|\cdot\|$.

2 Presentation and Proof of Main Results

The following theorem is the main result of this paper.

Theorem 2 *Suppose that $\Omega \subseteq \mathbf{R}^3$ is uniformly regular of the class C^3 for which the Poincaré inequality does not hold. Let $u_0 \in D(A^{1/4})$ and let either $||e^{-At}u_0|| \geq ct^{-1/8}$ or $c_1 t^{-\gamma} \geq ||e^{-At}u_0|| \geq c_2 t^{-(1+5\gamma)/8+\varepsilon}$ for every $t \geq t_0$, where $\gamma \in (0, 1/3)$, $\varepsilon \in (0, (1+5\gamma)/8 - \gamma)$ and c, c_1, c_2 and t_0 are positive constants. Let u be a global strong solution of (1), (2), (3), and (4). Then $A = D = 0$, where A and D are the numbers from Definition 1 and Theorem 1 and so*

$$\lim_{t\to\infty} \frac{||E_\lambda u(t)||}{||u(t)||} = 1 \tag{13}$$

for every $\lambda > 0$. Moreover,

$$\lim_{t\to\infty} \frac{|||E_\lambda u(t)|||_\beta}{|||u(t)|||_\beta} = 1 \text{ and } \lim_{t\to\infty} \frac{\|A^\beta u(t)\|}{\|u(t)\|} = 0 \tag{14}$$

for every $\lambda > 0$ and every $\beta \in (0, 1)$.

Remark 2 It seems to be quite difficult to characterize in some way the initial conditions u_0 which satisfy the assumptions in Theorem 2. On the other hand a construction of such u_0 is an easy task, see Appendix for one example.

The proof of Theorem 2 is a consequence of (6), Theorem 1 and the following Lemmas 2 and 3 and is postponed to the end of this section. The proofs of Lemmas 1, 2 and 3 are based on the techniques developed in [2, 3, 8]. Lemma 1 was proved in [2] (see Theorem 1.1) for the case of 3 and 4-dimensional domains and for suitable nonzero functions f on the right hand side of (1). The estimate (15) in our version of Lemma 1 is slightly better than the one derived in [2] due to the application of (6). In Lemmas 2 and 3 we present some lower estimates of the decay rates of the global strong solutions of (1), (2), (3), and (4). We use the technique from [3], where analogical results were presented for the case $\Omega = \mathbf{R}^\mathbf{n}$. The estimates from Lemmas 2 and 3 are weaker than the ones in [3] due to the fact that we work with general domains Ω. See in this connection Lemma 7 from [3] or Lemma 5.1 from [1].

Lemma 1 *Let $\alpha > 0$, $u_0 \in D(A^{1/4})$ and $||e^{-At}u_0|| \leq c_1 t^{-\alpha}$ for every $t > 0$, where c_1 is a positive constant. If u is a global strong solution of (1), (2), (3), and (4) then there exists $c > 0$ such that*

$$||u(t)|| \leq ct^{-\min(\alpha, 1/2)} \tag{15}$$

for every $t > 0$.

Proof Let the assumptions of Lemma 1 be satisfied. Using the idea by Schonbek of decomposing the frequency domain into two time dependent subsets, we obtain for any $r(t) > 0$

$$\frac{d}{dt}||u(t)||^2 + r(t)||u(t)||^2 \leq r(t)||E_{r(t)}u(t)||^2,\ t > 0. \tag{16}$$

We continue with the estimate of the right hand side of (16):

$$\begin{aligned}
&||E_{r(t)}u(t)|| \\
&\leq ||E_{r(t)}e^{-At}u_0|| + \int_0^t ||E_{r(t)}A^{1/2}e^{-A(t-s)}A^{-1/2}P_\sigma(u(s)\cdot\nabla u(s))||ds \\
&\leq ||e^{-At}u_0|| + \int_0^t \left(\int_0^{r(t)} \lambda e^{-2\lambda(t-s)}d||E_\lambda A^{-1/2}P_\sigma \mathrm{div}(u(s)u(s))||^2\right)^{1/2} ds \\
&\leq ||e^{-At}u_0|| + r(t)^{1/2}\int_0^t ||A^{-1/2}P_\sigma \mathrm{div}(u(s)u(s))||ds.
\end{aligned}$$

Since

$$||A^{-1/2}P_\sigma \mathrm{div}(uu)|| \leq c||uu|| = c||u||_4^2 \leq c||A^{3/8}u||^2 \leq c||u||^{1/2}||A^{1/2}u||^{3/2},$$

we get

$$\begin{aligned}
||E_{r(t)}u(t)|| &\leq ||e^{-At}u_0|| + cr(t)^{1/2}\int_0^t ||u(s)||^{1/2}||A^{1/2}u(s)||^{3/2}ds \\
&\leq ||e^{-At}u_0|| + cr(t)^{1/2}||u||^{1/2}_{L^2(0,t;L^2(\Omega))}||u||^{3/2}_{L^2(0,t;D(A^{1/2}))} \\
&\leq ||e^{-At}u_0|| + cr(t)^{1/2}t^{1/4}.
\end{aligned} \tag{17}$$

Inserting the last inequality into (16), we get

$$\frac{d}{dt}||u(t)||^2 + r(t)||u(t)||^2 \leq cr(t)\left(||e^{-At}u_0||^2 + r(t)t^{1/2}\right),\ t > 0. \tag{18}$$

Putting $r(t) = \beta/t$, where $\beta > 0$ is sufficiently large and multiplying (18) by t^β, we get for $t > 0$

$$||u(t)||^2 \leq ct^{-\beta}\left(\int_0^t \beta s^{\beta-1}||e^{-As}u_0||^2 ds + \beta^2/(\beta - 1/2)t^{\beta-1/2}\right). \tag{19}$$

Since $||e^{-As}u_0|| \to 0$ for $s \to \infty$, it follows from (19) that $||u(t)|| \to 0$ for $t \to \infty$ for any $u_0 \in D(A^{1/4})$. If we use the assumption $||e^{-At}u_0|| \leq ct^{-\alpha},\ t > 0$, we obtain

$$||u(t)||^2 \leq c(\beta t^{-2\alpha} + \beta^2/(\beta - 1/2)t^{-1/2}),\ t > 0. \tag{20}$$

If $\alpha \leq 1/4$ than $||u(t)|| \leq ct^{-\alpha}$ and the lemma is proved. Suppose that $\alpha > 1/4$. Then $||u(t)|| \leq ct^{-1/4}$ and repeating the proof from the beginning we get instead of (17) that

$$||E_{r(t)}u(t)|| \leq ||e^{-At}u_0|| + cr(t)^{1/2}\int_0^t ||u(s)||^{5/4}||Au(s)||^{3/4}ds \leq$$
$$||e^{-At}u_0|| + cr(t)^{1/2}(c + \int_1^t s^{-5/16}s^{-3/4}ds) \leq ||e^{-At}u_0|| + cr(t)^{1/2}.$$

So inserting the last estimate into (16) we arrive at the inequality

$$||u(t)||^2 \leq c(\beta t^{-2\alpha} + \beta^2/(\beta-1)t^{-1}),\ t > 0, \tag{21}$$

which completes the proof of the lemma. □

Lemma 2 *Let* $u_0 \in D(A^{1/4})$ *and* $||e^{-At}u_0|| \geq c_1 t^{-1/8}$ *for every* $t \geq t_0$, *where* c_1 *and* t_0 *are positive constants. If* u *is a global strong solution of (1), (2), (3), and (4) then there exists* $c > 0$ *such that* $||u(t)|| \geq ct^{-1/8}$ *for every* $t \geq 1$.

Proof Put $v = e^{-At}u_0$ and $w = u - v$. Proceeding in the same way as in the proof of Lemma 1 we get

$$\frac{d}{dt}||w(t)||^2 + r(t)||w(t)||^2 \leq r(t)||E_{r(t)}w(t)||^2 + ||\nabla v(t)||||u(t)||^{5/4}||Au(t)||^{3/4} \tag{22}$$

for every $t > 0$ and

$$||E_{r(t)}w(t)|| \leq cr(t)^{1/2}\int_0^t ||u(s)||^{5/4}||Au(s)||^{3/4}ds.$$

Putting again $r(t) = \beta/t$, $\beta > 0$ sufficiently large, we arrive at the inequality

$$||w(t)||^2 \leq ct^{-\beta}\int_0^t \tau^{\beta-2}\left(\int_0^\tau ||u(s)||^{5/4}||Au(s)||^{3/4}ds\right)^2 d\tau +$$
$$ct^{-\beta}\int_0^t \tau^\beta ||\nabla v(\tau)||||u(\tau)||^{5/4}||Au(\tau)||^{3/4}d\tau. \tag{23}$$

If we use the decay rates $||u(s)|| = o(1)$, $s \to \infty$, $||Au(s)|| = O(s^{-1})$, $s \to \infty$ and $||\nabla v(\tau)|| = O(\tau^{-1/2})$, $\tau \to \infty$, we get

$$\int_0^t \tau^{(\beta-2)}\left(\int_0^\tau ||u(s)||^{5/4}||Au(s)||^{3/4}ds\right)^2 d\tau = o(t^{\beta-1/2}),\ t \to \infty$$

and

$$\int_0^t \tau^\beta ||\nabla v(\tau)||||u(\tau)||^{5/4}||Au(\tau)||^{3/4}d\tau = o(t^{\beta-1/4}),\ t \to \infty$$

and so $||w(t)|| = o(t^{-1/8}),\ t \to \infty$. It concludes the proof of the lemma. □

Lemma 3 *Let $\gamma \in (0, 1/3)$, $u_0 \in D(A^{1/4})$ and $c_1 t^{-(1+5\gamma)/8+\varepsilon} \leq ||e^{-At}u_0|| \leq c_2 t^{-\gamma}$ for every $t \geq t_0$, where c_1, c_2 and t_0 are positive constants and $\varepsilon \in (0, (1+5\gamma)/8 - \gamma)$. If u is a global strong solution of (1), (2), (3), and (4), then there exists $c > 0$ such that $||u(t)|| \geq ct^{-(1+5\gamma)/8+\varepsilon}$ for every $t \geq 1$.*

Proof In the same way as in Lemma 2 one can derive (23). Let firstly $\gamma \in (0, 1/5]$. Using Lemma 1, the assumptions of Lemma 3 and the fact that $||\nabla v(\tau)|| \leq c\tau^{-1/2}$, $\tau > 0$, we get that

$$\int_0^\tau ||u(s)||^{5/4}||Au(s)||^{3/4} ds \leq c\tau^{1/4-5\gamma/4}, \ \tau > 0.$$

It follows elementarily from (23) that $||w(t)|| \leq ct^{-(1+5\gamma)/8}$ and the proof follows. If $\gamma \in (1/5, 1/3)$ then

$$\int_0^\tau ||u(s)||^{5/4}||Au(s)||^{3/4} ds \leq c < \infty, \quad \tau > 0$$

and we get again from (23) that $||w(t)|| \leq ct^{-(1+5\gamma)/8}$. The proof of the lemma follows immediately. □

Proof We are now prepared to prove Theorem 2. Let the assumptions of Theorem 2 be satisfied. It follows from Lemmas 2 and 3 that there exists $c > 0$ such that $||u(t)|| \geq ct^{-1/3}$ for every $t \geq 1$. Using (6) we get that $C(\beta) = 0$ for every $\beta \in [1/2, 1)$, where $C(\beta)$ was defined in Definition 1. Therefore, the equalities $A = D = 0$ follow from (7) in Theorem 1 and the validity of (13) and (14) follows immediately from (7) and (8). □

Acknowledgments Financial support of the Ministry of Education of the Czech Republic of the project MSM 6840770003 is gratefully acknowledged.

Appendix

Let $e^{-n} > a_n > a_{n+1} > 0$ for every $n \in N$. Choose $u_n \in H(E_{a_n} - E_{a_{n+1}})$ such that $||u_n|| = 1/n^2$. Then

$$||e^{-At}u_n|| \geq e^{-a_n t}/n^2$$

for every $n \in N$. Put $u_0 = \sum_{n=1}^{\infty} u_n$. Obviously, $u_0 \in D(A^{1/4})$ and

$$||e^{-At}u_0|| \geq ||e^{-At}u_n||$$

for every $n \in N$. Let c and α be arbitrary fixed positive numbers and put $K = \bigcup_{k=1}^{\infty} \left[(cek^2)^{1/\alpha}, e^k\right]$. Then there exists $t_0 > 0$ such that $[t_0, \infty) \subset K$. If $t \in K$, then $t \in \left[(cen^2)^{1/\alpha}, e^n\right]$ for some $n \in N$ and

$$||e^{-At}u_0|| \geq ||e^{-At}u_n|| \geq e^{-a_n t}/n^2 \geq e^{-1}/n^2 \geq c/t^\alpha.$$

Thus, $||e^{-At}u_0|| \geq c/t^\alpha$ for every $t \in [t_0, \infty)$. Moreover, multiplying u_0 by a sufficiently small constant and using the existence theorem from [5], we have the existence of a global strong solution of the Navier-Stokes equations with the initial condition u_0. By the choice $\alpha = 1/8$ we see that u_0 satisfies the assumptions of Theorem 2.

References

1. Borchers, W., Miyakawa, T.: Algebraic L^2 decay for Navier-Stokes flows in exterior domains. Acta Math. **165**, 189–227 (1990)
2. Borchers, W., Miyakawa, T.: L^2 decay for Navier-Stokes flows in unbounded domains, with application to exterior stationary flows. Arch. Rational Mech. Anal. **118**, 273–295 (1992)
3. Kajikiya, R., Miyakawa, T.: On L^2 decay of weak solutions of the Navier-Stokes equations in $\mathbf{R}^\mathbf{n}$. Math. Z. **192**, 135–148 (1986)
4. Kato, H.: *Perturbation Theory for Linear Operators.* Springer, Berlin, Heidelberg, New-York (1980)
5. Kozono, H., Ogawa, T.: Global strong solution and its decay properties for the Navier-Stokes equations in three dimensional domains with non-compact boundaries. Math. Z. **216**, 1–30 (1994)
6. Miyakawa, T.: On upper and lower bounds of rates of decay for nonstationary Navier-Stokes flows in the whole space. Hiroshima Math. J. **32**, 431–462 (2002)
7. Nečasová, Š., Rabier, P.J.: On the time decay of the solutions of the Navier-Stokes system. J. Math. Fluid Mech. **8**, 1–16 (2006)
8. Schonbek, M.E.: L^2 decay for weak solutions of the Navier-Stokes equations. Arch. Ration. Mech. Anal. **88**, 209–222 (1985)
9. Schonbek, M.E.: Lower bounds of rates of decay for solutions to the Navier-Stokes equations. J. Amer. Math. Soc. **4**, 423–449 (1991)
10. Schonbek, M.E.: Asymptotic behavior of solutions to the three-dimensional Navier-Stokes equations. Indiana Univ. Math. J. **41**, 809–823 (1992)
11. Skalák, Z.: Asymptotic behavior of modes in weak solutions to the homogeneous Navier-Stokes equations. WSEAS Trans. Math. **5**, 280–288 (2006)
12. Skalák, Z.: Asymptotic dynamics of modes in solutions to the homogeneous Navier-Stokes equations. Eng. Mech. **13**, 177–190 (2006)
13. Skalák, Z.: Some aspects of the asymptotic dynamics of solutions of the homogeneous Navier-Stokes equations in general domains. J. Math. Fluid Mech. doi 10.1007/s00021-009-0300-y
14. Skalák, Z.: Large time behavior of energy in exponentially decreasing solutions of the Navier-Stokes equations. Nonlinear Analysis **71**, 593–603 (2009)

A Selected Survey of the Mathematical Theory of 1D Flows

Ivan Straškraba

Abstract The global behavior of compressible fluid in a tube is investigated under physically realistic assumptions. Different initial and boundary conditions are discussed. General conditions are established, under which the fluid stabilizes to an equilibrium state. Motivation for this study is that apriori recognition of stabilization of the fluid is important in many situations arising in industrial applications. This contribution may serve as a partial survey of some results in this respect.

Keywords Compressible Navier-Stokes equations · Global behavior · Large data

1 Introduction and Main Results

Compressible flow in tubes is an important phenomenon appearing in many branches of industry as construction of hydraulic machinery, pipelines, power stations, etc. Contemporary technology requires more and more preliminary qualitative and quantitative analysis taking into account real physical aspects which cannot be ignored since expected dynamics of the system is highly oscillatory and sensitive to fluctuations in the model setting.

In the present paper we try to partially map the developments in the global in time analysis of compressible fluids in tubes under different external conditions.

To be more concrete, let us consider the system called shortly "barotropic", described by equations

$$\varrho(u_t + uu_x) + p(\varrho)_x - (\mu(\varrho)u_x)_x = \varrho f, \tag{1}$$

$$\varrho_t + (\varrho u)_x = 0, \quad x \in (0, 1), \quad t > 0, \tag{2}$$

$$u(0, t) = u(1, t) = 0, \quad t > 0, \tag{3}$$

$$u(x, 0) = u_0(x), \quad \varrho(x, 0) = \varrho_0(x), \quad x \in [0, 1]. \tag{4}$$

I. Straškraba (✉)
Mathematical Institute, Academy of Sciences of the Czech Republic, 11567 Prague 1, Czech Republic
e-mail: strask@math.cas.cz

R. Rannacher, A. Sequeira (eds.), *Advances in Mathematical Fluid Mechanics*, 581
DOI 10.1007/978-3-642-04068-9_32, © Springer-Verlag Berlin Heidelberg 2010

The unknown quantities are the density ϱ and the velocity u. The given data are the functional dependence $p = p(\varrho)$ between the density ϱ and the pressure p, viscosity coeffcient $\mu = \mu(\varrho)$ as a function of density (can be a constant which may play a decisive role), external force density $f = f(x)$ (+possibly an oscillatory part $\Delta f(x, t)$), and the initial distribution u_0 and ϱ_0 of the velocity and the density, respectively.

The problem of the behavior of $(\varrho(\cdot), u(\cdot))$ as t tends to infinity reaches to the papers like [7]. Further details about history of the global behavior of fluids can be found in the basic monograph of [1].

One of the principle questions is, whether, when, given regular initial data, the solution of (1), (2), (3), and (4) stabilizes to a rest state.

There are several variants of the initial boundary value problems. For example, instead of the Dirichlet boundary conditions, the free boundary condition

$$(\mu(\varrho)u_x - p(\varrho))|_{x=\ell(t)} = p_\Gamma(t) \quad \text{for } t > 0. \tag{5}$$

The function $\ell = \ell(t)$ may be, in one space dimension, reduced to, say 1, if we accept the Lagrangian mass coordinates. But if we hope to have, in the future, if there is any, attempt to attack any more dimensional problem, then it seems to be convenient to insist on more general formulation whether or not it is temporally rational.

If the temperature is included, then we consider for example, the system

$$\begin{aligned}
&\varrho_t + (\varrho u)_x = 0\\
&(\varrho u)_t + (\varrho u^2)_x - \mu u_{xx} + p_x = \varrho f\\
&\Big(\varrho\big(e + \frac{u^2}{2}\big)\Big)_t + \Big(\varrho u\big(e + \frac{u^2}{2}\big) + up\Big)_x - (\mu u u_x)_x + q_x = \varrho f u.
\end{aligned} \tag{6}$$

We may use the given constitutive relations

$$p(\varrho, e) = (\gamma - 1)\varrho e, \quad q(e, e_x) = -\kappa(e)e_x, \tag{7}$$

and the initial conditions for unknowns (ϱ, u, e) with boundary conditions as

$$u(0, t) = u(1, t) = e_x(0, t) = e_x(1, t) = 0. \tag{8}$$

An important question is, whether the limit in any of these cases exists or at least the $\omega-$limit set

$$\{(\varrho(t), u(t), \text{etc.}); t > 0\} \tag{9}$$

is compact in an appropriate space like $L^q(0, 1)$ (w.r.t. the space variable x), or whatever is possible to prove.

In an optimal case we expect a unique limit which is a steady state solution. For Eqs. (1), (2), and (3) with Dirichlet boundary condition for the velocity the steady state is given by the equations

$$u_s = 0 \quad \text{for all } x, t,$$
$$p(\varrho_s)_x = \varrho_s f \quad \text{for all } x, \qquad \int_0^1 \varrho_s\, dx = \int_0^1 \varrho_0\, dx. \tag{10}$$

It is known that this problem can have multiple solutions when we allow the density ϱ vanish for some $x \in (0, 1)$. The conditions under which it occurs or not are known (see [2, 8, 4, 5, 3, 9, 10]).

The regular case is when

$$\varrho_s(x) \geq \underline{\varrho_s} > 0,\ \ x \in (0, \ell). \tag{11}$$

Then the following theorem has been proved in [16]

Theorem 1 *Let the steady state density ϱ_s satisfy* (11), $p(\cdot)$ *be continuous, increasing and such that* $p(0) = 0$, $p(\infty) = \infty$, $p' \in L_{\text{loc}}(R^+)$, $rp'(r) = O(1)$ *as* $r \to 0^+$, *and* $p(r) = O(r^{\gamma_0})$ *as* $r \to 0^+$ *for some* $0 < \gamma_0 \leq 1$. *(Evidently, these conditions are satisfied for the most popular state functions* $p(r) = p_1 r^\gamma$ *with* $p_1 > 0$ *and* $\gamma > 0$.) *For simplicity assume* μ *to be a constant. Then, if in addition,* $1/p' \in L^\infty_{\text{loc}}(R^+)$ *and the initial density* ϱ_0 *belongs to* $W^1(0, 1)$, *then the following global in time estimate holds true:*

$$\begin{aligned}
&\|\varrho(\cdot, t) - \varrho_s(\cdot)\|_{L^2(0,1)} + \|u(\cdot, t)\|_{L^2(0,1)} \\
&\leq \text{const}\, e^{-at}\left(\|\varrho_0 - \varrho_s\|_{L^2(0,1)} + \|u_0\|_{L^2(0,1)} + \int_0^t e^{a\tau}\|\Delta f(\cdot, \tau)\|_{L^2(0,1)}\, d\tau\right) \\
&\qquad\qquad \text{for all } t \geq 0.
\end{aligned} \tag{12}$$

Here, a *is a constant depending on the magnitude of the data, and* Δf *is eventual oscillation component of the external force density which we initially assumed to be zero.*

On the other hand, the situation with vacuums is more singular, since at least an important estimate

$$\inf_{x,t} \varrho(x, t) > 0 \tag{13}$$

cannot be valid if we hope that $\varrho(x, t) \to \varrho_s(x)$ in a stronger sense when $\{\varrho_s(x) = 0\} \neq \emptyset$. The latter case is treated in our paper [11], which has been actually completely presented at the conference in Estoril, and we are able to prove the following theorem:

Theorem 2 *Let conditions concerning the function* $p(\cdot)$ *be as in the preceding Theorem and let there exist a unique steady density* ϱ_s *such that meas* $\{x; \varrho_s(x) = 0\} = 0$.

Then for any $t_0 \geq 0$ *there are positive constants* K *and* α *dependent only on the data such that*

$$\int_0^1 \left(\varrho u^2 + \varrho \Pi(\varrho, \varrho_s) + |\varrho - \varrho_s|^\beta\right) dx \tag{14}$$
$$\leq K\left\{e^{-\alpha(t-t_0)}\left[1 + \int_{t_0}^t e^{\alpha s}\|\Delta f(s)\|_2^2\, ds\right] + \int_t^\infty \|\Delta f(s)\|_2^2\right\}^{1/2},$$

where

$$\Pi(r,s) = \int_s^r \frac{p(\sigma) - p(s)}{\sigma^2}\, d\sigma, \quad r, s \geq 0$$

and $\beta \geq 2$ *if* $\gamma < 2$ *or* $\beta \geq \gamma$ *if* $\gamma \geq 2$ *is arbitrary but fixed.*

The method of proof is, among other, based on uniform apriori estimates, construction of an intermediate "quasistationary density" $\overline{\varrho}$ given by

$$p(\overline{\varrho}(x,t)) = \int_0^1 p(\varrho(\xi,t))\, d\xi + \int_0^1 \int_\xi^1 \varrho(\eta,t) f(\eta)\, d\eta\, d\xi - \int_x^1 \varrho(\xi,t) f(\xi)\, d\xi. \tag{15}$$

Notice, that $\overline{\varrho}$ satisfies

$$p(\overline{\varrho})_x = \varrho f, \quad x \in (0,1),\ t > 0, \quad \int_0^1 p(\overline{\varrho})\, dx = \int_0^1 p(\varrho)\, dx,\ t > 0. \tag{16}$$

Then, a "two layers" Lyapunov analysis is used. This means, that first we construct an auxiliary Lyapunov like functional containing the function $\overline{\varrho}$ (which is, of course determined by the data only implicitly since constructed via ϱ). Then by a series of estimates it is shown that this function has some appropriate asymptotics in time, and then it is used for the functional which has features of a real Lyapunov functional that can be used to establish the global in time rate of convergence in the sense of the preceding theorem.

2 Further Cases

Let us mention further variations of the model problem. First, we are able to modify our approach to the free boundary problem. The corresponding result in the regular case is given in our paper [17].

If it is assumed that the fluid leaks into vacuum, then the decay rate of the evolutionary solution is described in [20].

Another variant mentioned already above, is the problem with density dependent viscosity. When $\mu(\cdot)$ is regular and $\mu(0) > 0$, then we get the result quite analogous to the regular case for $\mu = \text{const}$.

On the other hand, when $\mu(0) = 0$ we have only conditional result assuming that the kinetic energy over layers given by $(x, t) \in (0, 1) \times (t - 1, t)$ decays to zero as t goes to infinity, but we have no idea how to prove that it is really true. The reason is that the dissipation of energy near possible vacuums is approaching zero which causes that we have no more tool to use it as before. There is a hope that careful balance of behavior of $\mu(\cdot)$ near zero with other data could give some result.

We use basically the method applied in [9, 10, 13] for the case of constant viscosity, but there is a considerable obstacle in the weakness of the dissipation term when the density is small if we allow the dependence of the viscosity be such that $\mu = \mu(\varrho)$, where ϱ can be zero at some points regardless how it is regular. Since, as it has been observed in [13], the density may asymptotically vanish even if it is strictly positive at any finite time we cannot in general to get the global estimates for density as in [14]. To overcome this obstacle we derive weaker uniform L^q estimates and find the play of the growth of function $p(\cdot)$ and that of $\mu(\cdot)$ that allows us to pass all steps analogously as in [14] under certain condition on the kinetic energy decay.

For related results for constant viscosity we refer to [15, 19] in one dimension, and to [4, 9, 10] in 2 or 3 dimensional case. The global existence results for the problem (1), (2), (3), and (4) with arbitrarily large data can be found in [6, 12, 18].

To be more detailed, let us present what we are able to prove.

First, let us make the following fundamental assumptions:

$$p(\cdot) \in C^1_{\mathrm{loc}}(0, \infty),\ p(0+) = p(0) = 0,\ p'(r) > 0 \quad \text{for} \quad r > 0,$$
$$\lim_{r\to\infty} p(r) = \infty; \tag{17}$$

$$\text{there exist } c > 0,\ \gamma > 1,\ 0 \le \alpha \le \gamma \text{ such that } c^{-1} r^{\alpha} \le \mu(r) \le c r^{\alpha}, \tag{18}$$
$$c^{-1} r^{\gamma} \le cr + r \int_1^r \frac{p(s)}{s^2}\, ds,$$
$$p(r) \le c(1 + r + r \int_1^r \frac{p(s)}{s^2}\, ds) \text{ for } r \ge 0;$$

$$\mu(\cdot) \in C^1_{\mathrm{loc}}(0, \infty) \cap C_{\mathrm{loc}}([0, \infty)),\ \mu(r) > 0 \qquad \text{for} \qquad r > 0; \tag{19}$$

$$f = f(x), \qquad f \in L^{\infty}(0, 1); \tag{20}$$

$$u_0 \in H^1(0, 1),\ u_0(0) = u_0(1) = 0,\ \varrho_0 \in H^1(0, 1),\ 0 < \alpha_0 \le \varrho_0(x)$$
$$\text{for } x \in [0, 1]. \tag{21}$$

The stationary problem corresponding to (1), (2), (3), and (4) is given by the equations

$$(\varrho u^2)_x + p(\varrho)_x - (\mu(\varrho)u_x)_x = \varrho f, \tag{22}$$
$$(\varrho u)_x = 0, \tag{23}$$
$$u(0) = u(1) = 0, \tag{24}$$
$$\int_0^1 \varrho \,\mathrm{d}x = 1, \qquad \varrho \ge 0. \tag{25}$$

While in the case of μ away from zero the only solutions of (22), (23), (24), and (25) are rest states $(u, \varrho) = (0, \varrho)$, this is not evident if $\mu(0) = 0$ [14]. Nevertheless, under certain conditions, we are able to show that despite of possible vacuums in the limit as $t \to \infty$ the evolution solutions stabilize to a rest state. The following two theorems give an essence of the merit.

Theorem 3 *Let the assumptions* (17)*,* (18)*,* (19)*,* (20)*, and* (21) *be satisfied. If*

$$\lim_{t\to\infty} \int_{t-1}^{t} \int_0^1 \varrho u^2 dx ds = 0,$$

then for any $q \in [1, \gamma)$ *and* $t_n \to \infty$ *there is a subsequence* $\{s_n\} \subset \{t_n\}$ *such that* $|\varrho(s_n) - \varrho_\infty|_q \to 0$ *as* $n \to \infty$*, where*

$$p(\varrho_\infty)_x = \varrho_\infty f, \quad \varrho_\infty \in W^{1,\infty}(0, 1), \tag{26}$$

$$\int_0^1 \varrho_\infty \, dx = \int_0^1 \varrho_0 \, dx := M_0. \tag{27}$$

If the rest state is uniquely determined (see [4, 3] for the optimal uniqueness conditions for the rest state)*, then*

$$\lim_{t\to\infty} \|\varrho(t) - \varrho_\infty\|_{L^q(0,1)} = 0, \tag{28}$$

and

$$\lim_{t\to\infty} \int_0^1 \varrho(t)|u(t)|^2 \, dx = 0. \tag{29}$$

Theorem 4 *Let, in addition to assumptions* (17)*,* (18)*,* (19)*,* (20)*, and* (21)*,* $\mu(0) > 0$*. Then, for any* $q \in [1, \infty)$ *and* $t_n \to \infty$*, there is a subsequence* $\{s_n\} \subset \{t_n\}$ *such that* $\|\varrho(s_n) - \varrho_\infty\|_{L^q(0,1)} \to 0$ *as* $n \to \infty$*, with* ϱ_∞ *satisfying* (27) *we have* (28)*, and* (29) *holds true.*

Remark In fact all steps can be retraced with a weak solution of the regularity $\varrho, \varrho u, \varrho u^2, p(\varrho), \mu(\varrho)u_x \in L^1((0, 1) \times (0, T))$ for any $T > 0$ if the generalized formulation is applied. Then the smoothness of data can be relaxed as for example in [18], where an appropriate existence theorem for weak solutions is given.

Acknowledgments This work was supported by the Grant Agency of the Czech Republic, Grant No. 201/108/0012 and by the Academy of Sciences of the Czech Republic, Institutional Research Plan No. AV0Z1090503.

References

1. S.N. Antontsev, A.V. Kazhikhov, V.N. Monakhov, *Boundary Value Problems of Mechanics of Nonhomogeneous Fluids (Russian)*. Nauka, Novosibirsk (1983)
2. H. Beirão da Veiga, An L^p−theory for the n−dimensional, stationary compressible Navier-Stokes equations, and the incompressible limit for compressible fluids, the equilibrium solutions. Commun. Math. Phys. **109**, 229–248 (1987)
3. E. Erban, On the static-limit solutions to the Navier-Stokes equations of compressible flow. J. Math. Fluid Mech. **3**, 393–407 (2001)
4. E. Feireisl, H. Petzeltová, On the zero-velocity-limit solutions to the Navier-Stokes equations of compressible flow. Manuscripta Math. **97**, 109–116 (1998)
5. E. Feireisl, H. Petzeltová, Large-time behaviour of solutions to the Navier-Stokes equations of compressible flow. Arch. Ration. Mech. Anal. **150**, 77–96 (1999)
6. S. Jiang, Global smooth solutions of the equations of a viscous, heat-conducting, one-dimensional gas with density-dependent viscosity. Math. Nachr. **190**, 169–183 (1998)
7. Ja.I. Kanel, On a model one-dimensional system for gas flow (Russian). Diff. Uravnenija **4**(4), 721–734 (1968)
8. V. Lovicar, I. Straškraba, Remark on cavitation solutions of stationary compressible Navier-Stokes equations in one dimension. Czechoslovak Math. J. **41**, 653–662 (1991)
9. A. Novotný, I. Straškraba, Stabilization of weak solutions to compressible Navier-Stokes equations. J. Math. Kyoto Univ. **40**(2), 217–245, (2000)
10. A. Novotný, I. Straškraba, Convergence to equilibria for compressible Navier-Stokes equations with large data. Ann. Mat. Pura Appl. **179**(4), 263–287 (2001)
11. P. Penel, I. Straškraba, Lyapunov analysis and stabilization to the rest state for solutions to the 1D barotropic compressible Navier-Stokes equations. CR Acad. Sci. Paris **395**(1), 67–72 (2007)
12. Sh. Smagulov, U.B. Zhanasbaeva, Estimates for the solution of a difference scheme for an equation of a barotropic gas with variable viscosity (Russian). DAN SSSR **299**(5), 1066–1068 (1988), also in Soviet Math. Dokl. **37**(2), 529–531 (1988)
13. I. Straškraba, Asymptotic development of vacuums for 1-D Navier-Stokes equations of compressible flow. Nonlin. World **3**, 519–535 (1996)
14. I. Straškraba, Global analysis of 1-D Navier-Stokes equations with density dependent viscosity. In: *Navier-Stokes Equations and Related Nonlinear Problems* (H. Amann et al., eds.), VSP, Utrecht, 371–389 (1998)
15. I. Straškraba, Large time behavior of solutions to compressible Navier-Stokes equations. In: *Navier-Stokes Equations: Theory and Numerical Methods* (R. Salvi, ed.), Pitman Res. Notes in Math. 388, Longman, Edinburgh, 125–138 (1998)
16. I. Straškraba, A. Zlotnik, On a decay rate for 1D-viscous compressible barotropic equations. J. Evol. Equat. **2**, 69–96 (2002)
17. I. Straškraba, A. Zlotnik, Global behavior of 1d-viscous compressible barotropic fluid with a free boundary and large data. J. Math. Fluid Mech. **5**, 119–143 (2003)
18. A.A. Zlotnik, A.A. Amosov, Generalized solutions in the large of equations of one-dimensional motion of a viscous barotropic gas (Russian). Doklady AN SSSR **299**(6), 1303–1307 (1988)
19. A.A. Zlotnik, N.Z. Bao, Properties and asymptotic behavior of solutions of a problem for one-dimensional motion of viscous barotropic gas (Russian). Mat. Zametki **55**(5), 51–68 (1994)
20. A. Zlotnik, Global behavior of 1-D viscous barotropic flows with free boundary and selfgravitation. Math. Meth. Appl. Sci. **26**, 671–690 (2003)

A Numerical Method for Nonstationary Stokes Flow

Werner Varnhorn

Abstract We consider a first order implicit time stepping procedure (Euler scheme) for the non-stationary Stokes equations in a cylindrical domain $(0, T) \times G$ where $G \subset \mathbb{R}^3$ is smoothly bounded. Using energy estimates we can prove optimal convergence properties in the Sobolev spaces $H^m(G)$ $(m = 0, 1, 2)$ uniformly for $t \in [0, T]$, provided that the solution of the Stokes equations has a certain degree of regularity. For the solution of the resulting Stokes resolvent boundary value problems we use a representation in form of hydrodynamical volume and boundary layer potentials, where the unknown source densities of the latter can be determined from uniquely solvable boundary integral equations' systems. For the numerical computation of the potentials and the solution of the boundary integral equations a boundary element method of collocation type is used. The main purpose of this paper is to combine these steps to an efficient numerical algorithm for non-stationary Stokes flow and illustrate its accuracy via different simulations of a model problem.

Keywords Stokes equations · Time stepping · Stokes resolvent potentials · Boundary element methods

1 Introduction and Notation

Let $T > 0$ be given and $G \subset \mathbb{R}^3$ be a bounded domain with a sufficiently smooth compact boundary S. In $(0, T)$ we consider the non-stationary Stokes equations

$$D_t v - \nu \Delta v + \nabla p = F, \quad \operatorname{div} v = 0, \quad v_{|S} = 0, \quad v_{|t=0} = v_0 \,. \tag{1}$$

These equations describe the linearized motion of a viscous incompressible fluid: The vector $v = (v_1(t, x), \; v_2(t, x), \; v_3(t, x))$ represents the velocity field and the scalar $p = p(t, x)$ the kinematic pressure function of the fluid at time $t \in (0, T)$ and at position $x \in G$. The constant $\nu > 0$ is the kinematic viscosity, and the

W. Varnhorn (✉)
Fachbereich Mathematik, Universität Kassel, 34109 Kassel, Germany
e-mail: varnhorn@mathematik.uni-kassel.de

R. Rannacher, A. Sequeira (eds.), *Advances in Mathematical Fluid Mechanics*,
DOI 10.1007/978-3-642-04068-9_33,

external force density F together with the initial velocity v_0 are the given data. The condition div $v = 0$ means the incompressibility of the fluid, and $v = 0$ on the boundary S expresses the no-slip condition, i. e. the fluid adheres to the boundary.

It is the aim of the present paper to develop a method for the numerical solution of (1). This method consists of three steps. In the first step, the implicit Euler method in time is used to transform (1) into a finite number of certain boundary value problems. In the second step, these boundary value problems are studied with methods of hydrodynamical potential theory. This leads to a representation of their solutions consisting of volume and surface potentials, where the unknown densities have to be determined from systems of boundary integral equations. In the third step, for the discretization of the boundary integral equations and the numerical computation of the potentials a boundary element method of collocation type and suitable quadrature methods are used.

Let us consider the following semi-discrete first order Euler approximation scheme for the Stokes equations (1): Setting

$$h = T/N > 0, \qquad t_k = k\,h \quad (k = 0, 1, \ldots, N)\,,$$

we approximate the solution v, p of (1) at time t_k by the solution $v^k, p^k (k = 1, 2, \ldots, N)$ of the following equations in G:

$$\begin{aligned} (v^k - v^{k-1})h^{-1} - \nu \Delta v^k + \nabla p^k &= h^{-1} \int_{(k-1)h}^{kh} F(t)dt\,, \\ \operatorname{div} v^k = 0, \qquad v^0 = v_0, &\qquad v^k_{|s} = 0\,. \end{aligned} \tag{2}$$

Here F and v_0 are the given data. Thus for every $k = 1, 2, 3, \ldots, N$ we have to determine in G the solution v^k, q^k of the Stokes resolvent boundary value problem

$$(\lambda - \Delta)v^k + \nabla q^k = F^{\lambda,k-1}, \qquad \operatorname{div} v^k = 0, \qquad v^k_{|s} = 0,$$

with $\lambda = (\nu h)^{-1} > 0$, $q^k = p^k/\nu$, and

$$F^{\lambda,k-1}(x) = \lambda \left(v^{k-1}(x) + \int_{(k-1)h}^{kh} F(t,x)dt \right). \tag{3}$$

Using methods of hydrodynamical potential theory we find a representation of the solution v^k, q^k in the form

$$(v^k(x), q^k(x)) = (V_\lambda F^{\lambda,k-1})(x) + (D_\lambda \Psi)(x), \quad x \in G\,. \tag{4}$$

Here $V_\lambda F^{\lambda,k-1}$ is a hydrodynamical volume potential with density $F^{\lambda,k-1}$, and $D_\lambda \Psi$ is a double layer potential with an unknown source density Ψ, which can be determined from the boundary integral equations

$$-(V_\lambda^* F^{\lambda,k-1})(x) \;=\; \frac{1}{2}\Psi(x) + (D_\lambda^*\Psi)(x) - (P_N\Psi)(x)\,, \quad x \in S\,. \tag{5}$$

Here the superscript $*$ indicates the velocity part of the above potentials. $(D_\lambda^*\Psi)$ is the direct value of the hydrodynamical double layer potential for the velocity, and P_N is a one-dimensional perturbation operator, which ensures that the solution Ψ is unique in the space of continuous vector fields on S. For the spatial discretization of (5) we use a boundary element method of collocation type as described in [6, 5].

At this point, let us introduce our notations. Throughout the paper, $G \subset \mathbb{R}^3$ is a bounded domain having a compact boundary S of class C^2. In the following, all functions are real valued. As usual, $C_0^\infty(G)$ denotes the space of smooth functions defined in G with compact support, and $L^2(G)$ is equipped with scalar product and norm

$$(f,g) \;=\; \int_G f(x)g(x)dx\,, \qquad ||f|| \;=\; (f,f)^{\frac{1}{2}}\,,$$

respectively. For functions $f, g \in L^2(G)$ we need the following well-known relations:

$$\begin{aligned} (f-g, f+g) &= ||f||^2 - ||g||^2, \\ (f-g, 2f) &= ||f||^2 - ||g||^2 + ||f-g||^2, \\ 2(f,g) \le 2\,||f||\,||g|| &\le ||f||^2 + ||g||^2\,. \end{aligned} \tag{6}$$

The Sobolev space $H^m(G)$ $(m = 0, 1, 2, \ldots)$ is the space of functions f such that $D^\alpha f \in L^2(G)$ for all $\alpha = (\alpha_1, \alpha_2, \alpha_3) \in \mathbb{N}_0^3$ with $|\alpha| = \alpha_1 + \alpha_2 + \alpha_3 \le m$. Its norm is denoted by

$$||f||_m \;=\; ||f||_{H^m(G)} \;=\; \left(\sum_{|\alpha|\le m} ||D^\alpha f||^2\right)^{\frac{1}{2}}\,,$$

where $D^\alpha = D_1^{\alpha_1} D_2^{\alpha_2} D_3^{\alpha_3}$ with $D_k = \frac{d}{dx_k}$ $(k = 1, 2, 3)$ is the distributional derivative. The completion of $C_0^\infty(G)$ with respect to $||\cdot||_m$ is denoted by $H_0^m(G)(H_0^0(G) = H^0(G) = L^2(G))$. If $f \in H_0^1(G)$, in particular, we have Poincaré's inequality

$$||f||^2 \;\le\; C_G||\nabla f||^2\,, \tag{7}$$

where here the constant $\lambda_1 = C_G^{-1}$ is the smallest eigenvalue of the Laplace operator $-\Delta$ in G with zero boundary condition.

The spaces $C_0^\infty(G)^3$, $L^2(G)^3$, $H^m(G)^3, \ldots$ are the corresponding spaces of vector fields $u = (u_1, u_2, u_3)$. Here norm and scalar product are denoted as in the scalar case, i. e. for example,

$$(u, v) = \sum_{k=1}^{3}(u_k, v_k)\,, \quad ||u|| \;=\; (u, u)^{\frac{1}{2}} \;=\; \int\limits_G |u(x)|^2 dx^{\,\frac{1}{2}}\,,$$

where $|u(x)| = (u_1(x)^2 + u_2(x)^2 + u_3(x)^2)^{\frac{1}{2}}$ is the Euclidian norm of $u(x) \in \mathbb{R}^3$. The completion of

$$C^\infty_{0,\sigma}(G)^3 \;=\; \{u \in C^\infty_0(G)^3 | \text{div}\, u \;=\; 0\}$$

with respect to the norm $|| \cdot ||$ and $|| \cdot ||_1$ are important spaces for the treatment of the Stokes equations. They are denoted by

$$H(G)^3\,, \quad V(G)^3\,,$$

respectively. In $H^1_0(G)^3$ and $V(G)^3$ we also use

$$(\nabla u, \nabla v) \;=\; \sum_{k,j=1}^{3}(D_k u_j, D_k v_j)\,, \qquad ||\nabla u|| \;=\; (\nabla u, \nabla u)^{\frac{1}{2}}$$

as scalar product and norm. Moreover, we need the B-valued spaces $C^m(J, B)$ and $H^m(a, b, B)$, $m \in \mathbb{N}_0$, where $J \subset \mathbb{R}$ with $a, b \in \mathbb{R}$ $(a < b)$, and where B is any of the spaces above. In case of $C^0(,)$ we simply write $C(,)$, and we use $H, V, H^m, \ldots$ instead of $H(G), V(G), H^m(G), \ldots$, if the domain of definition is clear from the context. Finally, let

$$P : L^2(G)^3 \;\longrightarrow\; H(G)^3 \tag{8}$$

denote the orthogonal projection. Then we have

$$L^2(G)^3 \;=\; H(G)^3 \oplus \{v \in L^2(G)^3 | v \;=\; \nabla p \text{ for some } p \in H^1(G)\}\,,$$

with means

$$(u, \nabla p) \;=\; 0 \quad \text{for all} \quad u \in V(G)^3 \quad \text{and} \quad p \in H^1(G)\,. \tag{9}$$

2 An Implicit Euler Scheme

Because the projection P from (8) commutes with the strong time derivative D_t, from the Stokes equations (1) we obtain the following evolution equations for the function $t \to v(t) \in H(G)^3$:

$$D_t v(t) - \nu P \Delta v(t) \;=\; PF(t)\,(t \in (0, T))\,, \qquad v(0) \;=\; v_0\,. \tag{10}$$

In this case, the condition div $v = 0$ and the boundary condition $v = 0$ on S are satisfied in the sense that we require $v(t) \in V(G)^3$ for all $t \in (0, T)$. Concerning the solvability of the evolution equations (10) it is known that for

$$v_0 \in H^2(G)^3 \cap V(G)^3 , \qquad F \in H^1(0, T, H(G)^3) \tag{11}$$

there is a unique solution v of (10) in G such that

$$v \in C([0, T], H^2(G)^3 \cap V(G)^3) ,\ D_t v \in C([0, T], H(G)^3) \cap L^2(0, T, H^1(G)^3), \tag{12}$$

and that there is some constant K depending only on G, ν, F, v_0 and not on $t \in [0, T]$ such that for all $t \in [0, T]$

$$\int_0^t ||\nabla D_\sigma v(\sigma)||^2 d\sigma \le K, \quad ||v(t)||_2 \le K, \quad ||D_t v(t)|| \le K. \tag{13}$$

Let us now consider the discrete equations under the weaker assumptions

$$v_0 \in H(G)^3 , \quad F \in L^2(0, T, H(G)^3) . \tag{14}$$

Using P as above and noting that $F = PF$ we obtain in $G(h = T/N > 0)$

$$(v^k - v^{k-1}) - h\nu P\Delta v^k \ = \int_{(k-1)h}^{kh} F(t)dt , \quad v^0 \ = \ v_0 . \tag{15}$$

It is known that under the above assumptions (14) there is a unique solution

$$v^k \in H^2(G)^3 \cap V(G)^3 \qquad (k = 1, 2, \dots , N) \tag{16}$$

of (15): If we define the Stokes operator A to be the extension of $-P\Delta$ in $H(G)^3$, then its domain of definition $D(A)$ is $H^2(G)^3 \cap V(G)^3$. Because $\lambda = (\nu h)^{-1} > 0$ belongs to the resolvent set of $-A$, the equations

$$v^k \ = \ (\lambda + A)^{-1} F^{\lambda,k-1} , \qquad F^{\lambda,k-1} \in H(G)^3$$

(see (12)) are uniquely solvable with $v^k \in H^2(G)^3 \cap V(G)^3$, as asserted.

To prove the convergence of the discrete equations (15) to the evolution equations (10) and to estimate the discretization error, we use the approach “stability + consistency → convergence”. Let us define

$$(\Pi v)\,(t_k) = v(t_k) - v(t_{k-1}) - \nu h P\Delta v(t_k)$$
$$\left(\Pi\{v^j\}\right)(t_k) = v^k - v^{k-1} - \nu h P\Delta v^k .$$

Then the discretization error

$$e^k \;=\; v^k - v(t_k) \tag{17}$$

satisfies the identity

$$e^k - e^{k-1} - \nu h P \Delta e^k \;=\; \big(\Pi\{v^j\}\big)(t_k) - (\Pi v)(t_k) \;=\; R^k, \tag{18}$$

which is used to obtain estimates of e^k in terms of the right hand side R^k ($\approx$ stability). Then the behavior of

$$\begin{aligned} R^k &= \int_{(k-1)h}^{kh} (D_t v(t) - \nu P \Delta v(t))dt - \{(v(t_k) - v(t_{k-1})) - h\nu P \Delta v(t_k)\} \\ &= \int_{(k-1)h}^{kh} -\nu P \Delta(v(t) - v(t_k))dt \\ &= -\nu P \Delta E^k \end{aligned} \tag{19}$$

as h tends to zero ($\approx$ consistency) follows from the regularity properties of the exact solution of the Stokes equations (1).

The next theorem describes the convergence properties of the implicit Euler scheme. Here the proposed C^2-regularity of the boundary S – necessary for the potential theoretical treatment of the resulting steady Stokes systems in the next step – can be weakened. A more detailed convergence analysis, including higher order schemes also for the non-linear equations, are given in [2, 4].

Theorem 1 *Let $T > 0$, $N \in \mathbb{N}$, and $G \subset \mathbb{R}^3$ be a bounded domain with a smooth boundary S of class C^2. Assuming (2), let v and $v^k (k = 1, 2, \ldots, N)$ denote the solution of (10) and (15), respectively. Then the discretization error e^k (see (17)) satisfies the following estimates:*

$$||e^k||^2 + \sum_{j=1}^{k} (h\nu||\nabla e^j||^2 + ||e^j - e^{j-1}||^2) \;\leq\; Kh^2,$$

$$||\nabla e^k||^2 + \sum_{j=1}^{k} (2(h\nu)^{-1}||e^j - e^{j-1}||^2 + \frac{1}{2}||\nabla(e^j - e^{j-1})||^2) \;\leq\; Kh\,.$$

Here the constant K depends only on G, ν, and the data. Moreover, we even have convergence with respect to the H^2-norm:

$$\max\{||e^k||_2 \mid k = 1, 2, \ldots, N\} \;=\; \circ(1) \;\; as \;\; h \longrightarrow 0 \;\; or \;\; N \longrightarrow \infty\,.$$

Proof From (18) and (19) we obtain for the defect e^k the identity

$$(e^k - e^{k-1}) - h\nu P \Delta e^k \;=\; -\nu P \Delta E^k\,. \tag{20}$$

Multiplying (20) scalar in L^2 by $2e^k$ and using (15) we obtain

$$||e^k||^2 \;-\; ||e^{k-1}||^2 \;+\; ||e^k - e^{k-1}||^2 \;+\; 2h\nu||\nabla e^k||^2 \;=\; 2\nu(\nabla E^k, \nabla e^k) \;\le\; 2\,(h\nu)^{\frac{1}{2}}||\nabla e^k||\,(h^{-1}\nu)^{\frac{1}{2}}||\nabla E^k|| \;\le\; h\nu||\nabla e^k||^2 + h^{-1}\nu||\nabla E^k||^2 \;=\; S_1 + S_2.$$

Because of

$$S_2 = h^{-1}\nu \left\| \int\limits_{(k-1)h}^{kh} \int\limits_{t}^{kh} D_\sigma \nabla v(\sigma) d\sigma dt \right\|^2 \le \nu \int\limits_{(k-1)h}^{kh} \left\| \int\limits_{(k-1)h}^{kh} |D_\sigma \nabla v(\sigma)| d\sigma \right\|^2 dt$$

$$\le \nu\, h \left\| \int\limits_{(k-1)h}^{kh} |\nabla v(\sigma)| d\sigma \right\|^2 \le \nu h^2 \int\limits_{(k-1)h}^{kh} ||D_\sigma \nabla v(\sigma)||^2 d\sigma\,,$$

we find

$$||e^k||^2 - ||e^{k-1}||^2 + ||e^k - e^{k-1}||^2 + h\nu||\nabla e^k||^2 \le \nu h^2 \int\limits_{(k-1)h}^{kh} ||D_\sigma \nabla v(\sigma)||^2 d\sigma \tag{21}$$

for all $k = 1, 2, \ldots, N$. Thus using $||e^0||^2 = 0$ and (13), the first estimate is proved. Next let us multiply (20) scalar in L^2 by $2(e^k - e^{k-1})$. Here we obtain

$$\begin{aligned}
&2||e^k - e^{k-1}||^2 + 2h\nu(\nabla e^k, \nabla(e^k - e^{k-1})) \\
&= 2||e^k - e^{k-1}||^2 + h\nu(||\nabla e^k||^2 - ||\nabla e^{k-1}||^2 + ||\nabla(e^k - e^{k-1})||^2) \\
&= 2\nu(\nabla E^k, \nabla(e^k - e^{k-1})) \\
&\le 2 \cdot \left(\frac{h\nu}{2}\right)^{\frac{1}{2}} ||\nabla(e^k - e^{k-1})|| \cdot (2h^{-1}\nu)^{\frac{1}{2}} ||\nabla E^k|| \\
&\le \frac{h\nu}{2}||\nabla(e^k - e^{k-1})||^2 + 2h^{-1}\nu||\nabla E^k||^2 \;=\; S_3 + 2S_2\,.
\end{aligned}$$

Using the above estimate for S_2 again, we have

$$2||e^k - e^{k-1}||^2 + h\nu(||\nabla e^k||^2 - ||\nabla e^{k-1}||^2) - \frac{h\nu}{2}||\nabla(e^k - e^{k-1})||^2$$

$$\leq 2\nu h^2 \int\limits_{(k-1)h}^{kh} ||D_\sigma \nabla v(\sigma)||^2 d\sigma \,,$$

hence

$$||\nabla e^k||^2 - ||\nabla e^{k-1}||^2 + 2(h\nu)^{-1}||e^k - e^{k-1}||^2 + \frac{1}{2}||\nabla(e^k - e^{k-1})||^2$$
$$\leq 2h \int\limits_{(k-1)h}^{kh} ||D_\sigma \nabla v(\sigma)||^2 d\sigma \,,$$

which implies the second estimate. Next we want to prove convergence with respect to the H^2-norm. From (20) we conclude

$$P\Delta e^k \;=\; (h\nu)^{-1}(e^k - e^{k-1}) + h^{-1} P\Delta E^k,$$

which implies

$$||P\Delta e^k||^2 \;\leq\; 2(h\nu)^{-2}||e^k - e^{k-1}||^2 + 2h^{-2}||P\Delta E^k||^2 \,. \tag{22}$$

By (3) we find the following estimate for the second term:

$$2h^{-2}||P\Delta E^k||^2 \leq 2h^{-2}\left\| \int\limits_{(k-1)h}^{kh} P\Delta(v(t) - v(t_k))dt \right\|^2$$
$$\leq 2 \max_{\substack{\sigma,\tau\in[0,T] \\ |\sigma-\tau|\leq h}} ||P\Delta(v(\sigma) - v(\tau))||^2$$
$$= \circ(1) \;\text{ as }\; h \longrightarrow 0\,.$$

It remains to show that also the first term of (22) tends to zero. Using

$$T^k \;=\; \frac{(e^k - e^{k-1})}{h} \qquad (k = 1, 2, \ldots, N)$$

for abbreviation, from (20) we obtain the identity

$$\begin{aligned} &T^k - T^{k-1} - h\nu P\Delta T^k \\ &= -h^{-1}\nu P\Delta \left\{ \int\limits_{(k-1)h}^{kh} (v(t) - v(t_k))dt - \int\limits_{(k-2)h}^{(k-1)h} (v(t) - v(t_{k-1}))dt \right\} \\ &= -h^{-1}\nu P\Delta G^k \,, \end{aligned}$$

where G^k is defined by the above term in brackets. Scalar multiplication in L^2 by $2T^k$ yields as above

$$||T^k||^2 - ||T^{k-1}||^2 + ||T^k - T^{k-1}||^2 + 2h\nu||\nabla T^k||^2 \;\le\; h\nu||\nabla T^k||^2 + h^{-3}\nu||\nabla G^k||^2, \tag{23}$$

hence

$$||T^k||^2 - ||T^{k-1}||^2 + ||T^k - T^{k-1}||^2 + h\nu||\nabla T^k||^2 \;\le\; h^{-3}\nu||\nabla G^k||^2 \,.$$

Because

$$G^k \;=\; -\int\limits_{(k-1)h}^{kh} \int\limits_{t}^{kh} (D_\sigma v(\sigma) - D_\sigma v(\sigma - h))d\sigma dt \,,$$

we find the estimate

$$||\nabla G^k||^2 \;\le\; h^3 \int\limits_{(k-1)h}^{kh} ||D_\sigma \nabla(v(\sigma) - v(\sigma - h))||^2 d\sigma \,.$$

Thus from (14) we obtain

$$||T^k||^2 - ||T^{k-1}||^2 + ||T^k - T^{k-1}||^2 + h\nu||\nabla T^k||^2 \;\le\; \nu \int\limits_{(k-1)h}^{kh} ||D_t \nabla(v(t) - v(t-h))||^2 dt \,,$$

and

$$\begin{aligned} &||T^k||^2 + \sum_{j=2}^{k}(||T^j - T^{j-1}||^2 + \nu h||\nabla T^j||^2) \\ &\le ||T^1||^2 + \nu \int\limits_{h}^{T} ||D_t \nabla(v(t) - v(t-h))||^2 dt \qquad (24) \\ &= \circ(1) \;\text{ as }\; h \longrightarrow 0 \,, \end{aligned}$$

because the integral vanishes as $h \to 0$, and because by (21) (note $||e^0|| = 0$)

$$||T^1||^2 = ||(e^1 - e^0)h^{-1}||^2 \le \nu \int_0^h ||D_t \nabla v(t)||^2 dt = \circ(1).$$

Thus (15) implies that also the first term of (22) tends to zero as $h \to 0$, hence $||P\Delta e^k||^2 = \circ(1)$ as $h \to 0$, and the asserted convergence with respect to the H^2-norm follows by means of Cattabriga's estimate. This proves the theorem. □

3 Hydrodynamical Potential Theory

Because every time step $t_k = kh$ $(k = 1, 2, \ldots, N \in \mathbb{N};\ h = \frac{T}{N} > 0)$ requires the solution of the boundary value problem (11), we consider for fixed h, k, and $\lambda = (h\nu)^{-1} > 0$ in G the system

$$(\lambda - \Delta)u + \nabla q = F, \quad \operatorname{div} u = 0, \quad u_{|s} = 0. \tag{25}$$

Let us define the formal differential operator of (1) by

$$S_\lambda : \begin{pmatrix} u \\ q \end{pmatrix} \longrightarrow S_\lambda \begin{matrix} u \\ q \end{matrix} = \begin{pmatrix} (\lambda - \Delta)u + \nabla q \\ \nabla \cdot u \end{pmatrix},$$

and let

$$S'_\lambda : \begin{pmatrix} u \\ q \end{pmatrix} \longrightarrow S'_\lambda \begin{matrix} u \\ q \end{matrix} = \begin{pmatrix} (\lambda - \Delta)u - \nabla q \\ -\nabla \cdot u \end{pmatrix},$$

denote its formally adjoint operator. To construct an explicit solution u, q of (25) with methods of potential theory, we first need the singular fundamental tensor $E_\lambda = (E^\lambda_{jk})_{j,k=1,\ldots,4}$, i.e. a solution of $S_\lambda E_\lambda = \delta I_4$ in the space of tempered distributions. Here δ is Dirac's in $\mathbb{R}^3$, I_4 the 4×4 unity matrix, and $S_\lambda E_\lambda = (SE^\lambda_1, SE^\lambda_3, SE^\lambda_4)$ with columns $E^\lambda_k = (E^\lambda_{jk})_{j=1,\ldots,4}$ for $k = 1, \ldots, 4$. It is well-known [6] that the fundamental tensor $E_\lambda = (E^\lambda_{jk}(x))_{j,k=1,\ldots,4}$ has the following form:

$$E^\lambda_{jk}(x) = \frac{1}{4\pi} \left\{ \frac{\delta_{jk}}{|x|} e_1(-\sqrt{\lambda}\,|x|) + \frac{x_j x_k}{|x|^3} e_2(-\sqrt{\lambda}\,|x|) \right\} \quad (k, j \ne 4)$$

$$e_1(\varepsilon) = \sum_{n=0}^{\infty} \frac{(n+1)^2}{(n+2)!} \varepsilon^n = \exp(\varepsilon)(1 - \varepsilon^{-1} + \varepsilon^{-2}) - \varepsilon^{-2}$$

$$e_2(\varepsilon) = \sum_{n=0}^{\infty} \frac{1-n^2}{(n+2)!} \varepsilon^n = \exp(\varepsilon)(-1 + 3\varepsilon^{-1} - 3\varepsilon^{-2}) + 3\varepsilon^{-2} \tag{26}$$

$$E^{\lambda}_{4k}(x) = E^{\lambda}_{k4}(x) = \frac{x_k}{4\pi|x|^3} \quad (k \neq 4),$$

$$E^{\lambda}_{44}(x) = \delta(x) + \frac{\lambda}{4\pi|x|}.$$

Using the exponential representation of the functions e_1, e_2 we obtain immediately the behavior of $E_\lambda(x)$ for $x \to 0$ and $x \to \infty$. Setting $r = |x|$ we have for $j, k \neq 4$:

$$\begin{aligned} E^{\lambda}_{jk}(x) &= O(r^{-1}) \quad \text{as} \quad r \longrightarrow 0 \\ E^{\lambda}_{jk}(x) &= O(r^{-3}) \quad \text{as} \quad r \longrightarrow \infty \quad (\lambda > 0) \\ E^{\lambda}_{4k}(x) &= O(r^{-2}) \quad \text{as} \quad r \longrightarrow 0 \quad \text{or} \quad r \longrightarrow \infty . \end{aligned} \tag{27}$$

Note that $E^{\lambda}_{jk}(\lambda > 0)$ decays stronger than $E^{0}_{jk}(j, k \neq 4)$ as $r \to \infty$.

Now using the right hand side F from (25) and the fundamental tensor E_λ, we can construct the hydrodynamical volume potential

$$(U(x), Q(x)) = \int_G < \begin{pmatrix} F(y) \\ 0 \end{pmatrix}, \quad E_\lambda(x-y) > dy, \tag{28}$$

which satisfies the equations $S_\lambda \begin{matrix} U \\ Q \end{matrix} = \binom{F}{0}$ in G due to its construction. Here and in the sequel, for $\xi \in \mathbb{R}^n$ and matrices $A = (A_{ji}) \in \mathbb{R}^n \times \mathbb{R}^m$ $(n, m \in \mathbb{N})$ we use

$$(\xi, A) = \left(\sum_{j=1}^{n} \xi_j A_{j1}, \ldots, \sum_{j=1}^{n} \xi_j A_{jm} \right),$$

obtaining a row with m components.

In order to represent the solution of (S_λ) by means of potentials we need the hydrodynamical Green's formulae. They are given in terms of the formal differential operators

$$S_\lambda : \begin{pmatrix} u \\ q \end{pmatrix} \longrightarrow S_\lambda \begin{matrix} u \\ q \end{matrix}, \qquad S'_\lambda : \begin{pmatrix} u \\ q \end{pmatrix} \longrightarrow S'_\lambda \begin{matrix} u \\ q \end{matrix}$$

from above, and their corresponding adjoint stress tensors, which are defined by

$$T : \begin{pmatrix} u \\ q \end{pmatrix} \longrightarrow T \begin{matrix} u \\ q \end{matrix} = (-\nabla u - (\nabla u)^T + q I_3),$$

$$T' : \begin{pmatrix} u \\ q \end{pmatrix} \longrightarrow T' \begin{matrix} u \\ q \end{matrix} = (-\nabla u - (\nabla u)^T - q I_3).$$

Here $(\nabla u)^T$ is the transposed matrix of $\nabla u = (D_i u_k)_{k,i=1,2,3}$ and I_3 the 3×3 unity matrix.

Let us assume that $u, v \in C^2(G)^3 \cap C^1(\overline{G})^3$ are divergence-free vector fields, that $q, p \in C^1(G) \cap C^0(\overline{G})$, and that $S_\lambda \begin{smallmatrix} u \\ q \end{smallmatrix}, S'_\lambda \begin{smallmatrix} v \\ p \end{smallmatrix} \in L^1(G)^3 (\lambda > 0)$. Then we have Green's first identity

$$\begin{aligned} &\int_G (S_\lambda \begin{matrix} u \\ q \end{matrix}, \begin{pmatrix} v \\ p \end{pmatrix}) dy \\ &= \int_S (T \begin{matrix} u \\ q \end{matrix} N, v) do_y + \int_G (\lambda u, v) dy + \int_G \frac{1}{2} (\nabla u + (\nabla u)^T,\ \nabla v + (\nabla v)^T) dy, \end{aligned} \tag{29}$$

and Green's second identity

$$\int_G \left\{ (S_\lambda \begin{matrix} u \\ q \end{matrix}, \begin{pmatrix} v \\ p \end{pmatrix}) - (\begin{pmatrix} u \\ q \end{pmatrix}, S'_\lambda \begin{matrix} v \\ p \end{matrix}) \right\} dy \;=\; \int_S \left\{ (T^u_q N, v) - (u, T'^v_p N) \right\} do_y \,. \tag{30}$$

Here we use

$$< \xi, \eta > = \sum_{k=1}^{n} \xi_k \eta_k \ \text{ for } \ \xi, \eta \in \mathbb{R}^n \ \text{ and } \ < A, B > = \sum_{i,k=1}^{n} A_{ik} B_{ik}$$

for matrices $A, B \in \mathbb{R}^n \times \mathbb{R}^n$ $(n \in \mathbb{N})$. The vector $N = N(y) \in \mathbb{R}^3$ denotes the exterior normal in $y \in S$ and $T^u_q N$ indicates the usual matrix vector product.

Now applying Green's second identity with a solution $u \in C^2(G)^3 \cap C^1(\overline{G})^3$, $q \in C^1(G) \cap C^0(\overline{G})$ of $S_\lambda \begin{smallmatrix} u \\ q \end{smallmatrix} = \binom{F}{0}$, and with v, p being the columns of the fundamental tensor E_λ, by cutting off the singularity in $x \in G$ we obtain the following representation (compare [3], p. 335) of u and q in $x \in G$ (N denotes the exterior normal on the C^2-boundary S):

$$\begin{aligned} &\int_G (\begin{pmatrix} F(y) \\ 0 \end{pmatrix}, E_\lambda(x-y)) dy - (u(x), q(x)) \\ &= \int_S (T^u_q(y) N(y), E^{(r)}_\lambda(x-y)) do_y - \int_S (u(y), T'_y E_\lambda(x-y) N(y)) do_y \,. \end{aligned} \tag{31}$$

Here $E^{(r)}_\lambda$ is the 3×4 matrix obtained from E_λ by eliminating the last row, and the product in the last boundary integral equation is defined as follows: Treating the 4 columns of E_λ with T' yields four 3×3 matrices, which, multiplied by N, give four columns with 3 components, hence a 3×4 matrix. The subscript y in T' means differentiation with respect to y.

The representation formula (31) suggests to introduce hydrodynamical boundary layer potentials for general vector valued source densities $\Psi = (\Psi_1, \Psi_2, \Psi_3) \in$

$C(S)^3$. For $x \in \mathbb{R}^3 \backslash S$ we define the single layer potential

$$(E_\lambda \Psi)(x) = \int_S (\Psi(y), E_\lambda^{(r)}(x-y)) do_y$$

and the double layer potential

$$(D_\lambda \Psi)(x) = \int_S (\Psi(y), T_y' E_\lambda(x-y) N(y)) do_y .$$

Because $E_\lambda = E_\lambda^T$, the single layer potential can be represented by

$$(E_\lambda \Psi)(x) = \int_S E_\lambda^{(c)}(x-y) \Psi(y) do_y . \quad (32)$$

Here the 4×3 matrix $E_\lambda^{(c)}$ is obtained from E_λ by eliminating the last column and $E_\lambda^{(c)} \Psi$ indicates the usual matrix vector product. If no confusion is possible, row representation and column representation will be identified. In order to develop a similar representation for the double layer potential we proceed as follows. Due to $D_{y_i} E_{jk}^\lambda(x-y) = -D_{x_i} E_{jk}^\lambda(x-y) (i, j = 1, 2, 3; k = 1, \ldots, 4)$ and observing the definition of T and T' we have $T_y' E_k^\lambda(x-y) = -T_x E_k^\lambda(x-y)$ where E_k^λ denotes the kth column of $E_\lambda (k = 1, \ldots, 4)$. Defining the 3×4 matrix $(D_\lambda(x, y))^T = -T_x E_\lambda(x-y) N(y)$, we first obtain the row vector

$$(D_\lambda \Psi)(x) = \int_{\partial G} < \psi(y), (D_\lambda(x, y))^T > do_y$$

and then the column

$$(D_\lambda \Psi)(x) = \int_{\partial G} D_\lambda(x, y) \Psi(y) do_y , \quad (33)$$

where the 4×3 matrix $D_\lambda(x, y)$ is defined by

$$D_\lambda(x, y) = (-T_x E_\lambda(x-y) N(y))^T = \left((-T_x E_k^\lambda(x-y))_{ij} N_j(y)\right)_{ki} .$$

Both the single layer potential (32) and the double layer potential (33) are analytic functions in $\mathbb{R}^3 \backslash S$ and satisfy there the homogeneous differential equations

$$S_\lambda \begin{matrix} u \\ q \end{matrix} = \begin{pmatrix} 0 \\ 0 \end{pmatrix} .$$

By elementary calculations we find (compare [6]) that the 4×3 kernel matrix $D_\lambda = (D^\lambda_{ki}(x, y))_{k=1,\ldots,4;i=1,2,3}$ of the double layer potential $D_\lambda \Psi$ has the following form: Setting $r = x - y$ and $N = N(y)$ we have

$$D^\lambda_{ki}(x, y) = -\frac{1}{4\pi}\left\{\frac{r_k N_i}{|<r|^3} d_1(-\sqrt{\lambda}|r|) - \left(\frac{N_k r_i}{|r|^3} + \delta_{ki}\frac{r \cdot N}{|r|^3}\right) d_2(-\sqrt{\lambda}|r|) + \right.$$

$$\left. \frac{r_k r_i r \cdot N}{|r|^5}(3 - 3d_1(-\sqrt{\lambda}|r|) + 2d_2(-\sqrt{\lambda|r|}))\right\},$$

$$d_1(\varepsilon) = \sum_{n=2}^{\infty} \frac{2(n^2-1)}{(n+2)!}\varepsilon^n = \exp(\varepsilon)(2 - 6\varepsilon^{-1} + 6\varepsilon^{-2}) - 6\varepsilon^{-2} + 1, \tag{34}$$

$$d_2(\varepsilon) = \sum_{n=2}^{\infty} \frac{n(n^2-1)}{(n+2)!}\varepsilon^n = \exp(\varepsilon)(\varepsilon - 3 + 6\varepsilon^{-1} - 6\varepsilon^{-2}),$$

$$D^\lambda_{4i}(x, y) = -\frac{1}{4\pi}\left\{6\frac{r_i r \cdot N}{|r|^5} + \frac{\lambda N_i}{|r|} - 2\frac{N_i}{|r|^3}\right\} - N_i \delta(r).$$

The series representation above yields $d_1(0) = d_2(0) = 0$, hence as $\lambda \to 0$ we obtain from (30) the well known (see [3], p. 336) double layer kernel matrix for the Stokes equations (S_0):

$$\begin{aligned} D^0_{ki}(x, y) &= -\frac{3}{4\pi}\frac{r_k r_i r \cdot N}{|r|^5} \qquad (k, i = 1, 2, 3), \\ D^0_{4i}(x, y) &= -\frac{1}{2\pi}\left(\frac{3r \cdot N r_i}{|r|^5} - \frac{N_i}{|r|^3}\right) - N_i \delta(r) \qquad (i = 1, 2, 3). \end{aligned} \tag{35}$$

It follows easily that the last term in d_1 comes from the pressure q. This term determines the decay for $r = |r| = |x - y| \to 0$ and $r \to \infty$. Hence for $k, i \neq 4$ we have $(\lambda > 0)$:

$$\begin{aligned} D^\lambda_{ki}(x, y) &= O(r^{-2}) \quad \text{as} \quad r \longrightarrow 0 \quad \text{or} \quad r \longrightarrow \infty \ (\lambda > 0), \\ D^\lambda_{4i}(x, y) &= O(r^{-3}) \quad \text{as} \quad r \longrightarrow 0, \\ D^\lambda_{4i}(x, y) &= O(r^{-1}) \quad \text{as} \quad r \longrightarrow \infty. \end{aligned} \tag{36}$$

In the following we consider the normal stresses of the single layer potential $E_\lambda \Psi$, which are defined in a neighborhood $U \subseteq \mathbb{R}^3$ of S for $x \in U \backslash S$ and $\Psi \in C(S)^3$ by

$$(H^*_\lambda \Psi)(x) = \int_S T_x(E^{(c)}_\lambda(x - y)\Psi(y))N(\tilde{x})do_y.$$

Here the superscript $*$ indicates a column vector with 3 components, and $N(\tilde{x})$ denotes the outward unit normal in $\tilde{x} \in S$, where $\tilde{x}$ is the unique projection of $x \in U \backslash S$ on S. Note that $S \in C^2$ allows the construction of parallel surfaces, which implies the existence of such a neighborhood U. If we use the representation

$$(H_\lambda^* \Psi)(x) = \int_S H_\lambda(x,y)\Psi(y)do_y \tag{37}$$

with some 3×3 matrix $H_\lambda(x,y)$, then

$$H_\lambda(x,y) = D_\lambda^{(r)}(y,x)^T$$

with $D_\lambda^{(r)}$ is obtained by eliminating the last row of the 4×3 matrix D_λ given above.

The next statements concern the continuity properties of the potentials, if $x \in \mathbb{R}^3 \backslash S$ approaches a point $z \in S$. For $x \in \mathbb{R}^3 \backslash S$ let

$$(E_\lambda^* \Psi)(x) = \int_{\partial G} E_\lambda^{(r,c)}(x-y)\Psi(y)do_y\,, \tag{38}$$

$$(D_\lambda^* \Psi)(x) = \int_{\partial G} D_\lambda^{(r)}(x,y)\Psi(y)do_y\,, \tag{39}$$

denote the single layer and the double layer potential corresponding to the velocity part of the potentials, respectively. Here $E_\lambda^{(r,c)}$ is the 3×3 matrix obtained from E_λ by eliminating the last row ($\approx r$) and the last column ($\approx c$). We first consider some potentials with special densities.

It is well known (see [3], p. 337) that for the case $\lambda = 0$ we have

$$(D_0^* \beta)(x) = \int_S D_0(x,y)\beta do_y = \begin{cases} \beta, \; x \in G\,, \\ \frac{1}{2}\beta, \; x \in S\,, \\ 0, \; x \in \mathbb{R}^3 \backslash \overline{G}\,, \end{cases} \tag{40}$$

where D_0 is the 3×3 matrix defined in (35) and $\beta \in \mathbb{R}^3$ is a constant column vector. For $\lambda > 0$, however,

$$(D_\lambda^* \beta)(x) = \lambda \int_G E_\lambda^{(r,c)}(x-y)\beta dy = \begin{cases} \beta, \; (x \in G)\,, \\ \frac{1}{2}\beta, \; (x \in S)\,, \\ 0, \; (x \in \mathbb{R}^3 \backslash \overline{G})\,. \end{cases} \tag{41}$$

Moreover, if N denotes the outward unit normal field on S, then for the single layer potential $E_\lambda N (\lambda > 0)$ with density N we have

$$(E_\lambda N)(x) \;=\; \int_S E_\lambda^{(c)}(x-y)N(y)do_y \;=\; \begin{cases} -\binom{0}{1}\ (x\in G)\,, \\ -\frac{1}{2}\binom{0}{1}\ (x\in S)\,, \\ \binom{0}{0}\ (x\in \mathbb{R}^3\backslash\overline{G})\,, \end{cases} \tag{42}$$

which follows from Green's second identity, and implies $(E_\lambda^* N)(x) = 0$ for all $x \in \mathbb{R}^3$.

Next let us study the continuity properties of potentials with general continuous source densities. Setting

$$w(z) \;=\; \lim_{\substack{x\to z\in S\\ x\in G}} w(x)\,, \qquad\qquad w(z) \;=\; \lim_{\substack{x\to z\in S\\ x\in \mathbb{R}^3\backslash\overline{G}}} w(x)\,,$$

we obtain on the boundary S the important relations

$$(E_\lambda^*\Psi)^i = E_\lambda^*\Psi \;=\; (E_\lambda^*\Psi)^e\,, \tag{43}$$

$$(D_\lambda^*\Psi)^i - D_\lambda^*\Psi = \frac{1}{2}\Psi \;=\; D_\lambda^*\Psi - (D_\lambda^*\Psi)^e\,, \tag{44}$$

$$(H_\lambda^*\Psi)^e - H_\lambda^*\Psi = \frac{1}{2}\Psi \;=\; H_\lambda^* - (H_\lambda^*\Psi)^i\,, \tag{45}$$

where $E_\lambda^*\Psi$, $D_\lambda^*\Psi$, and $H_\lambda^*\Psi$ are defined by (38), (39), and (37), respectively.

Now let $G^c = \mathbb{R}^3\backslash\overline{G}$ be the complementing exterior domain having the same boundary S as G. We consider the following boundary value problem: For a given boundary value $b \in C(S)^3$ find $u \in C^2(G)^3 \cap C(\overline{G})^3,\ q \in C^1(G)\cap C(\overline{G})$ satisfying

$$S_\lambda \begin{matrix} u \\ q \end{matrix} \;=\; \begin{pmatrix} 0 \\ 0 \end{pmatrix} \text{ in } G\,, \qquad\qquad u = b \text{ on } S\,. \tag{46}$$

We refer to this problem as to the interior hydrodynamic Dirichlet problem. Besides (46) we also consider the exterior hydrodynamic Neumann problem

$$S_\lambda \begin{matrix} u \\ q \end{matrix} \;=\; \begin{pmatrix} 0 \\ 0 \end{pmatrix} \text{ in } G^c\,, \qquad\qquad T_q^u N \;=\; b \text{ on } S\,, \tag{47}$$

being adjoint to (46). Using Green's first identity we can easily prove that regular solutions u, q of the exterior Neumann problem are uniquely determined provided that we require for $r = |x| \to \infty (\lambda > 0)$

$$u(x) \;=\; O(r^{-2})\,, \qquad \nabla u(x) \;=\; O(r^{-1})\,, \qquad q(x) \;=\; O(r^{-1})\,, \tag{48}$$

a condition, which takes into account the special decay properties of the potentials (compare (27) and (36)).

Concerning the interior Dirichlet problem, u is uniquely determined, while q is uniquely determined up to an additive constant only.

In the following we prove the existence of a solution u, q of the interior Dirichlet problem using the method of boundary integral equations. Let $b \in C(S)^3$ be given with

$$\int_S b \cdot N \, do \;=\; 0\,. \tag{49}$$

Choosing in $x \in G$ the ansatz $\binom{u}{q}(x) = (D_\lambda \Psi)(x)$ as double layer potential, due to the jump relations we obtain on S the weakly singular (S is of class C^2) boundary integral equations

$$b \;=\; \frac{1}{2}\,\Psi + (D^{*}\lambda\Psi) \;\text{ on }\; S\,, \tag{50}$$

which is a Fredholm system of the second kind on $C(S)^3$. To solve it we have to consider the corresponding homogeneous adjoint system

$$0 \;=\; \frac{1}{2}\,\Phi + (H_\lambda^{*}\Phi) \;\text{ on }\; S\,. \tag{51}$$

It follows from (18) that the normal vector $N \in C(S)^3$ is a solution: Due to $(H_\lambda^* N)(x) = (T(E_\lambda N))(x)N(\tilde{x}) = -N(\tilde{x})$ if $x \in G$ (for $\tilde{x}$ see above (37)) and $(H_\lambda^* N)(x) = 0$ if $x \in G^c$, from (21) we obtain

$$0 \;=\; \frac{1}{2}\,N + (H_\lambda^{*}N) \;\text{ on }\; S\,.$$

Moreover, if $\Phi \in C(S)^3$ is any solution of (51), then we have $\Phi \in \beta N$ with some constant $\beta \in \mathbb{R}$. To see this, consider the single layer potential $\binom{u}{q} = E_\lambda \Phi$ defined in (32). It decays as required in (48), and it solves the exterior Neumann problem (47) with zero boundary data due to (45) and (51). Thus we have $E_\lambda \Phi = \binom{0}{0}$ in G^c from the uniqueness statement, and $E_\lambda^* \Phi = 0$ on S using (43). This again implies that $E_\lambda \Phi$ also solves the interior Dirichlet problem with zero boundary data, and the corresponding uniqueness statement yields $E_\lambda \Phi = \binom{0}{\alpha}$ in G, with some constant $\alpha \in \mathbb{R}$. Because $H_\lambda^* \Phi = 0$ in G^c and $H_\lambda^* \Phi = \alpha N$ in G, the assertion follows by (45). Now using well known facts of Fredholm's theory on integral equations of second kind in spaces of continuous functions it follows that the condition (49) is necessary and sufficient for the existence of a solution $\Psi \in C(S)^3$ of (50).

Because (51) has a unique nontrivial solution $\Phi = N$, the homogeneous version of (50) has a nontrivial solution too. For numerical purposes, however, it is desirable to deal with uniquely solvable systems. This can be achieved as follows: Instead of (50) consider the boundary integral equations system

$$b \;=\; \frac{1}{2}\,\Psi + (D_\lambda^{*}\Psi) - (P_N\Psi) \;\text{ on }\; S \tag{52}$$

with the one-dimensional operator $P_n : C(S)^3 \to C(S)^3$ given by

$$(P_N \Psi)(x) \;=\; N(x) \int\limits_{\partial G} N \cdot \Psi do \,.$$

Because the normal field N forms a basis of the null space of the operator $\frac{1}{2} I_e + H_\lambda^*$ which is adjoint to $\frac{1}{2} I_3 + D_\lambda^*$, the system (52) is uniquely solvable ([7]). Moreover, the solution solves the system (50) too, provided the compatibility condition (49) is satisfied. Here the latter follows easily by multiplying (28) with N, integrating over S, and noting that

$$\int\limits_{\partial G} (D_\lambda^* \Psi) \cdot N \, do \;=\; \int\limits_{\partial G} \Psi \cdot (H_\lambda^* N) do \;=\; -\frac{1}{2} \int\limits_{\partial G} \Psi \cdot N \, do \,.$$

Thus we have shown

Theorem 2 *Let $b \in C(S)^3$ with (25) be given on a C^2-boundary S of a bounded domain $G \subseteq \mathbb{R}^3$, and let $0 < \lambda \in \mathbb{R}$. Then the interior hydrodynamic Dirichlet problem (22) has a solution $u \in C^2(G)^3 \cap C(\overline{G})^3$, $q \in C^1(G) \cap C(\overline{G})$. Here u is uniquely determined, while q is unique up to an additive constant, only. The solution u, q can be represented in G as a pure double layer potential $\binom{u}{q}(x) = (D_\lambda \Psi)(x)$, where the source density $\Psi \in C(S)^3$ is the unique solution of the second kind Fredholm boundary integral equations system*

$$b \;=\; \frac{1}{2} \Psi + (D_\lambda^* \Psi) - (P_N \Psi) \;\; on \;\; S \,.$$

Here $D_\lambda^* \Psi$ is the velocity part of $D_\lambda \Psi$ and $P_N : C(S)^3 \to C(S)^3$ is defined by

$$(P_N \Psi)(x) \;=\; N(x) \int\limits_{\partial G} N \cdot \Psi do \,.$$

4 A Boundary Element Method

Summarizing the results from the last two sections we find that the potential representation given in (28) defines an approximate solution $(v^k(x), q^k(x))$ of the Stokes equations (25) at time $t_k = kh$ $(k = 1, 2, \ldots, N)$. It depends on the solution Ψ of the boundary integral equations system (29), which – for each time step – has the form (52). For the discretization of (52) we choose a collocation procedure as described in [1, 5]. To be concrete, in the following let us restrict our considerations to the case of the unit ball $G \subseteq \mathbb{R}^3$ with boundary S and let us use the parametrization

$$f : S^\wedge = [0,1]^2 \longrightarrow S\,, \qquad f(\vartheta,\eta) = (x_1,x_2,x_3) \in S\,,$$

i.e. $x_1 = \sin(\pi\vartheta)\cos(2\pi\eta)$, $x_2 = \sin(\pi\vartheta)\sin(2\pi\eta)$, $x_3 = \cos(\pi\vartheta)$. For the sake of illustration, in the following we suppress some analytical problems due to the non-uniqueness of the inverse mapping f^{-1}. For $L \in \mathbb{N}$ let $\sigma = (2L)^{-1}$ and define on $S^\wedge$ a so-called collocation grid

$$C_\sigma^\wedge = \{x^\wedge = (i\sigma, j\sigma) | i, j = 0,\ldots,2L\}$$

consisting of $(2L+1)^2$ collocation points and an integration grid

$$J_\sigma^\wedge = \{((i+0.5)\sigma,\ (j+0.5)\sigma) \mid i, j = 0,\ldots,2L-1\}$$

consisting of $(2L)^2$ integration points. For $y^\wedge = ((i+0.5)\sigma,\ (j+0.5)\sigma) \in J_\sigma^\wedge$ let

$$Q_y^\wedge = \{(\vartheta,\eta) \mid i\sigma < \vartheta < (i+1)\sigma,\ j\sigma < \eta < (j+1)\sigma\}$$

be the square with length σ and center $y^\wedge$. The projections of these sets on S are denoted by

$$C_\sigma = f(C_\sigma^\wedge), \qquad J_\sigma = f(J_\sigma^\wedge), \qquad Q_y = f(Q_y^\wedge)\,.$$

Setting

$$\omega(\tau) = \begin{cases} \tau + 1 \text{ for } & -1 \le \tau \le 0\,, \\ 1 - \tau \text{ for } & 0 \le \tau \le 1\,, \\ \quad 0 & \text{elsewhere}\,, \end{cases}$$

for every $x^\wedge = (x_1, x_2) \in C_\sigma^\wedge$ let us define a bilinear B-spline

$$\xi^\wedge : S^\wedge \longrightarrow \mathbb{R}\,, \qquad \xi^\wedge(\vartheta,\eta) = \omega\left(\frac{(\vartheta - x_1)}{\sigma}\right)\omega\left(\frac{(\eta - x_2)}{\sigma}\right)\,.$$

These splines are used for interpolation: the interpolate $P_\sigma^\wedge \Phi^\wedge : S^\wedge \to \mathbb{R}^3$ of some vector function $\Phi^\wedge : S^\wedge \to \mathbb{R}^3$ is defined by

$$(P_\sigma^\wedge \Phi^\wedge)(\vartheta,\eta) = \sum_{x^\wedge \in C_\sigma^\wedge} \Phi^\wedge(x^\wedge)\xi^\wedge(\vartheta,\eta)\,,$$

and it holds $(P_\sigma^\wedge \Phi^\wedge)(u^\wedge) = \Phi^\wedge(z^\wedge)$ for all $z^\wedge \in C_\sigma^\wedge$. Analogously, we call

$$P_\sigma \Phi = (P_\sigma^\wedge(\Phi \circ f)) \circ f^{-1}$$

the interpolate of $\Phi : S \to \mathbb{R}^3$.

Let us now go back to the boundary integral equations system and look for an approximate solution

$$\Psi_\sigma \;=\; \Psi_\sigma^\wedge \circ f^{-1}\,,$$

where the vector function $\Psi_\sigma^\wedge : S^\wedge \to \mathbb{R}^3$ has the form

$$\Psi_\sigma^\wedge(\vartheta,\eta) \;=\; \sum_{x^\wedge \in C_\sigma^\wedge} \alpha(x^\wedge,\sigma)\xi^\wedge(\vartheta,\eta)\,.$$

Here the unknown coefficients $\alpha(x^\wedge,\sigma) \in \mathbb{R}^3$ have to be determined from the collocation procedure

$$P_\sigma b \;=\; P_\sigma(\frac{1}{2}\Psi_\sigma + (D^*_{\lambda,\sigma}\Psi_\sigma) - (P_{N,\sigma}\Psi_\sigma))\,, \tag{53}$$

where (compare (15) and (28))

$$(D^*_{\lambda,\sigma}\Psi_\sigma)(x) = \sum_{y\in J_\sigma} D_\lambda^{(r)}(x,y)\Phi_\sigma(y)|Q_y| \quad (x \notin J_\sigma)\,, \tag{54}$$

$$(P_{N,\sigma}\Psi_\sigma)(x) = N(x)\sum_{y\in J_\sigma} N(y)\cdot\Phi(y_\sigma)|Q|_y \quad (x\in S)\,, \tag{55}$$

and

$$|Q_y| \;=\; \int_{Q_y} do\,.$$

Hence integration has been replaced by a quadrature formula (midpoint rule). Thus considering (53) on the collocation grid only, we obtain a linear algebraic system for $3(2L+1)^2$ unknowns (3 components, $(2L+1)^2$ collocation points) with a non-sparse but diagonal-dominant system matrix, which is invertible for sufficiently small $\omega > 0$. This follows with the usual perturbation theory from the fact that (52) is uniquely solvable in $C(S)^3$. Moreover, the following estimates can be obtained in case of boundary values $b \in C(S)^3$ as in [1]:

$$\max_{x\in S}|\Psi(x) - \Psi_\sigma(x)| \le c(\lambda)\sigma\,\ln(\frac{1}{\sigma})\,, \tag{56}$$

$$\max_{x\in G_\sigma}|D^*_\lambda\Psi(x) - D^*_{\lambda,\sigma}\Psi_\sigma(x)| \le c(\lambda)\sigma\,\ln(\frac{1}{\sigma})\,. \tag{57}$$

Here $(G_\sigma)_{\sigma>0}$ is a family of subregions $G-\sigma$ exhausting G as $\sigma\to 0$.

Extending both grids from the boundary S into the domain G, the volume potentials can be approximated analogously, using the midpoint rule as quadrature formula instead of integration. In the following, we present some test calculations for the non-stationary Stokes equations (1) in the $3-d$ unit ball, which have been performed without using any symmetry property of the ball: Let

$$(t,x) \longrightarrow v(t,x) = (t+1)(\exp(-r^2) - \exp(-1)) \begin{pmatrix} x_3 - x_2 \\ x_1 - x_3 \\ x_1 - x_2 \end{pmatrix},$$

$$(t,x) \longrightarrow p(t,x) = \text{constant}, \quad r = (x_1^2 + x_2^2 + x_3^2)^{\frac{1}{2}}.$$

Then v, ∇p is the unique solution of a constructed non-stationary Stokes problem (1) with

$$\nu = 1, \qquad F = D_t v - \Delta v + \nabla p, \qquad v_0 = v(0).$$

The following numerical results illustrate the accuracy of our approach. The simulation runs with a time step size $h = 0.1$ and a spatial step size $\sigma \in \{\frac{1}{4}, \frac{1}{8}, \frac{1}{16}\}$ on a PC with single precision. Let $E(j)$, $j = 1, 2, 3$ denote the mean (over M collocation points) relative error (%), i. e.

$$E(j) = \frac{100}{M} \sum_{l=1}^{M} \left| \frac{v_j^{\mathrm{appr}}(x_l) - v_j^{\mathrm{exe}}(x_l)}{v_j^{\mathrm{exe}}(x_l)} \right|.$$

Development in time of $E(j)$ $(\sigma = \frac{1}{4})$

t	$j=1$	$j=2$	$j=3$
0.1	5.201	6.011	11.218
0.2	5.589	6.127	10.077
0.3	6.890	6.214	9.643
0.4	7.913	6.643	7.641
0.5	8.335	6.911	7.526
0.6	8.621	7.012	7.803
0.7	8.728	7.181	7.741
0.8	8.963	7.264	7.819
0.9	9.001	7.316	8.217
1.0	9.126	7.437	8.269

Development in time of $E(j)$ $(\sigma = \frac{1}{8})$

t	$j = 1$	$j = 2$	$j = 3$
0.1	2.627	3.074	6.664
0.2	2.764	2.808	5.216
0.3	3.442	3.140	4.338
0.4	3.920	3.413	3.982
0.5	4.133	3.541	3.907
0.6	4.255	3.611	3.910
0.7	4.353	3.659	3.940
0.8	4.434	3.698	3.988
0.9	4.494	3.727	4.047
1.0	4.537	3.768	4.114

Development in time of $E(j)$ $(\sigma = \frac{1}{16})$

t	$j = 1$	$j = 2$	$j = 3$
0.1	1.216	1.594	2.932
0.2	1.316	1.373	2.721
0.3	1.517	1.354	2.490
0.4	1.615	1.354	2.331
0.5	1.748	1.392	2.229
0.6	1.872	1.444	2.159
0.7	1.931	1.454	2.099
0.8	1.991	1.466	2.049
0.9	2.049	1.478	2.012
1.0	2.108	1.492	1.985

The results show the linear behavior of the spatial discretization, as expected from the convergence analysis.

Finally, let $E := \frac{1}{3}\sum_{j=1}^{3} E(j)$ denote the mean error of all three components in the first time step for $\sigma = \frac{1}{16}$. In this case we obtain:

h	1	$\frac{1}{2}$	$\frac{1}{4}$	$\frac{1}{8}$	$\frac{1}{16}$
E	13.701	6.817	3.306	1.652	0.901

These results show the linear behavior of the discretization error in time, as expected.

References

1. Hebeker, F. K.: Efficient boundary element methods for three-dimensional exterior viscous flow. Numer. Math. Part. Diff. Equa. **2**, 273–297 (1986)
2. Heywood, J. G., Rannacher R.: Finite element approximation of the nonstationary Navier-Stokes problem. II. Stability of solutions and error estimates uniform in time. Siam J. Numer. Anal. **23**, 750–777 (1986)
3. Odquist, F. K. G.: Über die Randwertaufgaben der Hydrodynamik zäher Flüssigkeiten. Math. Z. **32**, 329–375 (1930)
4. Rannacher, R.: On the numerical analysis of the nonstationary Navier-Stokes equations. The Navier-Stokes equations – Theory and numerical methods. Proc. Oberwolfach 1988, Berlin-Heidelberg-New York, Springer Lect. N. Math. **1431**, 180–193 (1990)
5. Varnhorn, W.: Efficient quadrature for a boundary element method to compute threedimensional Stokes flow. Int. J. Num. Meth. Fluids **9**, 185–191 (1989)
6. Varnhorn, W.: The Stokes Equations. Mathematical Research **76**, Akademie Verlag, Berlin (1994)
7. Varnhorn, W.: The boundary value problems of the Stokes resolvent equations in n dimensions. Math. Nachr. **269–270**, 210–230 (2004)

A New Criterion for Partial Regularity of Suitable Weak Solutions to the Navier-Stokes Equations

Jörg Wolf

Abstract In the present paper we study local properties of suitable weak solutions to the Navier-Stokes equation in a cylinder $Q = \Omega \times (0, T)$. Using the local representation of the pressure we are able to define a positive constant $\varepsilon_\star$ such that for every parabolic subcylinder $Q_R \subset Q$ the condition

$$R^{-2} \int\limits_{Q_R} |\mathbf{u}|^3 \, dxdt \;\le\; \varepsilon_*$$

implies $\mathbf{u} \in L^\infty(Q_{R/2})$. As one can easily check this condition is weaker then the well known Serrin's condition as well as the condition introduced by Farwig, Kozono and Sohr. Since our condition can be verified for suitable weak solutions to the Navier-Stokes system it improves the known results substantially.

Keywords Navier-Stokes equations · Partial regularity · Local regularity

1 Introduction and Main Result

Let Ω be a bounded domain in $\mathbb{R}^3$ with $\partial\Omega \in C^2$. For $T > 0$ we set $Q := \Omega \times]0, T[$. We consider an incompressible Newtonian fluid which is governed by the following Navier-Stokes system

$$\begin{aligned} \operatorname{div} \mathbf{u} &= 0 \quad \text{in} \quad Q, \\ \mathbf{u}_t + \operatorname{div}(\mathbf{u} \otimes \mathbf{u}) - \Delta \mathbf{u} + \nabla p &= 0 \quad \text{in} \quad Q, \\ \mathbf{u} &= 0 \quad \text{on} \quad \partial\Omega \times]0, T[, \\ \mathbf{u}(0) &= \mathbf{a} \quad \text{in} \quad \Omega, \end{aligned} \tag{1}$$

J. Wolf (✉)
Mathematical Institute, Humboldt University Berlin, 10099 Berlin, Germany
e-mail: jwolf@math.hu-berlin.de

R. Rannacher, A. Sequeira (eds.), *Advances in Mathematical Fluid Mechanics*,
DOI 10.1007/978-3-642-04068-9_34,

where $\mathbf{u} = (u_1, u_2, u_3)$ denotes the velocity field, p the pressure and $\mathbf{a} = (a_1, a_2, a_3)$ the initial velocity. The aim of the present paper is to introduce a new criterion beyond Serrin's class which guarantees interior regularity. At the same time, this result will improve the condition given by Farwig et al. [3] which has been obtained recently, using the notion of very weak solution. However our method to obtain the desired result will be entirely different from the one stated above and is based on local energy estimates as well as the representation of the local pressure for suitable weak solutions to the Navier-Stokes equations (1).

Throughout the paper the following standard notion will be used. By x we denote the points $(x_1, \ldots, x_n)$ in $\mathbb{R}^n$ $(n \in \mathbb{N})$. For $x, y \in \mathbb{R}^n$ by $x \cdot y$ we denote the scalar product $x_1 y_1 + \ldots + x_n y_n$ and by $|x| = (x \cdot x)^{1/2}$ the Euclidean norm in $\mathbb{R}^n$. By $\mathbb{M}^n$ we denote the space of all $n \times n$-matrices $\mathbf{A} = \{A_{ij}\}$. Given $\mathbf{A}, \mathbf{B} \in \mathbb{M}^n$ by $\mathbf{A} : \mathbf{B}$ we denote the scalar product $A_{ij} B_{ij}$.[1] Furthermore for $\mathbf{A} \in \mathbb{M}^n$ we define the norm $|\mathbf{A}| := (\mathbf{A} : \mathbf{A})^{1/2}$.

Weak solutions to (1). To begin with, let us introduce the function spaces which will be used in what follows. By $W^{m,q}(\Omega)$, $W^{m,q}_0(\Omega)\,(m = 1, 2, \ldots; 1 \le q < \infty)$ we denote the usual Sobolev spaces. Throughout the paper, we write $\mathbf{C}^\alpha(\Omega) := [C^\alpha(\Omega)]^3$, $\mathbf{L}^q(\Omega) := [L^q(\Omega)]^3$, $\mathbf{W}^{m,q}(\Omega) := [W^{m,q}(\Omega)]^3$ etc.

Next, by $\mathcal{D}_\sigma(\Omega)$ we denote the set of all solenoidal vector fields $\boldsymbol{\varphi} \in \mathbf{C}^\infty_0(\Omega)$. Then define

$$\begin{aligned} \mathbf{L}^2_\sigma(\Omega) &:= \text{closure of} \quad \mathcal{D}_\sigma(\Omega) \quad \text{in} \quad \mathbf{L}^2(\Omega), \\ \mathbf{W}^{1,2}_{0,\sigma}(\Omega) &:= \text{closure of} \quad \mathcal{D}_\sigma(\Omega) \quad \text{in} \quad \mathbf{W}^{1,2}(\Omega). \end{aligned}$$

Given a normed vector space X with norm $\|\cdot\|$, we denote by $L^s(a, b; X)\,(1 \le s \le \infty)\,(-\infty \le a < b \le \infty)$ the vector space of all Bochner measurable functions $z :]a, b[\to X$ such that

$$\int_a^b \|z(t)\|^s dt < \infty \quad \text{if } 1 \le s < \infty, \qquad \operatorname*{ess\,sup}_{]a,b[} \|z(t)\| < \infty \quad \text{if } s = \infty.$$

(see, e.g., [14, Chap. IV,1] for details).

Definition 1 Given $\mathbf{a} \in \mathbf{L}^2_\sigma(\Omega)$. A vector function $\mathbf{u} : Q \to \mathbb{R}^3$ is called a *weak solution* to (1) if

$$\mathbf{u} \in L^2(0, T; \mathbf{W}^{1,2}_{0,\sigma}(\Omega)) \cap L^\infty(0, T; \mathbf{L}^2_\sigma(\Omega))$$

and there holds the following integral identity

[1] Repeated subscripts imply summation over $1, \ldots, n$.

$$\int_Q \Big\{ -\mathbf{u}\cdot\partial_t\boldsymbol{\varphi} + (\mathbf{u}\cdot\nabla)\mathbf{u}\cdot\boldsymbol{\varphi} + \nabla\mathbf{u} : \nabla\boldsymbol{\varphi}\Big\} dxdt = \int_\Omega \mathbf{a}\cdot\boldsymbol{\varphi}(0)dx \tag{2}$$

for all $\boldsymbol{\varphi} \in C_0^\infty([0,T[;\mathcal{D}_\sigma(\Omega))$.

Remark 1 Let $\mathbf{u} : Q \to \mathbb{R}^3$ be a weak solution to (1). Then $\mathbf{u}$ can be redefined on a set of Lebesgue measure 0 such that $\mathbf{u} \in C_w([0,T[;\mathbf{L}^2_\sigma(\Omega))$, i.e. for all $t > 0$ there holds $\mathbf{u}(t) \in \mathbf{L}^2_\sigma(\Omega)$ such that

$$\lim_{s\to t}\int_\Omega \mathbf{u}(s)\cdot\boldsymbol{\xi}dx = \int_\Omega \mathbf{u}(t)\cdot\boldsymbol{\xi}dx \quad \forall\boldsymbol{\xi}\in\mathbf{L}^2_\sigma(\Omega).$$

In addition, we have

$$\mathbf{u}(t)\to\mathbf{a} \quad \text{in} \quad \mathbf{L}^2_\sigma(\Omega) \quad \text{as} \quad t\to 0^+.$$

Next, we recall the notion of a suitable weak solution which has been first introduced by Scheffer [9] and by Caffarelli-Kohn-Nirenberg [1].

Definition 2 A weak solution $\mathbf{u} : Q \to \mathbb{R}^3$ to (1) is called a *suitable weak solution* if there exist $p \in L^{3/2}(Q)$, such that

$$\int_Q \Big\{ -\mathbf{u}\cdot\frac{\partial\boldsymbol{\varphi}}{\partial t} - (\mathbf{u}\otimes\mathbf{u}) : \nabla\boldsymbol{\varphi} + \nabla\mathbf{u} : \nabla\boldsymbol{\varphi}\Big\} dxdt = \int_Q p\,\mathrm{div}\,\boldsymbol{\varphi}\,dxdt \tag{3}$$

for all $\boldsymbol{\varphi} \in \mathbf{C}_0^\infty(Q)$ together with the local energy inequality

$$\int_\Omega |\mathbf{u}(t)|^2\varphi(t)dx + 2\int_0^t\int_\Omega |\nabla\mathbf{u}|^2\varphi\,dxds$$
$$\le \int_0^t\int_\Omega |\mathbf{u}|^2\Big\{\frac{\partial\varphi}{\partial t} + \Delta\varphi\Big\}dxds + \int_0^t\int_\Omega (|\mathbf{u}|^2 + 2p)\mathbf{u}\cdot\nabla\varphi\,dxds$$

for almost all $0 < t < \infty$ and for all nonnegative functions $\varphi \in C_0^\infty(Q)$.

Remark 2 1. The existence of a suitable weak solution to (1) is closely related to the geometric properties of the domain Ω. In case of the whole space $\Omega = \mathbb{R}^3$ using the theory of singular integrals the existence of a pressure can be proved just by solving the Cauchy problem $-\Delta p = \mathrm{div}\,\mathrm{div}(\mathbf{u}\otimes\mathbf{u})$. For a bounded domain with $\partial\Omega \in C^2$ one obtains an appropriate pressure based on the L^q-theory for the non-stationary Stokes system treating the nonlinear term $\mathrm{div}(\mathbf{u}\otimes\mathbf{u}) = (\mathbf{u}\cdot\nabla)\mathbf{u}$ as a right hand side of the corresponding system (cf. [14]). For unbounded domains the problem appears to be rather difficult. There are various examples such as exterior domains, aperture domains, etc. for which the existence of a suitable weak solution is known. For a general unbounded domain with uniformly C^2-boundary the problem has been solved recently by Farwig et al. in [2].

2. If $\Omega \subset \mathbb{R}^3$ is a general open set, the notion of a suitable weak solution does not make any sense, since a pressure may not exist as a function but only as a distribution in time (cf. [15]). However using the local pressure method introduced in [18] one can construct a weak solution which obeys a local energy estimate in terms of $|\mathbf{u} + \nabla p_h|^2$ instead of $|u|^2$, where p_h denotes the harmonic part of the pressure. This allows us to extent the result of the paper to any open set Ω.

Statement of the main result. For $x_0 \in \mathbb{R}^3$ and $0 < R < \infty$ we define the open ball

$$B_R(x_0) := \{x \in \mathbb{R}^3 \mid |x - x_0| < R\}.$$

Given $t_0 \in \mathbb{R}$ and $0 < R < \infty$ we set

$$I_R(t_0) :=]t_0 - R^2, t_0[.$$

If no confusion can arise we write B_R (I_R resp.) in place of $B_R(x_0)$ ($I_R(t_0)$ resp.). By $Q_R = Q_R(x_0, t_0)$ we denote the parabolic cylinder

$$Q_R := B_R(x_0) \times I_R(t_0).$$

We prove the following main result concerning local regularity of suitable weak solutions to the Navier-Stokes equations

Theorem 1 *For every* $3 \le s, q \le \infty$ *there exists a constant* $\varepsilon_\star = \varepsilon_\star(s, q) > 0$ *with the following property: Let* $\mathbf{u}$ *be a suitable weak solution to the Navier-Stokes equations* (1). *Suppose that for a given cylinder* $Q_R(x_0, t_0) \subset Q$ *we have*

$$\|\mathbf{u}\|_{L^s(t_0 - R^2, t_0; \mathbf{L}^q(B_R(x_0)))} \le R^{\frac{2}{s} + \frac{3}{q} - 1} \varepsilon_\star. \tag{4}$$

Then $\mathbf{u}$ is Hölder continuous on $Q_{R/2}(x_0, t_0)$.

Historical Remarks The mathematical theory of the Navier-Stokes equations has been initiated by Leray's historical paper [7], where hestudied the existence of weak solutions and their structure for the case $\Omega = \mathbb{R}^n$. Later Hopf [5] introduced a Galerkin method to get weak solutions to the system (1) in a bounded domain. In both cases these weak solutions satisfy the so called energy inequality. Unfortunately, it is not known whether this weak solutions are unique or not. By this reason the regularity properties of weak solutions may depend on the construction of the weak solution. The first results of existence and partial regularity of suitable weak solutions are due to V. Scheffer [9, 10] and Caffarelli-Kohn-Nirenberg [1]. Later the partial regularity of suitable weak solutions of the Navier-Stokes system has been established by various authors. For more details on this subject we refer to the papers [16, 8, 6, 11, 17].

An alternative condition which guarantees the local regularity is the so called Serrin's condition. It says that if a weak solution $\mathbf{u} : Q \to \mathbb{R}^3$ to (1) satisfies

$$\mathbf{u} \in L^s(t_0 - R^2, t_0; L^q(B_R)), \quad \frac{2}{s} + \frac{3}{q} \leq 1, \quad q > 3, \tag{5}$$

where $Q_R = B_R(x_0) \times]t_0 - R^2, t_0[\subset Q$, then $\mathbf{u}$ is bounded on $Q_{R/2}$.

Recently, based on the theory of very weak solutions Farwig et al. [3] have shown that for $2 < s \leq q < \infty$ with $\frac{2}{s} + \frac{3}{q} \leq 1 + \frac{1}{q}$ there exists an absolute constant $\varepsilon_\star > 0$, such that for every subcylinder $Q_R \subset Q$ the condition

$$\|\mathbf{u}\|_{L^s(t_0 - R^2, t_0; \mathbf{L}^q(B_R))} \leq R^{\frac{2}{s} + \frac{3}{q} - 1} \varepsilon_\star \tag{6}$$

implies that $\mathbf{u}$ is bounded on $Q_{R/2}$. Clearly, this is a generalization of Serrin's condition above. However both condition's (5) and (6) cannot be verified by a given suitable weak solution since the only information we have is $\mathbf{u} \in L^s(0, T; \mathbf{L}^r(\Omega))$ for all $2 \leq s, r \leq \infty$ with $\frac{2}{s} + \frac{3}{r} \leq \frac{3}{2}$.

Clearly, the main theorem provides a new condition on $\mathbf{u}$ which uses the given energy norm of the weak solution only and therefore represents a substantial improvement of the conditions which has been known so far.

The paper is organized as follows. In Sect. 2 introducing the decomposition of the space $L^s(G) = A^s(G) \otimes B^s(G)$ which is due to Simader we provide the main tools for introducing a local pressure. In addition, we list few useful properties of harmonic functions. Next, in Sect. 3 considering the heat equation we present a generalization of the fundamental estimates for caloric functions. The aim of Sect. 4 is to derive a Caccioppoli-type inequality on the basis of the local energy inequality. In particular, we are able to replace the pressure term by the corresponding quantities evolving $\mathbf{u}$ and $\nabla \mathbf{u}$ only. This method cannot be found in the literature and seems to be new. Finally, in Sect. 5 we will complete the proof of Theorem 1.

2 Preliminary Lemmas

In this section we list a few lemmas which will be used below. Throughout let $G \subset \mathbb{R}^3$ be an open and bounded set with $\partial G \in C^2$. We start with a suitable decomposition of the space $L^s(G)\,(1 < s < \infty)$. For, we define,

$$A^s(G) := \{\Delta v \mid v \in W_0^{2,s}(G)\},$$
$$B^s(G) := \{p_h \in L^s(G) \mid \Delta p_h = 0 \text{ in } G\}.$$

The following result is due to Simader and can be found in [12].

Lemma 1 *For every* $1 < s < \infty$ *there holds*

$$L^s(G) = A^s(\Omega) \oplus B^s(G). \tag{7}$$

Next, by means of [12] (Chap. III, Theorem 3.4) one gets the

Lemma 2 *Let* $\mathbf{g} \in \mathbf{L}^s(B_R)\left(\frac{6}{5} \le s \le 2\right)$ *and* $q_0 \in A^2(B_R)$ *with*

$$\int_{B_R} \mathbf{g} \cdot \nabla\varphi dx = \int_{B_R} q_0 \Delta\varphi dx \quad \forall \varphi \in C_0^\infty(B_R). \tag{8}$$

Then $q_0 \in W^{1,s}(B_R)$ *and there exists a constant* C_s*, such that*

$$\|\nabla q_0\|_{\mathbf{L}^s(B_R)} \le C_s \|\mathbf{g}\|_{\mathbf{L}^s(B_R)}. \tag{9}$$

(for the proof we refer to [12,13])

For reader's convenience we present a Caccioppoli-type inequality for harmonic functions, which will be used frequently below

Lemma 3 *There exists an absolute constant* $c > 0$*, such that*

$$\|q\|^2_{L^3(B_{R/3})} + R^2\|\nabla q\|^2_{\mathbf{L}^3(B_{R/3})} + R^3\|D^2 q\|^2_{\mathbf{L}^2(B_{R/3})} \le cR^{-2}\|q\|^2_{L^{3/2}(B_{R/2})} \tag{10}$$

for all $q \in B^{3/2}(B_{R/2})$.

Proof First, we consider the case $R = 1$. Let $\varphi \in C^\infty(\mathbb{R}^3)$ be a cut-off function with $0 \le \varphi \le 1$ in $\mathbb{R}^3$, $\varphi \equiv 1$ on $B_{1/3}$, $\varphi \equiv 0$ in $\mathbb{R}^3 \setminus B_{1/2}$ and $|D^2\varphi| + |\nabla\varphi| \le c_0$. After applying integration by parts one easily estimates

$$\int_{B_{1/2}} |\nabla q|^2 \varphi^6 dx \le c \int_{B_{1/2}} q^2 \varphi^4 dx.$$

On the other hand, by the aid of Hölder's inequality together with Sobolev's inequality one gets

$$\begin{aligned}\int_{B_{1/2}} q^2\varphi^4 dx &\le \|q\|_{L^{3/2}(B_{1/2})}\left(\int_{B_{1/2}} q^3\varphi^{12} dx\right)^{1/3} \\ &\le c\|q\|^2_{L^{3/2}(B_{1/2})} + c\|q\|_{L^{3/2}(B_{1/2})}\left(\int_{B_{1/2}} |\nabla q|^2\varphi^6 dx\right)^{1/2}.\end{aligned}$$

Combining the two inequalities above using Young's inequality gives

$$\int_{B_{1/2}} |\nabla q|^2 \varphi^6 dx \le c\|q\|^2_{L^{3/2}(B_{1/2})}. \tag{11}$$

Similarly, one proves

$$\int\limits_{B_{1/2}} |D^2 q|^2 \varphi^8 dx \le c \int\limits_{B_{1/2}} |\nabla q|^2 \varphi^6 dx \le c\|q\|^2_{L^{3/2}(B_{1/2})}. \tag{12}$$

Finally, making use of Sobolev's embedding theorem taking into account (11) and (12) one gets

$$\begin{aligned}\Bigg(\int\limits_{B_{1/2}} |\nabla q|^3 \varphi^{12}\Bigg)^{2/3} &\le c \int\limits_{B_{1/2}} |\nabla(\nabla q \varphi^4)|^2 dx \\ &\le c \int\limits_{B_{1/2}} |\nabla q|^2 \varphi^6 + |D^2 q|^2 \varphi^8 dx \le c\|q\|^2_{L^{3/2}(B_{1/2})}. \end{aligned} \tag{13}$$

Thus, (10) is obtained by (12) and (13).

For the general case $0 < R < \infty$ the assertion easily follows from the case $R = 1$ by using a standard scaling argument. □

3 Fundamental Estimates for Caloric Functions

The aim of this section is to establish a fundamental estimate which plays a crucial role in proving Theorem 1. Let us start with the definition of a caloric functions

Definition 3 Let $D \subset \mathbb{R}^4$ be an open set. A function $\varphi : D \to \mathbb{R}$ is called *caloric* in D if $\varphi \in C^\infty(D)$ and there holds

$$\varphi_t - \Delta\varphi = 0 \quad \text{in} \quad D. \tag{14}$$

Remark 3 Let $\varphi \in L^2(I_1; L^2_{\text{loc}}(B_1))$ such that

$$\int\limits_{Q_1} -\varphi\psi_t + \nabla\varphi \cdot \nabla\psi \, dxdt = 0 \quad \forall\, \psi \in C^\infty_0(Q_1).$$

Using the standard mollification argument together with the Caccioppoli inequality (15) for caloric functions (see Lemma 4 below) one easily deduces that $\varphi \in C^\infty(Q_1)$ and thus φ is caloric.

Next, we present the Caccioppoli inequalities which holds for caloric functions

Lemma 4 *For each $k \in \mathbb{N}$ there exists a constant $c_k > 0$, such that*

$$\sup_{t \in I_r} \|D^k \varphi(t)\|^2_{L^2(B_r)} \le \frac{c_k}{(\varrho - r)^{2k}} \|\varphi\|^2_{L^2(Q_\varrho)} \quad \forall\, 0 < r < \varrho < 1 \tag{15}$$

for every caloric $\varphi \in C^\infty(Q_1)$.

Now, we are in a position to prove the following important fundamental estimate for caloric functions

Lemma 5 *There exists an absolute constant* $c_* > 0$ *such that for every caloric function* $\varphi \in C^\infty(Q_1)$ *there holds*

$$\|\varphi\|^2_{L^3(I_\tau;L^{9/4}(B_\tau))} \le c_*\tau^4 \|\varphi\|^2_{L^3(I_{1/2},0;L^{9/4}(B_{1/2}))} \quad \forall\, 0 < \tau \le 1. \tag{16}$$

Proof Obviously, the assertion holds for all $\tau \in \left[\frac{1}{4}, 1\right]$. Therefore without loss of generality we can restrict ourself to the case $0 < \tau < \frac{1}{4}$. By means of Sobolev's embedding theorem one gets

$$\|\varphi\|^2_{L^3(I_\tau;L^{9/4}(B_\tau))} \le c\tau^4 \sup_{t\in I_{1/4}} \|\varphi(t)\|^2_{L^\infty(B_{1/4})} \le c\tau^4 \sup_{t\in I_{1/4}} \|\varphi(t)\|^2_{W^{2,2}(B_{1/4})}.$$

Applying (15) with $r = \frac{1}{4}$ and $\varrho = \frac{1}{2}$ it follows that

$$\|\varphi\|^2_{L^3(I_\tau;L^{9/4}(B_\tau))} \le c\tau^4 \|\varphi\|^2_{L^2(I_{1/2};L^2(B_{1/2}))}.$$

To finish the proof, we estimate the right hand side of the last inequality by using Jensen's inequality. □

We complete this section by establishing a fundamental estimate for local solutions to the Stokes system, which plays an essential role in the regularity theory of weak solutions to the Navier-Stokes equations. We have the following

Lemma 6 *Let* $\mathbf{U} \in \mathbf{L}^3(I_R; L^{9/4}(B_R))$ *and* $p_h \in L^{3/2}(I_R; L^{3/2}(B_R))$ *with* $\Delta p_h = 0$ *in* $I_R \times B_R$*, such that*

$$\int_{Q_R} -\mathbf{U}\cdot\boldsymbol{\varphi}_t + \nabla\mathbf{U} : \nabla\boldsymbol{\varphi}\, dxdt = \int_{Q_R} p_h \operatorname{div}\boldsymbol{\varphi}\, dxdt \tag{17}$$

for every $\varphi \in \mathbf{C}^\infty_0(Q_R)$*. Then*

$$\begin{aligned} &R^{-2}\tau^{-2}\|\mathbf{U}\|^2_{L^3(I_{\tau R};\mathbf{L}^{9/4}(B_{\tau R}))} \\ &\quad \le c\tau^{2/3}\Big\{R^{-2}\|\mathbf{U}\|^2_{L^3(I_R;\mathbf{L}^{9/4}(B_R))} + R^{-16/3}\|\tilde{p}_h\|^2_{L^3(I_R;L^{3/2}(B_R))}\Big\} \end{aligned} \tag{18}$$

for every $0 < \tau < 1$ *with an absolute constant* $c > 0$*, where*

$$\tilde{p}_h(t) := \int_{t_0-R^2}^{t} p_h(s)ds, \quad t \in I_R.$$

Proof As above using an appropriate linear transformation it will be sufficient to prove the estimate (18) for the case $R = 1$ and $(x_0, t_0) = (0, 0)$. Furthermore, it is readily seen that the assertion is trivially fulfilled for $\tau \in \left[\frac{1}{4}, 1\right[$. Thus, we may assume $0 < \tau < \frac{1}{4}$.

First, define $\mathbf{V} := \mathbf{U} + \nabla \tilde{p}_h$. Since p_h is harmonic from (17) one infers

$$\int_{Q_1} -\mathbf{V} \cdot \boldsymbol{\varphi}_t + \nabla \mathbf{V} : \nabla \boldsymbol{\varphi} \, dxdt = 0 \quad \forall \boldsymbol{\varphi} \in \mathbf{C}_0^\infty(Q_1). \tag{19}$$

According to Remark 3 $\mathbf{V}$ is a caloric function. Thus, from Lemma 5 it follows that

$$\|\mathbf{V}\|^2_{L^3(I_\tau;\mathbf{L}^{9/4}(B_\tau))} \le c\tau^4 \|\mathbf{V}\|^2_{L^3(I_{1/2};\mathbf{L}^{9/4}(B_{1/2}))}. \tag{20}$$

Next, using the triangular inequality making use of (10) (cf. Lemma 3) one estimates

$$\begin{aligned} \|\mathbf{U}\|^2_{L^3(I_\tau;\mathbf{L}^{9/4}(B_\tau))} \le c\tau^4 \Big\{ \|\mathbf{U}\|^2_{L^3(I_{1/2};\mathbf{L}^{9/4}(B_{1/2}))} + \|\tilde{p}_h\|^2_{L^3(I_1;L^{3/2}(B_1))} \Big\} \\ + c\|\nabla \tilde{p}_h\|^2_{L^3(I_1;\mathbf{L}^{9/4}(B_\tau))}. \end{aligned} \tag{21}$$

In order to estimate the last term fix $t \in I_1$. Recalling that $\tilde{p}_h(t)$ is harmonic in B_1 once more using (10) it follows

$$\begin{aligned} \|\nabla \tilde{p}_h(t)\|^3_{\mathbf{L}^{9/4}(B_\tau)} &\le c\tau^4 \sup_{x \in B_{1/4}} |\nabla \tilde{p}_h(x,t)|^3 \\ &\le c\tau^4 \|\nabla \tilde{p}_h(t)\|^3_{\mathbf{L}^2(B_{1/2})} \le c\tau^4 \|\tilde{p}_h(t)\|^3_{L^{3/2}(B_1)}. \end{aligned}$$

Then, integrating both sides of this inequality over the interval I_1 gives

$$\|\nabla \tilde{p}_h\|^2_{L^3(I_1;\mathbf{L}^{9/4}(B_\tau))} \le c\,\tau^{8/3} \|\tilde{p}_h\|^2_{L^3(I_1;L^{3/2}(B_1))}. \tag{22}$$

Finally estimating the last term on the right of (21) by (22) leads to (18). □

4 Caccioppoli-Type Inequality

In the present section we are going to prove a Caccioppoli-type inequality for suitable weak solutions to the Navier-Stokes equations. Hereby, the pressure p will be estimated in terms of $\mathbf{u}$ and $\nabla \mathbf{u}$, which remarks a new type of estimate and serves as a main ingredient for the proof of Theorem 1. Throughout let $\{\mathbf{u}, p\}$ denote a suitable weak solution to the Navier-Stokes equations. First, we introduce the main quantities which are invariant under the natural scaling of the Navier-Stokes equation. Given $(x_0, t_0) \in Q$ for $0 < \varrho < \min\{\mathrm{dist}(x_0, \partial\Omega), t_0^{1/2}\}$ we define

$$\begin{aligned}
\Phi(\varrho) &:= \varrho^{-4/3}\|\mathbf{u}\|^2_{\mathbf{L}^3(Q_\varrho)},\\
\Psi(\varrho) &:= \varrho^{-2}\|\mathbf{u}\|^2_{L^3(I_\varrho;\mathbf{L}^{9/4}(B_\varrho))},\\
A(\varrho) &:= \varrho^{-1}\|\nabla\mathbf{u}\|^2_{\mathbf{L}^2(Q_\varrho)},\\
B(\varrho) &:= \varrho^{-1}\|\mathbf{u}\|^2_{L^3(I_\varrho;\mathbf{L}^{18/5}(B_\varrho))}.
\end{aligned}$$

Then we have the

Lemma 7 *There exists an absolute constant $c_1 > 0$, such that*

$$A(R/4) + B(R/4) \le c_1\Big\{\Psi(R) + [\Phi(R)]^{3/2} + [\Phi(R)]^3\Big\} \tag{23}$$

holds for all $Q_R \subset Q$.

Proof Let $Q_R \subset Q$ be fixed. Let $\varphi \in C^\infty(\mathbb{R}^4)$ denote a cut-off function, such that $0 \le \varphi \le 1$ in $\mathbb{R}^4$, $\varphi \equiv 0$ in $]-\infty, t_0 - R^2/4[\times(\mathbb{R}^3\setminus B_{R/3})$, $\varphi \equiv 1$ on $[t_0 - R^2/16, \infty[\times B_{R/4}$ with $|\varphi_t| + |D^2\varphi| + |\nabla\varphi|^2 \le \dfrac{c_0}{R^2}$.

Since $\{\mathbf{u}, p\}$ is a suitable weak solution to the Navier-Stokes equations, we have the local energy inequality

$$\begin{aligned}
&\int\limits_{B_{R/2}} |\mathbf{u}(t)|^2\varphi^4 dx + 2\int\limits_0^t\int\limits_\Omega |\nabla\mathbf{u}|^2\varphi^4\,dxdt\\
&\quad\le \int\limits_0^t\int\limits_{B_{R/2}} |\mathbf{u}|^2\Big\{\frac{\partial\varphi^4}{\partial t} + \Delta\varphi^4\Big\}dxdt\\
&\qquad + \int\limits_0^t\int\limits_{B_{R/2}} (|\mathbf{u}|^2 + 2p)\mathbf{u}\cdot\nabla\varphi^4\,dxdt.
\end{aligned} \tag{24}$$

Recalling that

$$L^{3/2}(B_{R/2}) = A^{3/2}(B_{R/2}) \oplus B^{3/2}(B_{R/2}),$$

there exist unique functions

$$\begin{aligned}
p_{0,R/2} &\in L^{3/2}(0, T; A^{3/2}(B_{R/2})),\\
p_{h,R/2} &\in L^{3/2}(0, T; B^{3/2}(B_{R/2}))
\end{aligned}$$

such that

$$p(t) - p(t)_{B_{R/2}} = p_{0,R/2}(t) + p_{h,R/2}(t) \quad \text{f.a.a.} \quad t \in]0,T[.$$

On the other hand, one clearly finds $t_1 \in I_R$ such that

$$\|\mathbf{u}(t_1)\|^3_{L^{3/2}(B_R)} = \frac{1}{R^2}\int_{I_R} \|\mathbf{u}(s)\|^3_{L^{3/2}(B_R)} ds. \tag{25}$$

Define,

$$\tilde{p}_{h,R/2}(t) := \int_{t_1}^{t} p_{h,R/2}(s)ds, \quad t \in I_R.$$

Set $\boldsymbol{v} := \mathbf{u} + \nabla \tilde{p}_{h,R/2}$. Using this notation one can rewrite the local energy inequality (24) as follows

$$\begin{aligned}
&\int_{B_{R/2}} |\boldsymbol{v}(t)|^2 \varphi^4(t) dx + 2\int_0^t \int_{B_{R/2}} |\nabla \boldsymbol{v}|^2 \varphi^4 \, dxdt \\
&\quad \le \int_0^t \int_{B_{R/2}} |\boldsymbol{v}|^2 \left\{ \frac{\partial \varphi^4}{\partial t} + \Delta \varphi^4 \right\} dxdt \\
&\qquad + \int_0^t \int_{B_{R/2}} (|\mathbf{u}|^2 \mathbf{u} + 2p_{0,R/2}\boldsymbol{v}) \cdot \nabla \varphi^4 \, dxdt \\
&\qquad + \int_0^t \int_{B_{R/2}} (\mathbf{u}\cdot\nabla)\mathbf{u} \cdot \nabla \tilde{p}_{h,R/2} \varphi^4 \, dxdt \\
&\quad = I + II + III
\end{aligned} \tag{26}$$

for almost all $t \in I_{R/2}$.

Firstly, by means of Caccioppoli's inequality (cf. Lemma 3) we have

$$\begin{aligned}
I &\le c\,R^{-2}\|\mathbf{u}\|^2_{\mathbf{L}^2(Q_R)} + c\,R^{-2}\|\varphi\nabla\tilde{p}_{h,R/2}\|^2_{L^2(I_{R/2};\mathbf{L}^2(B_{R/2}))} \\
&\le c\,R^{-2}\|\mathbf{u}\|^2_{\mathbf{L}^2(Q_R)} + cR^{-4}\|\tilde{p}_{h,R/2}\|^2_{L^2(I_{R/2};L^2(B_{R/3}))} \\
&\le cR\Big\{\Psi(R) + P_h(R/2)\Big\},
\end{aligned}$$

where

$$P_h(\varrho) := \varrho^{-16/3}\|\tilde{p}_{h,\varrho}\|^2_{L^3(I_\varrho;L^{3/2}(B_\varrho))}.$$

Secondly, using Hölder's and Young's inequality one estimates

$$\begin{aligned} II &\le cR^{-1}\|\mathbf{u}\|^3_{\mathbf{L}^3(Q_R)} + cR^{-1}\|p_{0,R/2}\|^{3/2}_{L^{3/2}(Q_R)} \\ &\qquad\qquad + cR^{-1}\|\nabla \tilde{p}_{h,R/2}\|^3_{L^3(I_{R/2};\mathbf{L}^3(B_{R/3}))} \\ &\le cR\Big\{[\Phi(R)]^{3/2} + [P_h(R/2)]^{3/2}\Big\}. \end{aligned}$$

By a similar reasoning one estimates

$$III \le cR\Big\{[\Phi(R)]^{3/2} + [P_h(R/2)]^{3/2}\Big\}.$$

Inserting the estimates of I, II and III into (26) leads to

$$\begin{aligned} &\operatorname*{ess\,sup}_{t\in I_{R/4}} \int\limits_{B_{R/4}} |\boldsymbol{v}(t)|^2 dx + \int\limits_{Q_{R/4}} |\nabla \boldsymbol{v}|^2 dxdt \\ &\quad \le c\, R\Big\{\Psi(R) + P_h(R/2) + [\Phi(R)]^{3/2} + [P_h(R/2)]^{3/2}\Big\}. \end{aligned} \tag{27}$$

In addition, by the aid of Sobolev's embedding theorem using multiplicative inequalities together with (27) one verifies

$$\begin{aligned} &\|\boldsymbol{v}\|^2_{L^3(I_{R/4};\mathbf{L}^{18/5}(B_{R/4}))} \\ &\quad \le c\Big\{\operatorname*{ess\,sup}_{t\in I_{R/4}} \int\limits_{B_{R/4}} |\boldsymbol{v}(t)|^2 dx + \int\limits_{Q_{R/4}} |\nabla \boldsymbol{v}|^2 dxdt + R^{-2}\|\boldsymbol{v}\|^2_{L^2(Q_{R/4})}\Big\} \\ &\quad \le c\, R\Big\{\Psi(R) + P_h(R/2) + [\Phi(R)]^{3/2} + [P_h(R/2)]^{3/2}\Big\} \\ &\qquad\qquad + cR^{-2}\|\boldsymbol{v}\|^2_{L^2(Q_{R/4})}. \end{aligned}$$

Arguing as above we get

$$\|\boldsymbol{v}\|^2_{L^2(Q_{R/4})} \le cR\Big\{\Psi(R) + P_h(R/2)\Big\}.$$

Thus,

$$B(R/4) \le c\Big\{\Psi(R) + P_h(R/2) + [\Phi(R)]^{3/2} + [P_h(R/2)]^{3/2}\Big\}.$$

Analogously, by means of (10) taking into account (27) one infers

$$\begin{aligned} A(R/4) &\le 2R^{-1}\|\nabla \boldsymbol{v}\|^2_{\mathbf{L}^2(Q_{R/4})} + 2R^{-1}\|D^2\tilde{p}_{h,R/2}\|^2_{\mathbf{L}^2(Q_{R/4})} \\ &\le 2R^{-1}\|\nabla \boldsymbol{v}\|^2_{\mathbf{L}^2(Q_{R/4})} + c\, P_h(R/2) \end{aligned}$$

$$\leq c\Big\{\Psi(R) + P_h(R/2) + [\Phi(R)]^{3/2} + [P_h(R/2)]^{3/2}\Big\}.$$

Combining the last two estimates gives

$$\begin{aligned} B(R/4) + A(R/4) \\ \leq c\Big\{\Psi(R) + P_h(R/2) + [\Phi(R)]^{3/2} + [P_h(R/2)]^{3/2}\Big\}. \end{aligned} \tag{28}$$

Estimation of $P_h(R/2)$: Integrating $(1)_2$ over the interval $]t_1, t[$ $(t \in I_R)$ using integration by parts yields

$$\mathbf{u}(t) - \mathbf{u}(t_1) - \Delta\tilde{\mathbf{u}}(t) = -\operatorname{div}\mathbf{H}(t) - \nabla\tilde{p}(t) \quad \text{in} \quad B_R, \tag{29}$$

where

$$\begin{aligned} \tilde{\mathbf{u}}(t) &:= \int_{t_1}^{t} \mathbf{u}(s)ds, \\ \mathbf{H}(t) &:= \int_{t_1}^{t} \mathbf{u}(s) \otimes \mathbf{u}(s)ds, \\ \tilde{p}(t) &:= \int_{t_1}^{t} p(s)ds, \quad t \in I_R. \end{aligned}$$

Recalling (7) making use of [4] (Theorems III.3.1 and III.5.2) one estimates

$$\begin{aligned} \|\tilde{p}_{h,R/2}(t)\|_{L^{3/2}(B_{R/2})} &\leq c\|\tilde{p}(t) - \tilde{p}_{B_{R/2}}(t)\|_{L^{3/2}(B_{R/2})} \\ &\leq c\|\nabla\tilde{\mathbf{u}}(t)\|_{\mathbf{L}^{3/2}(B_{R/2})} + c\|\mathbf{H}(t)\|_{\mathbf{L}^{3/2}(B_{R/2})} \\ &\quad + cR\|\mathbf{u}(t) - \mathbf{u}(t_1)\|_{\mathbf{L}^{3/2}(B_{R/2})}. \end{aligned} \tag{30}$$

Fix $t \in I_R$ such that $\mathbf{H}(t) \in \mathbf{L}^{3/2}(B_R)$ and $\mathbf{u}(t) \in \mathbf{L}^2(B_R)$. Let $\boldsymbol{w} \in \mathbf{W}^{1,2}_{0,\sigma}(B_R)$ be a weak solution to the stationary Stokes problem

$$\begin{aligned} \operatorname{div}\boldsymbol{w} &= 0 \quad \text{in} \quad B_R, \\ -\Delta\boldsymbol{w} + \nabla q &= -\operatorname{div}\mathbf{H}(t) - \mathbf{u}(t) + \mathbf{u}(t_1) \quad \text{in} \quad B_R, \\ \boldsymbol{w} &= 0 \quad \text{on} \quad \partial B_R. \end{aligned} \tag{31}$$

From the well-known L^p-theory for the Stokes equation [13] one obtains the estimate

$$\|\nabla\boldsymbol{w}\|_{\mathbf{L}^{3/2}(B_R)} \leq c\|\mathbf{H}(t)\|_{\mathbf{L}^{3/2}(B_R)} + cR\|\mathbf{u}(t) - \mathbf{u}(t_1)\|_{\mathbf{L}^{3/2}(B_R)}. \tag{32}$$

On the other hand, setting $\mathbf{U} := \tilde{\mathbf{u}}(t) - \boldsymbol{w}$ combining (29) and (31) implies

$$\begin{aligned} \operatorname{div}\mathbf{U} &= 0 \quad \text{in} \quad B_R, \\ -\Delta\mathbf{U} + \nabla P &= 0 \quad \text{in} \quad B_R. \end{aligned} \tag{33}$$

In particular, from $(33)_2$ it follows that $\operatorname{curl}\mathbf{U}$ is harmonic in B_R. Let $\varphi \in C_0^\infty(B_R)$ denote a cut-off function such that $0 \le \varphi \le 1$ in B_R, $\varphi \equiv 1$ in $B_{R/2}$ and $|D^2\varphi| + |\nabla\varphi|^2 \le \frac{c}{R^2}$. Using integration by parts yields

$$\int\limits_{B_R} |\nabla \operatorname{curl}\mathbf{U}|^2 \varphi^4 dx \le \frac{c}{R^2} \int\limits_{B_R} |\operatorname{curl}\mathbf{U}|^2 \varphi^2 dx. \tag{34}$$

Once more applying integration by parts shows that

$$\begin{aligned} &\int\limits_{B_R} |\operatorname{curl}\mathbf{U}|^2 \varphi^2 dx \\ &\qquad \le \int\limits_{B_R} \varphi^2 \mathbf{U} \cdot \operatorname{curl}\operatorname{curl}\mathbf{U} dx + \frac{c}{R} \int\limits_{B_R} |\mathbf{U}|\, |\operatorname{curl}\mathbf{U}| \varphi dx. \end{aligned}$$

With help of Young's inequality together with (34) one arrives at

$$R^2 \int\limits_{B_R} |\nabla \operatorname{curl}\mathbf{U}|^2 \varphi^4 dx + \int\limits_{B_R} |\operatorname{curl}\mathbf{U}|^2 \varphi^2 dx \le \frac{c}{R^2} \int\limits_{B_{2R}} |\mathbf{U}|^2 dx. \tag{35}$$

Noticing that $-\Delta\mathbf{U} = \operatorname{curl}\operatorname{curl}\mathbf{U}$ in B_R applying integration by parts making use of (35) gives

$$\begin{aligned} \int\limits_{B_R} |\nabla\mathbf{U}|^2 \varphi^2 dx &= \int\limits_{B_R} \varphi^2 \mathbf{U} \cdot \operatorname{curl}\operatorname{curl}\mathbf{U} dx + \frac{1}{2} \int\limits_{B_R} |\mathbf{U}|^2 \Delta\varphi^2 dx \\ &\le \frac{c}{R^2} \int\limits_{B_R} |\mathbf{U}|^2 dx. \end{aligned}$$

Finally, with help of Hölder's inequality one obtains

$$\|\nabla\mathbf{U}\|_{\mathbf{L}^{3/2}(B_{R/2})} \le \frac{c}{R^{1/2}} \|\mathbf{U}\|_{\mathbf{L}^2(B_R)}. \tag{36}$$

Combining (32) and (36) shows that

$$\begin{aligned} \|\nabla\widetilde{\mathbf{u}}(t)\|_{\mathbf{L}^{3/2}(B_{R/2})} &\le c\|\mathbf{H}(t)\|_{\mathbf{L}^{3/2}(B_R)} \\ &\quad + cR\|\mathbf{u}(t) - \mathbf{u}(t_1)\|_{\mathbf{L}^{3/2}(B_R)} + \frac{c}{R^{1/2}} \|\mathbf{U}\|_{\mathbf{L}^2(B_R)}. \end{aligned} \tag{37}$$

Once more using (32) together with Sobolev's inequality yields

$$\begin{aligned}\frac{c}{R^{1/2}}\|\mathbf{U}\|_{\mathbf{L}^2(B_R)} &\leq \frac{c}{R^{1/2}}\|\widetilde{\mathbf{u}}\|_{\mathbf{L}^2(B_R)} + c\|\nabla \boldsymbol{w}\|_{\mathbf{L}^{3/2}(B_R)} \\ &\leq \frac{c}{R^{1/2}}\|\widetilde{\mathbf{u}}\|_{\mathbf{L}^2(B_R)} + c\|\mathbf{H}(t)\|_{\mathbf{L}^{3/2}(B_R)} \\ &\qquad + cR\|\mathbf{u}(t) - \mathbf{u}(t_1)\|_{\mathbf{L}^{3/2}(B_R)}. \end{aligned} \tag{38}$$

Now estimating the right hand side of (37) by (38) implies

$$\begin{aligned}\|\nabla\widetilde{\mathbf{u}}(t)\|_{\mathbf{L}^{3/2}(B_R)} &\leq c\|\mathbf{H}(t)\|_{\mathbf{L}^{3/2}(B_R)} \\ &\quad + cR\|\mathbf{u}(t) - \mathbf{u}(t_1)\|_{\mathbf{L}^{3/2}(B_R)} + \frac{c}{R^{1/2}}\|\widetilde{\mathbf{u}}(t)\|_{\mathbf{L}^2(B_R)}. \end{aligned} \tag{39}$$

Combining (30) and (39) applying Minkowski's inequality and Jensen's inequality yields

$$\begin{aligned}\|\tilde{p}_{h,R/2}(t)\|^3_{L^{3/2}(B_{R/2})} &\leq cR^2\|\mathbf{u}\|^6_{\mathbf{L}^3(Q_R)} + cR^{3/2}\|\mathbf{u}\|^3_{\mathbf{L}^2(Q_R)} \\ &\quad + cR^3\|\mathbf{u}(t) - \mathbf{u}(t_1)\|^3_{\mathbf{L}^{3/2}(B_R)}. \end{aligned} \tag{40}$$

Integrating both sides of this inequality over I_R dividing the result by R^8 gives

$$\begin{aligned}&R^{-8}\int\limits_{I_R} \|\tilde{p}_{h,R}(t)\|^3_{L^{3/2}(B_R)}dt \\ &\quad \leq cR^{-4}\|\mathbf{u}\|^6_{L^3(Q_R)} + cR^{-3}\int\limits_{I_R} \|\mathbf{u}(t)\|^3_{L^{9/4}(B_R)}dt. \end{aligned} \tag{41}$$

Hence,

$$P_h(R/2) \leq c(\Psi(R) + [\Phi(R)]^2). \tag{42}$$

Inserting this estimate into (28) using Jensen's inequality along with Young's inequality completes the proof of (23). □

5 Proof of Theorem 1

Fundamental estimate for $\Psi(R)$. Let $Q_R \subset Q$ be fixed. Let $\mathbf{W}$ denote the weak solution to the following parabolic problem

$$\begin{aligned}\mathbf{W}_t - \Delta\mathbf{W} &= -(\mathbf{u}\cdot\nabla)\mathbf{u} - \nabla p_{0,R/4} \quad \text{in} \quad B_{R/4}\times I_{R/4}, \\ \mathbf{W} &= 0 \quad \text{on} \quad \partial B_{R/4}\times I_{R/4}, \\ \mathbf{W}(t_0 - R^2/16) &= 0 \quad \text{in} \quad B_{R/4}. \end{aligned} \tag{43}$$

As in [19] one gets

$$\begin{aligned}\|\mathbf{W}\|_{L^3(I_{R/4};\mathbf{L}^{9/4}(B_{R/4}))} &\le c\,\|(\mathbf{u}\cdot\nabla)\mathbf{u}\|_{L^{6/5}(I_{R/4};\mathbf{L}^{9/7}(B_{R/4}))}\\ &\quad + c\,\|\nabla p_{0,R/4}\|_{L^{6/5}(I_R/4;\mathbf{L}^{9/7}(B_{R/4}))}\\ &\le c\|\mathbf{u}\|_{L^3(I_{R/4};\mathbf{L}^{18/5}(B_{R/4}))}\|\nabla\mathbf{u}\|_{\mathbf{L}^2(Q_{R/4})}.\end{aligned}$$

Hence,

$$R^{-2}\|\mathbf{W}\|^2_{L^3(I_{R/4};\mathbf{L}^{9/4}(B_{R/4}))} \le cA(R/4)B(R/4). \tag{44}$$

Next, setting $\mathbf{U} := \mathbf{u} - \mathbf{W}$ it follows that

$$\mathbf{U}_t - \Delta\mathbf{U} = -\nabla p_{h,R/4} \qquad \text{in} \quad Q_{R/4}.$$

According to (18) one estimates

$$\begin{aligned}&\tau^{-2}R^{-2}\|\mathbf{U}\|^2_{L^3(t_0-\tau^2R^2,t_0;\mathbf{L}^{9/4}(B_{\tau R}))} \le\\ &\quad\le c\tau^{2/3}R^{-2}\|\mathbf{U}\|^2_{L^3(t_0-R^2,t_0;\mathbf{L}^{9/4}(B_{R/4}))} + c\tau^{2/3}P_h(R/4)\end{aligned} \tag{45}$$

for every $0 < \tau < \frac{1}{4}$. Using triangular inequality together with (45) replacing τ by 4τ $\left(0 < \tau < \frac{1}{16}\right)$ therein yields

$$\begin{aligned}\Psi(4\tau R) &\le c\tau^{-2}R^{-2}\|\mathbf{U}\|^2_{L^3(t_0-\tau^2R^2,t_0;\mathbf{L}^{9/4}(B_{\tau R}))}\\ &\quad + c\tau^{-2}R^{-2}\|\mathbf{W}\|^2_{L^3(I_R;\mathbf{L}^{9/4}(B_{R/4}))}\\ &\le c\tau^{2/3}R^{-2}\|\mathbf{U}\|^2_{L^3(t_0-R^2/16,t_0;\mathbf{L}^{9/4}(B_{R/4}))}\\ &\quad + c\tau^{2/3}P_h(R/4) + c\tau^{-2}R^{-2}\|\mathbf{W}\|^2_{L^3(I_{R/4};\mathbf{L}^{9/4}(B_{R/4}))}.\end{aligned}$$

Once more applying triangular inequality along with (44) and Hölder's inequality implies

$$\Psi(4\tau R) \le c\tau^{2/3}(\Phi(R) + P_h(R/4)) + c\tau^{-2}A(R/4)B(R/4).$$

Taking into account (23) and (42) gives

$$\Psi(4\tau R) \le c\tau^{2/3}\Phi(R) + c\tau^{-2}\Big\{[\Phi(R)]^3 + [\Phi(R)]^6\Big\}. \tag{46}$$

On the other hand, using Jensen's inequality thanks to (23) we have

$$\Phi(\tau R) \le cB(\tau R) \le c\Psi(4\tau R) + c\,\tau^{-4}\Big\{[\Phi(R)]^{3/2} + [\Phi(R)]^3\Big\}.$$

Combining the last two inequalities gives

$$\Phi(\tau R) \le c_1 \tau^{2/3} \Phi(R) + c_2 \tau^{-4} \Big\{ [\Phi(R)]^{3/2} + [\Phi(R)]^6 \Big\} \tag{47}$$

with two positive constants c_1, c_2.

Next, fix $0 < \tau < \frac{1}{16}$, such that $\tau^{1/3} c_1 \le \frac{1}{2}$. Then choose $0 < \varepsilon_0 < 1$ such that $c\tau^{-4}\varepsilon_0^{1/2} \le \frac{\tau}{4}$. Now, assume $\Phi(R) \le \varepsilon_0$. Then in view of (47) one finds

$$\Phi(\tau R) \le \tau^{1/3} \Phi(R) \le \varepsilon_0.$$

By a standard iteration argument it follows that

$$\Phi(\varrho) \le c\Big(\frac{\varrho}{R}\Big)^{1/3} \quad \forall\, 0 < \varrho < R.$$

From this inequality together with (4.1) and (46) we get

$$\frac{1}{\varrho} \int\limits_{Q_\varrho} |\nabla \mathbf{u}|^2 dxdt = B(\varrho) \le c\Big\{ \Phi(\varrho) + [\Phi(\varrho)]^6 \Big\} \le c\Big(\frac{\varrho}{R}\Big)^{1/3}$$

for all $0 < \varrho \le R$. By the well-known Caffarelli-Kohn Nirenberg theorem this inequality implies that (x_0, t_0) is a regular point. More precisely, there exists a constant c_3 not depending on R such that $|\mathbf{u}| \le \frac{c_3}{R^5}$ a. e. in a neighborhood left to (x_0, t_0).

Finally, set $\varepsilon_* := 2^{-4/3}\varepsilon_0$. Assume $\Phi(R; x_0, t_0) \le \varepsilon_*$. Then for every $(y, s) \in Q_{R/2}(x_0, t_0)$ the cube $Q_{R/2}(y, s)$ lies in $Q_R(x_0, t_0)$. Thus, by the definition of Φ one obtains

$$\Phi(R/2; y, s) \le 2^{4/3} \Phi(R; x_0, t_0) \le 2^{4/3} \varepsilon_* = \varepsilon_0.$$

Therefore (y, s) is a regular point and for some constant c there holds $|\mathbf{u}| \le \frac{c}{R^5}$ a. e. in $\Phi(R/2; x_0, t_0)$.

References

1. Caffarelli, L., Kohn, R., Nirenberg, M.: Partial regularity of suitable weak solutions of the Navier-Stokes equations. Comm. Pure Appl. Math. **35**, 771–831 (1982)
2. Farwig, R., Kozono, H., Sohr, H.: An L^q-approach to Stokes and Navier-Stokes equations in general domains. Acta Math. **195**, 21–53 (2005)
3. Farwig, R., Kozono, H., Sohr, H.: *Energy-Based Regularity Criteria for the Navier-Stokes Equations*. J. Math. Fluid Mech. **8**(3), 428–442 (2008)

4. Galdi, G.P.: *An Introduction to the Mathematical Theory of the Navier-Stokes Equations—Vol. I: Linearized Steady Problems.* Springer-Verlag, New York (1994)
5. Hopf, E.: Über die Anfangswertaufgabe für die Hydrodynamischen Grundgleichungen. Math. Nachr. **4**, 213 (1950/1951)
6. Ladyzhenskaya, O.A., Seregin, G.A.: On partial regularity of suitable weak solutions to the three-dimensional Navier-Stokes equations. J. Math. Fluid Mech. **1**(4), 356–387 (1999)
7. Leray, J.: Sur le mouvements d'un liquide visqueux emplissant l'espace. Acta Math. **63**, 193–248 (1934)
8. Lin, F.H.: A new proof of the Caffarelli-Kohn-Nirenberg theorem. Comm. Pure Appl. Math. **51**, 241–257 (1998)
9. Scheffer, V.: Partial regularity of solutions to the Navier-Stokes equations. Pacific J. Math. **66**, 535–552 (1976)
10. Scheffer, V.: Hausdorff measure and the Navier-Stokes equations. Comm. Math. Phys. **55**, 97–102 (1977)
11. Seregin, G.A.: Differentiability properties of weak soluitons of the Navier-Stokes equations (English. Russian original). St. Petersbg. Math J. **14**(1), 147–178 (2003); trans. from Algebra Anal. **14**(1), 194–237 (2002)
12. Simader, G.C.: *On Dirichlet's Boundary Value Problem*. Lecture Notes Mathematics, Vol. 268. Springer, Berlin Heidelberg New York (1972)
13. Simader, G.C.; Sohr, H.: *The Dirichlet Problem for the Laplacian in Bounded and Unbounded Domains.* Pitman Research Notes in Mathematics Series, Vol. 360. Addison Wesley Longman Ltd, Harlow (1996)
14. Sohr, H.: *The Navier-Stokes Equations. An Elementary Functional Analytic Approach*. Birkhäuser, Basel (2001)
15. Sohr, H., von Wahl, W.: On the regularity of the pressure of weak solutions of the Navier-Stokes equations. Arch. Math. (Basel) **46**, 428–439 (1986)
16. Tian, G., Xin, Z.: Gradient estimation on Navier-Stokes equations. Commun. Anal. Geom. **7**(2), 221–257 (1999)
17. Vasseur, A.F.: A new proof of partial regularity of solutions to Navier-Stokes equations. NoDEA Nonlinear Differential Equations and Appl. **14**(5–6), 735–785 (2007)
18. Wolf, J.: Existence of weak solutions to the equations of non-stationary motion of non-Newtonian fluids with shear rate dependent viscosity. J. Math. Fluid Mech. **9**(1), 104–138 (2007)
19. Wolf, J.: A direct proof of the Caffarelli-Kohn-Nirenberg theorem. Banach Center Publ.: Parabolic and Navier-Stokes equation **81**, 533–552 (2008)

An In Vitro Device for Evaluation of Cellular Response to Flows Found at the Apex of Arterial Bifurcations

Zijing Zeng, Bong Jae Chung, Michael Durka, and Anne M. Robertson

Abstract Intracranial aneurysms (ICA) are abnormal dilations of the cerebral arteries, most commonly located at the apices of bifurcations. The ability of the arterial wall, particularly the endothelial cells forming the inner lining of the wall, to respond appropriately to hemodynamic stresses is critical to arterial health. ICA initiation is believed to be caused by a breakdown in this homeostatic mechanism leading to wall degradation. Due to the complex nature of this process, there is a need for both controlled in vitro and in vivo studies. Chung et al. developed an in vitro chamber for analyzing the response of biological cells to the hemodynamic wall shear stress fields generated by the impinging flows found at arterial bifurcations [6, 7]. Here, we build on this work and design an in vitro flow chamber that can be used to reproduce specific magnitudes of wall shear stress (WSS) and gradients of wall shear stress. Particular attention is given to reproducing spatial distributions of these functions that have been shown to induce pre-aneurysmal changes in vivo [38]. We introduce a measure of the gradient of the wall shear stress vector (WSSVG) which is appropriate for complex 3D flows and reduces to expected measures in simple 2D flows. The WSSVG is a scalar invariant and is therefore appropriate for use in constitutive equations for vessel remodeling in response to hemodynamic loads [34, 35].

Keywords Intracranial aneurysm · Wall shear stress gradient · Flow chamber · Bifurcation

A.M. Robertson (✉)
Department of Mechanical Engineering and Materials Science, McGowan Institute for Regenerative Medicine, Center for Vascular Remodeling and Regeneration (CVRR); University of Pittsburgh, Pittsburgh, PA 15261, USA
e-mail: rbertson@pitt.edu

R. Rannacher, A. Sequeira (eds.), *Advances in Mathematical Fluid Mechanics*,
DOI 10.1007/978-3-642-04068-9_35,

1 Introduction

Due to the broad audience of this special volume, we begin this manuscript with a general introduction and motivation for this work. The arterial system is in some sense an optimized network of vessels [40]. In particular, it appears that the vasculature is designed to maintain the wall shear stress in vessels in a specific range, e.g. [15]. This is reflected in both the geometry of the vasculature and also in its ability to locally modify the vessel caliber through dilation and remodeling in response to changes in shear stress [23, 30, 50]. Throughout much of the arterial system, the velocity field is predominantly parallel to the vessel centerline. However, there are locations such as bifurcations, regions of sudden expansion and highly curved segments where the hemodynamic loading is far from this idealized flow, e.g. [26, 36]. These regions may display recirculation, flow impingement, acceleration/deceleration, and points of flow separation. In these areas, the magnitude and direction of the wall shear stress vector, $\underline{t}_s$, may change in space and time and be far from that associated with the nearly uni-directional flow found in straighter, more uniform arteries. For this reason, these flows are often referred to as "disturbed flows."

The fact that pathological changes to the vessel wall are correlated with these flows suggests the nature of the stress vector in these areas is outside the "optimal range" and is challenging for the vasculature. For example, intimal thickening is found to be correlated with regions of very low and oscillating wall shear stress often found in the carotid artery sinus, e.g. [27]. The destructive remodeling of the vessel wall in these regions appears to be a maladaptive response to hemodynamics in this region.

The general nature of the term "disturbed flows" is misleading. It is now understood that the endothelial cells (EC) which line our arteries can distinguish between some types of complex flows. Their response to altered $\underline{t}_s$ includes changes in cell shape and alignment, changes in activation of ion channels, intercellular signaling, gene expression changes at the level of transcription and protein synthesis (see, e.g. [2, 9, 16, 36, 41]). These local responses can trigger a cascade of large scale events such as vasodilation, and vessel remodeling.

Because of the importance of the EC in both the normal maintenance of the arterial wall as well as pathological changes associated with disease, numerous in vivo and in vitro studies have been directed at understanding the coupling between $\underline{t}_s$ and EC response. Various hemodynamic parameters have been introduced with the intent of replacing this complex vector function with scalar quantities that capture the most significant features of $\underline{t}_s$ for a given biomechanical response. One such parameter is the magnitude of $\underline{t}_s$ which is nearly uniformly accepted as an appropriate measure of $\underline{t}_s$. It is simply denoted as WSS.

Another hemodynamic feature of interest is the surface gradient of the wall shear stress. The choice of a scalar measure for this quantity is less clear. This is particularly true for curved surfaces where the spatial gradient of $\underline{t}_s$ has an out of plane contribution. A variety of scalar functions of the spatial gradient of $\underline{t}_s$ are used in the literature. Unfortunately, they are all denoted as WSSG, confounding comparison of results from different groups [5, 22, 25]. In most cases, a non-negative quantity is used, which cannot capture the dependence of the biological response on the sign of the gradient. In Sect. 2.1.1, we introduce a new measure of the wall shear stress gradient denoted as WSSVG rather than WSSG to emphasize that it is dependent on the gradient of the wall shear stress vector not the gradient of the WSS. This parameter has a number of advantages. It is appropriate for complex 3D flows and reduces to expected measures in simple 2D flows. The sign of WSSVG reflects the increasing and decreasing nature of $\underline{t}_s$. In addition, this measure is a scalar invariant of a second order tensor, so will be appropriate for use in constitutive equations for vessel remodeling in response to hemodynamic loads (e.g. [34, 35]).

There is substantial evidence to support the hypothesis that hemodynamics also play an important role in the initiation and development of intracranial aneurysms (ICA), (see, e.g. [14, 19, 20, 24, 44, 45]). An ICA is a pathological condition of cerebral arteries characterized by degeneration of the internal elastic lamina (IEL) and media, accompanied by local enlargements of the arterial wall, typically into a saccular shape. Cerebral aneurysms are predominantly found at the apices of bifurcations and outer bends of highly curved vessels in or near the circle of Willis, a network of vessels at the base of the brain. At both these locations, the blood impinges on the arterial wall where it is redirected with strong spatial variations in $\underline{t}_s$ downstream of the impingement point.

Earlier computational work suggested that the impulse of the incoming flow on the apex region could directly damage even healthy arterial walls [11]. It was later shown that the results supporting this conjecture were unphysical due to the use of perfectly sharp corners in the study [18]. The local increase in pressure at the apex is on the order of a few mmHg, much smaller than the normal variation in pressure throughout the vasculature [6]. Since cerebral aneurysms can form in humans in the absence of hypertension, we conjecture the role of elevated hemodynamic pressures in aneurysm formation is to hasten mechanical damage and ultimate failure of an IEL previously weakened by biochemical factors. The magnitude and spatial distribution of $\underline{t}_s$ at the apex of the bifurcation is drastically different from the seemingly desired distribution of more uniform flow. It has been conjectured that some aspect of $\underline{t}_s$ at the apex of the bifurcation initiates a cascade of biochemical activities that lead to the degradation of the IEL and media, rather than directly damaging the wall. For example, the character of $\underline{t}_s$ may lead to an imbalance in the production of enzymes responsible for natural remodeling and turnover of the extracellular matrix.

Motivated by diseases such as atherosclerosis as well as the frequent onset of intimal hyperplasia following bypass surgery, numerous in vitro and in vivo studies have been performed to explore the role of WSS and WSSVG in pathological changes to the arterial wall (e.g. [5, 29, 41]). While some in vitro chambers are designed to isolate the effect of specific parameters, others attempt to reproduce a specific "disturbed" flow found in vivo. For example, parallel plate and cone-and-plate flow chambers have been used to study the role of WSS under conditions for which there is no spatial or temporal gradient in $\underline{t}_s$. A backward facing step was introduced into these chambers to recreate the recirculating flow associated with intimal hyperplasia in vivo [10], including a reattachment point and regions of deaccelerating and accelerating flow. DePaola et al. appear to be the first to conjecture that endothelial cells may be sensitive to the gradient of $\underline{t}_s$ [10].

Recent in vivo work suggests both the WSS and the WSSVG play an important role in aneurysm initiation. Significantly, the sign of the gradient in $\underline{t}_s$ has been reported to be important for pre-aneurysmal changes [39]. However, the chambers designed for atherosclerosis do not reproduce the salient hemodynamic features found at the apices of bifurcations where aneurysms tend to form. In particular, the WSS field downstream of the stagnation point is monotonic and the surface gradient of $\underline{t}_s$ is much smaller than that found at the apex of bifurcations. There is a pressing need for an in vitro flow chamber which reproduces the WSS and WSSVG fields associated with aneurysm formation in vivo.

An in vitro T-chamber for studies of cellular response to apex flows was first introduced by Robertson et al. [6, 7]. This chamber well approximates the WSS field found in idealized human cerebral bifurcations and forms the starting place for the present work. In this work, we design a T-chamber which successfully reproduces specific profiles in both WSS and WSSVG found to be associated with pre-aneurysm changes in canine arterial bifurcations [38, 39].

2 Methods

2.1 Governing Equations

We perform numerical simulations in an idealized arterial bifurcation as well as in segments of an in vitro flow chamber. For both cases, the fluid is idealized as incompressible, homogeneous and linearly viscous (Newtonian) and the flow is modeled as steady and isothermal. The relevant governing equations are therefore the incompressibility condition and equation of linear momentum. Referred to rectangular Cartesian coordinates, x_i, the governing equations in the fluid domain, Ω, are

$$\left.\begin{aligned} v_{i,i} &= 0, \\ \varrho\, v_{i,j} v_j &= -\, p_{,i} + \mu\, v_{i,jj}, \end{aligned}\right\} \text{ in } \Omega \tag{1}$$

where v_i are the components of the velocity vector $\underline{v}$, p is the combined term representing the Lagrange multiplier arising from the incompressibility constraint (equivalent to the mechanical pressure) and the gravitational potential, μ is the constant viscosity and ϱ is the constant mass density. The notation $()_{,i}$ denotes $\partial()/\partial x_i$ and repeated indices imply summation over the values of the index $i = 1, 2, 3$.

The bounding surface of Ω is composed of rigid walls where the velocity is prescribed to be zero, as well as N inflow and outflow surfaces. The locations of these N surfaces are somewhat arbitrary, arising when we truncate the physical domain in order to make the computational problem tractable. The choice of boundary conditions on these surfaces is not unique from the physical or mathematical perspective.

We will specify the velocity on surfaces $\bar{\Gamma}_\alpha$ and the modified stress vector $\underline{t}'$ on surfaces denoted as Γ_α where $\alpha \in [0, 1, 2, ..N - 1]$. The choice of these surfaces and the corresponding conditions are problem specific and therefore will be given below for particular simulations. The modified stress vector is defined as

$$t_i' \equiv (-p\delta_{ij} + \mu v_{i,j})n_j \tag{2}$$

where n_j are the components of the outward normal to the surface Γ_α. It is physically reasonable and computationally straightforward in appropriately chosen FEM formulations to prescribe $\underline{t}'$ to be parallel to $\underline{n}$ on inlet and outlet surfaces, so that from (2),

$$(-p\delta_{ij} + \mu v_{i,j})n_j = Cn_i \qquad \text{on } \Gamma_\alpha. \tag{3}$$

For a discussion of the implementation of (3) using the finite element method see, for example [3], for a comparison of this condition with other inflow/outflow conditions see [17], and for numerical and some mathematical aspects of this boundary condition, see [21]. More recently, Galdi has addressed the mathematical properties of the system (1) for the case of steady and unsteady flows when condition (3) is applied at all inflow and outflow surfaces [13]. Kučera and Skalák have considered the unsteady problem with more general boundary conditions [28]. An early discussion of physical anomalies arising when the usual Cauchy stress vector rather than the modified stress vector is specified at outflow boundaries is given in [33].

2.1.1 Flow Parameters: Wall Shear Stress and Wall Shear Stress Gradient

In this section, we give a more precise meaning to the scalar quantities called the wall shear stress and wall shear stress gradient. The central considerations are (i) that these quantities be physically meaningful based on known biological data and (ii) that they are scalar invariants. This last point is important when these quantities are used in constitutive equations for destructive remodeling and damage of the arterial wall such at the model proposed in [34, 35].

We now consider the fluid domain to be surrounded by a solid domain Ω' (the wall), Fig. 1. Consider an arbitrary point P on the interface of these domains $\partial\Omega$ with unit normal $\underline{n}$ directed into the fluid domain. The wall shear stress vector, $\underline{t}_s$ at P is defined as

$$\underline{t}_s = \underline{t} - \underline{t} \cdot \underline{n}\,\underline{n}. \tag{4}$$

We would like the WSS to be a scalar function of $\underline{t}_s$ with dimensions of stress. Since a scalar valued function of a vector is invariant if and only if it can be expressed as a function of its inner product (e.g. [48]), the choice of WSS is clear,

$$\text{WSS} = |\underline{t}_s| = \sqrt{\underline{t}_s \cdot \underline{t}_s}. \tag{5}$$

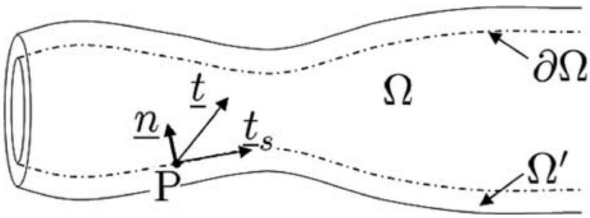

Fig. 1 Schematic of the vessel lumen and arterial wall

To our knowledge, there is only one work which does not use this definition [22].

We denote the spatial gradient of $\underline{t}_s$ with respect to surface coordinates as $\text{grad}_s\underline{t}_s$. For curved surfaces, $\text{grad}_s\underline{t}_s$ may not be a two dimensional tensor because the gradient of the surface base vectors may not lie on the surface. For example, consider the surface of a cylinder of circular cross section which is parameterized in terms of standard cylindrical components (θ, z). The $\text{grad}_s\underline{t}_s$ has an $\underline{e}_r \otimes \underline{e}_\theta$ component. We do not expect the biological cells to be sensitive to a purely geometric contribution of this kind, so we define a modified gradient of the wall shear stress vector as

$$\underline{G} = \text{grad}_s\underline{t}_s \;-\; \underline{n} \otimes (\underline{n} \cdot \text{grad}_s\underline{t}_s). \tag{6}$$

The quantity $\underline{G}$ is a two dimensional second order tensor with two principal invariants $\text{tr}(\underline{G})$ and $\det\underline{G}$, (e.g. [48]). Based on physical motivations elaborated on below, we define the $WSSVG$ as,

$$\text{WSSVG} \;=\; \text{tr}\,\underline{G}. \tag{7}$$

We emphasize that WSSVG is an invariant of the gradient of the wall shear stress *vector* and not the gradient of the WSS. To avoid confusion, we do not use the notation WSSG. As we will see below, this is an important distinction and necessary to ensure the WSSVG captures the desired physical behavior.

To attain a clearer understanding of the physical meaning of these quantities, we consider the special case of 2D flow of an incompressible linearly viscous fluid over a flat surface. Using 2D rectangular coordinates (x_1, x_2), we define a solid boundary at $x_2 = 0$ with normal $\underline{e}_2$ into the fluid and consider velocity fields of the form, $\underline{v} = v_1(x_1, x_2)\underline{e}_1 + v_2(x_1, x_2)\underline{e}_2$. For such flows,

$$\text{2D flow}: \qquad \underline{t}_s \;=\; t_{s1}\underline{e}_1 \;=\; \mu\,\frac{\partial v_1}{\partial x_2}\underline{e}_1, \quad \text{WSS} \;=\; \mu\left|\frac{\partial v_1}{\partial x_2}\right| \quad \text{at } x_2 = 0, \tag{8}$$

where we have made use of the no-slip condition. We see the WSS has the expected meaning of the magnitude of the viscous drag per unit area on the wall by the fluid. Furthermore, for these 2D flows,

$$\left[\text{grad}_s \underline{t}_s\right] = \begin{bmatrix} \mu \dfrac{\partial^2 v_1}{\partial x_1 \partial x_2} & 0 \\ 0 & 0 \end{bmatrix}, \quad \text{at } x_2 = 0. \tag{9}$$

For flat plates, Eq. (6) simplifies to $\underline{G} = \text{grad}_s \underline{t}_s$. It therefore follows directly from (7) that,

$$\text{2D flow :} \qquad \text{WSSVG} = \mu \frac{\partial^2 v_1}{\partial x_1 \partial x_2}. \tag{10}$$

The second principal invariant, $\det(\text{grad}_s \underline{t}_s)$, is zero for these 2D flows and so the choice to use the trace invariant is clear. A linear dependence on this invariant is consistent with the desired dimensions of WSSVG. It is clear from (10) that WSSVG is capable of distinguishing between increasing and decreasing t_{s1} through its sign.

The difference in using the surface gradient of WSS rather than the surface gradient of the stress vector is clear if we consider a special case of the 2D flow which is symmetric about the plane $x_1 = 0$. As an example, consider flows for which the fluid impinges on the plate with $v_1(-x_1, x_2) = -v_1(x_1, x_2)$ and $v_2(-x_1, x_2) = v_2(x_1, x_2)$. The idealized 2D flow fields we consider below for the apex region of the T-chamber display this symmetry. From the perspective of the response of the endothelial cells to flow of this type, we would like our "measured" WSSVG to display a symmetry about the plane $x_1 = 0$ as well. It follows directly from the result (10), that $\text{WSSVG}(-x_1, x_2) = \text{WSSVG}(x_1, x_2)$, as desired. Note that grad_s WSS is an odd function of x_1 and so would predict different behavior on either side of the symmetry plane.

2.2 *Flow in Idealized Bifurcation Models*

The T-chamber developed here is designed to reproduce shear stress fields which are typical of the apex region of cerebral arterial bifurcations. With this in mind, we briefly review the central features of such flows. Unsteady and steady flows in arterial bifurcations have been the subject of intense research, due to their relevance in atherosclerosis and other vascular diseases (see, e.g. [4, 18, 27, 51]). Here, we concentrate on flow in the apex region of bifurcations, where cerebral aneurysms are most likely to form.

Quantitative features of the bifurcation flow, such as the distribution of WSS, are dependent on the bifurcation geometry as well as the flow and fluid parameters. One such idealized bifurcation model with two planes of symmetry is shown in Fig. 2a, b. The bifurcation geometry was created using a parametric model for human cerebral bifurcations [6, 49]. Approximate solutions to (1) were obtained using the finite element method, implemented in ADINA (Automatic Dynamic Incremental Nonlinear Analysis, Watertown, MA). The velocity was prescribed to be zero on the lateral (rigid) walls. Boundary condition (3) was applied at the inlet and outlet surfaces with $C = 0$ on (Γ_1, Γ_2) and C set equal to a positive constant on Γ_0, chosen such that a Reynolds number (Re) of 255 was achieved, where

$$\mathrm{Re} = \varrho \bar{V} D / \mu, \tag{11}$$

D is the diameter at Γ_0 and $\bar{V} = 4Q/(\pi D^2)$ is the average velocity at the same location. For these studies, we choose parameters $\varrho = 1.05\,\mathrm{g/cm^3}$ and $\mu = 0.035\,\mathrm{g/(cm\,s)}$, $D = 4\,\mathrm{mm}$ and from (11), $\bar{V} = 21\,\mathrm{cm/s}$. The diameter of both daughter branches was set to 2.4 mm. These values are relevant for cerebral aneurysm formation.

As blood travels up the parent branch into the bifurcation region it impinges on the wall as it splits to flow into the two daughter branches, Fig. 2c. The blood then follows the curved geometry of the bifurcation into the daughter branches. The fluid close to the apex accelerates as it leaves the neighborhood of the impingement point, Fig. 2c. Displayed in Fig. 2d are the surface stress vectors $\underline{t}_s$ and iso-WSS contours

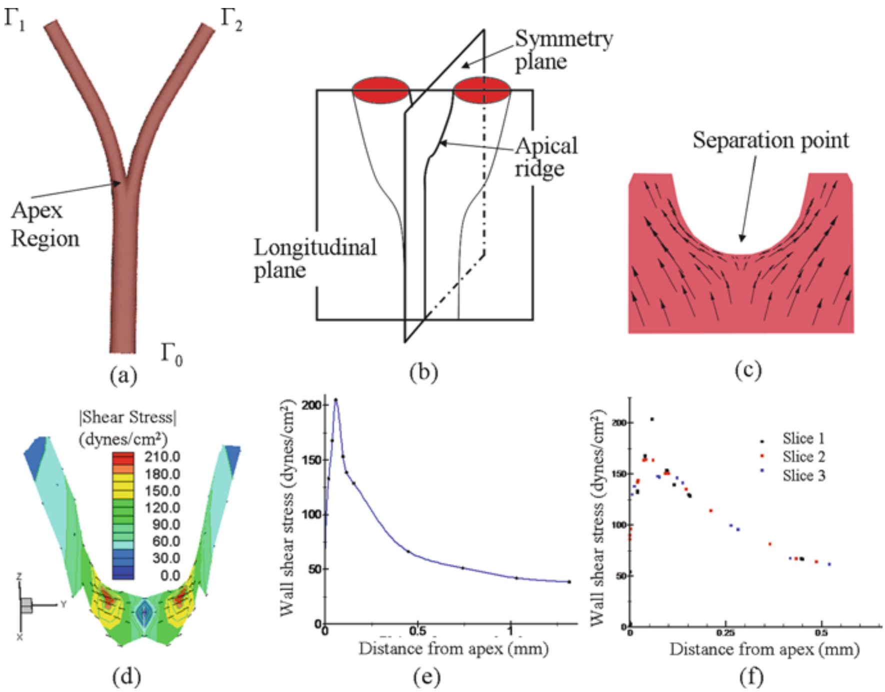

Fig. 2 Flow in an idealized bifurcation model. (**a**) Idealized geometry and computational domain Ω. (**b**) Schematic of cutting planes for bifurcation. (**c**) Velocity vectors in longitudinal plane of apex region. (**d**) Contours of the WSS (dynes/cm^2) with vectors $\underline{t}_s$ superimposed on iso-contours. (**e**) WSS along apical ridge defined by the intersection of apex and longitudinal plane. Distance is measured from impingement point. (**f**) WSS along apical ridge (slice 1) and planes parallel and separated by 0.04 and 0.08 mm from the longitudinal plane (slice 2 and 3, respectively)

for a saddle shaped region in the neighborhood of the bifurcation. In Fig. 2e, WSS along the apical ridge (formed by the intersection of saddle region and the longitudinal plane) is plotted as a function of distance from the impingement point. As can be seen in these two figures, WSS is non-monotonic, increasing from zero at the impingement point to a local maximum value and then decreasing again.

It is clear from Fig. 2d that the WSS field is fairly two dimensional in nature in the bifurcation region. To assess this further, consider the WSS at points denoted as slice 1 in Fig. 2f, corresponding to the curve in Fig. 2e. The WSS along two other curves is shown (labeled slice 2 and 3) in Fig. 2f. These correspond to the curves formed by the intersection of the saddle region with planes parallel to the longitudinal plane, separated from it by distances of 0.04 and 0.08 mm, respectively. If the stress field was perfectly two-dimensional, these curves would be identical. Though the maximum drops slightly with distance from the longitudinal plane, the WSS can be seen to be close to two-dimensional in this region. Furthermore the direction of vectors $\underline{t}_s$ are approximately tangent to these planes, Fig. 2d. This near two-dimensionality is likely due to the fact that the principal radii of curvature at the apex, are of opposite sign. Our in vitro chamber makes use of this near two dimensionality in the neighborhood of the apex.

Meng et al. [39] evaluated the response of vascular tissue to sudden exposure to apical $\underline{t}_s$ fields. Artificial bifurcations were surgically created from native segments of common carotid arteries in dogs. Using CFD analysis in reconstructions of these vessels, they obtained WSS fields similar in form to those shown in Fig. 2e. They divided the apex into three distinct hemodynamic regions which we denote as Regions A,B,C. Region A displays WSS $\leq$ 20 dynes/cm^2, Region B displays WSS $>$ 20 dynes/cm^2, and positive WSSVG and Region C displays WSS $>$ 20 dynes/cm^2 and negative WSSVG. Distinct histological responses were found in these regions. Significantly, in five of six cases, Region B displayed pre-aneurysmal changes including a thinned wall, disrupted IEL, reduction in SMCs and loss of endothelium. However, these same changes were not found in region C where the WSS magnitude was equally high though the WSSVG was of a negative sign. In that work, elevated WSS and positive elevated WSSVG were found to be important for aneurysm initiation.

2.3 Rationale Behind Design of Fluid Domain in the Bifurcation Chamber

The geometric features of the T-chamber designed by Chung and collaborators [6, 7] well approximates the WSS field found in an idealized human cerebral bifurcations. This chamber forms the starting place of the present work. Motivated by the in vivo results just discussed, this T-chamber was modified to reproduce the quantitative features of both the WSS and WSSVG of the range reported in [39]. Many tests of cellular function provide only a relative measure (e.g. Western blotting, etc.) and so it is desirable to build the chamber to recreate both the bifurcation stress field as well as control fields. We introduce two control regions for exposure of cells to constant WSS.

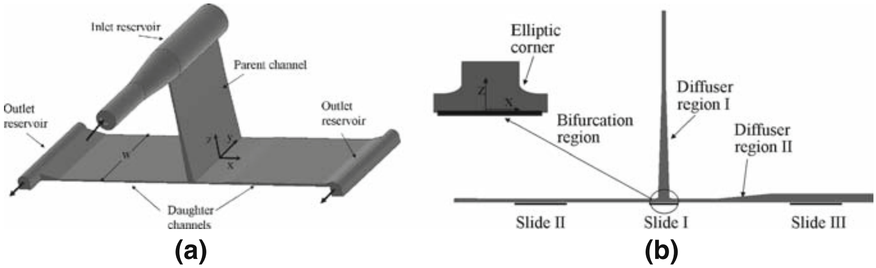

Fig. 3 Schematic of main features of fluid domain in flow chamber. (**a**) Entire 3D fluid domain (**b**) 2D cross section of fluid domain without reservoirs

A schematic of the general geometric features of the T-chamber are shown in Fig. 3, where the chamber orientation is inverted relative to the bifurcations shown in Fig. 2. Culture medium flows into the inlet reservoir, moves down the parent (vertical) channel, flows into the two daughter channels, into the outlet reservoirs and finally out of the chamber, Fig. 3a. Three separate slide regions are specified on the bottom plate: one in the region of the T-junction (slide I), two in control regions of constant WSS (slides II and III), Fig. 3b. Distinct slide banks are used to decrease contamination of the final biological cells from each test region with those from the transition regions. In addition, cross communication between cells in the different regions will be lessened.

Following [8], we define *Active Test Region*s, ATR-I, ATR-II, ATR-III, where the wall shear stress is within a chosen percentage of the desired 2D flow field for slides I, II and III. For ATR-II and ATR-III, the desired stress field will be a constant, corresponding to the solution for steady, fully developed, 2D, channel flow,

$$\tau_{fd_{2D}} = \frac{6Q\mu}{wh^2} = \frac{4V_o\mu}{h}, \tag{12}$$

where Q is the volumetric flow rate, V_o is the centerline (maximum) velocity, w is the channel width and h is the channel height. It follows from the exact analytic solution for 2D flow that $V_o = 3Q/(2hw)$. In the bifurcation slide, (slide I), the desired 2D field will correspond to the 2D bifurcation flow field, discussed in more detail below.

In summary, the T-chamber should meet the following criterion:

Design Criteria

1. A 2D WSS and WSSVG field is created on slide I which, with proper choice of flow rates, is relevant to (i) the apex of human cerebral arterial bifurcations and (ii) values for canine models in which pre-aneurysmal changes were reported.
2. Geometry of the flow domain creates nearly constant WSS fields on slides II and III. For example, supra-physiological WSS and physiological stress levels could be created in ATR-II and ATR-III, respectively.

3. The shear stress field should be approximately two dimensional in a large percentage of the chamber. In particular, the width of chamber should be chosen to provide sufficient quantities of cells for meaningful biological analysis in the bifurcation region.
4. The thickness of the daughter channels should be machined to sufficient tolerance to obtain acceptable errors in WSS and WSSVG.
5. The flow chamber should be easily assembled.
6. The total volume of the chamber fluid domain should be minimized to reduce the cost of the testing fluid, chamber body material and lessen the dilution of cellular byproducts.
7. The components of the chamber should be suitable for repeated autoclaving during sterilization.

A variety of perfusion fluids are used in the literature. In general, they have approximately the same properties as water. In other cases, an attempt is made to match the viscosity and density of blood. We take this latter approach and set $\mu = 0.032\,\text{g/(cm s)}$, $\varrho = 1.02\,\text{g/cm}^3$. These values are within the range reported for normal blood at 37°C at shear rates higher than $400\,\text{s}^{-1}$, (e.g. [42]). We use these latter values here.

It should be recalled, that the solution (12) is for a 2D channel not a channel with a finite width. An analytic series solution exists for fully developed flow in channels of rectangular cross section and can be used to assess the error in using (12), [8]. The velocity is diminished in a boundary layer near the wall, so that for a given flow rate, the average velocity and WSS will generally be higher outside the boundary layer in the finite channel compared with the idealized 2D solution given in (12). The difference between the WSS outside this boundary layer and that in of the 2D solution can be controlled through the channel geometric ratio $\beta = h/w$, [8]. For the geometries used here, this error is less than 2% and so it is convenient to simply estimate the WSS in slides II and III using (12).

3 T-Chamber Design: Analysis and Results

3.1 Fluid Domain

A 2D computational analysis was used to select the relevant 2D chamber geometric parameters in Fig. 4a such as the channel heights (h_0, h_1, h_2) and the shape of the bifurcation region. Next, the length of the daughter channel between the bifurcation region and the constant WSS regions s_1 and s_2 was chosen to assure the flow is nearly fully developed when it reaches slides II and III. Finally a 3D analysis was performed to design the inlet and outlet reservoirs to diminish the effects of the fluid entering and exiting the chamber. These reservoirs are essential for obtaining a nearly 2D flow in the test regions. The final design was then checked using a comprehensive CFD study of the full 3D chamber.

3.1.1 Bifurcation Region

Criterion 1 was the central factor in the design of the bifurcation region. The 2D computational domain for these studies was composed of the parent channel, the bifurcation region and symmetric daughter branches of constant height, h_1, Fig. 4a. The modified stress vector $\underline{t}'$ was set to zero at the inlet and a parabolic profile with

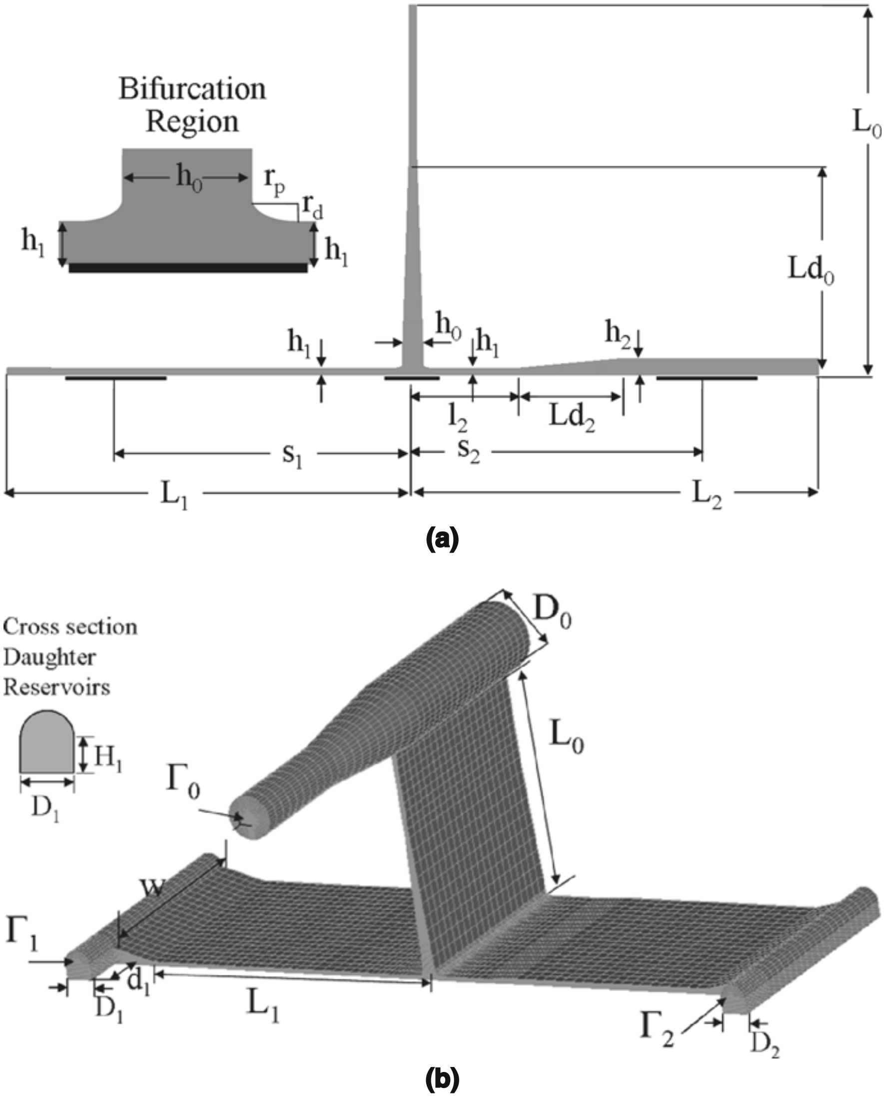

Fig. 4 Geometric parameters considered in chamber design. (**a**) 2D domain (no reservoirs), (**b**) full 3D domain

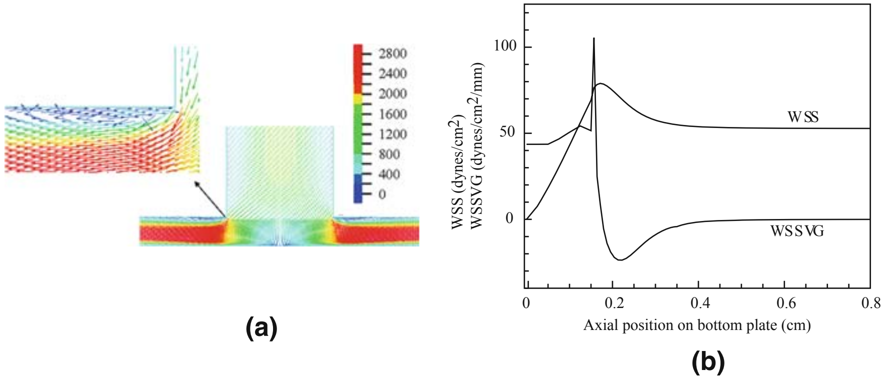

Fig. 5 Flow through a bifurcation with sharp corners (2D simulation). In (**a**), velocity vectors in bifurcation region with vortex seen downstream of sharp corner. In (**b**) WSS distribution along centerline of bottom plate in region $x \in [0.0, 0.8]$ cm. Here, $Q = 4518$ ml/min, $[h_0, h_1, h_2] = [1.0, 0.3, 0.3]$ mm

the desired flow rate was specified at each outlet. The FEM mesh was composed of structured quadrilateral elements (between 250 and 500K elements).

The WSS distribution on slide I was found to be quite sensitive to the shape of the juncture between the parent and daughter branches (the outer corner of the bifurcation) and the design of this region required the most intense evaluation. A simple sharp corner has been used in a recent T-chamber designs [47]. However, as seen in Fig. 5a below and Fig. 1 of [47], corners of this type can produce standing vortices. The qualitative nature of the WSSVG is altered by these vortices, Fig. 5b. Furthermore, these vortices can potentially be shed and washed downstream, creating additional errors in the imposed WSS and WSSVG fields on the bottom plate. Instabilities of this kind will not be captured in steady simulations.

These vortices can be removed by rounding the sharp corner to form a section of an ellipse, Fig. 6. The elliptical geometry can be characterized by the ellipticity, $\varepsilon = \sqrt{(r_p^2 - r_d^2)/r_p^2}$, where r_p and r_d are the half length of the major axis, Fig. 4a. The original chamber introduced in [6, 7], provided a good match with the WSS distribution in the idealized bifurcation using a circular corner ($\varepsilon = 0$), but there were quantitative differences in the WSS from those reported in [38]. In particular, for the canine model, the maximum in WSS ($\mathrm{WSS}_{\max}$) is found 2–3 mm from the bifurcation point, nearly twice the distance of that in the T–chamber with a circular corner. By elongating the circular corner (increasing ε), while holding other variables fixed, the location of the maximum in WSS shifts downstream. This effect can be seen Fig. 7 where 2D solutions for the WSS and WSSVG on the bottom plate are shown for a circular corner ($\varepsilon = 0$) and an elliptical corner with ε increased to $\sqrt{3}/2$. Comparison of Figs. 7 and 8 demonstrates the effect of increasing flowrate on the WSS and WSSVG profiles. The location where the WSSVG changes sign is relatively insensitive to flowrate, while both $\mathrm{WSS}_{\max}$ and $\mathrm{WSSVG}_{\max}$ increase with increasing Q. As can be seen in Fig. 9, the $\mathrm{WSS}_{\max}$ is quite sensitive to the channel

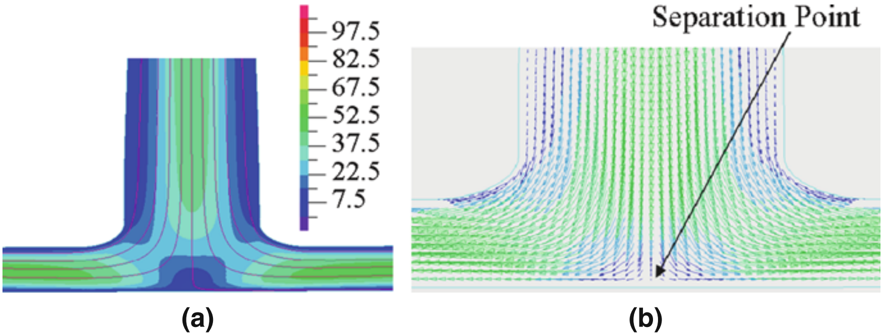

Fig. 6 Flow through a bifurcation with elliptical corner (2D simulation). In (**a**), magnified view of bifurcation with streamlines superimposed on iso-velocity contours (mm/s). In (**b**), magnified view of velocity vectors in bifurcation region. Here, $Q = 1333$ ml/min and geometric parameters are given in Table 1

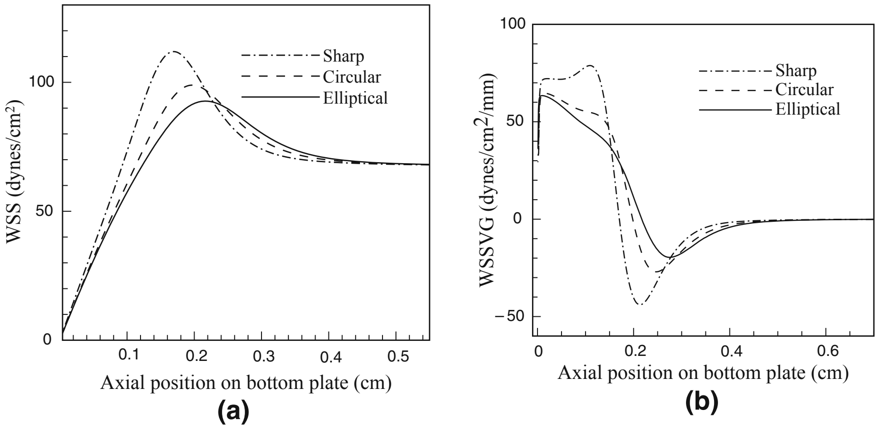

Fig. 7 Comparison of (**a**) WSS and (**b**) WSSVG on the *bottom plate* of T-chambers with elliptical, circular and sharp corners, (2D simulations) $Q = 1333$ ml/min, $\varepsilon = \sqrt{3}/2$, $R_c = 0.5$ mm, with all other geometric parameters given in Table 1

height of the daughter branch. As h_1 is narrowed from 0.8 to 0.4 mm for fixed h_0, the WSS_{max} more than doubles with a very slight downstream shift in its location. It was found that by adding a slight taper to the channel upstream of the bifurcation, the magnitude and location of the $WSSVG_{max}$ could be easily controlled with little change in WSS_{max}, making it possible to closely match specific WSS and WSSVG profiles.

Using these trends as guidelines, it was possible to select ε, h_0, h_1 and the parent channel taper in such a away to obtain bifurcation WSS and WSSVG values that capture the main quantitative features of a given arterial bifurcation. For example, shown in Fig. 10 is a comparison between WSS and WSSVG profiles

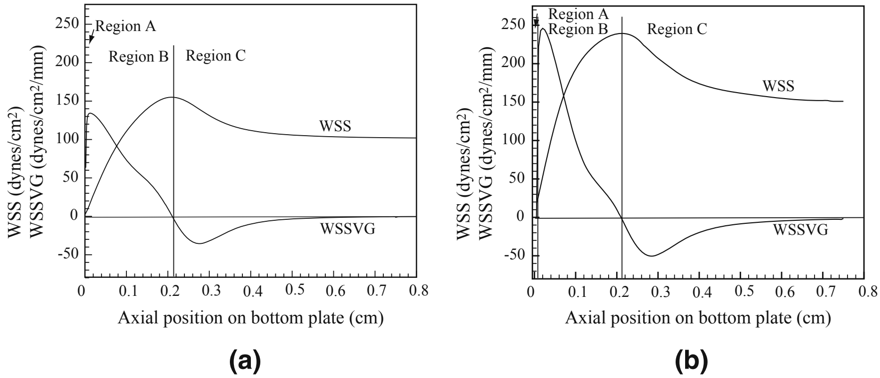

Fig. 8 WSS and WSSVG distribution along *centerline* of bottom plate in bifurcation region (2D simulations) with elliptical outer bifurcation $\varepsilon = \sqrt{3}/2$, $h_0, h_1, h_2 = [3.0, 0.8, 1.2]$ mm and all other geometric parameters given in Table 1. Two flowrates are considered: (**a**) $Q = 2000$ ml/min, (**b**) $Q = 2400$ ml/min. Region A is defined by WSS ≤ 20 dynes/cm^2, Region B by WSS > 20 dynes/cm^2 and positive WSSVG and Region C by WSS > 20 dynes/cm^2 and negative WSSVG

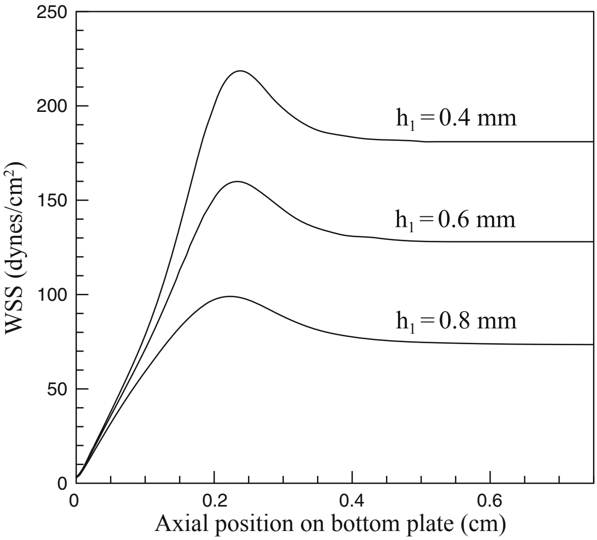

Fig. 9 WSS distribution along *centerline* of bottom plate in bifurcation region for $h_1 = [0.4, 0.6, 0.8]$ mm, (2D simulations) with elliptical outer bifurcation $\varepsilon = \sqrt{3}/2$, $Q = 1333$ ml/min. All other geometric parameters are given in Table 1

for a representative canine data set from [39] and results from a T-chamber model, designed to obtain a quantitative match of this data.

3.1.2 Test Regions II and III

The chambers are designed to be run with an equal flow split between the two daughter branches. This ensures the flow in the bifurcation region is nearly symmetric

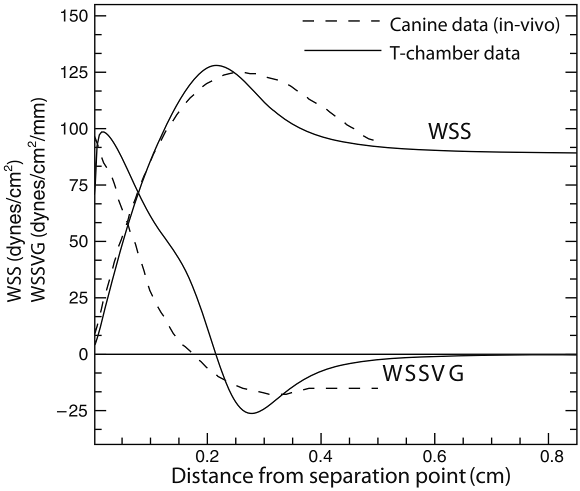

Fig. 10 WSS and WSSVG profiles in bifurcation region of canine model and T-chamber. T-chamber flowrate and geometry chosen to approximate maximum in WSS and WSSVG in canine data as well as qualitative shapes of curves. In T-chamber study $L_{d0} = 18$ mm and $Q = 1750$ ml/min, (2D simulations). All other geometric parameters are given in Table 1

about the plane $x = 0$. In this case, the flowrate in each daughter channel is $Q_d = Q/2$. The transition regions between slides I and the slides in the daughter branches are designed to achieve nearly fully developed flow prior to slides II and III. Assuming the flow is approximately 2D, the WSS on each daughter slide can then be calculated directly from (12). A 2D CFD analysis was performed to select the geometry of the diffuser and slide location that would guarantee the flow to be nearly fully developed on both slides. Values for the current chamber are shown in Table 1.

Table 1 Values (in mm) of geometric parameters for T-chamber, Fig. 4. The ellipticity (ε) is $\sqrt{3}/2$. The slide widths (in the flow direction) for slides I, II and III are 15, 25 and 25 mm, respectively

h_0	h_1	h_2	L_0	$L_1 = L_2$	w	l_2	Ld_0	Ld_2	$s_1 = s_2$	D_0	$D_1 = D_2$	$d_1 = d_2$
3.0	0.8	1.2	50	70	48	14	30	7.5	45	16	6	15

3.2 Reservoir Design

As discussed in detail in [8], the size of the ATR is influenced by the magnitude of the lateral wall effects as well as entrance and exit effects. While simply increasing the length of the chamber segments upstream of the test regions will generally lead to a more 2D flow it will also increase the volume of perfusion fluid. The cellular byproducts of the cells in the chamber are sometimes evaluated from samples of the perfusion fluid obtained during experiments [12]. By decreasing the volume of fluid, the cost of the experiment can be decreased and it will be possible to obtain higher concentrations of these materials.

Parametric studies were performed to design the shape and size of the reservoirs and diffusers for the parent and daughter channels. The 3D computational domain for these studies consisted of the inlet/exit to the reservoir, the inlet/daughter reservoir and the adjacent parent/daughter channel, Fig. 4b. A uniform velocity profile was applied at the inlet/outlet of the computational domain and the modified traction vector was set to zero at the outlet/inlet. The width of the channel was set to 48 mm to provide a large quantity of slides for cell culture while matching readily available slip cover and slide lengths.

The inlet reservoirs decreased the incoming momentum of the flow from the tubing and help to redistribute it across the width of the chamber, thereby contributing to the 2D nature of the flow. The shape of the reservoir has a significant impact on its effectiveness [8]. Following [7, 8], we chose cylindrical reservoirs with incoming flow perpendicular to the flow direction in the neighboring channel, Fig. 4b. For the inlet flow, a reservoir of circular cross section with $D_0 = 16$ mm was found to provide a good balance between damping effects and volume requirements. The reservoir design was found to be very effective at damping the momentum of the flow entering the inlet reservoir thereby diminishing the length of the parent channel needed to ensure the flow is nearly 2D in the test regions. Figure 11a displays the iso-velocity (magnitude) contours in the symmetry plane ($x = 0$) of the inlet reservoir and parent channel. The damping of the inlet jet can be seen within the reservoir. The diffuser effectively converts the incoming jet to a nearly 2D flow, a short distance downstream of the diffuser. There are two slight modifications in this

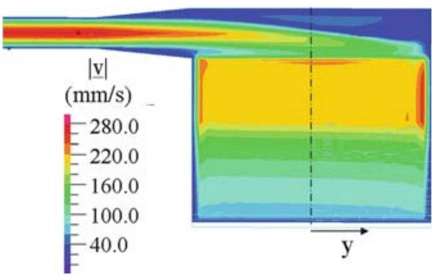

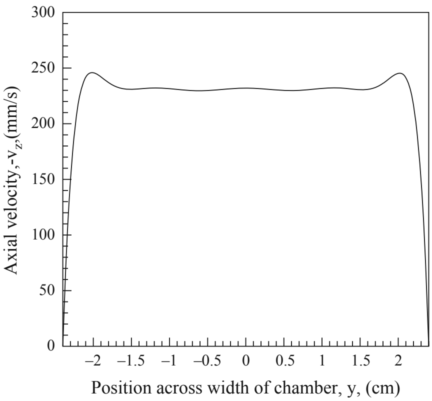

Fig. 11 Evaluation of transition to fully developed flow in parent channel (3D simulations) with (**a**) iso-velocity contours in yz-plane (mm/s) and (**b**) axial velocity ($-v_z$) as a function of y just upstream of bifurcation slide ($x = 0$, $z = 36$ mm), with $Q = 1333$ ml/min, $[h_0, h_1, h_2] = [3.0, 0.8, 1.2]$ mm and all other geometric parameters are given in Table 1. Coordinate system show in Fig. 3

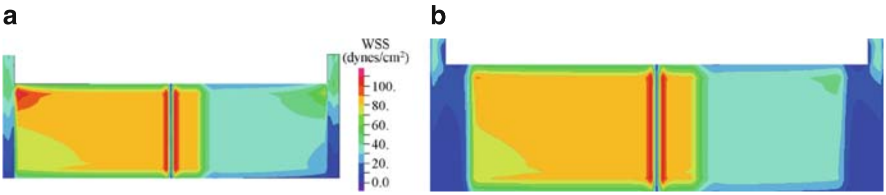

Fig. 12 WSS (dynes/cm^2) contours on *bottom surface* of flow domain, (3D simulation) for chamber (**a**) without diffusers and (**b**) with diffusers at outlet reservoirs. Geometric parameters are given in Table 1 and $Q = 2000$ ml/min

inlet reservoir design from that in [7, 8]. In the earlier chamber, a constant radius extension of the reservoir was used on both sides of the channel. Here, the constant radius inlet extension was replaced by a diffuser. The opposing extension on the inlet reservoir was found to have little impact on the flow and was removed in the current chamber.

The addition of two outlet diffusers upstream of the daughter reservoirs was found to significantly lessen the upstream influence of the reservoirs, Fig. 12. These reservoirs were designed independently from the parent reservoir and, for simplicity, were chosen to be identical. The cross section shape of is the union of a half circle of diameter D_1 and a rectangle of height H_1, Fig. 4b. The value of the geometric parameters used in the final chamber design are given in Table 1.

3.2.1 Methods of Decreasing Fluid Volume

The fluid domain can potentially be reduced in volume by decreasing the reservoir and channel volumes. Careful design of the reservoirs was used to diminish the entrance and exit lengths of the neighboring flow and therefore the lengths (and volume) of each channel. It was found that a region in the parent branch adjacent to the inlet reservoir could be narrowed to a thickness $h_p = 1/3h_0$ and then gradually expanded over a length Ld_0 to the desired value of h_0, Fig. 4a. Due to the gradual nature of the taper, these alteration to the parent channel had no measurable effect on the velocity field, WSS, or WSSVG in the bifurcation region. Values chosen for this chamber are given in Table 1. The total chamber volume is 25.8 ml.

3.3 Validation of T-Chamber Design

The design of the various sections of the chamber were performed for subsets of the entire final chamber geometry. It was therefore necessary to perform a 3D analysis for the full 3D chamber, including the inlet port and reservoirs. This corresponds to the complete computational domain shown in Fig. 4b using the geometric parameters in Table 1. A uniform velocity profile corresponding to the flowrate Q_d was prescribed at each of the outlets (Γ_1, Γ_2) to ensure equal flow division. The modified

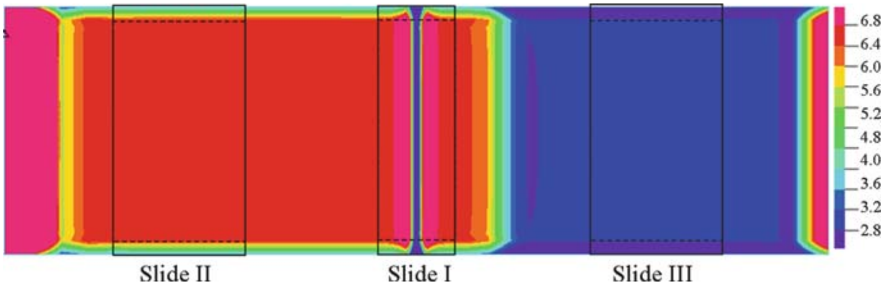

Fig. 13 WSS (dynes/cm^2) contours on bottom surface of flow domain, with labeled slide regions (3D simulation). Geometric parameters are given in Table 1 and $Q = 1333$ ml/min

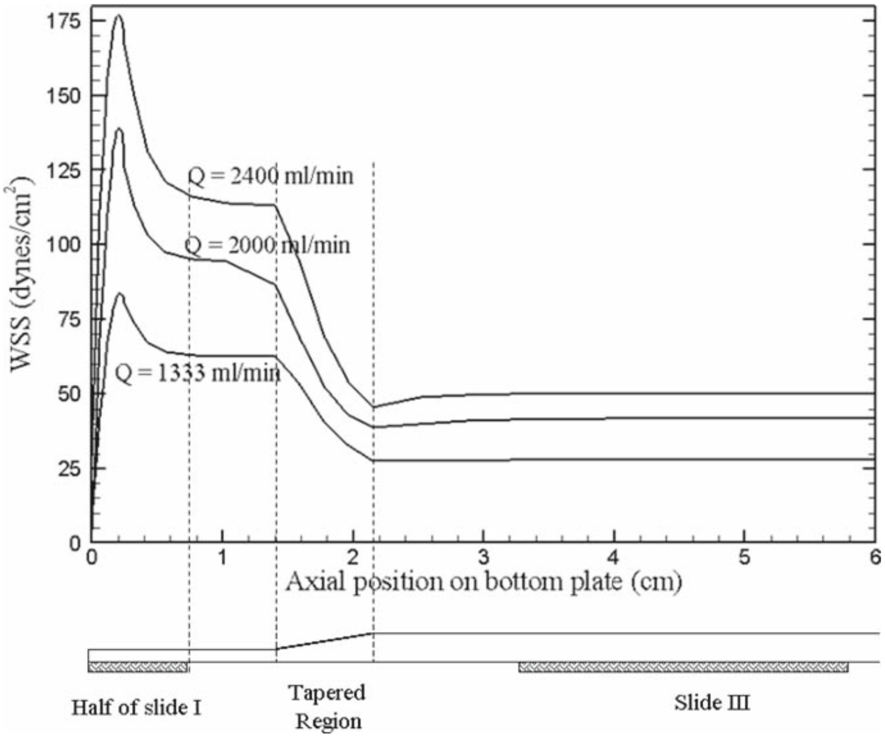

Fig. 14 WSS (dynes/cm^2) along centerline of *bottom plate* for flowrates, Q = [1333, 2000, 2400] ml/min with the geometry given in Table 1

traction vector was set to zero at the inlet, Γ_1. Approximately 70K structured hexahedral elements were used for these 3D studies. The results of this validation study are shown in Figs. 13 and 14.

The WSS on the bottom plate and reservoirs is shown in Fig. 13. The boundaries of ATR-II and III based on a criterion that the WSS be within 10% of the desired 2D value are drawn. The slide locations are drawn in solid lines with the lateral boundaries of the ATR drawn as dashed lines. The slide widths in the direction of flow are 15, 25 and 25 mm for slides I, II and III, respectively. For studies with $Q =$ 1333 ml/min, the desired WSS values in ATR-II and ATR-III, are 70 dynes/cm^2 and 31 dynes/cm^2, respectively. Due to the no-slip condition at the lateral walls, there is a boundary layer where the WSS differs substantially from the 2D value. Conservatively, a domain excluding a 3 mm wide strip on each lateral side of the slides will satisfy the ATR criterion. Shown in Fig. 13 are the slide regions, all within the appropriate ATR. Necessarily, the slide must extend beyond the lateral boundaries of the ATR. This can be addressed either by removing these cells from the slide after testing and prior to genetic analysis, or by bounding the domain occupied by the cells (see, e.g. [37]). The effect of varying the flowrate on the WSS distribution on the bottom surface of the final flow chamber (geometric parameters in Table 1), is shown in Fig. 14. The three slides can be seen to be well located for all three flowrates tested.

When the chamber is placed within a flow loop for testing, the flow division can be controlled by downstream flow regulators. 2D CFD studies were performed to investigate the possible impact of imbalances in this split. Shown in Fig. 15 are results of a conservative study, in which a deviation of $\pm 10\%$ from the desired value was imposed. While the change in flow magnitude is reflected in the magnitude of the WSS, it is clear that the locations of both the impingement point and the maximum in WSS are nearly insensitive to an imbalance of this magnitude. Therefore, the interpretation of the three regions within slide I will not be jeopardized if an experimental error of this kind is introduced.

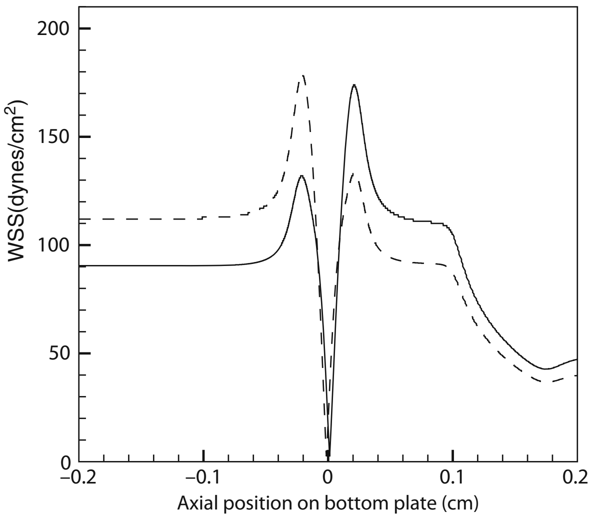

Fig. 15 Evaluation of the effect of a flow imbalance relative to a balanced flow $Q_1 = Q_2 = Q_n$. WSS along the bottom plate for imbalances $(Q_1, Q_2) = (1.1, 0.9)\ Q_n$ (*solid line*) and $(Q_1, Q_2) =$ $(0.9, 1.1)\ Q_n$ (*dashed line*). Geometric parameters are given in Table 1 and $Q_n = 1000$ ml/min

4 Assembly Design and Manufacture

The 3D assembly design of the flow chamber is shown in Fig. 16a, generated using Pro/ENGINEER Wildfire package (PTC Inc). The entire chamber is composed of four plates which we denote as A, B, C, D from the top to bottom in Fig. 16(a) and an inlet adaptor. The breakdown of the upper chamber into three layers was necessary for precise machining of the parent channel which has a very high aspect ratio ($w/h_0 = 16$, $w/h_{in} = 48$) and two different cross sectional shapes (constant and tapered). Machining of this channel through layers A,B,C was the most demanding aspect of the manufacturing process. The daughter branches, daughter diffusers and daughter reservoirs were machined from the underside of Plate C. These three plates were cut to a tolerance of $\pm 0.002''$ (0.051 mm) using CNC milling (Atlantic Diecasting, NY). The inlet reservoir of diameter D_0 was drilled in the top piece. The slide slots were machined to a tolerance of $\pm 0.003''$ (0.076 mm) on the upper side of layer D using CNC milling (Swanson School of Engineering, University of Pittsburgh), Fig. 16a, b. These slots were custom cut to fit the slides to minimize any change in height along the bottom boundary of the fluid domain. Standard AS-568A o-rings were used to seal all sections of the T-chamber, Fig. 16a. The o-rings were chosen to have 20–30% compression to ensure a positive seal while still allowing the mating pieces to properly seat against each other. Precision ground alignment pins were used to assure proper alignment of the pieces during assembly. They were placed at opposite corners of the parts, which is sufficient for alignment on a plane. Another critical aspect of the design was the decision to avoid any glued parts which

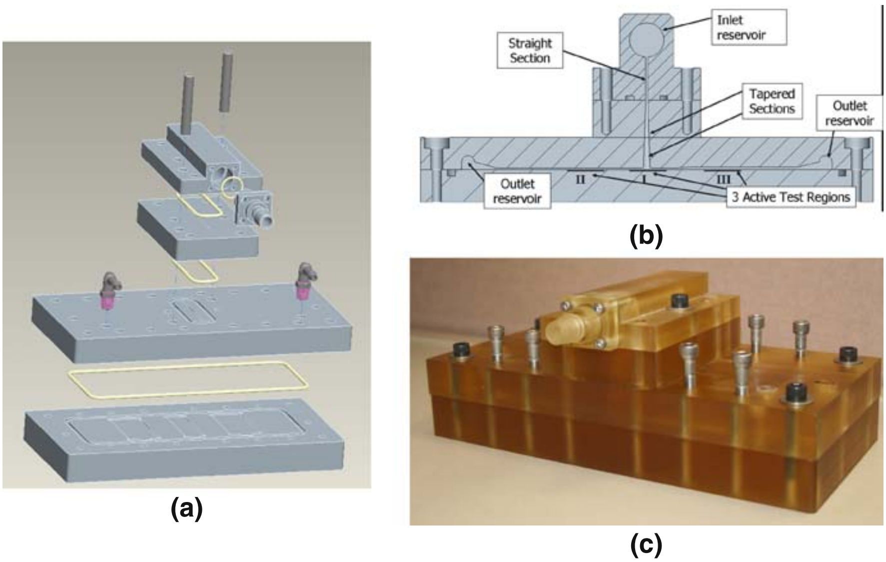

Fig. 16 (**a**) Exploded view of final T-chamber assembly design.(**b**) Cross section view of assembly design of flow chamber. (**c**) Photograph of manufactured T-chamber

could cause warping during autoclaving or potentially leak contaminants into the test chamber. Instead, the pieces were held together by stainless steel, standard hex, quarter 20 (1/4–20″) bolts (McMaster), Fig. 16c. Polysulfone was chosen for the chamber material due to its easy machinability and its ability to withstand autoclave conditions (120°C, 15 psi, 30 min). The final manufactured T-chamber is shown in Fig. 16c. Significantly, the tolerance for the channel heights h_0, h_1, h_2 are all set by the machining tolerances. This is in contrast to the use of gaskets to set the height in some channels.

5 Discussion

Cerebral aneurysms typically form at the apex region of arterial bifurcations. Hemodynamic stresses are believed to play an important role in the initiation of this pathology. Recent work in a canine model identified an association between pre-aneurysmal changes and a combination of elevated WSS and WSSVG in bifurcations formed from a naive vessel. This study was the first to connect in vivo histological changes with specific WSS and WSSVG profiles. The flow chamber designed here provides a tool for exploring these results in a controlled setting.

Most studies of endothelial cell response to mechanical stresses have been motivated by a desire to better understand the role of hemodynamics in the genesis and development of atherosclerosis. A number of researchers have developed in vitro chambers to evaluate the response of cellular components of the arterial wall (e.g. endothelial and smooth muscle cells) to homogeneous stress fields or recirculating flow fields of the type associated with atherosclerotic plaque formation. In early work in this field, DePaola et al., designed a step flow chamber which created a recirculating region [10]. At the edge of this region, the flow impinges on the wall and then separates – part of the flow circulating backward toward the step and the remainder moving downstream. However, the magnitude of the WSS and WSSVG fields in this flow are much smaller than those associated with aneurysm formation.

In this work, we have used parametric CFD studies to design a T-chamber capable of reproducing the qualitative and quantitative features of the WSS and WSSVG fields studied in [39]. The geometry of the flow domain was chosen using 2D and 3D CFD analyses. Building on earlier work for a parallel plate flow chamber [8] and the work in [6, 7], the magnitude of entrance and exit effects were controlled through careful design of chamber reservoirs. A full 3D analysis including all chambers was used to validate the final design. The chamber material was chosen for its easy machinability and its capability to withstand the high temperatures necessary for standard sterilization procedures.

To our knowledge, three previous T-chambers have been constructed [6, 8, 43, 46, 47]. The current chamber builds on that in [6, 8] with several principal changes. It is capable of generating a good approximating of both the WSS and WSSVG fields reported in [38, 39] and conjectured to lead to pre-aneurysmal changes. Secondly, an elliptical rather than circular corner is used at the bifurcation in order to shift the maximum in WSS further away from the impingement point. Thirdly, the chamber is designed so that it does not require any adhesives which could impact the cellular response. As in [6, 8], the height of the chamber is machined into the plates, and is not set by the width of a gasket as has been done in some earlier chambers.

Several features distinguish this T-chamber from that in [46, 47] including (i) the use of inlet and outlet reservoirs to diminish entrance and exit effects, (ii) confinement of wall effects to less than 5% of the chamber width, (iii) avoidance of vortex formation in the bifurcation region, and (iv) the use of three separate test regions for built in controls. Both T-chambers are directed at obtaining nearly 2D flow in the test regions (approximately independent of y, Fig. 3). This is particularly import due to inter-endothelial cell communication which is known to occur through both humoral exchange and via gap junctions. Furthermore, if the cells are to be removed from the slides for later analysis, the cells outside the ATR will contaminate the data. The effects of the entrance flow, exit flow and walls preclude complete 2D flow in the slide regions. Fortunately, the lateral wall effects can be diminished by lowering the aspect ratio of the chamber [8]. A boundary layer thickness defined by a WSS less than 90% of the centerline value can be estimated from the exact solution for fully developed flow in a channel [8]. For the current chamber, β (the channel thickness to width ratio) is quite small: 0.017, 0.025 and 0.0625 in the daughter and parent branches with a corresponding boundary layer thickness of 4.2% or less of the chamber width. However, for a parent value of $\beta = 0.15$ such as is found in [46, 47], the boundary layer on each side of the channel will rise to nearly 10% of the chamber width. The effect can be even more dramatic in the non-monotonic region at the apex, (e.g. Fig. 2 of [47]). The reservoirs significantly diminish the effect of the inlet and outlet flow for the chamber. The absence of reservoirs can result in large entrance and exit lengths which cannot be predicted by simple boundary layer theory [1, 8]. The chamber used in [46, 47] does not employ reservoirs. The inlets and outlets were omitted from the CFD analysis in [46, 47], so the impact of this design choice is not known. The connection of an inlet tube of circular cross section to a rectangular channel in the parent branch in their chamber will be expected to have a significant downstream influence.

Many tests of cell functionality provide only a relative measure of a particular response. To address this issue, we have included two control sections within the T-chamber. In the current chamber, the control flows are for a WSS of two different magnitudes. By switching out the bottom plate it is possible to change these controls. Other control flows of interest include flow over a backward facing step and constant WSSVG flows.

The apex region of the current chamber was carefully designed to avoid generating vortices at the outer walls of the bifurcation. Even for steady flows, these vortices will change the WSS profile on the bottom plate [46, 47]. Clearly this will be even more problematic if the vortices become unstable and are washed downstream.

A variety of WSSG definitions are used in the literature, unfortunately confounding comparison of results from different groups. As in this work, several researchers consider the $\underline{G} = \text{grad}_s \underline{t}_s$ to be of primary importance, (e.g. [5, 26, 32]). In these works, an orthogonal surface basis composed of a unit vector in the time averaged direction of $\underline{t}_s$ (for a cardiac cycle) and its perpendicular component are introduced. The WSSG is then defined as the square root of the sum of the squares of the diagonal elements of $\underline{G}$ using this basis. In contrast in [22], $\underline{G}$ is replaced with the 3D gradient of the full stress vector $\underline{t}$. For both these definitions, a non-negative quantity is used for the WSSG. In [25], the WSSG was approximated by the change in WSS divided by the change in axial position. In other works, particularly those with 2D flows in mind, the WSSG is not clearly defined. The variation in definitions may be one reason why groups have reported different correlations between biological markers for intimal hyperplasia and WSSG.

In this work, we have introduced a new measure of the gradient of the wall shear stress, denoted as WSSVG to distinguish it from these definitions of WSSG and to emphasize that it is not a measure of the gradient of WSS. We feel the WSSVG definition (7) has some advantages. It differentiates between increasing and decreasing shear stress through the sign of the WSSVG. It has been shown to be a scalar invariant of $\mathrm{grad}_s \underline{t}_s$ and it does not require calculation of the time averaged direction of WSS a priori. These last two points will become important if the WSSVG is to be incorporated into constitutive equations of the arterial wall, for example, to capture destructive remodeling during aneurysm formation [34, 35]. Furthermore, when the definition (7) is specialized to 2D flows over a flat surface, the sign of the gradient enters in a physically meaningful way.

In the future, it may be of interest to use this chamber for unsteady flows. In preliminary studies, we have found little difference between WSS and WSSVG results for steady simulations and the corresponding time averaged values for unsteady simulations using the same time averaged flow rates. It will also be useful to study the cellular response in real time. Modifications can be made to the bottom plate to achieve this objective.

Acknowledgments The authors would like to thank Andy Holmes of the Swanson Center for Product Innovation at the University of Pittsburgh for his valuable suggestions on the design and manufacture of the T-chamber. A number of undergraduates from the Department of Mechanical Engineering and Materials Science at the University of Pittsburgh have worked on an earlier version of the T-chamber as part of their senior design project and as undergraduate researchers. In particular, the authors would like to acknowledge John Barrow, Jason Larkin and David Remic [31]. A.M. Robertson would like to thank the Aachen Institute for Advanced Study in Computational Engineering Science (AICES) of the University of Aachen for a visiting professorship which she held during the period this paper was written.

References

1. Anderson, E., Falls, T., Sorkin, A., Tate, M.: The imperative for controlled mechanical stresses in unraveling cellular mechanisms of mechanotransduction. BioMed. Eng. OnLine **5**, 27 (2006) doi: 10.1186/1475-925X-5-27
2. Barbee, K., Davies, P., Lal, R.: Shear stress-induced reorganization of the surface topography of living endothelial cells imaged by atomic force microscopy. Circ. Res. **74**(1), 163–171 (1994)
3. Bathe, K.: *Finite Element Procedures*. Prentice Hall, Prentice (1996)

4. Berger, S.A., Lou, L.D.: Flows in stenotic vessels. Annu. Rev. Fluid Mech. **32**, 347–382 (2000)
5. Buchanan, J.R., Kleinstreuer, C., Truskey, G.A., Lei, M.: Relation between non-uniform hemodynamics and sites of altered permeability and lesion growth at the rabbit aorto-celiac junction. Atherosclerosis **143**(1), 27–40 (1999)
6. Chung, B.J.: The study of blood flow in arterial bifurcations: the influence of hemodynamics on endothelial cell response to vessel wall mechanics. Ph.D. thesis, University of Pittsburgh (2004)
7. Chung, B.J., Robertson, A.M.: A novel flow chamber to evaluate endothelial cell response to flow at arterial bifurcations. In: Annual meeting of the Biomedical Engineering Society (BMES), p. 6P5.113. Nashville, Tennessee (2003)
8. Chung, B.J., Robertson, A.M., Peters, D.G.: The numerical design of a parallel plate flow chamber for investigation of endothelial cell response to shear stress. Comput. Struct. **81**, 535–546 (2003). doi:10.1016/S0045-7949(02)00416-9
9. Davies, P.F., Shi, C., Depaola, N., Helmke, B.P., Polacek, D.C.: Hemodynamics and the focal origin of atherosclerosis: A spatial approach to endothelial structure, gene expression, and function. Ann. N.Y. Acad. Sci. **947**, 7–16; discussion 16–17 (2001)
10. DePaola, N., Gimbrone, M., Davies, P.F., Dewey, C.: Vascular endothelium responds to fluid shear stress gradients. [erratum appears in Arterioscler Thromb 1993 Mar;13(3):465]. Arterio. Thromb. **12**(11), 1254–1257 (1992)
11. Foutrakis, G.N., Yonas, H., Sclabassi, R.J.: Saccular aneurysm formation in curved and bifurcating arteries. Am. J. Neuroradiol. **20**(7), 1309–1317 (1999)
12. Frangos, J.A., McIntire, L., Eskin, S.G.: Shear stress induced stimulation of mammalian cell metabolism. Biotechnol. Bioeng. **32**, 1053–1060 (1988)
13. Galdi, G.P.: Mathematical problems in classical and non-newtonian fluid mechanics. In: G.P. Galdi, R. Rannacher, A.M. Robertson, S. Turek (eds.) *Hemodynamical Flows: Modeling, Analysis and Simulation*, Oberwolfach Seminars, vol. 37. Birkhäuser, Cambridge (2008)
14. Gao, L., Hoi, Y., Swartz, D.D., Kolega, J., Siddiqui, A., Meng, H.: Nascent aneurysm formation at the basilar terminus induced by hemodynamics. Stroke J. Cereb. Circ. **39**(7), 2085–2090 (2008)
15. Glagov, S., Zarins, C., Giddens, D., Ku, D.N.: Hemodynamics and atherosclerosis: insights and perspectives gained from studies of human arteries. Arch. Pathol. Lab. Med. **112**, 1018–1031 (1988)
16. Goode, T., Davies, P., Reidy, M., Bowyer, D.: Aortic endothelial cell morphology observed in situ by scanning electron microscopy during atherogenesis in the rabbit. Atherosclerosis **27**(2), 235–51 (1977)
17. Gresho, P.M.: Some current CFD issues relevant to the incompressible Navier-Stokes equations. Comput. Methods Appl. **87**, 201–252 (1991)
18. Haljasmaa, I., Robertson, A.M., Galdi, G.P.: On the effect of apex geomery on wall shear stress and pressure in two-dimensional models of arterial bifurcations. Math. Models Methods Appl. S. **11**(3), 499–520 (2001)
19. Hashimoto, N., Handa, H., Nagata, I., Hazama, F.: Experimentally induced cerebral aneurysms in rats: Part V. Relation of hemodynamics in the circle of Willis to formation of aneurysms. Surg. Neurol. **13**(1), 41–45 (1980)
20. Hassler, O.: Experimental carotid ligation followed by aneurysmal formation and other morphological changes in the circle of Willis. J. Neurosurg. **20**, 1–7 (1963)
21. Heywood, J.G., Rannacher, R., Turek, S.: Artificial boundaries and flux and pressure conditions for the incompressible Navier-Stokes equations. Int. J. Numer. Methods Fluids **22**, 325–352 (1996)
22. Huo, Y., Guo, X., Kassab, G.S.: The flow field along the entire length of mouse aorta and primary branches. Ann. Biomed. Eng. **36**(5), 685–699 (2008)
23. Kamiya, A., Togawa, T.: Adaptive regulation of wall shear stress to flow change in the canine carotid artery. Am. J. Physiol. **239**, H14–H21 (1980)
24. Kayembe, K., Sasahara, M., Hazama, F.: Cerebral aneurysms and variations in the circle of Willis. Stroke **15**, 846–850 (1984)

25. Keynton, R.S., Evancho, M.M., Sims, R.L., Rodway, N.V., Gobin, A., Rittgers, S.E.: Intimal hyperplasia and wall shear in arterial bypass graft distal anastomoses: An in vivo model study. J. Biomech. Eng. **123**(5), 464–473 (2001)
26. Kleinstreuer, C., Hyun, S., Buchanan, J.R., J, Longest, P.W., Archie J.P., J, Truskey, G.A.: Hemodynamic parameters and early intimal thickening in branching blood vessels. Crit. Rev. Biomed. Eng. **29**(1), 1–64 (2001)
27. Ku, D.N.: Blood flow in arteries. Annu. Rev. Fluid Mech. **29**(1), 399–434 (1997)
28. Kučera, P., Skalák, Z.: Local solutions to the Navier-Stokes equations with mixed boundary conditions. Acta Appl. Math. **54**(3), 275–288 (1998) 10.1023/A:1006185601807
29. LaMack, J.A., Himburg, H.A., Li, X.M., Friedman, M.H.: Interaction of wall shear stress magnitude and gradient in the prediction of arterial macromolecular permeability. Ann. Biomed. Eng. **33**(4), 457–464 (2005)
30. Langille, B.L.: Arterial remodeling: relation to hemodynamics. Can. J. Physiol. Pharmacol. **74**(7), 834–841 (1996)
31. Larkin, J., Barrow, J., Durka, M., Remic, D., Zeng, Z., Robertson, A.M.: Design of a flow chamber to explore the initiation and development of cerebral aneurysms. In: Annual Fall Meeting of the Biomedical Engineering Society (BMES). Los Angeles, CA (2007)
32. Lei, M., Archie, J.P., Kleinstreuer, C.: Computational design of a bypass graft that minimizes wall shear stress gradients in the region of the distal anastomosis. J. Vasc. Surg. **25**(4), 637–646 (1997)
33. Leone, J.M., Gresho, P.M.: Finite element simulations of steady, two-dimensional, viscous incompressible flow over a step. J. Comput. Phys. **41**(1), 167–191 (1981) doi: 10.1016/0021-9991(81)90086-3
34. Li, D., Robertson, A.M.: A structural multi-mechanism damage model for cerebral arterial tissue and its finite element implementation. Proceedings of the ASME 2008 Summer Bioengineering Conference (SBC-2008) (2008)
35. Li, D., Robertson, A.M.: A structural multi-mechanism damage model for cerebral arterial tissue. J. Biomech. Eng. **131**(10), 101013 (2009), doi:10.1115/1-3202559.
36. Malek, A.M., Izumo, S.: Mechanism of endothelial cell shape change and cytoskeletal remodeling in response to fluid shear stress. J. Cell Sci. **109**, 713–726 (1996)
37. McCann, J., Peterson, S., Plesniak, M., Webster, T., Haberstroh, K.: Non-uniform flow behavior in a parallel plate flow chamber alters endothelial cell responses. Ann. Biomed. Eng. **33**(3), 328–336 (2005) 10.1007/s10439-005-1735-9
38. Meng, H., Swartz, D.D., Wang, Z., Hoi, Y., Kolega, J., Metaxa, E.M., Szymanski, M.P., Yamamoto, J., Sauvageau, E., Levy, E.I.: A model system for mapping vascular responses to complex hemodynamics at arterial bifurcations in vivo. Neurosurgery **59**(5), 1094–1100; discussion 1100–1101 (2006)
39. Meng, H., Wang, Z., Hoi, Y., Gao, L., Metaxa, E., Swartz, D.D., Kolega, J.: Complex hemodynamics at the apex of an arterial bifurcation induces vascular remodeling resembling cerebral aneurysm initiation. Stroke **38**(6), 1924–1931 (2007)
40. Murray, C.D.: The physiological principle of minimum work. Proc. Natl. Acad. Sci. USA **12**(3), 207–214 (1926)
41. Nagel, T., Resnick, N., Dewey, C., Forbes, J., Gimbrone Michael, A., Jr.: Vascular endothelial cells respond to spatial gradients in fluid shear stress by enhanced activation of transcription factors. Arterio. Thromb. Vasc. Biol. **19**(8), 1825–1834 (1999)
42. Robertson, A.M., Sequeira, A., Kameneva, M.: Hemorheology. In: G.P. Galdi, R. Rannacher, A.M. Robertson, S. Turek (eds.) *Hemodynamical Flows: Modeling, Analysis and Simulation*, Oberwolfach Seminars, vol. 37. Birkhäuser, Cambridge (2008)
43. Sakamoto, N., Ohashi, T., Sato, M.: High shear stress induces production of matrix metalloproteinase in endothelial cells. In: Proceedings of the ASME 2008 Summer Bioengineering Conference (SBC2008). Marco Island, Florida (2008)
44. Sasaki, T., Kodama, N., Itokawa, H.: Aneurysm formation and rupture at the site of anastomosis following bypass surgery. J. Neurosurg. **85**, 500–502 (1996)

45. Sekhar, L.N., Heros, R.C.: Origin, growth, and rupture of saccular aneurysms: A review. Neurosurgery **8**, 248 –260 (1981)
46. Szymanski, M.: Endothelial cell layer subjected to flow mimickng the apex of an arterial bifurcation. Ph.d., State University of New York at Buffalo (2007)
47. Szymanski, M., Metaxa, E., Meng, H., Kolega, J.: Endothelial cell layer subjected to impinging flow mimicking the apex of an arterial bifurcation. Ann. Biomed. Eng. **36**(10), 1681–1689 (2008)
48. Truesdell, C., Noll, W.: Non-linear field theories of mechanics. In: S. Flugge (ed.) *Handbuch der Physik*, vol. III/3. Springer-Verlag, Berlin (1965)
49. Zakaria, H., Robertson, A.M., Kerber, C.: A parametric model for studies of flow in arterial bifurcations. Ann. Biomed. Eng. **36**(9), 1515–1530 (2008)
50. Zamir, M.: Optimality principles in arterial branching. J. Theor. Biol. **62**(1), 227–251 (1976)
51. Zheng, L., Yang, W.: Biofluid dynamics at arterial bifurcations. Crit. Rev. Biomed. Eng. **19**, 455–493 (1992)